2017

Azaborines: Unique Isosteres Of Aromatic And Heteroaromatic Systems

Geraint H. M. Davies
University of Pennsylvania, ghdavie@gmail.com

Azaborines: Unique Isosteres Of Aromatic And Heteroaromatic Systems

Abstract
The azaborine motif provides a unique opportunity to develop core isosteres by inserting B-N units in place of C=C bonds within aromatic scaffolds. These boron/nitrogen-containing heteroaromatic systems provide molecular frameworks that have similar, but not identical, geometrical shapes and electronic distributions to the analogous all carbon systems. Synthetic routes to the 1,3,2-benzodiazaborole core have been developed utilizing entirely bench-stable starting materials, including organotrifluoroborates, enabling a wider array of substrate analogues under facile reaction conditions. The physical, structural, and electronic properties of these compounds were explored computationally to understand the influence of the B-N replacement on structure, aromaticity, and the isosteric viability of these analogues. The class of azaborininones could similarly be accessed from both organotrifluoroborates and boronic acids. An inexpensive, common reagent, SiO2, was found to serve as both a fluorophile and desiccant to facilitate the annulation process across three different azaborininone platforms. Computationally-derived pKa values, NICS aromaticity calculations, and electrostatic potential surfaces revealed a unique isoelectronic/isostructural relationship between these azaborines and their carbon isosteres that changed based on boron connectivity. The 2,1-borazaronaphthalene motif can be accessed through robust methods of synthesis and subsequent functionalization strategies, affording an ideal platform to use for a variety of applications. However, the initial scope of substructures for this archetype has been limited by the lack of nitrogen-containing heteroaryls that can be incorporated within them. Modified reaction conditions enabled greater tolerance to provide access to a wider range of substructures. Additionally, computational and experimental studies of solvent decomposition demonstrate that substitution off boron is important to stability.

Post-annulation derivitization of the azaborine cores can allow access to higher order functionalized structures. A method for functionalizing the 2,1-borazaronaphthalene scaffold using ammonium alkylbis(catecholato)silicates via photoredox/nickel dual catalysis was found to be highly effective. By forging Csp3–Csp2 bonds via this approach, alkyl fragments with various functional groups can be introduced to the azaborine core, affording previously inaccessible heterocyclic isosteres in good to excellent yields. These conditions provide sensitive functional group tolerance, even permitting the cross-coupling of unprotected primary and secondary amines. Regioselective C-H borylation and subsequent cross-coupling of the 2,1-borazaronaphthalene core could also be achieved. Although 2,1-borazaronaphthalene is closely related to naphthalene in terms of structure, the argument is made that the former has electronic similarities to indole. Based on that premise, iridium-mediated C-H activation has enabled facile installation of a versatile, nucleophilic coupling handle at a previously inaccessible site of 2,1-borazaronaphthalenes. A variety of substituted 2,1-borazaronaphthalene cores can be successfully borylated and further cross-coupled in a facile manner to yield diverse C(8)-substituted 2,1-borazaronaphthalenes.

Degree Type
Dissertation

Degree Name
Doctor of Philosophy (PhD)

Graduate Group
Chemistry

AZABORINES: UNIQUE ISOSTERES OF AROMATIC AND HETEROAROMATIC SYSTEMS

Geraint H. M. Davies

A DISSERTATION

in

Chemistry

Presented to the Faculties of the University of Pennsylvania

in

Partial Fulfillment of the Requirements for the
Degree of Doctor of Philosophy

2017

Supervisor of Dissertation

_____

Gary A. Molander
Hirschmann-Makineni Professor of Chemistry

Graduate Group Chairperson

_____

Gary A. Molander
Hirschmann-Makineni Professor of Chemistry

Dissertation Committee:

David M. Chenoweth, Assistant Professor of Chemistry
Donna M. Huryn, Adjunct Professor of Chemistry
Daniel J. Mindiola, Presidential Professor of Chemistry

AZABORINES: UNIQUE ISOSTERES OF AROMATIC AND HETEROAROMATIC SYSTEMS

To Mom, Dad, and Evan

ACKNOWLEDGEMENTS

I would like to start by recognizing my advisor, Professor Gary Molander, for his guidance and patience. As a member of his research group I have had the freedom to explore and grow in many directions, often diverting from the standard practices of the lab. Through the trials and tribulations of graduate school, Gary has continually provided a stable environment for me to learn and develop into the researcher I am today.

I am also grateful for my committee members, Professors David Chenoweth, Donna Huryn and Daniel Mindiola. They have helped to steer me in productive pathways though their suggestions and discussions within my committee meetings.

Within the Molander group, Dr. Steve Wisniewski and Dr. Kaitlin (Traister) Rosen showed me the ins and outs of the lab. Even after they have gone on to successful careers, their guidance is still felt, as both of their dissertations have sat on my desk throughout the writing process. More recently, Dr. Matthieu Jouffroy and Dr. Chris Kelly had been great friends, mentors and colleagues, providing support for both my projects and career development. I would also like to acknowledge all of those that have worked with me on the azaborine projects - Casey Howshall, Asma Mukhtar, Melissa Ramirez, Borna Saeednia, Jennifer Saouaf, Fatemeh 'Zahra' Sherafat, Xie Wang, Minrui Xu, Zhaozhao Zhou - and to the rest of the Molander group for creating an atmosphere where I have been able to be successful.

Within the department, I would like to thank several friends who have helped me throughout my time at Penn; Melissa Grenier, Tyler Higgins, Dr. Simon Lang, Roy Malamakal, Dr. Bruno Melillo, Mike Nicastri, Dr. James Phelan, David Primer, Dr. Jerome Robinson, Chris Walters, and Dr. Ryan Walvoord. Dr. Simon Berrett (UPenn-Merck Screening Center) and Dr. George Furst (NMR) have also been valuable resources within the department. And a special thanks to Chris Jeffrey for being a voice of reason and source of constant help throughout my tenure at Penn.

Outside of the Penn Chemistry Department, there have been so many people who have helped me along the way. From my first exposure to research, that set me on this path, at Princeton University in the laboratory of Professor Erik Sorensen with mentors Professor Chris Jeffrey (University of Reno, Nevada) and Dr. John Malona (Celgene), to the opportunity to experience process research at Bristol-Myers Squibb under the guidance of Dr. Omid Soltani (Seattle Genetic) and Dr. Caroline Wei, as well as the foundation of my early training at Emory University in the research group of Professor Simon Blakey. I would be remiss to not mention both the Penn Running Club and Philadelphia Runner Track Club for providing me an outlet away from chemistry.

And finally and most importantly, I need thank my family. My dad, for inspiring my decision to pursue organic chemistry, and from whom I can still benefit from 'homework' help even at the culmination of my graduate career. My mum, who has always demonstrated by example that it is possible to do whatever one sets their mind to, no matter how difficult the task ahead. And to my brother Evan, who

has embarked in his own Ph.D journey in engineering, for not only being a supportive sibling, but for also providing critical input on some of the fundamental mathematics for the computational projects I have undertaken.

Thank you.

ABSTRACT

AZABORINES: UNIQUE ISOSTERES OF AROMATIC AND HETEROAROMATIC SYSTEMS

Geraint H. M. Davies

Gary A. Molander

The azaborine motif provides a unique opportunity to develop core isosteres by inserting B-N units in place of C=C bonds within aromatic scaffolds. These

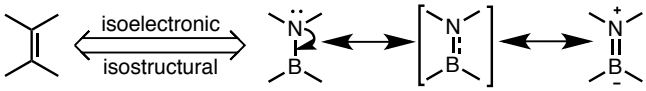

boron/nitrogen-containing heteroaromatic systems provide molecular frameworks that have similar, but not identical, geometrical shapes and electronic distributions to the analogous all carbon systems. Synthetic routes to the 1,3,2-benzodiazaborole core have been developed utilizing entirely bench-stable starting materials, including organotrifluoroborates, enabling a wider array of substrate analogues under facile reaction conditions. The physical, structural, and electronic properties

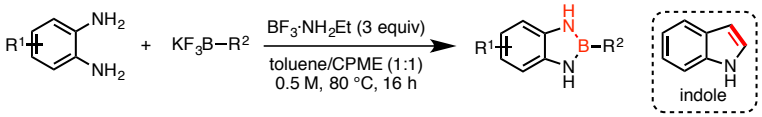

of these compounds were explored computationally to understand the influence of the B-N replacement on structure, aromaticity, and the isosteric viability of these analogues. The class of azaborininones could similarly be accessed from both organotrifluoroborates and boronic acids. An inexpensive, common reagent, SiO_2, was found to serve as both a fluorophile and desiccant to facilitate the annulation

process across three different azaborininone platforms. Computationally-derived pK_a values, NICS aromaticity calculations, and electrostatic potential surfaces

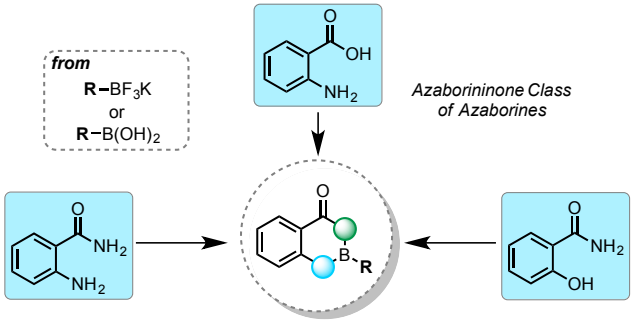

revealed a unique isoelectronic/isostructural relationship between these azaborines and their carbon isosteres that changed based on boron connectivity. The 2,1-borazaronaphthalene motif can be accessed through robust methods of synthesis and subsequent functionalization strategies, affording an ideal platform to use for a variety of applications. However, the initial scope of substructures for this archetype has been limited by the lack of nitrogen-containing heteroaryls that can be incorporated within them. Modified reaction conditions enabled greater tolerance to provide access to a wider range of substructures. Additionally, computational and experimental studies of solvent decomposition demonstrate that substitution off boron is important to stability.

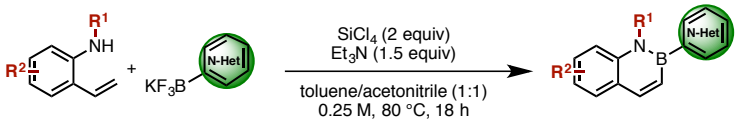

Post-annulation derivitization of the azaborine cores can allow access to higher order functionalized structures. A method for functionalizing the 2,1-borazaronaphthalene scaffold using ammonium alkylbis(catecholato)silicates *via* photoredox/nickel dual catalysis was found to be highly effective. By forging C_{sp^3}–

C_{sp}^2 bonds *via* this approach, alkyl fragments with various functional groups can be introduced to the azaborine core, affording previously inaccessible heterocyclic isosteres in good to excellent yields. These conditions provide sensitive functional group tolerance, even permitting the cross-coupling of unprotected primary and

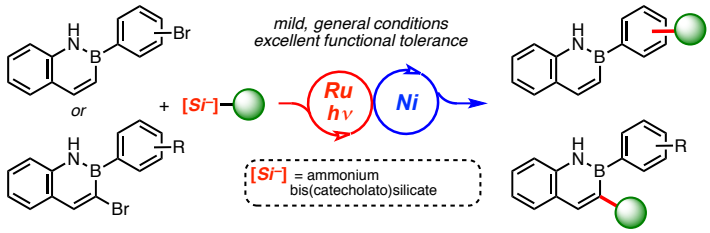

secondary amines. Regioselective C-H borylation and subsequent cross-coupling of the 2,1-borazaronaphthalene core could also be achieved. Although 2,1-borazaronaphthalene is closely related to naphthalene in terms of structure, the argument is made that the former has electronic similarities to indole. Based on that premise, iridium-mediated C-H activation has enabled facile installation of a versatile, nucleophilic coupling handle at a previously inaccessible site of 2,1-borazaronaphthalenes. A variety of substituted 2,1-borazaronaphthalene cores can be successfully borylated and further cross-coupled in a facile manner to yield diverse C(8)-substituted 2,1-borazaronaphthalenes.

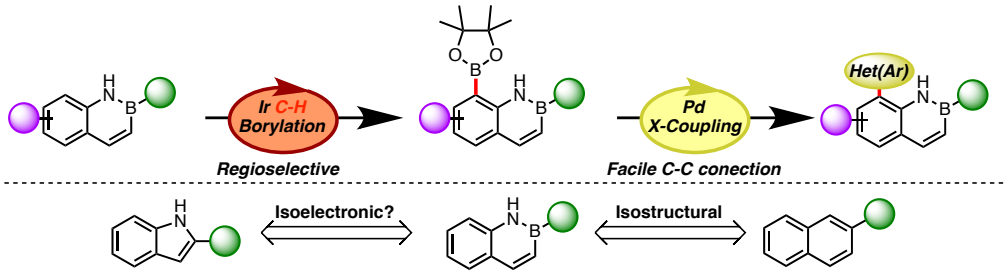

TABLE OF CONTENTS

LIST OF ABBREVIATIONS

δ	Chemical shift in parts per million
%Δ	Percent change
° C	Digress Celsius
^{11}B	Boron nuclear magnetic resonance
^{13}C	Carbon nuclear magnetic resonance
^{13}C {^{1}H}	Carbon nuclear magnetic resonance, proton decoupled
^{19}F	Fluorine nuclear magnetic resonance
^{19}F {^{1}H}	Fluorine nuclear magnetic resonance, proton decoupled
^{1}H	Hydrogen nuclear magnetic resonance
Å	Angstrom
ADME	Absorption, distribution, metabolism, and excretion
Alk	Alkyl
Aq	Aqueous
Ar	Aryl
B_2Pin_2	Bis(pinacolato)diboron
B	Boron
B3LYP	Becke, 3-parameter, Lee-Yang-Par
BCl_3	Boron trichloride
BF_3	Boron trifluoride
$BF_3•Et_2O$	Boron trifluoride diethyl etherate
$BF_3•Et_2O$	Boron trifluoride ethylamine complex
BF_3K	Potassium trifluoroborate
Boc	*tert*-Butyloxycarbonyl
$B(OH)_2$	Boronic acid
Br	Bromine
br	Broad
C	Carbon
Cat	Catechol
$CDCl_3$	Deuterated chloroform
CF_3	Trifluoromethyl

$CFCl_3$	Trichlorofluoromethane
CH_2Cl_2	Methylene dichloride
CI-TOF	Chemical ionization – time of flight mass spectrometry
Cl	Chloride
cm	Centimeters
CN	Cyano
CPME	Cyclopentyl methyl ether
Cs_2CO_3	Cesium carbonate
D	Daltons
d	Doublet
DCE	1,2-Dichloroethane
DMA	Dimethylacetamide
DME	Dimethoxyethane
DMF	Dimethylformamide
DMSO	Dimethyl sulfoxide
DMSO-d_6	Deuterated dimethyl sulfoxide
D_2O	Deuterium oxide
dtbbpy	4,4'-Di-*tert*-butyl-2,2'-dipyridyl
EI-TOF	Electron impact – time of flight mass spectrometry
Equiv	Equivalence
ESI-TOF	Electron spray ionization – time of flight mass spectrometry
Et	Ethyl
Et_3N	Triethylamine
EtOAc	Ethyl acetate
EtOH	Ethanol
Et_2O	Diethyl ether
F	Fluorine
FTIR-ATR	Fourier transform infrared spectroscopy – attenuated total reflectance
G	Gibbs free energy
GC-MS	Gas chromatography – mass spectrometry
GIAO	Gauge-independent atomic orbital
H	Hydrogen

h	Hours
hν	Light
HCl	Hydrogen chloride
H_2O	Water
HMDS	Hexamethyldisilazide
HOMO	Highest occupied molecular orbital
HPLC	High Pressure Liquid Chromatography
HRMS	High Resolution Mass Spectrometry
HTE	High-Throughput Experimentation
IC_{50}	Half maximal inhibitory concentration
IS	Internal Standard
Ile	Isoleucine
i-PrOH	Isopropyl alcohol
IR	Infrared spectroscopy
$[Ir(\mu\text{-}Cl)(COD)]_2$	Bis(1,5-cyclooctadiene)diiridium(I) dichloride
$[Ir(\mu\text{-}OMe)(COD)]_2$	Bis(1,5-cyclooctadiene)di-μ-methoxydiiridium(I)
J	Coupling constant
K	Kelvin
kcals	Kilocalories
K_2CO_3	Potassium carbonate
KHMDS	Potassium hexamethyldisilazide
kJ	Kilojoules
Lys	Lysine
LUMO	Lowest unoccupied molecular orbital
M	Molar concentration
m	Multiplet
M+ / M-	Molecular ion
μM	Micromolar
Me	Methyl
MeOH	Methanol
MeCN	Acetonitrile
MeCy	Methylcyclohexane

MeTHF	2-Methyltetrahydrofuran
mg	Milligrams
$MgSO_4$	Magnesium sulfate
MHz	Megahertz
min	Minutes
mmol	Millimoles
Mn	Manganese
mol	Mole
MP	Melting point
MTBE	Methyl *tert*-butyl ether
N	Nitrogen
$NaBF_4$	Sodium tetrafluoroborate
$NaHCO_3$	Sodium bicarbonate
Na_2CO_3	Sodium carbonate
Na_2SO_4	Sodium sulfate
NaOH	Sodium hydroxide
NH_4Cl	Ammonium chloride
Ni	Nickel
$NiCl_2$(dme)	Nickel(II) chloride ethylene glycol dimethyl ether complex
NICS	Nucleus-independent chemical shift
NMR	Nuclear magnetic resonance
nM	Nanomolar
O	Oxygen
Pd	Palladium
PDE	phosphodiesterase
pH	Potential of hydrogen
Ph	Phenyl
pIC_{50}	-log(IC_{50})
ppm	Parts per million
PPh_3	Triphenylphosphine
Prod	Product
Pt	Platinum

q	Quartet
R	Generic group
R^2	Coefficient of determination
RCM	Ring closing metathesis
rt	Room temperature
$Ru(bpy)_3(PF_6)_2$	Tris(2,2'-bipyridine)ruthenium(II) hexafluorophosphate
$RuCl_2(PPh_3)_3$	Dichlorotris(triphenylphosphine)ruthenium(II)
Rxn	Reaction
S	Sulfur
s	Singlet
SET	Single electron transfer
sept	Septet
Si	Silicon
$SiCl_4$	Silicon tetrachloride
SiO_2	Silicone dioxide (silica gel)
SM	Starting material
SMe_2	Dimethyl sulfide
t	Triplet
t-BuOH	*tert*-Butyl alcohol
THF	Tetrahydrofuran
Try	Tyrosine
TMS	Tetramethylsilane
TMSCl	Trimethylsilyl chloride
XPhos	2-Dicyclohexylphosphino-2′,4′,6′-triisopropylbiphenyl
XPhos-Pd-G2	2nd generation XPhos precatalyst

CHAPTER 1 – THE AZABORINE ISOSTERE

1.1 – Isosterism as it applies to boron/nitrogen containing heterocycles

Isosterism, first proposed by Irving Langmuir in his treatise "Isomorphism, Isosterism and Covalence",[1] is a fundamental concept in small molecule design that relies on the relative similarities and differences of various compounds. In Langmuir's case, he noticed the surprising similarity of the physical properties of carbon dioxide (CO_2) and nitrous oxide (N_2O) - critical temperature and pressure, viscosity, thermal conductivity, dielectric constant, and density – despite having fundamentally different atomic construction. The origins of this phenomenon stems from the underlying electrostatic similarities of these two compounds. Advances in orbital theory since the time of Langmuir have resulted in a more comprehensive understanding of the classical theory of isosteres, which are defined as molecules or fragments that contain the same peripheral electron sphere.[2]

A subset of isosterism, which is of particular interest in the modern era, is bioisosterism, wherein different structural motifs are compared and categorized based on biological function.[3] The application of bioisosteres, coupled with computational methods for comparing fragment properties, has been instrumental in the advancement of new therapeutic candidates. Classes of isosteres include molecules with fluorine or deuterium at positions previously occupied by hydrogen, specifically at sites prone to oxidation. Thiol or amino groups can be interchanged with hydroxyl groups, based on their capacity for hydrogen bonding. sp^2-Hybridized substructures can also be efficiently exchanged (C=S, C=O, C=NH and C=C) and can

be further extended to the corresponding aromatic ring systems (furan, thiophene, pyrole, oxazole, pyrazole, and imidazole). For aromatic six-membered rings, insertion of nitrogen is one of the few options that retains both ring size and aromaticity. This is ultimately a limited isostere because it introduces a basic motif that is capable of chemistries not common to all-carbon arenes.

One strategy to overcome this limitation is to consider fundamental isosteres of a C=C that could be exchanged within the ring system. One such example is the comparison of a C=C bond to that of a B-N bond (Figure 1.1). Donation of the Lewis basic lone pair of nitrogen into the Lewis acidic empty orbital of boron allows pseudo double-bond character. Both C=C and B-N subunits contain the same

Figure 1.1: B-N isosterism for C=C

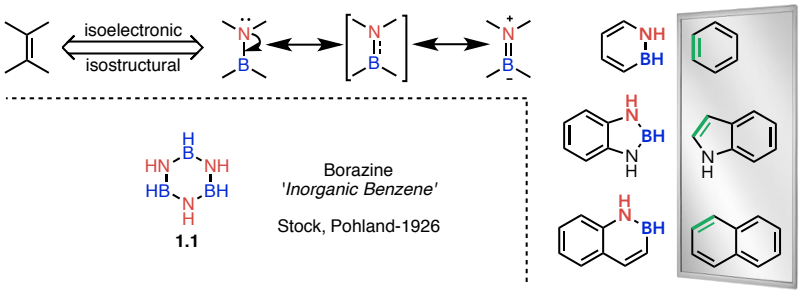

electron count and have similar structural features (four external bonds, two on each side). This class of compounds dates back to 1926 with the discovery of borazine (**1.1**),[4] known as "inorganic benzene", composed of alternating B-N bonds. Organic variants, where *one* B-N bond is inserted into a carbon-based aromatic system, coined azaborines, were initially studied in attempts to understand aromaticity. As the field matured and synthetic viability for accessing these classes of molecule improved, the potential applications of these systems began to be

realized.[5] An early example of this was a report detailing the antibacterial activity of diazaborine **1.2** (Figure 1.2), which binds to the enoyl reductase of *Escherichia coli*.[6] A crystal structure of the compound in the active site revealed an unusual, tetravalent coordination between the boron and an alcohol of a nicotinamide ribose also present in the binding pocket (**1.3**), which provided additional hydrogen bond contacts. Although spatially viable, the carbon analogues show no appreciable activity, demonstrating the potential of the azaborine scaffold to provide normally inaccessible pharmacological activity. There is growing interest in the application of boron isosteres to medicinally relevant systems, as these substuctures can open up new intellectual property space and offer new avenues for binding.[7]

Figure 1.2: Diazaborine biological activity *via* tetravalent coordination of boron in the enoyl reductase binding pocket of *Escherichia coli*

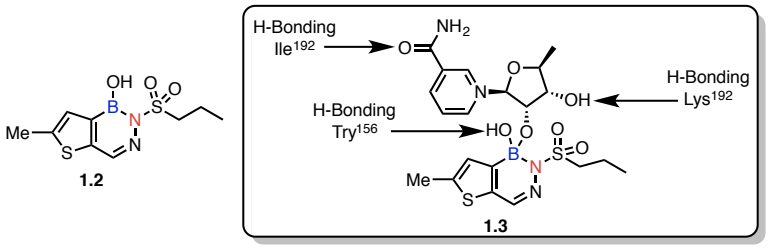

1.2 – Computational analysis of azaborine isosterism

When considering how to verify the proposed azaborines as isosteres, computational modeling offers an easy entry point.[8] By comparing predicted structural parameters, it is possible to gain insight into the viability of a potential isostere prior to physical testing. As most of the early interest in azaborines was predicated on understanding aromaticity, and considering the significance of applying these molecules as heteroaromatic isosteres, computational studies

predominantly focused on understanding the aromatic properties of the B-N containing structures. A useful barometer for understanding aromaticity is nucleus-independent chemical shielding (NICS) calculations,[9] which provide a quantitative correlation for aromaticity using a "theoretical nuclei" at the center of a ring system to probe electron shielding. Typically, evaluations are done at a distances of 0.0 angstrom [NICS(0)] and 1 angstrom [NICS(0)] from the plane of the ring system. A more negative NICS value indicates greater electron shielding *via* a stronger ring current and thus more π-electron delocalization. Enhanced delocalization is indicative of greater aromatic character. Because of ring current effects, only rings of similar size can be compared.

This method was applied in computational studies of different B-N 6-membered analogues of benzene (Figure 1.3).[10] It was observed that boron and nitrogen-containing aromatic systems had higher charge separation caused by reduced delocalization effects on aromatic topology. This observation was dependent on the position of the heteroatoms within the aromatic systems. Furthermore, the computed structural stability of these molecules was dominated by the sigma bonds, not the pi bonds. From the aromaticity calculations (NICS), it was found that generally the B-N ring fused systems were less aromatic but that the higher aromatic azaborine isomers corresponded to less energetic stability.

Figure 1.3: NICS values (ppm) for 6-membered azaborines

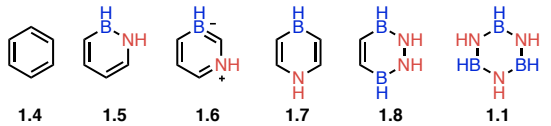

	1.4	1.5	1.6	1.7	1.8	1.1
NICS(0)	-8.20	-5.08	-6.36	-4.85	-2.72	-2.06
NICS(1)	-10.25	-7.00	-8.55	-3.54	-4.81	-2.78

This analysis has been separately verified in other studies of the 1,2- 1,3- and 1,4-azaborine (**1.5**, **1.6**, and **1.7,** respectively), where an inverse correlation of aromaticity versus stability was also observed.[11] In examining calculated resonance stabilization energies, it was noticed that the 1,3-benzene azaborine (**1.6**) demonstrated greater resonance stabilization (~3 kcal/mol) compared to the 1,2-azaborine (**1.5**), which correlated to the increased NICS values. It is suggested that the greater aromaticity is due to the inability of the zwitterionic 1,3-azaborine to reside in an uncharged resonance form, leading to greater delocalization. Additionally, comparison of molecular orbital contributions to magnetic field induction and poly-electron population analysis for these azaborine analogues of benzene supports the notion that only 1,3-azaborine (**1.6**) contains fully delocalized pi electrons,[12] and that a hydroxyl substitution has an effect on the aromaticity and stability of the mono-hydrated azaborines.[13]

1.3 – Synthetic methods to access azaborine isosteres

Interest in azaborines has borne synthetic strategies to a variety of different scaffolds (Figure 1.4). Five-membered azaborine ring systems (**1.9**) have been made from chelation of either ethylenediamine derivatives followed by oxidation[14a] or diimines followed by reduction.[14b] Additionally, cyclopentadienide mimics (**1.10**) have been synthesized on metal templates.[15] The 1,2-azaborine (**1.5**) can be constructed from the coordination of allyltrifluoroborate and allylamine, which undergoes ring closing metathesis (RCM), followed by oxidation.[16] Isosteric 1,3-azaborine (**1.6**) can be accessed through a similar strategy.[11,17] The 1,4-azaborine (**1.7**) can be synthesized by rhodium catalyzed 2+2+2 cyclization of alkynes[18a] or

through the lithiation of diallylamine with dichloroborane followed by tautomerization. [18b] Both bicyclic (**1.16**) [18c] and tricyclic (**1.24**) [18d] extended 1,4-azaborine ring systems have been synthesized by similar synthetic strategies.

In the case of bicyclic systems, an isoindole-like azaborine (**1.11**), synthesized by chelating borane with 2-(aminomethyl)pyridine, can undergo reversible aromaticity, switching between the rings.[19] The 1,3,2-benzodiazaborininone (**1.12**), which has been the interest of our group and others,

Figure 1.4: Core azaborine molecular scaffolds

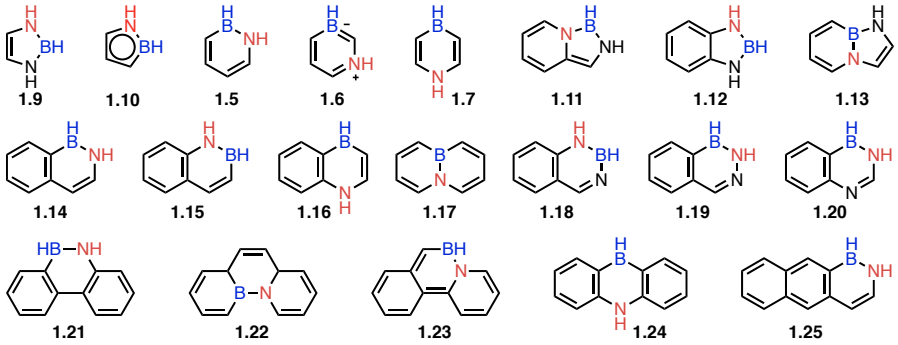

is typically accessed through coordination of phenylenediamines.[5d,20] Synthesis of a fused BN-indole ring system (**1.13**), has been accomplished through chelation of an allyl-dichloroborane to an allyl-diamine followed by RCM, and subsequent oxidation to the azaborine.[21] The 1,2-borazaronaphthalene (**1.14**) can be cyclized from phenethylimines and tribromoborane.[22] Inversely, the 2,1-borazaronaphthalene (**1.15**), our group's initial interest in azaborines, can be accessed from organotrifluoroborates *via in situ* generation of a dihaloborane in a 6-π cyclization with *o*-aminostyrenes.[23a] More recently this core has been synthesized from 2-(phenylethynyl)anilines and dichloroboranes[23b]. A fused BN-naphthalene (**1.17**) can be derived from a bis-allylchloroborane and diallylamine that can undergo double

RCM followed by oxidation with palladium on carbon.[24] Diamino 6,6-azaborine scaffolds have been obtained by amide tautomerization after anthranilamide coordination of boron (**1.18**)[25] or from the condensation of hydrazines with 2-formylphenylboronic acids to access **1.19**, which has been used as a fluorescent tag for bacteria.[26] A 2,4-diamino-substituted bicyclic scaffold **1.20** can also be accessed from 2-amino-phenylboronic esters.[27]

One of the pioneering azaborine scaffolds, reported by Dewar, was the 9,10-azaboraphenanthrene (**1.21**), accessed through a Lewis acid-mediated cyclization event.[28] The tricyclic variants of the azaborine motif have continued to be of interest because of the potential material applications of the extended π-systems. A similar phenanthroline-base azaborine system (**1.22**) could also be synthesized from boracylcohexadiene and 2-ethynylpyridines.[29] Furthermore, a photo-elimination strategy has enabled access to **1.23.**[30] Aside from the previously mentioned 1,4-azaborine derivative of anthracene (**1.24**), an isomeric, tricyclic B-N ring system, **1.25**, can be accessed through a strategy similar to the 2,1-borazaronaphthalenes *via* cyclization of 2-amino-vinylnaphthalene.[31]

Although a broad scope of accessible azaborine cores exists, there are some limitations to current synthetic methods. The primary problem is the lack of functional group diversification and the use of sensitive reagents. Furthermore, many of the procedures have undesired steps to manipulate oxidation state, and access to many of the azaborine structural classes require significant synthetic effort, increasing the barrier to practical application.

1.4 – Applications of azaborine scaffolds

Even with these synthetic barriers, azaborines have some interesting potential applications based on their physical and material properties, as well as some early assessment of their practical biological viability. One recent interest has been in their photophysical properties for optoelectronic materials.[32] The polarization caused by the replacement of a C=C for a B-N allows localization of singularly occupied molecular orbitals from the triplet state, which has potential for organic light emitting diodes.[33] As a result, azaborines present a means of triplet energy control, allowing higher efficiencies and extended excited state lifetimes (Figure 1.5-A). This is demonstrated in the effect of the extended conjugation of boron and nitrogen on opposite termini of a luminescent superbenzene structure (**1.26**).[34] This donor-acceptor substitution provides a larger charge transfer band resulting in a higher fluorescence quantum yield. A class of small molecule, highly fluorescent azaborine chromophores (**1.27**) has been demonstrated to have strong visible absorption, sharp fluorescence, and efficient quantum yields. Compared to similar carbonyl analogues, the azaborine chromophores demonstrated higher molar absorption.[35] Additionally, the 1,9-diaza-9-borazaphenalene motif (**1.28**) has been imbedded into zigzag-edged graphene nanoribbons, and the N-B-N within dibenzophenalenes offers heightened chemical stability. Moreover, the dipole created within the system allows post-synthetic modifications *via* selective electrophilic bromination and subsequent cross-coupling.[36]

Figure 1.5: Photophysically viable azaborine small molecules and polymers

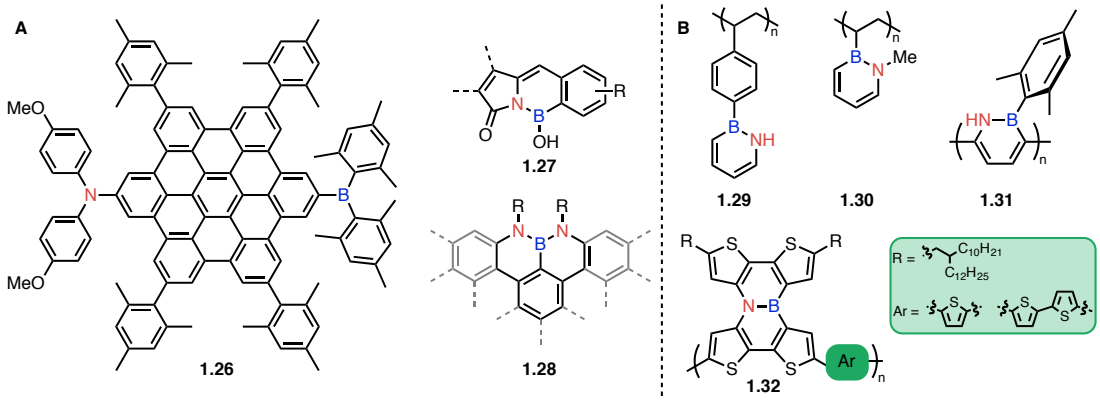

Further extensions of the photophysical properties have been considered by using azaborine polymer scaffolds (Figure 1.5-B). Simple chain radical polymerization of vinyl azaborine monomers yielded high molecular weight polymers (**1.29**, **1.30**) and demonstrated a bathochromic shift in absorption and emission bands.[37a,b] A syn-arranged, conjugated backbone polymer (**1.31**) was accessed *via* Suzuki cross-coupling of a bifunctional (bromo-boryl) A-B type monomer of 1,2-azaborine and displayed the same trends in absorption and emission. Moreover, computational studies found that the HOMO-LUMO energy gap for this polymer decreased with chain length.[37c] Furthermore, BN-substituted tetrathienonaphthalene polymers (**1.32**) could be synthesized from the dibrominated monomers in a Stille coupling polycondensation with bis-stannylthiophenes. These polymers demonstrated improved stability and decreased HOMO levels, which are beneficial properties for organic field-effect transistors.[37d]

Another beneficial application of azaborines has been their use in energy storage technology as liquid-phase hydrogen transfer carriers (Figure 1.6).[38a] Using the hydrogenated 1,2 azaborine (**1.33**), this system is able to undergo exothermic

trimerization (**Rxn 1**) followed by endothermic aromatization (**Rxn 2**) to release hydrogen, which allows for a highly conserved dehydrogenation process.[38b] In a profile of several aromatics as potential hydrogen storage materials, heteroatoms were observed to affect the thermodynamics of hydrogen extursion. While incorporation of sulfur and oxygen were found to have a negative influence on this process, nitrogen improved the thermodynamics in favor of dehydrogenation. Furthermore, when moving to the azaborine substrates (**1.05** and **1.36**) there was an additional shift in favor of dehydrogenation (free energy ΔG of hydrogenation -2.7 and -2.9 kJ/mol H_2, respectively, compared to –29.5 for pyridine).[38c]

Figure 1.6: Azaborine application to hydrogen storage

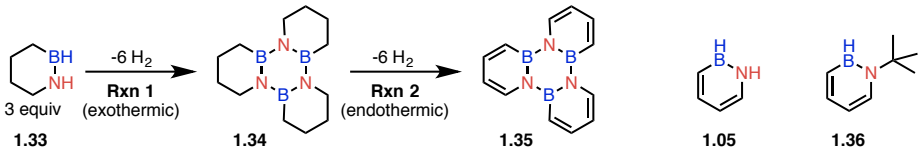

An alternative application of azaborines is their use as ligands for transition metal catalysis (Figure 1.7). Considering the small stereoelectronic factors that affect catalysis, the azaborine isosteres present a facile way of developing electronically modified ligands of similar structural frameworks. Furthermore, the desymmetrized azaborine cores present an opportunity to develop ligand derivatives that fine-tune catalyst activity. An azaboryl-ruthenium catalyst (**1.37**) has been synthesized that behaves similarly to cyclopentadienyl complexes. (Figure 1.7-A) The electron rich 1,2-azaboryl ligand binds such that the ruthenium is preferentially closer to the intra-ring carbon and nitrogen atoms and positioned farther from the boron atom, causing the two external triphenylphosphine ligands

to be non-symmetrical.[15a] This catalyst has been used in the 2+2 cycloaddition of norbornene analogues to form the exo-cycloadduct (Figure 1.7-C), and further used in atom transfer radical addition (Figure 1.7-D). Additional ligands have been synthesized from the benzo-fused-1,4-azaborine structures (Figure 1.7-B) including **1.38**, which chelates platinum in a η^2-L-type binding, atypical of the analogous naphthyl-pyridine ligands.[18c] Additionally, a phosphine-functionalized 1,4-azaborine (**1.39**) has been used in palladium-catalyzed trans-hydroboration of enynes (Figure 1.7-E).[39]

Figure 1.7: Azaborines as ligands for catalysis

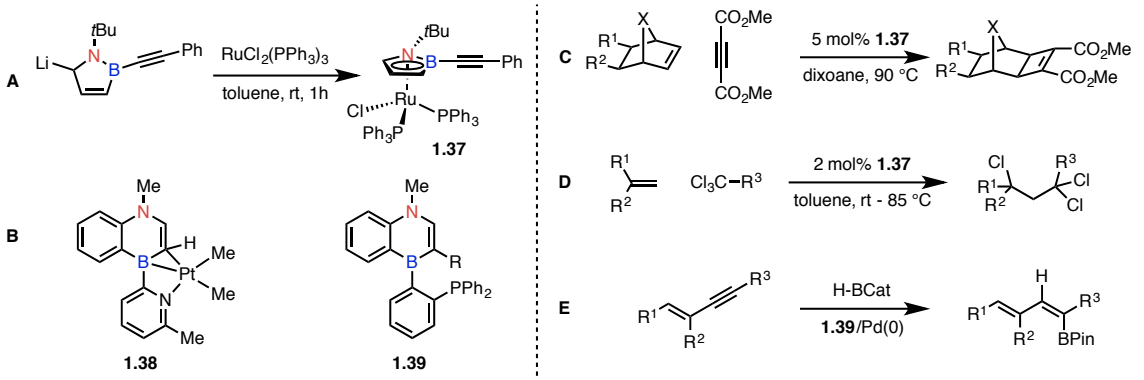

One of the most valuable applications for isosteres is their contribution to the design of new medicines. Initial drug targets are identified in a variety of ways, including library and fragment screening of natural products, or herbal remedies that present unusual or targeted effects.[2,3,40] Rarely are the initial candidates viable for the clinic because of unwanted background activity, lack of desired physical or chemical properties, or a myriad other unexpected hurdles. Implementation of isosteric variations can transform medicinally relevant structures to reliable clinical candidates by suppressing undesired properties while retaining other useful traits.

Azaborines present a useful aromatic structural/electronic isosteric variant that also has the potential to provide new modes of binding to biological targets.[41]

The 1,2-azaborine (**1.5**) has been demonstrated to bind an aryl recognition site of T4 phage lysozymes effectively (Figure 1.8).[42] Based on the enhanced dipole moment of **1.5**, along with the potential for hydrogen bonding presented by the N-H (calculated pK_a of ~24), it was proposed that the azaborine might display unique binding. In the nonpolar L99A lysosome (leucine to alanine mutation at position 99) pocket, similar binding was observed between the azaborine and benzene. However, in the L99A/M102Q lysosome (additional methionine to glutamine mutation at position 102) cavity, which presents a more polar binding pocket, there is evidence for hydrogen bonding of the azaborine to the glutamine[102] residue of the macromolecule. This hydrogen bonding and the enhanced dipole moment are demonstrated in the preferred thermodynamic binding free energy of the azaborine (-6.40 kcal/mol) compared to benzene (-5.96 kcal/mol) in the polar L99A/M102Q binding pocket, which is reversed in the nonpolar L99A mutant (azaborine: -5.04, benzene: -5.54).

Figure 1.8: Biologically relevant 1,2-azaborines

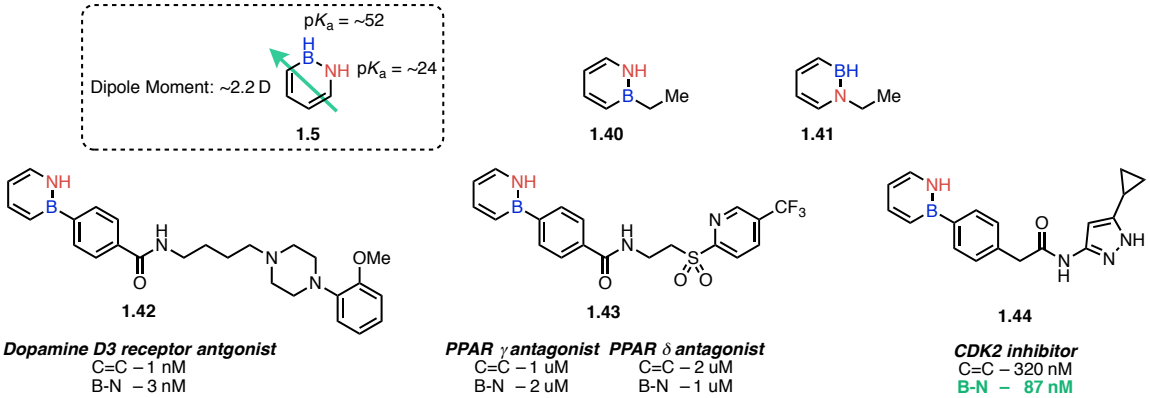

Regioisomeric 1,2-azaborine cores with an ethyl side chain displayed markedly different inhibition of ethylbenzene dehydrogenase. The *B*-ethyl-1,2-azaborine **1.40** (IC_{50} - 100 μM) was 50 times less potent than the *N*-ethyl-1,2-azaborine **1.41** (IC_{50} – 2.8 μM), though in neither case was any enzymatic turnover observed. Calculated energy for radical and carbocation formation for the azaborine were >20 kcal/mol higher than ethylbenzene, suggesting a much higher barrier for the associated hydroxylation event. Molecular mechanics modeling was utilized to understand this phenomenon. The *N*-ethyl-1,2-azaborine binding pose in the active site was the same as ethyl benzene. However, the *B*-ethyl-1,2-azaborine was slightly angled based on modeling, corroborating the weaker inhibition. In further studies of the *N*-ethyl **1.41**, it appears to be a mixed-type inhibitor, displaying lower competitive (K_{ic}: 0.55 μM - comparable to ethylbenzene) than uncompetitive inhibition (K_{iu} – 9 μM), suggestive of a potential second binding site. [43]

More elaborated 1,2-azaborine derivatives have been profiled for their specific medicinal relevance.[44] In this case, 1,2-azaborine-based biphenyl acids and amides were demonstrated to be both air- and water stable and have improved solubility in water compared to their all-carbon analogues, caused by the previously mentioned dipole moment. They also have additional potential hydrogen bonding contacts from the N-H of the azaborine scaffold. These benefits can be transferred to improved *in vivo* oral availability, suggesting lower clearance and longer terminal half-life. To probe their activity, azaborine dopamine D3 antagonist **1.42**, PPAR γ and δ antagonist **1.43**, and CDK2 inhibitor **1.44** were compared to the all carbon

analogues. For both the dopamine D3 antagonist and the PPAR γ and δ antagonists both classes of compounds displayed comparable activity. Interestingly, in the case the CDK2 inhibitor there was a three-fold increase in potency for the azaborine. In docking studies of the CDK2 binding, it was observed that the N-H in the azaborine analogue exhibited additional hydrogen-bonding contact to the backbone of a neighboring isoleucine.

The 2,1-borazaronaphthalene core also has potential biological applications (Figure 1.9-A). Two isomeric azaborine derivatives (**1.45**, **1.46**) were compared to propranolol, a commercially available β-blocker drug.[45] Stability tests under normal atmosphere indicate these derivatives display good stability at both pH 7.4 and in DMSO , as well as 80% stability in 0.1 M NaOH after 2 days. However, both azaborines immediately degraded in 0.1 M HCl. This degradation could be caused by protonation of the nitrogen, leading to dearomatization of the B-N ring. Though a possible caviat, this limitation can be solved by formulation strategies.[46] Tested in a screen of 26 receptors for both agonist and antagonist activity, **1.45** was found to be 10 fold less potent than propranolol for the *β*2 adrenergic receptor, while **1.46** had comparable activity. *In vitro* physicochemical and ADME studies demonstrated that both azaborines were more lypophilic that propranolol, had good cell permeability, and readily crossed the blood-brain barrier. Additionally, **1.46** had improved stability in human liver microsomes, suggesting potentially useful benefits for azaborine mimetics.

Figure 1.9: Biologically relevant 2,1-borazaronaphthalenes

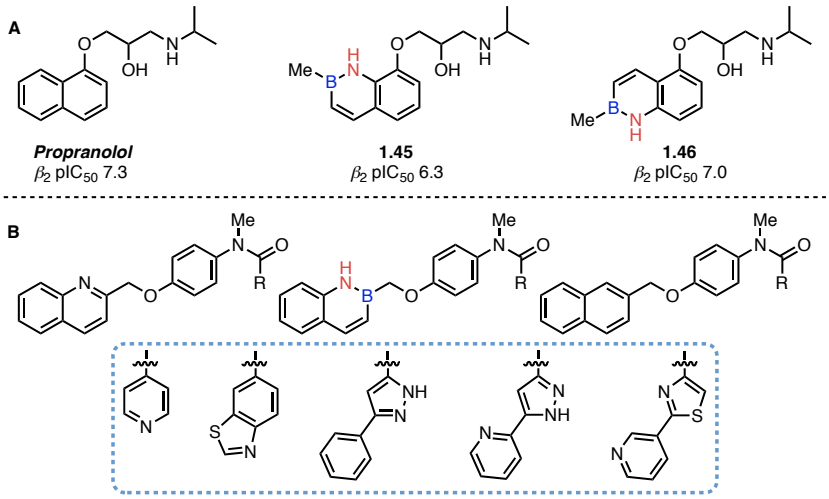

1,2-Borazaronaphthalene derivatives have also been tested for phosphodiesterase (PDE) enzyme inhibition (Figure 1.9-B), which hold potential therapeutic value for Parkinson's, Huntington's, schizophrenia and obsessive compulsive disorder.[47] Historically, quinolones have been shown to be efficient binders, owing to an H-bond acceptor capacity, while naphthalene was hypothesized to be inefficient. The 2,1-borazaronaphthalene could be considered a compromise, where the polarized B-N bond demonstrates some protic character in the N-H bond. In a cross comparison of quinoline, 2,1-borazaronaphthalene, and naphthalene analogues for metabolic stability, lipophilicity and PDE1-A potency, neither the azaborine nor the naphthalene variants show particularly high activity in most cases, though a couple of azaborine derivatives demonstrated nanomolar potency. In general, the azaborine derivatives had physiochemical properties between those of quinolone and naphthalene in terms of metabolic stability, lipophilicity and potency.

1.5 – Conclusions

With the considerable potential for the azaborine scaffolds, improved methods to access a diversity of structural motifs are required to support the growth of the field. Of critical importance, new synthetic strategies must provide rapid access to azaborine cores and use mild reaction conditions, amenable to large substrate scopes. Additionally, methods that can employ bench-stable, commercially available starting materials would lower the barrier of access to this class of molecules. It would be of added benefit if strategies would allow access to azaborine cores that can be used as precursors for further diversification to permit the incorporation of additional functional appendages. These incremental advancements would provide greater access to diverse azaborine isosteres.

1.6 – References

1. Langmuir, I. *J. Am. Chem. Soc.* **1919**, *41*, 1543.
2. Patani, G. A.; LaVoie, E. J. *Chem. Rev.* **1996**, *96*, 3147.
3. Meanwell, N. A. *J. Med. Chem.* **2011**, *54*, 2529.
4. Stock, A.; Pohland, E. *Ber. Dtsch. Chem. Ges.* **1926**, *59*, 2215.
5. *For reviews on azaborines*: a) Weber, L. *Coord. Chem. Rev.* **2008**, *252*, 1. b) Dosdet, M. J. D.; Piers, W. E. *Can. J. Chem.* **2009**, *87*, 8. c) Campbell, P. G.; Marwitz. A. J. V.; Liu, S.-Y. *Angew. Chem., Int. Ed.* **2012**, *51*, 6074. d) Abbey, E. R.; Liu, S.-Y. *Org. Biomol. Chem.* **2013**, *11*, 2060. e) Weber, L.; Böhling, L. *Coord. Chem. Rev.* **2015**, *284*, 236. f) Wang, X.-Y.; Wang, J.-Y.; Pei, J. *Chem. Eur. J.* **2015**, *21*, 3528. g) Morgan, M. M.; Piers, W. E. *Dalton Trans.* **2016**, *45*, 5920.

6. Baldock, C.; Rafferty, J. B.; Sedelnikova, S. E.; Baker, P. J.; Stuitje, A. R.; Slabas, A. R.; Hawkes, T. R.; Rice, D. W. *Science* **1996**, *274*, 2107.

7. *For interest in the boron atom for biological systems*: a) Hunter, P. *EMBO Rep.* **2009**, *10*, 125. b) Baker, S. J.; Tomsho, J. W.; Benkovic, S. J. *Chem. Soc. Rev.* **2011**, *40*, 4279. c) Hernandez, V.; Crépin, C.; Palencia, A.; Cusack, S.; Akama, T.; Baker, S. J.; Bu, W.; Feng, L.; Freund, Y. R.; Liu, L.; Meewan, M.; Mohan, M.; Mao, W.; Rock, F. L.; Sexton, H.; Sheoran, A.; Zhang, Y.; Zhang, Y.-K.; Zhou, Y.; Nieman, J. A.; Anugula, M. R.; Keramane, E. M.; Savariraj, K.; Reddy, D. S.; Sharma, R.; Subedi, R.; Singh, R.; O'Leary, A.; Simon, N. L.; De Marsh, Peter, L.; Mushtaq, S.; Warner, M.; Livermore, D. M.; Alley, M. R. K.; Plattnera, J. J. *Antimicrob. Agents Chemother.* **2013**, *57*, 1394. d) Ramachandran, P. V. *Future Med. Chem.* **2013**, *5*, 611. e) Fu, H.; Fang, H.; Sun, J.; Wang, H.; Liu, A.; Sun, J.; Wu, Z. *Curr. Med. Chem.* **2014**, *21*, 3271. f) Chen, Z.; Tian, Z.; Kallio, K.; Oleson, A. L.; Ji. A.; Borchardt, D.; Jiang, D.; Remington, S. J.; Ai, H. *J Am. Chem. Soc.* **2016**, *138*, 4900.

8. a) Carvalho, I.; Borges, Á. D. L.; Bernardes, L. S. C. *J. Chem. Educ.* **2005**, *82*, 588. b) Eid, S. Zalewski, A.; Smieško, M.; Ernst, B.; Vedani, A. *Int. J. Mol. Sci.* **2013**, *14*, 684. c) Firth, N. C.; Brown, N.; Blagg, J. *J. Chem. Inf. Model.* **2012**, *52*, 2516.

9. a) Clark, T.; Kranz, *J. Org. Chem.* **1992**, *57*, 5492. b) Chen, Z.; Wannere, C. S.; Corminboeuf, C.; Puchta, R.; Schleyer, P. v. R. *Chem. Rev.* **2005**, *105*, 3842.

10. Ghosh, D.; Periyasamy, G.; Pati, S. K. *Phys. Chem. Chem. Phys.* **2011**, *13*, 20627.

11. Xu, S.; Mikulas, T. C.; Zakharov, L. N.; Dixon, D. A.; Liu, S.-L. *Angew. Chem., Int. Ed.* **2013**, *52*, 7527.

12. Papadopoulos, A. G.; Charistos, N. D.; Kyriakidou, K.; Sigalas, M. P. *J. Phys. Chem. A* **2015**, *119*, 10091.

13. Srivastava, A. K.; Pandey, S. K.; Misra, N. *Mol. Phys.* **2016**, *114*, 1763.

14. a) Meriam, J. S.; Niedenzu, K. *J. Organomet. Chem.* **1973**, *51*, 21. b) Weber, L.; Schmid, G. *Angew. Chem., Int. Ed.* **1974**, *13*, 467.

15. a) Liu, Z.; Xu, J.; Ruan, W.; Fu, C.; Zhang, H.-J.; Wen, T.-B. *Dalton Trans.* **2013**, *42*, 11976. b) Liu, S.-Y.; Hills I. D.; Fu, G. C. *Organometallics* **2002**, *21*, 4323.

16. Abbey, E. R.; Lamm, A. N.; Baggett, A. W.; Zakharov, L. N.; Liu, S.-Y. *J. Am. Chem. Soc.* **2013**, *135*, 12908.

17. a) Xu, S.; Zakharov, L. N.; Liu, S.-Y. *J. Am. Chem. Soc.* **2011**, *133*, 20152.

18. a) Braunschweig, H.; Damme, A.; Jimenez-Halla, J. O. C.; Pfaffinger, B.; Radacki, K.; Wolf, J. *Angew. Chem., Int. Ed.* **2012**, *51*, 10034. b) Liu, X.; Zhang, Y.; Li, B.; Zakharove, L. N.; Vasiliu, M.; Dixon, D. A.; Liu, S.-Y. *Angew. Chem., Int. Ed.* **2016**, *55*, 8333. c) Xu, S.; Haeffner, F. Bo, L.; Zakharove, L. N.; Liu, S.-Y. *Angew. Chem., Int. Ed.* **2014**, *53*, 6795. d) Igarashi, T.; Tobisu, M.; Chatani, N. *Angew. Chem., Int. Ed.* **2017**, *56*, 2069.

19. Gellrich, U.; Diskin-Posner, Y.; Shimon, L. J. W.; Milstein, D. *J. Am. Chem. Soc.* **2016**, *138*, 13307.

20. Davies, G. H. M.; Molander, G. A. *J. Org. Chem.* **2016**, *81*, 3771.

21. Abbey, E. R.; Zakharov, L. N.; Liu, S.-Y. *J. Am. Chem. Soc.* **2011**, *133*, 11508.

22. Liu, W.; Wu, P.; Li, J.; Cui, C. *J. Org. Chem.* **2015**, *80*, 3737.

23. a) Wisniewski, S. R.; Guenther, C. L.; Argintaru, O. A.; Molander, G. A. *J. Org. Chem.* **2014**, *79*, 365. b) Zhuang, F.-D.; Han, J.-M.; Tang, S.; Yang, J.-H.; Chen, Q.-

R.; Wang, J.-Y.; Pei, J. *Organometallics* **2016,** *ASAP*, DIO: 10.1021/acs.organomet.6b00811.

24. a) Dohr, A. D.; Kampf, J. W.; Ashe, A. J. *Organometallics* **2014**, *33*, 1318. b) Su, F.; Lv, L.; Huang, M.; Shou, Z.; Fang, X. *Org. Lett.* **2014**, *16*, 5024.
25. Yale, H. L. *J. Heterocyclic Chem.* **1971**, *8*, 193.
26. a) Yang, J.; Johnson, B. J.; Letourneau, A. A.; Vogels, C. M.; Decken, A.; Baerlocher, F. J.; Westcott, S. A.; *Aust. J. Chem.* **2015**, *68*, 366. b) Bandyopadhyay, A.; Cambray, S.; Gao, J. *J. Am. Chem. Soc.* **2017**, *139*, 871.
27. Suchy, M.; Hudson, R. H. E. *J. Org. Chem.* **2014**, *79*, 3336.
28. Dewar, M. J. S.; Kubba, V. P.; Pettit, R. *J. Chem. Soc.* **1958**, 3073.
29. Bosdet, M. J. D.; Jaska, C. A.; Piers, W. E.; Sorensen, T. S.; Parvez, M. *Org. Lett.* **2007**, *9*, 1395.
30. Lu, J.-S., Ko, S.-B.; Walters N. R.; Kang, Y.; Sauriol, F.; Wang, S. *Angew. Chem., Int. Ed.* **2013**, *52*, 4544.
31. Van de Wouw, H. L.; Lee, J. Y.; Klausen, R. S. *Org. Biomol. Chem.* **2016**, *14*, 3256.
32. Wang, J.-Y.; Pei, J. *Chin. Chem. Lett.* **2016**, *27*, 1139.
33. Hashimoto, S.; Ikurta, T.; Shiren, K.; Nakatsuka, S.; Ni, J.; Nakamura, M.; Hatakeyama, T. *Chem. Mater.* **2014**, *26*, 6265.
34. Kurata, R.; Kaneda, K.; Ito, A. *Org. Lett.* **2017**, *19*, 392.
35. Saint-Louis, C. J.; Magill, L. L.; Wilson, J. A.; Schroeder, A. R.; Harrell, S. E.; Jackson, N. S.; Trindell, J. A.; Kim, S.; Fisch, A. R.; Munro, L. Catalano, V. J.; Webster, C. E.; Vaughan, P. P.; Molek, K. S.; Schrock, A. K.; Huggins, M. T. *J. Org. Chem. Soc.* **2016**, *81*, 10955.

36. Wang, X.; Zhang, F.; Schellhammer, K. S.; Machata, P.; Ortmann, F.; Cuniberti, G.; Fu, Y.; Hunger, J.; Tang, R.; Popov, A. A.; Berger, R.; Müllen, K.; Feng, X. *J. Am. Chem. Soc.* **2016**, *138*, 11606.

37. a) Thiedemann, B.; Gliese, P. J.; Hoffmann, J.; Lawrence, P. G.; Sönnichsen, F. D.; Staubitz, A. *Chem. Commun.* **2017**, *Advance Article*, DOI: 10.1039/C6CC08599G. b) Wan, W.-M.; Baggett, A. W.; Cheng, F.; Lin, H.; Liu, S.-Y.; Jäkle, F. *Chem. Commun.* **2016**, *52*, 13616. c) Bagget, A. W.; Gou, F.; Li, B.; Liu, S.-Y. Jäkle, F. *Angew. Chem., Int. Ed.* **2015**, *54*, 11191. d) Wang, X.-Y.; Ahuang, F.-D.; Wang, J.-Y.; Pei, J. *Chem. Commun,* **2015**, *51*, 17532.

38. a) Zhu, Q.-L.; Xu, Q. *Energy Environ. Sci.* **2015**, *8*, 478. b) Brooks, K. P.; Bowden, M. E.; Karkamkar, A. J.; Houghton, A. Y.; Autrey, S. T. *J. Power Sources* **2016**, *324*, 170. c) Müller, K.; Völkl, J.; Arlt, W. *Energy Technol.* **2013**, *1*, 20.

39. Xu, S.; Zhang, Y.; Li, B.; Liu, S.-Y. *J. Am. Chem. Soc.* **2016**, *138*, 14566.

40. a) Nicolaou, C. A.; Brown, N. *Drug Discov. Today* **2013**, *10*, 427. b) Lima, L. M.; Berreiro, E. J. *Curr. Med. Chem.* **2005**, *12*, 23. c) Hughes, J. P.; Rees, S.; Kalindjina, S. B.; Philpott, K. L. *Br. J. Pharmacol.* **2011**, *162*, 1239.

41. Baker, S. J.; Ding, C. Z.; Akama, T.; Zhang, Y.-K.; Herandez, V.; Xia, Y. *Future Med. Chem.* **2009**, *1*, 1275.

42. Lee, H.; Fischer, M.; Shoichet, B. K.; Liu, Liu, S.-Y. *J. Am. Chem. Soc.* **2016**, *138*, 12021.

43. Knack, D. H.; Marshall, J. L.; Harlow, G. P.; Dudzik A.; Szaleniec, M.; Liu, S.-Y.; Heider, J. *Angew. Chem., Int. Ed.* **2013**, *52*, 2599.

44. Zhao, P.; Nettleton, D. O.; Karki, R. G.; Zécri, F. J.; Liu, S.-Y. *Chem. Med. Chem.* **2017**, *12*, 358.

45. Rombouts, F. J. R.; Tovar, F.; Austin, N.; Tresadern, G.; Trabanco, A. A. *J. Med. Chem.* **2015**, *58*, 9287.

46. a) Pérez, Y A.; Usista, C. M.; Martínez, J. I.; Nava, M. D. C. D.; Rodríguez, F. A. R. *Polymers* **2016**, *8*, 214. b) Bikiaris, D.; Koutris, E.; Karavas, E. *Recent Pat. Drug Deliv. Formul.* **2007**, *1*, 201.

47. Vlasceanu, A.; Jessing, M.; Kilburn, J. P. *Bioorg. Med. Chem.* **2015**, *23*, 4453.

CHAPTER 2 – SYNTHETIC METHODS TO ACCESS AZABORINE CORES

2.1 – Introduction

The preparation of boron-based heteroaromatic species greatly expands the library of heterocyclic structures and can redefine the reactivity profile of these conjugated systems.[1] Although historically studied as a means to understand aromaticity,[2] boron-based aromatic systems have been recognized as a viable, emerging area for expanding molecular diversity.[3] Particularly privileged among these boron-based cores is the azaborine scaffold in which a B-N bond is integrated into the aromatic system.[4] The B−N bond serves as a surrogate for a C=C bond in arenes or heteroarenes, providing structural mimicry with unique electronic properties, and therefore chemical reactivity. The unique disconnections, wholly unavailable in the corresponding carbon analogues, provide opportunities for dissonant synthetic routes to bicyclic systems. Additionally, the interchange between B−N and C=C bonds is particularly attractive for drug discovery, as the boron can adopt a tetrahedral geometry to present alternative binding contacts for enzymatic targets.[5] Taken together, not only could this enhance potency of existing scaffolds, but it could also lead to new pharmacophores. Indeed, oxaboroles[6] and azaboroles[7] have been shown to have unique modes of bioactivity. Methods to construct new or unexplored boron heterocyclic species could dramatically improve the quality of drug discovery libraries.

2.2 – Access to functionalized 1,3,2-benzodiazaborole cores

The indole structural motif has a demonstrated prominence in biological targets,[8] and therefore accessing isosteric species would be of value for both

academic and pharmaceutical applications. Currently, there are two known azaborine isosteres of indole: (*i*) the 1,3,2-benzodiazaborole (**2.1**), where the 2-3 carbon-carbon double bond is replaced by a B-N bond;[9] and (*ii*) the "fused" B-N indole[10] (**2.2**), in which the adjacent bond in the bicycle is exchanged (Figure 2.1). The indole-azaborine **2.1** is particularly valuable because it provides access to an indole isostere in one-step *via* chelation of a boron species between the amino groups of *o*-phenylenediamine.[11] Literature reports have revealed the incorporation of different substituents on boron through the use of alkyl-amino,-[11a], trialkyl-[11b] or alkyl-dichloroboranes[12a] and, in later contributions, via condensation reactions with boronic acids[12b-e] or electron deficient boronate esters.[12f] The major limitation of the currently available methods is the requirement of air- and/or moisture-sensitive

Figure 2.1: Indole isosteres

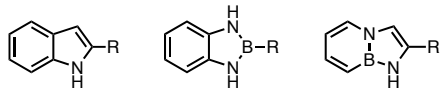

Indole **2.1** **2.2**

boron precursors that limit the diversity within these indole isosteres.

Leveraging organotrifluoroborates[13] as bench-stable precursors for the synthesis of azaborines[14] presents a straightforward method that would enable access to a library of molecules through activation of the organotrifluoroborate precursors using a fluorophile (e.g., chlorosilane reagents)[15] and subsequent reaction with *o*-aminostyrene derivatives. Application of this strategy to the indole azaborines was envisioned to provide an easily accessible, robust route toward the 1,3,2-benzodiazaborole core in a similar fashion.

2.2.1 – Synthetic results and discussion

Initial screening of reaction conditions, using *o*-phenylenediamine (**2.3**) and phenyltrifluoroborate (**2.4**), indicated that reactive silicon fluorophiles could be directly applied to the synthesis of 1,3,2-benzodiazaboroles (Table 2.1). Silicon tetrachloride has been previously demonstrated to react with potassium organotrifluoroborates, generating highly reactive dichloroborane species,[15] which let to good conversion to **2.5** (Table 2.1, entry 1). In exploring more user-friendly

Table 2.1: Optimization of the Fluorophile for Reaction Conditions

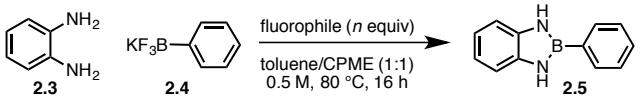

Entry	Fluorophile	Equiv	Prod:IS[a]
1	$SiCl_4$	1	4.60
2	TMSCl	1	2.49
3	BCl_3 (1.5 M in hexane)	3	4.21
4	$BH_3{\cdot}SMe_2$	3	1.21
5	$BF_3{\cdot}MeCN$	3	1.85
6	$BF_3{\cdot}SMe_2$	3	1.60
7	$BF_3{\cdot}THF$	3	0.42
8	$BF_3{\cdot}OEt_2$	3	0.43
9	$BF_3{\cdot}NH_2Et$	3	6.85
10	$BF_3{\cdot}NH_2Et$	2	5.55
11	$BF_3{\cdot}NH_2Et$	1	3.80

[a]Product:Internal Standard ratios determined by GCMS using 4,4'-di-*tert*-butylbiphenyl as internal standard.

fluorophiles, which have recently been shown to activate organotrifluoroborates,[16] it was observed that trivalent, electron-poor, boron species could also promote the reaction (Table 2.1, entries 3–11), and were more effective when used in excess. With boron fluorophiles, initial organotrifluoroborate deprotection generates a difluoroborane species that has significantly poorer reactivity when compared to the dichloroborane intermediates,[17] thereby requiring excess boron reagent to abstract both of the remaining fluorides. The best results were obtained when using

three equivalents of boron trifluoride ethylamine complex as the fluorophile (Table 2.1, entry 9), a particularly appealing reagent because it was the sole reagent tested that was a bench-stable solid.

These modified reaction conditions were then applied to prepare 1,3,2-benzodiazaborole analogues using various potassium aryltrifluoroborates (Table 2.2). Besides alkyl groups (**2.6, 2.7, 2.8**) and halogens (**2.9, 2.10, 2.11**), the relatively mild reaction conditions were tolerant of vinyl (**2.12**), ether (**2.13, 2.14, 2.15, 2.16, 2.18**) and ester (**2.17**) functional groups. Although steric hindrance at either the ortho position of the aryltrifluoroborate (**2.6, 2.7, 2.9, 2.13, 2.16**) or on

Table 2.2: Scope of Reaction with (Hetero)aryltrifluoroborates

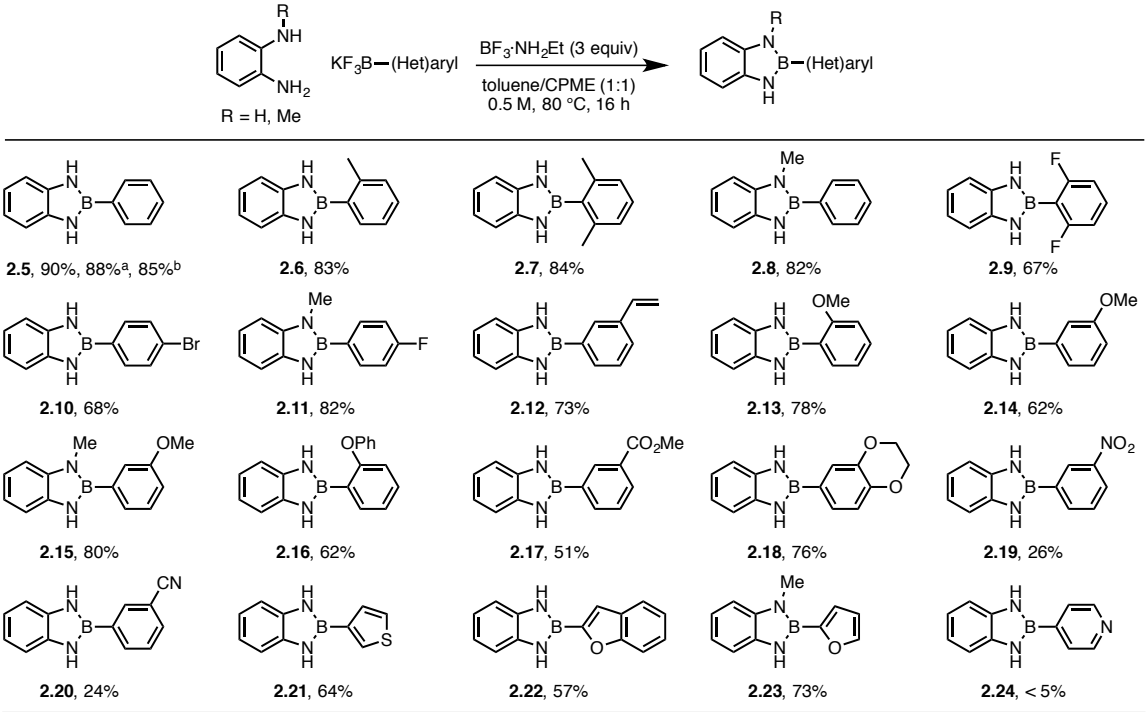

[a]Reaction run under ambient atmosphere. [b]Reaction run on 30 mmol scale.

one of the diamine nitrogen atoms (**2.8, 2.11, 2.23**) did not deeply affect the reaction, the presence of some electron-withdrawing substituents such as nitro

(**2.19**) or cyano (**2.20**) groups resulted in lower yields. Heteroaryltrifluoroborates containing sulfur– (**2.21**) or oxygen– (**2.22, 2.23**) atoms were well tolerated. Unfortunately, the method could not be extended to nitrogen-containing heteroaryls such as pyridyl subunits (**2.24**).

The utility of this protocol, using all air-stable starting materials, consequently allowed the reaction to proceed even in the absence of a nitrogen purge of the reaction vessel or solvents (88% under air *versus* 90% under argon for **2.5**). It important to note that for several of the reactions, the only purification required was a basic aqueous (sat. $NaHCO_3$) workup followed by extraction with ethyl acetate, thus highlighting the ease of access toward these cores. In most remaining cases, the only additional purification required was passage through a flash plug of silica gel.

Desymmetrization of the starting phenylenediamine enabled the synthesis of unsymmetrical azaborine cores (Table 2.3). Use of functionalized phenylenediamines allowed the facile introduction of versatile synthetic handles

Table 2.3: Scope of Reaction with Substituted *o*-Phenylenediamines

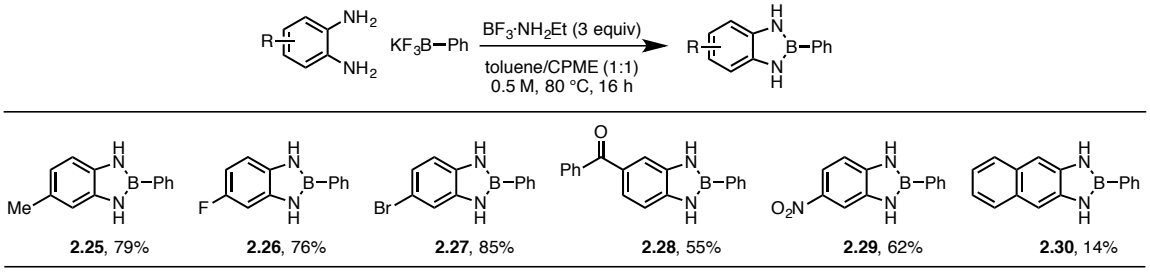

2.25, 79% **2.26**, 76% **2.27**, 85% **2.28**, 55% **2.29**, 62% **2.30**, 14%

such as bromo (**2.27**), carbonyl (**2.28**), or nitro (**2.29**) groups. Some difficulty was encountered when using 2,3-naphthalenediamine (**2.30**), presumably because of the heterogeneity of the reaction mixture under these reaction conditions.

The scope of the method was further advanced to other C_{sp}^2-hybridized as well as C_{sp}^3-hybridized groups on the boron atom (Table 2.4). Alkenyltrifluoroborates were well tolerated under these conditions (Table 2.4, left), affording the corresponding azaborines in good yields (**2.31, 2.32, 2.33**). An alkynyltrifluoroborate was also utilized to demonstrate that the procedure could be extended to *sp*-hybridized centers (**2.34**). *N*-Methylation of the diamine did not affect the reaction (**2.35, 2.36**), and the presence of a bulky *N*-phenyl group was tolerated when using sterically small organotrifluoroborates (**2.37, 2.38, 2.46**). However, only starting diamine was observed when attempting to cyclize such substrates with larger aliphatic or aryl substituents on the organoboron precursors.

Table 2.4: Scope of Alkyl- and Alkenyltrifluoroborates

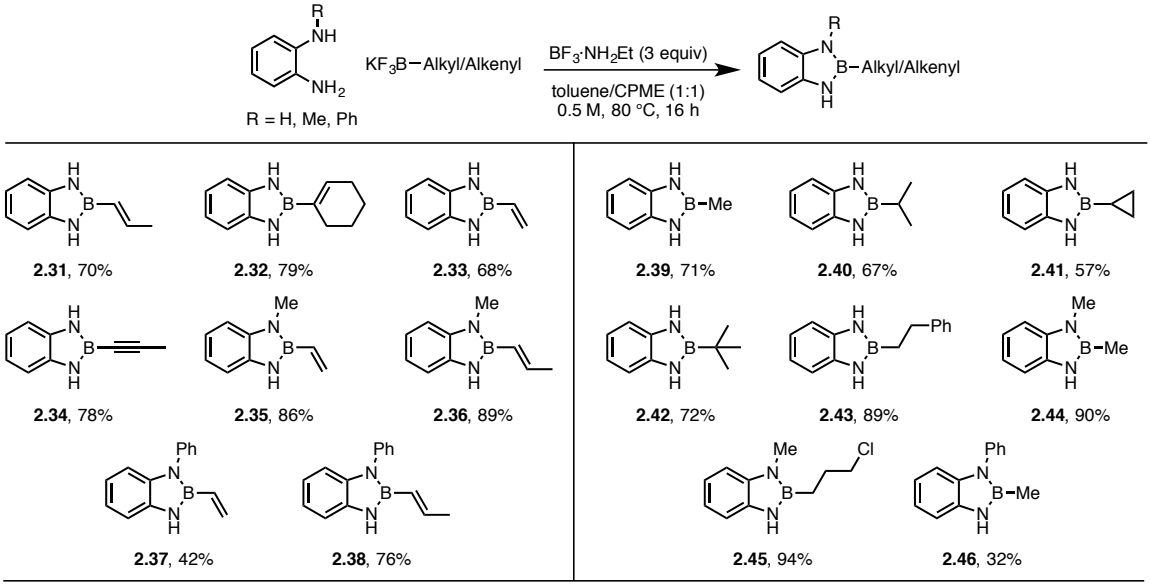

Substituted azaborine compounds with C_{sp}^3-hybridized units on the boron (Table 2.4, right) were found to be less stable than their C_{sp2}-hybridized counterparts. The *B*-alkyl compounds, when subjected to the standard workup,

readily decomposed in the presence of water. This problem was overcome by foregoing the aqueous workup and directly subjecting the reaction mixture to a flash plug of silica, allowing access to pure material in moderate (**2.41**) to good yields (**2.44**). Once isolated and stored as solids on the bench top, no degradation of the products were observed. Using this modified workup procedure, primary (**2.39, 2.43, 2.44, 2.45, 2.46**), secondary (**2.40, 2.41**), and tertiary (**2.42**) alkyl-substituted azaborines were isolated. *N*-Alkylated diamines could be used as reaction partners, affording the corresponding azaborines, often in very good yields (**2.44, 2.45, 2.46**).

2.2.2 – Physical properties and computationally derived results

With the primary objective of the project achieved (development of a straightforward method for synthesis of the 1,3,2-benzodiazaborole core involving only bench-stable partners), attention was next focused on understanding the potential value and versatility of these indole isosteres. Initially, the pK_a of the azaborine N-H was determined *via* bracketing experiments, an NMR experiment, in which a substrate is initially deprotonated *via* strong base and subsequently exposed to proton sources of known acidity (Figure 2.2). The monoalkylated 1,3,2-benzodiazaborole **2.8** was found to have a pK_a of approximately 18.2 (in DMSO), because it was observed to (*i)* remain fully deprotonated in the presence of trifluoroacetamide (pK_a of 17.2), (*ii)* fully reprotonated in the presence of pyrazole (pK_a of 19.6) and (*iii*) was observed as a mixture of protonated and unprotonated in *N,N*-dimethylacetoacetamide (pK_a of 18.2). This value falls slightly lower than the pK_a for indole (20.9)[18] and significantly below the "fused" B-N indole (around 30)[10].

Considering the pK_a for aniline (30.6) or phenylacetamide (21.5), the lower pK_a suggests that 1,3,2-benzodiazaborole core is better at inductively stabilizing the negative charge generated upon deprotonation.

Figure 2.2: pK_a bracketing experiment

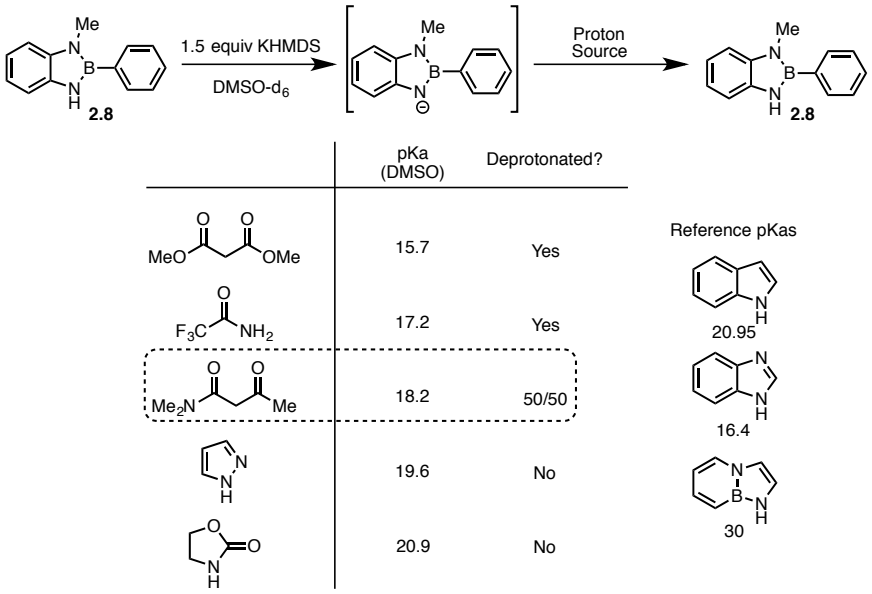

Computational models were further studied as a means of assessing the structural and electronic correlation between azaborine cores and indole. Liu,[19] and more recently Northrop,[12c] have looked at various computational methods for analyzing the core of the indole-azaborine systems, however our interest was on aromatic perturbations caused by core substitution. All calculations were carried out using Gaussian 09,[20] and the structures were visualized *via* WebMO.[21] Geometry optimizations were performed in the gas-phase at the B3LYP/6-311+G(2d,p) level of theory.[22] Stationary points were characterized by frequency analysis at 298 K. To probe the ring current in these systems, NICS values were determined at the GIAO-B3LYP/6-311+G(2d,p) level of theory at distances 0.0 Å [(A(0) and B(0)] and 1 Å

[(A(1) and B(1)] from each ring system as well from the center of the bicyclic systems [Center (1)] in the perpendicular direction (Figure 2.3).

Figure 2.3: NICS values calculated

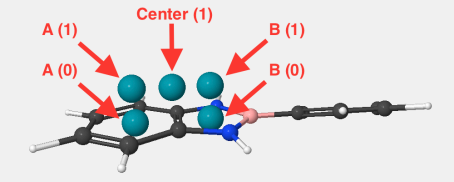

The electrostatic potentials of indole azaborines and their carbon analogs were initially evaluated (Figure 2.4). A pictorial comparison of the electrostatic potential maps for both the 1,3,2-benzodiazaborole core and the "fused" B-N indole core explored by Liu[10] to similar 6-5 aromatic ring systems suggested that they most closely resemble the indole framework. It is visually apparent that both azaborines present a greater likeness to indole [compare 2-methyl-indole (**2.47**) and 2-methyl-benzimidazole (**2.48**) to their azaborine analogs **2.39** and **2.49**], supporting the notion that the B-N bond displays some of the electronic properties of a C=C bond. An even stronger likeness can be seen when comparing *N*-alkylated azaborines **2.44**, **2.50**, **2.51** and **2.53**, respectively. The strong similarity between the electrostatic potential maps in these isosteric systems presumably results from enhanced electron availability from the methylated nitrogen within the 5-membered ring. In the case of **2.44**, although this increased electron availability would enhance electron density, it would also reduce competitive conjugation of the lone pairs of the now desymmetrized nitrogen atoms. Computationally, this is observed by a slight lengthening of the MeN-B bond (1.439 Å) as compared to the HN-B bond (1.435 Å). This factor is also noticed in the indole and "fused" B-N indole

2.52, though to lesser extents (Figure 2.5). When taken together, these factors lead to an electronic hybrid between **2.50** and **2.51** where the dimethylated 1,3,2-benzodiazaborole **2.44** core closely resembles the A ring of **2.51** while having a more similar B ring to **2.50**.

Figure 2.4: Electrostatic potentials (from +31.38 kcal/mol to -31.38 kcal/mol) of the 1,3,2-benzodiazaborole compared to indole

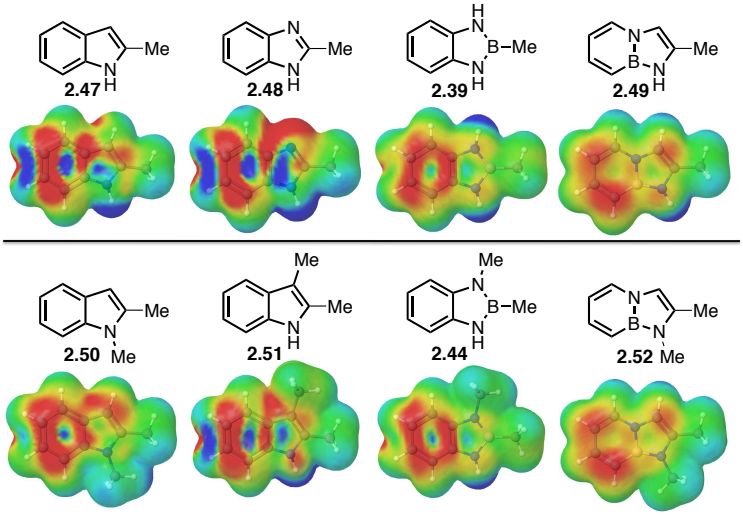

Nuclear independent chemical shift (NICS) calculations[23] were performed to assess the relative aromatic character of each ring (Table 2.5). NICS calculations provide quantitative correlations for aromaticity using a "theoretical nuclei" at the center of a ring system to probe electron shielding. A more negative NICS value indicates greater electron shielding *via* a stronger ring current and thus more π-electron delocalization. Enhanced delocalization is indicative of greater aromatic character. Because of ring current effects, only rings of similar size can be compared.[24] Across a selection of several molecules (Table 2.5), a few preliminary trends for the indole-azaborines can be ascertained. Initially, an increase in aromaticity in the A-ring from *o*-phenylenediamine **2.3** to the cyclized azaborine

products was observed (Table 2.5, right). This is presumably caused by the nitrogen lone pairs becoming locked in plane with the rest of the π-cloud upon annulation. Furthermore, the A-rings of the 1,3,2-benzodiazaborole **2.39** share similar NICS values to the corresponding indole **2.47** and benzimidazole **2.48**. However, when examining the B-ring, there is a lower electron shielding effect for the azaborine, presumably caused by incomplete π–delocalization with the B-N bond. This is confirmed by the NICS calculation for "fused" B-N indole **2.49**, where lower electron shielding occurs in both rings caused by the conjoined B-N bond. Similar values for related compounds have been observed by Liu.[19] Furthermore, B-ring deshielding is perturbed by the hybridization of groups bound to boron (**2.5, 2.31, 2.34, 2.39**), presumably caused by a change in orbital overlap or the electron-donating character of these functional groups. This hybridization effect has been previously observed within the benzene-azaborine scaffold,[25] where *sp*-hybridized groups generally induce shielding relative to their phenyl counterpart.

Table 2.5: NICS Comparisons (ppm) of 1,3,2-Benzodiazaborole and its Relative Carbon Isosteres[a]

	NICS(0) A Ring	NICS(1) A Ring	NICS(0) B Ring	NICS(1) B Ring	NICS(1) Center		NICS(0) A Ring	NICS(1) A Ring	NICS(0) B Ring	NICS(1) B Ring	NICS(1) Center
 **2.3**	-8.57	-8.73	-	-	-	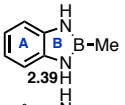 **2.39**	-9.60	-10.20	-6.86	-5.61	-14.30
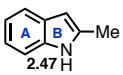 **2.47**	-9.20	-10.46	-10.57	-8.96	-16.22	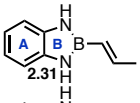 **2.31**	-9.42	-10.09	-6.93	-5.60	-14.21
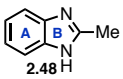 **2.48**	-9.82	-10.83	-9.23	-9.06	-16.16	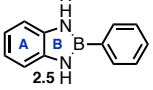 **2.5**	-9.34	-9.96	-6.32	-5.30	-14.02
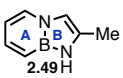 **2.49**	-6.21	-7.65	-9.31	-7.41	-13.08	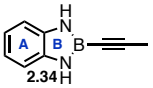 **2.34**	-9.55	-10.27	-7.80	-6.05	-14.48

[a]All structures are fully optimized to local minima [B3LYP/6-311+G(2d,p)].

The application of a facile synthetic approach to the 1,3,2-benzodiazaboroles highlights the ability to synthesize these azaborine cores *via* bench-stable reagents in a reaction tolerant of atmospheric conditions. Furthermore, the simple workup and purification conditions employed enable rapid access to molecules with valuable isosteric potential. The physical and computational data suggest that this class of azaborine compounds indeed demonstrates aromatic tendencies, which could be leveraged for potential applications of this core isostere of indole.

2.3 – Synthesis and structural analysis of the azaborininone

Considering the success of the 1,3,2-benzodiazaborole[26] scaffolds, we were interested in expanding into new polyheteroatom-based azaborinyl systems. Of particular interest was the azaborininone family (Figure 2.5). These underexplored, carbonyl-bearing, boron-heterocyclic scaffolds chelate a boron atom between a carboxylate or amide and a secondary aryl hydroxyl or amino group, thus establishing a 6,6-bicyclic ring system. The three resulting classes of azaborininones have been very sporadically explored,[27] and have shown applications as boron protecting/directing groups for C-H activation,[27e-g] as well as potential promise as therapeutics given their known abilities as insect chemosterilants.[27h] Development of a concise, robust synthetic method applicable to the entire family of azaborininones would be highly attractive. In addition to overcoming a synthetic challenge, the three core systems provide future opportunities to explore the reactivity of an entirely new library of boron-containing compounds. In parallel to these synthetic studies, computational investigation of the azaborininone family

could provide additional understanding as to how the substitution of O-B and N-B affect the structural and electronic properties of these molecules.

Figure 2.5 Azaborininones, their possible isosteric counterparts, and their requisite starting points

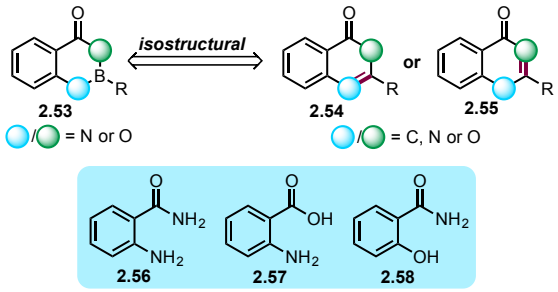

2.3.1 – Synthetic development of azaborininones

Early synthetic efforts centered on accessing 1,3,2-benzodiazaborininones derived from anthranilamide **2.56**. Using the conditions established from prior work with the similar 3,1,2-benzodiazaboroles,[26] the defluorinative annulation with phenyltrifluoroborate was met with success (Figure 2.6-A), affording **2.59**. Unfortunately, the fluorophile used (BF_3•NH_2Et) to facilitate the cyclization proved unsuccessful in reactions with anthranilic acid, **2.57** (Figure 2.6-B), or salicylamide, **2.58** (Figure 2.6-C), likely because the strong Lewis acidity of BF_3 diminished the already weak nucleophilicity of these systems. Thus, although the boron trifluoride-based approach would grant access to one core, alternative conditions were required to access the remaining two cores reliably. Given the known affinity of SiO_2 for fluoride in the context of organotrifluoroborates,[28] this reagent was considered as an alternative to BF_3•NH_2Et in enabling mild, defluorinative annulation. Not only would this mitigate the requirement of an excess boron trifluoride reagent, but it

would also employ an extraordinarily inexpensive, readily available reagent already found in virtually any organic laboratory.

Figure 2.6: Application of BF_3•NH_2Et conditions to azaborininones

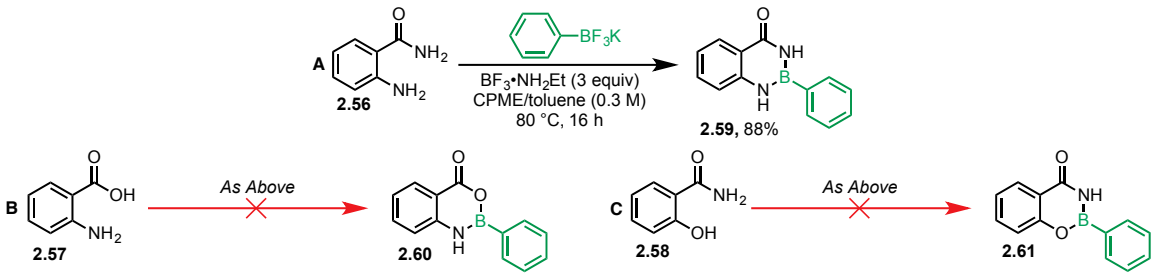

A brief screening of alternative additives in reaction with **2.56** and potassium phenyltrifluoroborate revealed SiO_2 to be the optimal fluorophile (Table 2.6). Importantly, these same conditions could be extended to both anthranilic acid and salicylamide without modification. Upon further study of SiO_2 as a fluorophile,

Table 2.6: Fluorophilic Reagent Optimization

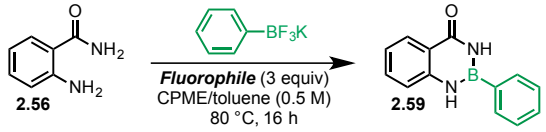

entry	fluorophile	% Consumption
1	BF_3•NH_2Et	100%
2	hexamethyldisilazane (HMDS)	8%
3	SiO_2	100%
4	Florisil	84%
5	alumina (basic)	40%
6	lithium silicate	26%

[a]Conversion determined by ^1H NMR spectroscopy

oven-dried SiO_2 was determined to be more effective and allowed the reaction temperature to be lowered to 60 °C. In addition to being a fluorophilic agent, SiO_2 is known to convert organotrifluoroborates to their corresponding boronic acids,[28] suggesting a potential reaction intermediate for the annulation. Exposure of phenylboronic acid in place of phenyltrifluoroborate (Figure 2.7) to the optimized

conditions resulted in conversion to **2.59**, validating this hypothesis. This finding also explains the benefit observed of dried SiO_2, as this can improve the ability of SiO_2 to act as a desiccant in the annulation (whose byproduct is H_2O). This indicates two viable mechanisms; one proceeding through a difluoro-organoborane and the

Figure 2.7: Azaborininone annulation *via* boronic acid

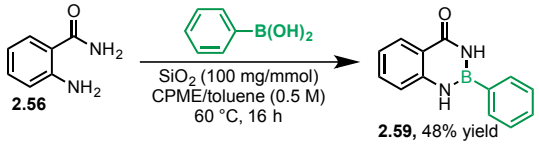

other *via* a boronic acid. Both may be operative under SiO_2-mediated annulation, but only the former is possible when using the anhydrous BF_3•NH_2Et conditions.

With two complementary conditions in hand, the scope of each approach was assessed. In the case of the 1,3,2-benzodiazaborininones (Table 2.7) derived from

Table 2.7: Synthesis of 1,3,2-Benzodiazaborininones *via* Defluorinative Annulation

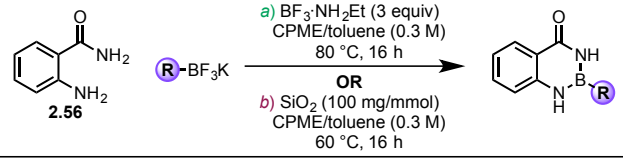

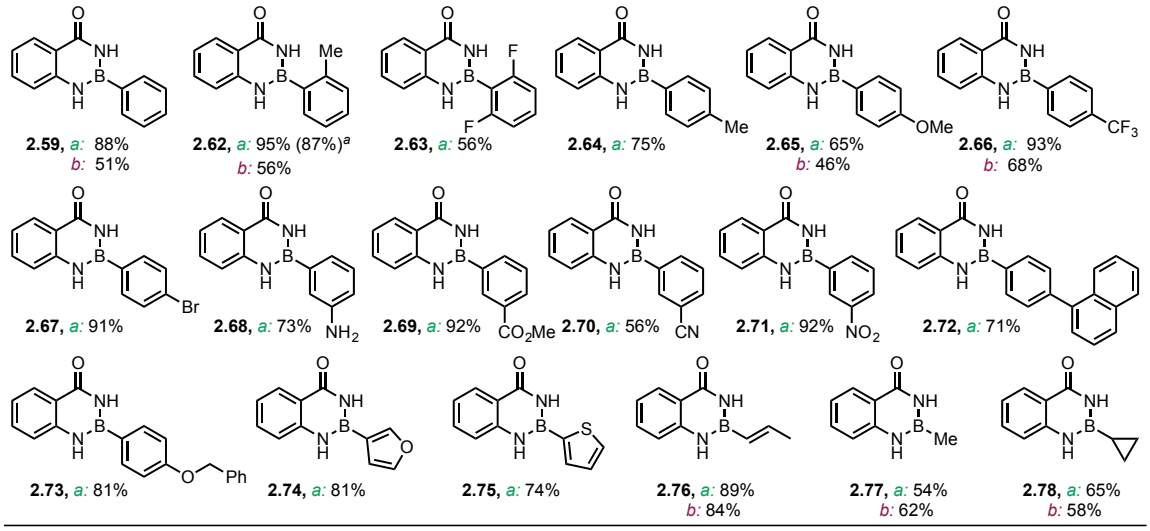

[a]Yield on 7 mmol scale (see Experimental Section for detailed reaction conditions).

anthranilamide and the corresponding potassium organotrifluoroborates, a variety of annulated products could be accessed using either protocol. Typically, the BF_3•NH_2Et conditions outperformed SiO_2-mediated cyclizations (compare yields for **2.59, 2.62, 2.65, 2.66, 2.76-2.78**). Various functional groups were amenable to the annulation, including ethers (**2.65, 2.73**), amines (**2.68**), esters (**2.69**), and cyano groups (**2.70**). Furthermore, polycyclic (**2.72**) and heterocyclic (**2.74**, **2.75**) species could be accessed, as well as non-aryl organotrifluoroborates (**2.76-2.78**). Finally, the BF_3•NH_2Et conditions were readily scalable to furnish gram quantities of **2.62**.

Utilization of the SiO_2-based conditions enabled initial entry to the mixed N,O-azaborininone classes. Starting from anthranilic acid (**2.57**), a variety of 1,3,2-benzoxazaborininones could be synthesized (Table 2.8). A range of potassium organotrifluoroborates were competent in the synthesis of this class of oxazaborininones, and functional group tolerance remained high. In addition to retaining the functional group tolerance seen with 1,3,2-benzodiazaborininones,

Table 2.8: Synthesis of 3,1,2-Benzoxazaborininones via Defluorinative Annulation

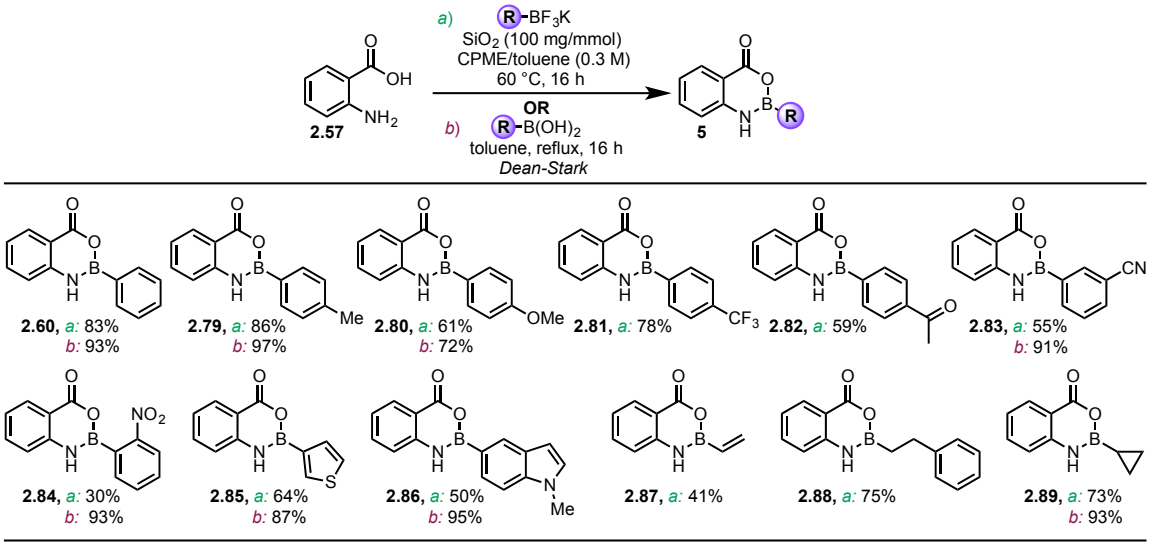

additional substrates containing ketones (**2.82**) and indoles (**2.86**) were demonstrated to be amenable to cyclization. Alkenyl- (**2.87**) and alkyl-3,1,2-benzoxazaborinine substrates (**2.88, 2.89**) could also readily be prepared. Oftentimes, inconsistent conversion was observed upon isolation of the products, as **2.57** would remain even after purification by silica plug. Using ^{1}H NMR spectroscopy, these compounds were determined to be intolerant to water, and they readily hydrolyzed to the corresponding boronic acid and **2.57** in a quantifiable manner (Figure 2.8).[27e,29] However, apart from hydrolysis, these systems were found to be stable in organic solutions even at elevated temperatures. With this in mind, conditions involving boronic acids were considered, capitalizing on azeotropic water removal to drive cyclization.[27e,30] These conditions (denoted conditions *b* in Table 2.8) provide a complementary route that in many cases gives equal to superior yields, likely because of the irreversibility of annulation because of the removal of water *via* Dean-Stark conditions. Although not explored for every substrate, this approach was most useful for systems prone to hydrolysis (**2.60,**

Figure 2.8: Water stability study of 2-phenyl-3,1,2-benzoxazaborininone

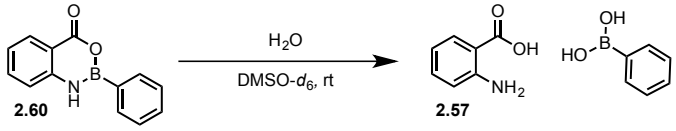

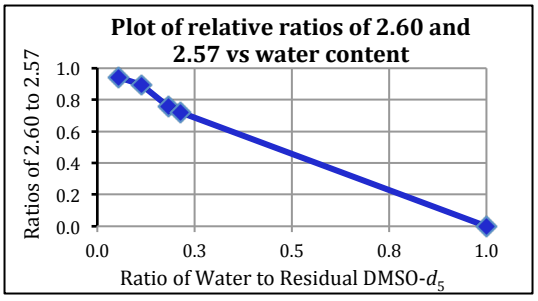

Integrals				Ratios	
2.60	**2.57**	**H_2O**	**DMSO**	**2.60 to 2.57**	**H_2O to DMSO**
1.00	0.06	0.94	1.00	0.06	0.06
1.00	0.12	0.89	1.02	0.15	0.13
1.00	0.32	0.76	1.19	0.34	0.22
1.00	0.39	0.72	1.12	0.42	0.27
0.00	1.00	0.00	1.00	66.7	0.99

2.79, 2.80, 2.83-2.86, 2.89).

The isomeric 1,3,2-benzoxaborininones (Table 2.9) could also be accessed from salicylamide (2.58). These substrates were typically the lowest-yielding members of the azaborininone family. This can be attributed to the diminished nucleophilicity of an amidyl nitrogen relative to an aniline, combined with lability of *O*-borylated phenols. In this case, a significant yield difference exists between the SiO_2 conditions (*a*) and the Dean-Stark condensation (*b*). Again, this likely relates to the unique electronics of this azaborininone class, which is more prone to degradation *via* hydrolysis. Despite this, many, if not all, of the boryl substitution patterns tolerated with other members of the azaborininone family could be accessed with this more sensitive core. Not surprisingly, the azeotropic protocol fared far better with these systems. Indeed, in some cases, such as the acetophenone derivative **2.93,** azeotropic condensation was the only way to effect annulation.

Table 2.9: Synthesis of 1,3,2-Benzoxazaborininones *via* Defluorinative Annulation

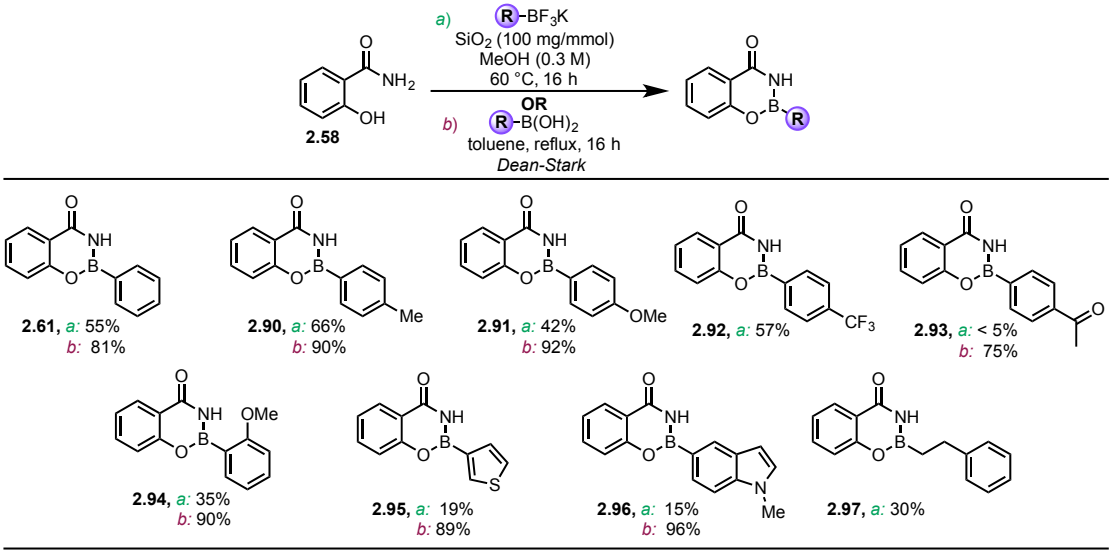

2.3.2 – Computational evaluation of azaborininones

In parallel to developing a user-friendly synthesis of this underexplored azaborine class, we sought to evaluate their electronic properties. More specifically, we hoped to discern what, if any, isostructural (or isoelectronic) character these systems possessed. Indeed, many possible isosteres were envisioned, such as isochromones for 3,1,2-benzoxazaborininones or isoquinolinones for 1,3,2-benzodiazaborole. Compounds were initially considered on an isostructural basis, focusing on the structural similarities, comparing B-N/C=C and the analogous B-O/C=N. Given the prior successes in analyzing the 1,3,2-benzodiazaborole core using quantum mechanical calculations,[26] computational modeling was used to glean insight. All calculations were carried out using Gaussian 09,[20] and the structures were visualized *via* WebMO.[21] Geometry optimizations were performed in the gas phase at the B3LYP/6–311+G(2d,p) level of theory.[22] The method used for calculations involving thermochemical values (e.g., computed pK_a) of the various systems involved (i) geometry optimization and vibrational frequency calculations in the gas phase at the B3LYP/6–311+G(2d,p) level of theory and (ii) geometry optimization and vibrational frequency calculations in implicit water (H_2O) using PCM[31] at the B3LYP/6–311+G(2d,p) level of theory. Stationary points were characterized by frequency analysis at 298.15 K, with structures at energy minima showing no imaginary frequencies. To probe the ring current in these systems, nuclear independent chemical shift (NICS) values were determined at the GIAO-B3LYP/6-311+G(2d,p) level of theory at distances of 0.0 Å [A(0) and B(0)] and 1 Å

[A(1) and B(1)] from each ring system as well as from the center of the bicyclic systems [Center(1)] in the perpendicular direction.[23]

Initial computational investigations focused on the truncated cores (i.e., without functionalization on boron) to explore the structural and electronic features in comparison to isostructural compounds (Table 2.10). 1,3,2-Benzodiazaborininone **2.98**, isoquinolinone **2.101** and quinolinone **2.102** were identified as likely isosteres. A pictorial comparison of the electrostatic potential maps of these isosteres with the truncated 1,3,2-benzodiazaborininone **2.98** seemed to indicate that this system was a hybrid of both structures. This is not altogether surprising given that nitrogen is well-known to participate in electron-donation to boron. Indeed, the B-N bond lengths in the 1,3,2-benzodiazaborininone are quite uniform despite the nitrogen atoms being in vastly different electronic environments. This is corroborated in the slight contraction seen in the C=O bond as compared to isoquinolinone (**2.101**), indicating diminished nitrogen participation in the carbonyl π-system. NICS calculations, which provide a quantitative correlation for aromaticity using "theoretical nuclei" at the center of a ring system to probe electron shielding, were used for further elucidations.[23] Specifically, NICS(1) values were highlighted based on their improved ability to observe a π-delocalized aromatic ring current. NICS studies indicated that, relative to its isosteres, 1,3,2-benzodiazaborininone **2.98** has less aromatic character in its B ring. This finding is in agreement with prior work by our group and others, wherein boryl-based aromatic systems display diminished aromatic character when compared to their indole counterparts.[23a, 26] This effect is less pronounced in the adjoined carbon ring

but is still observed. NICS values between the two possible isosteres of this system are relatively similar, with **2.102** having slightly less aromatic character and thus

Table 2.10: Comparison of the Azaborininone Family with their Structural Isosteres[a]

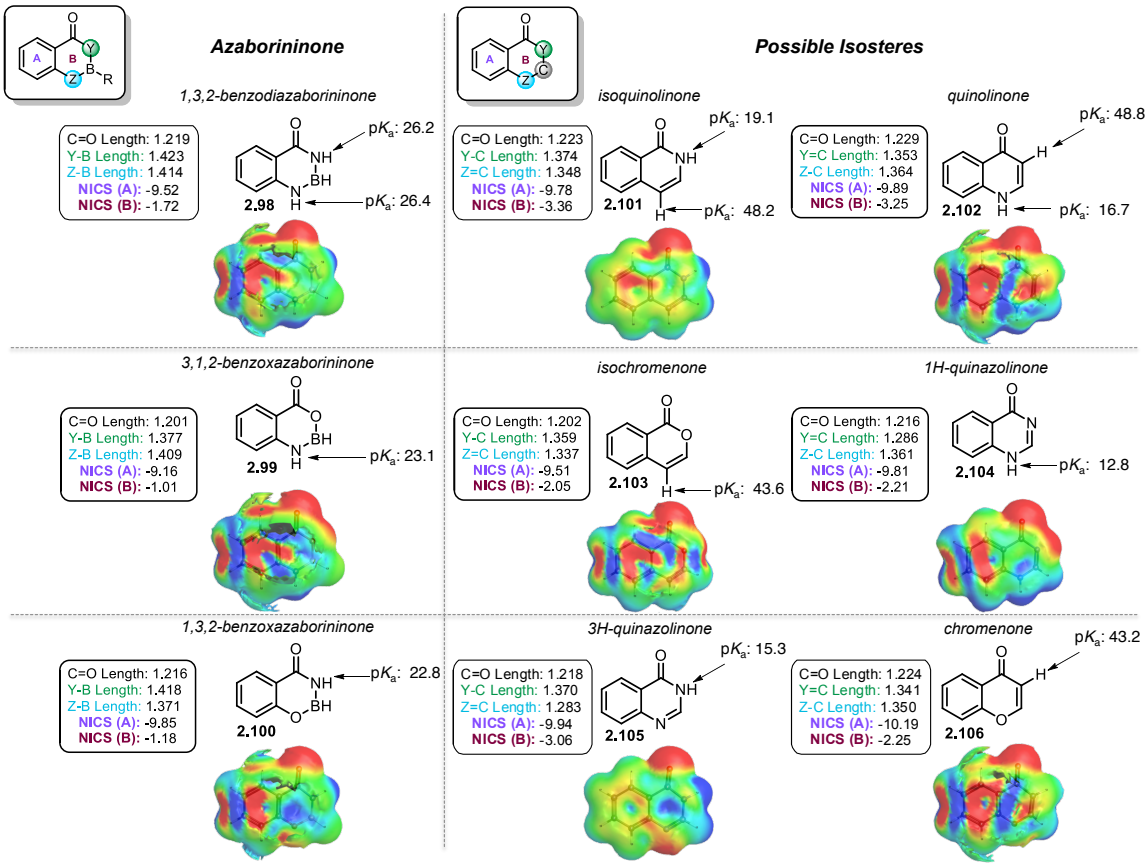

[a]All distances given in angstroms (Å), and the electrostatic potentials range from +31.38 kcals/mol to -31.38 kcals/mol. NICS(1) values are given in ppm.

more similarity to **2.98**. Because of the aforementioned inherent stability issues of these systems, experimentally-derived pK_a values were unobtainable, and thus theoretical values were pursued.[32] The computed pK_as of **2.98** are quite uniform, indicative of a strong electron donation to boron by both nitrogen atoms. The pK_as are notably higher than their isosteres, a consequence of the competitive donation by both nitrogen atoms into boron and the lack of a resonance contributor in the B

ring to delocalize negative charge. Indeed, approximating this situation by averaging pK_as of **2.101** gives a value of 33.7, which is within a few orders of magnitude of the pK_a of **2.98.** Repeating this with **2.102** gives an even closer value, 32.8. Combining the NICS data with the pK_a, suggests that **2.98** represents a unique hybrid between **2.101** and **2.102**, with a slight electronic bias toward **2.102**.

Moving to 3,1,2-benzoxazaborininone **2.99** and 1,3,2-benzoxazaborininones **2.100**, similar trends were observed. As a whole these mixed N,O systems displayed less aromatic character and were more acidic. This increased acidity can be attributed to a lower secondary orbital overlap with boron by the secondary heteroatom (in this case oxygen). The lower participation of electron donation by oxygen likely also relates to the observed, less negative, NICS values for the B rings of these systems. However, the isosteric character of these two systems was not as uniform. Using electrostatic potentials, **2.99** more closely resembles isochromone **2.103**, whereas **2.100** appears to be more of a hybrid of **2.105** and **2.106**. These trends are also borne out in the NICS analysis, wherein **2.100** has slightly more aromatic character than **2.99**, indicating more oxygen participation in the ring system, thus providing more plausibility to B-O/C–N mimicry. The relatively longer B-N bond seen in **2.100** also is in line with enhanced oxygen participation. However, the NICS value for the B ring of **2.100** more closely aligns with the B ring of **2.106**. The exact opposite is true for the A ring, thus supporting the notion that **2.100** is a hybrid of the two systems.

To probe the role of electronics in these systems further, substitution on boron was next explored (Table 2.11). Four representative *B*-aryl groups were

selected that not only provided a range of electronic environments but were also prepared during the synthetic studies to allow correlative studies. In general, adding a *B*-aryl group led to diminished aromatic character for all members of the azaborininone family, as the boron is in favorable π-orbital overlap with the external ring. In particular, the 1,3,2-benzoxazaborininones showed the most significant disparity in the NICS values of the B ring from its truncated system. The diminished delocalization in this system and the lower values observed for the isomeric 3,1,2-benzoxazaborininone class may increase the electrophilic character of boron. Ultimately, this increase may relate to their observed experimental instability. Electronically, the 1,3,2-benzodiazaborininones were the least sensitive to electronic changes, suggesting the overriding participation of both nitrogen atoms in this core. The 3,1,2-benzoxazaborininones seemed to be most influenced by electronic changes and appeared to gain aromatic character with more electron-deficient *B*-arenes.

Table 2.11: NICS Analysis of Electronically Disparate Azaborininones Divided by Class

1,3,2-benzodiazaborininones	OMe	Me		CF_3
	NICS(1) (A): -9.08 NICS(1) (B): -1.30	NICS(1) (A): -9.16 NICS(1) (B): -1.29	NICS(1) (A): -9.10 NICS(1) (B): -1.31	NICS(1) (A): -9.29 NICS(1) (B): -1.22
3,1,2-benzoxazaborininones	OMe	Me		CF_3
	NICS(1) (A): -8.74 NICS(1) (B): -0.39	NICS(1) (A): -8.91 NICS(1) (B): -0.50	NICS(1) (A): -8.76 NICS(1) (B): -0.49	NICS(1) (A): -9.01 NICS(1) (B): -0.55
1,3,2-benzoxazaborininones	OMe	Me		CF_3
	NICS(1) (A): -9.54 NICS(1) (B): -0.64	NICS(1) (A): -9.53 NICS(1) (B): -0.56	NICS(1) (A): -9.51 NICS(1) (B): -0.64	NICS(1) (A): -9.57 NICS(1) (B): -0.60

As a means of correlating some of the observed computational trends with experimental data, NICS calculations were compared with experimental data. Although pK_as would have been ideal, the instability of these systems to strongly basic environments prohibited such a correlative study. Instead, IR and NMR spectroscopy were used as a means of quantitatively comparing calculations to experiment. Initially, the computed IR stretching for C=O were compared against the NICS values for both rings, to determine if the double bond character of the carbonyl would be influenced by the aromatic character of the ring and the relative electron-donation propensity of the adjacent heteroatom with boron. It was observed that, whereas the amide-containing 1,3,2-benzoxazaborininones and 1,3,2-benzodiazaborininones were readily comparable, the 3,1,2-benzoxazaborininones did not trend with the other members of the azaborininone class (Figure 2.9). This is not altogether that surprising given the pseudo-α,β-unsaturated character of the structures (*via* C-N/C=C isosterism) possible with the former two systems, which is

Figure 2.9: Plots of computed C=O IR stretch vs NICS values for both the A and B rings of various azaborininones

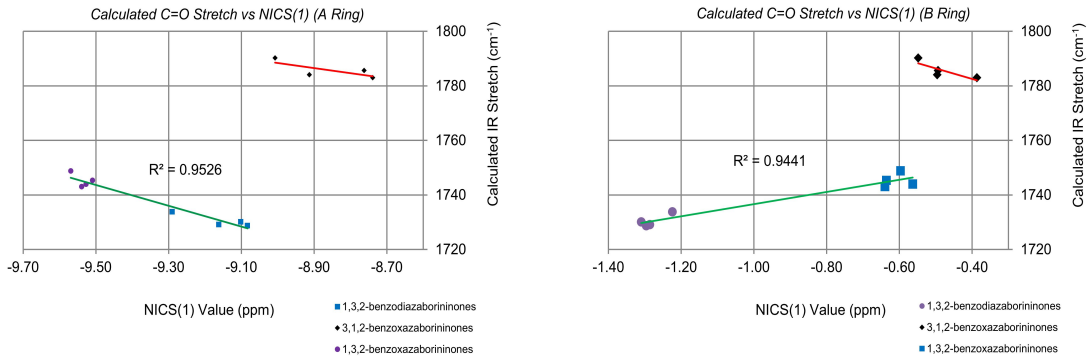

not possible in the latter. This trend is also in agreement with the findings of the truncated systems. Whereas the amide-based systems usually are hybrid structures

and very much electronically related, the ester-like 3,1,2-benzoxazaborininones are more like their isochromenone isosteres. Comparison of the experimental values for these systems provided some level of correlation but, because of their complex IR spectrum, the correlations were less than ideal (See Supporting Information for details). For a more precise correlation, ^{13}C NMR was used, which would be quite sensitive to electronic changes. Experimental NMR values correlated well with NICS(1) values in both rings, indicating the electronic shielding trends observed computationally may indeed occur in these systems experimentally (Figure 2.10). In general, the distribution of these values was self-consistent within each structural class (i.e., bimodal for the two classes plotted). Although the B rings shows aromatic character, the values observed for the A ring are more analogous to aromatic systems [NICS(1) value of benzene is -10.20].[23b] This is similarly reflected in these

Figure 2.10: Plots of experimental ^{13}C NMR values vs computed NICS values for both the A and B rings of various 1,3,2-benzoxazaborininones and 1,3,2-benzodiazaborininones.

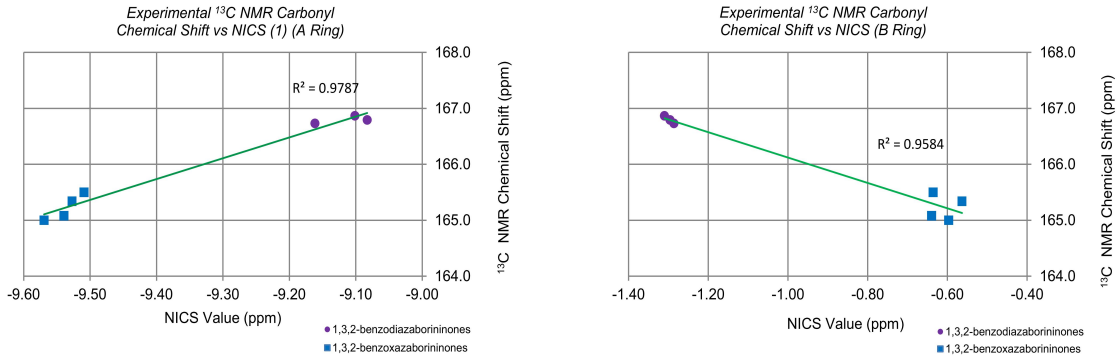

studies, with the A ring showing a stronger correlation than the B ring. Thus, this provides some level of experimental validation of the trends observed in the NICS studies.

This modular approach to the synthesis of the azaborininone family of azaborines provides a set of simple conditions enabling various organotrifluoroborates to undergo facile defluorinative annulation facilitated by inexpensive fluorophiles. Alternatively, boronic acids also undergo annulation *via* a more classical condensation route. Three classes, 1,3,2-benzodiazaborininones, 1,3,2-benzoxazaborininones, and 3,1,2-benzoxazaborininones, can be prepared using these approaches. Computational methods revealed some similarities to possible carbon isosteres. Whereas 1,3,2-benzodiazaborininones and 3,1,2-benzoxazaborininones appear to represent a hybrid between their plausible isosteres, the 1,3,2-benzoxazaborininones seem to align closely with isochromenones. Correlations between computed NICS values and experimentally derived trends provide support for these computed values.

2.4 – Stability studies and access to challenging 2,1-borazaronaphthalene cores

The Molander group's initial foray into azaborines began with 2,1-borazaronaphthalene, an isostuctural relative of naphthalene.[14] Previously, this class of azaborines had been accessed from 2-aminostyrene (**2.107**) and dihalo-boranes,[33] however with limited substrate tolerance (Figure 2.11-A). It is proposed that the annulation proceeds *via* an initial coordination with the borane, followed by a 6-π annulation and proton elimination to generate the 2,1-borazaronaphthalene (**2.108**). Our group developed a method to capitalize on this mechanistic pathway, while vastly expanding the scope of substituted 2,1-borazaronaphthalenes by leveraging organotriflouroborates as the synthetic source of boron (Figure 2.11-

B).[13] In the presence of silicon tetrachloride, it was established that trifluoroborates readily exchange to the di-halo species,[15] which is well suited to undergo annulation to form the azaborine under mild conditions.

Figure 2.11: Annulation of 2,1-borazaronaphthalene

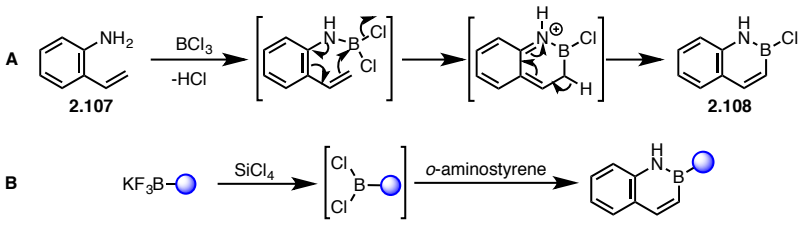

B-Aryl 2,1-borazaronaphthalenes have been demonstrated to have good thermal stability, along with tolerance to both acid (pH 2 at 37 °C) and base (Cs_2CO_3/H_2O at 60 °C).[34] Further studies that focused on the medicinal viability of the 2,1-borazaronaphthalene have subsequently found that *B*-Me 2,1-borazaronaphthalene derivatives showed good stability in base (>80% stability in 0.1 N NaOH), but showed a tendency to degrade in acid (0.1 N HCl). However, it is noted that overall this class of compounds represent a potential "bioisosteric replacement for naphthalene in drug discovery programs".[35]

2.4.1 – Stability studies of 2,1-borazaronaphthalene

One negative feature observed within our own program was a tendency of the azaborine to gradually decompose in solution. Monitoring by ^{1}H NMR, 2-methyl-2,1-borazaronaphthalene (**2.109**), was noted to decompose in both deuterated chloroform and DMSO, within a week's time (Figure 2.12). A more rapid decomposition was observed for a Boc-protected tetrahydropyridine derivative (**2.110**), which was concerning as this compound presented a more biologically

relevant scaffold (Figure 2.13). These findings were surprising as no decomposition was ever observed for compounds that were stored on the benchtop as a solid. However, the lack of long term solution stability presents a critical problem as many of the screening libraries at pharmaceutical companies are stored as solutions for easy dosing, causing a barrier to use.[36]

Figure 2.12: Time decomposition of 2-methyl-2,1-borazaronaphthalene

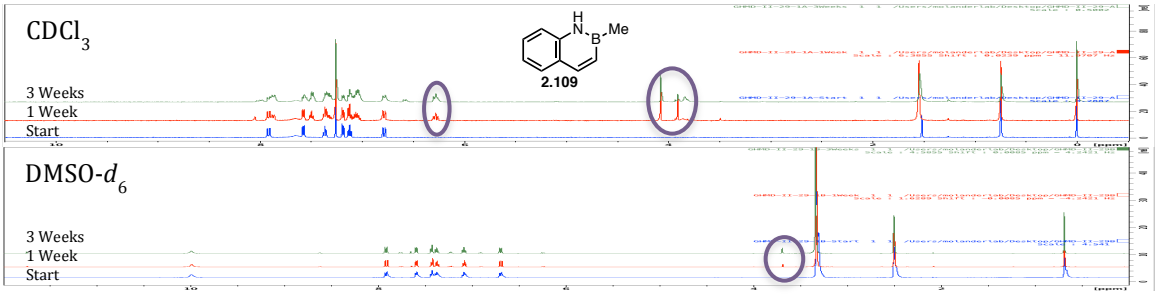

Figure 2.13: Time decomposition of 4-(2,1-borazaronaphthyl)methyl-1-(*tert*-butoxycarbonyl)-1,2,3,6-tetrahydropyridine

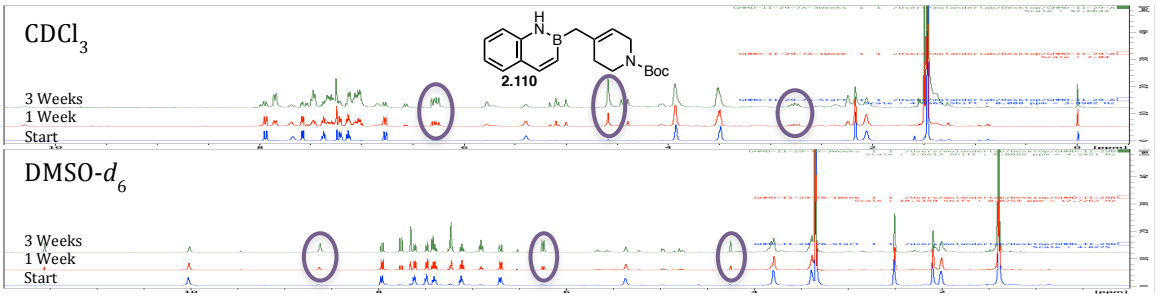

In an attempt to understand the features associated with stability, three electronically varied *B*-aryl 2,1-borazaronaphthalene cores were studied over the period of a month (Figures 2.14, 2.15 and 2.16). As can be observed when compared to the *B*-alkyl **2.109** and **2.110**, aryl substitution off boron is exceedingly more stable. Nevertheless, over a month's time, decomposition could be observed (circled in purple). From this data, a decomposition rate could be derived in comparison to an internal standard (4,4'-di-*tert*-butylbiphenyl) (Figure 2.17), which was then

translated to a value for the percent change of product to internal standard ratio (%Δ of Prod:IS). From this data, it was observed that the more electron deficient aryl ring (**2.113**) had a higher tendency for decomposition, as compared to the electron neutral (**2.111**) or electron rich substrates (**2.112**).

Figure 2.14: Time study of 2-phenyl-2,1-borazaronaphthalene

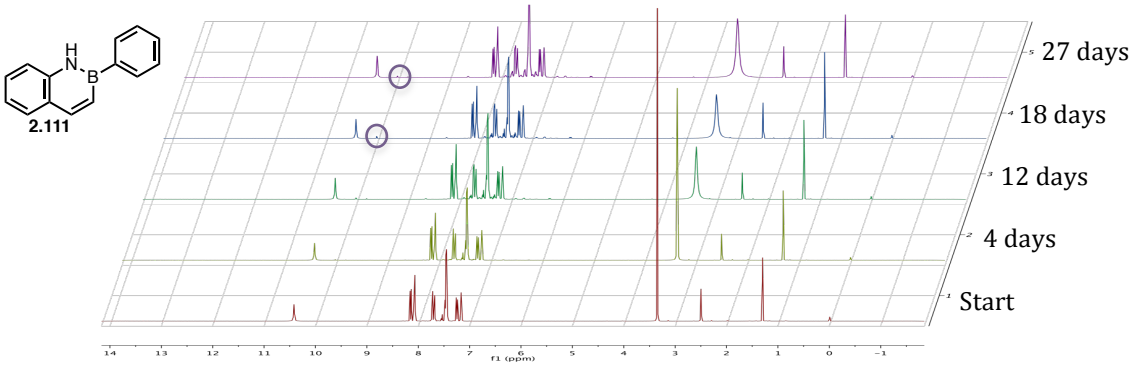

Figure 2.15: Time study of 2-(4-(methoxy)phenyl)-2,1-borazaronaphthalene

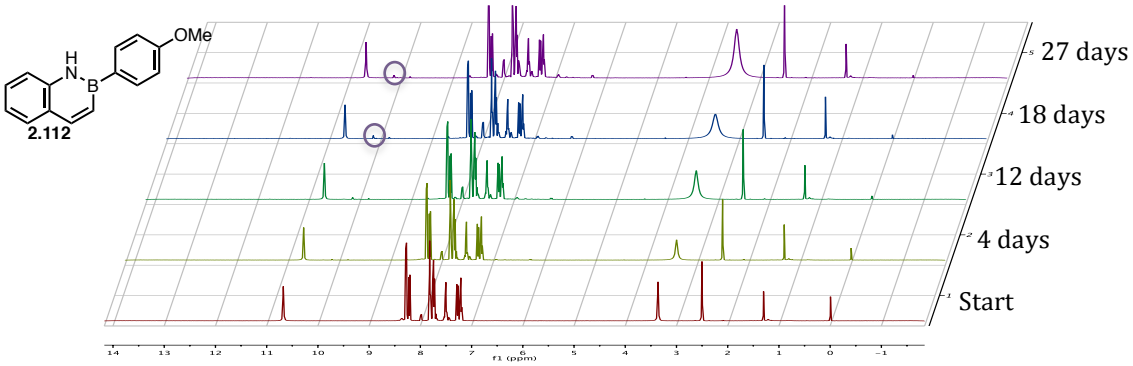

Figure 2.16: Time study of 2- (4-(trifluoromethyl)phenyl)-phenyl-2,1-borazaronaphthalene

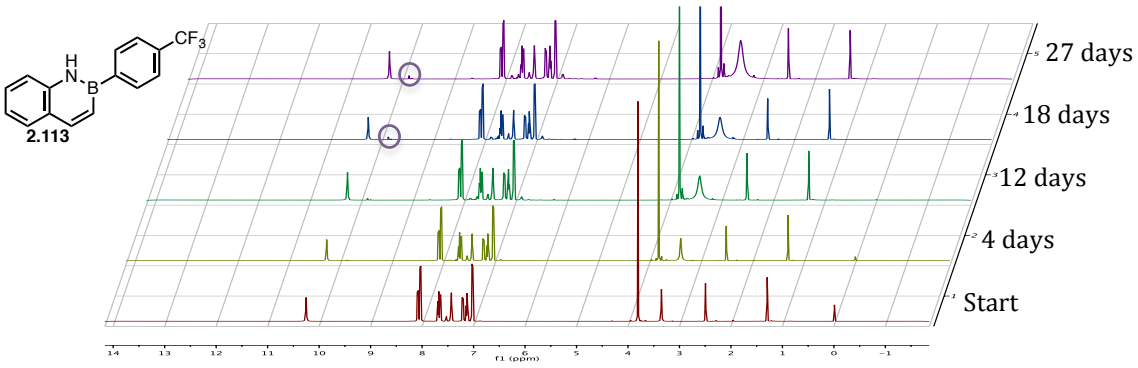

Figure 2.17: Decomposition rates for *B*-aryl 2,1-borazaronaphthalenes

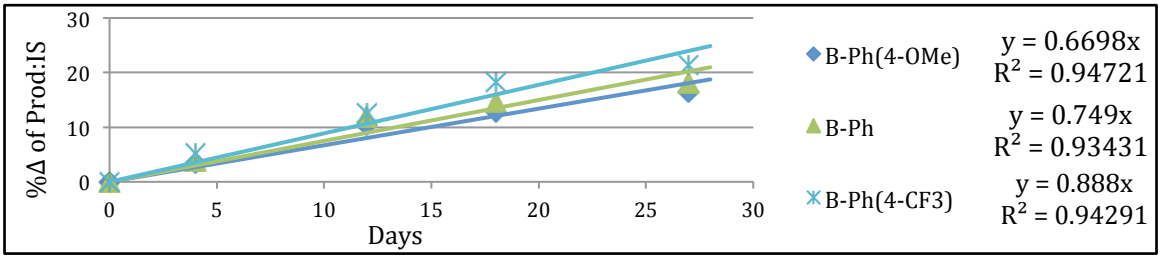

Because electronic variation of the 2,1-borazaronaphthalene compounds presented different rates of decompositions, it was considered whether the experimental rates could be correlated to computational values, which would allow us to develop a model of factors for degradation. Computational comparisons of a subset of *B*-arylated molecules with different electronic functional groups (Figure 2.18) could provide a structural-electronic trend that could then be tied back to the

Figure 2.18: Compounds compared *via* computational studies

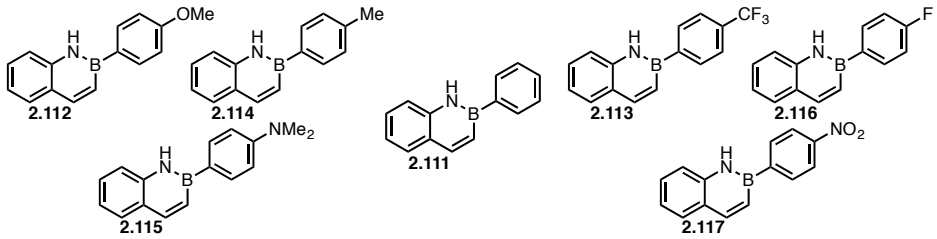

actual degradation data. Initially, ground state geometry-optimized core structures were derived at the B3LYP/6-311+G(2d,p) level of theory[20] using Gaussian 09[21] visualized *via* WebMO[22]. To assess aromaticity, NICS values[23] were determined for both A and B rings and the center of the azaborine core at distances of 0.0 Å [(A(0), B(0) and Center(0)] and 1 Å [(A(1), B(1) and Center(1)] (Figure 2.19).

Figure 2.19: Computational points of interest

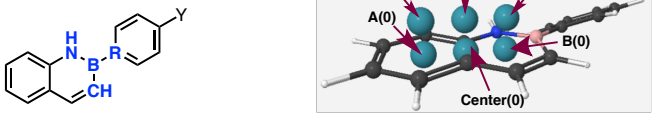

Comparing the geometry optimized 2,1-borazaronaphthalene structures, the bond lengths presented an initial structural correlation. When comparing the bond lengths most critically influenced by electronic changes, the boron-aryl fragment (B–R) was found to have an inverse relationship to the length of both the boron-nitrogen (B–N) and boron-carbon (B–C) bonds within the azaborine core (Figure 2.20). The shorter B-R bond lengths were attributed to electron rich substituents, which would provide better orbital overlap with boron's empty orbital. Consequently, those systems would have less electron donation from the azaborine ring, resulting in elongated B–N and B-C bond lengths.

Figure 2.20: Correlation of B–R bond length of both B–N and B–C[a]

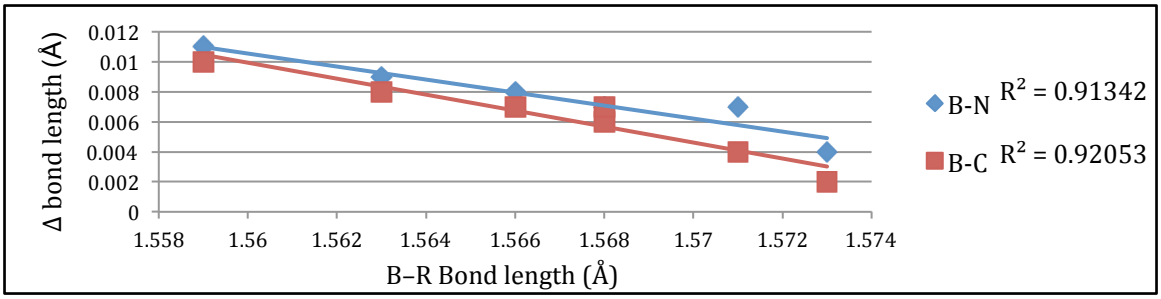

[a]Relative bond lengths were compared to the 2*H*-2,1-borazaronaphthalene as the standard

This was corroborated when comparing the bond length to NICS values, where both increasing B–N and B–C (Figure 2.21 and 2.22) bond lengths trended with less negative NICS values (deceasing aromaticity). The B–R bond, however, showed the opposite trend (Figure 2.23). This was consistent across both rings (A and B) along with the center of the azaborine core (Center), both in the plane of the ring system [NICS(0)] as well as 1 Å above [NICS(1)]. Relating back to the substrates, compounds with electron-withdrawing groups (**2.113, 2.116, 2.11)** have shorter B–N and B–C bond lengths and higher aromaticity values, suggesting

greater delocalization of electrons within the azaborine core. Conversely, the compounds with electron-donating groups (**2.112, 2.114, 2.115**) have longer B–N and B–C bond lengths and lower aromaticity values, presumably since there is more π-donation from the external aryl ring.

Figure 2.21: B–N Bond lengths vs NICS aromaticity[a]

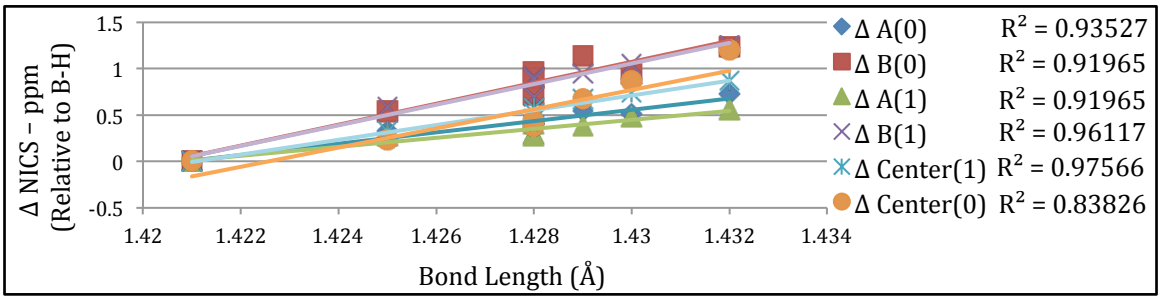

[a]Relative NICS values were compared to the 2*H*-2,1-borazaronaphthalene as a standard

Figure 2.22: B–C Bond lengths vs NICS aromaticity[a]

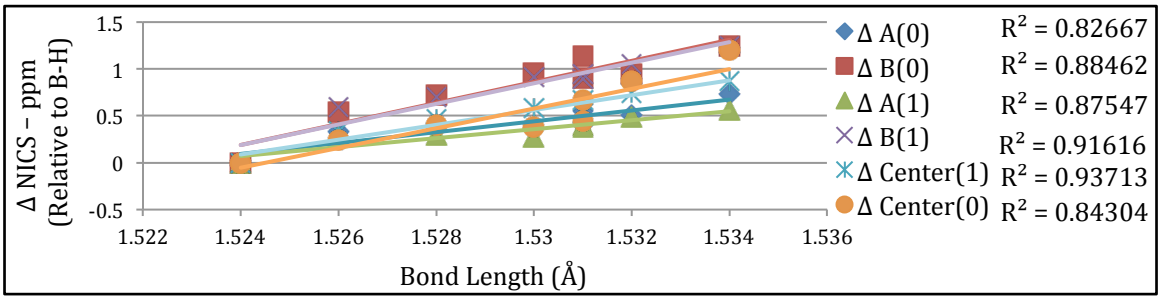

[a]Relative NICS values were compared to the 2*H*-2,1-borazaronaphthalene as a standard

Figure 2.23: B–R Bond lengths vs NICS aromaticity[a]

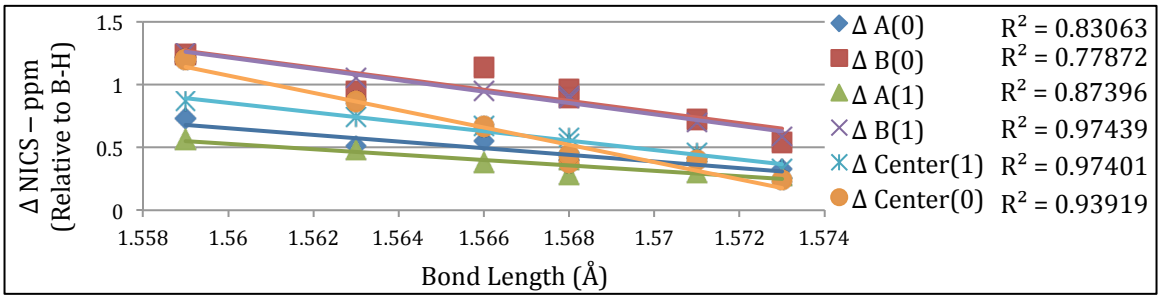

[a]Relative NICS values were compared to the 2*H*-2,1-borazaronaphthalene as a standard

With an understanding of the structural correlation to aromaticity, we considered whether this would correlate to the rate of decomposition data obtained for **2.111**, **2.112**, and **2.113**. Gratifyingly, good correlation was observed between both the changes in B–C and B–R bond lengths as well as in several of the NICS values (Figure 2.24). Correlation to B–N bond length was limited by the lack of accuracy available *via* calculation, as two of the computational compounds were too similar to actually calculate a difference. As expected, there was an inverse trend for rate of decomposition between the B–C and B–R bond lengths; for the former, the longer bond lengths coincided with slower decomposition, while this trend was reversed for the latter. For the NICS values, there was good correlation between B-rings, at both the plane of the molecule and 1 Å above, as well as with the NICS (1)

Figure 2.24: Correlation of bond lengths and NICS aromaticity to rate of decomposition[a]

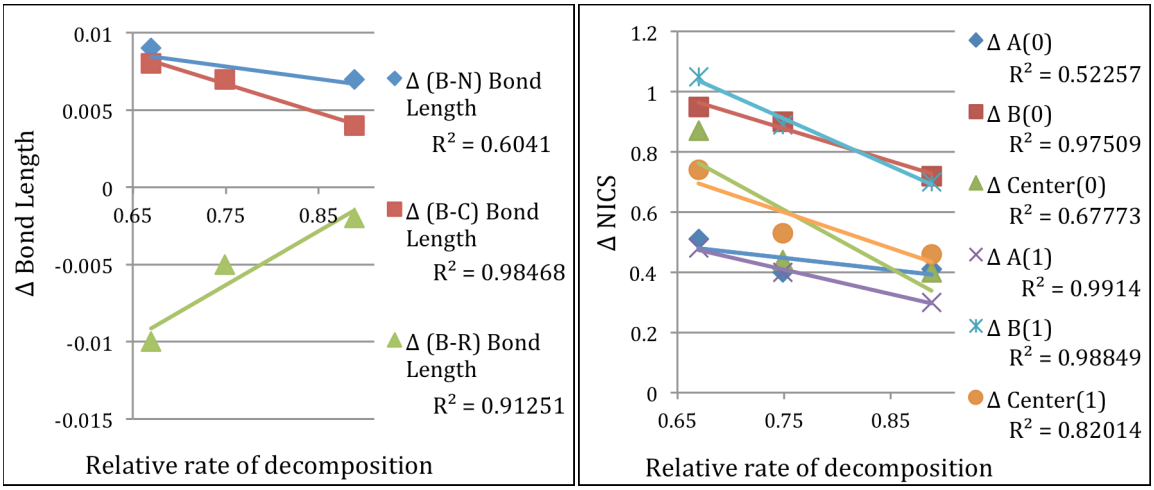

[a]Relative bond lengths and NICS values were compared to the 2*H*-2,1-borazaronaphthalene as the standard. Rate of decomposition was derived as the slope for decomposition for **2.111**, **2.112** and **2.113**

for the A-ring. These would be the computed positions expected to be the most sensitive to electronic perturbations. The B-ring is closest to the electronic variation, causing a direct influence. Correlation in the A-ring NICS values suggests that there

is good electronic cross-talk between the rings, highlighted by the NICS(1) values, which provided a better benchmark for π-cloud aromaticity because of the favorable proximity to the delocalized electrons.[23] The center values can become obscured by σ-bond interference, demonstrated by the lower statistical fit.

Unusual was the counterintuitive relationship between the decomposition rate and the aromaticity values; the azaborine with the highest rate of decomposition also had the highest aromaticity. This is opposite from most text-book chemistry, in which it is understood that increasing aromaticity encourages stability.[37] We are not the first to observe this phenomenon in the context of azaborines,[25,38] and while aromaticity (especially when considered from ring current delocalization) is an important component when considering compound stability, it does not take into consideration other factors important to overall compound stability, including σ-bond influences and modes of decomposition. Critically, the most important factor correlating with stability was the substitution off of boron (B-R). Aryl substituents were far more tolerable and remain mostly intact after a month in solution, compared to *B*-alkyl 2,1-borazaronaphthalenes, which showed significant decomposition after one week. It is important to reiterate that as a solid on the bench-top, none of these compounds were observed to show any decomposition. Additionally, during the time of this study, it was observed that the decomposition likely proceeds *via* a light mediated pathway. When samples were left in solution, with no exposure to light, even *B*-alkyl samples were found to be stable for extended time periods.

2.4.2 – Access to nitrogen-containing, *B*-heteroaryl 2,1-borazaronaphthalenes

Confident that the stability of the 2,1-borazaronaphthalene core was improved with *B*-aromatic substitution, we assessed the diversity of substrates at our disposal. One deficiency within the initial synthetic scope for accessing the 2,1-borazaronaphthalene core was the lack of nitrogen-containing heterocyclic functional motifs, particularly substituted off of boron.[14] Considering the diverse use of heterocycles and their recognition as "privileged structures" for modulation of biological systems, this presented a significant limitation of the system.[39] A recent solution to address this problem was reported by Rombouts *et al*. using microwave (μW) conditions, which allowed the annulation of pyridyl styrenes in high yields.[40] Furthermore, they reported select examples of pyridyltrifluoroborates being successful in the annulation under their conditions. Despite this recent advance, we were interested in finding a widely applicable set of conditions that would allow the incorporation of a diverse array of nitrogen-containing heterocyclic substructures.

Using the standard reaction conditions previously developed by our group for accessing the 2,1-borazaronaphthalene core,[14] initial attempts to condense nitrogen-containing trifluoroborates with *o*-aminostyrene derivatives were met with no success. To understand why nitrogen heterocyclic trifluoroborates were incompatible with the reported conditions, pyridine was added in increasing amounts to the reaction of 2-aminostyrene (**2.118**) with phenyltrifluoroborate (**2.119**) (Table 2.12). As is evident from the results presented, pyridine has a marked inhibitory effect on the reaction, which intensifies with increasing amounts of this additive. With evidence in hand of the direct inhibition caused by added

pyridine in the formation of 2-phenyl-2,1-borazaronaphthalene (**2.120**), we surmised that the presence of Lewis basic sites in the nitrogen-containing heterocyclic trifluoroborates explained the previous lack of success observed in using them as partners for azaborine synthesis.[41] It was therefore anticipated that increasing the loading of $SiCl_4$ would allow the reaction to proceed in the case of heteroaryl-containing trifluoroborates.

Table 2.12: Effect of Pyridine on the Synthesis of 2,1-Borazaronaphthalene

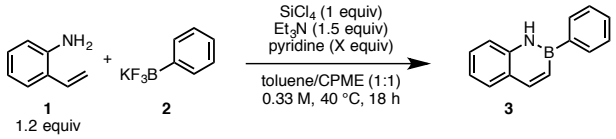

Added Pyridine	Prod : SM[a]
0	Full conversion
0.5	66 : 34
1.0	8 : 92
2.0	**no reaction**

[a]Ratios determined by GCMS

By adjusting the reaction conditions (Table 2.13, in bold), using two equivalents of $SiCl_4$, exchanging cyclopentyl methyl ether (CPME) for acetonitrile, and increasing both the dilution and temperature to improve solubility, the substrate scope was explored. In early condition development, it was observed that some of the heteroaromatic 2,1-borazaronaphthalene cores exhibited poor solubility, most probably because of the high tendency toward π-stacking in extended aromatic systems.[42] To mitigate this, substitutions off the styrenyl nitrogen helped facilitate both the reaction progress and purification by increasing the solubility of the resulting compounds. Upon reaction completion, products could be isolated by initial filtration of solid byproducts followed by column

chromatography to afford cyclized 2,1-borazaronaphthalenes. With this viable set of conditions to isolate products, we started investigating the scope for the *N*-benzyl-2-aminostyrene precursor.

Table 2.13: Nitrogen-containing *B*-Heterocyclic 2,1-Borazaronaphthalenes from *N*-Benzyl-2-aminostyrene

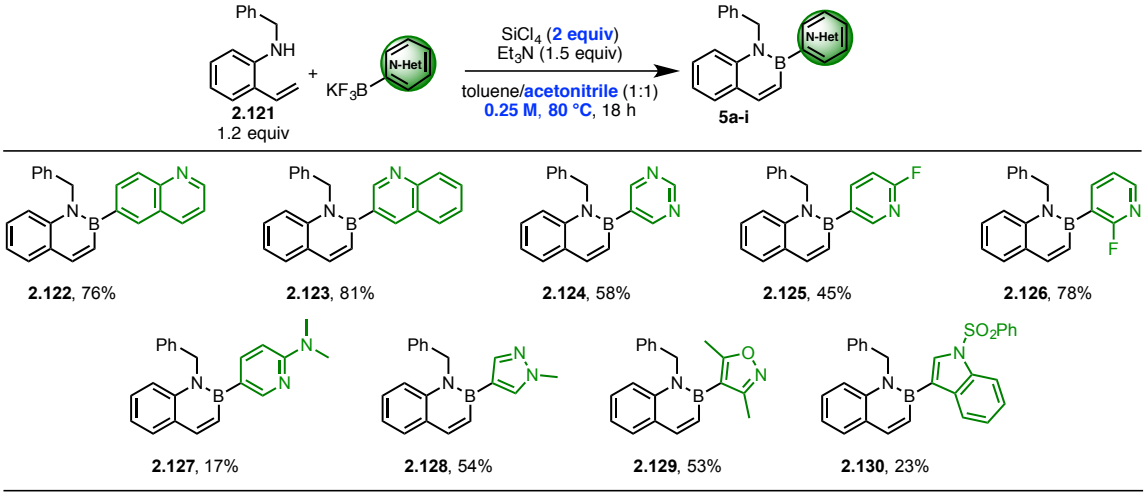

Under these conditions, quinolinyl- (**2.122, 2.123**), pyrimidinyl- (**2.124**) and substituted pyridinyl- (**2.125-2.127**) trifluoroborates were all tolerated in the cyclization process, as well as pyrazolyl- (**2.128**), isoxazolyl- (**2.129**), and indolyl- (**2.130**) derivatives. It was observed that the substitution pattern of pyridine had an effect on yield (**2.125** compared to **2.126**), presumably caused by a combination of electronic effects.

Various other *N*-substituted 2-aminostyrenes could also be used in the annulation (Table 2.14). *N*-Methylated 2,1-borazaronaphthalenes could be synthesized (**2.131-2.139**), but were consistently lower yielding compared to *N*-benzyl systems. Examples that had substituents more likely to disrupt π-π interactions more effectively, such as morpholine (**2.136**) or *N*-methylated pyrazole

(**2.139**), demonstrated higher product isolation. As previously mentioned, there was a consistent effect of the substitution pattern off of pyridine when comparing **2.134** and **2.135** to the corresponding benzylated compounds **2.125** and **2.126**. Isoquinoline variants (**2.133, 2.146**) could also be formed in modest yield using various *N*-alkylated 2-aminostyrene partners. Other substituents tolerated off of the styrenyl nitrogen included 4-*t*-Bu-phenyl (**2.141**), allyl (**2.142**), arylated alkyl (**2.144-2.146**) as well as unsubstituted N-H (**2.143**).

Table 2.14: 2,1-Borazaronaphthalene Annulation with Nitrogen-modified 2-Aminostyrene

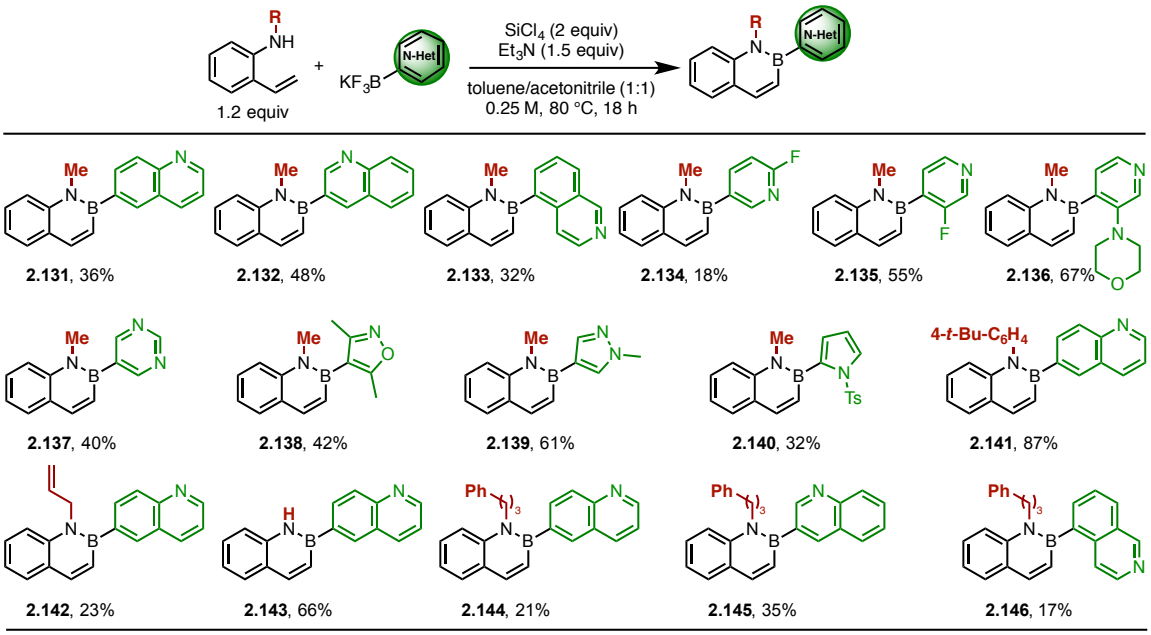

In addition, pre-installed functional groups could be employed on the aminostyrene to develop more elaborated cores (Table 2.15). Fluorinated motifs (**2.147-2.149**), including trifluoromethyl (**2.147**) and trifluoromethyl ether (**2.148**) were tolerated, as well as isopropyl (**2.150**) and nitrile (**2.151**) substituents. Typically those substrates incorporating substituents with more sp^3 character

tended to be isolated in higher yield, continuing to suggest the influence of π interactions on the effectiveness of the reaction or isolation process. Aminopyridyl styrenes, similar to those previously reported,[40] were also amenable to these conditions (**2.152-2.155**).

Table 2.15: Substituted 2-Aminostyrene Derivatives for *B*-Heterocyclic 2,1-Borazaronaphthalenes

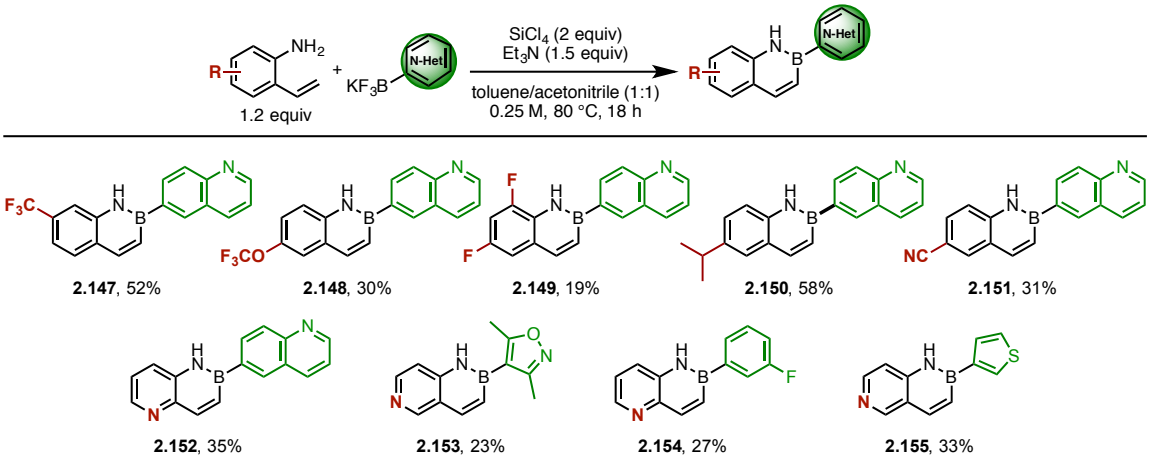

These modified reaction conditions offer a significant increase in the substrate group tolerability for the 2,1-borazaronaphthalene annulation of various *o*-aminostyrenes and organotrifluoroborates. The ability to access nitrogen-containing substructures provides greater viability for this class of isosteres, enabling the incorporation of more bio-relevant functional groups. Considering that the conditions were not optimized for each individual substrate, the capacity to access such diversity affords a reliable method to gain rapid entry to versatile 2,1-borazaronaphthalene compounds that can continue to propagate the value of this class of isosteres.

2.5 – Conclusions

An emphasis on developing reliable, robust synthetic strategies to provide access to azaborine cores is fundamental to their potential application. In developing these methods to access core scaffolds rapidly for the 1,3,2-benzodiazaborole, azaborininones and nitrogen-containing 2,1-borazaronaphthalene, the barrier is lowered to access these classes of molecules for functional uses. Computational evaluations suggest that aromaticity calculations (NICS) provide a consistent method to analyze azaborine classes for a better understanding of their structural composition and isosteric viability and have been further demonstrated to have viable correlation to experimental data. Through these studies, it was observed that the boron substitution is important to the stability of the systems, with *B*-aryl systems found to be consistently more stable. It is important to note that many of these substructures, even though quite simple, have all-carbon isosteres that would be difficult to access, speaking volumes about the ability of the method described to allow access to new chemical space.

2.6 – Experimental Section

General considerations: All reactions were carried out under an inert atmosphere of nitrogen or argon in oven-dried glassware, unless otherwise noted. Toluene and cyclopentyl methyl ether (CPME) were dried using a J. C. Meyer solvent system. MeCN was purchased dry and used as received. Et_3N was distilled prior to use and stored over activated molecular sieves. *O*-Phenylenediamine (99%) was recrystallized from toluene. All other reagents were purchased commercially and

used as received, unless otherwise noted. Standard flash chromatography procedures were followed using 32-63 μm silica gel. Column chromatography was performed by Combiflash(R) using RediSep Rf Gold Normal-Phase Silica(R) columns or Alumina Basic columns. Melting points (°C) are uncorrected. HRMS data (ESI-, EI- or CI-TOF) were recorded using CH_2Cl_2, MeCN or MeOH as the solvent. IR spectra were recorded using FTIR-ATR of the neat oil or solid products. NMR spectra (^1H, ^{13}C $\{^1H\}$, ^{11}B, ^{19}F $\{^1H\}$) were performed at 298 K. ^1H (500.4 MHz) and ^{13}C $\{^1H\}$ (125.8 MHz) NMR chemical shifts are reported relative to internal TMS (δ = 0.00 ppm) or to residual protiated solvent. Any observed splitting in the ^{13}C $\{^1H\}$ NMR spectra, is due to ^{13}C-^{19}F coupling. ^{11}B (128.4 MHz) and ^{19}F $\{^1H\}$ NMR (470.8 MHz) chemical shifts were referenced to external BF_3•Et_2O (0.0 ppm) and $CFCl_3$ (0.0 ppm), respectively. Data are presented as follows: chemical shift (ppm), multiplicity (s = singlet, d = doublet, t = triplet, q = quartet, sept = septet, m = multiplet, br = broad), coupling constant *J* (Hz) and integration.

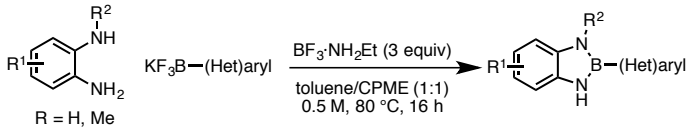

General procedure for synthesis of aryl 1,3,2-benzodiazaboroles (2.5-2.30). Diamine (1 equiv, 1 mmol), organotrifluoroborate (1 equiv, 1 mmol), and BF_3·NH_2Et (3 equiv, 3 mmol) were added to an oven-dried Biotage microwave vial with a stir bar. The vial was sealed with a cap, which was lined with a disposable Teflon septum, and the reaction vessel was subsequently evacuated and purged three times with argon. A 1:1 mixture of CPME (1 mL) and toluene (1 mL) was

added, and the reaction was heated to 80 °C. Upon stirring overnight, the reaction was diluted with 5 mL of saturated $NaHCO_3$ and extracted with EtOAc (2 x 5 mL). The organic phase was washed with brine and dried ($MgSO_4$), before being condensed under vacuum to afford the azaborine.

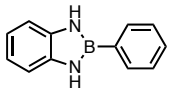

2-Phenyl-2,3-dihydro-1H-1,3,2-benzodiazaborole (**2.5**). 30 mmol scale reaction run in a 200 mL round bottom flask. Obtained as a tan solid (4.949 g, 85%); mp: 198-200 °C; ^{1}H NMR ($CDCl_3$, 500.4 MHz): δ 7.76-7.74 (m, 2H), 7.49 – 7.41 (m, 3H), 7.14 (dd, J = 5.3, 3.4 Hz, 2H), 6.99 (ddd J = 5.6, 3.3 Hz, 0.9 Hz, 2H), 6.79 (s, 2H) ppm; ^{13}C {^{1}H} NMR ($CDCl_3$, 125.8 MHz): δ 136.4, 133.2, 129.9, 128.3, 119.5, 111.3 ppm; ^{11}B NMR (MeCN, 128.4 MHz): δ 28.5 ppm; IR: ν = 3441, 3418, 1421, 746, 699, 597 cm^{-1}; HRMS (ESI+) m/z calc. for $C_{12}H_{12}BN_2$ $[M + H]^+$ 195.1094, found 195.1100.

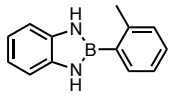

2-(o-Tolyl)-2,3-dihydro-1H-1,3,2-benzodiazaborole (**2.6**). Obtained as a tan solid (173 mg, 83%); mp: 107-110 °C; ^{1}H NMR ($CDCl_3$, 500.4 MHz): δ 7.65 (d, J = 7.3 Hz, 1H), 7.36 (t, J = 7.3 Hz, 1H), 7.28 (d, J = 7.3 Hz, 2H), 716 (dd, J = 5.6, 3.4 Hz, 2H), 7.02 (dd, J = 5.6, 3.4 Hz, 2H), 6.73 (s, 2H), 2.59 (s, 3H) ppm; ^{13}C {^{1}H} NMR ($CDCl_3$, 125.8 MHz): δ 142.0, 136.2, 134.4, 130.0, 129.6, 125.4, 119.5, 111.2, 23.1 ppm; ^{11}B

NMR (MeCN, 128.4 MHz): δ 28.6. IR: ν = 3457, 3423, 1605, 1416, 1351, 740, 612 cm^{-1}; HRMS (CI) m/z calc. for $C_{13}H_{14}BN_2$ $[M + H]^+$ 209.1250, found 209.1242.

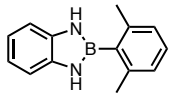

2-(2,6-Dimethylphenyl)-2,3-dihydro-1H-1,3,2-benzodiazaborole (**2.7**). Obtained as a tan solid (186 mg, 84%); mp: 124-126 °C; ^1H NMR ($CDCl_3$, 500.4 MHz): δ 7.24 (t, *J* = 7.7 Hz, 1H), 7.15 (dd, 5.4, 3.6 Hz, 2H), 7.08 (d, *J* = 7.7 Hz, 2H), 7.01 (dd, *J* = 5.4, 3.4 Hz, 2H), 6.54 (s, 2H), 2.33 (s, 6H) ppm; ^{13}C $\{^1H\}$ NMR ($CDCl_3$, 125.8 MHz): δ 141.8, 136.2, 128.9, 126.4, 119.3, 111.2, 23,2 ppm; ^{11}B NMR (MeCN, 128.4 MHz): δ 29.5 ppm; IR: ν = 3421, 3054, 2925, 1440, 1352, 739, 617 cm^{-1}; HRMS (CI) m/z calc. for $C_{14}H_{14}BN_2$ $[M - H]^-$ 221.1250, found 221.1257.

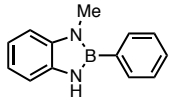

1-Methyl-2-phenyl-2,3-dihydro-1H-1,3,2-benzodiazaborole (**2.8**). 3 mmol scale reaction run in a 20 mL microwave vial. Obtained as a dark red solid (171 mg, 82%); mp: 84-88 °C; ^1H NMR ($CDCl_3$, 500.4 MHz): δ 7.74-7.70 (m, 2H), 7.47-7.44 (m, 3H), 7.18-7.07 (m, 3H), 7.03 (td, *J* = 7.6, 1.3 Hz, 1H), 6.66 (s, 1H), 3.52 (s, 3H) ppm; ^{13}C $\{^1H\}$ NMR ($CDCl_3$, 125.8 MHz): δ 139.1, 135.9, 133.8, 129.2, 128.2, 119.3, 119.3, 110.1, 106.8, 30.0 ppm; ^{11}B NMR (MeCN, 128.4 MHz): δ 28.8 ppm; IR: ν = 3431, 3054, 3045, 1409, 736, 703, 587 cm^{-1}; HRMS (CI) m/z calc. for $C_{13}H_{13}BN_2$ $[M]^+$ 208.1172, found 208.1172.

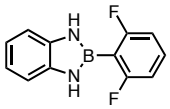

2-(2,6-Difluorophenyl)-2,3-dihydro-1H-1,3,2-benzodiazaborole (**2.9**). Product further purified *via* a plug of silica with hexane/EtOAc (4:1) as eluent. Obtained as a tan solid (154 mg, 67%); mp: 148-151 °C; ^{1}H NMR (DMSO-d_6, 500.4 MHz): δ 9.01 (s, 2H), 7.54 (tt, J = 8.2, 6.9 Hz, 1H), 7.18 (dd, J = 5.7, 3.3 Hz, 2H), 7.16 – 7.12 (m, 2H), 6.96 – 6.74 (m, 2H) ppm; ^{13}C {^{1}H} NMR ($CDCl_3$, 125.8 MHz): δ 167.0 (dd, J = 247.5, 13.4 Hz), 135.7, 132.2 (t, J = 11.3 Hz), 119.7, 111.5, 111.4 (dd, J = 23.1, 5.6 Hz) ppm; ^{19}F {^{1}H} NMR ($CDCl_3$, 282.4 MHz): δ -103.0 ppm; ^{11}B NMR (MeCN, 128.4 MHz): δ 24.6 ppm; IR: ν = 3450, 3054, 1624, 1453, 979, 779, 735, 590 cm^{-1}; HRMS (CI) m/z calc. for $C_{12}H_9BN_2F_2$ $[M]^+$ 230.0827, found 230.0827.

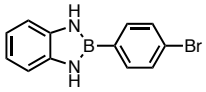

2-(4-Bromophenyl)-2,3-dihydro-1H-1,3,2-benzodiazaborole (**2.10**). Obtained as a tan solid (184 mg, 68 %), mp: 216-218 °C; ^{1}H NMR ($CDCl_3$, 500.4 MHz): δ 7.61-7.54 (m, 4H), 7.12 (dd, J = 5.4, 3.3 Hz, 2H), 6.99 (dd, J = 5.3, 4.4 Hz, 2H), 6.76 (s, 2H) ppm; ^{13}C {^{1}H} NMR ($CDCl_3$, 125.8 MHz): δ 136.3, 134.8, 131.5, 124.5, 119.7, 111.4 ppm; ^{11}B NMR (MeCN, 128.4 MHz): δ 28.2 ppm; IR: ν = 3418, 1584, 1427, 1275, 751, 599 cm^{-1}; HRMS (CI) m/z calc. for $C_{12}H_{10}BN_2Br$ $[M]^+$ 272.0120, found 272.0133.

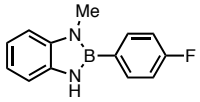

2-(4-Fluorophenyl)-1-methyl-2,3-dihydro-1H-1,3,2-benzodiazaborole (**2.11**). Obtained as a brown solid (185 mg, 82%); mp: 114-115 °C; ^{1}H NMR ($CDCl_3$, 500.4 MHz): δ 7.68 (dd, J = 8.8, 5.7 Hz, 2H), 7.19-7.12 (m, 2H), 7.12-7.03 (m, 3H), 7.00 (t, J = 6.8 Hz, 1H), 6.61 (s, 1H), 3.48 (s, 3H) ppm; ^{13}C {^{1}H} NMR ($CDCl_3$, 125.8 MHz): δ 163.8 (d, J = 248.4 Hz), 139.0, 135.8, 135.6 (d, J = 7.9 Hz), 119.4, 119.4, 115.4 (d, J = 19.9 Hz), 110.9, 108.9, 30.0 ppm; ^{19}F {^{1}H} NMR ($CDCl_3$, 282.4 MHz): δ -112.5 ppm; ^{11}B NMR (MeCN, 128.4 MHz): δ 28.0 ppm; IR: ν = 3437, 3054, 2910, 1596, 1397, 1217, 830, 738, 576 cm^{-1}; HRMS (CI) m/z calc. for $C_{13}H_{12}BN_2F$ $[M]^+$ 226.1078, found 226.1080.

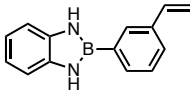

2-(3-Vinylphenyl)-2,3-dihydro-1H-1,3,2-benzodiazaborole (**2.12**). Obtained as a light brown solid (162 mg, 73%); mp: 119-121 °C; ^{1}H NMR (DMSO-d_6, 500.4 MHz): δ 9.16 (s, 2H), 8.05 (s, 1H), 7.80 (d, J = 7.2 Hz, 1H), 7.48 (d, J = 7.7 Hz, 1H), 7.40 (t, J = 7.5 Hz, 1H), 7.09 – 7.02 (m, 2H), 6.84 – 6.81 (m, 2H), 6.77 (dd, J = 17.5, 10.8 Hz, 1H), 5.92 (d, J = 17.6 Hz, 1H), 5.31 (d, J = 10.9 Hz, 1H) ppm; ^{13}C {^{1}H} NMR (DMSO-d_6, 125.8 MHz): δ 137.1, 136.9, 136.5, 133.0, 131.1, 128.2, 127.3, 118.3, 114.1, 110.8 ppm; ^{11}B NMR (MeCN, 128.4 MHz): δ 28.5 ppm; IR: ν = 3445, 3425, 3054, 1353,

904, 746, 688, 564 cm^{-1}; HRMS (CI) m/z calc. for $C_{14}H_{14}BN_2$ $[M + H]^+$ 221.1250, found 221.1244.

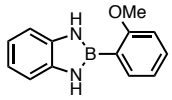

2-(2-Methoxyphenyl)-2,3-dihydro-1H-1,3,2-benzodiazaborole (**2.13**). Obtained as a tan solid (175 mg, 78%); mp: 123-124 °C; ^{1}H NMR (DMSO-d_6, 500.4 MHz): δ 8.77 (s, 2H), 7.86 (d, J = 7.2 Hz, 1H), 7.39 (t, J = 7.7 Hz, 1H), 7.11 (dd, J = 5.7, 3.3 Hz, 2H), 7.05 – 6.95 (m, 2H), 6.81 (dd, J = 5.8, 3.2 Hz, 2H), 3.89 (s, 3H) ppm; ^{13}C {^{1}H} NMR (DMSO-d_6, 125.8 MHz): δ 163.2, 136.9, 135.3, 131.0, 120.1, 118.0, 110.7, 110.4, 55.0 ppm; ^{11}B NMR (MeCN, 128.4 MHz): δ 27.4 ppm; IR: ν = 3460, 3423, 1598, 1418, 1243, 743, 619 cm^{-1}; HRMS (CI) m/z calc. for $C_{13}H_{14}BN_2O$ $[M+H]^+$ 225.1199, found 225.1201.

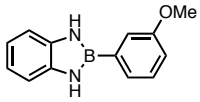

2-(3-Methoxyphenyl)-2,3-dihydro-1H-1,3,2-benzodiazaborole (**2.14**). Product further purified *via* recrystallization from boiling toluene. Obtained as a brown solid (139 mg, 62%); mp: 150-152 °C; ^{1}H NMR (DMSO-d_6, 500.4 MHz): 9.11 (s, 2H), 7.51 (s, 1H), 7.47 (d, J = 7.1 Hz, 1H), 7.33 (td, J = 7.7, 2.1 Hz, 1H), 7.06 (dt, J = 5.6, 2.6 Hz, 2H), 6.96 (d, J = 8.1 Hz, 1H), 6.82 (dt, J = 5.6, 2.7 Hz, 2H), 3.81 (s, 3H) ppm; ^{13}C {^{1}H} NMR (DMSO-d_6, 125.8 MHz): δ 156.9, 137.1, 129.0, 125.6, 118.5, 118.3, 115.0, 110.7,

54.9 ppm; ^{11}B NMR (MeCN, 128.4 MHz): δ 28.4 ppm; IR: ν = 3414, 1425, 750, 698, 634 cm^{-1}; HRMS (CI) m/z calc. for $C_{13}H_{14}BN_2O$ $[M+H]^+$ 225.1199, found 225.1201.

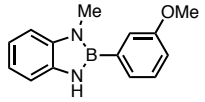

2-(3-Methoxyphenyl)-1-methyl-2,3-dihydro-1H-1,3,2-benzodiazaborole (**2.15**). Obtained as a dark brown solid (191 mg, 80%); mp: 86-88 °C; ^{1}H NMR ($CDCl_3$, 500.4 MHz): δ 7.40 (t, J = 7.4 Hz, 1H), 7.30 (d, J = 7.4 Hz, 1H), 7.25 (s, 1H), 7.14-7.04 (m, 3H), 7.03-6.97 (m, 2H), 6.66 (s, 1H), 3.87 (s, 3H), 3.51 (s, 3H) ppm; ^{13}C {^{1}H} NMR ($CDCl_3$, 125.8 MHz): δ 159.4, 139.0, 135.8, 129.5, 126.1, 119.32, 199.31, 119.2, 114.5, 110.9, 108.9, 55.3, 30.0 ppm; ^{11}B NMR (MeCN, 128.4 MHz): δ 28.4 ppm; IR: ν = 3427, 1575, 1402, 1254, 749, 702, 608 cm^{-1}; HRMS (CI) m/z calc. for $C_{14}H_{16}BN_2O$ $[M +H]^+$ 239.1356, found 239.1359.

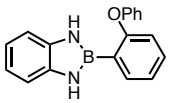

2-(2-Phenoxyphenyl)-2,3-dihydro-1H-1,3,2-benzodiazaborole (**2.16**). Product further purified *via* a plug of silica with hexane/EtOAc (4:1) as eluent. Obtained as a brown solid (178 mg, 62%); mp: 81-83 °C; ^{1}H NMR ($CDCl_3$, 500.4 MHz): δ 7.79-7.75 (m, 1H), 7.41-7.32 (m, 3H), 7.17 (dt, J = 11.4, 7.3 Hz, 2H), 7.12-7.07 (m, 4H), 7.03 (s, 2H), 6.96 (d, J = 3.2 Hz, 1H), 6.95 (d, J = 3.3 Hz, 1H), 6.89-6.86 (m, 1H) ppm; ^{13}C {^{1}H} NMR ($CDCl_3$, 125.8 MHz): δ 161.8, 157.2, 136.3, 135.1, 131.4, 130.1, 123.8, 123.3, 119.6, 119.4, 118.1, 111.2 ppm; ^{11}B NMR ($CDCl_3$, 128.4 MHz): δ 27.1 ppm; IR: ν =

3431, 3186, 2946, 2865, 1458, 1274, 738, 575 cm^{-1}; HRMS (CI) m/z calc. for $C_{18}H_{15}BN_2ONa$ $[M + Na]^+$ 309.1175, found 309.1181.

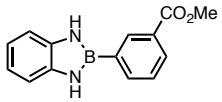

2-(4-(Methoxycarbonyl)phenyl)-2,3-dihydro-1H-1,3,2-benzodiazaborole (**2.17**). Obtained as a tan solid (130 mg, 51%); mp: 171-172 °C; ^1H NMR (DMSO-d_6, 500.4 MHz): δ 9.33 (s, 2H), 8.54 (s, 1H), 8.16 (d, J = 7.9 Hz, 1H), 7.99 (dt, J = 8.1, 1.7 Hz, 1H), 7.58 (td, J = 7.6, 1.7 Hz, 1H), 7.16 – 7.02 (m, 2H), 6.83 (dt, J = 5.6, 2.5 Hz, 2H), 3.90 (s, 3H) ppm; ^{13}C {^1H} NMR (DMSO-d_6, 125.8 MHz): δ 166.6, 138.1, 137.1, 134.0, 130.0, 129.3, 128.3, 118.4, 111.0, 52.1 ppm; ^{11}B NMR (MeCN, 128.4 MHz): δ 28.0 ppm; IR: ν = 3424, 3404, 2950, 1701, 1431, 1282, 1263, 741, 690 cm^{-1}; HRMS (CI) m/z calc. for $C_{14}H_{14}BN_2O_2$ $[M + H]^+$ 253.1148, found 253.1137.

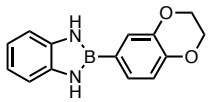

2-(2,3-Dihydrobenzo[b][1,4]dioxin-6-yl)-2,3-dihydro-1H-1,3,2-benzodiazaborole (**2.18**). Obtained as a tan solid (191 mg, 76%); mp: 199-201 °C; ^1H NMR ($CDCl_3$, 500.4 MHz): δ 7.24 -7.20 (m, 2H), 7.10 (dd, J =5.3, 3.4 Hz, 2H), 6.98-6.93 (m, 3H), 6.68 (s, 2H), 4.30 (s, 4H) ppm; ^{13}C {^1H} NMR ($CDCl_3$, 125.8 MHz): δ 145.3, 143.6, 136.5, 126.5, 121.9, 119.4, 117.4, 111.1, 64.7, 64.5 ppm; ^{11}B NMR (MeCN, 128.4 MHz): δ 28.5 ppm; IR: ν = 3446, 3416, 2995, 2940, 2875, 1575, 1245, 1126,

745, 547cm^{-1}; HRMS (CI) m/z calc. for $C_{14}H_{14}BN_2O_2$ [M + H]$^+$ 253.1148, found 253.1157.

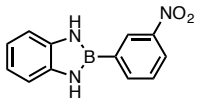

2-(3-Nitrophenyl)-2,3-dihydro-1H-1,3,2-benzodiazaborole (**2.19**). Product further purified *via* a plug of silica with hexane/EtOAc (4:1) as eluent. Obtained as a tan solid (62 mg, 26%); mp: 210-211 °C; ^{1}H NMR (DMSO-d_6, 500.4 MHz): δ 9.46 (s, 2H), 8.79 (s, 1H), 8.32 (d, J = 7.1 Hz, 1H), 8.25 (d, J = 7.7 Hz, 1H), 7.74 (t, J = 7.7 Hz, 1H), 7.09 (dd, J = 5.8, 3.1 Hz, 2H), 6.86 (dt, J = 5.7, 3.1 Hz, 2H) ppm; ^{13}C {^{1}H} NMR (DMSO-d_6, 125.8 MHz): δ 147.6, 139.7, 136.9, 129.5, 127.5, 123.9, 118.7, 111.1 ppm; ^{11}B NMR (MeCN, 128.4 MHz): δ 27.7 ppm; IR: ν = 3397, 1620, 1429, 1346, 1270, 737, 687 cm^{-1}; HRMS (CI) m/z calc. for $C_{12}H_{11}BN_3O_2$ [M+H]$^+$ 240.0944, found 240.0937.

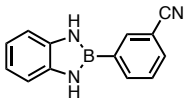

2-(3-Cyanophenyl)-2,3-dihydro-1H-1,3,2-benzodiazaborole (**2.20**). Obtained as a tan solid (53 mg, 24%); mp: 195-196 °C; ^{1}H NMR ($CDCl_3$, 500.4 MHz): δ 8.01 (s, 1H), 7.94 (dt, J = 7.5, 1.3 Hz, 1H), 7.71 (dt, J = 7.8, 1.5 Hz, 1H), 7.54 (td, J = 7.6, 0.7 Hz, 1H), 7.19 – 7.13 (m, 2H), 7.01 (dd, J = 5.7, 3.1 Hz, 2H), 6.86 (s, 2H) ppm; ^{13}C {^{1}H} NMR ($CDCl_3$, 125.8 MHz): δ 137.2, 136.7, 136.1, 133.0, 129.0, 120.1, 119.1, 112.7, 111.7 ppm; ^{11}B NMR (MeCN, 128.4 MHz): δ 27.6 ppm; IR: ν = 3415, 3378, 3065,

2232, 1434, 1273, 745, 693, 561 cm^{-1}; HRMS (CI) m/z calc. for $C_{13}H_{11}BN_3$ $[M+H]^+$ 220.1046, found 220.1048.

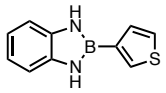

2-(Thiophen-3-yl)-2,3-dihydro-1H-1,3,2-benzodiazaborole (**2.21**). Obtained as a tan solid (128 mg, 64%); mp: 221-222 °C; ^1H NMR ($CDCl_3$, 500.4 MHz): δ 7.75 – 7.73 (m, 1H), 7.45 (dd, J = 4.7, 2.6 Hz, 1H), 7.42 (d, J = 4.6 Hz, 1H), 7.11 (dd, J = 7.5, 3.8 Hz, 2H), 6.97 (dd, J = 5.7, 3.3 Hz, 2H), 6.70 (s, 2H) ppm; ^{13}C $\{^1H\}$ NMR ($CDCl_3$, 125.8 MHz): δ 136.3, 131.9, 131.2, 126.1, 119.5, 111.2 ppm; ^{11}B NMR (MeCN, 128.4 MHz): δ 26.4 ppm; IR: ν = 3427, 1431, 740, 662, 600 cm^{-1}; HRMS (CI) m/z calc. for $C_{10}H_9BN_2S$ $[M]^+$ 200.0580, found 200.0601.

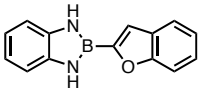

2-(2-Benzofuranyl)-2,3-dihydro-1H-1,3,2-benzodiazaborole (**2.22**). Obtained as a tan solid (132 mg, 57%); mp: 220-222 °C; ^1H NMR ($CDCl_3$, 500.4 MHz): δ 7.66 (d, J = 7.9 Hz, 1H), 7.56 (d, J = 8.2 Hz, 1H), 7.39 – 7.32 (m, 1H), 7.29 – 7.23 (m, 2H), 7.16 (dd, J = 7.4, 3.7 Hz, 2H), 7.01 (dd, J = 5.8, 3.2 Hz, 2H), 6.96 (s, 2H) ppm; ^{13}C $\{^1H\}$ NMR (DMSO-d_6, 125.8 MHz): δ 156.5, 136.7, 128.0, 125.0, 122.7, 121.5, 118.7, 115.5, 111.2, 111.1 ppm; ^{11}B NMR (MeCN, 128.4 MHz): δ 24.8 ppm; IR: ν = 3436, 1569, 1411, 1337, 735, 602 cm^{-1}; HRMS (CI) m/z calc. for $C_{14}H_{12}BN_2O$ $[M+H]^+$ 235.1043, found 235.1053.

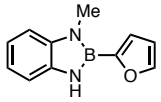

2-(Furan-2-yl)-1-methyl-2,3-dihydro-1H-1,3,2-benzodiazaborole (**2.23**). Product further purified *via* a plug of silica with hexane/EtOAc (4:1) as eluent. Obtained as a brown solid (144 mg, 73%); mp: 73-75 °C; ^{1}H NMR ($CDCl_3$, 500.4 MHz): δ 7.75 (s, 1H), 7.60 (d, J = 1.4 Hz, 1H), 7.06-7.03 (m, 3H) 6.99 (dt, J =7.4, 1.4 Hz, 1H), 6.66 (s, 1H), 6.57 (s, 1H) 3.49 (s, 3H) ppm; ^{13}C {^{1}H} NMR ($CDCl_3$, 125.8 MHz): δ 147.4, 143.2, 138.9, 119.2, 119.1, 113.2, 110.8, 108.6, 30.0 ppm; ^{11}B NMR (MeCN, 128.4 MHz): δ 26.4 ppm; IR: ν = 3431, 3054, 2947, 1478, 1345, 733, 541 cm^{-1}; HRMS (CI) m/z calc. for $C_{11}H_{11}BN_2O$ $[M]^+$ 198.0964, found 198.0965.

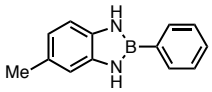

5-Methyl-2-phenyl-2,3-dihydro-1H-1,3,2-benzodiazaborole (**2.25**). Obtained as a tan solid (164 mg, 79%); mp: 212-214 °C; ^{1}H NMR ($CDCl_3$ with 1% TMS, 500.4 MHz): δ 7.74-7.71 (m, 2H), 7.44-7.41 (m, 3H), 7.00 (dd, J = 7.9, 3.4 Hz, 1H), 6.94 (s, 1H), 6.79 (d, J = 7.9 Hz, 1H), 6.69 (s, 2H), 2.40 (d, J = 3.4 Hz, 3H) ppm; ^{13}C {^{1}H} NMR ($CDCl_3$ with 1% TMS, 125.8 MHz,): δ 136.6, 134.2, 133.1, 129.8, 129.0, 128.3, 120.1, 112.0, 110.8, 21.5 ppm; ^{11}B NMR (MeCN, 128.4 MHz): δ 28.6 ppm; IR: ν = 3440, 3054, 2915, 1603, 1419, 805, 695, 569 cm^{-1}; HRMS (CI) m/z calc. for $C_{13}H_{14}BN_2$ $[M+H]^+$ 209.1250, found 209.1247.

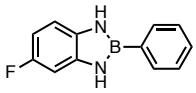

5-Fluoro-2-phenyl-2,3-dihydro-1H-1,3,2-benzodiazaborole (**2.26**). Obtained as a brown solid (160 mg, 76%); mp: 186-188 °C; ^{1}H NMR ($CDCl_3$, 500.4 MHz): δ 7.73-7.70 (m, 2H), 7.47-7.41 (m, 3H), 6.98 (dd, J = 8.4, 4.9 Hz, 1H), 6.85 (dd, J = 9.3, 2.5 Hz, 1H), 6.78 (s, 1H), 6.71 – 6.66 (m, 2H) ppm; ^{13}C {^{1}H} NMR ($CDCl_3$, 125.8 MHz): δ 157.9 (d, J = 233.9 Hz), 136.9 (d, J = 11.9 Hz), 133.1, 132.6, 130.0, 128.4, 110.7 (d, J = 9.9 Hz), 105.8 (d, J = 24.1 Hz), 99.0 (d, J = 26.8 Hz) ppm; ^{19}F {^{1}H} NMR ($CDCl_3$, 282.4 MHz): δ -124.9 ppm; ^{11}B NMR (MeCN, 128.4 MHz): δ 29.2 ppm; IR: ν = 3441, 1424, 1365, 1255, 1139, 700, 587 cm^{-1}; HRMS (CI) m/z calc. for $C_{12}H_{11}BN_2F$ $[M + H]^+$ 213.0999, found 213.1000.

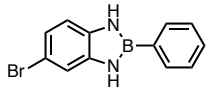

5-Bromo-2-phenyl-2,3-dihydro-1H-1,3,2-benzodiazaborole (**2.27**). 8 mmol scale reaction run in a 20 mL microwave vial. Obtained as a brown solid. (1.64 g, 76%); mp: 157-159 °C; ^{1}H NMR ($CDCl_3$, 500.4 MHz): δ 7.77 – 7.63 (m, 2H), 7.45 (d, J = 6.0 Hz, 3H), 7.24 (s, 1H), 7.12 – 7.05 (m, 1H), 6.97 (d, J = 7.9 Hz, 1H), 6.77 (s, 2H) ppm; ^{13}C {^{1}H} NMR ($CDCl_3$, 125.8 MHz): δ 137.8, 135.5, 133.2, 130.2, 128.4, 122.2, 114.3, 112.2, 112.0 ppm; ^{11}B NMR (MeCN, 128.4 MHz): δ 28.8 ppm; IR: ν = 3435, 1599, 1420, 803, 697, 566 cm^{-1}; HRMS (CI) m/z calc. for $C_{12}H_{10}BBrN_2$ $[M]^+$ 272.0120, found 272.0127.

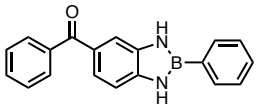

5-Phenylcarbonyl-2-phenyl-2,3-dihydro-1H-1,3,2-benzodiazaborole (**2.28**). 8 mmol scale reaction run in a 20 mL microwave vial. Product further purified *via* recrystallization from boiling toluene. Obtained as a burnt-orange solid (1.31 g, 55%); mp: 186-187 °C; ^{1}H NMR (DMSO-d_6, 500.4 MHz): δ 9.68 (s, 1H), 9.44 (s, 1H), 7.96 – 7.85 (m, 2H), 7.74 – 7.66 (m, 2H), 7.66 – 7.59 (m, 1H), 7.58 – 7.51 (m, 3H), 7.45 (t, J = 4.6 Hz, 3H), 7.39 (dd, J = 8.1, 2.5 Hz, 1H), 7.19 (dd, J = 8.4, 2.8 Hz, 1H) ppm; ^{13}C {^{1}H} NMR (DMSO-d_6, 125.8 MHz): δ 195.4, 142.0, 139.0, 137.0, 133.5, 131.3, 129.8, 128.2, 128.0, 127.5, 122.7, 112.6, 110.3 ppm; ^{11}B NMR (MeCN, 128.4 MHz): δ 30.2 ppm; IR: ν = 3460, 3372, 1603, 1428, 1287, 707, 630 cm^{-1}; HRMS (CI) m/z calc. for $C_{19}H_{16}BN_2O$ $[M+H]^+$ 299.1356, found 299.1348.

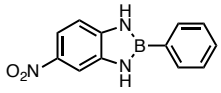

5-Nitro-2-phenyl-2,3-dihydro-1H-1,3,2-benzodiazaborole (**2.29**). Product further purified *via* recrystallization from boiling toluene. Obtained as an orange solid (148 mg, 62%); mp: 195-196 °C; ^{1}H NMR (DMSO-d_6, 500.4 MHz): δ 9.97 (s, 1H), 9.70 (s, 1H), 7.94 – 7.86 (m, 4H), 7.50 – 7.45 (m, 3H), 7.20 (d, J = 8.5 Hz, 1H) ppm; ^{13}C {^{1}H} NMR (DMSO-d_6, 125.8 MHz): δ 143.7, 139.8, 137.1, 133.6, 130.2, 128.1, 116.0, 110.1, 105.9 ppm; ^{11}B NMR (MeCN, 128.4 MHz): δ 31.0 ppm; IR: ν = 3435, 3415,

3380, 1610, 1435, 1303, 695, 631 cm^{-1}; HRMS (ESI-) m/z calc. for $C_{12}H_9BN_3O_2$ $[M-H]^-$ 238.0788, found 238.0788.

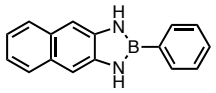

2-Phenyl-2,3-dihydro-1H-1,3,2-naphthodiazaborole (**2.30**). Product further purified *via* recrystallization from boiling toluene. Obtained as a tan solid (33.5 mg, 14%); mp: >250 °C; ^1H NMR (DMSO-d_6, 500.4 MHz): δ 9.30 (s, 2H), 8.00 – 7.95 (m, 2H), 7.77 (dd, J = 6.6, 3.3 Hz, 2H), 7.48 – 7.44 (m, 3H), 7.42 (s, 2H), 7.22 (dd, J = 6.9, 3.1 Hz, 2H) ppm; ^{13}C $\{^1H\}$ NMR (DMSO-d_6, 125.8 MHz): δ 139.0, 133.7, 129.9, 128.6, 128.0, 126.4, 122.0, 105.4 ppm; ^{11}B NMR (MeCN, 128.4 MHz): δ 30.8 ppm; IR: ν = 3429, 1435, 862, 695, 588 cm^{-1}; HRMS (CI) m/z calc. for $C_{16}H_{14}BN_2$ $[M+H]^+$ 245.1250, found 245.1252.

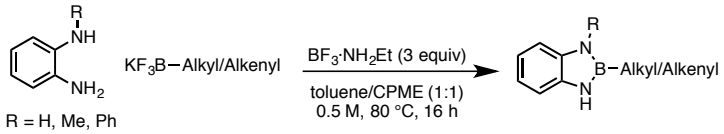

General procedure for synthesis of alkyl and alkenyl 1,3,2-benzodiazaboroles (2.31-2.46). Diamine (1 equiv, 1 mmol), organotrifluoroborate (1 equiv, 1 mmol), and BF_3•NH_2Et (3 equiv, 3 mmol) were added to an oven-dried Biotage microwave vial with stir bar. The vial was sealed with a cap, which was lined with a disposable Teflon septum. The reaction vessel was subsequently evacuated and purged three times with argon. A 1:1 mixture of CPME (1 mL) and toluene (1 mL) was added, and the reaction was heated to 80 °C. Upon stirring overnight, the reaction was diluted with 2 mL of hexane and run though a two inch

silica plug, with 10% EtOAc in hexane as eluent. The reaction was then condensed under vacuum to afford the azaborine compound.

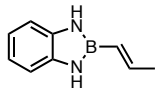

(E)-2-(Prop-1-en-1-yl)-2,3-dihydro-1H-1,3,2-benzodiazaborole (**2.31**). Obtained as a brown solid (110 mg, 70%); mp: 72-74 °C; ^{1}H NMR ($CDCl_3$, 500.4 MHz): δ 7.05 (dd, J = 5.7, 3.3 Hz, 2H), 6.94 (dd, J = 5.8, 3.2 Hz, 2H), 6.60 – 6.33 (m, 3H), 5.90 (d, J = 17.7 Hz, 1H), 1.95 (d, J = 6.4 Hz, 3H) ppm; ^{13}C {^{1}H} NMR ($CDCl_3$, 125.8 MHz): δ 143.8, 136.3, 119.1, 110.9, 22.1 ppm; ^{11}B NMR ($CDCl_3$, 128.4 MHz): δ 27.0 ppm; IR: ν = 3385, 3185, 1500, 1272, 743 cm^{-1}; HRMS (CI) m/z calc. for $C_9H_{12}BN_2$ $[M+H]^+$ 159.1094, found 159.1100.

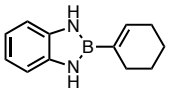

2-(Cyclohex-1-en-1-yl)-2,3-dihydro-1H-1,3,2-benzodiazaborole (**2.32**). Obtained as a brown solid (156 mg, 79%); mp: 123-125 °C; ^{1}H NMR ($CDCl_3$, 500.4 MHz): δ 7.03 (dd, J = 5.6, 3.2 Hz, 2H), 6.92 (dd, J = 5.6, 3.2 Hz, 2H), 6.41 (s, 3H), 2.29-2.25 (m, 2H), 2.21-2.16 (m, 2H), 1.74-1.67 (m, 4H) ppm; ^{13}C {^{1}H} NMR ($CDCl_3$, 125.8 MHz): δ 138.0, 136.3, 119.0, 110.8, 27.3, 26.7, 22.8, 22.4 ppm; ^{11}B NMR ($CDCl_3$, 128.4 MHz): δ 27.9 ppm; IR: ν = 3430, 2923, 2852, 1627, 1431, 738, 594 cm^{-1}; HRMS (CI) m/z calc. for $C_{12}H_{16}BN_2$ $[M + H]^+$ 199.1407, found 199.1411.

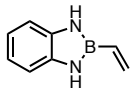

2-Vinyl-2,3-dihydro-1H-1,3,2-benzodiazaborole (**2.33**). Product further purified *via* a plug of silica with hexane/EtOAc (4:1) as eluent. Obtained as a tan solid (97 mg, 68%); mp: 106-108 °C; ^{1}H NMR ($CDCl_3$, 500.4 MHz): δ 7.05 (dt, J = 7.3, 3.6 Hz, 2H), 6.94 (dd, J = 5.7, 3.2 Hz, 2H), 6.52 (s, 2H), 6.31 (dd, J_{trans} = 20.0, J_{cis} = 13.7 Hz, 1H), 6.08 – 5.85 (m, 2H) ppm; ^{13}C {^{1}H} NMR ($CDCl_3$, 125.8 MHz): δ 136.1, 131.8, 119.4, 111.1 ppm; ^{11}B NMR (MeCN, 128.4 MHz): δ 27.5 ppm; IR: ν = 3415, 3054, 1615, 1407, 1270, 954, 750, 631 cm^{-1}; HRMS (CI) m/z calc. for $C_8H_9BN_2$ $[M]^+$ 144.0859, found 144.0849.

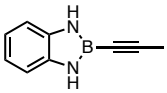

2-(1-Propynyl)-2,3-dihydro-1H-1,3,2-benzodiazaborole (**2.34**). Obtained as a white solid (122 mg, 78%); mp: 130-131 °C; ^{1}H NMR ($CDCl_3$, 500.4 MHz): δ 7.06-7.03 (m, 2H), 6.96 (dd, J = 5.7, 3.2 Hz, 2H), 6.59 (s, 2H), 2.02 (s, 3H) ppm; ^{13}C {^{1}H} NMR ($CDCl_3$, 125.8 MHz): δ 135.5, 119.7, 111.2, 5.0 ppm; ^{11}B NMR (MeCN, 128.4 MHz): δ 20.2 ppm; IR: ν = 3422, 3057, 2204, 1418, 1352, 1266, 729, 624 cm^{-1}; HRMS (CI) m/z calc. for $C_9H_9BN_2$ $[M]^+$ 156.0859, found 156.0844.

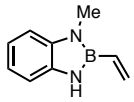

1-Methyl-2-vinyl-2,3-dihydro-1H-1,3,2-benzodiazaborole (**2.35**). Obtained as a dark red oil (136 mg, 86%); ^{1}H NMR ($CDCl_3$, 500.4 MHz): δ 7.05 (d, J = 7.4 Hz, 1H), 7.02-6.99 (m, 2H), 6.96 (dt, J = 7.1, 2.7 Hz, 1H), 6.50 (s, 1H), 6.41 (dd, J = 18.6, 15.5 Hz, 1H), 5.98 (d, J = 18.6 Hz, 2H), 3.40, (s, 3H) ppm; ^{13}C {^{1}H} NMR ($CDCl_3$, 125.8 MHz): δ 135.8, 131.8, 119.2, 119.1, 110.7, 108.5, 29.5 ppm; ^{11}B NMR (MeCN, 128.4 MHz): δ 26.71 ppm; IR: ν = 3428, 3054, 2930, 1614, 1443, 1399, 1010, 733 cm^{-1}; HRMS (CI) m/z calc. for $C_9H_{12}BN_2$ $[M + H]^+$ 159.1094, found 159.1090.

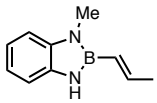

(E)-1-Methyl-2-(prop-1-en-1-yl)-2,3-dihydro-1H-1,3,2-benzodiazaborole (**2.36**). Obtained as a dark brown solid (153 mg, 89%); mp: 81-85 °C; ^{1}H NMR ($CDCl_3$, 500.4 MHz): δ 7.02 (d, J = 7.5 Hz, 1H), 6.99 (d, J = 3.4 Hz, 2H), 6.94 (dd, J = 7.0, 4.3 Hz, 1H), 6.49-6.42 (dd, J = 18.0, 6.0 Hz, 1H), 6.40 (s, 1H), 5.98 (dd, J = 18.0, 1.8 Hz, 1H), 3.37 (s, 3H), 1.96 (dd, J = 6.0, 1.8 Hz, 3H) ppm; ^{13}C {^{1}H} NMR ($CDCl_3$, 125.8 MHz): δ 143.7, 138.9, 136.0, 118.9, 118.8, 110.4, 108.2, 29.4, 22.3 ppm; ^{11}B NMR (MeCN, 128.4 MHz): δ 27.0 ppm; IR: ν = 3424, 2905, 1645, 1412, 1240, 984, 733 cm^{-1}; HRMS (CI) m/z calc. for $C_{10}H_{14}BN_2$ $[M + H]^+$ 173.1250, found 173.1254.

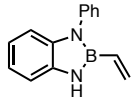

1-Phenyl-2-vinyl-2,3-dihydro-1H-1,3,2-benzodiazaborole (**2.37**). 10 mmol scale reaction run in a 50 mL round bottom flask. Product was further purified *via* combiflash with hexane/EtOAc as solvents. Obtained as a deep red oil (0.93 g, 42%); ^{1}H NMR ($CDCl_3$, 500.4 MHz): δ 7.47 (t, J = 7.1 Hz, 2H), 7.40 – 7.29 (m, 3H), 7.13 (d, J = 7.7 Hz, 1H), 7.07 (d, J = 7.9 Hz, 1H), 7.01 (t, J = 7.4 Hz, 1H), 6.94 (t, J = 7.6 Hz, 1H), 6.70 (s, 1H), 6.25 (dd, J_{trans} = 20.1, J_{cis} = 13.9 Hz, 1H), 5.99 – 5.84 (m, 2H) ppm; ^{13}C {^{1}H} NMR ($CDCl_3$, 125.8 MHz): δ 140.6, 137.8, 135.7, 132.4, 129.4, 126.9, 120.1, 119.3, 111.3, 110.1 ppm; ^{11}B NMR (MeCN, 128.4 MHz): δ 26.7 ppm; IR: ν = 3430, 3054, 1596, 1396, 1269, 736, 696 cm^{-1}; HRMS (CI) m/z calc. for $C_{14}H_{14}BN_2$ $[M+H]^+$ 221.1250, found 221.1254.

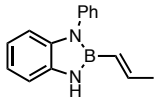

(E)-1-Phenyl-2-(1-propenyl)-2,3-dihydro-1H-1,3,2-benzodiazaborole (**2.38**). Product further purified *via* a plug of silica with hexane/EtOAc (4:1) as eluent. Obtained as a red solid (178 mg, 76%); mp: 61-63 °C; ^{1}H NMR ($CDCl_3$, 500.4 MHz): δ 7.53 – 7.43 (m, 2H), 7.40 – 7.29 (m, 3H), 7.13 – 7.08 (m, 1H), 7.08 – 7.03 (m, 1H), 7.03 – 6.97 (m, 1H), 6.96 – 6.90 (m, 1H), 6.59 (s, 1H), 6.49 – 6.34 (m, 1H), 5.84 (d, J = 18.9 Hz, 1H), 1.91 – 1.84 (m, 3H) ppm; ^{13}C {^{1}H} NMR ($CDCl_3$, 125.8 MHz): δ 144.5, 140.8, 138.0, 136.0, 129.3, 127.0, 125.9, 119.9, 119.1, 111.0, 109.8, 22.2 ppm; ^{11}B

NMR ($CDCl_3$, 128.4 MHz): δ 26.8 ppm; IR: ν = 3387, 1597, 1495, 1315, 746, 691 cm^{-1}; HRMS (CI) m/z calc. for $C_{14}H_{13}BN_2$ $[(M+H)-CH_3]^+$ 220.1172, found 220.1172.

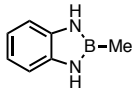

2-Methyl-2,3-dihydro-1H-1,3,2-benzodiazaborole (**2.39**). Product further purified *via* a plug of silica with hexane/EtOAc (4:1) as eluent. Obtained as a tan solid (94 mg, 71%); mp: 67-68 °C; ^1H NMR ($CDCl_3$, 500.4 MHz): δ 7.00 (dd, J = 5.7, 3.2 Hz, 2H), 6.91 (dd, J = 5.7, 3.2 Hz, 2H), 6.30, (s, 2H), 0.63 (s, 3H) ppm; ^{13}C $\{^1H\}$ NMR ($CDCl_3$, 125.8 MHz): δ 136.4, 118.9, 110.5 ppm; ^{11}B NMR (MeCN, 128.4 MHz): δ 30.3 ppm; IR: ν = 3421, 3385, 3054, 2905, 1612, 1263, 739, 600 cm^{-1}; HRMS (CI) m/z calc. for $C_7H_8BN_2$ $[M - H]^-$ 131.0781, found 131.0783.

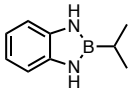

2-Isopropyl-2,3-dihydro-1H-1,3,2-benzodiazaborole (**2.40**). Product further purified *via* a plug of silica with hexane/EtOAc (4:1) as eluent. Obtained as a tan solid (107 mg, 67%); mp: 78-79 °C; ^1H NMR ($CDCl_3$, 500.4 MHz): δ 7.07 – 6.97 (m, 2H), 6.94 – 6.86 (m, 2H), 6.31 (s, 2H), 1.52 (sept, J = 7.4 Hz, 1H), 1.15 (d, J = 6.7 Hz, 6H) ppm; ^{13}C $\{^1H\}$ NMR ($CDCl_3$, 125.8 MHz): δ 136.2, 119.0, 110.8, 20.1 ppm; ^{11}B NMR (MeCN, 128.4 MHz): δ 32.4 ppm; IR: ν = 3432, 3385, 3186, 2945, 1458, 1431, 1274, 738, 576 cm^{-1}; HRMS (CI) m/z calc. for $C_9H_{13}BN_2$ $[M]^+$ 160.1172 found 160.1177.

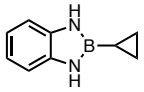

2-Cyclopropyl-2,3-dihydro-1H-1,3,2-benzodiazaborole (**2.41**). Product further purified *via* a plug of silica with hexane/EtOAc (4:1) as eluent. Obtained as a dark brown solid (90 mg, 57%); mp: 64-66 °C; ^{1}H NMR ($CDCl_3$, 500.4 MHz): δ 7.01 – 6.94 (m, 2H), 6.92 – 6.86 (m, 2H), 6.15 (s, 2H), 0.82 (dt, J = 9.4, 3.8 Hz, 2H), 0.50 (dd, J = 6.6, 3.8 Hz, 2H), 0.21 (tt, J = 9.4, 6.3 Hz, 1H) ppm; ^{13}C {^{1}H} NMR ($CDCl_3$, 125.8 MHz): δ 136.3, 118.9, 110.5, 5.6 ppm; ^{11}B NMR (MeCN, 128.4 MHz): δ 31.2 ppm; IR: ν = 3414, 2998, 2925, 1440, 900, 733, 588 cm^{-1}; HRMS (CI) m/z calc. for $C_9H_{11}BN_2$ $[M]^+$ 158.1015, found 158.1008.

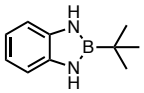

2-(tert-Butyl)-2,3-dihydro-1H-1,3,2-benzodiazaborole (**2.42**). 0.5 mmol scale reaction. Product further purified *via* a plug of silica with hexane/EtOAc (4:1) as eluent. Obtained as a tan solid (63 mg, 72%); mp: 90-91 °C; ^{1}H NMR ($CDCl_3$, 500.4 MHz): δ 7.05 – 6.99 (m, 2H), 6.95 – 6.88 (m, 2H), 6.26 (s, 2H), 1.13 (s, 9H) ppm; ^{13}C {^{1}H} NMR ($CDCl_3$, 125.8 MHz): δ 136.2, 119.1, 110.8, 100.1, 29.1 ppm; ^{11}B NMR ($CDCl_3$, 128.4 MHz): δ 33.08 ppm; IR: ν = 3438, 3390, 3345, 3194, 2939, 1477, 1435, 585, 568 cm^{-1}; HRMS (CI) m/z calc. for $C_{10}H_{15}BN_2$ $[M]^+$ 174.1328, found 174.1328.

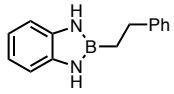

2-Phenethyl-2,3-dihydro-1H-1,3,2-benzodiazaborole (**2.43**). Obtained as a brown solid (198 mg, 89%); mp: 112-114 °C; ^{1}H NMR ($CDCl_3$, 500.4 MHz): δ 7.31 (t, J = 7.5 Hz, 2H), 7.27 (d, J = 1.4 Hz, 2H), 7.21 (t, J = 7.2 Hz, 1H), 7.00 (dd, J = 5.7, 3.2 Hz, 2H), 6.91 (dd, J = 5.7, 3.2 Hz, 2H), 6.29 (s, 2H), 2.90 (t, J = 8.1 Hz, 2H), 1.59 (t, J = 8.1 Hz, 2H) ppm; ^{13}C {^{1}H} NMR ($CDCl_3$, 125.8 MHz): δ 144.4, 136.2, 128.6, 128.1, 125.9, 119.0, 110.7, 32.0 ppm; ^{11}B NMR (MeCN, 128.4 MHz): δ 31.0 ppm; IR: ν = 3433, 2925, 1434, 1267, 732, 593 cm^{-1}; HRMS (CI) m/z calc. for $C_{14}H_{15}BN_2$ $[M]^+$ 222.1328, found 222.1328.

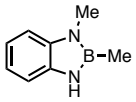

1,2-Dimethyl-2,3-dihydro-1H-1,3,2-benzodiazaborole (**2.44**). 5 mmol scale reaction run in a 20 mL microwave vial. Obtained as a dark brown solid (0.66 g, 90%); mp: 80-82 °C; ^{1}H NMR ($CDCl_3$, 500.4 MHz): δ 7.04 – 6.96 (m, 3H), 6.96 – 6.90 (m, 1H), 6.29 (s, 1H), 3.31 (s, 3H), 0.65 (s, 3H) ppm; ^{13}C {^{1}H} NMR ($CDCl_3$, 125.8 MHz): δ 138.8, 136.1, 118.7, 118.5, 110.1, 107.9, 29.2 ppm; ^{11}B NMR (MeCN, 128.4 MHz): δ 30.3 ppm; IR: ν = 3425, 3054, 2910, 1615, 1413, 1368, 1356, 732, 586 cm^{-1}; HRMS (CI) m/z calc. for $C_8H_{11}BN_2$ $[M]^+$ 146.1051, found 146.1021.

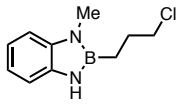

2-(3-Chloropropyl)-1-methyl-2,3-dihydro-1H-1,3,2-benzodiazaborole (**2.45**). Obtained as a brown oil (194 mg, 94%); ^{1}H NMR ($CDCl_3$, 500.4 MHz): δ 7.03 – 6.87 (m, 3H), 6.93 (dt, J = 6.93, 2.5 Hz, 1H), 6.26 (s, 1H), 3.60 (t, J = 6.7 Hz, 2H), 3.31 (s, 3H), 2.08 – 1.98 (m, 2H), 1.36 (t, J = 8.0 Hz, 2H) ppm; ^{13}C {^{1}H} NMR ($CDCl_3$, 125.8 MHz): δ 138.7, 135.9, 119.0, 118.8, 110.4, 108.2, 47.4, 29.3, 29.3 ppm; ^{11}B NMR (MeCN, 128.4 MHz): δ 30.6 ppm; IR: ν = 3327, 2928, 1617, 1307, 1052, 910, 731 cm^{-1}; HRMS (CI) m/z calc. for $C_{10}H_{14}BN_2Cl$ $[M]^+$ 208.0939, found 208.0939.

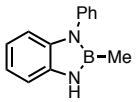

2-Methyl-1-phenyl-2,3-dihydro-1H-1,3,2-benzodiazaborole (**2.46**). 10 mmol scale reaction run in a 50 mL round bottom flask. Product was further purified *via* combiflash with hexane/EtOAc as solvents. Obtained as a deep red oil (0.93 g, 32%); ^{1}H NMR ($CDCl_3$, 500.4 MHz): δ 7.46 (t, J = 7.9 Hz, 2H), 7.37 – 7.28 (m, 3H), 7.06 (dt, J = 10.9, 7.9 Hz, 2H), 6.97 (t, J = 7.7 Hz, 1H), 6.91 (t, J = 7.7 Hz, 1H), 6.48 (s, 1H), 0.64 (s, 3H) ppm; ^{13}C {^{1}H} NMR ($CDCl_3$, 125.8 MHz): δ 141.0, 137.7, 136.0, 129.3, 126.6, 125.7, 119.6, 118.9, 110.7, 109.6 ppm; ^{11}B NMR (MeCN, 128.4 MHz): δ 30.6 ppm; IR: ν = 3433, 1597, 1409, 1356, 1271, 734, 697 cm^{-1}; HRMS (CI) m/z calc. for $C_{13}H_{14}BN_2$ $[M+H]^+$ 209.1250, found 209.1250.

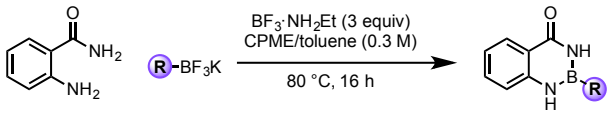

Procedure A – Cyclization of potassium organotrifluoroborates activated with BF_3·$EtNH_2$ to form 1,3,2-benzodiazaborininones. To a microwave vial with a stir bar was added anthranilamide (1.0 equiv) and the appropriate potassium organotrifluoroborate (1.05 equiv) along with BF_3·$EtNH_2$ (3.0 equiv). The reaction vessel was capped and purged with argon, upon which CPME and toluene were added in a 1:1 mixture (3 mL/mmol). The reaction was then heated at 80 °C for 16 h. Upon cooling to rt, the reaction mixture was washed with an aqueous solution of $NaHCO_3$, extracted with EtOAc, and dried ($MgSO_4$), before being concentrated to afford the azaborininone product. If needed, the product was further purified by passage of the crude matter through a short pad of silica, using a 9:1 mixture of hexane/EtOAc as eluent.

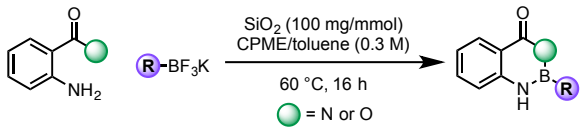

Procedure B-1 – Cyclization of potassium organotrifluoroborates activated with SiO_2 to form azaborininones. To a microwave vial with a stir bar was added anthranilamide or anthranilic acid (1.0 equiv) and potassium organotrifluoroborates (1.05 equiv) along with oven-dried SiO_2 (100 mg/mmol). The reaction vessel was capped and purged with argon, upon which CPME and toluene were added in a 1:1 mixture (3 mL/mmol). The reaction was then heated at 60 °C for 16 h. Upon cooling to rt, the reaction mixture was filtered through a short

pad of Celite and flushed with MeOH, before being concentrated. If needed, the solid was further washed with EtOAc for purification to afford the azaborininone product.

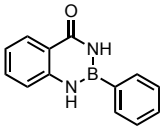

2-Phenyl-1,3,2-benzodiazaborininone (**2.59**). Obtained as a white solid by procedure A (195 mg, 88%, 1.0 mmol scale) and procedure B-1 (113 mg, 51%, 1.0 mmol scale); mp: 206-208 °C; ^{1}H NMR ($CDCl_3$, 500.4 MHz): δ 8.27 (d, *J* = 7.9 Hz, 1H), 7.70 (d, *J* = 7.5 Hz, 2H), 7.61 – 7.44 (m, 5H), 7.18 (t, *J* = 7.6 Hz, 1H), 7.12 (d, *J* = 8.1 Hz, 1H), 6.81 (s, 1H) ppm; ^{13}C {^{1}H} NMR ($CDCl_3$, 125.8 MHz): δ 166.9, 144.4, 134.1, 132.0, 131.2, 129.4, 128.7, 122.1, 119.1, 117.8 ppm; ^{11}B NMR ($CDCl_3$, 128.4 MHz): δ 29.4 ppm; IR: ν = 3347, 3245, 1635, 1612, 1526, 1484, 1270, 747, 686 cm^{-1}; HRMS (CI) m/z calc. for $C_{13}H_{11}BN_2O$ $[M]^+$ 223.1043, found 223.1043.

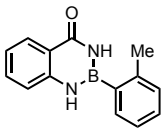

2-(o-Tolyl)-1,3,2-benzodiazaborininone (**2.62**). Obtained as a white solid by procedure A after recrystallization from EtOAc (1.43 g, 87%, 7.0 mmol scale) and procedure B-1 (132 mg, 56%, 1.0 mmol scale); mp: 168-169 °C; ^{1}H NMR ($CDCl_3$, 500.4 MHz): δ 8.25 (d, *J* = 7.9 Hz, 1H), 7.55 (t, *J* = 7.6 Hz, 1H), 7.45 (d, *J* = 7.2 Hz, 1H), 7.34 (t, *J* = 7.5 Hz, 1H), 7.30 (s, 1H), 7.23 (d, *J* = 6.1 Hz, 2H), 7.18 (t, *J* = 7.6 Hz, 1H), 7.07 (d, *J* = 8.1 Hz, 1H), 6.72 (s, 1H), 2.48 (s, 3H) ppm; ^{13}C {^{1}H} NMR ($CDCl_3$, 125.8 MHz): δ 166.5, 144.4, 140.9, 134.0, 132.7, 130.1, 130.1, 129.3, 125.6, 122.1, 119.0, 117.7, 22.6 ppm; ^{11}B NMR ($CDCl_3$, 128.4 MHz): δ 30.7 ppm; IR: ν = 3385, 3210,

1614, 1516, 1484, 1455, 745, 723 cm^{-1}; HRMS (ESI+) m/z calc. for $C_{14}H_{14}BN_2O$ $[M+H]^+$ 237.1199, found 237.1193.

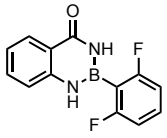

2-(2,6-Fluorophenyl)-1,3,2-benzodiazaborininone (**2.63**). Obtained as a beige solid by procedure A after recrystallization from EtOAc (150 mg, 58%, 1.0 mmol scale); mp: 164-165 °C; ^{1}H NMR (acetone-d_6, 500.4 MHz): δ 8.59 (s, 1H), 8.55 (s, 1H), 8.15 (d, J = 7.9 Hz, 1H), 7.64 – 7.50 (m, 2H), 7.42 (d, J = 8.1 Hz, 1H), 7.18 (t, J = 7.5 Hz, 1H), 7.05 (t, J = 7.8 Hz, 2H) ppm; ^{13}C {^{1}H} NMR (DMSO-d_6, 125.8 MHz): δ 165.9, 164.8 (dd, J = 244.6, 13.7 Hz), 145.4, 133.9, 133.1 (t, J = 10.1 Hz), 128.4, 121.8, 119.4, 118.5, 111.6 (dd, J = 22.7, 5.3 Hz) ppm; ^{19}F {^{1}H} NMR (acetone-d_6, 470.8 MHz): δ -103.6 ppm; ^{11}B NMR (acetone-d_6, 128.4 MHz): δ 28.0 ppm; IR: ν = 3438, 3362, 1666, 1616, 1454, 982, 762, 750, 720 cm^{-1}; HRMS (ESI+) m/z calc. for $C_{13}H_{10}BN_2OF_2$ $[M+H]^+$ 259.0854, found 259.0862.

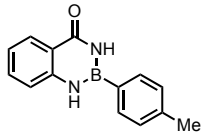

2-(p-Tolyl)-1,3,2-benzodiazaborininone (**2.64**). Obtained as a white solid by procedure A (177 mg, 75%, 1.0 mmol scale); mp: 255-256 °C; ^{1}H NMR ($CDCl_3$, 500.4 MHz): δ 8.26 (d, J = 7.8 Hz, 1H), 7.61 (d, J = 7.8 Hz, 2H), 7.56 (t, J = 7.7 Hz, 1H), 7.51 (s, 1H), 7.31 (d, J = 7.6 Hz, 2H), 7.18 (t, J = 7.6 Hz, 1H), 7.11 (d, J = 8.1 Hz, 1H), 6.76 (s, 1H), 2.43 (s, 3H) ppm; ^{13}C {^{1}H} NMR ($CDCl_3$, 125.8 MHz): δ 166.7, 144.5, 141.6, 134.0, 132.0, 129.6, 129.4, 122.0, 119.1, 117.7, 21.8 ppm; ^{11}B NMR ($CDCl_3$, 128.4

MHz): δ 29.5 ppm; IR: ν = 3321, 3247, 1635, 1615, 1486, 1364, 1342, 1272, 752, 719, 477 cm^{-1}; HRMS (EI) m/z calc. for $C_{14}H_{13}BN_2O$ $[M]^+$ 236.1121, found 236.1136.

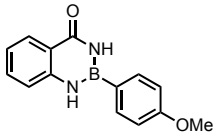

2-(4-Methoxyphenyl)-1,3,2-benzodiazaborininone (**2.65**). Obtained as a white solid by procedure A (82 mg, 65%, 0.5 mmol scale) and procedure B-1 (58 mg, 68%, 0.5 mmol scale); mp: 215-217 °C; ^{1}H NMR ($CDCl_3$, 500.4 MHz): δ 8.26 (d, *J* = 7.9 Hz, 1H), 7.65 (d, *J* = 8.5 Hz, 2H), 7.56 (dt, *J* = 7.8, 1.5 Hz, 1H), 7.52 (s, 1H), 7.17 (t, *J* = 7.6 Hz, 1H), 7.10 (d, *J* = 8.1 Hz, 1H), 7.02 (d, *J* = 8.5 Hz, 2H), 6.73 (s, 1H), 3.88 (s, 3H) ppm; ^{13}C {^{1}H} NMR ($CDCl_3$, 125.8 MHz): δ 166.8, 162.2, 144.6, 134.0, 133.7, 129.4, 121.9, 119.0, 117.6, 114.4, 55.4 ppm; ^{11}B NMR ($CDCl_3$, 128.4 MHz): δ 29.2 ppm; IR: ν = 3352, 3290, 1640, 1602, 1507, 1487, 1242, 1179, 753 cm^{-1}; HRMS (ESI+) m/z calc. for $C_{14}H_{14}{}^{10}BN_2O_2$ $[M+H]^+$ 252.1185, found 252.1187.

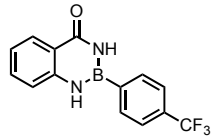

2-(4-(Trifluoromethyl)phenyl)-1,3,2-benzodiazaborininone (**2.66**). Obtained as a white solid by procedure A (270 mg, 93%, 1.0 mmol scale) and procedure B-1 (197 mg, 68%, 1.0 mmol scale); mp: >260 °C; ^{1}H NMR (DMSO-d_6, 500.4 MHz): δ 9.80 (s, 1H), 9.45 (s, 1H), 8.23 (d, *J* = 7.5 Hz, 2H), 8.04 (d, *J* = 7.7 Hz, 1H), 7.77 (d, *J* = 7.6 Hz, 2H), 7.57 (t, *J* = 7.4 Hz, 1H), 7.43 (d, *J* = 7.9 Hz, 1H), 7.11 (t, *J* = 7.7 Hz, 1H) ppm; ^{13}C {^{1}H} NMR (DMSO-d_6, 125.8 MHz): δ 166.7, 145.6, 134.3, 133.8, 130.9 (q, *J* = 31.7 Hz), 128.3, 124.6 (q, *J* = 272.2 Hz), 124.6 (q, *J* = 3.4 Hz), 121.5, 119.3, 118.6 ppm; ^{19}F

{^{1}H} NMR (DMSO-d_6, 470.8 MHz): δ -63.1 ppm; ^{11}B NMR ($CDCl_3$, 128.4 MHz): δ 28.5 ppm; IR: ν = 3333, 3245, ,1630, 1616, 1316, 1110, 1066, 763, 526 cm^{-1}; HRMS (ESI+) m/z calc. for $C_{14}H_{11}BN_2OF_3$ $[M+H]^+$ 291.0917, found 291.0916.

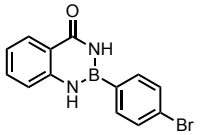

2-(4-Bromophenyl)-1,3,2-benzodiazaborininone (**2.67**). Obtained as a white solid by modification to procedure A as **2.67** was not particularly soluble in EtOAc. As a result, some product could be collected as a precipitate from the aqueous workup (273 mg, 91%, 1.0 mmol scale); mp: >260 °C; ^{1}H NMR (DMSO-d_6, 500.4 MHz): δ 9.73 (s, 1H), 9.36 (s, 1H), 8.04 – 7.95 (m, 3H), 7.65 (d, J = 8.3 Hz, 2H), 7.60 – 7.53 (m, 1H), 7.40 (d, J = 8.0 Hz, 1H), 7.10 (t, J = 7.3 Hz, 1H) ppm; ^{13}C {^{1}H} NMR (DMSO-d_6, 125.8 MHz): δ 166.6, 145.7, 135.8, 133.8, 131.1, 128.3, 125.0, 121.3, 119.2, 118.5 ppm; ^{11}B NMR (THF, 128.4 MHz): δ 29.4 ppm; IR: ν = 3331, 3240, 1615, 1486, 1269, 753, 717, 528 cm^{-1}; HRMS (ESI+) m/z calc. for $C_{13}H_{11}BN_2OBr$ $[M+H]^+$ 301.0148, found 301.0157.

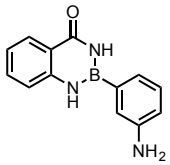

2-(3-Aminophenyl)-1,3,2-benzodiazaborininone (**2.68**). Obtained as a tan solid by modification to procedure A as **2.68** was minimally soluble in EtOAc. As a result, the product could be collected directly as a precipitate from the aqueous workup (173 mg, 73%, 1.0 mmol scale); mp: 210-213 °C; ^{1}H NMR (DMSO-d_6, 500.4 MHz): δ

9.38 (s, 1H), 9.17 (s, 1H), 7.99 (d, *J* = 7.9 Hz, 1H), 7.61 – 7.50 (m, 1H), 7.42 (d, *J* = 8.2 Hz, 1H), 7.19 – 7.12 (m, 2H), 7.12 – 7.04 (m, 2H), 6.70 (d, *J* = 7.7 Hz, 1H), 4.92 (s, 2H) ppm; ^{13}C {^{1}H} NMR (DMSO-d_6, 125.8 MHz): δ 166.6, 148.3, 146.0, 133.6, 128.7, 128.2, 121.5, 121.0, 119.1, 118.5, 116.6, 99.9 ppm; ^{11}B NMR (MeCN, 128.4 MHz): δ 30.1 ppm; IR: ν = 3395, 3292, 3211, 1657, 1608, 1526, 1484, 757, 509 cm^{-1}; HRMS (ESI+) m/z calc. for $C_{13}H_{12}BN_3ONa$ [M+Na]$^+$ 260.0971, found 260.0984.

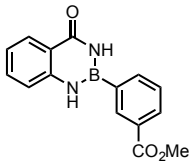

2-(3-(Methoxycarbonyl)phenyl)-1,3,2-benzodiazaborininone (**2.69**). Obtained as a white solid by modification to procedure A as **2.69** was not particularly soluble in EtOAc. As a result some product was also collected as a precipitate from the aqueous workup (258 mg, 92%, 1.0 mmol scale); mp: 234-235 °C; ^{1}H NMR (DMSO-d_6, 500.4 MHz): δ 9.82 (s, 1H), 9.48 (s, 1H), 8.63 (s, 1H), 8.27 (d, *J* = 7.4 Hz, 1H), 8.05 (d, *J* = 7.8 Hz, 1H), 8.01 (d, *J* = 7.8 Hz, 1H), 7.63 – 7.54 (m, 2H), 7.44 (d, *J* = 8.1 Hz, 1H), 7.10 (t, *J* = 7.5 Hz, 1H), 3.89 (s, 3H) ppm; ^{13}C {^{1}H} NMR (DMSO-d_6, 125.8 MHz): δ 166.9, 166.6, 145.8, 138.5, 134.5, 133.8, 131.4, 129.7, 128.6, 128.3, 121.3, 119.3, 118.6, 52.5 ppm; ^{11}B NMR (THF, 128.4 MHz): δ 29.5 ppm; IR: ν = 3320, 3226, 2951, 1716, 1623, 1487, 1289, 749, 690 cm^{-1}; HRMS (ESI+) m/z calc. for $C_{15}H_{14}BN_2O_3$ [M+H]$^+$ 281.1097, found 281.1092.

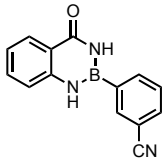

2-(3-Cyanophenyl)-1,3,2-benzodiazaborininone (**2.70**). Obtained as a white solid by procedure A after purifying *via* plug of silica gel with EtOAc/hexane (1:1) as eluent (138 mg, 56%, 1.0 mmol scale); mp: > 260 °C; ^{1}H NMR (DMSO-d_6, 500.4 MHz): δ 9.84 (s, 1H), 9.47 (s, 1H), 8.48 (s, 1H), 8.35 (t, *J* = 6.6 Hz, 1H), 8.01 (d, *J* = 7.5 Hz, 1H), 7.93 (d, *J* = 6.9 Hz, 1H), 7.66 (t, *J* = 7.5 Hz, 1H), 7.58 (d, *J* = 7.1 Hz, 1H), 7.40 (d, *J* = 7.1 Hz, 1H), 7.16 – 7.03 (m, 1H) ppm; ^{13}C {^{1}H} NMR (DMSO-d_6, 125.8 MHz): δ 166.6, 145.6, 138.2, 137.3, 134.1, 133.9, 129.2, 128.3, 121.5, 119.4, 119.3, 118.6, 111.6 ppm; ^{11}B NMR (THF, 128.4 MHz): δ 29.3 ppm; IR: ν = 3365, 3197, 2230, 1651, 1619, 1485, 760, 699, 687 cm^{-1}; HRMS (ESI+) m/z calc. for $C_{14}H_{11}BN_3O$ $[M+H]^+$ 248.0995, found 248.0991.

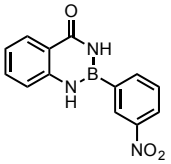

2-(3-Nitrophenyl)-1,3,2-benzodiazaborininone (**2.71**). Obtained as a beige solid by procedure A (123 mg, 92%, 0.5 mmol scale); mp: >260 °C; ^{1}H NMR (DMSO-d_6, 500.4 MHz): δ 9.97 (s, 1H), 9.62 (s, 1H), 8.92 (s, 1H), 8.46 (d, *J* = 7.4 Hz, 1H), 8.31 (dd, *J* = 8.2, 1.4 Hz, 1H), 8.02 (d, *J* = 7.9 Hz, 1H), 7.74 (t, *J* = 7.8 Hz, 1H), 7.63 – 7.55 (m, 1H), 7.44 (d, *J* = 8.1 Hz, 1H), 7.13 (t, *J* = 7.5 Hz, 1H) ppm; ^{13}C {^{1}H} NMR (DMSO-d_6, 125.8 MHz): δ 166.6, 148.1, 145.6, 140.3, 140.3, 133.9, 129.7, 128.3, 125.4, 121.6, 119.3, 118.6 ppm; ^{11}B NMR (THF, 128.4 MHz): δ 29.1 ppm; IR: ν = 3325, 1614, 1515,

1484, 1345, 1269, 763, 679 cm^{-1}; HRMS (ESI-) m/z calc. for $C_{13}H_9BN_3O_3$ $[M-H]^-$ 266.0737, found 266.0747.

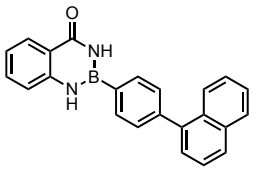

2-(4-(Naphthalen-1-yl)phenyl)-1,3,2-benzodiazaborininone (**2.72**). Obtained as a beige solid by procedure A (247 mg, 71%, 1.0 mmol scale); mp: 255-256 °C; ^1H NMR (DMSO-d_6, 500.4 MHz): δ 9.76 (s, 1H), 9.42 (s, 1H), 8.20 (d, J = 7.8 Hz, 2H), 8.01 (t, J = 8.7 Hz, 2H), 7.96 (d, J = 8.2 Hz, 1H), 7.82 (d, J = 8.3 Hz, 1H), 7.61 – 7.52 (m, 5H), 7.52 – 7.43 (m, 3H), 7.10 (t, J = 7.4 Hz, 1H) ppm; ^{13}C $\{^1H\}$ NMR (DMSO-d_6, 125.8 MHz): δ 166.8, 146.0, 142.5, 139.7, 133.9, 133.8, 133.8, 131.1, 129.6, 128.8, 128.3, 128.2, 127.3, 126.8, 126.3, 125.9, 125.5, 121.2, 119.2, 118.6 ppm; ^{11}B NMR (THF, 128.4 MHz): δ 29.9 ppm; IR: ν = 3320, 1657, 1316, 1533, 1511, 1485, 1358, 798, 774, 760, 716 cm^{-1}; HRMS (ESI-) m/z calc. for $C_{23}H_{16}BN_2O$ $[M-H]^-$ 347.1356, found 347.1357.

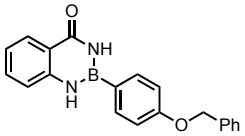

2-(4-(Benzyloxy)phenyl)-1,3,2-benzodiazaborininone (**2.73**). Obtained as a white solid by procedure A (265 mg, 81%, 1.0 mmol scale); mp: 249-251 °C; ^1H NMR (DMSO-d_6, 500.4 MHz): δ 9.57 (s, 1H), 9.20 (s, 1H), 8.07 – 7.94 (m, 3H), 7.54 (t, J = 7.6 Hz, 1H), 7.46 (d, J = 7.7 Hz, 2H), 7.43 – 7.37 (m, 3H), 7.33 (t, J = 7.3 Hz, 1H), 7.11 – 7.03 (m, 3H), 5.17 (s, 2H) ppm; ^{13}C $\{^1H\}$ NMR (DMSO-d_6, 125.8 MHz): δ 166.7, 160.8,

146.0, 137.3, 135.5, 133.7, 128.8, 128.3, 128.2, 128.0, 120.9, 118.9, 118.4, 114.7, 69.4 ppm; ^{11}B NMR (THF, 128.4 MHz): δ 29.6 ppm; IR: ν = 3404, 3302, 1645, 1622, 1604, 1486, 1214, 996, 759, 721 cm^{-1}; HRMS (ESI+) m/z calc. for $C_{20}H_{18}BN_2O_2$ $[M+H]^+$ 329.1461, found 329.1458.

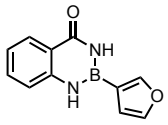

2-(Furan-3-yl)-1,3,2-benzodiazaborininone (**2.74**). Obtained as a light brown solid by procedure A (172 mg, 81%, 1.0 mmol scale); mp: 190-192 °C; ^{1}H NMR ($CDCl_3$, 500.4 MHz): δ 8.25 (d, *J* = 7.9 Hz, 1H), 8.00 (s, 1H), 7.90 (s, 1H), 7.60 (s, 1H), 7.55 (t, *J* = 8.2 Hz, 1H), 7.27 (s, 1H), 7.17 (t, *J* = 7.5 Hz, 1H), 7.09 (d, *J* = 8.1 Hz, 1H), 6.68 (s, 1H) ppm; ^{13}C {^{1}H} NMR ($CDCl_3$, 125.8 MHz): δ 167.0, 148.6, 144.5, 144.1, 134.0, 129.3, 121.9, 119.1, 117.5, 111.7 ppm; ^{11}B NMR (EtOAc, 128.4 MHz): δ 28.2 ppm; IR: ν = 3347, 3250, 1636, 1610, 1516, 1487, 1150, 754, 732, 668, 527 cm^{-1}; HRMS (ESI+) m/z calc. for $C_{11}H_{10}BN_2O_2$ $[M+H]^+$ 213.0835, found 213.0836

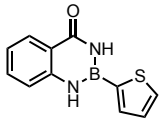

2-(Thiophen-2-yl)-1,3,2-benzodiazaborininone (**2.75**). Obtained as a white solid by procedure A (169 mg, 74%, 1.0 mmol scale); mp: 211-213 °C; ^{1}H NMR (DMSO-d_6, 500.4 MHz): δ 9.71 (s, 1H), 9.26 (s, 1H), 7.99 (dd, *J* = 11.2, 2.5 Hz, 2H), 7.92 (d, *J* = 4.6 Hz, 1H), 7.55 (td, *J* = 7.8, 1.5 Hz, 1H), 7.41 (d, *J* = 8.1 Hz, 1H), 7.29 (dd, *J* = 4.6, 3.5 Hz, 1H), 7.09 (t, *J* = 7.5 Hz, 1H) ppm; ^{13}C {^{1}H} NMR (DMSO-d_6, 125.8 MHz): δ 166.4, 145.8, 136.7, 133.8, 132.8, 129.0, 128.3, 121.2, 119.2, 118.5 ppm; ^{11}B NMR

(EtOAc, 128.4 MHz): δ 27.7 ppm; IR: ν = 3315, 3240, 1614, 1530, 1486, 1264, 1025, 753, 698, 687, 474 cm^{-1}; HRMS (ESI+) m/z calc. for $C_{11}H_{10}BN_2OS$ $[M+H]^+$ 229.0607, found 229.0618.

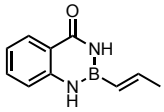

(E)-2-(Prop-1-en-1-yl)-1,3,2-benzodiazaborininone (**2.76**). Obtained as an off-white solid by procedure A (166 mg, 89%, 1.0 mmol scale) and procedure B-1 (156 mg, 84%, 1.0 mmol scale); mp: 142-143 °C; ^{1}H NMR (DMSO-d_6, 500.4 MHz): δ 9.25 (s, 1H), 8.91 (s, 1H), 7.93 (d, *J* = 7.8 Hz, 1H), 7.55 – 7.45 (m, 1H), 7.22 (d, *J* = 8.2 Hz, 1H), 7.02 (t, *J* = 7.5 Hz, 1H), 6.77 (dq, *J* = 18.7, 6.3 Hz, 1H), 5.69 (dd, *J* = 17.9, 1.7 Hz, 1H), 1.86 (d, *J* = 6.3 Hz, 3H) ppm; ^{13}C {^{1}H} NMR (DMSO-d_6, 125.8 MHz): δ 166.4, 145.9, 145.7, 133.5, 128.3, 120.7, 119.1, 118.1, 22.1 ppm; ^{11}B NMR (EtOAc, 128.4 MHz,): δ 28.4 ppm; IR: ν = 3315, 3201, 1608, 1517, 1485, 1362, 986, 754 cm^{-1}; HRMS (ESI+) m/z calc. for $C_{10}H_{12}BN_2O$ $[M+H]^+$ 187.1043, found 187.1048.

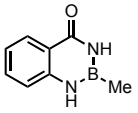

2-Methyl-1,3,2-benzodiazaborininone (**2.77**). Obtained as a white solid by procedure A after purifying *via* plug of silica gel with EtOAc/hexane (1:1) as eluent (86 mg, 54%, 1.0 mmol scale) and procedure B-1 (86 mg, 62%, 1.0 mmol scale); mp: 181-182 °C; ^{1}H NMR ($CDCl_3$, 500.4 MHz): δ 8.20 (d, *J* = 6.8 Hz, 1H), 7.50 (t, *J* = 6.8 Hz, 1H), 7.12 (t, *J* = 7.2 Hz, 2H), 6.98 (d, *J* = 7.3 Hz, 1H), 6.40 (s, 1H), 0.59 (s, 3H) ppm; ^{13}C {^{1}H} NMR ($CDCl_3$, 125.8 MHz): δ 166.5, 144.4, 133.8, 129.2, 121.6, 118.7, 117.2 ppm; ^{11}B NMR ($CDCl_3$, 128.4 MHz): δ 32.3 ppm; IR: ν = 3267, 3190, 1609, 1519, 1486,

1364, 909, 749 cm^{-1}; HRMS (CI) m/z calc. for $C_8H_9BN_2O$ $[M]^+$ 160.0808, found 160.0808.

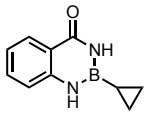

2-Cyclopropyl-1,3,2-benzodiazaborininone (**2.78**). Obtained as a white solid by procedure A (121 mg, 65%, 1.0 mmol scale) and procedure B-1 (108 mg, 58%, 1.0 mmol scale); mp: 186-188 °C; ^1H NMR (DMSO-d_6, 500.4 MHz): δ 8.98 (s, 1H), 8.50 (s, 1H), 7.90 (dd, J = 7.9, 1.4 Hz, 1H), 7.47 (td, J = 7.8, 1.6 Hz, 1H), 7.17 (d, J = 8.0 Hz, 1H), 6.99 (t, J = 7.5 Hz, 1H), 0.68 (dt, J = 9.2, 2.5 Hz, 2H), 0.65 – 0.59 (m, 2H), 0.05 (ddd, J = 9.2, 6.5, 2.9 Hz, 1H) ppm; ^{13}C {^1H} NMR (DMSO-d_6, 125.8 MHz): δ 166.2, 145.8, 133.4, 128.2, 120.4, 118.7, 117.8, 5.4 ppm; ^{11}B NMR (EtOAc, 128.4 MHz): δ 30.4 ppm; IR: ν = 3380, 3308, 3189, 1615, 1557, 1488, 1393, 1254, 752 cm^{-1}; HRMS (ESI+) m/z calc. for $C_{10}H_{12}BN_2O$ $[M+H]^+$ 187.1043, found 187.1048.

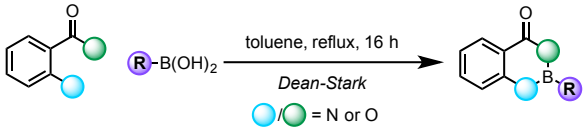

Procedure C – Condensation of boronic acids to form oxazaborininones. To a round-bottomed flask with a stir bar was added the appropriate boronic acid (1 equiv) and either anthranilic acid or salicylamide (1 equiv) followed by toluene (4 mL/mmol). The flask was equipped with a Dean-Stark trap, and the reaction was heated to reflux. The reaction was stirred at this temperature overnight. After this time, the solvent was removed *in vacuo* by rotary evaporation, giving a crude solid.

The resulting solid was further purified by washing with hexane/EtOAc (1:1), affording the desired, pure oxazaborininone.

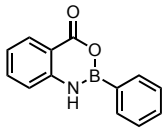

2-Phenyl-3,1,2-benzoxazaborininone (**2.60**). Obtained as a white solid by procedure B-1 (367 mg, 83%, 2.0 mmol scale) and procedure C (650 mg, 93%, 3.0 mmol scale); mp: 211-212 °C; ^{1}H NMR ($CDCl_3$, 500.4 MHz): δ 8.21 (d, *J* = 7.8 Hz, 1H), 7.95 (d, *J* = 6.9 Hz, 2H), 7.64 – 7.59 (m, 1H), 7.58 – 7.53 (m, 1H), 7.48 (t, *J* = 7.4 Hz, 2H), 7.20 (t, *J* = 7.5 Hz, 1H), 7.09 (d, *J* = 8.1 Hz, 1H), 6.89 (s, 1H) ppm; ^{13}C {^{1}H} NMR (DMSO-d_6, 125.8 MHz): δ 161.8, 146.1, 135.8, 133.8, 131.8, 130.1, 128.3, 122.2, 118.1, 114.9 ppm; ^{11}B NMR ($CDCl_3$, 128.4 MHz): δ 28.9 ppm; IR: ν = 3315, 1685, 1613, 1484, 1431, 1271, 1227, 750, 692 cm^{-1}; HRMS (ESI+) m/z calc. for $C_{13}H_{11}BNO_2$ $[M+H]^+$ 224.0883, found 224.0904.

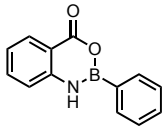

2-(p-Tolyl)-3,1,2-benzoxazaborininone (**2.79**). Obtained as an off-white solid by procedure B-1 (408 mg, 86%, 2.0 mmol scale) and procedure C (230 mg, 97%, 2.0 mmol scale); mp: 220-221 °C; ^{1}H NMR (DMSO-d_6, 500.4 MHz): δ 9.66 (s, 1H), 7.94 (d, *J* = 7.9 Hz, 1H), 7.88 (d, *J* = 7.8 Hz, 2H), 7.67 – 7.62 (m, 1H), 7.33 (d, *J* = 8.1 Hz, 1H), 7.29 (d, *J* = 7.6 Hz, 2H), 7.13 (t, *J* = 7.6 Hz, 1H), 2.35 (s, 3H) ppm; ^{13}C {^{1}H} NMR (DMSO-d_6, 125.8 MHz): δ 161.4, 145.7, 141.3, 135.5, 133.6, 129.7, 128.7, 121.8, 117.7, 114.4, 21.3 ppm; ^{11}B NMR (MeCN, 128.4 MHz): δ 29.2 ppm; IR: ν = 3307,

1701, 1613, 1485, 1280, 756, 695, 626 cm^{-1}; HRMS (ESI+) m/z calc. for $C_{14}H_{13}BNO_2$ $[M+H]^+$ 238.1039, found 238.1033.

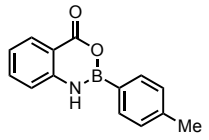

2-(4-Methoxyphenyl)-3,1,2-benzoxazaborininone (**2.80**). Obtained as a white solid by procedure B-1 (154 mg, 61%, 1.0 mmol scale) and procedure C after an additional wash with *t*-BuOH (364 mg, 72%, 2.0 mmol scale); mp: 205-206 °C; ^{1}H NMR ($CDCl_3$, 500.4 MHz): δ 8.18 (d, *J* = 7.8 Hz, 1H), 7.88 (d, *J* = 8.5 Hz, 2H), 7.61 – 7.54 (m, 1H), 7.16 (t, *J* = 7.5 Hz, 1H), 7.04 (d, *J* = 8.1 Hz, 1H), 6.99 (d, *J* = 8.6 Hz, 2H), 6.75 (s, 1H), 3.87 (s, 3H) ppm; ^{13}C {^{1}H} NMR ($CDCl_3$, 125.8 MHz): δ 162.5, 161.8, 146.2, 135.9, 135.8, 130.1, 122.1, 118.0, 114.7, 114.1, 55.5 ppm; ^{11}B NMR ($CDCl_3$, 128.4 MHz): δ 28.6 ppm; IR: ν = 3340, 1698, 1599, 1428, 1281, 1251, 1224, 1180, 753, 693 cm^{-1}; HRMS (ESI+) m/z calc. for $C_{14}H_{13}BNO_3$ $[M+H]^+$ 254.0988, found 254.0984.

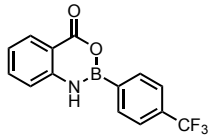

2-(4-(Trifluoromethyl)phenyl)-3,1,2-benzoxazaborininone (**2.81**). Obtained as a white solid by procedure B-1 (226 mg, 78%, 1.0 mmol scale); mp: >260 °C; ^{1}H NMR (DMSO-d_6, 500.4 MHz): δ 9.50 (s, 1H), 8.12 (d, *J* = 7.8 Hz, 2H), 7.93 (d, *J* = 7.7 Hz, 1H), 7.81 (d, *J* = 7.9 Hz, 2H), 7.62 (t, *J* = 7.4 Hz, 1H), 7.28 (d, *J* = 8.1 Hz, 1H), 7.09 (t, *J* = 7.5 Hz, 1H) ppm; ^{13}C NMR (DMSO-d_6, 126 MHz): δ 162.1, 146.7, 136.0, 134.5, 131.4 (q, *J* = 31.4 Hz), 130.4, 124.9 (q, *J* = 272 Hz), 125.0 (q, *J* = 3.5 Hz), 122.0, 118.2,

115.0 ppm; ^{19}F {^{1}H} NMR (DMSO-d_6, 470.8 MHz): δ -61.3 ppm; ^{11}B NMR (EtOAc, 128.4 MHz): δ 28.8 ppm; IR: ν = 3307, 1686, 1615, 1326, 1265, 1149, 1108, 1071, 759, 635 cm^{-1}; HRMS (ESI+) m/z calc. for $C_{14}H_{10}BNO_2F_3$ $[M+H]^+$ 292.0757, found 292.30753.

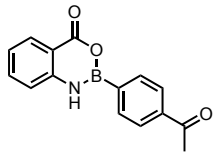

2-(4-Acetylphenyl)-3,1,2-benzoxazaborininone (**2.82**). Obtained as a white solid by procedure B-1 (313 mg, 59%, 2.0 mmol scale); mp: 252-253 °C; ^{1}H NMR (DMSO-d_6, 500.4 MHz): δ 9.64 (s, 1H), 8.09 (d, J = 7.9 Hz, 2H), 8.03 (d, J = 7.9 Hz, 2H), 7.96 (d, J = 7.8 Hz, 1H), 7.65 (t, J = 7.5 Hz, 1H), 7.32 (d, J = 8.1 Hz, 1H), 7.13 (t, J = 7.5 Hz, 1H), 2.62 (s, 3H) ppm; ^{13}C {^{1}H} NMR (DMSO-d_6, 125.8 MHz): δ 198.7, 162.0, 146.5, 139.2, 136.1, 134.1, 130.3, 128.0, 122.3, 118.3, 115.1, 27.5 ppm; ^{11}B NMR (acetone-d_6, 128 MHz): δ 27.6 ppm; IR: ν = 3308, 1668, 1614, 1484, 1399, 1261, 1233, 760, 628 cm^{-1}; HRMS (ESI+) m/z calc. for $C_{15}H_{13}BNO_3$ $[M+H]^+$ 266.0988, found 266.0983.

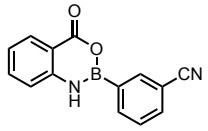

2-(3-Cyanophenyl)-3,1,2-benzoxazaborininone (**2.83**). Obtained as an off-white solid by procedure B-1 (136 mg, 55%, 1.0 mmol scale) and procedure C (677 mg, 91%, 3.0 mmol scale); mp: >260 °C; ^{1}H NMR (DMSO-d_6, 500.4 MHz): δ 9.33 (s, 1H), 8.26 (s, 1H), 8.15 (d, J = 7.5 Hz, 1H), 7.90 (d, J = 7.6 Hz, 2H), 7.64 (t, J = 7.6 Hz, 1H), 7.59 (t, J = 7.5 Hz, 1H), 7.21 (d, J = 8.1 Hz, 1H), 7.06 (t, J = 7.5 Hz, 1H) ppm; ^{13}C

{^{1}H} NMR (DMSO-d_6, 125.8 MHz): δ 162.1, 146.8, 138.1, 137.2, 136.0, 134.5, 130.4, 129.6, 121.8, 119.5, 118.1, 114.8, 111.8 ppm; ^{11}B NMR (acetone-d_6, 128 MHz): δ 27.1 ppm; IR: ν = 3313, 2235, 1694, 1621, 1526, 1483, 1279, 753, 688, 524 cm^{-1}; HRMS (ESI+) m/z calc. for $C_{14}H_{10}BN_2O_2$ $[M+H]^+$ 249.0835, found 249.0836.

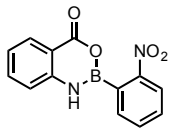

2-(2-Nitrophenyl)-3,1,2-benzoxazaborininone (**2.84**). Obtained as a light yellow solid by procedure B-1 (81 mg, 30%, 1.0 mmol scale) and procedure C (498 mg, 93%, 2.0 mmol scale); mp: 210-211 °C; ^{1}H NMR (DMSO-d_6, 500.4 MHz): δ 9.43 (s, 1H), 8.25 (d, J = 8.2 Hz, 1H), 7.98 (d, J = 7.8 Hz, 1H), 7.92 – 7.85 (m, 2H), 7.76 (t, J = 7.3 Hz, 1H), 7.65 (t, J = 7.5 Hz, 1H), 7.19 – 7.13 (m, 2H) ppm; ^{13}C {^{1}H} NMR (DMSO-d_6, 125.8 MHz): δ 161.8, 151.3, 146.5, 136.3, 135.1, 134.3, 131.6, 130.4, 123.8, 122.5, 118.2, 114.8 ppm; ^{11}B NMR (methanol-d_4, 128 MHz): δ 27.0 ppm; IR: ν = 3348, 1698, 1510, 1484, 1342, 1266, 756, 724, 695 cm^{-1}; HRMS (ESI+) m/z calc. for $C_{13}H_{10}BN_2O_4$ $[M+H]^+$ 269.0734, found 269.0741.

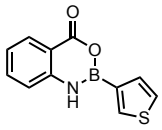

2-(Thiophen-3-yl)-3,1,2-benzoxazaborininone (**2.85**). Obtained as an off-white solid by procedure B-1 (147 mg, 64%, 1.0 mmol scale) and procedure C after washing with *t*-BuOH (400 mg, 87%, 3.0 mmol scale); mp: 227-229 °C; ^{1}H NMR ($CDCl_3$, 500.4 MHz): δ 8.19 (d, J = 7.9 Hz, 1H), 8.13 (s, 1H), 7.60 (t, J = 7.7 Hz, 1H), 7.53 (d, J = 4.8 Hz, 1H), 7.49 – 7.43 (m, 1H), 7.19 (t, J = 7.6 Hz, 1H), 7.07 (d, J = 8.1 Hz,

1H), 6.77 (s, 1H) ppm; ^{13}C {^{1}H} NMR (DMSO-d_6, 125.8 MHz): δ 161.7, 146.1, 136.7, 135.9, 131.6, 130.1, 127.0, 122.2, 118.0, 114.9 ppm; ^{11}B NMR ($CDCl_3$, 128.4 MHz): δ 27.0 ppm; IR: ν = 3295, 1694, 1619, 1524, 1483, 1273, 1096, 695, 658, 521 cm^{-1}; HRMS (ESI+) m/z calc. for $C_{11}H_9BNO_2S$ $[M+H]^+$ 230.0447, found 230.0445.

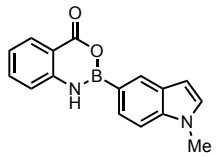

2-(1-Methyl-1H-indol-5-yl)-3,1,2-benzoxazaborininone (**2.86**). Obtained as a white solid by procedure B-1 (138 mg, 50%, 1.0 mmol scale) and procedure C (524 mg, 95%, 2.0 mmol scale); mp: >260 °C; ^{1}H NMR (DMSO-d_6, 500.4 MHz): δ 9.65 (s, 1H), 8.28 (s, 1H), 7.95 (d, J = 7.8 Hz, 1H), 7.79 (d, J = 8.3 Hz, 1H), 7.64 (t, J = 8.3 Hz, 1H), 7.53 (d, J = 8.3 Hz, 1H), 7.38 – 7.34 (m, 2H), 7.12 (t, J = 7.5 Hz, 1H), 6.53 (d, J = 2.8 Hz, 1H), 3.81 (s, 3H) ppm; ^{13}C {^{1}H} NMR (DMSO-d_6, 125.8 MHz): δ 161.9, 146.4, 138.8, 135.8, 130.6, 130.1, 128.3, 127.6, 126.4, 122.0, 118.0, 114.7, 109.8, 101.5, 32.9 ppm; ^{11}B NMR (acetone-d_6, 128 MHz): δ 28.7 ppm; IR: ν = 3285, 1693, 1612, 1520, 1485, 1293, 1268, 1175, 753, 717, 697 cm^{-1}; HRMS (ESI+) m/z calc. for $C_{16}H_{14}BN_2O_3$ $[M+H]^+$ 277.1148, found 277.1147.

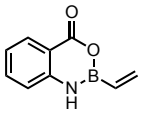

2-Vinyl-3,1,2-benzoxazaborininone (**2.87**). Obtained as an off-white solid by procedure B-1 (142 mg, 41%, 2.0 mmol scale); mp: 140-141 °C; ^{1}H NMR ($CDCl_3$, 500.4 MHz): 8.14 (d, J = 8.6 Hz, 1H), 7.55 (td, J = 7.7, 1.5 Hz, 1H), 7.15 (t, J = 7.6 Hz, 1H), 6.98 (d, J = 8.1 Hz, 1H), 6.51 (s, 1H), 6.41 (dd, J = 19.1, 3.6 Hz, 1H), 6.16 (dd, J =

13.6, 3.4 Hz, 1H), 6.07 (dd, *J* = 19.1, 13.6 Hz, 1H) ppm; ^{13}C {^{1}H} NMR ($CDCl_3$, 125.8 MHz): δ 161.8, 144.2, 137.2, 135.5, 131.1, 122.9, 117.1, 115.6 ppm; ^{11}B NMR ($CDCl_3$, 128.4 MHz): δ 27.6 ppm; IR: ν = 3265, 1706, 1618, 1516, 1486, 1351, 1283, 1175. 755, 694 cm^{-1}; HRMS (ESI+) m/z calc. for $C_9H_9BNO_2$ $[M+H]^+$ 174.0726, found 174.0730.

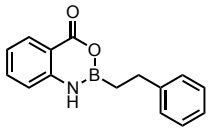

2-Phenethyl-3,1,2-benzoxazaborininone (**2.88**). Obtained as a yellow solid by procedure B-1 (377 mg, 75%, 2.0 mmol scale); mp: 100-102 °C; ^{1}H NMR ($CDCl_3$, 500.4 MHz): δ 8.12 (d, *J* = 7.9 Hz, 1H), 7.52 (td, *J* = 8.2, 1.5 Hz, 1H), 7.30 (t, *J* = 7.5 Hz, 2H), 7.26 – 7.23 (m, 2H), 7.22 – 7.17 (m, 1H), 7.13 (t, *J* = 7.6 Hz, 1H), 6.84 (d, *J* = 8.0 Hz, 1H), 6.23 (s, 1H), 2.91 (t, *J* = 8.0 Hz, 2H), 1.50 (t, *J* = 8.0 Hz, 2H) ppm; ^{13}C {^{1}H} NMR ($CDCl_3$, 125.8 MHz): δ 161.9, 144.1, 143.6, 135.5, 131.0, 128.7, 128.1, 126.1, 122.8, 116.8, 115.2, 29.8 ppm; ^{11}B NMR ($CDCl_3$, 128.4 MHz): δ 32.7 ppm; IR: ν = 3118, 1689, 1619, 1520, 1489, 1276, 1131, 757, 693 cm^{-1}; HRMS (ESI+) m/z calc. for $C_{15}H_{15}BNO_2$ $[M+H]^+$ 252.1196, found 252.1196.

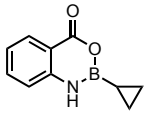

2-Cyclopropyl-3,1,2-benzoxazaborininone (**2.89**). Obtained as a beige solid by procedure B-1 after washing with 5:1 hexane/EtOAc instead of straight EtOAc (137 mg, 73%, 1.0 mmol scale) and procedure C (516 mg, 92%, 3.0 mmol scale); mp: 155-156 °C; ^{1}H NMR ($CDCl_3$, 500.4 MHz): δ 8.07 (d, *J* = 7.8 Hz, 1H), 7.52 (t, *J* = 7.7 Hz, 1H),

7.08 (t, *J* = 7.6 Hz, 1H), 6.94 (d, *J* = 8.1 Hz, 1H), 6.58 (s, 1H), 0.82 – 0.71 (m, 4H), 0.02 (tt, *J* = 8.7, 6.6 Hz, 1H) ppm; ^{13}C {^{1}H} NMR ($CDCl_3$, 125.8 MHz): δ 162.1, 144.4, 135.3, 130.7, 122.0, 116.5, 114.8, 5.0 ppm; ^{11}B NMR ($CDCl_3$, 128.4 MHz): δ 32.3 ppm; IR: ν = 3270, 1699, 1615, 1515, 1486, 1442, 1163, 755 cm^{-1}; HRMS (ESI+) m/z calc. for $C_{10}H_{11}BNO_2$ $[M+H]^+$ 188.0883, found 187.0925.

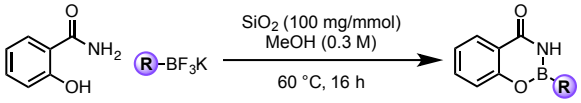

Procedure B-2 – Cyclization of potassium trifluoroborates activated with silica gel to form 1,3,2-benzoxazaborininones. To a microwave vial with a stir bar was added salicylamide (1.0 equiv) and the appropriate potassium organotrifluoroborates (1.05 equiv) along with oven-dried silica gel (100 mg/mmol). The reaction vessel was capped and purged with argon, and subsequently dry MeOH was added (3 mL/mmol). The reaction was then heated at 60 °C for 16 h. Upon cooling to rt, the reaction mixture was filtered through a short pad of Celite and flushed with additional MeOH. Removal of the solvent *in vacuo* afforded the desired 1,3,2-benzoxazaborininone product.

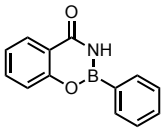

2-Phenyl-1,3,2-benzoxazaborininone (**2.61**). Obtained as a white solid by procedure B-2 after recrystallization from $CHCl_3$ (123 mg, 55%, 1.0 mmol scale) and procedure C (2.75 g, 81%, 10.0 mmol scale); mp: 195-196 °C; ^{1}H NMR ($CDCl_3$, 500.4 MHz): δ 8.25 (s, 1H), 8.22 (dd, *J* = 7.8, 1.6 Hz, 1H), 8.01 (d, *J* = 6.8 Hz, 2H), 7.70 – 7.64

(m, 1H), 7.61 – 7.56 (m, 1H), 7.52 (t, *J* = 7.3 Hz, 2H), 7.41 (d, *J* = 8.2 Hz, 1H), 7.32 (t, *J* = 7.5 Hz, 1H) ppm; ^{13}C {^{1}H} NMR ($CDCl_3$, 125.8 MHz): δ 165.3, 155.8, 134.8, 133.3, 132.1, 128.4, 128.3, 123.7, 119.5, 119.1 ppm; ^{11}B NMR (128.4 MHz, $CDCl_3$): δ 32.2 ppm; IR: ν = 3202, 3101, 1688, 1471, 11373, 1276, 1245, 758, 629 cm^{-1}; HRMS (ESI+) m/z calc. for $C_{13}H_{11}BNO_2$ $[M+H]^+$ 224.0883, found 224.0880.

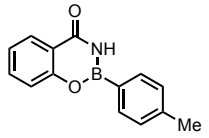

2-(p-Tolyl)-1,3,2-benzoxazaborininone (**2.90**). Obtained as a white solid by procedure B-2 after recrystallization from $CHCl_3$ (156 mg, 66%, 1.0 mmol scale) and procedure C (1.32 g, 90%, 5.0 mmol scale); mp: 200-202 °C; ^{1}H NMR ($CDCl_3$, 500.4 MHz): δ 8.20 (dd, *J* = 7.8, 1.7 Hz, 1H), 7.97 (s, 1H), 7.87 (d, *J* = 7.9 Hz, 2H), 7.66 (td, *J* = 7.8, 1.7 Hz, 1H), 7.39 (d, *J* = 8.3 Hz, 1H), 7.34 – 7.28 (m, 3H), 2.44 (s, 3H) ppm; ^{13}C {^{1}H} NMR ($CDCl_3$, 125.8 MHz): δ 165.1, 155.9, 142.6, 134.8, 133.3, 129.1, 128.3, 123.6, 119.4, 119.1, 21.7 ppm; ^{11}B NMR ($CDCl_3$, 128.4 MHz): δ 30.7 ppm; IR: ν = 3210, 3098, 1667, 1609, 1454, 1372, 1276, 860, 760 cm^{-1}; HRMS (ESI+) m/z calc. for $C_{14}H_{13}BNO_2$ $[M+H]^+$ 238.1039, found 238.1031.

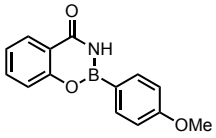

2-(4-Methoxyphenyl)-1,3,2-benzoxazaborininone (**2.91**). Obtained as a white solid by procedure B-2 after recrystallization from $CHCl_3$ (106 mg, 42%, 1.0 mmol scale) and procedure C (466 mg, 92%, 2.0 mmol scale); mp: 231-233 °C; ^{1}H NMR ($CDCl_3$, 500.4 MHz): δ 8.19 (d, *J* = 8.2 Hz, 1H), 7.89 (d, *J* = 8.3 Hz, 2H), 7.66 (t, *J* = 7.7

Hz, 1H), 7.58 (s, 1H), 7.38 (d, *J* = 8.3 Hz, 1H), 7.30 (t, *J* = 7.3 Hz, 1H), 7.03 (d, *J* = 8.3 Hz, 2H), 3.90 (s, 3H) ppm; ^{13}C {^{1}H} NMR ($CDCl_3$, 125.8 MHz): δ 164.8, 162.9, 155.9, 135.1, 134.8, 128.4, 123.5, 119.3, 119.0, 113.9, 55.1 ppm; ^{11}B NMR (THF, 128.4 MHz): δ 31.2 ppm; IR: ν = 3203, 1680, 1471, 1454, 1373, 1334, 1247, 756, 708 cm^{-1}; HRMS (ESI+) m/z calc. for $C_{14}H_{13}BNO_3$ $[M+H]^+$ 254.0991, found 254.0991.

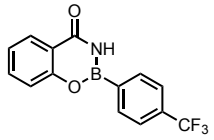

2-(4-(Trifluoromethyl)phenyl)-1,3,2-benzoxazaborininone (**2.92**). Obtained as a white solid by procedure B-2 after recrystallization from $CHCl_3$ (167 mg, 57%, 1.0 mmol scale); mp: 245-246 °C; ^{1}H NMR ($CDCl_3$, 500.4 MHz): δ 8.21 (dd, *J* = 7.8, 1.6 Hz, 1H), 8.08 (d, *J* = 8.0 Hz, 2H), 7.97 (s, 1H), 7.76 (d, *J* = 8.2 Hz, 2H), 7.69 (td, *J* = 7.6, 1.5 Hz, 1H), 7.42 (d, *J* = 8.3 Hz, 1H), 7.34 (t, *J* = 7.6 Hz, 1H) ppm; ^{13}C {^{1}H} NMR ($CDCl_3$, 125.8 MHz): δ 165.0, 155.8, 135.4, 134.0 (q, *J* = 32.5 Hz), 133.8, 128.7, 125.2 (q, *J* = 3.7 Hz), 124.3, 124.0 (d, *J* = 272.5 Hz), 119.7, 119.4 ppm; ^{19}F {^{1}H} NMR ($CDCl_3$, 470.8 MHz): δ -63.2 ppm; ^{11}B NMR (MeCN, 128.4 MHz): δ 31.6 ppm; IR: ν = 3172, 3100, 1683, 1614, 1323, 1108, 1097, 1069, 865, 835, 755, 636 cm^{-1}; HRMS (ESI+) m/z calc. for $C_{14}H_{10}BNO_2F_3$ $[M+H]^+$ 292.0757, found 292.0750.

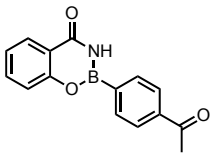

2-(4-Acetylphenyl)-1,3,2-benzoxazaborininone (**2.93**). Obtained as a white solid by procedure C (398 mg, 75%, 2.0 mmol scale); mp: 236-238 °C; ^{1}H NMR

($CDCl_3$, 500.4 MHz): δ 8.21 (dd, *J* = 7.8, 1.7 Hz, 1H), 8.06 (dd, *J* = 10.3, 8.5 Hz, 4H), 7.91 (s, 1H), 7.69 (td, *J* = 7.8, 1.7 Hz, 1H), 7.42 (d, *J* = 8.2 Hz, 1H), 7.34 (t, *J* = 7.5 Hz, 1H), 2.67 (s, 3H) ppm; ^{13}C {^1H} NMR ($CDCl_3$, 125.8 MHz): δ 197.9, 164.7, 155.6, 139.7, 135.1, 133.5, 128.5, 127.8, 124.0, 119.4, 119.1, 26.7 ppm; ^{11}B NMR (THF, 128.4 MHz): δ 31.4 ppm; IR: ν = 3158, 3100, 2985, 1687, 1673, 1402, 1258, 864, 753, 619 cm^{-1}; HRMS (ESI+) m/z calc. for $C_{15}H_{13}BNO_3$ $[M+H]^+$ 266.0988 found 266.0990.

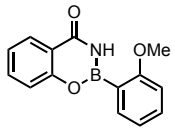

2-(2-Methoxyphenyl)-1,3,2-benzoxazaborininone (**2.94**). Obtained as a white solid by procedure B-2 after further washing with acetone (89 mg, 35%, 1.0 mmol scale) and procedure C (454 mg, 90%, 2.0 mmol scale); mp: 169-171 °C; ^1H NMR (THF-d_8, 500.4 MHz): δ 8.59 (s, 1H), 8.12 (dd, *J* = 7.8, 1.6 Hz, 1H), 8.06 (dd, *J* = 7.4, 1.6 Hz, 1H), 7.67 – 7.62 (m, 1H), 7.56 – 7.46 (m, 1H), 7.38 (dd, *J* = 8.3, 0.6 Hz, 1H), 7.27 (t, *J* = 7.5 Hz, 1H), 7.06 (t, *J* = 7.4 Hz, 2H), 3.97 (s, 3H) ppm; ^{13}C {^1H} NMR (THF-d_8, 125.8 MHz): δ 165.2, 163.0, 155.9, 135.6, 134.0, 133.4, 127.9, 123.0, 120.2, 118.6, 110.2, 54.6 ppm; ^{11}B NMR (THF-d_8, 128.4 MHz): δ 31.4 ppm; IR: ν = 3397, 1694, 1598, 1468, 1420, 1365, 1243, 767, 752 cm^{-1}; HRMS (ESI+) m/z calc. for $C_{14}H_{13}BNO_3$ $[M+H]^+$ 254.0988, found 254.0981.

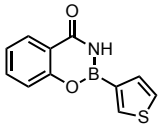

2-(Thiophen-3-yl)-1,3,2-benzoxazaborininone (**2.95**). Obtained as a white solid by procedure B-2 after further washing with acetone (44 mg, 19%, 1.0 mmol scale) and procedure C (408 mg, 89%, 2.0 mmol scale); mp: 215-217 °C; ^{1}H NMR ($CDCl_3$, 500.4 MHz): δ 8.24 – 8.18 (m, 2H), 8.11 (s, 1H), 7.70 – 7.63 (m, 1H), 7.60 (dd, *J* = 4.8, 0.9 Hz, 1H), 7.50 (dd, *J* = 4.8, 2.7 Hz, 1H), 7.38 (d, *J* = 8.3 Hz, 1H), 7.31 (t, *J* = 7.5 Hz, 1H) ppm; ^{13}C {^{1}H} NMR ($CDCl_3$, 125.8 MHz): δ 165.3, 155.9, 136.5, 134.9, 130.7, 128.4, 126.4, 123.6, 119.4, 119.0 ppm; ^{11}B NMR ($CDCl_3$, 128.4 MHz): δ 29.7 ppm; IR: ν = 3163, 3102, 1679, 1469, 1385, 1263, 1244, 760, 662 cm^{-1}; HRMS (ESI+) m/z calc. for $C_{11}H_9BNO_2S$ $[M+H]^+$ 230.0447, found 230.0463.

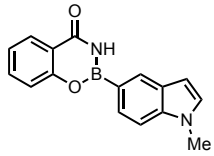

2-(1-Methyl-1H-indol-5-yl)-1,3,2-benzoxazaborininone (**2.96**). Obtained as a beige solid by procedure B-2 after recrystallization from $CHCl_3$ (41 mg, 15%, 1.0 mmol scale) and procedure C (528 mg, 95%, 2.0 mmol scale); mp: 244-246 °C; ^{1}H NMR ($CDCl_3$, 500.4 MHz): δ 8.27 (s, 1H), 8.19 (dd, *J* = 7.8, 1.7 Hz, 1H), 7.75 (d, *J* = 8.3 Hz, 1H), 7.70 – 7.62 (m, 2H), 7.43 (dd, *J* = 12.4, 8.3 Hz, 2H), 7.28 (t, *J* = 7.5 Hz, 1H), 7.12 (d, *J* = 3.1 Hz, 1H), 6.61 (s, 1H), 3.85 (s, 3H) ppm; ^{13}C {^{1}H} NMR ($CDCl_3$, 125.8 MHz): δ 165.0, 156.1, 139.0, 134.7, 129.5, 128.5, 128.3, 127.4, 125.8, 123.3, 119.4, 119.0, 109.2, 101.9, 32.8 ppm; ^{11}B NMR ($CDCl_3$, 128.4 MHz): δ 29.9 ppm; IR: ν = 3210, 2185, 3097, 1680, 1601, 1372, 1242, 1184, 1177, 759, 622, 598 cm^{-1}; HRMS (ESI+) m/z calc. for $C_{16}H_{14}BN_2O_2$ $[M+H]^+$ 277.1148, found 277.1157.

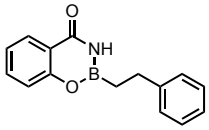

2-Phenethyl--1,3,2-benzoxazaborininone (**2.97**). Obtained as a white solid by procedure B-2 after further washing with acetone (75 mg, 30%, 1.0 mmol scale); mp: 115-116 °C; ^{1}H NMR ($CDCl_3$, 500.4 MHz): δ 8.13 (dd, *J* = 7.8, 1.6 Hz, 1H), 7.65 – 7.59 (m, 1H), 7.40 (s, 1H), 7.33 – 7.25 (m, 6H), 7.21 (t, *J* = 7.2 Hz, 1H), 2.93 (t, *J* = 8.1 Hz, 2H), 1.53 (t, *J* = 8.1 Hz, 2H) ppm; ^{13}C {^{1}H} NMR ($CDCl_3$, 125.8 MHz): δ 164.6, 155.7, 143.2, 134.7, 128.4, 128.3, 127.8, 125.9, 123.5, 119.3, 118.8, 29.4 ppm; ^{11}B NMR (acetonitrile, 128.4 MHz): δ 32.7 ppm; IR: ν = 3105, 2928, 1688, 1468, 1373, 1348, 752, 731, 699 cm^{-1}; HRMS (CI) m/z calc. for $C_{15}H_{15}BNO_2$ $[M+H]^+$ 252.1196, found 252.1194.

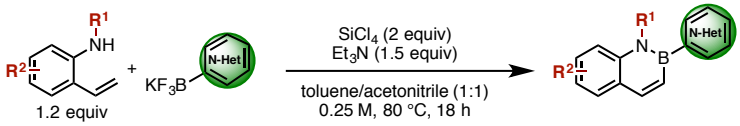

General procedure for synthesis of nitrogen-containing heteroaryl-2,1-borazaronaphthalenes: Potassium heteroaryltrifluoroborate (1.0 equiv) was introduced into a microwave vial with a stirring bar. The vial was sealed with a Teflon-coated septum cap, then evacuated and purged with N_2 four times. An MeCN/toluene mixture (0.25 M, 1:1, *v*/*v*) and 2-aminostyrene (1.2 equiv) were introduced *via* syringe, followed by NEt_3 (1.5 equiv) and $SiCl_4$ (2.0 equiv). The resulting suspension was heated to 80 °C under vigorous stirring for 18 h. The vial was then cooled to rt, and the reaction mixture was neutralized by using saturated

$NaHCO_3$ aqueous solution. The resulting solid was filtered off, and the remaining solution was extracted with EtOAc/H_2O, dried ($MgSO_4$) and concentrated under vacuum. The crude material was purified through a short plug of silica and flushed with hexanes/EtOAc mixture (20 times solvent volume, 4:1, *v*/*v*). Solvents were removed *in vacuo* to obtain a crude material that was further purified by automated column chromatography on silica gel or basic alumina, eluting with a gradient method of CH_2Cl_2 and hexanes, starting at 100% hexanes to 10:90 hexanes/CH_2Cl_2.

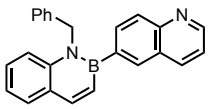

1-Benzyl-2-(quinolin-6-yl)-2,1-borazaronaphthalene (**2.122**). Purified on silica gel and obtained as a white solid (131.0 mg, 76%, 0.5 mmol scale); mp: 105-106 °C; ^{1}H NMR ($CDCl_3$, 500.4 MHz): δ 8.89-8.90 (m, 1H), 8.17-8.20 (d, *J* = 11.3 Hz, 1H), 8.02-8.06 (m, 2 H), 7.95 (s, 1H), 7.86-7.88 (d, *J* = 8.4 Hz, 1H), 7.74-7.75 (d, *J* = 7.6 Hz, 1H), 7.30-7.39 (m, 5H), 7.22-7.26 (m, 2H), 7.10-7.15 (m, 3H), 5.46 (s, 2H) ppm; ^{13}C {^{1}H} NMR ($CDCl_3$, 125.8 MHz): δ 150.4, 148.1, 145.7, 141.1, 139.0, 136.2, 133.4, 132.4, 130.4, 128.8, 128.8, 128.3, 127.8, 127.4, 127.0, 125.7, 121.3, 121.0, 117.0, 52.6 ppm; ^{11}B NMR ($CDCl_3$, 128.4 MHz): δ 36.7 ppm; IR: ν = 1605, 1588, 1547, 1492, 1455, 1410, 1353, 1229, 1181, 1143, 1118, 982, 840, 814, 798, 765, 748, 698, 476, 465 cm^{-1}; HRMS (ESI+) m/z calc. for $C_{24}H_{19}BN_2Na$ $[M + Na]^+$ 369.1539, found 369.1547.

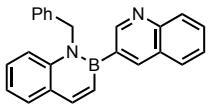

1-Benzyl-2-(quinolin-3-yl)-2,1-borazaronaphthalene (**2.123**). Purified on silica gel and obtained as a white solid (140.8 mg, 81%, 0.5 mmol scale); mp: 94-95 °C; ^{1}H

NMR ($CDCl_3$, 500.4 MHz): δ 9.07 (s, 1 H), 8.27 (s, 1H), 8.20-8.22 (d, *J* = 11.3 Hz, 1H), 8.07-8.09 (d, *J* = 8.5 Hz, 1H), 7.75-7.76 (d, *J* = 7.6 Hz, 1H), 7.68-7.70 (m, 2H), 7.48-7.51 (t, *J* = 8 Hz, 1H), 7.39-7.40 (m, 2H), 7.32-7.29 (m, 2H), 7.26-7.23 (m, 2H), 7.15-7.12 (m, 3H), 5.48 (s, 2H) ppm; ^{13}C {^1H} NMR ($CDCl_3$, 125.8 MHz): δ 153.7, 147.7, 146.0, 141.2, 140.7, 138.7, 130.5, 129.5, 129.2, 128.9 (2 x C), 128.0, 127.7, 127.4, 127.1, 126.4, 125.6, 121.5, 117.0, 52.6 ppm; ^{11}B NMR ($CDCl_3$, 128.4 MHz): δ 36.1 ppm; IR: ν = 1608, 1593, 1550, 1491, 1452, 1415, 1347, 1282, 1226, 943, 913, 856, 812, 789, 761, 731, 695, 477 cm^{-1}; HRMS (ESI+) m/z calc. for $C_{24}H_{19}BN_2Na$ $[M + Na]^+$ 369.1539, found 369.1534.

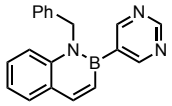

1-Benzyl-2-(pyrimidin-5-yl)-2,1-borazaronaphthalene (**2.124**). Purified on silica gel and obtained as a brown solid (86.2 mg, 58%, 0.5 mmol scale); mp: 123-124 °C; ^1H NMR ($CDCl_3$, 500.4 MHz): δ 9.18 (s, 1H), 8.82 (s, 2H), 8.21-8.23 (d, *J* = 11.3 Hz, 1H), 7.75-7.76 (d, *J* = 7.5 Hz, 1H), 7.40 (m, 2H), 7.24-7.31 (m, 4H), 7.08-7.09 (d, *J* = 7.5 Hz, 2H), 7.03-7.05 (d, *J* = 11.3 Hz, 1H), 5.40 (s, 2H) ppm; ^{13}C {^1H} NMR ($CDCl_3$, 125.8 MHz): δ 160.1, 158.2, 146.6, 140.9, 138.0, 130.6, 129.2, 129.0, 127.4, 127.3, 125.3, 121.8, 116.9, 52.5 ppm; ^{11}B NMR ($CDCl_3$, 128.4 MHz): δ 34.9 ppm; IR: ν = 1611, 1592, 1568, 1543, 1493, 1452, 1403, 1354, 1280, 1251, 1218, 1138, 962, 810, 762, 725, 695, 638, 482, 463 cm^{-1}; HRMS (ESI+) m/z calc. for $C_{19}H_{17}BN_3$ $[M + H]^+$ 298.1516, found 298.1508.

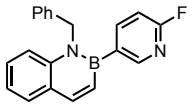

1-Benzyl-2-(6-fluoropyridin-3-yl)-2,1-borazaronaphthalene (**2.125**). Purified on silica gel and obtained as a brown solid (70.3 g, 45%, 0.5 mmol scale); mp: 93-94 °C; ^{1}H NMR ($CDCl_3$, 500.4 MHz): δ 8.34 (d, *J* = 1.85 Hz, 1H), 8.17-8.15 (d, *J* = 11.3 Hz, 1H), 7.88-7.84 (td, *J* = 8.5, 2.1 Hz, 1H), 7.73-7.72 (d, *J* = 7.6 Hz, 1H), 7.37-7.36 (m, 2H), 7.31-7.28 (t, *J* = 7.2 Hz, 2H), 7.25-7.21 (m, 2H), 7.09-7.08 (d, *J* = 7.3 Hz, 2H), 7.02-7.00 (d, *J* = 11.3 Hz, 1H), 6.87-6.85 (dd, *J* = 8.2, 2.3 Hz, 1H), 5.38 (s, 2H) ppm; ^{13}C {^{1}H} NMR ($CDCl_3$, 125.8 MHz): δ 163.8 (d, *J* = 239.7 Hz), 151.3 (d, *J* = 13.5 Hz), 146.1, 145.2 (d, *J* = 7.3 Hz), 141.0, 138.4, 130.4, 129.0 (2 x C), 127.3, 127.1, 125.4, 121.5, 116.9, 108.8 (d, *J* = 35.3 Hz), 52.4 ppm; ^{19}F {^{1}H} NMR ($CDCl_3$, 470.8 MHz): δ -68.5 ppm; ^{11}B NMR ($CDCl_3$, 128.4 MHz): δ 35.6 ppm; IR: ν = 1611, 1575, 1550, 1482, 1451, 1412, 1346, 1277, 1233, 1146, 1056, 964, 834, 805, 761, 727, 695, 645, 478, 463 cm^{-1}; HRMS (ESI+) m/z calc. for $C_{20}H_{17}BN_2F$ $[M + H]^+$ 315.1469, found 315.1458.

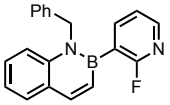

1-Benzyl-2-(2-fluoropyridin-3-yl)-2,1-borazaronaphthalene (**2.126**). Purified on silica gel and obtained as a yellow solid (122.3 mg, 78%, 0.5 mmol scale); mp: 108-109 °C; ^{1}H NMR ($CDCl_3$, 500.4 MHz): δ 8.18-8.19 (dd, *J* = 4.5, 2.0 Hz, 1H), 8.15-8.13 (d, *J* = 11.3 Hz, 1H), 7.76-7.70 (m, 2H), 7.39-7.33 (m, 2H), 7.24-7.17 (m, 4H), 7.10-7.07 (m, 1H), 7.04-7.03 (d, *J* = 7.7 Hz, 2H), 7.00-6.98 (d, *J* = 11.3 Hz, 1H), 5.33 (s, 2H) ppm; ^{13}C {^{1}H} NMR ($CDCl_3$, 125.8 MHz): δ 164.5 (d, *J* = 235.2 Hz), 147.7 (d, *J* = 14.5 Hz), 145.9, 144.7 (d, *J* = 8.5 Hz), 140.8, 138.2, 130.4, 128.8, 128.7, 127.4, 127.0,

125.5, 121.5, 121.0 (d, J = 3.8 Hz), 117.0, 52.6 ppm; ^{19}F {^{1}H} NMR ($CDCl_3$, 470.8 MHz): δ -58.1 ppm; ^{11}B NMR ($CDCl_3$, 128.4 MHz): δ 35.1 ppm; IR: ν = 1609, 1592, 1549, 1494, 1416, 1400, 1367, 1350, 1286, 1244, 1219, 1192, 962, 804, 764, 750, 744, 734, 706, 696 cm^{-1}; HRMS (ESI+) m/z calc. for $C_{20}H_{16}BN_2FNa$ $[M + Na]^+$ 337.1288, found 337.1285.

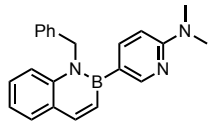

1-Benzyl-2-(4-(N,N-dimethylamino)pyridin-5-yl)-2,1-borazaronaphthalene (**2.127**). Purified on silica gel and obtained as a pale yellow solid (28.9 mg, 17%, 0.5 mmol scale); mp: 139-140 °C; ^{1}H NMR ($CDCl_3$, 500.4 MHz): δ 8.43 (m, 1H), 8.09-8.07 (d, J = 11.4 Hz, 1H), 7.67-7.65 (d, J = 8.4 Hz, 1H), 7.62-7.60 (dd, J = 8.6, 2.2 Hz, 1H), 7.31-7.27 (m, 4H), 7.23-7.20 (m, 1H), 7.17-7.14 (m, 3H), 7.09-7.07 (d, J = 11.4 Hz, 1H), 6.48-6.46 (dd, J = 8.6, 0.7 Hz, 1H), 5.47 (s, 2H), 3.07 (s, 6H) ppm; ^{13}C {^{1}H} NMR ($CDCl_3$, 125.8 MHz): δ 159.0, 152.8, 145.0, 142.2, 141.5, 139.2, 130.2, 128.9, 128.4, 127.3, 126.9, 125.7, 120.8, 116.9, 105.4, 52.5, 37.9 ppm; ^{11}B NMR ($CDCl_3$, 128.4 MHz): δ 34.0 ppm; IR: ν = 1588, 1549, 1510, 1495, 1453, 1412, 1385, 1344, 1272, 1242, 1223, 1145, 953, 805, 765, 759, 737, 730, 694, 478 cm^{-1}; HRMS (ESI+) m/z calc. for $C_{22}H_{23}BN_3$ $[M + H]^+$ 340.1985, found 340.1989.

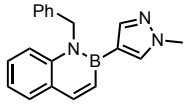

1-Benzyl-2-(1-methyl-1H-pyrazol-4-yl)-2,1-borazaronaphthalene (**2.128**). Purified on silica gel and obtained as a yellow solid (80.7 mg, 54%, 0.5 mmol scale);

mp: 116-117 °C; ^{1}H NMR ($CDCl_3$, 500.4 MHz): δ 8.05-8.03 (d, *J* = 11.5 Hz, 1H), 7.69 (s, 1H), 7.65-7.64 (d, *J* = 7.5 Hz, 1H), 7.46 (s, 1H), 7.33-7.30 (m, 4H), 7.26-7.24 (m, 1H), 7.20-7.19 (d, *J* = 7.5 Hz, 2H), 7.17-7.11 (m, 2H), 5.51 (s, 2H), 3.88 (s, 3H) ppm; ^{13}C {^{1}H} NMR ($CDCl_3$, 125.8 MHz): δ 145.0, 144.8, 141.9, 138.6, 135.4, 130.1, 129.0, 128.5, 127.0, 127.0, 125.8, 120.7, 116.2, 52.6, 38.6 ppm; ^{11}B NMR ($CDCl_3$, 128.4 MHz): δ 33.4 ppm; IR: ν = 1604, 1591, 1548, 1533, 1487, 1460, 1411, 1376, 1347, 1327, 1299, 1218, 1177, 934, 896, 808, 761, 730, 696, 674 cm^{-1}; HRMS (ESI+) m/z calc. for $C_{19}H_{18}BN_3Na$ $[M + Na]^+$ 322.1491, found 322.1470.

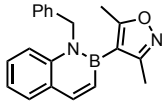

1-Benzyl-2-(3,5-dimethylisoxazole-4-yl)-2,1-borazaronaphthalene (**2.129**). Purified on silica gel and obtained as a pale yellow solid (83.0 mg, 53%, 0.5 mmol scale); mp: 110-111 °C; ^{1}H NMR ($CDCl_3$, 500.4 MHz): δ 8.14-8.12 (d, *J* = 11.3 Hz, 1H), 7.73-7.71 (d, *J* = 7.7 Hz, 1H), 7.45-7.35 (m, 2H), 7.23-7.20 (m, 3H), 7.18-7.15 (m, 1H), 6.97-6.96 (d, *J* = 7.4 Hz, 2H), 6.93-6.91 (d, *J* = 11.3 Hz, 1H), 5.36 (s, 2H), 2.20 (s, 3H), 2.15 (s, 3H) ppm; ^{13}C {^{1}H} NMR ($CDCl_3$, 125.8 MHz): δ 169.8, 162.0, 145.8, 141.1, 138.1, 130.4, 128.7, 128.6, 127.4, 127.0, 125.6, 121.5, 117.0, 52.2, 12.8, 12.2 ppm; ^{11}B NMR ($CDCl_3$, 128.4 MHz): δ 34.6 ppm; IR: ν = 1589, 1547, 1492, 1415, 1402, 1356, 1288, 1259, 1209, 1133, 1055, 1028, 958, 896, 818, 769, 733, 697, 481, 468 cm^{-1}; HRMS (ESI+) m/z calc. for $C_{20}H_{20}BN_2O$ $[M + H]^+$ 315.1669, found 315.1674.

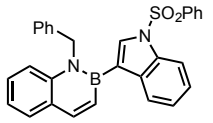

1-Benzyl-2-(1-(phenylsulfonyl)-1H-indol-3-yl)-2,1-borazaronaphthalene (**2.130**). Purified on silica gel and obtained as a white solid (53.4 mg, 23%, 0.5 mmol scale); mp: 74-75 °C; ^{1}H NMR ($CDCl_3$, 500.4 MHz): δ 8.15-8.13 (d, *J* = 11.4 Hz, 1H), 8.03-8.01 (d, *J* = 8.3 Hz, 1H), 7.74-7.69 (m, 3H), 7.58-7.57 (d, *J* = 7.9 Hz, 1H), 7.49-7.46 (td, *J* = 7.5, 1.0 Hz, 1H), 7.41-7.38 (m, 3H), 7.35-7.32 (m, 5H), 7.30-7.27 (m, 1H), 7.24-7.20 (m, 2H), 7.14-7.11 (d, *J* = 11.3 Hz, 1H), 7.10-7.08 (d, *J* = 7.35 Hz, 2H), 5.41 (s, 2H) ppm; ^{13}C {^{1}H} NMR ($CDCl_3$, 125.8 MHz): δ 145.4, 141.6, 138.9, 138.3, 135.6, 134.5, 133.6, 130.4, 129.1, 128.9, 128.9, 128.7, 127.3, 127.1, 126.7, 125.6, 124.4, 123.3, 122.4, 121.3, 116.9, 113.5, 52.7 ppm; ^{11}B NMR ($CDCl_3$, 128.4 MHz): δ 34.0 ppm; IR: ν = 1609, 1592, 1551, 1445, 1412, 1368, 1175, 1130, 1087, 1021, 984, 809, 765, 746, 726, 686, 596, 587, 569, 551 cm^{-1}; HRMS (ESI+) m/z calc. for $C_{29}H_{24}BN_2O_2S$ $[M + H]^+$ 475.1652, found 475.1645.

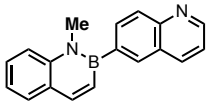

1-Methyl-2-(quinolin-6-yl)-2,1-borazaronaphthalene (**2.131**). Purified by basic alumina column and obtained as a pale yellow oil (48.0 mg, 36%, 0.5 mmol scale); ^{1}H NMR ($CDCl_3$, 500.4 MHz): δ 9.30 (s, 1H), 8.44-8.43 (d, *J* = 5.9 Hz, 1H), 8.13-8.11 (d, *J* = 11.3 Hz, 1H), 7.99-7.98 (d, *J* = 8.2 Hz, 1H), 7.79-7.77 (t, *J* = 6.2 Hz, 2H), 7.68-7.60 (m, 3H), 7.48-7.47 (d, *J* = 5.8 Hz, 1H), 7.35-7.32 (t, *J* = 7.6 Hz, 1H), 6.96-6.94 (d, *J* = 11.3 Hz, 1H), 3.54 (s, 3H) ppm; ^{13}C {^{1}H} NMR ($CDCl_3$, 125.8 MHz): δ 153.1,

145.0, 142.8, 142.2, 137.7, 134.4, 130.4, 128.9, 128.4, 127.2, 127.0, 126.8, 121.7, 121.4, 115.1, 37.1 ppm; ^{11}B NMR ($CDCl_3$, 128.4 MHz): δ 36.6 ppm; IR: ν = 1608, 1590, 1549, 1455, 1409, 1336, 1289, 1266, 1238, 1215, 1174, 1135, 1101, 1044, 830, 805, 760, 734, 674, 480 cm^{-1}; HRMS (ESI+) m/z calc. for $C_{18}H_{16}BN_2$ $[M + H]^+$ 271.1407, found 271.1400.

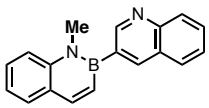

1-Methyl-2-(quinolin-3-yl)-2,1-borazaronaphthalene (**2.132**). Purified by basic alumina column and obtained as a yellow solid (65.1 mg, 48%, 0.5 mmol scale); mp: 101-102 °C; ^{1}H NMR ($CDCl_3$, 500.4 MHz): δ 9.16 (s, 1H), 8.39 (s, 1H), 8.17-8.11 (m, 2H), 7.87-7.85 (d, *J* = 8.1 Hz, 1H), 7.75-7.72 (m, 2H), 7.67-7.62 (m, 1H), 7.22-7.65 (m, 2H), 7.33-7.30 (m, 1H), 7.04-7.01 (d, *J* = 11.3 Hz, 1H), 3.78 (s, 3H) ppm; ^{13}C {^{1}H} NMR ($CDCl_3$, 125.8 MHz): δ 154.2, 147.6, 145.3, 142.2, 141.1, 130.3, 129.4, 129.2, 128.9, 127.9, 127.8, 126.9, 126.4, 121.3, 115.1, 36.9 ppm; ^{11}B NMR ($CDCl_3$, 128.4 MHz): δ 35.4 ppm; IR: ν = 1608, 1590, 1549, 1483, 1409, 1343, 1316, 1288, 1215, 1190, 1141, 1120, 1023, 947, 912, 807, 788, 753, 693, 484 cm^{-1}; HRMS (ESI+) m/z calc. for $C_{18}H_{16}BN_2$ $[M + H]^+$ 271.1407, found 271.1409.

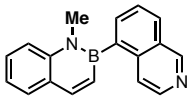

2-(Isoquinolin-5-yl)-1-methyl-2,1-borazaronaphthalene (**2.133**). Purified by basic alumina column and obtained as a yellow oil (43.1 mg, 32%, 0.5 mmol scale); ^{1}H NMR ($CDCl_3$, 500.4 MHz): δ 9.30 (s, 1H), 8.44-8.43 (d, *J* = 5.8 Hz, 1H), 8.14-8.11 (d, *J* = 11.3 Hz, 1H), 8.00-7.98 (d, *J* = 8.2 Hz, 1H), 7.79-7.77 (t, *J* = 5.6 Hz, 2H), 7.68-7.60

(m, 3H), 7.48-7.47 (d, *J* = 5.9 Hz, 1H), 7.35-7.32 (t, *J* = 7.0 Hz, 1H), 6.96-6.94 (d, *J* = 11.3 Hz, 1H), 3.55 (s, 3H) ppm; ^{13}C {^{1}H} NMR ($CDCl_3$, 125.8 MHz): δ 153.1, 145.0, 142.7, 142.2, 137.7, 134.4, 130.4, 128.9, 128.4, 127.2, 127.1, 126.8, 121.6, 121.4, 115.1, 37.1 ppm; ^{11}B NMR ($CDCl_3$, 128.4 MHz): δ 36.5 ppm; IR: ν = 1608, 1590, 1550, 1455, 1445, 1424, 1409, 1336, 1289, 1238, 1215, 1174, 1135, 1101, 1044, 830, 805, 760, 739, 674 cm^{-1}; HRMS (ESI+) m/z calc. for $C_{18}H_{16}BN_2$ $[M + H]^+$ 271.1407, found 271.1389.

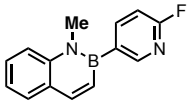

2-(6-Fluoropyridin-3-yl)-1-methyl-2,1-borazaronaphthalene (**2.134**). Purified by basic alumina column and obtained as a brown oil (21.5 g, 18%, 0.5 mmol scale); ^{1}H NMR ($CDCl_3$, 500.4 MHz): δ 8.43 (s, 1H), 8.10-8.08 (d, *J* = 11.3 Hz, 1H), 8.02-7.08 (td, *J* = 8.4, 2.1 Hz, 1H), 7.74-7.72 (d, *J* = 7.7 Hz, 1H), 7.65-7.58 (m, 2H), 7.32-7.29 (td, *J* = 7.8, 1.2 Hz, 1H), 7.02-7.00 (dd, *J* = 8.2, 2.6 Hz, 1H), 6.92-6.90 (d, *J* = 11.3 Hz, 1H), 3.72 (s, 3H) ppm; ^{13}C {^{1}H} NMR ($CDCl_3$, 125.8 MHz): δ 163.7 (d, *J* = 239.3 Hz), 151.7 (d, *J* = 13.3 Hz), 145.9 (d, *J* = 7.1 Hz), 145.4, 142.1, 130.4, 129.0, 126.9, 121.4, 115.2, 108.9 (d, *J* = 35.3 Hz), 36.7 ppm; ^{19}F {^{1}H} NMR ($CDCl_3$, 470.8 MHz): δ -68.9 ppm; ^{11}B NMR ($CDCl_3$, 128.4 MHz): δ 35.0 ppm; IR: ν = 1608, 1581, 1552, 1482, 1470, 1444, 1412, 1342, 1289, 1241, 1213, 1123, 984, 853, 830, 802, 763, 740, 633, 486 cm^{-1}; HRMS (ESI+) m/z calc. for $C_{14}H_{13}BN_2F$ $[M + H]^+$ 239.1156, found 239.1161.

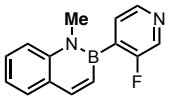

2-(3-Fluoropyridin-4-yl)-1-methyl-2,1-borazaronaphthalene (**2.135**). Purified by basic alumina column and obtained as a brown solid (65.1 mg, 55%, 0.5 mmol scale); mp: 97-98 °C; ^{1}H NMR ($CDCl_3$, 500.4 MHz): δ 8.49 (s, 1H), 8.47-8.46 (dd, *J* = 4.6, 2.3 Hz, 1H), 8.12-8.10 (d, *J* = 11.3 Hz, 1H), 7.75-7.73 (dd, *J* = 7.7, 1.2 Hz, 1H), 7.66-7.64 (d, *J* = 8.4 Hz, 1H), 7.62-7.59 (td, *J* = 6.9, 1.4 Hz, 1H), 7.39-7.37 (t, *J* = 4.8 Hz, 1H), 7.33-7.30 (td, *J* = 7.8, 0.8 Hz, 1H), 6.90-6.87 (d, *J* = 11.3 Hz, 1H), 3.63 (s, 3H) ppm; ^{13}C {^{1}H} NMR ($CDCl_3$, 125.8 MHz): δ 160.7 (d, *J* = 250.6 Hz), 145.7, 144.9 (d, *J* = 3.0 Hz), 141.8, 137.5 (d, *J* = 27.1 Hz), 130.4, 129.1, 128.3 (d, *J* = 5.6 Hz), 127.0, 121.6, 115.1, 37.1 ppm; ^{19}F {^{1}H} NMR ($CDCl_3$, 470.8 MHz): δ -118.8 ppm; ^{11}B NMR ($CDCl_3$, 128.4 MHz): δ 33.2 ppm; IR: ν = 1611, 1586, 1552, 1442, 1410, 1346, 1282, 1237, 1202, 1054, 1001, 842, 798, 755, 664, 586, 574, 548, 525, 482 cm^{-1}; HRMS (ESI+) m/z calc. for $C_{14}H_{13}BN_2F$ $[M + H]^+$ 239.1156, found 239.1166.

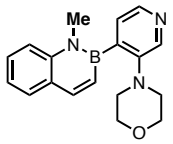

1-Methyl-2-(2-(morpholino)pyridin-3-yl)-2,1-borazaronaphthalene (**2.136**). Purified by basic alumina column and obtained as a colorless oil (102.1 mg, 67%, 0.5 mmol scale); ^{1}H NMR ($CDCl_3$, 500.4 MHz): δ 8.28-8.27 (dd, *J* = 4.9 2.0 Hz, 1H), 8.05-8.03 (d, *J* = 11.3 Hz, 1H), 7.70-7.69 (dd, *J* = 7.7, 1.2 Hz, 1H), 7.61-7.55 (m, 3H), 7.29-7.25 (td, *J* = 7.8, 1.3 Hz, 1H), 6.94-6.92 (d, *J* = 11.3 Hz, 1H), 6.85-6.83 (dd, *J* = 7.1, 5.0 Hz, 1H), 3.60 (s, 7H), 3.27 (s, 4H) ppm; ^{13}C {^{1}H} NMR ($CDCl_3$, 125.8 MHz): δ 156.3, 140.2, 138.3, 135.7, 135.1, 123.2, 121.8, 119.7, 114.1, 108.4, 107.9, 60.0, 42.9, 29.7 ppm; ^{11}B NMR ($CDCl_3$, 128.4 MHz): δ 34.7 ppm; IR: ν = 1609, 1590, 1572, 1551,

1455, 1408, 1364, 1335, 1286, 1231, 1217, 1116, 980, 941, 925, 908, 808, 785, 762, 728 cm^{-1}; HRMS (ESI+) m/z calc. for $C_{18}H_{21}BN_3O$ $[M + H]^+$ 306.1778, found 306.1771.

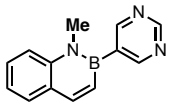

1-Methyl-2-(pyrimidin-5-yl)-2,1-borazaronaphthalene (**2.137**). Purified by basic alumina column and obtained as a brown solid (44.5 mg, 40%, 0.5 mmol scale); mp: 109-110 °C; ^1H NMR ($CDCl_3$, 500.4 MHz): δ 9.25 (s, 1H), 8.94 (s, 2H), 8.15-8.12 (d, *J* = 11.3 Hz, 1H), 7.76-7.74 (d, *J* = 7.8 Hz, 1H), 7.70-7.62 (m, 2H), 7.35-7.32 (t, *J* = 6.8 Hz, 1H), 6.95-6.92 (d, *J* = 11.3 Hz, 1H), 3.75 (s, 3H) ppm; ^{13}C $\{^1H\}$ NMR ($CDCl_3$, 125.8 MHz): δ 160.6, 157.9, 145.9, 141.9, 130.5, 129.2, 127.0, 121.7, 115.2, 36.8 ppm; ^{11}B NMR ($CDCl_3$, 128.4 MHz): δ 34.3 ppm; IR: ν = 1610, 1591, 1571, 1547, 1459, 1408, 1351, 1340, 1291, 1215, 1188, 1137, 1106, 980, 801, 754, 728, 647, 637, 484 cm^{-1}; HRMS (ESI+) m/z calc. for $C_{13}H_{13}BN_3$ $[M + H]^+$ 222.1203, found 222.1201.

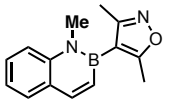

1-Methyl-2-(3,5-dimethylisoxazole-4-yl)-2,1-borazaronaphthalene (**2.138**). Purified by basic alumina column and obtained as a white solid (49.5 mg, 42%, 0.5 mmol scale); mp: 86-87 °C; ^1H NMR ($CDCl_3$, 500.4 MHz): δ 8.06-8.04 (d, *J* = 11.3 Hz, 1H), 7.73-7.72 (d, *J* = 7.7 Hz, 1H), 7.64-7.57 (m, 2H), 7.32-7.25 (td, *J* = 7.0, 1.2 Hz, 1H), 6.87-6.84 (d, *J* = 11.3 Hz, 1H), 3.65 (s, 3H), 2.37 (s, 3H), 2.26 (s, 3H) ppm; ^{13}C $\{^1H\}$ NMR ($CDCl_3$, 125.8 MHz): δ 170.3, 162.2, 145.0, 142.3, 130.3, 128.8, 126.9,

121.4, 115.1, 36.8, 12.9, 12.2 ppm; ^{11}B NMR ($CDCl_3$, 128.4 MHz): δ 33.7 ppm; IR: ν = 1591, 1551, 1463, 1444, 1415, 1404, 1360, 1336, 1291, 1279, 1253, 1217, 1207, 1131, 972, 891, 813, 767, 738, 485 cm^{-1}; HRMS (ESI+) m/z calc. for $C_{14}H_{16}BN_2O$ [M + H]$^+$ 239.1356, found 239.1354.

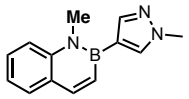

1-Methyl-2-(1-methyl-1H-pyrazol-4-yl)-2,1-borazaronaphthalene (**2.139**). Purified by basic alumina column and obtained as a brown solid (67.4 mg, 61%, 0.5 mmol scale); mp: 82-83 °C; ^{1}H NMR ($CDCl_3$, 500.4 MHz): δ 7.94-7.92 (d, *J* = 11.3 Hz, 1H), 7.84 (s, 1H), 7.64-7.61 (m, 2H), 7.54-7.48 (m, 2H), 7.23-7.18 (m, 1H), 6.98-6.95 (d, *J* = 11.4 Hz, 1H), 3.96 (s, 3H), 3.79 (s, 3H) ppm; ^{13}C {^{1}H} NMR ($CDCl_3$, 125.8 MHz): δ 144.7, 144.1, 142.6, 135.6, 129.9, 128.4, 126.5, 120.5, 114.7, 38.5, 36.5 ppm; ^{11}B NMR ($CDCl_3$, 128.4 MHz): δ 31.9 ppm; IR: ν = 1608, 1590, 1552, 1531, 1495, 1460, 1438, 1409, 1361, 1342, 1322, 1214, 1176, 1148, 1118, 940, 801, 757, 688, 677 cm^{-1}; HRMS (ESI+) m/z calc. for $C_{13}H_{15}BN_3$ [M + H]$^+$ 224.1359, found 224.1370.

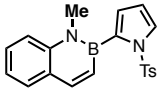

1-Methyl-2-(1-tosyl-1H-pyrrol-2-yl)-2,1-borazaronaphthalene (**2.140**). Purified by basic alumina column and obtained as a white solid (57.9 mg, 32%, 0.5 mmol scale); mp: 122-123 °C; ^{1}H NMR ($CDCl_3$, 500.4 MHz): δ 8.00-7.98 (d, *J* = 11.3 Hz, 1H), 7.71-7.69 (d, *J* = 7.6 Hz, 1H), 7.59-7.54 (m, 2H), 7.51-7.50 (d, *J* = 8.4 Hz, 2H), 7.46-7.45 (dd, *J* = 3.1, 1.4 Hz, 1H), 7.28-7.25 (m, 1H), 7.17-7.15 (d, *J* = 8.4 Hz, 2H), 6.69-6.67 (d, *J* = 11.3 Hz, 1H), 6.40-6.38 (t, *J* = 3.2 Hz, 1H), 6.30-6.29 (q, *J* = 1.5 Hz,

1H), 3.49 (s, 3H), 2.35 (s, 3H) ppm; ^{13}C {^{1}H} NMR ($CDCl_3$, 125.8 MHz): δ 144.5, 144.0, 142.1, 136.3, 130.1, 129.5, 128.6, 127.0, 126.9, 123.8, 121.0, 120.2, 115.1, 113.7, 37.3, 21.5 ppm; ^{11}B NMR ($CDCl_3$, 128.4 MHz): δ 32.8 ppm; IR: ν = 1612, 1594, 1554, 1456, 1411, 1359, 1293, 1168, 1058, 1034, 951, 807, 756, 727, 701, 672, 588, 539, 489 cm^{-1}; HRMS (ESI+) m/z calc. for $C_{20}H_{20}BN_2O_2S$ $[M + H]^+$ 363.1339, found 363.1335.

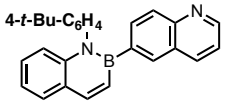

1-(4-(tert-Butyl)phenyl)-2-(quinolin-6-yl)-2,1-borazaronaphthalene (**2.141**). Purified by basic alumina column and obtained as a brown solid (167.8 mg, 87%, 0.5 mmol scale); mp: 157-158 °C; ^{1}H NMR ($CDCl_3$, 500.4 MHz): δ 8.83 (s, 1H), 8.23-8.21 (d, *J* = 11.3 Hz, 1H), 7.93-7.92 (d, *J* = 7.9 Hz, 1H), 7.83-7.81 (d, *J* = 8.3 Hz, 1H), 7.75-7.73 (d, *J* = 7.5 Hz, 1H), 7.67 (s, 1H), 7.51-7.50 (d, *J* = 8.3 Hz, 1H), 7.41-7.34 (m, 3H), 7.29-7.22 (m, 3H), 7.11-7.08 (m, 3H), 1.34 (s, 9H) ppm; ^{13}C {^{1}H} NMR ($CDCl_3$, 125.8 MHz): δ 150.5, 150.4, 147.9, 145.5, 142.8, 140.8, 136.2, 134.6, 134.4, 129.7, 128.8, 128.3, 127.6, 127.3, 126.3, 126.1, 121.3, 120.6, 117.8, 34.6, 31.4 ppm; ^{11}B NMR ($CDCl_3$, 128.4 MHz): δ 34.1 ppm; IR: ν = 1604, 1594, 1545, 1506, 1486, 1410, 1321, 1291, 1281, 1258, 1170, 1150, 894, 837, 807, 794, 770, 758, 581, 550 cm^{-1}; HRMS (ESI+) m/z calc. for $C_{27}H_{26}BN_2$ $[M + H]^+$ 389.2189, found 389.2201.

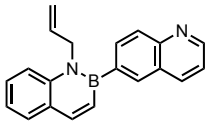

1-Allyl-2-(quinolin-6-yl)-2,1-borazaronaphthalene (**2.142**). Purified by basic alumina column and obtained as a yellow solid (33.6 mg, 23%, 0.5 mmol scale); mp: 85-86 °C; ^{1}H NMR ($CDCl_3$, 500.4 MHz): δ 9.28 (s, 1H), 8.41-8.40 (d, *J* = 5.7 Hz, 1H), 8.14-8.11 (d, *J* = 11.3 Hz, 1H), 7.98-7.96 (d, *J* = 7.9 Hz, 1H), 7.77-7.76 (d, *J* = 6.8 Hz, 2H), 7.64-7.58 (m, 2H), 7.55-7.52 (t, *J* = 7.0 Hz, 1H), 7.49-7.48 (d, *J* = 5.9 Hz, 1H), 7.31-7.28 (t, *J* = 7.6 Hz, 1H), 6.95-6.93 (d, *J* = 11.3 Hz, 1H), 5.93-5.86 (m, 1H), 5.11-5.09 (d, *J* = 10.6 Hz, 1H), 4.91-4.88 (d, *J* = 17.3 Hz, 1H), 4.71-4.67 (dd, *J* = 15.2, 2.0 Hz, 1H), 4.58-4.54 (dd, *J* = 17.2, 2.1 Hz, 1H) ppm; ^{13}C {^{1}H} NMR ($CDCl_3$, 125.8 MHz): δ 153.0, 145.2, 142.6, 141.1, 137.6, 134.9, 133.5, 130.5, 128.6, 128.4, 127.3, 127.1, 126.7, 121.7, 121.3, 116.6, 116.2, 51.0 ppm; ^{11}B NMR ($CDCl_3$, 128.4 MHz): δ 37.1 ppm; IR: ν = 1608, 1590, 1547, 1455, 1409, 1358, 1333, 1283, 1245, 1219, 1174, 1134, 1049, 937, 918, 833, 809, 761, 675, 473 cm^{-1}; HRMS (ESI+) m/z calc. for $C_{20}H_{18}BN_2$ $[M + H]^+$ 297.1563, found 297.1566.

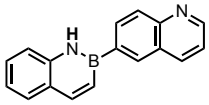

2-(Quinolin-6-yl)-2,1-borazaronaphthalene (**2.143**). Purified by basic alumina column and obtained as a white solid (84.6 mg, 66%, 0.5 mmol scale); mp: 226-227 °C; ^{1}H NMR (DMSO-d_6, 500.4 MHz): δ 10.7 (s, 1H), 8.94 (s, 1H), 8.69 (s, 1H), 8.48-8.44 (m, 2H), 8.24-8.22 (d, *J* = 11.3 Hz, 1H), 8.12-8.10 (d, *J* = 8.2 Hz, 1H), 7.80-7.73 (m, 2H), 7.59-7.51 (m, 2H), 7.42-7.40 (d, *J* = 11.1 Hz, 1H), 7.22-7.21 (m, 1H) ppm; ^{13}C {^{1}H} NMR (DMSO-d_6, 125.8 MHz): δ 150.9, 148.5, 145.5, 140.9, 136.4, 134.3, 135.6, 129.1, 128.5, 128.0, 127.7, 125.2, 121.5, 120.8, 118.7 ppm; ^{11}B NMR (Acetone-d_6,

128.4 MHz): δ 32.7 ppm; IR: ν = 1615, 1597, 1568, 1496, 1456, 1448, 1346, 1320, 1288, 1268, 1219, 1178, 1159, 872, 828, 802, 791, 765, 753 cm^{-1}; HRMS (ESI+) m/z calc. for $C_{17}H_{14}BN_2$ $[M + H]^+$ 257.1250, found 257.1245.

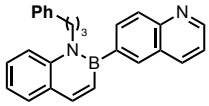

1-(3-Phenylpropyl)-2-(quinolin-6-yl)-2,1-borazaronaphthalene (**2.144**). Purified by basic alumina column and obtained as a yellow oil (39.1 mg, 21%, 0.5 mmol scale); ^1H NMR ($CDCl_3$, 500.4 MHz): δ 9.29 (s, 1H), 8.41-8.40 (d, *J* = 5.9 Hz, 1H), 8.10-8.07 (d, *J* = 11.2 Hz, 1H), 7.98-7.96 (d, *J* = 8.1 Hz, 1H), 7.76-7.71 (m, 2H), 7.64-7.61 (t, *J* = 7.0 Hz, 1H), 7.53-7.50 (t, *J* = 7.1 Hz, 1H), 7.46-7.42 (m, 2H), 7.30-7.27 (t, *J* = 7.5 Hz, 1H), 7.13-7.09 (m, 3H), 6.89-6.86 (m, 3H), 4.10-4.04 (m, 1H), 3.90-3.84 (m, 1H), 2.40-2.37 (t, *J* = 7.4 Hz, 2H), 2.03-1.94 (m, 2H) ppm; ^{13}C $\{^1H\}$ NMR ($CDCl_3$, 125.8 MHz): δ 153.0, 145.1, 142.5, 140.8, 140.7, 137.5, 133.6, 130.8, 128.7, 128.4, 128.2, 128.0, 127.5, 127.0, 126.8, 125.9, 121.6, 121.2, 115.4, 47.9, 33.0, 31.3 ppm; ^{11}B NMR ($CDCl_3$, 128.4 MHz): δ 37.0 ppm; IR: ν = 1608, 1590, 1549, 1494, 1453, 1411, 1353, 1279, 1259, 1216, 1171, 1043, 1030, 830, 806, 763, 741, 698, 674, 475 cm^{-1}; HRMS (ESI+) m/z calc. for $C_{26}H_{24}BN_2$ $[M + H]^+$ 375.2033, found 375.2031.

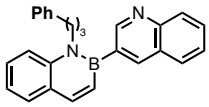

1-(3-Phenylpropyl)-2-(quinolin-3-yl)-2,1-borazaronaphthalene (**2.145**). Purified by basic alumina column and obtained as a colorless oil (65.3 mg, 35%, 0.5 mmol scale); ^1H NMR ($CDCl_3$, 500.4 MHz): δ 9.10-9.09 (d, *J* = 1.3 Hz, 1H), 8.26 (s, 1H), 8.17-8.15 (d, *J* = 8.4 Hz, 1H), 8.09-8.07 (d, *J* = 11.3 Hz, 1H), 7.82-7.80 (d, *J* = 8.1 Hz,

1H), 7.76-7.71 (m, 2H), 7.58-7.55 (t, *J* = 7.6 Hz, 1H), 7.52-7.49 (t, *J* = 7.3 Hz, 1H), 7.46-7.44 (d, *J* = 8.5 Hz, 1H), 7.27-7.23 (m, 1H), 7.12-7.09 (m, 2H), 7.06-7.05 (d, *J* = 7.1 Hz, 1H), 7.02-7.01 (d, *J* = 7.3 Hz, 2H), 6.95-6.93 (d, *J* = 11.2 Hz, 1H), 4.21-4.18 (m, 2H), 2.57-2.54 (t, *J* = 7.4 Hz, 2H), 2.16-2.10 (m, 2H) ppm; ^{13}C {^{1}H} NMR ($CDCl_3$, 125.8 MHz): δ 153.3, 147.5, 145.4, 140.7, 140.6, 140.0, 130.7, 129.3, 129.3, 128.8, 128.3, 128.1, 127.9, 127.9, 127.4, 126.4, 126.0, 121.2, 115.4, 47.5, 33.0, 31.5 ppm; ^{11}B NMR ($CDCl_3$, 128.4 MHz): δ 34.9 ppm; IR: ν = 1608, 1591, 1549, 1486, 1453, 1412, 1347, 1280, 1217, 1189, 1125, 1026, 949, 910, 808, 788, 763, 749, 698, 477 cm^{-1}; HRMS (ESI+) m/z calc. for $C_{26}H_{24}BN_2$ $[M + H]^+$ 375.2033, found 375.2045.

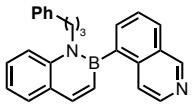

2-(Isoquinolin-5-yl)-1-(3-phenylpropyl)-2,1-borazaronaphthalene (**2.146**). Purified by basic alumina column and obtained as a colorless oil (29.3 mg, 17%, 0.5 mmol scale); ^{1}H NMR ($CDCl_3$, 500.4 MHz): δ 9.29 (s, 1H), 8.41-8.40 (d, *J* = 5.8 Hz, 1H), 8.10-8.07 (d, *J* = 11.3 Hz, 1H), 7.98-7.96 (d, *J* = 8.1 Hz, 1H), 7.76-7.71 (m, 2H), 7.64-7.61 (t, *J* = 8.1 Hz, 1H), 7.53-7.50 (td, *J* = 8.5, 1.5 Hz, 1H), 7.46-7.41 (m, 2H), 7.30-7.27 (t, *J* = 7.1 Hz, 1H), 7.13-7.09 (m, 3H), 6.89-6.86 (m, 3H), 4.10-4.04 (m, 1H), 3.90-3.84 (m, 1H), 2.41-2.38 (t, *J* = 7.4 Hz, 2H), 2.04-1.94 (m, 2H) ppm; ^{13}C {^{1}H} NMR ($CDCl_3$, 125.8 MHz): δ 153.1, 145.1, 142.6, 140.8, 140.7, 137.5, 133.6, 130.8, 128.8, 128.5, 128.2, 128.0, 127.5, 127.0, 126.8, 125.9, 121.6, 121.2, 115.4, 48.0, 33.3, 31.3 ppm; ^{11}B NMR ($CDCl_3$, 128.4 MHz): δ 36.6 ppm; IR: ν = 1608, 1590, 1548, 1453, 1411, 1352,

1259, 1216, 1171, 1134, 1106, 1042, 1030, 829, 805, 762, 740, 698, 675, 474 cm^{-1}; HRMS (ESI+) m/z calc. for $C_{26}H_{24}BN_2$ $[M + H]^+$ 375.2033, found 375.2025.

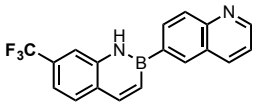

2-(Quinolin-6-yl)-7-(trifluoromethyl)-2,1-borazaronaphthalene (**2.147**). Purified by basic alumina column and obtained as a white solid (83.8 mg, 52%, 0.5 mmol scale); mp: 173-174 °C; ^1H NMR ($CDCl_3$, 500.4 MHz): δ 8.96-8.95 (dd, *J* = 4.2, 1.7 Hz, 1H), 8.43 (br s, 1H), 8.38 (s, 1H), 8.24-8.19 (m, 4H), 7.79-7.77 (d, *J* = 8.1 Hz, 1H), 7.68 (s, 1H), 7.52-7.42 (m, 3H) ppm; ^{13}C $\{^1H\}$ NMR ($CDCl_3$, 125.8 MHz): δ 151.1, 149.2, 145.1, 139.6, 136.5, 133.7, 132.6, 130.4, 130.2, 129.1, 128.1, 127.8, 121.4, 117.6, 115.5 ppm; ^{19}F $\{^1H\}$ NMR ($CDCl_3$, 470.8 MHz): δ -62.2 ppm; ^{11}B NMR ($CDCl_3$, 128.4 MHz): δ 32.7 ppm; IR: ν = 1619, 1571, 1459, 1358, 1329, 1249, 1219, 1167, 1150, 1123, 1070, 924, 835, 772 cm^{-1}; HRMS (ESI+) m/z calc. for $C_{18}H_{13}BN_2F_3$ $[M + H]^+$ 325.1124, found 325.1121.

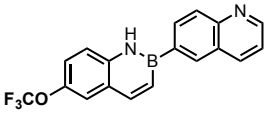

2-(Quinolin-6-yl)-6-(trifluoromethoxy)-2,1-borazaronaphthalene (**2.148**). Purified by basic alumina column and obtained as a white solid (51.4 mg, 30%, 0.5 mmol scale); mp: 204-205 °C; ^1H NMR (DMSO-d_6, 500.4 MHz): δ 10.9 (s, 1H), 8.97-8.96 (m, 1H), 8.71 (s, 1H), 8.48-8.45 (t, *J* = 8.0 Hz, 2H), 8.30-8.27 (d, *J* = 11.6 Hz, 1H), 8.14-8.12 (d, *J* = 8.5 Hz, 1H), 7.91-7.89 (d, *J* = 8.9 Hz, 1H), 7.81 (s, 1H), 7.60-7.51 (m,

3H) ppm; ^{13}C {^{1}H} NMR (DMSO-d_6, 125.8 MHz): δ 151.0, 148.6, 144.8, 141.9, 139.7, 136.4, 134.5, 133.5, 128.1, 127.7, 125.5, 121.8, 121.6, 120.7, 120.3 ppm; ^{19}F {^{1}H} NMR ($CDCl_3$, 470.8 MHz): δ -57.0 ppm; ^{11}B NMR ($CDCl_3$, 128.4 MHz): δ 32.2 ppm; IR: ν = 1572, 1457, 1251, 1225, 1205, 1177, 1156, 1123, 996, 975, 942, 899, 876, 832, 801, 767, 754, 740, 478, 463 cm^{-1}; HRMS (ESI+) m/z calc. for $C_{18}H_{13}BN_2OF_3$ [M + H]$^+$ 341.1073, found 341.1062.

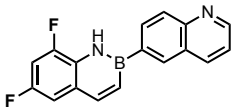

6,8-Difluoro-2-(quinolin-6-yl)-2,1-borazaronaphthalene (**2.149**). Purified by basic alumina column and obtained as a white solid (27.2 mg, 19%, 0.5 mmol scale); mp: 243-244 °C; ^{1}H NMR ($CDCl_3$, 500.4 MHz): δ 8.95-8.94 (dd, *J* = 4.2, 1.7 Hz, 1H), 8.42 (br s, 1H), 8.34 (s, 1H), 8.23-8.18 (m, 3H), 8.07-8.05 (d, *J* = 11.6 Hz, 1H), 7.48-7.45 (d, *J* = 11.6 Hz, 1H), 7.43-7.40 (dd, *J* = 8.3, 4.3 Hz, 1H), 7.15-7.14 (d, *J* = 8.8 Hz, 1H), 7.08-7.03 (td, *J* = 8.4, 2.6 Hz, 1H) ppm; ^{13}C {^{1}H} NMR ($CDCl_3$, 125.8 MHz): δ 155.9 (dd, *J* = 241.8, 11.7 Hz), 151.4 (dd, *J* = 246.3, 13.1 Hz), 151.1, 149.2, 144.2 (t, *J* = 3.7, 3.1 Hz), 136.5, 133.6, 132.6, 129.1, 128.1, 126.9 (dd, *J* = 9.5, 4.5 Hz), 125.8 (d, *J* = 12.9 Hz), 121.3, 109.3 (dd, *J* = 21.5, 3.8 Hz), 103.1 (dd, *J* = 28.3, 22.3 Hz) ppm; ^{19}F {^{1}H} NMR ($CDCl_3$, 470.8 MHz): δ -119.8, -133.0 ppm; ^{11}B NMR ($CDCl_3$, 128.4 MHz): δ 32.0 ppm; IR: ν = 1567, 1455, 1438, 1403, 1289, 1242, 1177, 1111, 1040, 978, 890, 829, 794, 769, 741, 707, 682, 647, 617, 594 cm^{-1}; HRMS (ESI+) m/z calc. for $C_{17}H_{12}BN_2F_2$ [M + H]$^+$ 293.1062, found 293.1051.

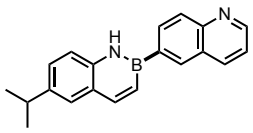

6-Isopropyl-2-(quinolin-6-yl)-2,1-borazaronaphthalene (**2.150**). Purified by basic alumina column and obtained as a white solid (85.3 mg, 58%, 0.5 mmol scale); mp: 148-149 °C; ^{1}H NMR ($CDCl_3$, 500.4 MHz): δ 8.92-8.91 (dd, *J* = 4.1, 1.7 Hz, 1H), 8.33 (m, 2H), 8.18-8.14 (m, 4H), 7.50 (s, 1H), 7.39-7.30 (m, 4H), 3.05-2.97 (m, 1H), 1.32 (s, 3H), 1.31 (s, 3H) ppm; ^{13}C {^{1}H} NMR ($CDCl_3$, 125.8 MHz): δ 150.7, 149.0, 145.8, 141.8, 138.4, 136.4, 133.2, 132.9, 128.8, 128.1, 127.4, 126.5, 125.7, 121.1, 118.2, 33.6, 24.2 ppm; ^{11}B NMR ($CDCl_3$, 128.4 MHz): δ 32.2 ppm; IR: ν = 1568, 1453, 1441, 1422, 1287, 1235, 1223, 1187, 1176, 1123, 838, 830, 822, 810, 803, 777, 755, 725, 707, 464 cm^{-1}; HRMS (ESI+) m/z calc. for $C_{20}H_{20}BN_2$ $[M + H]^+$ 299.1720, found 299.1723.

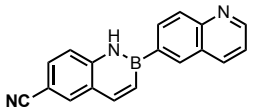

2-(Quinolin-6-yl)-6-carbonitrile-2,1-borazaronaphthalene (**2.151**). Purified by basic alumina column and obtained as a white solid (43.0 mg, 31%, 0.5 mmol scale); mp: 150-151 °C; ^{1}H NMR (DMSO-d_6, 500.4 MHz): δ 11.0 (s, 1 H), 8.97 (s,1H), 8.73 (s, 1H), 8.47-8.46 (d, *J* = 7.5 Hz, 2H), 8.32 (s, 1H), 8.29-8.26 (d, *J* = 11.6 Hz, 1H), 8.14-8.12 (d, *J* = 8.3 Hz, 1H), 7.93-7.86 (q, *J* = 23.6, 8.3 Hz, 2H), 7.60-7.54 (m, 2H) ppm; ^{13}C {^{1}H} NMR (DMSO-d_6, 125.8 MHz): δ 151.2, 148.7, 144.7, 143.7, 136.5, 134.9, 134.4, 133.5, 130.7, 128.2, 127.7, 125.1, 121.6, 119.9, 119.4, 102.9 ppm; ^{11}B NMR ($CDCl_3$, 128.4 MHz): δ 33.2 ppm; IR: ν = 2221, 1613, 1597, 1576, 1461, 1343, 1321, 1298,

1244, 1212, 1180, 1171, 900, 877, 868, 832, 797, 770, 744, 574 cm^{-1}; HRMS (ESI+) m/z calc. for $C_{18}H_{13}BN_3$ $[M + H]^+$ 282.1203, found 282.1206.

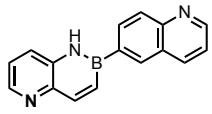

2-(Quinolin-6-yl)-6,5-borazaroquinoline (**2.152**). Purified by basic alumina column and obtained as a white solid (45.1 mg, 35%, 0.5 mmol scale); mp: 176-177 °C; ^1H NMR (DMSO-d_6, 500.4 MHz): δ 10.8 (br s, 1H), 8.95 (s, 1H), 8.72 (s, 1H), 8.54-8.46 (m, 3H), 8.33-8.30 (d, J = 11.2 Hz, 1H), 8.16-8.11 (dd, J = 16.6, 7.3 Hz, 2H), 7.71-7.69 (d, J = 10.8 Hz, 1H), 7.59-7.53 (m, 2H) ppm; ^{13}C {^1H} NMR (DMSO-d_6, 125.8 MHz): δ 151.1, 148.6, 146.6, 143.6, 142.3, 136.8, 136.5, 134.6, 133.5, 128.1, 127.7, 126.2, 123.3, 121.6 ppm; ^{11}B NMR ($CDCl_3$, 128.4 MHz): δ 32.6 ppm; IR: ν = 1598, 1567, 1460, 1445, 1374, 1353, 1321, 1264, 1240, 1219, 1194, 1182, 1116, 826, 791, 767, 741, 622, 588, 478 cm^{-1}; HRMS (ESI+) m/z calc. for $C_{16}H_{13}BN_3$ $[M + H]^+$ 258.1203, found 258.1198.

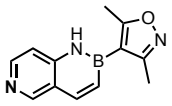

2-(3,5-Dimethylisoxazole-4yl)-6,5-borazaroisoquinoline (**2.153**). Purified by basic alumina column and obtained as a white solid (25.7 mg, 23%, 0.5 mmol scale); mp: 200-2017 °C; ^1H NMR ($CDCl_3$, 500.4 MHz): δ 8.90 (s, 1H), 8.50 (d, J = 5.7 Hz, 1H), 8.14 (d, J = 11.6 Hz, 1H), 8.06 (br s, 1H), 7.22 (d, J = 5.7 Hz, 1H), 7.15 (d, J = 11.7 Hz, 1H), 2.60 (s, 3H), 2.46 (s, 3H) ppm; ^{13}C {^1H} NMR ($CDCl_3$, 125.8 MHz): δ 174.0, 162.1, 151.8, 147.7, 144.6, 143.5, 121.4, 112.7 ppm; ^{11}B NMR ($CDCl_3$, 128.4 MHz): δ 31.7

ppm; IR: ν = 3368, 3276, 2930, 1630, 1518, 1399, 1083, 967, 823, 798 cm^{-1}; HRMS (ESI+) m/z calc. for $C_{12}H_{13}BN_3O$ $[M + H]^+$ 226.1152, found 226.1150.

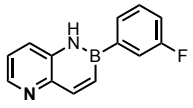

2-(3-Fluorophenyl)-6,5-borazaroquinoline (**2.154**). Purified by basic alumina column and obtained as a white solid (30.9 mg, 27%, 0.5 mmol scale); mp: 246-247 °C; ^1H NMR ($CDCl_3$, 500.4 MHz): δ 8.61-8.59 (dd, *J* = 4.4, 1.4 Hz, 1H), 8.39-8.37 (d, *J* = 11.8 Hz, 1H), 8.07 (br s, 1H), 7.70-7.67 (td, *J* = 7.9, 0.7 Hz, 2H), 7.59-7.58 (dd, *J* = 9.6, 2.5 Hz, 1H), 7.53-7.51 (dd, *J* = 11.9, 2.2 Hz, 1H), 7.48-7.44 (m, 1H), 7.41-7.38 (dd, *J* = 8.2, 4.4 Hz, 1H), 7.18-7.14 (m, 1H) ppm; ^{13}C $\{^1H\}$ NMR ($CDCl_3$, 125.8 MHz): δ 163.0 (d, *J* = 245.1 Hz), 147.1, 144.0, 143.1, 135.8, 130.0 (d, *J* = 6.9 Hz), 128.3 (d, *J* = 3.2 Hz), 125.9, 123.0, 119.0 (d, *J* = 18.8 Hz), 116.8 (d, *J* = 20.3 Hz). ^{19}F $\{^1H\}$ NMR ($CDCl_3$, 470.8 MHz): δ -113.5 ppm; ^{11}B NMR ($CDCl_3$, 128.4 MHz): δ 31.7 ppm; IR: ν = 1596, 1568, 1445, 1418, 1377, 1323, 1289, 1261, 1236, 1226, 1198, 1164, 880, 868, 825, 799, 786, 753, 746, 689 cm^{-1}; HRMS (ESI+) m/z calc. for $C_{13}H_{11}BN_2F$ $[M + H]^+$ 225.0999, found 225.1009.

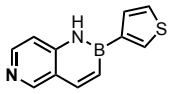

2-(Thiophen-3-yl)-6,5-borazaroisoquinoline (**2.155**). Purified by basic alumina column and obtained as a white solid (34.9 mg, 33%, 0.5 mmol scale); mp: 165-166 °C; ^1H NMR ($CDCl_3$, 500.4 MHz): δ 8.87 (s, 1H), 8.50-8.48 (d, *J* = 5.7 Hz, 1H), 8.13-8.06 (m, 2H), 7.99 (dd, *J* = 2.5, 1.0 Hz, 1H), 7.58-7.57 (dd, *J* = 4.8, 1.0 Hz, 1H), 7.50-7.49 (dd, *J* = 4.8, 2.7 Hz, 1H), 7.31-7.29 (dd, *J* = 11.6, 1.7 Hz, 1H), 7.21-7.20 (d, *J*

= 5.7 Hz, 1H) ppm; ^{13}C {^{1}H} NMR ($CDCl_3$, 125.8 MHz): δ 151.6, 147.5, 144.9, 143.3, 133.7, 130.3, 126.4, 121.9, 112.6 ppm; ^{11}B NMR ($CDCl_3$, 128.4 MHz): δ 31.1 ppm; IR: ν = 1623, 1568, 1516, 1465, 1426, 1385, 1325, 1204, 1172, 1129, 1077, 1043, 976, 939, 911, 827.8, 786, 755, 693, 557 cm^{-1}; HRMS (ESI+) m/z calc. for $C_{11}H_{10}BN_2S$ $[M + H]^+$ 213.0658, found 213.0656.

2.7 – References

1) Maitlis, P. M. *Chem. Rev.* **1962**, *62*, 223.

2) Balaban, A. T.; Oniciu, D. C.; Katritzky, A. R. *Chem. Rev.* **2004**, *104*, 2777.

3) Chinchill, R.; Nájera, C.; Yus, M. *Chem. Rev.* **2004**, *104*, 2667.

4) *Reviews on azaborines*: a) Campbell, P. G.; Marwits, A. J. V.; Liu, S.-Y. *Angew. Chem., Int. Ed.* **2012**, *51,* 6074. b) Bosdet, M. J. D.; Piers, W. E. *Can. J. Chem.* **2009**, *87*, 8. c) Bosdet, M. J. D.; Jaska, C. A.; Piers, W. E.; Sorensen, T. S.; Parvez, M. *Org. Lett.* **2007**, *9*, 1395. d) Vlasceanu, A.; Jessing, M.; Kilburn, J. P. *Bioorg. Med. Chem.* **2015**, *23*, 4453.

5) *Applications of azaborines*: a) Baldock, C.; Rafferty, J. B.; Sedelnikova, S. E.; Baker, P. J.; Stuitje, A. R.; Slabas, A. R.; Hawkes, T. R.; Rice, D. W. *Science* **1996**, *274*, 2107. b) Liu, L.; Marwitz, A. J.; Matthews, B. W.; Liu, S. Y. *Angew. Chem., Int. Ed.* **2009**, *48*, 6817. c) Zhao, P.; Nettleton, D. O.; Karki, R. G.; Zécri, F. J.; Liu, S.-L. *Chem. Med. Chem.* **2017**, *12*, 358.

6) a) Li, X.; Zhang, Y.-K.; Plattner, J. J.; Mao, W.; Alley, M.R.K.; Xia, Y.; Hernandez, V.; Zhou, Y.; Ding, C. Z.; Li, J.; Shao, Z.; Zhang, H.; Xu, M. *Bioorg. Med. Chem. Lett.* **2013**, *23*, 963. b) Nare, B.; Wring, S.; Bacchi, C.; Beaudet, B.; Bowling, T.; Brun,

R.; Chen, D.; Ding, C.; Freund, Y.; Gaukel, E.; Hussain, A.; Jarnagin, K.; Jenks, M.; Kaiser, M.; Mercer, M.; Mejia, E.; Noe, A.; Orr, M.; Parham, R.; Plattner, J.; Randolph, R.; Rattendi, D.; Rewerts, C.; Sligar, J.; Nigel Yarlett, N.; Don, R.; Jacobs, R. *Antimicrob. Agents Chemother*. **2010**, *54*, 4379.

7) a) Davie, M. C.; Franzblau, S. G.; Martin A. R. *Bioorg. Med. Chem. Lett.* **1998**, *8*, 843. b) Baker, S. J.; Ding, C. Z.; Akama, T.; Zhang, Y.-K.; Hernandez, V.; Xia, Y. *Future Med. Chem.* **2009**, *1*, 2375.

8) Kaushi, N. K.; Kaushik, N.; Attri, P.; Kumar, N.; Kim, C. H.; Verma, A. K.; Choi, E. H. *Molecules* **2013**, *18*, 6620.

9) Weber, L. *Coord. Chem. Rev.* **2008**, *252*, 1.

10) Abbey, E. R.; Zakharov, L. N.; Liu, S.-Y. *J. Am. Chem. Soc.* **2011**, *133*, 11508.

11) a) Hawthorne, M. F. *J. Am. Chem. Soc.* **1961**, *83*, 831. b) Ulmschneider, D.; Goubeau, J. *Chem. Ber.* **1957**, *90*, 2733.

12) a) Dewar, M. J. S.; Kubba, V. P.; Pettit, R. *J. Chem. Soc.* **1958**, 3073**.** b) Kaupp, G.; Naimi-Jamal, M. R.; Stepanenko, V. *Chem. Eur. J*. **2003**, *9,* 4156. c) Nyilas, E.; Soloway, A. H. *J. Am. Chem. Soc.* **1959**, *81*, 2681. d) Slabber, C. A.; Grimmer, C. D.; Robinson, R. S. *J. Organomet. Chem.* **2013**, *723*, 122. e) Goldberg, A. R.; Northrop, B. H*. J. Org. Chem.* **2016**, *81*, 969. f) Lee, Y.-S.; Cheon, C.-H. *Adv. Synth. Catal.* **2015**, *13*, 2951.

13) Molander, G. A. *J. Org. Chem.* **2015**, *80*, 7837.

14) Wisniewski, S. R.; Guenther, C. L.; Argintaru, O. A.; Molander, G. A. *J. Org. Chem.* **2014**, *79*, 365.

15) Kim, B. J.; Matteson, D. S. *Angew. Chem. Int. Ed.* **2004**, *43*, 3056.

16) a) Ramadhar, T. R.; Bansagi, J.; Batey, R. A. *J. Org. Chem.* **2013**, *78*, 1216. b) Noda H.; Bode, J. W. *J. Am. Chem. Soc.* **2015**, *137*, 3958.

17) Plumley, J. A.; Evanseck, J. D. *J. Phys. Chem. A* **2009**, *113*, 5985.

18) Bordwell, F. G.; Drucker, G. E.; Fried, H. E. *J. Org. Chem.* **1981**, *46*, 632.

19) Chrostawska, A.; Xu, S.; Maziére, A.; Bokenvitz, K.; Li, B.; Abbey, E. R.; Cargelos, A.; Graciaa, A.; Liu, S.-Y. *J. Am. Chem. Soc.* **2014**, *136*, 11813.

20) Frisch, M. J.; Trucks, G. W.; Schlegel, H. B.; Scuseria, G. E.; Robb, M. A.; Cheeseman, J. R.; Scalmani, G.; Barone, V.; Mennucci, B.; Petersson, G. A.; Nakatsuji, H.; Caricato, M.; Li, X.; Hratchian, H. P.; Izmaylov, A. F.; Bloino, J.; Zheng, G.; Sonnenberg, J. L.; Hada, M.; Ehara, M.; Toyota, K.; Fukuda, R.; Hasegawa, J.; Ishida, M.; Nakajima, T.; Honda, Y.; Kitao, O.; Nakai, H.; Vreven, T.; Montgomery, J. A., Jr.; Peralta, J. E.; Ogliaro, F.; Bearpark, M.; Heyd, J. J.; Brothers, E.; Kudin, K. N.; Staroverov, V. N.; Kobayashi, R.; Normand, J.; Raghavachari, K.; Rendell, A.; Burant, J. C.; Iyengar, S. S.; Tomasi, J.; Cossi, M.; Rega, N.; Millam, J. M.; Klene, M.; Knox, J. E.; Cross, J. B.; Bakken, V.; Adamo, C.; Jaramillo, J.; Gomperts, R.; Stratmann, R. E.; Yazyev, O.; Austin, A. J.; Cammi, R.; Pomelli, C.; Ochterski, J. W.; Martin, R. L.; Morokuma, K.; Zakrzewski, V. G.; Voth, G. A.; Salvador, P.; Dannenberg, J. J.; Dapprich, S.; Daniels, A. D.; Farkas, Ö.; Foresman, J. B.; Ortiz, J. V.; Cioslowski, J.; Fox, D. J. *Gaussian 09*, revision D.01; Gaussian, Inc.: Wallingford CT, 2009.

21) Schmidt, J.R.; Polik, W.F. *WebMO Enterprise*, version 14.0.004e; WebMO LLC: Holland, MI, USA, 2013; *http://www.webmo.net*.

22) a) Becke, A. D. *J. Chem. Phys*. **1993**, *98*, 5648. b) Lee, C.; Yang, W.; Parr, R. G. *Phys. Rev. B: Condens. Matter Mater. Phys.* **1988**, *37*, 785. c) Vosko, S. H.; Wilk, L.; Nusair, M. *Can. J. Phys.* **1980**, *58*, 1200. d) Stephens, P. J.; Devlin, F. J.; Chabalowski, C. F.; Frisch, M. J. *J. Phys. Chem*. **1994**, *98*, 11623. e) Ditchfield, R.; Hehre, W. J.; Pople, J. A. *J. Chem. Phys.* **1971**, *54*, 724. f) Hehre, W. J.; Ditchfield, R.; Pople, J. A. *J. Chem. Phys.* **1972**, *56*, 2257. g) Hariharan, P. C.; Pople, J. A. *Theor. Chim. Acta* **1973**, *28*, 213.

23) a) Clark, T.; Kranz, *J. Org. Chem.* **1992**, *57*, 5492. b) Chen, Z.; Wannere, C. S.; Corminboeuf, C.; Puchta, R.; Schleyer, P. v. R. *Chem. Rev.* **2005**, *105*, 3842.

24) Stanger, A. *Phys. Chem. Chem. Phys.* **2011**, *13*, 12652.

25) Xu, S.; Mikulas, T. C.; Zakharov, L. N.; Dixon, D. A.; Liu, S.-Y. *Angew. Chem., Int. Ed.* **2013**, *52*, 7527.

26) Davies, G. H. M.; Molander, G. A. *J. Org. Chem.* **2016**, *81*, 3771.

27) a) Yale, H. L. *J. Heterocyclic Chem.* **1971**, *8*, 193. b) Cragg, R. H.; Miller, T. J. *J. Organomet. Chem.* **1985**, *294*, 1. c) Churches, Q. I.; Hooper, J. F.; Hutton, C. A.; *J. Org. Chem.* **2015**, *80*, 5428. d) Mahdavi, M.; Asadi, M.; Saeedi, M.; Tehrani M. H.; Sara Mirfazli, S. S.; Abbas Shafiee, A.; Foroumadi A. *Synth. Commun.* **2013**, *43*, 2936. e) Ihara, H.; Koyanagi, M.; Suginome, M. *Org. Lett.* **2011**, *13*, 2662. f) Ihara, H.; Ueda, A.; Suginome, M. *Chem. Lett.* **2011**, *40*, 916. g) Koyanagi, M.; Sichenauer, N.; Ihara, H.; Yamamoto, T.; Suginome, M. *Chem. Lett.* **2013**, *42*, 541. h) Settepani, J. A.;Stokes, J. B.; Borkovec, A. *J. Med. Chem.* **1970**, *13*, 128.

28) Molander, G. A.; Cavalcanti, L. N.; Canturk, B.; Pan, P.-S.; Kennedy, L. E. *J. Org. Chem.* **2009**, *74*, 7364.

29) Ashley, J. D.; Stefanick, J. F.; Schroeder, V. A.; Suckow, M. A.; Kiziltepe, T.; Bilgicer B. *J. Med. Chem.* **2014**, *57*, 5282.

30) Murugan, K.; Chinnapattu, M.; Khan, F.-R. N.; Lyer, P. S. *RCS Adv.* **2015**, *5*, 36902.

31) a) Miertuš S. *Chem. Phys.* **1981**, *55*, 117. b) Tomasi, J.; Mennucci, B.; Cammi, R. *Chem. Rev.* **2005**, *105*, 2999.

32) *Computationally derived pK_a studies*: a) Liptak, M. D.; Shields, G. C. *J. Am. Chem. Soc.* **2001**, *123*, 7314. b) Muckerman, J. T.; Skone, J. H.; Ning, M.; Wasada-Tsutsui, Y. *Biochim. Biophys. Acta* **2013**, *1827*, 882. c) Casasnovas, R.; Fernández, D.; Ortega-Castro, J.; Frau, J.; Donoso, J.; Muñoz, F. *Theor. Chem. Acc.* **2011**, *130*, 1. d) Baggett, A. W.; Vasiliu, M.; Li, B.; Dixon, D. A.; Liu, S.-L. *J. Am. Chem. Soc.* **2015**, *137*, 5536.

33) a) Dewar, M. J. S.; Dietz, R. *J. Chem. Soc.* **1959**, 2728. b) Currel, B.R.; Gerrard, W.; Khodabocus, M. *J. Organomet. Chem.* **1967**, *8*, 411. c) Atkinson, I. B.; Clapp, D. B.; Beck, C.A.; Currell, B. R. *J. Chem. Soc., Dalton Trans.* **1972**, 182.

34) a) Molander, G. A.; Wisniewski, S. R. *J. Org. Chem.* **2014**, *79*, 6663. b) Dewar, M. J. S.; Dietz, R. *Tetrahedron* **1961**, *15*, 26.

35) Rombouts, F. J. R.; Tovar, F.; Austin, N.; Tresadern, G.; Trabanco, A. A. *J. Med. Chem.* **2015**, *58*, 9287.

36) Macarron, R.; Banks, M. N.; Bojanic, D.; Burns, D. J.; Cirovic, D. A.; Garyantes, T.; Green, D. V. S.; Herzberg, R. P.; Janzen, W. P.; Paslay, J. W.; Schopfer, U.; Sittampalam, G. S. *Nat. Rev. Drug Descov.* **2011**, *10*, 188.

37) Morrison, R. T.; Boyd, R. N. *Organic Chemistry*, 6th ed.; Prentice-Hall: Eaglewood Cliffs, New Jersey, 1992.

38) Ghosh, D.; Periyasamy, G.; Pati, S. K. *Phys. Chem. Chem. Phys.* **2011**, *13*, 20627.

39) *Reviews of N-heterocyclic influence on biological availability:* a) Bua, R.; Shrivastava, S.; Sonwane, S. K.; Srivastava, S. K. *Advan. Biol. Res.* **2011**, *5*, 120. b) Welsch, M. E.; Snyder, S. A.; Stockwell, B. R. *Curr. Opin. Chem. Biol.* **2010**, *14*, 347.

40) Casado, M. R. S.; Jiménez, M. C.; Bueno, M. A.; Barriol, M.; Leenaerts, J. E.; Pagliuca, C.; Lamenca, C. M.; Lucas A. I. D.; García, A.; Trabanco A. A.; Rombouts F. J. R. *Eur. J. Org. Chem.* **2015**, *23*, 5221.

41) a) Jolibois, H.; Doucet, A.; Dubry, J. L. J. *Inorg. Nucl. Chem. Lett.* **1976**, *12*, 759. b) Rami, T.; Hensen, K. *J. Inorg. Nucl. Chem.* **1971**, *33*, 937.

42) Martinez, C. R.; Iverson, B. L. *Chem. Sci.* **2012**, *3*, 2191.

This chapter contains adaptations with permission from the following publications:

1) Davies, G. H. M.; Molander, G. A. *J. Org. Chem.* **2016**, *81*, 3771.
2) Davies, G. H. M.; Mukhtar, A.; Fatemeh, S.; Kelly, C. B.; Molander, G. A.; *J. Org. Chem.* **2017**, *82*, 5380.
3) Davies, G. H. M.; Zhou, Z.-Z.; Jouffroy, M.; Molander, G. A. *J. Org. Chem.* **2017**, *82*, 549.

CHAPTER 3 – NEW STRATEGIES FOR FUNCTIONALIZATION OF THE 2,1-BORAZARONAPHTHALENE CORE

3.1 – Introduction

The versatility of the 2,1-borazaronaphthalene class of azaborines arises from the desymmetrization of the heterocyclic core, providing access to several modes of functionalization (Figure 3.1).[1] The Molander group's initial synthetic report demonstrates that annulation of various *o*-aminostyrene and trifluoroborate derivatives can provide diverse substitution off boron and nitrogen.[1a] Additional diversity off boron can be established utilizing halo-methyl boron derivatives in

Figure 3.1: Strategies to functionalize the 2,1-borazaronaphthalene core

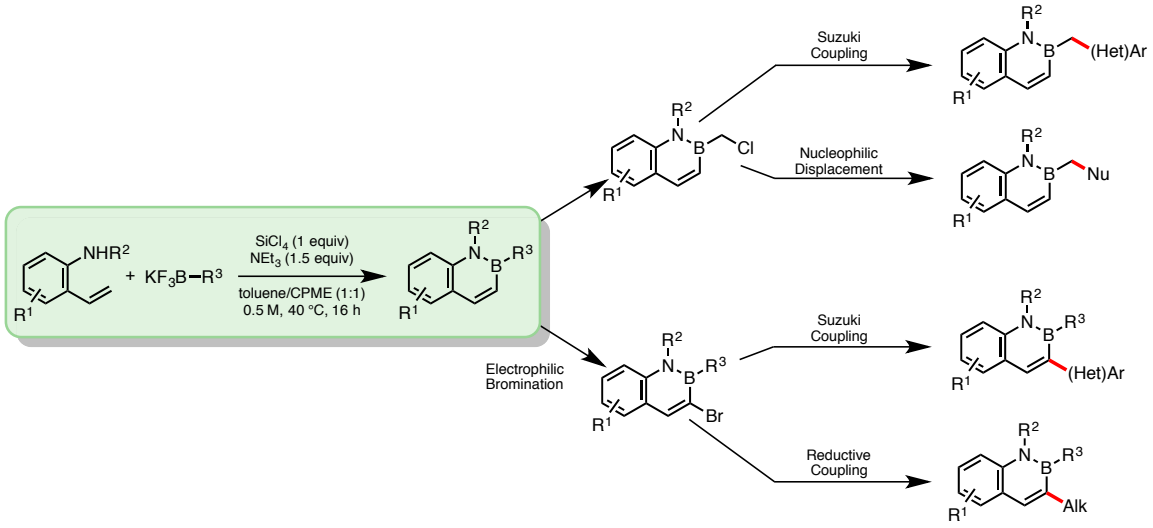

both nucleophilic substitution and cross coupling strategies.[1b,c] Based on the electronics of the ring system, selective bromination occurs at the C(3)-position followed by secondary bromination at C(6) (Figure 3.2). These brominated cores can be functionalized by both traditional cross coupling[1d,e] and reductive coupling strategies[1f] to install a myriad of functional groups. Employed in an iterative fashion,

Figure 3.2: Selectivity for bromination of 2,1-borazaronaphthalene[a]

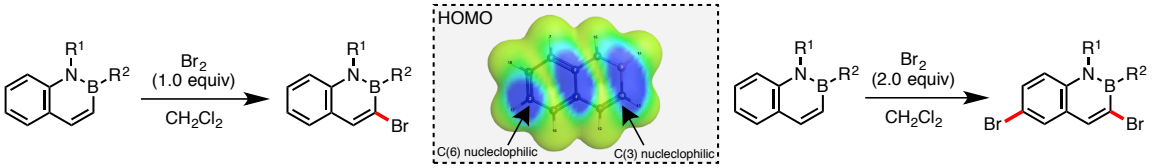

[a]HOMO electron density map generated at B3LYP/6-311+G(2d,p) level of theory[2] (from +0.251 kcal/mol to +0.063 kcal/mol) in Gaussian 09[3], visualized *via* WebMO[4]

this strategy has been successfully applied to the sequential 3,6-difunctionalization of 2,1-borazaronaphthalene cores.[1d] Recently, (C)4-position halogenation has been achieved when accessing the 2,1-borazaronaphthalene from the corresponding 2-

Figure 3.3: 2,3,4-Arylated 2,1-borazaronaphthalene strategy

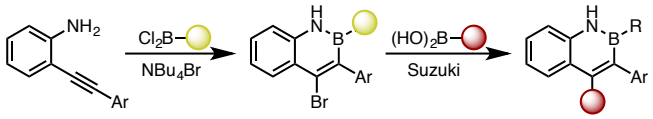

alkynyl-anilines with dichloroboranes, which can also undergo cross-coupling (Figure 3.3).[1k] Overall, these methods provide a platform to develop analogue diversity that has been beneficial toward several applications of the 2,1-borazaronaphthalene core.[5] However, there still remain gaps within the synthetic strategies for functionalizing the 2,1-borazaronaphthalene core, which create limits to its overall viability. Improvements to the existing strategies of diversification as well as exploration of novel methods to access new sites of functionalization would serve to expand the utility of the 2,1-borazaronaphthalene scaffold.

3.2 – Elaboration of the 2,1-borazaronapthalene core *via* photoredox/nickel dual catalysis

The introduction of functionalized alkyl moieties to the 2,1-borazaronaphthalene is attractive, particularly for medicinal chemistry applications.[5a,5b,6] Addition of such groups could provide a means of increasing

solubility of drug candidates, hence improving their ADME (Absorption, Distribution, Metabolism, and Excretion) properties.[7] The installation of alkyl groups has been demonstrated at the C(3)-position of the 2,1-borazaronaphthalene *via* Ni-catalyzed reductive coupling of 1˚ and 2˚ alkyl iodides (Figure 3.4).[1g] Though this protocol enabled the formation of $C_{sp}{}^3$–$C_{sp}{}^2$ bonds between the naphthalene isostere core and an alkyl side chain, these conditions required excess terminal reductant, were intolerant of protic functional groups, and were limited by the accessibility/high cost of alkyl iodides.

Figure 3.4: Nickel catalyzed reductive cross-coupling

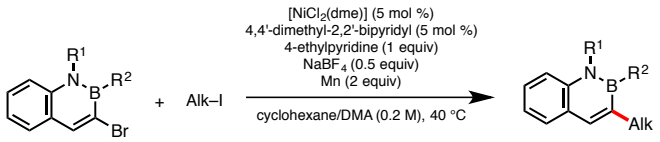

Recently, our group and others reported a new synthetic paradigm to enable the formation of C–C bonds under extremely mild reaction conditions: i.e., visible light photoredox/Ni dual catalytic cross-coupling.[8,9] Utilization of this reaction manifold has allowed the formation of $C_{sp}{}^3$–$C_{sp}{}^2$ bonds between benzylic,[8a,10] secondary alkyl,[9a,10] primary alkyl,[10] α-alkoxy,[8d,9a,f] and α-amino[8b,9c,d,f] $C_{sp}{}^3$–hybridized radical precursors with a variety of (hetero)aryl and/or alkenyl halide electrophiles. These radical precursors are oxidizable species such as organotrifluoroborates, carboxylic acids, and alkylsilicates. The latter, specifically ammonium alkylbis(catecholato)silicates,[10a,b] represent practical, highly versatile radical precursors because of their low oxidation potentials, the innocuous by-products generated during single electron transfer (SET) mediated fragmentation,

and the near-neutral reaction conditions. The mechanism (Figure 3.5) is proposed to go through an initial excitation of the photocatalyst by light, which can then undergo an SET event with the silicate, resulting in homolytic fragmentation to the alkyl radical. This radical can then coordinate to a nickel(0) complex, which then undergoes oxidative addition with the aryl bromide to generate a nickel(III) species. Subsequent reductive elimination establishes the formation of the new C_{sp^3}–C_{sp^2} bond, followed by symbiotic single electron reduction of the nickel center/oxidation of the photocatalyst to turn over the catalytic system. Taken together, photoredox/Ni dual catalysis employing ammonium alkylsilicates offers a versatile cross-coupling approach that displays excellent functional group tolerance and ease of operation.[10a,b] With this newly developed paradigm in mind and the goal of accessing more highly elaborated and functionalized 2,1-borazaronaphthalene cores, we assessed whether these substrates were amenable to this means of C_{sp^3}–C_{sp^2} bond formation.

Figure 3.5: Photoredox/nickel mechanistic pathway

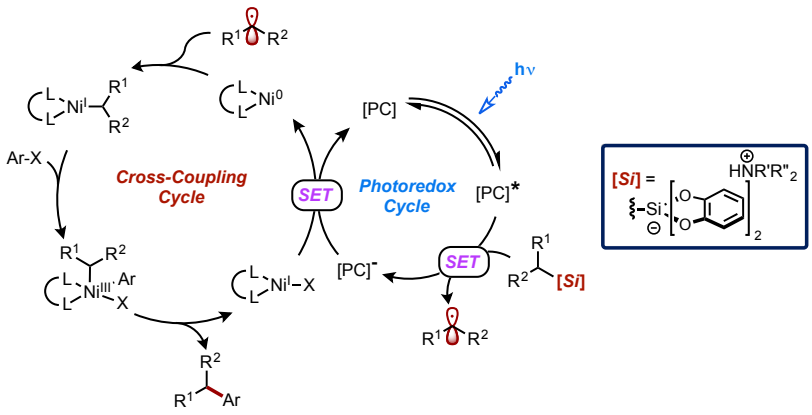

Using the previously reported reaction conditions for the cross-coupling of aryl bromides with silicates {2 mol % $[Ru(bpy)_3](PF_6)_2$, 5 mol % $[NiCl_2(dme)]$, 5 mol

% dtbbpy in DMF (0.1 M)}, the reaction of 2-(4-bromophenyl)-2,1-borazaronaphthalene **3.1** with cyclohexylsilicate[10a] affords coupled product **3.2** in 97% isolated yield (Table 3.1) (dtbbpy: 4,4'-di-*tert*-butyl-2,2'-dipyridyl; bpy: 2,2'-dipyridyl). Substrate **3.1** was further coupled with various silicates, affording alkylated azaborines **3.2-3.15** in excellent yield with both 2º and 1º alkylsilicates. Bicyclic, 3,3,3-trifluoropropyl, and isobutyl fragments were amenable to cross-

Table 3.1: Photoredox Cross-coupling of Ammonium Alkylbis(catecholato)silicates with 2-(4-Bromophenyl)-2,1-borazaronaphthalene

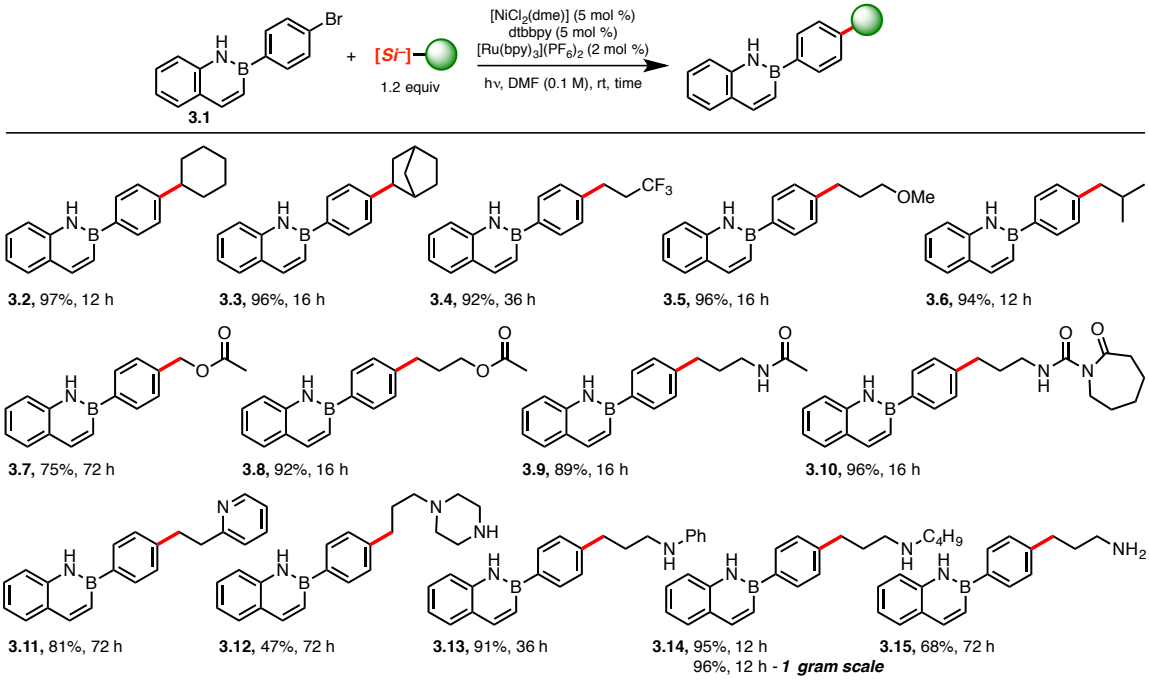

[a]Reaction carried out on 3.5 mmol using blue LEDs; all other reactions were carried out on a 0.5 mmol scale.

coupling (**3.3, 3.4, 3.6**) as were radicals containing various functional groups, including an ether (**3.5**), ester (**3.7, 3.8**), amide (**3.9**) and even a lactam (**3.10**). Alkylsilicates containing Lewis basic residues such as pyridyl (**3.11**), benzylalkylamino (**3.13**) and secondary alkylamino (**3.14**) were similarly well

tolerated. In the case of piperazine- (**3.12**) and primary amine- (**3.15**) containing silicates, lower yields were obtained (47% and 68%, respectively), with unreacted bromoazaborine remaining even after extended reaction time.[10a] The late-stage incorporation of these basic substituents may be highly attractive to medicinal chemists seeking to improve the ADME properties of prospective azaborine targets. To assess further the robustness of the described protocol, the synthesis of the amine-containing compound **3.14** was scaled to one gram (3.5 mmol). Neither the yield nor the reaction time was compromised in this transformation, demonstrating the scalability of this reaction.

The azaborine scope was further extended to *meta* and *ortho* substituted 2-(bromophenyl)-2,1-borazaronaphthalenes (Table 3.2). It appeared that the position of the bromine atom on the *B*-aryl group did not affect the reaction, affording coupled products in excellent yields (**3.16-3.21**). Interestingly, *ortho*-substituted azaborines (**3.19-3.21**) were isolated as oils, whereas nearly all other compounds (with the exception of **3.12**) were obtained as fluffy powders. This disparity is most

Table 3.2: Photoredox Cross-coupling of Ammonium Alkylbis(catecholato)silicates with *meta* and *ortho* Substituted 2,1-Borazaronaphthalene

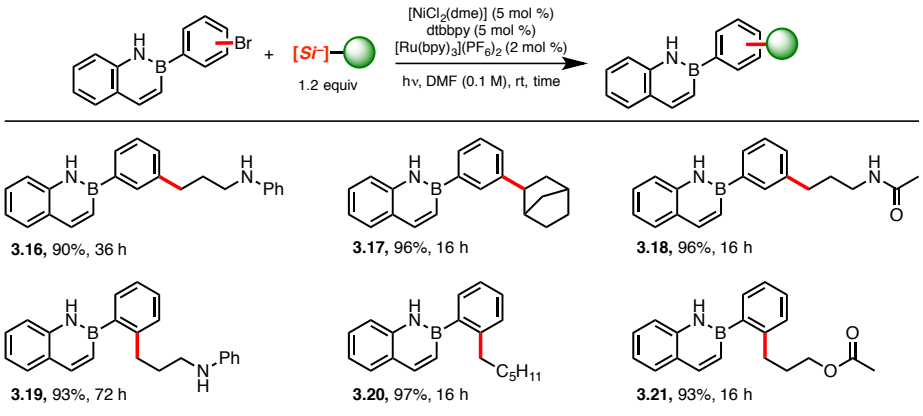

likely due to a perturbation of the molecular packing caused by the steric constraints imparted by *ortho* substitution. Positioning of an alkyl chain at this position on the *B*-aryl group likely prevents coplanarity, disrupting intermolecular π–stacking.

Photoredox/Ni cross-coupling of the brominated azaborinyl ring was further examined. In this case, *B*-aryl 2,1-borazaronaphthalenes were focused on, considering their aforementioned higher stability, especially in the presence of light. In general, brominated azaborines were found to be excellent electrophiles in this type of cross-coupling, affording coupled product in good to excellent yields (Table 3.3). Indeed, a variety of functional groups could be installed at the 3-position on the

Table 3.3: 2,1-Borazaronaphthalene Scope with both Primary and Secondary Ammonium Alkylbis(catecholato)silicates

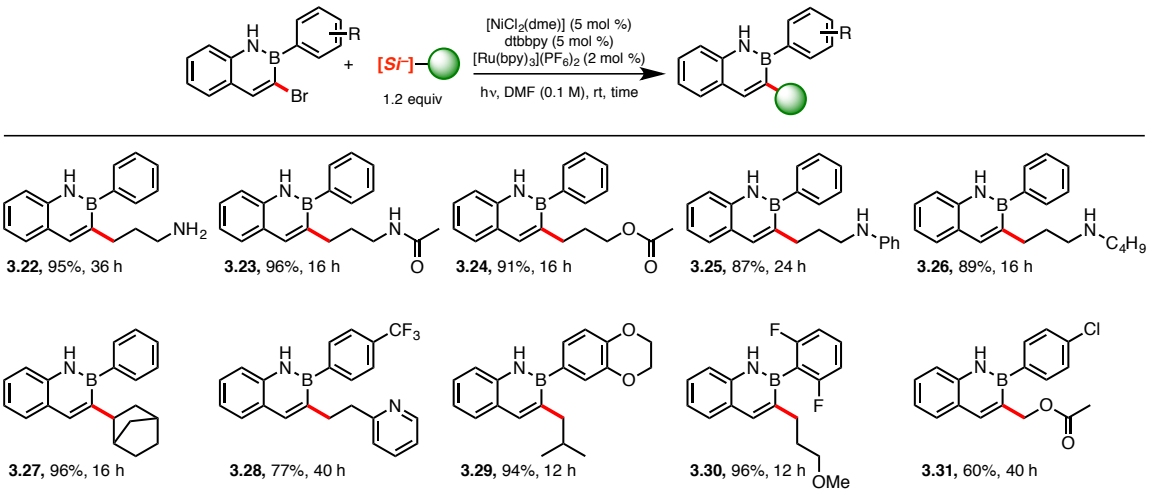

azaborine core (**3.22**–**3.31**). Notably, reaction times were often shorter when performing these couplings. Such acceleration may be due to improved rates of oxidative addition into the C–Br bond, illustrating the lower aromatic character of the azaborines relative to that of all-carbon arenes. Substitution on the aryl group off the boron did not seem to affect cross-coupling. *B*-4-Trifluoromethylphenyl (**3.28**)

and *B*-benzodioxanyl substituents (**3.29**) were both well tolerated. An *ortho*-difluoro-substituted azaborine (**3.30**) did not impede the reaction and afforded near-quantitative reactivity. Whereas selectivity can sometimes be problematic when using dihalogenated systems in transition metal catalyzed cross-couplings, complete selectivity for the bromine over the chlorine atom was observed in the case of **3.31**, leaving the latter intact for further modification.

The use of ammonium alkylsilicates in photoredox/Ni dual catalysis allowed several 2,1-borazaronaphthalene derivatives to be efficiently alkylated. This selective, high yielding, and very mild approach to azaborinyl functionalization enables the rapid construction of a library of naphthalene isosteres with numerous types of functional groups at room temperature and in near-neutral conditions. The modular nature for constructing the borazaronaphthalene core, combined with the selective and regiocomplementary means of elaboration, provides a means to access chemical space in a manner that is challenging, if not impossible, to achieve in the parent naphthalene systems themselves. The method developed further adds to this versatility, and may allow enhancement of ADME properties of target structures, thus improving the viability of azaborines as potential isosteres for drug molecules.

3.3 – Regioselective diversification of 2,1-borazaronaphthalene *via* C-H activation

The well-established strategies of functionalizing the 2,1-borazaronaphthalene offers a variety of options for diversification (Figure 3.6) off nitrogen, boron, C(3), and C(4), with an iterative pathway to access C(6). However, access to substitution of the remaining positions of 2,1-borazaronaphthalene has

continued to be challenging. This was exemplified in the synthesis of 2,1-borazaronaphthalene mimetics of propranolol,[5a] where C(5) and C(8) ethereally-substituted 2,1-borazaronaphthalene derivatives required pre-installation of the oxygen functional group, followed by protection, deprotection, and two subsequent modification steps to introduce the desired side chain. Although such a synthesis might be tolerated from an exploratory chemical design viewpoint, this strategy

Figure 3.6: Functionalization strategies for the 2,1-borazaronapthalene

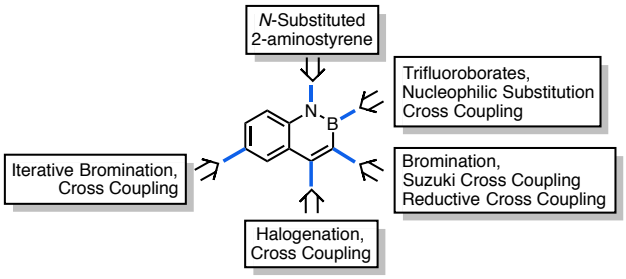

would be inefficient for a more expansive molecular diversity study, costing significant time, effort, and material.

3.3.1 – Iridium catalyzed C-H borylation selectivity

When considering ways to expand the 2,1-borazaronaphthalene motif, installing a *nucleophilic* coupling handle directly on the azaborine core would be beneficial. This would present an alternative approach to those employing an *electrophilic*, brominated core, opening up a wide array of complementary transformations.[11] One major drawback to most classical methods for installing nucleophilic coupling partners is that they are often derived from the corresponding halides, effectively passing through the electrophilic coupling partner in a detrimental synthetic step. A direct C-H borylation would circumvent that limitation and lead directly to a readily diversifiable handle on the azaborine core.[12] Inspired

by the report of the borylation of 1,2-dihydro-1,2-azaborine,[13] along with the diversity of methods for bicyclic systems, it was envisioned that iridium catalyzed C-H borylation would provide a versatile platform capable of high regioselectivity.

Structurally, the 2,1-borazaronaphthalene is isosteric to naphthalene, which diborylates to yield a mixture of 2,6- or 2,7-disubstituted isomers (Figure 3.7-A)[14] owing to a lack of inherent directing preference. Quinolines, which have a similar atomic placement to 2,1-borazaronaphthalenes, undergo C(8)-borylation using silica-supported phosphine ligands (Figure 3.7-B1).[15] With traditional amine ligands, borylation of quinoline is predominantly favored at the C(4)-position (Figure 3.7-B2), with subsequent addition at either the C(6)- or C(7)-positions.[16] Indoles, which possess an aromatic N-H functional unit with a geometric tradeoff to a 6,5-ring system, typically borylate at the C(2)-position.[17] However, introducing

Figure 3.7: Comparison of C-H borylation pathways[a] and bromination of 2-phenyl-2,1-borazaronaphthalene and 2-phenylindole

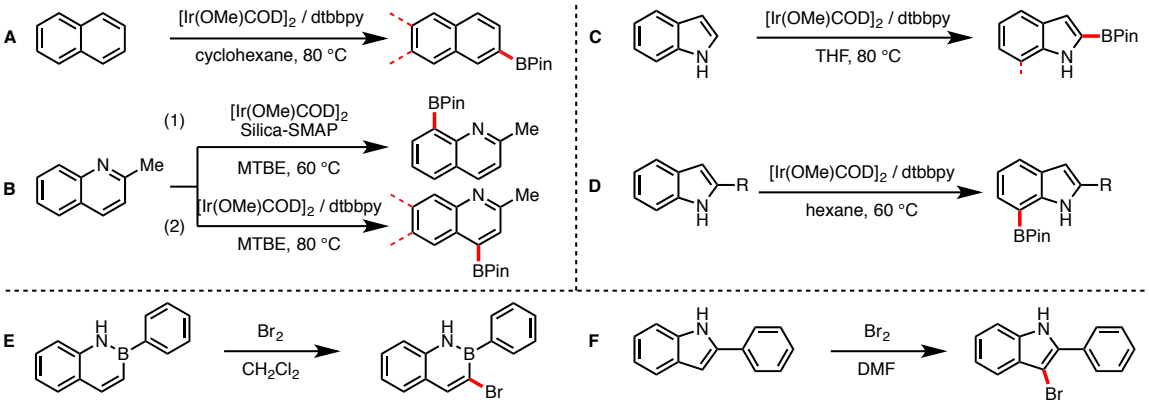

[a]First site of borylation depicted in bold; second site of borylation depicted by dotted line

substitution at the C(2)-position of indole, which is consonant with *B*-substitution on 2,1-borazaronaphthalenes, causes exclusive borylation at the C(7)-position (Figure 3.7-D).[18] Furthermore, it is interesting to note the similarity between the

electrophilic bromination patterns of 2-phenyl-2,1-borazaronaphthalene and 2-phenylindole, as both brominate at the 3-position (Figure 3.7-E,F).[1d, 19]

Considering these three representative bicyclic models for 2,1-borazaronaphthalene, computationally derived electrostatic potential maps were compared to determine their surface electronic similarities (Figure 3.8). Cursory observation validates the archetypal resemblance of the 2-phenyl-2,1-borazaronaphthalene (Figure 3.8-A) to 2-phenylnaphthalene (Figure 3.8-C). However, with our interest in leveraging the desymmetrization of the azaborine core, a deeper look into the distribution of electron density across the surface of the molecules yields a clear likeness to 2-phenylindole (Figure 3.8-B). In both the azaborine and indole electrostatic potential maps, a significant density of electrons resides around the N–H bond, not seen in either of the other structures (Figure 3.8-C and D). Also, there appears to be a distinct similarity in the asymmetric distribution of the partially electron-deficient region within the bicyclic cores. Encouraged by the

Figure 3.8: Electrostatic potentials (from +31.38 kcals/mol to -15.69 kcals/mol) for bicyclic systems[a]

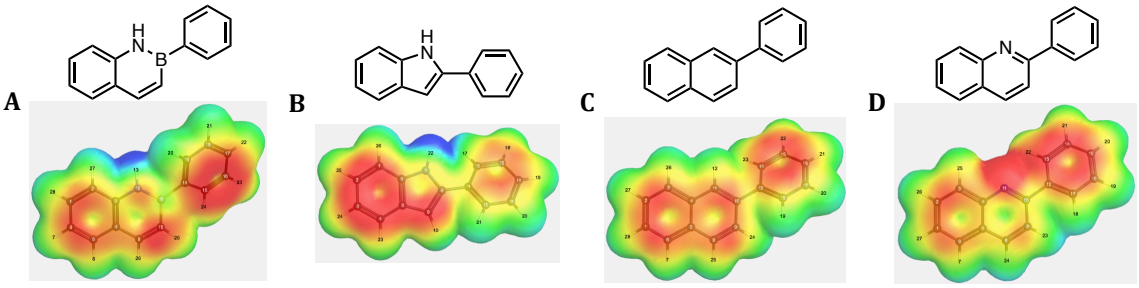

[a]Calculations performed at B3LYP/6-31G(d) level of theory[2] using Gaussian 09[3] visualized *via* WebMO[4]

congruence of the electrostatic potentials and the comparable reactivity profile for electrophilic bromination, indole could be considered electronically comparable and

potentially useful in providing a foundation to predict the selectivity of C-H borylation of 2-phenyl-2,1-borazaronaphthalene.

The iridium-catalyzed borylation of 2-substituted indoles and similarly structured aniline scaffolds have been extensively studied by Smith and co-workers, with the anilines proposed to go through a mechanism in which outer-sphere hydrogen-bond coordination of the nitrogen occurs to direct the C-H functionalization.[18,20] The nitrogen of indole is suggested to be incorporated in the mechanism, providing selectivity for the C(7)-position. Computational elucidation of the iridium-catalyzed C-H borylation of several aromatic systems indicates that the transition state for C-H activation, which is predictive of the regioselectivity, contains "significant proton transfer character".[21] It was surmised that the relative anionic stability of the different C-H centers of the 2,1-borazaronaphthalene core, a trait of proton transfer processes, could predict the site of C-H borylation in these systems. This method is analogous to Liu's use of theoretically derived pK_a values in justifying the site selectivity for C-H borylation of 1,2-dihydro-1,2-azaborine.[13]

To validate this approach, computational comparisons of the anion stability at various positions around 2-phenylindole were used as a representative system (see Supporting Information for complete anionic stability studies). Surprisingly, both the C(3)-position and the *ortho*-site of the external phenyl ring were more anionically stabilized than the known C(7)-borylation site (Table 3.4). However, it is well documented that those sites are inaccessible based on steric factors, considering the steric bulk of the iridium catalyst.[19] Anionic stability only accounts for the electronic factors of the C-H activation event, thus steric constraints must

Table 3.4: Free Energy Calculation of Relative Anionic Stability[a]

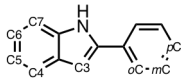

2-Phenylindole[b]

Location	ΔG (kcals/mol)
i-C3	-13.68
i-C4	-3.91
i-C5	0.0
i-C6	-2.76
i-C7	-10.96
i-*o*C	-12.47
i-*m*C	-8.43
i-*p*C	-9.40

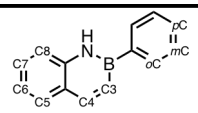

2-Phenyl-2,1-borazaronaphthalene

Location	ΔG (kcals/mol)
b-C3	-1.45
b-C4	-3.54
b-C5	-6.51
b-C6	-3.48
b-C7	-6.55
b-C8	-13.41
b-*o*C	-1.62
b-*m*C	0.00
b-*p*C	-0.03

[a]All structures are fully optimized to local minima [B3LYP/6-31G(d)]. [b]Grayed-out values are sterically nonviable

also be entertained. Removing these two nonviable sites, the theoretical method correctly predicted the C(7)-site for borylation. Applying this method to 2-phenyl-2,1-borazaronaphthalene, the C(8)-position appeared to be significantly more amenable to anionic charge stabilization that any other position. Considering this predicted site of borylation in the azaborine has no foreseeable steric constraints, this functionalization method was anticipated to provide access to a previously unattainable position of the 2,1-borazronaphthalene.

3.3.2 – C-H borylation condition optimization

Excited by the potential regioselectivity of the C-H activation strategy, high throughput experimentation (HTE) was leveraged to survey the various reported C-H borylation conditions for optimal regioselectivity for the 2,1-borazaronaphthalene system.[12f] Initial optimization screening focused on identifying the optimal ligand source for the C-H borylation, along with comparing four solvents and two iridium

sources (Figure 3.9). From this screen, comparing internal standard (4,4′-di-*tert*-butylbiphenyl) to starting material ratios (IS/SM) to find lead reaction conditions, it was observed that full conversion of starting material could be achieved with [Ir(μ-OMe)(COD)]$_2$ in THF using bi-dentate amine ligands **L2**, **L6** or **L7**. The iridium chloride dimer showed no consumption of starting 2,1-borazaronaphthalene, as well as deviation from bipyridine and phenanthroline ligand classes. These conditions provided a valuable starting point to optimze the reaction conditions further.

Figure 3.9: Initial screening of iridium-catalyzed C-H borylation conditions for 2,1-borazaronaphthalene

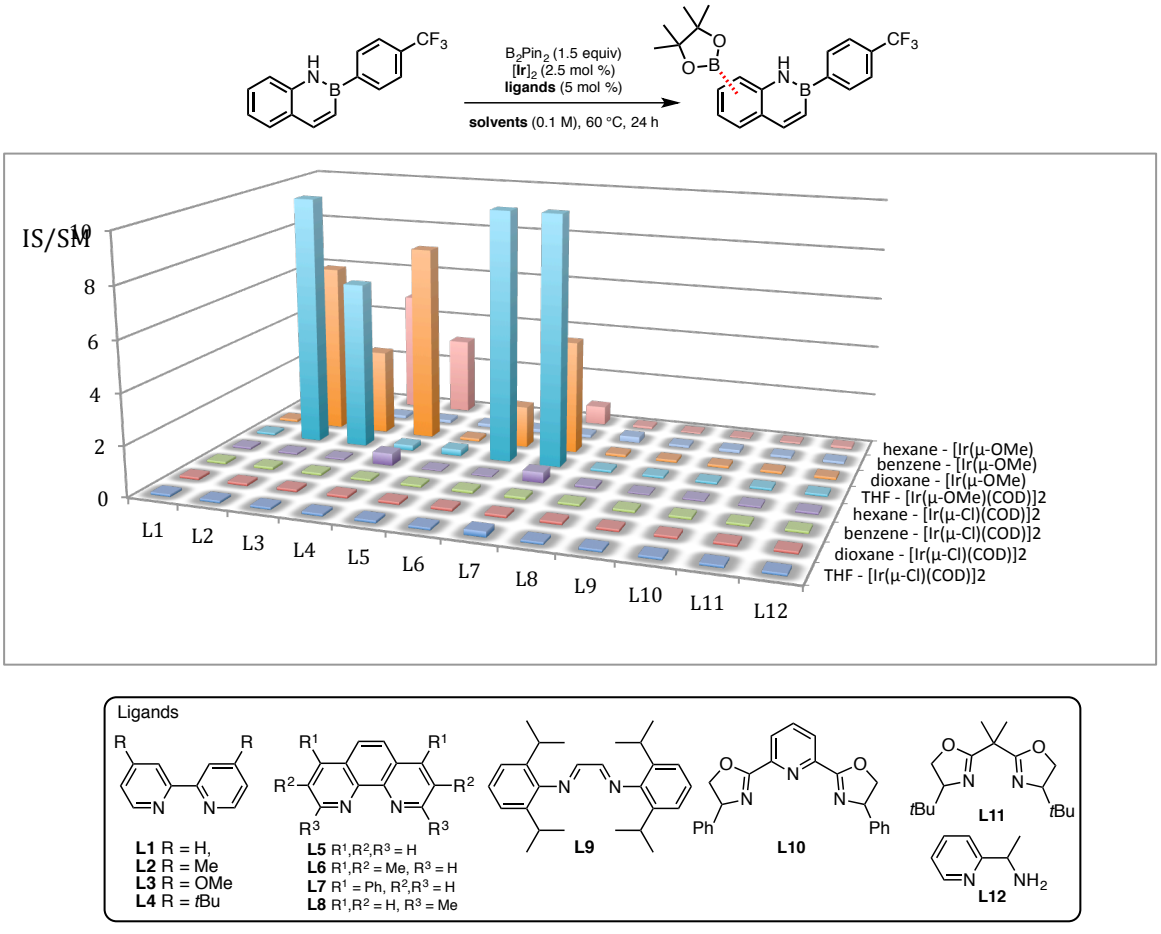

In total, close to 450 conditions (see Appendix A2.3 for complete screening details) were screened to verify the best ligands classes, solvents and relative ratios of reaction components. Bipyridine- and phenanthroline-based ligands were consistently superior to other nitrogen-containing homobidentate ligands, while diphosphine ligands showed minimal conversion.[12g] It was further determined that catalyst loading was optimal at 4 mol % with a 1:1.25 metal-to-ligand ratio. A slight excess (1.05 equiv) of B_2Pin_2 was required for the reaction to go to completion. However, significant excess led to an increase of diborylated product. As previously observed, solvent played an important role in controlling selectivity, with non-polar solvents such as hexane and methylcyclohexane proving optimal.

Upon validation of these conditions on benchtop scale, it was observed that higher reaction concentration coincided with increased diborylation. Temperature also played a significant role in sequestering the *N*-borylated byproduct and preventing significant diborylation. However, given that the solubility of some of the substrates in methylcyclohexane was very low at room temperature, poorly soluble substrates required elevated temperatures (40 °C *vs* 80 °C) for the reaction to proceed. NMR analysis of the isolated, monoborylated compound indicated exclusive borylation at the previously predicted (C)8-position, and this was later confirmed via single crystal X-ray diffraction analysis (Figure 3.10).

Figure 3.10: X-Ray crystal structure of C(8)-borylated 2,1-borazaronaphthalene

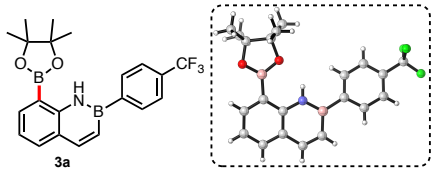

3.3.3 – C-H borylation substrate scope

With conditions for C-H borylation at the (C)8 position of 2,1-borazaronaphthalene established, the applicability to various substrates was considered, starting with boron substitution (Table 3.5). A variety of different *B*-aryl-2,1-borazaronaphthalene substructures (**3.32**-**3.42**) were tolerated with various levels of success. Electronic diversification off the aryl substituent seemed to have little impact on the reaction outcome (compare **3.32**, **3.35**, **3.39**). However, the substitution pattern off the *B*-aryl subunit did influence the effectiveness of the reaction, with *para*-substitution being preferred over either *meta*- or *ortho*-substitution (compare **3.35** to **3.36**, and **3.39**, **3.40**, and **3.41**). Furan (**3.44**) was tolerated, albeit modestly, as it presents a competing site for C-H borylation.[23] Alkyl-substituted 2,1-borazaronaphthalenes (**3.45-3.49**) were typically well tolerated, presumably because of the increased solubility in the reaction solvent. In almost all cases, the mass balance for the reaction consisted exclusively of starting material, product, and various amounts of a single diborylated byproduct, suggesting that re-optimization for a specific substrate would provide a high return of product.

Table 3.5: Borylation Scope of *B*-Substituted 2,1-Borazaronaphthalenes

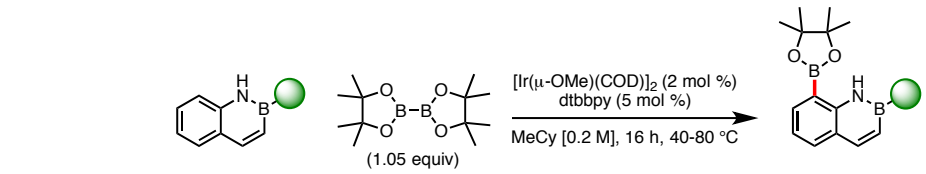

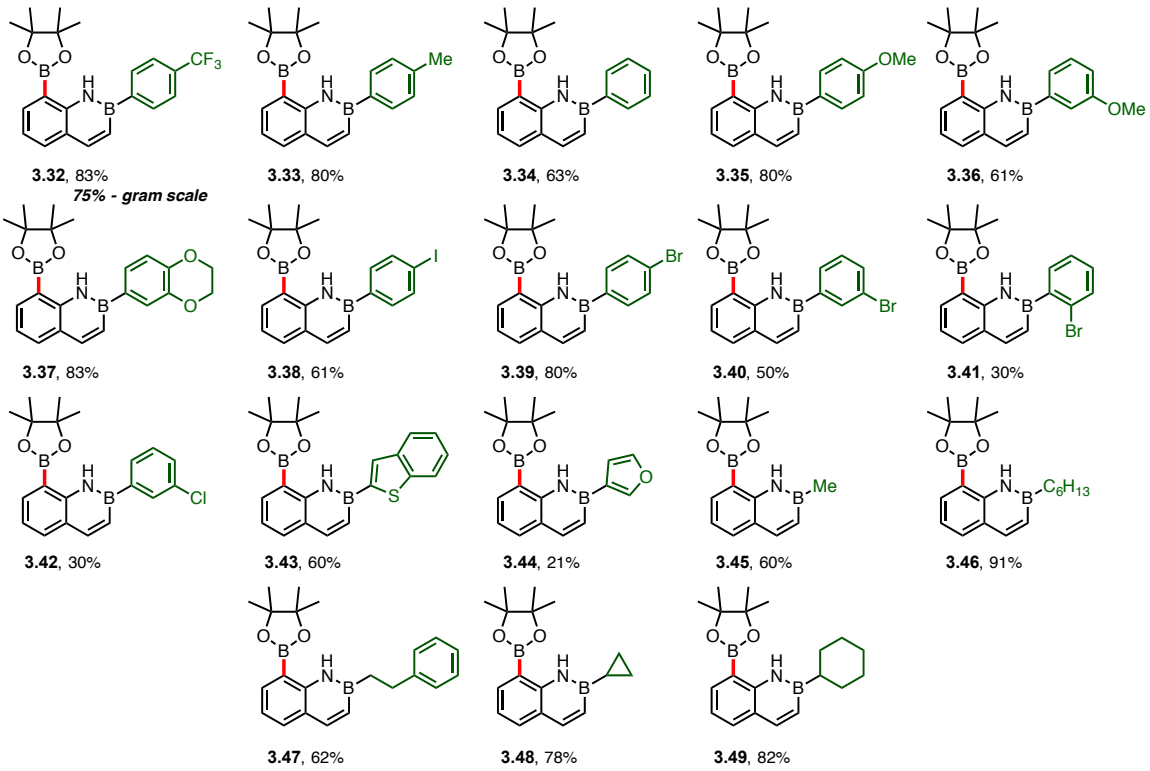

More elaborate 2,1-borazaronaphthalenes were next explored and found to be competent in the selective C-H borylation process (Table 3.6). 3-Bromo-2,1-borazaronaphthalenes (**3.50** and **3.51**) and the 3,6-di-brominated core (**3.52**) were tolerated, along with aryl substitution at the 3-position (**3.53**), a cross-coupled product derived from **3.50**.[1d] 7-Fluoro-2,1-borazaronaphthalene was also suitable in the selective reaction, providing **3.54** in modest yield. However, no other substituent at the 7-positions (e.g., *i*-Pr, Me) allowed productive borylation. Presumably, the steric constraints imparted by substitution at this position prevent accessibility by the bulky catalyst. Functionalization at the 6-position was well

tolerated, including cyano (**3.55**), trifluoromethyl (**3.56**), isopropyl (**3.57**), and trifluoromethoxy (**3.58**) groups. Compounds with electrophilic coupling handles, either installed off the boron subunit (**3.38-3.42**) or the brominated borazaronaphthalene core (**3.50**, **3.51**, **3.52**), provide potential lynchpins for rapid

Table 3.6: Borylation of Elaborated 2,1-Borazaronaphthtalene Scaffolds

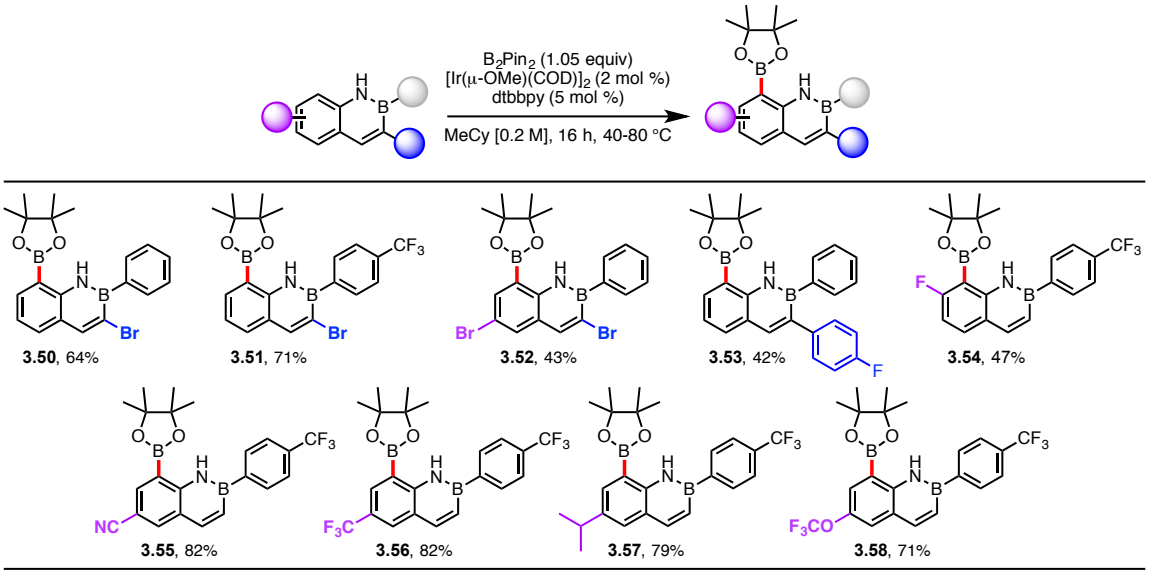

core diversification. One such avenue could be photoredox cross-coupling, which has demonstrated tolerance of aryl borinates[24] and has already been applied with great success to azaborines.[1h]

As previously mentioned, the exclusive byproduct affecting yields came from di-borylation. Fortuitously, the second C–H borylation event *again* occurred regioselectively, this time at the C(6)-position (Figure 3.11). When increasing the

Figure 3.11: X-Ray validation of 6,8-diborylated 2,1-borazaronaphthalene

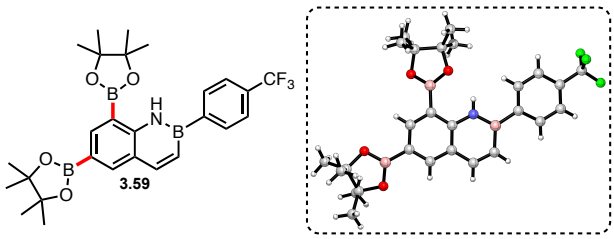

amount of B_2Pin_2 in the reaction, this product can be exclusively observed (Table 3.7). These diborylated cores (**3.59-3.61**) might be further applicable in divergent functionalization, capitalizing on the stereoelectronic disparities between the sites of borylation, similar to prior work of selective cross-coupling of poly-borylated molecules.[25]

Table 3.7: Diborylation of 2,1-Borazaronaphthalene Cores

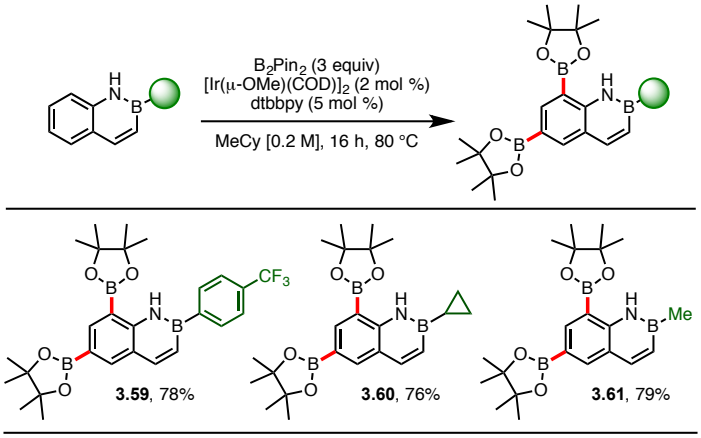

While screening the borylation of the 2,1-borazaronaphthalenes, one observed phenomenon was the formation of the *N*-borylation product. Although only observed in trace amounts at elevated temperatures and lower ligand to metal ratios, similar products have previously been noted and used as an *in situ* "traceless" directing group for the C(3) borylation of indoles.[20a] To probe whether this byproduct was an intermediate of the reaction pathway, the *N*-deuterated 2,1-borazaronaphthalene **3.62** was synthesized and subjected to the borylation conditions (Figure 3.12-A). No scrambling of the deuterium was observed in the crude reaction mixture. The C(8)-borylated, *N*-deuterated product **3.63** could be isolated, suggesting that the N–H insertion, required to obtain the *N*-borylated

product, is not part of the mechanistic pathway for borylation at the C(8)-position. However, it does appear that the N–H is intrinsically valuable for the regiospecificity of the borylation. When the *N*-methyl-2,1-borazaronaphthalene **3.64** was subjected

Figure 3.12: Experimental data of mechanistic value

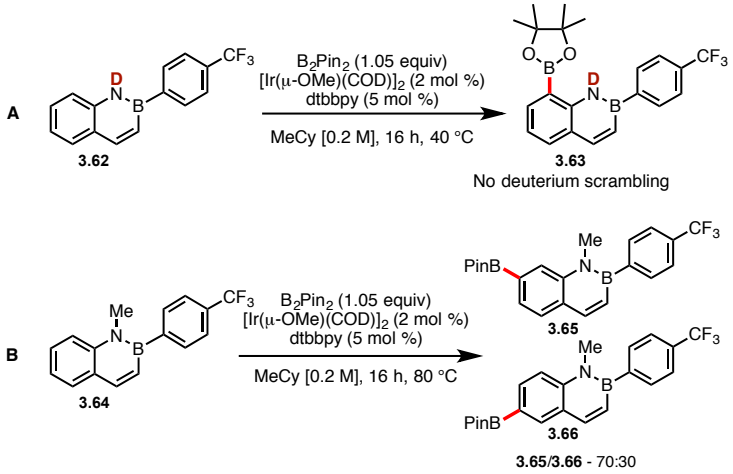

to the borylation reaction, complete conversion was observed to an inseparable mixture of two regioisomeric products (Figure 3.12-B). Analysis by 2D NMR suggests that none of the C(8)-borylated product was obtained. Rather, the isomers obtained were the C(7)-borylated **3.65** and C(6)-borylated **3.66** 2,1-borazaronaphthalenes, with the major product being the C(7)-borylated isomer. The relative ratio of observed products concurs with the computational model as the C(7)-position has greater favorable anionic charge stabilization compared to the C(6)-positions. It is interesting to note that while C(7) is the second most favorable point of anionic stabilization, C(6) ranks fifth, behind both C(5) and C(4). The lack of observed borylation at those sites could be explained by a peri-interaction,[26] marginally disfavoring those sites. This further suggests that the N–H could play a fundamental role in enabling the C(8)-borylation event, consistent with the outer-

sphere hydrogen-bond coordination model used to explain the *ortho*-C–H borylation for similarly structured anilines.[20b]

3.3.4 – Cross-coupling of 8-borylated 2-1-borazaronaphthalenes

With a diverse array of borylated compounds in hand, the viability of the subsequent Suzuki-Miyaura cross-coupling reaction was studied. Taking insight from conditions previously established for the inverted coupling of brominated 2,1-borazaronaphthalenes with organotrifluoborates,[1d] with only minor modification to the solvent and ligand choice, the reaction worked exceedingly well. It was observed that alcoholic solvent mixtures with water were highly effective (Table 3.8), and that sterically bulky alcohols produced the best results (entries **3** and **4**), avoiding proto-deborylation.

Table 3.8: Solvent Optimization of Cross-coupling[a]

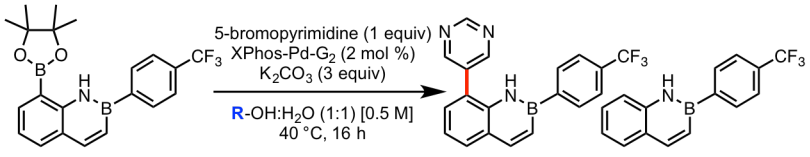

	Alcohol	**3.32** : IS	**3.67** : IS	**Des-Br** : IS
1	MeOH	0.07	1.93	0.02
2	EtOH	0.08	2.18	0.18
3	*i*-PrOH	0.07	2.54	0
4	*t*-BuOH	0.03	2.62	0
5	phenol	0.00	0.30	1.40
6	cyclohexanol	0.00	1.63	1.53

[a]Product ratios determined by HPLC using 4,4'-di-*tert*-butylbiphenyl as internal standard (IS)

These optimized conditions were then tested on a variety of the borylated 2,1-borazaronaphthalene cores, focusing on adding heterocyclic diversity to a variety of substituted azaborine substrates (Table 3.9). Across the board, yields were generally excellent, with several of the reactions proceeding nearly

Table 3.9: Cross-coupling of (Hetero)aryl Bromides with 8-Borylated 2,1-Borazaronaphthalene Cores

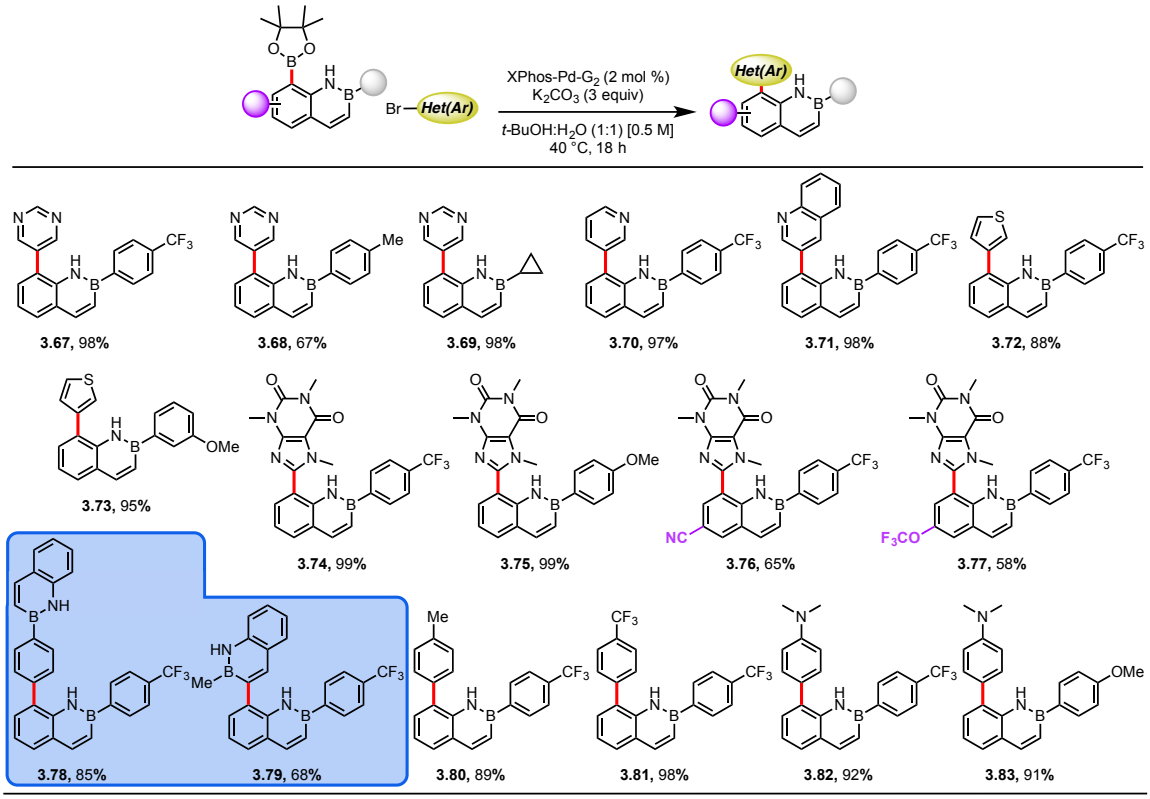

quantitatively (**3.67, 3.69, 3.70, 3.71, 3.74, 3.75, 3.81**). Indeed, for reactions that went to full conversion, often the only purification required was simple aqueous workup followed by rapid purification through a plug of silica to remove the palladium catalyst. In most cases, yield losses corresponded to the required use of column chromatography, owing to incomplete reaction. 5-Bromopyrimidine cross-coupled well with various 8-borylated 2,1-borazaronaphthalene analogues (**3.67**, **3.68**, **3.69**). Pyridine (**3.70**), quinoline (**3.71**), and thiophene (**3.72** and **3.73**) substrates also worked well. Although highly functionalized cores such as caffeine could easily be installed with little difficulty (**3.74**, **3.75**), substitution on the all-carbon ring of the azaborine core seemed to hinder the reaction (**3.76**, **3.77**).

Standard aryl bromides could also be cross-coupled in high yields (**3.80-3.83**), including challenging electron rich *N,N*-dimethylamino derivatives (**3.82**, **3.83**). Unusual substructures were synthesized using both nucleophilic and electrophilic 2,1-borazaronaphthalene derivatives that could be conjoined to generate heterodimeric-azaborines (**3.78**, **3.79**).

This protocol for selective C-H borylation and subsequent cross coupling of 2,1-borazaronaphthalene allows late-stage functionalization at a previously inaccessible position. Furthermore, there appears to be correlation of 2,1-borazaronaphthalene to indole, suggesting an alternative isostereic comparison. Computational methods accounting for the electronic factors of proton transfer-like C-H activation were able to identify the potential site of borylation, while high throughput experimentation could rapidly identify viable reaction conditions. Subjecting the substrate to excess B_2Pin_2 resulted in the exclusive formation of a diborylated adduct, providing an unprecedented opportunity for chemoselective functionalization in the all-carbon ring. Furthermore, it was demonstrated that the N–H is imperative for selectivity, although the reaction is most probably not going through a productive N-H insertion pathway. The resulting borylated substrates could be further cross-coupled using mild Suzuki-Miyaura conditions to provide highly elaborated azaborine scaffolds.

3.4 Conclusions

These developed methods open up new opportunities for the diversification of 2,1-borazaronaphthalene and thus entry into unexplored isostereic space. The advantage of this azaborine core is the unique electronic directing capacity,

inaccessible in the isostructural naphthalene, presenting various highly selective methods of functionalization (Figure 3.13). Applying the photoredox/nickel dual-catalysis using alkylbis(catecholato)-silicates with the brominated azaborine core

Figure 3.13: Functionalization of the 2,1-borazaronaphthalene

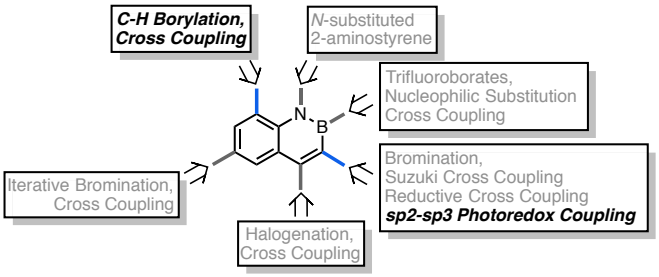

presents an unparalleled method for installing alkyl functional groups off the 2,1-borazaronaphthalene core. The incredibly mild conditions for the $C_{sp}{}^3$–$C_{sp}{}^2$ coupling allow the installation of sensitive functional groups and those of high interest for biologically relevant molecular scaffolds. The iridium catalyzed C-H borylation presents a strategy for functionalization at a position previously inaccessible, and the ensuing Suzuki-Miyaura cross-coupling demonstrates the variety of diverse analogues that can be accessed from the borylated 2,1-borazaronaphthalene core. These methods, combined with the previous functionalization pathways, provide a versatile toolbox to access a variety of analogues for potentially diverse applications.

3.5 – Experimental Section

General considerations: All reactions were carried out under an inert atmosphere of nitrogen or argon in oven-dried glassware, unless otherwise noted. Conventional solvents (THF, Et_2O, CH_2Cl_2, toluene, CPME) were dried using a J. C.

Meyer solvent system. DMF (99.9%, extra dry) was used as received. [$NiCl_2$(dme)] was purchased from commercial sources, and all other reagents were purchased commercially and used as received, unless otherwise noted. Column chromatography was performed by Combiflash(R) using RediSep Rf Gold Normal-Phase Silica(R) columns. Photoredox reactions were irradiated with blue LED strips, and the temperature was controlled using an external fan. Melting points (°C) are uncorrected. Mass spectra (ESI-, EI- or CI-TOF) were recorded using CH_2Cl_2, MeCN or MeOH as the solvent. NMR Spectra (^{1}H, ^{13}C {^{1}H}, ^{11}B, ^{19}F{^{1}H}) were performed at 298 K. ^{1}H (500.4 MHz) and ^{13}C{^{1}H} (125.8 MHz) NMR chemical shifts are reported relative to internal TMS (δ = 0.00 ppm) or to residual protiated solvent. ^{11}B (128.4 MHz) and ^{19}F{^{1}H} NMR (470.8 MHz) chemical shifts were referenced to external BF_3•Et_2O (0.0 ppm) and $CFCl_3$ (0.0 ppm), respectively. Data are presented as follows: chemical shift (ppm), multiplicity (s = singlet, d = doublet, t = triplet, q = quartet, sept = septet, m = multiplet, br = broad), coupling constant *J* (Hz) and integration. Ammonium organobis(catecholato)silicates[10] and 2,1-borazaronaphthalenes[1a] were prepared according to literature procedures.

Experimental procedure for photoredox/Ni cross-coupling of brominated 2,1-borazaronaphthalenes

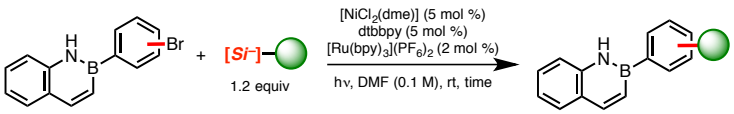

0.5 mmol scale reaction: To an 8 mL clear glass vial equipped with a Teflon-coated magnetic stir bar was added 4,4'-di-*tert*-butyl-2,2'-bipyridine (6.7 mg, 0.025 mmol),

and [$NiCl_2$(dme)] (5.5 mg, 0.025 mmol). The vial was capped and purged with nitrogen, then 1.5 mL of THF was introduced. The resulting suspension was heated briefly with a heat gun until the nickel complex and ligand were fully solubilized, yielding a pale green solution. The solution was cooled in an ice bath, resulting in the immediate precipitation of an evergreen solid. Solvents were then evaporated in vacuo to give a fine coating of the ligated nickel complex. Once dry, brominated 2,1-borazaronaphthalene (0.5 mmol, 1.0 equiv) (liquid aryl bromides were added at the time of solvent addition), organosilicates (0.6 mmol, 1.2 equiv), and [$Ru(bpy)_3$](PF_6)$_2$ (8.6 mg, 0.01 mmol) were added in succession. The vial was then capped and purged four times. Under an inert atmosphere, DMF (5 mL) was introduced. The vial containing all the reagents was further sealed with parafilm and stirred approximately 4 cm away from the LED strips (Figure 3.14). A fan was blown across the reaction setup to suppress the heat generated by the latter (the reaction temperatures were estimated to be ~30 °C). After 12 h, an aliquot was taken and analyzed by HPLC to monitor reaction completion. The crude reaction mixture was poured into a separatory funnel and diluted with H_2O (20 mL). The resulting suspension was extracted with EtOAc (3 × 10 mL), and the combined organic extracts were washed with a saturated solution of Na_2CO_3 (2 × 20 mL) then H_2O (20 mL), dried ($MgSO_4$) and concentrated. The residue was purified by column chromatography on silica gel, eluting with EtOAc and hexanes, to obtain products in pure form. In the case of primary and secondary alkylamine-containing compounds, the residue was purified by column chromatography on silica gel, eluting with MeOH and CH_2Cl_2 containing NH_4OH (1 %, *v*/*v*).

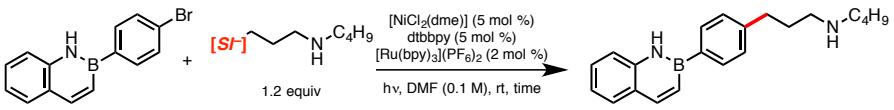

Gram scale reaction: To a 100 mL round bottom flask equipped with a Teflon-coated magnetic stir bar was added [$NiCl_2$(dme)] (39 mg, 0.18 mmol) and 4,4'-di-*tert*-butyl-2,2'-bipyridine (47 mg, 0.18 mmol). The flask was capped and purged with nitrogen, then 3.0 mL of THF was introduced. The resulting suspension was heated briefly with a heat gun until the nickel and ligand were fully solubilized, yielding a pale green solution. The solution was cooled in an ice bath, resulting in the immediate precipitation of an evergreen solid. Solvents were then evaporated in vacuo to give a fine coating of the ligated nickel complex. Once dry, 2,1-borazaronaphthalene **3.1** (1.000 g, 3.52 mmol), bis(catecholato)3-(butylammonio)propyl silicate (1.949 g, 4.23 mmol) and [$Ru(bpy)_3$](PF_6)$_2$ (61 mg, 0.07 mmol) were added in succession. The vial was then capped and purged four times. Under an inert atmosphere, DMF (35 mL) was introduced. The vial containing all the reagents was further sealed with parafilm and stirred in the presence of coiled blue LEDs (Figure 3.14). A fan was blown across the reaction setup to suppress the heat generated by the LEDs, stabilizing at 30 °C after 1 h. Reaction completion was monitored by sampling the reaction mixture and analyzing by HPLC. After completion (4 h), the crude reaction mixture was diluted with EtOAc (40 mL), filtered through approximately 6 cm x 4 cm cylindrical plug of Celite, washing with EtOAc (40 mL). The resulting solution was concentrated, retaken in EtOAc (50 mL), poured into a separatory funnel, and washed with a saturated

solution of Na_2CO_3 (2 × 40 mL) then H_2O (40 mL), dried ($MgSO_4$) and concentrated. The residue was purified by column chromatography on silica gel, eluting with MeOH and CH_2Cl_2 containing NH_4OH (1%, *v*/*v*), to obtain azaborine **3.14** in pure form (1070 mg, 96%).

Figure 3.14: 0.5 mmol (left) and gram (right) scale photoredox cross-coupling reaction set-up.

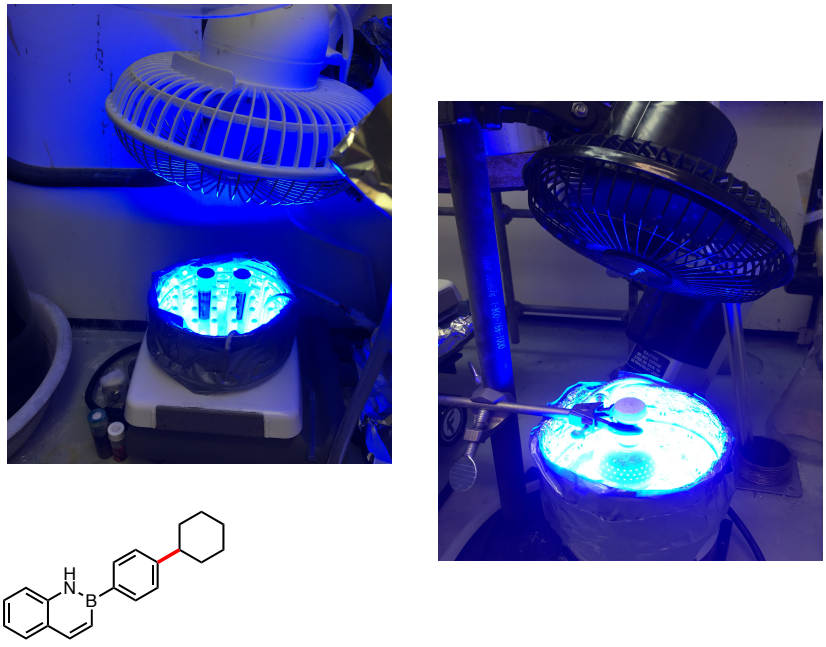

2-(4-Cyclohexylphenyl)-2,1-borazanaphthalene (**3.2**): obtained as a white powder (139 mg, 97%); mp = 144-146C; ^{1}H NMR ($CDCl_3$, 500.4 MHz): δ 8.12 (d, *J* = 10.5 Hz, 2 H), 7.87 (d, *J* = 8.4 Hz, 2 H), 7.66 (d, *J* = 8.4 Hz, 1 H), 7.44 (dd, *J* = 7.4, 7.4 Hz, 1 H), 7.37–7.32 (m, 3 H), 7.30–7.26 (m, 1 H), 7.19 (ddd, *J* = 7.6, 7.4, 1.1 Hz, 1 H), 2.62–2.53 (m, 1 H), 1.96–1.85 (m, 4 H), 1.78 (d, *J* = 6.0 Hz, 1 H), 1.52–1.37 (m, 4 H), 1.34–1.27 (m, 1 H) ppm; ^{13}C {^{1}H} NMR (acetone-d_6, 125.8 MHz): δ 149.3, 145.1, 141.1, 133.2, 129.1, 128.1, 126.4, 125.6, 120.5, 118.5, 44.5, 34.2, 26.6, 25.9 ppm; ^{11}B NMR (acetone, 128.4 MHz): δ 34.6 ppm; IR: ν = 2920, 2849, 1612, 1596, 1564, 1439,

1404, 1388, 1347, 1284, 1218, 1174, 978, 808, 755, 737 cm^{-1}; HRMS (ESI+) m/z calc. for $C_{20}H_{23}BN$ $[M + H]^+$ 288.1924, found 288.1924.

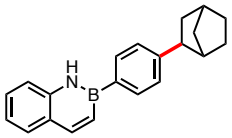

2-(4-(exo-Bicyclo[2.2.1]heptan-2-yl)phenyl)-2,1-borazanaphthalene (**3.3**): obtained as a white powder (143 mg, 96%); mp = 158-161 °C; ^1H NMR (acetone-d_6, 500.4 MHz): δ 9.67 (br s, 1 H), 8.15 (d, *J* = 12.5 Hz, 1 H), 7.96 (d, *J* = 7.2 Hz, 2 H), 7.69–7.63 (m, 2 H), 7.43 (dd, *J* = 7.2, 7.9 Hz, 1 H), 7.33–7.24 (m, 3 H), 7.16 (dd, *J* = 6.6, 7.2 Hz, 1 H), 2.82–2.76 (m, 1 H), 2.37–2.34 (m, 2 H), 1.82–1.75 (m, 1 H), 1.73–1.68 (m, 1 H), 1.64–1.54 (m, 3 H), 1.43–1.36 (m, 1 H), 1.31–1.28 (m, 1 H), 1.21–1.18 (m, 1 H) ppm; ^{13}C {^1H} NMR (acetone-d_6, 125.8 MHz): δ 148.8, 145.1, 141.1, 133.1, 129.0, 128.1, 126.6, 125.6, 120.5, 118.4, 47.2, 42.9, 38.6, 36.6, 35.6, 30.2, 28.5 ppm; ^{11}B NMR (acetone, 128.4 MHz): δ 34.0 ppm; IR: ν = 2947, 2866, 1612, 1594, 1440, 1403, 1388, 1345, 1284, 1209, 1143, 978, 941, 806, 756, 697 cm^{-1}; HRMS (ESI-) m/z calc. for $C_{21}H_{21}BN$ $[M - H]^-$ 298.1767, found 298.1763.

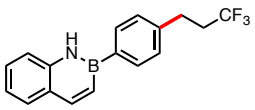

2-(4-(3,3,3-Trifluoropropyl)phenyl)-2,1-borazanaphthalene (**3.4**): obtained as a white powder (138 mg, 92%) using silicate **11a**; mp = 149-151 °C; ^1H NMR (acetone-d_6, 500.4 MHz): δ 9.73 (br s, 1 H), 8.17 (d, *J* = 11.3 Hz, 1 H), 8.00 (d, *J* = 7.7 Hz, 2 H), 7.70–7.63 (m, 2 H), 7.44 (dd, *J* = 7.5, 7.6 Hz, 1 H), 7.39 (d, *J* = 8.4 Hz, 2 H), 7.30–7.25 (m, 1 H), 7.17 (dd, *J* = 7.4, 7.4 Hz, 1 H), 2.95–2.89 (m, 2 H), 2.62–2.50 (m, 2

H) ppm; ^{13}C {^{1}H} NMR ($CDCl_3$, 125.8 MHz): δ 145.5, 140.5, 140.0, 133.1, 129.4, 128.3, 128.1, 126.7 (q, *J* = 276.3 Hz), 125.7, 121.0, 118.1, 35.5 (q, *J* = 28.7 Hz), 28.2 (q, *J* = 2.73 Hz) ppm; ^{11}B NMR (acetone, 128.4 MHz): δ 33.9 ppm; ^{19}F {^{1}H} NMR (acetone-d_6, 470.8 MHz): –67.0 ppm; IR: ν = 1607, 1564, 1438, 1385, 1330, 1304, 1284, 1255, 1224, 1155, 1115, 1082, 975, 811, 760, 732 cm^{-1}; HRMS (ESI+) m/z calc. for $C_{17}H_{16}BNF_3$ [M + H]$^+$ 302.1328, found 302.1334.

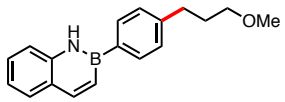

2-(4-(3-Methoxypropyl)phenyl)-2,1-borazanaphthalene (**3.5**): obtained as an off white powder (133 mg, 96%); mp = 76-78 °C; ^{1}H NMR (acetone-d_6, 500.4 MHz): δ 9.69 (br s, 1 H), 8.15 (d, *J* = 11.7 Hz, 1 H), 7.97 (d, *J* = 7.4 Hz, 2 H), 7.69–7.64 (m, 2 H), 7.44 (dd, *J* = 7.0, 7.0 Hz, 1 H), 7.30–7.28 (m, 3 H), 7.17 (dd, *J* = 7.6, 7.5 Hz, 1 H), 3.36 (t, *J* = 5.8 Hz, 2 H), 3.28 (s, 3 H), 2.70 (t, *J* = 7.2 Hz, 2 H), 1.87 (dt, *J* = 7.2, 5.8 Hz, 2 H) ppm; ^{13}C {^{1}H} NMR (acetone-d_6, 125.8 MHz): δ 145.2, 143.6, 141.1, 133.2, 129.1, 128.2, 128.1, 125.6, 120.6, 118.5, 71.4, 57.5, 32.0, 31.2 ppm; ^{11}B NMR (acetone, 128.4 MHz): δ 34.3 ppm; IR: ν = 1605, 1595, 1562, 1437, 1389, 1346, 1282, 1208, 1193, 1118, 1067, 977, 952, 942, 813, 801 cm^{-1}; HRMS (ESI+) m/z calc. for $C_{18}H_{20}BNO$ [M]$^+$ 277.1638, found 277.1632.

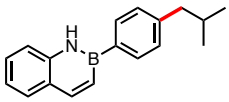

2-(4-Isobutylphenyl)-2,1-borazanaphthalene (**3.6**): obtained as a white powder (122 mg, 94%); mp = 108-111 °C; ^{1}H NMR (acetone-d_6, 500.4 MHz): δ 9.67 (br s, 1 H), 8.15 (d, *J* = 11.5 Hz, 1 H), 7.96 (d, *J* = 7.9 Hz, 2 H), 7.69–7.63 (m, 2 H), 7.44

(ddd, *J* = 7.4, 7.4, 1.0 Hz, 1 H), 7.29 (dd, *J* = 11.9, 1.0 Hz, 1 H), 7.25 (d, *J* = 8.2 Hz, 2 H), 7.17 (dd, *J* = 7.2, 7.3 Hz, 1 H), 2.52 (d, *J* = 7.0 Hz, 2 H), 1.91 (sept, *J* = 6.7 Hz, 1 H), 0.92 (d, *J* = 6.6 Hz, 6 H) ppm; ^{13}C {^{1}H} NMR (acetone-d_6, 125.8 MHz): δ 145.2, 142.9, 141.1, 133.0, 129.1, 128.7, 128.2, 125.6, 120.6, 118.5, 45.1, 30.0, 21.8 ppm; ^{11}B NMR (acetone, 128.4 MHz): δ 34.2 ppm; IR: ν = 2952, 2865, 1612, 1596, 1566, 1460, 1440, 1402, 1384, 1346, 1284, 1200, 1118, 978, 813, 791 cm^{-1}; HRMS (ESI+) m/z calc. for $C_{18}H_{21}BN$ [M + H]$^+$ 262.1767, found 262.1769.

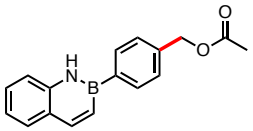

2-(4-(Acetoxymethyl)phenyl)-2,1-borazanaphthalene (**3.7**): obtained as a white powder (104 mg, 75%) using silicate **11b**; mp = 94-97 °C; ^{1}H NMR (acetone-d_6, 500.4 MHz): δ 9.79 (br s, 1 H), 8.18 (d, *J* = 11.6 Hz, 1 H), 8.05 (d, *J* = 8.0 Hz, 2 H), 7.70–7.64 (m, 2 H), 7.49–7.42 (m, 3 H), 7.29 (dd, *J* = 11.5, 2.1 Hz, 1 H), 7.18 (ddd, *J* = 7.9, 7.1, 1.1 Hz, 1 H), 5.15 (s, 2 H), 2.07 (s, 3 H) ppm; ^{13}C {^{1}H} NMR (acetone-d_6, 125.8 MHz): δ 170.0, 145.4, 141.0, 137.7, 133.2, 129.1, 128.3, 127.5, 125.6, 120.8, 118.6, 65.5, 19.9 ppm; ^{11}B NMR (acetone, 128.4 MHz): δ 33.4 ppm; IR: ν = 1738, 1609, 1595, 1563, 1437, 1377, 1361, 1226, 1152, 1117, 1039, 1018, 988, 977, 939, 806 cm^{-1}; HRMS (ESI+) m/z calc. for $C_{17}H_{16}BNNaO_2$ [M + Na]$^+$ 300.1172, found 300.1169.

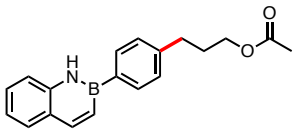

2-(4-(3-Acetoxypropyl)phenyl)-2,1-borazanaphthalene (**3.8**): obtained as an off white powder (141 mg, 92%); mp = 70-72 °C; ^{1}H NMR (acetone-d_6, 500.4 MHz): δ

9.70 (br s, 1 H), 8.15 (d, *J* = 8.6 Hz, 1 H), 7.98 (d, *J* = 7.8 Hz, 2 H), 7.69 (d, *J* = 8.1 Hz, 1 H), 7.66 (d, *J* = 8.1 Hz, 1 H), 7.45 (ddd, *J* = 8.1, 6.7, 1.3 Hz, 1 H), 7.31 (d, *J* = 7.8 Hz, 2 H), 7.28 (dd, *J* = 11.5, 1.8 Hz, 1 H), 7.17 (ddd, *J* = 8.0, 7.0, 1.3 Hz, 1 H), 4.07 (t, *J* = 6.6 Hz, 2 H), 2.74 (t, *J* = 7.7 Hz, 2 H), 2.00 (s, 3 H), 2.00–1.95 (m, 2 H) ppm; ^{13}C {^{1}H} NMR (acetone-d_6, 125.8 MHz): δ 170.1, 145.2, 142.9, 141.0, 133.2, 129.1, 128.2, 128.0, 125.6, 120.6, 118.5, 63.2, 31.8, 30.1, 19.9 ppm; ^{11}B NMR (acetone, 128.4 MHz): δ 34.7 ppm; IR: ν = 3354, 1717, 1610, 1562, 1444, 1403, 1388, 136, 1344, 1253, 1191, 1154, 1033, 1002, 979, 815 cm^{-1}; HRMS (ESI+) m/z calc. for $C_{19}H_{20}BNNaO_2$ [M + Na]$^+$ 328.1485, found 328.1481.

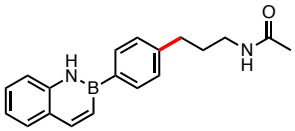

2-(4-(3-Acetamidopropyl)phenyl)-2,1-borazanaphthalene (**3.9**): obtained as an off white powder (135 mg, 89%); mp = 157-159 °C; ^{1}H NMR ($CDCl_3$, 500.4 MHz): δ 8.17 (br s, 1 H), 8.13 (d, *J* = 11.3 Hz, 1 H), 7.86 (d, *J* = 7.8 Hz, 2 H), 7.68 (d, *J* = 8.3 Hz, 1 H), 7.45 (ddd, *J* = 7.9, 7.2, 1.4 Hz, 1 H), 7.35 (d, *J* = 8.5 Hz, 1 H), 7.30 (d, *J* = 7.5 Hz, 2 H), 7.27 (dd, *J* = 11.6, 2.1 Hz, 1 H), 7.20 (ddd, *J* = 7.9, 7.0, 0.9 Hz, 1 H), 5.49 (br s, 1 H), 3.33 (td, *J* = 6.8, 6.5 Hz, 2 H), 2.72 (t, *J* = 7.7 Hz, 2 H), 1.96 (s, 3 H), 1.90 (tt, *J* = 7.7, 6.8 Hz, 2 H) ppm; ^{13}C {^{1}H} NMR ($CDCl_3$, 125.8 MHz): δ 170.0, 145.4, 143.0, 140.1, 133.0, 132.9, 129.4, 128.3, 125.6, 120.9, 118.1, 39.3, 33.3, 31.0, 23.3 ppm; ^{11}B NMR (acetone, 128.4 MHz): δ 34.1 ppm; IR: ν = 1633, 1606, 1595, 1551, 1435, 1404, 1366, 1344, 1301, 1281, 1200, 1182, 810, 757, 745, 719 cm^{-1}; HRMS (ESI+) m/z calc. for $C_{19}H_{22}BN_2O$ [M + H]$^+$ 305.1825, found 305.1816.

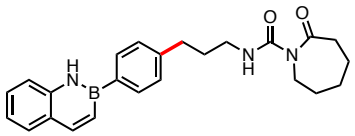

2-(4-(3-(2-Oxoazepane-1-carboxamido)propyl)phenyl)-2,1-borazanaphthalene (**3.10**): obtained as an off white powder (192 mg, 96%); mp = 131-133 °C; ^{1}H NMR (DMSO-d_6, 500.4 MHz): δ 10.34 (br s, 1 H), 9.22 (br s, 1 H), 8.11 (d, *J* = 11.4 Hz, 1 H), 7.99 (d, *J* = 8.0 Hz, 2 H), 7.71 (d, *J* = 8.3 Hz, 1 H), 7.66 (d, *J* = 8.0 Hz, 1 H), 7.44 (t, *J* = 7.6 Hz, 1 H), 7.29 (d, *J* = 7.1 Hz, 2 H), 7.22 (d, *J* = 11.1 Hz, 1 H), 7.14 (t, *J* = 7.1 Hz, 1 H), 3.90 (d, *J* = 2.1 Hz, 2 H), 3.18–3.24 (m, 2 H), 2.71–2.68 (m, 2 H), 2.62 (t, *J* = 4.3 Hz, 2 H), 1.85–1.80 (m, 2 H), 1.68–1.62 (m, 4 H), 1.58–1.53 (m, 2 H) ppm; ^{13}C {^{1}H} NMR (DMSO-d_6, 125.8 MHz): δ 179.4, 154.6, 145.5, 143.3, 141.4, 133.9, 129.4, 128.6, 128.3, 125.5, 120.9, 119.0, 43.2, 39.9, 39.3, 33.0, 30.9, 28.7, 28.3, 23.4 ppm; ^{11}B NMR (acetone, 128.4 MHz): δ 33.9 ppm; IR: ν = 3390, 3258, 1686, 1651, 1614, 1568, 1524, 1451, 1440, 1396, 1351, 1289, 1205, 1174, 1159, 814, 776, 748 cm^{-1}; HRMS (ESI+) m/z calc. for $C_{24}H_{29}BN_3O_2$ $[M + H]^+$ 402.2344, found 402.2353.

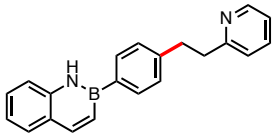

2-(4-(2-Pyridin-2-yl)ethyl)phenyl)-2,1-borazanaphthalene (**3.11**): obtained as an off white powder (125 mg, 81%); mp = 117-119 °C; ^{1}H NMR (acetone-d_6, 500.4 MHz): δ 9.73 (br s, 1 H), 8.52 (d, *J* = 4.9 Hz, 1 H), 8.16 (d, *J* = 11.2 Hz, 1 H), 7.95 (d, *J* = 7.3 Hz, 2 H), 7.69–7.60 (m, 3 H), 7.44 (ddd, *J* = 7.9, 7.4, 1.4 Hz, 1 H), 7.32–7.26 (m, 3 H), 7.21 (d, *J* = 8.0 Hz, 1 H) 7.19–7.12 (m, 2 H), 3.13–3.08 (m, 4 H) ppm; ^{13}C {^{1}H} NMR (acetone-d_6, 125.8 MHz): δ 161.1, 149.1, 145.2, 143.3, 141.1, 136.0, 133.2,

129.1, 128.2, 128.1, 125.6, 122.7, 121.0, 120.6, 118.5, 39.6, 35.5 ppm; ^{11}B NMR (acetone, 128.4 MHz): δ 34.2 ppm; IR: ν = 3372, 1605, 1593, 1565, 1471, 1431, 1404, 1386, 1347, 1282, 1229, 1199, 1139, 977, 808, 756, 745 cm^{-1}; HRMS (ESI+) m/z calc. for $C_{21}H_{20}BN_2$ $[M + H]^+$ 311.1720, found 311.1724.

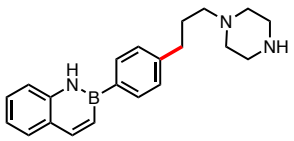

2-(4-(3-(Piperazin-1-yl)propyl)phenyl)-2,1-borazanaphthalene (**3.12**): obtained as a colorless oil (78 mg, 47%) using silicate **11c**; ^{1}H NMR (acetone-d_6, 500.4 MHz): δ 8.16 (br s, 1 H), 8.13 (d, *J* = 11.5 Hz, 1 H), 7.66 (d, *J* = 7.7 Hz, 2 H), 7.66 (dd, *J* = 8.0, 1.1 Hz, 1 H), 7.44 (ddd, *J* = 8.3, 6.9, 1.2 Hz, 1 H), 7.35–7.30 (m, 3 H), 7.29 (d, *J* = 12 H, 1 H), 7.20 (t, *J* = 7.4 Hz, 1 H), 2.96–2.90 (m, 4 H), 2.71 (t, *J* = 7.7 Hz, 2 H), 2.51–2.37 (m, 6 H), 2.32–2.20 (br s, 1 H), 1.89 (tt, *J* = 8.5, 6.7 Hz, 2 H) ppm; ^{13}C {^{1}H} NMR (acetone-d_6, 125.8 MHz): δ 145.3, 143.9, 140.2, 132.8, 129.4, 128.4, 128.3, 125.6, 120.9, 118.1, 58.6, 54.5, 46.0, 33.7, 28.2 ppm; ^{11}B NMR (acetone, 128.4 MHz): δ 34.2 ppm; IR: ν = 2939, 2806, 1612, 1595, 1563, 1437, 1345, 1283, 1233, 1217, 1199, 1188, 1142, 1116, 979, 801 cm^{-1}; HRMS (ESI+) m/z calc. for $C_{21}H_{27}BN_3$ $[M + H]^+$ 332.2298, found 332.2307.

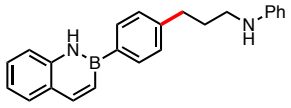

2-(4-(3-(Phenylamino)propyl)phenyl)-2,1-borazanaphthalene (**3.13**): obtained as a white powder (154 mg, 91%); mp = 110-111 °C; ^{1}H NMR (acetone-d_6, 500.4 MHz): δ 9.69 (br s, 1 H), 8.16 (d, *J* = 11.0 Hz, 1 H), 7.98 (d, *J* = 7.8 Hz, 2 H), 7.67

(t, *J* = 8.6 Hz, 2 H), 7.44 (ddd, *J* = 8.2, 7.2, 1.5 Hz, 1 H), 7.34–7.26 (m, 3 H), 7.17 (ddd, *J* = 8.0, 6.8, 1.2 Hz, 1 H), 7.10–7.05 (m, 2 H), 6.61 (dd, *J* = 8.2, 1.1 Hz, 2 H), 6.56 (t, *J* = 7.3 Hz, 1 H), 4.85 (br s, 1 H), 3.18–3.12 (m, 2 H), 2.78 (t, *J* = 7.7 Hz, 2 H), 2.00–1.94 (m, 2 H) ppm; ^{13}C {^{1}H} NMR (acetone-d_6, 125.8 MHz): δ 149.1, 145.2, 143.6, 141.1, 133.2, 129.1, 128.8, 128.2, 128.1, 125.6, 120.6, 118.5, 115.9, 112.2, 42.8, 33.2, 30.9 ppm; ^{11}B NMR (acetone, 128.4 MHz): δ 34.4 ppm; IR: ν = 3350, 1596, 1561, 1503, 1480, 1438, 1405, 1311, 1282, 1236, 1183, 1163, 1148, 1118, 810, 757, 743 cm^{-1}; HRMS (ESI+) m/z calc. for $C_{23}H_{24}BN_2$ [M + H]$^+$ 339.2033, found 339.2032.

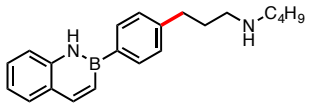

2-(4-(3-(Butylamino)propyl)phenyl)-2,1-borazanaphthalene (**3.14**): obtained as a light brown powder (152 mg, 95%) using silicate **11d**; mp = 90-92 °C; ^{1}H NMR ($CDCl_3$, 500.4 MHz): δ 8.18–8.12 (m, 2 H), 7.88 (d, *J* = 7.8 Hz, 2 H), 7.67 (d, *J* = 7.8 Hz, 1 H), 7.46 (ddd, *J* = 8.6, 6.4, 1.4 Hz, 1 H), 7.36–7.27 (m, 4 H), 7.21 (ddd, *J* = 8.1, 7.5, 1.3 Hz, 1 H), 2.77–2.69 (m, 4 H), 2.64 (t, *J* = 7.2 Hz, 2 H), 2.19 (br s, 1 H), 1.90 (tt, *J* = 7.8, 7.2 Hz, 2 H), 1.51 (tt, *J* = 8.0, 7.2 Hz, 2 H), 1.40–1.33 (m, 2 H), 0.95 (t, *J* = 7.5 Hz, 3 H) ppm; ^{13}C {^{1}H} NMR ($CDCl_3$, 125.8 MHz): δ 145.3, 143.8, 140.2, 132.8, 129.4, 128.3, 128.2, 125.6, 120.9, 118.1, 49.7, 49.5, 33.7, 32.2, 31.5, 20.4, 13.9 ppm; ^{11}B NMR (acetone, 128.4 MHz): δ 34.6 ppm; IR: ν = 2988, 1608, 1597, 1563, 1437, 1405, 1345, 1282, 1234, 1211, 1183, 1103, 977, 881, 796, 758, 733 cm^{-1}; HRMS (ESI+) m/z calc. for $C_{21}H_{28}BN_2$ [M + H]$^+$ 319.2346, found 319.2351.

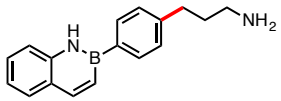

2-(4-(3-Aminopropyl)phenyl)-2,1-borazanaphthalene (**3.15**): obtained as a white powder (89 mg, 68%); mp = 120-123 °C; ^{1}H NMR (acetone-d_6, 500.4 MHz): δ 9.71 (br s, 1 H), 8.15 (d, *J* = 11.6 Hz, 1 H), 7.96 (d, *J* = 7.9 Hz, 2 H), 7.69–7.65 (m, 2 H), 7.43 (ddd, *J* = 8.5, 6.8, 1.4 Hz, 1 H), 7.31–7.26 (m, 3 H), 7.16 (ddd, *J* = 8.1, 6.8, 1.4 Hz, 1 H), 3.21 (t, *J* = 6.8 Hz, 2 H), 2.72 (t, *J* = 7.1 Hz, 2 H), 1.95–1.71 (m, 4 H) ppm; ^{13}C {^{1}H} NMR (acetone-d_6, 125.8 MHz): δ 145.1, 144.1, 141.1, 133.1, 129.1, 128.2, 128.1, 125.6, 120.5, 118.5, 50.2, 33.4, 32.5 ppm; ^{11}B NMR (acetone, 128.4 MHz): δ 34.2 ppm; IR: ν = 2941, 1651, 1609, 1575, 1455, 1417, 1349, 1287, 1208, 1193, 978, 941, 893, 813, 790, 759 cm^{-1}; HRMS (ESI+) m/z calc. for $C_{17}H_{20}BN_2$ $[M + H]^+$ 263.1720, found 263.1711.

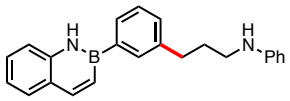

2-(3-(3-(Phenylamino)propyl)phenyl)-2,1-borazanaphthalene (**3.16**): obtained as a white powder (153 mg, 90%); mp = 72-75 °C; ^{1}H NMR ($CDCl_3$, 500.4 MHz): δ 8.18 (d, *J* = 11.3 Hz, 1 H), 8.14 (br s, 1 H), 7.81 (dt, *J* = 7.2, 1.2 Hz, 1 H), 7.78 (s, 1 H), 7.70 (dd, *J* = 7.9, 1.3 Hz, 1 H), 7.51–7.44 (m, 2 H), 7.38–7.30 (m, 3 H), 7.27–7.20 (m, 3 H), 6.75 (tt, *J* = 7.2, 1.0 Hz, 1 H), 6.65 (dd, *J* = 8.4, 0.8 Hz, 2 H), 3.67 (s, 1 H), 3.24 (t, *J* = 7.1 Hz, 2 H), 2.87 (t, *J* = 7.6 Hz, 2 H), 2.06 (tt, *J* = 7.6, 7.1 Hz, 2 H) ppm; ^{13}C {^{1}H} NMR ($CDCl_3$, 125.8 MHz): δ 148.3, 145.5, 141.3, 140.1, 132.8, 130.4, 129.7, 129.4, 129.2, 128.3 [× 2], 125.7, 121.0, 118.2, 117.2, 112.7, 43.4, 33.5, 31.2 ppm; ^{11}B NMR (acetone, 128.4 MHz): δ 34.5 ppm; IR: ν = 3325, 1599, 1579, 1561, 1507, 135,

1389, 1346, 1334, 1283, 1262, 1245, 1210, 1184, 1153, 795, 762 cm^{-1}; HRMS (ESI+) m/z calc. for $C_{23}H_{24}BN_2$ $[M + H]^+$ 339.2033, found 339.2036.

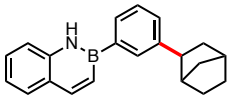

2-(3-(exo-Bicyclo[2.2.1]heptan-2-yl)phenyl)-2,1-borazanaphthalene (**3.17**): obtained as a light brown powder (143 mg, 96%); mp = 114-116 °C; ^1H NMR ($CDCl_3$, 500.4 MHz): δ 8.13 (d, *J* = 11.7 Hz, 2 H), 7.75 (s, 1 H), 7.70 (d, *J* = 7.5 Hz, 1 H), 7.65 (d, *J* = 7.7 Hz, 1 H), 7.43 (ddd, *J* = 8.6, 7.2, 1.4 Hz, 1 H), 7.39 (t, *J* = 7.4 Hz, 1 H), 7.35–7.30 (m, 2 H), 7.27 (dd, *J* = 11.6, 2.2 Hz, 1 H), 7.18 (ddd, *J* = 7.9, 7.0, 1.1 Hz, 1 H), 2.84 (dd, *J* = 8.3, 5.8 Hz, 1 H), 2.45–2.43 (m, 1 H), 2.41–2.37 (m, 1 H), 1.86–1.80 (m, 1 H), 1.79–1.73 (m, 1 H), 1.67–1.55 (m, 3 H), 1.44–1.38 (m, 1 H), 1.34–1.28 (m, 1 H), 1.26–1.20 (m, 1 H) ppm; ^{13}C $\{^1H\}$ NMR ($CDCl_3$, 125.8 MHz): δ 147.2, 145.4, 140.2, 131.8, 129.8, 129.5, 128.4, 128.3, 128.2, 125.8, 121.0, 118.3, 47.6, 43.1, 39.2, 36.9, 36.2, 30.7, 29.0 ppm; ^{11}B NMR (acetone, 128.4 MHz): δ 34.5 ppm; IR: ν = 2948, 2866, 1613, 1595, 1561, 1435, 1349, 1288, 1267, 1244, 1210, 1188, 1119, 818, 791, 756 cm^{-1}; HRMS (ESI-) m/z calc. for $C_{21}H_{21}BN$ $[M - H]^-$ 298.1767, found 298.1756.

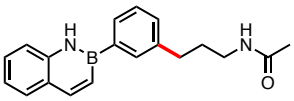

2-(3-(3-Acetamidopropyl)phenyl)-2,1-borazanaphthalene (**3.18**): obtained as an off white powder (146 mg, 96%); mp = 77-78 °C; ^1H NMR ($CDCl_3$, 500.4 MHz): δ 8.49 (br s, 1 H), 8.11 (d, *J* = 11.4 Hz, 1 H), 7.76–7.71 (m, 2 H), 7.63 (d, *J* = 8.0 Hz, 1 H), 7.44–7.41 (m, 2 H), 7.37 (t, *J* = 7.5 Hz, 1 H), 7.26–7.21 (m, 2 H), 7.19–7.15 (m, 1 H), 5.65 (br s, 1 H), 3.30 (td, *J* = 6.6, 6.7 Hz, 2 H), 2.70 (t, *J* = 7.4 Hz, 2 H), 1.94 (s, 3 H),

1.87 (tt, *J* = 7.7, 7.1 Hz, 2 H) ppm; ^{13}C {^{1}H} NMR ($CDCl_3$, 125.8 MHz): δ 170.2, 145.4, 140.8, 140.4, 132.8, 130.6, 129.6, 129.3, 128.3, 128.2, 125.6, 120.9, 118.4, 39.3, 33.1, 31.0, 23.3 ppm; ^{11}B NMR (acetone, 128.4 MHz): δ 34.7 ppm; IR: ν = 3321, 1649, 1613, 1595, 1562, 1436, 1412, 1386, 1366, 1347, 1285, 1242, 1207, 1181, 810, 785, 759 cm^{-1}; HRMS (ESI+) m/z calc. for $C_{19}H_{21}BN_2NaO$ $[M + Na]^+$ 327.1645, found 327.1635.

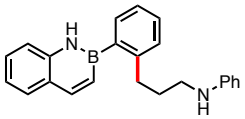

2-(2-(3-(Phenylamino)propyl)phenyl)-2,1-borazanaphthalene (**3.19**): obtained as a light yellow oil (158 mg, 93%); ^{1}H NMR ($CDCl_3$, 500.4 MHz): δ 8.08 (d, *J* = 11.7 Hz, 1 H), 7.92 (br s, 1 H), 7.66 (d, *J* = 8.3 Hz, 1 H), 7.48–7.44 (m, 1 H), 7.40 (ddd, *J* = 8.2, 7.1, 1.5 Hz, 1 H), 7.37–7.32 (m, 1 H), 7.28–7.23 (m, 2 H), 7.19 (ddd, *J* = 7.9, 7.0, 1.1 Hz, 1 H), 7.15 (d, *J* = 8.3 Hz, 1 H), 7.09–7.02 (m, 3 H), 6.64 (tt, *J* = 7.3, 1.1 Hz, 1 H), 6.38 (dd, *J* = 8.6, 1.1 Hz, 2 H), 3.37 (br s, 1 H), 3.03 (t, *J* = 6.8 Hz, 2 H), 2.90 (t, *J* = 7.6 Hz, 2 H), 1.85 (tt, *J* = 7.6, 6.8 Hz, 2 H) ppm; ^{13}C {^{1}H} NMR ($CDCl_3$, 125.8 MHz): δ 148.2, 144.9, 140.0, 133.0 ,129.4, 129.1, 128.7, 128.6, 128.4 [× 2], 125.5, 125.3, 121.2, 118.3, 117.2, 112.7, 43.4, 33.6, 31.9 ppm; ^{11}B NMR (acetone, 128.4 MHz): δ 36.1 ppm; IR: ν = 3331, 1614, 1597, 1559, 1504, 1430, 1345, 1320, 1280, 1262, 1235, 1203, 1179, 978, 907, 811, 746 cm^{-1}; HRMS (ESI+) m/z calc. for $C_{23}H_{24}BN_2$ $[M + H]^+$ 339.2033, found 339.2034.

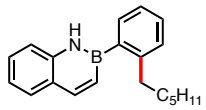

2-(2-Hexylphenyl)-2,1-borazanaphthalene (**3.20**): obtained as a colorless oil (140 mg, 97%); ^{1}H NMR ($CDCl_3$, 500.4 MHz): δ 8.09 (d, *J* = 11.4 Hz, 1 H), 7.93 (br s, 1 H), 7.67 (d, *J* = 8.3 Hz, 1 H), 7.47 (dd, *J* = 7.3, 1.3 Hz, 1 H), 7.43 (ddd, *J* = 8.4, 6.8, 1.2 Hz, 1 H), 7.33 (ddd, *J* = 7.6, 7.4, 1.3 Hz, 1 H), 7.29–7.16 (m, 4 H), 7.07 (dd, *J* = 11.4, 2.1 Hz, 1 H), 2.77 (t, *J* = 8.3 Hz, 2 H), 1.60–1.51 (m, 2 H), 1.31–1.17 (m, 6 H), 0.8 (t, *J* = 6.8 Hz, 3 H) ppm; ^{13}C {^{1}H} NMR ($CDCl_3$, 125.8 MHz): δ 146.3, 144.7, 140.1, 133.0, 129.5, 128.7, 128.5, 128.3, 125.4, 125.3, 121.1, 118.2, 36.2, 32.7, 31.7, 29.3, 22.6, 14.1 ppm; ^{11}B NMR (acetone, 128.4 MHz): δ 36.3 ppm; IR: ν = 2952, 2924, 2854, 1614, 1596, 1559, 1430, 1383, 1345, 1278, 1232, 1213, 1203, 1114, 978, 809 cm^{-1}; HRMS (ESI-) m/z calc. for $C_{20}H_{23}BN$ $[M - H]^-$ 288.1924, found 288.1942.

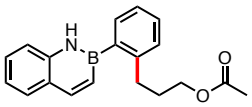

2-(2-(3-Acetoxypropyl)phenyl)-2,1-borazanaphthalene (**3.21**): obtained as a colorless oil (142 mg, 93%); ^{1}H NMR ($CDCl_3$, 500.4 MHz): δ 8.10 (d, *J* = 11.2 Hz, 1 H), 7.80 (br s, 1 H), 7.68 (d, *J* = 8.0 Hz, 1 H), 7.50–7.41 (m, 2 H), 7.37–7.30 (m, 2 H), 7.28–7.24 (m, 2 H), 7.22 (ddd, *J* = 8.0, 7.0, 1.2 Hz, 1 H), 7.06 (dd, *J* = 11.6, 1.8 Hz, 1 H), 3.99 (t, *J* = 6.6 Hz, 2 H), 2.87 (t, *J* = 7.8 Hz, 2 H), 1.91–1.85 (m, 2 H), 1.84 (s, 3 H) ppm; ^{13}C {^{1}H} NMR ($CDCl_3$, 125.8 MHz): δ 171.1, 144.8, 144.4, 140.2, 133.0, 129.4, 128.6, 128.5, 128.4, 125.6, 125.3, 121.2, 118.3, 63.8, 32.3, 31.2, 20.7 ppm; ^{11}B NMR (acetone, 128.4 MHz): δ 36.1 ppm; IR: ν = 1723, 1614, 1596, 1560, 1432, 1286,

1365, 1347, 1236, 1031, 979, 908, 812, 753, 729, 662 cm^{-1}; HRMS (ESI+) m/z calc. for $C_{19}H_{21}BNO_2$ $[M + H]^+$ 306.1665, found 306.1666.

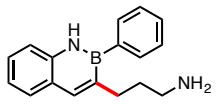

3-(3-Aminopropyl)-2-phenyl-2,1-borazanaphthalene (**3.22**): obtained as a brown oil (124 mg, 95%); ^1H NMR ($CDCl_3$, 500.4 MHz): δ 7.95 (br s, 1 H), 7.86 (s, 1 H), 7.70–7.65 (m, 2 H), 7.63 (dd, *J* = 7.8, 0.9 Hz, 1 H), 7.48–7.37 (m, 4 H), 7.27 (d, *J* = 7.4 Hz, 1 H), 7.20 (t, *J* = 7.5 Hz, 1 H), 2.78 (t, *J* = 7.6 Hz, 2 H), 2.68 (t, *J* = 7.6 Hz, 2 H), 1.72 (br s, 2 H), 1.66 (tt, *J* = 7.6 Hz, 2 H) ppm; ^{13}C $\{^1H\}$ NMR ($CDCl_3$, 125.8 MHz): δ 141.9, 139.0, 132.3, 128.7, 128.4, 127.9, 127.4, 125.3, 121.1, 117.6, 41.8, 34.9, 32.4 ppm; ^{11}B NMR (acetone, 128.4 MHz): δ 36.1 ppm; IR: ν = 2926, 2854, 1661, 1614, 1597, 1567, 1453, 1427, 1372, 1347, 1285, 1240, 1208, 945, 909, 751 cm^{-1}; HRMS (ESI+) m/z calc. for $C_{17}H_{20}BN_2$ $[M + H]^+$ 263.1720, found 263.1724.

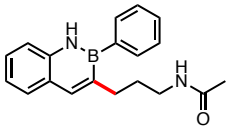

3-(3-Acetamidopropyl)-2-phenyl-2,1-borazanaphthalene (**3.23**): obtained as an off white solid (146 mg, 96%); mp = 92-93 °C; ^1H NMR ($CDCl_3$, 500.4 MHz): δ 7.99 (br s, 1 H), 7.83 (s, 1 H), 7.65 (dd, *J* = 7.6, 1.4 Hz, 2 H), 7.60 (d, *J* = 7.7 Hz, 1 H), 7.46–7.40 (m, 3 H), 7.37 (ddd, *J* = 8.3, 6.8, 1.4 Hz, 1 H), 7.26 (d, *J* = 7.8 Hz, 1 H), 7.17 (ddd, *J* = 7.9, 7.3, 1.1 Hz, 1 H), 5.26 (br s, 1 H), 3.13 (td, *J* = 6.4, 6.3 Hz, 2 H), 2.73 (t, *J* = 7.6 Hz, 2 H), 1.80 (s, 3 H), 1.63 (tt, *J* = 7.4, 7.2 Hz, 2 H) ppm; ^{13}C $\{^1H\}$ NMR ($CDCl_3$, 125.8 MHz): δ 169.9, 142.5, 139.1, 132.3, 128.8, 128.4, 128.0, 127.6, 125.3, 121.1, 117.7, 39.0, 32.1, 31.1, 23.2 ppm; ^{11}B NMR (acetone, 128.4 MHz): δ 35.8 ppm; IR: ν = 3281,

1650, 1614, 1597, 1565, 1453, 1429, 1365, 1347, 1286, 1239, 1208, 948, 752, 731, 701 cm^{-1}; HRMS (ESI+) m/z calc. for $C_{19}H_{22}BN_2O$ $[M + H]^+$ 305.1825, found 305.1830.

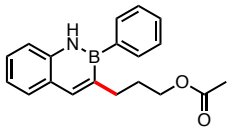

3-(3-Acetoxypropyl)-2-phenyl-2,1-borazanaphthalene (**3.24**): obtained as a thick white wax (139 mg, 91%); ^1H NMR ($CDCl_3$, 500.4 MHz): δ 7.93 (br s, 1 H), 7.85 (s, 1 H), 7.67 (dd, *J* = 7.8, 1.6 Hz, 2 H), 7.62 (d, *J* = 7.7 Hz, 1 H), 7.46–7.41 (m, 3 H), 7.39 (ddd, *J* = 8.2, 7.2, 1.4 Hz, 1 H), 7.26 (d, *J* = 8.2 Hz, 1 H), 7.19 (ddd, *J* = 7.8, 7.1, 1.0 Hz, 1 H), 4.02 (t, *J* = 6.6 Hz, 2 H), 2.80 (t, *J* = 7.9 Hz, 2 H), 1.98 (s, 3 H), 1.81 (tt, *J* = 7.8, 6.4 Hz, 2 H) ppm; ^{13}C $\{^1H\}$ NMR ($CDCl_3$, 125.8 MHz): δ 171.1, 142.3, 139.1, 132.3, 128.8, 128.4, 128.0, 127.6, 125.3, 121.2, 117.7, 64.1, 31.4, 29.9, 20.9 ppm; ^{11}B NMR (acetone, 128.4 MHz): δ 36.2 ppm; IR: ν = 1721, 1614, 1597, 1567, 1452, 1427, 1385, 1364, 1347, 1238, 1035, 999, 946, 918, 854, 751 cm^{-1}; HRMS (ESI+) m/z calc. for $C_{19}H_{20}BNNaO_2$ $[M + Na]^+$ 328.1485, found 328.1496.

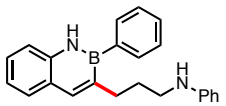

3-(3-(Phenylamino)propyl)-2-phenyl-2,1-borazanaphthalene (**3.25**): obtained as a brown oil (147 mg, 87%); ^1H NMR ($CDCl_3$, 500.4 MHz): δ 8.00 (br s, 1 H), 7.96 (s, 1 H), 7.79–7.75 (m, 2 H), 7.72 (d, *J* = 8.0 Hz, 1 H), 7.58–7.54 (m, 3 H), 7.48 (t, *J* = 7.4 Hz, 1 H), 7.33–7.21 (m, 4 H), 6.78 (t, *J* = 7.2 Hz, 1 H), 6.59 (d, *J* = 8.1 Hz, 2 H), 3.51 (br s, 1 H), 3.15 (t, *J* = 7.0 Hz, 2 H), 2.94 (t, *J* = 7.5 Hz, 2 H), 1.87 (tt, *J* = 7.5, 7.0 Hz, 2 H)

ppm; ^{13}C {^{1}H} NMR ($CDCl_3$, 125.8 MHz): δ 148.4, 142.3, 139.2, 132.4, 129.2, 128.9, 128.6, 128.1, 127.6, 125.4, 121.3, 117.8, 117.0, 112.7, 43.5, 32.7, 31.0 ppm; ^{11}B NMR (acetone, 128.4 MHz): δ 35.9 ppm; IR: ν = 1613, 1600, 1565, 1504, 1473, 1451, 1423, 1345, 1320, 1282, 1255, 1240 ,1206, 1179, 944, 765 cm^{-1}; HRMS (ESI+) m/z calc. for $C_{23}H_{24}BN_2$ $[M + H]^+$ 339.2031, found 339.2033.

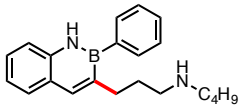

3-(3-(Butylamino)propyl)-2-phenyl-2,1-borazanaphthalene (**3.26**): obtained as a light brown powder (141 mg, 89%); ^{1}H NMR ($CDCl_3$, 500.4 MHz): δ 7.98 (br s, 1 H), 7.88 (s, 1 H), 7.70 (dd, *J* = 7.8, 1.5 Hz, 2 H), 7.65 (d, *J* = 8.2 Hz, 1 H), 7.49–7.43 (m, 3 H), 7.40 (ddd, 8.1, 7.4, 1.7 Hz, 1 H), 7.27 (d, *J* = 8.3 Hz, 1 H), 7.21 (ddd, *J* = 7.8, 7.2, 1.0 Hz, 1 H), 2.79 (t, *J* = 8.1 Hz, 2 H), 2.62 (t, *J* = 7.3 Hz, 2 H), 2.54 (t, *J* = 7.5 Hz, 2 H), 1.98 (br s, 1 H), 1.73 (tt, *J* = 7.5, 7.3 Hz, 2 H), 1.48–1.40 (m, 2 H), 1.37–1.27 (m, 2 H), 0.92 (t, *J* = 7.5 Hz, 3 H) ppm; ^{13}C {^{1}H} NMR ($CDCl_3$, 125.8 MHz): δ 142.0, 139.1, 132.3, 128.7, 128.4, 127.9, 127.4, 125.4, 121.1, 117.6, 49.6, 49.4, 32.8, 32.0, 31.3, 20.4, 14.0 ppm; ^{11}B NMR (acetone, 128.4 MHz): δ 35.0 ppm; IR: ν = 2954, 2927, 2857, 1615, 1597, 1567, 1454, 1423, 1346, 1283, 1240, 1207, 954, 943, 910, 764 cm^{-1}; HRMS (ESI+) m/z calc. for $C_{21}H_{28}BN_2$ $[M + H]^+$ 319.2346, found 319.2333.

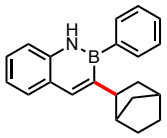

3-(exo-Bicyclo[2.2.1]heptan-2-yl)-2-phenyl-2,1-borazanaphthalene (**3.27**): obtained as an off white solid (144 mg, 96%); mp = 60-62 °C; ^{1}H NMR ($CDCl_3$, 500.4

MHz): δ 7.84 (br s, 1 H), 7.81 (s, 1 H), 7.68–7.61 (m, 3 H), 7.46–7.38 (m, 3 H), 7.34 (ddd, *J* = 8.2, 6.9, 1.5 Hz, 1 H), 7.22–7.19 (m, 1 H), 7.17 (ddd, *J* = 8.1, 6.9, 1.1 Hz, 1 H), 2.98 (dd, *J* = 8.9, 6.0 Hz, 1 H), 2.35–2.33 (m, 1 H), 2.32–2.30 (m, 1 H), 1.66–1.44 (m, 5 H), 1.30–1.23 (m, 1 H), 1.21–1.11 (m, 2 H) ppm; ^{13}C {^{1}H} NMR ($CDCl_3$, 125.8 MHz): δ 138.6, 137.4, 132.4, 1291, 128.1, 127.8, 127.2, 125.4, 121.1, 117.5, 44.9, 42.4, 38.7, 37.2, 35.5, 30.2, 29.0 ppm; ^{11}B NMR (acetone, 128.4 MHz): δ 36.6 ppm; IR: ν = 2946, 2866, 1612, 1597, 1563, 1453, 1419, 1345, 1307, 1235, 1206, 940, 909, 763, 747, 700 cm^{-1}; HRMS (ESI+) m/z calc. for $C_{21}H_{23}BN$ [M + H]$^+$ 300.1924, found 300.1928.

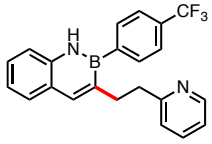

3-(2-Pyridin-2-yl)ethyl)-2-(4-trifluoromethylphenyl)-2,1-borazanaphthalene (**3.28**): obtained as a white solid (145 mg, 77%); mp = 100-102 °C; ^{1}H NMR (acetone-d_6, 500.4 MHz): δ 9.71 (br s, 1 H), 8.44 (d, *J* = 4.2 Hz, 1 H), 8.01–7.87 (m, 3 H), 7.71 (d, *J* = 8.6 Hz, 2 H), 7.67 (d, *J* = 7.7 Hz, 1 H), 7.61 (d, *J* = 7.8 Hz, 1 H), 7.57 (ddd, *J* = 7.8, 7.7, 1.8 Hz, 1 H), 7.40 (ddd, *J* = 7.9, 7.5, 1.7 Hz, 1 H), 7.18 (t, *J* = 7.9 Hz, 1 H), 7.09–7.00 (m, 2 H), 3.13 (d, *J* = 8.6 Hz, 2 H), 2.93 (dd, *J* = 9.6, 7.3 Hz, 2 H) ppm; ^{13}C {^{1}H} NMR (acetone-d_6, 125.8 MHz): δ 161.5, 149.0, 142.5, 139.8, 135.9, 133.2, 129.4 (q, *J* = 32.4 Hz), 128.7, 127.6, 125.5, 124.7 (q, *J* = 271.8 Hz), 124.0 (q, *J* = 4.0 Hz), 122.5, 121.1, 120.9, 118.2, 39.5, 34.9 ppm; ^{11}B NMR (acetone, 128.4 MHz): δ 35.2 ppm; ^{19}F {^{1}H} NMR (acetone-d_6, 470.8 MHz): –62.9 ppm; IR: ν = 1595, 1571, 1459, 1438, 1322, 1293, 1150, 1112, 1104, 1063, 1019, 969, 953, 835, 763, 749 cm^{-1}; HRMS (ESI+) m/z calc. for $C_{22}H_{19}BF_3N_2$ [M + H]$^+$ 379.1593, found 379.1599.

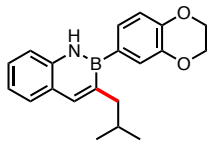

3-(Isobutyl)-2-(2,3-dihydro-1,4-benzodioxin-6-yl)-2,1-borazanaphthalene (**3.29**): obtained as a white solid (78 mg, 94%), starting from **1f** (69 mg, 0.26 mmol); mp = 76-79 °C; ^{1}H NMR ($CDCl_3$, 500.4 MHz): δ 8.09 (br s, 1 H), 7.77 (s, 1 H), 7.60 (d, *J* = 7.5 Hz, 1 H), 7.33 (ddd, *J* = 8.2, 7.0, 1.1 Hz, 1 H), 7.20 (d, *J* = 8.3 Hz, 1 H), 7.15 (t, *J* = 7.2 Hz, 1 H), 8.97 (dd, *J* = 5.8, 3.2 Hz, 1 H), 6.92–6.86 (m, 2 H), 4.26–4.17 (m, 4 H), 2.52 (d, *J* = 7.2 Hz, 2 H), 1.67 (tsept, 6.6, 7.2 Hz, 1 H), 0.79 (d, *J* = 6.6 Hz, 6 H) ppm; ^{13}C {^{1}H} NMR ($CDCl_3$, 125.8 MHz): δ 145.3, 143.1, 142.3, 138.8, 128.7, 127.1, 125.8, 125.4, 121.3, 121.0, 117.6, 117.5, 64.3, 64.2, 45.1, 29.2, 22.6 ppm; ^{11}B NMR (acetone, 128.4 MHz): δ 36.5 ppm; IR: ν = 2946, 1614, 1597, 1565, 1454, 1437, 1422, 1377, 1280, 1252, 1217, 1200, 1093, 1082, 930, 895, 843 cm^{-1}; HRMS (ESI+) m/z calc. for $C_{20}H_{23}BNO_2$ $[M + H]^+$ 320.1822, found 320.1836.

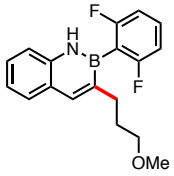

3-(3-Methoxypropyl)-2-(2,6-difluorophenyl)-2,1-borazanaphthalene (**3.30**): obtained as a white solid from (150 mg, 96%); mp = 71-74 °C; ^{1}H NMR (acetone-d_6, 500.4 MHz): δ 9.91 (br s, 1 H), 7.96 (s, 1 H), 7.71 (d, *J* = 9.1 Hz, 1 H), 7.61 (d, *J* = 8.0 Hz, 1 H), 7.47–7.40 (m, 2 H), 7.22 (ddd, *J* = 8.1, 7.0, 1.1 Hz, 1 H), 7.03–6.95 (m, 2 H), 3.25 (t, *J* = 6.7 Hz, 2 H), 3.15 (s, 3 H), 2.63 (t, *J* = 8.2 Hz, 2 H), 1.69 (tt, *J* = 8.3, 6.7 Hz, 2 H) ppm; ^{13}C {^{1}H} NMR ($CDCl_3$, 125.8 MHz): δ 164.4 (dd, *J* = 238.9, 16.7 Hz), 141.7,

139.4, 131.0 (t, *J* = 10.1 Hz), 128.7, 127.5, 125.6, 121.3, 118.1, 110.7 (dd, *J* = 21.8, 5.7 Hz), 71.8, 57.3, 31.4, 30.6 ppm; ^{11}B NMR (acetone, 128.4 MHz): δ 33.6 ppm; ^{19}F {^{1}H} NMR (acetone-d_6, 470.8 MHz): –103.2 ppm; IR: ν = 3274, 1617, 1573, 1462, 1444, 1227, 1213, 1110, 1101, 1060, 976, 966, 943, 852, 777, 760 cm^{-1}; HRMS (ESI+) m/z calc. for $C_{18}H_{19}BF_2NO$ $[M + H]^+$ 314.1528, found 314.1536.

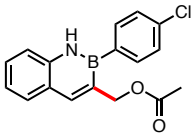

3-(Acetoxymethyl)-2-(4-chlorophenyl)-2,1-borazanaphthalene (**3.31**): obtained as a white solid (94 mg, 60%); mp = 121-123 °C; ^{1}H NMR (acetone-d_6, 500.4 MHz): δ 9.73 (br s, 1 H), 8.13 (s, 1 H), 7.76–7.71 (m, 3 H), 7.65 (d, *J* = 8.7 Hz, 1 H), 7.50–7.42 (m, 3 H), 7.22 (ddd, *J* = 8.2, 6.7, 1.1 Hz, 1 H), 5.19 (s, 2 H), 2.03 (s, 3 H) ppm; ^{13}C {^{1}H} NMR (acetone-d_6, 125.8 MHz): δ 169.9, 142.9, 140.5, 134.6, 134.2, 129.2, 128.6, 127.7, 124.6, 121.2, 118.3, 66.2, 20.0 ppm; ^{11}B NMR (acetone, 128.4 MHz): δ 34.9 ppm; IR: ν = 3324, 1720, 1616, 1587, 1575, 1454, 1431, 1367, 1340, 1246, 1210, 1100, 1088, 1034, 1013, 961, 792 cm^{-1}; HRMS (ESI+) m/z calc. for $C_{17}H_{15}BClNNaO_2$ $[M + Na]^+$ 334.0782, found 334.0796.

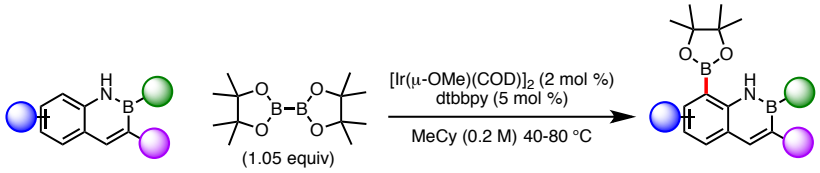

Experimental Procedure for Iridium Catalyzed C-H Borylation of 2,1-Borazaronaphthalenes. In a microwave vial with stir bar, 2,1-borazaronaphthalene (0.5 mmol, 1.0 equiv) and B_2Pin_2 (133.3 mg, 0.53 mmol, 1.05

equiv) were added. The reaction vessel was capped and purged with argon followed by the addition of 1 mL of degassed methylcyclohexane. In a separate vial, [Ir(μ-OMe)(COD)]$_2$ (6.6 mg, 0.01 mmol, 2 mol %) and di-*t*-Bu-bipyridine (6.7 mg, 0.025 mmol, 5 mol %) were precomplexed under an inert atmosphere in 1 mL degassed methylcyclohexane, stirring 30 min at rt as the mixture turned magenta. The catalyst mixture was then added to the reaction mixture *via* syringe. The reaction was then heated and run for 16 h while being monitored by HPLC for completion. Upon cooling, the reaction mixture was condensed and adhered to silica, which was directly subjected to purification by automated silica gel column chromatography with a gradient solution of hexane/EtOAc as the mobile phase.

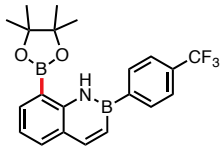

8-(4,4,5,5-Tetramethyl-1,3,2-dioxaboryl)-2-(4-(trifluoromethyl)phenyl)-2,1-borazaronaphthalene (**3.32**): Reaction was run at 40 °C, and the product was obtained as a white solid (166 mg, 83%, 0.5 mmol scale); mp: 135-137 °C; ^{1}H NMR ($CDCl_3$, 500.4 MHz): δ 10.61 (s, 1H), 8.21 (d, *J* = 11.4 Hz, 1H), 8.12 (d, *J* = 7.7 Hz, 2H), 8.05 (d, *J* = 7.2 Hz, 1H), 7.82 (d, *J* = 7.8 Hz, 1H), 7.78 (d, *J* = 7.6 Hz, 2H), 7.32 (d, *J* = 11.5 Hz, 1H), 7.29 – 7.23 (m, 1H), 1.51 (s, 12H) ppm; ^{13}C {^{1}H} NMR ($CDCl_3$, 125.8 MHz): δ 146.3, 145.6, 137.0, 133.4, 133.0, 131.1 (q, *J* = 32.0 Hz), 125.3, 124.7 (q, *J* = 4.0 Hz), 124.4 (q, *J* = 272.1 Hz), 120.6, 84.3, 25.0 ppm; ^{19}F {^{1}H} NMR ($CDCl_3$, 470.8 MHz): δ -62.7 ppm; ^{11}B NMR ($CDCl_3$, 128.4 MHz): δ 30.8 (br, 2B) ppm; IR: ν = 3355,

2984, 1600, 1321, 1307, 1127, 1104, 786 cm^{-1}; HRMS (EI) m/z calc. for $C_{21}H_{22}B_2NO_2F_3$ $[M]^+$ 399.1789, found 399.1798.

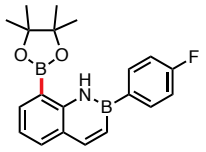

2-(p-Tolyl)-8-(4,4,5,5-tetramethyl-1,3,2-dioxaboryl)-2,1-borazaronaphthalene (**3.33**): Reaction was run at 80 °C for 24 h, and obtained as a white solid (552 mg, 80%, 2.0 mmol scale); mp: 105-108 °C; ^1H NMR ($CDCl_3$, 500.4 MHz): δ 10.46 (s, 1H), 8.12 (d, *J* = 11.5 Hz, 1H), 7.97 (dd, *J* = 7.2, 1.4 Hz, 1H), 7.92 (d, *J* = 7.8 Hz, 2H), 7.76 (d, *J* = 7.6 Hz, 1H), 7.38 – 7.30 (m, 3H), 7.18 (t, *J* = 7.4 Hz, 1H), 2.44 (s, 3H), 1.47 (s, 12H) ppm; ^{13}C $\{^1H\}$ NMR ($CDCl_3$, 125.8 MHz): δ 145.9, 145.5, 139.4, 136.6, 133.3, 132.9, 132.6, 128.9, 119.9, 84.1, 25.0, 21.5 ppm; ^{11}B NMR ($CDCl_3$, 128.4 MHz): δ 33.2, 30.5 ppm; IR: ν = 3351, 2973, 1599, 1565, 1355, 1307, 1138, 775 cm^{-1}; HRMS (EI) m/z calc. for $C_{21}H_{25}B_2NO_2$ $[M]^+$ 345.2071, found 345.2077.

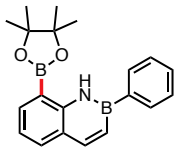

2-Phenyl-8-(4,4,5,5-tetramethyl-1,3,2-dioxaboryl)-2,1-borazaronaphthalene (**3.34**): Reaction was run at 40 °C, and the product was obtained as a white solid (104 mg, 63%, 0.5 mmol scale); mp: 131-133 °C; ^1H NMR ($CDCl_3$, 500.4 MHz): δ 10.58 (s, 1H), 8.20 (d, *J* = 11.5 Hz, 1H), 8.09 (d, *J* = 7.4 Hz, 2H), 8.06 (d, *J* = 7.2 Hz, 1H), 7.83 (d, *J* = 7.8 Hz, 1H), 7.62 – 7.51 (m, 3H), 7.38 (dd, *J* = 11.5, 1.9 Hz, 1H), 7.26 (t, *J* =

7.4 Hz, 1H), 1.53 (s, 12H) ppm; ^{13}C {^{1}H} NMR ($CDCl_3$, 125.8 MHz): δ 145.9, 145.7, 136.8, 133.4, 132.9, 129.5, 128.2, 125.3, 120.2, 84.2, 25.0 ppm; ^{11}B NMR ($CDCl_3$, 128.4 MHz): δ 30.8 (br, 2B) ppm; IR: ν = 3348, 2981, 1599, 1354, 1305, 1138, 1125, 793, 746 cm^{-1}; HRMS (EI) m/z calc. for $C_{20}H_{23}B_2NO_2$ $[M]^+$ 331.1915, found 331.1921.

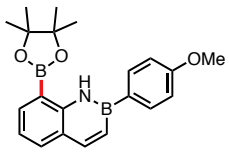

2-(4-Methoxyphenyl)-8-(4,4,5,5-tetramethyl-1,3,2-dioxaboryl)-2,1-borazaronaphthalene (**3.35**): Reaction was run at 40 °C, and the product was obtained as an off-white solid (144 mg, 80%, 0.5 mmol scale); mp: 95-98 °C; ^{1}H NMR ($CDCl_3$, 500.4 MHz): δ 10.40 (s, 1H), 8.11 (d, *J* = 11.5 Hz, 1H), 8.01 – 7.95 (m, 3H), 7.76 (dd, *J* = 7.9, 1.6 Hz, 1H), 7.27 (s, 1H), 7.18 (t, *J* = 7.4 Hz, 1H), 7.06 (d, *J* = 8.3 Hz, 2H), 3.91 (s, 3H), 1.49 (s, 12H) ppm; ^{13}C {^{1}H} NMR ($CDCl_3$, 125.8 MHz): δ 160.9, 146.0, 145.3, 136.6, 134.4, 133.3, 125.1, 119.9, 113.7, 84.1, 55.1, 25.0 ppm; ^{11}B NMR ($CDCl_3$, 128.4 MHz): δ 31.4 (br, 2B) ppm; IR: ν = 3354, 2975, 1597, 1355, 1308, 1252, 1178, 1138, 1125, 800, 788 cm^{-1}; HRMS (ESI+) m/z calc. for $C_{21}H_{26}B_2NO_3$ $[M + H]^+$ 362.2099, found 362.2109.

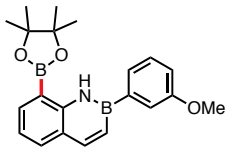

2-(3-Methoxyphenyl)-8-(4,4,5,5-tetramethyl-1,3,2-dioxaboryl)-2,1-borazaronaphthalene (**3.36**): Reaction was run at 80 °C, and the product was obtained as a white solid (91 mg, 61%, 0.41 mmol scale); mp: 96-98 °C; ^{1}H NMR ($CDCl_3$, 500.4 MHz): δ 10.48 (s, 1H), 8.17 (dd, *J* = 11.6, 9.1 Hz, 1H), 8.02 (t, *J* = 7.1 Hz,

1H), 7.84 – 7.75 (m, 1H), 7.63 (d, *J* = 7.4 Hz, 1H), 7.57 (t, *J* = 4.4 Hz, 1H), 7.46 (t, *J* = 7.8 Hz, 1H), 7.35 – 7.28 (m, 1H), 7.22 (dd, *J* = 14.8, 7.4 Hz, 1H), 7.05 (dd, *J* = 8.3, 2.8 Hz, 1H), 3.95 (s, 3H), 1.49 (s, 12H) ppm; ^{13}C {^{1}H} NMR ($CDCl_3$, 125.8 MHz): δ 159.5, 145.8, 145.7, 136.8, 133.4, 129.2, 125.3 (2 x C), 120.2, 117.9, 115.2, 84.1, 55.1, 25.0 ppm; ^{11}B NMR ($CDCl_3$, 128.4 MHz): δ 31.0 (br, 2B) ppm; IR: ν = 3355, 2965, 1603, 1462, 1358, 1303, 1265, 1142, 1126, 774 cm^{-1}; HRMS (ESI+) m/z calc. for $C_{21}H_{26}B_2NO_3$ $[M + H]^+$ 362.2099, found 362.2092.

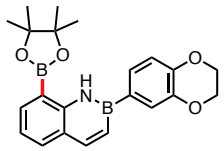

2-(2,3-Dihydrobenzo[1,4]dioxine)-8-(4,4,5,5-tetramethyl-1,3,2-dioxaboryl)-2,1-borazaronaphthalene (**3.37**): Reaction was run at 40 °C, and the product was obtained as a yellow oil (162 mg, 83%, 0.5 mmol scale); ^{1}H NMR ($CDCl_3$, 500.4 MHz): δ 10.46 (s, 1H), 8.14 (d, *J* = 11.6 Hz, 1H), 8.01 (dd, *J* = 7.2, 1.6 Hz, 1H), 7.79 (dd, *J* = 7.7, 1.6 Hz, 1H), 7.58 (d, *J* = 1.6 Hz, 1H), 7.56 (dd, *J* = 7.9, 1.6 Hz, 1H), 7.29 (dd, *J* = 11.7, 1.9 Hz, 1H), 7.21 (t, *J* = 7.4 Hz, 1H), 7.05 (d, *J* = 7.9 Hz, 1H), 4.35 (s, 4H), 1.52 (s, 12H) ppm; ^{13}C {^{1}H} NMR ($CDCl_3$, 125.8 MHz): δ 146.0, 145.4, 145.1, 143.6, 136.6, 133.3, 126.2, 125.1, 121.7, 112.0, 117.2, 84.2, 64.6, 64.3, 25.0 ppm; ^{11}B NMR ($CDCl_3$, 128.4 MHz): δ 30.5 (br, 2B) ppm; IR: ν = 3347, 2981, 1598, 1309, 1281, 1126, 1066, 801, 795 cm^{-1}; HRMS (ESI+) m/z calc. for $C_{22}H_{25}B_2NO_4$ $[M]^+$ 389.1970, found 389.1987.

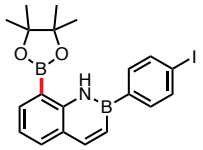

2-(4-Iodophenyl)-8-(4,4,5,5-tetramethyl-1,3,2-dioxaboryl)-2,1-borazaronaphthalene (**3.38**): Reaction was run at 40 °C, and the product was obtained as an off-while solid (139 mg, 61%, 0.5 mmol scale); mp: 114-115 °C; ^{1}H NMR ($CDCl_3$, 500.4 MHz): δ 10.48 (s, 1H), 8.15 (d, *J* = 11.5 Hz, 1H), 7.99 (dd, *J* = 7.1, 1.6 Hz, 1H), 7.85 (d, *J* = 8.0 Hz, 2H), 7.78 (dd, *J* = 7.7, 1.5 Hz, 1H), 7.72 (d, *J* = 8.0 Hz, 2H), 7.25 (dd, *J* = 11.5, 1.9 Hz, 1H), 7.21 (t, *J* = 7.4 Hz, 1H), 1.47 (s, 12H) ppm; ^{13}C {^{1}H} NMR ($CDCl_3$, 125.8 MHz): δ 146.0, 145.7, 137.2, 136.9, 134.5, 133.4, 125.2, 120.3, 96.4, 84.2, 25.0 ppm; ^{11}B NMR ($CDCl_3$, 128.4 MHz): δ 31.3 (br, 2B) ppm; IR: ν = 3347, 2984, 1600, 1352, 1306, 1124, 792, 775 cm^{-1}; HRMS (EI) m/z calc. for $C_{20}H_{22}B_2NO_2I$ $[M + Na]^+$ 457.0881, found 457.0906.

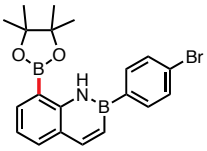

2-(4-Bromophenyl)-8-(4,4,5,5-tetramethyl-1,3,2-dioxaboryl)-2,1-borazaronaphthalene (**3.39**): Reaction was run at 40 °C, and the product was obtained as a white solid (164 mg, 80%, 0.5 mmol scale); mp: 132-135 °C; ^{1}H NMR ($CDCl_3$, 500.4 MHz): δ 10.53 (s, 1H), 8.18 (d, *J* = 11.5 Hz, 1H), 8.04 (dd, *J* = 7.2, 1.6 Hz, 1H), 7.89 (d, *J* = 8.0 Hz, 2H), 7.81 (dd, *J* = 7.8, 1.5 Hz, 1H), 7.68 (d, *J* = 8.0 Hz, 2H), 7.33 – 7.21 (m, 2H), 1.51 (s, 12H) ppm; ^{13}C {^{1}H} NMR ($CDCl_3$, 125.8 MHz): δ 146.0, 145.7, 136.9, 134.4, 133.4, 131.3, 125.3, 124.2, 120.4, 84.2, 25.0 ppm; ^{11}B NMR ($CDCl_3$, 128.4 MHz): δ 30.4 (br, 2B) ppm; IR: ν = 3340, 2976, 1601, 1353, 1307, 1138, 1125,

794, 777 cm^{-1}; HRMS (ESI+) m/z calc. for $C_{20}H_{23}B_2NO_2Br$ $[M + H]^+$ 410.1098, found 410.1092.

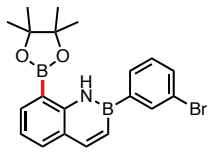

2-(3-Bromophenyl)-8-(4,4,5,5-tetramethyl-1,3,2-dioxaboryl)-2,1-borazaronaphthalene (**3.40**): Reaction was run at 40 °C, and the product was obtained as a white solid (102 mg, 50%, 0.5 mmol scale); mp: 211-213 °C; ^1H NMR ($CDCl_3$, 500.4 MHz): δ 10.62 (s, 1H), 8.24 – 8.15 (m, 2H), 8.03 (d, *J* = 6.5 Hz, 1H), 7.96 (d, *J* = 7.0 Hz, 1H), 7.81 (d, *J* = 7.7 Hz, 1H), 7.61 (d, *J* = 8.2 Hz, 1H), 7.39 (t, *J* = 7.5 Hz, 1H), 7.33 – 7.20 (m, 2H), 1.52 (s, 12H) ppm; ^{13}C $\{^1H\}$ NMR ($CDCl_3$, 125.8 MHz): δ 146.1, 145.7, 136.9, 135.4, 133.4, 132.2, 131.6, 129.9, 125.3, 123.1, 120.4, 84.3, 25.0 ppm; ^{11}B NMR ($CDCl_3$, 128.4 MHz): δ 31.3 (br, 2B) ppm; IR: ν = 3354, 2964, 1602, 1358, 1307, 1125, 776 cm^{-1}; HRMS (ESI+) m/z calc. for $C_{20}H_{23}B_2NO_2Br$ $[M + H]^+$ 410.1098, found 410.1086.

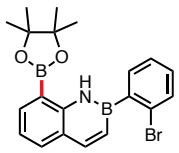

2-(2-Bromophenyl)-8-(4,4,5,5-tetramethyl-1,3,2-dioxaboryl)-2,1-borazaronaphthalene (**3.41**): Reaction was run at 40 °C, and the product was obtained as a yellow solid (62 mg, 30%, 0.5 mmol scale); mp: 89-90 °C; ^1H NMR ($CDCl_3$, 500.4 MHz): δ 10.42 (s, 1H), 8.16 (d, *J* = 11.5 Hz, 1H), 8.02 (d, *J* = 6.5 Hz, 1H), 7.81 (d, *J* = 7.7 Hz, 1H), 7.67 (dd, *J* = 11.5, 7.3 Hz, 2H), 7.40 (t, *J* = 7.6 Hz, 1H), 7.29 – 7.21 (m, 3H), 1.42 (s, 12H) ppm; ^{13}C $\{^1H\}$ NMR ($CDCl_3$, 125.8 MHz): δ 145.3, 145.1,

136.9, 135.9, 133.4, 132.6, 129.9, 127.5, 126.6, 125.0, 120.5, 84.2, 24.9 ppm; ^{11}B NMR ($CDCl_3$, 128.4 MHz): δ 31.8 (br, 2B) ppm; IR: ν = 3338, 2991, 1597, 1354, 1141, 1126, 819, 757 cm^{-1}; HRMS (ESI+) m/z calc. for $C_{20}H_{23}B_2NO_2Br$ $[M + H]^+$ 410.1098, found 410.1085.

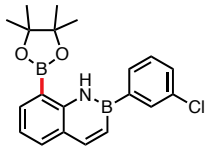

2-(3-Chlorophenyl)-8-(4,4,5,5-tetramethyl-1,3,2-dioxaboryl)-2,1-borazaronaphthalene (**3.42**): Reaction was run at 80 °C, and the product was obtained as a white solid (56 mg, 30%, 0.33 mmol scale); mp: 118-120 °C; ^{1}H NMR ($CDCl_3$, 500.4 MHz): δ 10.60 (s, 1H), 8.18 (d, *J* = 11.6 Hz, 1H), 8.05 – 7.95 (m, 2H), 7.92 – 7.86 (m, 1H), 7.80 (d, *J* = 7.8 Hz, 1H), 7.47 – 7.41 (m, 2H), 7.30 – 7.27 (m, 1H), 7.23 (t, *J* = 7.5 Hz, 1H), 1.50 (s, 12H) ppm; ^{13}C {^{1}H} NMR ($CDCl_3$, 125.8 MHz): δ 146.1, 145.7, 136.8, 134.5, 133.3, 132.5, 131.0, 129.5, 129.3, 125.2, 120.4, 84.3, 25.0 ppm; ^{11}B NMR ($CDCl_3$, 128.4 MHz): δ 30.9 (br, 2B) ppm; IR: ν = 3352, 2971, 1602, 1359, 1307, 1141, 1125, 778, 760 cm^{-1}; HRMS (ESI+) m/z calc. for $C_{20}H_{23}B_2NO_2Cl$ $[M + H]^+$ 366.1603, found 366.1608.

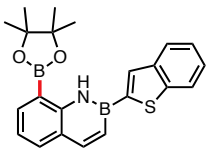

2-(Benzothiophen-2-yl)-8-(4,4,5,5-tetramethyl-1,3,2-dioxaboryl)-2,1-borazaronaphthalene (**3.43**): Reaction was run at 80 °C, and the product was obtained as a white solid (117 mg, 60%, 0.5 mmol scale); mp: 163-164 °C; ^{1}H NMR ($CDCl_3$, 500.4 MHz): δ 10.52 (s, 1H), 8.16 (d, *J* = 11.5 Hz, 1H), 8.03 – 7.96 (m, 3H),

7.95 – 7.90 (m, 1H), 7.79 (d, *J* = 7.4 Hz, 1H), 7.43 – 7.36 (m, 2H), 7.30 (dd, *J* = 11.5, 1.9 Hz, 1H), 7.23 (t, *J* = 7.4 Hz, 1H), 1.53 (s, 12H) ppm; ^{13}C {^{1}H} NMR ($CDCl_3$, 125.8 MHz): δ 145.8, 145.7, 143.1, 141.5, 136.9, 133.4, 131.0, 125.4, 124.6, 124.0, 123.9, 122.5, 120.4, 84.3, 25.0 ppm; ^{11}B NMR ($CDCl_3$, 128.4 MHz): δ 30.5 (br, 2B) ppm; IR: ν = 3335, 2976, 1597, 1353, 1307, 1137, 798 cm^{-1}; HRMS (ESI+) m/z calc. for $C_{22}H_{24}B_2NO_2S$ $[M + H]^+$ 388.1714, found 388.1715.

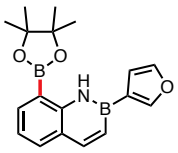

2-(Furan-3-yl)-8-(4,4,5,5-tetramethyl-1,3,2-dioxaboryl)-2,1-borazaronaphthalene (**3.44**): Reaction was run at 80 °C, and the product was obtained as a white solid (33 mg, 21%, 0.5 mmol scale); mp: 195-197 °C; ^{1}H NMR ($CDCl_3$, 500.4 MHz): δ 10.44 (s, 1H), 8.13 (d, *J* = 11.4 Hz, 1H), 7.80 (s, 1H), 7.66 (d, *J* = 7.8 Hz, 1H), 7.45 (t, *J* = 7.6 Hz, 1H), 7.30 (d, *J* = 8.1 Hz, 1H), 7.24 – 7.14 (m, 2H), 7.03 (s, 1H), 1.51 (s, 12H) ppm; ^{13}C {^{1}H} NMR ($CDCl_3$, 125.8 MHz): δ 147.1, 145.0, 140.5, 129.3, 128.1, 125.5, 120.5, 118.0, 116.0, 84.8, 24.9 ppm; ^{11}B NMR ($CDCl_3$, 128.4 MHz): δ 27.4 (br, 2B) ppm; IR: ν = 3348, 2971, 1574, 1560, 1451, 1303, 1138, 778 cm^{-1}; HRMS (ESI+) m/z calc. for $C_{18}H_{22}B_2NO_3$ $[M + H]^+$ 322.1786, found 322.1793.

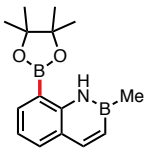

2-Methyl-8-(4,4,5,5-tetramethyl-1,3,2-dioxaboryl)-2,1-borazaronaphthalene (**3.45**): Reaction was run at 80 °C, and the product was obtained as a thick yellow oil (80 mg, 60%, 0.5 mmol scale); ^{1}H NMR ($CDCl_3$, 500.4 MHz): δ 9.68 (s, 1H), 7.92 (d, *J*

= 9.5 Hz, 2H), 7.70 (d, *J* = 7.8 Hz, 1H), 7.13 (t, *J* = 7.7 Hz, 1H), 6.80 (d, *J* = 11.4 Hz, 1H), 1.44 (s, 12H), 0.79 (s, 3H) ppm; ^{13}C {^{1}H} NMR ($CDCl_3$, 125.8 MHz): δ 145.8, 144.1, 136.3, 133.2, 124.6, 119.5, 83.9, 24.9 ppm; ^{11}B NMR ($CDCl_3$, 128.4 MHz): δ 36.5, 30.0 ppm; IR: ν = 3358, 2984, 1601, 1354, 1311, 1136, 1101, 760 cm^{-1}; HRMS (ESI+) m/z calc. for $C_{15}H_{22}B_2NO_2$ $[M + H]^+$ 270.1837, found 270.1827.

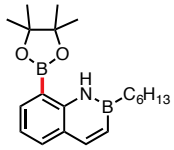

2-Hexyl-8-(4,4,5,5-tetramethyl-1,3,2-dioxaboryl)-2,1-borazaronaphthalene (**3.46**): Reaction was run at 40 °C, and the product was obtained as a white solid (65 mg, 91%, 0.21 mmol scale); mp: 127-130 °C; ^{1}H NMR ($CDCl_3$, 500.4 MHz): δ 9.85 (s, 1H), 7.98 – 7.92 (m, 2H), 7.76 – 7.68 (m, 1H), 7.15 (t, *J* = 7.4 Hz, 1H), 6.82 (d, *J* = 11.4 Hz, 1H), 1.73 – 1.65 (m, 2H), 1.48 – 1.43 (m, 14H), 1.42 – 1.33 (m, 6H), 0.95 (t, *J* = 6.7 Hz, 3H) ppm; ^{13}C {^{1}H} NMR ($CDCl_3$, 125.8 MHz): δ 145.9, 144.0, 136.2, 133.2, 124.8, 119.6, 83.9, 32.3, 32.0, 25.4, 24.9, 22.6, 14.1 ppm; ^{11}B NMR ($CDCl_3$, 128.4 MHz): δ 37.5, 29.8 ppm; IR: ν = 3354, 2921, 1600, 1354, 1303, 1137, 762 cm^{-1}; HRMS (ESI+) m/z calc. for $C_{20}H_{32}B_2NO_2$ $[M + H]^+$ 340.2623, found 3340.2630.

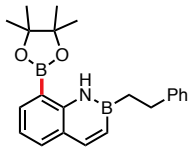

2-Phenethyl-8-(4,4,5,5-tetramethyl-1,3,2-dioxaboryl)-2,1-borazaronaphthalene (**3.47**): Reaction was run at 40 °C, and the product was obtained as a white solid (111 mg, 62%, 0.5 mmol scale); mp: 58-60 °C; ^{1}H NMR ($CDCl_3$, 500.4 MHz): δ 9.91 (s, 1H), 8.00 – 7.91 (m, 2H), 7.72 (d, *J* = 7.7 Hz, 1H), 7.36 – 7.29 (m, 4H), 7.23 – 7.11 (m,

2H), 6.84 (dd, *J* = 11.5, 1.9 Hz, 1H), 3.01 (t, *J* = 8.3 Hz, 2H), 1.71 (t, *J* = 8.3 Hz, 2H), 1.43 (s, 12H) ppm; ^{13}C {^{1}H} NMR ($CDCl_3$, 125.8 MHz): δ 145.7, 145.2, 144.4, 136.4, 133.3, 128.2, 128.0, 127.9, 125.3, 124.8, 119.8, 84.0, 31.5, 24.9 ppm; ^{11}B NMR ($CDCl_3$, 128.4 MHz): δ37.8, 31.5 ppm; IR: ν = 3349, 2978, 1598, 1355, 1311, 1137, 1127, 759 cm^{-1}; HRMS (ESI+) m/z calc. for $C_{22}H_{28}B_2NO_2$ $[M + H]^+$ 360.2306, found 360.2305.

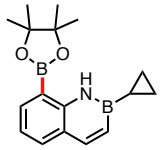

2-Cyclopropyl-8-(4,4,5,5-tetramethyl-1,3,2-dioxaboryl)-2,1-borazaronaphthalene (**3.48**): Reaction was run at 80 °C, and the product was obtained as a white solid (115 mg, 78%, 0.5 mmol scale); mp: 75-76 °C; ^{1}H NMR ($CDCl_3$, 500.4 MHz): δ 9.61 (s, 1H), 8.04 – 7.84 (m, 2H), 7.69 (dd, *J* = 7.7, 1.6 Hz, 1H), 7.13 (t, *J* = 7.4 Hz, 1H), 6.62 (dd, *J* = 11.6, 1.9 Hz, 1H), 1.45 (s, 12H), 0.97 – 0.80 (m, 2H), 0.72 – 0.57 (m, 2H), 0.37 (tt, *J* = 8.8, 6.0 Hz, 1H) ppm; ^{13}C {^{1}H} NMR ($CDCl_3$, 125.8 MHz): δ 145.9, 144.5, 136.4, 133.2, 124.7, 119.4, 83.9, 24.9, 6.3 ppm; ^{11}B NMR ($CDCl_3$, 128.4 MHz): δ 37.3, 30.0 ppm; IR: ν = 3356, 2979, 1598, 1353, 1297, 1135, 1109, 794, 774 cm^{-1}; HRMS (ESI+) m/z calc. for $C_{17}H_{24}B_2NO_2$ $[M + H]^+$ 296.1993, found 296.1990.

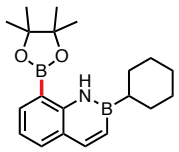

2-Cyclohexyl-8-(4,4,5,5-tetramethyl-1,3,2-dioxaboryl)-2,1-borazaronaphthalene (**3.49**): Reaction was run at 40 °C, and the product was obtained as a yellow solid (138 mg, 82%, 0.5 mmol scale); mp: 69-70 °C; ^{1}H NMR

($CDCl_3$, 500.4 MHz): δ 9.94 (s, 1H), 8.07 – 7.87 (m, 2H), 7.72 (d, *J* = 7.3 Hz, 1H), 7.15 (t, *J* = 7.4 Hz, 1H), 6.88 (dd, *J* = 11.5, 1.9 Hz, 1H), 2.08 – 1.97 (m, 2H), 1.85 – 1.71 (m, 3H), 1.54 – 1.38 (m, 18H) ppm; ^{13}C {^1H} NMR ($CDCl_3$, 125.8 MHz): δ 145.7, 144.4, 136.2, 133.2, 124.8, 119.6, 83.9, 29.6, 27.7, 27.2, 24.9 ppm; ^{11}B NMR ($CDCl_3$, 128.4 MHz): δ 40.2, 31.8 ppm; IR: ν = 3356, 2917, 1599, 1356, 1309, 1137, 1124, 800 cm^{-1}; HRMS (EI) m/z calc. for $C_{20}H_{29}B_2NO_2$ $[M + Na]^+$ 337.2384, found 337.2386.

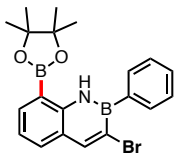

3-Bromo-2-phenyl-8-(4,4,5,5-tetramethyl-1,3,2-dioxaboryl)-2,1-borazaronaphthalene (**3.50**): Reaction was run at 80 °C, and the product was obtained as a white solid (130 mg, 64%, 0.5 mmol scale); mp: 72-74 °C; ^1H NMR ($CDCl_3$, 500.4 MHz): δ 10.48 (s, 1H), 8.49 (s, 1H), 8.22 – 8.14 (m, 2H), 8.06 (dd, *J* = 7.1, 1.5 Hz, 1H), 7.75 (d, *J* = 7.8 Hz, 1H), 7.64 – 7.50 (m, 3H), 7.27 (t, *J* = 7.5 Hz, 1H), 1.47 (s, 12H) ppm; ^{13}C {^1H} NMR ($CDCl_3$, 125.8 MHz): δ 147.1, 144.9, 137.1, 133.6, 132.5, 129.3, 127.8, 124.7, 121.0, 84.4, 25.0 ppm; ^{11}B NMR ($CDCl_3$, 128.4 MHz): δ 30.6 (br, 2B) ppm; IR: ν = 3338, 2974, 1597, 1373, 1344, 1309, 1132, 698 cm^{-1}; HRMS (EI) m/z calc. for $C_{20}H_{22}B_2NO_2Br$ $[M]^+$ 409.1020, found 409.1041.

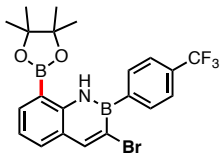

3-Bromo-8-(4,4,5,5-tetramethyl-1,3,2-dioxaboryl)-2-(4-(trifluoromethyl)phenyl)-2,1-borazaronaphthalene (**3.51**): Reaction was run at 80 °C,

and the product was obtained as an off-white solid (169 mg, 71%, 0.5 mmol scale); mp: 122-124 °C; ^{1}H NMR ($CDCl_3$, 500.4 MHz): δ 10.50 (s, 1H), 8.46 (s, 1H), 8.20 (d, *J* = 7.4 Hz, 2H), 8.08 (d, *J* = 7.0 Hz, 1H), 7.79 (d, *J* = 7.5 Hz, 2H), 7.73 (d, *J* = 7.6 Hz, 1H), 7.28 (t, *J* = 7.1 Hz, 1H), 1.47 (s, 12H) ppm; ^{13}C {^{1}H} NMR ($CDCl_3$, 125.8 MHz): δ 147.4, 144.6, 137.4, 133.7, 132.5, 131.0 (q, *J* = 32.1 Hz), 124.8, 124.4 (q, *J* = 271.8 Hz), 124.3 (q, *J* = 3.9 Hz), 121.4, 84.5, 24.9 ppm; ^{19}F {^{1}H} NMR ($CDCl_3$, 470.8 MHz): δ -62.6 ppm; ^{11}B NMR ($CDCl_3$, 128.4 MHz): δ 32.0 (br, 2B) ppm; IR: ν = 3340, 2980, 1598, 1558, 1320, 1120, 1068, 761 cm^{-1}; HRMS (EI) m/z calc. for $C_{21}H_{21}B_2NO_2F_3Br$ $[M]^+$ 477.0894, found 477.0891.

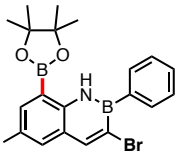

3,6-Dibromo-2-phenyl-8-(4,4,5,5-tetramethyl-1,3,2-dioxaboryl)-2,1-borazaronaphthalene (**3.52**): Reaction was run at 80 °C, and the product was obtained as a white solid (52 mg, 43%, 0.25 mmol scale); mp: 136-138 °C; ^{1}H NMR ($CDCl_3$, 500.4 MHz): δ 10.34 (s, 1H), 8.35 (s, 1H), 8.13 – 8.03 (m, 3H), 7.82 (s, 1H), 7.54 – 7.47 (m, 3H), 1.44 (s, 12H) ppm; ^{13}C {^{1}H} NMR ($CDCl_3$, 125.8 MHz): δ 145.8, 143.4, 139.2, 134.0, 133.5, 129.5, 127.8, 126.3, 113.8, 84.8, 24.9 ppm; ^{11}B NMR ($CDCl_3$, 128.4 MHz): δ 32.7, 30.7 ppm; IR: ν = 3550, 2975, 1593, 1555, 1416, 1370, 1312, 1141, 848, 793 cm^{-1}; HRMS (EI) m/z calc. for $C_{20}H_{21}B_2NO_2Br_2$ $[M]^+$ 487.0125, found 487.0122.

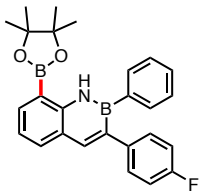

3-(4-Fluorophenyl)-2-phenyl-8-(4,4,5,5-tetramethyl-1,3,2-dioxaboryl)-2,1-borazaronaphthalene (**3.53**): Reaction was run at 60 °C, and the product was obtained as a light brown solid (45 mg, 42%, 0.25 mmol scale); mp: 164-165 °C; ^{1}H NMR ($CDCl_3$, 500.4 MHz): δ 10.39 (s, 1H), 8.03 – 7.96 (m, 2H), 7.83 (d, *J* = 7.1 Hz, 1H), 7.57 (d, *J* = 7.9 Hz, 2H), 7.39 – 7.29 (m, 5H), 7.24 (t, *J* = 7.4 Hz, 1H), 7.03 (t, *J* = 8.8 Hz, 2H), 1.46 (s, 12H) ppm; ^{13}C {^{1}H} NMR ($CDCl_3$, 125.8 MHz): δ 161.7 (d, *J* = 244.2 Hz), 145.2, 143.7, 140.5, 136.7, 133.6, 133.4, 130.1 (d, *J* = 7.8 Hz), 128.6, 127.7, 124.7, 120.6, 114.7 (d, *J* = 21.1 Hz), 84.2, 24.9 ppm; ^{19}F {^{1}H} NMR ($CDCl_3$, 470.8 MHz): δ -111.7 ppm; ^{11}B NMR ($CDCl_3$, 128.4 MHz): δ 34.0, 31.2 ppm; IR: ν = 3348, 2970, 2915, 1600, 1446, 1346, 1310, 1131, 760 cm^{-1}; HRMS (EI) m/z calc. for $C_{26}H_{26}B_2NO_2F$ $[M]^+$ 425.2134, found 425.2144.

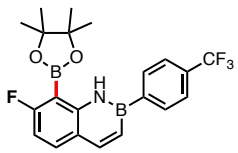

7-Fluoro-8-(4,4,5,5-tetramethyl-1,3,2-dioxaboryl)-2-(4-(trifluoromethyl)phenyl)-2,1-borazaronaphthalene (**3.54**): Reaction was run at 80 °C, and the product was obtained as brown cystals (98 mg, 47%, 0.5 mmol scale); mp: 132-135 °C; ^{1}H NMR ($CDCl_3$, 500.4 MHz): δ 10.80 (s, 1H), 8.15 (d, *J* = 11.5 Hz, 1H), 8.08 (d, *J* = 7.8 Hz, 2H), 7.79 – 7.70 (m, 3H), 7.23 (dd, *J* = 11.5, 1.4 Hz, 1H), 6.95 (t, *J* = 9.0 Hz, 1H), 1.51 (s, 12H) ppm; ^{13}C {^{1}H} NMR ($CDCl_3$, 125.8 MHz): δ 168.6 (d, *J* =

254.2 Hz), 146.6 (d, *J* = 11.2 Hz), 145.9, 135.14 (d, *J* = 11.7 Hz), 132.9, 131.2 (q, *J* = 32.2 Hz), 124.7 (q, *J* = 3.7 Hz), 124.3 (q, *J* = 272.2 Hz), 122.2, 109.5 (d, *J* = 26.8 Hz), 84.1, 24.9 ppm; ^{19}F {^{1}H} NMR ($CDCl_3$, 470.8 MHz): δ -62.7, -97.1 ppm; ^{11}B NMR ($CDCl_3$, 128.4 MHz): δ 33.6, 30.2 ppm; IR: ν = 3345, 2982, 1599, 1320, 1208, 1162, 1138, 1119, 1066, 802 cm^{-1}; HRMS (EI) m/z calc. for $C_{21}H_{21}B_2NO_2F_4$ $[M]^+$ 417.1695, found 417.1695.

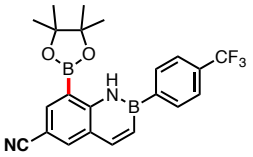

6-Cyano-8-(4,4,5,5-tetramethyl-1,3,2-dioxaboryl)-2-(4-(trifluoromethyl)phenyl)-2,1-borazaronaphthalene (**3.55**): Reaction was run at 80 °C for 24 h, and the product was obtained as a white solid (202 mg, 93%, 1.0 mmol scale); mp: 195-196 °C; ^{1}H NMR ($CDCl_3$, 500.4 MHz): δ 10.66 (s, 1H), 8.22 (d, *J* = 1.6 Hz, 1H), 8.15 (d, *J* = 11.6 Hz, 1H), 8.12 – 8.05 (m, 3H), 7.76 (d, *J* = 7.9 Hz, 2H), 7.41 (dd, *J* = 11.7, 1.2 Hz, 1H), 1.49 (s, 12H) ppm; ^{13}C {^{1}H} NMR ($CDCl_3$, 125.8 MHz): δ 147.7, 145.4, 139.2, 137.3, 133.1, 131.8 (q, *J* = 32.0 Hz), 125.2, 124.9 (q, *J* = 3.7 Hz), 124.1 (q, *J* = 271.4, Hz), 119.0, 104.2, 85.0, 25.0 ppm; ^{19}F {^{1}H} NMR ($CDCl_3$, 470.8 MHz): δ -62.9 ppm; ^{11}B NMR ($CDCl_3$, 128.4 MHz): δ 33.7, 30.3 ppm; IR: ν = 3346, 2985, 2928, 1719, 1608, 1395, 1317, 1135, 1118, 792 cm^{-1}; HRMS (EI) m/z calc. for $C_{22}H_{21}B_2N_2O_2F_3$ $[M]^+$ 424.1741, found 424.1750.

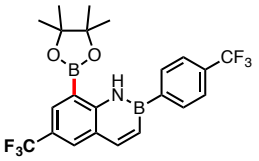

8-(4,4,5,5-Tetramethyl-1,3,2-dioxaboryl)-6-(trifluoromethyl)-2-(4-trifluoromethyl)phenyl)-2,1-borazaronaphthalene (**3.56**): Reaction was run at 80 °C, and the product was obtained as a white solid (140 mg, 82%, 0.5 mmol scale); mp: 160-162 °C; ^{1}H NMR ($CDCl_3$, 500.4 MHz): δ 10.66 (s, 1H), 8.23 (d, *J* = 1.3 Hz, 1H), 8.20 (d, *J* = 11.6 Hz, 1H), 8.09 (d, *J* = 7.8 Hz, 2H), 8.05 (s, 1H), 7.77 (d, *J* = 7.8 Hz, 2H), 7.39 (dd, *J* = 11.6, 1.5 Hz, 1H), 1.51 (s, 12H) ppm; ^{13}C {^{1}H} NMR ($CDCl_3$, 125.8 MHz): δ 147.3, 146.0, 133.0, 133.0 (q, *J* = 3.7 Hz), 131.5 (q, *J* = 32.1 Hz), 130.3 (q, *J* = 3.8 Hz), 124.8 (q, *J* = 3.8 Hz), 124.7, 124.4 (q, *J* = 272.2 Hz), 124.2 (q, *J* = 271.8 Hz), 122.8 (q, *J* = 32.7 Hz), 84.8, 25.0 ppm; ^{19}F {^{1}H} NMR ($CDCl_3$, 470.8 MHz): δ -61.3, -62.8 ppm; ^{11}B NMR ($CDCl_3$, 128.4 MHz): δ 33.5, 31.0 ppm; IR: ν = 3350, 2985, 1618, 1581, 1319, 1142, 1113, 1067, 793 cm^{-1}; HRMS (EI) m/z calc. for $C_{22}H_{21}B_2NO_2F_6$ $[M]^+$ 467.1663, found 467.1652.

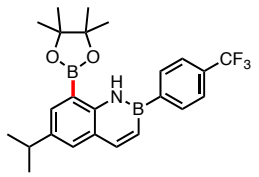

6-Isopropyl-8-(4,4,5,5-tetramethyl-1,3,2-dioxaboryl)-2-(4-(trifluoromethyl)phenyl)-2,1-borazaronaphthalene (**3.57**): Reaction was run at 80 °C, and the product was obtained as a white solid (174 mg, 79%, 0.5 mmol scale); mp: 198-202 °C; ^{1}H NMR ($CDCl_3$, 500.4 MHz): δ 10.54 (s, 1H), 8.18 (d, *J* = 11.5 Hz, 1H), 8.09 (d, *J* = 8.0 Hz, 2H), 7.90 (d, *J* = 2.1 Hz, 1H), 7.74 (d, *J* = 8.0 Hz, 2H), 7.65 (d, *J* = 2.0

Hz, 1H), 7.28 (dd, *J* = 11.4, 2.1 Hz, 1H), 3.06 (sept, *J* = 6.9 Hz, 1H), 1.49 (s, 12H), 1.35 (d, *J* = 6.9 Hz, 6H) ppm; ^{13}C {^{1}H} NMR ($CDCl_3$, 125.8 MHz): δ 146.2, 144.0, 140.9, 135.9, 132.9, 130.9 (q, *J* = 32.2 Hz), 130.5, 125.4, 124.7 (q, *J* = 3.8 Hz), 124.4 (q, *J* = 272.1 Hz), 84.2, 33.5, 25.0, 24.2 ppm; ^{19}F {^{1}H} NMR ($CDCl_3$, 470.8 MHz): δ -62.7 ppm; ^{11}B NMR ($CDCl_3$, 128.4 MHz): δ 30.5 (br, 2B) ppm; IR: ν = 3350, 2954, 1572, 1332, 1163, 1120, 1067, 789 cm^{-1}; HRMS (EI) m/z calc. for $C_{24}H_{28}B_2NO_2F_3$ $[M]^+$ 441.2285, found 441.2253.

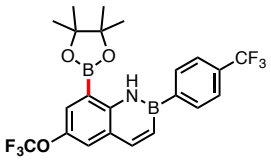

8-(4,4,5,5-Tetramethyl-1,3,2-dioxaboryl)-6-(trifluoromethoxy)-2-(4-(trifluoromethyl)phenyl)-2,1-borazaronaphthalene (**3.58**): Reaction was run at 80 °C, and the product was obtained as a white solid (171 mg, 71%, 0.5 mmol scale); mp: 117-119 °C; ^{1}H NMR ($CDCl_3$, 500.4 MHz): δ 10.57 (s, 1H), 8.15 (d, *J* = 11.6 Hz, 1H), 8.08 (d, *J* = 7.8 Hz, 2H), 7.85 (d, *J* = 2.4 Hz, 1H), 7.75 (d, *J* = 8.0 Hz, 2H), 7.64 (d, *J* = 2.0 Hz, 1H), 7.37 (dd, *J* = 11.6, 1.8 Hz, 1H), 1.49 (s, 12H) ppm; ^{13}C {^{1}H} NMR ($CDCl_3$, 125.8 MHz): δ 145.5, 144.0, 142.5, 132.9, 131.3 (q, *J* = 32.2 Hz), 129.6, 126.0, 124.8, 124.8 (q, *J* = 3.8 Hz), 124.2 (q, *J* = 271.0 Hz), 120.5 (q, *J* = 256.2 Hz), 84.7, 25.0 (q, *J* = 79.7 Hz) ppm; ^{19}F {^{1}H} NMR ($CDCl_3$, 470.8 MHz): δ -58.0, -62.8 ppm; ^{11}B NMR ($CDCl_3$, 128.4 MHz): δ 30.0 (br, 2B) ppm; IR: ν = 3353, 2981, 1574, 1315, 1259, 1155, 1140, 1106, 1067, 774 cm^{-1}; HRMS (EI) m/z calc. for $C_{22}H_{21}B_2NO_3F_6$ $[M]^+$ 483.1612, found 483.1620.

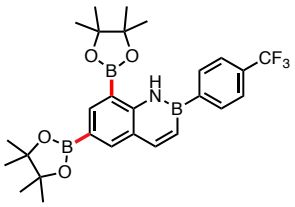

6,8-Bis(4,4,5,5-tetramethyl-1,3,2-dioxaboryl)-2-(4-(trifluoromethyl)phenyl)-2,1-borazaronaphthalene (**3.59**): 3.0 equiv of B_2Pin_2 (381 mg, 1.5 mmol) was used in the reaction run at 80 °C, and the product was obtained as a white solid (203 mg, 78%, 0.5 mmol scale); mp: 220-222 °C; ^{1}H NMR ($CDCl_3$, 500.4 MHz): δ 10.69 (s, 1H), 8.49 (s, 1H), 8.34 (s, 1H), 8.24 (dd, *J* = 11.6, 2.9 Hz, 1H), 8.12 (d, *J* = 6.3 Hz, 2H), 7.77 (d, *J* = 6.5 Hz, 2H), 7.30 (d, *J* = 11.6 Hz, 1H), 1.50 (s, 12H), 1.43 (s, 12H) ppm; ^{13}C {^{1}H} NMR ($CDCl_3$, 125.8 MHz): δ 147.8, 146.7, 143.2, 141.0, 133.0 (2 x C), 131.2 (q, *J* = 31.9 Hz), 124.7 (q, *J* = 3.1 Hz), 124.4 (q, *J* = 272.3 Hz), 84.2, 83.7, 25.0, 24.8 ppm; ^{19}F {^{1}H} NMR ($CDCl_3$, 470.8 MHz): δ -62.6 ppm; ^{11}B NMR ($CDCl_3$, 128.4 MHz): δ 30.3 (br, 3B) ppm; IR: ν = 3352, 2981, 1605, 1345, 1321, 1164, 1138 cm^{-1}; HRMS (ESI+) m/z calc. for $C_{27}H_{34}B_3NO_4F_3$ $[M + H]^+$ 526.2719, found 526.2724.

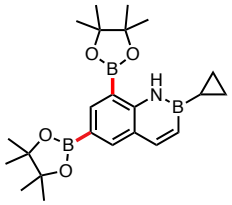

2-Cyclopropyl-6,8-bis(4,4,5,5-tetramethyl-1,3,2-dioxaboryl)-2,1-borazaronaphthalene (**3.60**): 3.0 equiv of B_2Pin_2 (381 mg, 1.5 mmol) was used in the reaction run at 80 °C, and the product was obtained as a white solid (160 mg, 76%, 0.5 mmol scale); mp: 120-124 °C; ^{1}H NMR ($CDCl_3$, 500.4 MHz): δ 9.66 (s, 1H), 8.33 (s, 1H), 8.15 (s, 1H), 7.92 (d, *J* = 11.7 Hz, 1H), 6.57 (d, *J* = 11.9 Hz, 1H), 1.42 (s, 12H),

1.37 (s, 12H), 0.90 – 0.87 (m, 2H), 0.63 (dd, *J* = 6.0, 2.2 Hz, 2H), 0.40 – 0.28 (m, 1H) ppm; ^{13}C {^{1}H} NMR ($CDCl_3$, 125.8 MHz): δ 148.1, 144.8, 142.6, 140.7, 124.1, 83.9, 83.5, 24.9, 24.8, 14.0, 6.3, 6.0 ppm; ^{11}B NMR ($CDCl_3$, 128.4 MHz): δ 38.0, 30.2 (br, 2B) ppm; IR: ν = 3358, 2978, 1605, 1360, 1342, 1313, 1138, 851, 774 cm^{-1}; HRMS (ESI+) m/z calc. for $C_{23}H_{35}B_3NO_4$ $[M + H]^+$ 422.2845, found 422.2849.

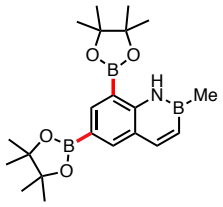

2-Methyl-6,8-bis(4,4,5,5-tetramethyl-1,3,2-dioxaboryl)-2,1-borazaronaphthalene (**3.61**): 3.0 equiv of B_2Pin_2 (381 mg, 1.5 mmol) was used in the reaction run at 80 °C, and the product was obtained as a white solid (156 mg, 79%, 0.5 mmol scale); mp: 167-170 °C; ^{1}H NMR ($CDCl_3$, 500.4 MHz): δ 9.80 (s, 1H), 8.38 (s, 1H), 8.21 (s, 1H), 7.97 (d, *J* = 11.5 Hz, 1H), 6.80 (d, *J* = 12.5 Hz, 1H), 1.44 (s, 12H), 1.39 (s, 12H), 0.81 (s, 3H) ppm; ^{13}C {^{1}H} NMR ($CDCl_3$, 125.8 MHz): δ 148.1, 144.5, 142.6, 140.8, 124.1, 83.9, 83.5, 24.9, 24.8 ppm; ^{11}B NMR ($CDCl_3$, 128.4 MHz): δ 37.6, 30.5 (br, 2B) ppm; IR: ν = 3354, 2981, 1605, 1340, 1313, 1270, 1139, 758 cm^{-1}; HRMS (ESI+) m/z calc. for $C_{21}H_{33}B_3NO_4$ $[M + H]^+$ 396.2689, found 396.2693.

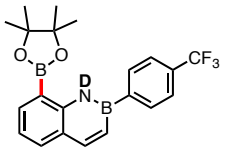

N-Deuterio-8-(4,4,5,5-tetramethyl-1,3,2-dioxaboryl)-2-(4-(trifluoromethyl)phenyl)-2,1-borazaronaphthalene (**3.63**): Reaction was run at 40 °C, and the products was obtained as a white solid (81.4 mg, 41%, 0.5 mmol scale); mp:

139-140 °C; ^{1}H NMR ($CDCl_3$, 500.4 MHz): δ 8.20 (d, *J* = 11.5 Hz, 1H), 8.10 (d, *J* = 7.8 Hz, 2H), 8.02 (d, *J* = 7.1 Hz, 1H), 7.81 (d, *J* = 7.7 Hz, 1H), 7.75 (d, *J* = 7.9 Hz, 2H), 7.30 (d, *J* = 11.5 Hz, 1H), 7.24 (t, *J* = 7.4 Hz, 1H), 1.49 (s, 12H) ppm; ^{13}C {^{1}H} NMR ($CDCl_3$, 125.8 MHz): δ 146.2, 145.5, 137.0, 133.4, 132.9, 131.0 (q, *J* = 32.2 Hz), 125.3, 124.7 (q, *J* = 3.7 Hz), 124.3 (q, *J* = 272.1 Hz), 120.5, 84.2, 25.0 ppm; ^{19}F {^{1}H} NMR ($CDCl_3$, 470.8 MHz): δ -62.7 ppm; ^{11}B NMR ($CDCl_3$, 128.4 MHz): δ 33.0 (br, 2B) ppm; IR: ν = 2983, 1603, 1555, 1374, 1323, 1305, 1163, 1109, 1067, 761 cm^{-1}; HRMS (EI) m/z calc. for $C_{21}H_{21}DB_2NO_2F_3$ $[M]^+$ 400.1852, found 400.1877.

Deuteration of 2,1-borazaronaphthalene:

N-Deuterio-2-(4-(trifluoromethyl)phenyl)-2,1-borazaronaphthalene (**3.62**)

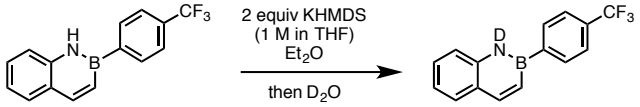

To a microwave vial with a stir bar, 2-(4-(trifluoromethyl)phenyl)-2,1-borazaronaphthalene (273 mg, 1 mmol, 1 equiv) was added. The vial was capped and purged with argon. Et_2O (3 mL) was added followed by KHMDS (2 mL of a 1 M solution in THF, 2 equiv). The reaction was stirred for 20 min at rt, at which time D_2O (3 mL) was added dropwise and stirred for an additional 30 min. The reaction mixture was then extracted with EtOAc (5 mL) and dried ($MgSO_4$). Removal of the solvent afforded 218 mg (80%) of a yellow solid; mp: 149-150 °C; ^{1}H NMR ($CDCl_3$, 500.4 MHz): δ 8.19 (d, *J* = 11.5 Hz, 1H), 8.00 (d, *J* = 7.7 Hz, 2H), 7.71 (d, *J* = 7.8 Hz, 2H), 7.69 (d, *J* = 7.9 Hz, 1H), 7.48 (t, *J* = 7.2 Hz, 1H), 7.37 (d, *J* = 8.1 Hz, 1H), 7.30 – 7.19 (m, 2H) ppm; ^{13}C {^{1}H} NMR ($CDCl_3$, 125.8 MHz): δ 146.1, 139.7, 132.8, 131.2 (q, *J* = 32.1 Hz), 129.5, 128.6, 125.7, 124.7 (q, *J* = 3.7 Hz), 124.3 (q, *J* = 272.0 Hz), 121.4,

118.2 ppm; ^{19}F {^{1}H} NMR ($CDCl_3$, 470.8 MHz): δ -62.7 ppm; ^{11}B NMR ($CDCl_3$, 128.4 MHz): δ 33.0 ppm; IR: ν = 2923, 2502, 1612, 1325, 1118, 1108, 1071, 812, 762, 643 cm^{-1}; HRMS (EI) m/z calc. for $C_{15}H_{10}DBNF_3$ $[M]^+$ 274.0999, found 274.1018.

Experimental Procedure for Palladium-catalyzed Cross-Coupling of 8-Borylated 2,1-Borazaronaphthalenes

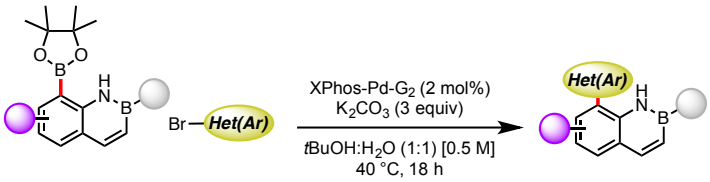

To a microwave vial with a stir bar was added borylated 2,1-borazaronaphthalene (1.0 equiv), solid aryl bromide (1.1 equiv), K_2CO_3 (3.0 equiv) and XPhos-Pd-G2 catalyst (2 mol %). The reaction vial was then capped and purged with argon. A solvent mixture of degassed *t*-BuOH/H_2O (1:1 – 2 mL/mmol) was added followed by any liquid aryl bromides (1.1 equiv). The reaction vessel was then heated at 40 °C for 18 h. Upon cooling, the solution was washed with H_2O, extracted with CH_2Cl_2, further washed with saturated NH_4Cl, dried (Na_2SO_4), and concentrated *in vacuo*. If required, the product was further purified by automated column chromatography with silica gel and hexane/EtOAc as eluent to yield 8-substituted 2,1-borazaronaphthalenes.

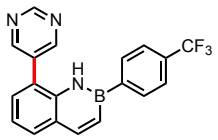

8-(Pyrimidin-5-yl)-2-(4-(trifluoromethyl)phenyl)-2,1-borazaronaphthalene (**3.67**): Obtained as a light brown solid (172 mg, 98%, 0.5 mmol scale); mp: 97-99

°C; ^{1}H NMR ($CDCl_3$, 500.4 MHz): δ 9.39 (s, 1H), 8.99 (s, 2H), 8.27 (d, *J* = 11.5 Hz, 1H), 8.19 (s, 1H), 7.84 – 7.80 (m, 3H), 7.66 (d, *J* = 7.9 Hz, 2H), 7.42 (dd, *J* = 7.2, 1.1 Hz, 1H), 7.37 (t, *J* = 7.6 Hz, 1H), 7.33 (dd, *J* = 11.6, 1.6 Hz, 1H) ppm; ^{13}C {^{1}H} NMR ($CDCl_3$, 125.8 MHz): δ 158.7, 158.6, 157.5, 146.6, 137.2, 132.9, 132.2, 131.8 (q, *J* = 32.4 Hz), 131.2, 130.4, 126.5, 125.1 (q, *J* = 3.6 Hz), 124.3 (q, *J* = 272.2 Hz), 123.6, 121.8 ppm; ^{19}F {^{1}H} NMR ($CDCl_3$, 470.8 MHz): δ -62.9 ppm; ^{11}B NMR ($CDCl_3$, 128.4 MHz): δ 33.4 ppm; IR: ν = 3409, 3285, 2980, 1568, 1323, 1162, 1117, 1065, 827, 757 cm^{-1}; HRMS (ESI+) m/z calc. for $C_{19}H_{14}BF_3N_3$ $[M+H]^+$ 352.1223, found 352.1222.

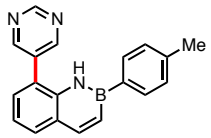

8-(Pyrimidin-5-yl)-2-(p-tolyl)-2,1-borazaronaphthalene (**3.68**): Obtained as a white solid (100.3 mg, 67%, 0.5 mmol scale); mp: 102-104 °C; ^{1}H NMR ($CDCl_3$, 500.4 MHz): δ 9.39 (s, 1H), 8.99 (s, 2H), 8.19 (d, *J* = 11.6 Hz, 1H), 8.13 (s, 1H), 7.77 (dd, *J* = 7.8, 1.5 Hz, 1H), 7.67 – 7.61 (m, 2H), 7.41 – 7.28 (m, 3H), 7.24 (d, *J* = 7.6 Hz, 2H), 2.39 (s, 3H) ppm; ^{13}C {^{1}H} NMR ($CDCl_3$, 125.8 MHz): δ 158.5, 157.5, 145.8, 140.3, 137.5, 132.8, 132.5, 131.0, 130.0, 129.3, 126.4, 123.3, 121.2, 21.7 ppm; ^{11}B NMR ($CDCl_3$, 128.4 MHz): δ 32.3 ppm; IR: ν = 3403, 3031, 1597, 1549, 1436, 1401, 1191, 760, 726, 721, 692 cm^{-1}; HRMS (EI) m/z calc. for $C_{19}H_{16}BN_3$ $[M]^+$ 297.1437, found 297.1453.

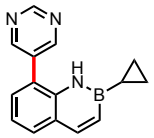

2-Cyclopropyl-8-(pyrimidin-5-yl)-2,1-borazaronaphthalene (**3.69**): Obtained as a beige solid (60.6 mg, 98%, 0.25 mmol scale); mp: 135-137 °C; ^{1}H NMR ($CDCl_3$, 500.4 MHz): δ 9.34 (s, 1H), 8.92 (s, 2H), 7.95 (d, *J* = 11.5 Hz, 1H), 7.66 (d, *J* = 7.5 Hz, 1H), 7.59 (s, 1H), 7.29 (dd, *J* = 7.3, 1.5 Hz, 1H), 7.22 (t, *J* = 7.5 Hz, 1H), 6.49 (dd, *J* = 11.7, 1.6 Hz, 1H), 0.83 (m, 2H), 0.55 (m, 2H), 0.11(m, 1H) ppm; ^{13}C {^{1}H} NMR ($CDCl_3$, 125.8 MHz): δ 158.3, 157.5, 144.9, 137.4, 132.7, 130.9, 129.7, 125.9, 122.6, 120.6, 6.3 ppm; ^{11}B NMR ($CDCl_3$, 128.4 MHz): δ 36.7 ppm; IR: ν = 3277, 3023, 2995, 1605, 1565, 1453, 1411, 1356, 827, 768 cm^{-1}; HRMS (EI) m/z calc. for $C_{15}H_{14}BN_3$ $[M]^+$ 247.1281, found 247.1306.

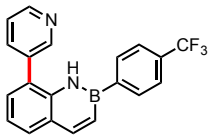

8-(Pyridin-3-yl)-2-(4-(trifluoromethyl)phenyl)-2,1-borazaronaphthalene (**3.70**): Obtained as a yellow solid (170 mg, 97%, 0.5 mmol scale); mp: 55-56 °C; ^{1}H NMR ($CDCl_3$, 500.4 MHz): δ 8.86 (d, *J* = 1.6 Hz, 1H), 8.79 (dd, *J* = 4.8, 1.5 Hz, 1H), 8.37 (s, 1H), 8.26 (d, *J* = 11.5 Hz, 1H), 7.90 (dt, *J* = 7.7, 1.8 Hz, 1H), 7.81 (d, *J* = 7.8 Hz, 2H), 7.77 (d, *J* = 7.8 Hz, 1H), 7.65 (d, *J* = 7.8 Hz, 2H), 7.54 (dd, *J* = 7.5, 5.0 Hz, 1H), 7.44 (dd, *J* = 7.3, 1.2 Hz, 1H), 7.34 (t, *J* = 7.6 Hz, 1H), 7.30 (dd, *J* = 11.6, 1.8 Hz, 1H) ppm; ^{13}C {^{1}H} NMR ($CDCl_3$, 125.8 MHz): δ 150.5, 149.8, 146.7, 137.2, 137.1, 133.9, 132.9, 131.5 (q, *J* = 32.3 Hz), 130.3, 130.1, 127.4, 126.3, 125.0 (q, *J* = 4.0 Hz), 124.2, 123.3 (q, *J* = 270.9 Hz), 121.6 ppm; ^{19}F {^{1}H} NMR ($CDCl_3$, 470.8 MHz): δ -62.8 ppm; ^{11}B

NMR ($CDCl_3$, 128.4 MHz): δ 33.3 ppm; IR: ν = 3398, 3029, 2970, 2931, 1601, 1567, 1320, 1119, 1104, 1065 cm^{-1}; HRMS (ESI+) m/z calc. for $C_{20}H_{15}BF_3N_2$ $[M+H]^+$ 351.1280, found 351.1301.

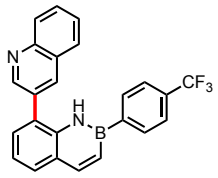

8-(Quinolin-3-yl)-2-(4-(trifluoromethyl)phenyl)-2,1-borazaronaphthalene

(**3.71**): Obtained as a white solid (197 mg, 98%, 0.5 mmol scale); mp: 138-140 °C; ^1H NMR ($CDCl_3$, 500.4 MHz): δ 9.15 (d, *J* = 2.1 Hz, 1H), 8.49 (s, 1H), 8.38 (d, *J* = 1.7 Hz, 1H), 8.29 (dd, *J* = 13.5, 10.1 Hz, 1H), 7.94 (d, *J* = 8.1 Hz, 1H), 7.86 (t, *J* = 7.7 Hz, 1H), 7.83 – 7.77 (m, 3H), 7.69 (t, *J* = 7.4 Hz, 1H), 7.61 (d, *J* = 7.8 Hz, 1H), 7.54 (dd, *J* = 7.3, 1.1 Hz, 1H), 7.39 (t, *J* = 7.6 Hz, 1H), 7.33 (dd, *J* = 11.5, 1.6 Hz, 1H) ppm; ^{13}C $\{^1H\}$ NMR ($CDCl_3$, 125.8 MHz): δ 151.3, 147.9, 146.7, 137.5, 136.4, 132.9, 131.5 (q, *J* = 32.2 Hz), 131.1, 130.5, 130.4, 130.4, 129.7, 128.1, 128.1, 127.8, 127.5, 126.4, 125.0 (q, *J* = 3.6 Hz), 124.4 (q, *J* = 272.0 Hz), 121.7 ppm; ^{19}F $\{^1H\}$ NMR ($CDCl_3$, 470.8 MHz): δ -62.9 ppm; ^{11}B NMR ($CDCl_3$, 128.4 MHz): δ 31.6 ppm; IR: ν = 3402, 3012, 2969, 2935, 1561, 1319, 1160, 1110, 1065, 821, 751 cm^{-1}; HRMS (ESI+) m/z calc. for $C_{24}H_{17}BF_3N_2$ $[M+H]^+$ 401.1437, found 401.1426.

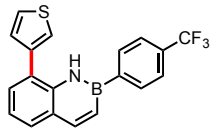

8-(Thiophen-3-yl)-2-(4-(trifluoromethyl)phenyl)-2,1-borazaronaphthalene

(**3.72**): Obtained as a white solid (156.3 mg, 88%, 0.5 mmol scale); mp: 95-96 °C; ^1H

NMR ($CDCl_3$, 500.4 MHz): δ 8.79 (s, 1H), 8.25 (d, *J* = 11.5 Hz, 1H), 7.87 (d, *J* = 7.8 Hz, 2H), 7.73 – 7.66 (m, 3H), 7.63 (dd, *J* = 4.9, 3.0 Hz, 1H), 7.53 – 7.49 (m, 2H), 7.36 (dd, *J* = 4.9, 1.2 Hz, 1H), 7.32 – 7.27 (m, 2H) ppm; ^{13}C {^1H} NMR ($CDCl_3$, 125.8 MHz): δ 146.4, 138.2, 137.3, 132.7 (2 x C), 131.2 (q, *J* = 32.2 Hz), 129.4, 129.2, 128.3, 127.5, 125.9, 124.8 (q, *J* = 3.8 Hz), 124.2 (q, *J* = 272.0 Hz), 123.6, 121.1 ppm; ^{19}F {^1H} NMR ($CDCl_3$, 470.8 MHz): δ -62.7 ppm; ^{11}B NMR ($CDCl_3$, 128.4 MHz): δ 33.0 ppm; IR: ν = 3397, 3096, 3047, 3016, 1600, 1566, 1324, 1102, 1066, 752 cm^{-1}; HRMS (EI) m/z calc. for $C_{19}H_{13}BF_3NS$ $[M]^+$ 355.0814, found 355.0829.

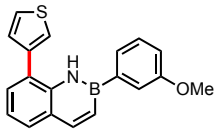

8-(Thiophen-3-yl)-2-(3-methoxyphenyl)-2,1-borazaronaphthalene (**3.73**): Obtained as a white solid (150 mg, 95%, 0.5 mmol scale); mp: 85-86 °C; ^1H NMR ($CDCl_3$, 500.4 MHz): δ 8.76 (s, 1H), 8.20 (d, *J* = 11.5 Hz, 1H), 7.67 (d, *J* = 7.8 Hz, 1H), 7.61 (dd, *J* = 4.7, 3.0 Hz, 1H), 7.51 (d, *J* = 2.1 Hz, 1H), 7.48 (dd, *J* = 7.5, 1.1 Hz, 1H), 7.40 – 7.34 (m, 3H), 7.33 (d, *J* = 2.5 Hz, 1H), 7.29 (dd, *J* = 11.5, 1.7 Hz, 1H), 7.24 (t, *J* = 7.7 Hz, 1H), 6.98 (dt, *J* = 7.3, 2.3 Hz, 1H), 3.86 (s, 3H) ppm; ^{13}C {^1H} NMR ($CDCl_3$, 125.8 MHz): δ 159.7, 146.1, 138.6, 137.8, 129.6, 129.4, 129.3, 128.7, 127.5, 126.1, 126.0, 125.1, 123.8, 120.9, 118.2, 115.2, 55.3 ppm; ^{11}B NMR ($CDCl_3$, 128.4 MHz): δ 34.7 ppm; IR: ν = 3384, 2920, 1597, 1565, 1436, 1264, 1255, 755, 720 cm^{-1}; HRMS (ESI+) m/z calc. for $C_{19}H_{17}BNOS$ $[M+H]^+$ 318.1124, found 318.1106.

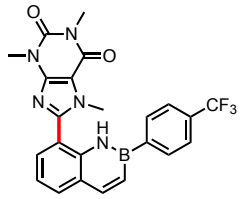

2-(4-(Trifluoromethyl)phenyl)-8-(1,3,7-trimethyl-2,6-dioxo-2,3,6,7-tetrahydro-1H-purin-8-yl)-2,1-borazaronaphthalene (**3.74**): Obtained as a white solid (233 mg, 99%, 0.5 mmol scale); mp: >260 °C; ^{1}H NMR ($CDCl_3$, 500.4 MHz): δ 11.04 (s, 1H), 8.26 (d, *J* = 11.6 Hz, 1H), 8.04 (d, *J* = 7.7 Hz, 2H), 7.87 (d, *J* = 7.7 Hz, 1H), 7.70 (d, *J* = 7.9 Hz, 2H), 7.67 (dd, *J* = 7.7, 1.2 Hz, 1H), 7.44 – 7.32 (m, 2H), 4.15 (s, 3H), 3.76 (s, 3H), 3.49 (s, 3H) ppm; ^{13}C {^{1}H} NMR ($CDCl_3$, 125.8 MHz): δ 155.6, 151.8, 149.6, 148.0, 146.3, 139.3, 133.2, 132.7, 131.8 (q, *J* = 32.3 Hz), 129.5, 127.2, 125.1 (q, *J* = 3.4 Hz), 124.4 (q, *J* = 272.1 Hz), 120.4, 115.0, 108.8, 35.1, 30.1, 28.4 ppm; ^{19}F {^{1}H} NMR ($CDCl_3$, 470.8 MHz): δ -62.8 ppm; ^{11}B NMR ($CDCl_3$, 128.4 MHz): δ 33.0 ppm; IR: ν = 3312, 2950, 1698, 1658, 1539, 1323, 1164, 1108, 1067 cm^{-1}; HRMS (ESI+) m/z calc. for $C_{23}H_{20}BF_3N_5O_2$ $[M+H]^+$ 466.1662, found 466.1668.

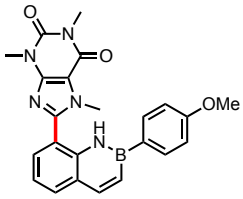

2-(4-Methoxyphenyl)-8-(1,3,7-trimethyl-2,6-dioxo-2,3,6,7-tetrahydro-1H-purin-8-yl)-2,1-borazaronaphthalene (**3.75**): Recrystallized from toluene and obtained as a white solid (212 mg, 99%, 0.5 mmol scale); mp: >260 °C; ^{1}H NMR ($CDCl_3$, 500.4 MHz): δ 10.76 (s, 1H), 8.14 (d, *J* = 11.6 Hz, 1H), 7.89 (d, *J* = 8.5 Hz, 2H), 7.79 (d, *J* = 7.7

Hz, 1H), 7.61 (dd, *J* = 7.2, 1.0 Hz, 1H), 7.36 (dd, *J* = 11.5, 1.5 Hz, 1H), 7.29 (t, *J* = 7.7 Hz, 1H), 7.00 (d, *J* = 8.5 Hz, 2H), 4.13 (s, 3H), 3.87 (s, 3H), 3.77 (s, 3H), 3.49 (s, 3H). $^{13}C\{^{1}H\}$ NMR ($CDCl_3$, 125.8 MHz): δ 161.3, 155.3, 151.6, 149.7, 147.7, 145.0, 139.5, 134.4, 132.2, 128.9, 126.7, 119.4, 114.3, 113.8, 108.4, 55.1, 34.7, 29.7, 28.3 ppm; ^{11}B NMR ($CDCl_3$, 128.4 MHz): δ 31.6 ppm; IR: ν = 3305, 2939, 1703, 1662, 1598, 1442, 1243, 1179, 1026 cm^{-1}; HRMS (EI) m/z calc. for $C_{23}H_{23}BNSO_3$ $[M+H]^+$ 428.1894, found 428.1891.

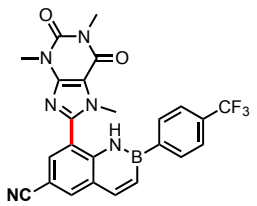

6-Cyano-2-(4-(trifluoromethyl)phenyl)-8-(1,3,7-trimethyl-2,6-dioxo-2,3,6,7-tetrahydro-1H-purin-8-yl)-2,1-borazaronaphthalene (**3.76**): Obtained as a light yellow solid (79.7 mg, 65%, 0.25 mmol scale); mp: >260 °C; ^{1}H NMR ($CDCl_3$, 500.4 MHz): δ 11.35 (s, 1H), 8.23 (d, *J* = 11.6 Hz, 1H), 8.17 (s, 1H), 8.04 (d, *J* = 7.5 Hz, 2H), 7.88 (d, *J* = 1.5 Hz, 1H), 7.73 (d, *J* = 7.8 Hz, 2H), 7.53 (d, *J* = 11.5 Hz, 1H), 4.20 (s, 3H), 3.75 (s, 3H), 3.49 (s, 3H) ppm; $^{13}C\{^{1}H\}$ NMR ($CDCl_3$, 125.8 MHz): δ 155.5, 151.6, 147.8, 147.1, 145.4, 141.8, 136.4, 133.4, 132.5 (q, *J* = 32.4 Hz), 131.1, 127.2, 125.2 (q, *J* = 3.8 Hz), 124.18 (q, *J* = 118.4 Hz), 116.3, 109.1, 104.1, 35.1, 30.0, 28.4 ppm; ^{11}B NMR ($CDCl_3$, 128.4 MHz): δ 34.0 ppm; $^{19}F\{^{1}H\}$ NMR ($CDCl_3$, 470.8 MHz): δ -62.9 ppm; IR: ν = 3308, 2962, 2230, 1712, 1674, 1327, 1166, 1101, 1070, 779 cm^{-1}; HRMS (ESI+) m/z calc. for $C_{24}H_{19}BN_6O_2F_3$ $[M+H]^+$ 491.1615, found 491.1636.

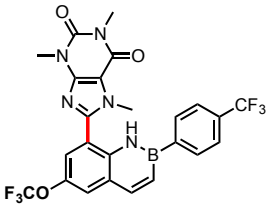

6-(Trifluoromethoxy)-2-(4-(trifluoromethyl)phenyl)-8-(1,3,7-trimethyl-2,6-dioxo-2,3,6,7-tetrahydro-1H-purin-8-yl)-2,1-borazaronaphthalene (**3.77**): Obtained as a white solid (81 mg, 58%, 0.25 mmol scale); mp: 209-210 °C; ^{1}H NMR ($CDCl_3$, 500.4 MHz): δ 11.13 (s, 1H), 8.21 (d, *J* = 11.6 Hz, 1H), 8.03 (d, *J* = 7.8 Hz, 2H), 7.74 – 7.67 (m, 3H), 7.55 (d, *J* = 2.3 Hz, 1H), 7.47 (dd, *J* = 11.6, 1.6 Hz, 1H), 4.17 (s, 3H), 3.75 (s, 3H), 3.48 (s, 3H) ppm; ^{13}C {^{1}H} NMR ($CDCl_3$, 125.8 MHz): δ 155.5, 151.6, 147.9, 147.8, 145.5, 141.8, 137.9, 133.2, 132.1 (q, *J* = 32.5 Hz), 127.7, 125.1 (q, *J* = 3.7 Hz), 124.2, 124.0 (q, *J* = 274.8 Hz), 122.5, 120.8 (q, *J* = 257.6 Hz), 116.0, 109.0, 34.9, 30.0, 28.3 ppm; ^{19}F {^{1}H} NMR ($CDCl_3$, 470.8 MHz): δ -58.3, -62.9 ppm; ^{11}B NMR ($CDCl_3$, 128.4 MHz): δ 32.8 ppm; IR: ν = 3302, 3047, 2951, 1702, 1663, 1326, 1267, 1257, 1166, 1106 cm^{-1}; HRMS (ESI+) m/z calc. for $C_{24}H_{19}BN_5O_3F_6$ $[M+H]^+$ 550.1485, found 550.1480.

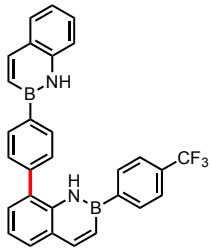

8-(4-(2,1-Borazaronaphthalen-2-yl)phenyl)-2-(4-(trifluoromethyl)phenyl)-2,1-borazaronaphthalene (**3.78**): Obtained as an off white solid (202 mg, 85%, 0.5 mmol scale); mp: 138-140 °C; ^{1}H NMR ($CDCl_3$, 500.4 MHz): δ 8.76 (s, 1H), 8.21-8.29 (m,

3H), 8.16 (d, *J* = 7.6 Hz, 2H), 7.84 (d, *J* = 7.8 Hz, 2H), 7.73 (t, *J* = 9.9 Hz, 2H), 7.70 (d, *J* = 7.7 Hz, 2H), 7.66 (d, *J* = 7.8 Hz, 2H), 7.52 (d, *J* = 7.0 Hz, 1H), 7.49 (t, *J* = 7.2 Hz, 1H), 7.41 (d, *J* = 8.8 Hz, 1H), 7.39 – 7.29 (m, 3H), 7.26 (t, *J* = 7.8 Hz, 1H) ppm; ^{13}C {^{1}H} NMR ($CDCl_3$, 125.8 MHz): δ146.7, 146.1, 140.3, 139.3, 137.2, 133.9, 133.0, 131.4 (q, *J* = 30.9Hz), 131.2, 129.8, 129.8, 129.5, 129.4, 128.8, 128.1, 126.2, 126.0, 125.0, 125.0 (q, *J* = 4.6 Hz), 124.5 (q, *J* = 273.0 Hz), 121.5, 121.4, 118.5 ppm; ^{19}F {^{1}H} NMR ($CDCl_3$, 470.8 MHz): δ -62.8 ppm; ^{11}B NMR ($CDCl_3$, 128.4 MHz): δ 33.8 ppm; IR: ν = 3385, 3397, 2954, 2931, 1598, 1562, 1437, 1322, 1167, 1117, 1066, 808, 757 cm^{-1}; HRMS (EI) m/z calc. for $C_{29}H_{21}B_2F_3N_2$ $[M]^+$ 476.1843, found 476.1857.

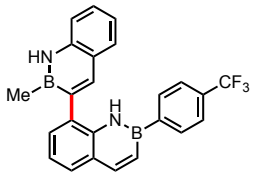

8-(2-Methyl-2,1-borazaronaphthalen-3-yl)-2-(4-(trifluoromethyl)phenyl)-2,1-borazaronaphthalene (**3.79**): Obtained as a white solid (70 mg, 68%, 0.25 mmol scale); mp: 159-161 °C; ^{1}H NMR ($CDCl_3$, 500.4 MHz): δ 8.42 (s, 1H), 8.28 (d, *J* = 11.5 Hz, 1H), 8.04 (s, 1H), 8.01 (s, 1H), 7.81 (d, *J* = 7.7 Hz, 2H), 7.68 (t, *J* = 6.1 Hz, 2H), 7.61 (d, *J* = 7.7 Hz, 2H), 7.52 (t, *J* = 7.6 Hz, 1H), 7.39 – 7.33 (m, 2H), 7.33 – 7.22 (m, 3H), 0.64 (s, 3H) ppm; ^{13}C {^{1}H} NMR ($CDCl_3$, 125.8 MHz): δ 146.8, 144.6, 140.3, 137.2, 134.0, 132.9, 131.2 (q, *J* = 32.3 Hz), 129.8, 129.1, 128.9, 128.2, 125.8, 124.9 (q, *J* = 3.2 Hz), 124.5 (q, *J* = 272.0 Hz), 121.5, 121.2, 117.9 ppm; ^{19}F {^{1}H} NMR ($CDCl_3$, 470.8 MHz): δ -62.8 ppm; ^{11}B NMR ($CDCl_3$, 128.4 MHz): δ 35.57, 30.9 ppm; IR: ν = 3377, 1559, 1320, 1101, 1063, 759, 752, 717cm^{-1}; HRMS (EI) m/z calc. for $C_{24}H_{19}B_2N_2F_3$ $[M]^+$ 414.1686, found 414.1686.

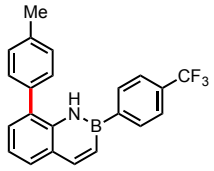

8-(p-Tolyl)-2-(4-(trifluoromethyl)phenyl)-2,1-borazaronaphthalene (**3.80**): Obtained as a white solid (162.1 mg, 89%, 0.5 mmol scale); mp: 92-93 °C; ^{1}H NMR ($CDCl_3$, 500.4 MHz): δ 8.70 (s, 1H), 8.26 (d, *J* = 11.5 Hz, 1H), 7.84 (d, *J* = 7.8 Hz, 2H), 7.71 (d, *J* = 7.8 Hz, 1H), 7.67 (d, *J* = 7.9 Hz, 2H), 7.49 – 7.43 (m, 3H), 7.41 (d, *J* = 7.9 Hz, 2H), 7.30 (t, *J* = 7.6 Hz, 2H), 2.51 (s, 3H) ppm; ^{13}C {^{1}H} NMR ($CDCl_3$, 125.8 MHz): δ 146.4, 138.0, 137.1, 134.8, 132.7, 131.2 (q, *J* = 32.3 Hz), 131.1, 130.1, 129.5, 129.2, 128.9, 125.9, 124.7 (q, *J* = 3.8 Hz), 123.2 (q, *J* = 271.9 Hz), 121.1, 21.2 ppm; ^{19}F {^{1}H} NMR ($CDCl_3$, 470.8 MHz): δ -62.8 ppm; ^{11}B NMR ($CDCl_3$, 128.4 MHz): δ 33.1 ppm; IR: ν = 3403, 3031, 2923, 2856, 1600, 1567, 1322, 1104, 1065, 753 cm^{-1}; HRMS (EI) m/z calc. for $C_{22}H_{17}BF_3N$ $[M]^+$ 363.1406, found 363.1399.

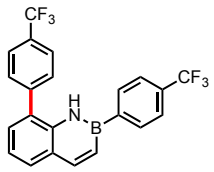

2,8-Bis(4-(trifluoromethyl)phenyl)-2,1-borazaronaphthalene (**3.81**): Obtained as a white solid (204 mg, 98%, 0.5 mmol scale); mp: 105-106 °C; ^{1}H NMR ($CDCl_3$, 500.4 MHz): δ 8.47 (s, 1H), 8.27 (d, *J* = 11.5 Hz, 1H), 7.87 (d, *J* = 8.1 Hz, 2H), 7.81 (d, *J* = 7.8 Hz, 2H), 7.76 (d, *J* = 7.7 Hz, 1H), 7.71 (d, *J* = 8.0 Hz, 2H), 7.67 (d, *J* = 7.9 Hz, 2H), 7.44 (dd, *J* = 7.3, 1.3 Hz, 1H), 7.38 – 7.27 (m, 2H) ppm; ^{13}C {^{1}H} NMR ($CDCl_3$, 125.8 MHz): δ ^{13}C NMR (126 MHz, $CDCl_3$) δ 146.7, 141.9, 136.9, 132.9, 131.4 (q, *J* = 32.3 Hz), 130.6 (q, *J* = 32.5 Hz), 130.2, 130.1, 129.9, 129.7, 126.6 (q, *J* = 3.7 Hz), 126.3,

125.0 (q, *J* = 3.8 Hz), 124.4 (q, *J* = 271.9 Hz), 124.2 (q, *J* = 272.0 Hz), 121.5 ppm; ^{19}F {^{1}H} NMR ($CDCl_3$, 470.8 MHz): δ -62.5, -62.8 ppm; ^{11}B NMR ($CDCl_3$, 128.4 MHz): δ 31.5 ppm; IR: ν = 3405, 3035, 2939, 1566, 1323, 1098, 1067, 1016, 818, 755 cm^{-1}; HRMS (EI) m/z calc. for $C_{22}H_{14}BNF_6$ $[M]^+$ 417.1123, found 417.1129.

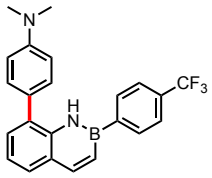

8-(4-(Dimethylamino)phenyl)-2-(4-(trifluoromethyl)phenyl)-2,1-borazaronaphthalene (**3.82**): Obtained as a white solid (180.4 mg, 92%, 0.5 mmol scale); mp: 114-115 °C; ^{1}H NMR ($CDCl_3$, 500.4 MHz): δ 8.82 (s, 1H), 8.25 (d, *J* = 11.5 Hz, 1H), 7.86 (d, *J* = 7.8 Hz, 2H), 7.68 – 7.63 (m, 3H), 7.47 – 7.41 (m, 3H), 7.30 – 7.22 (m, 2H), 6.93 (d, *J* = 8.5 Hz, 2H), 3.08 (s, 6H) ppm; ^{13}C {^{1}H} NMR ($CDCl_3$, 125.8 MHz): δ 150.1, 146.5, 137.3, 132.8, 132.6, 131.4, 131.0 (q, *J* = 32.2 Hz), 130.1, 129.5, 128.3, 126.4 (q, *J* = 272.1 Hz), 125.8, 124.7 (q, *J* = 3.9 Hz), 121.1, 112.9, 40.4 ppm; ^{19}F {^{1}H} NMR ($CDCl_3$, 470.8 MHz): δ 62.8 ppm; ^{11}B NMR ($CDCl_3$, 128.4 MHz): δ 32.9 ppm; IR: ν = 3386, 3045, 2893, 2804, 1601, 1565, 1522, 1321, 1115, 1103, 1064 cm^{-1}; HRMS (ESI+) m/z calc. for $C_{23}H_{20}BF_3N_2$ $[M]^+$ 393.1750, found 393.1763.

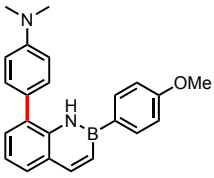

8-(4-(Dimethylamino)phenyl)-2-(4-methoxyphenyl)-2,1-borazaronaphthalene (**3.83**): Obtained as a light gray solid (161 mg, 91%, 0.5 mmol scale); mp: 140-142

°C; ^{1}H NMR ($CDCl_3$, 500.4 MHz): δ 8.71 (s, 1H), 8.18 (d, *J* = 11.6 Hz, 1H), 7.75 (d, *J* = 8.5 Hz, 2H), 7.62 (d, *J* = 7.6 Hz, 1H), 7.47 (d, *J* = 8.7 Hz, 2H), 7.40 (dd, *J* = 7.3, 1.4 Hz, 1H), 7.29 (d, *J* = 11.8 Hz, 1H), 7.23 (t, *J* = 7.5 Hz, 1H), 6.99 (d, *J* = 8.5 Hz, 2H), 6.95 (d, *J* = 8.4 Hz, 1H), 3.86 (s, 3H), 3.09 (s, 6H) ppm; ^{13}C {^{1}H} NMR ($CDCl_3$, 125.8 MHz): δ 161.1, 150.4, 145.8, 137.9, 134.4, 131.3, 130.4, 129.5, 128.4, 125.8 (d, *J* = 5.2 Hz), 120.7, 114.0, 113.2, 77.0, 55.3, 40.7 ppm; ^{11}B NMR ($CDCl_3$, 128.4 MHz): δ 33.8 ppm; IR: ν = 3381, 2962, 2927, 2835, 1595, 1558, 1433, 1237, 1179, 819, 759 cm^{-1}; HRMS (ESI+) m/z calc. for $C_{23}H_{24}BN_2O$ $[M+H]^+$ 335.1982, found 335.1989.

3.6 – References

1. *For 2,1-borazaronaphthalene synthetic methods:* a) Wisniewski, S. R.; Guenther, C. L.; Argintaru, O. A.; Molander, G. A. *J. Org. Chem*. **2014**, *79*, 365. b) Molander, G. A.; Wisniewski, S. R.; Amani, J. *Org. Lett.* **2014**, *16*, 5636. c) Molander, G. A.; Amani, J.; Wisniewski, S. R. *Org. Lett.* **2014**, *16*, 6024. d) Molander, G. A.; Wisniewski, S. R. *J. Org. Chem*. **2014**, *79*, 6663. e) Molander, G. A.; Wisniewski, S. R.; Etemadi-Davan, E. *J. Org. Chem.* **2014**, *79*, 11199. f) Molander, G. A.; Wisniewski, S. R. *J. Org. Chem.* **2014**, *79*, 8339. g) Molander, G. A.; Wisniewski, S. R.; Traister, K. M. *Org. Lett.* **2014**, *16*, 3692. h) Jouffroy, M.; Davies, G. H. M.; Molander, G. A. *Org. Lett.* **2016**, *18*, 1606. i) Davies, G. H. M.; Zhou, Z.-Z.; Jouffroy, M.; Molander, G. A. *J. Org. Chem.* **2017**, *82*, 549. j) Casado, M. R. S.; Jimeńez, M. C.; Bueno, M. A.; Barriol, M.; Leenaerts, J. E.; Pagliuca, C.; Lamenca, C. M.; Lucas, A. I. D.; García, A.; Trabanco, A. A.; Rombouts, F. J. R. *Eur. J. Org. Chem*. **2015**, *23*, 5221. k) Zhuang, F.-D.; Han, J.-M.; Tang, S.; Yang, J.-H.; Chen, Q.-

R.; Wang, J.-Y.; Pei, J. *Organometallics* **2016,** *ASAP*, DOI: 10.1021/acs.organomet.6b00811.

2. a) Becke, A. D. J. *Chem. Phys*. **1993**, *98*, 5648. b) Lee, C.; Yang, W.; Parr, R. G. *Phys. Rev. B: Condens. Matter Mater. Phys.* **1988**, *37*, 785. c) Vosko, S. H.; Wilk, L.; Nusair, M. *Can. J. Phys.* **1980**, *58*, 1200. d) Stephens, P. J.; Devlin, F. J.; Chabalowski, C. F.; Frisch, M. J. *J. Phys. Chem*. **1994**, *98*, 11623. e) Ditchfield, R.; Hehre, W. J.; Pople, J. A. *J. Chem. Phys.* **1971**, *54*, 724. f) Hehre, W. J.; Ditchfield, R.; Pople, J. A. *J. Chem. Phys.* **1972**, *56*, 2257. g) Hariharan, P. C.; Pople, J. A. *Theor. Chim. Acta* **1973**, *28*, 213.

3. Frisch, M. J.; Trucks, G. W.; Schlegel, H. B.; Scuseria, G. E.; Robb, M. A.; Cheeseman, J. R.; Scalmani, G.; Barone, V.; Mennucci, B.; Petersson, G. A.; Nakatsuji, H.; Caricato, M.; Li, X.; Hratchian, H. P.; Izmaylov, A. F.; Bloino, J.; Zheng, G.; Sonnenberg, J. L.; Hada, M.; Ehara, M.; Toyota, K.; Fukuda, R.; Hasegawa, J.; Ishida, M.; Nakajima, T.; Honda, Y.; Kitao, O.; Nakai, H.; Vreven, T.; Montgomery, J. A., Jr.; Peralta, J. E.; Ogliaro, F.; Bearpark, M.; Heyd, J. J.; Brothers, E.; Kudin, K. N.; Staroverov, V. N.; Kobayashi, R.; Normand, J.; Raghavachari, K.; Rendell, A.; Burant, J. C.; Iyengar, S. S.; Tomasi, J.; Cossi, M.; Rega, N.; Millam, J. M.; Klene, M.; Knox, J. E.; Cross, J. B.; Bakken, V.; Adamo, C.; Jaramillo, J.; Gomperts, R.; Stratmann, R. E.; Yazyev, O.; Austin, A. J.; Cammi, R.; Pomelli, C.; Ochterski, J. W.; Martin, R. L.; Morokuma, K.; Zakrzewski, V. G.; Voth, G. A.; Salvador, P.; Dannenberg, J. J.; Dapprich, S.; Daniels, A. D.; Farkas, Ö.; Foresman, J. B.; Ortiz, J. V.; Cioslowski, J.; Fox, D. J. *Gaussian 09*, revision D.01; Gaussian, Inc.: Wallingford CT, 2009.

4. Schmidt, J.R.; Polik, W.F. *WebMO Enterprise*, version 14.0.004e; WebMO LLC: Holland, MI, USA, 2013; http://www.webmo.net.

5. *Applications of 2,1-borazaronaphthalene*: a) Rombouts, F. J. R.; Tovar, F.; Austin, N.; Tresadern, G.; Trabanco, A. A. *J. Med. Chem.* **2015**, *58*, 9287. b) Vlasceanu, A.; Jessing, M.; Kilburn, J. P. *Bioorg. Med. Chem.* **2015**, *23*, 4453. c) Saint-Louis, C. J.; Magill, L. L.; Wilson, J. A.; Schroeder, A. R.; Harrell, S. E.; Jackson, N. S.; Trindell, J. A.; Kim, S.; Fisch, A. R.; Munro, L.; J. Catalano, V. J.; Webster, C. E.; Vaughan, P. P.; Molek, K. S.; Schrock, A. K.; Huggins, M. T. *J. Org. Chem.* **2016**, *81*, 10955. d) Xu, S.; Zhang, Y.; Li, B.; Liu, S.-Y. *J. Am. Chem. Soc.* **2016**, *138*, 14566.

6. Foye, W. O.; Lemke, T. L.; Williams, D. A. *Foye's Principles of Medicinal Chemistry*; Wolters Kluwer Health/Lippincott Williams & Wilkins: Philadelphia, 2013.

7. a) Kerns, E. H.; Di, L. *Drug-like Properties: Concepts, Structure Design and Methods*; 1st Edn, Elsevier: Burlington, MA, 2008. b) Leeson, P. *Nature* **2012**, *481*, 455. c) Manallack, D. T.; Prankerd, R. J.; Yuriev, E.; Oprea, T. I.; Chalmers D. K. *Chem. Soc. Rev.* **2013**, *42*, 485.

8. *Seminal reports of photoredox dual catalysis*: *(*a) Tellis, J. C.; Primer, D. N.; Molander, G. A. *Science* **2014**, *345*, 433. (b) Zuo, Z. W.; Ahneman, D. T.; Chu, L. L.; Terrett, J. A.; Doyle, A. G.; MacMillan, D. W. C. *Science* **2014**, *345*, 437. (c) Kalyani, D.; McMurtrey, K. B.; Neufeldt, S. R.; Sanford, M. S. *J. Am. Chem. Soc.* **2011**, *133*, 18566. (d) Ye, Y.; Sanford, M. S. *J. Am. Chem. Soc.* **2012**, *134*, 9034. (e) Sahoo, B.; Hopkinson, M. N.; Glorius, F. *J. Am. Chem. Soc.* **2013**, *135*, 5505.

9. *Recent advance in photoredox dual catalysis*: a) Primer, D. N.; Karakaya, I.; Tellis, J. C.; Molander, G. A. *J. Am. Chem. Soc.* **2015**, *137*, 2195. b) Karakaya, I.; Primer,

D. N.; Molander, G. A. *Org. Lett.* **2015**, *17*, 3294. c) El Khatib, M.; Serafim, R. A. M.; Molander, G. A. *Angew. Chem., Int. Ed.* **2016**, *55*, 254. d) Rueping, M.; Koenigs, R. M.; Poscharny, K.; Fabry, D. C.; Leonori, D.; Vila, C. *Chem.–Eur. J.* **2012**, *18*, 5170. e) Shu, X. Z.; Zhang, M.; He, Y.; Frei, H.; Toste, F. D. *J. Am. Chem. Soc.* **2014**, *136*, 5844. f) Noble, A.; McCarver, S. J.; MacMillan, D. W. C. *J. Am. Chem. Soc.* **2015**, *137*, 624. g) Chu, L.; Lipshultz, J. M.; MacMillan, D. W. C. *Angew. Chem., Int. Ed.* **2015**, *54*, 7929. h) Le, C. C.; MacMillan, D. W. C. *J. Am. Chem. Soc.* **2015**, *137*, 11938.

10. a) Jouffroy, M.; Primer, D. N.; Molander, G. A. *J. Am. Chem. Soc.* **2016**, *138*, 475. b) Patel, N. R.; Kelly, C. B.; Jouffroy, M.; Molander, G. A. *Org. Lett.* **2016**, *18*, 764**.** c) Corce, V.; Chamoreau, L.-M.; Derat, E.; Goddard, J.-P.; Ollivier, C.; Fensterbank, L. *Angew. Chem., Int. Ed.* **2015**, *54*, 11414.

11. a) Scott, H. K.; Aggarwall, V. K. *Chem. Eur. J.* **2011**, *17*, 13124. b) Molander, G. A. *J. Org. Chem.* **2015**, *80*, 7837.

12. *References and reviews of C-H borylation strategies*: a) Mkhalid, I. A. I.; Barnard, J. H.; Marder, T. B.; Murphy, J. M.; Hartwig, J. F. *Chem. Rev.* **2010**, *110*, 890. b) Hartwig, J. F. *Acc. Chem. Res.* **2012**, *45*, 864. c) Ros A.; Fernández, R.; Lassaletta, J. M. *Chem. Soc. Rev.* **2014**, *43*, 3229. d) Amaike, K.; Loach, R. P.; Movassaghi, M. *Org. Synth.* **2015**, *92*, 373. e) Shinokubo, H. *Proc. Jpn. Acad. Ser. B Phys. Biol. Sci.* **2014**, *90*, 1. f) Preshlokc, S. M.; Ghaffari, B.; Maligres, P, E.; Krska, S. W.; Maleczka, R. E., Jr.; Smith, M. R., III *J. Am. Chem. Soc.* **2013**, *135*, 7572. g) Saito, Y.; Segawa, Y.; Itami, K. *J. Am. Chem. Soc.* **2015**, *137*, 5193.

13. Baggett, A. W.; Vasiliu, M.; Li, B.; Dixon, D. A.; Liu, S.-L. *J. Am. Chem. Soc.* **2015**, *137*, 5536.

14. Coventry, D. N.; Batsanov, A. S.; Goeta, A. E.; Howard, J. A. K.; Marder, T. B.; Perutz, R. N. *Chem. Commun.* **2005**, 2172.

15. Konishi, S.; Kawamorita, S.; Iwai, T.; Steel, P. G.; Marder, T. B.; Masaya S. *Chem. Asian J.* **2014**, *9*, 434.

16. Tajuddin, H.; Harrisson, P.; Bitterlich, B.; Collings, J. C.; Sim, N.; Batsanov, A. S.; Cheung, M. S.; Kawamorita, S.; Maxwell, A. C.; Shukla, L.; Morris, J.; Lin, Z.; Marder, T. B.; Steel, P. G. *Chem. Sci.* **2012**, *3*, 3505.

17. Robbins, D. W.; Boebel, T. A.; Hartwig, J. F. *J. Am. Chem. Soc.* **2010**, *132*, 4068.

18. Paul, S.; Chotana, G. A.; Holmes, D.; Reichle, R. C.; Maleczka, R. E., Jr., Smith, M. R., III *J. Am. Chem. Soc.* **2006**, *128*, 15552.

19. Bocchi, V.; Palla, G.; *Synthesis* **1982**, *12*, 1096.

20. a) Preshlock, S. M.; Plattner, D. L.; Malegres, P. E.; Krska, S. W.; Maleczka, R. E., Jr.; Smith, M. R., III *Angew. Chem., Int. Ed.* **2013**, *52*, 12915. b) Roosen, P. C.; Kallepalli, B. A.; Chattopadhyay, B.; Singleton, D. A.; Maleczka, R. E., Jr.; Smith, M. R., III *J. Am. Chem. Soc.* **2012**, *134*, 11350.

21. Vanchura, B. A.; Preshlock, S. M.; Roosen, P. C.; Kallepalli, V. A.; Staples, R. J.; Maleczka, R. E., Jr.; Singleton, D. A.; Smith, M. R., III. *Chem. Commun.* **2010**, *46*, 7724.

22. Larsen, M. A.; Hartwig, J. F. *J. Am. Chem. Soc.* **2014**, *136*, 4287.

23. Ishiyama, T.; Takagi, J.; Yonekawa, Y.; Hartwig, J. F.; Miyaura, N. *Adv. Synth. Catal.* **2003**, *345*, 1103.

24. Vara, B. A.; Jouffroy, M.; Molander, G. A.; *Chem. Sci.* **2017**, *8*, 530.

25. Crudden, C. M.; Ziebenhaus, C.; Rygus, J. P. G.; Ghozati, K.; Unsworth, P. J.; Nambo, M.; Voth, S.; Hutchinson, M.; Laberge, V. S.; Maekawa, Y.; Imao, D. *Nat. Chem.* **2016**, *7*, DOI: 10.1038/ncomms11065.

26. a) Balasubramaniyan, V. *Chem. Rev.* **1966**, *66*, 567. b) Chu, J.-H.; Tsai, S.-L.; Wu, M.-J. *Synthesis* **2009**, *22*, 3757.

This chapter contains adaptations with permission from the following publications:

1) Jouffroy, M.; Davies, G. H. M.; Molander, G. A. *Org. Lett.* **2016**, *18*, 1606.

APPENDIX A1 –SUPPORTING DATA FOR CHAPTER 2

A1.1 – Computational data relevant for Chapter 2.2

Figure A1.1: Bond lengths of 1,3,2-benzodiazaboroles and isosteres

		Bond Lenghts (Angstroms)												
Name	Structure	1-2	2-3	3-4	4-5	5-6	6-7	7-8	8-9	4-9	9-1	1-10	2-11	3-12
2.49	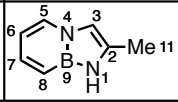	1.391	1.358	1.398	1.361	1.367	1.425	1.374	1.502	1.460	1.441	-	1.490	-
2.53	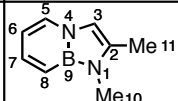	1.395	1.360	1.395	1.360	1.367	1.425	1.375	1.503	1.459	1.441	1.449	1.491	-
2.3	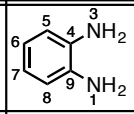	-	-	1.390	1.396	1.389	1.389	1.389	1.396	1.412	1.390	-	-	-
2.5	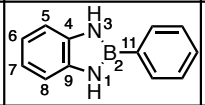	1.437	1.437	1.393	1.388	1.395	1.395	1.395	1.388	1.410	1.393	-	1.555	-
2.31	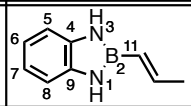	1.439	1.438	1.392	1.387	1.395	1.395	1.395	1.388	1.411	1.392	-	1.545	-
2.34	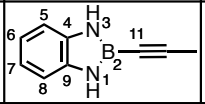	1.435	1.435	1.395	1.388	1.394	1.396	1.394	1.388	1.411	1.392	-	1.516	-
2.39	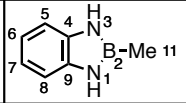	1.436	1.437	1.394	1.387	1.395	1.395	1.395	1.387	1.410	1.395	-	1.570	-
2.52	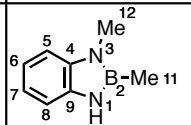	1.435	1.439	1.395	1.388	1.397	1.394	1.396	1.386	1.411	1.393	-	1.571	1.447
2.47	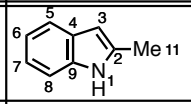	1.385	1.368	1.435	1.401	1.385	1.405	1.387	1.393	1.418	1.380	-	1.491	-
2.50	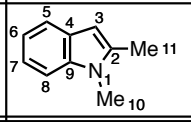	1.391	1.370	1.432	1.400	1.386	1.404	1.388	1.394	1.418	1.381	1.447	1.492	-
2.51	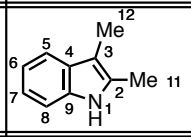	1.389	1.372	1.441	1.401	1.386	1.404	1.387	1.393	1.416	1.377	-	1.492	1.497
2.48	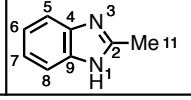	1.380	1.307	1.389	1.395	1.388	1.404	1.389	1.391	1.410	1.384	-	1.490	-

Figure A1.2: Atomic Coordinates for [B3LYP/6-311+G(2d,p)] optimized geometry value of total energy of 2-methyl "fused" BN-indole (**2.49**)

Center Number	Atomic Number	Atomic Type	Coordinates (Angstroms) X	Y	Z
1	6	0	0.061521	-0.006736	-0.293402
2	6	0	0.026108	-0.005984	1.196650
3	7	0	1.184309	0.070195	1.964019
4	5	0	0.833886	0.050056	3.361158
5	6	0	1.507411	0.095995	4.703417
6	6	0	0.683631	0.044685	5.802465
7	6	0	-0.734874	-0.047212	5.699994
8	6	0	-1.361471	-0.089888	4.486349
9	7	0	-0.623315	-0.044193	3.344410
10	6	0	-1.055517	-0.074521	2.015347
11	1	0	-2.097266	-0.142358	1.746517
12	1	0	-2.438253	-0.159685	4.386583
13	1	0	-1.338515	-0.084642	6.597101
14	1	0	1.106559	0.073806	6.802844
15	1	0	2.578183	0.165513	4.863009
16	1	0	2.088680	0.128069	1.528711
17	1	0	-0.947445	-0.072416	-0.700708
18	1	0	0.636327	-0.855134	-0.678396
19	1	0	0.523123	0.906663	-0.682067

E_{Tot}: -406.713074625 Hartree

Figure A1.3: Atomic Coordinates for [B3LYP/6-311+G(2d,p)] optimized geometry value of total energy of 1,2-dimethyl "fused" BN-indole (**2.53**)

Center Number	Atomic Number	Atomic Type	Coordinates (Angstroms) X	Y	Z
1	6	0	-0.136410	0.058875	0.068043
2	6	0	-0.003242	0.035924	1.553349
3	7	0	1.232605	-0.004042	2.199654
4	5	0	1.001376	-0.016612	3.621816
5	6	0	1.807011	-0.053776	4.890304
6	6	0	1.095399	-0.050830	6.066660
7	6	0	-0.328743	-0.014845	6.105920
8	6	0	-1.073973	0.019223	4.960844
9	7	0	-0.451432	0.018981	3.751251
10	6	0	-1.006383	0.049807	2.472056
11	1	0	-2.070398	0.079358	2.300793
12	1	0	-2.157287	0.046891	4.968923
13	1	0	-0.841380	-0.014131	7.058718
14	1	0	1.616558	-0.076616	7.019669
15	1	0	2.890295	-0.082277	4.945317
16	6	0	2.497298	-0.027895	1.492329
17	1	0	3.306378	-0.058325	2.220248
18	1	0	2.634299	0.863513	0.872941
19	1	0	2.588011	-0.908824	0.850038
20	1	0	-1.189178	0.088528	-0.212803
21	1	0	0.352893	0.934028	-0.370533
22	1	0	0.309492	-0.827334	-0.393944

E_{Tot}: -446.028825381 Hartree

Figure A1.4: Atomic Coordinates for [B3LYP/6-311+G(2d,p)] optimized geometry value of total energy of *o*-phenylenediamine (**2.3**)

Center Number	Atomic Number	Atomic Type	Coordinates (Angstroms) X	Y	Z
1	6	0	0.074437	0.000000	0.017709
2	6	0	0.074437	0.000000	1.406791
3	6	0	1.284070	0.000000	2.090296
4	6	0	2.507404	0.000000	1.418094
5	6	0	2.507404	0.000000	0.006406
6	6	0	1.284070	0.000000	-0.665796
7	1	0	1.290506	0.000000	-1.751241
8	7	0	3.696462	0.000000	-0.713252
9	1	0	3.672354	0.000000	-1.716100
10	1	0	4.599595	0.000000	-0.282739
11	7	0	3.696462	0.000000	2.137752
12	1	0	4.599595	0.000000	1.707239
13	1	0	3.672354	0.000000	3.140600
14	1	0	1.290506	0.000000	3.175741
15	1	0	-0.856541	0.000000	1.959820
16	1	0	-0.856541	0.000000	-0.535320

E_{Tot}: -343.061786471 Hartree

Figure A1.5: Atomic Coordinates for [B3LYP/6-311+G(2d,p)] optimized geometry value of total energy of 2-phenyl-2,3-dihydro-1*H*-1,3,2-benzodiazaborole (**2.5**)

Center Number	Atomic Number	Atomic Type	Coordinates (Angstroms) X	Y	Z
1	6	0	-0.135947	-0.131735	-0.230355
2	6	0	-0.128905	-0.210850	1.162039
3	6	0	1.090689	-0.128176	1.818503
4	6	0	2.291079	0.026479	1.094404
5	6	0	2.279343	0.107514	-0.290691
6	6	0	1.051122	0.026612	-0.946425
7	1	0	1.020267	0.086913	-2.027418
8	1	0	3.200129	0.228145	-0.849994
9	7	0	3.342735	0.069288	2.007386
10	5	0	2.829171	-0.049469	3.343764
11	7	0	1.407625	-0.169253	3.174660
12	1	0	0.696194	-0.320088	3.869360
13	6	0	3.632469	-0.048637	4.675675
14	6	0	5.004421	-0.342573	4.701525
15	6	0	5.725686	-0.344259	5.889682
16	6	0	5.088944	-0.047985	7.090838
17	6	0	3.729241	0.248162	7.093369
18	6	0	3.015067	0.245862	5.901048
19	1	0	1.958546	0.492166	5.924897
20	1	0	3.227140	0.483727	8.024652
21	1	0	5.648490	-0.048252	8.018926
22	1	0	6.783827	-0.579061	5.880263
23	1	0	5.518592	-0.589155	3.778313
24	1	0	4.288929	0.220621	1.701915
25	1	0	-1.053051	-0.331744	1.715718
26	1	0	-1.077654	-0.193343	-0.761889

E_{Tot}: -598.536528558 Hartree

Figure A1.6: Atomic Coordinates for [B3LYP/6-311+G(2d,p)] optimized geometry value of total energy of (*E*)-2-(prop-1-en-1-yl)-1*H*-1,3,2-benzodiazaborole (**2.31**)

Center Number	Atomic Number	Atomic Type	Coordinates (Angstroms) X	Y	Z
1	6	0	0.056090	0.109224	-0.139391
2	6	0	0.062896	0.162354	1.356725
3	6	0	1.096250	-0.142763	2.149448
4	5	0	1.094875	-0.085210	3.693221
5	7	0	0.034159	0.291170	4.589924
6	6	0	0.475955	0.196822	5.906742
7	6	0	-0.170629	0.450385	7.108062
8	6	0	0.540040	0.264363	8.293977
9	6	0	1.867068	-0.165527	8.276090
10	6	0	2.521236	-0.421680	7.070965
11	6	0	1.818347	-0.238041	5.888956
12	7	0	2.195885	-0.409384	4.559682
13	1	0	3.121864	-0.717688	4.315890
14	1	0	3.552574	-0.755702	7.059620
15	1	0	2.398338	-0.302838	9.209926
16	1	0	0.052371	0.457150	9.241775
17	1	0	-1.201798	0.784622	7.126303
18	1	0	-0.903638	0.586168	4.378974
19	1	0	2.015214	-0.458490	1.652977
20	1	0	-0.875568	0.482833	1.809382
21	1	0	-0.715416	-0.577197	-0.504455
22	1	0	1.020098	-0.217350	-0.533895
23	1	0	-0.175444	1.090989	-0.566203

E_{Tot}: -484.170539338 Hartree

Figure A1.7: Atomic Coordinates for [B3LYP/6-311+G(2d,p)] optimized geometry value of total energy of 2-(1-propynyl)-2,3-dihydro-1*H*-1,3,2-benzodiazaborole (**2.34**)

Center Number	Atomic Number	Atomic Type	Coordinates (Angstroms) X	Y	Z
1	6	0	0.080755	-0.117035	0.000000
2	6	0	1.531567	-0.241677	0.000000
3	6	0	2.734870	-0.345928	0.000000
4	5	0	4.245261	-0.476700	0.000000
5	7	0	5.214653	0.580808	0.000000
6	6	0	6.496087	0.036646	0.000000
7	6	0	7.745552	0.640846	0.000000
8	6	0	8.874480	-0.177293	0.000000
9	6	0	8.754035	-1.567743	0.000000
10	6	0	7.501214	-2.179533	0.000000
11	6	0	6.374295	-1.369443	0.000000
12	7	0	5.018327	-1.685148	0.000000
13	1	0	4.695020	-2.637503	0.000000
14	1	0	7.410710	-3.259749	0.000000
15	1	0	9.645963	-2.182244	0.000000
16	1	0	9.858788	0.274695	0.000000
17	1	0	7.842216	1.720529	0.000000
18	1	0	5.059899	1.574550	0.000000
19	1	0	-0.223795	0.932468	0.000000
20	1	0	-0.352477	-0.593419	-0.883379
21	1	0	-0.352477	-0.593419	0.883379

E_{Tot}: -482.932836614 Hartree

Figure A1.8: Atomic Coordinates for [B3LYP/6-311+G(2d,p)] optimized geometry value of total energy of 2-methyl-2,3-dihydro-1*H*-1,3,2-benzodiazaborole (**2.39**)

Center Number	Atomic Number	Atomic Type	Coordinates (Angstroms) X	Y	Z
1	6	0	-0.052185	0.000429	0.015223
2	5	0	0.080676	-0.003933	1.579635
3	7	0	1.284111	-0.003486	2.362414
4	6	0	0.968013	-0.000579	3.720857
5	6	0	1.775220	0.001192	4.848588
6	6	0	1.161178	0.003532	6.101572
7	6	0	-0.228571	0.003774	6.218510
8	6	0	-1.043959	0.001620	5.086198
9	6	0	-0.437259	-0.000435	3.838895
10	7	0	-0.976905	-0.003292	2.553156
11	1	0	-1.972066	-0.004175	2.406513
12	1	0	-2.123997	0.001728	5.180791
13	1	0	-0.683572	0.005619	7.201479
14	1	0	1.774251	0.005137	6.994518
15	1	0	2.855828	0.000895	4.760748
16	1	0	2.239841	-0.004660	2.048738
17	1	0	0.916249	-0.078744	-0.484492
18	1	0	-0.670641	-0.829370	-0.340635
19	1	0	-0.526523	0.919751	-0.343304

E_{Tot}: -406.749628439 Hartree

Figure A1.9: Atomic Coordinates for [B3LYP/6-311+G(2d,p)] optimized geometry value of total energy of 1,2-dimethyl-2,3-dihydro-1*H*-1,3,2-benzodiazaborole (**2.52**)

Center Number	Atomic Number	Atomic Type	Coordinates (Angstroms) X	Y	Z
1	6	0	0.052092	0.009832	-0.334484
2	7	0	0.059788	0.012954	1.112687
3	6	0	1.249831	-0.008073	1.840342
4	6	0	2.571506	-0.034061	1.416150
5	6	0	3.577148	-0.051084	2.385056
6	6	0	3.265606	-0.042245	3.743384
7	6	0	1.937649	-0.016081	4.174188
8	6	0	0.936352	0.000852	3.216335
9	7	0	-0.450907	0.027555	3.336147
10	5	0	-1.048156	0.035941	2.030852
11	6	0	-2.579714	0.064162	1.681545
12	1	0	-3.205254	0.078692	2.577361
13	1	0	-2.879032	-0.809522	1.093616
14	1	0	-2.845581	0.945185	1.088534
15	1	0	-0.898593	0.037394	4.236713
16	1	0	1.697607	-0.009223	5.231471
17	1	0	4.062754	-0.055810	4.476628
18	1	0	4.614423	-0.071451	2.073499
19	1	0	2.822610	-0.041080	0.362567
20	1	0	-0.976590	0.028521	-0.691261
21	1	0	0.537297	-0.886583	-0.733797
22	1	0	0.570938	0.885247	-0.737813

E_{Tot}: -446.067218958 Hartree

Figure A1.10: Atomic Coordinates for [B3LYP/6-311+G(2d,p)] optimized geometry value of total energy of 2-methylindole (**2.47**)

Center Number	Atomic Number	Atomic Type	Coordinates (Angstroms) X	Y	Z
1	6	0	0.018083	0.000000	0.106874
2	6	0	0.009337	0.000000	1.597791
3	7	0	1.192623	0.000000	2.318229
4	6	0	0.916256	0.000000	3.670603
5	6	0	1.770261	0.000000	4.770884
6	6	0	1.192048	0.000000	6.031720
7	6	0	-0.203878	0.000000	6.190868
8	6	0	-1.049185	0.000000	5.093262
9	6	0	-0.495117	0.000000	3.806684
10	6	0	-1.038265	0.000000	2.478036
11	1	0	-2.081806	0.000000	2.204429
12	1	0	-2.124854	0.000000	5.227958
13	1	0	-0.621895	0.000000	7.190465
14	1	0	1.828051	0.000000	6.908782
15	1	0	2.847820	0.000000	4.651303
16	1	0	2.112741	0.000000	1.912066
17	1	0	-1.003051	0.000000	-0.273100
18	1	0	0.525317	0.883136	-0.294767
19	1	0	0.525317	-0.883136	-0.294767

E_{Tot}: -403.255153596 Hartree

Figure A1.11: Atomic Coordinates for [B3LYP/6-311+G(2d,p)] optimized geometry value of total energy of 1,2-dimethylindole (**2.50**)

Center Number	Atomic Number	Atomic Type	Coordinates (Angstroms) X	Y	Z
1	6	0	-0.012400	0.000000	0.094205
2	7	0	0.072907	0.000000	1.538574
3	6	0	1.260100	0.000000	2.244845
4	6	0	2.576280	0.000000	1.784613
5	6	0	3.589070	0.000000	2.733666
6	6	0	3.297818	0.000000	4.107451
7	6	0	1.988046	0.000000	4.560684
8	6	0	0.944637	0.000000	3.627419
9	6	0	-0.484154	0.000000	3.717731
10	6	0	-0.984097	0.000000	2.442717
11	6	0	-2.408725	0.000000	1.999327
12	1	0	-3.059131	0.000000	2.873487
13	1	0	-2.655884	0.882923	1.401464
14	1	0	-2.655884	-0.882923	1.401464
15	1	0	-1.078801	0.000000	4.617809
16	1	0	1.774303	0.000000	5.623543
17	1	0	4.113056	0.000000	4.821203
18	1	0	4.622537	0.000000	2.408354
19	1	0	2.809538	0.000000	0.726604
20	1	0	-1.055187	0.000000	-0.213701
21	1	0	0.469346	0.887466	-0.325686
22	1	0	0.469346	-0.887466	-0.325686

E_{Tot}: -442.573440367 Hartree

Figure A1.12: Atomic Coordinates for [B3LYP/6-311+G(2d,p)] optimized geometry value of total energy of 2,3-dimethylindole (**2.51**)

Center Number	Atomic Number	Atomic Type	Coordinates (Angstroms) X	Y	Z
1	6	0	0.000000	0.000000	0.000000
2	6	0	0.000000	0.000000	1.490943
3	7	0	1.187491	0.000000	2.204427
4	6	0	0.919061	0.000000	3.558399
5	6	0	1.779505	0.000000	4.653652
6	6	0	1.208698	0.000000	5.917858
7	6	0	-0.186271	0.000000	6.085192
8	6	0	-1.038001	0.000000	4.992563
9	6	0	-0.491489	0.000000	3.702756
10	6	0	-1.042421	0.000000	2.377318
11	6	0	-2.087549	0.000000	2.109836
12	1	0	-2.692627	0.010030	2.766283
13	1	0	-2.291019	0.010030	1.543530
14	1	0	-2.824344	0.010030	2.056761
15	1	0	-2.112862	0.000000	5.133566
16	1	0	-0.598417	0.000000	7.087223
17	1	0	1.849835	0.000000	6.791175
18	1	0	2.856344	0.000000	4.527753
19	1	0	2.105211	0.000000	1.792874
20	1	0	-1.023345	0.000000	-0.373978
21	1	0	0.504869	0.883136	-0.404610
22	1	0	0.504869	-0.883136	-0.404610

E_{Tot}: -442.583243305 Hartree

Figure A1.13: Atomic Coordinates for [B3LYP/6-311+G(2d,p)] optimized geometry value of total energy of 2-methylbenzimidazole (**2.48**)

Center Number	Atomic Number	Atomic Type	Coordinates (Angstroms) X	Y	Z
1	6	0	0.046943	0.177156	0.066225
2	6	0	0.018558	-0.283794	1.482826
3	7	0	1.134879	-0.234103	2.292376
4	6	0	0.769724	-0.731238	3.530990
5	6	0	1.464814	-0.919565	4.720682
6	6	0	0.750987	-1.457126	5.784240
7	6	0	-0.606873	-1.792828	5.659939
8	6	0	-1.292715	-1.601535	4.469003
9	6	0	-0.593572	-1.062772	3.388990
10	7	0	-1.024806	-0.770264	2.101795
11	1	0	-2.339818	-1.859186	4.369409
12	1	0	-1.126114	-2.209718	6.514445
13	1	0	1.253119	-1.620815	6.730077
14	1	0	2.512567	-0.662257	4.822030
15	1	0	2.044790	0.103102	2.025005
16	1	0	0.318574	1.234312	-0.004390
17	1	0	0.768502	-0.393811	-0.525128
18	1	0	-0.941927	0.042369	-0.366736

E_{Tot}: -419.31208368 Hartree

A1.2 – Spectral data relevant to Chapter 2.2

Figure A1.14: ^{1}H NMR ($CDCl_3$, 500.4 MHz) of 2-Phenyl-2,3-dihydro-1*H*-1,3,2-benzodiazaborole (**2.5**)

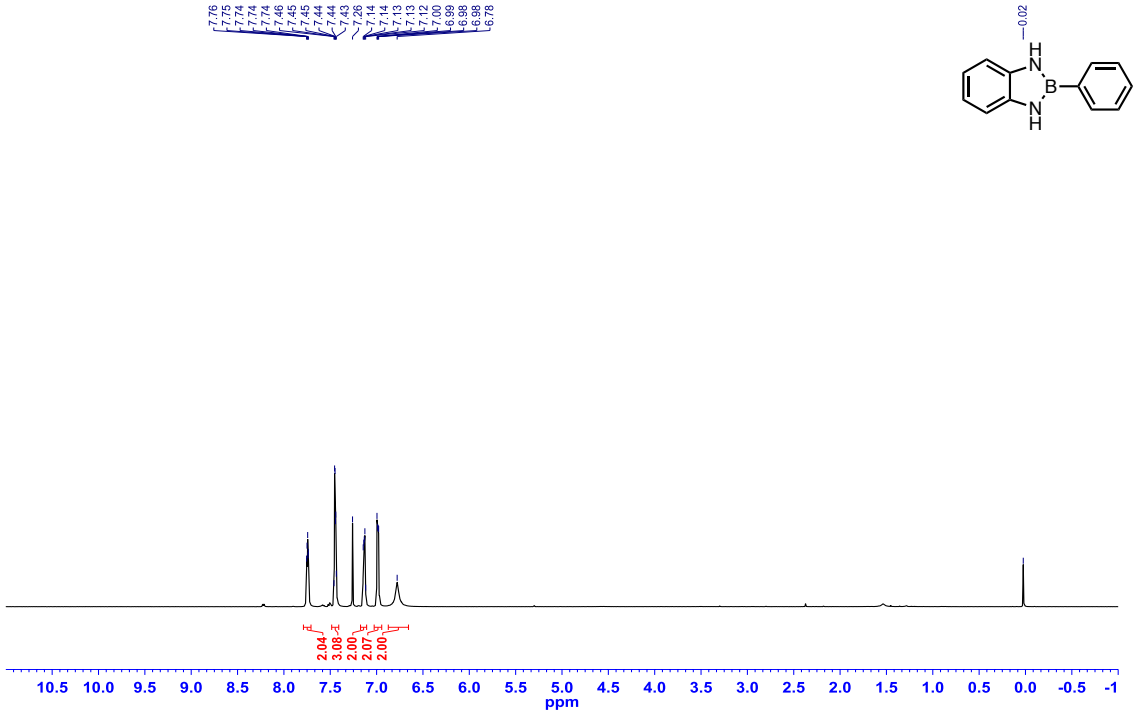

Figure A1.15: ^{13}C {^{1}H} NMR ($CDCl_3$, 125.8 MHz) of 2-Phenyl-2,3-dihydro-1*H*-1,3,2-benzodiazaborole (**2.5**)

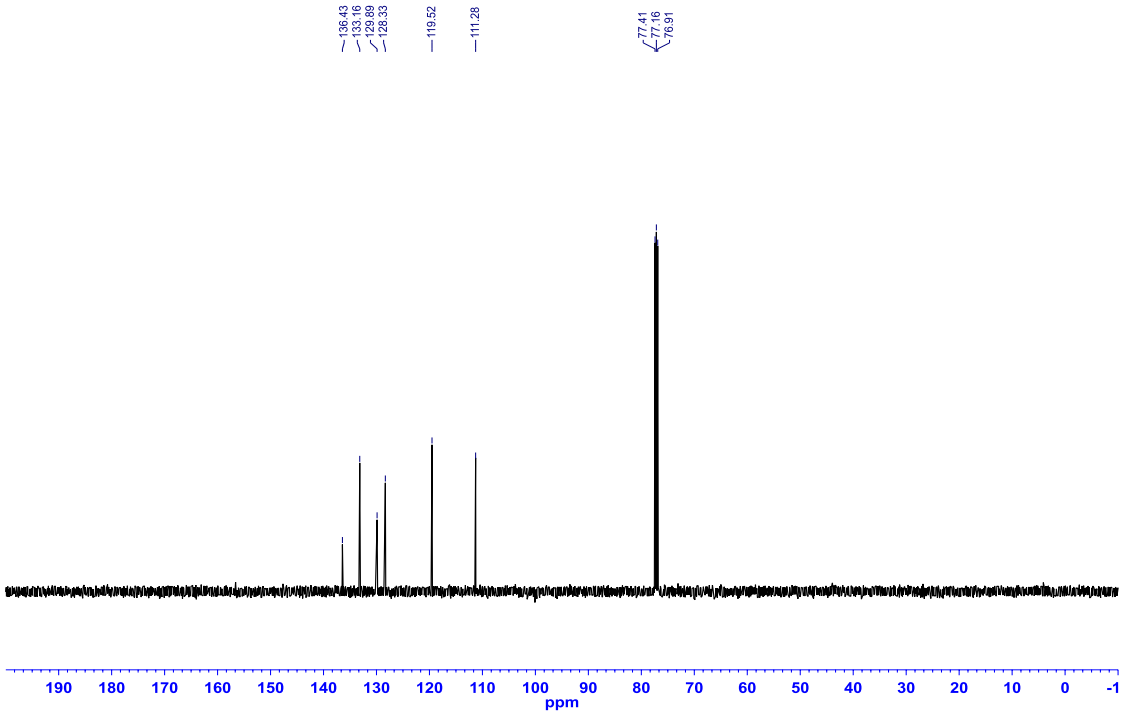

Figure A1.16: ^{11}B NMR (MeCN, 128.4 MHz) of 2-Phenyl-2,3-dihydro-1*H*-1,3,2-benzodiazaborole (**2.5**)

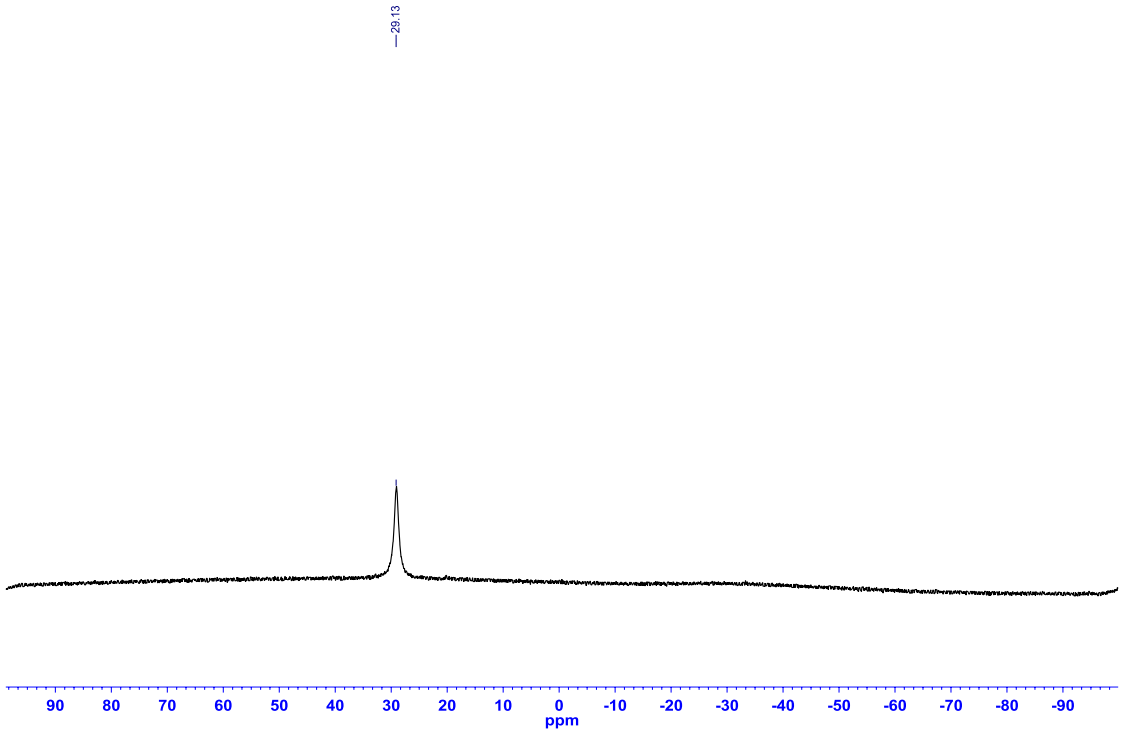

Figure A1.17: ^{1}H NMR ($CDCl_3$, 500.4 MHz) of 2-(*o*-tolyl)-2,3-dihydro-1*H*-1,3,2-benzodiazaborole (**2.6**)

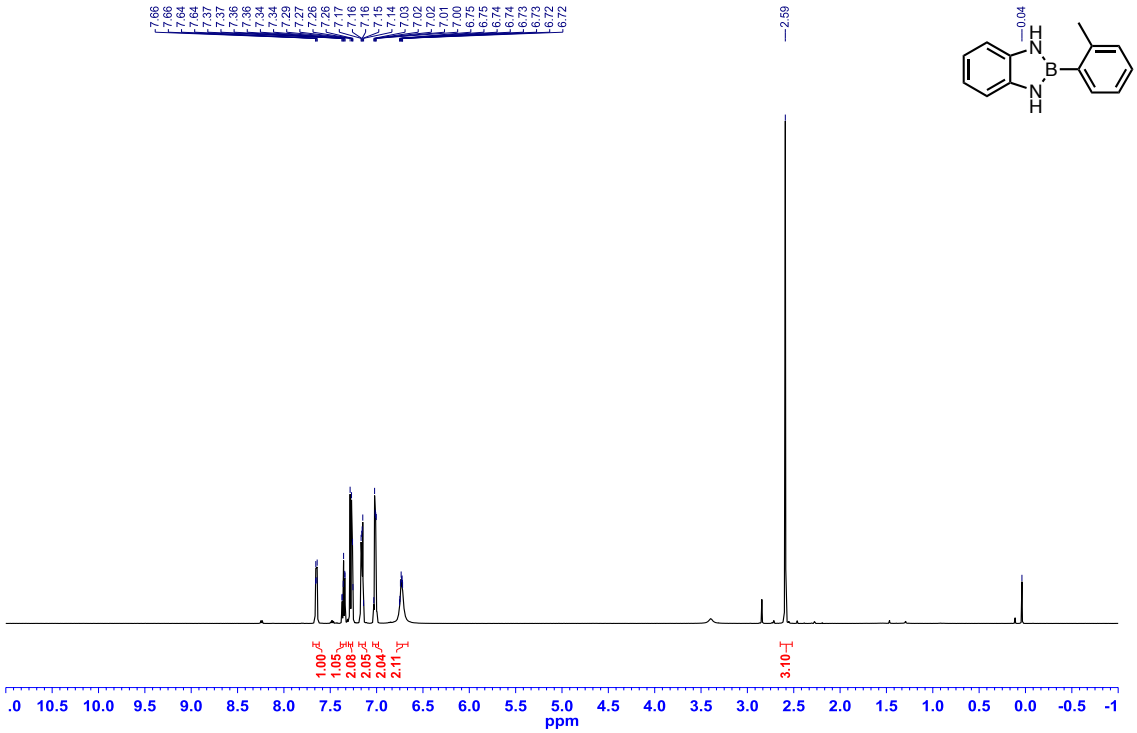

Figure A1.18: ^{13}C {^{1}H} NMR ($CDCl_3$, 125.8 MHz) of 2-(*o*-tolyl)-2,3-dihydro-1*H*-1,3,2-benzodiazaborole (**2.6**)

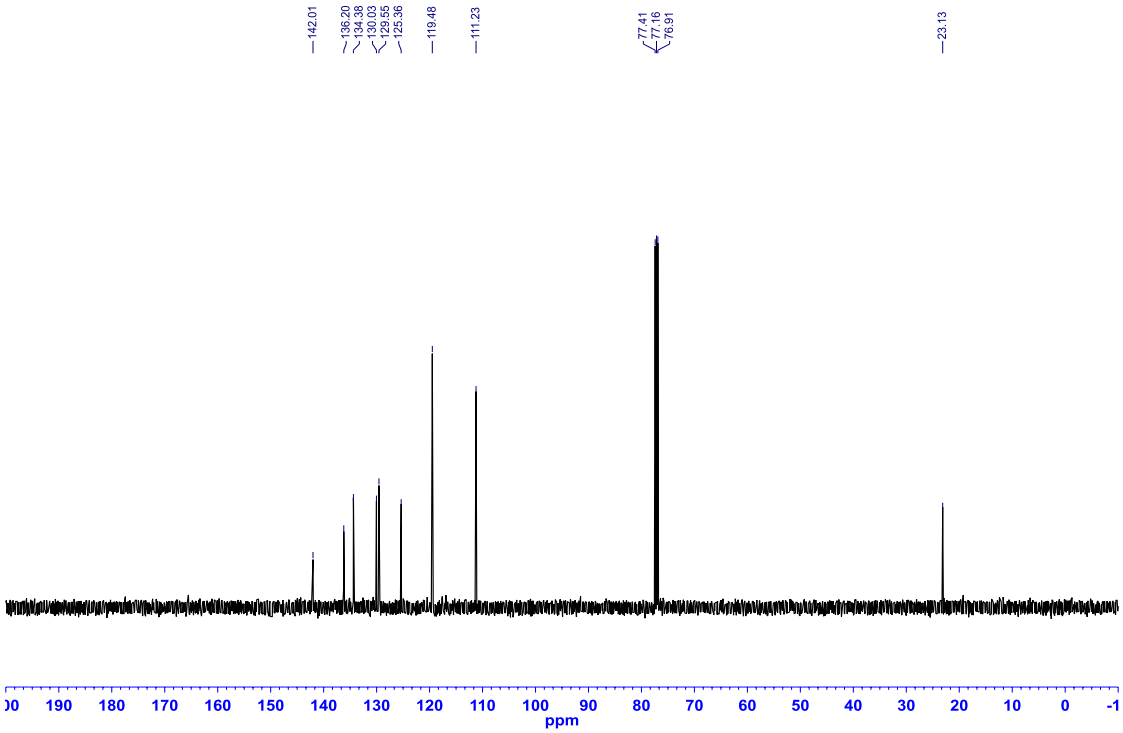

Figure A1.19: ^{11}B NMR (MeCN, 128.4) of 2-(*o*-tolyl)-2,3-dihydro-1*H*-1,3,2-benzodiazaborole (**2.6**)

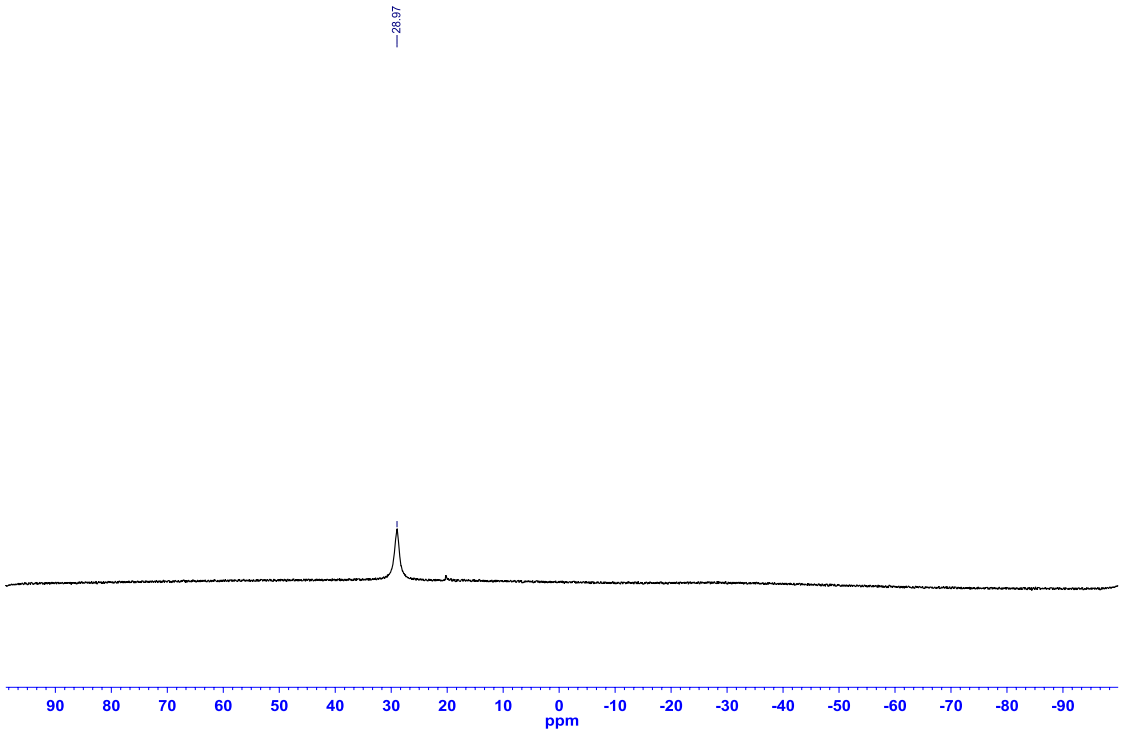

Figure A1.20: ^{1}H NMR ($CDCl_3$, 500.4 MHz) of 2-(2,6-dimethylphenyl)-2,3-dihydro-1*H*-1,3,2-benzodiazaborole (**2.7**)

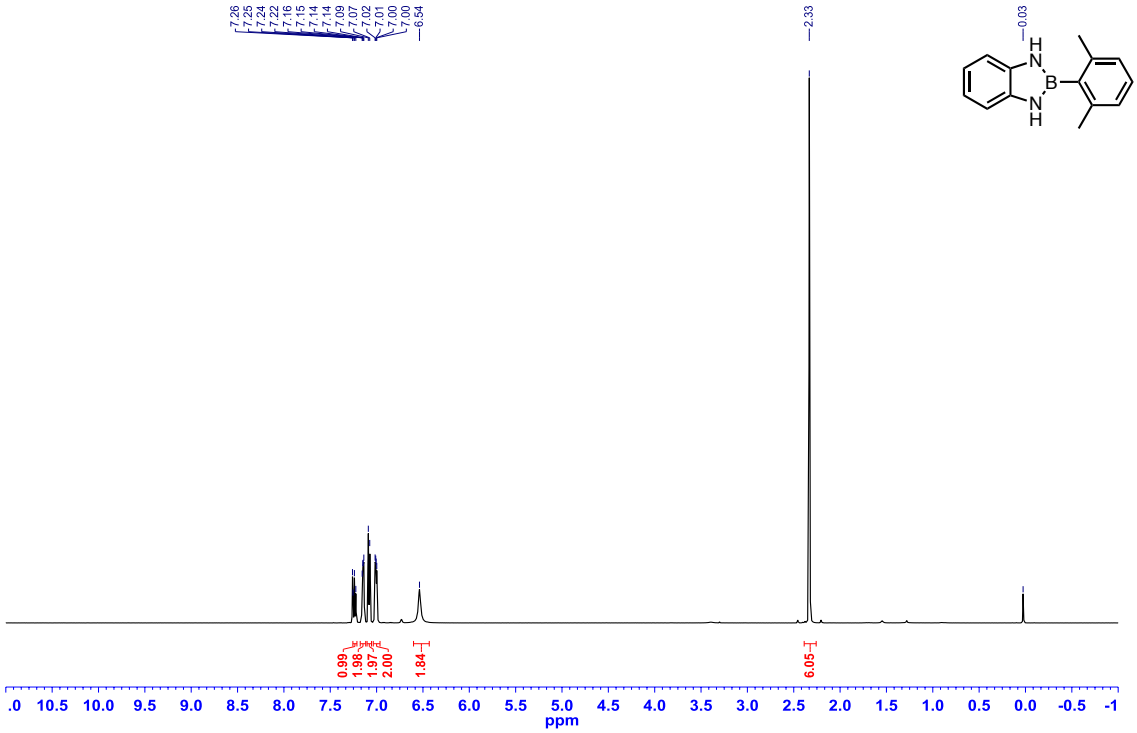

Figure A1.21: ^{13}C {^{1}H} NMR ($CDCl_3$, 125.8 MHz) of 2-(2,6-dimethylphenyl)-2,3-dihydro-1*H*-1,3,2-benzodiazaborole (**2.7**)

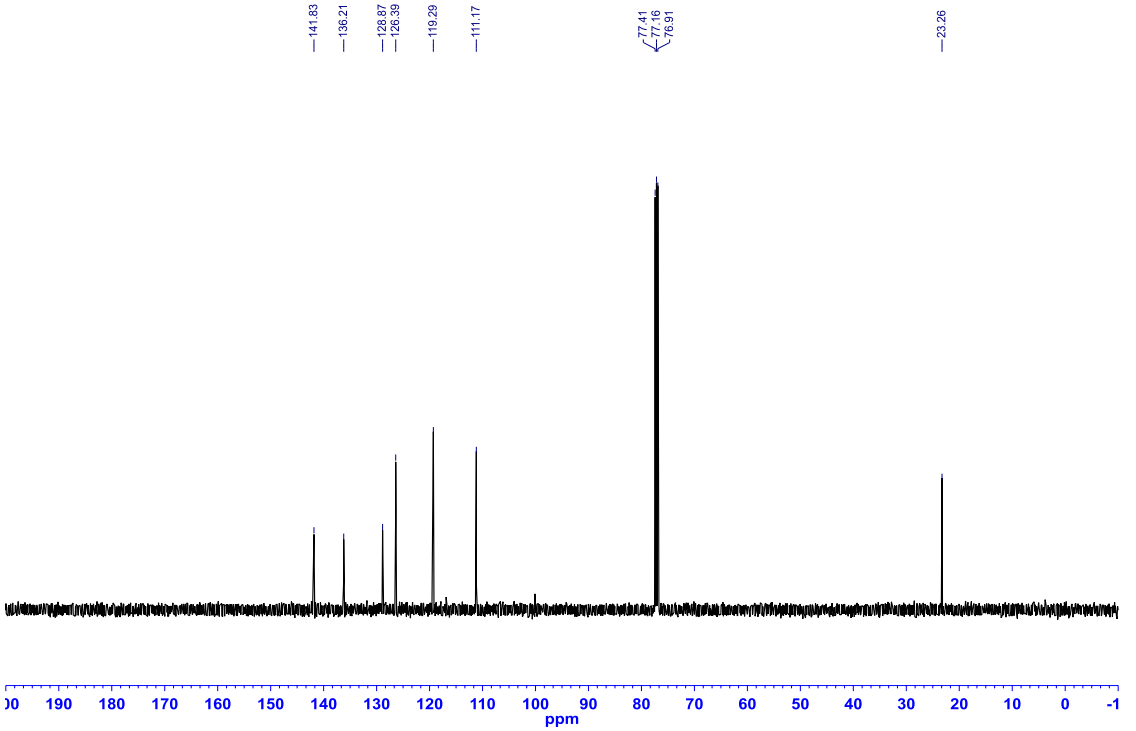

Figure A1.22: ^{11}B NMR (MeCN, 128.4 MHz) of 2-(2,6-dimethylphenyl)-2,3-dihydro-1*H*-1,3,2-benzodiazaborole (**2.7**)

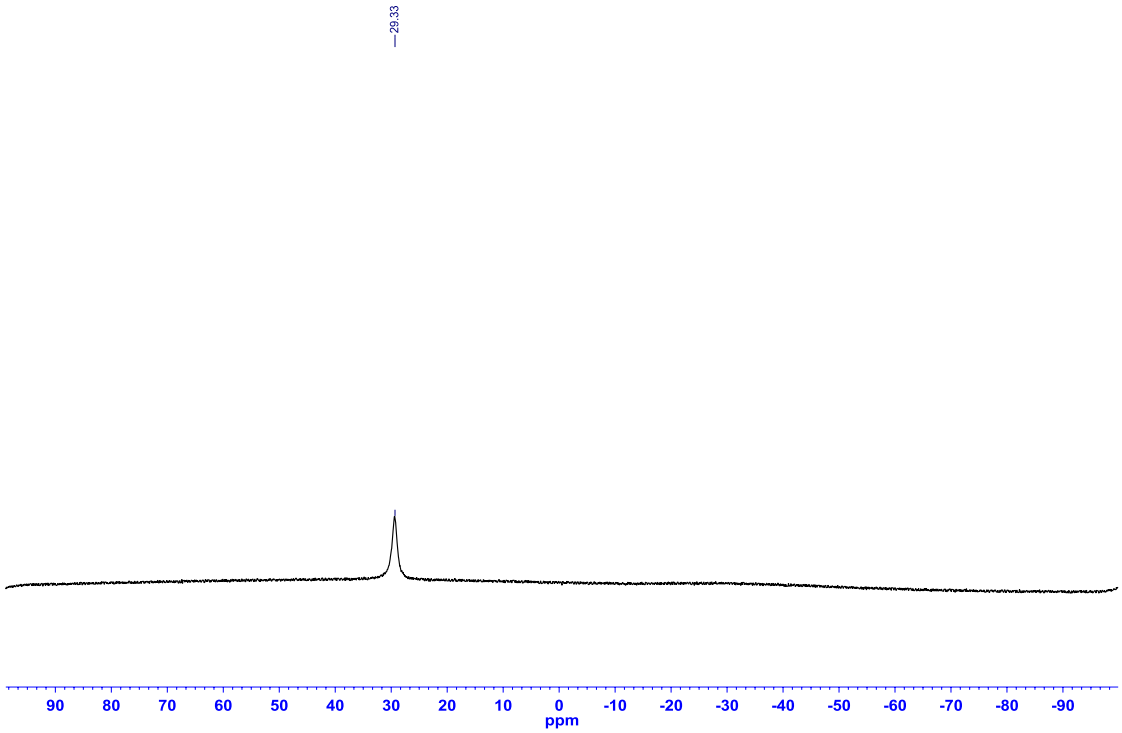

Figure A1.23: ^{1}H NMR ($CDCl_3$, 500.4 MHz) of 1-methyl-2-phenyl-2,3-dihydro-1*H*-1,3,2-benzodiazaborole (**2.8**)

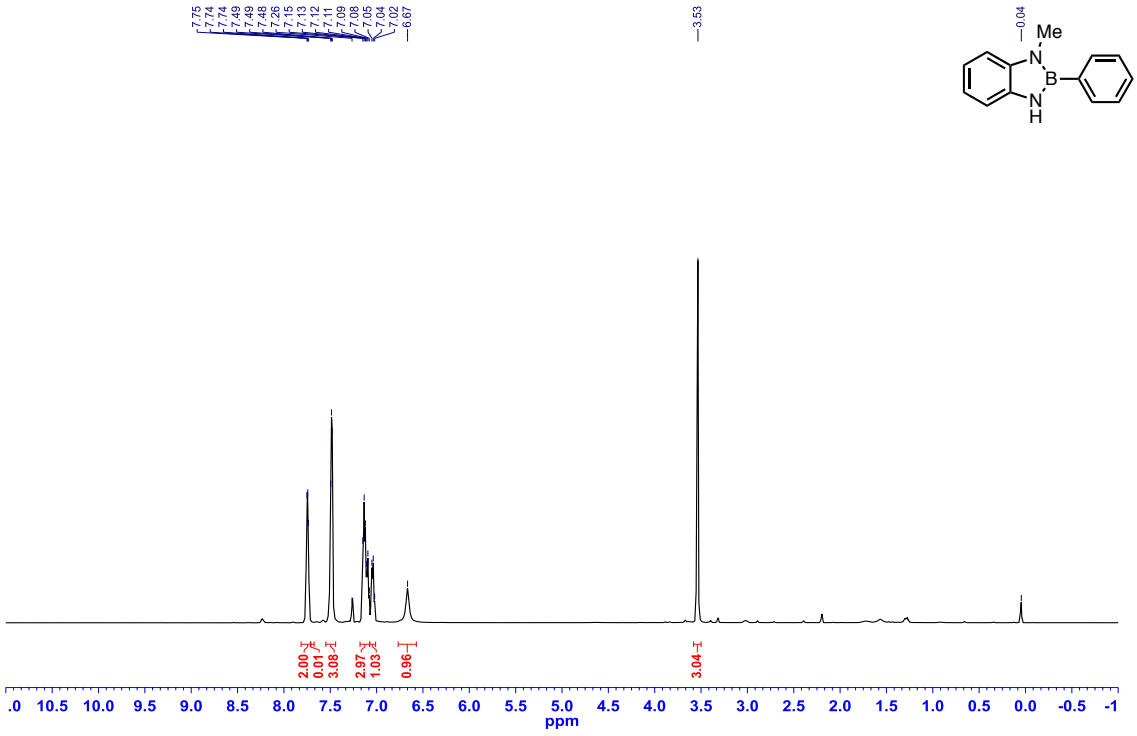

Figure A1.24: ^{13}C {^{1}H} NMR ($CDCl_3$, 125.8 MHz) of 1-methyl-2-phenyl-2,3-dihydro-1*H*-1,3,2-benzodiazaborole (**2.8**)

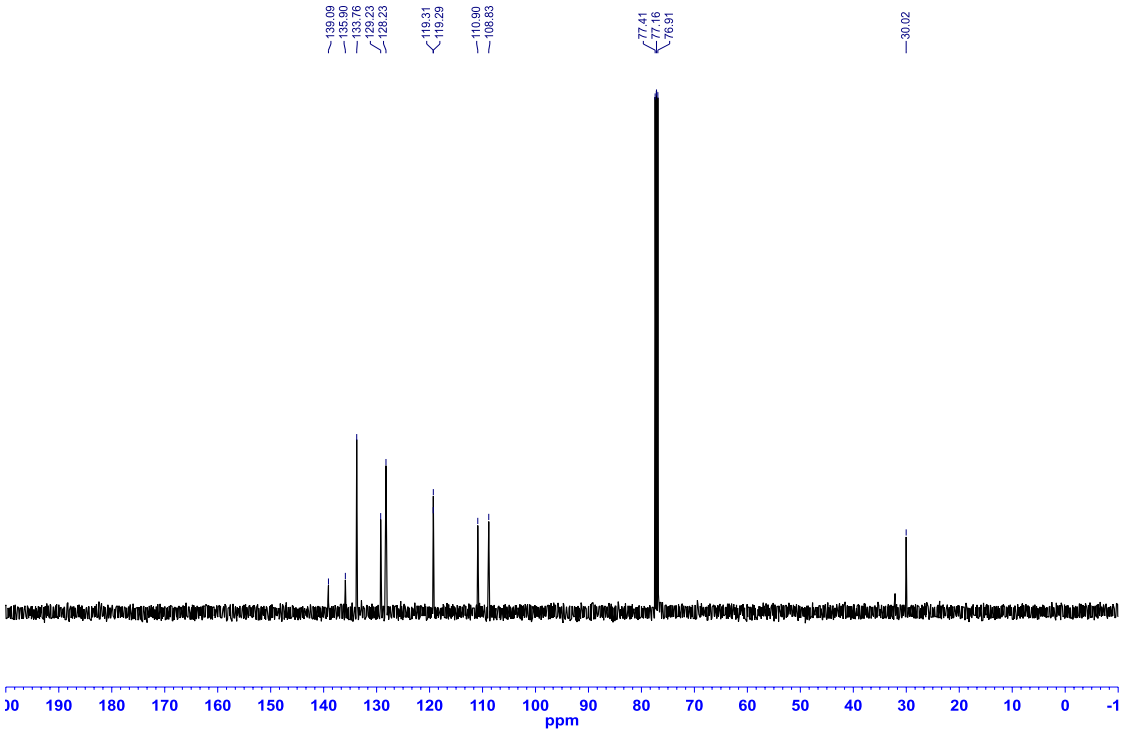

Figure A1.25: ^{11}B NMR (MeCN, 128.4) of 1-methyl-2-phenyl-2,3-dihydro-1*H*-1,3,2-benzodiazaborole (**2.8**)

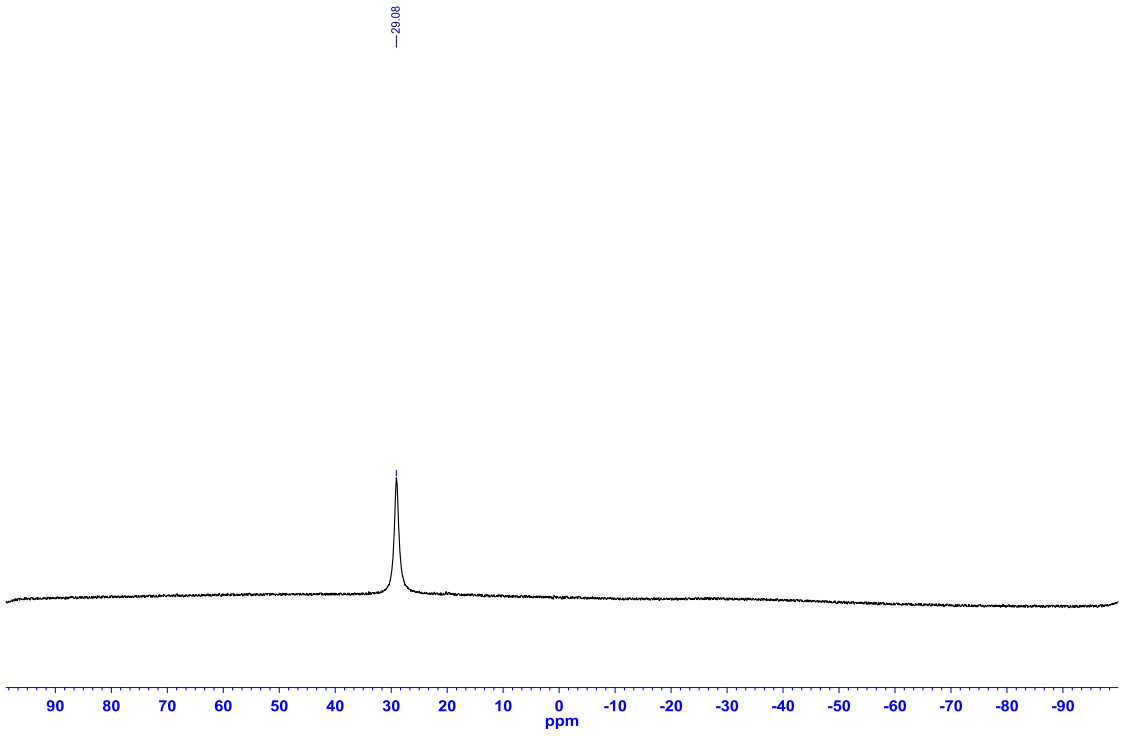

Figure A1.26: ^{1}H NMR (DMSO-d_6, 500.4 MHz) of 2-(2,6-difluorophenyl)-2,3-dihydro-1*H*-1,3,2-benzodiazaborole (**2.9**)

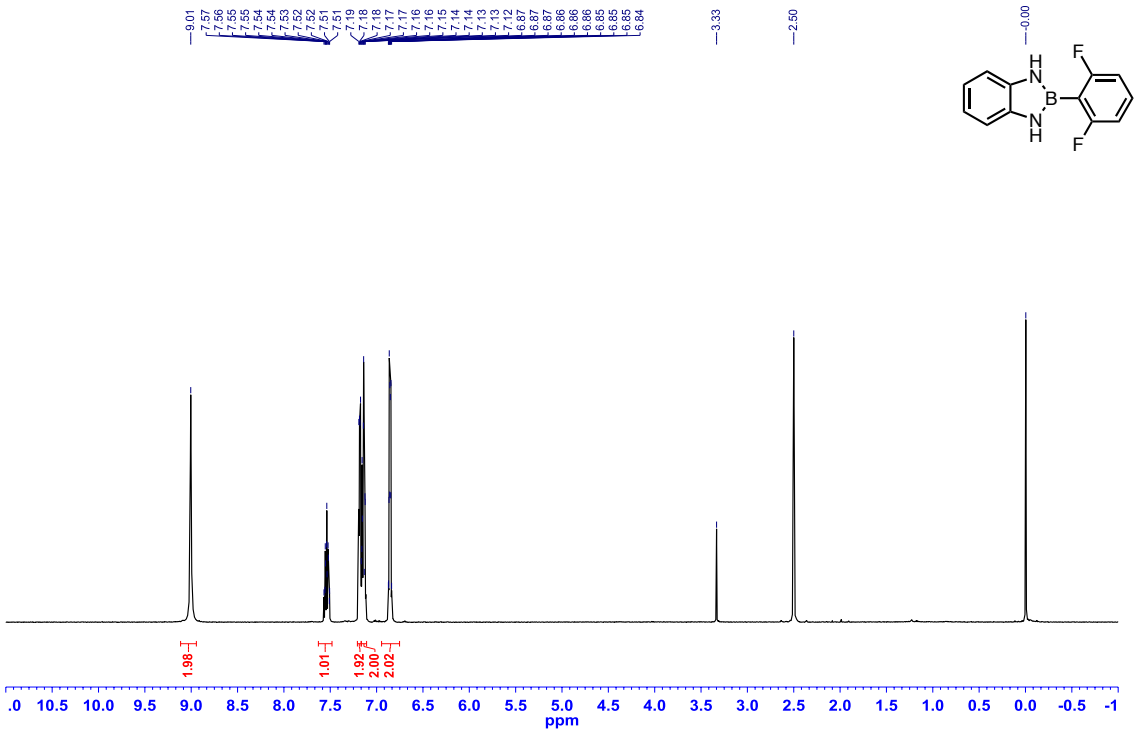

Figure A1.27: ^{13}C {^{1}H} NMR ($CDCl_3$, 125.8 MHz) of 2-(2,6-difluorophenyl)-2,3-dihydro-1*H*-1,3,2-benzodiazaborole (**2.9**)

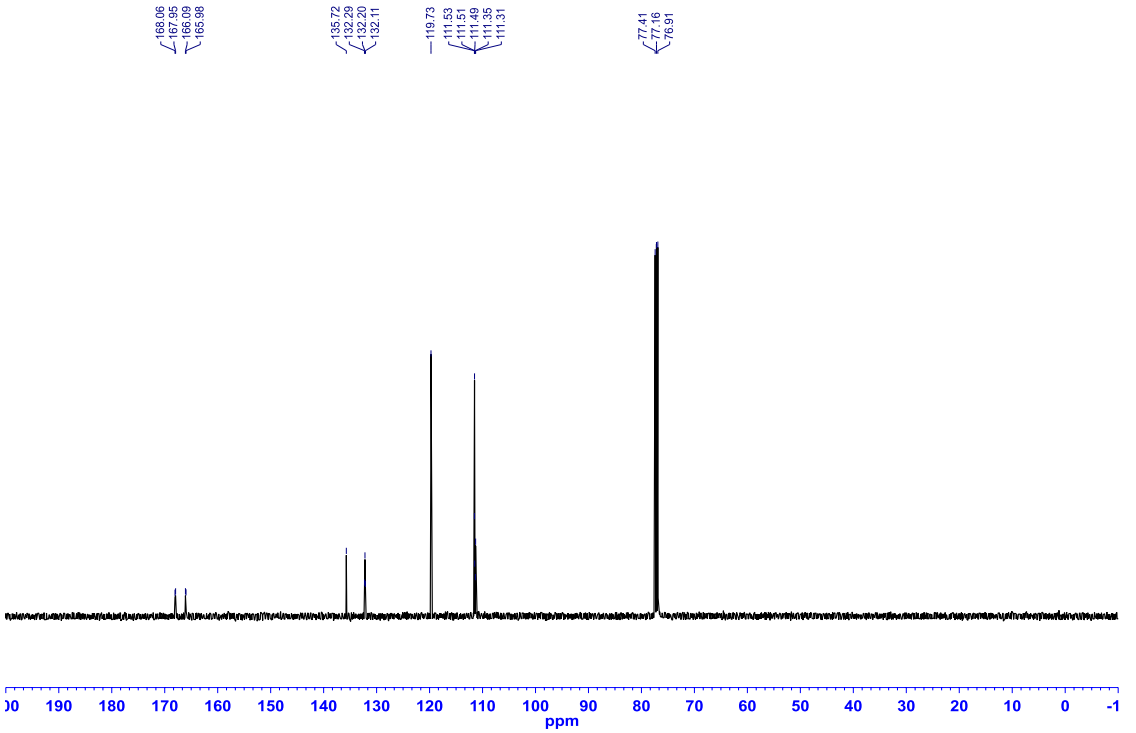

Figure A1.28: ^{19}F {^{1}H} NMR ($CDCl_3$, 282.4 MHz) of 2-(2,6-difluorophenyl)-2,3-dihydro-1*H*-1,3,2-benzodiazaborole (**2.9**)

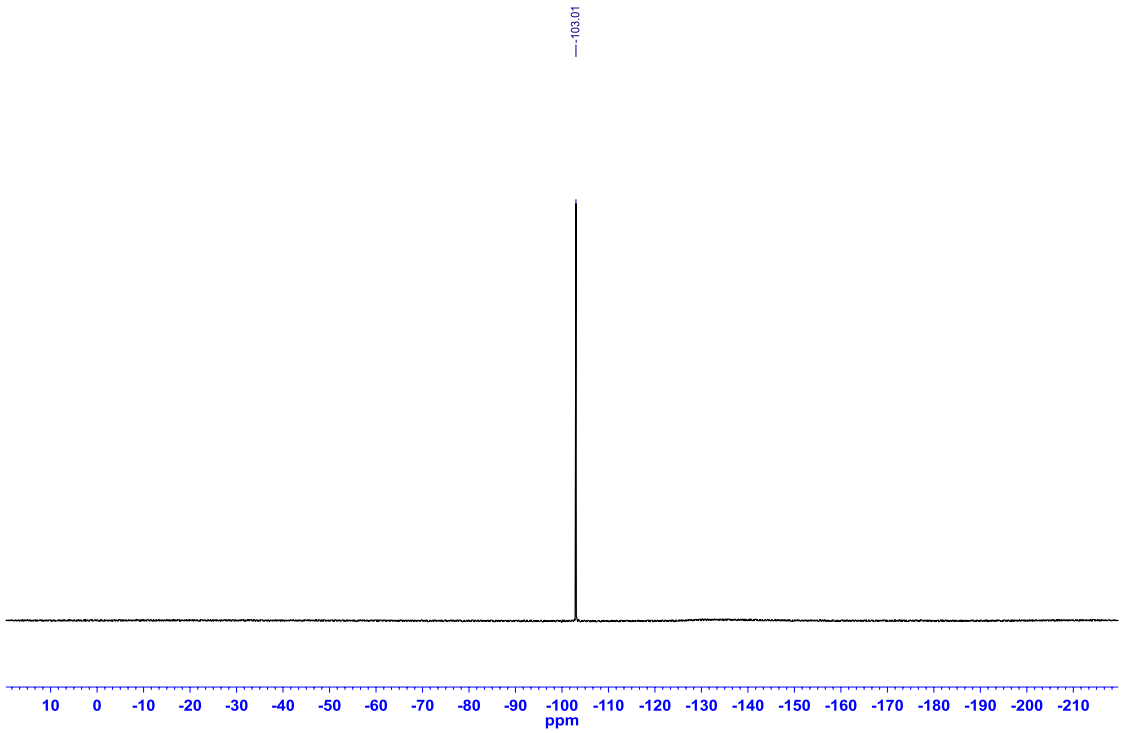

Figure A1.29: ^{11}B NMR (MeCN, 128.4 MHz) of 2-(2,6-difluorophenyl)-2,3-dihydro-1*H*-1,3,2-benzodiazaborole (**2.9**)

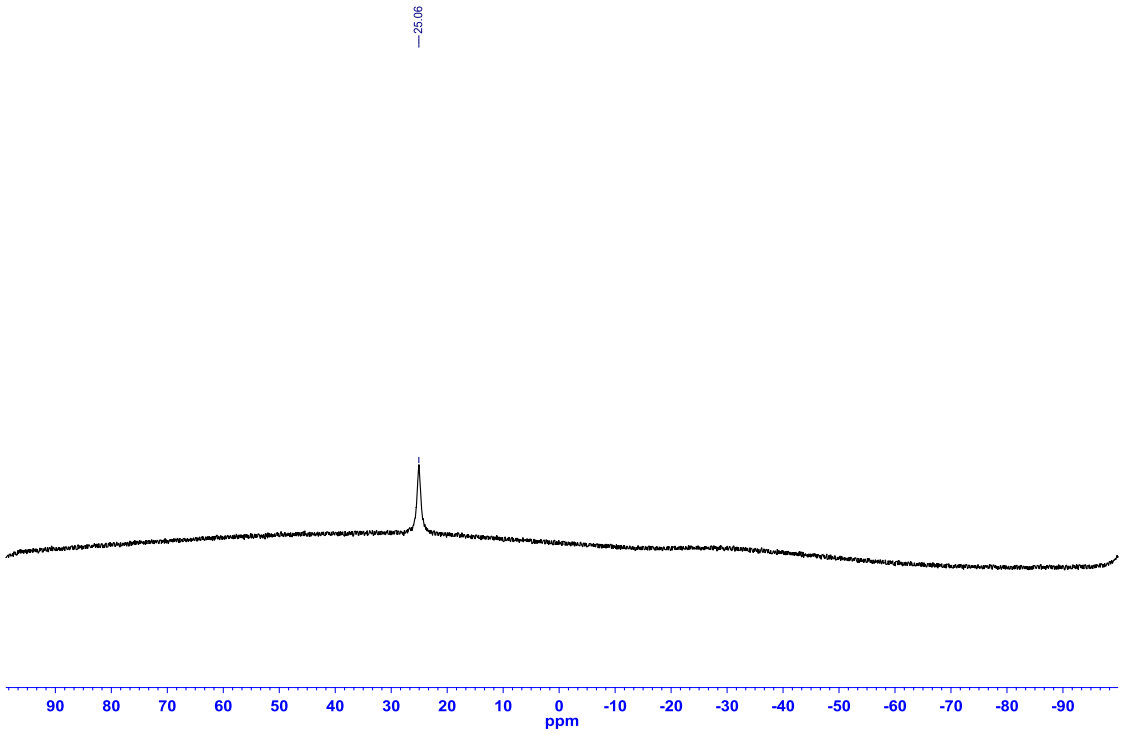

Figure A1.30: ^{1}H NMR ($CDCl_3$, 500.4 MHz) of 2-(4-bromophenyl)-2,3-dihydro-1*H*-1,3,2-benzodiazaborole (**2.10**)

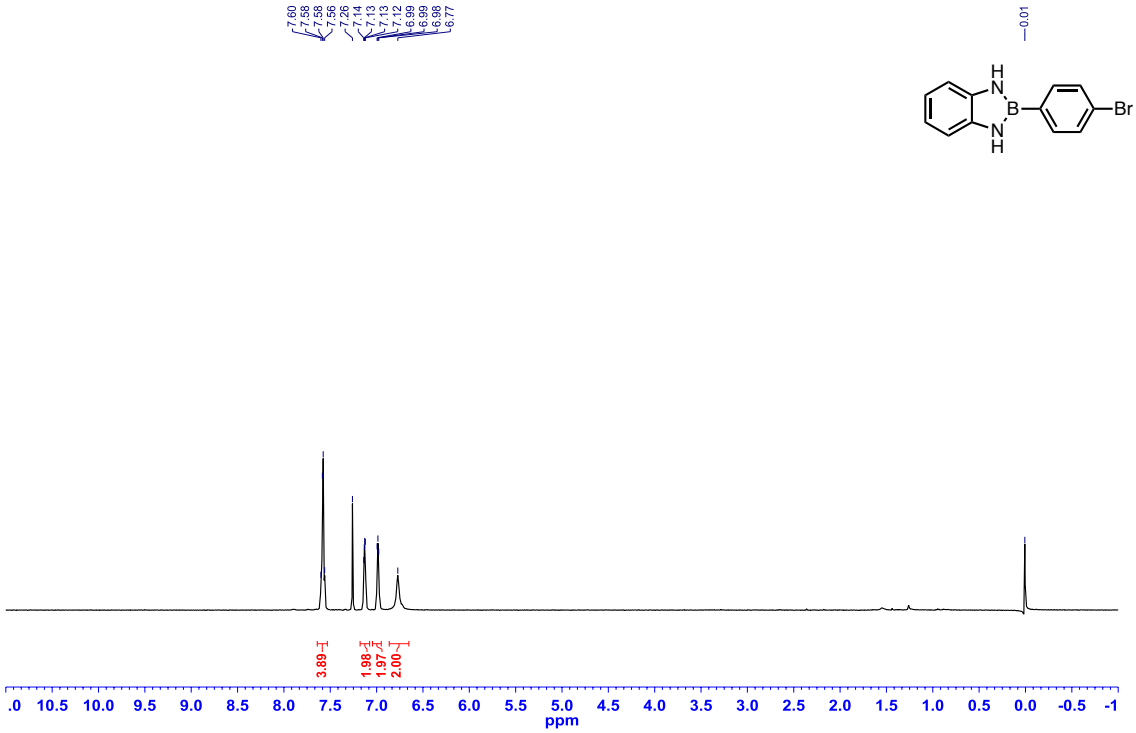

Figure A1.31: ^{13}C {^{1}H} NMR ($CDCl_3$, 125.8 MHz) of 2-(4-bromophenyl)-2,3-dihydro-1*H*-1,3,2-benzodiazaborole (**2.10**)

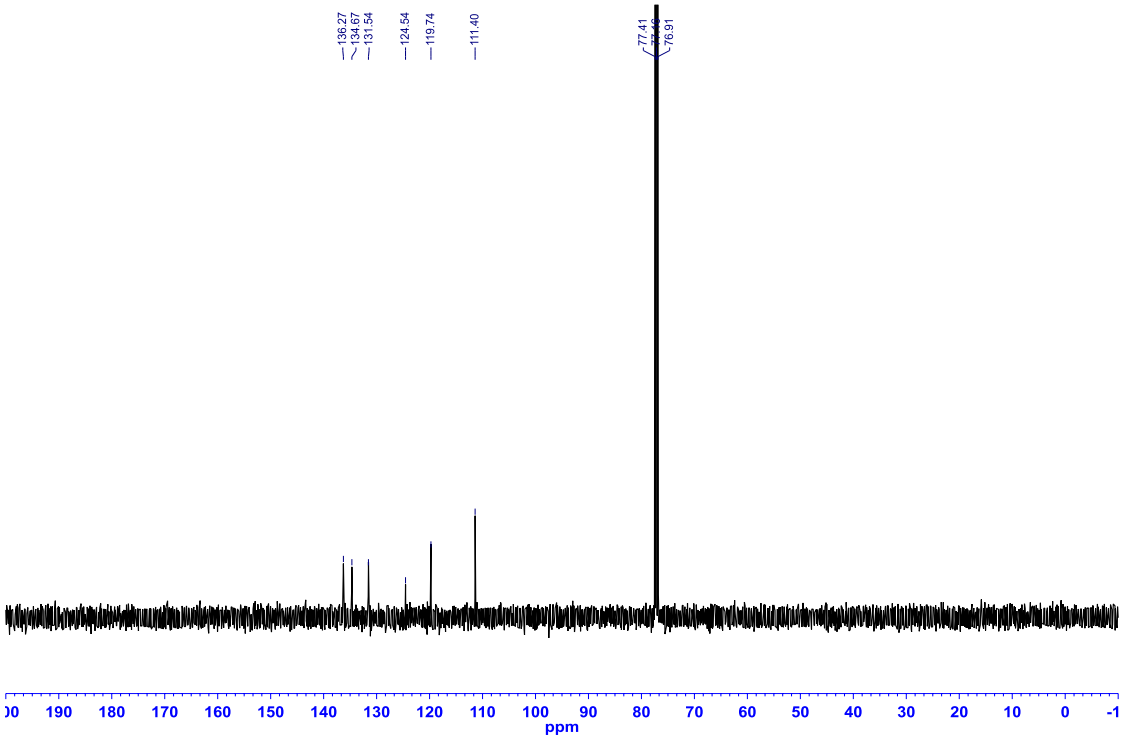

Figure A1.32: ^{11}B NMR (MeCN, 128.4 MHz) of 2-(4-bromophenyl)-2,3-dihydro-1*H*-1,3,2-benzodiazaborole (**2.10**)

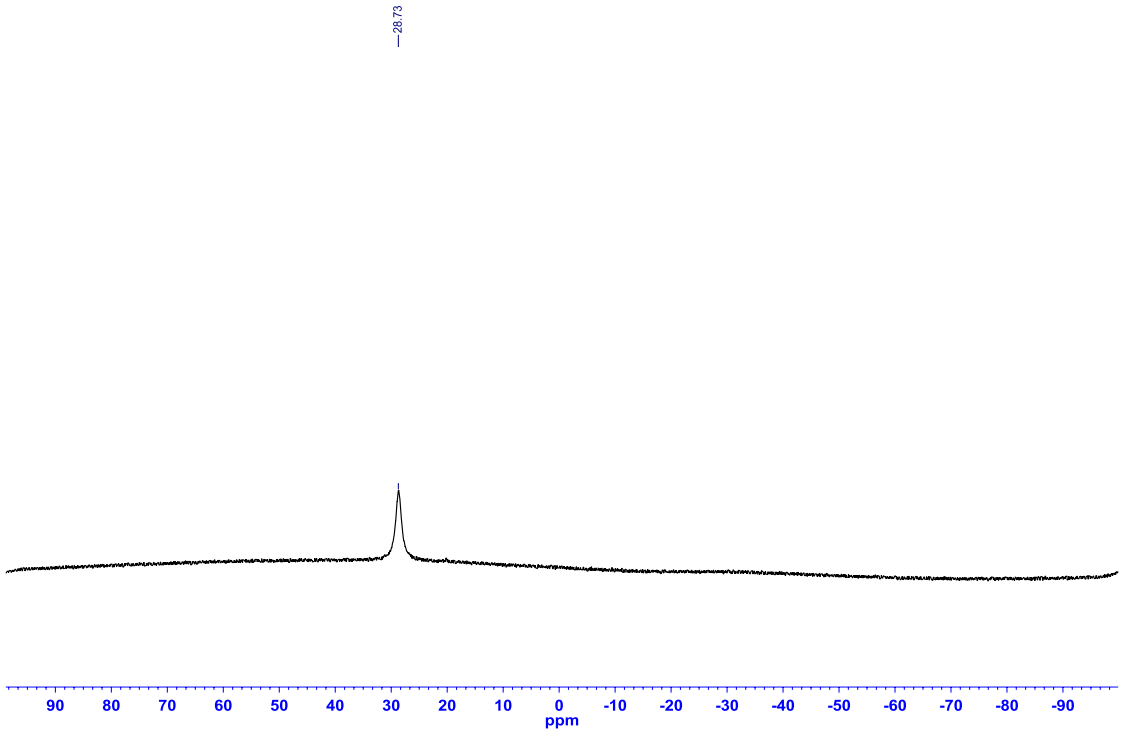

Figure A1.33: ^{1}H NMR ($CDCl_3$, 500.4 MHz) of 2-(4-fluorophenyl)-1-methy-2,3-dihydro-1*H*-1,3,2-benzodiazaborole (**2.11**)

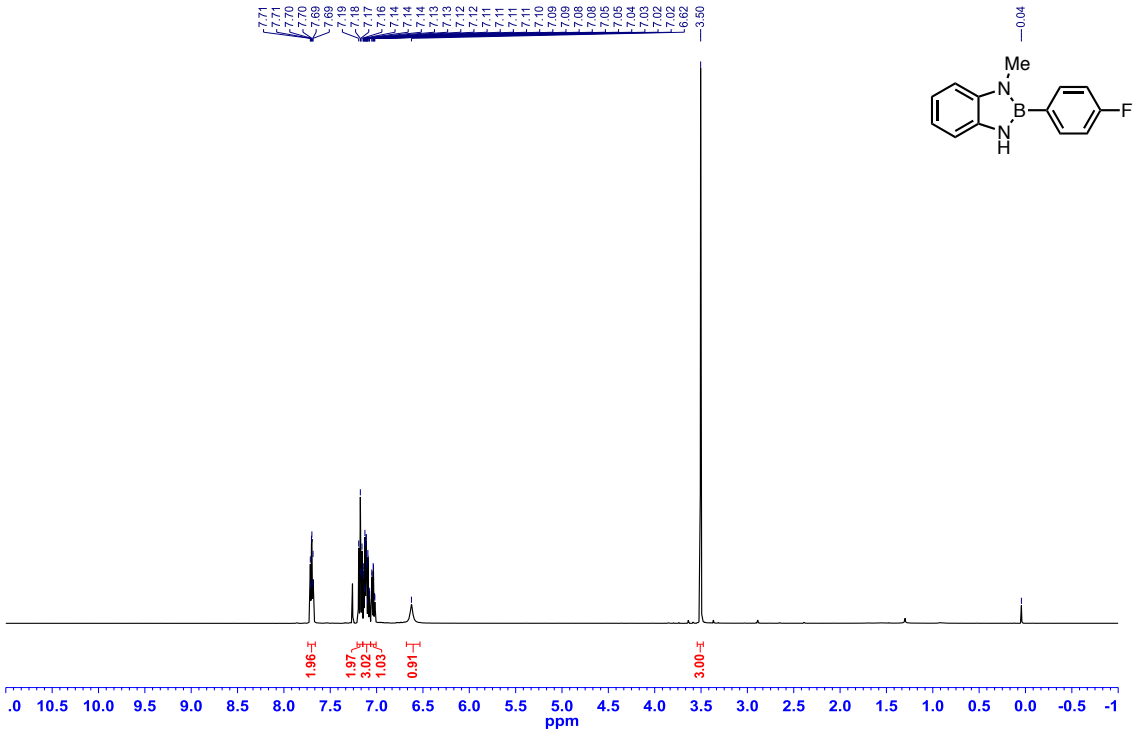

Figure A1.34: ^{13}C {^{1}H} NMR ($CDCl_3$, 125.8 MHz) of 2-(4-fluorophenyl)-1-methy-2,3-dihydro-1*H*-1,3,2-benzodiazaborole (**2.11**)

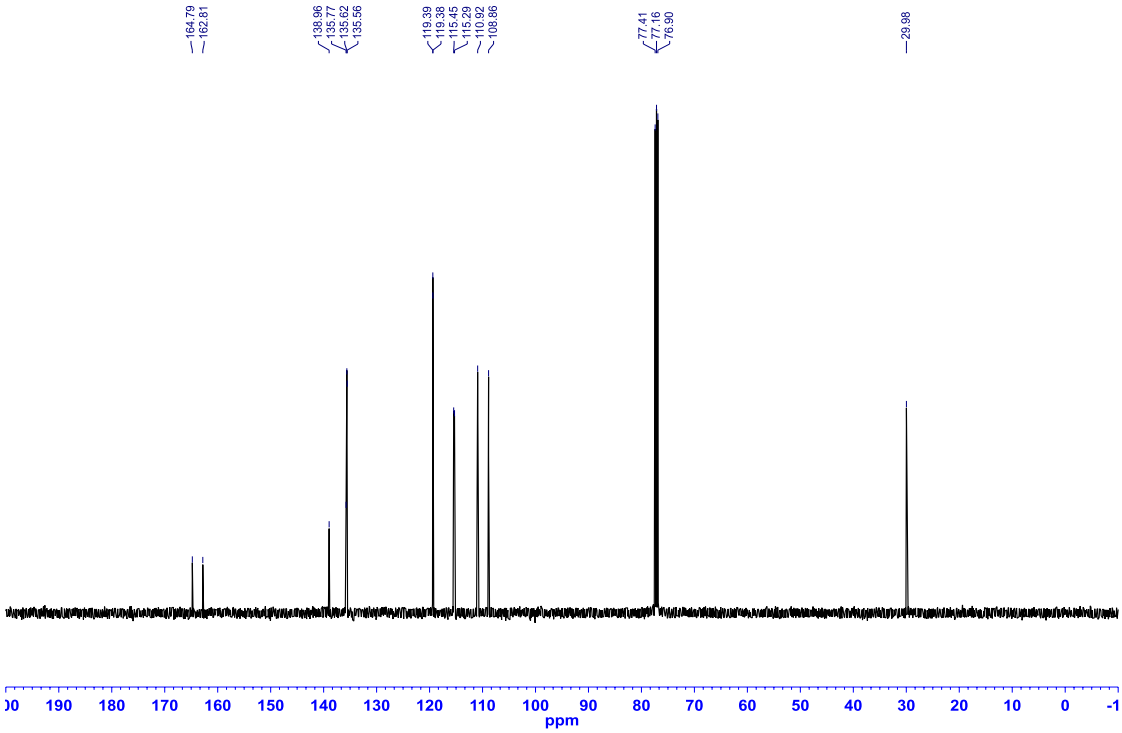

Figure A1.35: ^{19}F {^{1}H} NMR ($CDCl_3$, 282.4 MHz) of 2-(4-fluorophenyl)-1-methy-2,3-dihydro-1*H*-1,3,2-benzodiazaborole (**2.11**)

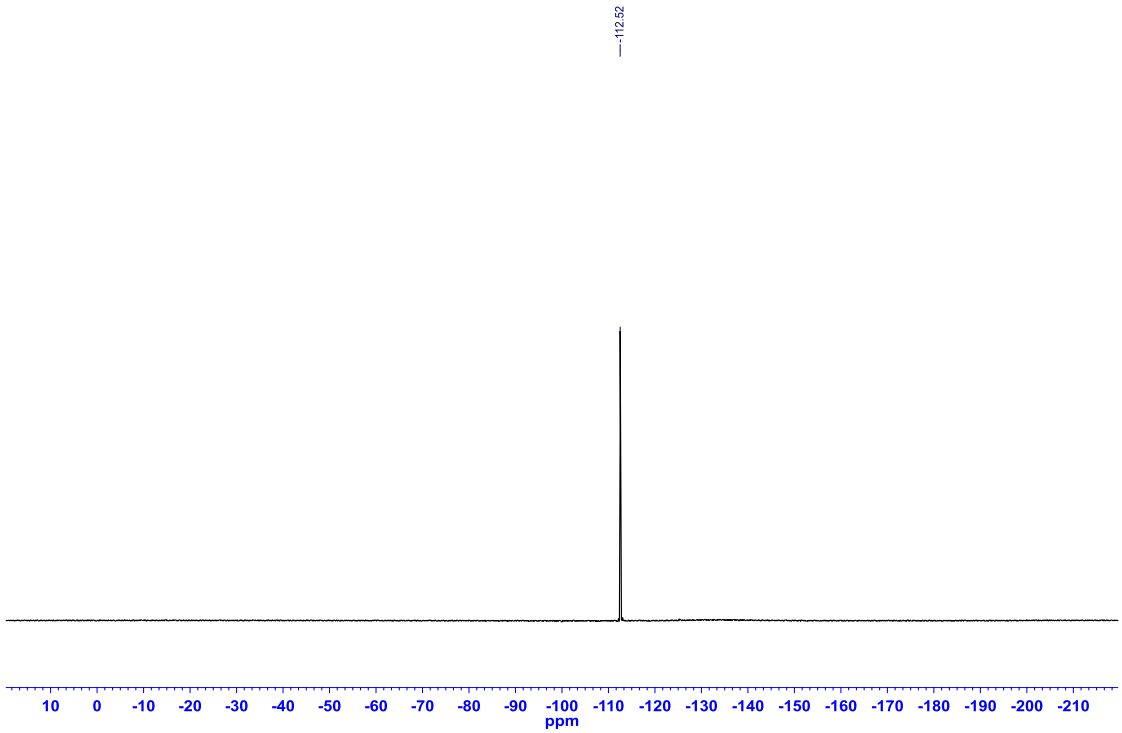

Figure A1.36: ^{11}B NMR (MeCN, 128.4 MHz) of 2-(4-fluorophenyl)-1-methy-2,3-dihydro-1*H*-1,3,2-benzodiazaborole (**2.11**)

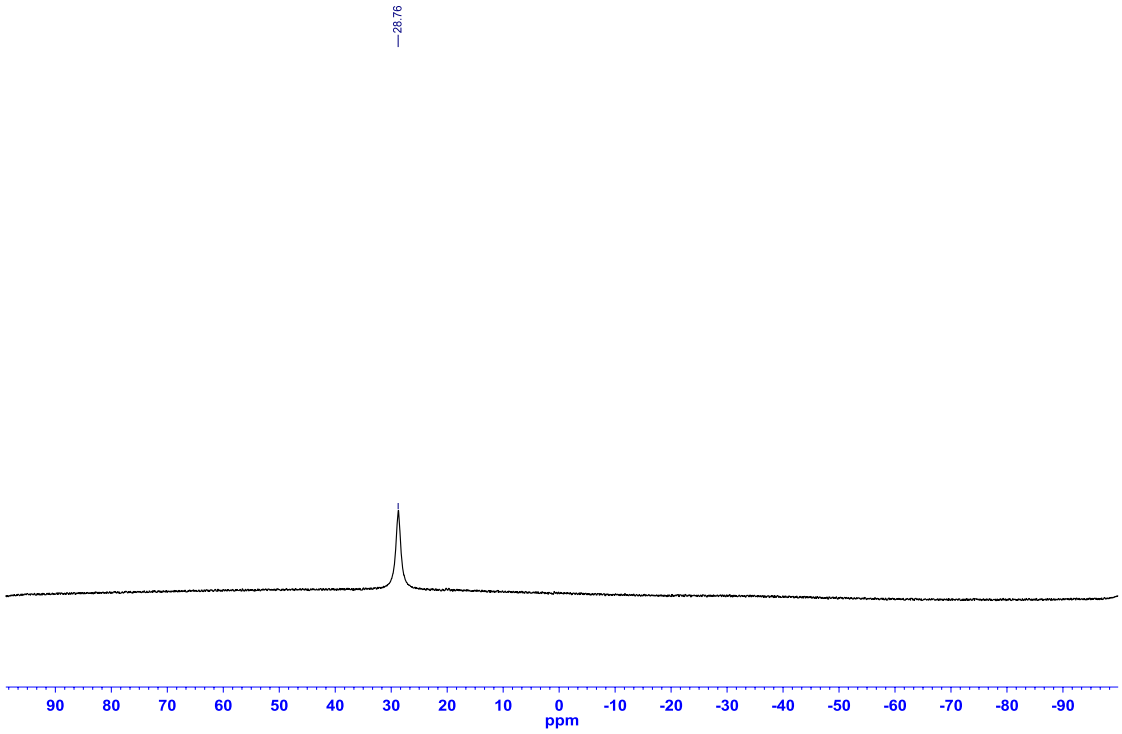

Figure A1.37: ^{1}H NMR (DMSO-d_6, 500.4 MHz) of 2-(3-vinylphenyl)-2,3-dihydro-1*H*-1,3,2-benzodiazaborole (**2.12**)

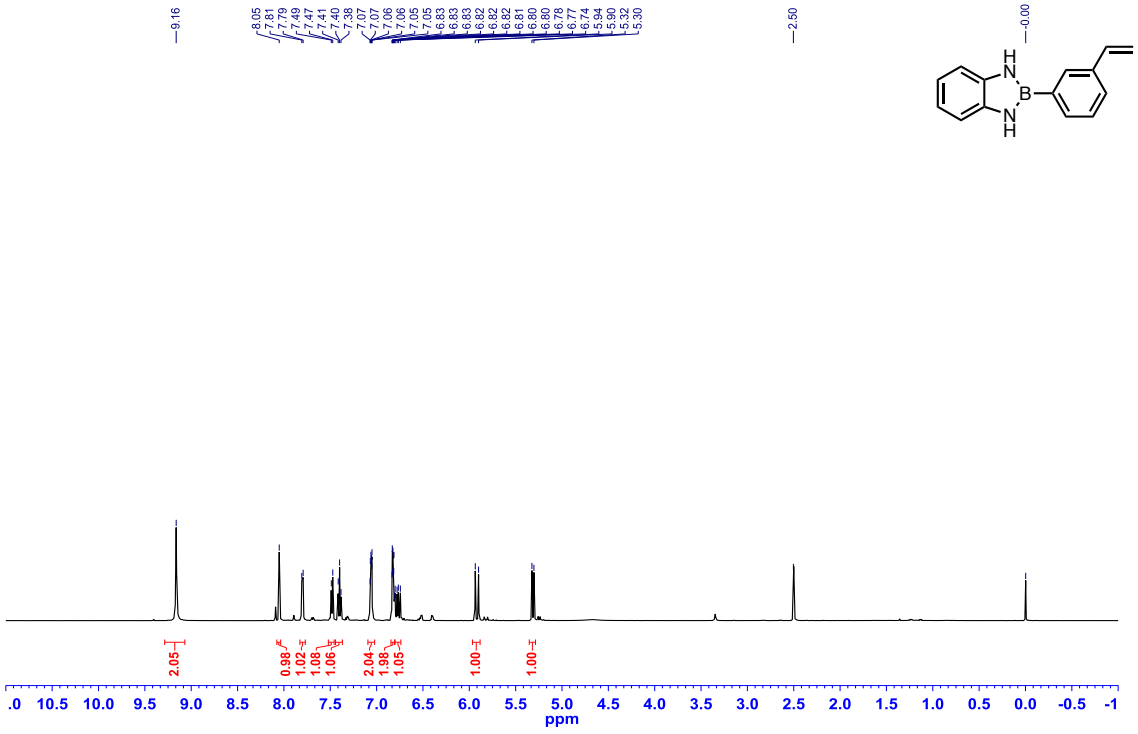

Figure A1.38: ^{13}C {^{1}H} NMR (DMSO-d_6, 125.8 MHz) of 2-(3-vinylphenyl)-2,3-dihydro-1*H*-1,3,2-benzodiazaborole (**2.12**)

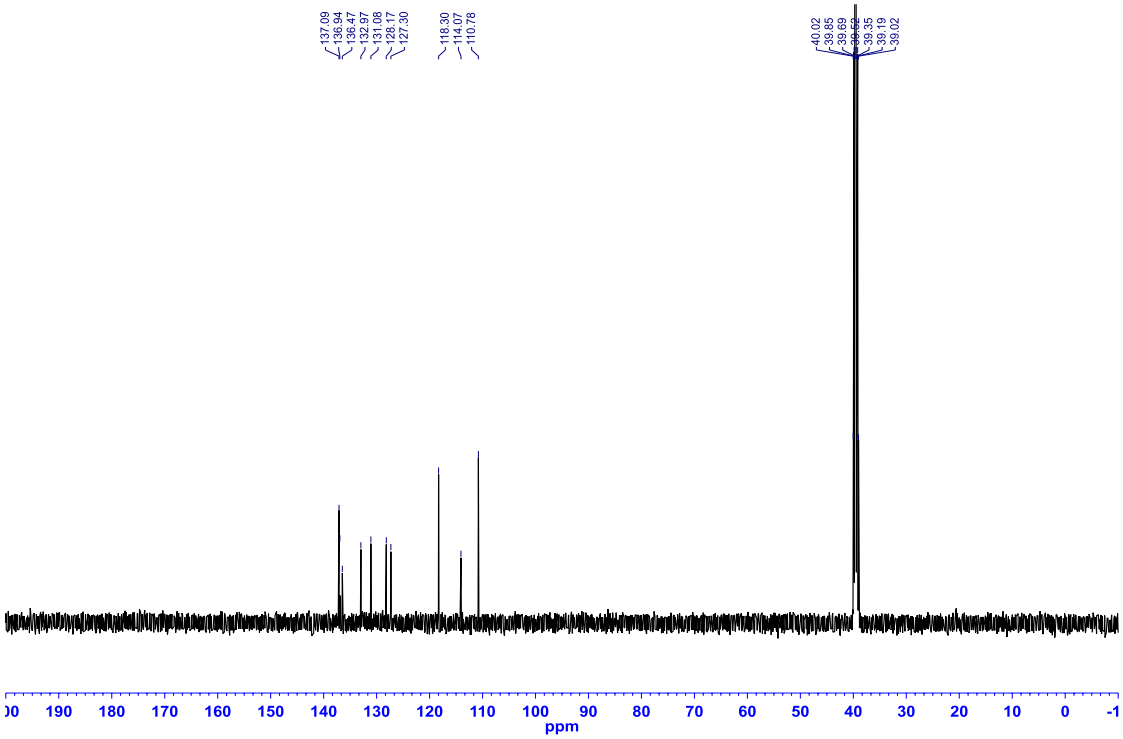

Figure A1.39: ^{11}B NMR (MeCN, 128.4 MHz) of 2-(3-vinylphenyl)-2,3-dihydro-1*H*-1,3,2-benzodiazaborole (**2.12**)

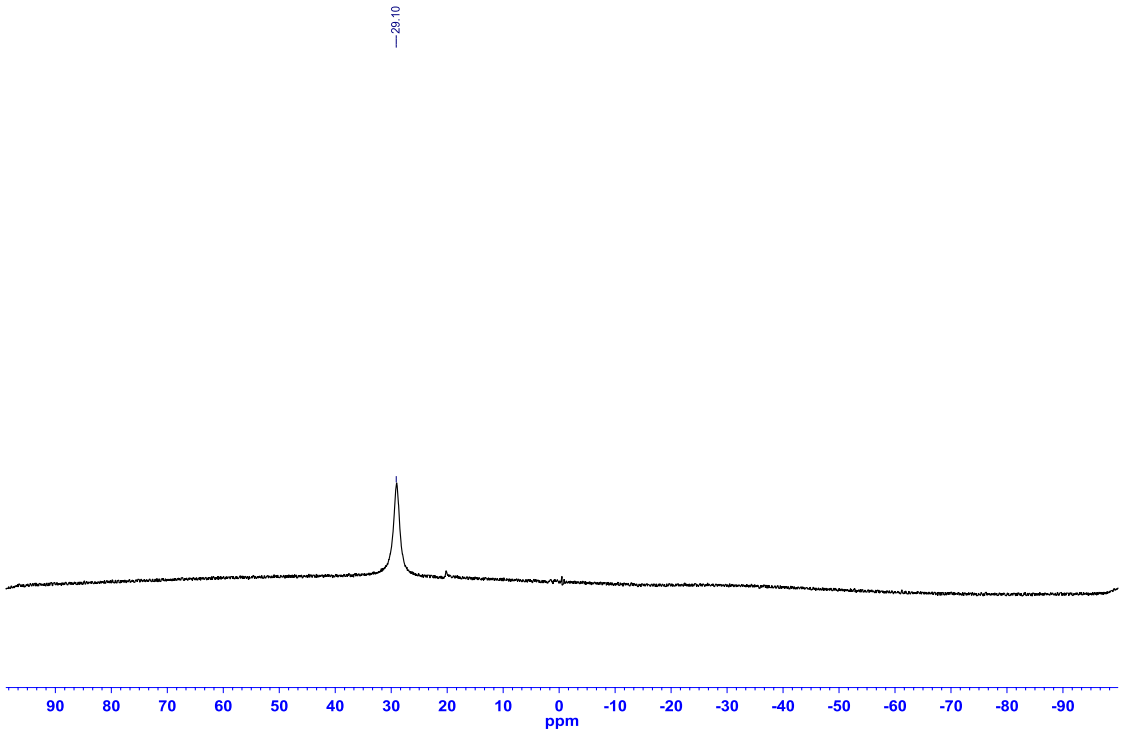

Figure A1.40: ^{1}H NMR (DMSO-d_6, 500.4 MHz) of 2-(2-methoxyphenyl)-2,3-dihydro-1*H*-1,3,2-benzodiazaborole (**2.13**)

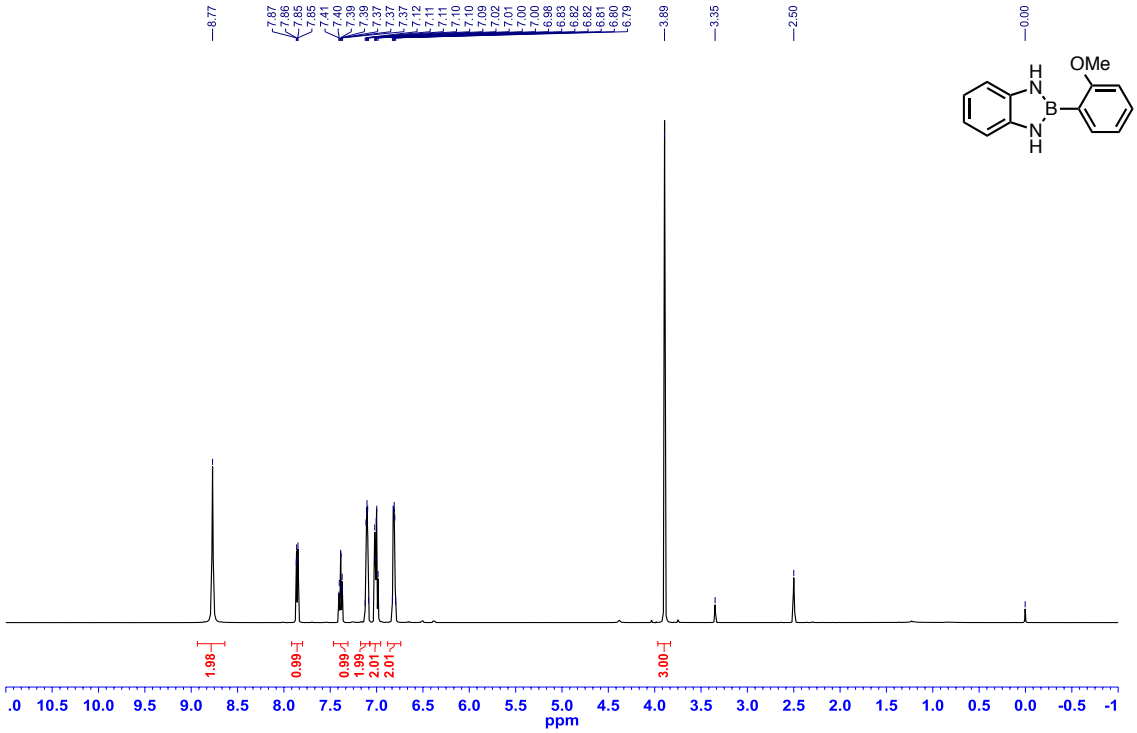

Figure A1.41: ^{13}C {^{1}H} NMR (DMSO-d_6, 125.8 MHz) of 2-(2-methoxyphenyl)-2,3-dihydro-1*H*-1,3,2-benzodiazaborole (**2.13**)

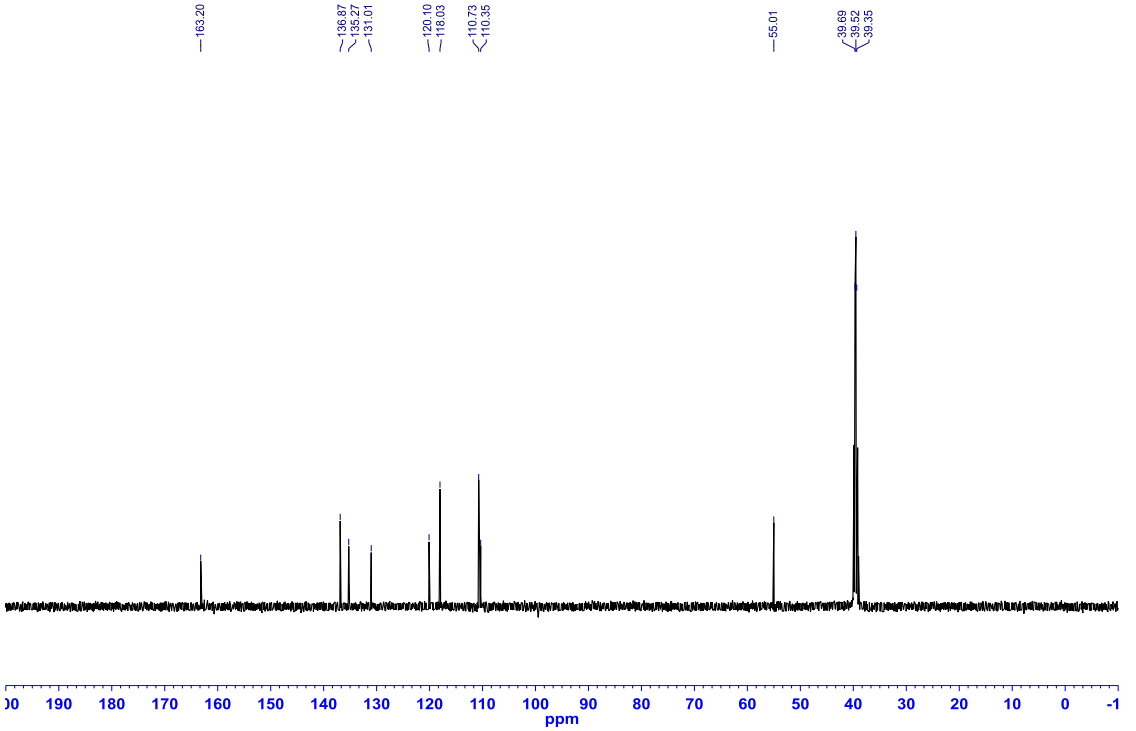

Figure A1.42: ^{11}B NMR (MeCN, 128.4 MHz) of 2-(2-methoxyphenyl)-2,3-dihydro-1*H*-1,3,2-benzodiazaborole (**2.13**)

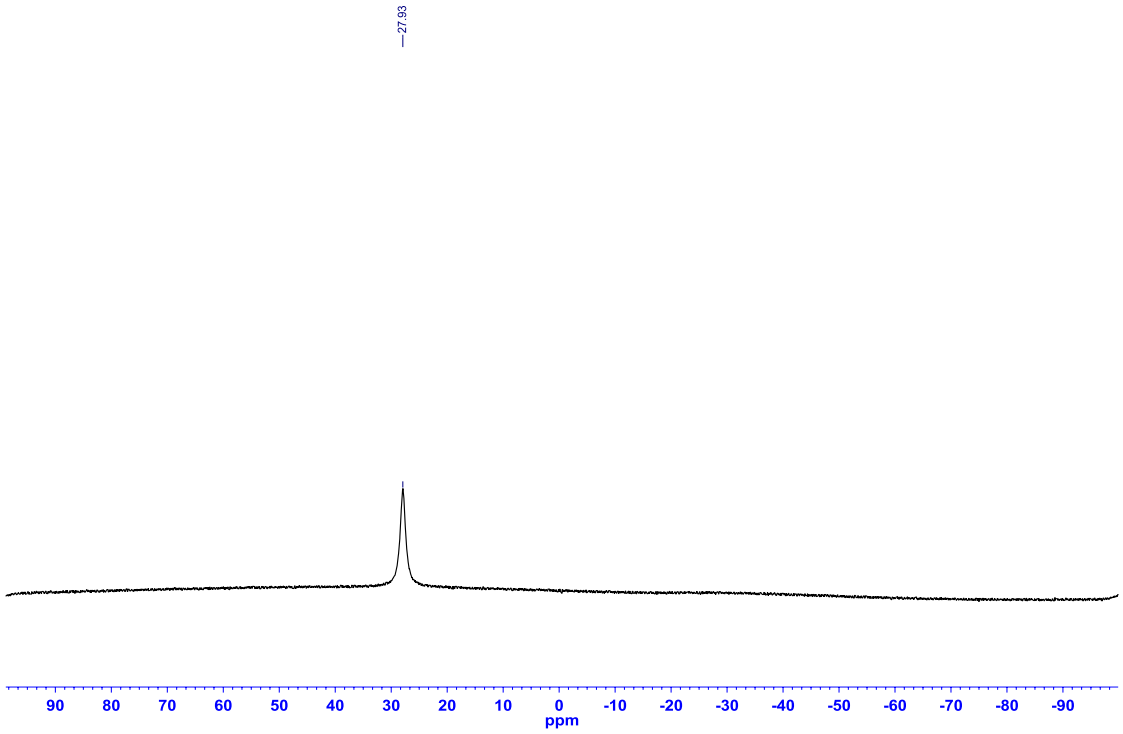

Figure A1.43: ^{1}H NMR (DMSO-d_6, 500.4 MHz) of 2-(3-methoxyphenyl)-2,3-dihydro-1*H*-1,3,2-benzodiazaborole (**2.14**)

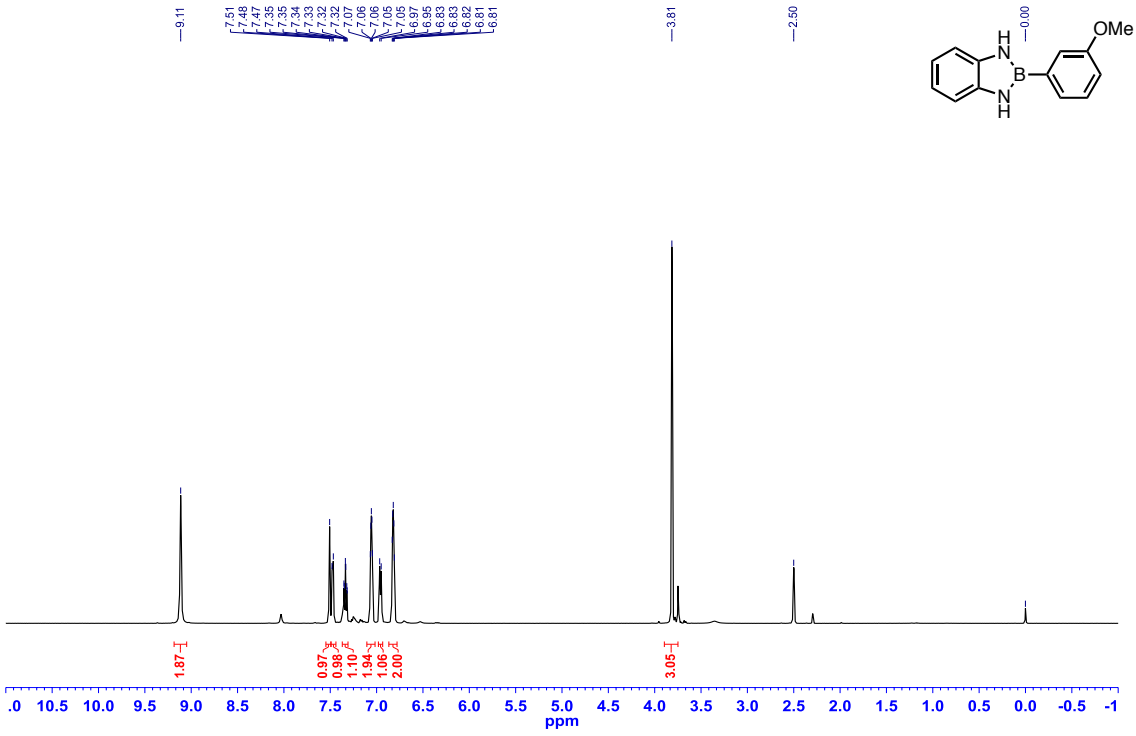

Figure A1.44: ^{13}C {^{1}H} NMR (DMSO-d_6, 125.8 MHz) of 2-(3-methoxyphenyl)-2,3-dihydro-1*H*-1,3,2-benzodiazaborole (**2.14**)

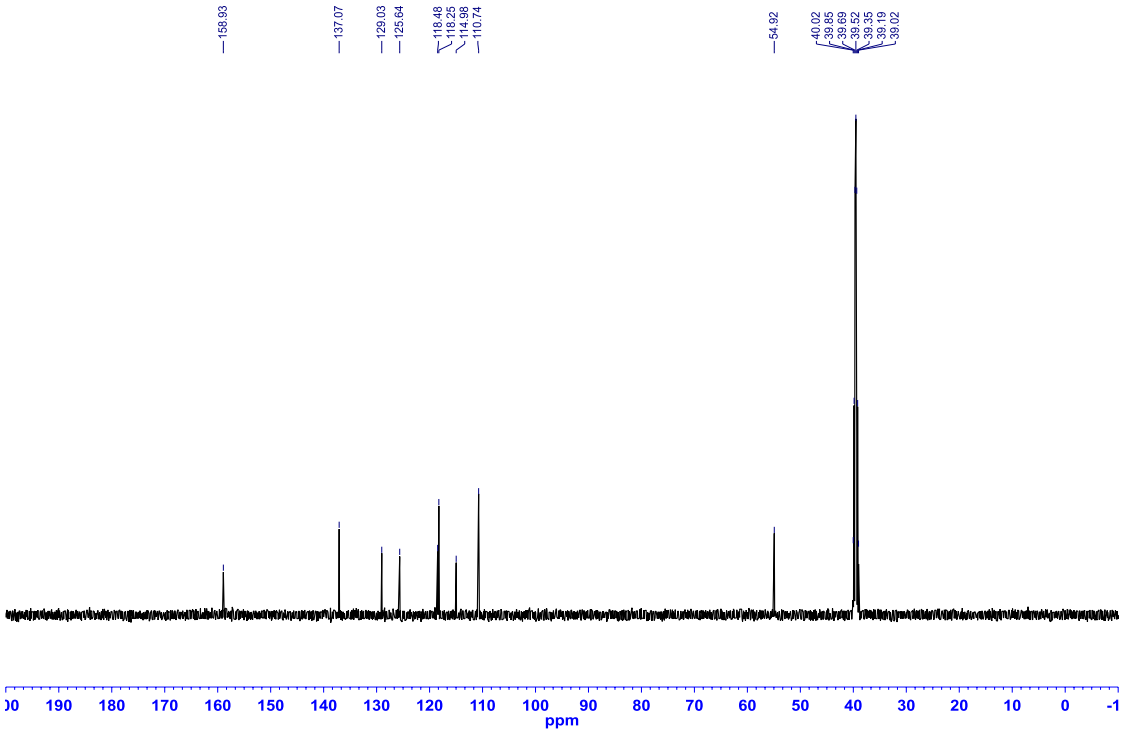

Figure A1.45: ^{11}B NMR (MeCN, 128.4 MHz) of 2-(3-methoxyphenyl)-2,3-dihydro-1*H*-1,3,2-benzodiazaborole (**2.14**)

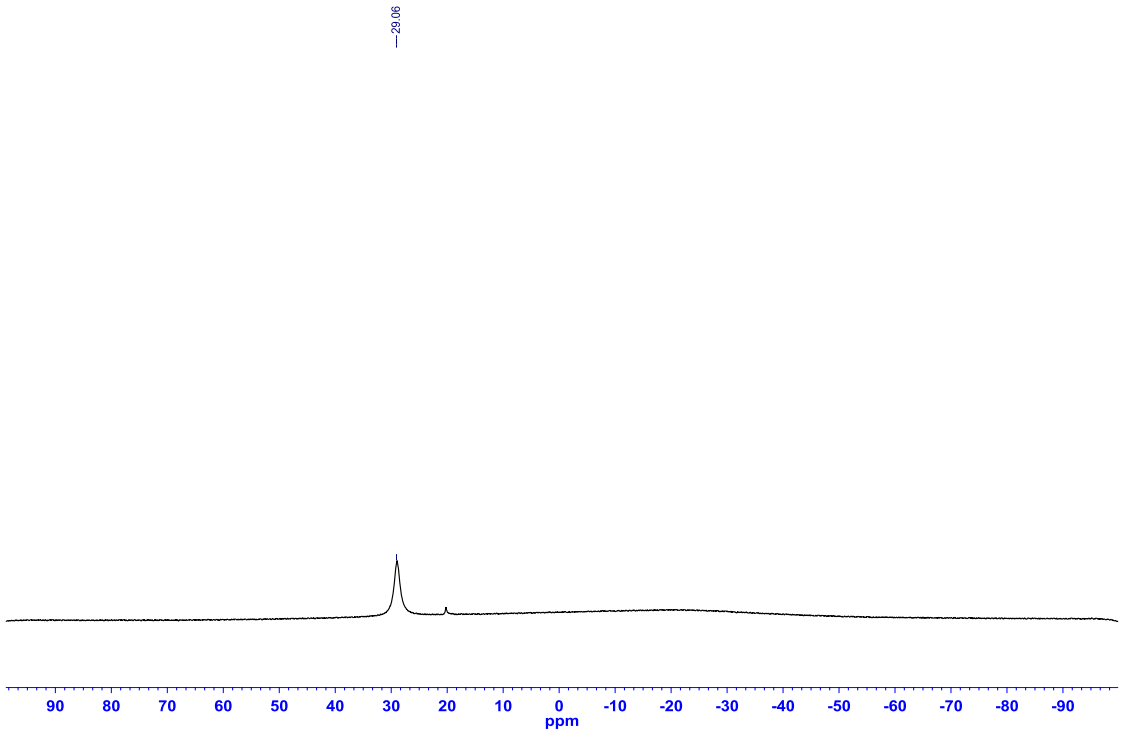

Figure A1.46: ^{1}H NMR ($CDCl_3$, 500.4 MHz) of 2-(3-methoxyphenyl)-1-methyl-2,3-dihydro-1*H*-1,3,2-benzodiazaborole (**2.15**)

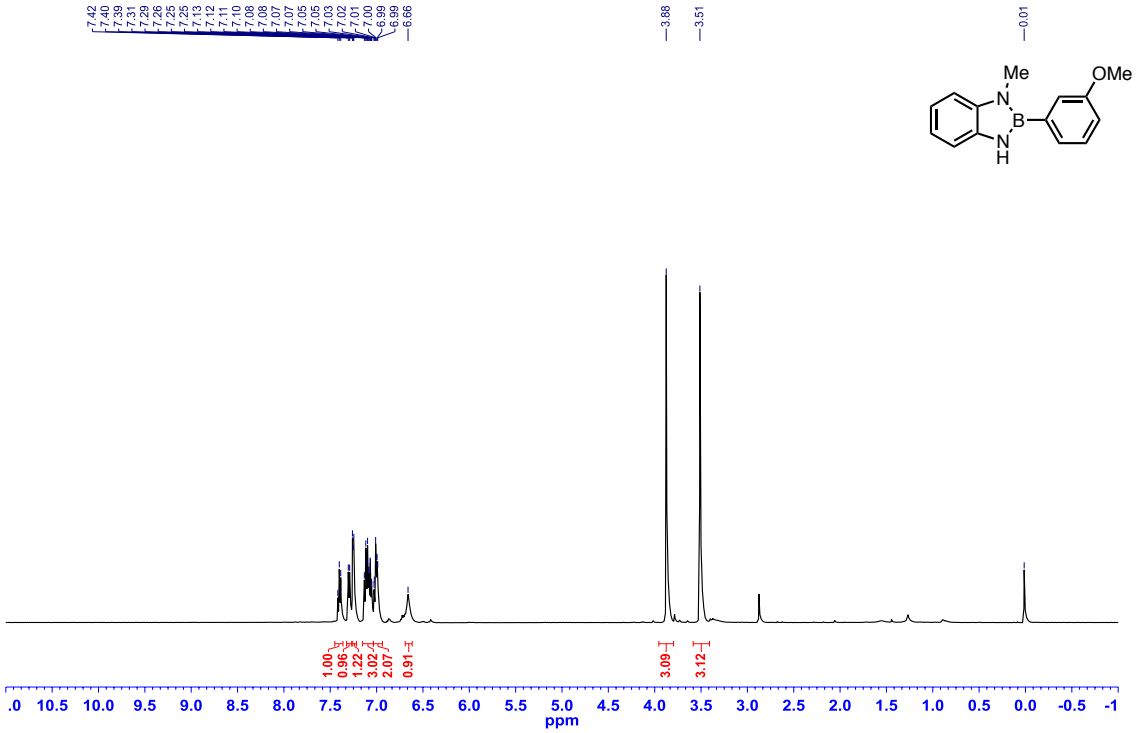

Figure A1.47: ^{13}C {^{1}H} NMR ($CDCl_3$, 125.8 MHz) of 2-(3-methoxyphenyl)-1-methyl-2,3-dihydro-1*H*-1,3,2-benzodiazaborole (**2.15**)

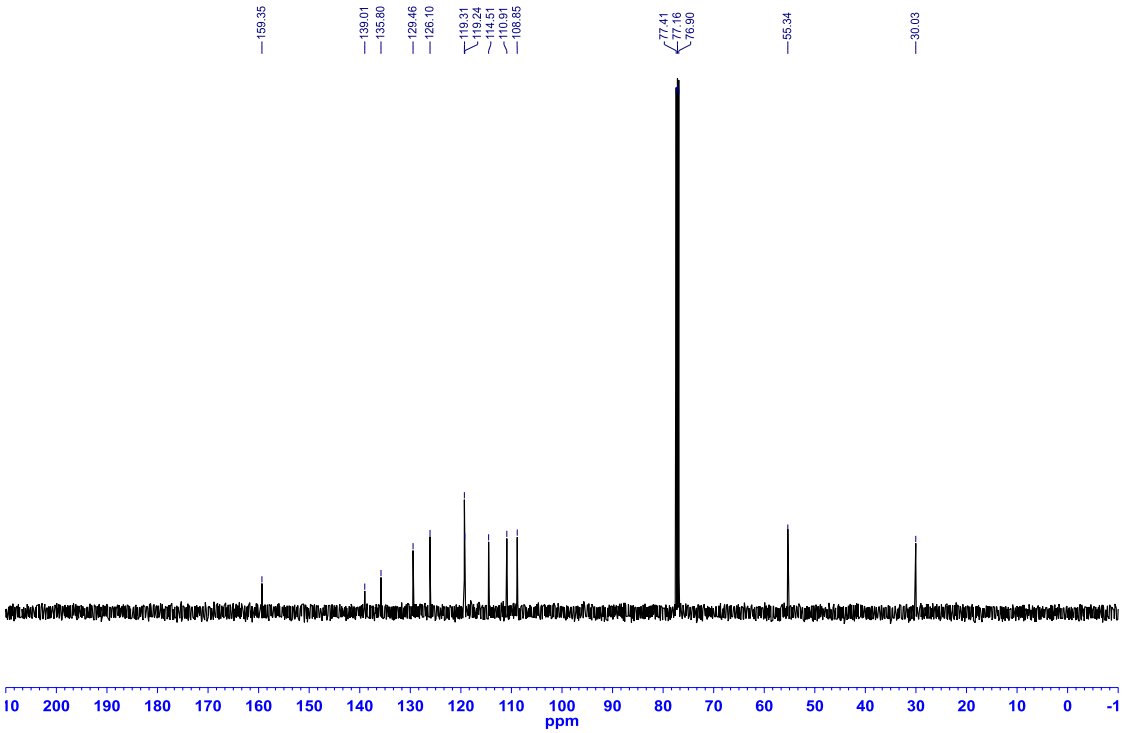

Figure A1.48: ^{11}B NMR (MeCN, 128.4 MHz) of 2-(3-methoxyphenyl)-1-methyl-2,3-dihydro-1*H*-1,3,2-benzodiazaborole (**2.15**)

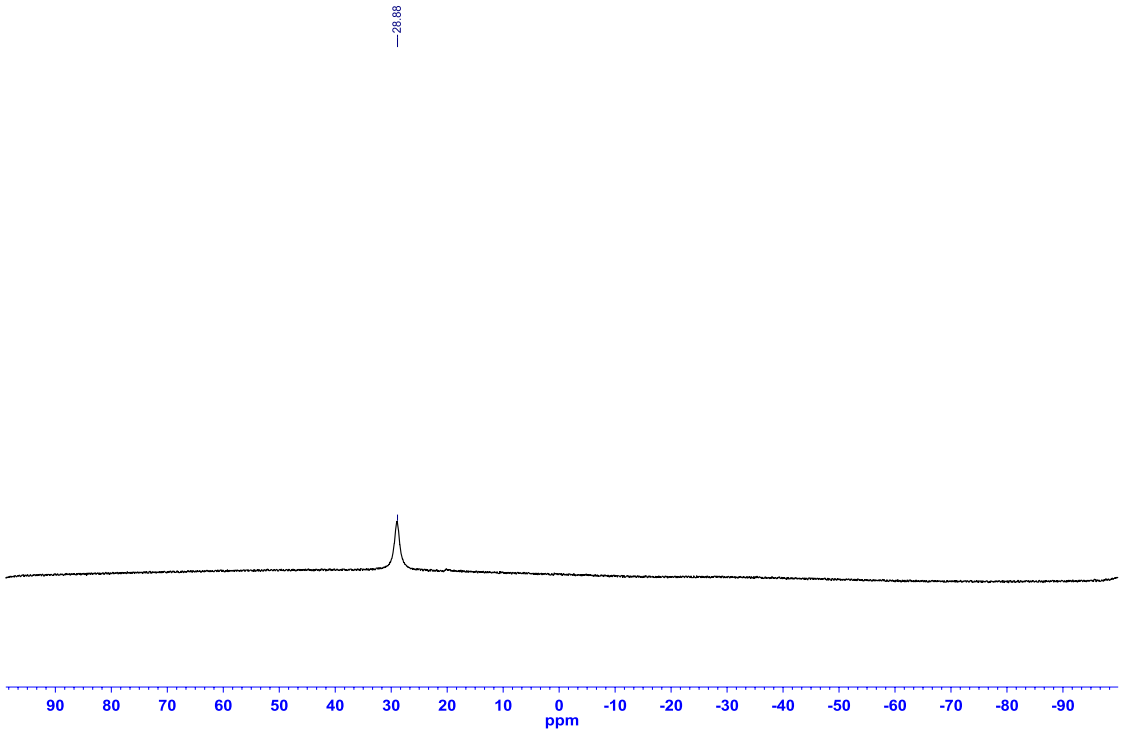

Figure A1.49: ^{1}H NMR ($CDCl_3$, 500.4 MHz) of 2-(2-phenoxyphenyl)-2,3-dihydro-1*H*-1,3,2-benzodiazaborole (**2.16**)

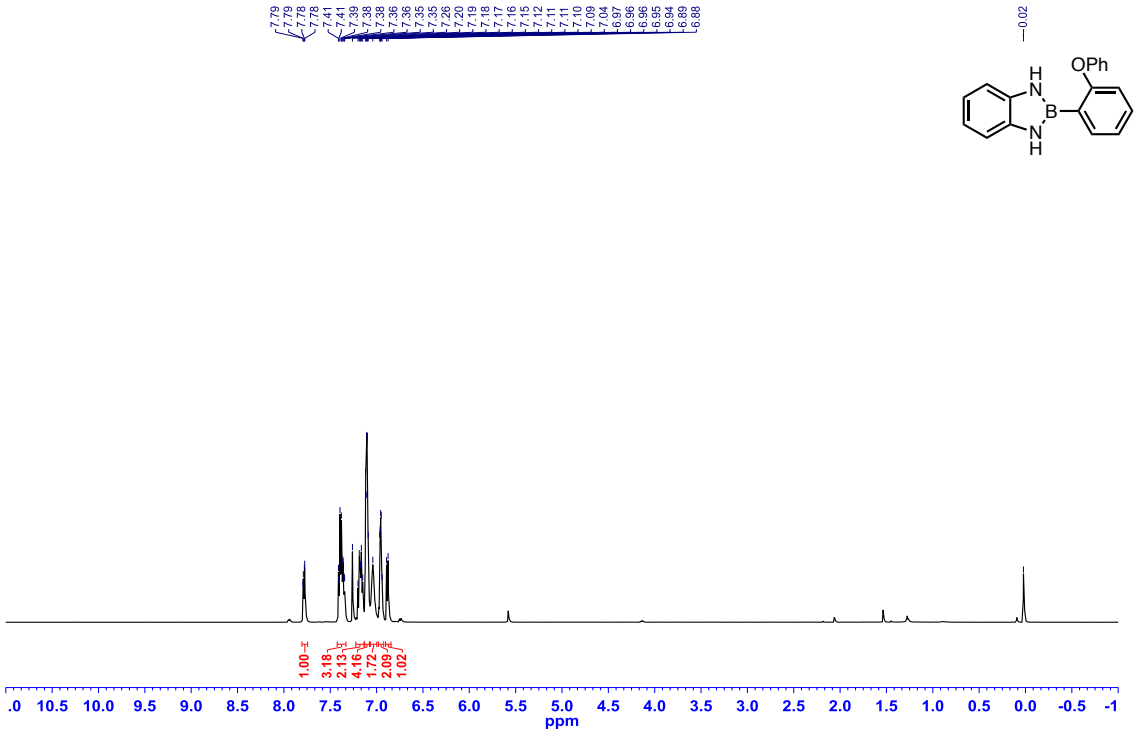

Figure A1.50: ^{13}C {^{1}H} NMR ($CDCl_3$, 125.8 MHz) of 2-(2-phenoxyphenyl)-2,3-dihydro-1*H*-1,3,2-benzodiazaborole (**2.16**)

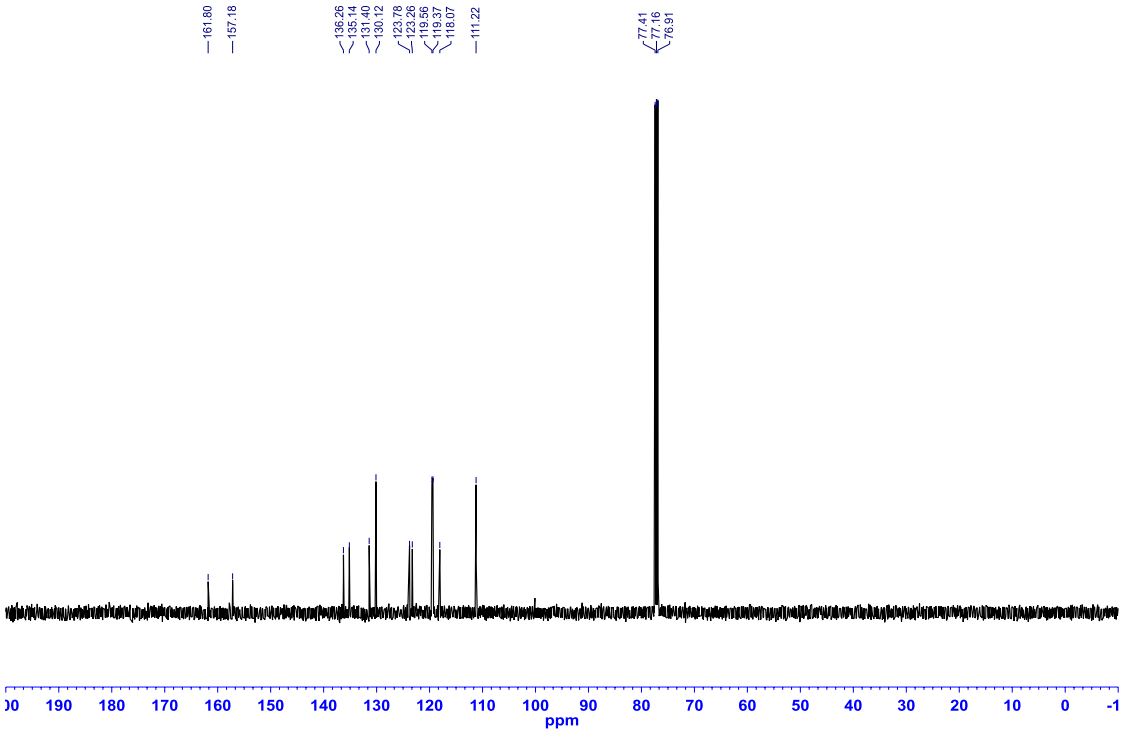

Figure A1.51: ^{11}B NMR ($CDCl_3$, 128.4 MHz) of 2-(2-phenoxyphenyl)-2,3-dihydro-1*H*-1,3,2-benzodiazaborole (**2.16**)

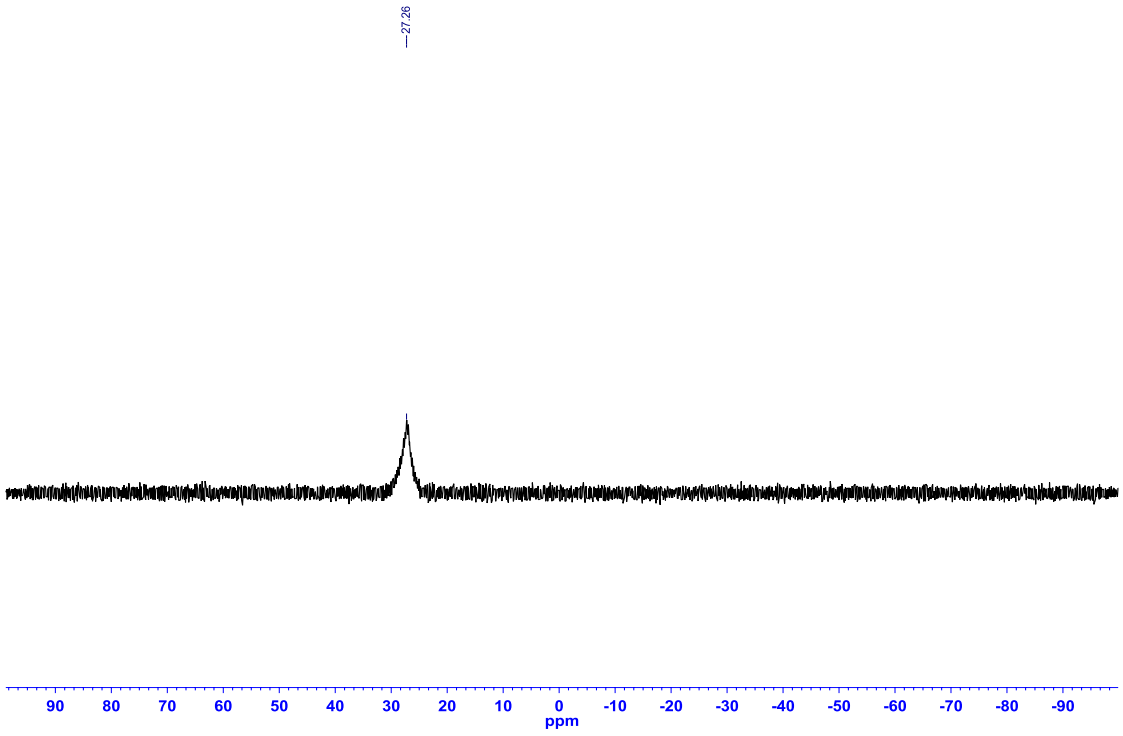

Figure A1.52: ^{1}H NMR (DMSO-d_6, 500.4 MHz) of 2-(4-(methoxycarbonyl)phenyl)-2,3-dihydro-1*H*-1,3,2-benzodiazaborole (**2.17**)

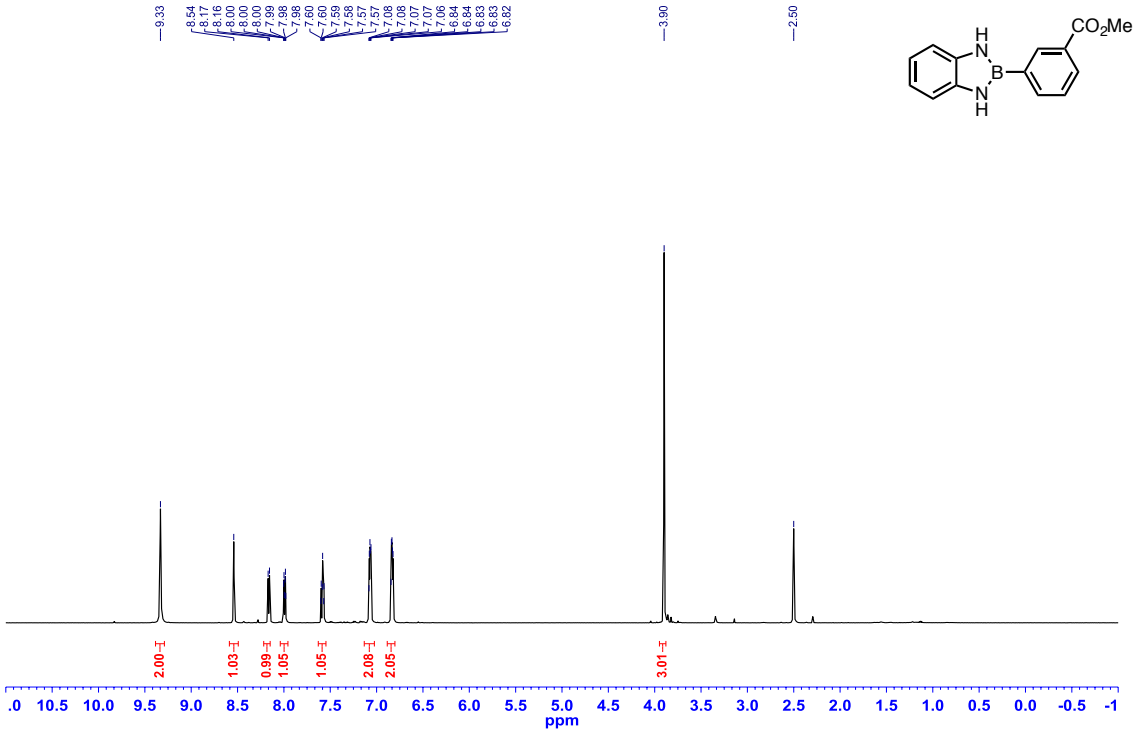

Figure A1.53: ^{13}C {^{1}H} NMR (DMSO-d_6, 125.8 MHz) of 2-(4-(methoxycarbonyl)phenyl)-2,3-dihydro-1*H*-1,3,2-benzodiazaborole (**2.17**)

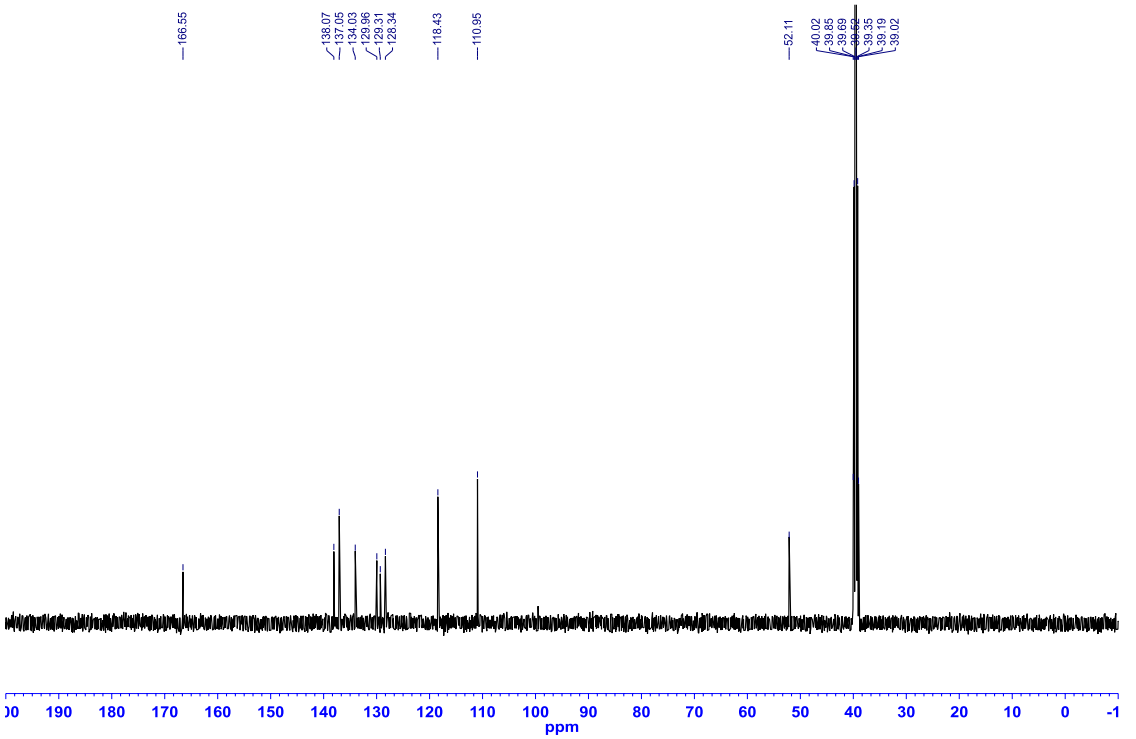

Figure A1.54: ^{11}B NMR (MeCN, 128.4 MHz) of 2-(4-(methoxycarbonyl)phenyl)-2,3-dihydro-1*H*-1,3,2-benzodiazaborole (**2.17**)

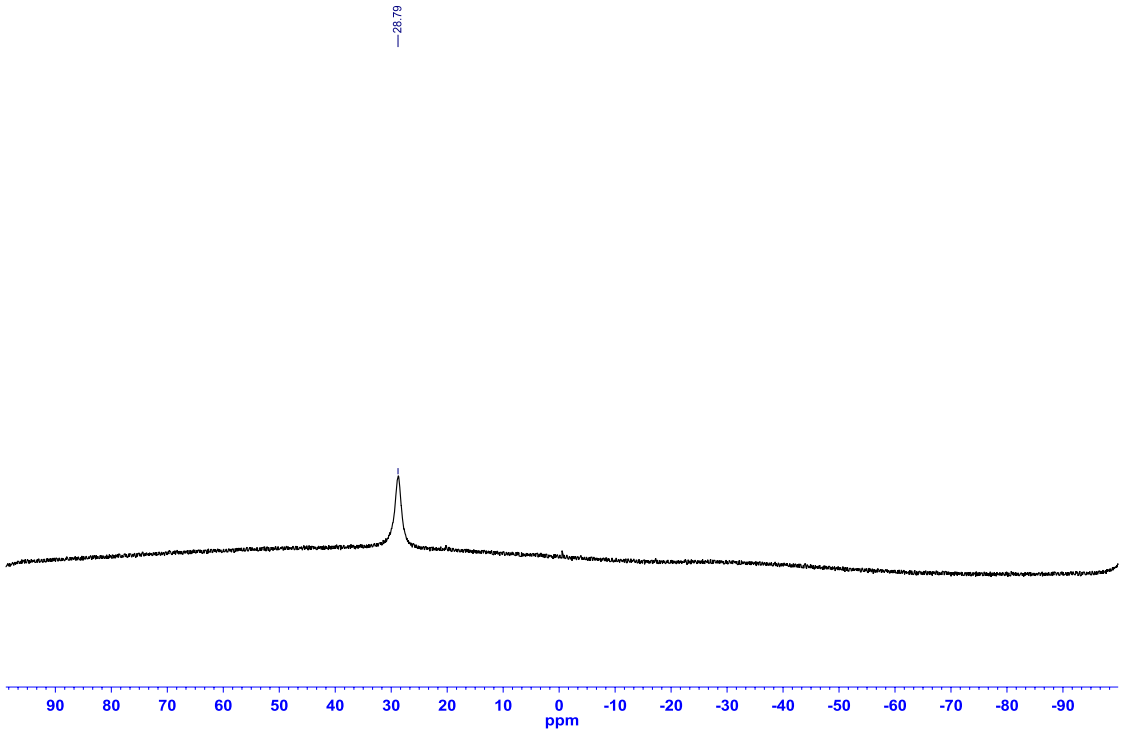

Figure A1.55: ^{1}H NMR ($CDCl_3$, 500.4 MHz) of 2-(2,3-dihydrobenzo[1,4]dioxin-5-yl)-1-methyl-2,3-dihydro-1*H*-1,3,2-benzodiazaborole (**2.18**)

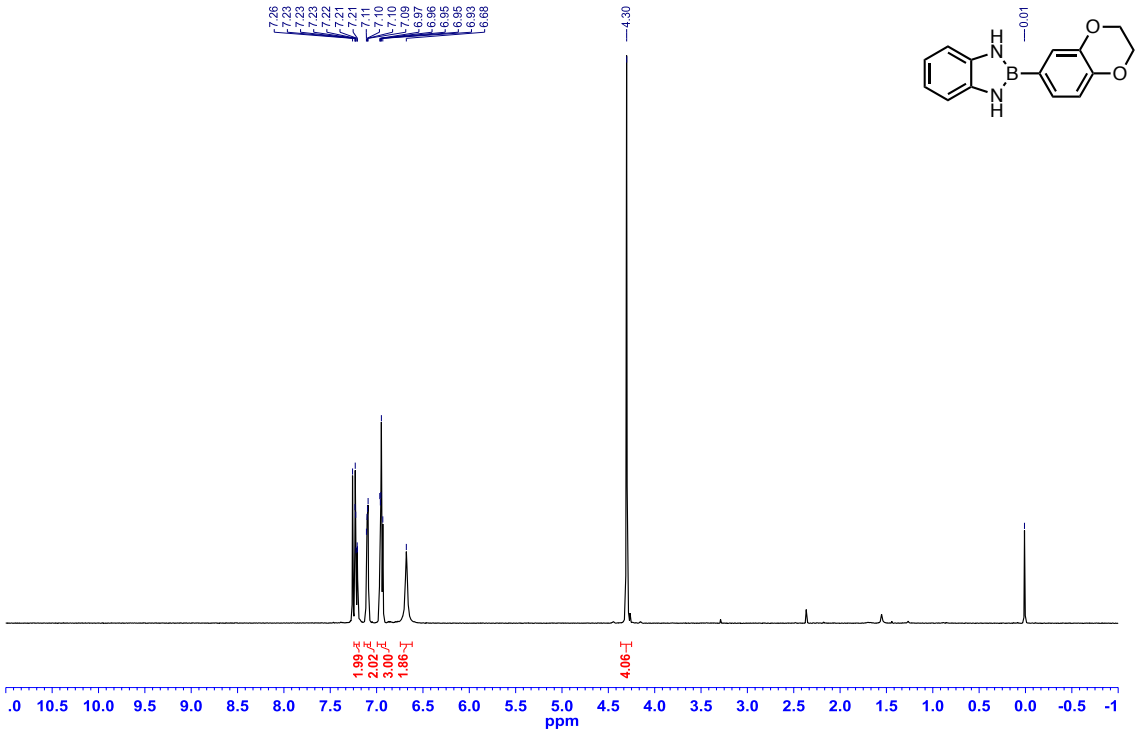

Figure A1.56: ^{13}C {^{1}H} NMR ($CDCl_3$, 125.8 MHz) of 2-(2,3-dihydrobenzo[1,4]dioxin-5-yl)-1-methyl-2,3-dihydro-1*H*-1,3,2-benzodiazaborole (**2.18**)

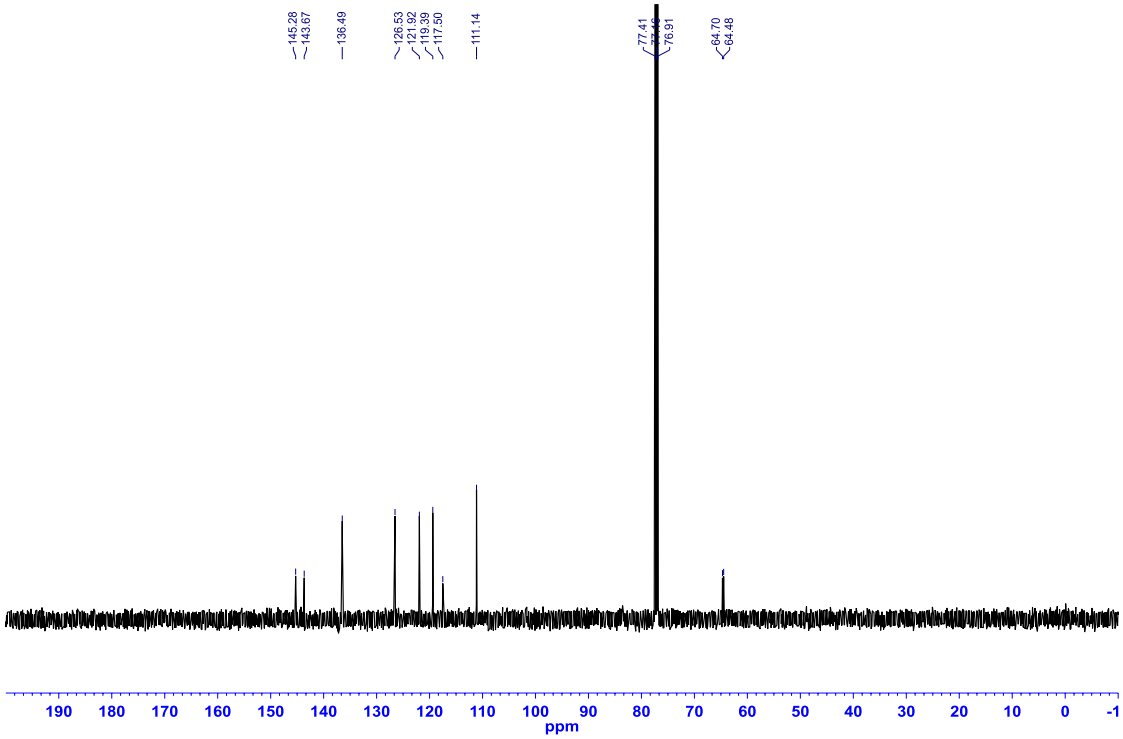

Figure A1.57: ^{11}B NMR (MeCN, 128.4 MHz) of 2-(2,3-dihydrobenzo[1,4]dioxin-5-yl)-1-methyl-2,3-dihydro-1*H*-1,3,2-benzodiazaborole (**2.18**)

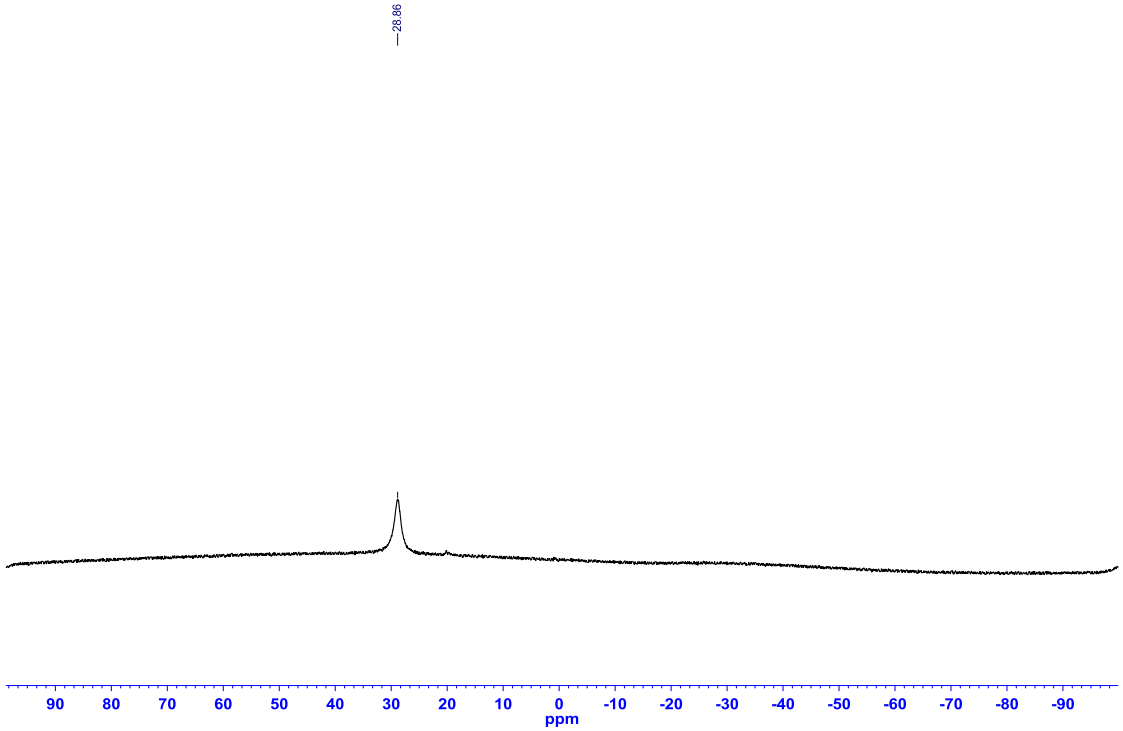

Figure A1.58: ^{1}H NMR (DMSO-d_6, 500.4 MHz) of 2-(3-nitrophenyl)-2,3-dihydro-1*H*-1,3,2-benzodiazaborole (**2.19**)

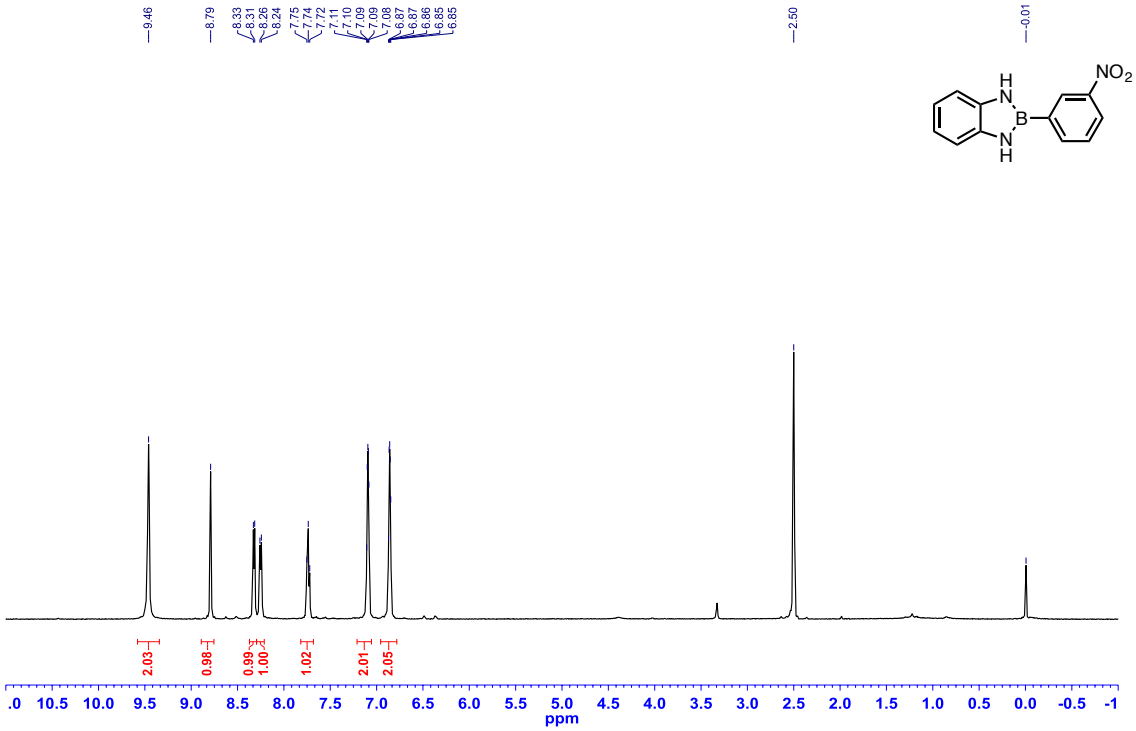

Figure A1.59: ^{13}C {^{1}H} NMR (DMSO-d_6, 125.8 MHz) of 2-(3-nitrophenyl)-2,3-dihydro-1*H*-1,3,2-benzodiazaborole (**2.19**)

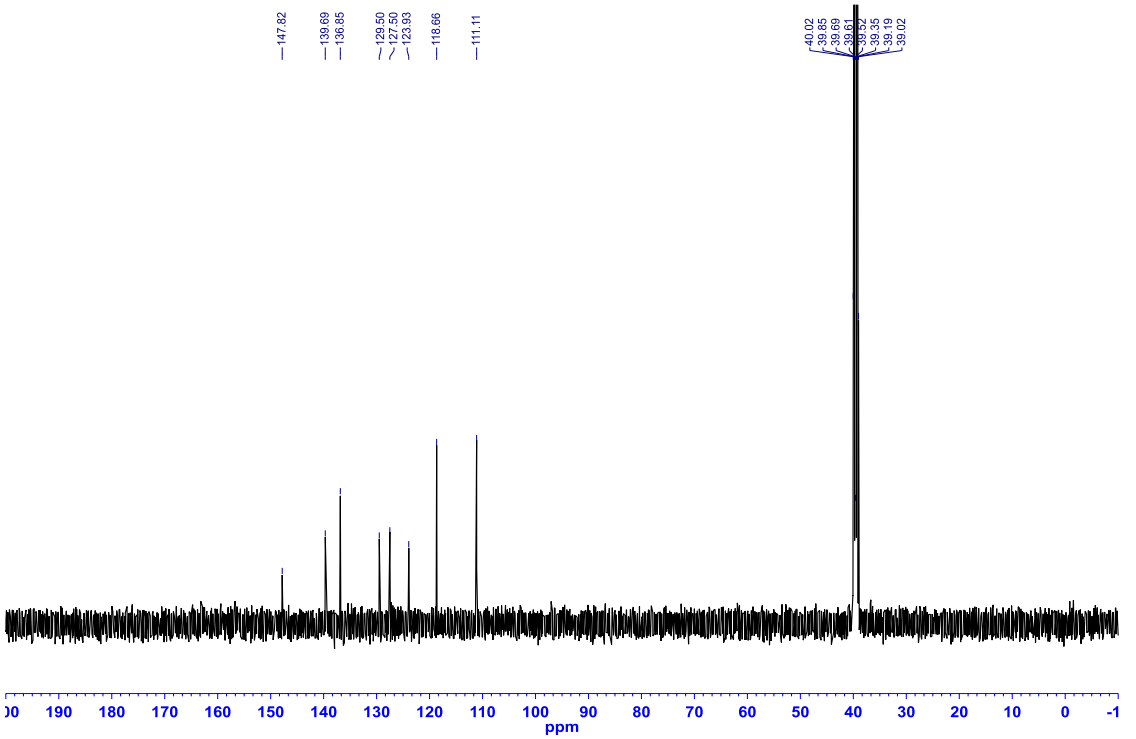

Figure A1.60: ^{11}B NMR (MeCN, 128.4 MHz) of 2-(3-nitrophenyl)-2,3-dihydro-1*H*-1,3,2-benzodiazaborole (**2.19**)

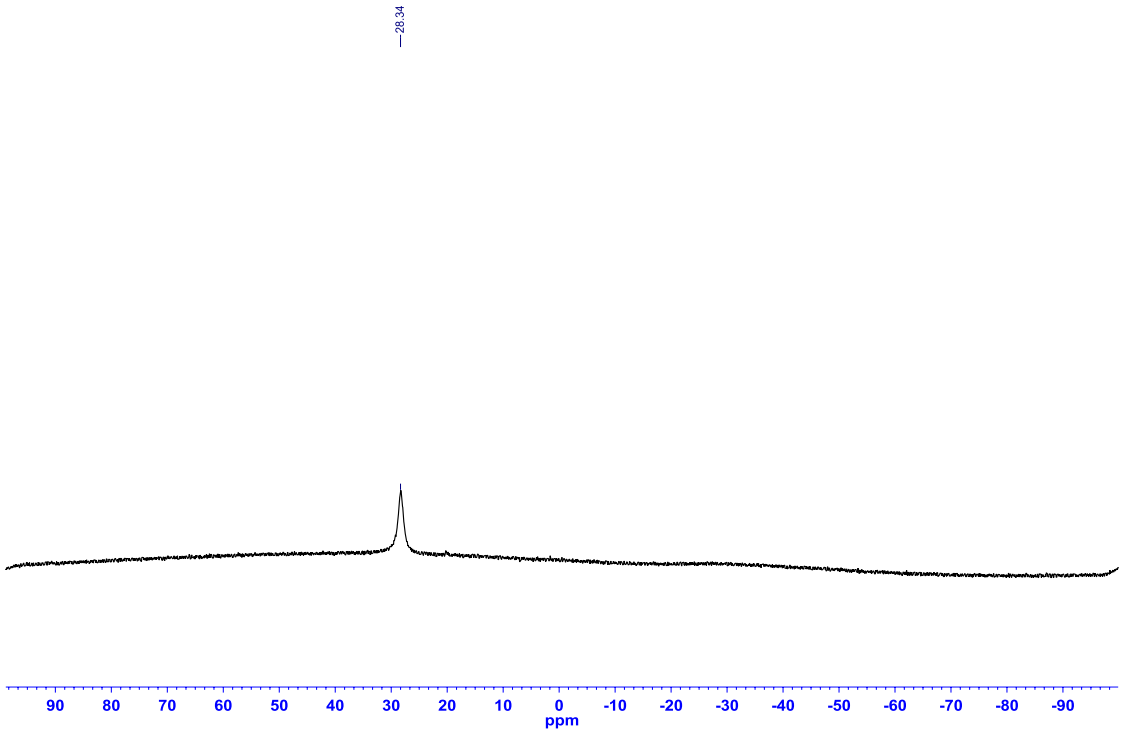

Figure A1.61: ^{1}H NMR ($CDCl_3$, 500.4 MHz) of 2-(3-cyanophenyl)-2,3-dihydro-1*H*-1,3,2-benzodiazaborole (**2.20**)

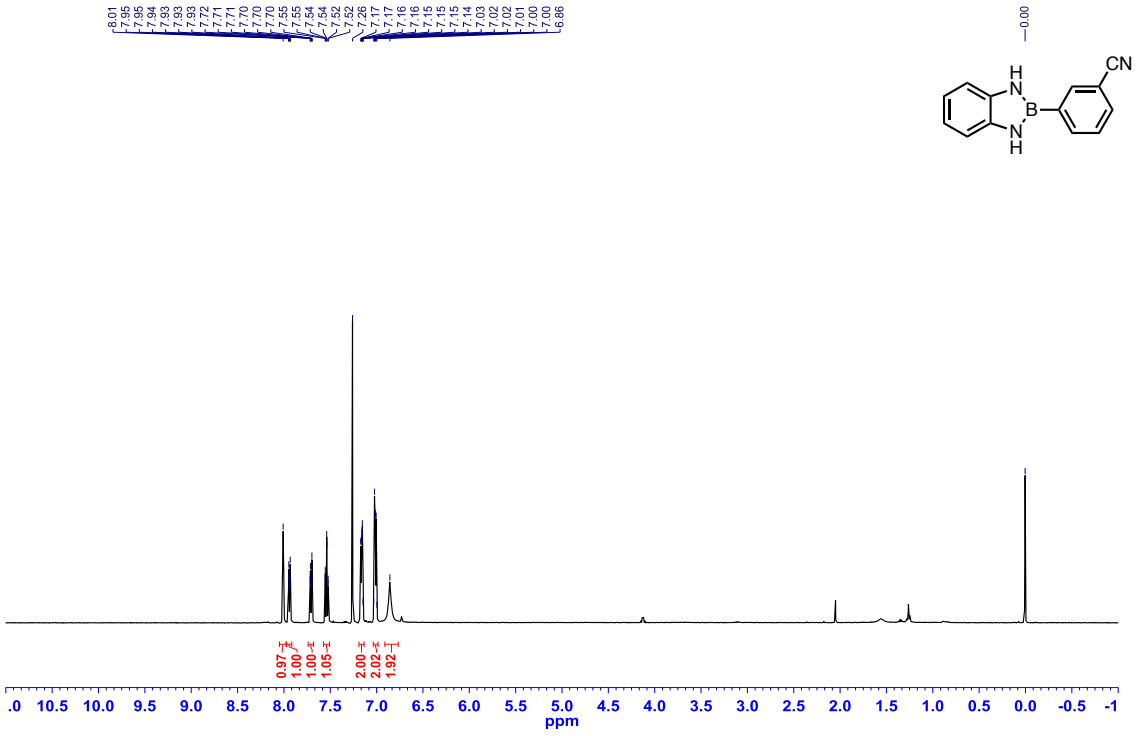

Figure A1.62: ^{13}C {^{1}H} NMR ($CDCl_3$, 125.8 MHz) of 2-(3-cyanophenyl)-2,3-dihydro-1*H*-1,3,2-benzodiazaborole (**2.20**)

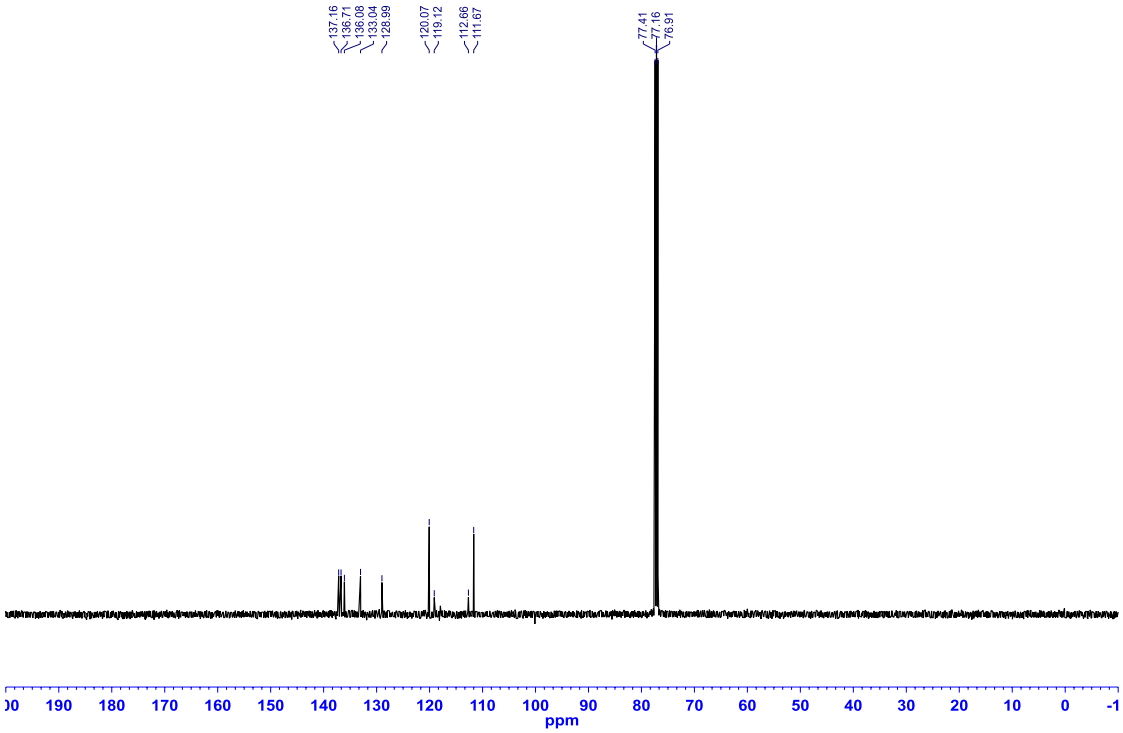

Figure A1.63: ^{11}B NMR ($CDCl_3$, 128.4 MHz) of 2-(3-cyanophenyl)-2,3-dihydro-1*H*-1,3,2-benzodiazaborole (**2.20**)

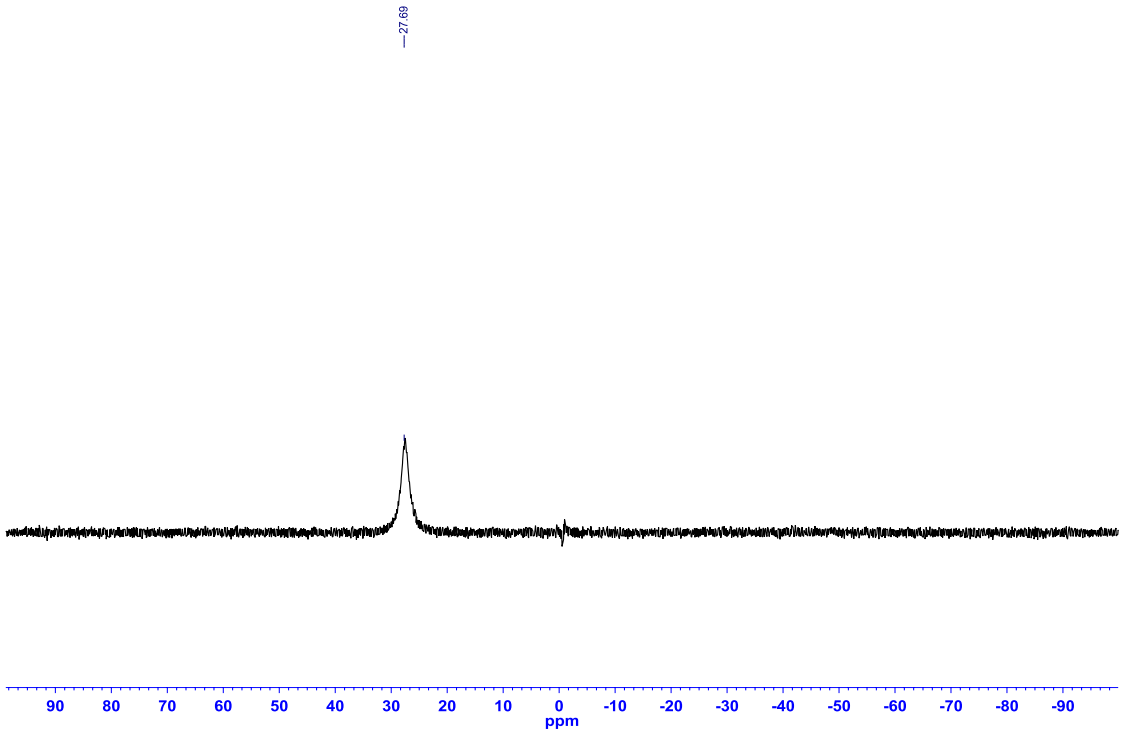

Figure A1.64: ^{1}H NMR ($CDCl_3$, 500.4 MHz) of 2-(3-thienyl)-2,3-dihydro-1*H*-1,3,2-benzodiazaborole (**2.21**)

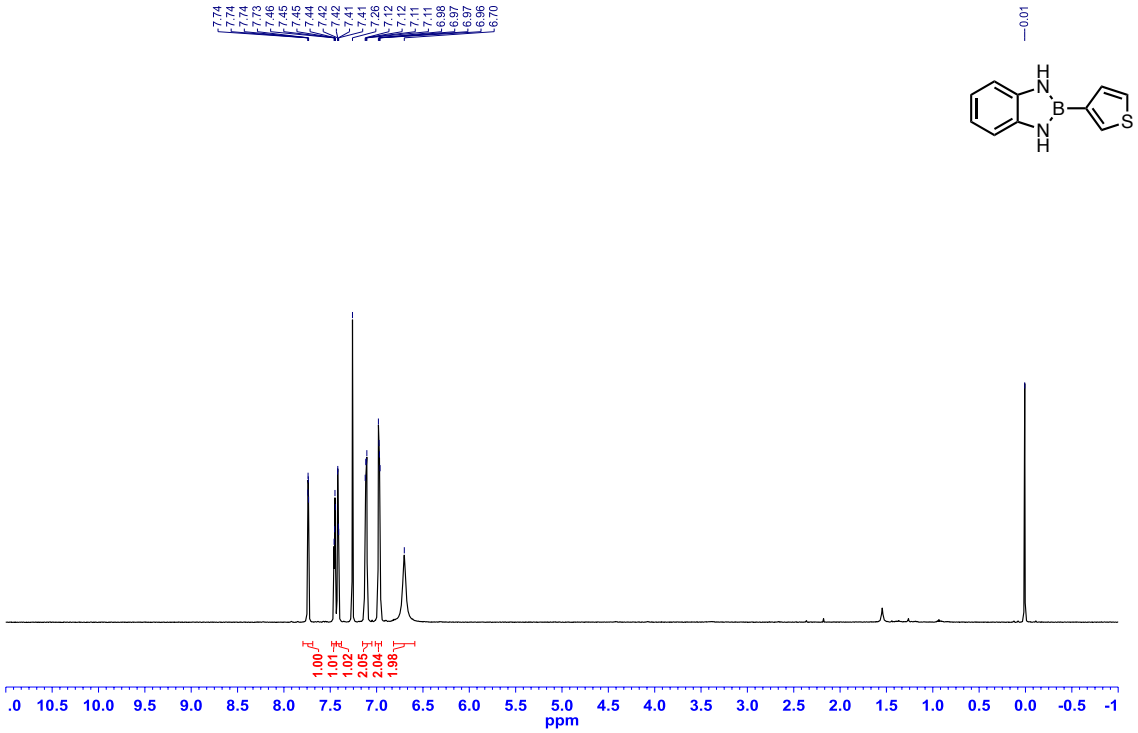

Figure A1.65: ^{13}C {^{1}H} NMR ($CDCl_3$, 125.8 MHz) of 2-(3-thienyl)-2,3-dihydro-1*H*-1,3,2-benzodiazaborole (**2.21**)

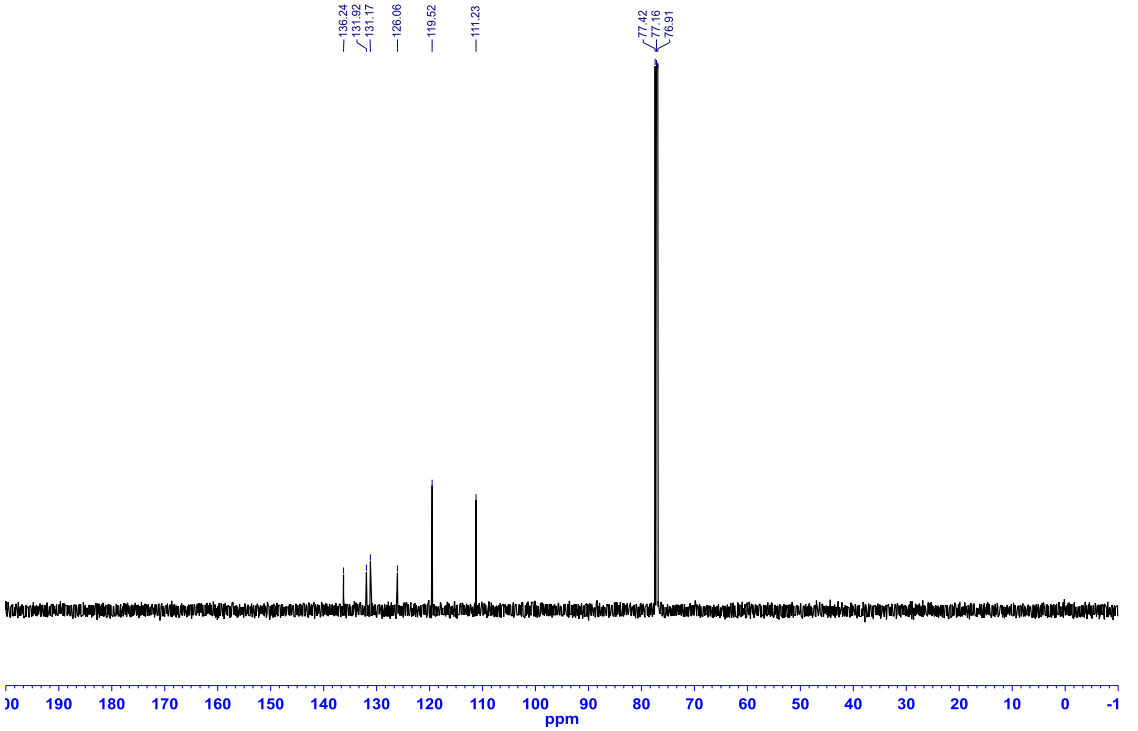

Figure A1.66: ^{11}B NMR (MeCN, 128.4 MHz) of 2-(3-thienyl)-2,3-dihydro-1*H*-1,3,2-benzodiazaborole (**2.21**)

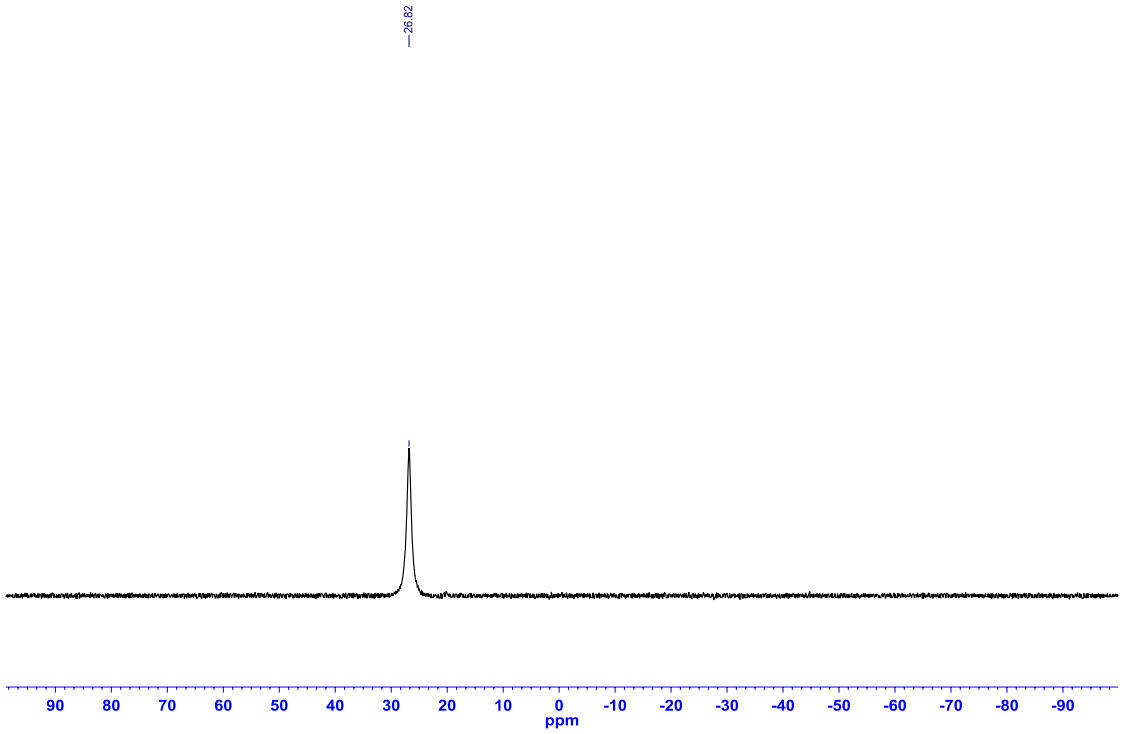

Figure A1.67: ^{1}H NMR ($CDCl_3$, 500.4 MHz) of 2-(2-benzofuranyl)-2,3-dihydro-1*H*-1,3,2-benzodiazaborole (**2.22**)

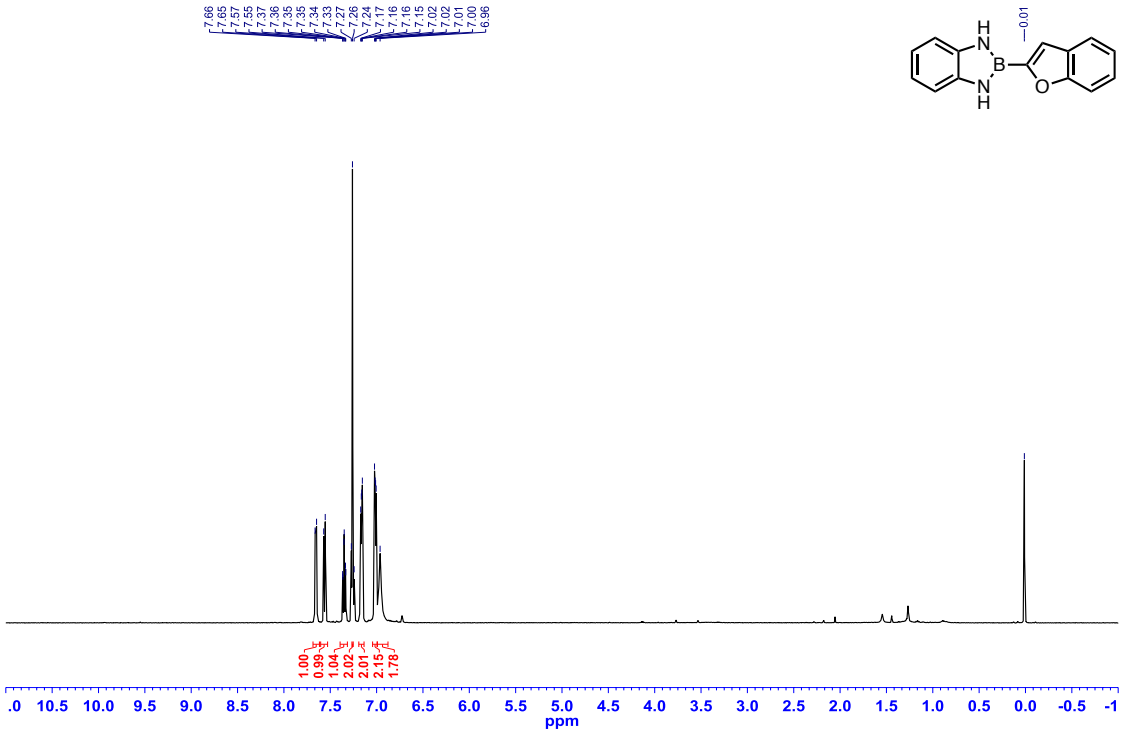

Figure A1.68: ^{13}C {^{1}H} NMR (DMSO-d_6, 125.8 MHz) of 2-(2-benzofuranyl)-2,3-dihydro-1*H*-1,3,2-benzodiazaborole (**2.22**)

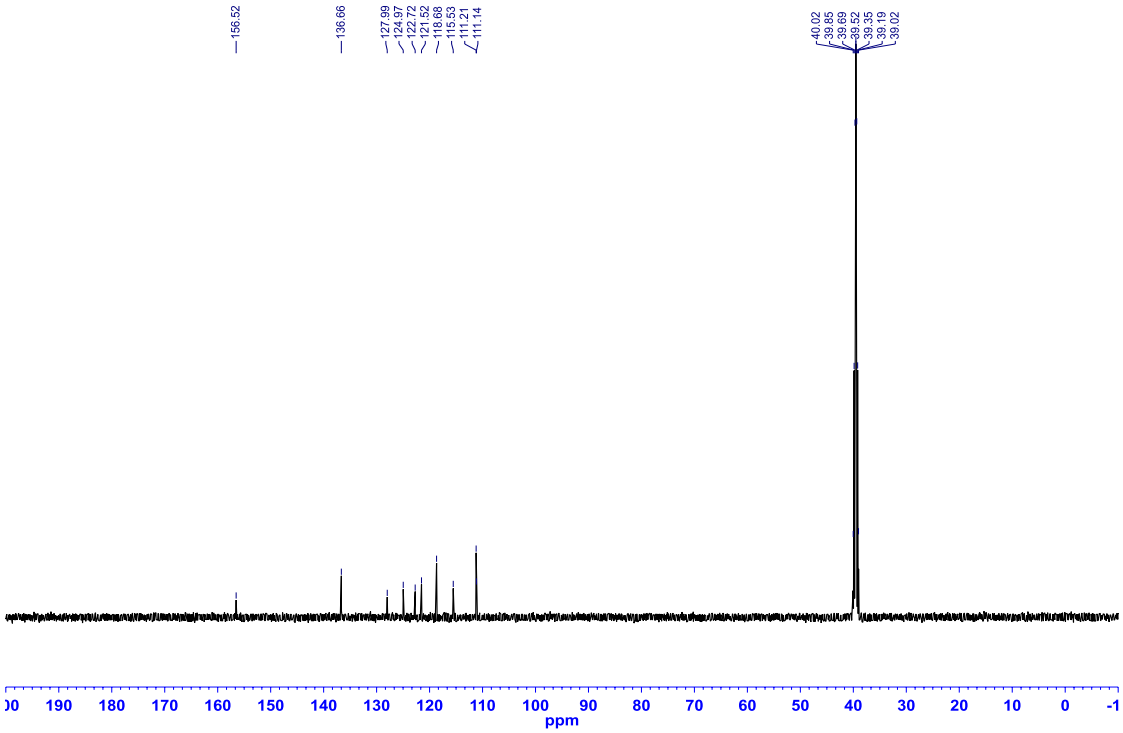

Figure A1.69: ^{11}B NMR (MeCN, 128.4 MHz) of 2-(2-benzofuranyl)-2,3-dihydro-1*H*-1,3,2-benzodiazaborole (**2.22**)

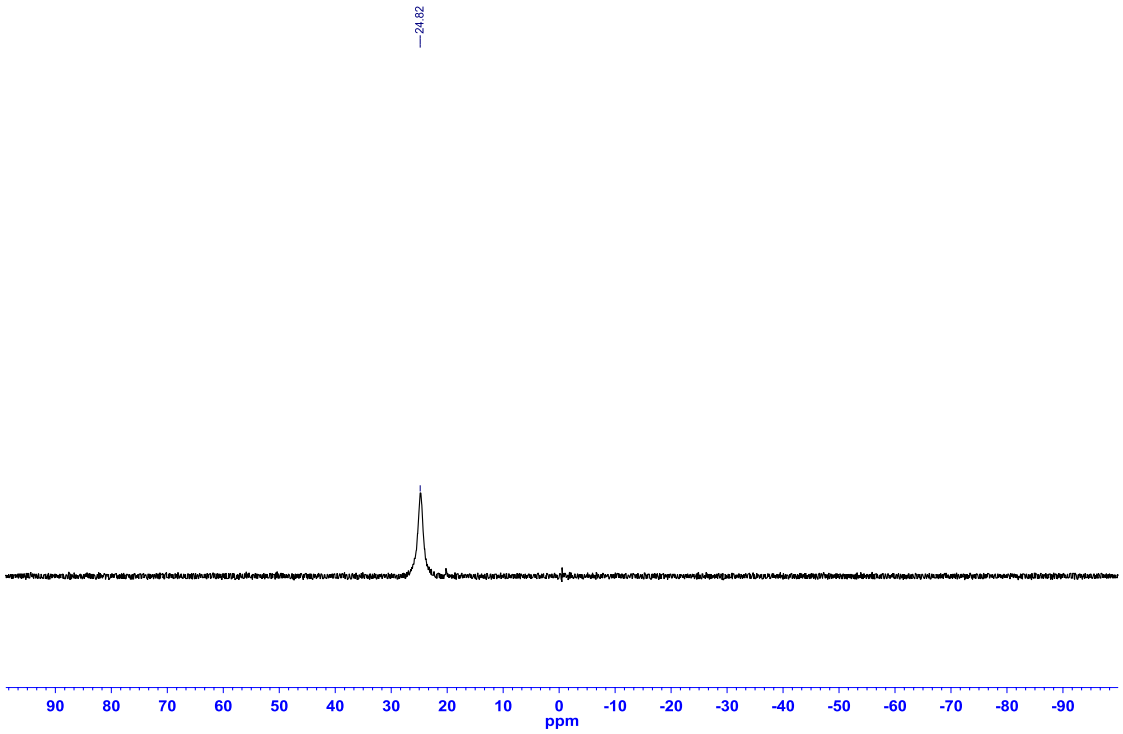

Figure A1.70: ^{1}H NMR ($CDCl_3$, 500.4 MHz) of 2-(2-furyl)-1-methyl-2,3-dihydro-1*H*-1,3,2-benzodiazaborole (**2.23**)

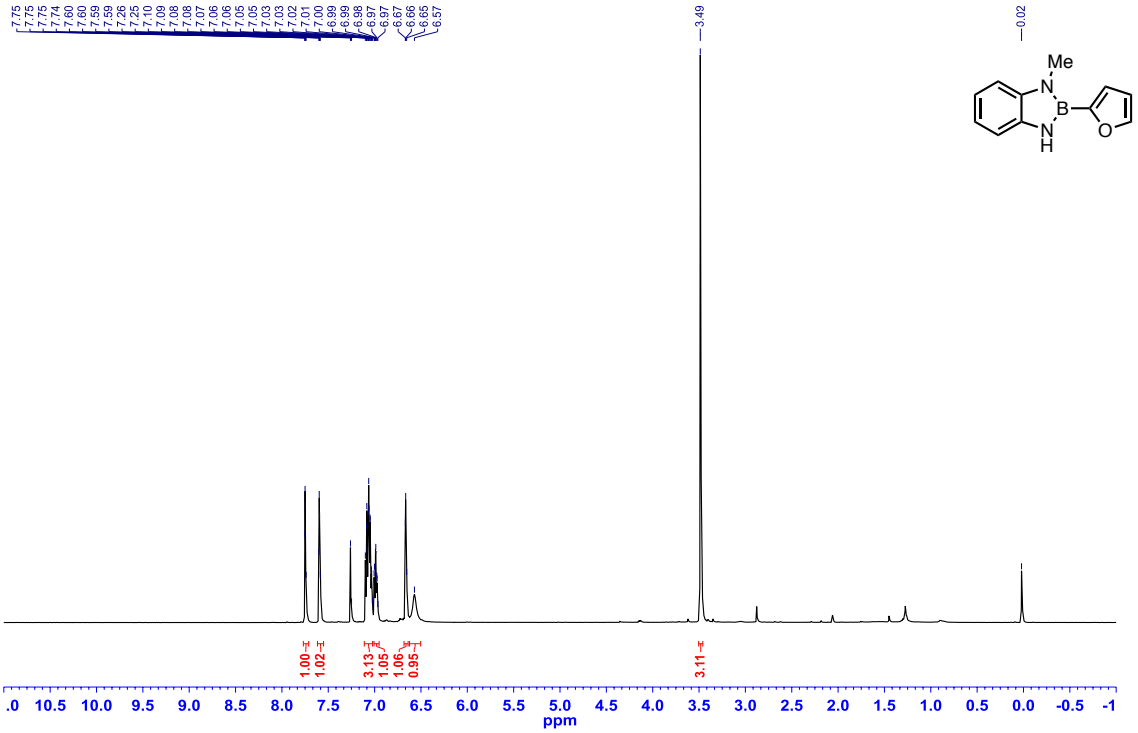

Figure A1.71: ^{13}C {^{1}H} NMR ($CDCl_3$, 125.8 MHz) of 2-(2-furyl)-1-methyl-2,3-dihydro-1*H*-1,3,2-benzodiazaborole (**2.23**)

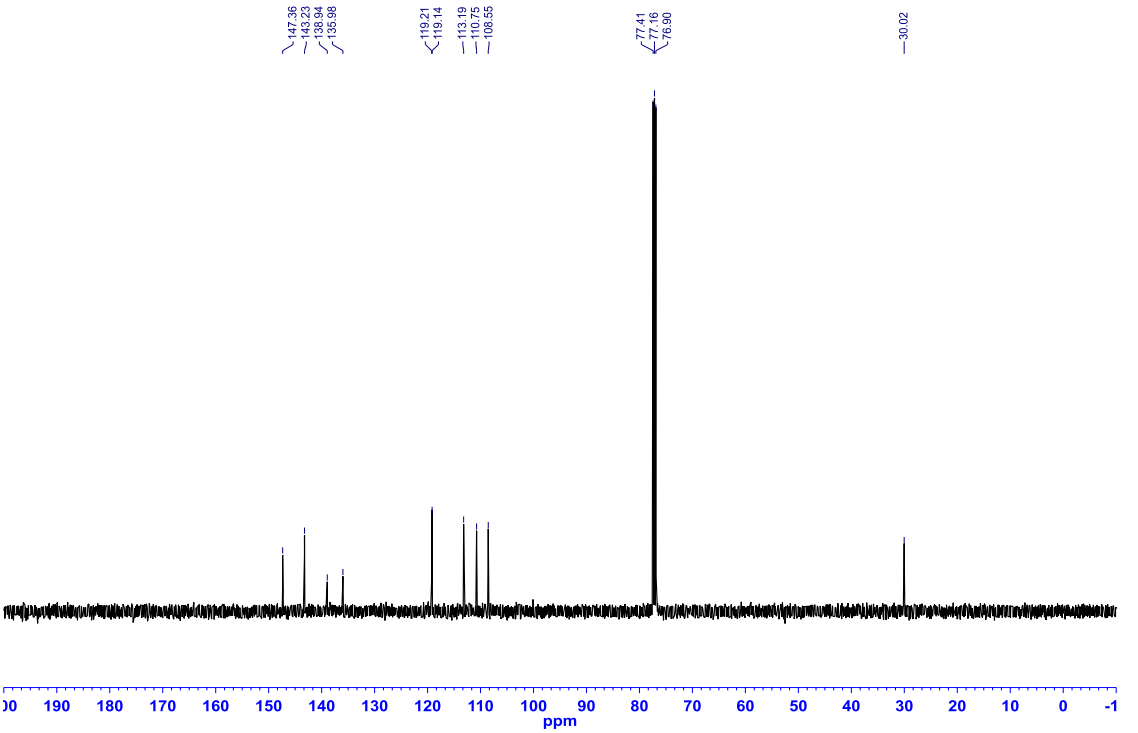

Figure A1.72: ^{11}B NMR (MeCN, 128.4 MHz) of 2-(2-furyl)-1-methyl-2,3-dihydro-1*H*-1,3,2-benzodiazaborole (**2.23**)

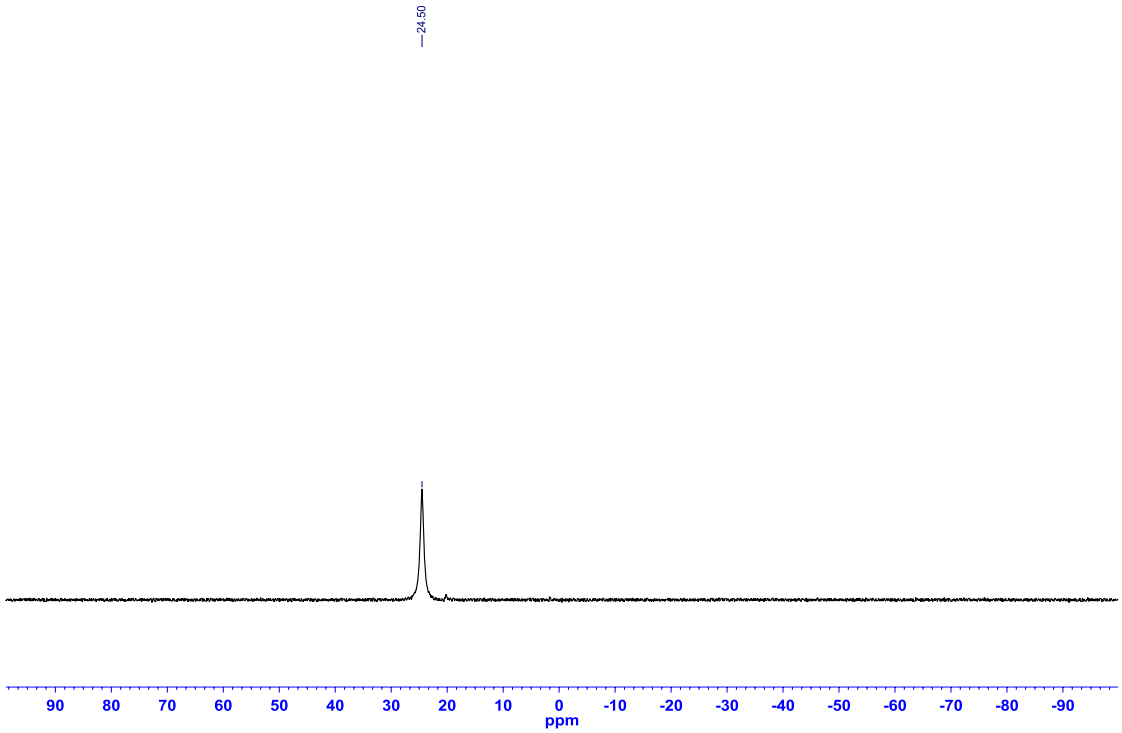

Figure A1.73: ^{1}H NMR ($CDCl_3$ with 1% TMS, 500.4 MHz) of 5-methyl-2-phenyl-2,3-dihydro-1*H*-1,3,2-benzodiazaborole (**2.25**)

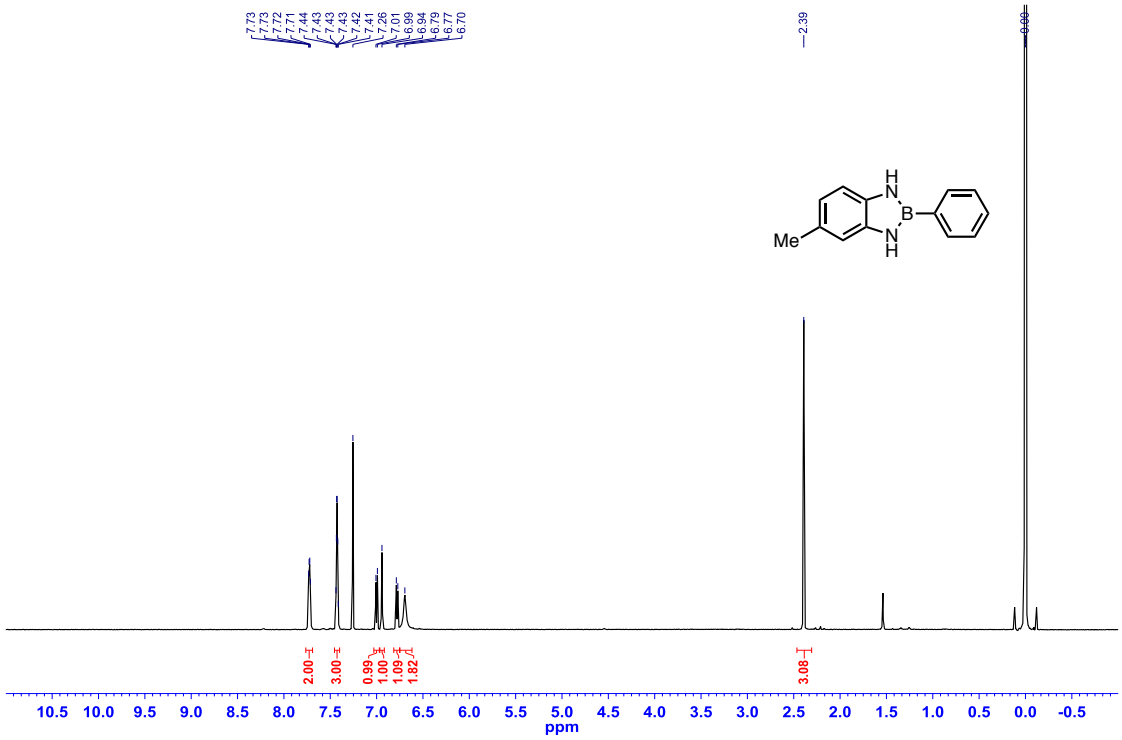

Figure A1.74: ^{13}C {^{1}H} NMR ($CDCl_3$, 125.8 MHz) of 5-methyl-2-phenyl-2,3-dihydro-1*H*-1,3,2-benzodiazaborole (**2.25**)

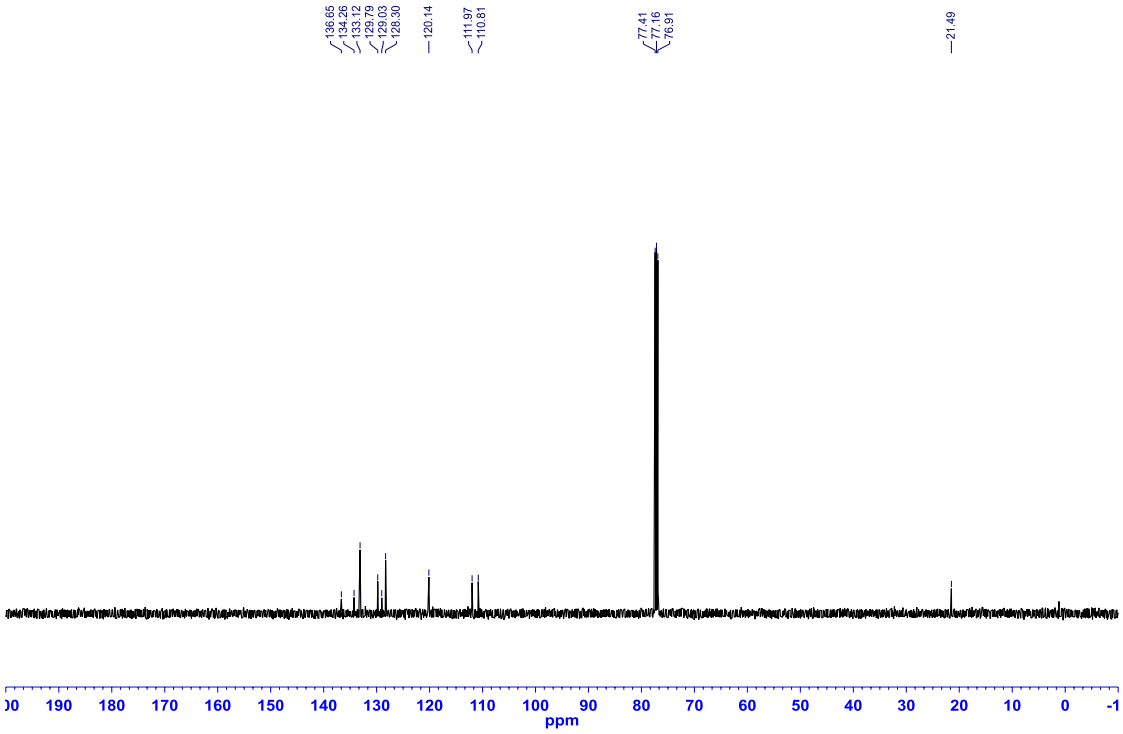

Figure A1.75: ^{11}B NMR (MeCN, 128.4 MHz) of 5-methyl-2-phenyl-2,3-dihydro-1*H*-1,3,2-benzodiazaborole (**2.25**)

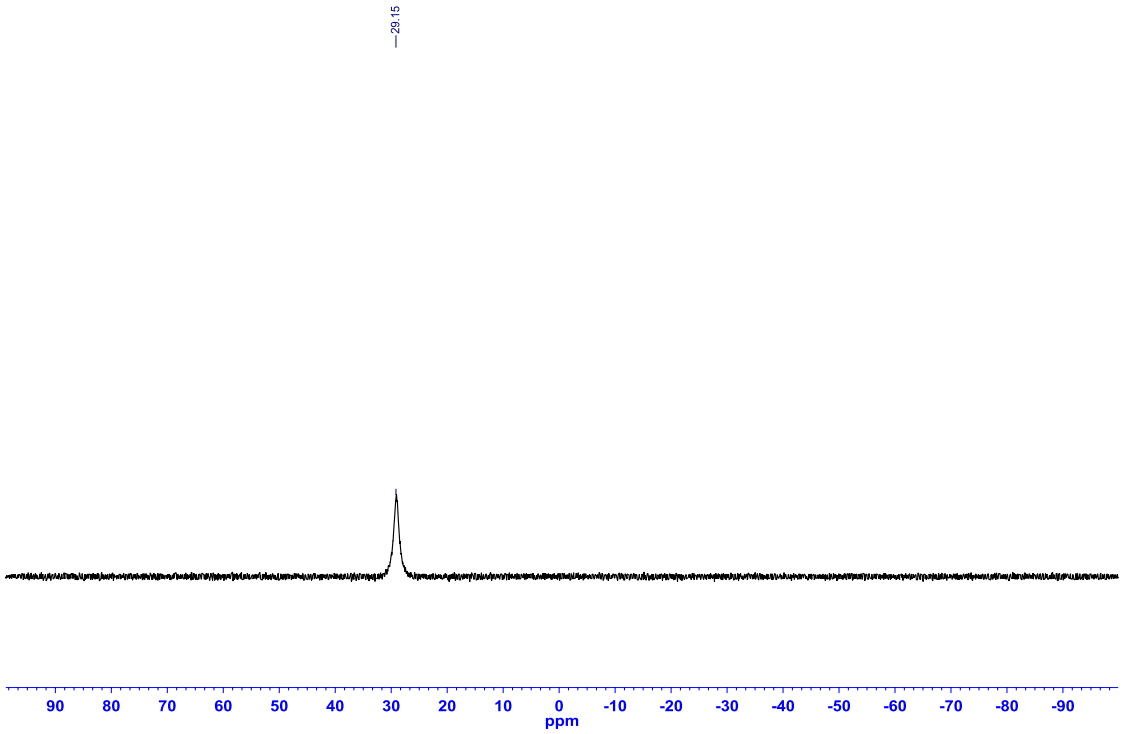

Figure A1.76: ^{1}H NMR ($CDCl_3$, 500.4 MHz) of 5-fluoro-2-phenyl-2,3-dihydro-1*H*-1,3,2-benzodiazaborole (**2.26**)

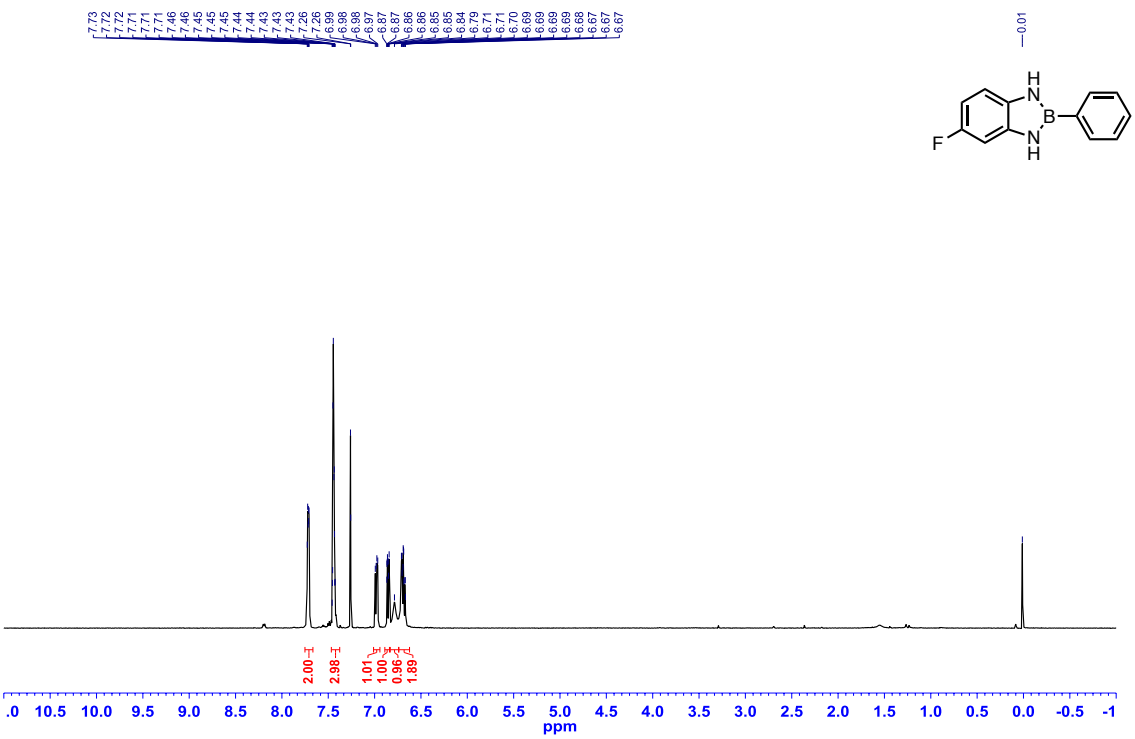

Figure A1.77: ^{13}C {^{1}H} NMR ($CDCl_3$, 125.8 MHz) of 5-fluoro-2-phenyl-2,3-dihydro-1*H*-1,3,2-benzodiazaborole (**2.26**)

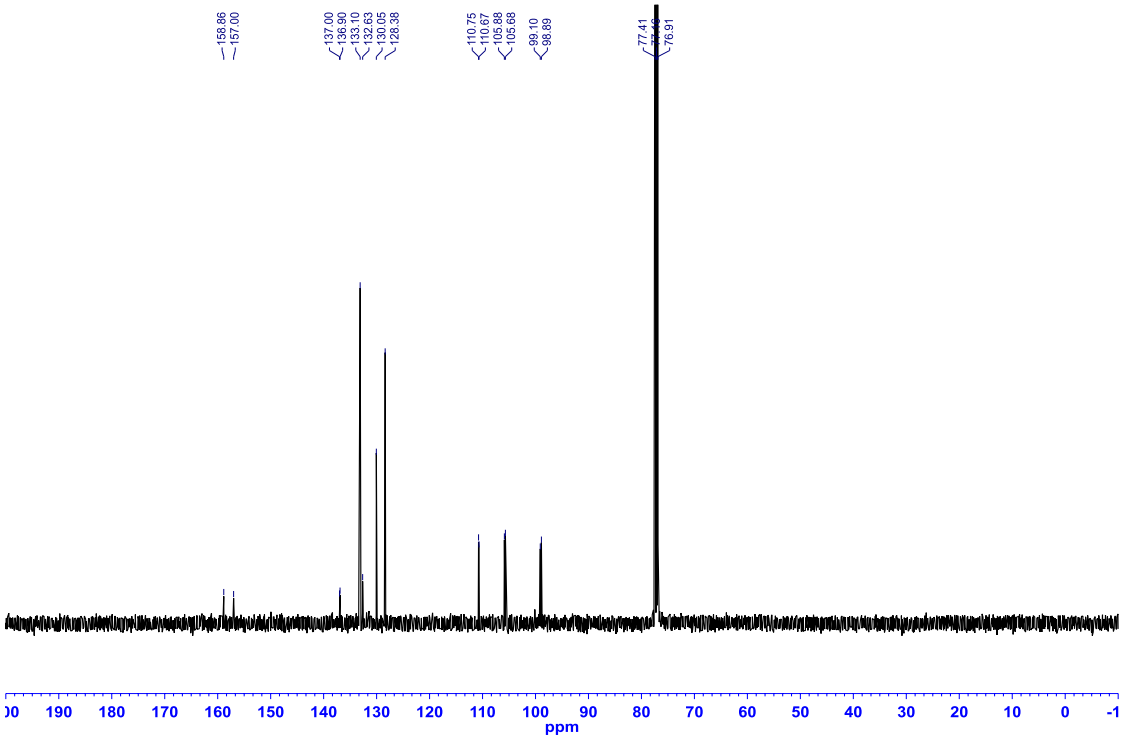

Figure A1.78: ^{19}F {^{1}H} NMR ($CDCl_3$, 282.4 MHz) of 5-fluoro-2-phenyl-2,3-dihydro-1*H*-1,3,2-benzodiazaborole (**2.26**)

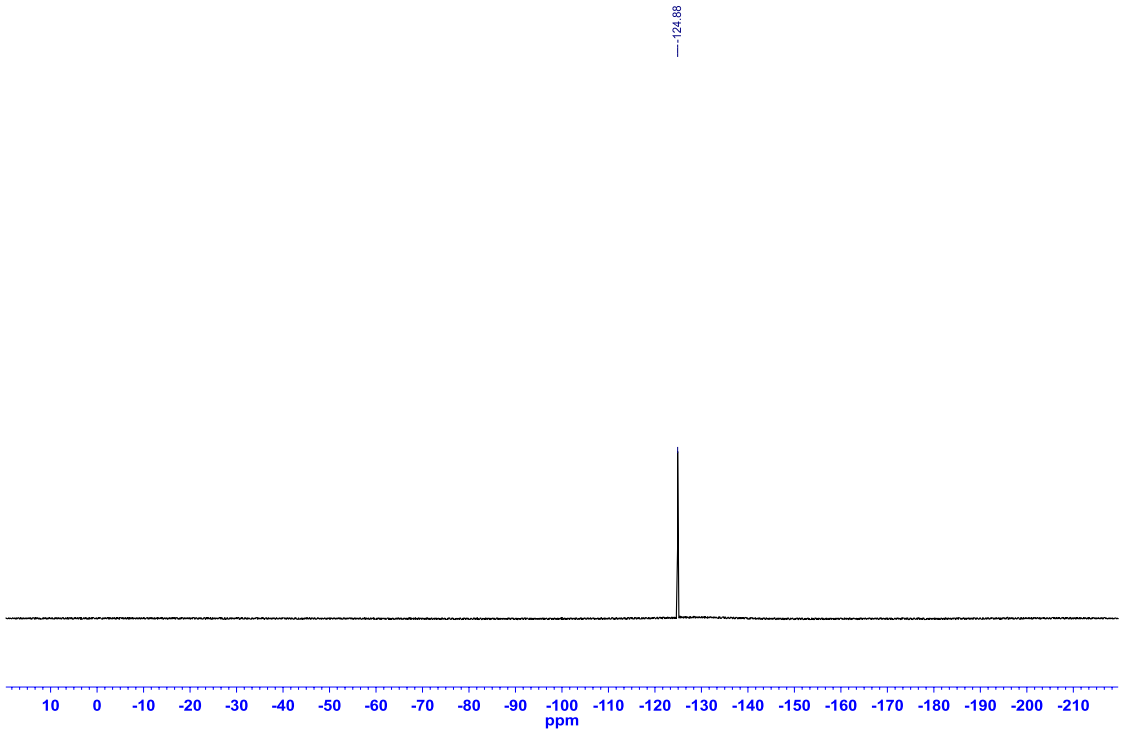

Figure A1.79: ^{11}B NMR (MeCN, 128.4) of 5-fluoro-2-phenyl-2,3-dihydro-1*H*-1,3,2-benzodiazaborole (**2.26**)

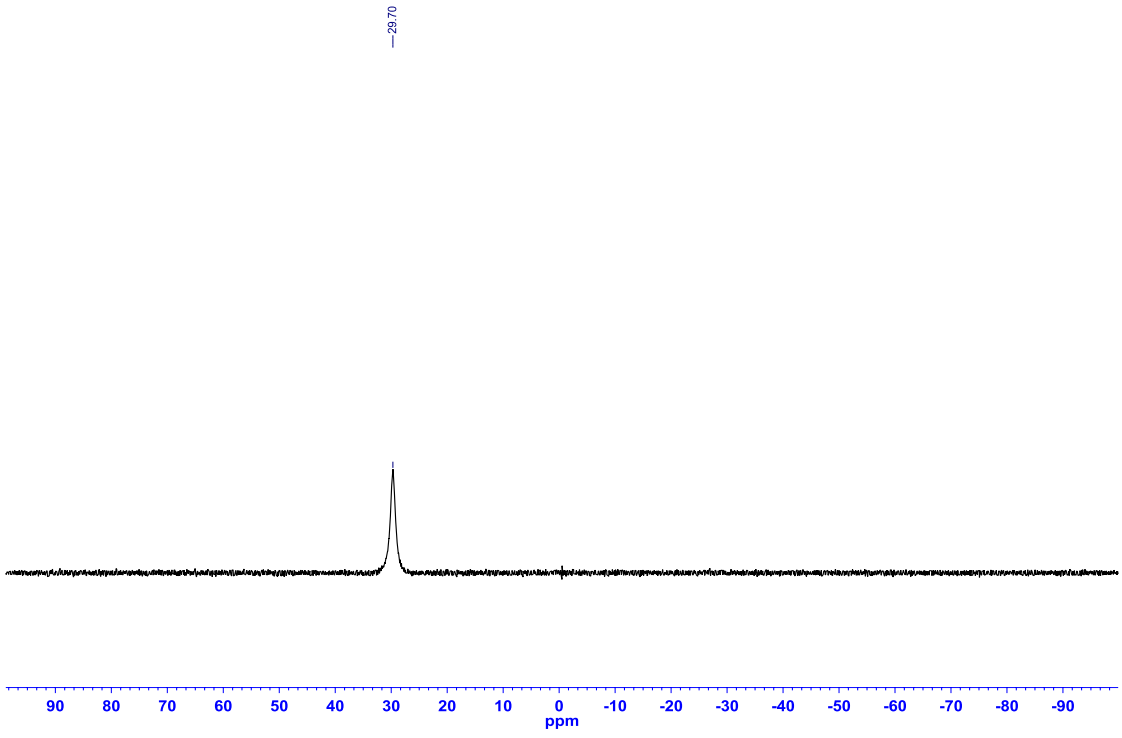

Figure A1.80: ^{1}H NMR ($CDCl_3$, 500.4 MHz) of 5-bromo-2-phenyl-2,3-dihydro-1*H*-1,3,2-benzodiazaborole (**2.27**)

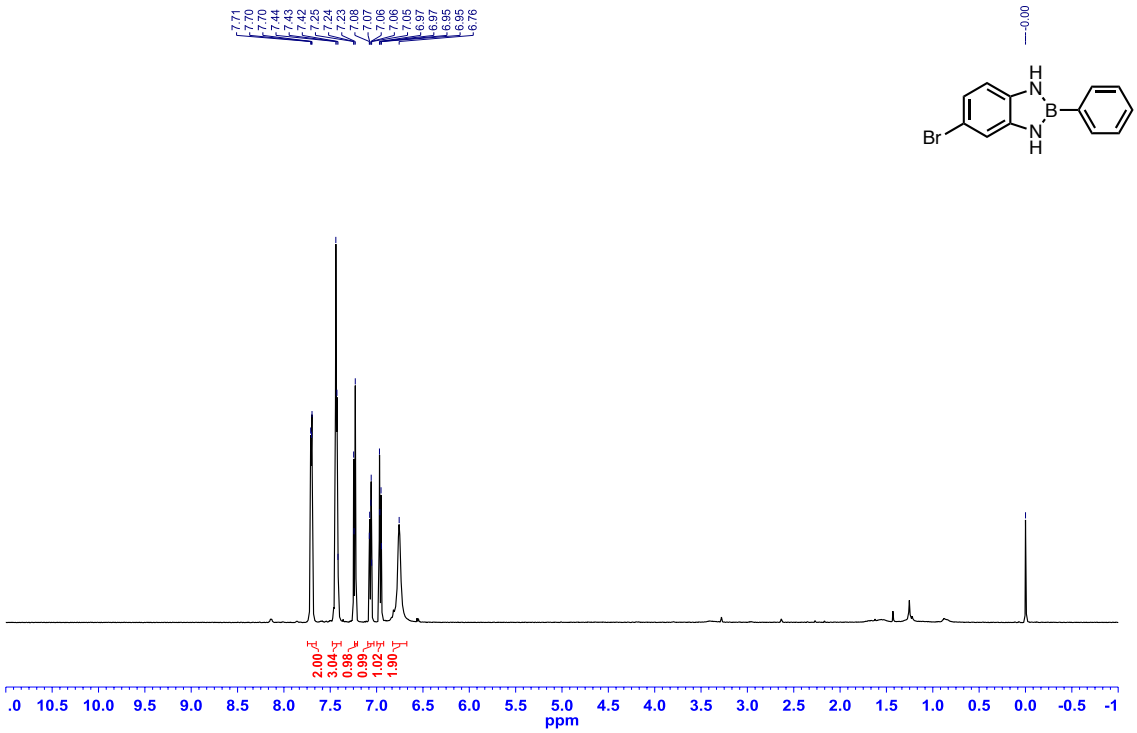

Figure A1.81: ^{13}C {^{1}H} NMR ($CDCl_3$, 125.8 MHz) of 5-bromo-2-phenyl-2,3-dihydro-1*H*-1,3,2-benzodiazaborole (**2.27**)

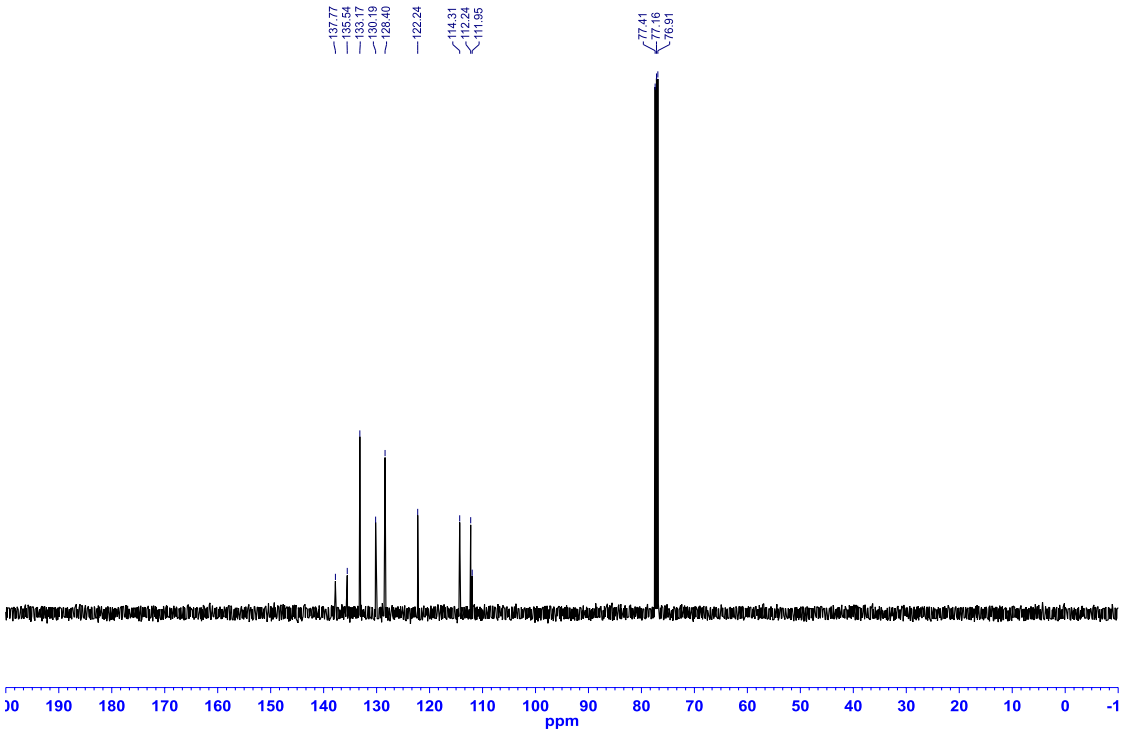

Figure A1.82: ^{11}B NMR (MeCN, 128.4 MHz) of 5-bromo-2-phenyl-2,3-dihydro-1*H*-1,3,2-benzodiazaborole (**2.27**)

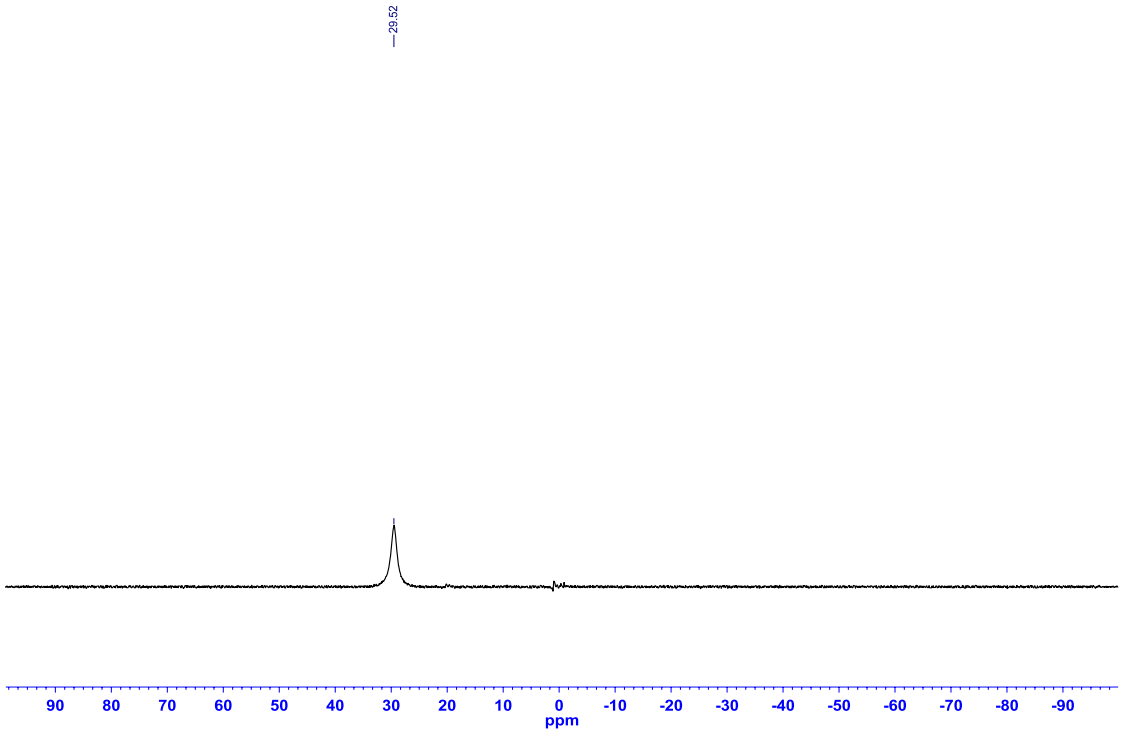

Figure A1.83: ^{1}H NMR (DMSO-d_6, 500.4 MHz) of 5-phenylcarbonyl-2-phenyl-2,3-dihydro-1*H*-1,3,2-benzodiazaborole (**2.28**)

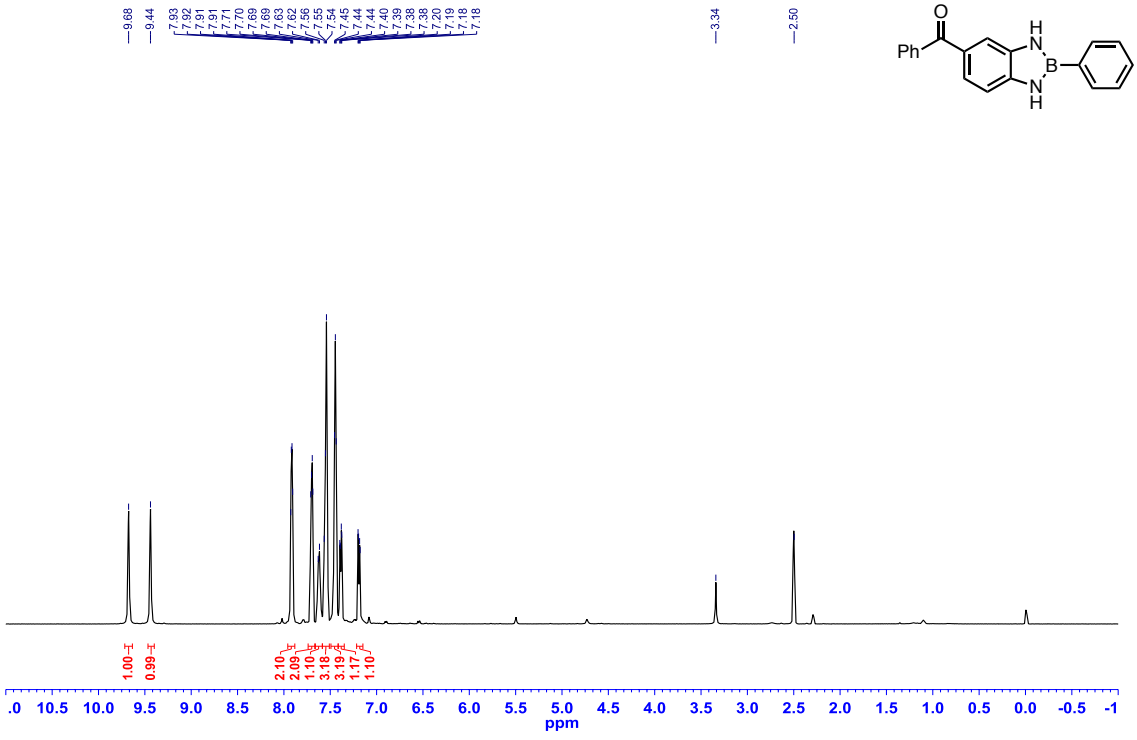

Figure A1.84: ^{13}C {^{1}H} NMR (DMSO-d_6, 125.8 MHz) of 5-phenylcarbonyl-2-phenyl-2,3-dihydro-1*H*-1,3,2-benzodiazaborole (**2.28**)

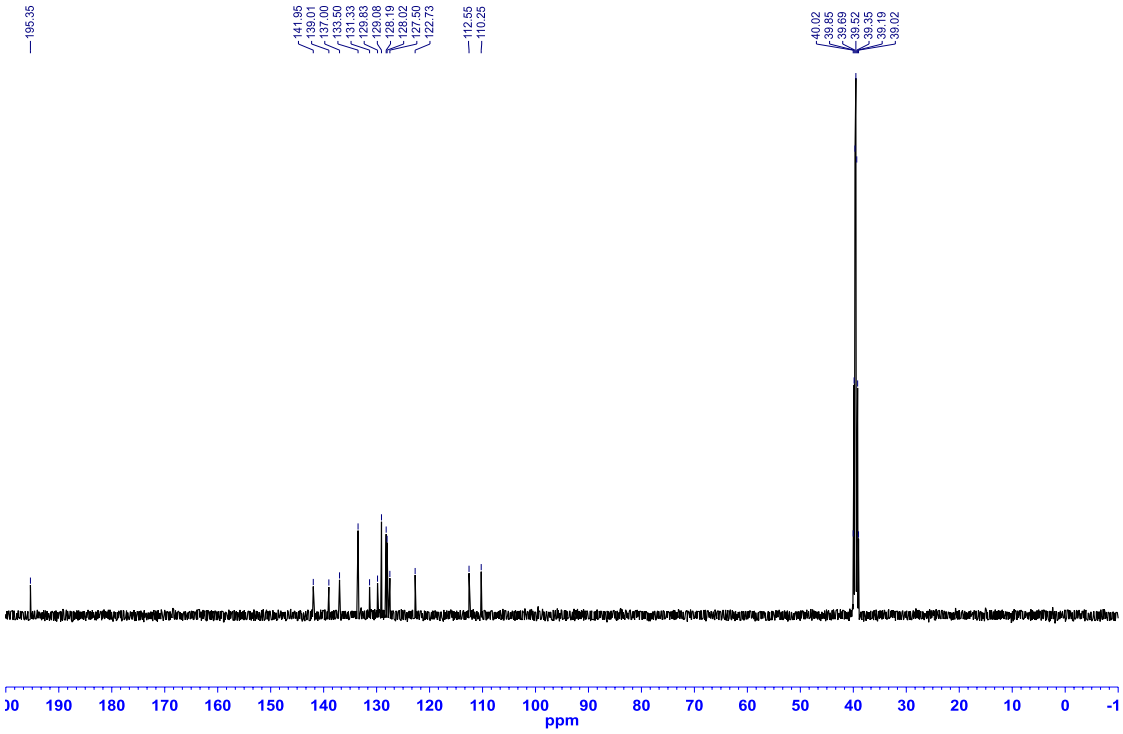

Figure A1.85: ^{11}B NMR (MeCN, 128.4 MHz) of 5-phenylcarbonyl-2-phenyl-2,3-dihydro-1*H*-1,3,2-benzodiazaborole (**2.28**)

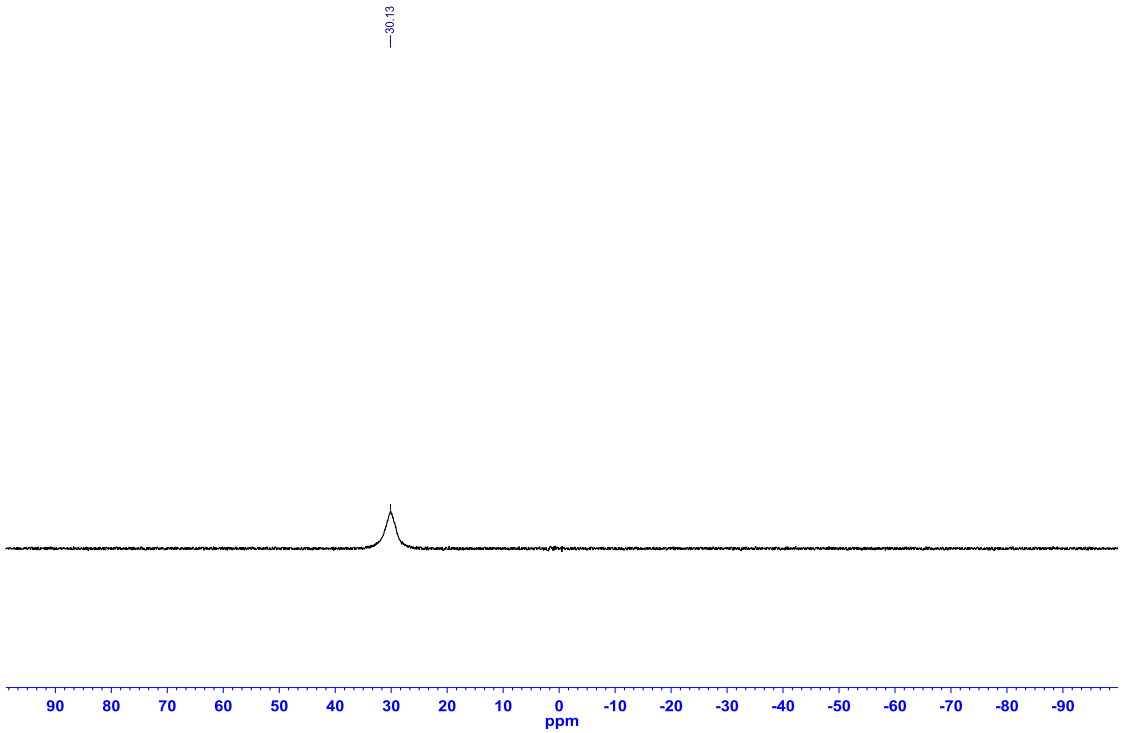

Figure A1.86: ^{1}H NMR (DMSO-d_6, 500.4 MHz) of 5-nitro-2-phenyl-2,3-dihydro-1*H*-1,3,2-benzodiazaborole (**2.29**)

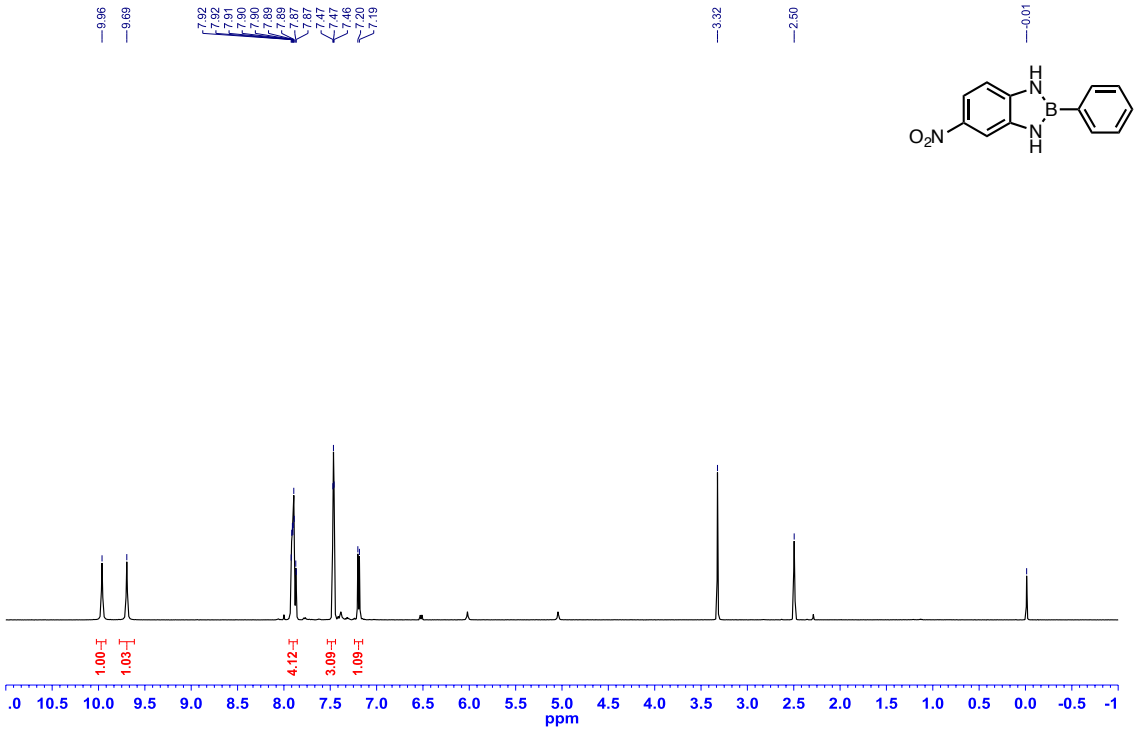

Figure A1.87: ^{13}C {^{1}H} NMR (DMSO-d_6, 125.8 MHz) of 5-nitro-2-phenyl-2,3-dihydro-1*H*-1,3,2-benzodiazaborole (**2.29**)

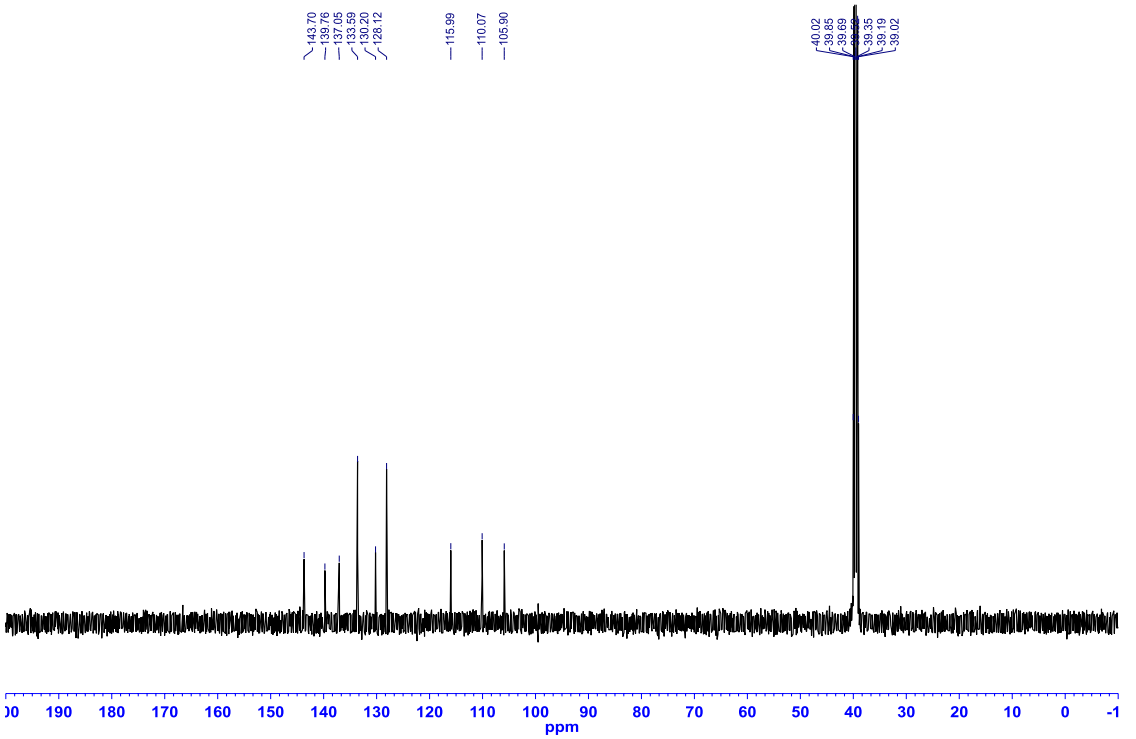

Figure A1.88: ^{11}B NMR (MeCN, 128.4 MHz) of 5-nitro-2-phenyl-2,3-dihydro-1*H*-1,3,2-benzodiazaborole (**2.29**)

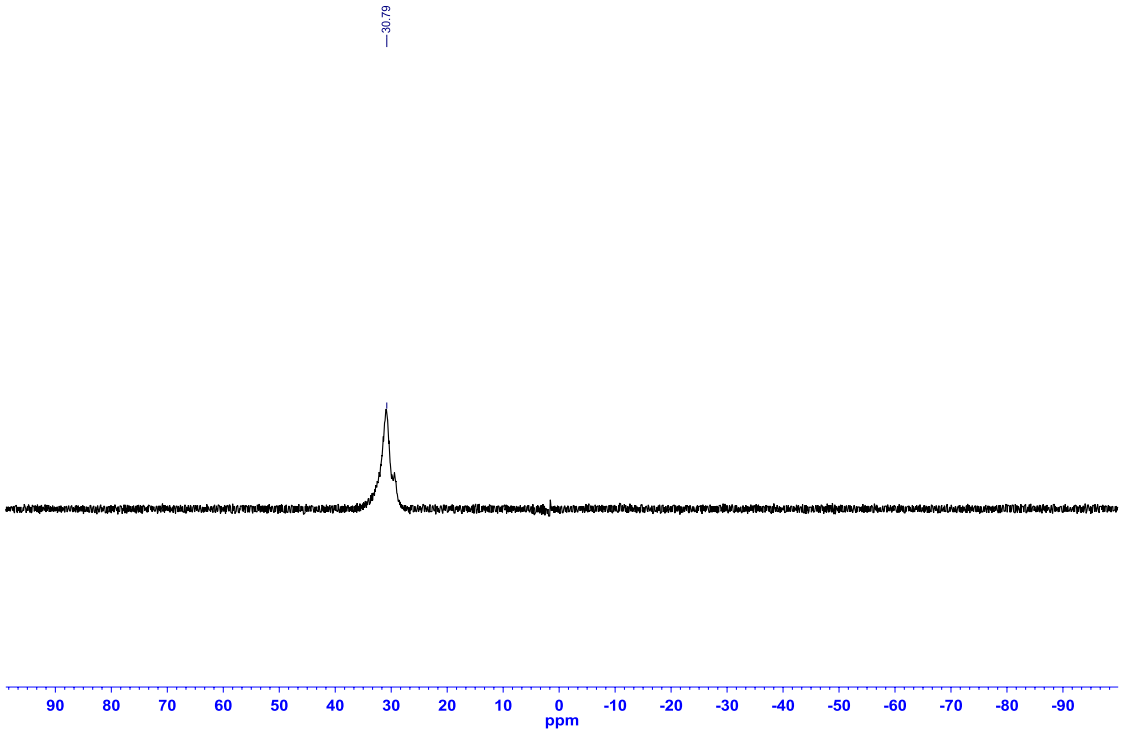

Figure A1.89: ^{1}H NMR (DMSO-d_6, 500.4 MHz) of 2-phenyl-2,3-dihydro-1*H*-1,3,2-naphthodiazaborole (**2.30**)

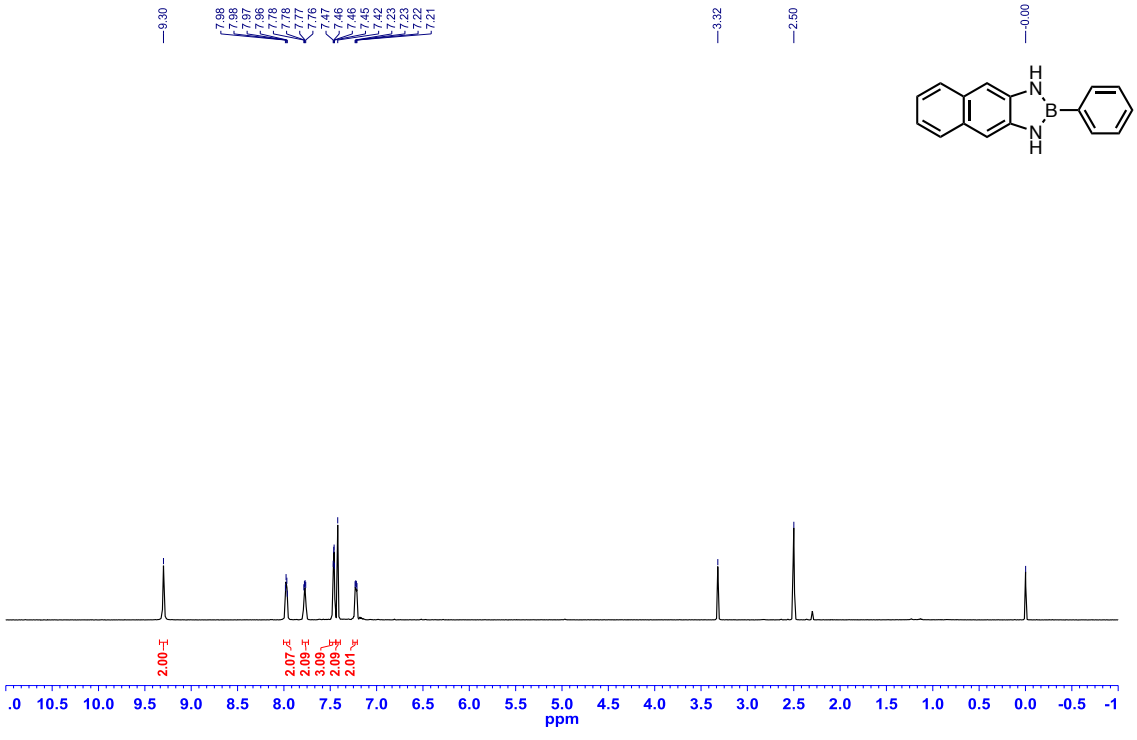

Figure A1.90: ^{13}C {^{1}H} NMR (DMSO-d_6, 125.8 MHz) of 2-phenyl-2,3-dihydro-1*H*-1,3,2-naphthodiazaborole (**2.30**)

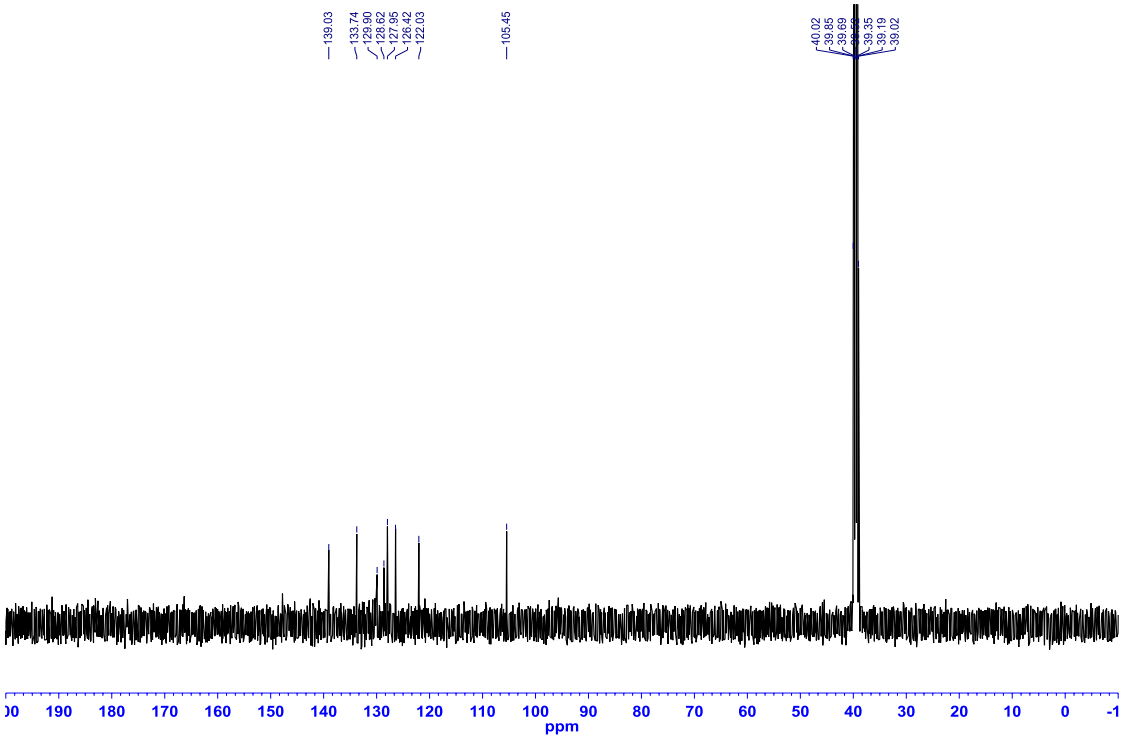

Figure A1.91: ^{11}B NMR (MeCN, 128.4 MHz) of 2-phenyl-2,3-dihydro-1*H*-1,3,2-naphthodiazaborole (**2.30**)

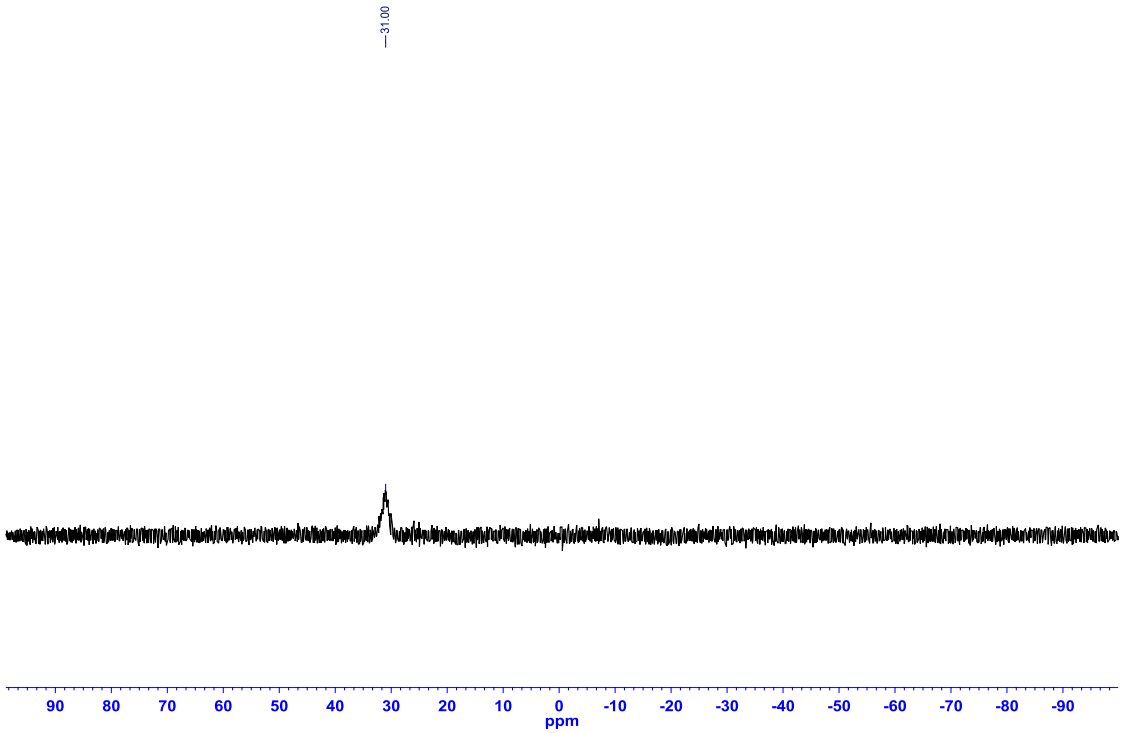

Figure A1.92: ^{1}H NMR ($CDCl_3$, 500.4 MHz) of (*E*)-2-(1-propenyl)-2,3-dihydro-1*H*-1,3,2-benzodiazaborole (**2.31**)

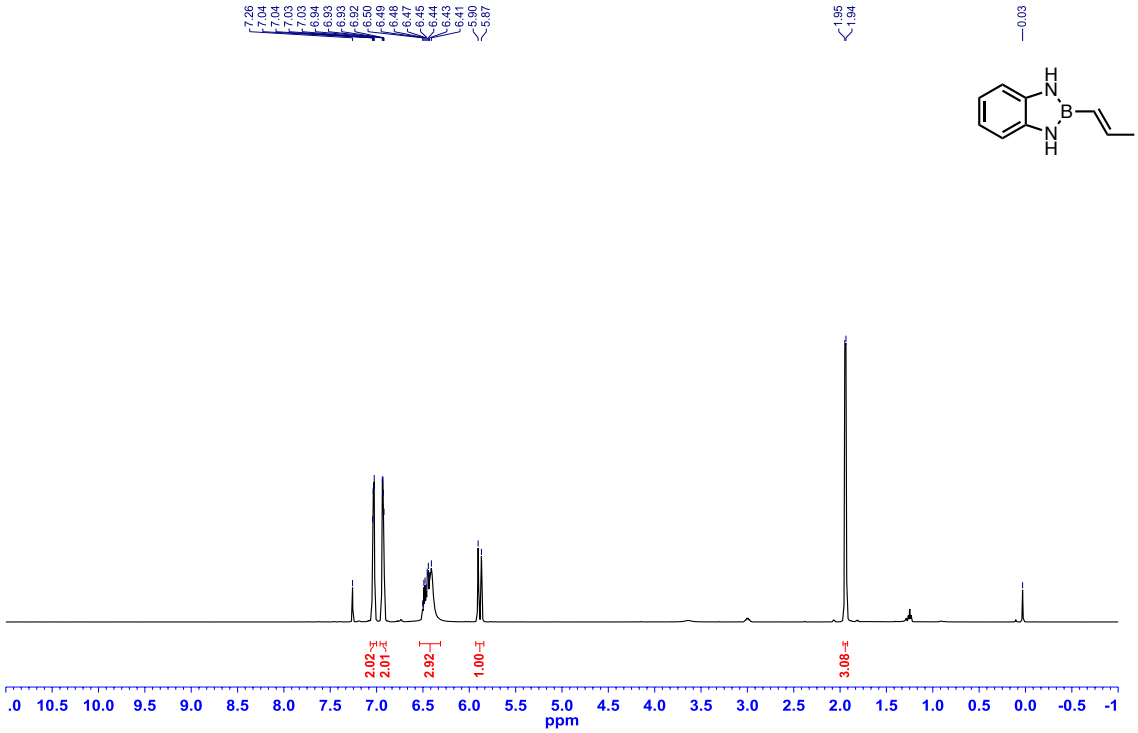

Figure A1.93: ^{13}C {^{1}H} NMR ($CDCl_3$, 125.8 MHz) of (*E*)-2-(1-propenyl)-2,3-dihydro-1*H*-1,3,2-benzodiazaborole (**2.31**)

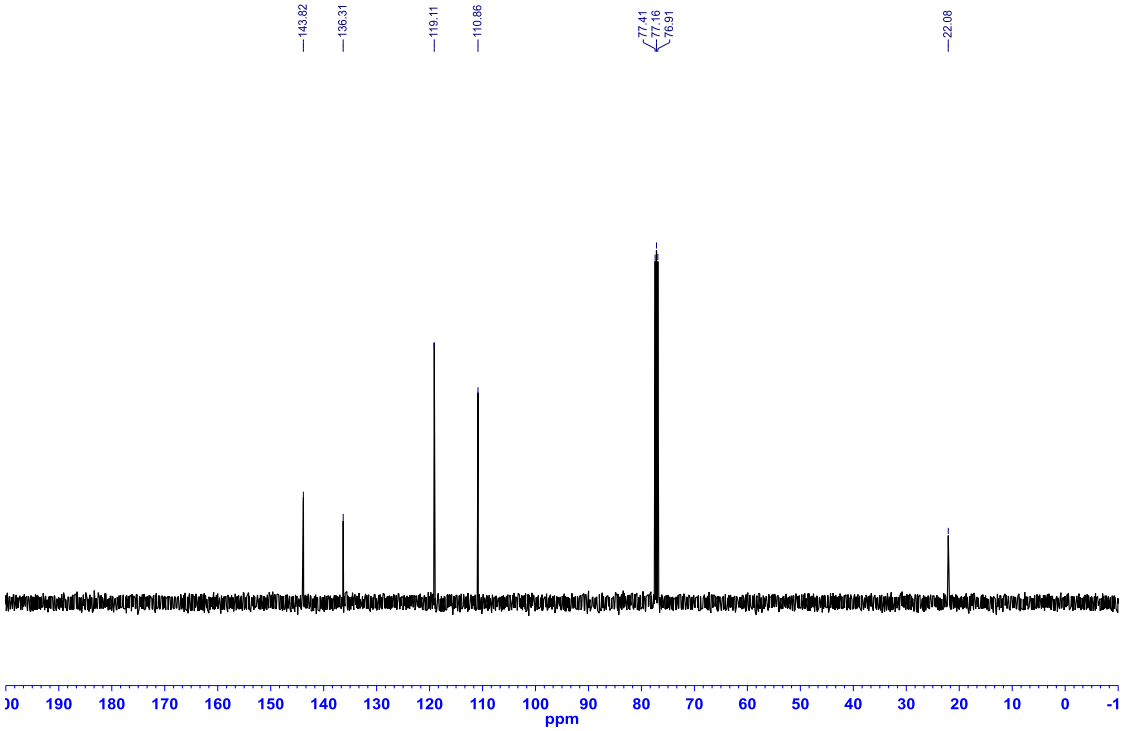

Figure A1.94: ^{11}B NMR ($CDCl_3$, 128.4 MHz) of (*E*)-2-(1-propenyl)-2,3-dihydro-1*H*-1,3,2-benzodiazaborole (**2.31**)

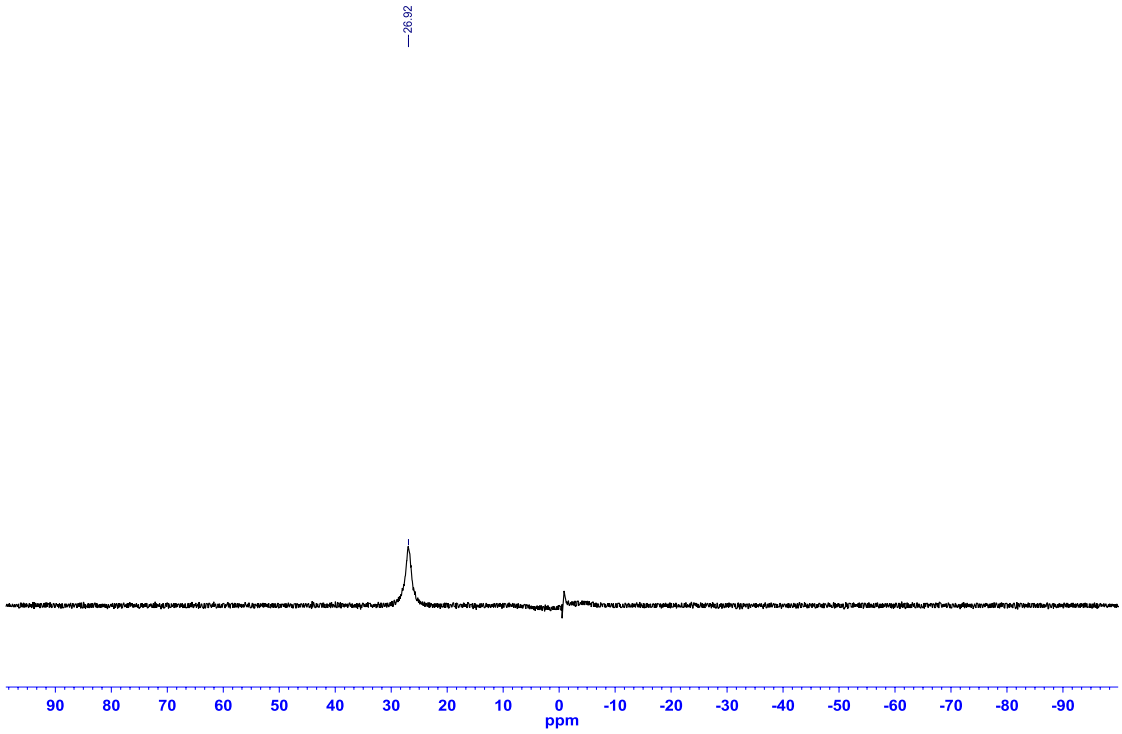

Figure A1.95: ^{1}H NMR ($CDCl_3$, 500.4 MHz) of 2-(1-cyclohexenyl)-2,3-dihydro-1*H*-1,3,2-benzodiazaborole (**2.32**)

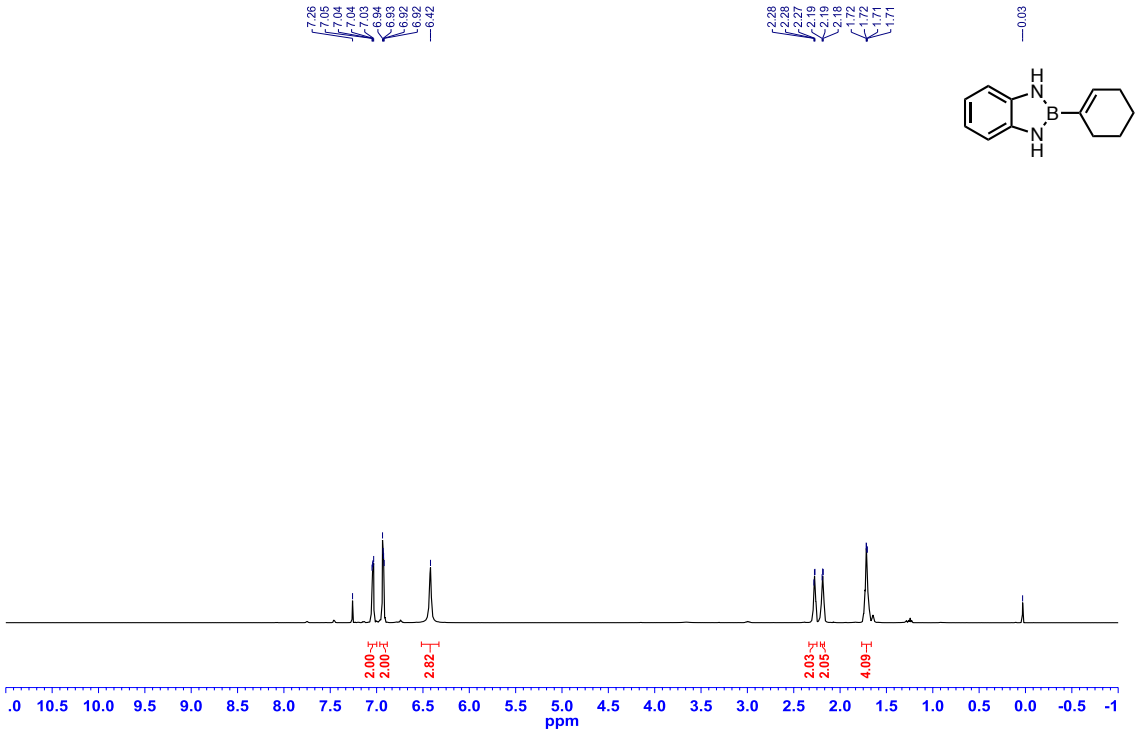

Figure A1.96: ^{13}C {^{1}H} NMR ($CDCl_3$, 125.8 MHz) of 2-(1-cyclohexenyl)-2,3-dihydro-1*H*-1,3,2-benzodiazaborole (**2.32**)

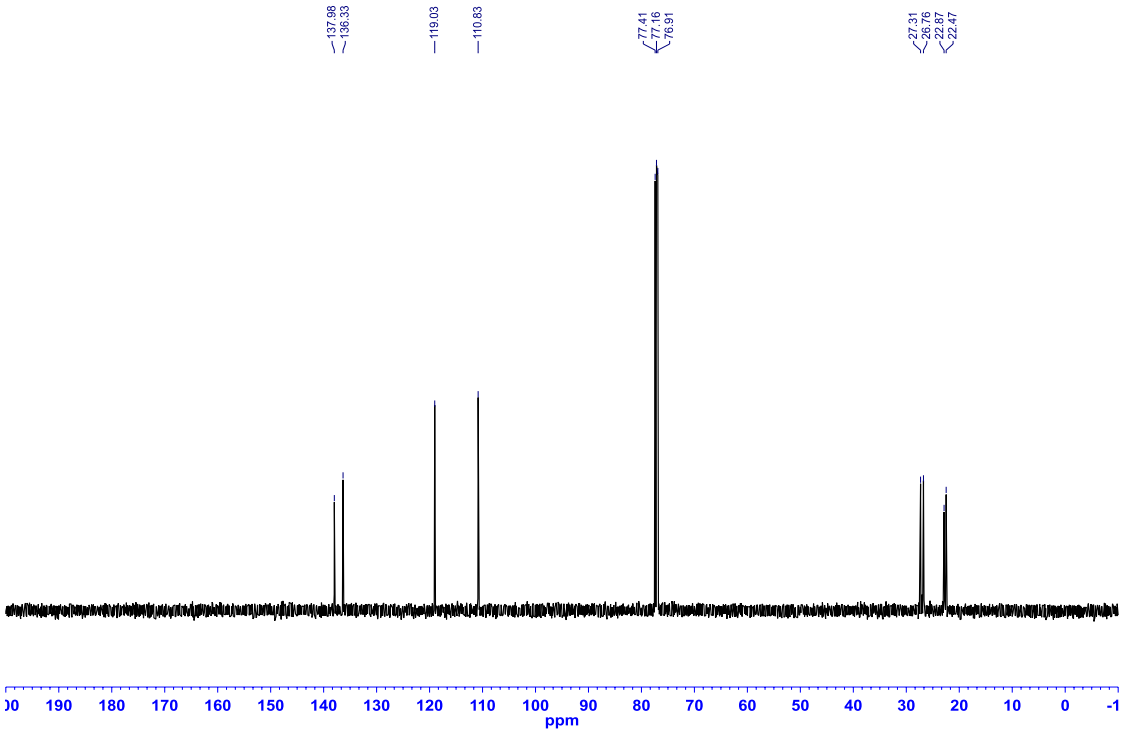

Figure A1.97: ^{11}B NMR ($CDCl_3$, 128.4 MHz) of 2-(1-cyclohexenyl)-2,3-dihydro-1*H*-1,3,2-benzodiazaborole (**2.32**)

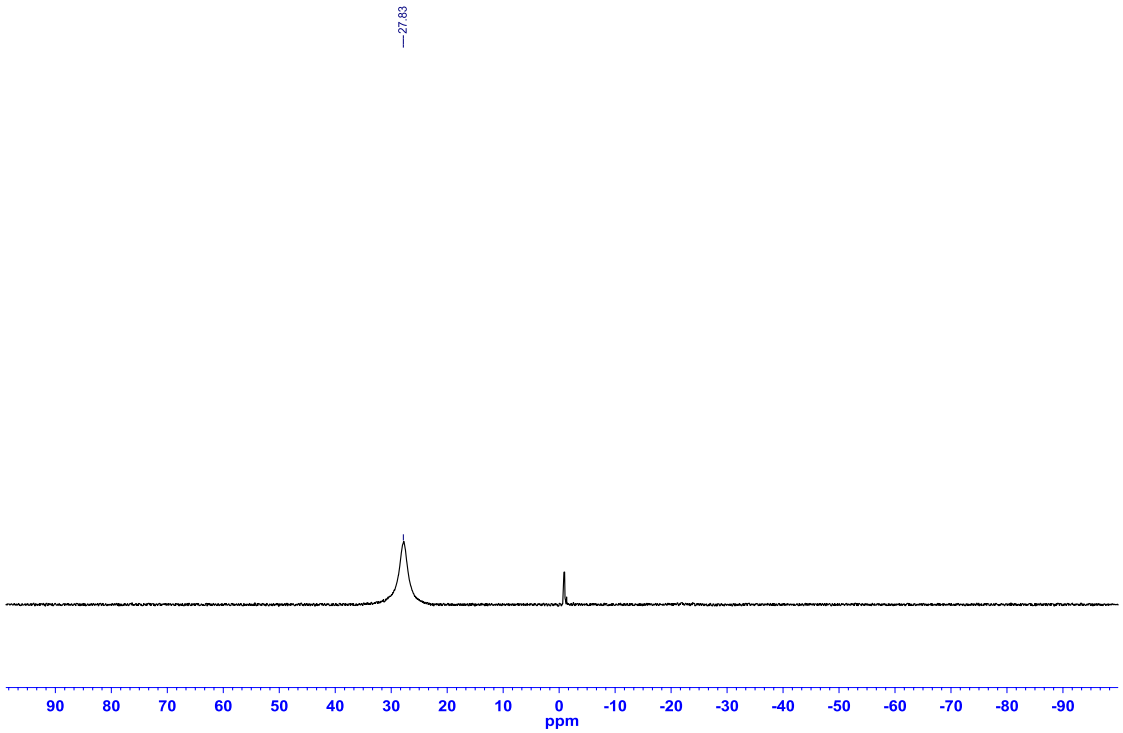

Figure A1.98: ^{1}H NMR ($CDCl_3$, 500.4 MHz) of 2-vinyl-2,3-dihydro-1*H*-1,3,2-benzodiazaborole (**2.33**)

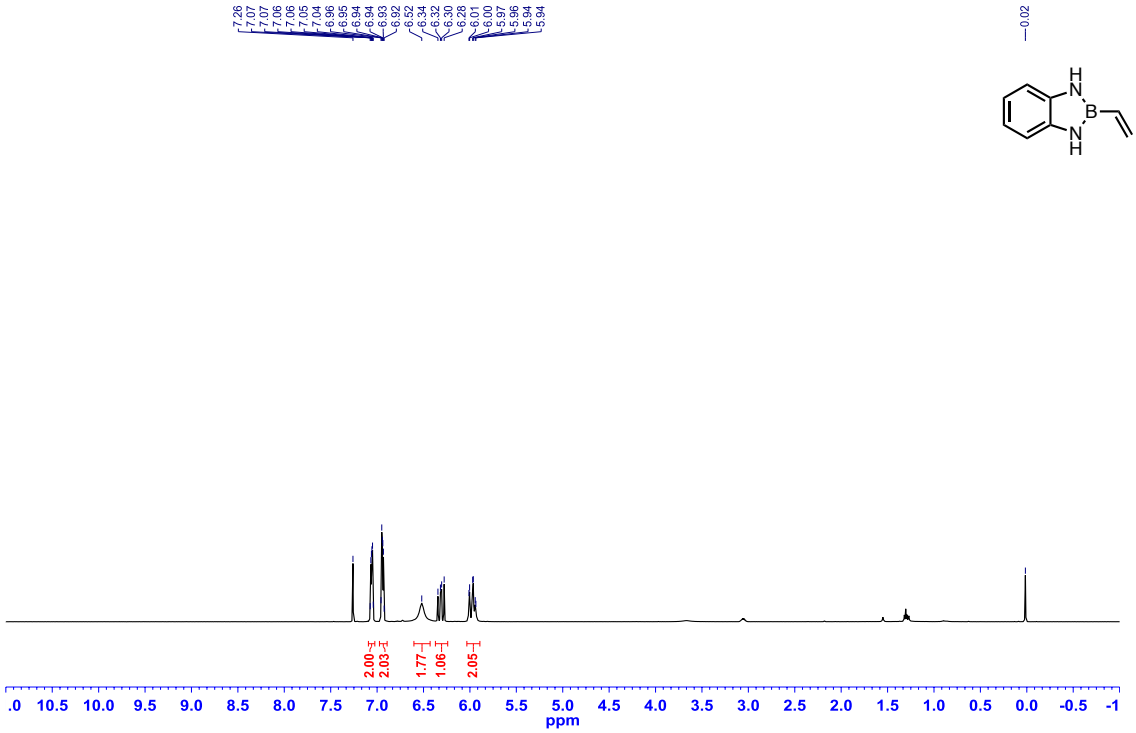

Figure A1.99: ^{13}C {^{1}H} NMR ($CDCl_3$, 125.8 MHz) of 2-vinyl-2,3-dihydro-1*H*-1,3,2-benzodiazaborole (**2.33**)

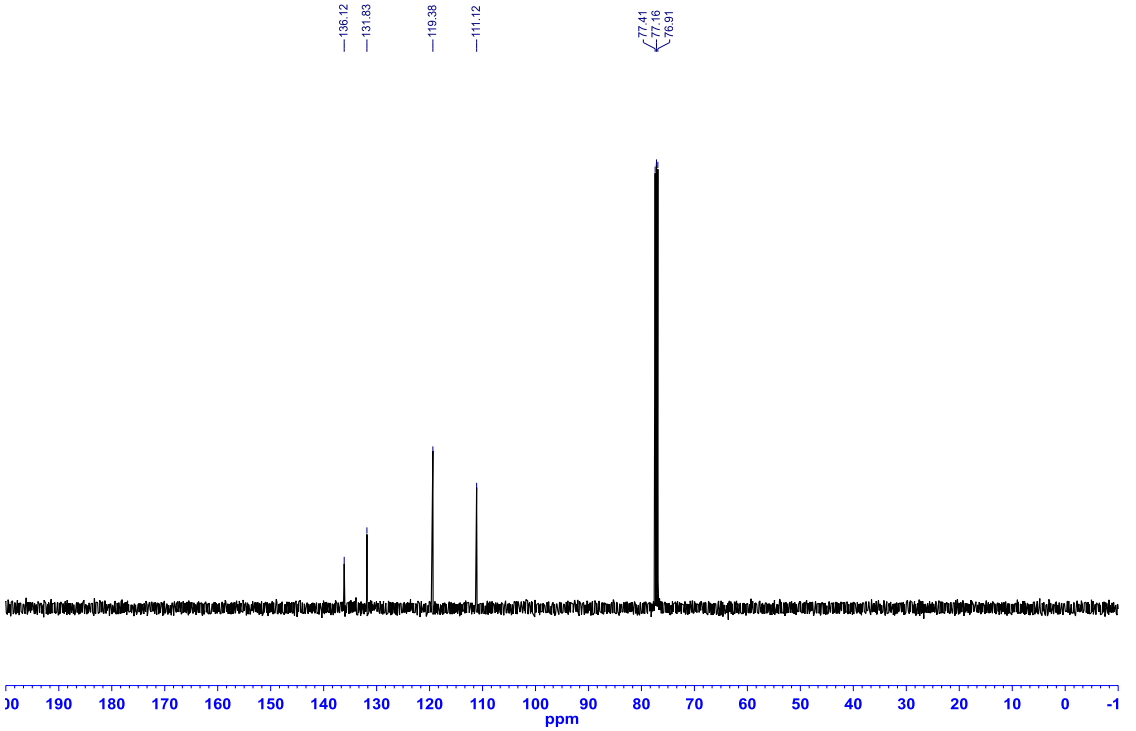

Figure A1.100: ^{11}B NMR (MeCN, 128.4 MHz) of 2-vinyl-2,3-dihydro-1*H*-1,3,2-benzodiazaborole (**2.33**)

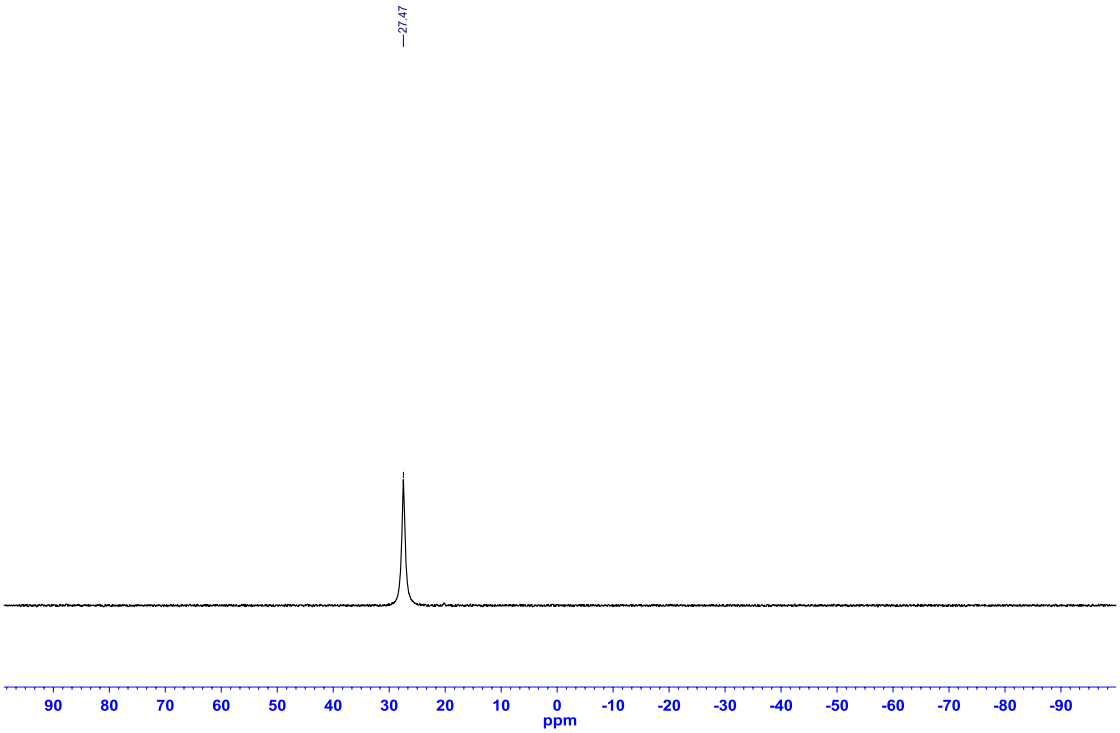

Figure A1.101: ^{1}H NMR ($CDCl_3$, 500.4 MHz) of 2-(1-propynyl)-2,3-dihydro-1*H*-1,3,2-benzodiazaborole (**2.34**)

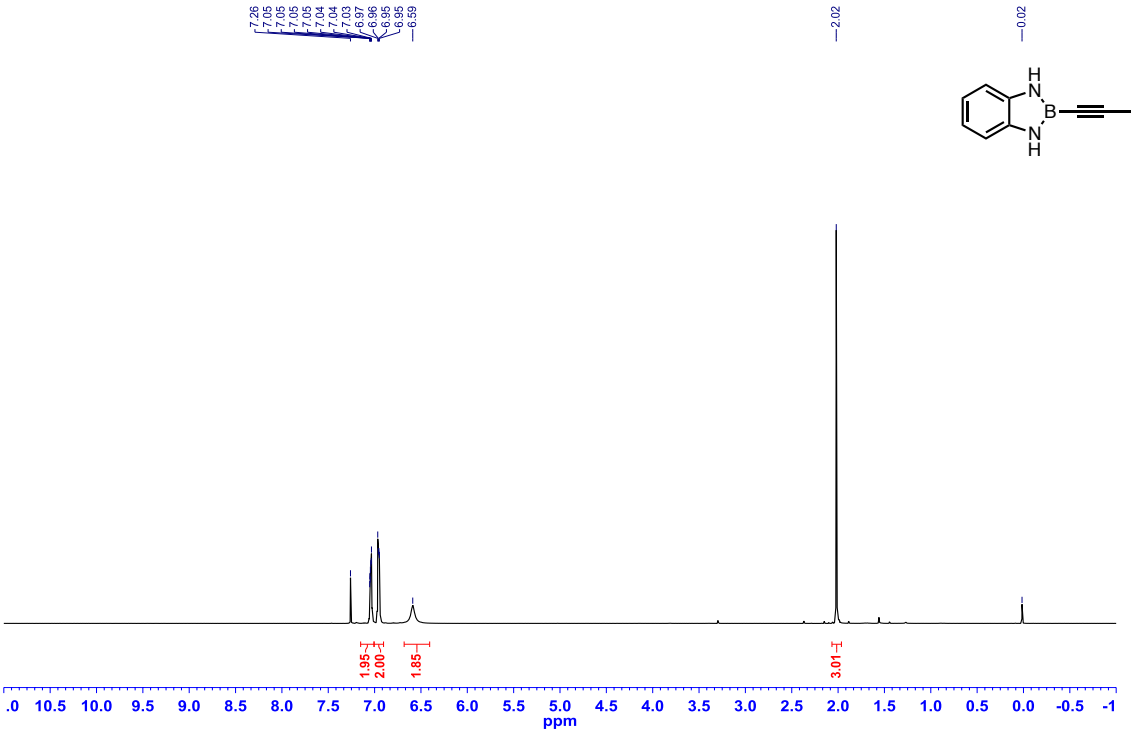

Figure A1.102: ^{13}C {^{1}H} NMR ($CDCl_3$, 125.8 MHz) of 2-(1-propynyl)-2,3-dihydro-1*H*-1,3,2-benzodiazaborole (**2.34**)

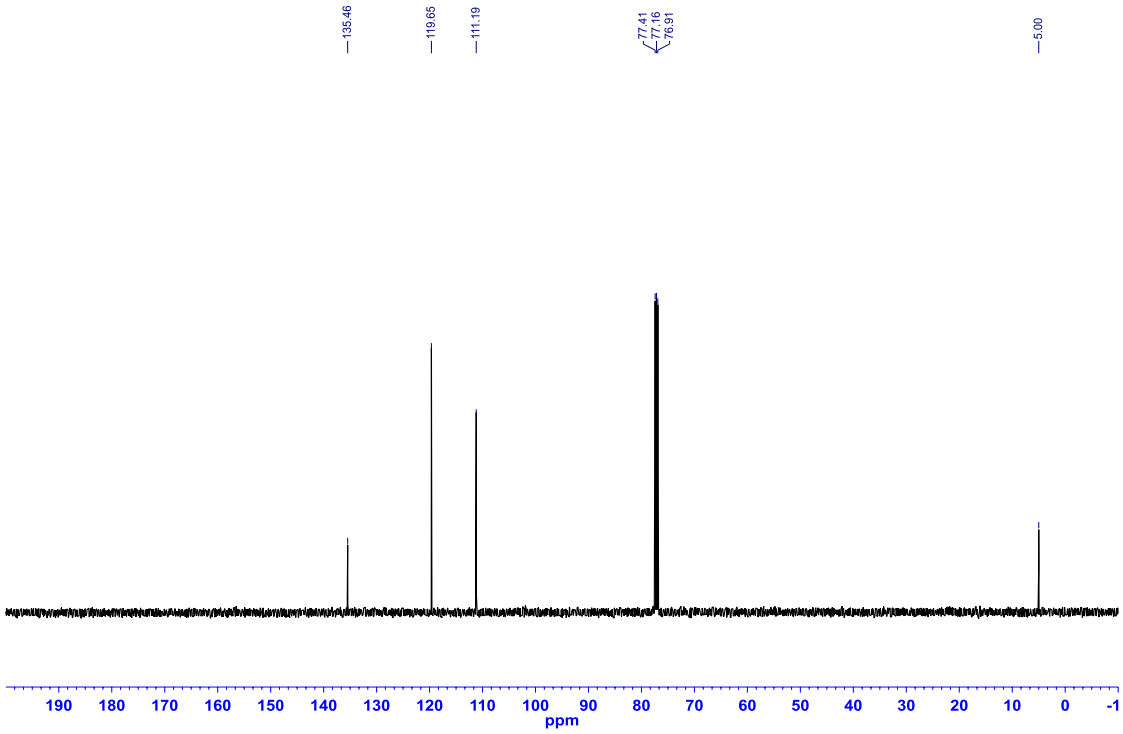

Figure A1.103: ^{11}B NMR (MeCN, 128.4 MHz) of 2-(1-propynyl)-2,3-dihydro-1*H*-1,3,2-benzodiazaborole (**2.34**)

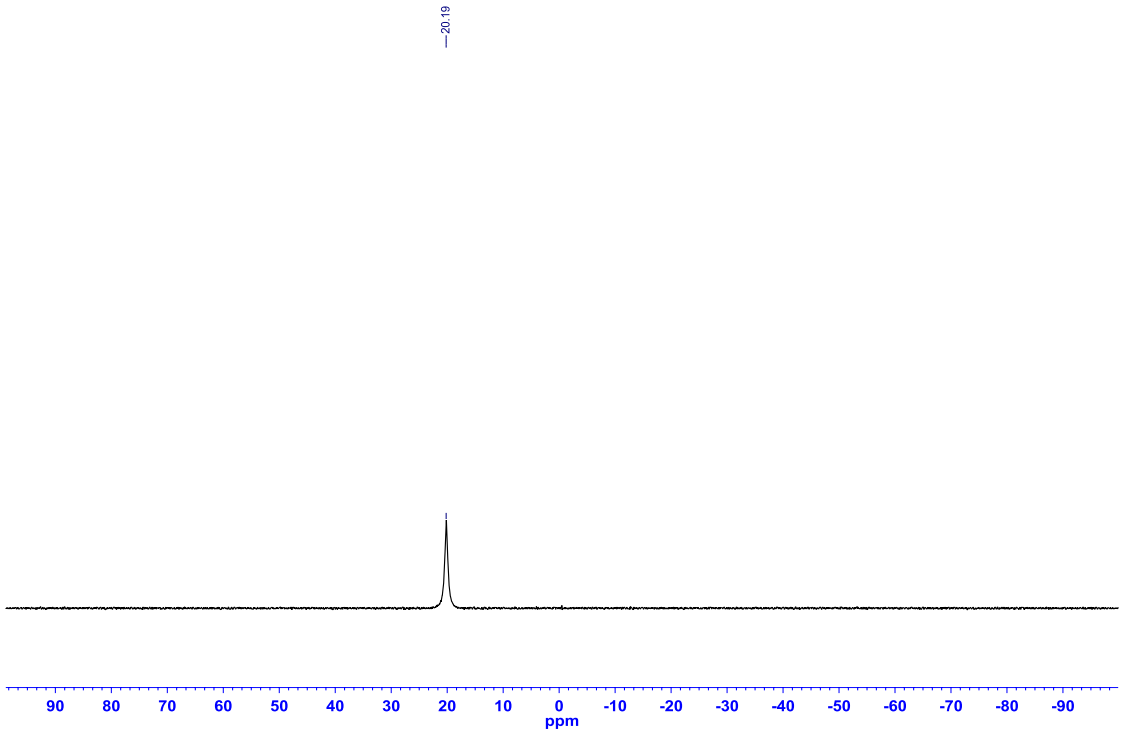

Figure A1.104: ^{1}H NMR ($CDCl_3$, 500.4 MHz) of 1-methyl-2-vinyl-2,3-dihydro-1*H*-1,3,2-benzodiazaborole (**2.35**)

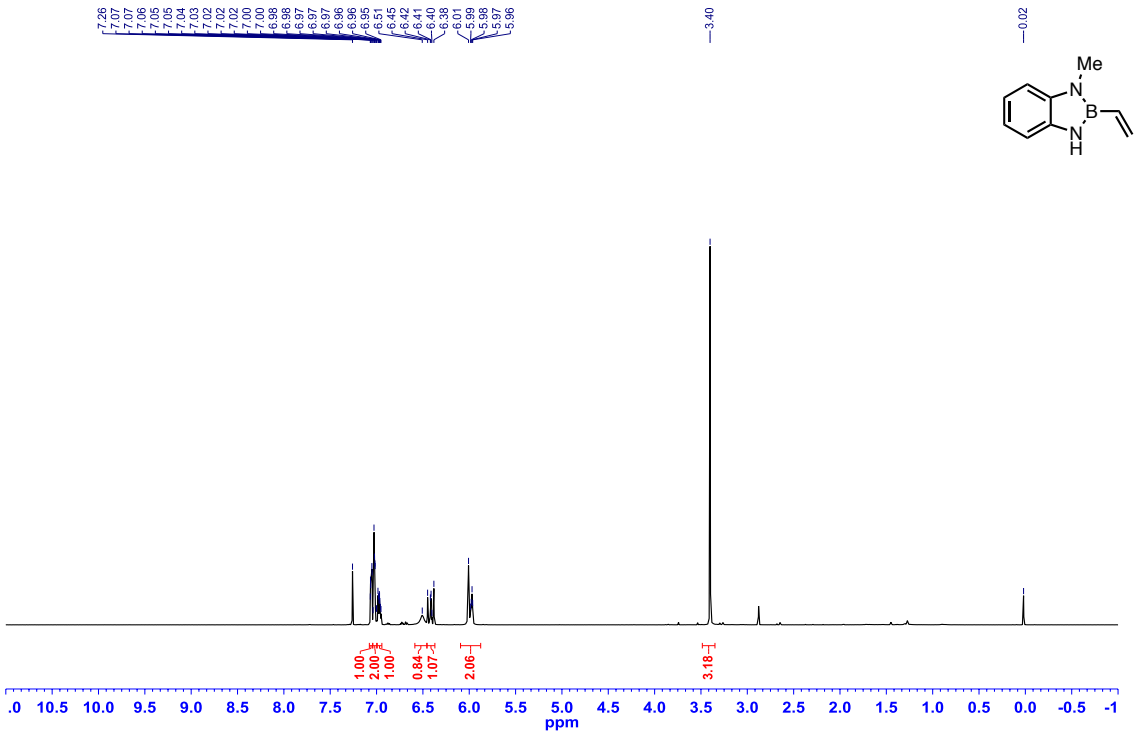

Figure A1.105: ^{13}C {^{1}H} NMR ($CDCl_3$, 125.8 MHz) of 1-methyl-2-vinyl-2,3-dihydro-1*H*-1,3,2-benzodiazaborole (**2.35**)

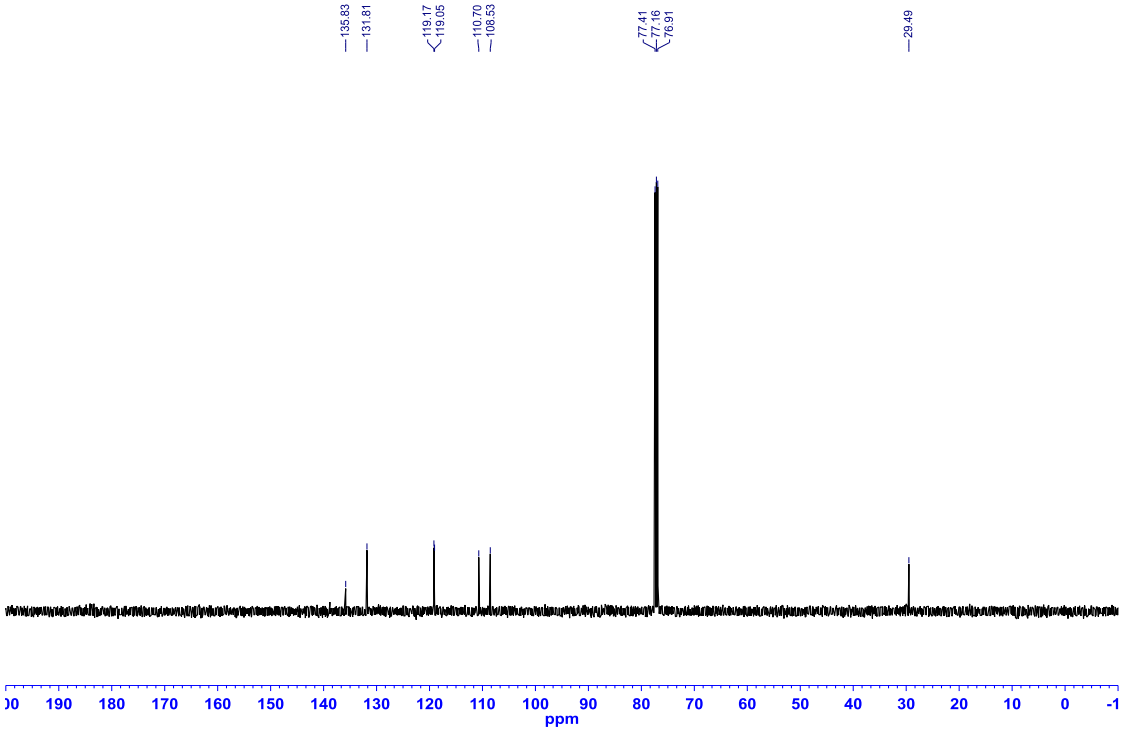

Figure A1.106: ^{11}B NMR (MeCN, 128.4 MHz) of 1-methyl-2-vinyl-2,3-dihydro-1*H*-1,3,2-benzodiazaborole (**2.35**)

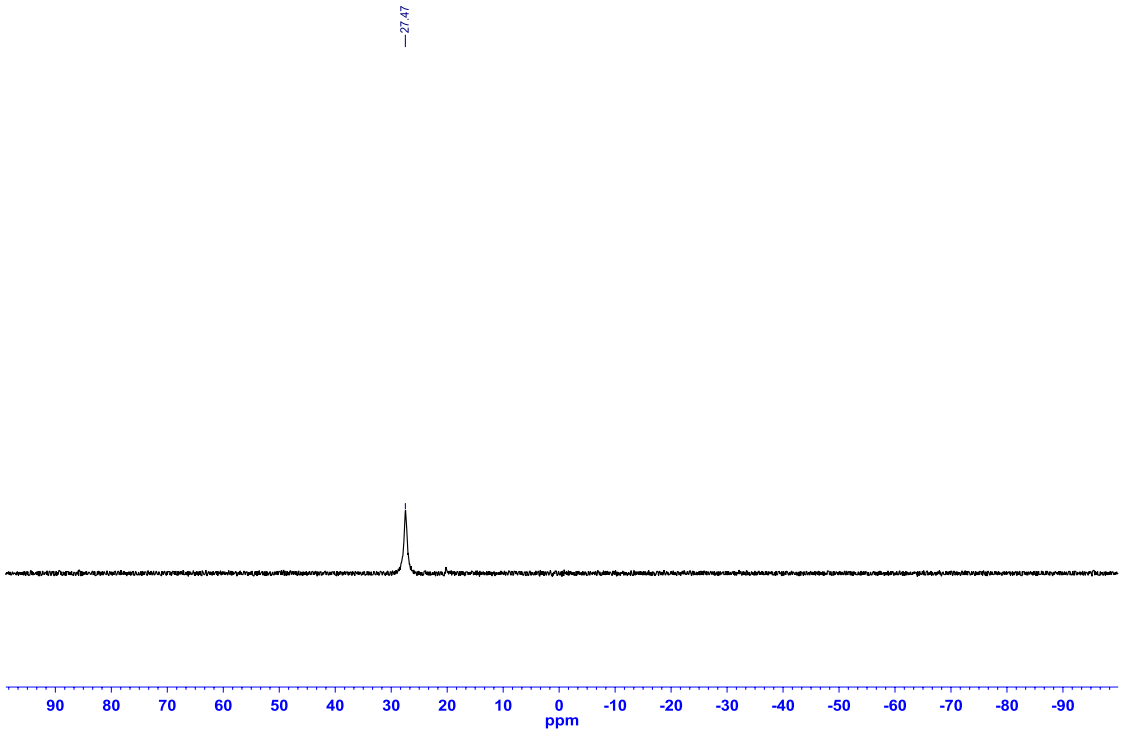

Figure A1.107: ^{1}H NMR ($CDCl_3$, 500.4 MHz) of (*E*)-1-methyl-2-(1-propenyl)-2,3-dihydro-1*H*-1,3,2-benzodiazaborole (**2.36**)

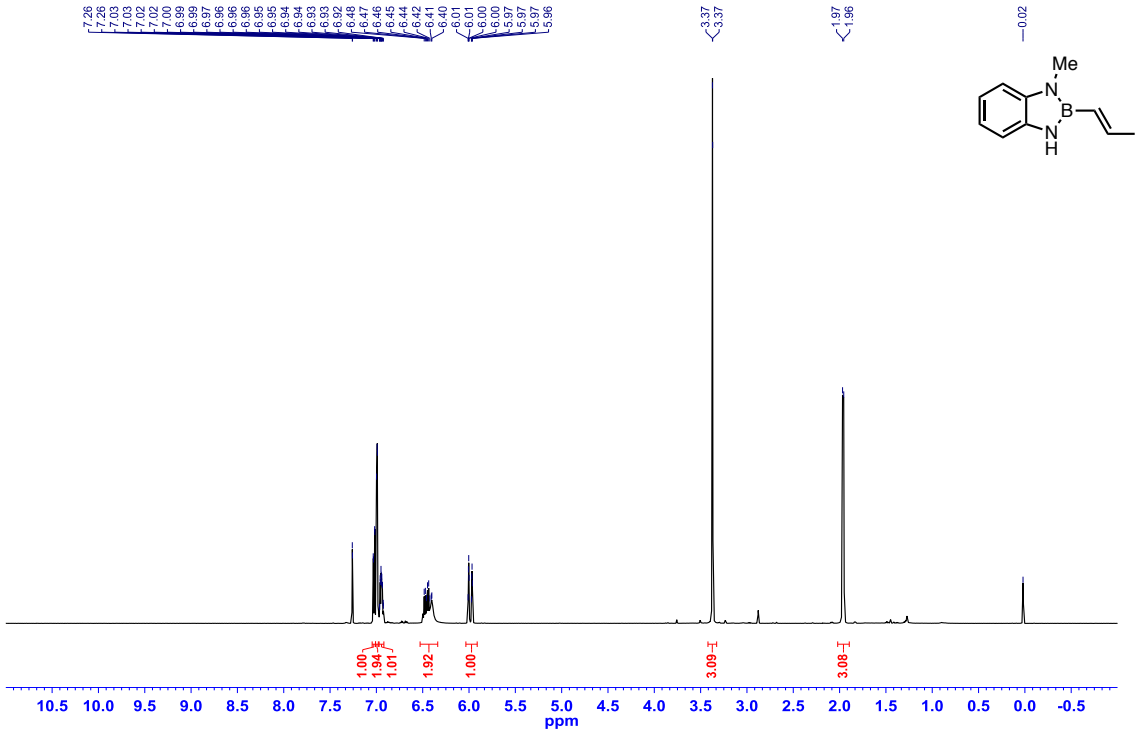

Figure A1.108: ^{13}C {^{1}H} NMR ($CDCl_3$, 125.8 MHz) of (*E*)-1-methyl-2-(1-propenyl)-2,3-dihydro-1*H*-1,3,2-benzodiazaborole (**2.36**)

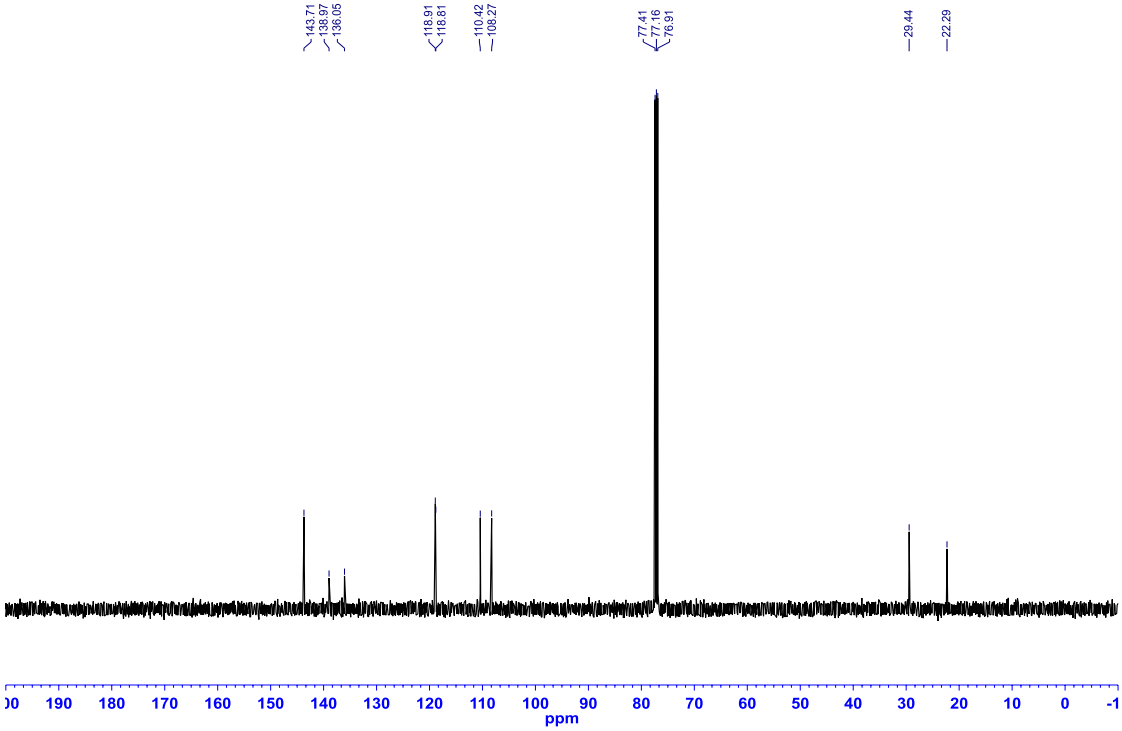

Figure A1.109: ^{11}B NMR (MeCN, 128.4 MHz) of (*E*)-1-methyl-2-(1-propenyl)-2,3-dihydro-1*H*-1,3,2-benzodiazaborole (**2.36**)

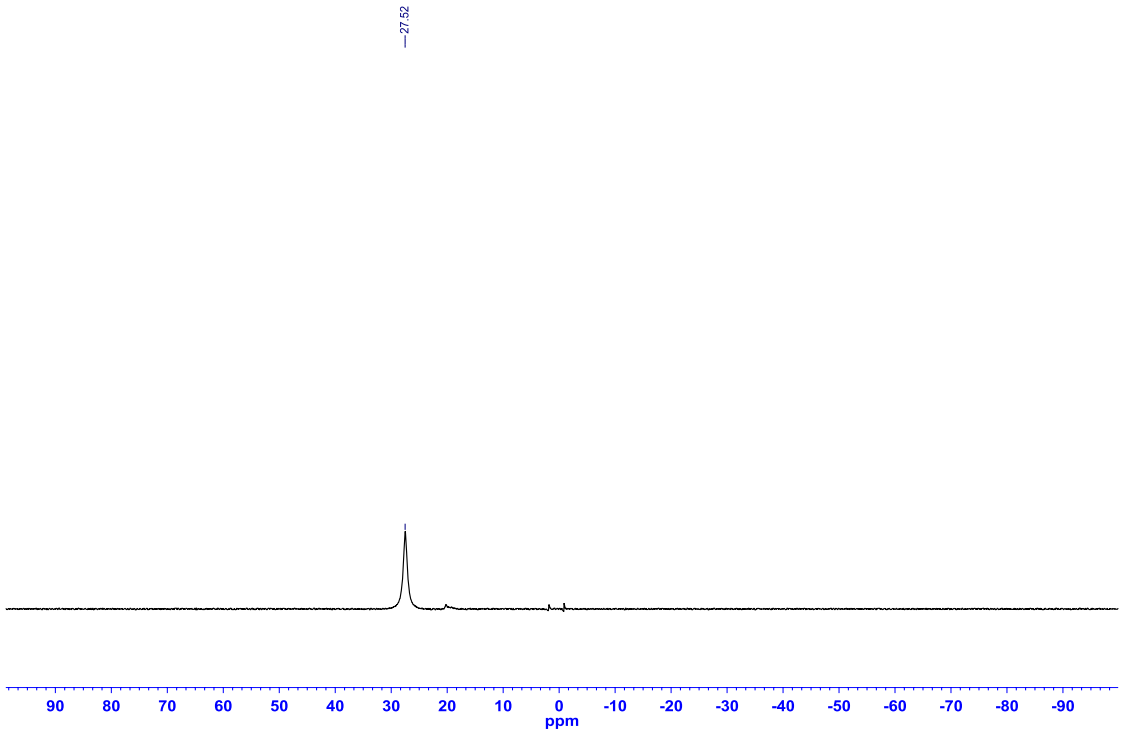

Figure A1.110: ^{1}H NMR ($CDCl_3$, 500.4 MHz) of 1-phenyl-2-vinyl-2,3-dihydro-1*H*-1,3,2-benzodiazaborole (**2.37**)

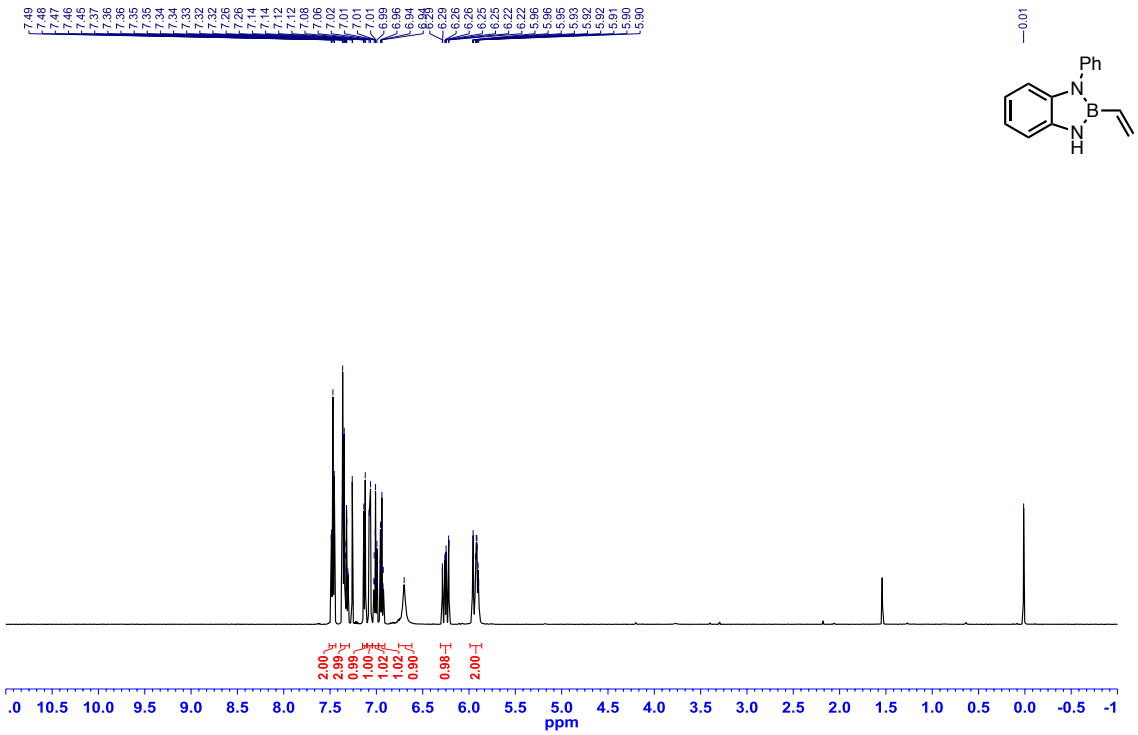

Figure A1.111: ^{13}C {^{1}H} NMR ($CDCl_3$, 125.8 MHz) of 1-phenyl-2-vinyl-2,3-dihydro-1*H*-1,3,2-benzodiazaborole (**2.37**)

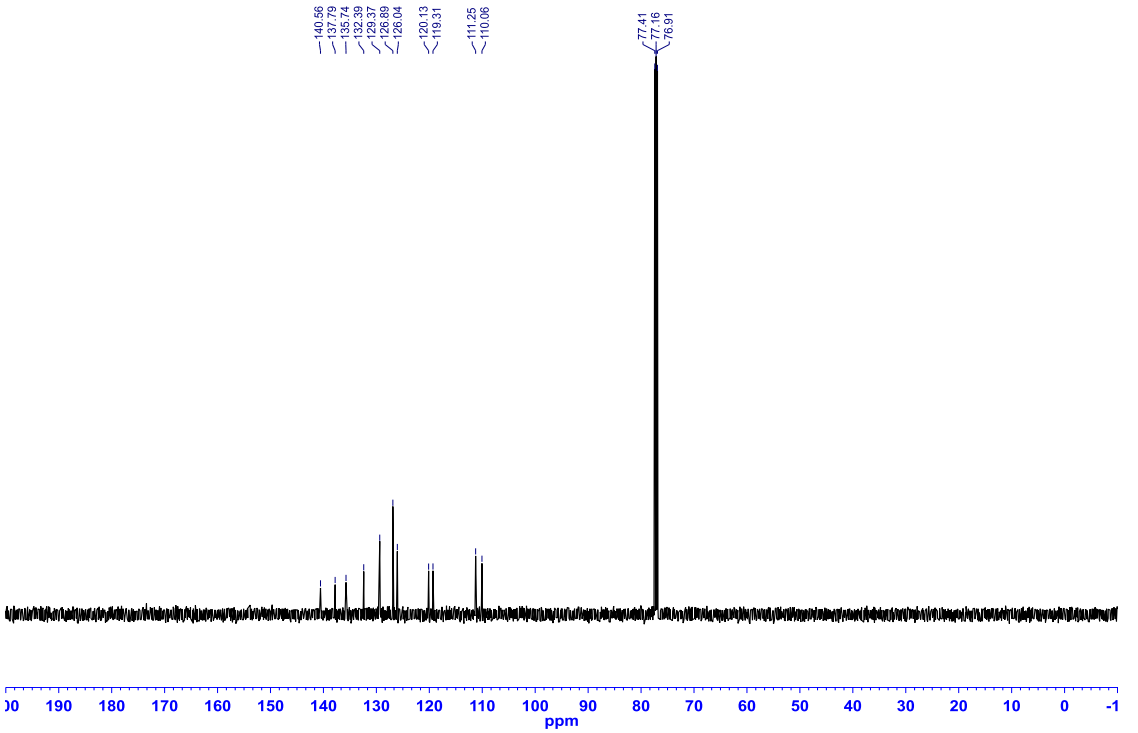

Figure A1.112: ^{11}B NMR (MeCN, 128.4 MHz) of 1-phenyl-2-vinyl-2,3-dihydro-1*H*-1,3,2-benzodiazaborole (**2.37**)

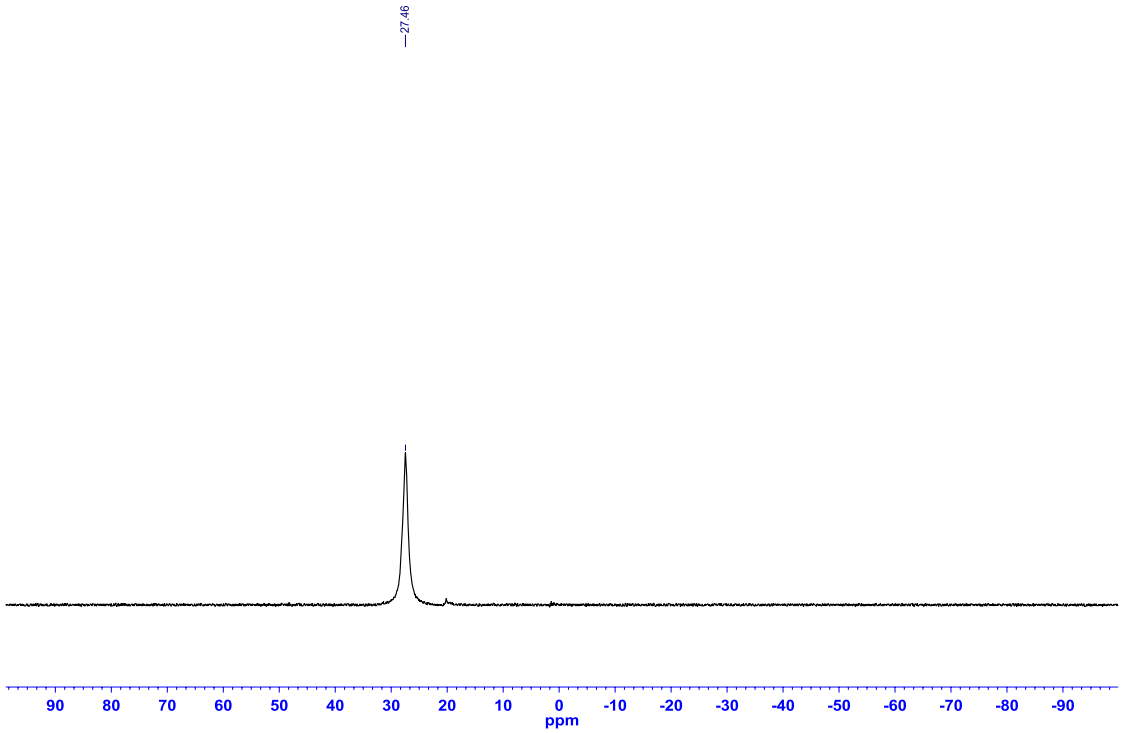

Figure A1.113: ^{1}H NMR ($CDCl_3$, 500.4 MHz) of (*E*)-1-phenyl-2-(1-propenyl)-2,3-dihydro-1*H*-1,3,2-benzodiazaborole (**2.38**)

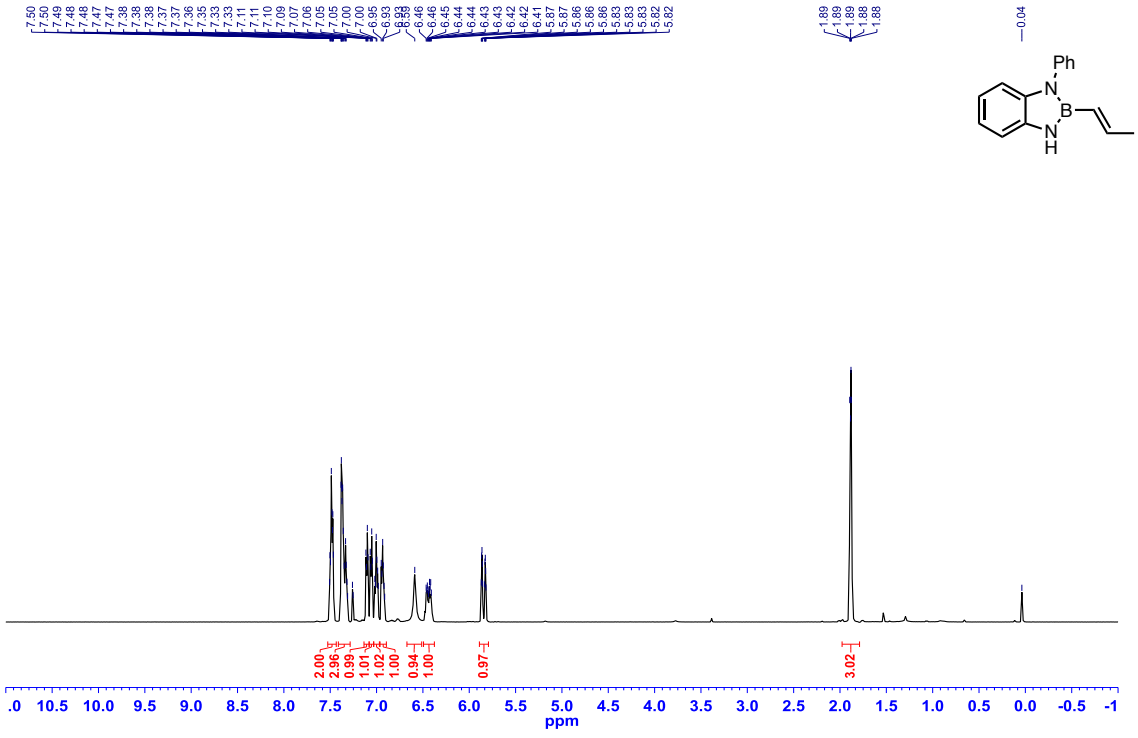

Figure A1.114: ^{13}C {^{1}H} NMR ($CDCl_3$, 125.8 MHz) of (*E*)-1-phenyl-2-(1-propenyl)-2,3-dihydro-1*H*-1,3,2-benzodiazaborole (**2.38**)

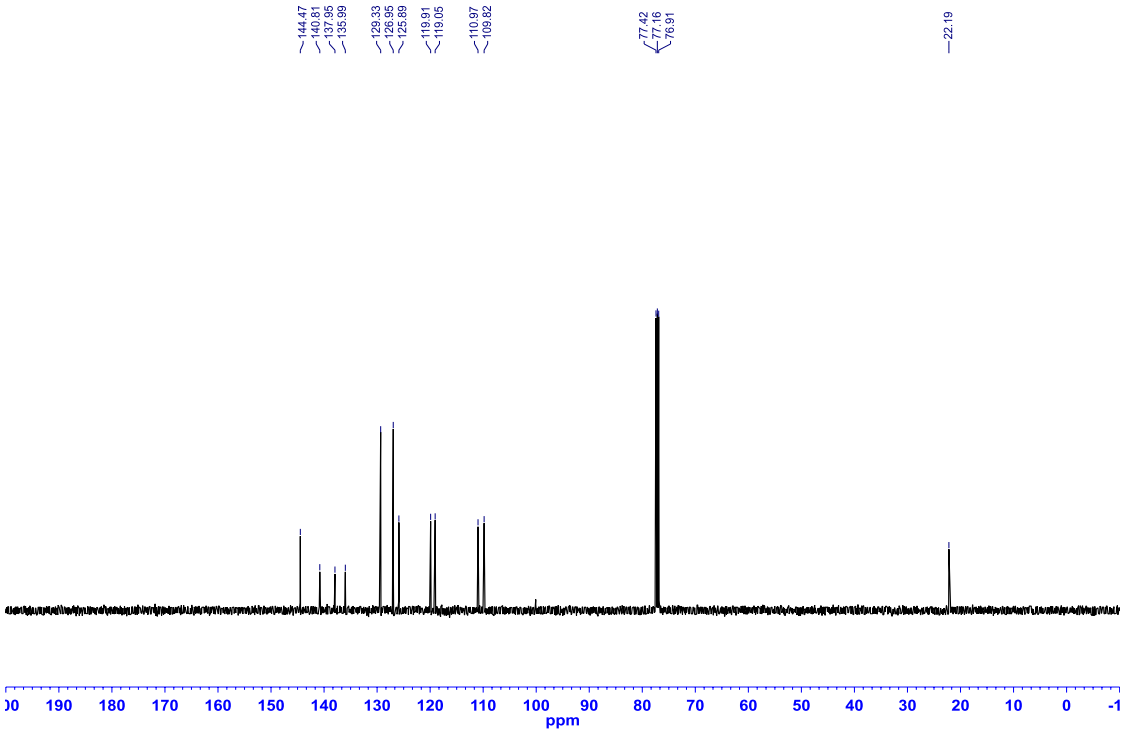

Figure A1.115: ^{11}B NMR ($CDCl_3$, 128.4 MHz) of (*E*)-1-phenyl-2-(1-propenyl)-2,3-dihydro-1*H*-1,3,2-benzodiazaborole (**2.38**)

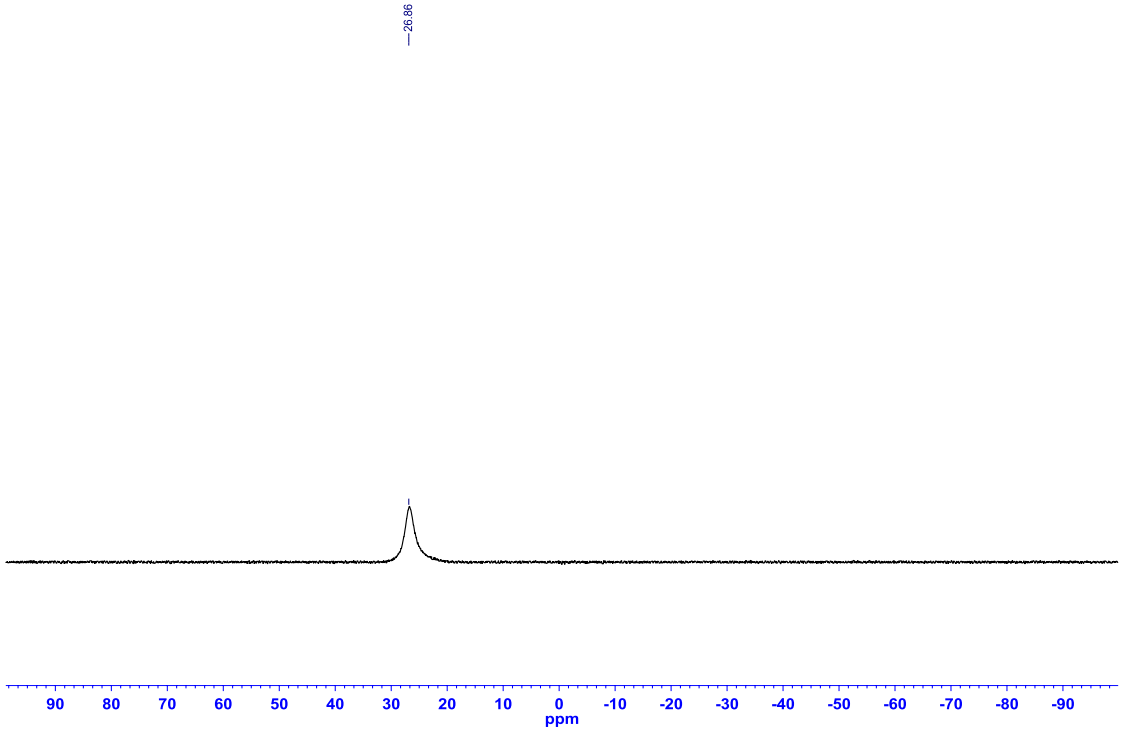

Figure A1.116: ^{1}H NMR ($CDCl_3$, 500.4 MHz) of 2-methyl-2,3-dihydro-1*H*-1,3,2-benzodiazaborole (**2.39**)

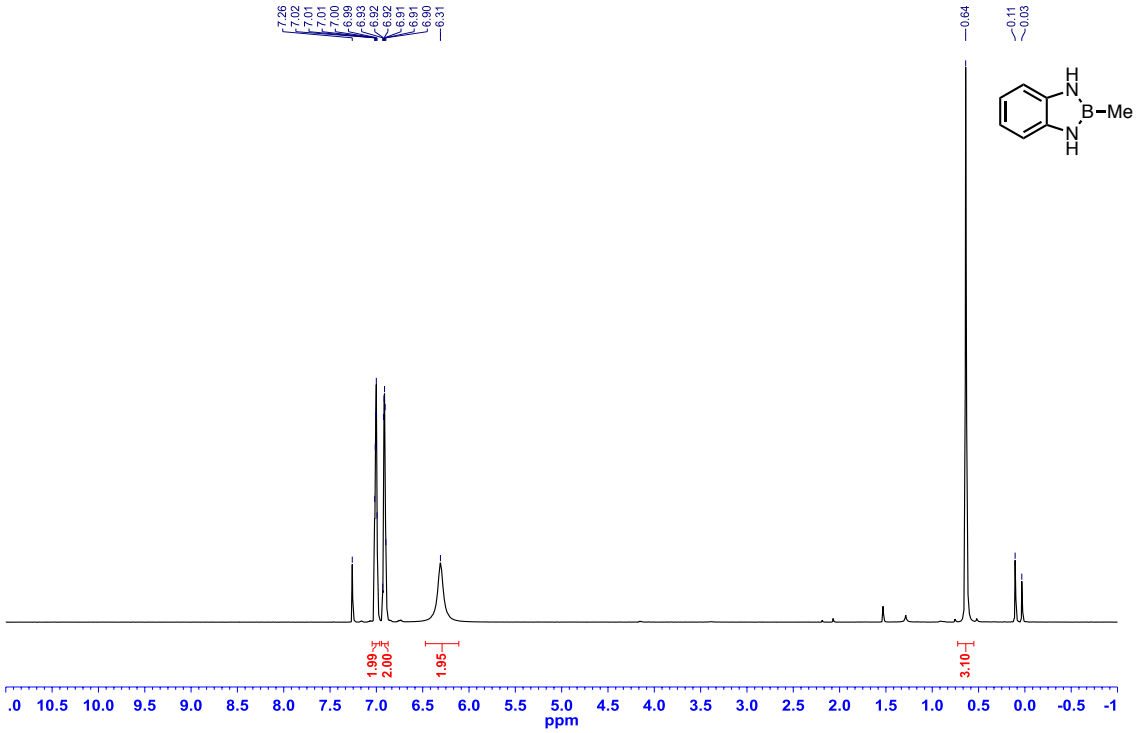

Figure A1.117: ^{13}C {^{1}H} NMR ($CDCl_3$, 125.8 MHz) of 2-methyl-2,3-dihydro-1*H*-1,3,2-benzodiazaborole (**2.39**)

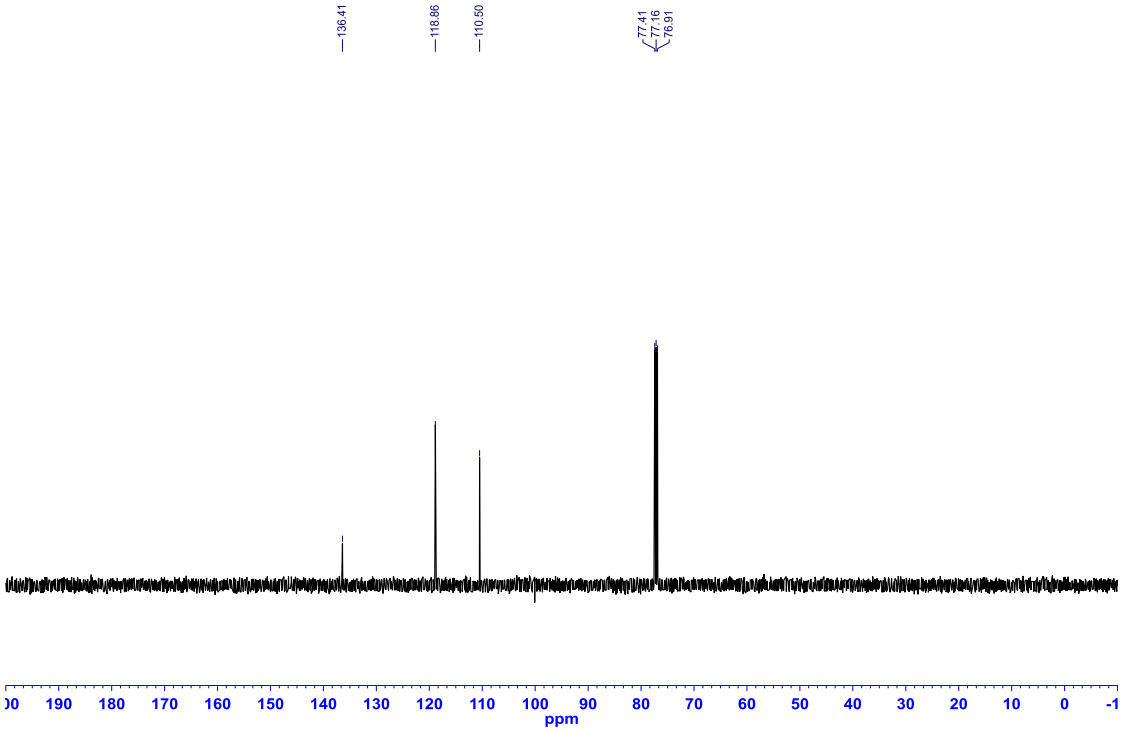

Figure A1.118: ^{11}B NMR ($CDCl_3$, 128.4 MHz) of 2-methyl-2,3-dihydro-1*H*-1,3,2-benzodiazaborole (**2.39**)

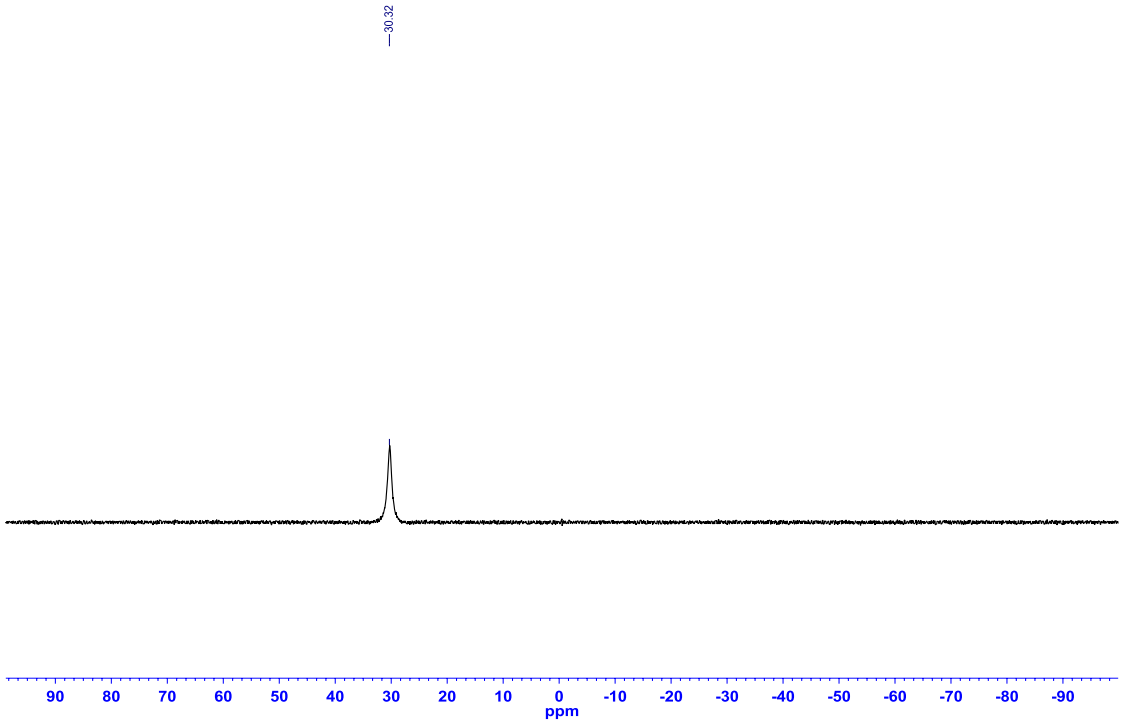

Figure A1.119: ^{1}H NMR ($CDCl_3$, 500.4 MHz) of 2-isopropyl-2,3-dihydro-1*H*-1,3,2-benzodiazaborole (**2.40**)

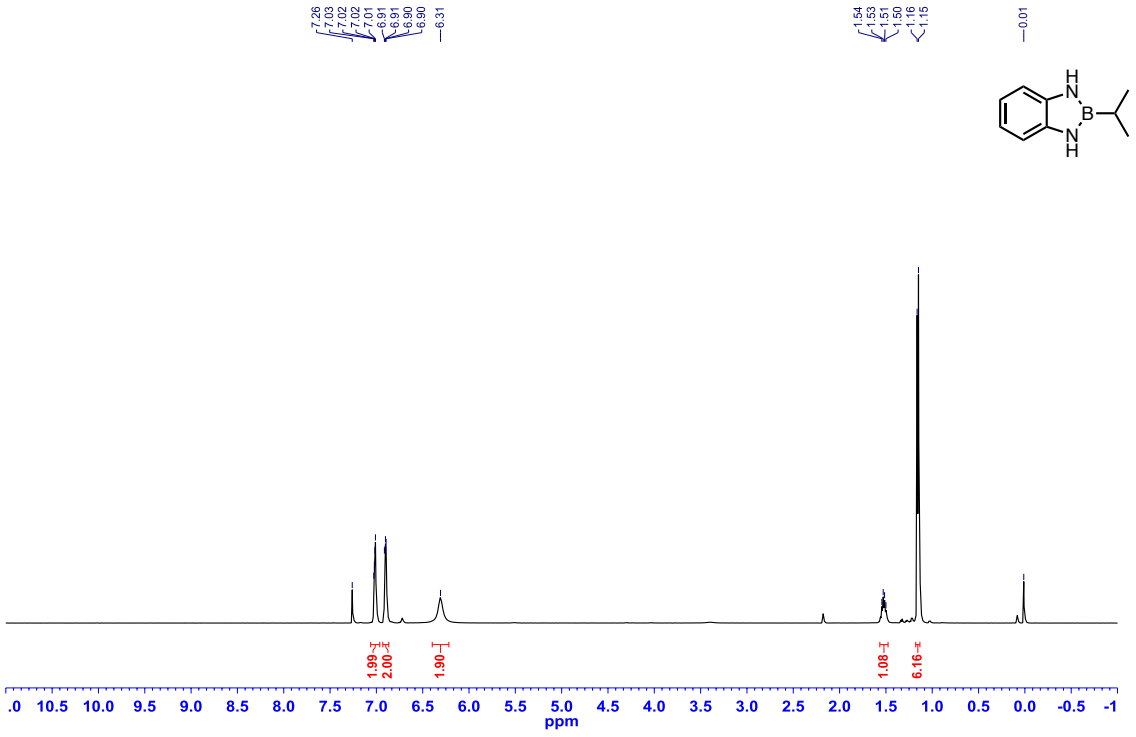

Figure A1.120: ^{13}C {^{1}H} NMR ($CDCl_3$, 125.8 MHz) of 2-isopropyl-2,3-dihydro-1*H*-1,3,2-benzodiazaborole (**2.40**)

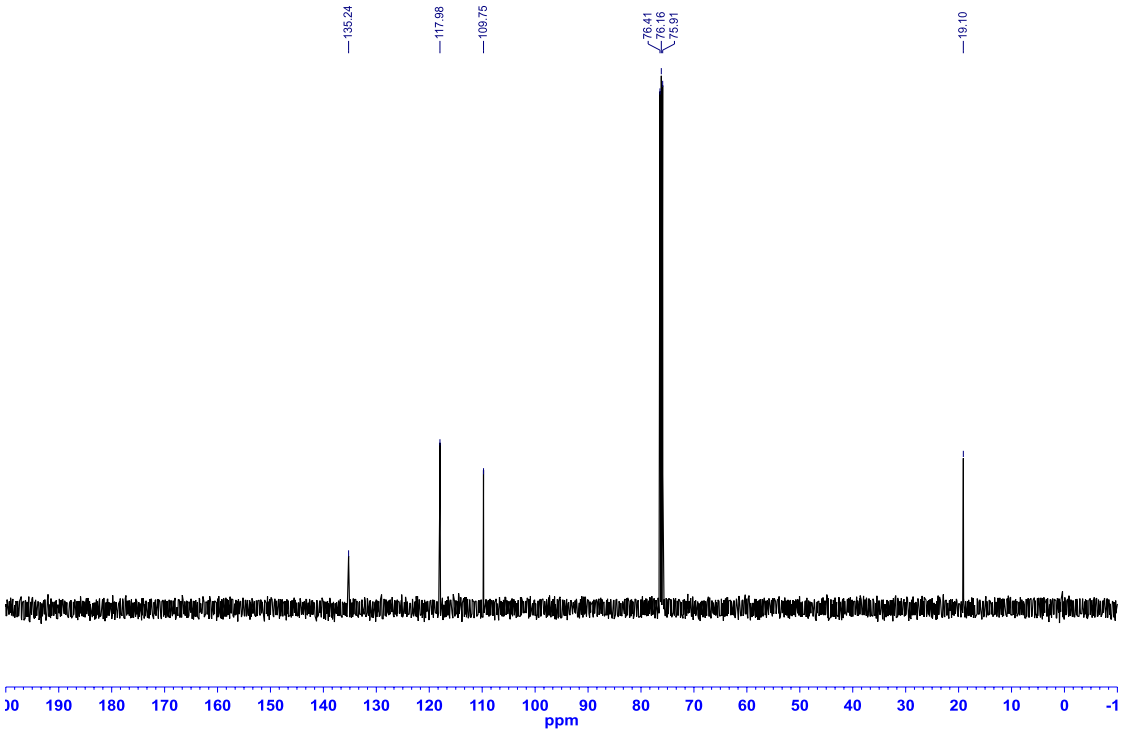

Figure A1.121: ^{11}B NMR ($CDCl_3$, 128.4 MHz) of 2-isopropyl-2,3-dihydro-1*H*-1,3,2-benzodiazaborole (**2.40**)

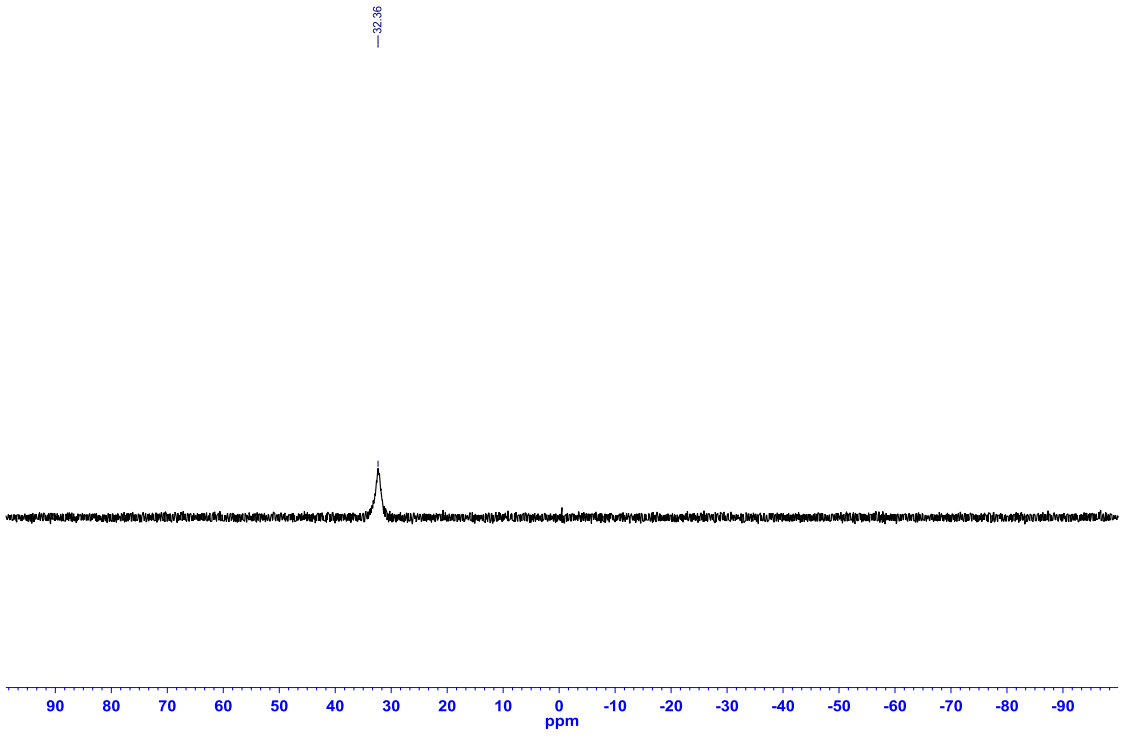

Figure A1.122: ^{1}H NMR ($CDCl_3$, 500.4 MHz) of 2-cyclopropyl_-2,3-dihydro-1*H*-1,3,2-benzodiazaborole (**2.41**)

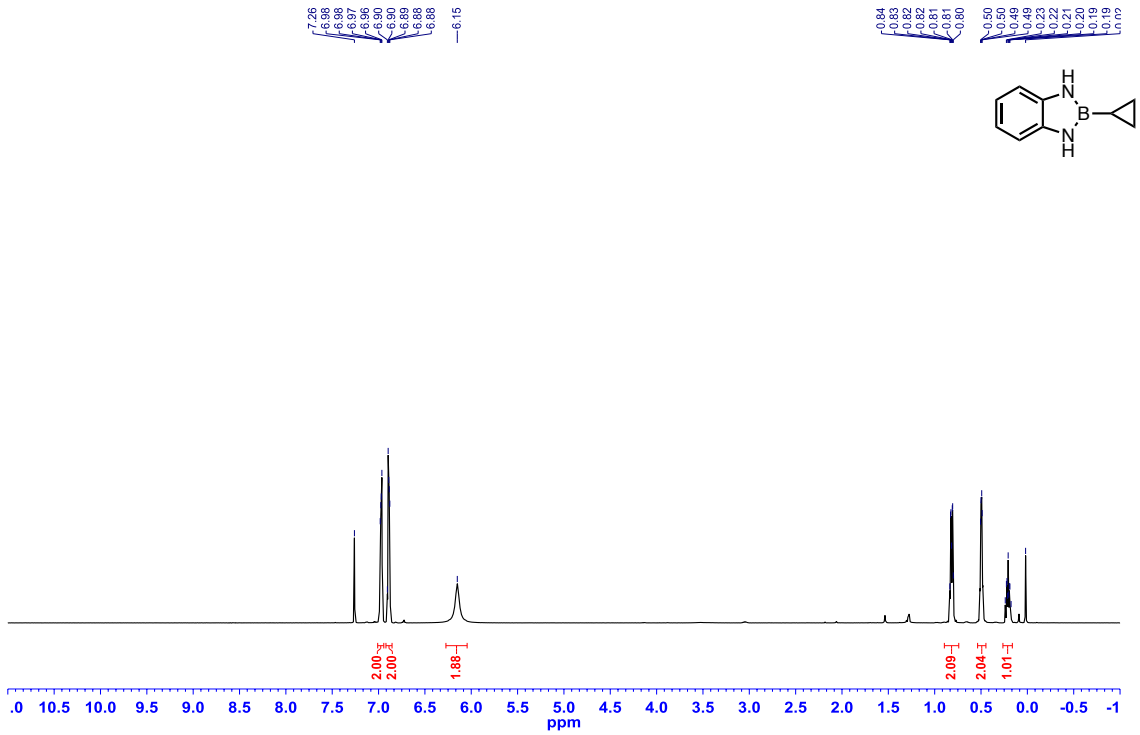

Figure A1.123: ^{13}C {^{1}H} NMR ($CDCl_3$, 125.8 MHz) of 2-cyclopropyl_-2,3-dihydro-1*H*-1,3,2-benzodiazaborole (**2.41**)

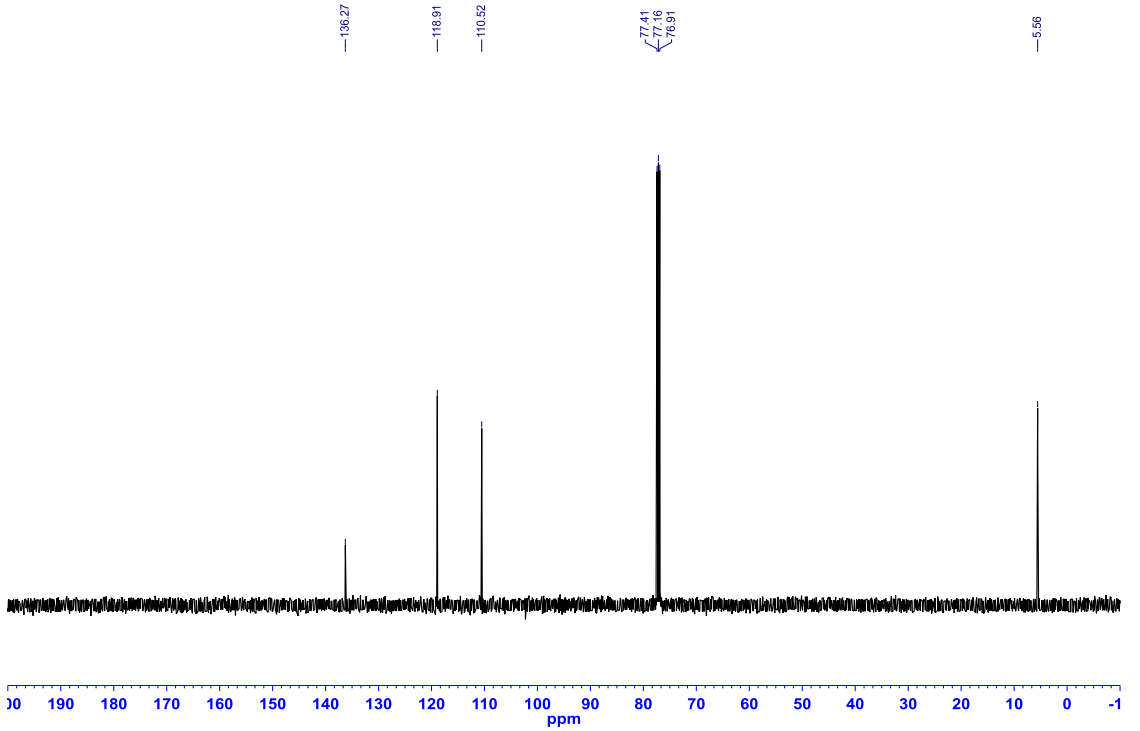

Figure A1.124: ^{11}B NMR (MeCN, 128.4 MHz) of 2-cyclopropyl_-2,3-dihydro-1*H*-1,3,2-benzodiazaborole (**2.41**)

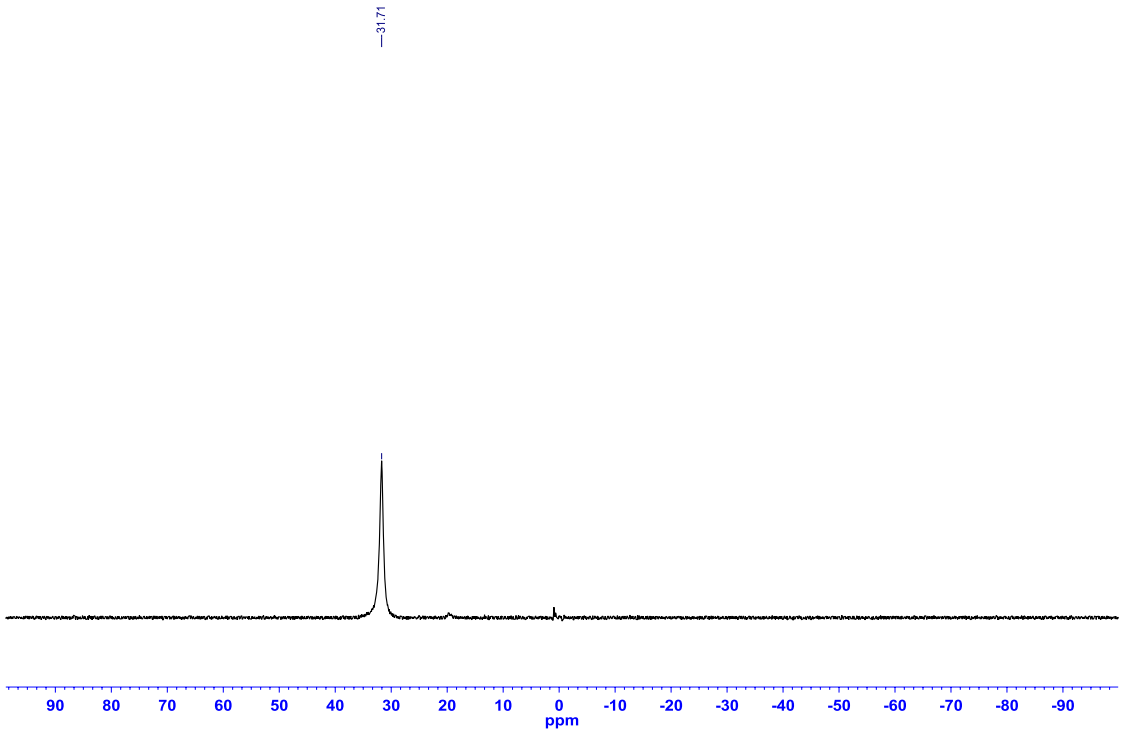

Figure A1.125: ^{1}H NMR ($CDCl_3$, 500.4 MHz) of 2-(*tert*-butyl)_-2,3-dihydro-1*H*-1,3,2-benzodiazaborole (**2.42**)

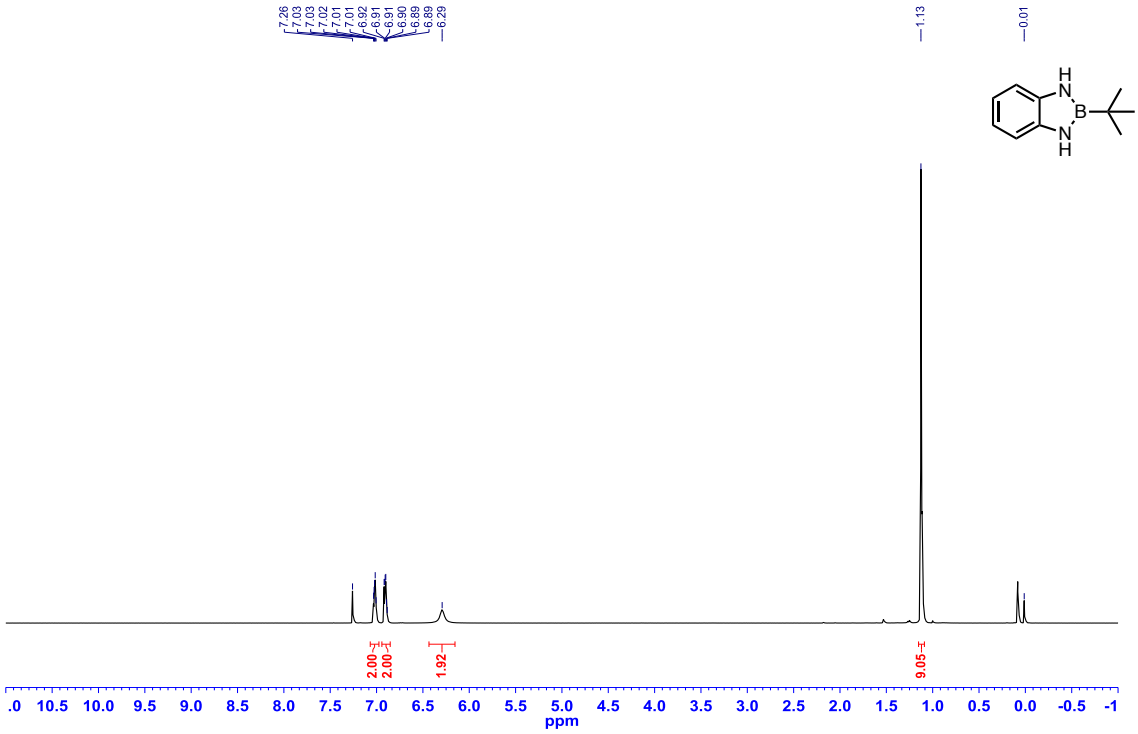

Figure A1.126: ^{13}C {^{1}H} NMR ($CDCl_3$, 125.8 MHz) of 2-(*tert*-butyl)_-2,3-dihydro-1*H*-1,3,2-benzodiazaborole (**2.42**)

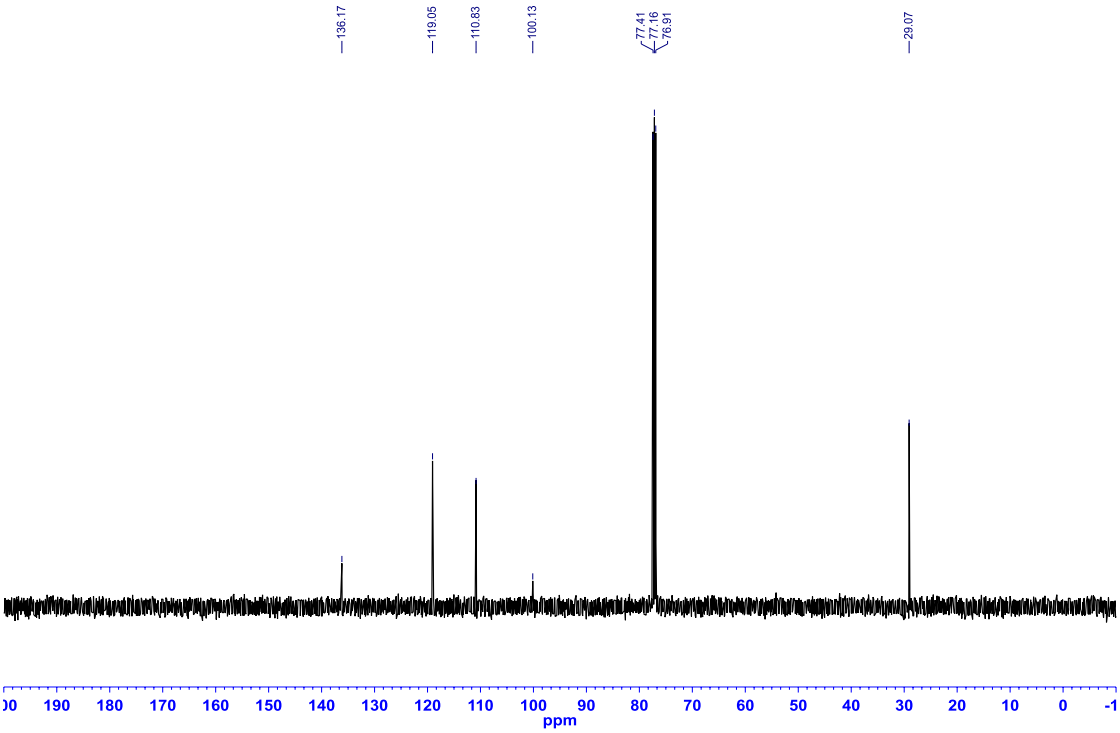

Figure A1.127: ^{11}B NMR ($CDCl_3$, 128.4 MHz) of 2-(*tert*-butyl)_-2,3-dihydro-1*H*-1,3,2-benzodiazaborole (**2.42**)

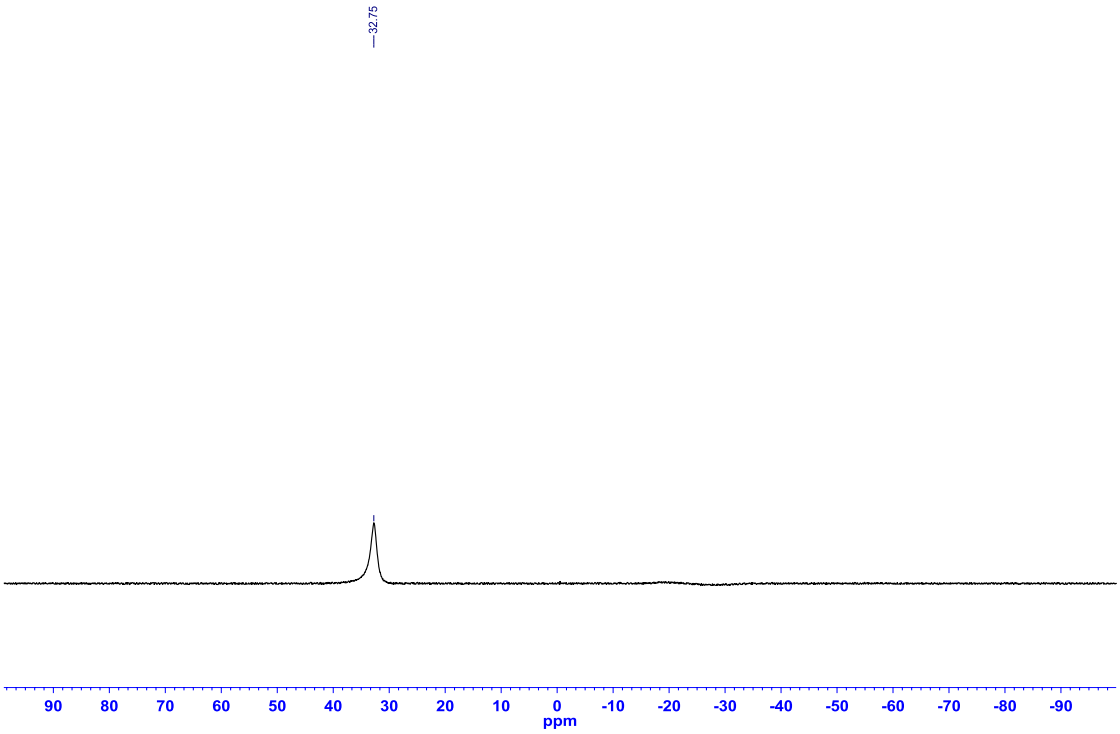

Figure A1.128: ^{1}H NMR ($CDCl_3$, 500.4 MHz) of 2-phenethyl-2,3-dihydro-1*H*-1,3,2-benzodiazaborole (**2.43**)

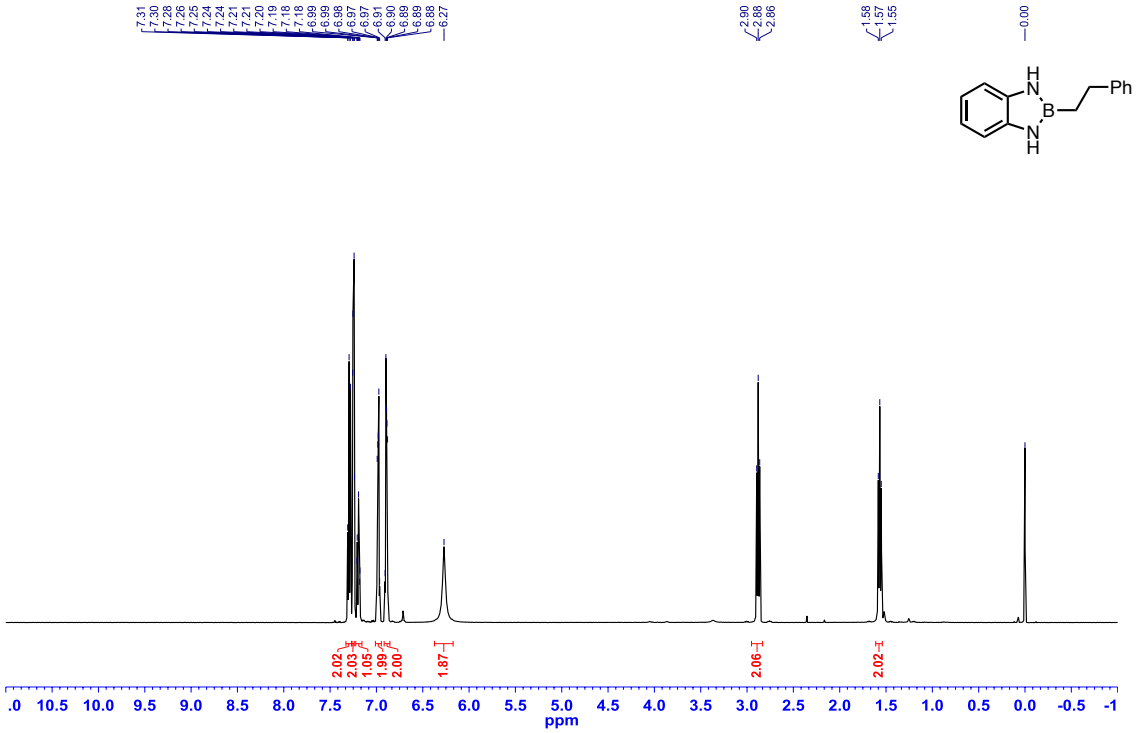

Figure A1.129: ^{13}C {^{1}H} NMR ($CDCl_3$, 125.8 MHz) of 2-phenethyl-2,3-dihydro-1*H*-1,3,2-benzodiazaborole (**2.43**)

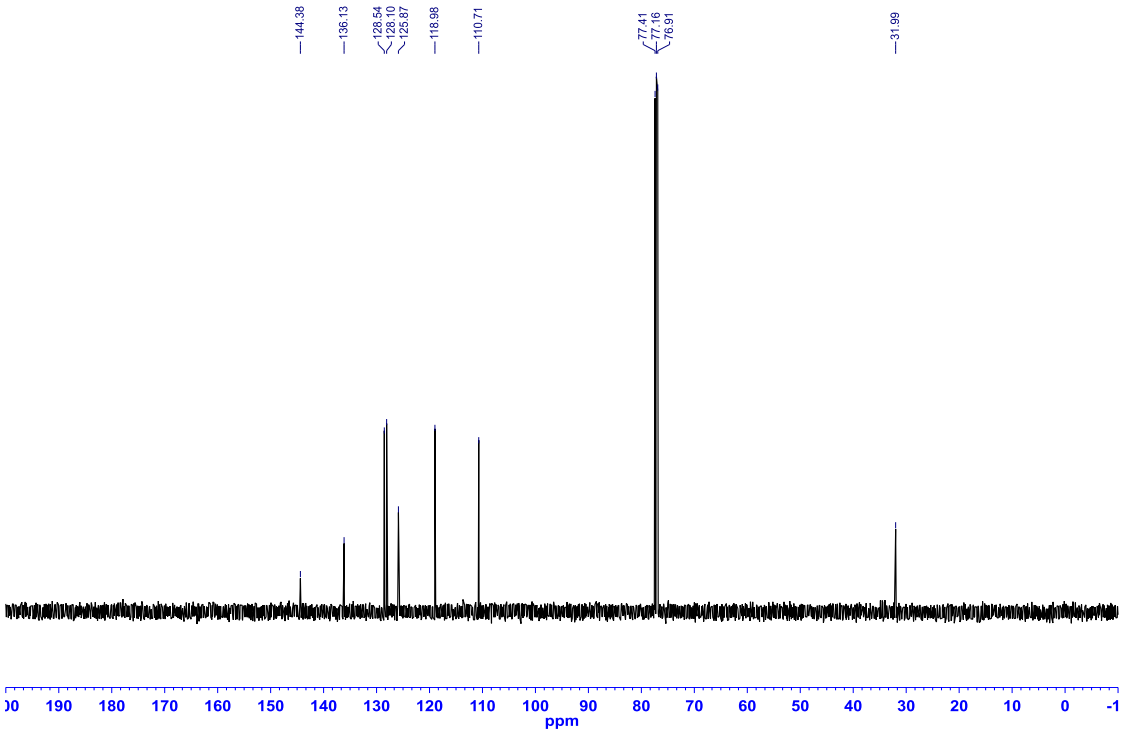

Figure A1.130: ^{11}B NMR (MeCN, 128.4) of 2-phenethyl-2,3-dihydro-1*H*-1,3,2-benzodiazaborole (**2.43**)

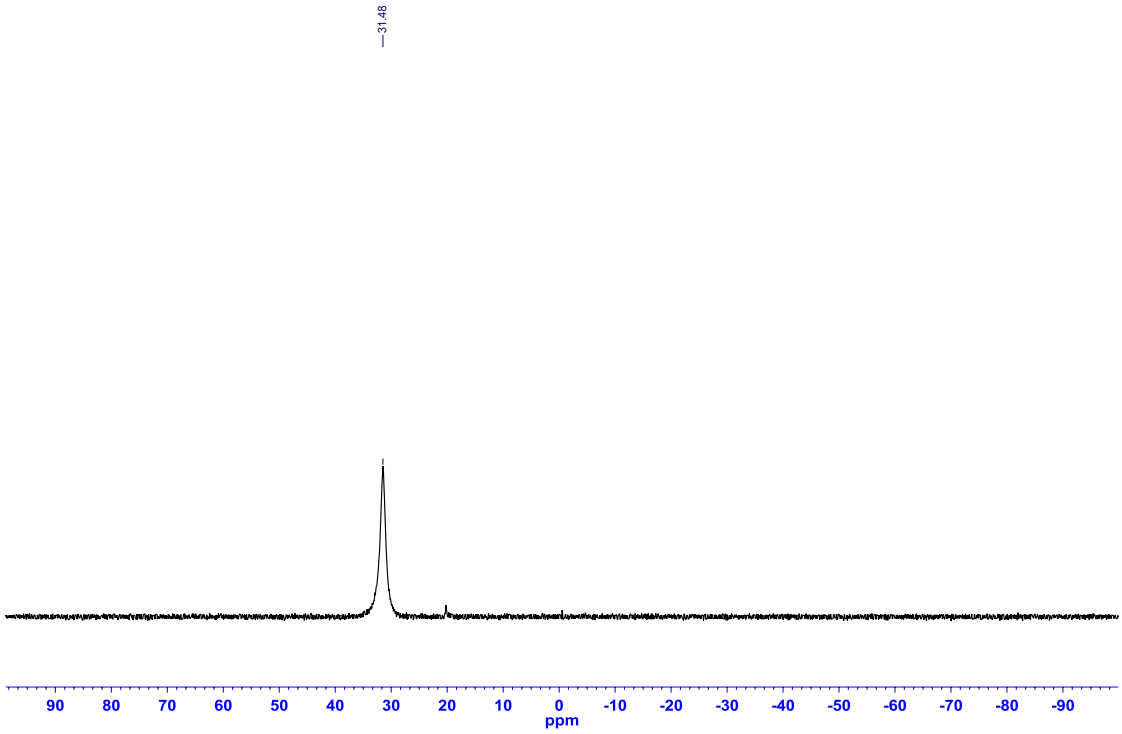

Figure A1.131: ^{1}H NMR ($CDCl_3$, 500.4 MHz) of 1,2-dimethyl-2,3-dihydro-1*H*-1,3,2-benzodiazaborole (**2.44**)

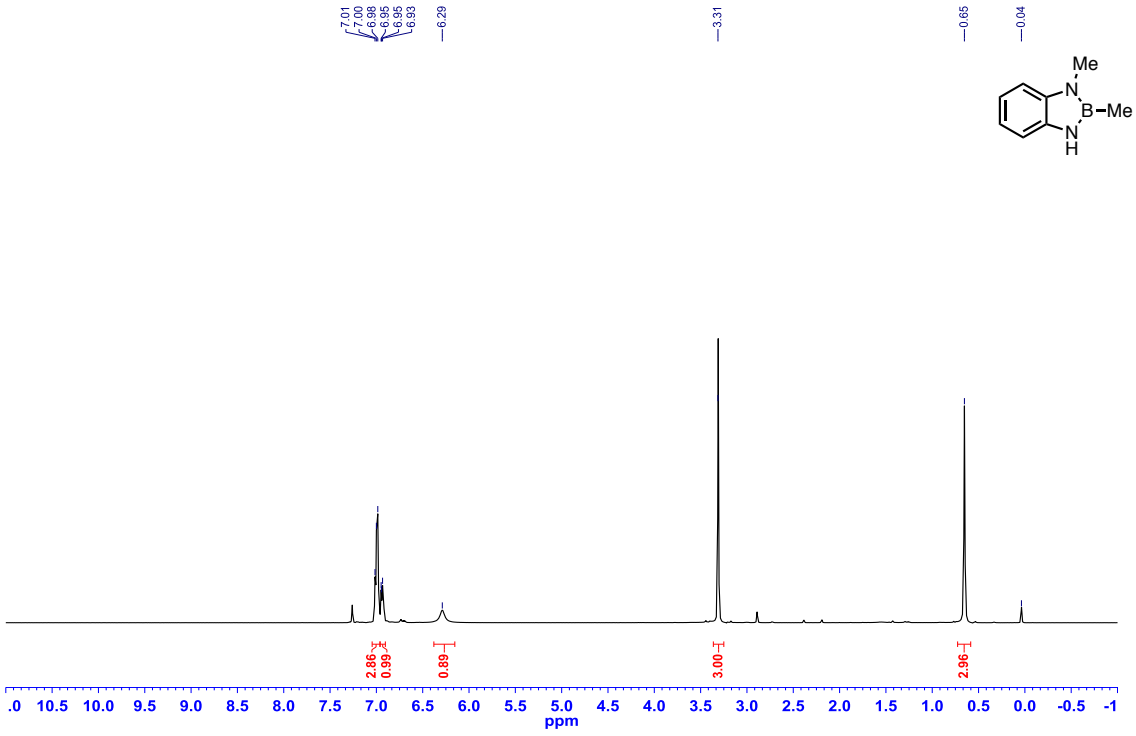

Figure A1.132: ^{13}C {^{1}H} NMR ($CDCl_3$, 125.8 MHz) of 1,2-dimethyl-2,3-dihydro-1*H*-1,3,2-benzodiazaborole (**2.44**)

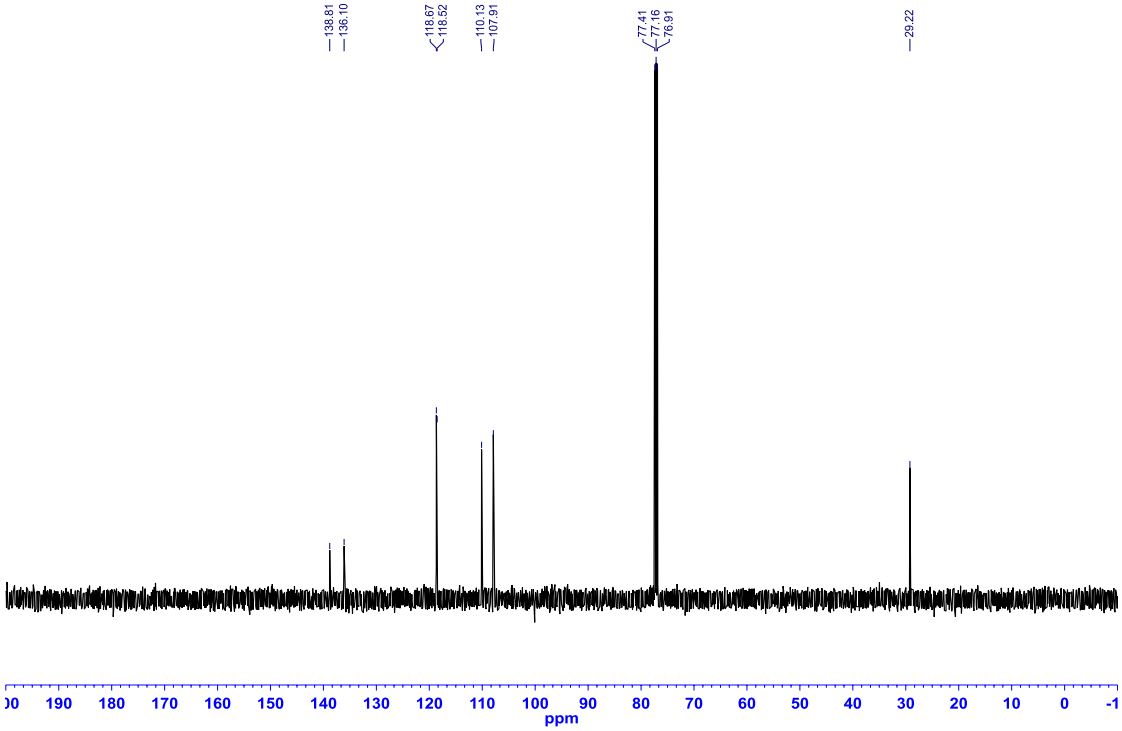

Figure A1.133: ^{11}B NMR (MeCN, 128.4 MHz) of 1,2-dimethyl-2,3-dihydro-1*H*-1,3,2-benzodiazaborole (**2.44**)

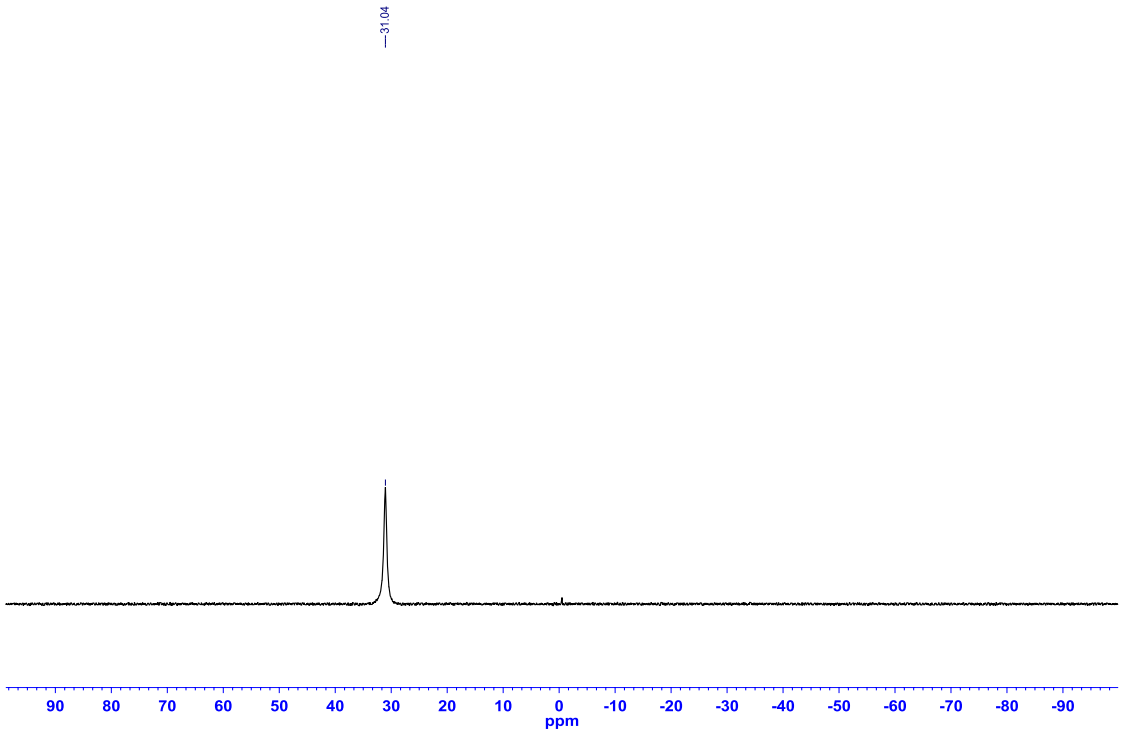

Figure A1.134: ^{1}H NMR ($CDCl_3$, 500.4 MHz) of 2-(3-chloropropyl)-1-methyl-2,3-dihydro-1*H*-1,3,2-benzodiazaborole (**2.45**)

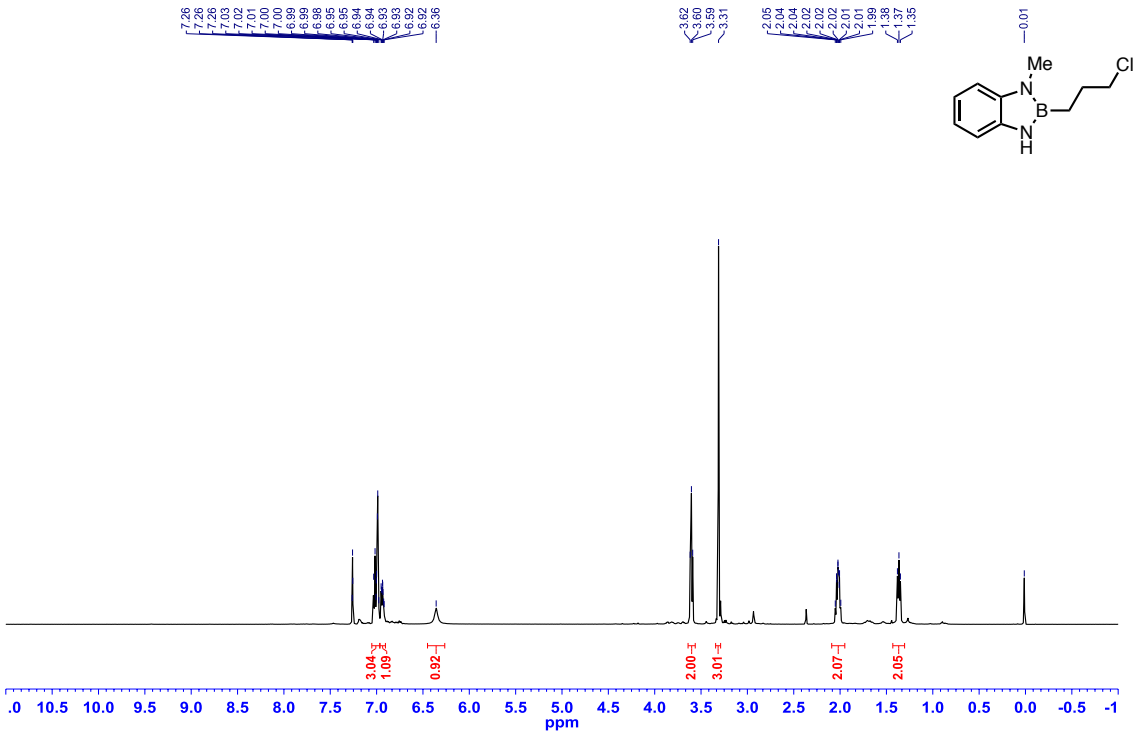

Figure A1.135: ^{13}C {^{1}H} NMR ($CDCl_3$, 125.8 MHz) of 2-(3-chloropropyl)-1-methyl-2,3-dihydro-1*H*-1,3,2-benzodiazaborole (**2.45**)

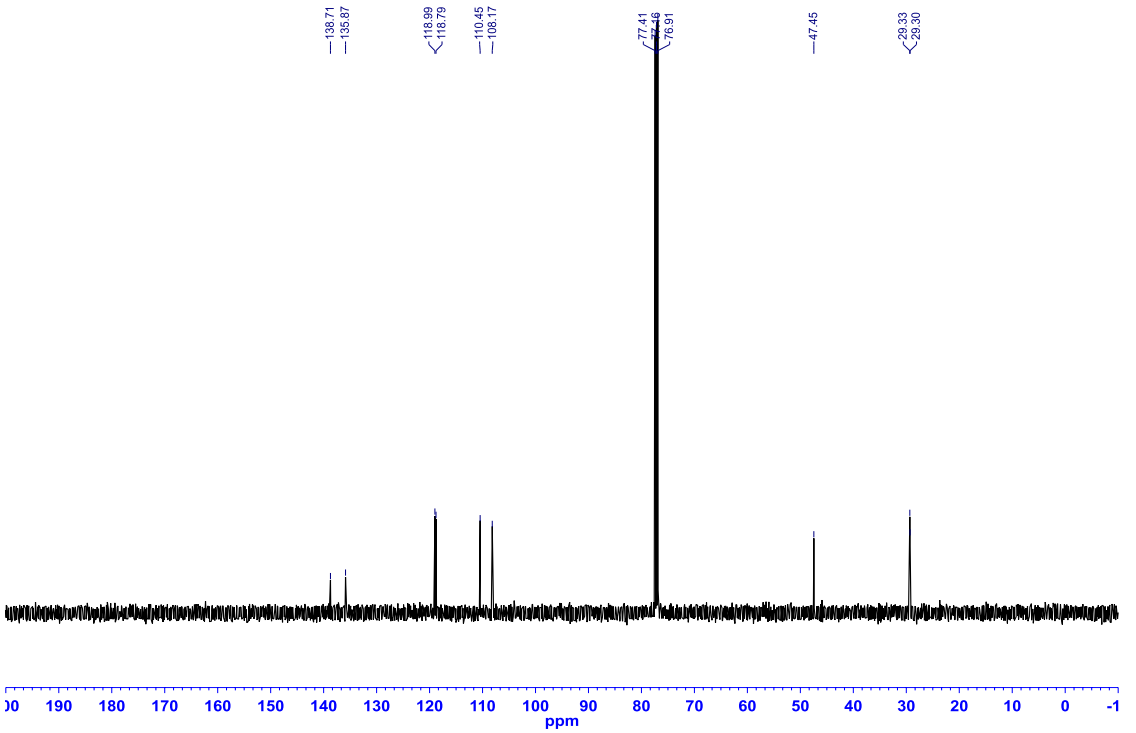

Figure A1.136: ^{11}B NMR ($CDCl_3$, 128.4 MHz) of 2-(3-chloropropyl)-1-methyl-2,3-dihydro-1*H*-1,3,2-benzodiazaborole (**2.45**)

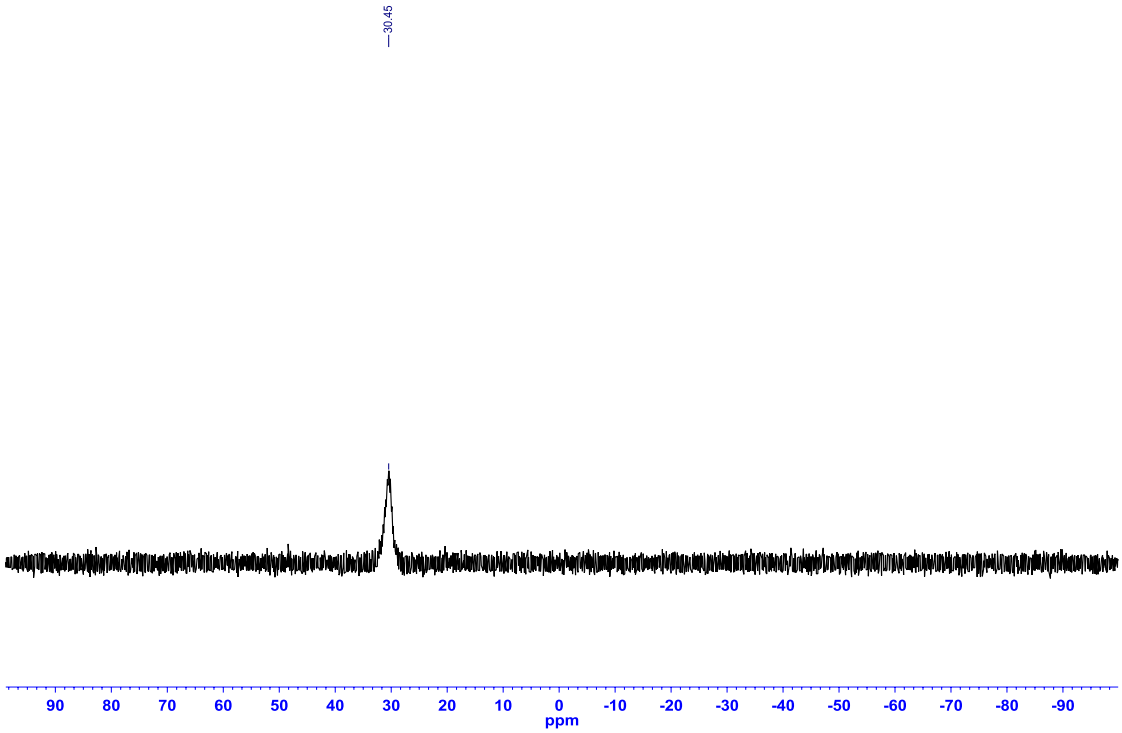

Figure A1.137: ^{1}H NMR ($CDCl_3$, 500.4 MHz) of 2-methyl-1-phenyl-2,3-dihydro-1*H*-1,3,2-benzodiazaborole (**2.46**)

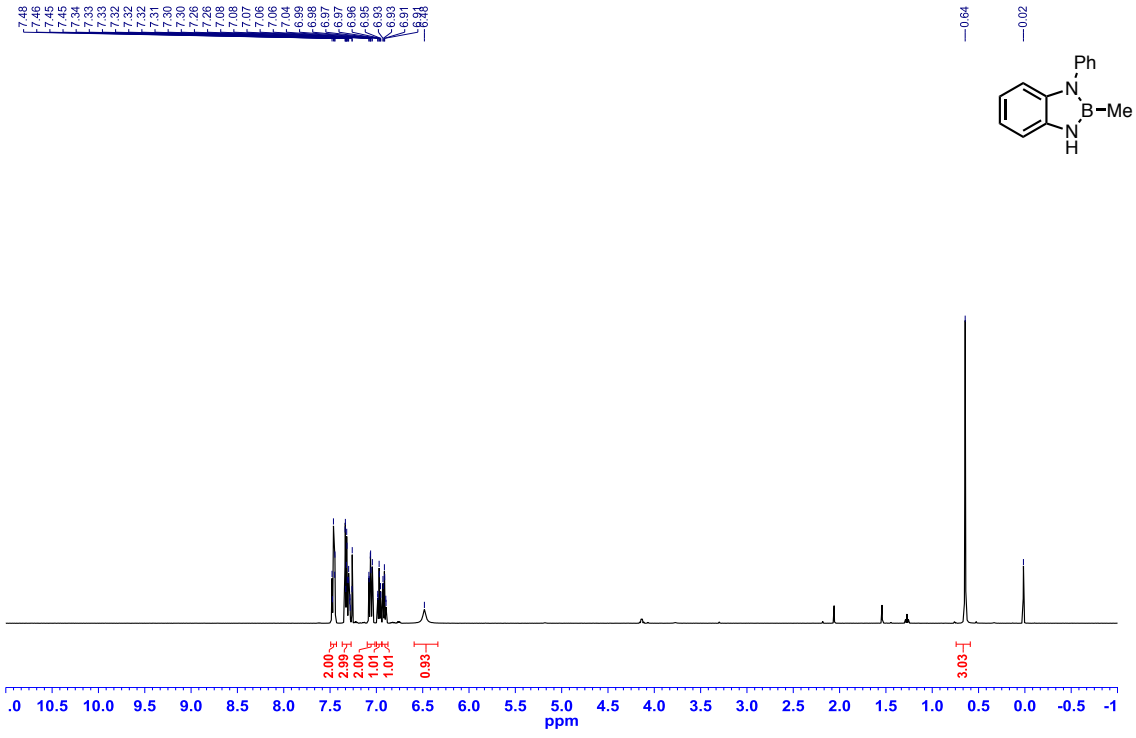

Figure A1.138: ^{13}C {^{1}H} NMR ($CDCl_3$, 125.8 MHz) of 2-methyl-1-phenyl-2,3-dihydro-1*H*-1,3,2-benzodiazaborole (**2.46**)

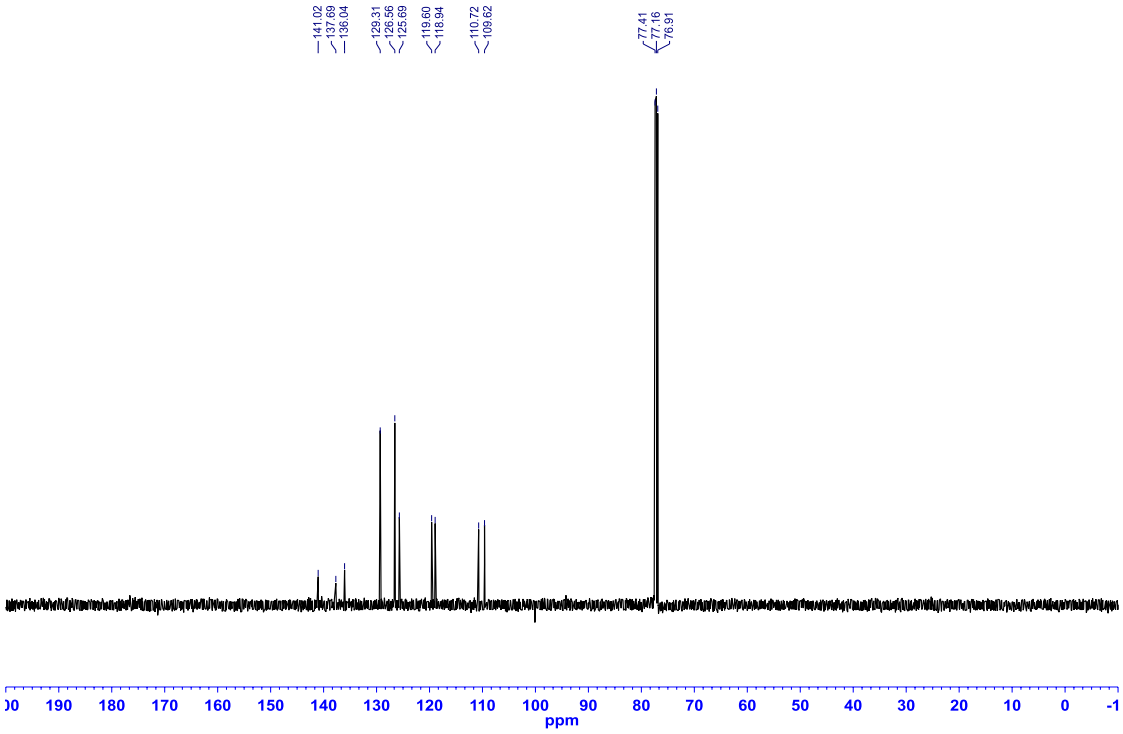

Figure A1.139: ^{11}B NMR (MeCN, 128.4 MHz) of 2-methyl-1-phenyl-2,3-dihydro-1*H*-1,3,2-benzodiazaborole (**2.46**)

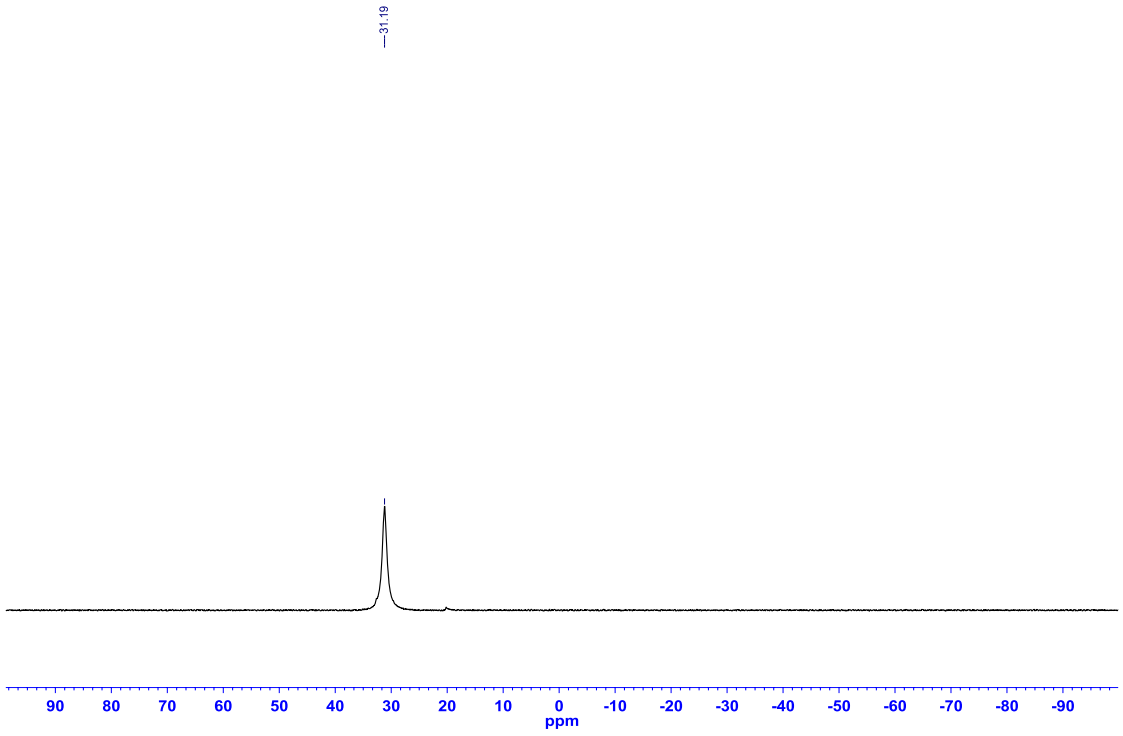

A1.3 – Computational data relevant for Chapter 2.3

Figure A1.140: Computed Properties for Truncated Azaborininones and Isosteres

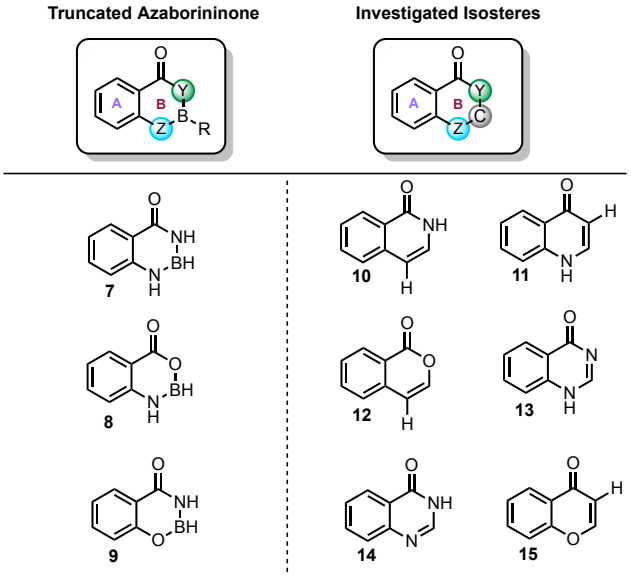

	Bond Length for Select B Ring Lengths (Å)				NICS (A Ring) (ppm)		NICS (B Ring) (ppm)	
Compound	**C=O**	**C-Y**	**Y-B**	**B-Z**	**NICS (1)**	**NICS (0)**	**NICS (1)**	**NICS (0)**
1,3,2-benzodiazaborininone (**2.98**)	1.219	1.392	1.423	1.414	-9.52	-8.12	-1.72	0.36
isoquinolinone (**2.101**)	1.223	1.392	1.374	1.348	-9.78	-7.56	-3.36	-1.22
quinolinone (**2.102**)	1.229	1.454	1.353	1.364	-9.89	-8.53	-3.25	-0.19
3,1,2-benzoxazaborininone (**2.99**)	1.201	1.379	1.377	1.409	-9.16	-7.82	-1.01	1.40
isochromenone (**2.103**)	1.202	1.392	1.359	1.337	-9.51	-7.37	-2.05	-0.60
1*H*-quinazolinone (**2.104**)	1.216	1.407	1.286	1.361	-9.81	-8.50	-2.21	1.62
1,3,2-benzoxazaborininone (**2.100**)	1.216	1.395	1.418	1.371	-9.85	-8.89	-1.18	1.24
3*H*-quinazolinone (**2.105**)	1.218	1.399	1.370	1.283	-9.94	-8.11	-3.06	-0.12
chromenone (**2.106**)	1.224	1.459	1.341	1.350	-10.19	-9.27	-2.25	-1.39

Figure A1.141: Computational Method and Data for pK_a of Truncated Cores

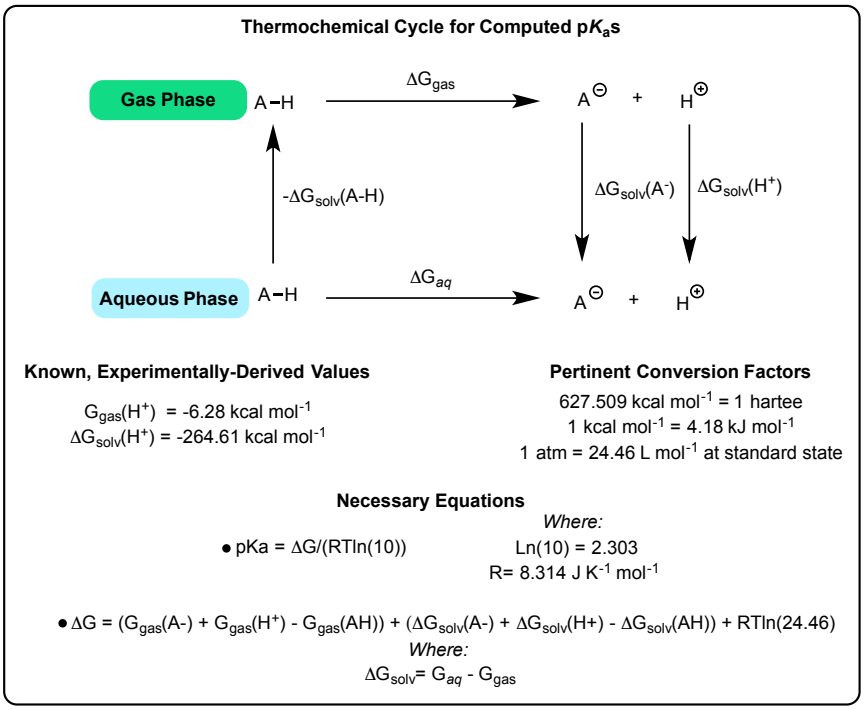

	G_{gas} (kcal mol^{-1})			G_{aq} (kcal mol^{-1})			ΔG_{solv} (kcal mol^{-1})			pK_a	
	A-H	**A$^-$(Y)**	**A$^-$(Z)**	**A-H**	**A$^-$(Y)**	**A$^-$(Z)**	**A-H**	**A$^-$(Y)**	**A$^-$(Z)**	**A-H(Y)**	**A-H (Z)**
2.98	-301642.86	-301294.10	-301286.77	-301649.85	-301345.15	-301344.86	-6.99	-51.06	-58.08	26.17	26.38
2.101	-299451.97	-299068.72	-299107.97	-299459.25	-299124.55	-299163.18	-7.28	-55.83	-55.21	48.16	19.85
2.102	-299442.96	-299109.59	-299054.06	-299453.13	-299161.37	-299117.62	-10.17	-51.78	-63.56	16.69	48.76
2.99	-314120.21	-313776.73	N/A	-314127.65	-313827.12	N/A	-7.44	-50.39	N/A	23.12	N/A
2.103	-311919.66	-311543.71	N/A	-311925.73	-311597.23	N/A	-6.07	-53.51	N/A	43.62	N/A
2.104	-309522.21	-309194.94	N/A	-309535.34	-309248.93	N/A	-13.13	-53.99	N/A	12.76	N/A
2.100	-314121.15	-313771.64	N/A	-314126.61	-313826.55	N/A	-5.46	-54.90	N/A	22.77	N/A
2.105	-309530.95	-309194.94	N/A	-309538.78	-309248.93	N/A	-7.83	-53.99	N/A	15.28	N/A
2.106	-311911.18	-311531.79	N/A	-311917.26	-311589.36	N/A	-6.08	-57.57	N/A	43.18	N/A

Figure A1.142: Computed properties for *B*-aryl azaborininone cores

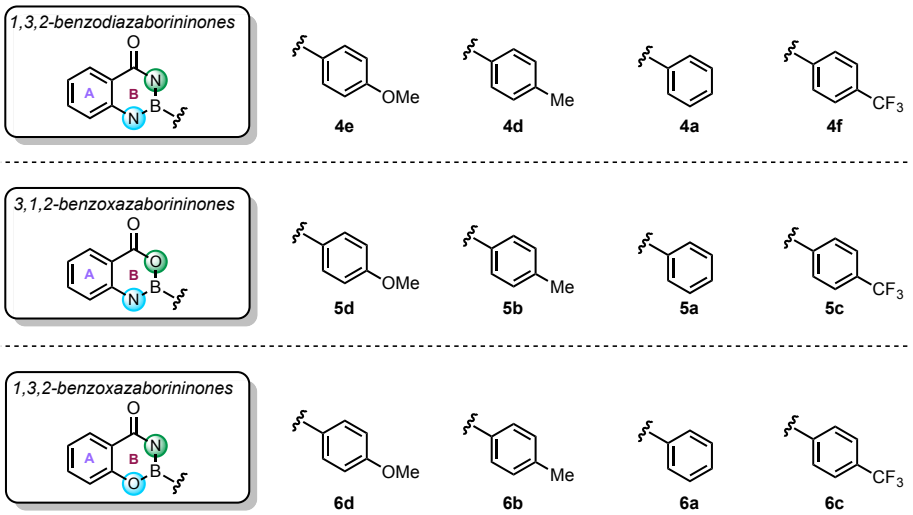

	Bond Length for Select B Ring Lengths (Å)					NICS (A Ring) (ppm)		NICS (B Ring) (ppm)		^{13}C NMR (ppm)[a]	IR C=O Stretch (cm^{-1})	
Compound	**C=O**	**C-Y**	**Y-B**	**B-Ar**	**B-Z**	**NICS (1)**	**NICS (0)**	**NICS (1)**	**NICS (0)**	**C=O**	**expt**	**calc**
1,3,2-benzodiazaborininones												
Phenyl (**2.56**)	1.220	1.390	1.431	1.563	1.422	-9.10	-7.69	-1.31	0.68	166.87	1634	1730
p-Tolyl (**2.64**)	1.220	1.389	1.432	1.561	1.423	-9.16	-7.77	-1.29	0.72	166.73	1637	1729
p-MeOC$_6$H$_4$ (**2.65**)	1.221	1.389	1.433	1.558	1.424	-9.08	-7.66	-1.30	0.63	166.79	1640	1729
p- F$_3$CC$_6$H$_4$ (**2.66**)	1.219	1.392	1.429	1.567	1.420	-9.29	-7.81	-1.22	0.73	–[b]	1630	1734
3,1,2-benzoxazaborininones												
Phenyl (**2.57**)	1.387	1.557	1.418	1.387	1.557	-8.76	-7.34	-0.49	1.98	–	1685	1786
p-Tolyl (**2.79**)	1.388	1.554	1.419	1.388	1.554	-8.91	-7.38	-0.50	2.01	–	1701	1784
p- MeOC$_6$H$_4$ (**2.80**)	1.389	1.550	1.421	1.389	1.550	-8.74	-7.28	-0.39	2.10	–	1698	1783
p-F$_3$CC$_6$H$_4$ (**2.81**)	1.384	1.561	1.416	1.384	1.561	-9.01	-7.52	-0.55	1.92	–	1686	1790
1,3,2-benzoxazaborininones												
Phenyl (**2.58**)	1.427	1.556	1.381	1.427	1.556	-9.51	-8.47	-0.64	1.79	165.50	1688	1745
p-Tolyl (**2.90**)	1.428	1.553	1.382	1.428	1.553	-9.53	-8.35	-0.56	2.16	165.34	1667	1744
p- MeOC$_6$H$_4$ (**2.91**)	1.429	1.549	1.384	1.429	1.549	-9.54	-8.49	-0.64	1.84	165.08	1680	1743
p- F$_3$CC$_6$H$_4$ (**2.92**)	1.424	1.561	1.379	1.424	1.561	-9.57	-8.43	-0.60	2.06	165.00	1683	1749

[a]Samples for ^{13}C NMR taken in $CDCl_3$, [b]Compound not soluble in $CDCl_3$

Figure A1.143: Additional plots of experimental and computational azaborininone correlations

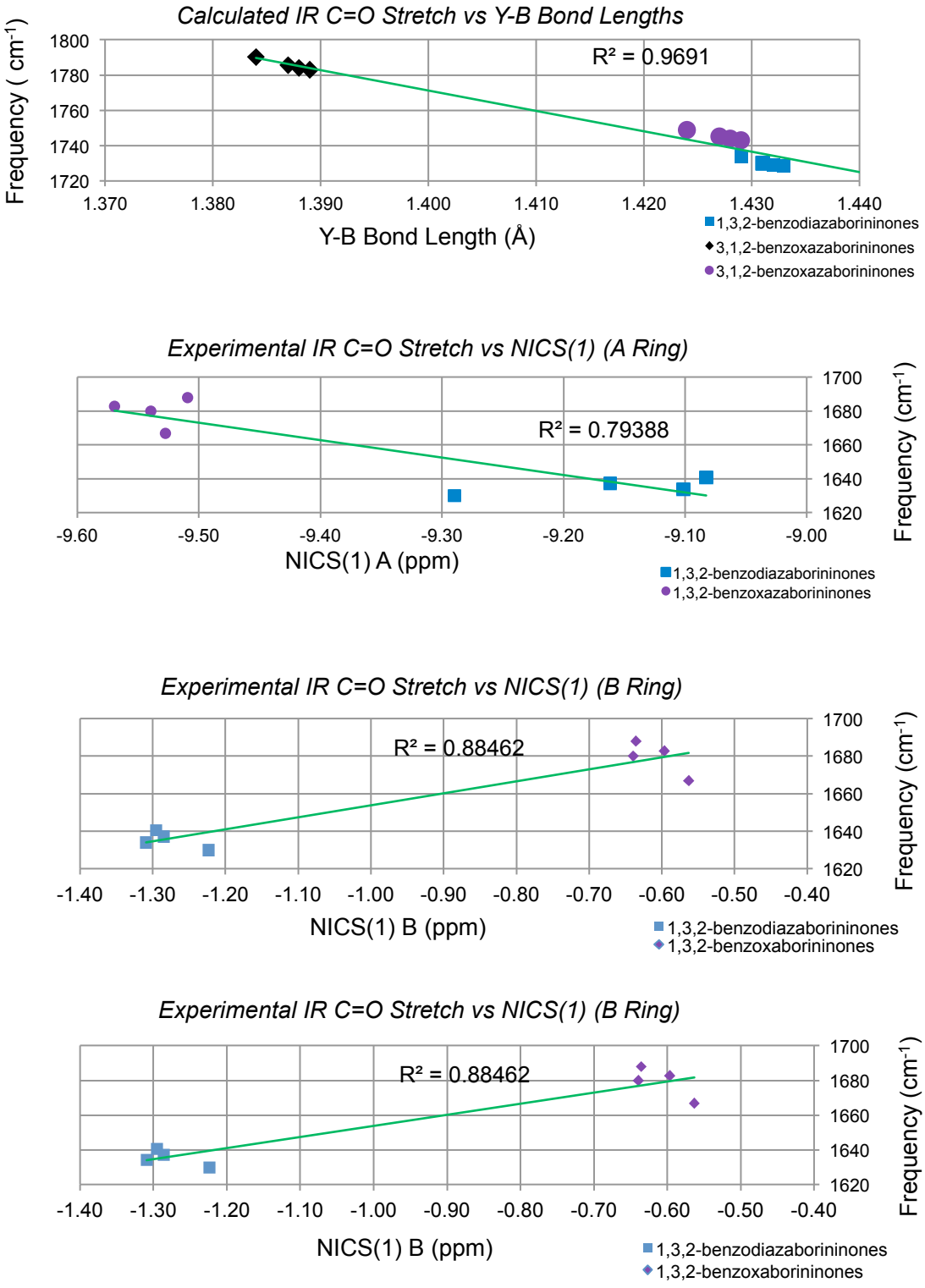

Figure A1.144: Atomic Coordinates for [B3LYP/6-311+G(2d,p)] optimized geometry value of total energy of 1,3,2-benzodiazaborininone (**2.98**) – gas phase

Center Number	Atomic Number	Atomic Type	Coordinates (Angstroms) X	Y	Z
1	6	0	0.040616	0.000000	0.020630
2	6	0	0.036171	0.000000	1.403336
3	6	0	1.251226	0.000000	2.094098
4	6	0	2.452492	0.000000	1.408049
5	6	0	2.464311	0.000000	0.007473
6	6	0	1.242922	0.000000	-0.693625
7	6	0	1.201856	0.000000	-2.174663
8	7	0	2.449562	0.000000	-2.792121
9	5	0	3.702816	0.000000	-2.117460
10	7	0	3.659200	0.000000	-0.703951
11	1	0	4.503393	0.000000	-0.153095
12	1	0	4.731252	0.000000	-2.708450
13	1	0	2.382468	0.000000	-3.801029
14	8	0	0.169307	0.000000	-2.823283
15	1	0	3.392611	0.000000	1.949195
16	1	0	1.257465	0.000000	3.177744
17	1	0	-0.899908	0.000000	1.947152
18	1	0	-0.880680	0.000000	-0.547750

E_{Tot}: -480.804266959 Hartree

Figure A1.145: Atomic Coordinates for [B3LYP/6-311+G(2d,p)] optimized geometry value of total energy of 1,3,2-benzodiazaborininone (**2.98**) – aqueous phase

Center Number	Atomic Number	Atomic Type	Coordinates (Angstroms) X	Y	Z
1	6	0	-0.002051	0.000000	-0.000566
2	6	0	-0.000970	0.000000	1.381472
3	6	0	1.219229	0.000000	2.067912
4	6	0	2.417372	0.000000	1.378279
5	6	0	2.424882	0.000000	-0.024423
6	6	0	1.198963	0.000000	-0.722261
7	6	0	1.160784	0.000000	-2.198337
8	7	0	2.395622	0.000000	-2.817844
9	5	0	3.655680	0.000000	-2.145118
10	7	0	3.615533	0.000000	-0.734466
11	1	0	4.462038	0.000000	-0.184340
12	1	0	4.677254	0.000000	-2.744396
13	1	0	2.338344	0.000000	-3.828173
14	8	0	0.116965	0.000000	-2.849788
15	1	0	3.359688	0.000000	1.913689
16	1	0	1.229712	0.000000	3.151336
17	1	0	-0.934376	0.000000	1.929627
18	1	0	-0.930954	0.000000	-0.555894

E_{Tot}: -480.815351469 Hartree

Figure A1.146: Atomic Coordinates for [B3LYP/6-311+G(2d,p)] optimized geometry value of total energy of 1,3,2-benzodiazaborinin-1-ide – gas phase

Center Number	Atomic Number	Atomic Type	Coordinates (Angstroms) X	Y	Z
1	6	0	-0.000825	0.000000	-0.006093
2	6	0	-0.008090	0.000000	1.375340
3	6	0	1.223941	0.000000	2.058404
4	6	0	2.415045	0.000000	1.370173
5	6	0	2.470869	0.000000	-0.058623
6	6	0	1.198579	0.000000	-0.732055
7	6	0	1.144114	0.000000	-2.198879
8	8	0	0.097230	0.000000	-2.866403
9	7	0	2.383192	0.000000	-2.798912
10	5	0	3.650537	0.000000	-2.076777
11	7	0	3.669152	0.000000	-0.683228
12	1	0	4.644246	0.000000	-2.762028
13	1	0	2.323721	0.000000	-3.808768
14	1	0	3.364832	0.000000	1.894329
15	1	0	1.233993	0.000000	3.145457
16	1	0	-0.943173	0.000000	1.924984
17	1	0	-0.925841	0.000000	-0.572142

E_{Tot}: -480.233984155 Hartree

Figure A1.147: Atomic Coordinates for [B3LYP/6-311+G(2d,p)] optimized geometry value of total energy of 1,3,2-benzodiazaborinin-1-ide – aqueous phase

Center Number	Atomic Number	Atomic Type	Coordinates (Angstroms) X	Y	Z
1	6	0	-0.000566	0.000000	0.000790
2	6	0	0.000811	0.000000	1.380350
3	6	0	1.234639	0.000000	2.058591
4	6	0	2.422698	0.000000	1.363272
5	6	0	2.467627	0.000000	-0.062316
6	6	0	1.198401	0.000000	-0.732840
7	6	0	1.142406	0.000000	-2.196559
8	8	0	0.084282	0.000000	-2.855994
9	7	0	2.368673	0.000000	-2.810351
10	5	0	3.638144	0.000000	-2.098809
11	7	0	3.666773	0.000000	-0.703666
12	1	0	4.628214	0.000000	-2.781045
13	1	0	2.312869	0.000000	-3.821464
14	1	0	3.369234	0.000000	1.893054
15	1	0	1.249536	0.000000	3.143499
16	1	0	-0.929769	0.000000	1.934595
17	1	0	-0.934003	0.000000	-0.549686

E_{Tot}: -480.315702925 Hartree

Figure A1.148: Atomic Coordinates for [B3LYP/6-311+G(2d,p)] optimized geometry value of total energy of 1,3,2-benzodiazaborinin-3-ide – gas phase

Center Number	Atomic Number	Atomic Type	Coordinates (Angstroms) X	Y	Z
1	6	0	0.023824	0.000000	-0.003649
2	6	0	0.003194	0.000000	1.385536
3	6	0	1.212950	0.000000	2.085651
4	6	0	2.415669	0.000000	1.398479
5	6	0	2.436424	0.000000	-0.008521
6	6	0	1.218268	0.000000	-0.724449
7	6	0	1.203707	0.000000	-2.245111
8	8	0	0.088069	0.000000	-2.799776
9	7	0	2.388484	0.000000	-2.890520
10	5	0	3.586404	0.000000	-2.181349
11	7	0	3.610924	0.000000	-0.725078
12	1	0	4.465758	0.000000	-0.189505
13	1	0	4.676933	0.000000	-2.706174
14	1	0	3.357431	0.000000	1.941455
15	1	0	1.215772	0.000000	3.171461
16	1	0	-0.939224	0.000000	1.923172
17	1	0	-0.890426	0.000000	-0.585746

E_{Tot}: -480.221482263 Hartree

Figure A1.149: Atomic Coordinates for [B3LYP/6-311+G(2d,p)] optimized geometry value of total energy of 1,3,2-benzodiazaborinin-3-ide – aqueous phase

Center Number	Atomic Number	Atomic Type	Coordinates (Angstroms) X	Y	Z
1	6	0	-0.008633	0.000000	0.000493
2	6	0	-0.000832	0.000000	1.386318
3	6	0	1.223533	0.000000	2.065138
4	6	0	2.413803	0.000000	1.360781
5	6	0	2.408098	0.000000	-0.045763
6	6	0	1.178914	0.000000	-0.741858
7	6	0	1.154543	0.000000	-2.243916
8	8	0	0.031778	0.000000	-2.816582
9	7	0	2.321551	0.000000	-2.913763
10	5	0	3.542690	0.000000	-2.213757
11	7	0	3.577052	0.000000	-0.776764
12	1	0	4.438056	0.000000	-0.249160
13	1	0	4.607518	0.000000	-2.774358
14	1	0	3.362701	0.000000	1.886806
15	1	0	1.243993	0.000000	3.149104
16	1	0	-0.931606	0.000000	1.940836
17	1	0	-0.943195	0.000000	-0.545854

E_{Tot}: -480.315341405 Hartree

Figure A1.150: Atomic Coordinates for [B3LYP/6-311+G(2d,p)] optimized geometry value of total energy of 3,1,2-benzoxazaborininone (**2.99**) – gas phase

Center Number	Atomic Number	Atomic Type	Coordinates (Angstroms) X	Y	Z
1	6	0	0.027351	0.000000	0.023468
2	6	0	0.033282	0.000000	1.420530
3	6	0	1.225967	0.000000	2.123344
4	6	0	2.442096	0.000000	1.433661
5	6	0	2.444369	0.000000	0.027431
6	6	0	1.228146	0.000000	-0.662849
7	1	0	1.259324	0.000000	-1.744634
8	6	0	3.710117	0.000000	-0.734205
9	8	0	4.865345	0.000000	0.018465
10	5	0	4.887655	0.000000	1.394997
11	7	0	3.665181	0.000000	2.095925
12	1	0	3.636135	0.000000	3.104262
13	1	0	5.933750	0.000000	1.953099
14	8	0	3.789436	0.000000	-1.932652
15	1	0	1.225036	0.000000	3.207698
16	1	0	-0.903963	0.000000	1.964272
17	1	0	-0.910313	0.000000	-0.517311

E_{Tot}: -500.67507438 Hartree

Figure A1.151: Atomic Coordinates for [B3LYP/6-311+G(2d,p)] optimized geometry value of total energy of 3,1,2-benzoxazaborininone (**2.99**) – aqueous phase

Center Number	Atomic Number	Atomic Type	Coordinates (Angstroms) X	Y	Z
1	6	0	0.000302	0.000000	-0.002531
2	6	0	0.004084	0.000000	1.397314
3	6	0	1.193145	0.000000	2.104609
4	6	0	2.413349	0.000000	1.419016
5	6	0	2.417790	0.000000	0.010715
6	6	0	1.201433	0.000000	-0.685440
7	1	0	1.226615	0.000000	-1.767157
8	6	0	3.682956	0.000000	-0.734109
9	8	0	4.831733	0.000000	0.014602
10	5	0	4.850834	0.000000	1.401041
11	7	0	3.627986	0.000000	2.089893
12	1	0	3.588972	0.000000	3.099184
13	1	0	5.899127	0.000000	1.950268
14	8	0	3.781389	0.000000	-1.941347
15	1	0	1.190592	0.000000	3.188067
16	1	0	-0.934421	0.000000	1.938364
17	1	0	-0.936529	0.000000	-0.544330

E_{Tot}: -500.686921703 Hartree

Figure A1.152: Atomic Coordinates for [B3LYP/6-311+G(2d,p)] optimized geometry value of total energy of 3,1,2-benzoxazaborinin-1-ide – gas phase

Center Number	Atomic Number	Atomic Type	Coordinates (Angstroms) X	Y	Z
1	6	0	0.002070	0.000000	-0.011196
2	6	0	0.012111	0.000000	1.397323
3	6	0	1.195355	0.000000	2.099558
4	6	0	2.464024	0.000000	1.442959
5	6	0	2.427397	0.000000	0.009118
6	6	0	1.208986	0.000000	-0.683613
7	1	0	1.246895	0.000000	-1.767191
8	6	0	3.684072	0.000000	-0.745630
9	8	0	3.768552	0.000000	-1.965578
10	8	0	4.815183	0.000000	0.002470
11	5	0	4.785054	0.000000	1.427350
12	7	0	3.608458	0.000000	2.161451
13	1	0	5.886808	0.000000	1.907716
14	1	0	1.204987	0.000000	3.184197
15	1	0	-0.930468	0.000000	1.938569
16	1	0	-0.935800	0.000000	-0.555430

E_{Tot}: -500.113499578 Hartree

Figure A1.153: Atomic Coordinates for [B3LYP/6-311+G(2d,p)] optimized geometry value of total energy of 3,1,2-benzoxazaborinin-1-ide – aqueous phase

Center Number	Atomic Number	Atomic Type	Coordinates (Angstroms) X	Y	Z
1	6	0	0.001636	0.000000	-0.000002
2	6	0	0.000753	0.000000	1.407682
3	6	0	1.180779	0.000000	2.118269
4	6	0	2.446433	0.000000	1.468227
5	6	0	2.425561	0.000000	0.037923
6	6	0	1.209007	0.000000	-0.666723
7	1	0	1.241806	0.000000	-1.749555
8	6	0	3.684281	0.000000	-0.699783
9	8	0	3.788379	0.000000	-1.922829
10	8	0	4.812979	0.000000	0.048264
11	5	0	4.778465	0.000000	1.473881
12	7	0	3.598031	0.000000	2.195541
13	1	0	5.874852	0.000000	1.959969
14	1	0	1.171664	0.000000	3.202500
15	1	0	-0.943993	0.000000	1.941073
16	1	0	-0.932388	0.000000	-0.548179

E_{Tot}: -500.194117299 Hartree

Figure A1.154: Atomic Coordinates for [B3LYP/6-311+G(2d,p)] optimized geometry value of total energy of 1,3,2-benzoxazaborininone (**2.100**) – gas phase

Center Number	Atomic Number	Atomic Type	Coordinates (Angstroms) X	Y	Z
1	6	0	0.039044	0.000000	0.022981
2	6	0	0.068318	0.000000	1.420287
3	6	0	1.274381	0.000000	2.102443
4	6	0	2.465115	0.000000	1.381576
5	6	0	2.453885	0.000000	-0.019034
6	6	0	1.225503	0.000000	-0.687893
7	1	0	1.238257	0.000000	-1.770376
8	6	0	3.719117	0.000000	-0.786010
9	7	0	4.859395	0.000000	0.017232
10	5	0	4.843789	0.000000	1.434745
11	8	0	3.637871	0.000000	2.087720
12	1	0	5.838553	0.000000	2.078177
13	1	0	5.721380	0.000000	-0.512041
14	8	0	3.785816	0.000000	-1.999811
15	1	0	1.316847	0.000000	3.184020
16	1	0	-0.859342	0.000000	1.980068
17	1	0	-0.908712	0.000000	-0.500334

E_{Tot}: -500.676972414 Hartree

Figure A1.155: Atomic Coordinates for [B3LYP/6-311+G(2d,p)] optimized geometry value of total energy of 1,3,2-benzoxazaborininone (**2.100**) – aqueous phase

Center Number	Atomic Number	Atomic Type	Coordinates (Angstroms) X	Y	Z
1	6	0	0.000323	0.000000	-0.000614
2	6	0	0.000069	0.000000	1.398038
3	6	0	1.191851	0.000000	2.105082
4	6	0	2.397535	0.000000	1.409097
5	6	0	2.417621	0.000000	0.007734
6	6	0	1.201527	0.000000	-0.686253
7	1	0	1.226864	0.000000	-1.768195
8	6	0	3.699574	0.000000	-0.725097
9	7	0	4.818104	0.000000	0.091725
10	5	0	4.774407	0.000000	1.510219
11	8	0	3.555023	0.000000	2.139126
12	1	0	5.754942	0.000000	2.172535
13	1	0	5.697802	0.000000	-0.409538
14	8	0	3.789002	0.000000	-1.946073
15	1	0	1.207563	0.000000	3.187407
16	1	0	-0.938767	0.000000	1.938150
17	1	0	-0.936172	0.000000	-0.543282

E_{Tot}: -500.685417254 Hartree

Figure A1.156: Atomic Coordinates for [B3LYP/6-311+G(2d,p)] optimized geometry value of total energy of 1,3,2-benzoxazaborinin-3-ide – gas phase

Center Number	Atomic Number	Atomic Type	Coordinates (Angstroms) X	Y	Z
1	6	0	0.000642	0.000000	0.003471
2	6	0	-0.014405	0.000000	1.401221
3	6	0	1.176273	0.000000	2.111593
4	6	0	2.398175	0.000000	1.427733
5	6	0	2.430259	0.000000	0.024400
6	6	0	1.216645	0.000000	-0.666254
7	1	0	1.271328	0.000000	-1.748729
8	6	0	3.757573	0.000000	-0.707956
9	8	0	3.729748	0.000000	-1.949727
10	7	0	4.873004	0.000000	0.051874
11	5	0	4.773471	0.000000	1.432653
12	8	0	3.538788	0.000000	2.152082
13	1	0	5.740206	0.000000	2.115276
14	1	0	1.189563	0.000000	3.195783
15	1	0	-0.958933	0.000000	1.936263
16	1	0	-0.931860	0.000000	-0.551303

E_{Tot}: -500.105329059 Hartree

Figure A1.157: Atomic Coordinates for [B3LYP/6-311+G(2d,p)] optimized geometry value of total energy of 1,3,2-benzoxazaborinin-3-ide – aqueous phase

Center Number	Atomic Number	Atomic Type	Coordinates (Angstroms) X	Y	Z
1	6	0	0.001204	0.000000	-0.001044
2	6	0	0.004473	0.000000	1.397709
3	6	0	1.202216	0.000000	2.094471
4	6	0	2.410466	0.000000	1.392313
5	6	0	2.429203	0.000000	-0.010162
6	6	0	1.204532	0.000000	-0.688766
7	1	0	1.224367	0.000000	-1.771120
8	6	0	3.741030	0.000000	-0.738458
9	8	0	3.729499	0.000000	-1.990899
10	7	0	4.870234	0.000000	-0.000965
11	5	0	4.783951	0.000000	1.390610
12	8	0	3.567700	0.000000	2.104325
13	1	0	5.740206	0.000000	2.115276
14	1	0	1.223419	0.000000	3.177688
15	1	0	-0.932083	0.000000	1.943062
16	1	0	-0.937466	0.000000	-0.541870

E_{Tot}: -500.193544554 Hartree

Figure A1.158: Atomic Coordinates for [B3LYP/6-311+G(2d,p)] optimized geometry value of total energy of isoquinolinone (**2.101**) – gas phase

Center Number	Atomic Number	Atomic Type	Coordinates (Angstroms) X	Y	Z
1	6	0	0.036395	0.000000	0.010161
2	6	0	0.038547	0.000000	1.411716
3	6	0	1.228615	0.000000	2.111606
4	6	0	2.460744	0.000000	1.431544
5	6	0	2.448394	0.000000	0.016605
6	6	0	1.233469	0.000000	-0.678900
7	1	0	1.263959	0.000000	-1.760940
8	6	0	3.707047	0.000000	-0.745932
9	7	0	4.853141	0.000000	0.043787
10	6	0	4.867682	0.000000	1.418149
11	6	0	3.720723	0.000000	2.125818
12	1	0	3.750346	0.000000	3.206501
13	1	0	5.846581	0.000000	1.877918
14	1	0	5.720804	0.000000	-0.473790
15	8	0	3.797542	0.000000	-1.965332
16	1	0	1.224487	0.000000	3.195671
17	1	0	-0.901750	0.000000	1.950656
18	1	0	-0.902534	0.000000	-0.529738

E_{Tot}: -477.315096123 Hartree

Figure A1.159: Atomic Coordinates for [B3LYP/6-311+G(2d,p)] optimized geometry value of total energy of isoquinolinone (**2.101**) – aqueous phase

Center Number	Atomic Number	Atomic Type	Coordinates (Angstroms) X	Y	Z
1	6	0	0.000264	0.000000	-0.001134
2	6	0	0.000825	0.000000	1.402605
3	6	0	1.189448	0.000000	2.103686
4	6	0	2.424252	0.000000	1.424267
5	6	0	2.415180	0.000000	0.007625
6	6	0	1.197537	0.000000	-0.688635
7	1	0	1.218512	0.000000	-1.770665
8	6	0	3.675538	0.000000	-0.742808
9	7	0	4.812533	0.000000	0.040053
10	6	0	4.828405	0.000000	1.414548
11	6	0	3.679535	0.000000	2.121262
12	1	0	3.706413	0.000000	3.201886
13	1	0	5.808630	0.000000	1.869520
14	1	0	5.689519	0.000000	-0.463932
15	8	0	3.766726	0.000000	-1.974141
16	1	0	1.184665	0.000000	3.187324
17	1	0	-0.940051	0.000000	1.939999
18	1	0	-0.938025	0.000000	-0.541700

E_{Tot}: -477.326922718 Hartree

Figure A1.160: Atomic Coordinates for [B3LYP/6-311+G(2d,p)] optimized geometry value of total energy of isoquinolin-4-ide – gas phase

Center Number	Atomic Number	Atomic Type	Coordinates (Angstroms) X	Y	Z
1	6	0	0.000764	0.000000	-0.010892
2	6	0	0.005966	0.000000	1.396475
3	6	0	1.196950	0.000000	2.090846
4	6	0	2.458431	0.000000	1.438121
5	6	0	2.420647	0.000000	0.008279
6	6	0	1.201797	0.000000	-0.690553
7	1	0	1.237404	0.000000	-1.774145
8	6	0	3.670501	0.000000	-0.755485
9	8	0	3.758664	0.000000	-1.998898
10	7	0	4.785545	0.000000	0.034228
11	6	0	4.788646	0.000000	1.446992
12	6	0	3.680392	0.000000	2.226522
13	1	0	5.807797	0.000000	1.835604
14	1	0	5.659416	0.000000	-0.477160
15	1	0	1.213010	0.000000	3.175405
16	1	0	-0.936542	0.000000	1.937095
17	1	0	-0.938523	0.000000	-0.554711

E_{Tot}: -476.689632014 Hartree

Figure A1.161: Atomic Coordinates for [B3LYP/6-311+G(2d,p)] optimized geometry value of total energy of isoquinolin-4-ide – aqueous phase

Center Number	Atomic Number	Atomic Type	Coordinates (Angstroms) X	Y	Z
1	6	0	0.000299	0.000000	0.000877
2	6	0	-0.002481	0.000000	1.406987
3	6	0	1.185724	0.000000	2.107545
4	6	0	2.447704	0.000000	1.458653
5	6	0	2.421142	0.000000	0.030863
6	6	0	1.203515	0.000000	-0.673777
7	1	0	1.231129	0.000000	-1.756694
8	6	0	3.675275	0.000000	-0.720940
9	8	0	3.763148	0.000000	-1.968383
10	7	0	4.790870	0.000000	0.060848
11	6	0	4.792870	0.000000	1.466689
12	6	0	3.676422	0.000000	2.239599
13	1	0	5.806983	0.000000	1.858492
14	1	0	5.672401	0.000000	-0.437890
15	1	0	1.179113	0.000000	3.192128
16	1	0	-0.946286	0.000000	1.941520
17	1	0	-0.935387	0.000000	-0.545876

E_{Tot}: -476.77950934 Hartree

Figure A1.162: Atomic Coordinates for [B3LYP/6-311+G(2d,p)] optimized geometry value of total energy of isoquinolin-2-ide – gas phase

Center Number	Atomic Number	Atomic Type	Coordinates (Angstroms) X	Y	Z
1	6	0	-0.000227	0.000000	-0.002293
2	6	0	-0.015493	0.000000	1.404309
3	6	0	1.165805	0.000000	2.114318
4	6	0	2.419329	0.000000	1.451174
5	6	0	2.428424	0.000000	0.028772
6	6	0	1.213075	0.000000	-0.667827
7	1	0	1.266001	0.000000	-1.750400
8	6	0	3.717811	0.000000	-0.717076
9	8	0	3.717839	0.000000	-1.963900
10	7	0	4.881679	0.000000	0.008112
11	6	0	4.812776	0.000000	1.344957
12	6	0	3.669424	0.000000	2.119912
13	1	0	3.726745	0.000000	3.203022
14	1	0	5.780037	0.000000	1.853512
15	1	0	1.148398	0.000000	3.200764
16	1	0	-0.963748	0.000000	1.934322
17	1	0	-0.933117	0.000000	-0.556698

E_{Tot}: -476.752323618 Hartree

Figure A1.163: Atomic Coordinates for [B3LYP/6-311+G(2d,p)] optimized geometry value of total energy of isoquinolin-2-ide – aqueous phase

Center Number	Atomic Number	Atomic Type	Coordinates (Angstroms) X	Y	Z
1	6	0	0.002547	0.000000	-0.000011
2	6	0	0.005282	0.000000	1.407772
3	6	0	1.195060	0.000000	2.101969
4	6	0	2.435847	0.000000	1.418133
5	6	0	2.429967	0.000000	-0.002299
6	6	0	1.201049	0.000000	-0.685556
7	1	0	1.219604	0.000000	-1.768132
8	6	0	3.707509	0.000000	-0.742904
9	8	0	3.710637	0.000000	-2.007617
10	7	0	4.871887	0.000000	-0.042019
11	6	0	4.829210	0.000000	1.310833
12	6	0	3.694191	0.000000	2.080868
13	1	0	3.753433	0.000000	3.162622
14	1	0	5.801068	0.000000	1.801746
15	1	0	1.193319	0.000000	3.186985
16	1	0	-0.935241	0.000000	1.947539
17	1	0	-0.937433	0.000000	-0.539521

E_{Tot}: -476.841303383 Hartree

Figure A1.164: Atomic Coordinates for [B3LYP/6-311+G(2d,p)] optimized geometry value of total energy of quinolinone (**2.102**) – gas phase

Center Number	Atomic Number	Atomic Type	Coordinates (Angstroms) X	Y	Z
1	6	0	-0.015242	0.000000	-0.006006
2	6	0	-0.007642	0.000000	1.400801
3	7	0	1.205888	0.000000	2.065786
4	6	0	2.392534	0.000000	1.393812
5	6	0	2.458339	0.000000	0.042450
6	6	0	1.255413	0.000000	-0.773844
7	8	0	1.275845	0.000000	-2.002940
8	1	0	3.416866	0.000000	-0.457357
9	1	0	3.277038	0.000000	2.018333
10	1	0	1.206509	0.000000	3.072798
11	6	0	-1.213952	0.000000	2.117232
12	6	0	-2.413452	0.000000	1.434688
13	6	0	-2.436130	0.000000	0.033169
14	6	0	-1.248806	0.000000	-0.670897
15	1	0	-1.229511	0.000000	-1.753563
16	1	0	-3.383193	0.000000	-0.491892
17	1	0	-3.343288	0.000000	1.990873
18	1	0	-1.197216	0.000000	3.202057

E_{Tot}: -477.300163192 Hartree

Figure A1.165: Atomic Coordinates for [B3LYP/6-311+G(2d,p)] optimized geometry value of total energy of quinolinone (**2.102**) – aqueous phase

Center Number	Atomic Number	Atomic Type	Coordinates (Angstroms) X	Y	Z
1	6	0	0.004519	0.000000	-0.005355
2	6	0	0.004434	0.000000	1.404374
3	7	0	1.209176	0.000000	2.076120
4	6	0	2.392115	0.000000	1.418807
5	6	0	2.465011	0.000000	0.060123
6	6	0	1.276796	0.000000	-0.754273
7	8	0	1.307493	0.000000	-1.999418
8	1	0	3.431865	0.000000	-0.424197
9	1	0	3.273261	0.000000	2.046045
10	1	0	1.205764	0.000000	3.085949
11	6	0	-1.206458	0.000000	2.116748
12	6	0	-2.401441	0.000000	1.429295
13	6	0	-2.418751	0.000000	0.024896
14	6	0	-1.230399	0.000000	-0.674979
15	1	0	-1.219713	0.000000	-1.757286
16	1	0	-3.364098	0.000000	-0.503096
17	1	0	-3.333716	0.000000	1.980749
18	1	0	-1.190238	0.000000	3.200408

E_{Tot}: -477.316904046 Hartree

Figure A1.166: Atomic Coordinates for [B3LYP/6-311+G(2d,p)] optimized geometry value of total energy of quinolin-1-ide – gas phase

Center Number	Atomic Number	Atomic Type	Coordinates (Angstroms) X	Y	Z
1	6	0	0.016628	0.000000	-0.009680
2	6	0	0.049649	0.000000	1.418416
3	7	0	1.199679	0.000000	2.151152
4	6	0	2.327471	0.000000	1.437232
5	6	0	2.436020	0.000000	0.054361
6	6	0	1.275664	0.000000	-0.778785
7	8	0	1.295912	0.000000	-2.033695
8	1	0	3.412278	0.000000	-0.419345
9	1	0	3.246409	0.000000	2.027233
10	6	0	-1.192828	0.000000	2.107245
11	6	0	-2.390448	0.000000	1.429702
12	6	0	-2.413343	0.000000	0.020550
13	6	0	-1.220927	0.000000	-0.674240
14	1	0	-1.196544	0.000000	-1.758403
15	1	0	-3.360582	0.000000	-0.509268
16	1	0	-3.323984	0.000000	1.985312
17	1	0	-1.160538	0.000000	3.191761

E_{Tot}: -476.755297232 Hartree

Figure A1.167: Atomic Coordinates for [B3LYP/6-311+G(2d,p)] optimized geometry value of total energy of quinolin-1-ide – aqueous phase

Center Number	Atomic Number	Atomic Type	Coordinates (Angstroms) X	Y	Z
1	6	0	0.000000	0.000000	0.000000
2	6	0	0.000000	0.000000	1.428478
3	7	0	1.132785	0.000000	2.187602
4	6	0	2.276779	0.000000	1.499943
5	6	0	2.417265	0.000000	0.119951
6	6	0	1.276478	0.000000	-0.739795
7	8	0	1.325730	0.000000	-1.993902
8	1	0	3.404213	0.000000	-0.331061
9	1	0	3.181833	0.000000	2.111029
10	6	0	-1.258067	0.000000	2.088401
11	6	0	-2.439706	0.000000	1.383355
12	6	0	-2.430020	0.000000	-0.025949
13	6	0	-1.221862	0.000000	-0.692990
14	1	0	-1.172424	0.000000	-1.776300
15	1	0	-3.364759	0.000000	-0.577522
16	1	0	-3.385836	0.000000	1.917237
17	1	0	-1.250856	0.000000	3.173374

E_{Tot}: -476.838434415 Hartree

Figure A1.168: Atomic Coordinates for [B3LYP/6-311+G(2d,p)] optimized geometry value of total energy of quinolin-3-ide – gas phase

Center Number	Atomic Number	Atomic Type	Coordinates (Angstroms) X	Y	Z
1	6	0	0.001601	0.095213	-0.029201
2	6	0	-0.024487	0.123678	1.384814
3	7	0	1.162669	0.227967	2.044867
4	6	0	2.367875	0.443214	1.332882
5	6	0	2.526251	0.412706	-0.008530
6	6	0	1.314245	0.111450	-0.765916
7	8	0	1.287154	-0.133937	-1.985319
8	1	0	3.182219	0.654174	2.032797
9	1	0	1.152537	0.309448	3.052041
10	6	0	-1.255071	0.042992	2.070135
11	6	0	-2.438971	-0.046595	1.365115
12	6	0	-2.429588	-0.063807	-0.038151
13	6	0	-1.219351	0.003510	-0.708393
14	1	0	-1.168964	-0.025648	-1.791058
15	1	0	-3.362714	-0.135003	-0.587397
16	1	0	-3.379694	-0.103062	1.904035
17	1	0	-1.261353	0.057343	3.156880

E_{Tot}: -476.664150187 Hartree

Figure A1.169: Atomic Coordinates for [B3LYP/6-311+G(2d,p)] optimized geometry value of total energy of quinolin-3-ide – aqueous phase

Center Number	Atomic Number	Atomic Type	Coordinates (Angstroms) X	Y	Z
1	6	0	0.002931	0.000000	-0.008302
2	6	0	0.002429	0.000000	1.404411
3	7	0	1.205269	0.000000	2.050820
4	6	0	2.398945	0.000000	1.346758
5	6	0	2.533577	0.000000	-0.012532
6	6	0	1.287133	0.000000	-0.755013
7	8	0	1.241455	0.000000	-2.016469
8	1	0	3.251941	0.000000	2.023372
9	1	0	1.219059	0.000000	3.060916
10	6	0	-1.212007	0.000000	2.121133
11	6	0	-2.410309	0.000000	1.441260
12	6	0	-2.431333	0.000000	0.034976
13	6	0	-1.242075	0.000000	-0.665320
14	1	0	-1.237774	0.000000	-1.748018
15	1	0	-3.378507	0.000000	-0.491344
16	1	0	-3.340909	0.000000	1.996817
17	1	0	-1.191585	0.000000	3.205542

E_{Tot}: -476.767911396 Hartree

Figure A1.170: Atomic Coordinates for [B3LYP/6-311+G(2d,p)] optimized geometry value of total energy of isochromenone (**2.103**) – gas phase

Center Number	Atomic Number	Atomic Type	Coordinates (Angstroms) X	Y	Z
1	6	0	0.028027	0.000000	0.012129
2	6	0	0.022151	0.000000	1.411557
3	6	0	1.209761	0.000000	2.120703
4	6	0	2.438749	0.000000	1.444150
5	6	0	2.437063	0.000000	0.034690
6	6	0	1.230027	0.000000	-0.671849
7	1	0	1.263641	0.000000	-1.753524
8	6	0	3.700769	0.000000	-0.715223
9	8	0	4.865870	0.000000	0.045811
10	6	0	4.838312	0.000000	1.404214
11	6	0	3.710178	0.000000	2.122568
12	1	0	3.763963	0.000000	3.202615
13	1	0	5.836618	0.000000	1.818387
14	8	0	3.816292	0.000000	-1.911200
15	1	0	1.200095	0.000000	3.204417
16	1	0	-0.921292	0.000000	1.944645
17	1	0	-0.907289	0.000000	-0.533589

E_{Tot}: -497.170550985 Hartree

Figure A1.171: Atomic Coordinates for [B3LYP/6-311+G(2d,p)] optimized geometry value of total energy of isochromenone (**2.103**) – aqueous phase

Center Number	Atomic Number	Atomic Type	Coordinates (Angstroms) X	Y	Z
1	6	0	-0.000154	0.000000	-0.001372
2	6	0	0.002352	0.000000	1.399953
3	6	0	1.193133	0.000000	2.103302
4	6	0	2.419023	0.000000	1.419431
5	6	0	2.410135	0.000000	0.008359
6	6	0	1.196827	0.000000	-0.692462
7	1	0	1.214909	0.000000	-1.774190
8	6	0	3.669037	0.000000	-0.734462
9	8	0	4.830574	0.000000	0.011815
10	6	0	4.817423	0.000000	1.377869
11	6	0	3.690016	0.000000	2.095737
12	1	0	3.744292	0.000000	3.175541
13	1	0	5.818760	0.000000	1.781999
14	8	0	3.791069	0.000000	-1.940470
15	1	0	1.190025	0.000000	3.186468
16	1	0	-0.938027	0.000000	1.937693
17	1	0	-0.938773	0.000000	-0.540807

E_{Tot}: -497.180298877 Hartree

Figure A1.172: Atomic Coordinates for [B3LYP/6-311+G(2d,p)] optimized geometry value of total energy of isochromen-4-ide – gas phase

Center Number	Atomic Number	Atomic Type	Coordinates (Angstroms) X	Y	Z
1	6	0	0.001948	0.000000	-0.010422
2	6	0	0.003659	0.000000	1.393859
3	6	0	1.194608	0.000000	2.093034
4	6	0	2.449157	0.000000	1.436477
5	6	0	2.419274	0.000000	0.016462
6	6	0	1.206623	0.000000	-0.688414
7	1	0	1.242862	0.000000	-1.771484
8	6	0	3.678227	0.000000	-0.745646
9	8	0	4.811109	0.000000	-0.022740
10	6	0	4.772278	0.000000	1.423203
11	6	0	3.688705	0.000000	2.200450
12	1	0	5.811797	0.000000	1.732012
13	8	0	3.748252	0.000000	-1.969366
14	1	0	1.208597	0.000000	3.177347
15	1	0	-0.940255	0.000000	1.931629
16	1	0	-0.935520	0.000000	-0.556771

E_{Tot}: -496.556783348 Hartree

Figure A1.173: Atomic Coordinates for [B3LYP/6-311+G(2d,p)] optimized geometry value of total energy of isochromen-4-ide – aqueous phase

Center Number	Atomic Number	Atomic Type	Coordinates (Angstroms) X	Y	Z
1	6	0	-0.000225	0.000000	0.000717
2	6	0	-0.000358	0.000000	1.403526
3	6	0	1.190871	0.000000	2.105208
4	6	0	2.441445	0.000000	1.448021
5	6	0	2.415987	0.000000	0.028801
6	6	0	1.202957	0.000000	-0.678504
7	1	0	1.226831	0.000000	-1.761014
8	6	0	3.673601	0.000000	-0.721910
9	8	0	4.809881	0.000000	-0.002093
10	6	0	4.780298	0.000000	1.436066
11	6	0	3.689573	0.000000	2.204752
12	1	0	5.818001	0.000000	1.747589
13	8	0	3.761804	0.000000	-1.947229
14	1	0	1.187038	0.000000	3.189472
15	1	0	-0.943126	0.000000	1.939317
16	1	0	-0.936402	0.000000	-0.544508

E_{Tot}: -496.642678107 Hartree

Figure A1.174: Atomic Coordinates for [B3LYP/6-311+G(2d,p)] optimized geometry value of total energy of 1*H*-quinazolinone (**2.104**) – gas phase

Center Number	Atomic Number	Atomic Type	Coordinates (Angstroms) X	Y	Z
1	6	0	0.035399	0.000000	0.030713
2	6	0	0.041965	0.000000	1.430415
3	6	0	1.234976	0.000000	2.129566
4	6	0	2.439781	0.000000	1.419599
5	6	0	2.451396	0.000000	0.018470
6	6	0	1.230780	0.000000	-0.664228
7	1	0	1.259384	0.000000	-1.746317
8	6	0	3.745958	0.000000	-0.711412
9	7	0	4.920288	0.000000	0.063989
10	6	0	4.825185	0.000000	1.346344
11	7	0	3.669048	0.000000	2.063800
12	1	0	3.707983	0.000000	3.071670
13	1	0	5.731183	0.000000	1.948993
14	8	0	3.798695	0.000000	-1.925826
15	1	0	1.241483	0.000000	3.213993
16	1	0	-0.894563	0.000000	1.974943
17	1	0	-0.906007	0.000000	-0.504212

E_{Tot}: -493.350802377 Hartree

Figure A1.175: Atomic Coordinates for [B3LYP/6-311+G(2d,p)] optimized geometry value of total energy of 1*H*-quinazolinone (**2.104**) – aqueous phase

Center Number	Atomic Number	Atomic Type	Coordinates (Angstroms) X	Y	Z
1	6	0	0.001881	0.000000	-0.001653
2	6	0	0.005732	0.000000	1.400790
3	6	0	1.194566	0.000000	2.104505
4	6	0	2.402101	0.000000	1.396791
5	6	0	2.417726	0.000000	-0.006429
6	6	0	1.196885	0.000000	-0.694626
7	1	0	1.215977	0.000000	-1.776458
8	6	0	3.712359	0.000000	-0.715056
9	7	0	4.874269	0.000000	0.054030
10	6	0	4.775489	0.000000	1.349852
11	7	0	3.624388	0.000000	2.046557
12	1	0	3.659042	0.000000	3.057165
13	1	0	5.677791	0.000000	1.952641
14	8	0	3.783881	0.000000	-1.944039
15	1	0	1.200459	0.000000	3.187808
16	1	0	-0.932379	0.000000	1.941894
17	1	0	-0.938721	0.000000	-0.537589

E_{Tot}: -493.372400975 Hartree

Figure A1.176: Atomic Coordinates for [B3LYP/6-311+G(2d,p)] optimized geometry value of total energy of 1*H*-quinazolin-1-ide – gas phase

Center Number	Atomic Number	Atomic Type	Coordinates (Angstroms) X	Y	Z
1	6	0	0.005131	0.000000	-0.005917
2	6	0	0.014016	0.000000	1.401052
3	6	0	1.205012	0.000000	2.094781
4	6	0	2.444814	0.000000	1.409286
5	6	0	2.428412	0.000000	-0.007833
6	6	0	1.205594	0.000000	-0.691801
7	1	0	1.240455	0.000000	-1.775341
8	6	0	3.719171	0.000000	-0.732848
9	7	0	4.854321	0.000000	0.044138
10	6	0	4.709267	0.000000	1.367093
11	7	0	3.613976	0.000000	2.118906
12	1	0	5.646352	0.000000	1.929212
13	8	0	3.762617	0.000000	-1.973264
14	1	0	1.227061	0.000000	3.179277
15	1	0	-0.925945	0.000000	1.945375
16	1	0	-0.937083	0.000000	-0.544084

E_{Tot}: -492.816175687 Hartree

Figure A1.177: Atomic Coordinates for [B3LYP/6-311+G(2d,p)] optimized geometry value of total energy of 1*H*-quinazolin-1-ide – aqueous phase

Center Number	Atomic Number	Atomic Type	Coordinates (Angstroms) X	Y	Z
1	6	0	0.001689	0.000000	-0.000079
2	6	0	0.002527	0.000000	1.406905
3	6	0	1.189766	0.000000	2.107282
4	6	0	2.427551	0.000000	1.424521
5	6	0	2.423210	0.000000	0.009566
6	6	0	1.200985	0.000000	-0.683544
7	1	0	1.222816	0.000000	-1.766251
8	6	0	3.715133	0.000000	-0.691656
9	7	0	4.843774	0.000000	0.080465
10	6	0	4.701111	0.000000	1.412157
11	7	0	3.600471	0.000000	2.141913
12	1	0	5.634966	0.000000	1.974580
13	8	0	3.783306	0.000000	-1.942682
14	1	0	1.197628	0.000000	3.191205
15	1	0	-0.939272	0.000000	1.944026
16	1	0	-0.937483	0.000000	-0.540385

E_{Tot}: -492.902733272 Hartree

Figure A1.178: Atomic Coordinates for [B3LYP/6-311+G(2d,p)] optimized geometry value of total energy of 3*H*-quinazolinone (**2.105**) – gas phase

Center Number	Atomic Number	Atomic Type	Coordinates (Angstroms) X	Y	Z
1	6	0	0.046423	0.000000	0.022780
2	6	0	0.081453	0.000000	1.424145
3	6	0	1.285990	0.000000	2.100143
4	6	0	2.494969	0.000000	1.387822
5	6	0	2.453976	0.000000	-0.024482
6	6	0	1.225780	0.000000	-0.695935
7	1	0	1.230040	0.000000	-1.778462
8	6	0	3.709360	0.000000	-0.779725
9	7	0	4.834398	0.000000	0.051425
10	6	0	4.773230	0.000000	1.419708
11	7	0	3.687348	0.000000	2.103384
12	1	0	5.732707	0.000000	1.928271
13	1	0	5.729852	0.000000	-0.419476
14	8	0	3.831077	0.000000	-1.991582
15	1	0	1.328462	0.000000	3.181814
16	1	0	-0.846761	0.000000	1.983381
17	1	0	-0.905068	0.000000	-0.494462

E_{Tot}: -493.365456343 Hartree

Figure A1.179: Atomic Coordinates for [B3LYP/6-311+G(2d,p)] optimized geometry value of total energy of 3*H*-quinazolinone (**2.105**) – aqueous phase

Center Number	Atomic Number	Atomic Type	Coordinates (Angstroms) X	Y	Z
1	6	0	-0.000375	0.000000	-0.001370
2	6	0	-0.001013	0.000000	1.401809
3	6	0	1.186099	0.000000	2.107630
4	6	0	2.414689	0.000000	1.426671
5	6	0	2.410286	0.000000	0.013526
6	6	0	1.197205	0.000000	-0.688642
7	1	0	1.220370	0.000000	-1.770749
8	6	0	3.684770	0.000000	-0.702275
9	7	0	4.784017	0.000000	0.147271
10	6	0	4.694465	0.000000	1.510161
11	7	0	3.588831	0.000000	2.170094
12	1	0	5.643149	0.000000	2.035062
13	1	0	5.697857	0.000000	-0.289066
14	8	0	3.832306	0.000000	-1.919629
15	1	0	1.194139	0.000000	3.190396
16	1	0	-0.942715	0.000000	1.937274
17	1	0	-0.938192	0.000000	-0.542341

E_{Tot}: -493.378040404 Hartree

Figure A1.180: Atomic Coordinates for [B3LYP/6-311+G(2d,p)] optimized geometry value of total energy of 3*H*-quinazolin-3-ide – gas phase

Center Number	Atomic Number	Atomic Type	Coordinates (Angstroms) X	Y	Z
1	6	0	-0.000056	0.000000	-0.002266
2	6	0	-0.012624	0.000000	1.404304
3	6	0	1.168064	0.000000	2.116301
4	6	0	2.416957	0.000000	1.449116
5	6	0	2.422601	0.000000	0.032337
6	6	0	1.210641	0.000000	-0.670420
7	1	0	1.261645	0.000000	-1.753266
8	6	0	3.725056	0.000000	-0.673315
9	8	0	3.785720	0.000000	-1.913174
10	7	0	4.847576	0.000000	0.120203
11	6	0	4.682220	0.000000	1.441332
12	7	0	3.576413	0.000000	2.176537
13	1	0	5.610618	0.000000	2.017724
14	1	0	1.173387	0.000000	3.200914
15	1	0	-0.960862	0.000000	1.934056
16	1	0	-0.934172	0.000000	-0.554463

E_{Tot}: -492.816176326 Hartree

Figure A1.181: Atomic Coordinates for [B3LYP/6-311+G(2d,p)] optimized geometry value of total energy of 3*H*-quinazolin-3-ide – aqueous phase

Center Number	Atomic Number	Atomic Type	Coordinates (Angstroms) X	Y	Z
1	6	0	0.001384	0.000000	-0.000337
2	6	0	0.002452	0.000000	1.406627
3	6	0	1.189819	0.000000	2.106814
4	6	0	2.427495	0.000000	1.423872
5	6	0	2.422910	0.000000	0.008914
6	6	0	1.200610	0.000000	-0.683977
7	1	0	1.222325	0.000000	-1.766693
8	6	0	3.714775	0.000000	-0.692566
9	8	0	3.782672	0.000000	-1.943563
10	7	0	4.843515	0.000000	0.079395
11	6	0	4.701019	0.000000	1.411136
12	7	0	3.600532	0.000000	2.141081
13	1	0	5.635001	0.000000	1.973357
14	1	0	1.197882	0.000000	3.190740
15	1	0	-0.939239	0.000000	1.943945
16	1	0	-0.937849	0.000000	-0.540540

E_{Tot}: -492.902733387 Hartree

Figure A1.182: Atomic Coordinates for [B3LYP/6-311+G(2d,p)] optimized geometry value of total energy of chromenone (**2.106**) – gas phase

Center Number	Atomic Number	Atomic Type	Coordinates (Angstroms) X	Y	Z
1	6	0	0.034118	0.000000	0.035419
2	6	0	0.079799	0.000000	1.435353
3	6	0	1.292198	0.000000	2.100637
4	6	0	2.468612	0.000000	1.353613
5	6	0	2.450235	0.000000	-0.043823
6	6	0	1.207966	0.000000	-0.692125
7	1	0	1.207143	0.000000	-1.774903
8	6	0	3.720609	0.000000	-0.804377
9	6	0	4.908851	0.000000	0.041634
10	6	0	4.808498	0.000000	1.379170
11	8	0	3.644216	0.000000	2.062224
12	1	0	5.652864	0.000000	2.055377
13	1	0	5.883609	0.000000	-0.426345
14	8	0	3.763654	0.000000	-2.027642
15	1	0	1.350737	0.000000	3.181476
16	1	0	-0.840781	0.000000	2.006383
17	1	0	-0.921774	0.000000	-0.473321

E_{Tot}: -497.157082805 Hartree

Figure A1.183: Atomic Coordinates for [B3LYP/6-311+G(2d,p)] optimized geometry value of total energy of chromenone (**2.106**) – aqueous phase

Center Number	Atomic Number	Atomic Type	Coordinates (Angstroms) X	Y	Z
1	6	0	0.000713	0.000000	-0.000849
2	6	0	0.001796	0.000000	1.401440
3	6	0	1.191963	0.000000	2.104763
4	6	0	2.391793	0.000000	1.395040
5	6	0	2.419929	0.000000	-0.003808
6	6	0	1.196320	0.000000	-0.691173
7	1	0	1.217694	0.000000	-1.773260
8	6	0	3.713274	0.000000	-0.711777
9	6	0	4.868431	0.000000	0.164374
10	6	0	4.727106	0.000000	1.501549
11	8	0	3.542227	0.000000	2.139963
12	1	0	5.550755	0.000000	2.201733
13	1	0	5.861297	0.000000	-0.264121
14	8	0	3.800292	0.000000	-1.943648
15	1	0	1.213410	0.000000	3.186853
16	1	0	-0.936305	0.000000	1.942448
17	1	0	-0.938710	0.000000	-0.538787

E_{Tot}: -497.166813033 Hartree

Figure A1.184: Atomic Coordinates for [B3LYP/6-311+G(2d,p)] optimized geometry value of total energy of chromen-3-ide – gas phase

Center Number	Atomic Number	Atomic Type	Coordinates (Angstroms) X	Y	Z
1	6	0	-0.087473	0.036604	-0.006930
2	6	0	-0.063086	0.028874	1.394457
3	6	0	1.140229	-0.045514	2.071881
4	6	0	2.345049	-0.121755	1.353988
5	6	0	2.340889	-0.098584	-0.051959
6	6	0	1.105552	-0.020515	-0.707297
7	1	0	1.128410	0.009062	-1.790851
8	6	0	3.640960	-0.081507	-0.800500
9	6	0	4.843048	-0.407318	-0.041961
10	6	0	4.692346	-0.443916	1.279450
11	8	0	3.483503	-0.214329	2.056090
12	1	0	5.450095	-0.660876	2.027176
13	8	0	3.618122	0.218906	-2.002555
14	1	0	1.180553	-0.055429	3.155243
15	1	0	-0.991278	0.079814	1.954970
16	1	0	-1.033997	0.094952	-0.534246

E_{Tot}: -496.536734759 Hartree

Figure A1.185: Atomic Coordinates for [B3LYP/6-311+G(2d,p)] optimized geometry value of total energy of chromen-3-ide – aqueous phase

Center Number	Atomic Number	Atomic Type	Coordinates (Angstroms) X	Y	Z
1	6	0	0.002258	0.000000	0.000170
2	6	0	0.008567	0.000000	1.403556
3	6	0	1.203219	0.000000	2.097013
4	6	0	2.410901	0.000000	1.386820
5	6	0	2.432438	0.000000	-0.015638
6	6	0	1.198768	0.000000	-0.690069
7	1	0	1.215438	0.000000	-1.772666
8	6	0	3.733978	0.000000	-0.730820
9	8	0	3.735719	0.000000	-1.980925
10	6	0	4.952173	0.000000	0.067725
11	6	0	4.767342	0.000000	1.397370
12	8	0	3.551827	0.000000	2.109818
13	1	0	5.549823	0.000000	2.150206
14	1	0	1.229018	0.000000	3.179870
15	1	0	-0.927374	0.000000	1.949644
16	1	0	-0.939182	0.000000	-0.535945

E_{Tot}: -496.629751374 Hartree

Figure A1.186: Atomic Coordinates for [B3LYP/6-311+G(2d,p)] optimized geometry value of total energy of 2-phenyl-1,3,2-benzodiazaborininone (**2.59**)

Center Number	Atomic Number	Atomic Type	Coordinates (Angstroms) X	Y	Z
1	6	0	0.000197	-0.003638	-0.000297
2	6	0	0.000184	0.004273	1.407428
3	6	0	1.266506	0.008245	2.175459
4	7	0	2.419666	-0.000721	1.399870
5	1	0	3.258883	0.036568	1.963459
6	5	0	2.471077	-0.008229	-0.030256
7	7	0	1.208759	-0.006709	-0.684478
8	1	0	1.143958	-0.060603	-1.689459
9	6	0	3.820378	-0.019910	-0.819213
10	6	0	4.967011	-0.632930	-0.292325
11	6	0	6.167032	-0.652217	-0.993728
12	6	0	6.251869	-0.047699	-2.243834
13	6	0	5.130646	0.571715	-2.786984
14	6	0	3.932419	0.580191	-2.082525
15	1	0	3.075892	1.084761	-2.518358
16	1	0	5.192031	1.051232	-3.756965
17	1	0	7.187032	-0.057674	-2.791264
18	1	0	7.035472	-1.139706	-0.566441
19	1	0	4.920906	-1.122389	0.675011
20	8	0	1.318107	0.024085	3.394469
21	6	0	-1.216099	0.009264	2.096637
22	6	0	-2.418682	0.003228	1.413832
23	6	0	-2.414070	-0.008270	0.016131
24	6	0	-1.222066	-0.011645	-0.685717
25	1	0	-1.225160	-0.019092	-1.770454
26	1	0	-3.351338	-0.014078	-0.527881
27	1	0	-3.355916	0.006331	1.955678
28	1	0	-1.179665	0.016821	3.178489

E_{Tot}: -711.932417191 Hartree

Figure A1.187: Atomic Coordinates for [B3LYP/6-311+G(2d,p)] optimized geometry value of total energy of 2-(*p*-tolyl)-1,3,2-benzodiazaborininone (**2.64**)

Center Number	Atomic Number	Atomic Type	Coordinates (Angstroms) X	Y	Z
1	6	0	-0.008030	-0.040266	0.036847
2	6	0	0.007563	-0.032608	1.543635
3	6	0	1.148831	0.347943	2.251925
4	6	0	1.151853	0.379377	3.640635
5	6	0	0.015564	0.037502	4.387753
6	6	0	-1.124655	-0.342796	3.664998
7	6	0	-1.128134	-0.382548	2.276970
8	1	0	-2.025996	-0.693876	1.753532
9	1	0	-2.025889	-0.637539	4.192872
10	5	0	0.019840	0.073031	5.948291
11	7	0	1.201187	-0.138389	6.712258
12	6	0	1.221802	-0.114929	8.100259
13	6	0	2.408221	-0.336099	8.812852
14	6	0	2.405744	-0.308497	10.195844
15	6	0	1.225267	-0.060496	10.902050
16	6	0	0.050601	0.156976	10.205304
17	6	0	0.029976	0.131778	8.807761
18	6	0	-1.248802	0.367788	8.098856
19	7	0	-1.165375	0.319684	6.713123
20	1	0	-2.052682	0.520021	6.270714
21	8	0	-2.304815	0.594710	8.667155
22	1	0	-0.883192	0.351357	10.717254
23	1	0	1.231702	-0.039900	11.984436
24	1	0	3.331250	-0.480984	10.732676
25	1	0	3.327940	-0.527811	8.270500
26	1	0	2.075412	-0.367104	6.264632
27	1	0	2.057440	0.697543	4.147817
28	1	0	2.045884	0.625243	1.708296
29	1	0	-0.656729	-0.827983	-0.350963
30	1	0	-0.381821	0.911347	-0.354330
31	1	0	0.992713	-0.190855	-0.371695

E_{Tot}: -751.261653146 Hartree

Figure A1.188: Atomic Coordinates for [B3LYP/6-311+G(2d,p)] optimized geometry value of total energy of 2-(4-methoxyphenyl)-1,3,2-benzodiazaborininone (**2.65**)

Center Number	Atomic Number	Atomic Type	Coordinates (Angstroms) X	Y	Z
1	6	0	0.026383	0.112703	0.189008
2	8	0	0.125946	-0.205784	1.570976
3	6	0	1.344790	-0.128251	2.169761
4	6	0	2.523874	0.244096	1.523400
5	6	0	3.714397	0.285095	2.243234
6	6	0	3.780825	-0.028277	3.605239
7	6	0	2.572013	-0.395197	4.224824
8	6	0	1.378402	-0.450807	3.530049
9	1	0	0.456327	-0.743121	4.016947
10	1	0	2.563716	-0.664031	5.276030
11	5	0	5.121641	0.029961	4.396423
12	7	0	6.388253	-0.151634	3.771628
13	6	0	7.590689	-0.105033	4.463421
14	6	0	8.814487	-0.294890	3.806885
15	6	0	10.001097	-0.245806	4.516201
16	6	0	9.999360	-0.006745	5.893333
17	6	0	8.795423	0.180250	6.547765
18	6	0	7.584578	0.132837	5.850919
19	6	0	6.316699	0.337413	6.588564
20	7	0	5.170045	0.269951	5.808379
21	1	0	4.333325	0.451795	6.346765
22	8	0	6.260874	0.556667	7.788122
23	1	0	8.753740	0.367382	7.613193
24	1	0	10.932238	0.030729	6.441380
25	1	0	10.939074	-0.394413	3.994024
26	1	0	8.822673	-0.479729	2.737912
27	1	0	6.456511	-0.378371	2.791492
28	1	0	4.610825	0.596628	1.716158
29	1	0	2.526090	0.506373	0.474657
30	1	0	-1.021815	-0.017208	-0.070591
31	1	0	0.322105	1.148339	-0.002447
32	1	0	0.637201	-0.560920	-0.419150

E_{Tot}: -826.493306457 Hartree

Figure A1.189: Atomic Coordinates for [B3LYP/6-311+G(2d,p)] optimized geometry value of total energy of 2-(4-(trifluoromethyl)phenyl)-1,3,2-benzodiazaborininone (**2.66**)

Center Number	Atomic Number	Atomic Type	Coordinates (Angstroms) X	Y	Z
1	6	0	-0.004903	-0.004122	0.000618
2	6	0	0.014829	-0.006178	1.503966
3	6	0	1.218752	0.007427	2.199294
4	1	0	2.155181	0.048096	1.659087
5	6	0	1.211272	-0.027404	3.588379
6	1	0	2.161911	-0.025294	4.110156
7	6	0	0.014953	-0.087188	4.315022
8	5	0	0.015709	-0.137254	5.880851
9	7	0	-0.965714	-0.855660	6.613051
10	6	0	-0.973890	-0.922137	8.001897
11	6	0	-1.953352	-1.652870	8.686613
12	6	0	-1.942761	-1.705156	10.068964
13	1	0	-2.706904	-2.274105	10.585317
14	6	0	-0.959530	-1.032813	10.800199
15	6	0	0.011199	-0.311078	10.130208
16	1	0	0.788549	0.221579	10.662888
17	6	0	0.020505	-0.246388	8.733606
18	6	0	1.078747	0.535010	8.054009
19	7	0	1.005115	0.532959	6.664054
20	1	0	1.725313	1.105787	6.243730
21	8	0	1.954669	1.145326	8.642812
22	1	0	-0.958673	-1.078068	11.881787
23	1	0	-2.719507	-2.175988	8.124431
24	1	0	-1.672748	-1.401258	6.144293
25	6	0	-1.183687	-0.101905	3.585653
26	1	0	-2.134256	-0.123769	4.107693
27	6	0	-1.191021	-0.058824	2.199363
28	1	0	-2.128672	-0.056872	1.657991
29	9	0	1.169294	0.389250	-0.530482
30	9	0	-0.265858	-1.237396	-0.497012
31	9	0	-0.960263	0.815417	-0.490837

E_{Tot}: -1049.08949152 Hartree

Figure A1.190: Atomic Coordinates for [B3LYP/6-311+G(2d,p)] optimized geometry value of total energy of 2-phenyl-3,1,2-benzoxazaborininone (**2.60**)

Center Number	Atomic Number	Atomic Type	Coordinates (Angstroms) X	Y	Z
1	6	0	0.047586	0.000000	-0.033438
2	6	0	0.009577	0.000000	1.363507
3	6	0	1.179103	0.000000	2.103943
4	6	0	2.418965	0.000000	1.454935
5	6	0	2.462992	0.000000	0.049859
6	6	0	1.270470	0.000000	-0.679761
7	1	0	1.337772	0.000000	-1.760023
8	6	0	3.753585	0.000000	-0.667234
9	8	0	4.876828	0.000000	0.123293
10	5	0	4.875032	0.000000	1.509850
11	7	0	3.614526	0.000000	2.160132
12	1	0	3.535398	0.000000	3.165030
13	6	0	6.243171	0.000000	2.252114
14	6	0	7.436965	0.000000	1.514644
15	6	0	8.674221	0.000000	2.147544
16	6	0	8.746100	0.000000	3.537013
17	6	0	7.575566	0.000000	4.290501
18	6	0	6.342367	0.000000	3.651474
19	1	0	5.447058	0.000000	4.265710
20	1	0	7.626264	0.000000	5.372966
21	1	0	9.710124	0.000000	4.032258
22	1	0	9.583267	0.000000	1.557633
23	1	0	7.386601	0.000000	0.432502
24	8	0	3.873704	0.000000	-1.863592
25	1	0	1.142741	0.000000	3.187832
26	1	0	-0.944290	0.000000	1.877669
27	1	0	-0.872320	0.000000	-0.603860

E_{Tot}: -731.80672836 Hartree

Figure A1.191: Atomic Coordinates for [B3LYP/6-311+G(2d,p)] optimized geometry value of total energy of 2-(*p*-tolyl)-3,1,2-benzoxazaborininone (**2.79**)

Center Number	Atomic Number	Atomic Type	Coordinates (Angstroms) X	Y	Z
1	6	0	-0.004321	0.003511	-0.037357
2	6	0	0.017378	-0.002694	1.469166
3	6	0	1.224322	-0.024439	2.171982
4	6	0	1.241437	-0.000697	3.559713
5	6	0	0.056699	0.043782	4.308028
6	5	0	0.039668	0.069977	5.861220
7	7	0	1.202042	0.048556	6.675691
8	6	0	1.134033	0.075156	8.061396
9	6	0	2.285081	0.054069	8.857749
10	6	0	2.173919	0.082068	10.237167
11	6	0	0.920674	0.131479	10.853579
12	6	0	-0.220038	0.152374	10.071539
13	6	0	-0.129027	0.124678	8.676877
14	6	0	-1.363903	0.147739	7.867459
15	8	0	-2.478203	0.189374	8.318268
16	8	0	-1.187524	0.118447	6.506947
17	1	0	-1.207212	0.190410	10.513681
18	1	0	0.844579	0.153104	11.933100
19	1	0	3.072731	0.065316	10.842342
20	1	0	3.261199	0.015786	8.386692
21	1	0	2.128085	0.012968	6.278786
22	6	0	-1.150417	0.061198	3.593014
23	6	0	-1.168941	0.036963	2.205548
24	1	0	-2.119917	0.046993	1.683435
25	1	0	-2.085429	0.091095	4.139519
26	1	0	2.206171	-0.020697	4.057735
27	1	0	2.159969	-0.062429	1.624316
28	1	0	-0.874377	-0.529509	-0.425354
29	1	0	-0.052183	1.027482	-0.421487
30	1	0	0.892790	-0.459625	-0.451786

E_{Tot}: -771.136065237 Hartree

Figure A1.192: Atomic Coordinates for [B3LYP/6-311+G(2d,p)] optimized geometry value of total energy of 2-(4-methoxyphenyl)-3,1,2-benzoxazaborininone (**2.80**)

Center Number	Atomic Number	Atomic Type	Coordinates (Angstroms) X	Y	Z
1	6	0	-0.024523	-0.000833	0.247556
2	8	0	0.098909	-0.003009	1.663890
3	6	0	1.343770	-0.002337	2.210069
4	6	0	2.530504	0.000384	1.474344
5	6	0	3.748083	0.000873	2.146170
6	6	0	3.833256	-0.001286	3.542654
7	6	0	2.618137	-0.003999	4.253751
8	6	0	1.397214	-0.004535	3.607902
9	1	0	0.466775	-0.006635	4.162023
10	1	0	2.643359	-0.005727	5.336724
11	5	0	5.180887	-0.000794	4.307529
12	7	0	6.459061	0.001709	3.686749
13	6	0	7.636850	0.002071	4.419505
14	6	0	8.892182	0.004587	3.799589
15	6	0	10.044292	0.004904	4.566572
16	6	0	9.974866	0.002740	5.962360
17	6	0	8.737265	0.000248	6.580217
18	6	0	7.561982	-0.000129	5.823465
19	6	0	6.254766	-0.002856	6.510420
20	8	0	5.151311	-0.002925	5.696033
21	8	0	6.108561	-0.004716	7.704471
22	1	0	8.644786	-0.001482	7.658600
23	1	0	10.881646	0.003011	6.553451
24	1	0	11.009629	0.006865	4.074084
25	1	0	8.954175	0.006290	2.716830
26	1	0	6.563027	0.003294	2.684185
27	1	0	4.649813	0.003033	1.541182
28	1	0	2.516807	0.002177	0.393549
29	1	0	-1.092789	-0.001736	0.043134
30	1	0	0.427889	0.894174	-0.189295
31	1	0	0.429941	-0.893361	-0.192212

E_{Tot}: -846.367991853 Hartree

Figure A1.193: Atomic Coordinates for [B3LYP/6-311+G(2d,p)] optimized geometry value of total energy of 2-(4-(trifluoromethyl)phenyl)-3,1,2-benzoxazaborininone (**2.81**)

Center Number	Atomic Number	Atomic Type	Coordinates (Angstroms) X	Y	Z
1	6	0	-0.091838	0.006484	0.078964
2	6	0	-0.046516	-0.011945	1.582002
3	6	0	1.194220	-0.018516	2.217462
4	6	0	1.254570	-0.014045	3.601812
5	6	0	0.091482	-0.002717	4.386412
6	6	0	-1.141428	0.004205	3.721530
7	6	0	-1.215636	0.000077	2.333823
8	1	0	-2.177227	0.003140	1.838492
9	1	0	-2.054765	0.011722	4.303152
10	5	0	0.125835	0.000855	5.946862
11	7	0	1.312569	-0.007959	6.719082
12	6	0	1.285781	-0.004352	8.108868
13	6	0	2.460909	-0.013152	8.867786
14	6	0	2.391724	-0.009153	10.250375
15	6	0	1.157238	0.003646	10.904928
16	6	0	-0.007573	0.012367	10.159190
17	6	0	0.041230	0.008485	8.762011
18	6	0	-1.218338	0.017761	7.992448
19	8	0	-1.081287	0.013242	6.623173
20	8	0	-2.319183	0.029227	8.473304
21	1	0	-0.980885	0.022290	10.632376
22	1	0	1.114032	0.006659	11.986421
23	1	0	3.308722	-0.016062	10.827597
24	1	0	3.422622	-0.023061	8.366773
25	1	0	2.227546	-0.017306	6.295872
26	1	0	2.234137	-0.021154	4.068115
27	1	0	2.103886	-0.031559	1.630309
28	9	0	-1.331778	-0.197234	-0.404568
29	9	0	0.335857	1.191263	-0.419526
30	9	0	0.707059	-0.943209	-0.459046

E_{Tot}: -1068.96369938 Hartree

Figure A1.194: Atomic Coordinates for [B3LYP/6-311+G(2d,p)] optimized geometry value of total energy of 2-phenyl-1,3,2-benzoxazaborininone (**2.61**)

Center Number	Atomic Number	Atomic Type	Coordinates (Angstroms) X	Y	Z
1	6	0	0.057486	0.000000	0.106202
2	6	0	0.143980	0.000000	1.500973
3	6	0	1.376968	0.000000	2.133460
4	6	0	2.538486	0.000000	1.365037
5	6	0	2.468354	0.000000	-0.033150
6	6	0	1.214649	0.000000	-0.651940
7	1	0	1.184225	0.000000	-1.734101
8	6	0	3.703019	0.000000	-0.847714
9	7	0	4.872819	0.000000	-0.095720
10	5	0	4.933126	0.000000	1.329913
11	8	0	3.736487	0.000000	2.019417
12	6	0	6.258423	0.000000	2.145931
13	6	0	7.518885	0.000000	1.530476
14	6	0	8.689470	0.000000	2.278624
15	6	0	8.623939	0.000000	3.668758
16	6	0	7.385279	0.000000	4.303124
17	6	0	6.218785	0.000000	3.548690
18	1	0	5.257863	0.000000	4.048939
19	1	0	7.330481	0.000000	5.385445
20	1	0	9.535466	0.000000	4.255009
21	1	0	9.651497	0.000000	1.780033
22	1	0	7.600657	0.000000	0.448441
23	1	0	5.702726	0.000000	-0.673460
24	8	0	3.719384	0.000000	-2.064635
25	1	0	1.461985	0.000000	3.212581
26	1	0	-0.759937	0.000000	2.098461
27	1	0	-0.910829	0.000000	-0.378043

E_{Tot}: -731.808284393 Hartree

Figure A1.195: Atomic Coordinates for [B3LYP/6-311+G(2d,p)] optimized geometry value of total energy of 2-(*p*-tolyl)-1,3,2-benzoxazaborininone (**2.90**)

Center Number	Atomic Number	Atomic Type	Coordinates (Angstroms) X	Y	Z
1	6	0	0.000956	-0.001500	-0.000069
2	6	0	-0.000753	-0.002219	1.506412
3	6	0	1.193188	0.035150	2.229231
4	6	0	1.186764	0.061072	3.617456
5	6	0	-0.010627	0.048974	4.345817
6	5	0	-0.046847	0.075438	5.898502
7	7	0	1.116859	0.110326	6.725347
8	6	0	1.111695	0.135343	8.115031
9	6	0	-0.243345	0.122880	8.708761
10	6	0	-1.378329	0.088470	7.889858
11	6	0	-2.654635	0.076772	8.447930
12	6	0	-2.794197	0.099529	9.826277
13	6	0	-1.670677	0.133897	10.656721
14	6	0	-0.405480	0.145377	10.097165
15	1	0	0.486147	0.171829	10.710543
16	1	0	-1.790773	0.151451	11.732569
17	1	0	-3.786914	0.090492	10.260497
18	1	0	-3.514133	0.050120	7.790394
19	8	0	-1.276679	0.065519	6.529496
20	8	0	2.141454	0.164631	8.763664
21	1	0	2.052773	0.119081	6.342420
22	6	0	-1.205104	0.007591	3.610155
23	6	0	-1.200313	-0.018838	2.223220
24	1	0	-2.141850	-0.054979	1.685248
25	1	0	-2.150417	-0.007194	4.139443
26	1	0	2.142062	0.088308	4.131707
27	1	0	2.138707	0.041958	1.697743
28	1	0	-0.153519	1.009983	-0.389051
29	1	0	-0.799302	-0.627834	-0.399380
30	1	0	0.949639	-0.364616	-0.398430

E_{Tot}: -771.137700603 Hartree

Figure A1.196: Atomic Coordinates for [B3LYP/6-311+G(2d,p)] optimized geometry value of total energy of 2-(4-methoxyphenyl)-1,3,2-benzoxazaborininone (**2.91**)

Center Number	Atomic Number	Atomic Type	Coordinates (Angstroms) X	Y	Z
1	6	0	0.185394	-0.010379	0.121224
2	8	0	0.196041	-0.031403	1.543346
3	6	0	1.393360	-0.024477	2.185713
4	6	0	2.635405	0.002212	1.548696
5	6	0	3.796153	0.006811	2.313675
6	6	0	3.768663	-0.014503	3.713414
7	6	0	2.500949	-0.041144	4.322725
8	6	0	1.334195	-0.046211	3.583631
9	1	0	0.362883	-0.066816	4.061738
10	1	0	2.413320	-0.058599	5.404104
11	5	0	5.089057	-0.008333	4.523329
12	7	0	5.152843	-0.028164	5.951067
13	6	0	6.321809	-0.023194	6.701409
14	6	0	7.556479	0.005317	5.886404
15	6	0	7.485283	0.024639	4.488305
16	6	0	8.647716	0.051524	3.720786
17	6	0	9.880463	0.059039	4.353427
18	6	0	9.967142	0.039970	5.748100
19	6	0	8.809718	0.013306	6.505588
20	1	0	8.839340	-0.001988	7.587630
21	1	0	10.935446	0.046051	6.232405
22	1	0	10.784449	0.079947	3.756317
23	1	0	8.563269	0.066038	2.641662
24	8	0	6.288589	0.017919	3.833949
25	8	0	6.308175	-0.040939	7.918850
26	1	0	4.323467	-0.047653	6.529325
27	1	0	4.753019	0.027628	1.805781
28	1	0	2.708501	0.019353	0.470319
29	1	0	0.684476	-0.891218	-0.292639
30	1	0	-0.863290	-0.020549	-0.167000
31	1	0	0.659820	0.895817	-0.266033

E_{Tot}: -846.369906127 Hartree

Figure A1.197: Atomic Coordinates for [B3LYP/6-311+G(2d,p)] optimized geometry value of total energy of 2-(4-(trifluoromethyl)phenyl)-1,3,2-benzoxazaborininone (**2.92**)

Center Number	Atomic Number	Atomic Type	Coordinates (Angstroms) X	Y	Z
1	6	0	0.000856	-0.002515	-0.000281
2	6	0	0.000720	-0.000440	1.503899
3	6	0	1.222379	0.045705	2.173593
4	6	0	1.244936	0.047307	3.559168
5	6	0	0.061388	0.003433	4.311190
6	5	0	0.061008	0.004163	5.872052
7	7	0	1.240462	0.045518	6.669186
8	6	0	1.261912	0.046029	8.062396
9	6	0	-0.080324	-0.000305	8.681351
10	6	0	-1.231072	-0.040354	7.885492
11	6	0	-2.495608	-0.084038	8.466240
12	6	0	-2.607747	-0.087611	9.847421
13	6	0	-1.468664	-0.047987	10.656067
14	6	0	-0.214947	-0.004691	10.073018
15	1	0	0.687790	0.026682	10.669582
16	1	0	-1.567944	-0.051208	11.734097
17	1	0	-3.591162	-0.121560	10.300865
18	1	0	-3.367574	-0.114382	7.825586
19	8	0	-1.154557	-0.038005	6.520827
20	8	0	2.304190	0.081830	8.687707
21	1	0	2.169421	0.077308	6.270541
22	6	0	-1.151381	-0.042282	3.612018
23	6	0	-1.188037	-0.044520	2.223034
24	1	0	-2.134706	-0.080120	1.701146
25	1	0	-2.080978	-0.076583	4.166243
26	1	0	2.209397	0.083963	4.053333
27	1	0	2.148256	0.080345	1.613052
28	9	0	0.607996	1.097928	-0.501664
29	9	0	0.670548	-1.067644	-0.498558
30	9	0	-1.241285	-0.039303	-0.519057

E_{Tot}: -1068.96507966 Hartree

A1.4 – Spectral data relevant to Chapter 2.3

Figure A1.198: ^{1}H NMR ($CDCl_3$, 500.4 MHz) of 2-phenyl-1,3,2-benzodiazaborininone (**2.59**)

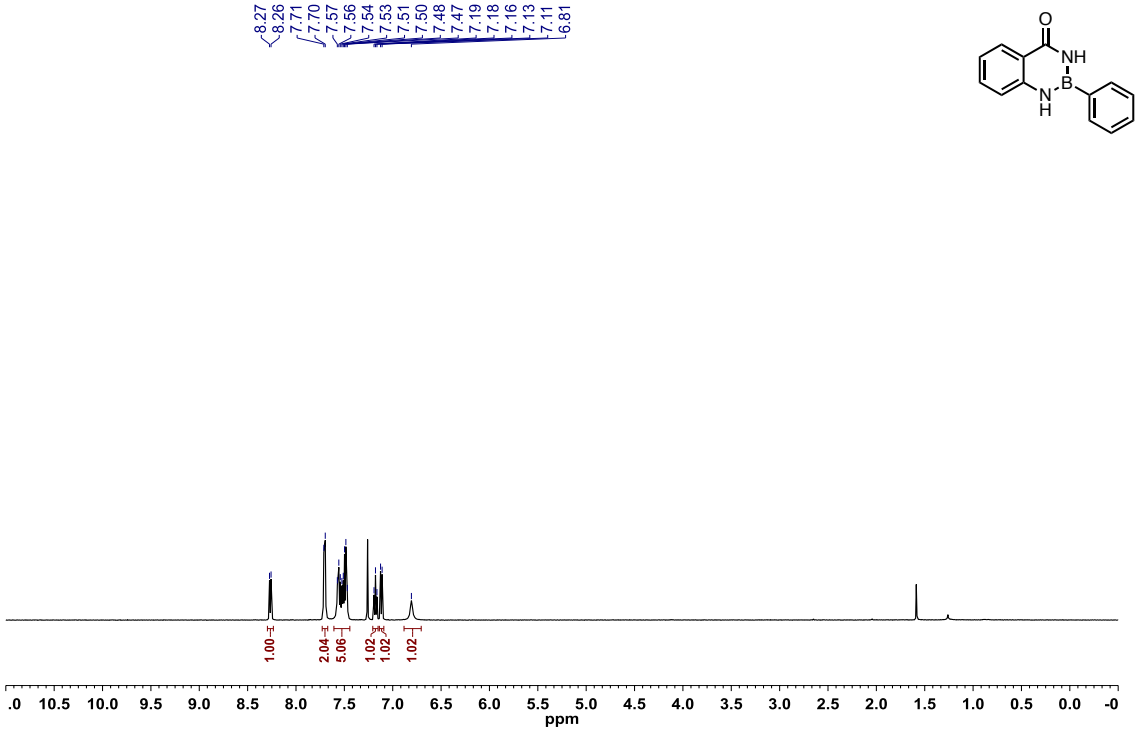

Figure A1.199: ^{13}C {^{1}H} NMR ($CDCl_3$, 125.8 MHz) of 2-phenyl-1,3,2-benzodiazaborininone (**2.59**)

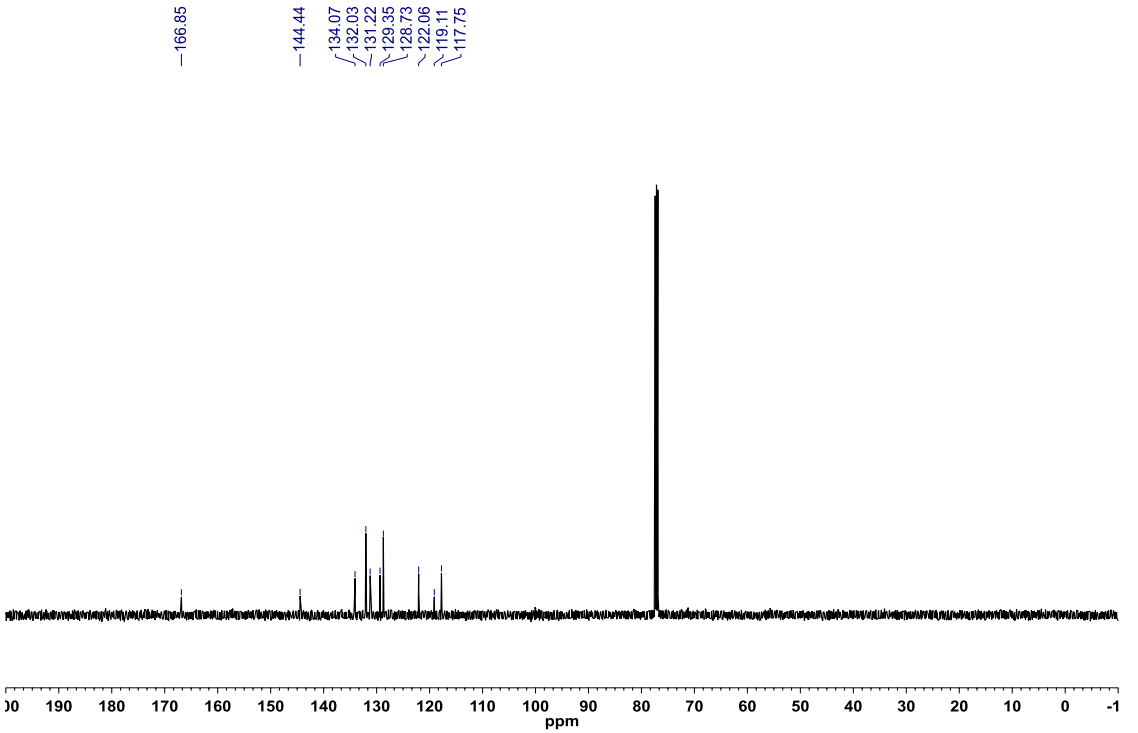

Figure A1.200: ^{11}B NMR ($CDCl_3$, 128.4 MHz) of 2-phenyl-1,3,2-benzodiazaborininone (**2.59**)

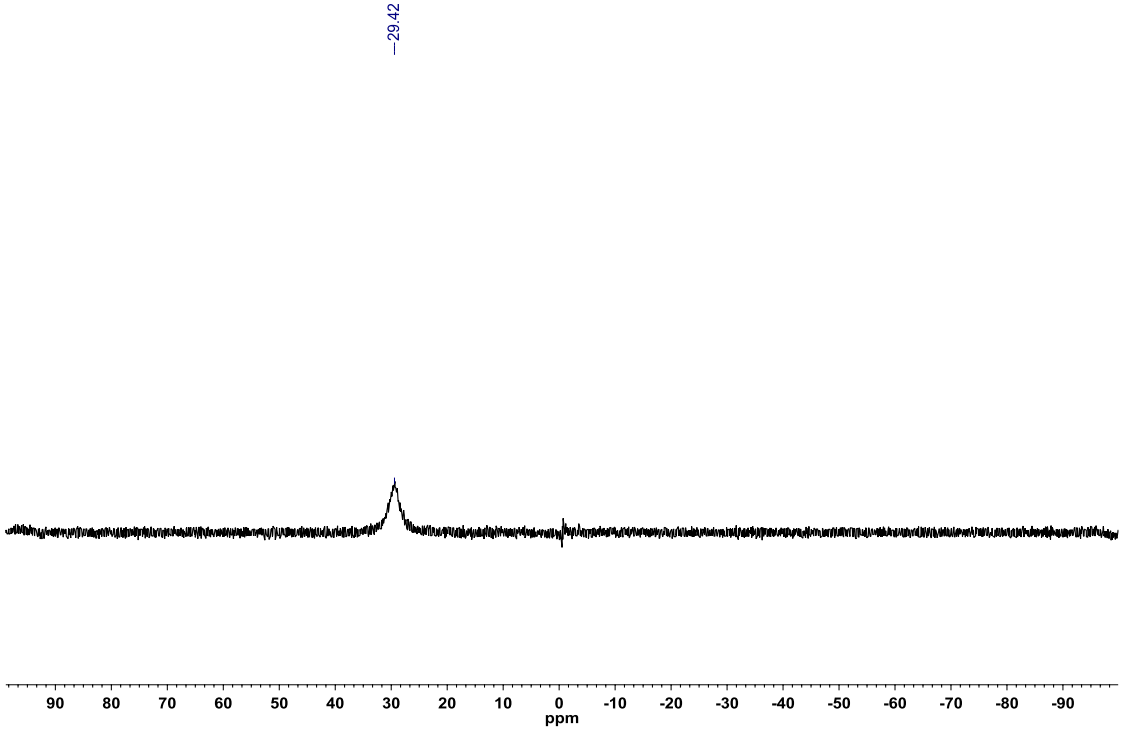

Figure A1.201: ^{1}H NMR ($CDCl_3$, 500.4 MHz) of 2-(*o*-tolyl)-1,3,2-benzodiazaborininone (**2.62**)

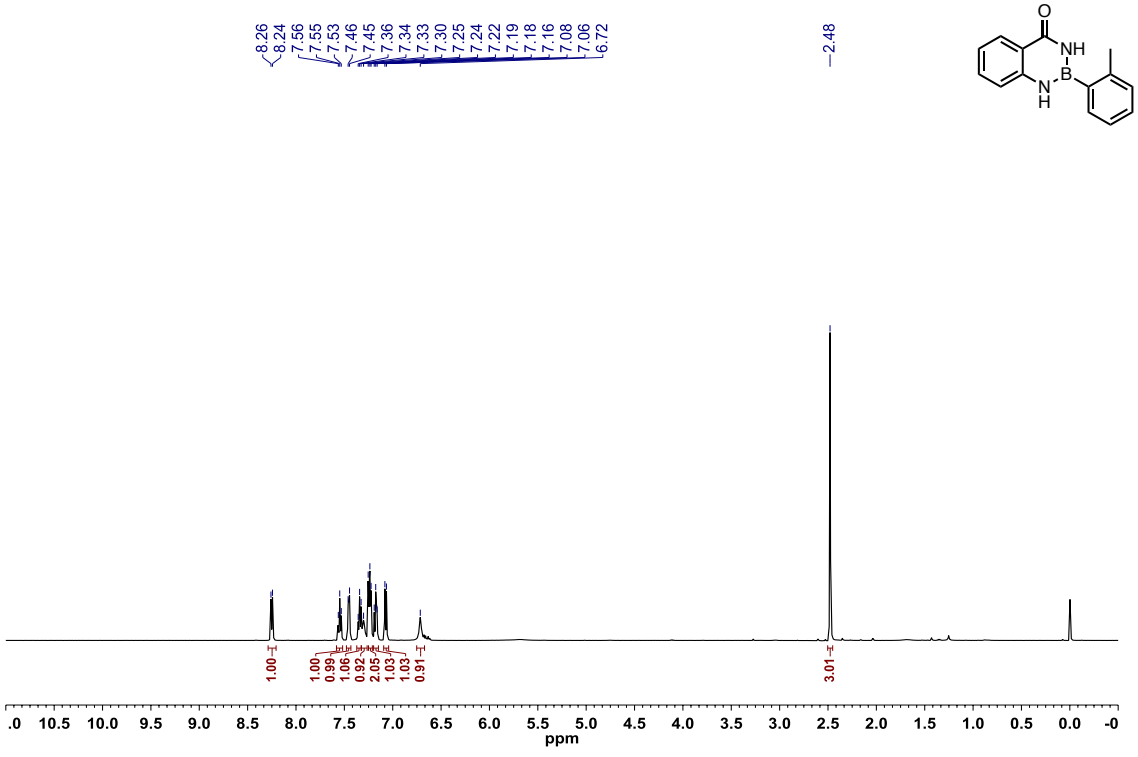

Figure A1.202: ^{13}C {^{1}H} NMR ($CDCl_3$, 125.8 MHz) of 2-(*o*-tolyl)-1,3,2-benzodiazaborininone (**2.62**)

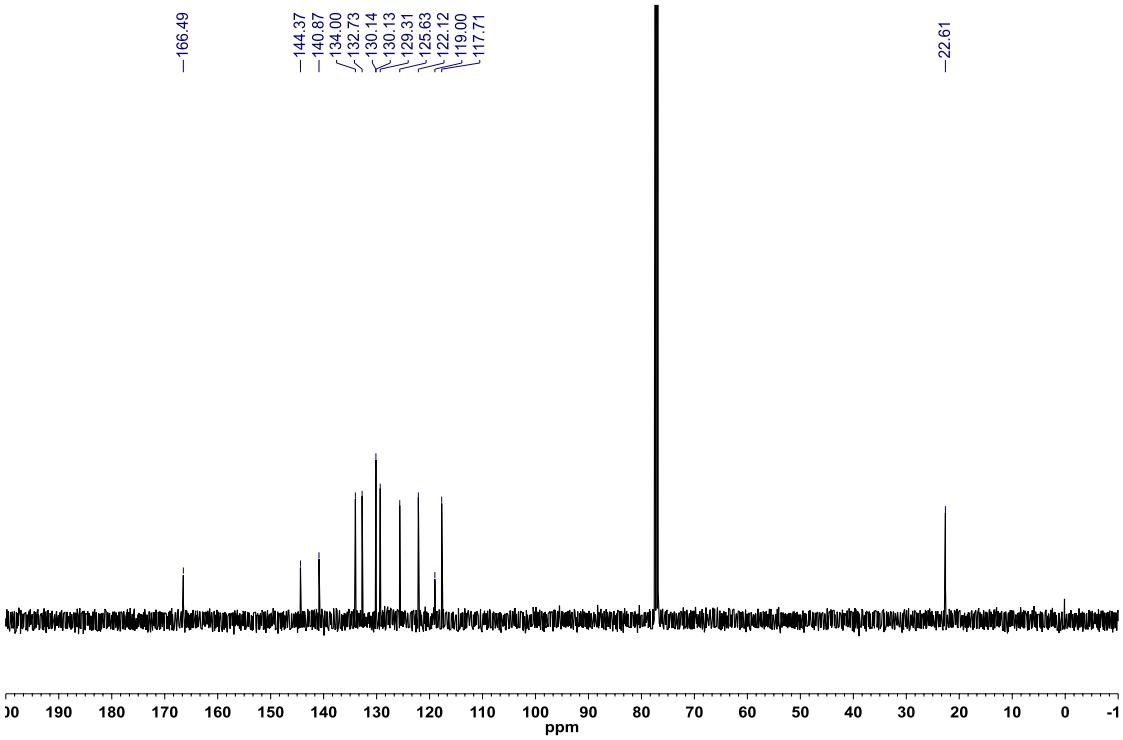

Figure A1.203: ^{11}B NMR ($CDCl_3$, 128.4 MHz) of 2-(*o*-tolyl)-1,3,2-benzodiazaborininone (**2.62**)

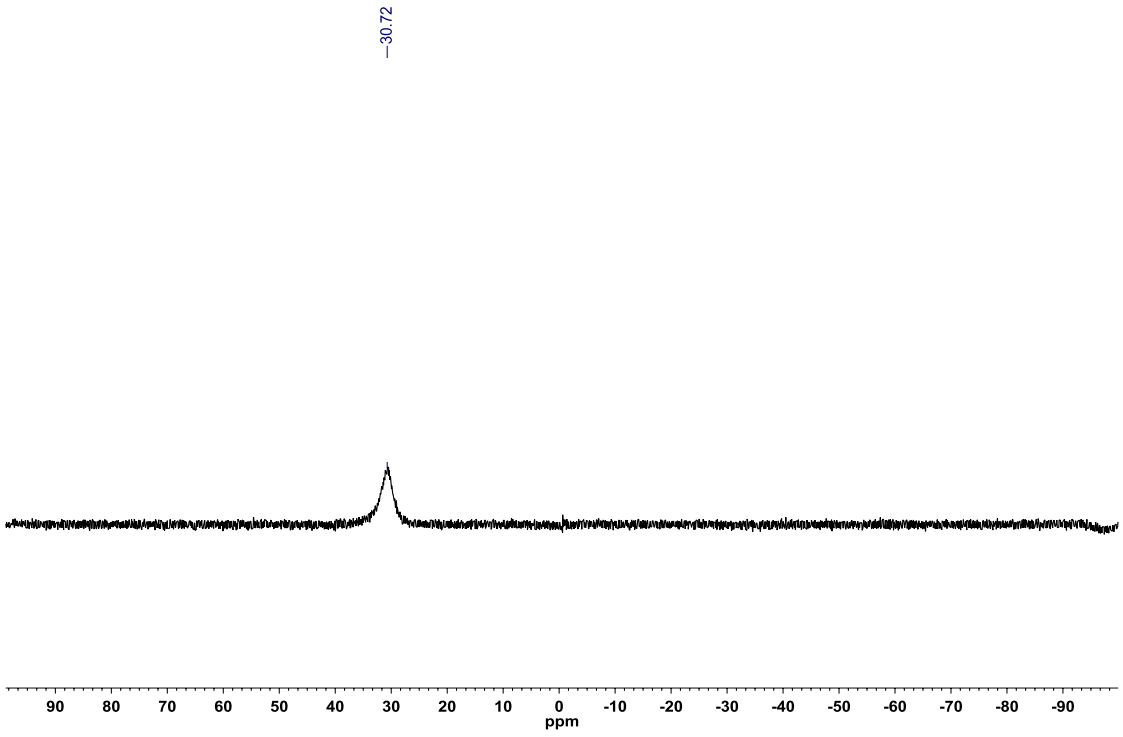

Figure A1.204: ^{1}H NMR (acetone-d_6, 500.4 MHz) of 2-(2,6-fluorophenyl)-1,3,2-benzodiazaborininone (**2.63**)

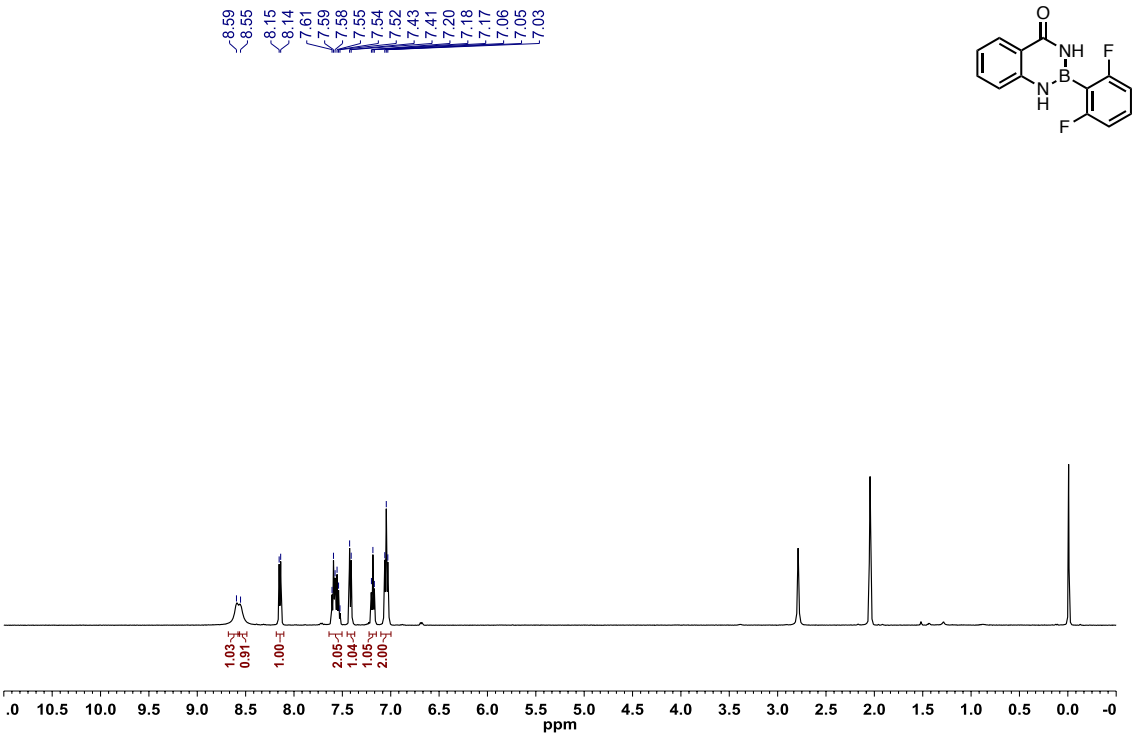

Figure A1.205: ^{13}C {^{1}H} NMR (DMSO-d_6, 125.8 MHz) of 2-(2,6-fluorophenyl)-1,3,2-benzodiazaborininone (**2.63**)

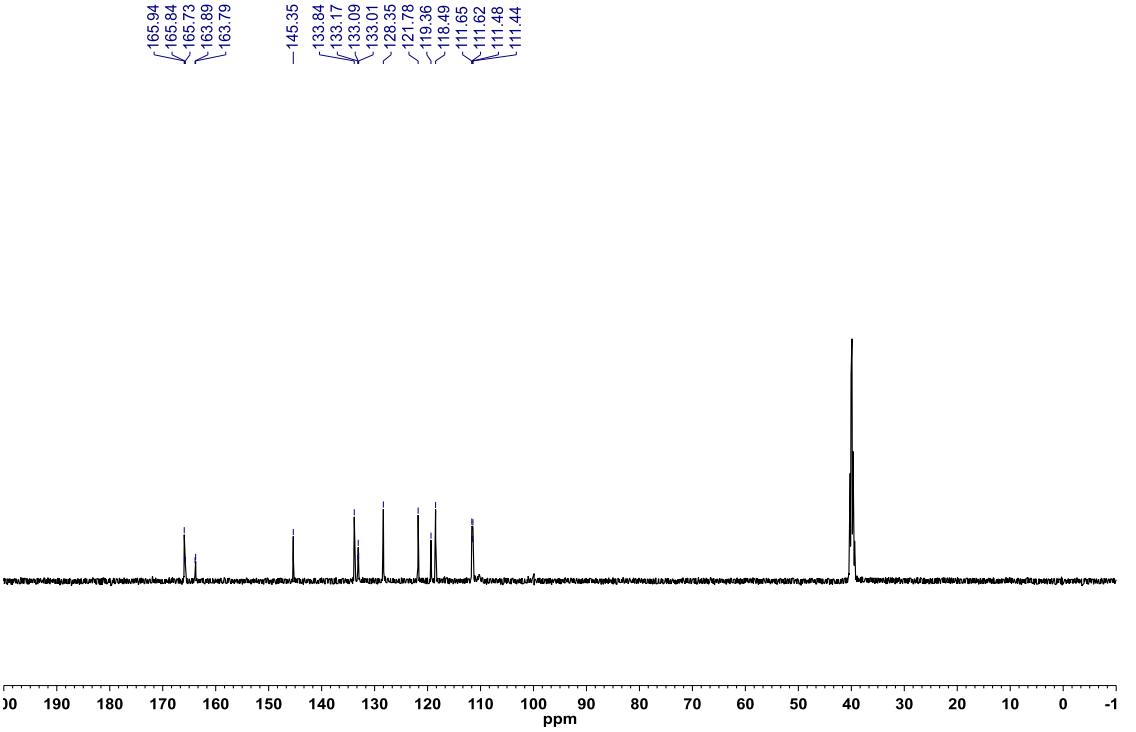

Figure A1.206: ^{19}F {^{1}H} NMR (acetone-d_6, 470.8 MHz) of 2-(2,6-fluorophenyl)-1,3,2-benzodiazaborininone (**2.63**)

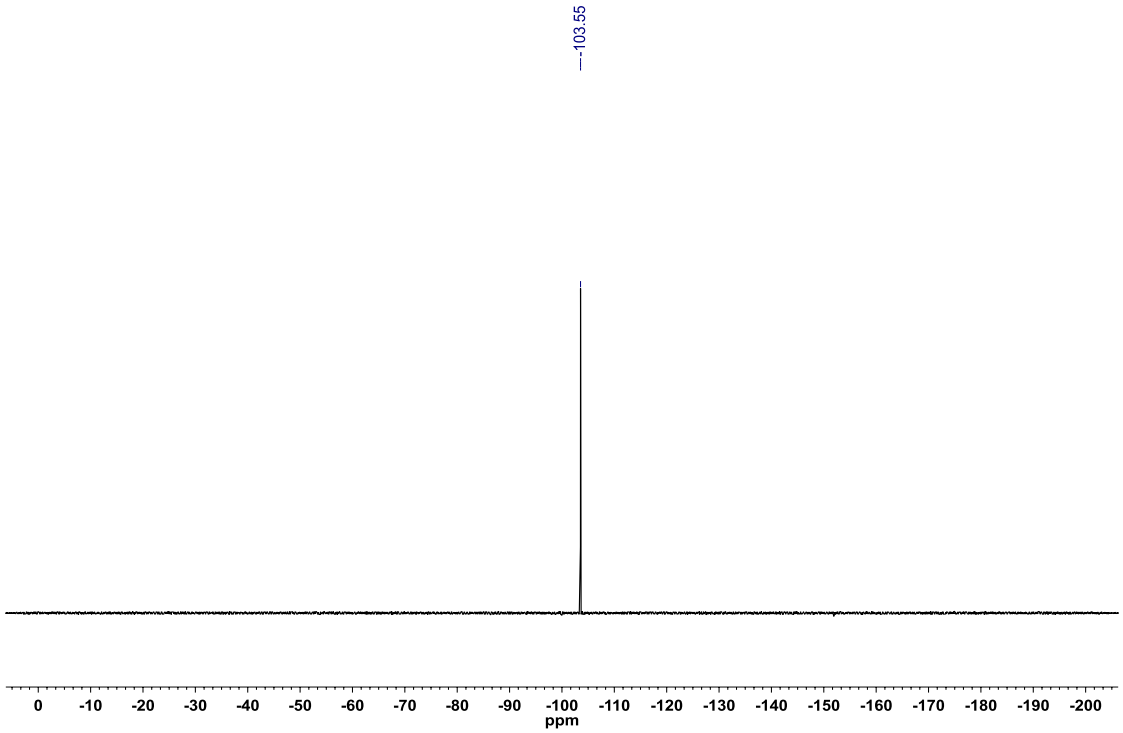

Figure A1.207: ^{11}B NMR (acetone-d_6, 128.4 MHz) of 2-(2,6-fluorophenyl)-1,3,2-benzodiazaborininone (**2.63**)

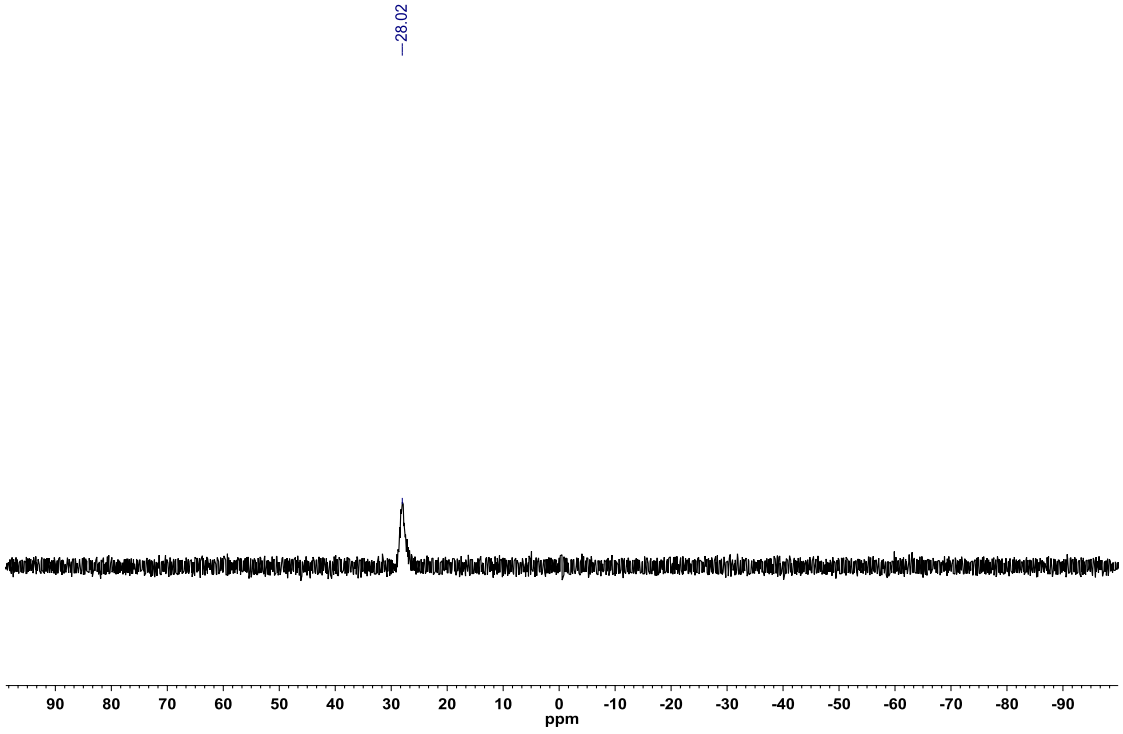

Figure A1.208: ^{1}H NMR ($CDCl_3$, 500.4 MHz) of 2-(*p*-tolyl)-1,3,2-benzodiazaborininone (**2.64**)

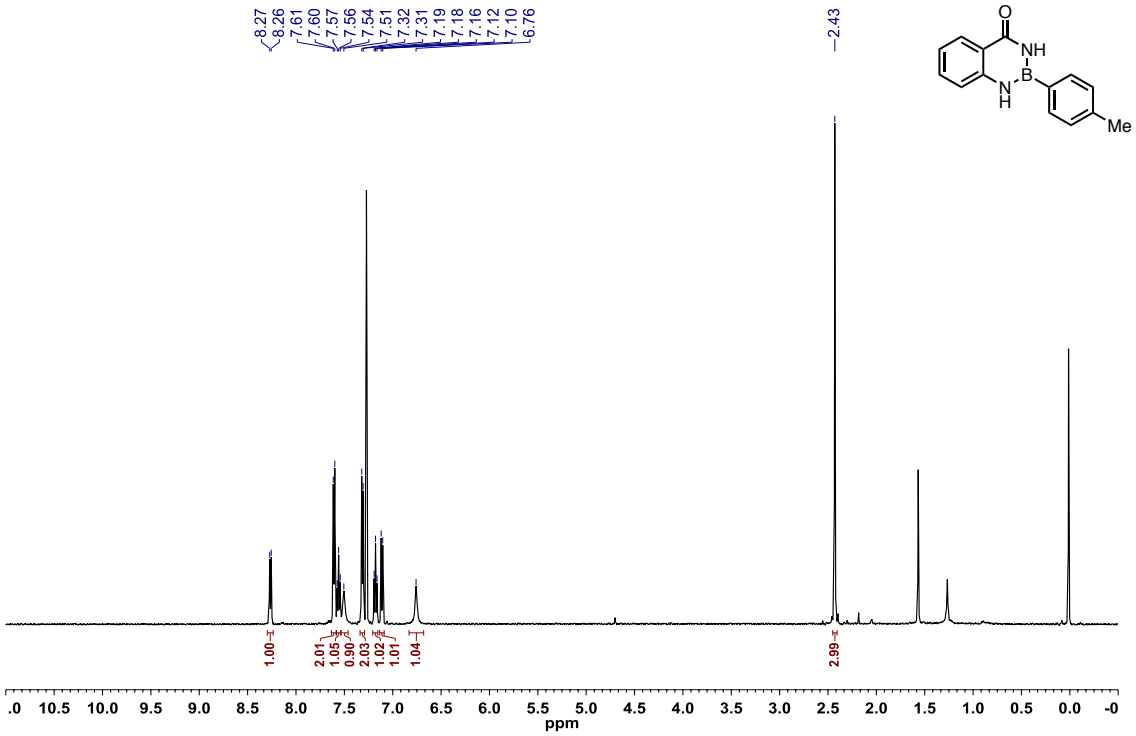

Figure A1.209: ^{13}C {^{1}H} NMR ($CDCl_3$, 125.8 MHz)) of 2-(*p*-tolyl)-1,3,2-benzodiazaborininone (**2.64**)

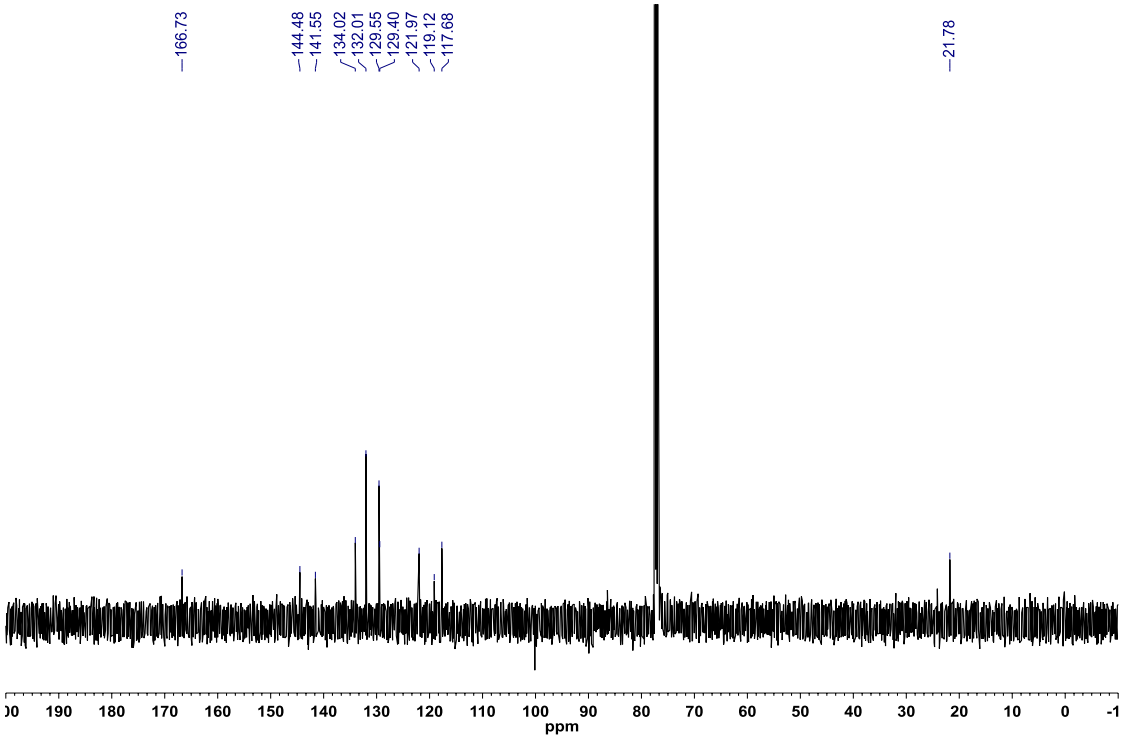

Figure A1.210: ^{11}B NMR ($CDCl_3$, 128.4 MHz)) of 2-(*p*-tolyl)-1,3,2-benzodiazaborininone (**2.64**)

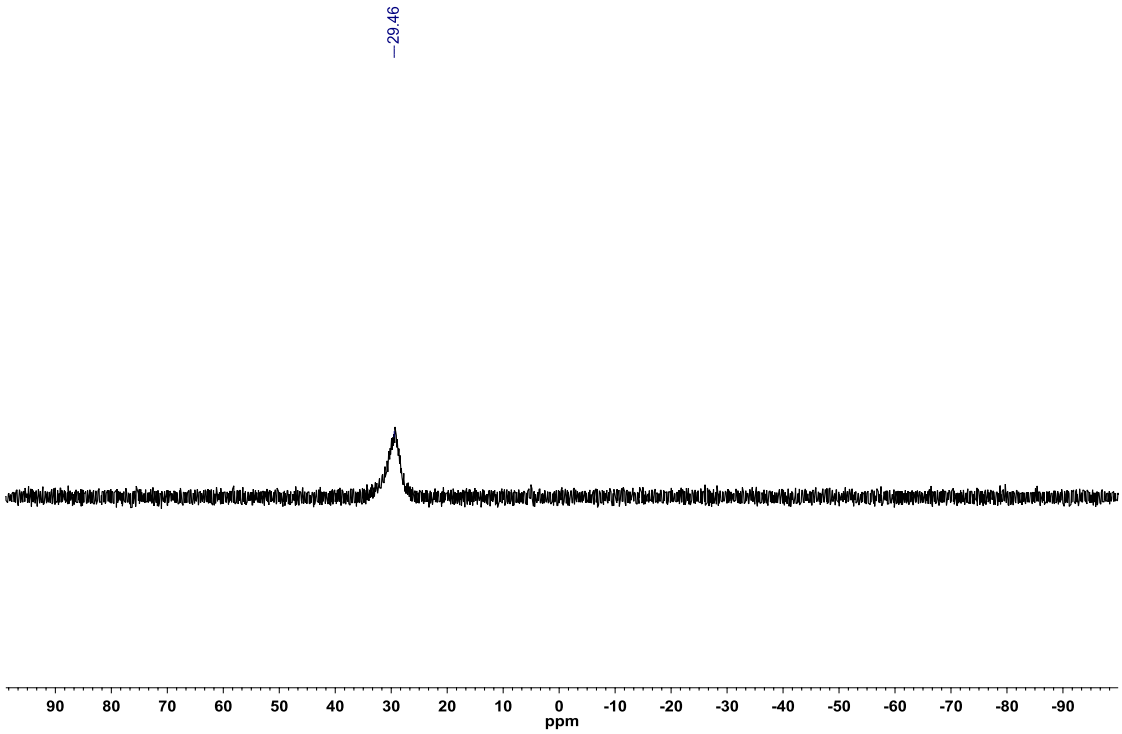

Figure A1.211: ^{1}H NMR ($CDCl_3$, 500.4 MHz) of 2-(4-methoxyphenyl)-1,3,2-benzodiazaborininone (**2.65**)

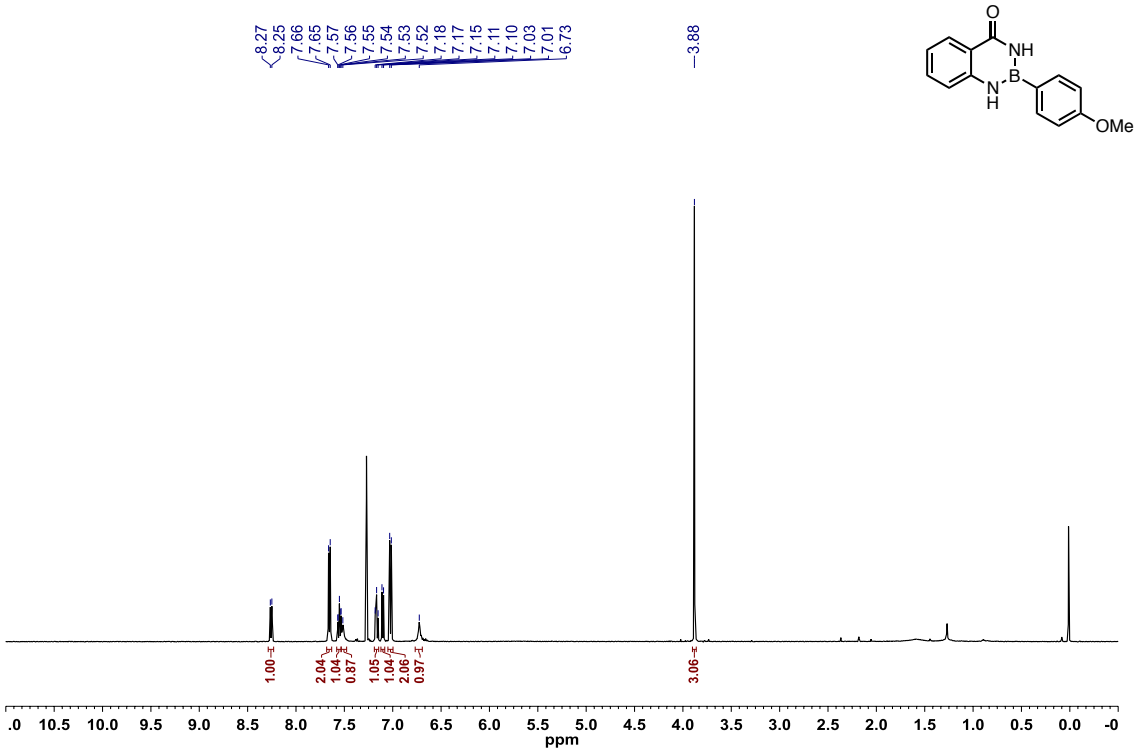

Figure A1.212: ^{13}C {^{1}H} NMR ($CDCl_3$, 125.8 MHz) of 2-(4-methoxyphenyl)-1,3,2-benzodiazaborininone (**2.65**)

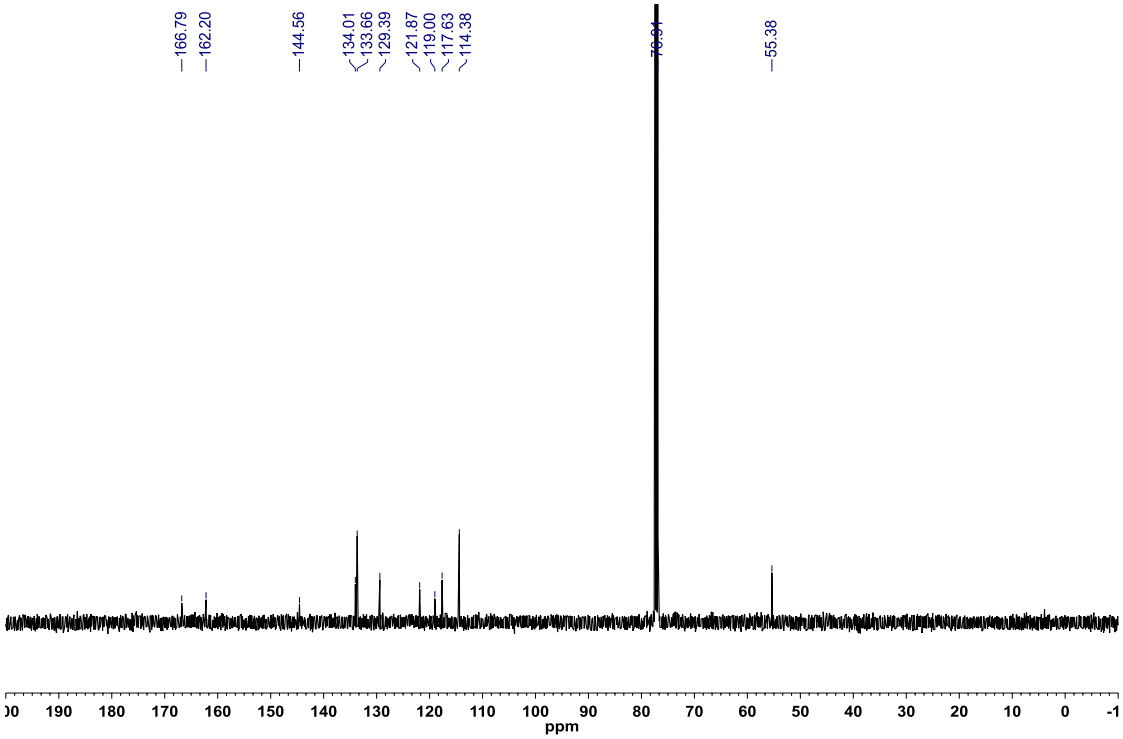

Figure A1.213: ^{11}B NMR ($CDCl_3$, 128.4 MHz) of 2-(4-methoxyphenyl)-1,3,2-benzodiazaborininone (**2.65**)

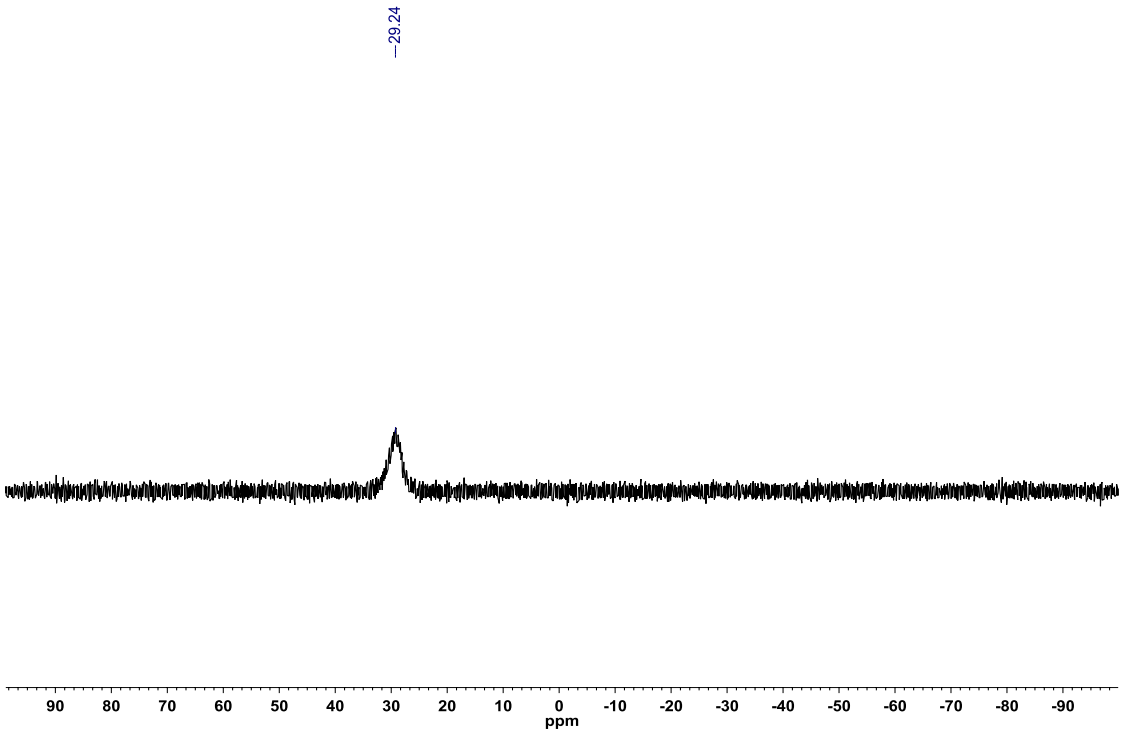

Figure A1.214: ^{1}H NMR (DMSO-d_6, 500.4 MHz) of 2-(4-(trifluoromethyl)phenyl)-1,3,2-benzodiazaborininone (**2.66**)

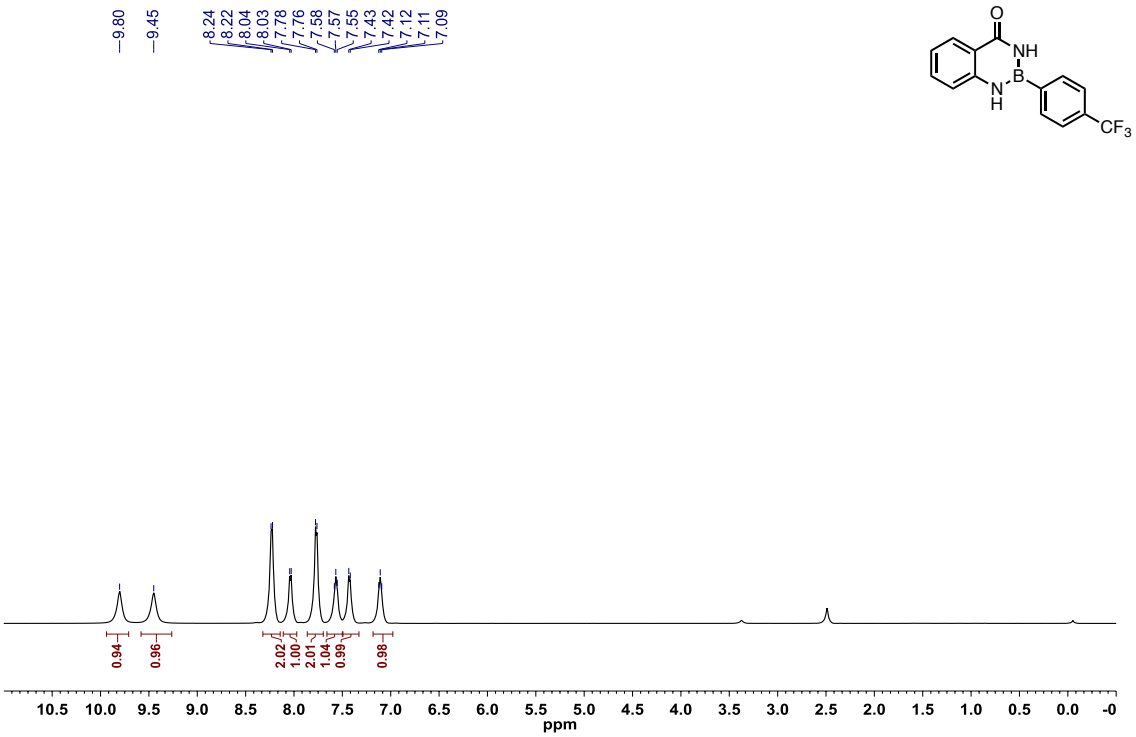

Figure A1.215: ^{13}C {^{1}H} NMR (DMSO-d_6, 125.8 MHz) of 2-(4-(trifluoromethyl)phenyl)-1,3,2-benzodiazaborininone (**2.66**)

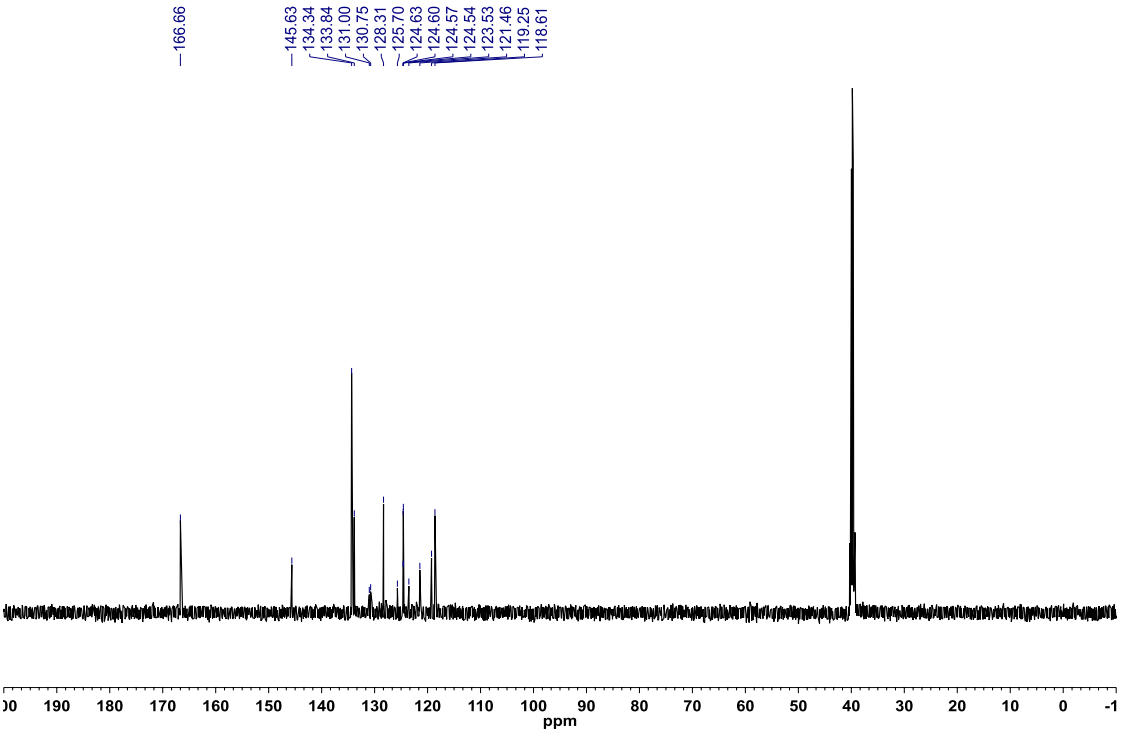

Figure A1.216: ^{19}F {^{1}H} NMR (DMSO-d_6, 470.8 MHz) of 2-(4-(trifluoromethyl)phenyl)-1,3,2-benzodiazaborininone (**2.66**)

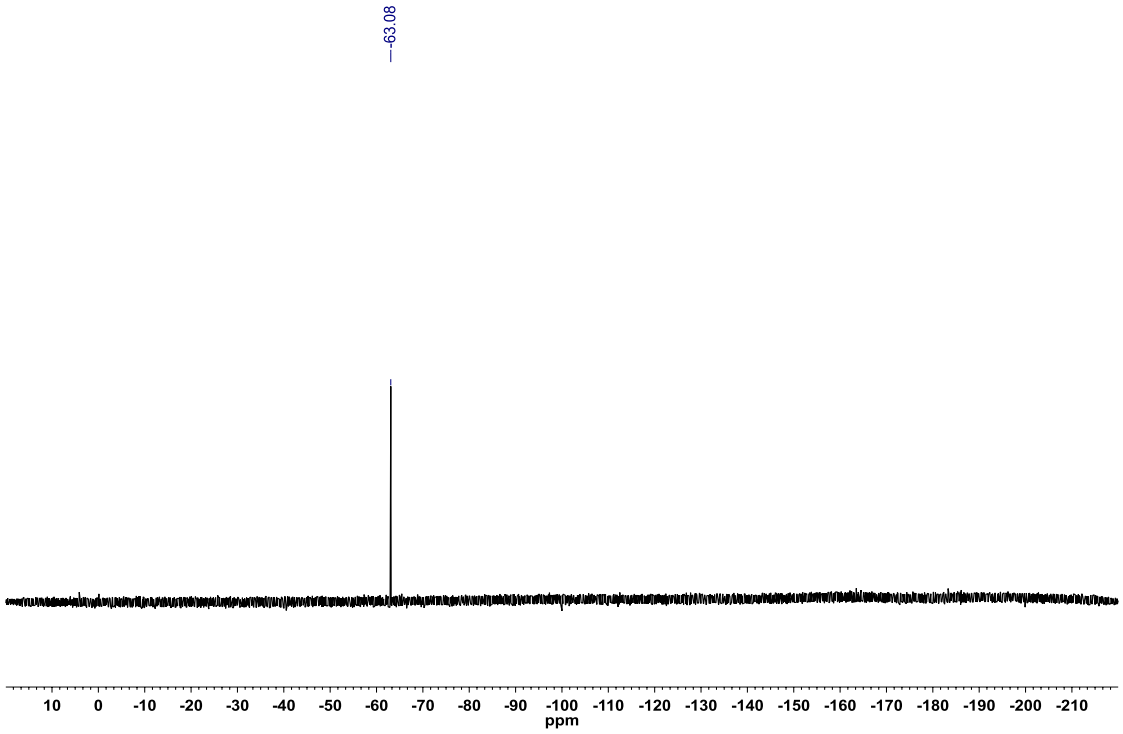

Figure A1.217: ^{11}B NMR ($CDCl_3$, 128.4 MHz) of 2-(4-(trifluoromethyl)phenyl)-1,3,2-benzodiazaborininone (**2.66**)

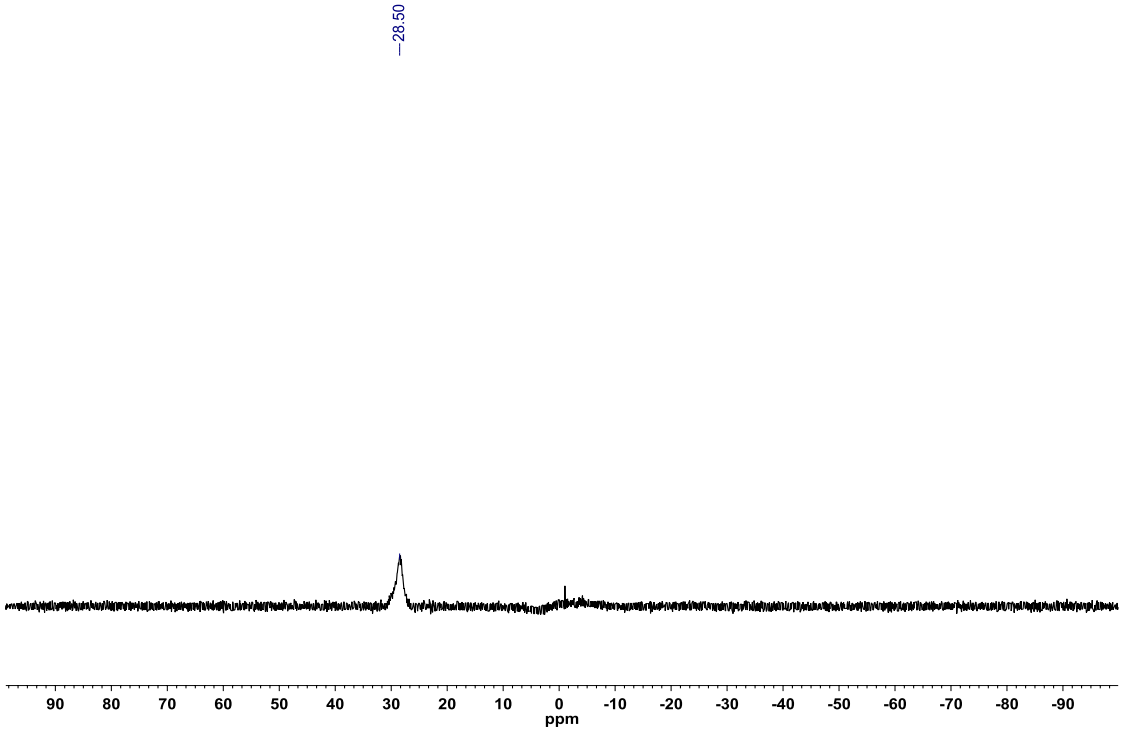

Figure A1.218: ^{1}H NMR (DMSO-d_6, 500.4 MHz) of 2-(4-bromophenyl)-1,3,2-benzodiazaborininone (**2.67**)

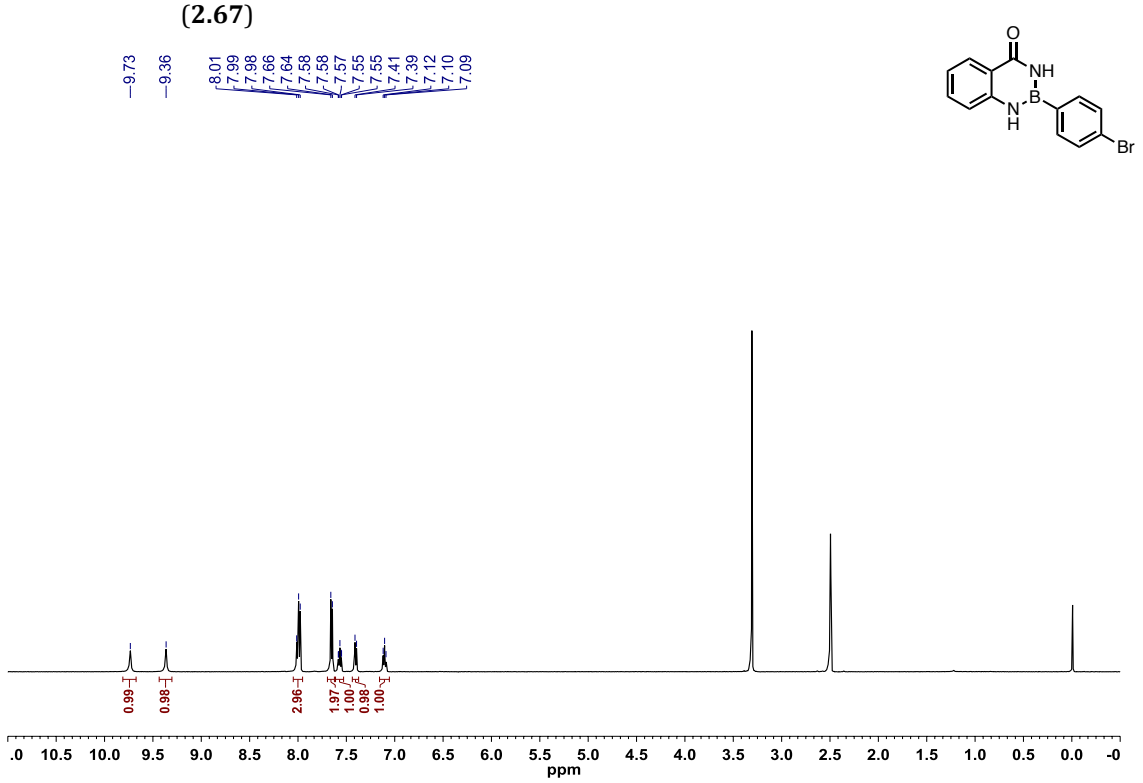

Figure A1.219: ^{13}C {^{1}H} NMR (DMSO-d_6, 125.8 MHz) of 2-(4-bromophenyl)-1,3,2-benzodiazaborininone (**2.67**)

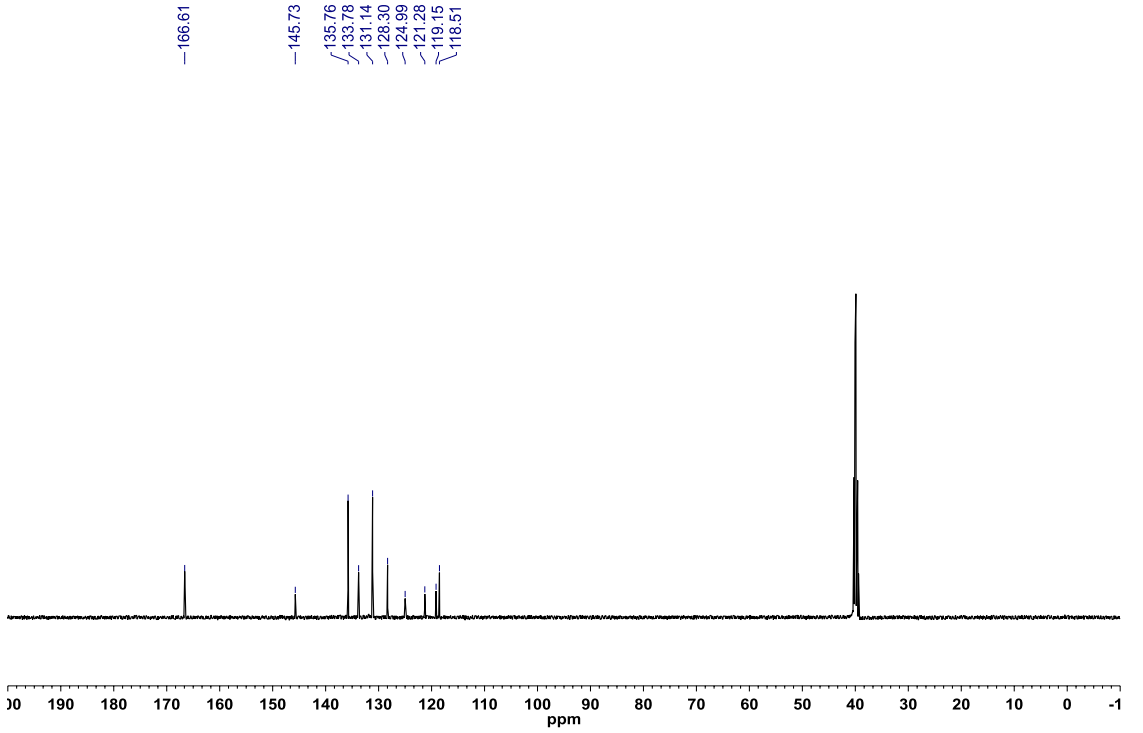

Figure A1.220: ^{11}B NMR (THF, 128.4 MHz) of 2-(4-bromophenyl)-1,3,2-benzodiazaborininone (**2.67**)

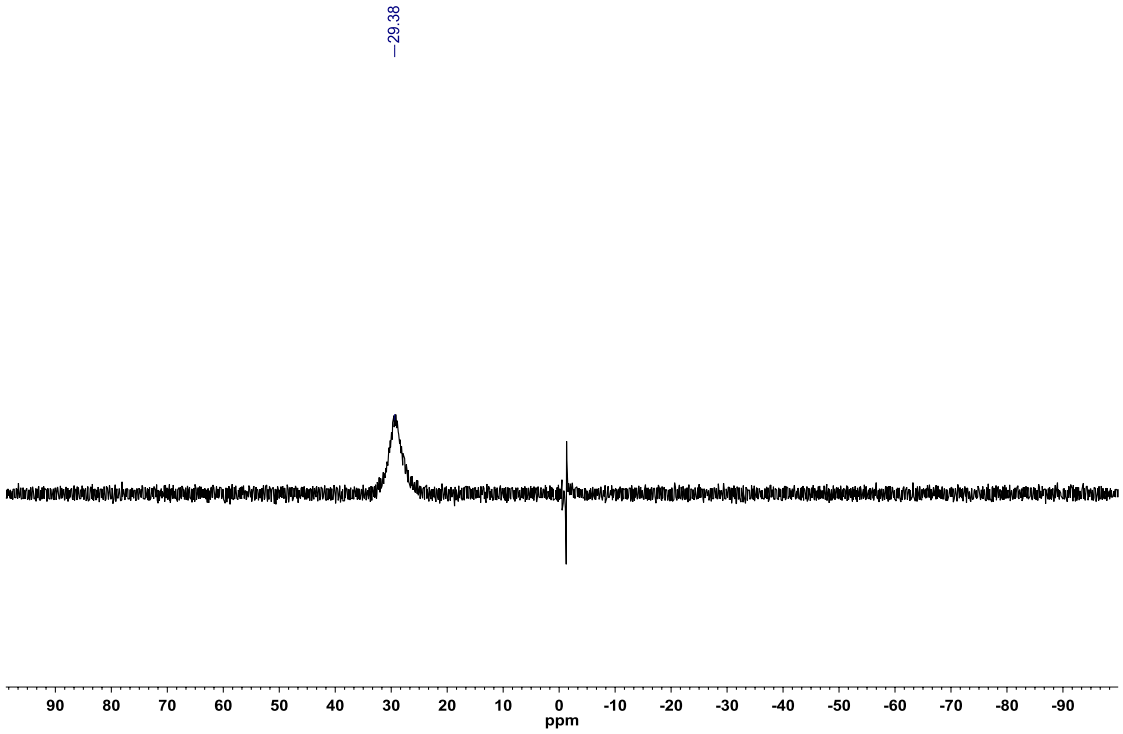

Figure A1.221: ^{1}H NMR (DMSO-d_6, 500.4 MHz) of 2-(3-aminophenyl)-1,3,2-benzodiazaborininone (**2.68**)

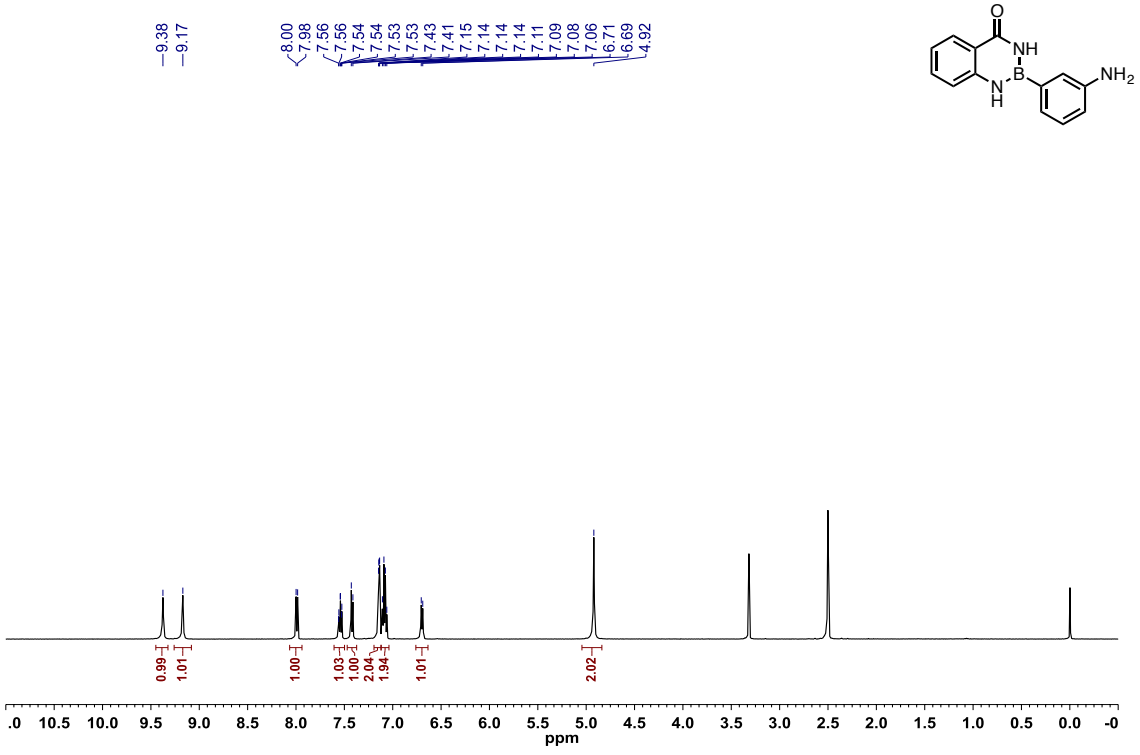

Figure A1.222: ^{13}C {^{1}H} NMR (DMSO-d_6, 125.8 MHz) of 2-(3-aminophenyl)-1,3,2-benzodiazaborininone (**2.68**)

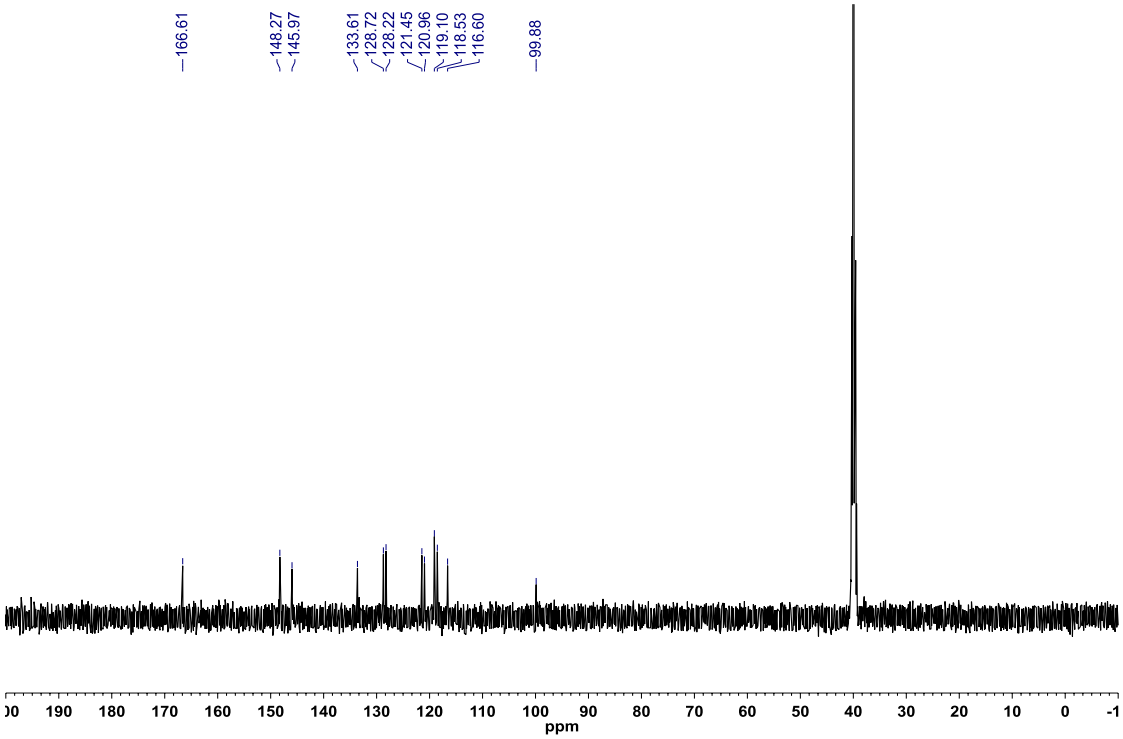

Figure A1.223: ^{11}B NMR (MeCN, 128.4 MHz) of 2-(3-aminophenyl)-1,3,2-benzodiazaborininone (**2.68**)

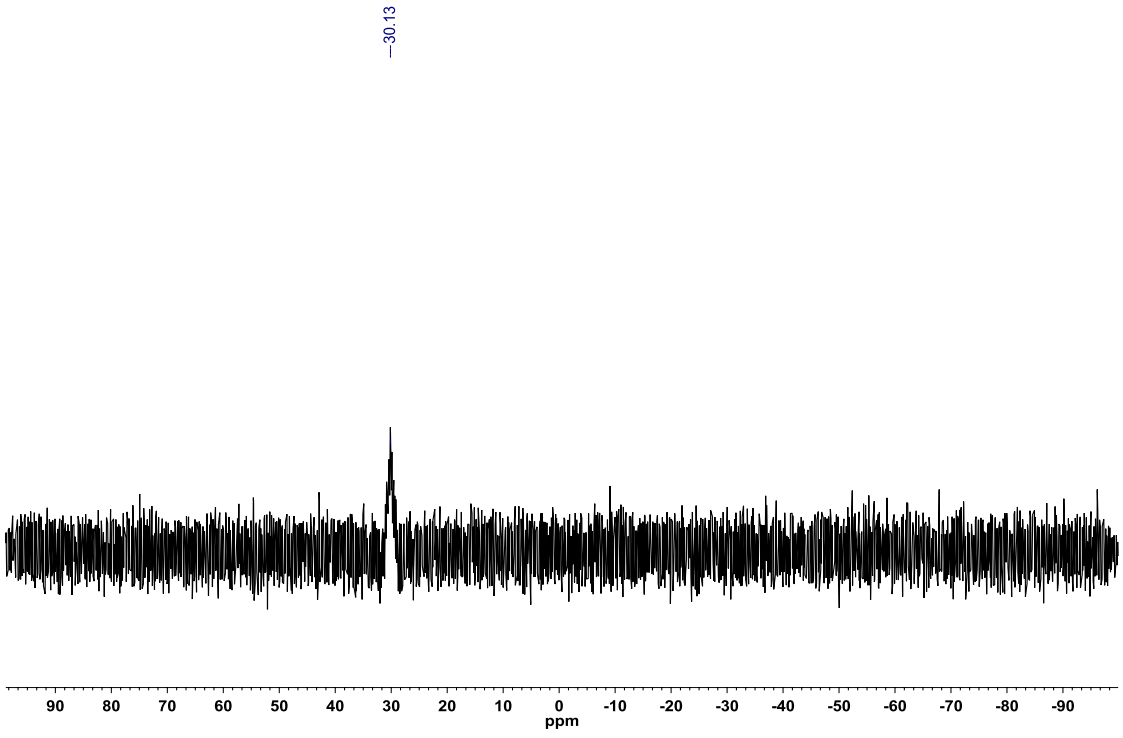

Figure A1.224: ^{1}H NMR (DMSO-d_6, 500.4 MHz) of 2-(3-(methoxycarbonyl)phenyl)-1,3,2-benzodiazaborininone (**2.69**)

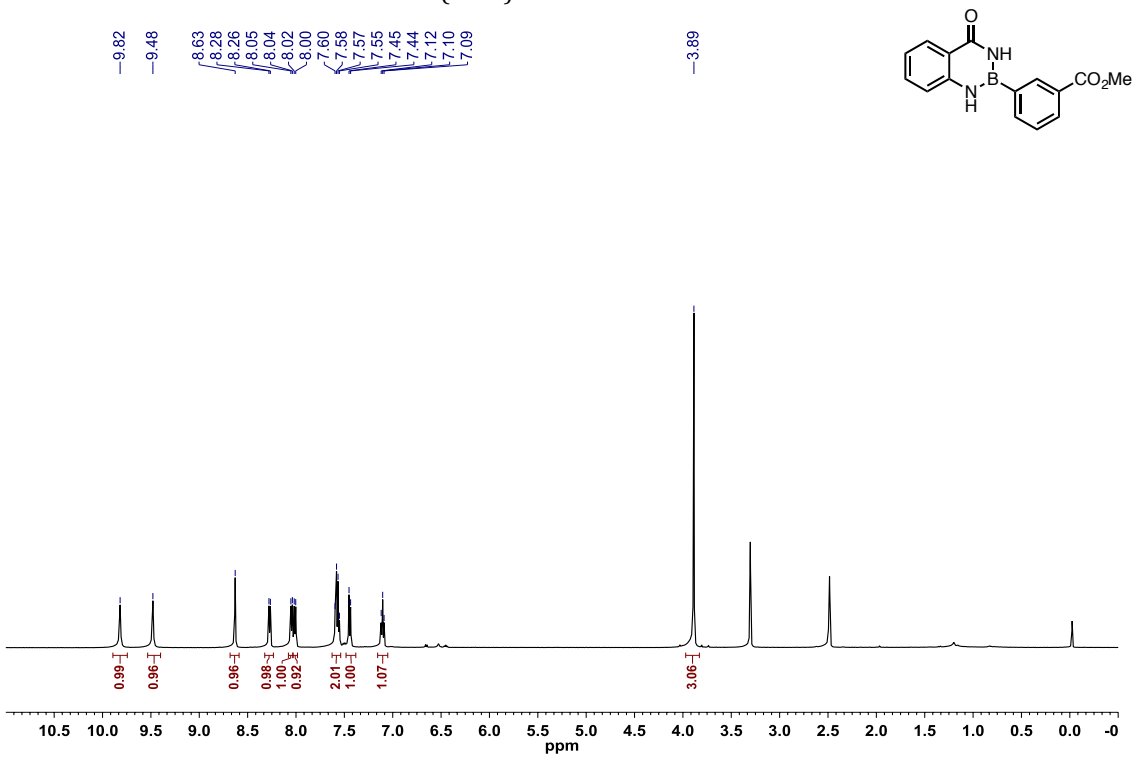

Figure A1.225: ^{13}C {^{1}H} NMR (DMSO-d_6, 125.8 MHz) of 2-(3-(methoxycarbonyl)phenyl)-1,3,2-benzodiazaborininone (**2.69**)

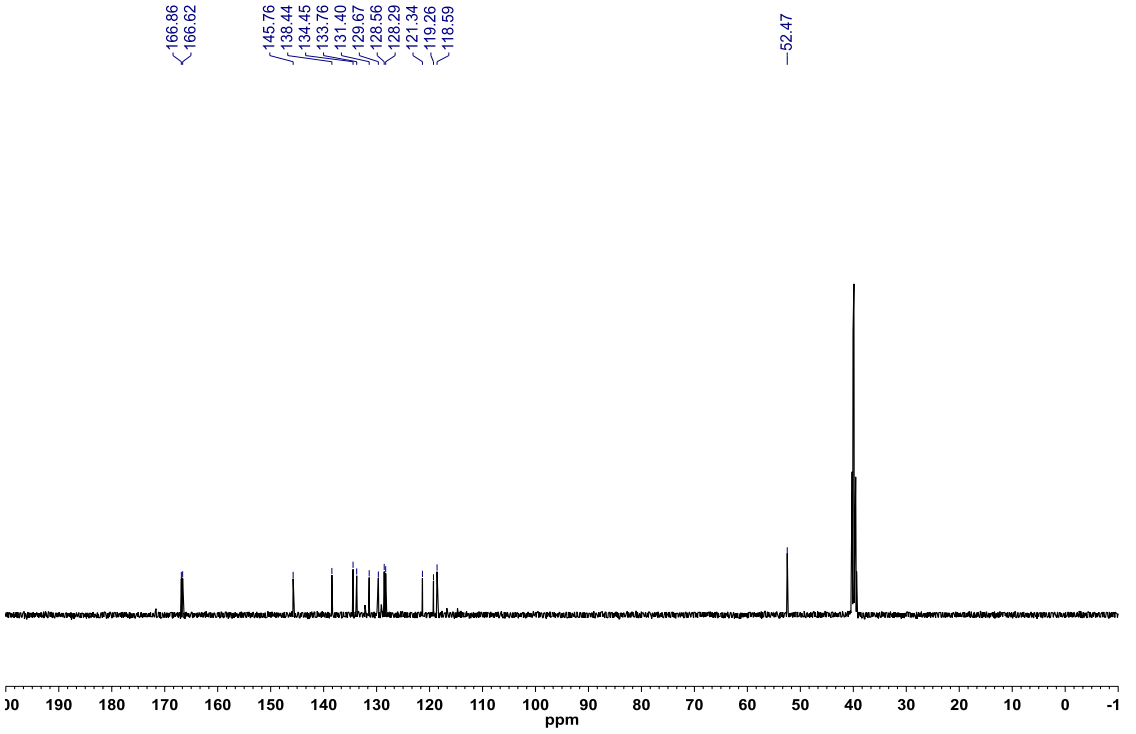

Figure A1.226: ^{11}B NMR (THF, 128.4 MHz) of 2-(3-(methoxycarbonyl)phenyl)-1,3,2-benzodiazaborininone (**2.69**)

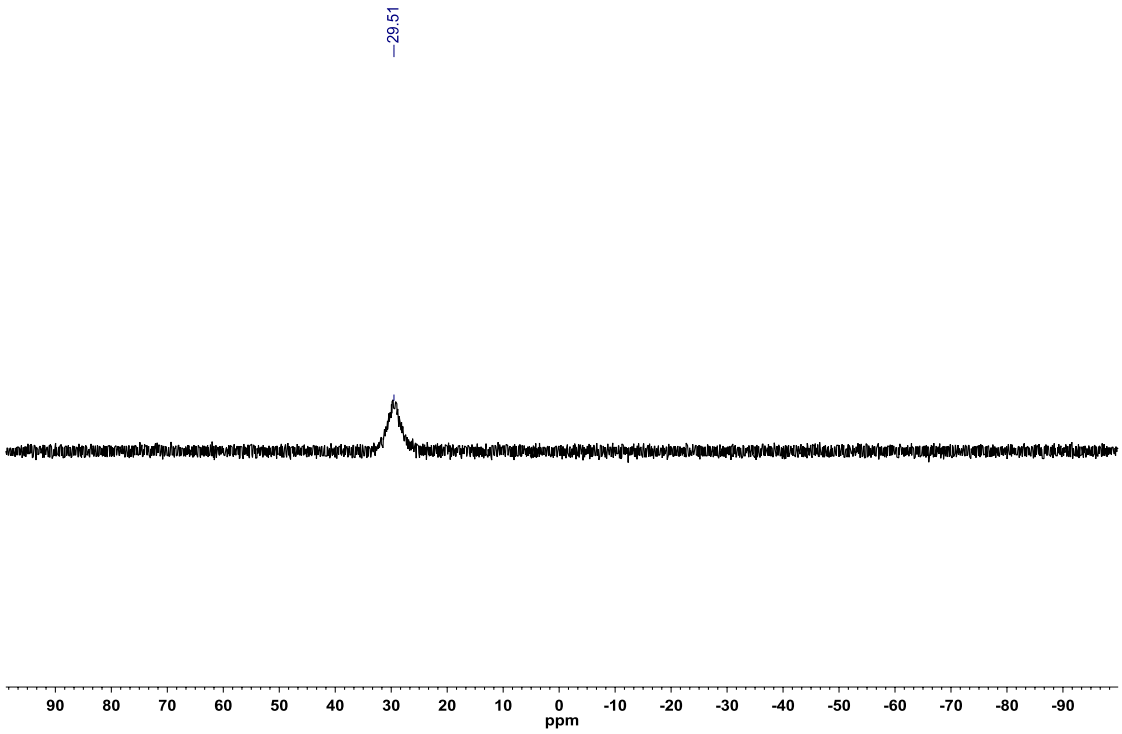

Figure A1.227: ^{1}H NMR (DMSO-d_6, 500.4 MHz) of 2-(3-cyanophenyl)-1,3,2-benzodiazaborininone (**2.70**)

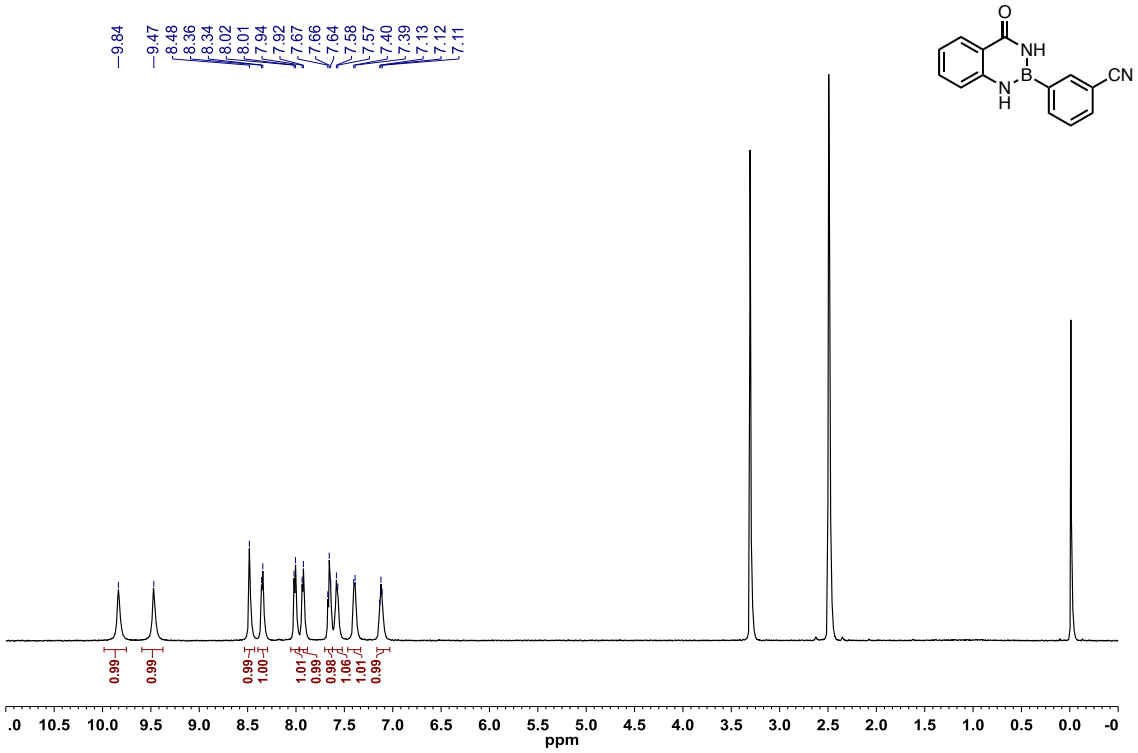

Figure A1.228: ^{13}C {^{1}H} NMR (DMSO-d_6, 125.8 MHz) of 2-(3-cyanophenyl)-1,3,2-benzodiazaborininone (**2.70**)

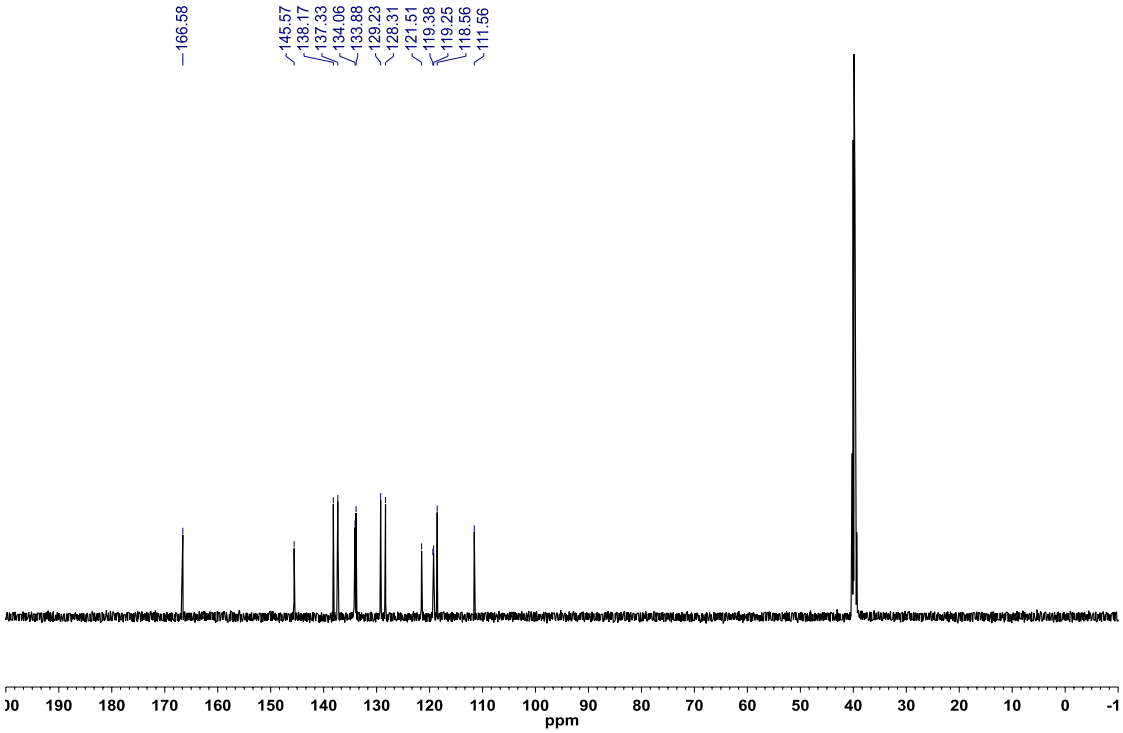

Figure A1.229: ^{11}B NMR (THF, 128.4 MHz) of 2-(3-cyanophenyl)-1,3,2-benzodiazaborininone (**2.70**)

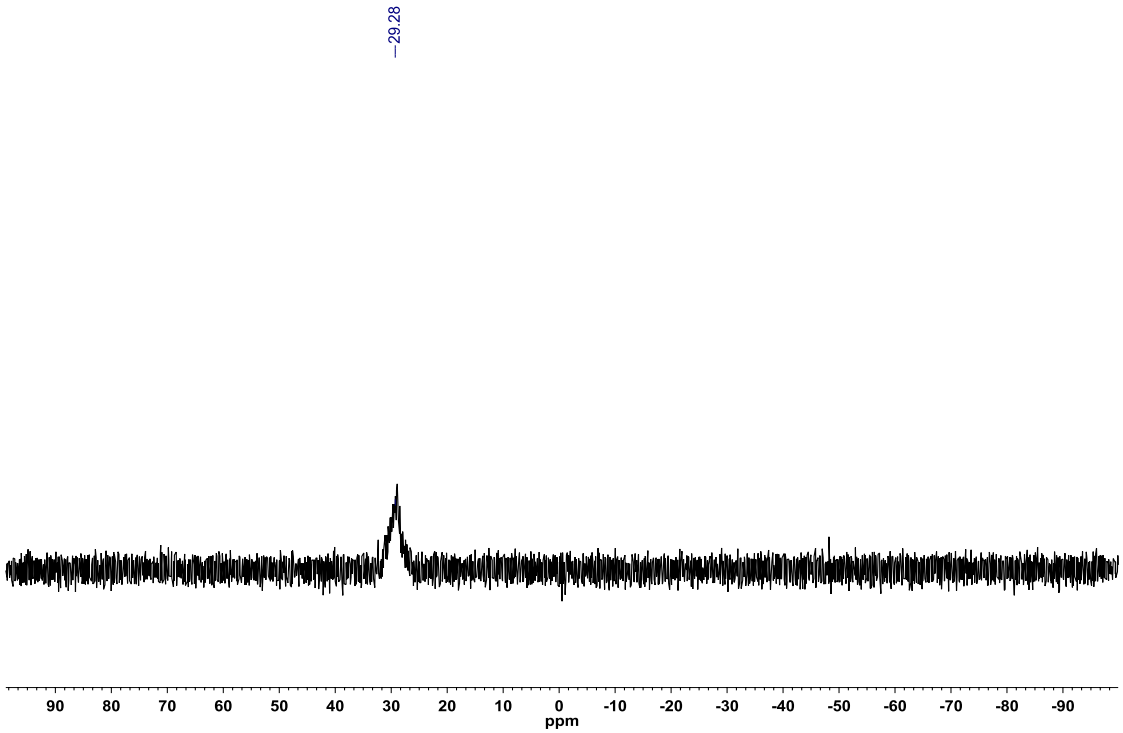

Figure A1.230: ^{1}H NMR (DMSO-d_6, 500.4 MHz) of 2-(3-nitrophenyl)-1,3,2-benzodiazaborininone (**2.71**)

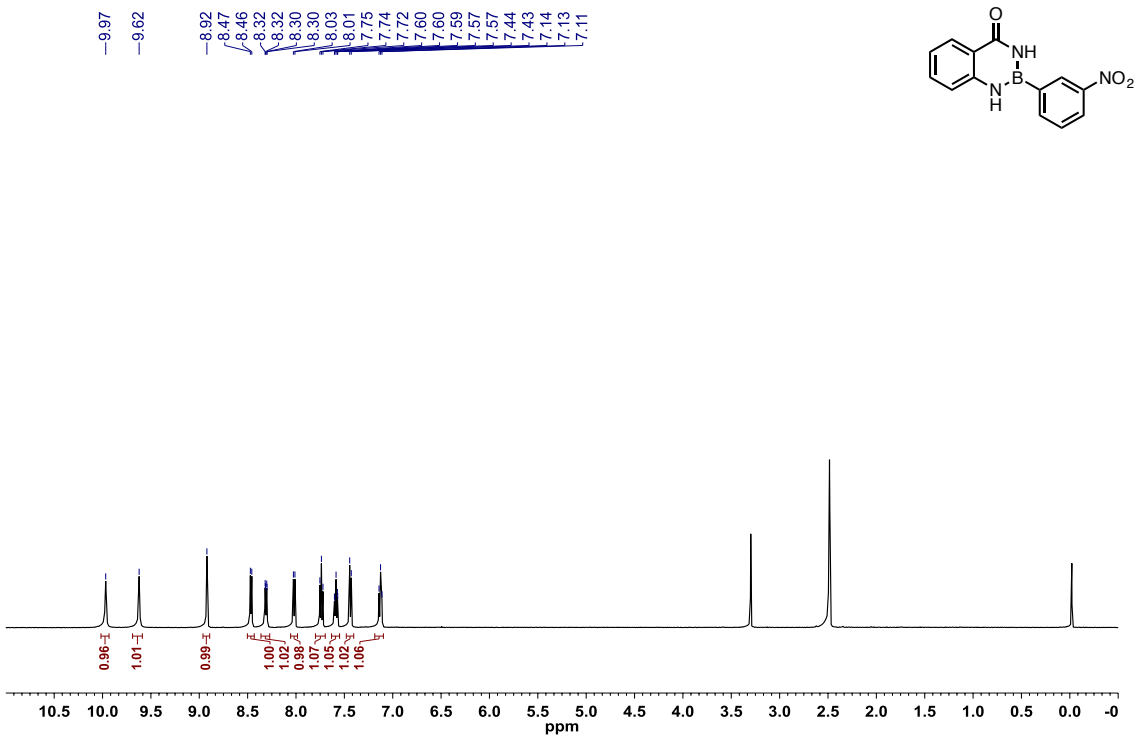

Figure A1.231: ^{13}C {^{1}H} NMR (DMSO-d_6, 125.8 MHz) of 2-(3-nitrophenyl)-1,3,2-benzodiazaborininone (**2.71**)

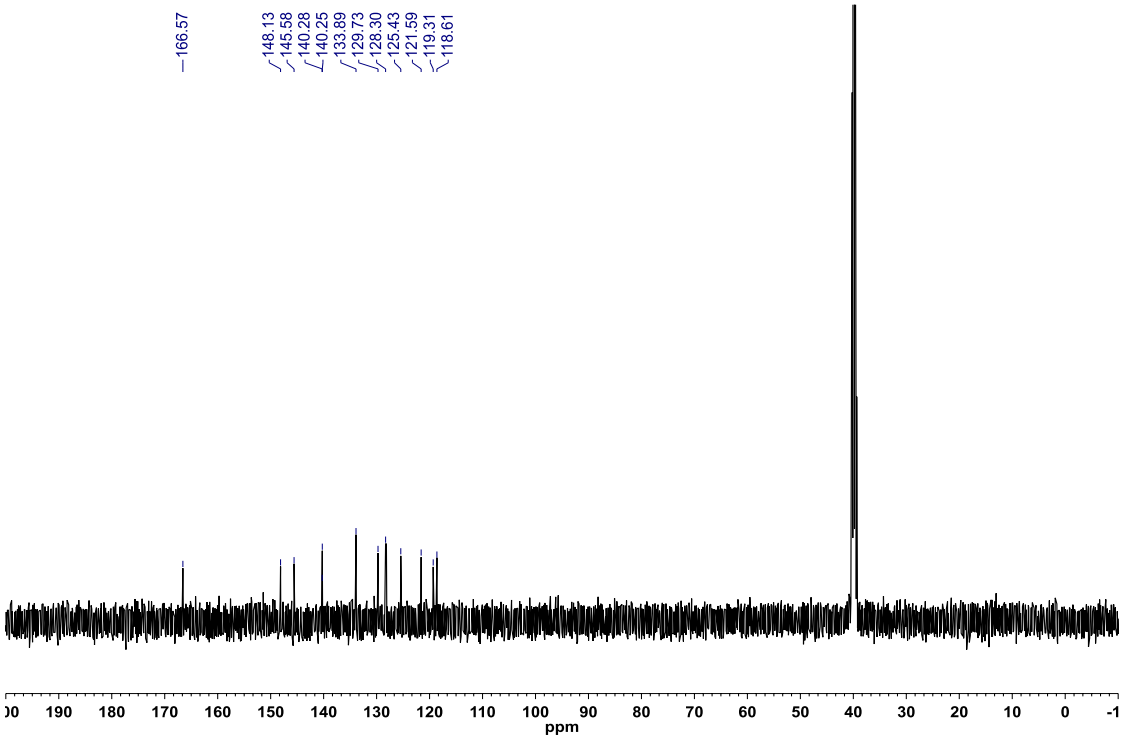

Figure A1.232: ^{11}B NMR (THF, 128.4 MHz) of 2-(3-nitrophenyl)-1,3,2-benzodiazaborininone (**2.71**)

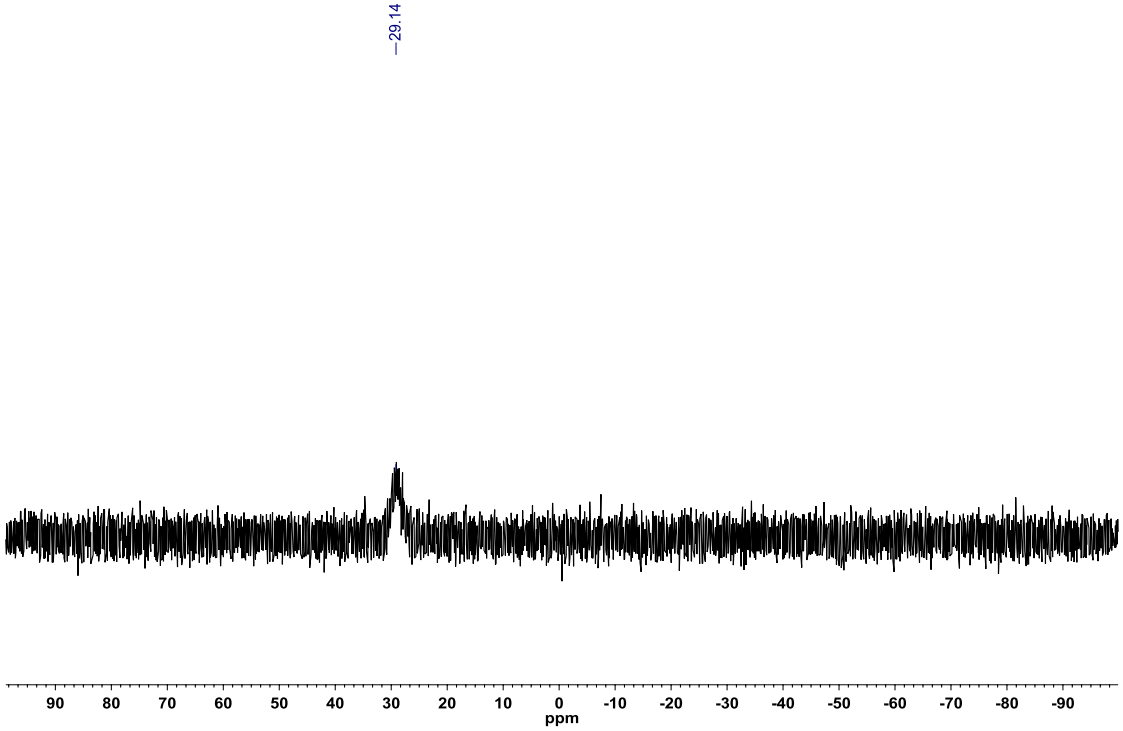

Figure A1.233: ^{1}H NMR (DMSO-d_6, 500.4 MHz) of 2-(4-(naphthalen-1-yl)phenyl)-1,3,2-benzodiazaborininone (**2.72**)

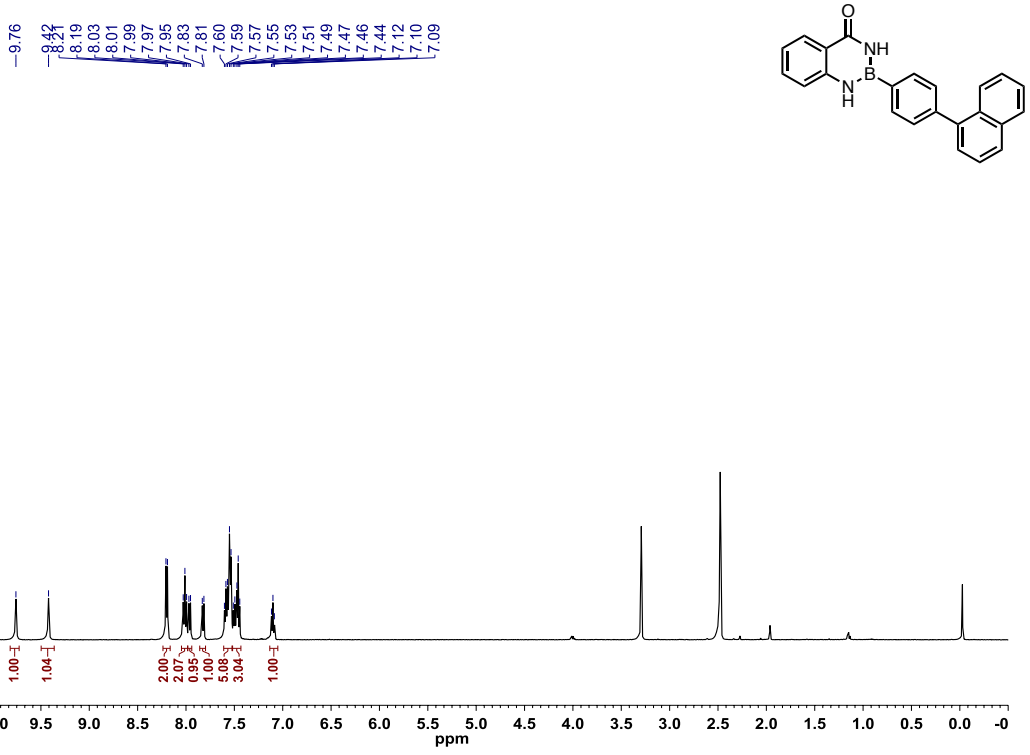

Figure A1.234: ^{13}C {^{1}H} NMR (DMSO-d_6, 125.8 MHz) of 2-(4-(naphthalen-1-yl)phenyl)-1,3,2-benzodiazaborininone (**2.72**)

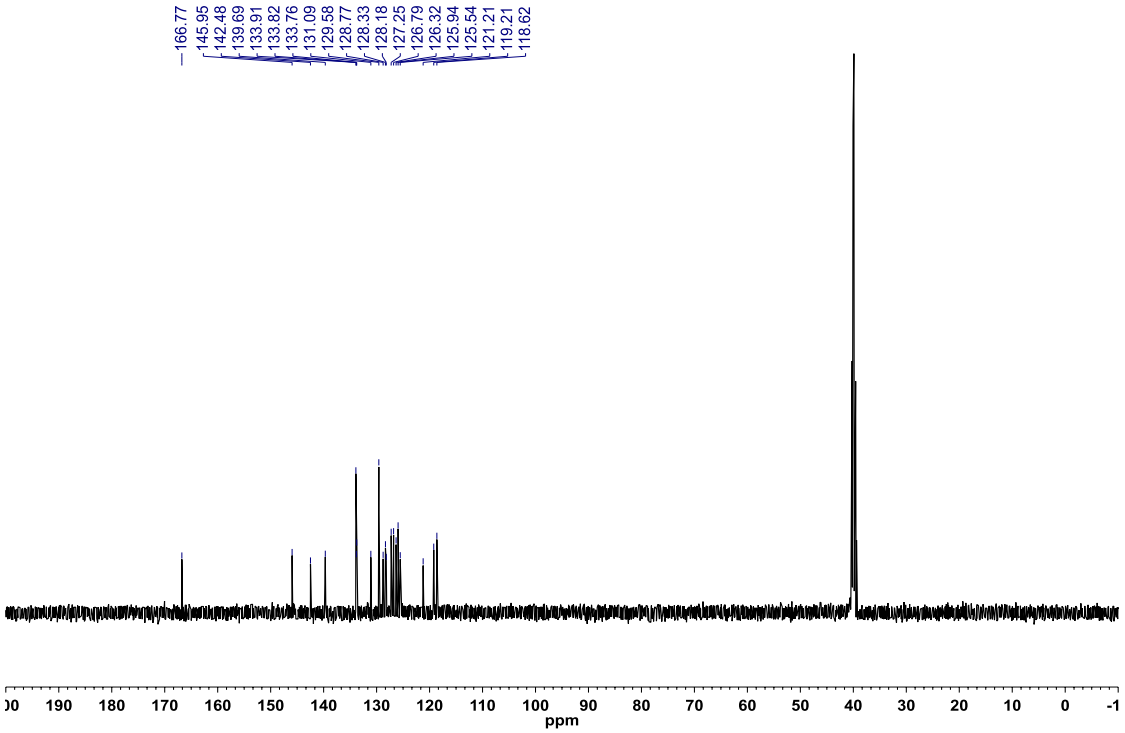

Figure A1.235: ^{11}B NMR (THF, 128.4 MHz) of 2-(4-(naphthalen-1-yl)phenyl)-1,3,2-benzodiazaborininone (**2.72**)

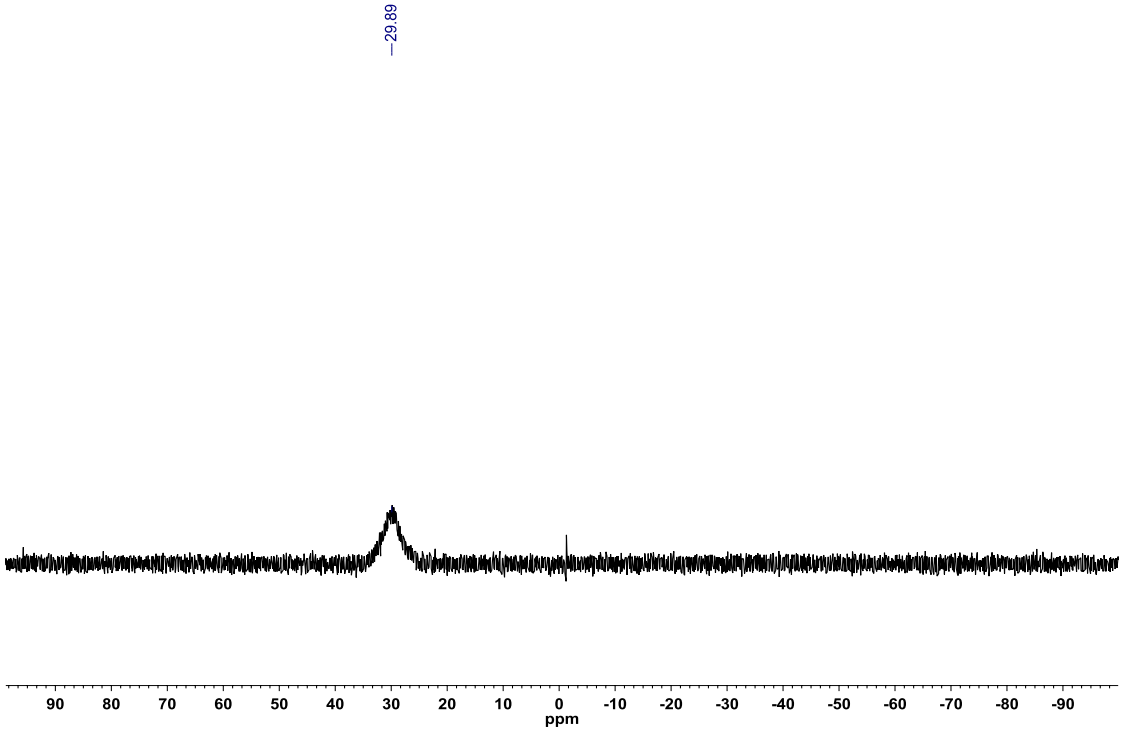

Figure A1.236: ^{1}H NMR (DMSO-d_6, 500.4 MHz) of 2-(4-(benzyloxy)phenyl)-1,3,2-benzodiazaborininone (**2.73**)

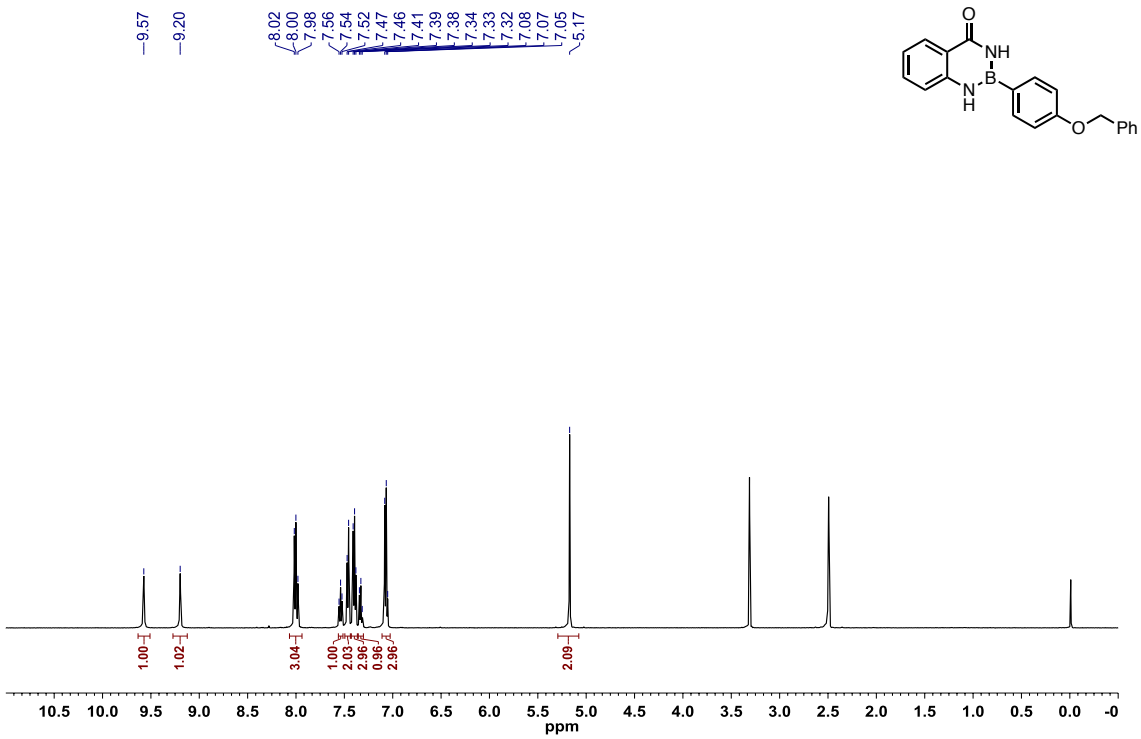

Figure A1.237: ^{13}C {^{1}H} NMR (DMSO-d_6, 125.8 MHz) of 2-(4-(benzyloxy)phenyl)-1,3,2-benzodiazaborininone (**2.73**)

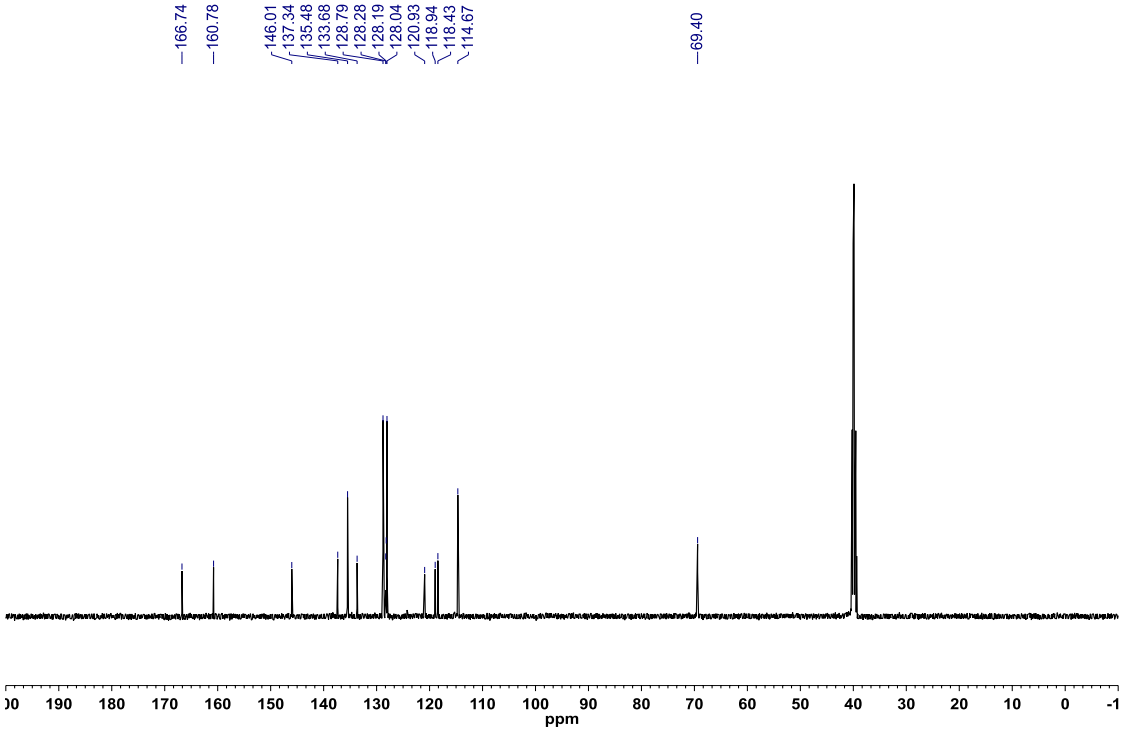

Figure A1.238: ^{11}B NMR (THF, 128.4 MHz) of 2-(4-(benzyloxy)phenyl)-1,3,2-benzodiazaborininone (**2.73**)

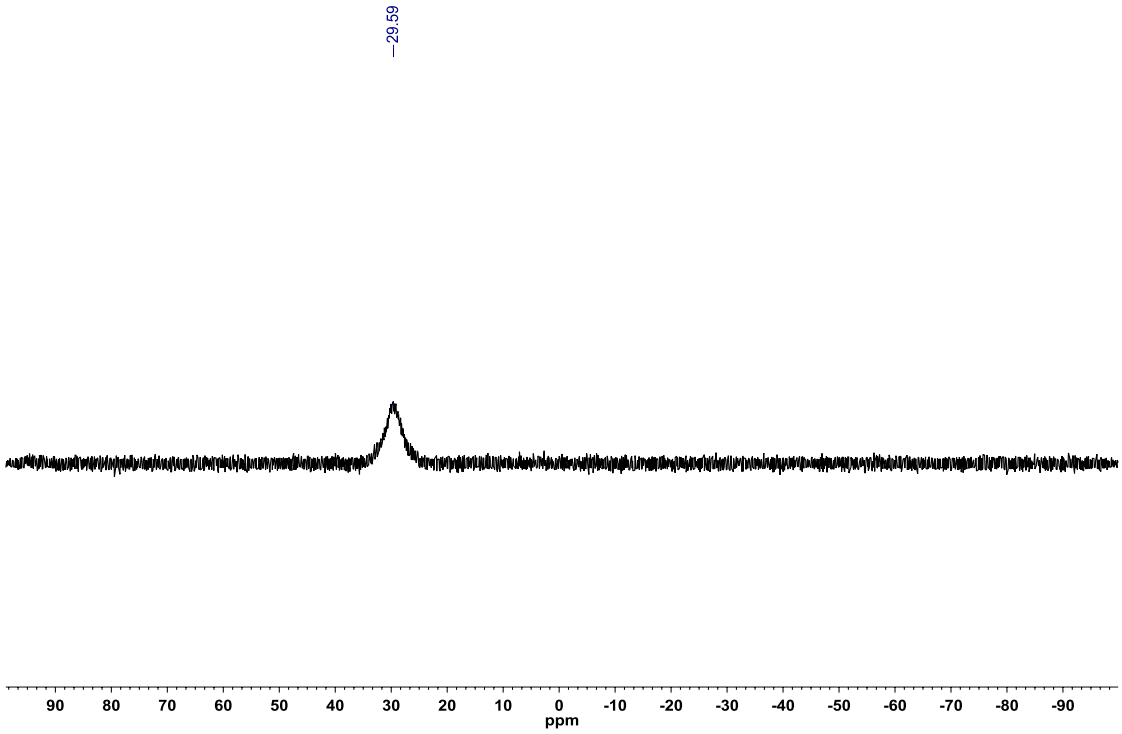

Figure A1.239: ^{1}H NMR ($CDCl_3$, 500.4 MHz) of 2-(furan-3-yl)-1,3,2-benzodiazaborininone (**2.74**)

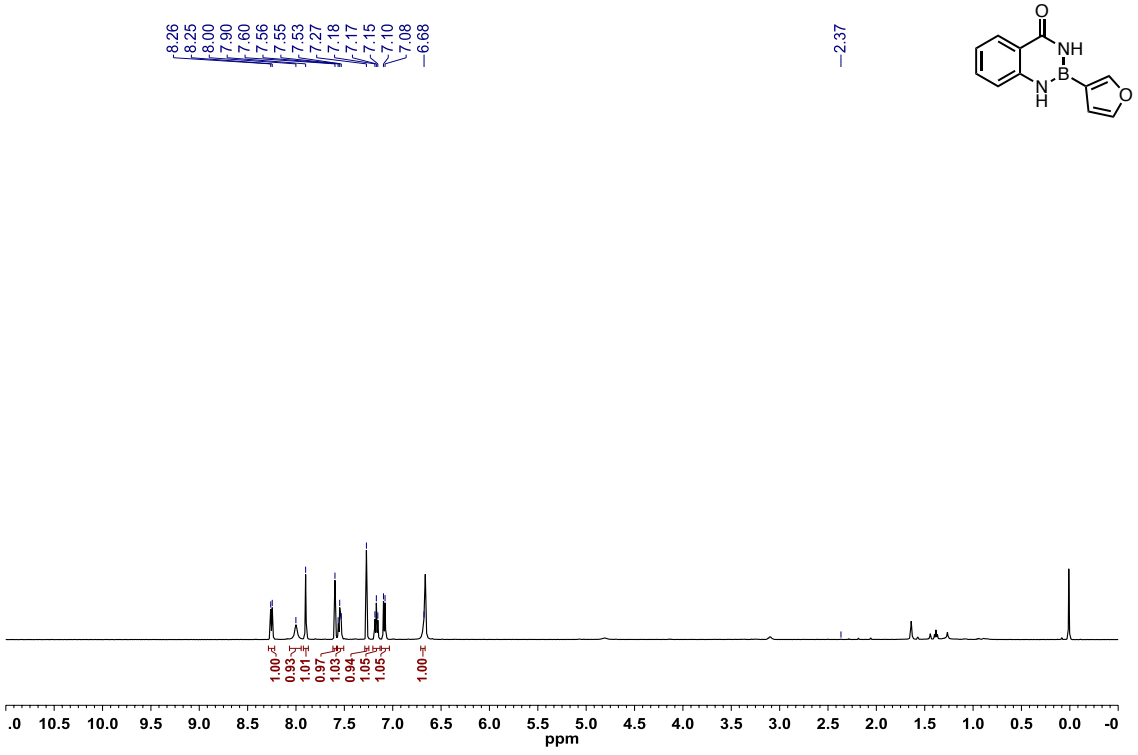

Figure A1.240: ^{13}C {^{1}H} NMR ($CDCl_3$, 125.8 MHz) of 2-(furan-3-yl)-1,3,2-benzodiazaborininone (**2.74**)

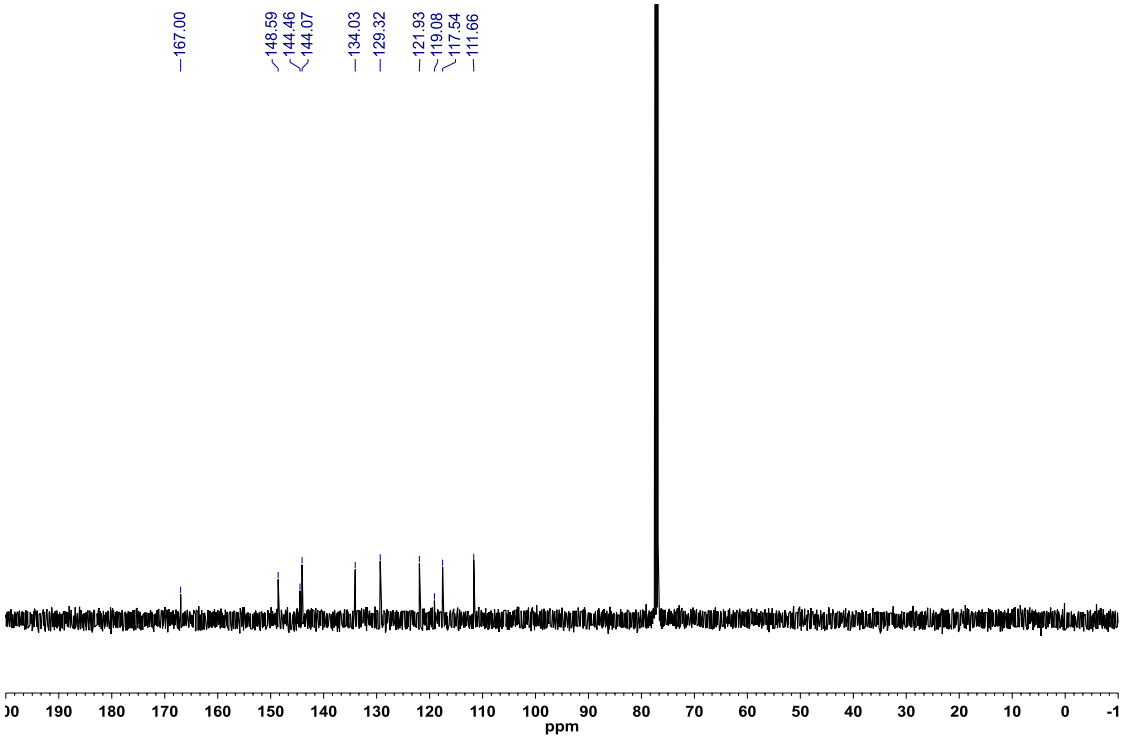

Figure A1.241: ^{11}B NMR (EtOAc, 128.4 MHz) of 2-(furan-3-yl)-1,3,2-benzodiazaborininone **(2.74)**

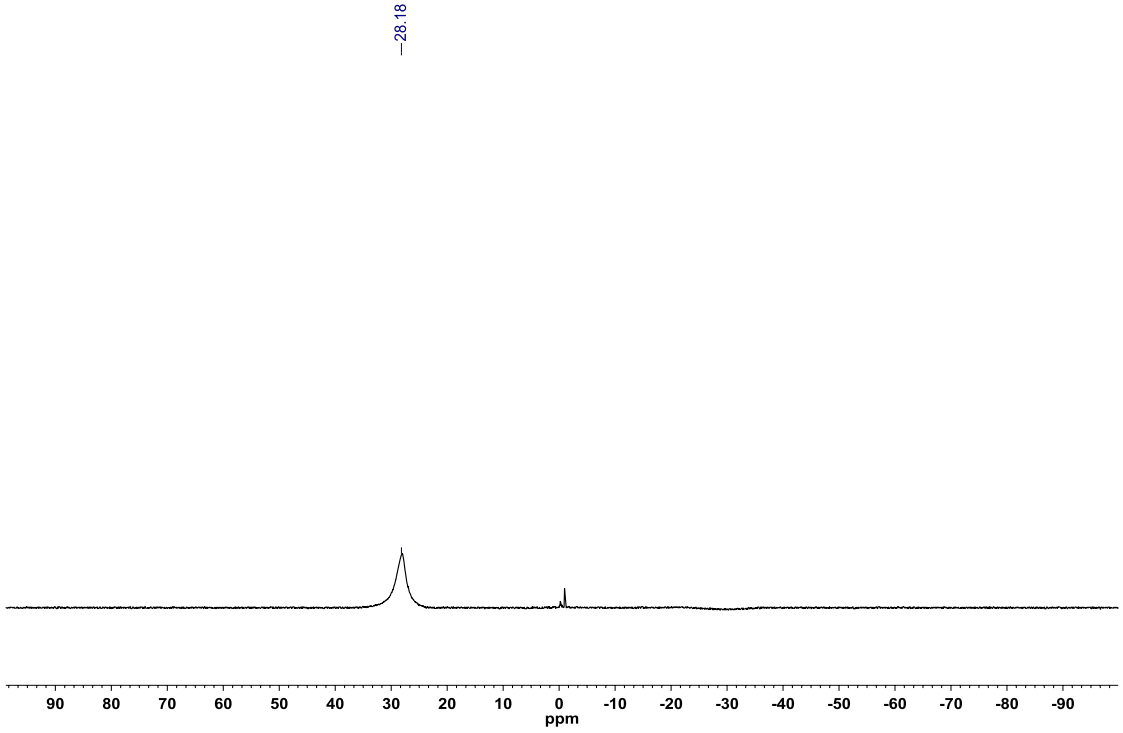

Figure A1.242: ^{1}H NMR (DMSO-d_6, 500.4 MHz) of 2-(thiophen-2-yl)-1,3,2-benzodiazaborininone (**2.75**)

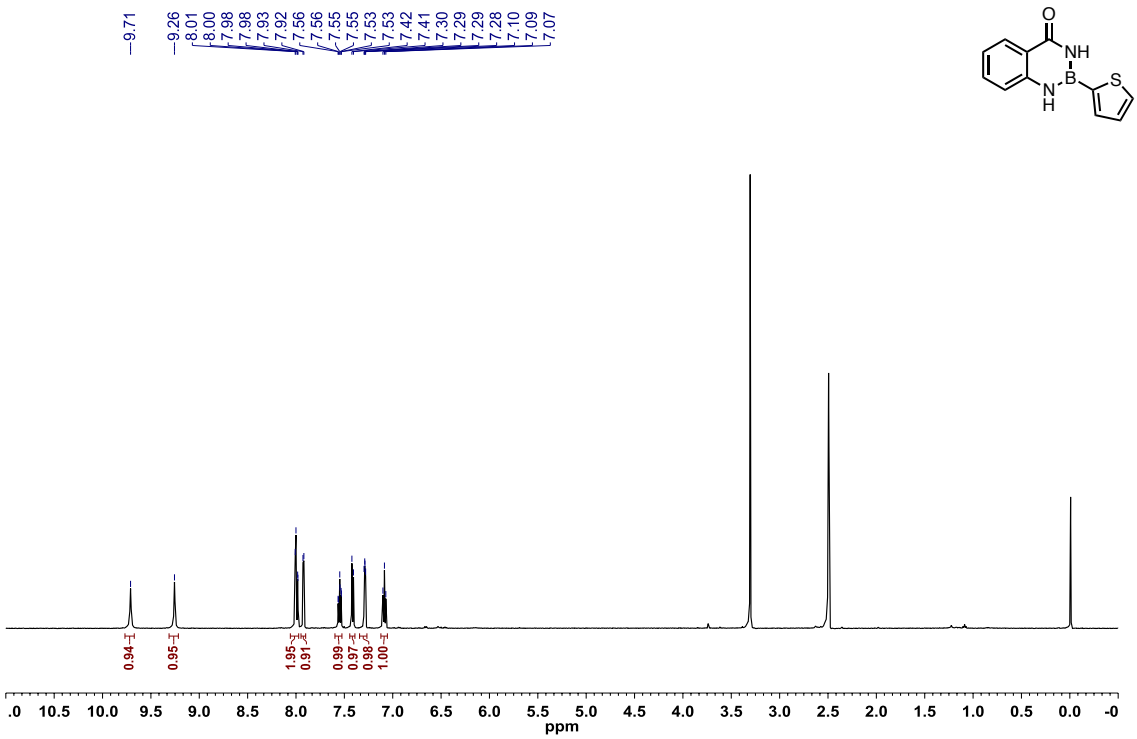

Figure A1.243: ^{13}C {^{1}H} NMR (DMSO-d_6, 125.8 MHz) of 2-(thiophen-2-yl)-1,3,2-benzodiazaborininone (**2.75**)

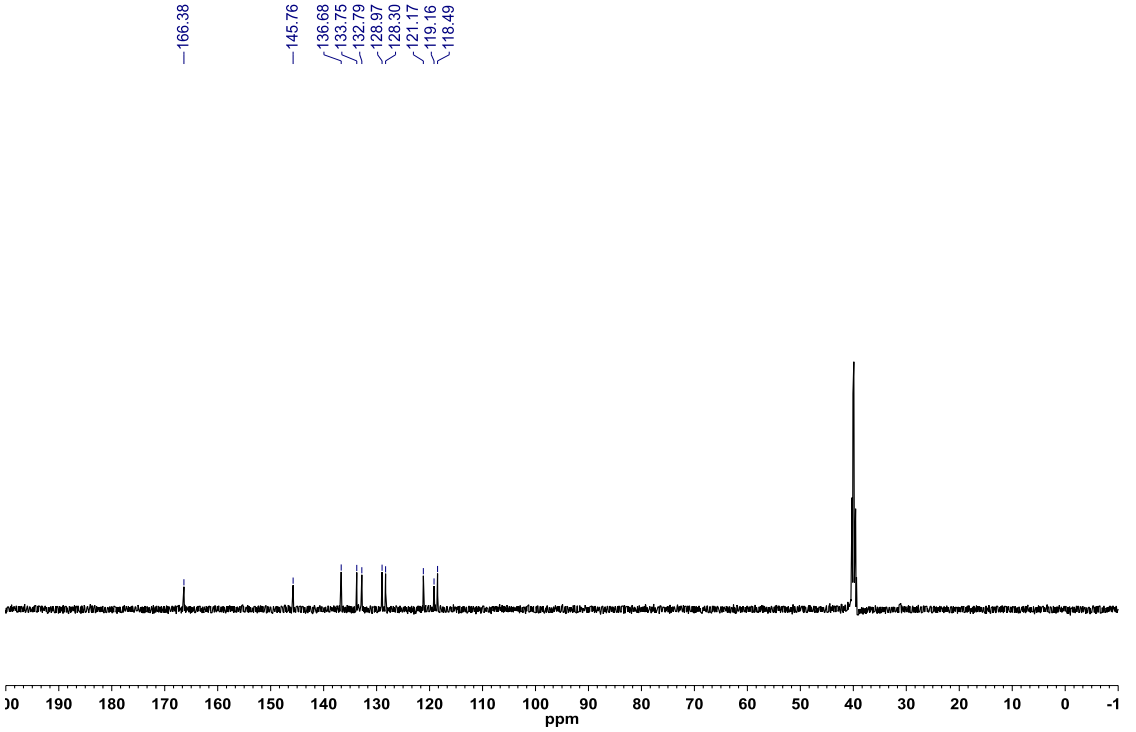

Figure A1.244: ^{11}B NMR (EtOAc, 128.4 MHz) of 2-(thiophen-2-yl)-1,3,2-benzodiazaborininone (**2.75**)

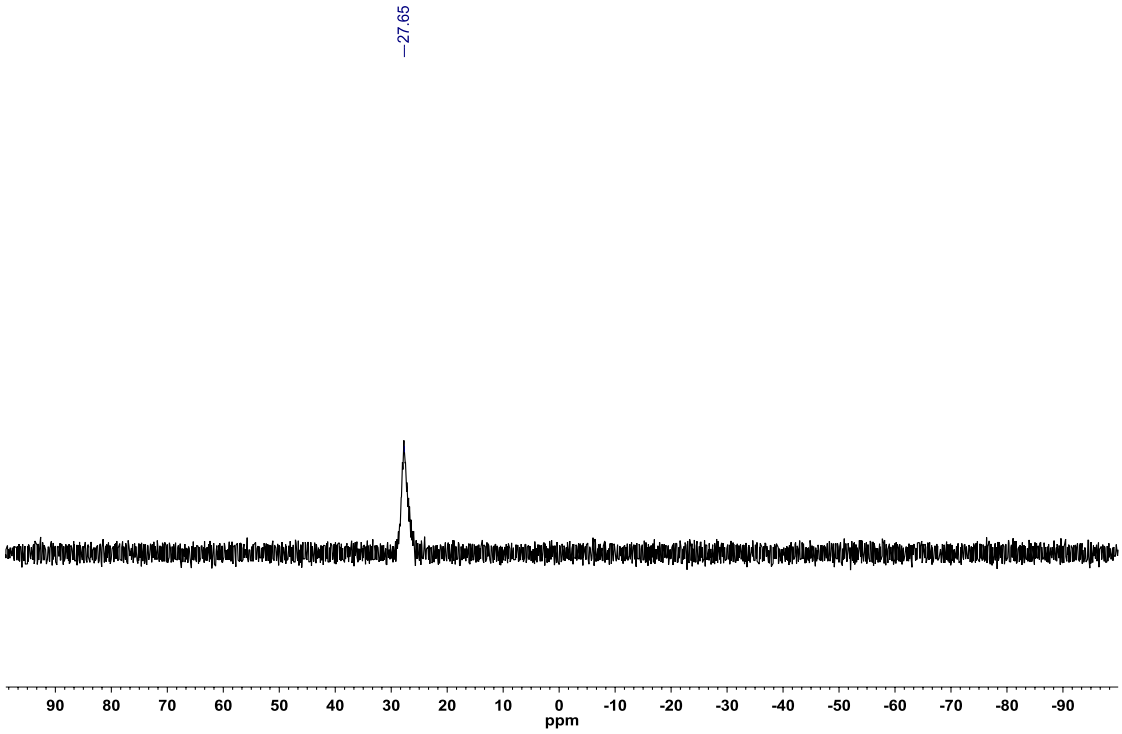

Figure A1.245: ^{1}H NMR (DMSO-d_6, 500.4 MHz) of (*E*)-2-(prop-1-en-1-yl)-1,3,2-benzodiazaborininone (**2.76**)

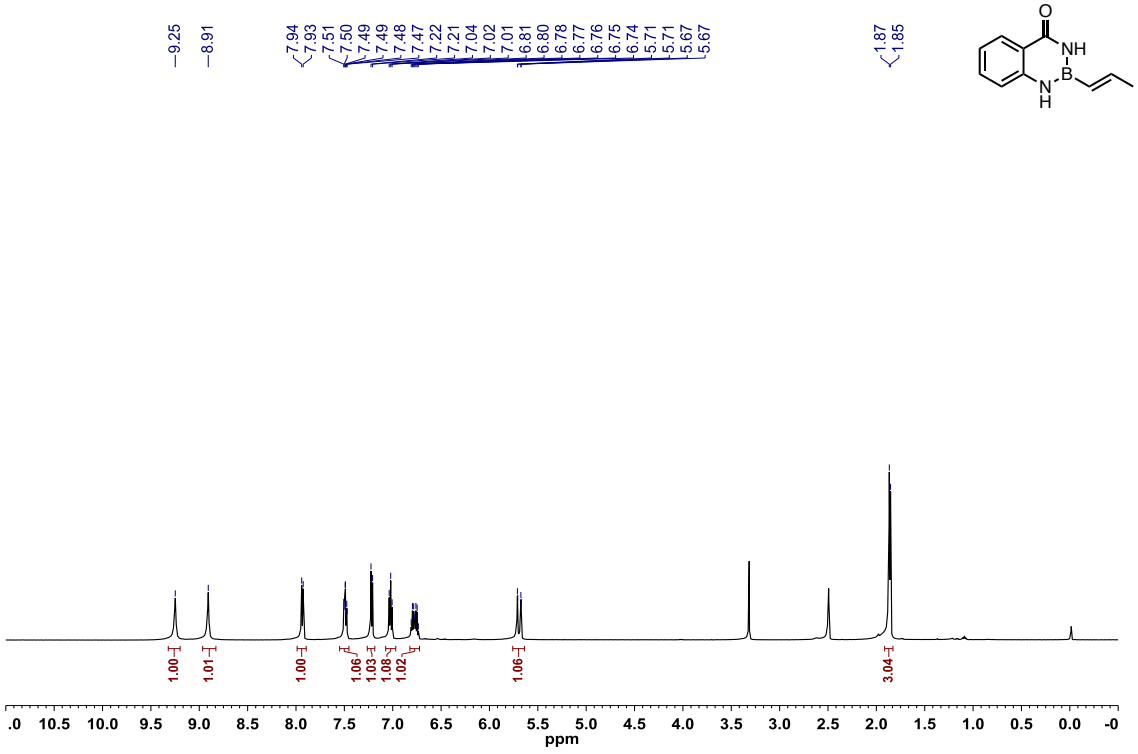

Figure A1.246: ^{13}C {^{1}H} NMR (DMSO-d_6, 125.8 MHz) of (*E*)-2-(prop-1-en-1-yl)-1,3,2-benzodiazaborininone (**2.76**)

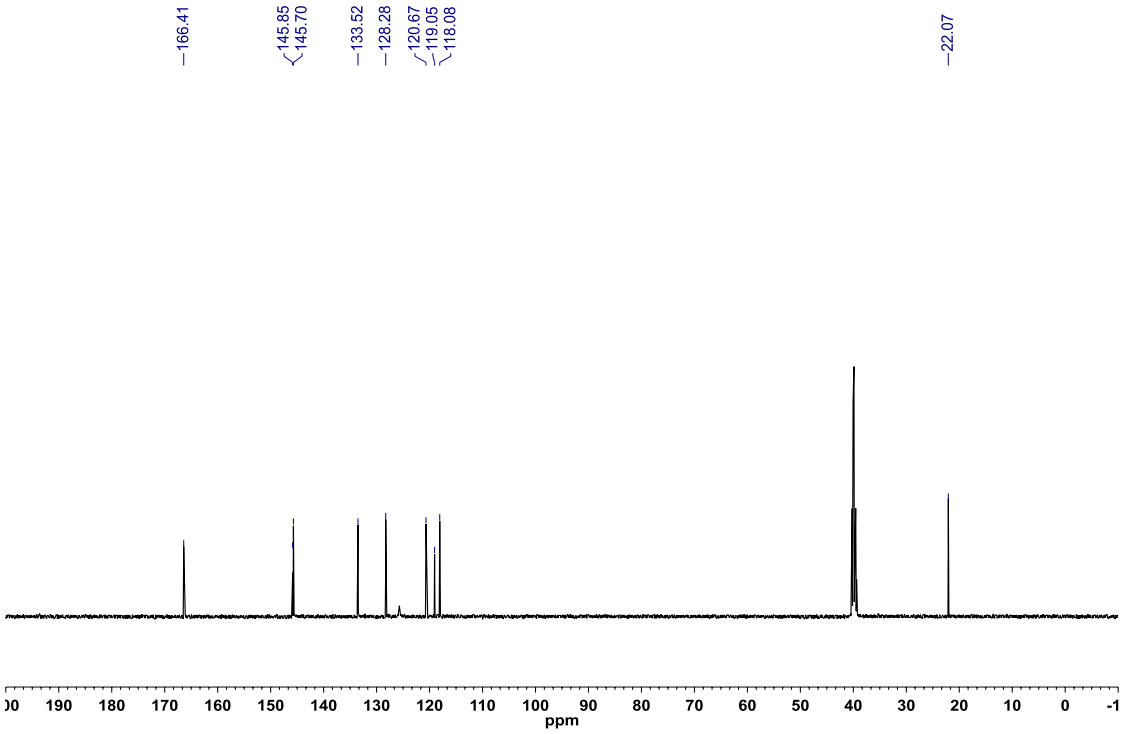

Figure A1.247: ^{11}B NMR (EtOAc, 128.4 MHz,) of (*E*)-2-(prop-1-en-1-yl)-1,3,2-benzodiazaborininone (**2.76**)

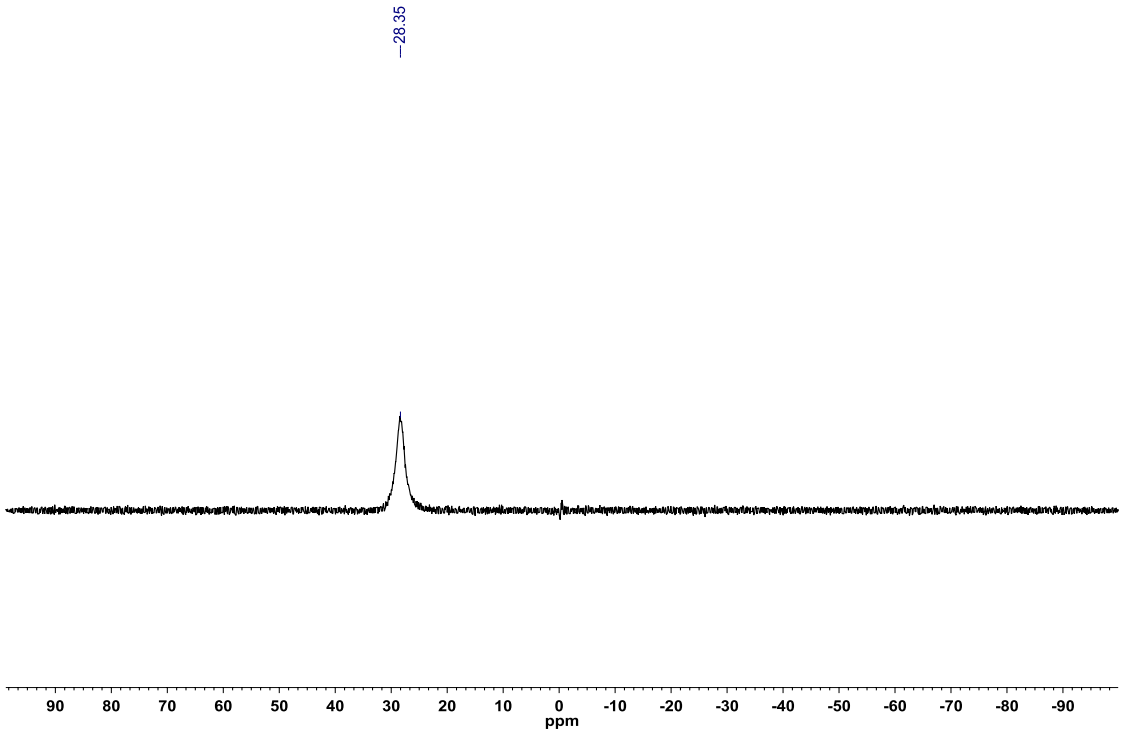

Figure A1.248: ^{1}H NMR ($CDCl_3$, 500.4 MHz) of 2-methyl-1,3,2-benzodiazaborininone (**2.77**)

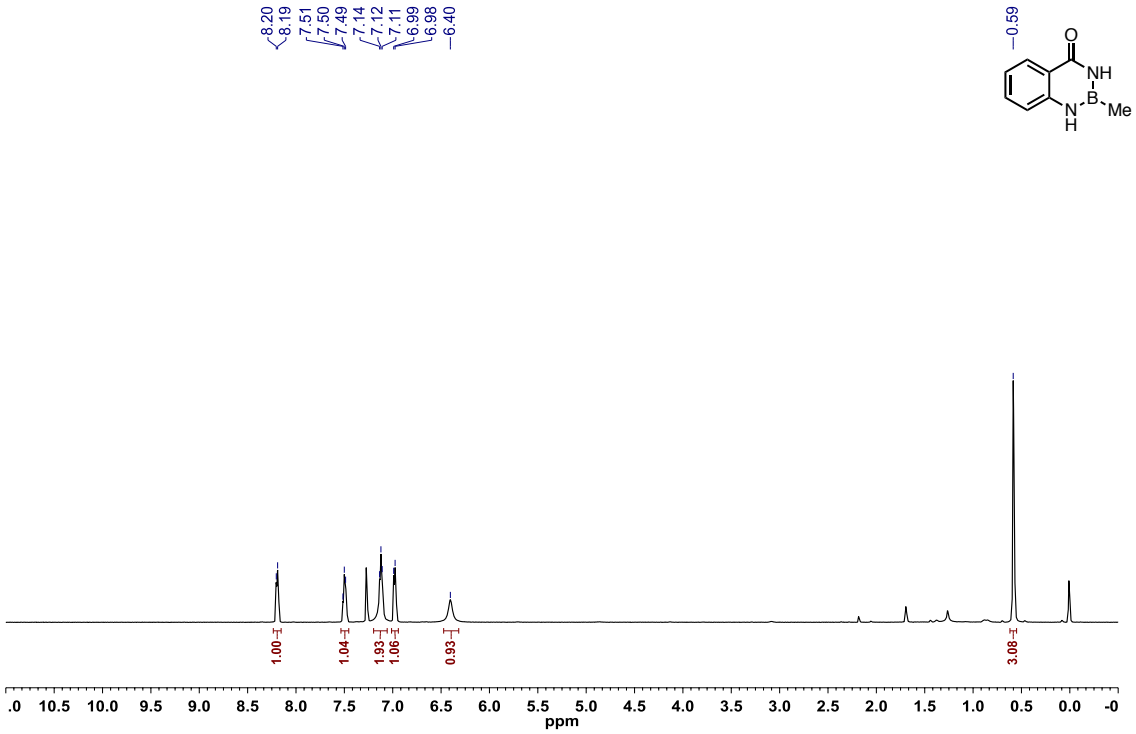

Figure A1.249: ^{13}C {^{1}H} NMR ($CDCl_3$, 125.8 MHz) of 2-methyl-1,3,2-benzodiazaborininone (**2.77**)

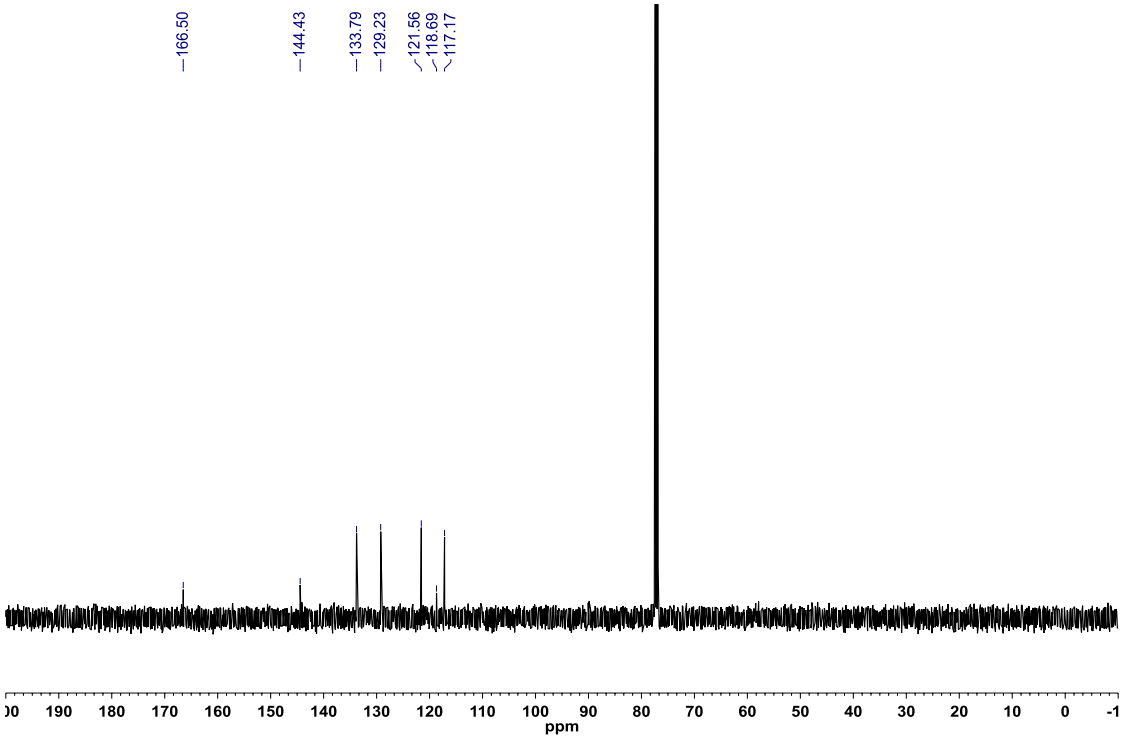

Figure A1.250: ^{11}B NMR ($CDCl_3$, 128.4 MHz) of 2-methyl-1,3,2-benzodiazaborininone (**2.77**)

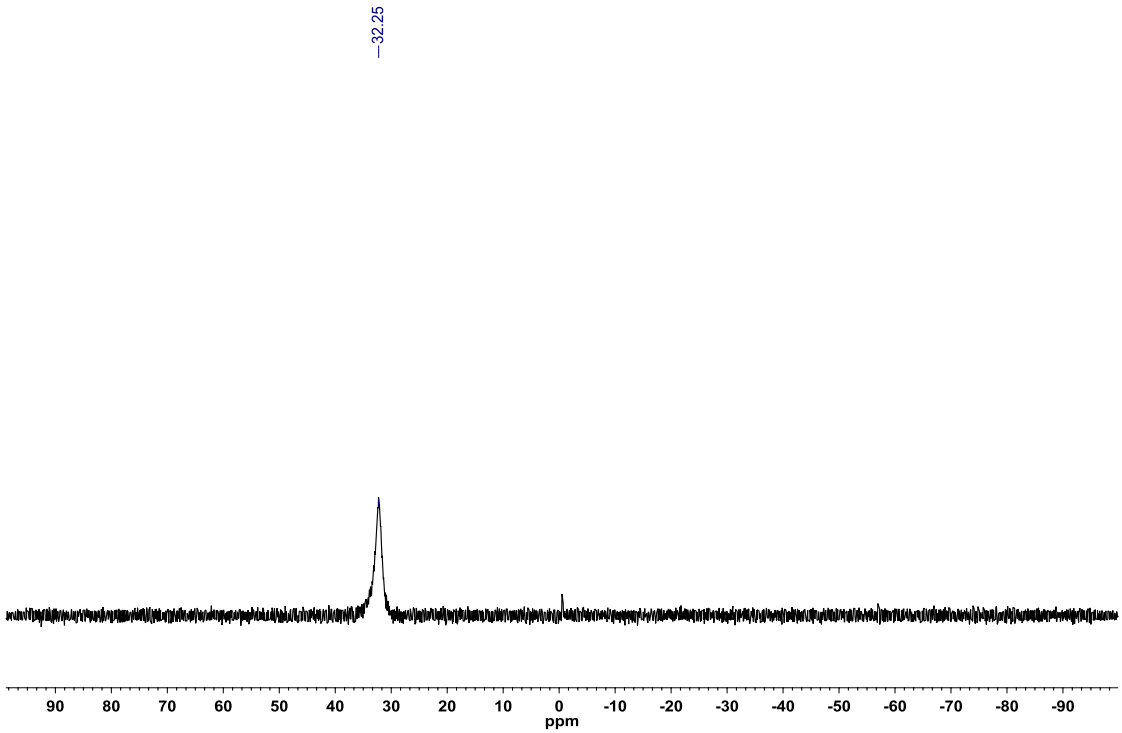

Figure A1.251: ^{1}H NMR (DMSO-d_6, 500.4 MHz) of 2-cyclopropyl-1,3,2-benzodiazaborininone (**2.78**)

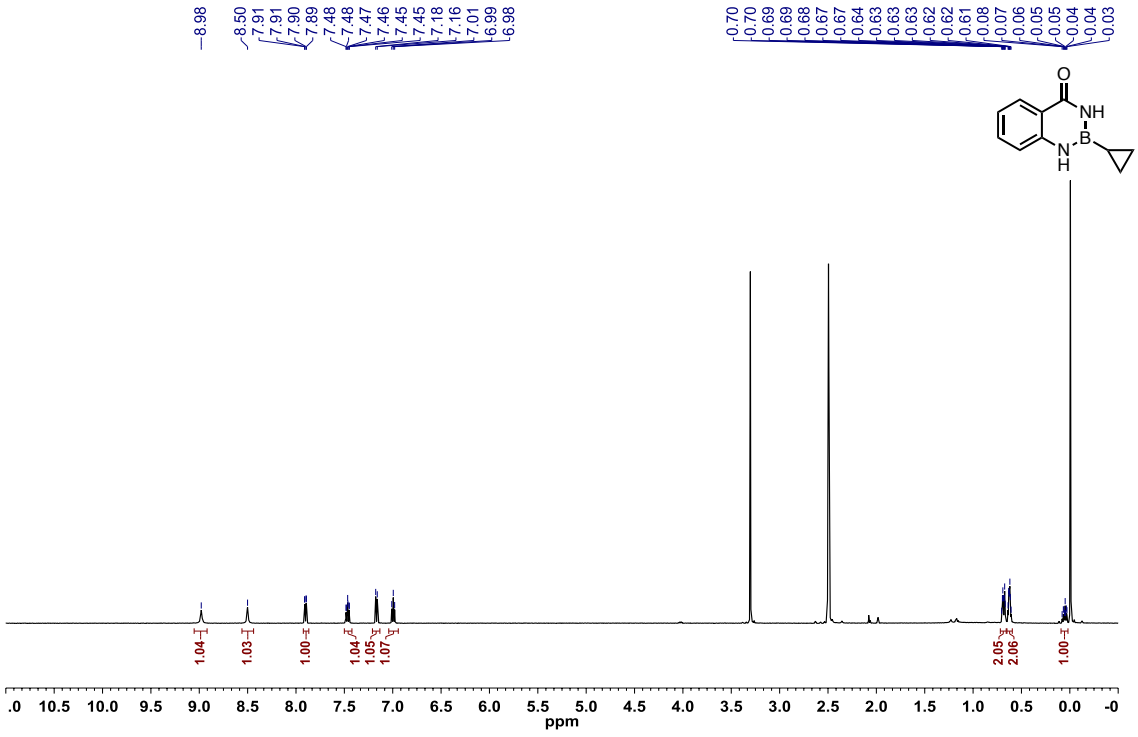

Figure A1.252: ^{13}C {^{1}H} NMR (DMSO-d_6, 125.8 MHz) of 2-cyclopropyl-1,3,2-benzodiazaborininone (**2.78**)

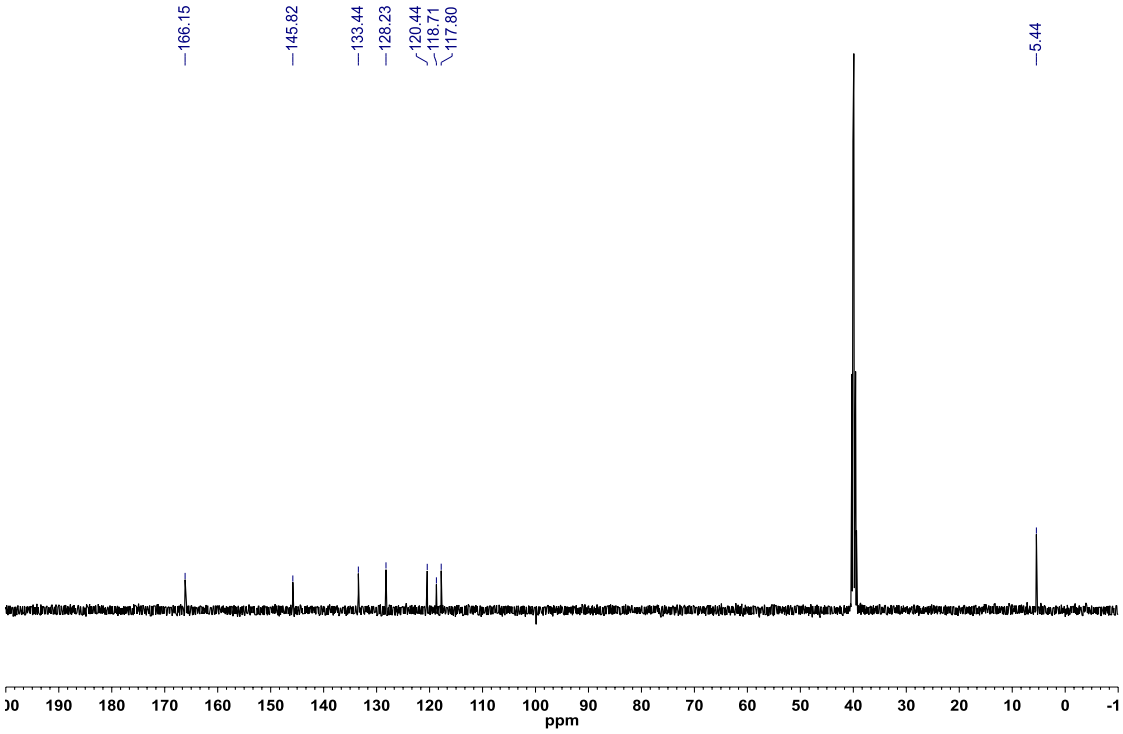

Figure A1.253: ^{11}B NMR (EtOAc, 128.4 MHz) of 2-cyclopropyl-1,3,2-benzodiazaborininone (**2.78**)

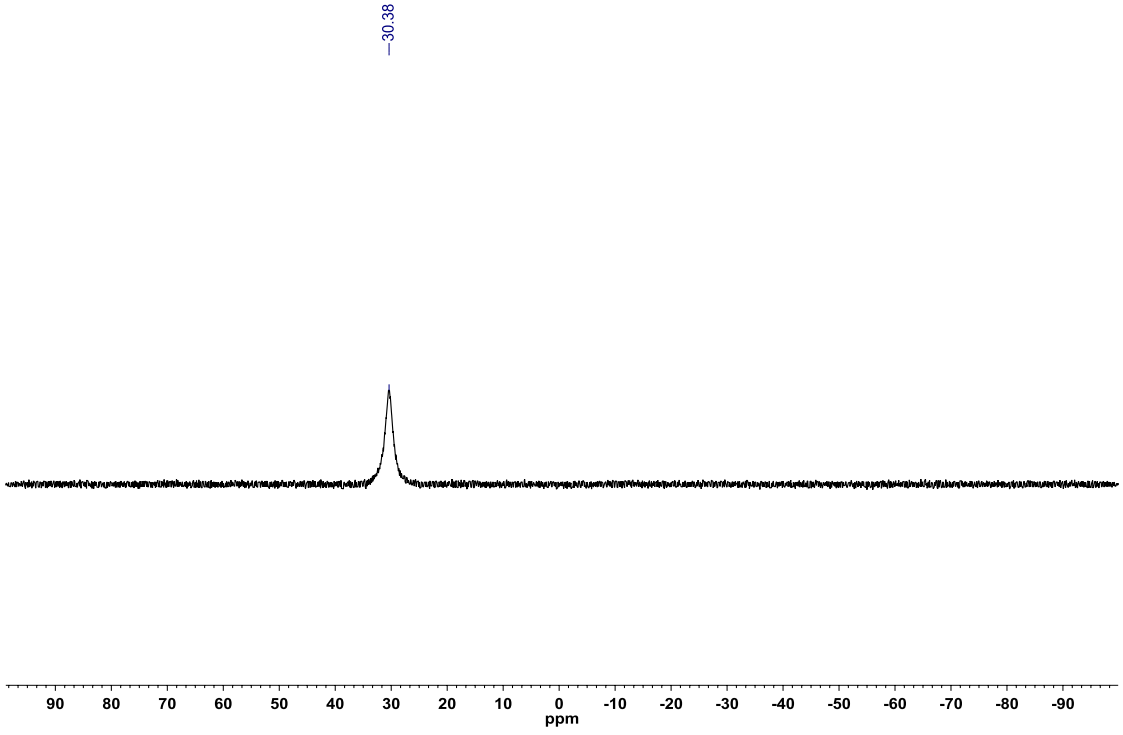

Figure A1.254: ^{1}H NMR ($CDCl_3$, 500.4 MHz) of 2-phenyl-3,1,2-benzoxazaborininone (**2.60**)

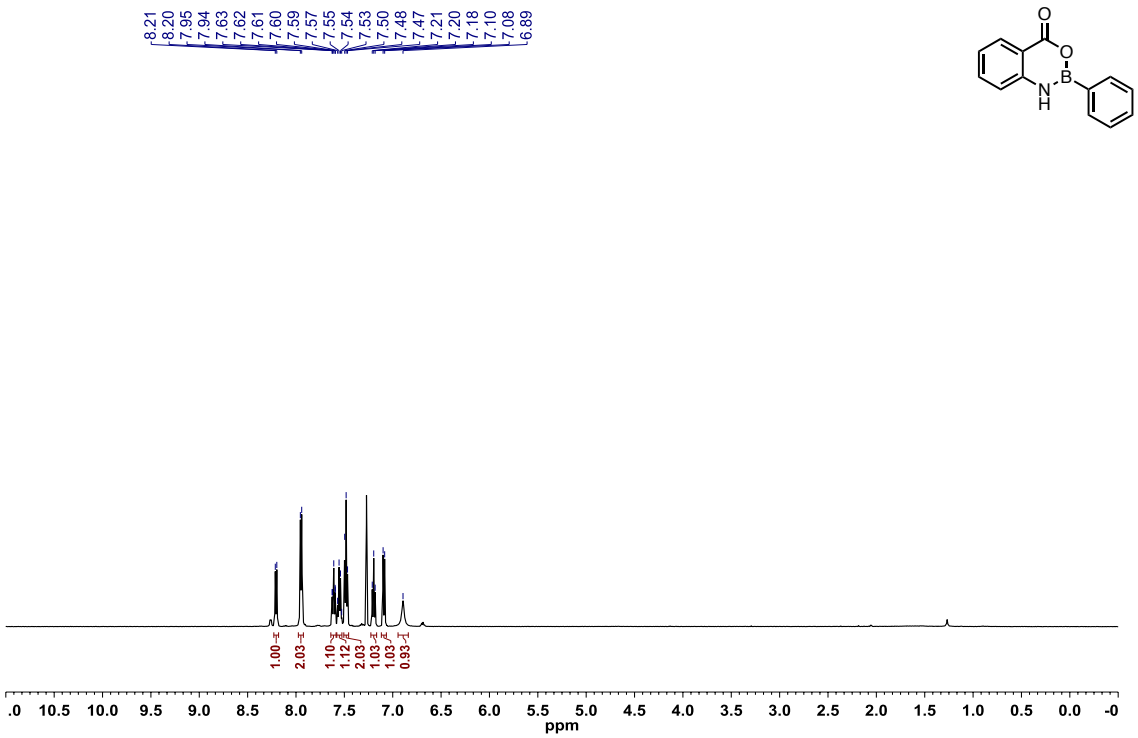

Figure A1.255: ^{13}C {^{1}H} NMR (DMSO-d_6, 125.8 MHz) of 2-phenyl-3,1,2-benzoxazaborininone (**2.60**)

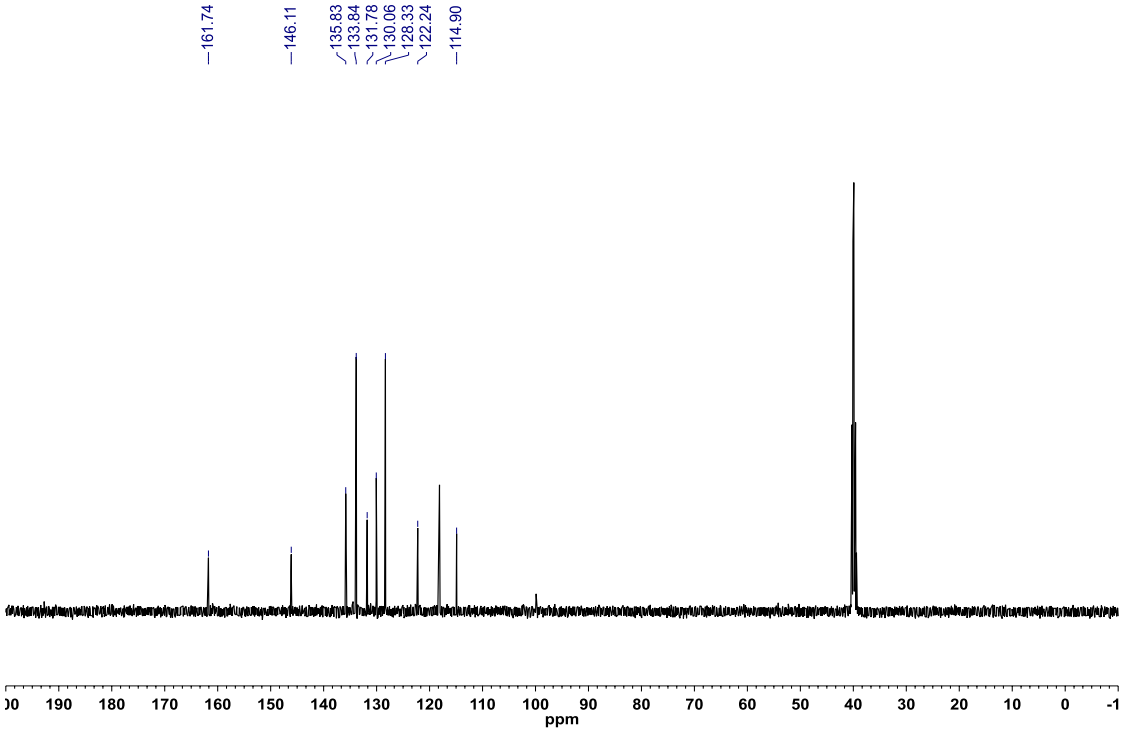

Figure A1.256: ^{11}B NMR ($CDCl_3$, 128.4 MHz) of 2-phenyl-3,1,2-benzoxazaborininone (**2.60**)

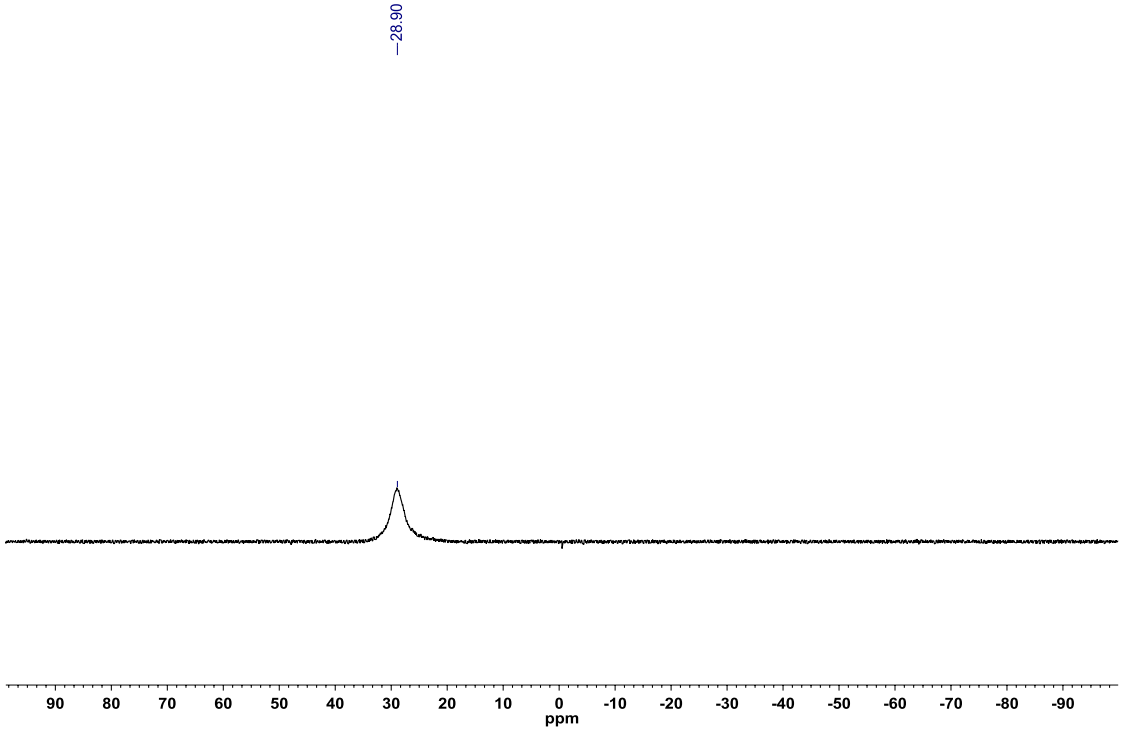

Figure A1.257: ^{1}H NMR (DMSO-d_6, 500.4 MHz) of 2-(*p*-tolyl)-3,1,2-benzoxazaborininone (**2.79**)

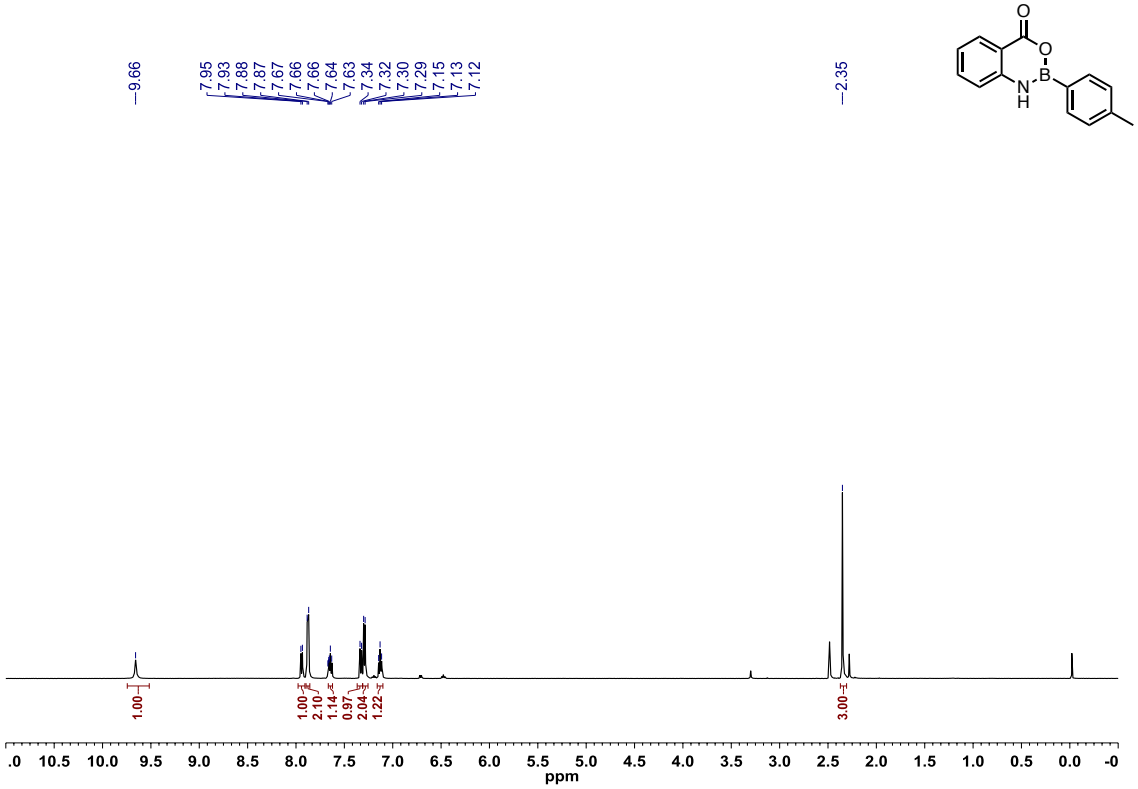

Figure A1.258: ^{13}C {^{1}H} NMR (DMSO-d_6, 125.8 MHz) of 2-(*p*-tolyl)-3,1,2-benzoxazaborininone (**2.79**)

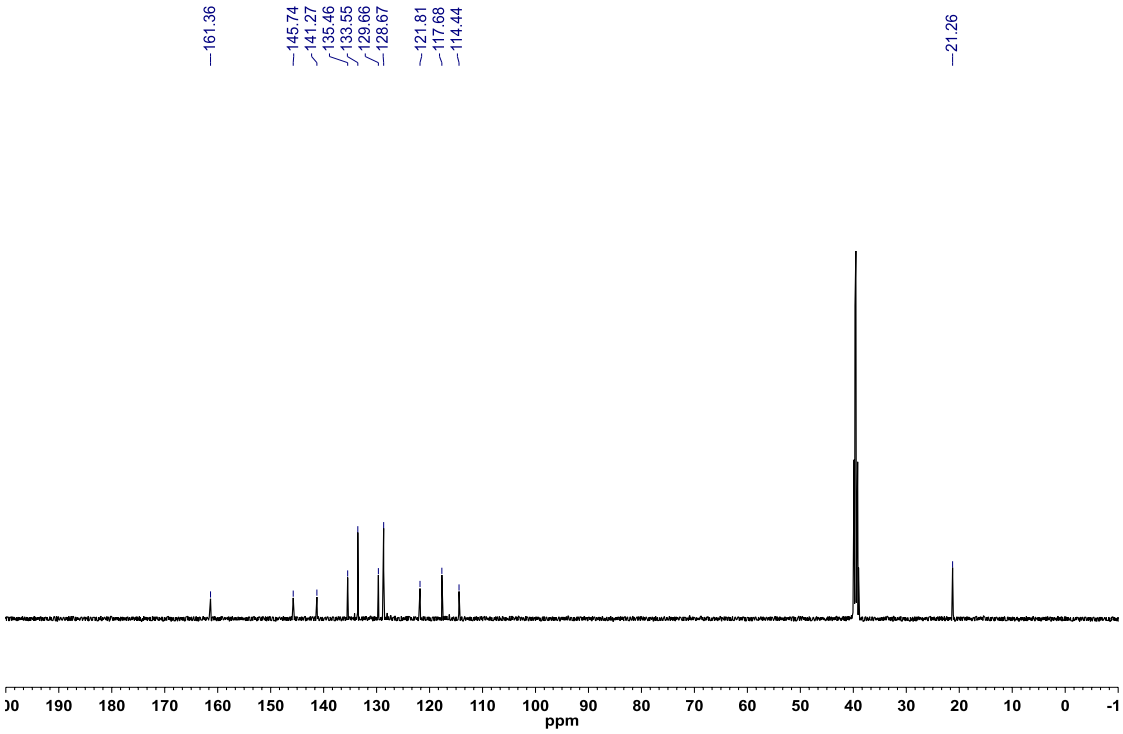

Figure A1.259: ^{11}B NMR (MeCN, 128.4 MHz) of 2-(*p*-tolyl)-3,1,2-benzoxazaborininone (**2.79**)

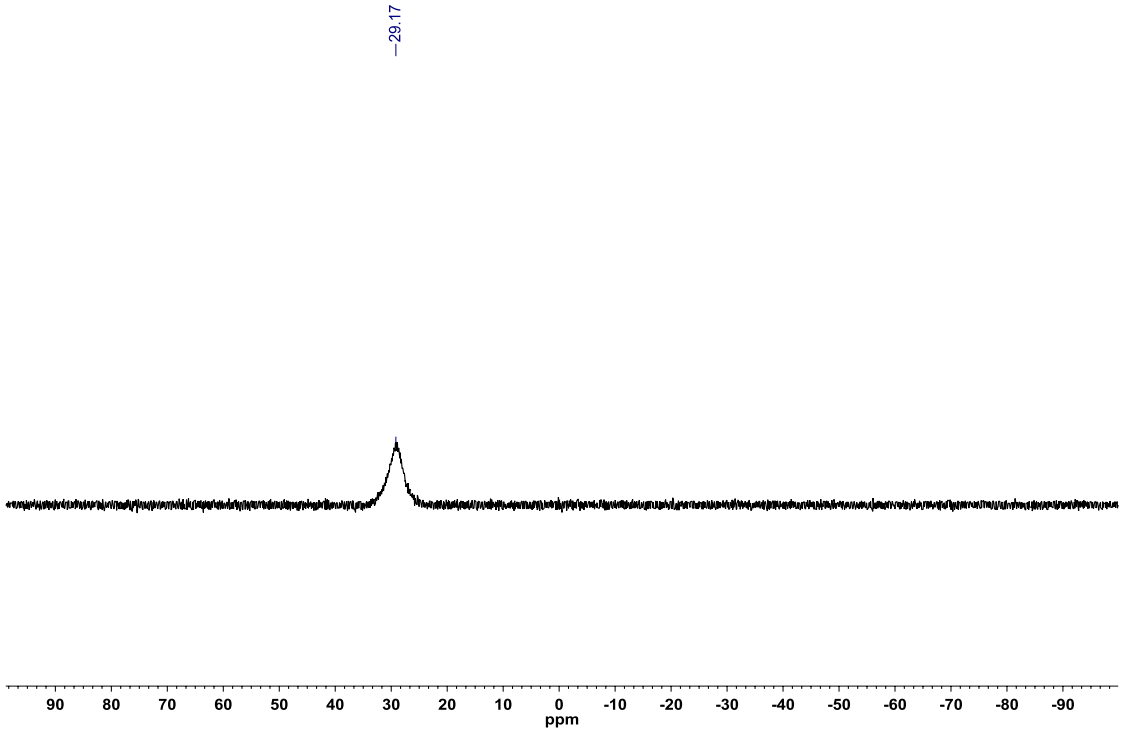

Figure A1.260: ^{1}H NMR ($CDCl_3$, 500.4 MHz) of 2-(4-methoxyphenyl)-3,1,2-benzoxazaborininone (**2.80**)

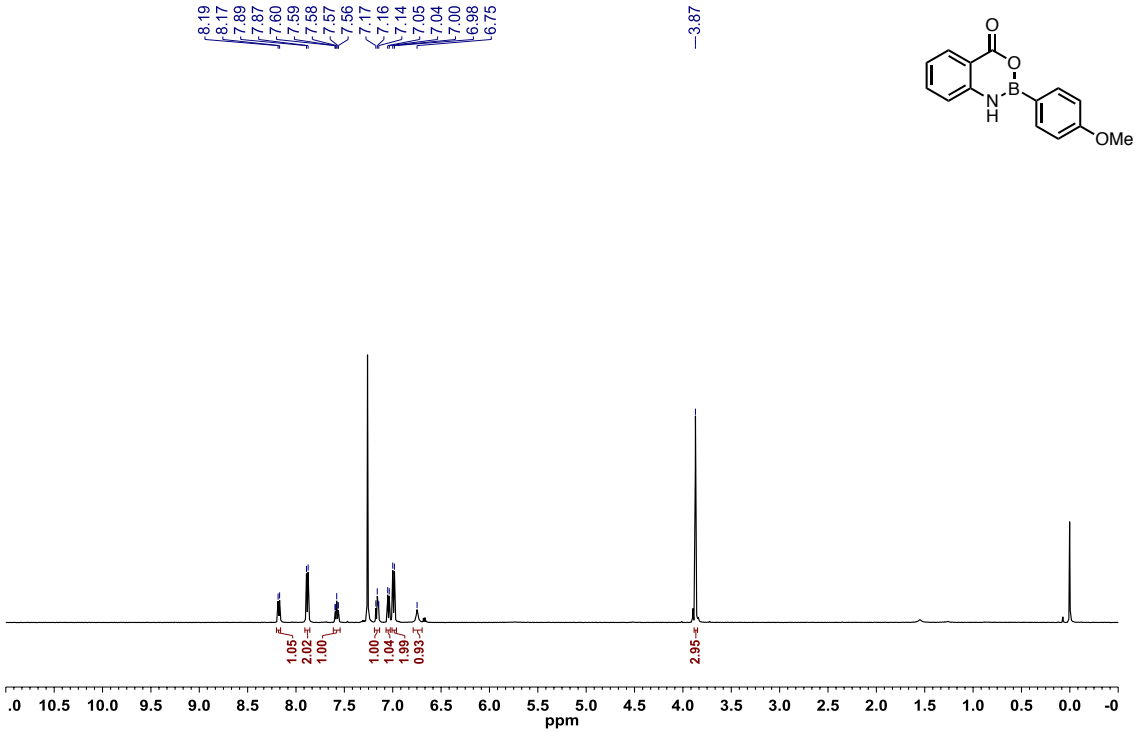

Figure A1.261: ^{13}C {^{1}H} NMR ($CDCl_3$, 125.8 MHz) of 2-(4-methoxyphenyl)-3,1,2-benzoxazaborininone (**2.80**)

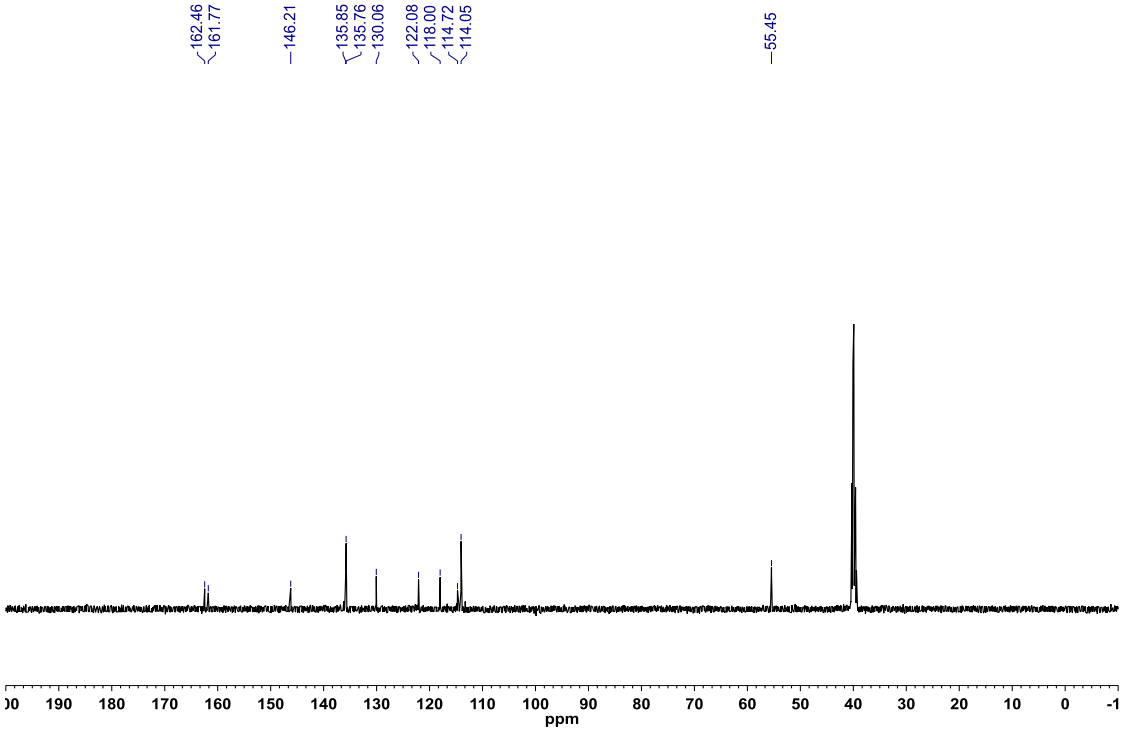

Figure A1.262: ^{11}B NMR ($CDCl_3$, 128.4 MHz) of 2-(4-methoxyphenyl)-3,1,2-benzoxazaborininone (**2.80**)

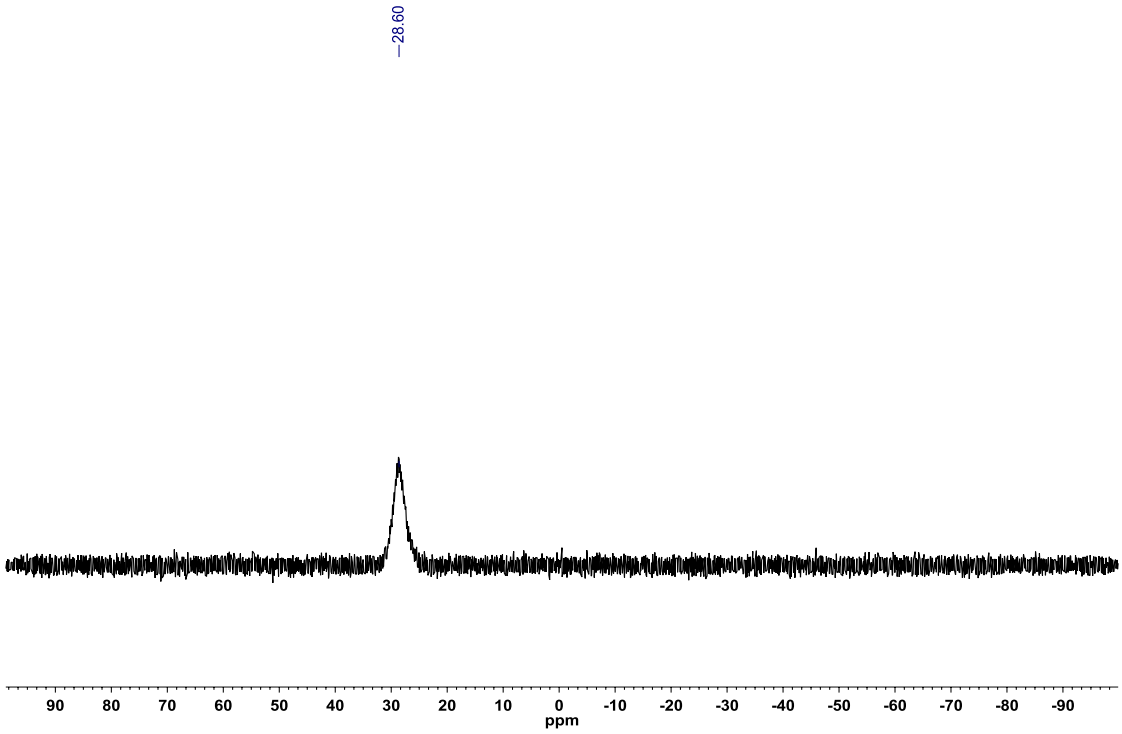

Figure A1.263: ^{1}H NMR (DMSO-d_6, 500.4 MHz) of 2-(4-(trifluoromethyl)phenyl)-3,1,2-benzoxazaborininone (**2.81**)

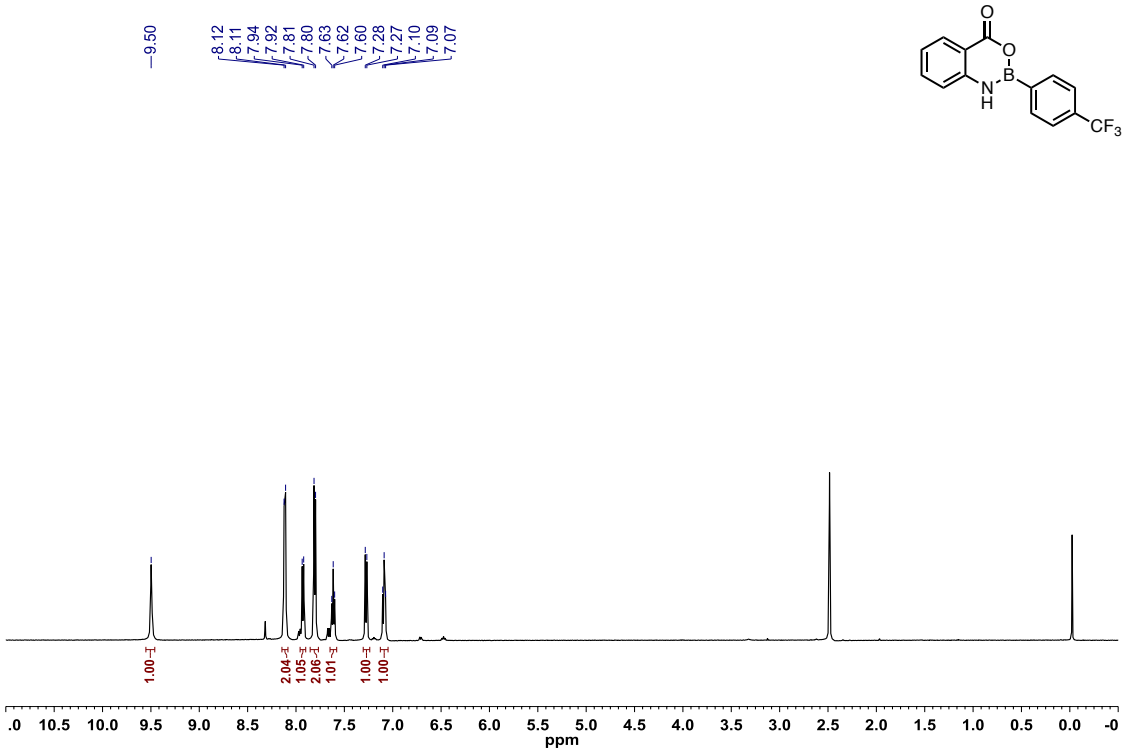

Figure A1.264: ^{13}C NMR (DMSO-d_6, 126 MHz) of 2-(4-(trifluoromethyl)phenyl)-3,1,2-benzoxazaborininone (**2.81**)

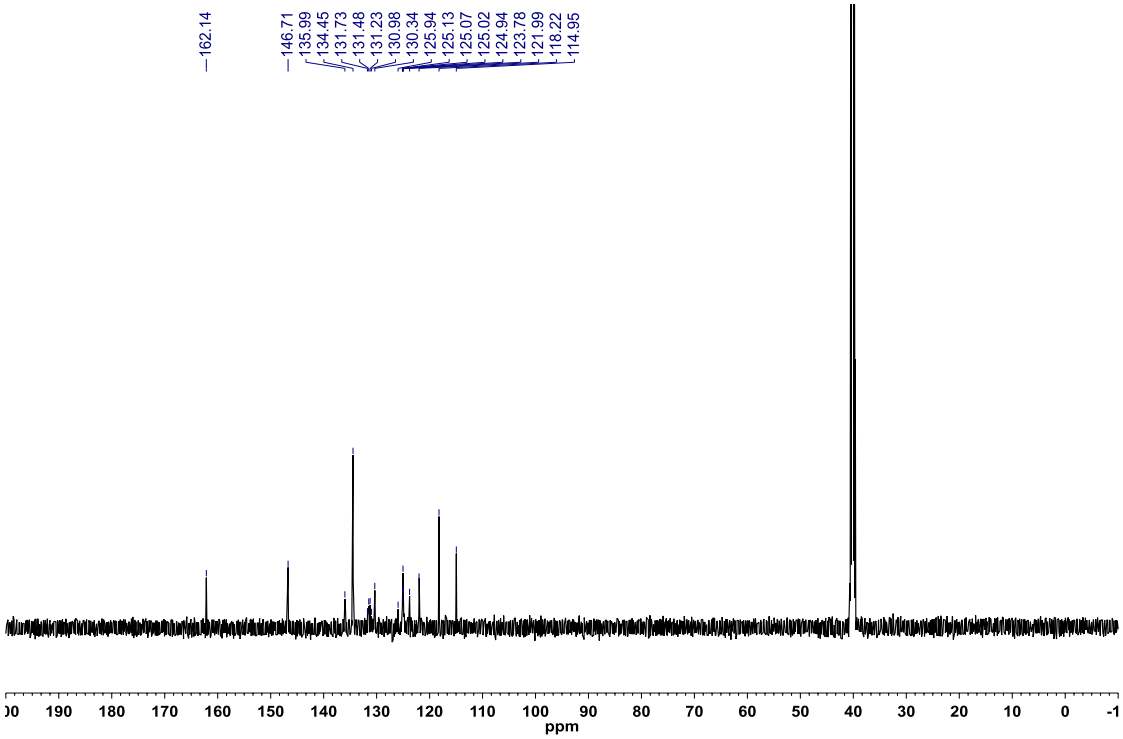

Figure A1.265: ^{19}F {^{1}H} NMR (DMSO-d_6, 470.8 MHz) of 2-(4-(trifluoromethyl)phenyl)-3,1,2-benzoxazaborininone (**2.81**)

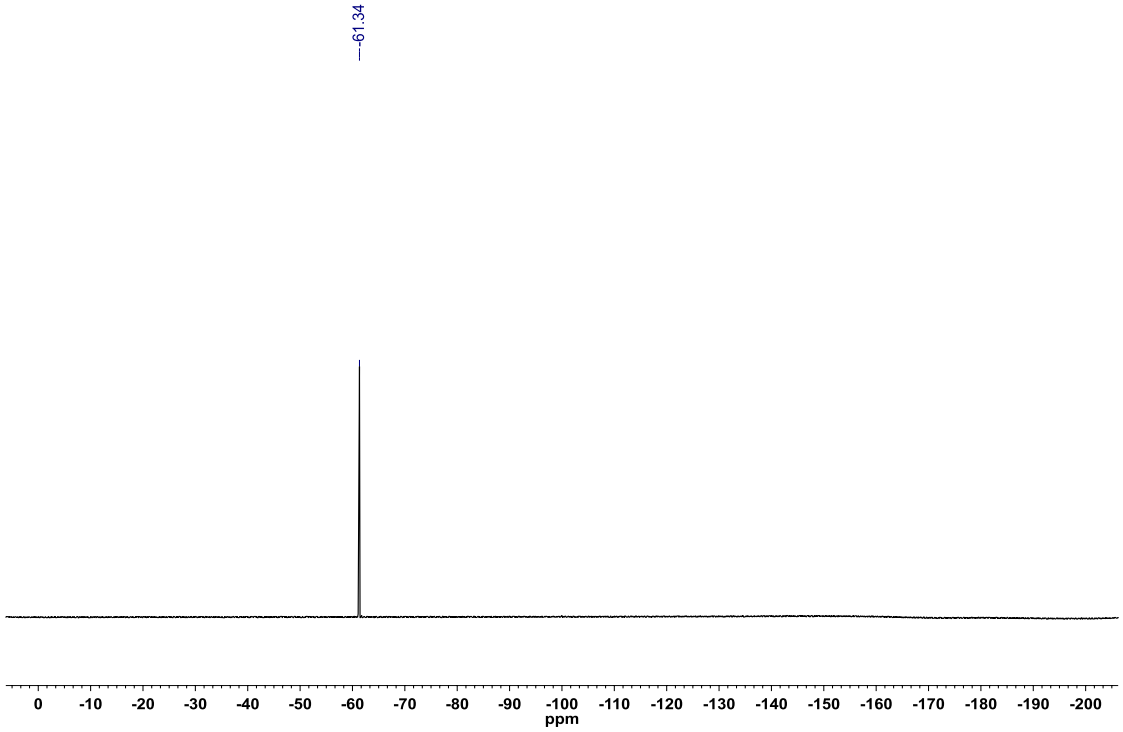

Figure A1.266: ^{11}B NMR (EtOAc, 128.4 MHz) of 2-(4-(trifluoromethyl)phenyl)-3,1,2-benzoxazaborininone (**2.81**)

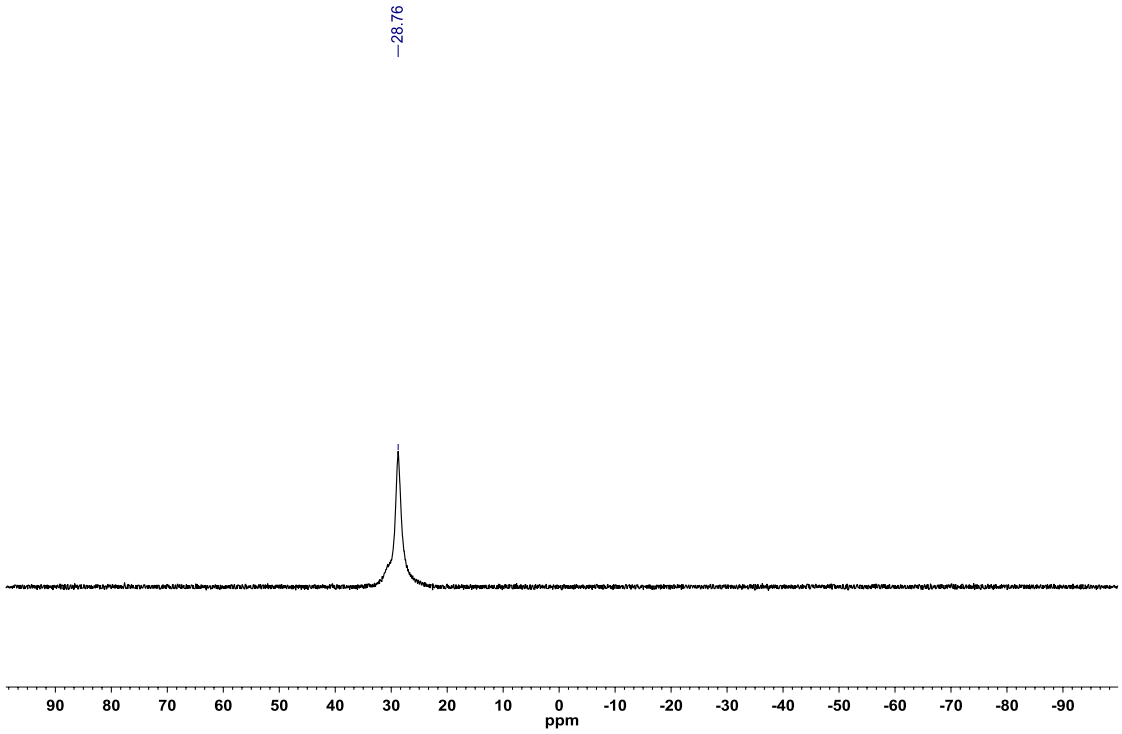

Figure A1.267: ^{1}H NMR (DMSO-d_6, 500.4 MHz) 2-(4-acetylphenyl)-3,1,2-benzoxazaborininone (**2.82**)

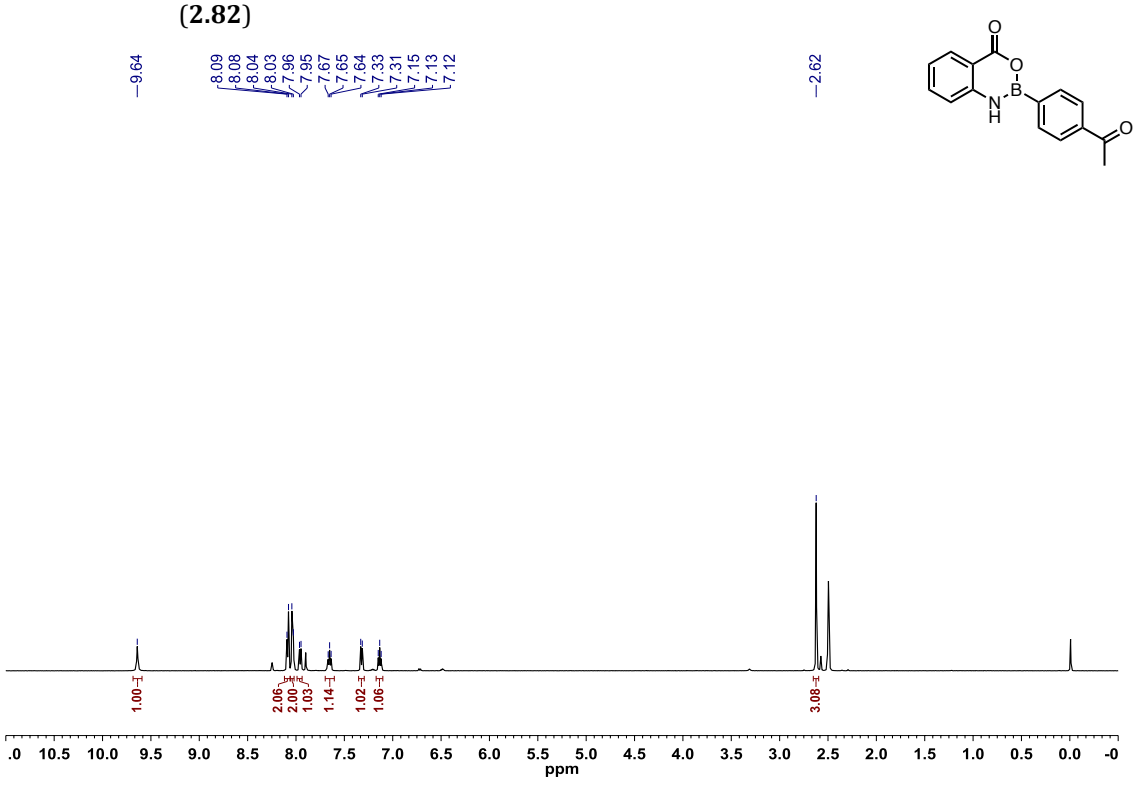

Figure A1.268: ^{13}C {^{1}H} NMR (DMSO-d_6, 125.8 MHz) 2-(4-acetylphenyl)-3,1,2-benzoxazaborininone (**2.82**)

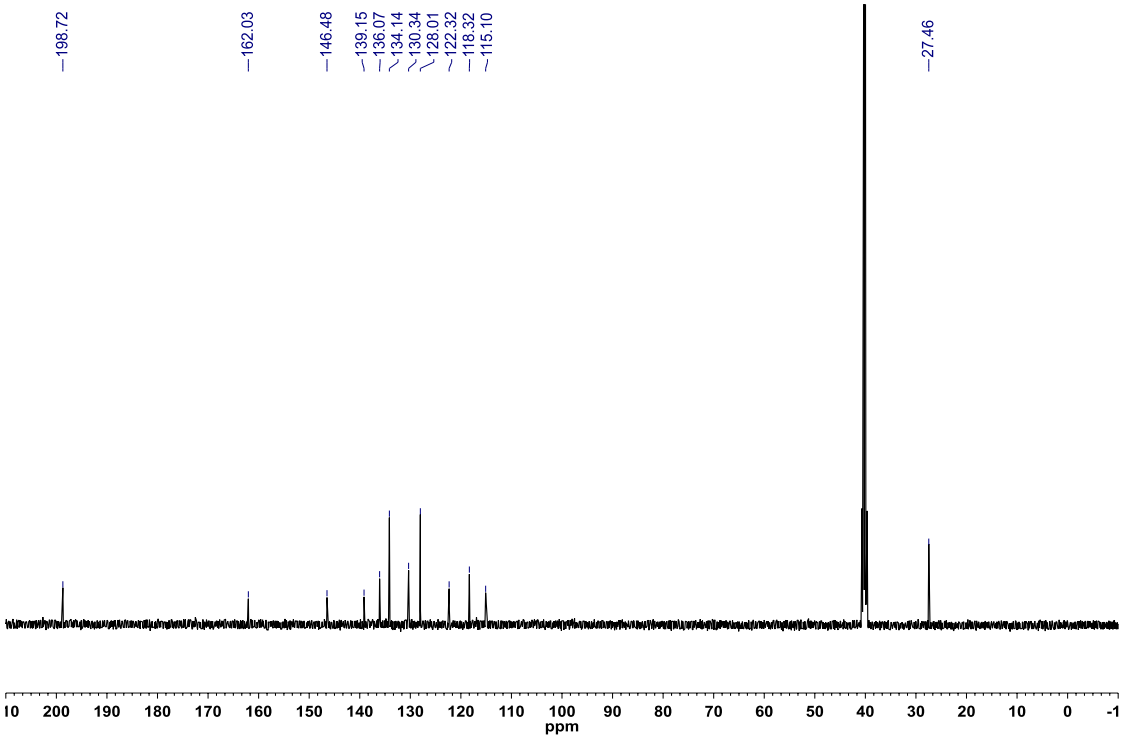

Figure A1.269: ^{11}B NMR (acetone-d_6, 128 MHz) 2-(4-acetylphenyl)-3,1,2-benzoxazaborininone (**2.82**)

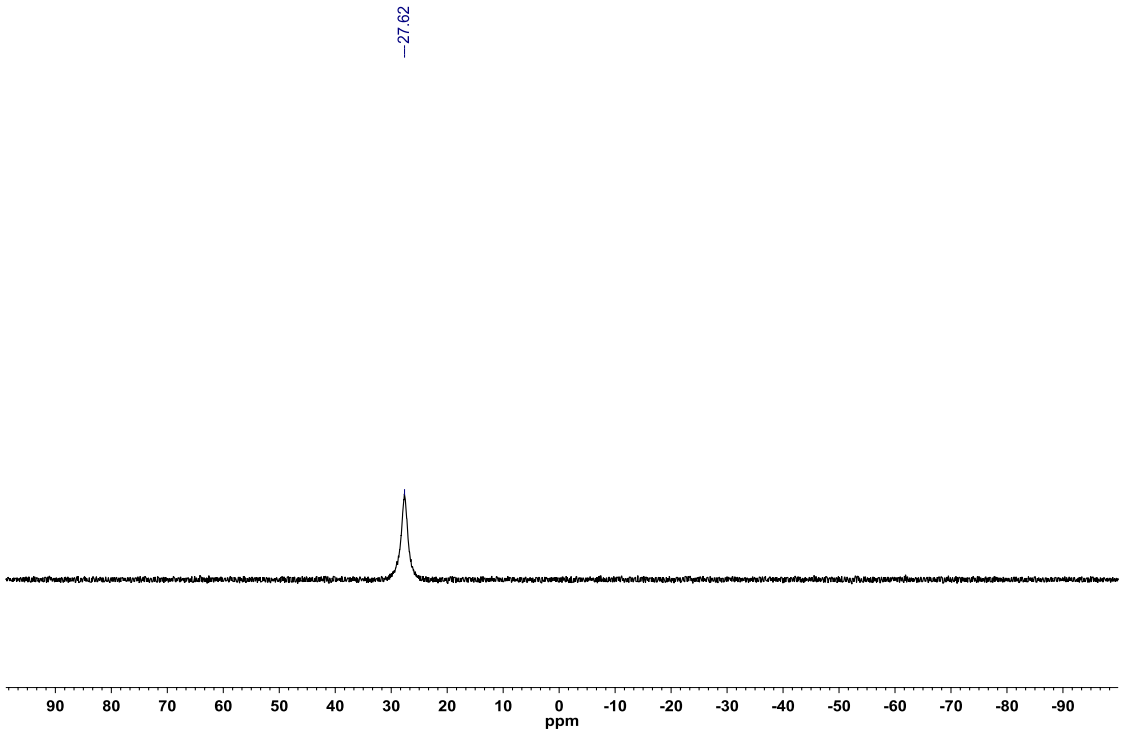

Figure A1.270: ^{1}H NMR (DMSO-d_6, 500.4 MHz) of 2-(3-cyanophenyl)-3,1,2-benzoxazaborininone (**2.83**)

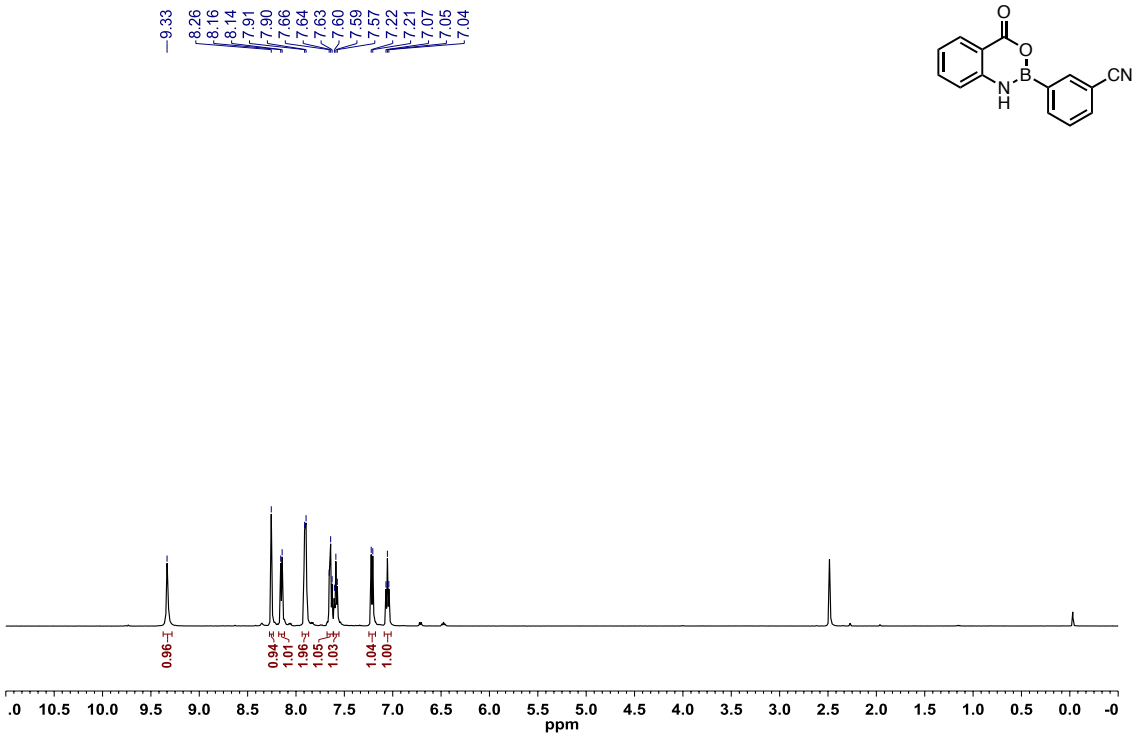

Figure A1.271: ^{13}C {^{1}H} NMR (DMSO-d_6, 125.8 MHz) of 2-(3-cyanophenyl)-3,1,2-benzoxazaborininone (**2.83**)

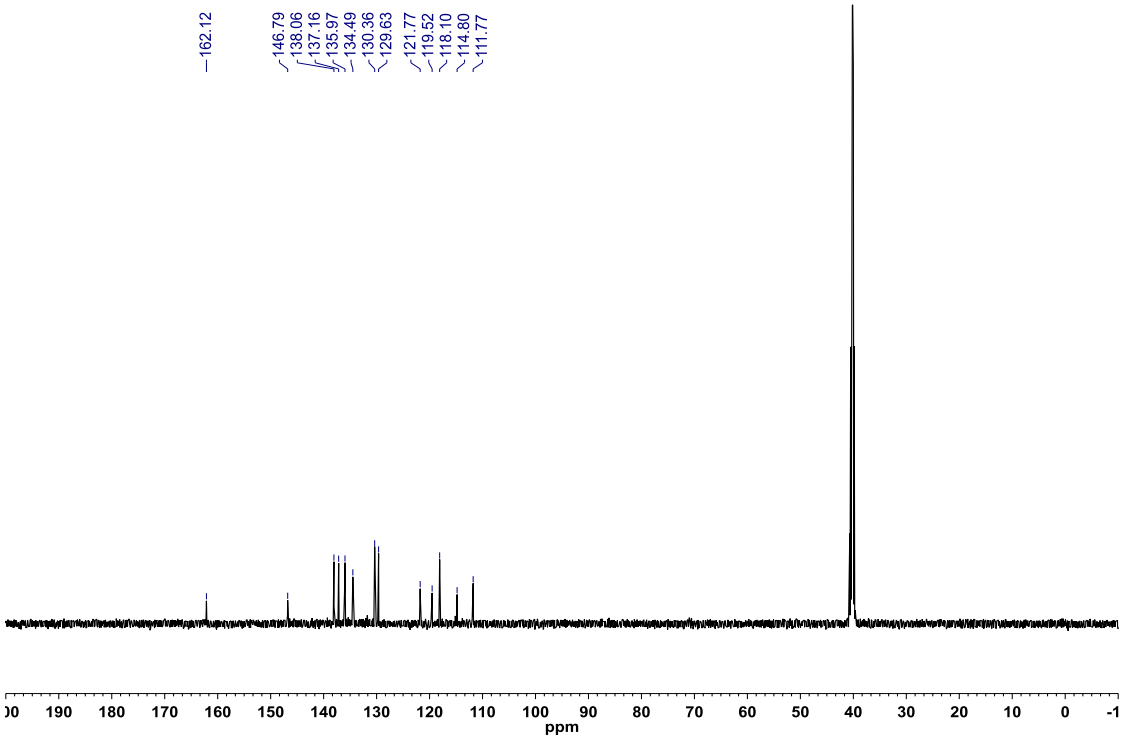

Figure A1.272: ^{11}B NMR (acetone-d_6, 128 MHz) of 2-(3-cyanophenyl)-3,1,2-benzoxazaborininone (**2.83**)

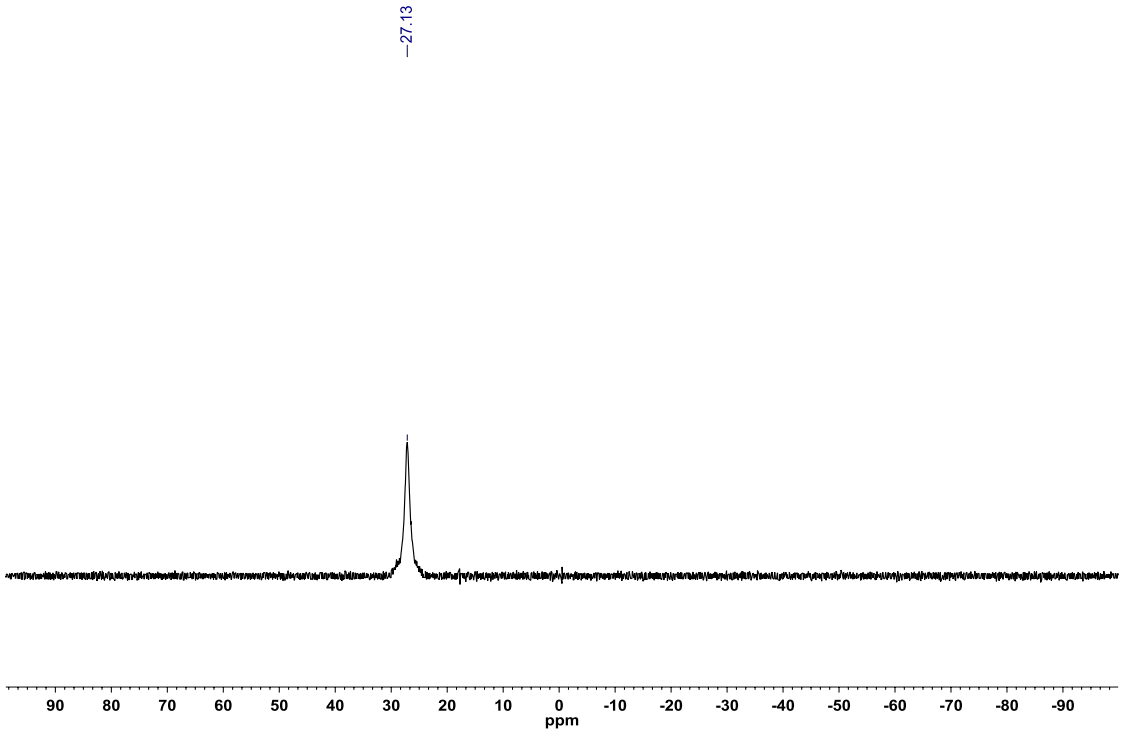

Figure A1.273: ^{1}H NMR (DMSO-d_6, 500.4 MHz) of 2-(2-nitrophenyl)-3,1,2-benzoxazaborininone (**2.84**)

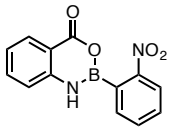

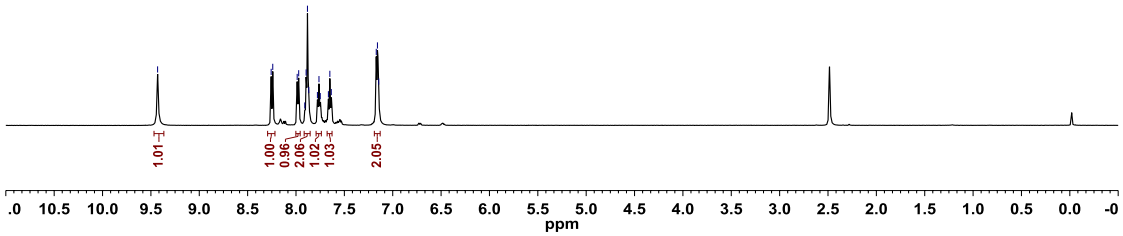

Figure A1.274: ^{13}C {^{1}H} NMR (DMSO-d_6, 125.8 MHz) of 2-(2-nitrophenyl)-3,1,2-benzoxazaborininone (**2.84**)

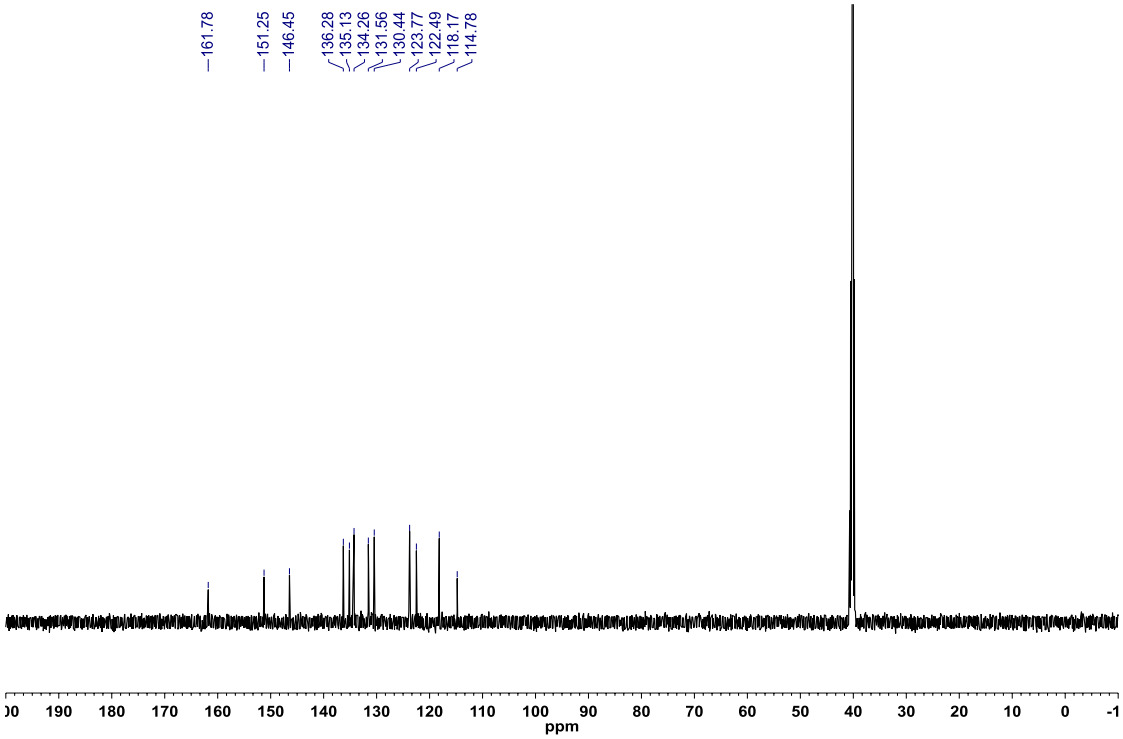

Figure A1.275: ^{11}B NMR (methanol-d_4, 128 MHz) of 2-(2-nitrophenyl)-3,1,2-benzoxazaborininone (**2.84**)

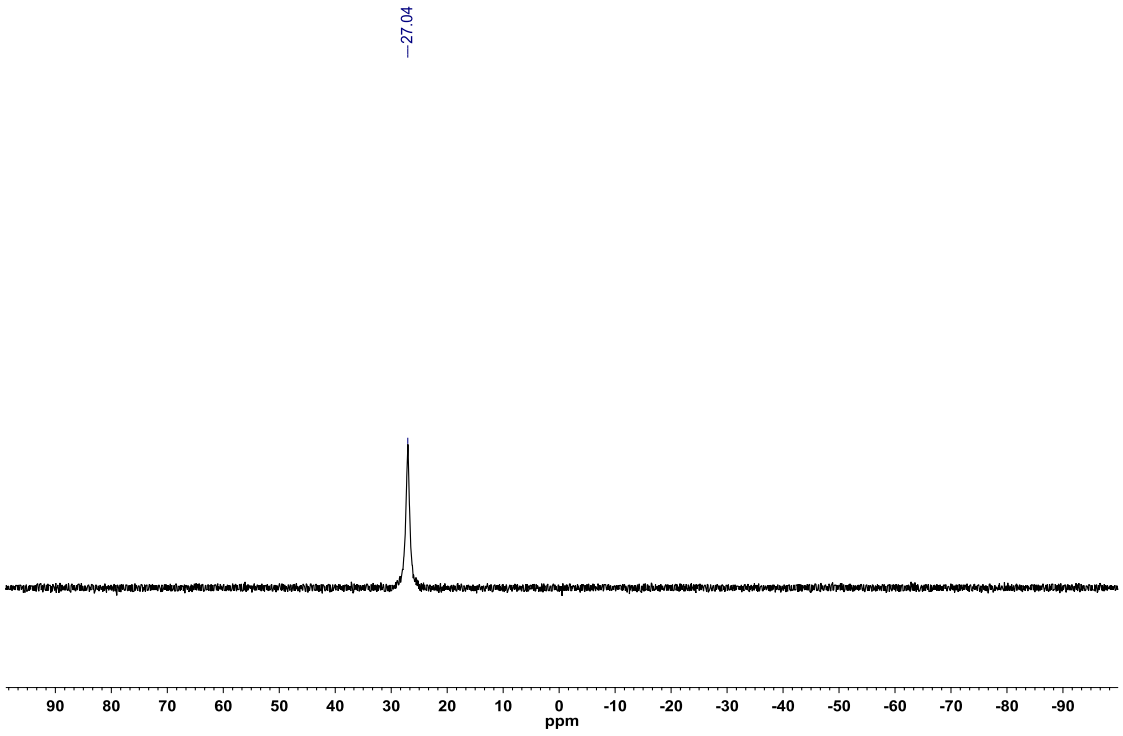

Figure A1.276: ^{1}H NMR ($CDCl_3$, 500.4 MHz) of 2-(thiophen-3-yl)-3,1,2-benzoxazaborininone (**2.85**)

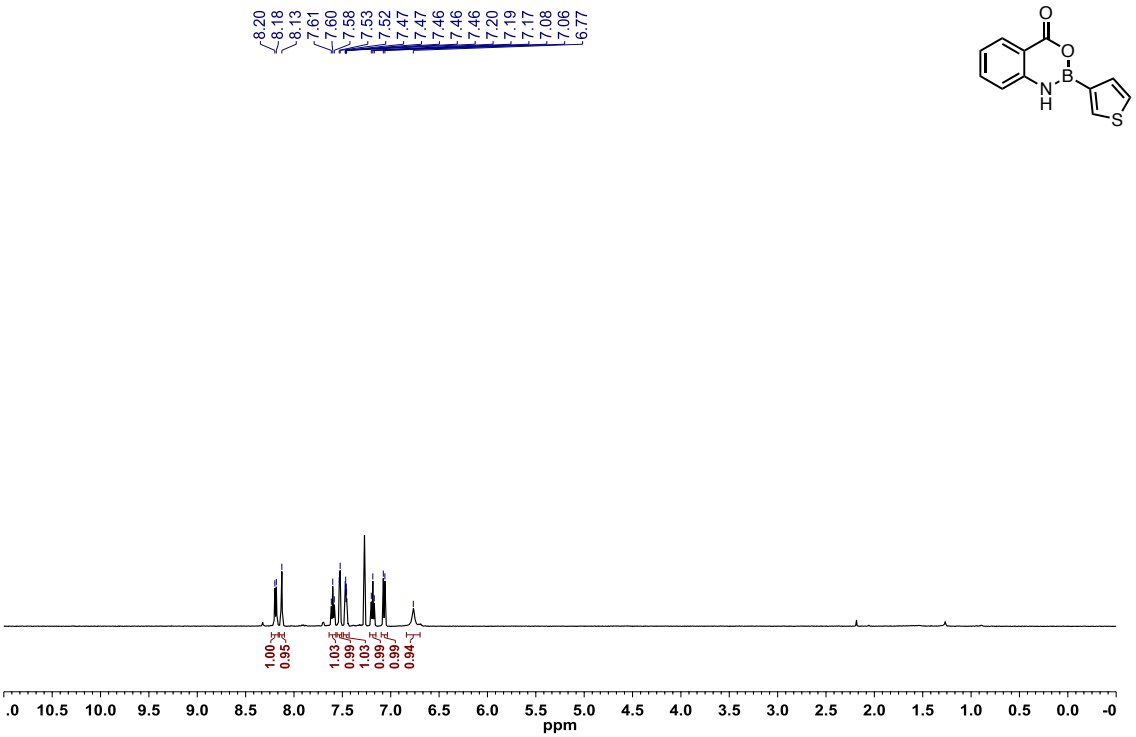

Figure A1.277: ^{13}C {^{1}H} NMR (DMSO-d_6, 125.8 MHz) of 2-(thiophen-3-yl)-3,1,2-benzoxazaborininone (**2.85**)

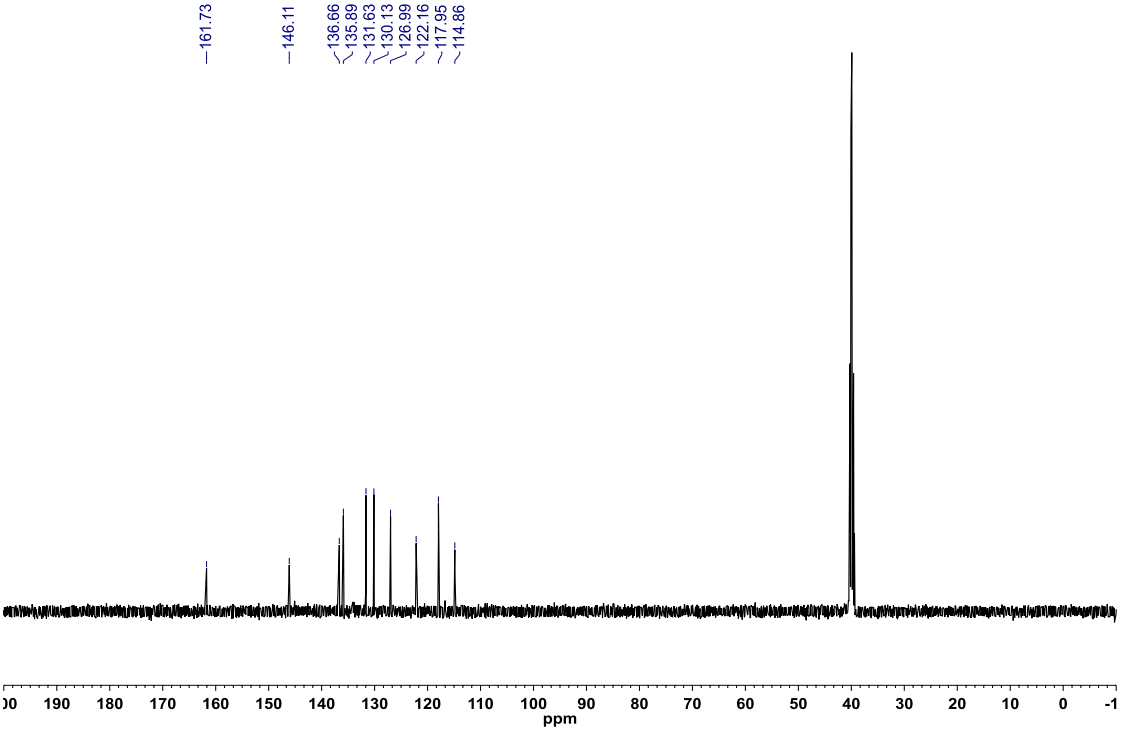

Figure A1.278: ^{11}B NMR ($CDCl_3$, 128.4 MHz) of 2-(thiophen-3-yl)-3,1,2-benzoxazaborininone (**2.85**)

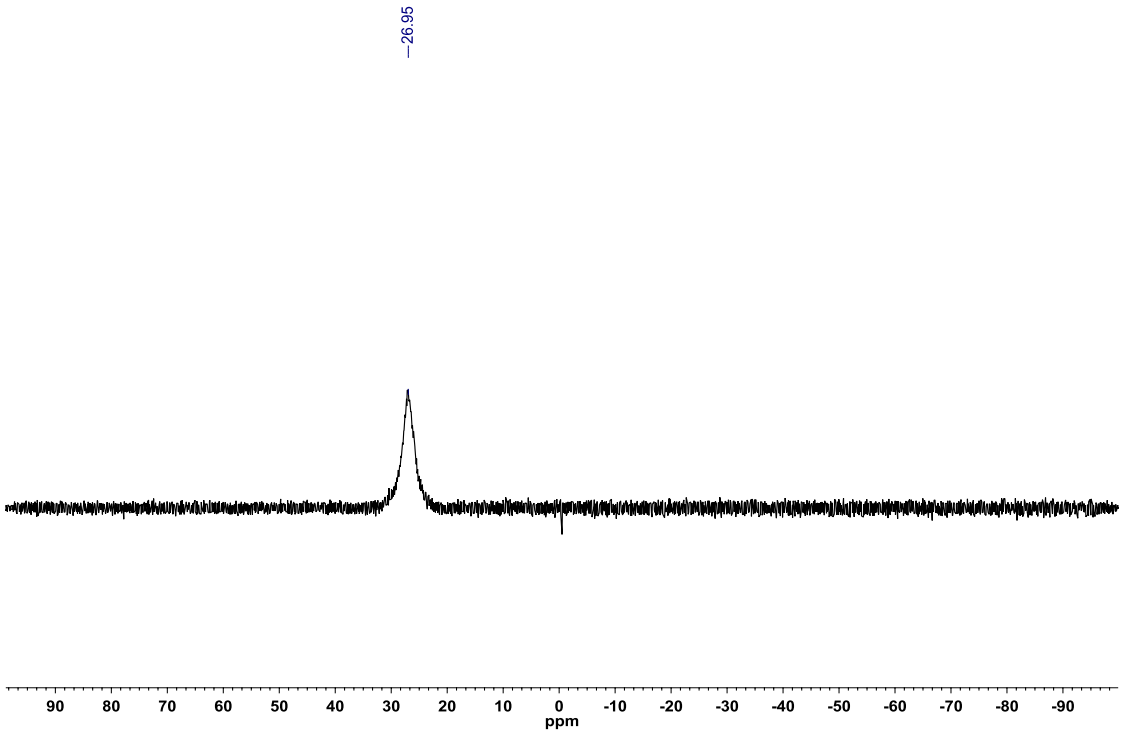

Figure A1.279: ^{1}H NMR (DMSO-d_6, 500.4 MHz) of 2-(1-methyl-1H-indol-5-yl)-3,1,2-benzoxazaborininone (**2.86**)

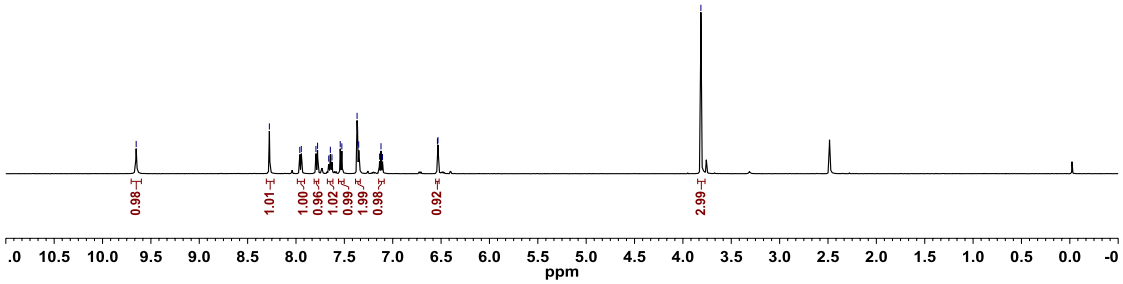

Figure A1.280: ^{13}C {^{1}H} NMR (DMSO-d_6, 125.8 MHz) of 2-(1-methyl-1H-indol-5-yl)-3,1,2-benzoxazaborininone (**2.86**)

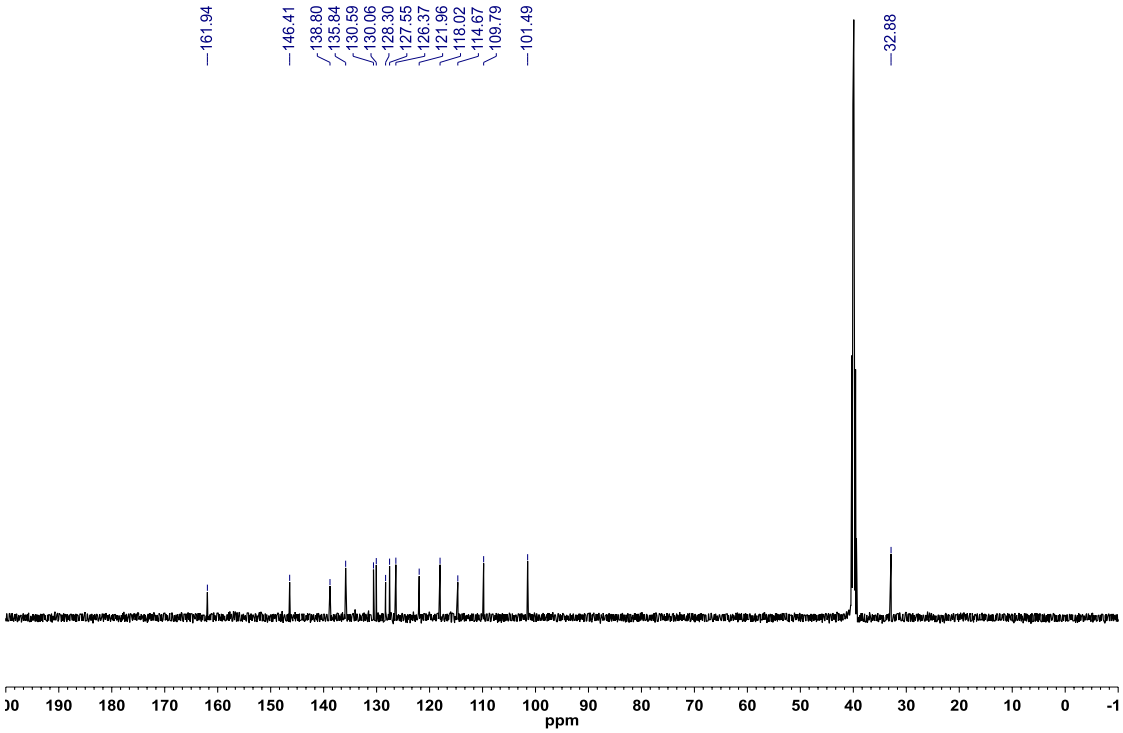

Figure A1.281: ^{11}B NMR (acetone-d_6, 128 MHz) of 2-(1-methyl-1H-indol-5-yl)-3,1,2-benzoxazaborininone (**2.86**)

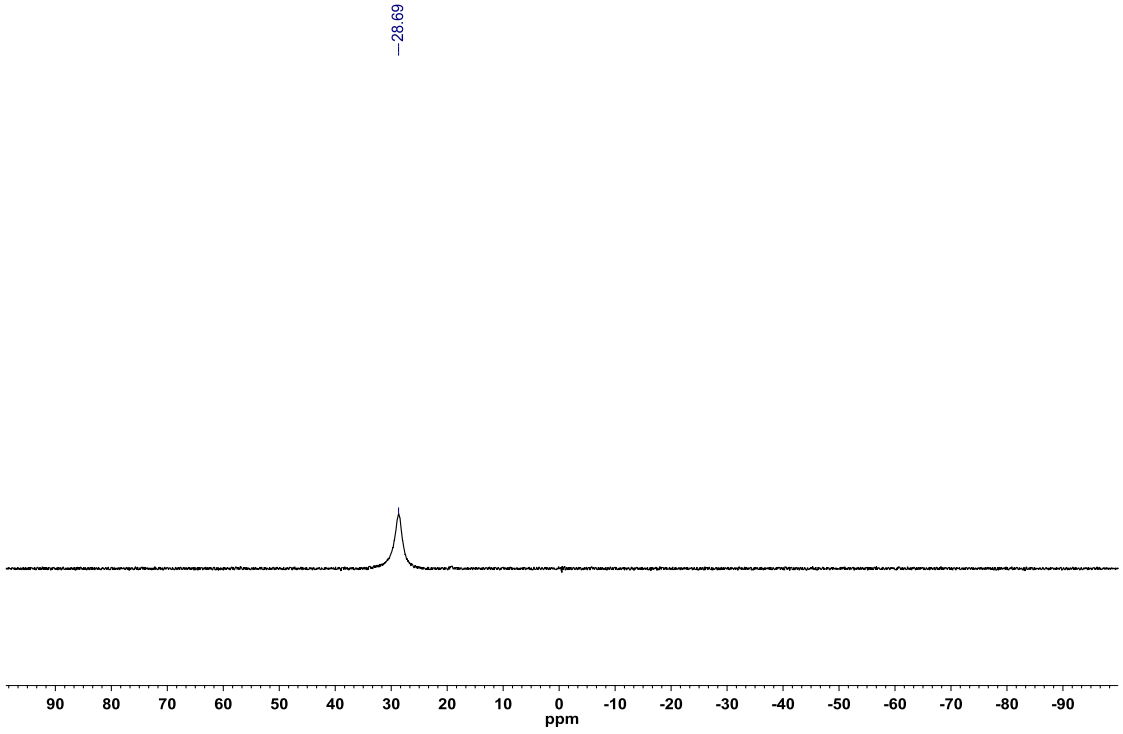

Figure A1.282: ^{1}H NMR ($CDCl_3$, 500.4 MHz) of 2-vinyl-3,1,2-benzoxazaborininone (**2.87**)

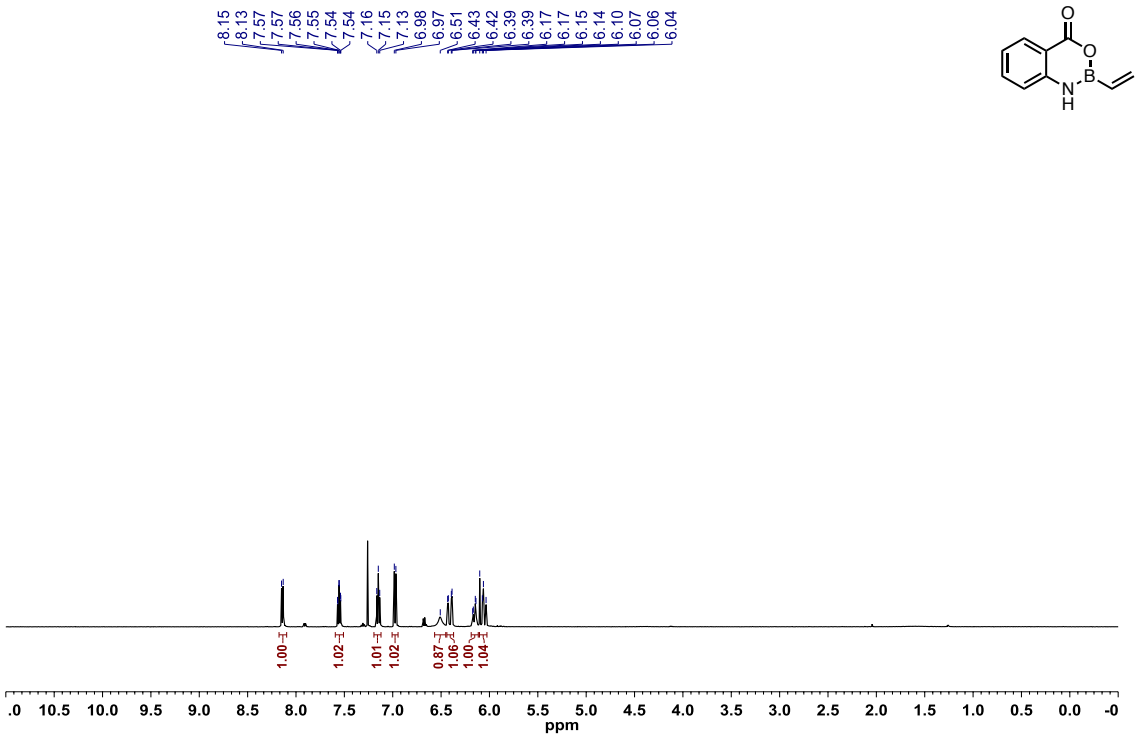

Figure A1.283: ^{13}C {^{1}H} NMR ($CDCl_3$, 125.8 MHz) of 2-vinyl-3,1,2-benzoxazaborininone (**2.87**)

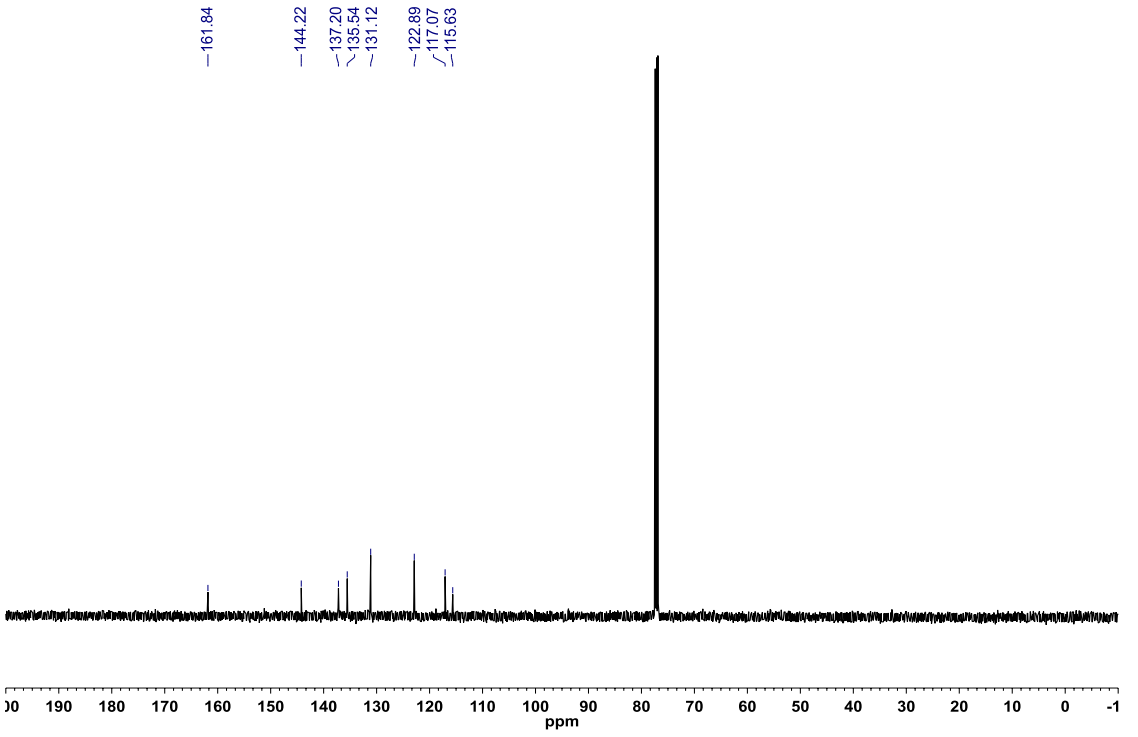

Figure A1.284: ^{11}B NMR ($CDCl_3$, 128.4 MHz) of 2-vinyl-3,1,2-benzoxazaborininone (**2.87**)

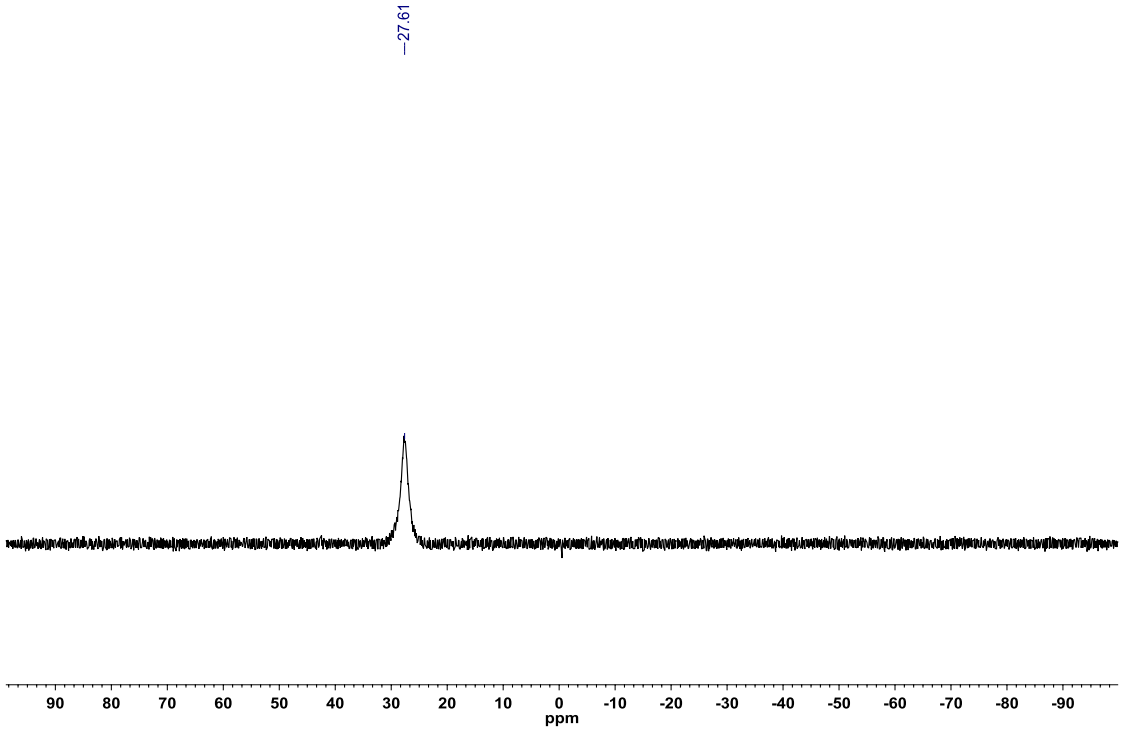

Figure A1.285: ^{1}H NMR ($CDCl_3$, 500.4 MHz) of 2-phenethyl-3,1,2-benzoxazaborininone (**2.88**)

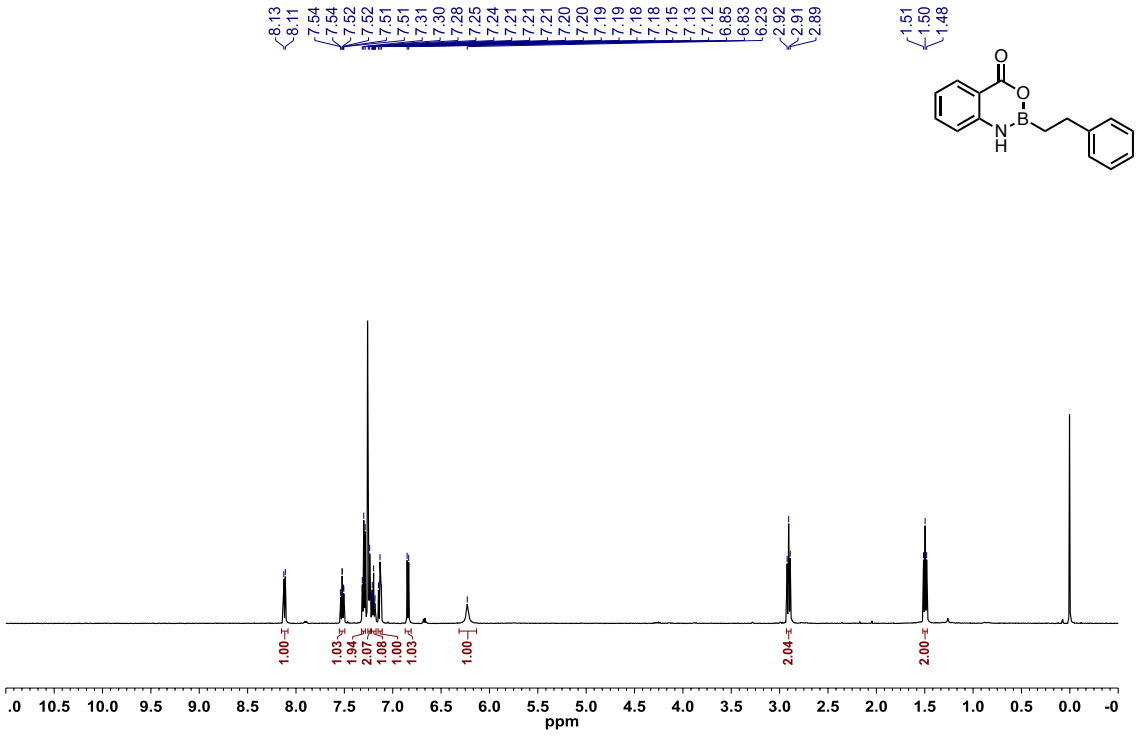

Figure A1.286: ^{13}C {^{1}H} NMR ($CDCl_3$, 125.8 MHz) of 2-phenethyl-3,1,2-benzoxazaborininone (**2.88**)

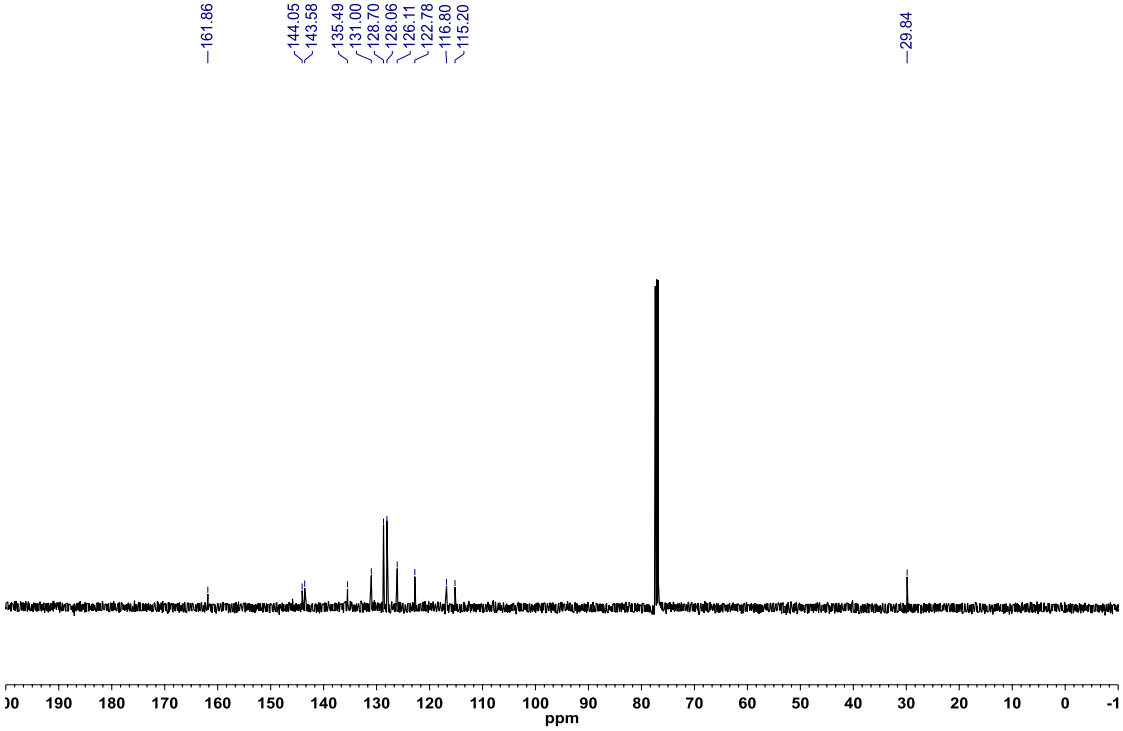

Figure A1.287: ^{11}B NMR ($CDCl_3$, 128.4 MHz) of 2-phenethyl-3,1,2-benzoxazaborininone (**2.88**)

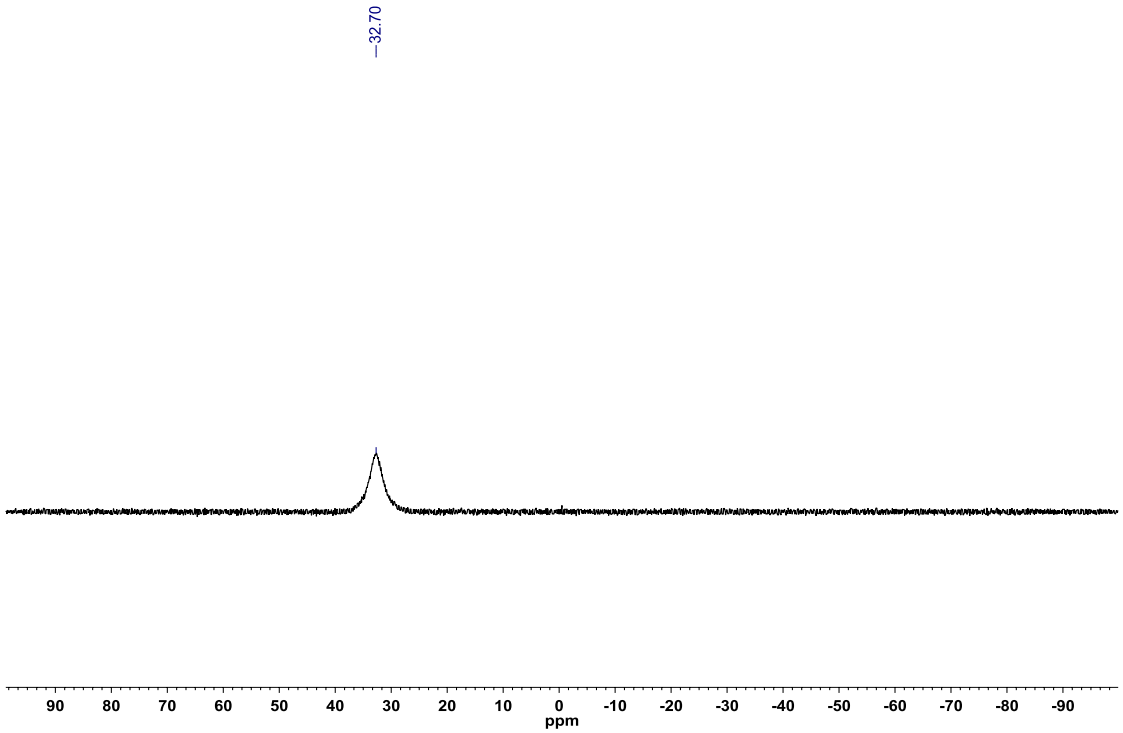

Figure A1.288: ^{1}H NMR ($CDCl_3$, 500.4 MHz) of 2-cyclopropyl-3,1,2-benzoxazaborininone (**2.89**)

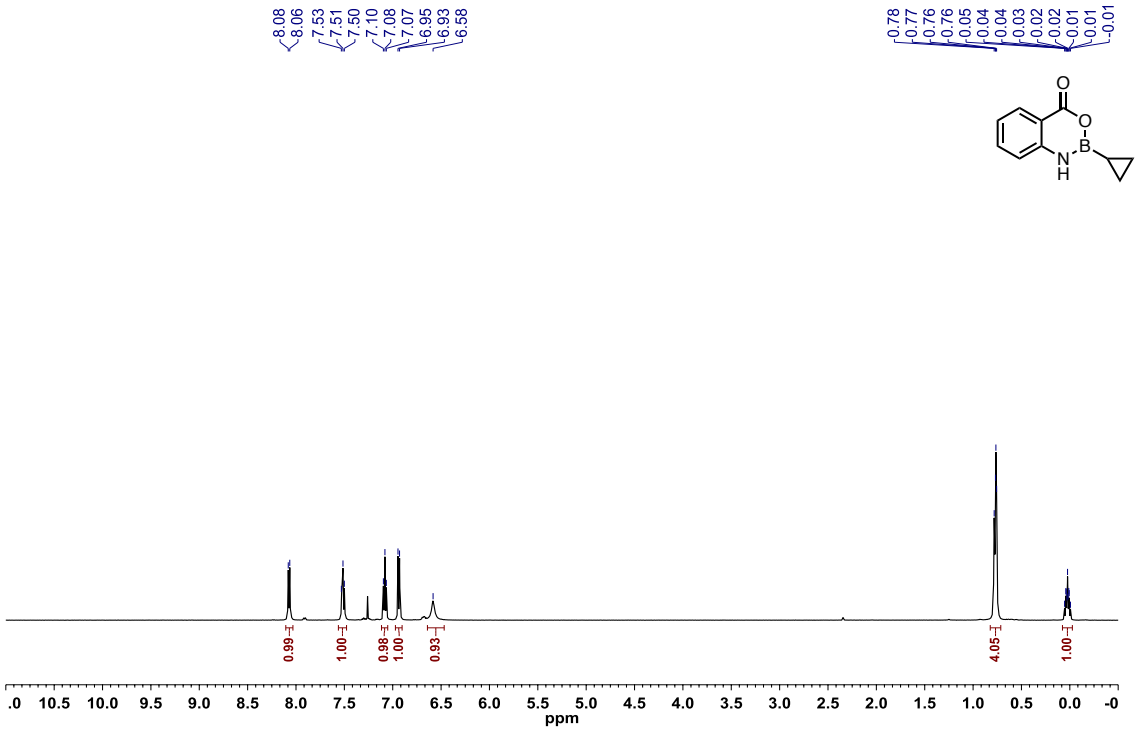

Figure A1.289: ^{13}C {^{1}H} NMR ($CDCl_3$, 125.8 MHz) of 2-cyclopropyl-3,1,2-benzoxazaborininone (**2.89**)

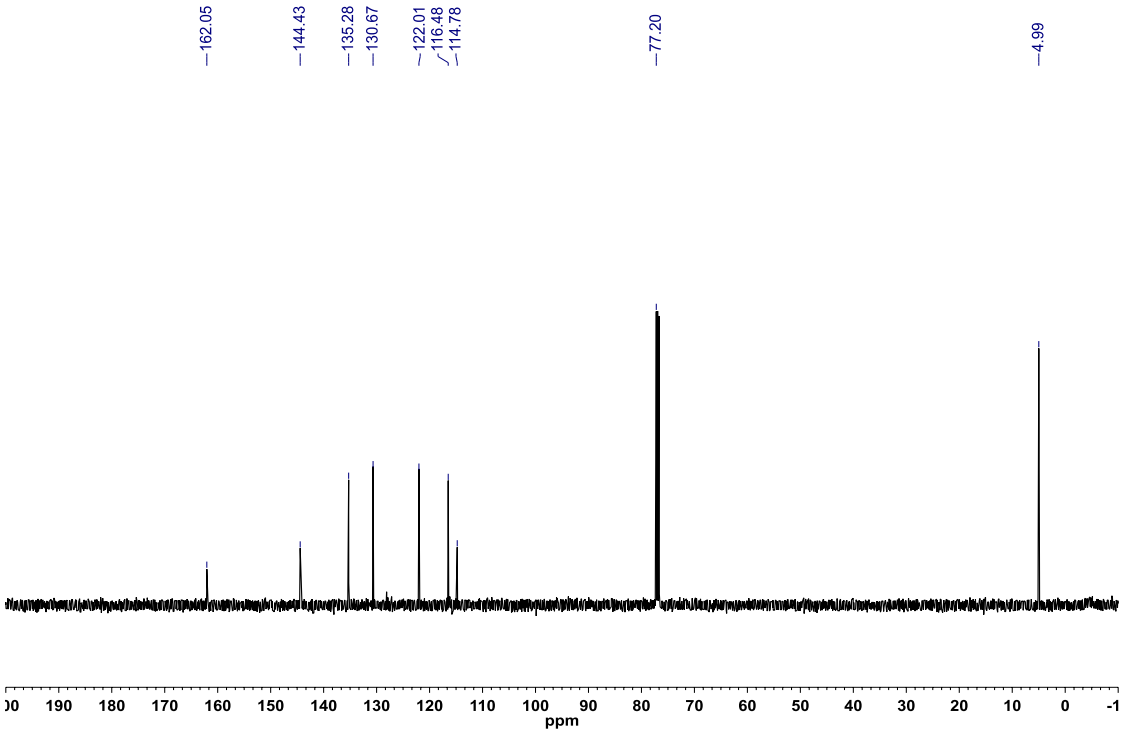

Figure A1.290: ^{11}B NMR ($CDCl_3$, 128.4 MHz) of 2-cyclopropyl-3,1,2-benzoxazaborininone (**2.89**)

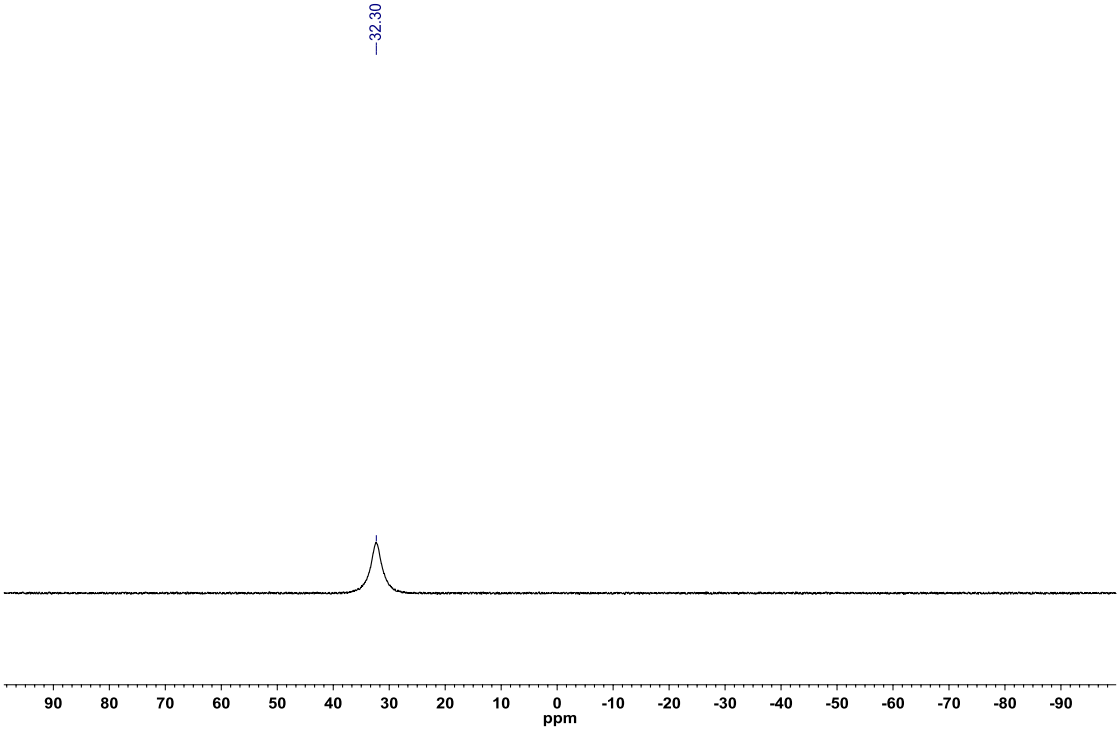

Figure A1.291: ^{1}H NMR ($CDCl_3$, 500.4 MHz) of 2-phenyl-1,3,2-benzoxazaborininone (**2.61**)

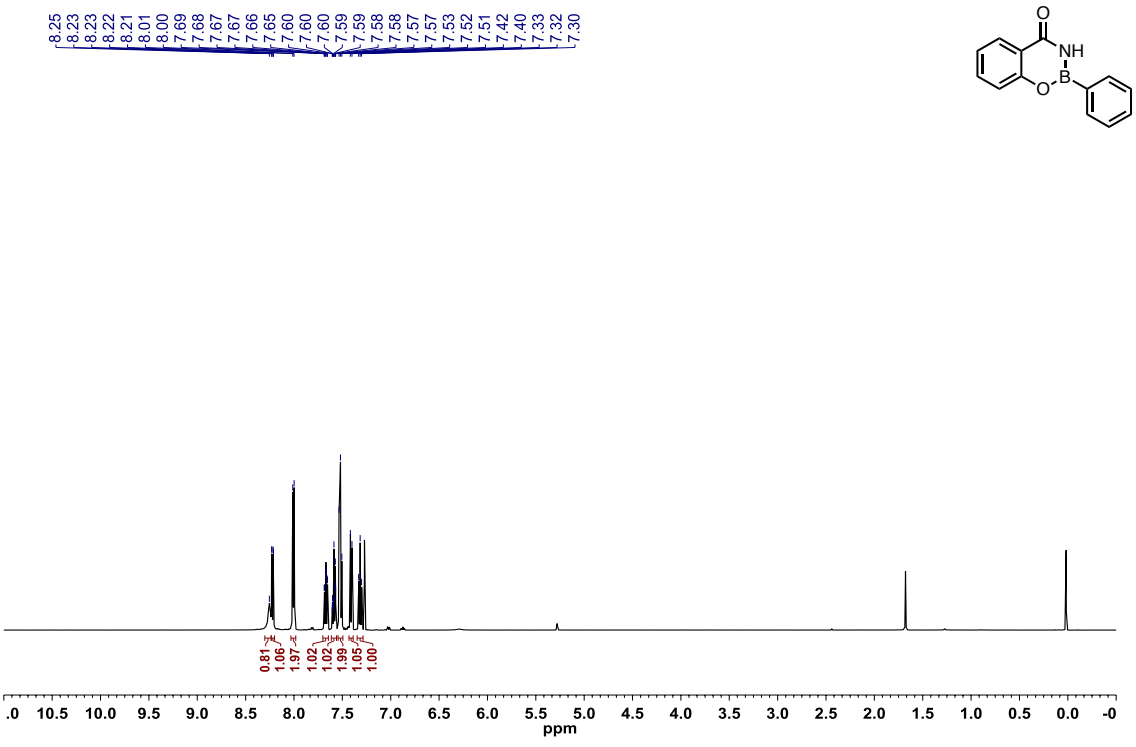

Figure A1.292: ^{13}C {^{1}H} NMR ($CDCl_3$, 125.8 MHz) of 2-phenyl-1,3,2-benzoxazaborininone (**2.61**)

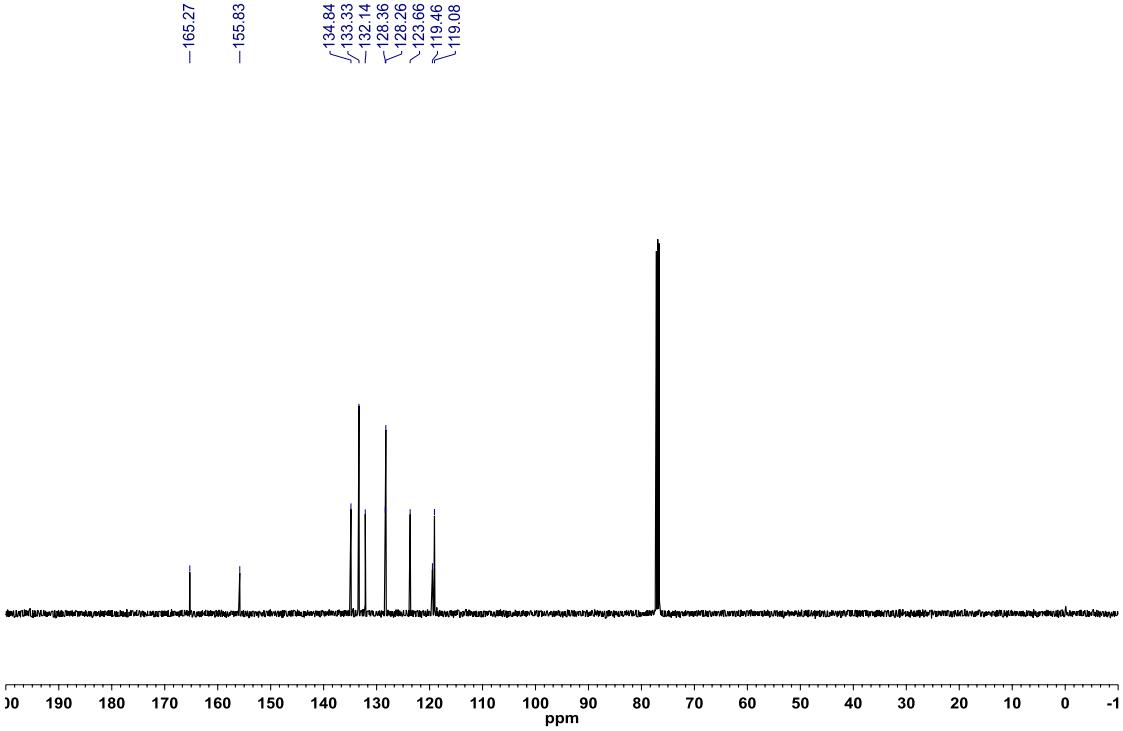

Figure A1.293: ^{11}B NMR (128.4 MHz, $CDCl_3$) of 2-phenyl-1,3,2-benzoxazaborininone (**2.61**)

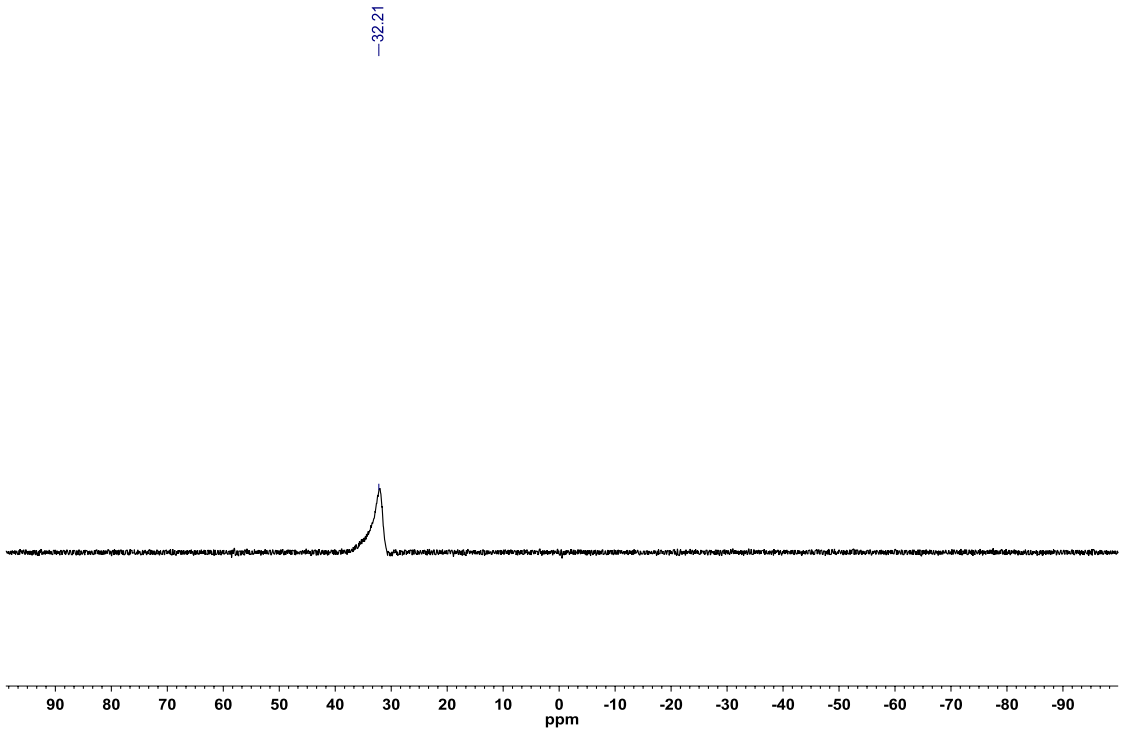

Figure A1.294: ^{1}H NMR ($CDCl_3$, 500.4 MHz) of 2-(*p*-tolyl)-1,3,2-benzoxazaborininone (**2.90**)

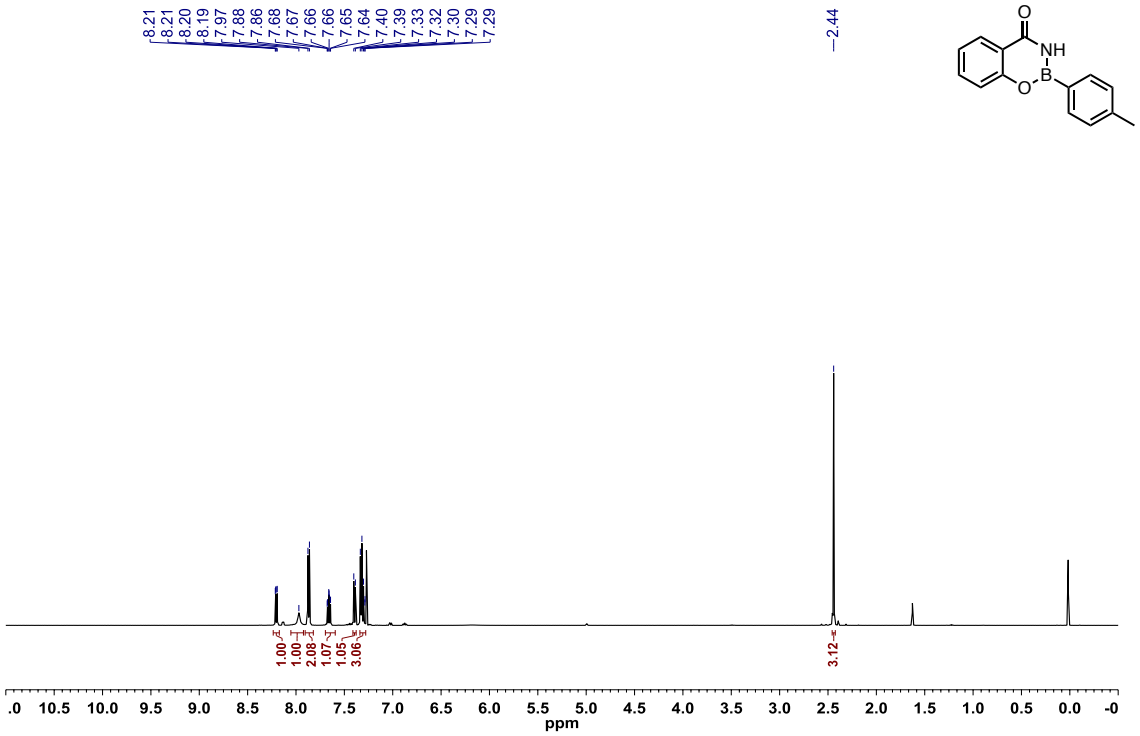

Figure A1.295: ^{13}C {^{1}H} NMR ($CDCl_3$, 125.8 MHz) of 2-(*p*-tolyl)-1,3,2-benzoxazaborininone (**2.90**)

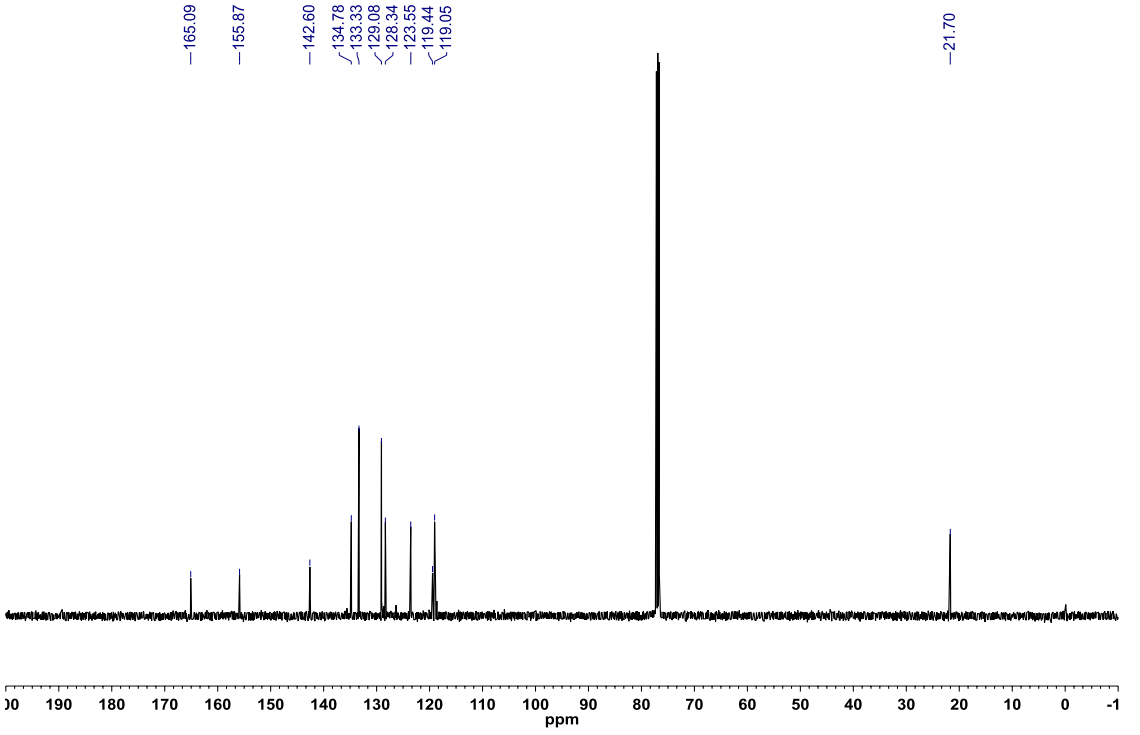

Figure A1.296: ^{11}B NMR ($CDCl_3$, 128.4 MHz) of 2-(*p*-tolyl)-1,3,2-benzoxazaborininone (**2.90**)

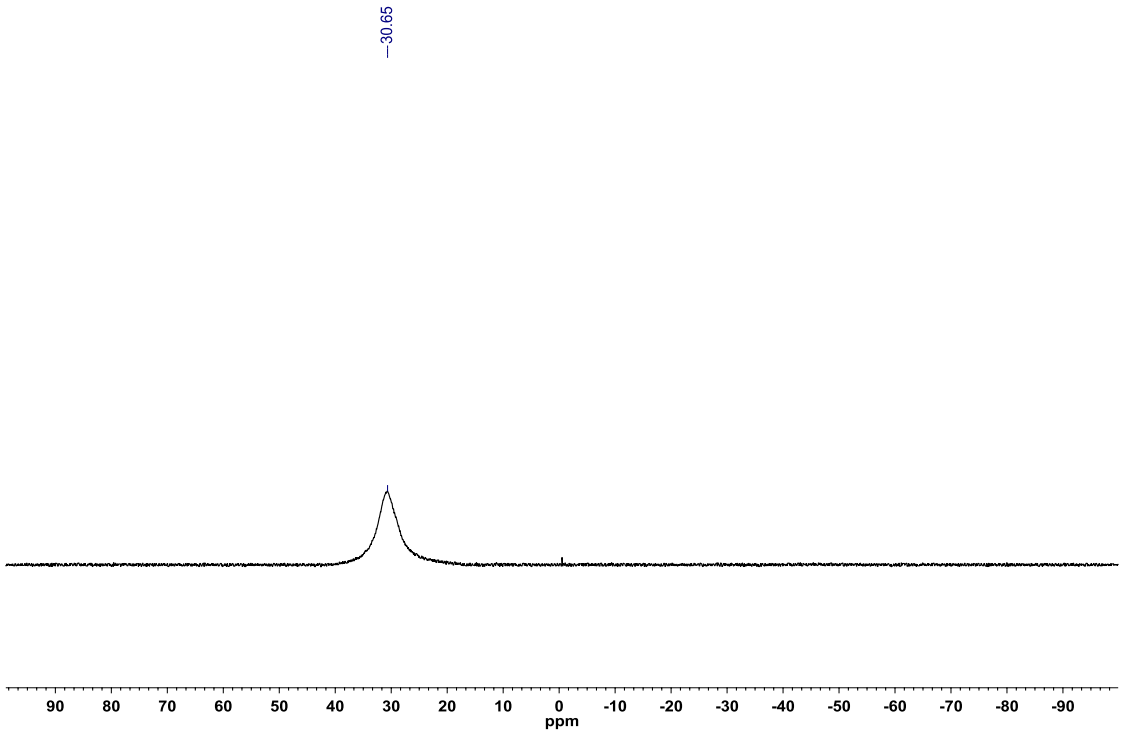

Figure A1.297: ^{1}H NMR ($CDCl_3$, 500.4 MHz) of 2-(4-methoxyphenyl)-1,3,2-benzoxazaborininone (**2.91**)

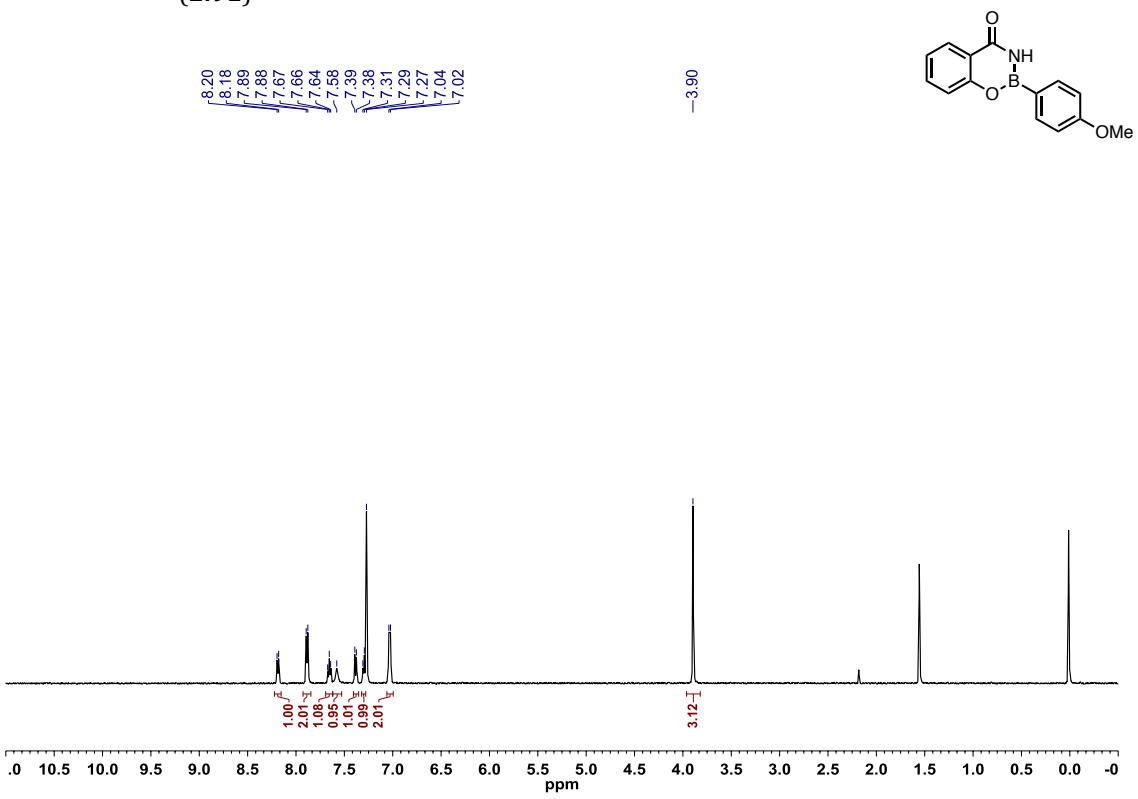

Figure A1.298: ^{13}C {^{1}H} NMR ($CDCl_3$, 125.8 MHz) of 2-(4-methoxyphenyl)-1,3,2-benzoxazaborininone (**2.91**)

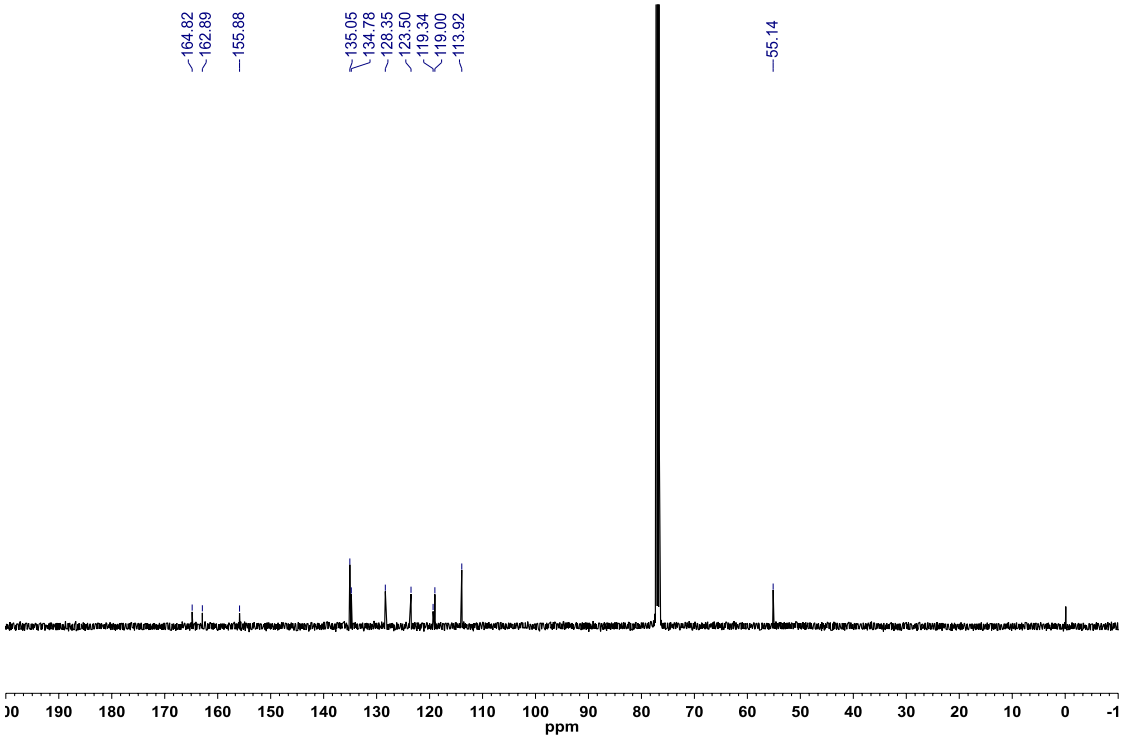

Figure A1.299: ^{11}B NMR (THF, 128.4 MHz) of 2-(4-methoxyphenyl)-1,3,2-benzoxazaborininone (**2.91**)

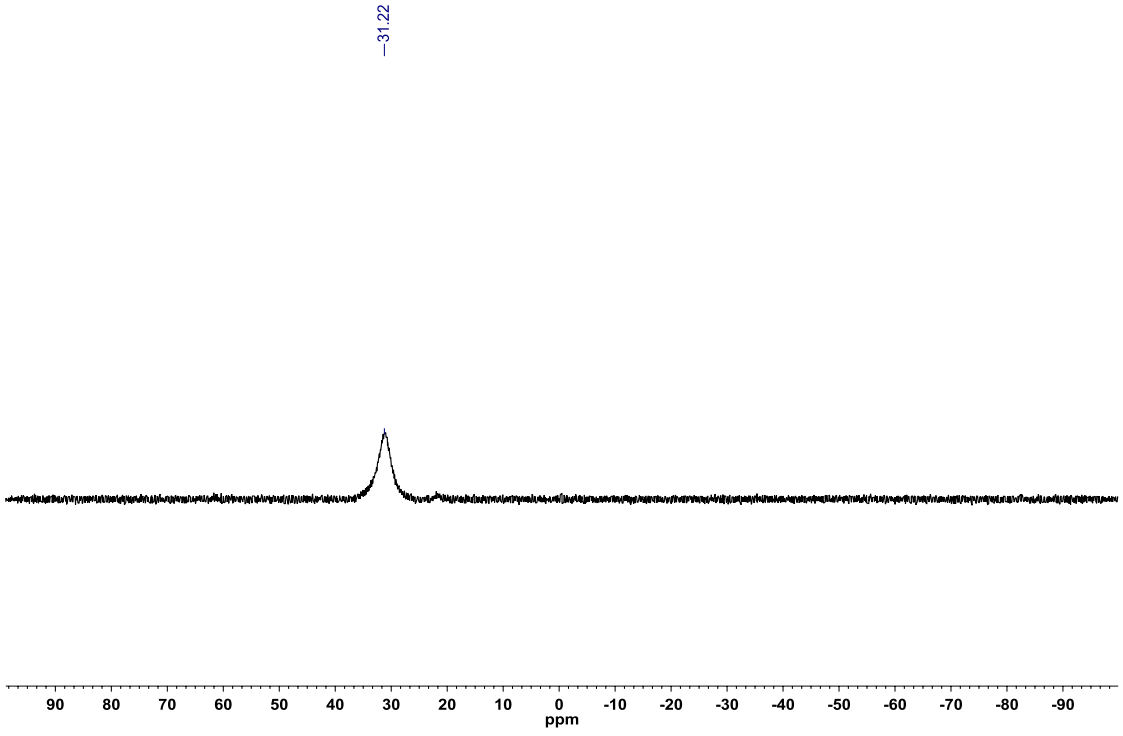

Figure A1.300: ^{1}H NMR ($CDCl_3$, 500.4 MHz) of 2-(4-(trifluoromethyl)phenyl)-1,3,2-benzoxazaborininone (**2.92**)

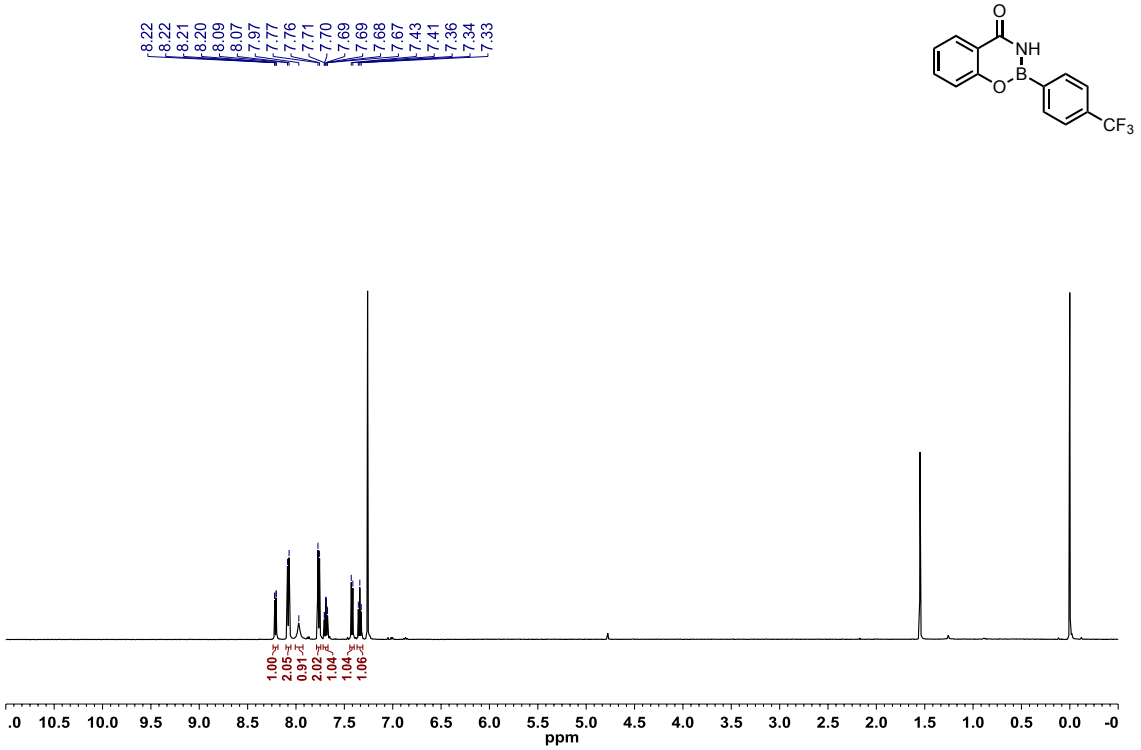

Figure A1.301: ^{13}C {^{1}H} NMR ($CDCl_3$, 125.8 MHz) of 2-(4-(trifluoromethyl)phenyl)-1,3,2-benzoxazaborininone (**2.92**)

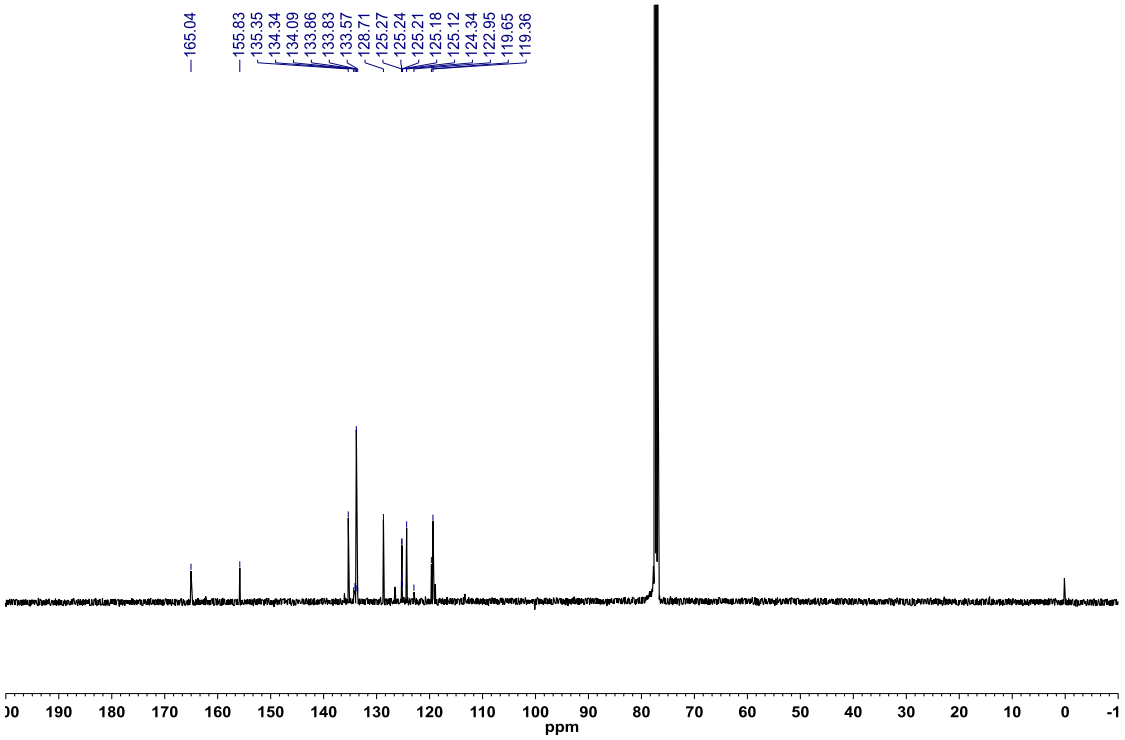

Figure A1.302: ^{19}F {^{1}H} NMR ($CDCl_3$, 470.8 MHz) of 2-(4-(trifluoromethyl)phenyl)-1,3,2-benzoxazaborininone (**2.92**)

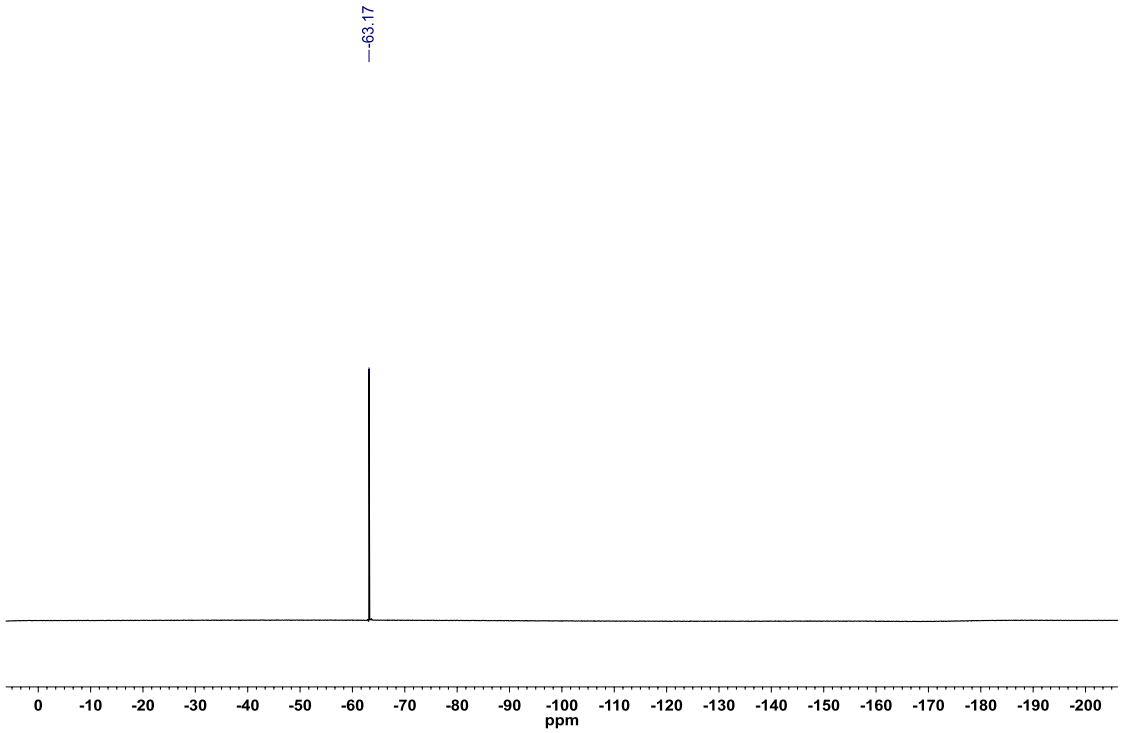

Figure A1.303: ^{11}B NMR (MeCN, 128.4 MHz) of 2-(4-(trifluoromethyl)phenyl)-1,3,2-benzoxazaborininone (**2.92**)

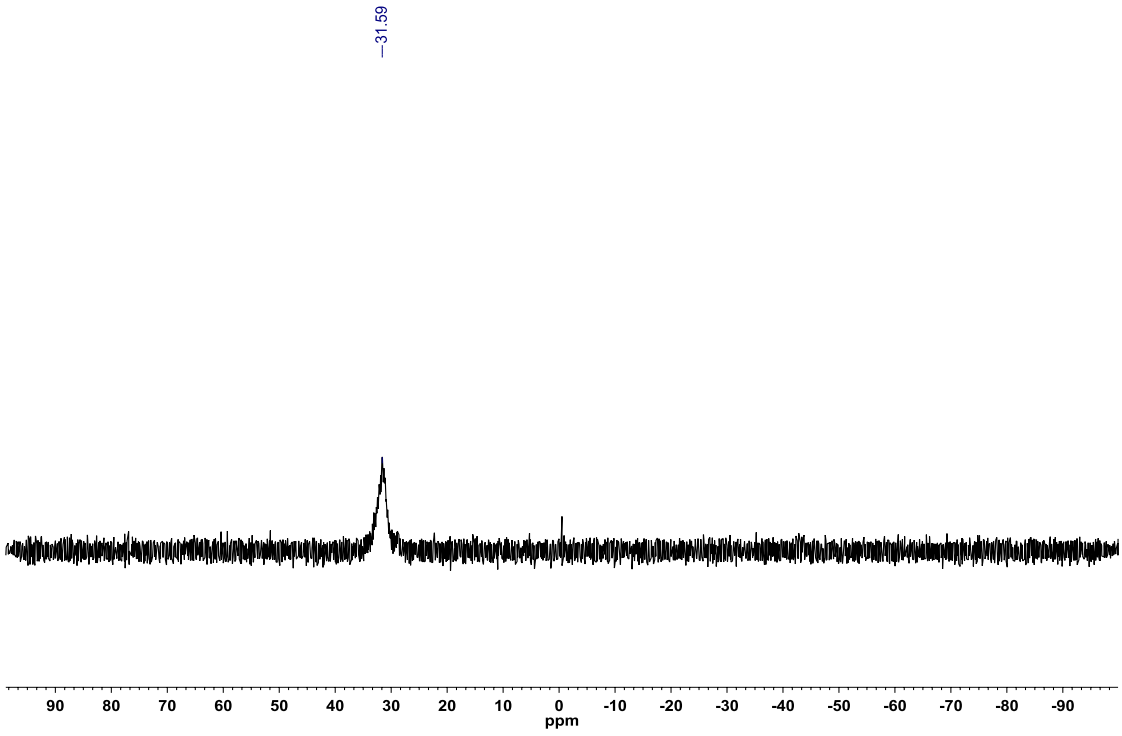

Figure A1.304: ^{1}H NMR ($CDCl_3$, 500.4 MHz) of 2-(4-acetylphenyl)-1,3,2-benzoxazaborininone (**2.93**)

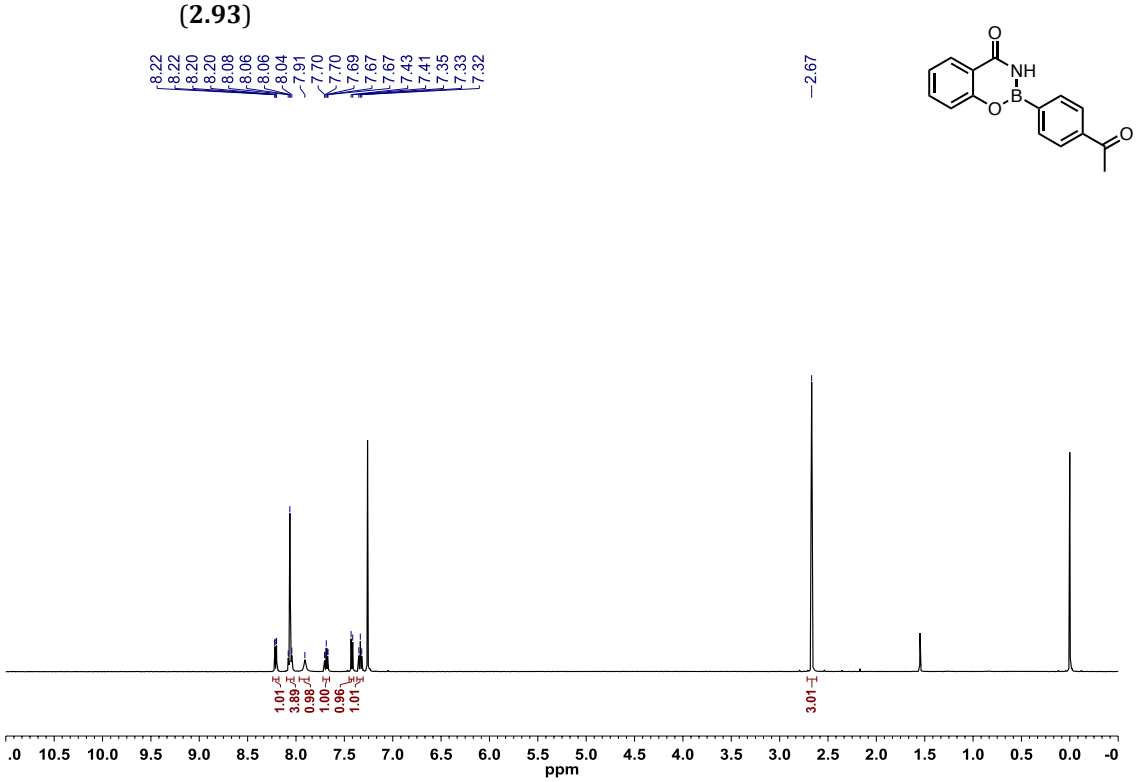

Figure A1.305: ^{13}C {^{1}H} NMR ($CDCl_3$, 125.8 MHz) of 2-(4-acetylphenyl)-1,3,2-benzoxazaborininone (**2.93**)

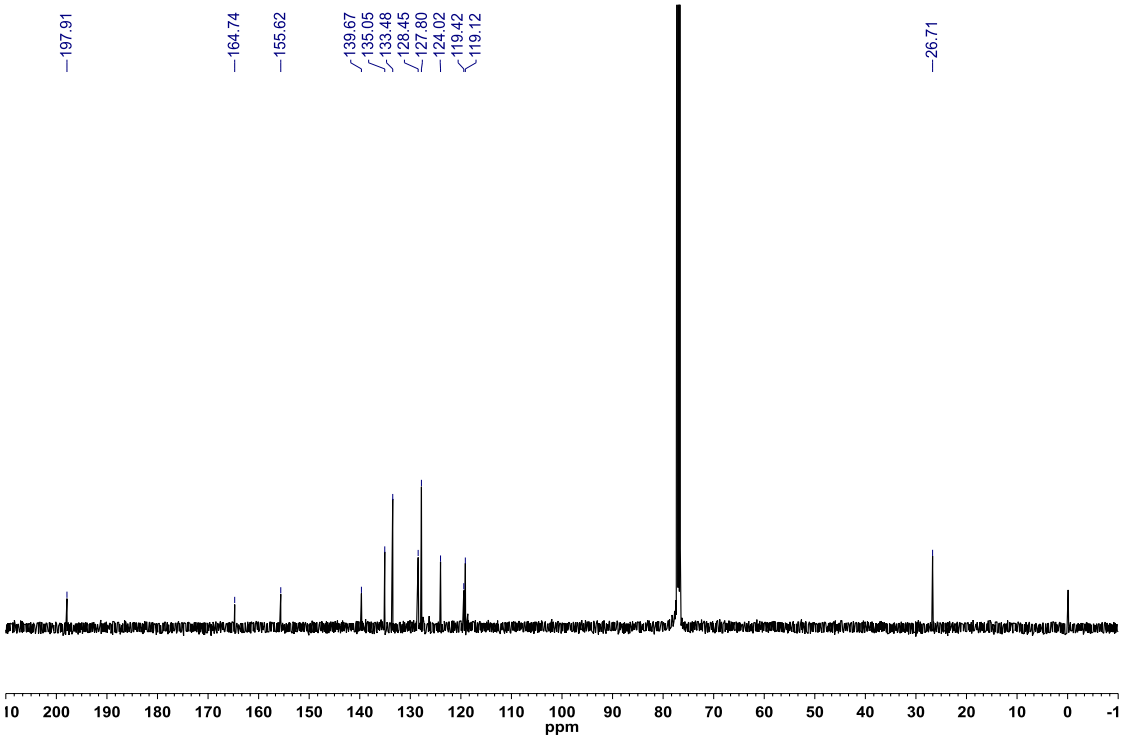

Figure A1.306: ^{11}B NMR (THF, 128.4 MHz) of 2-(4-acetylphenyl)-1,3,2-benzoxazaborininone (**2.93**)

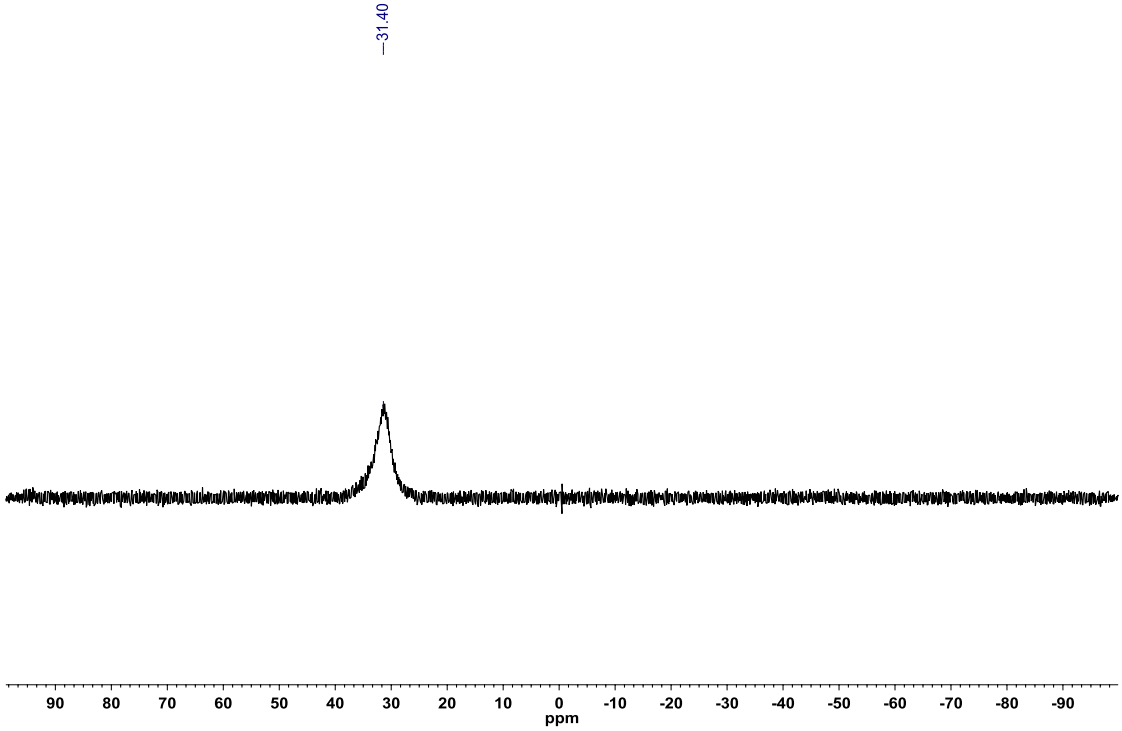

Figure A1.307: ^{1}H NMR (THF-d_8, 500.4 MHz) of 2-(2-methoxyphenyl)-1,3,2-benzoxazaborininone (**2.94**)

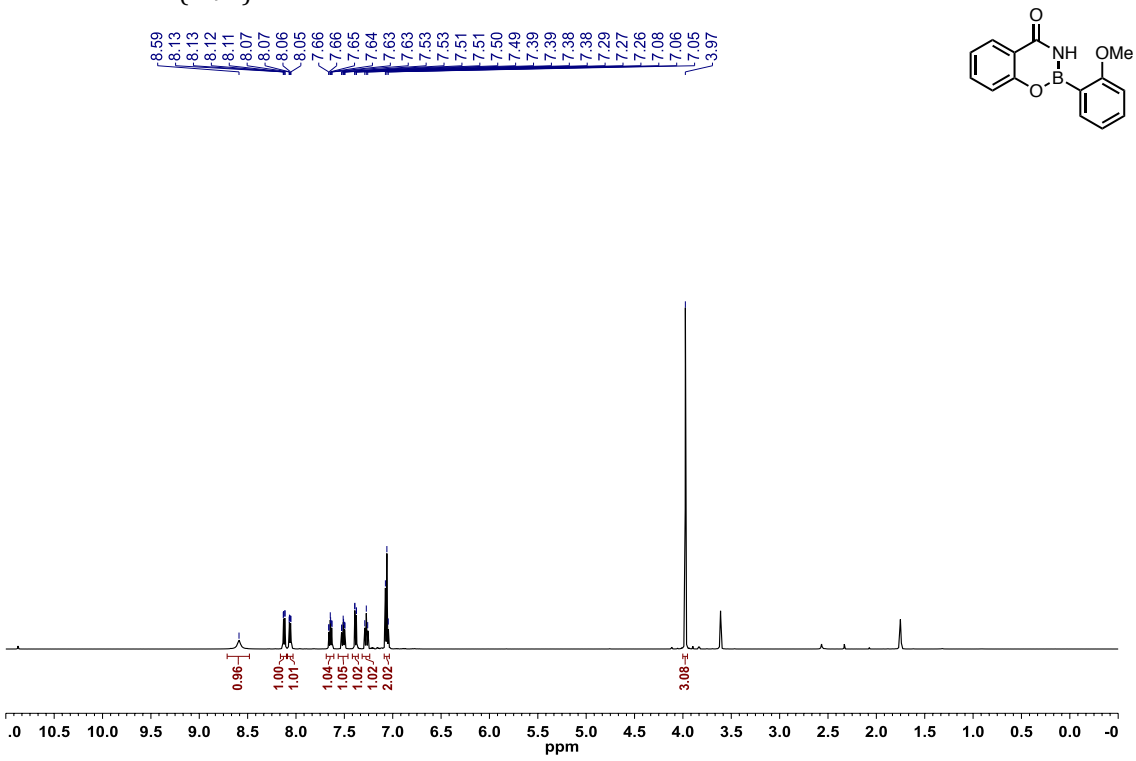

Figure A1.308: ^{13}C {^{1}H} NMR (THF-d_8, 125.8 MHz) of 2-(2-methoxyphenyl)-1,3,2-benzoxazaborininone (**2.94**)

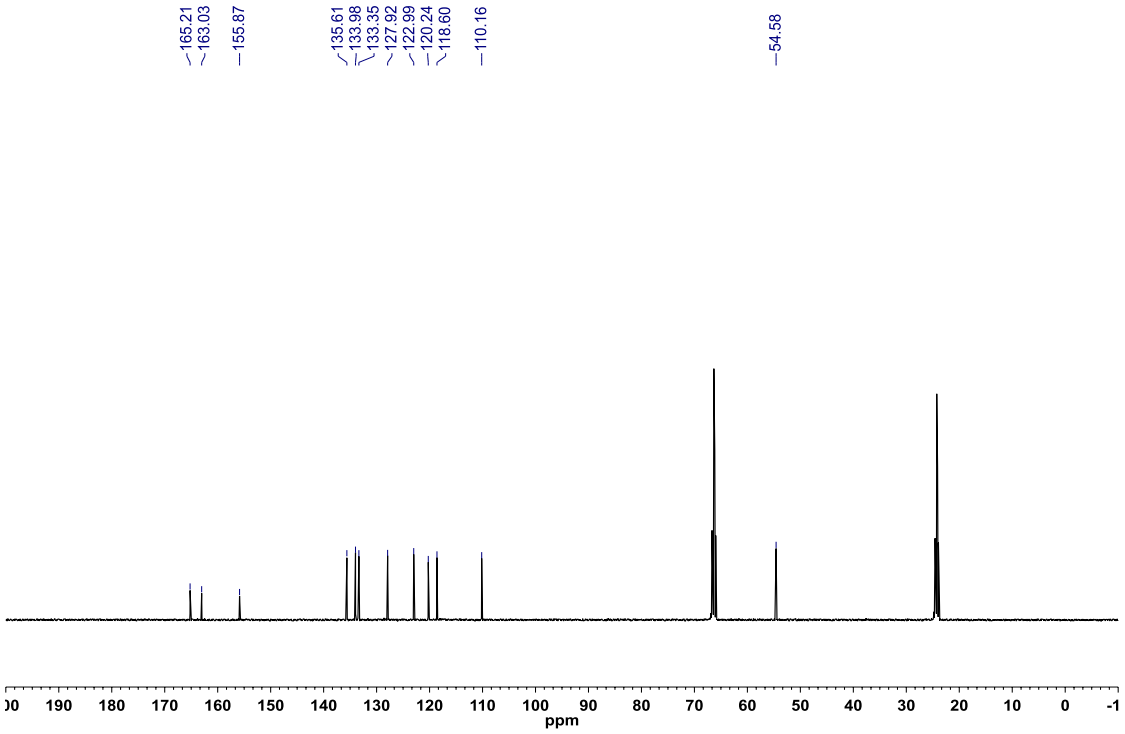

Figure A1.309: ^{11}B NMR (THF-d_8, 128.4 MHz) of 2-(2-methoxyphenyl)-1,3,2-benzoxazaborininone (**2.94**)

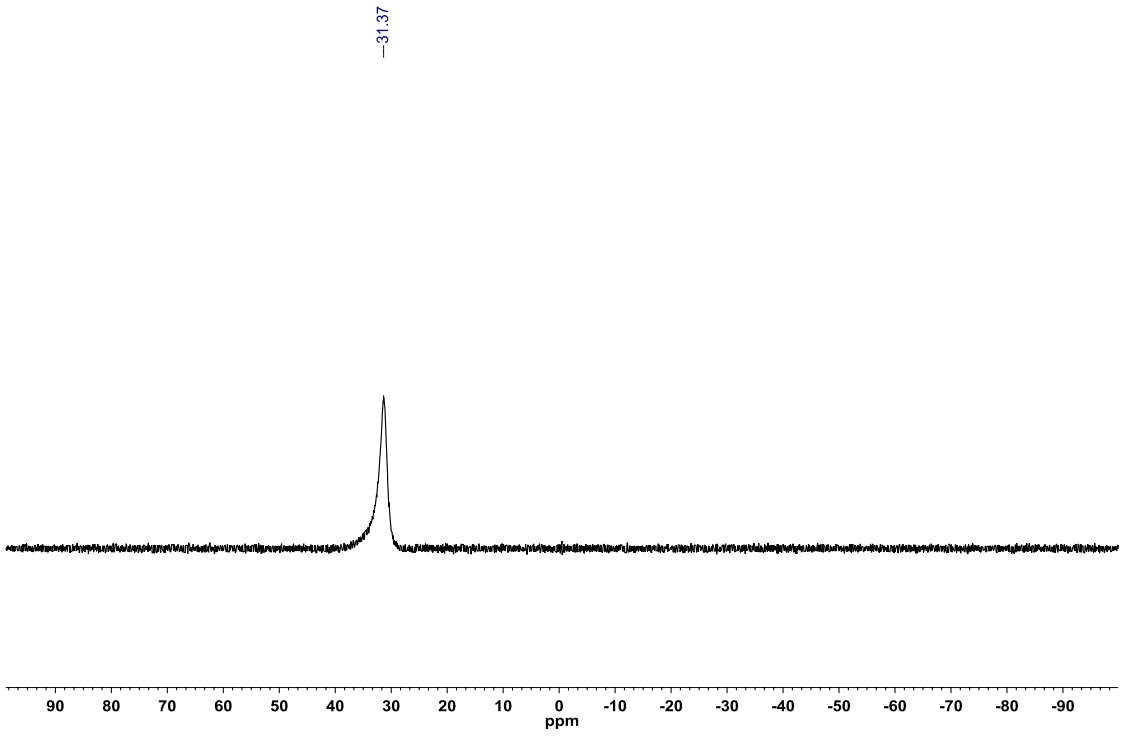

Figure A1.310: ^{1}H NMR ($CDCl_3$, 500.4 MHz) of 2-(thiophen-3-yl)-1,3,2-benzoxazaborininone (**2.95**)

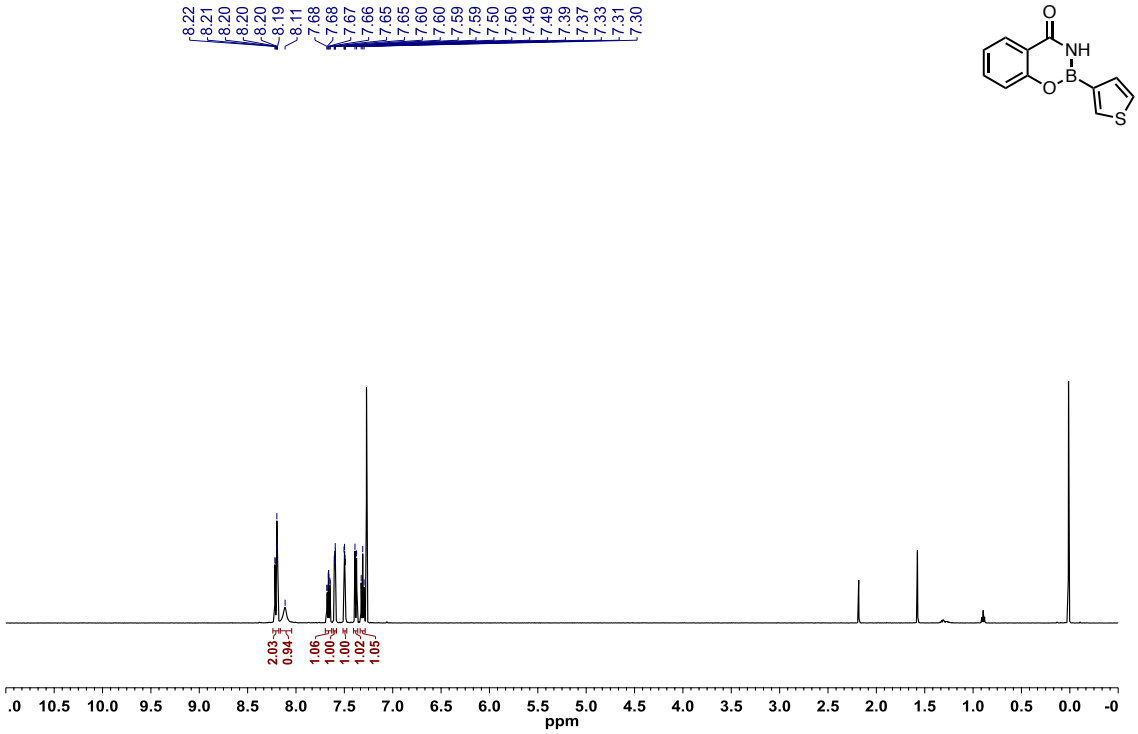

Figure A1.311: ^{13}C {^{1}H} NMR ($CDCl_3$, 125.8 MHz) of 2-(thiophen-3-yl)-1,3,2-benzoxazaborininone (**2.95**)

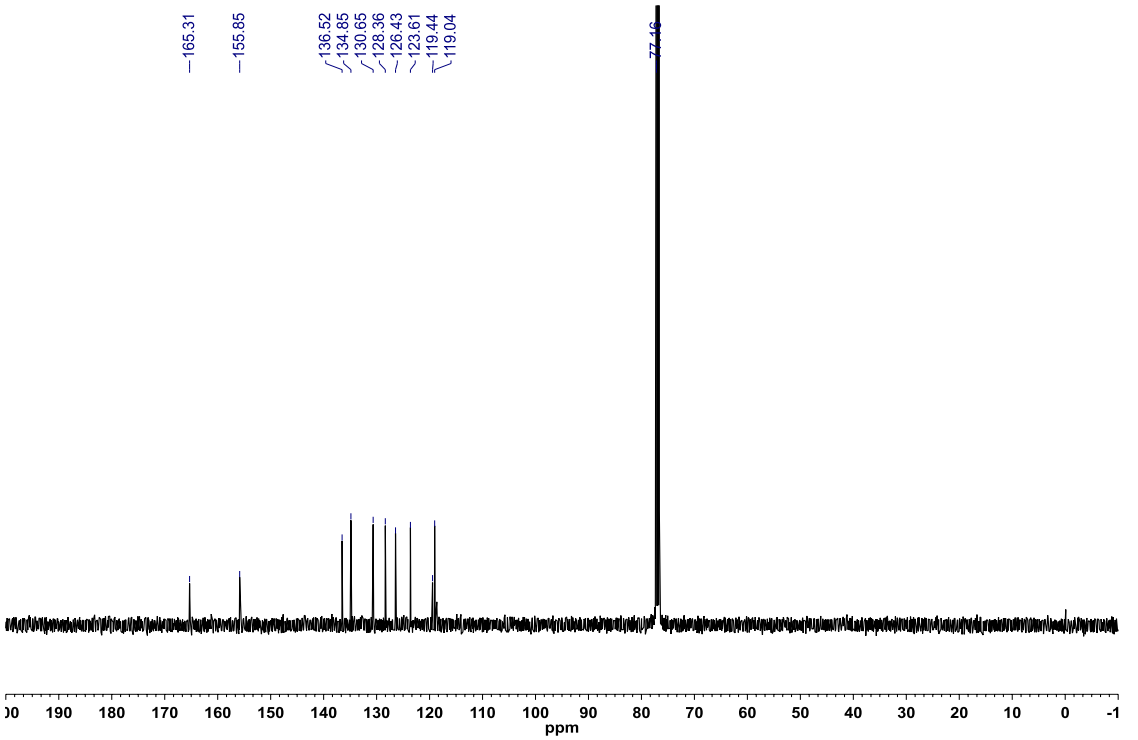

Figure A1.312: ^{11}B NMR ($CDCl_3$, 128.4 MHz) of 2-(thiophen-3-yl)-1,3,2-benzoxazaborininone (**2.95**)

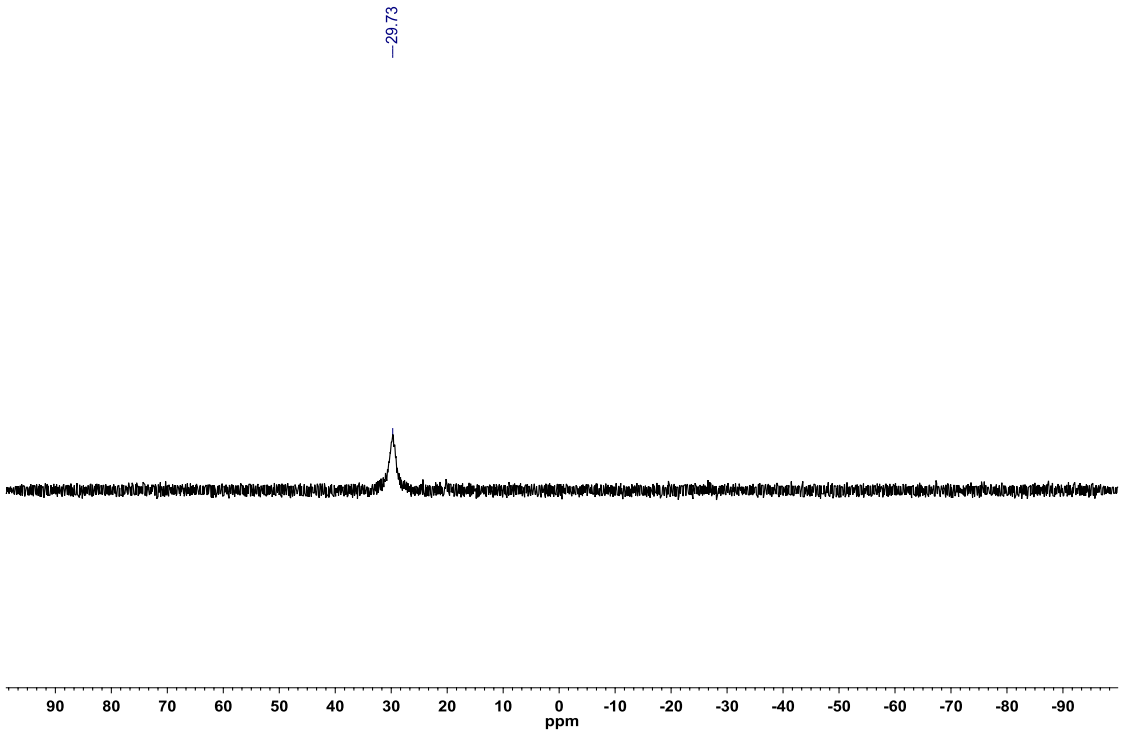

Figure A1.313: ^{1}H NMR ($CDCl_3$, 500.4 MHz) of 2-(1-methyl-1H-indol-5-yl)-1,3,2-benzoxazaborininone (**2.96**)

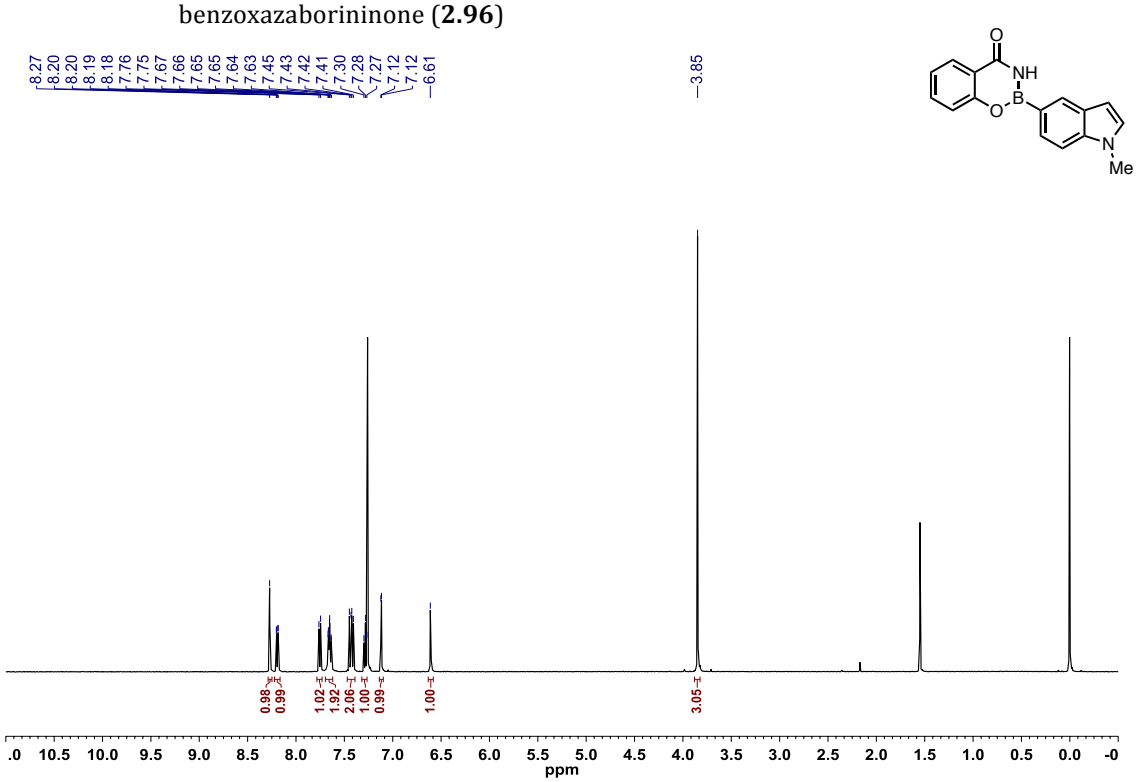

Figure A1.314: ^{13}C {^{1}H} NMR ($CDCl_3$, 125.8 MHz) of 2-(1-methyl-1H-indol-5-yl)-1,3,2-benzoxazaborininone (**2.96**)

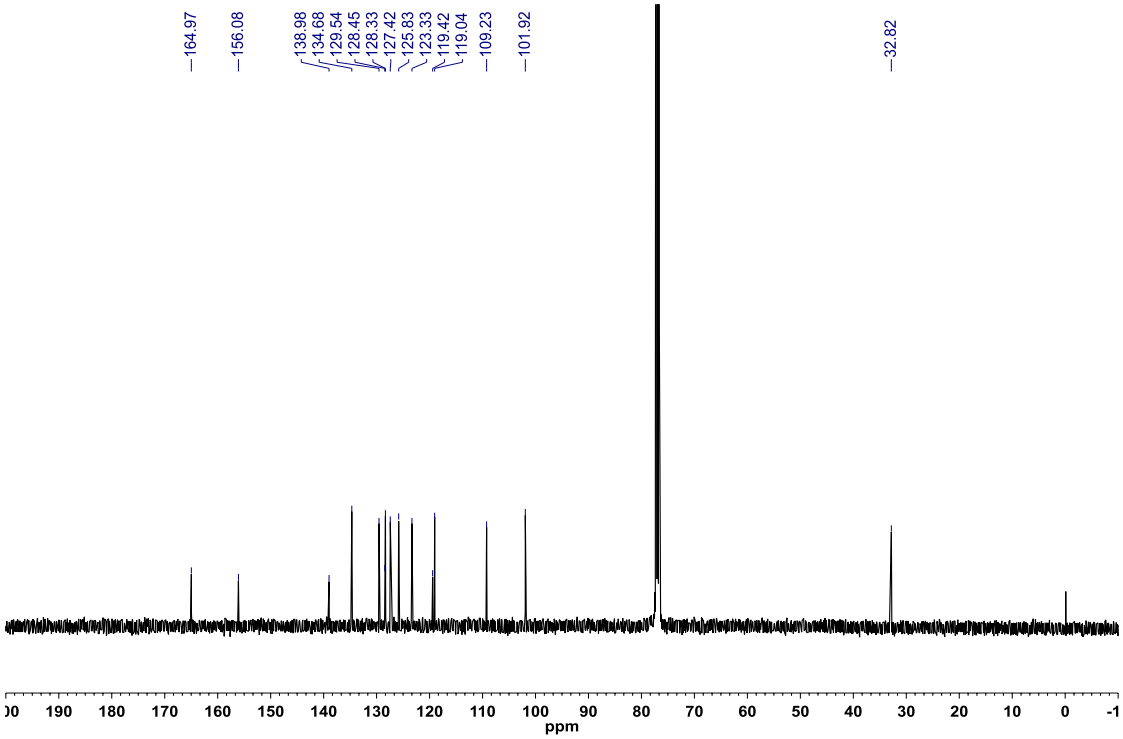

Figure A1.315: ^{11}B NMR ($CDCl_3$, 128.4 MHz) of 2-(1-methyl-1H-indol-5-yl)-1,3,2-benzoxazaborininone (**2.96**)

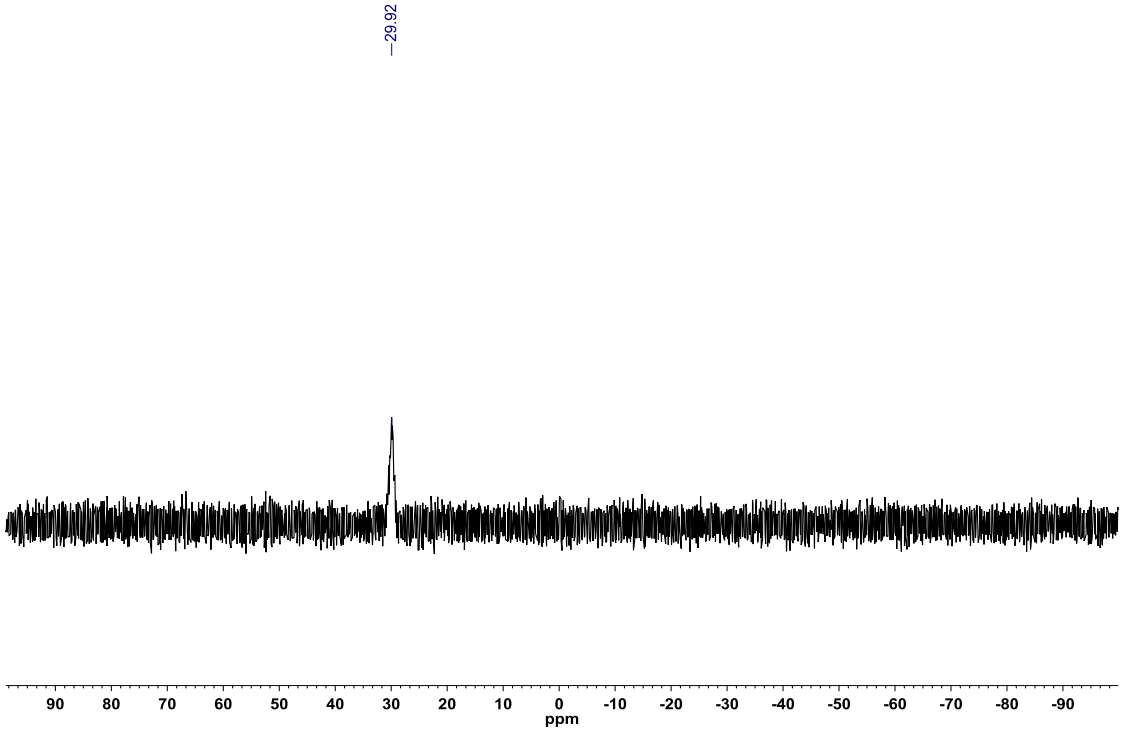

Figure A1.316: ^{1}H NMR ($CDCl_3$, 500.4 MHz) of 2-phenethyl-1,3,2-benzoxazaborininone (**2.97**)

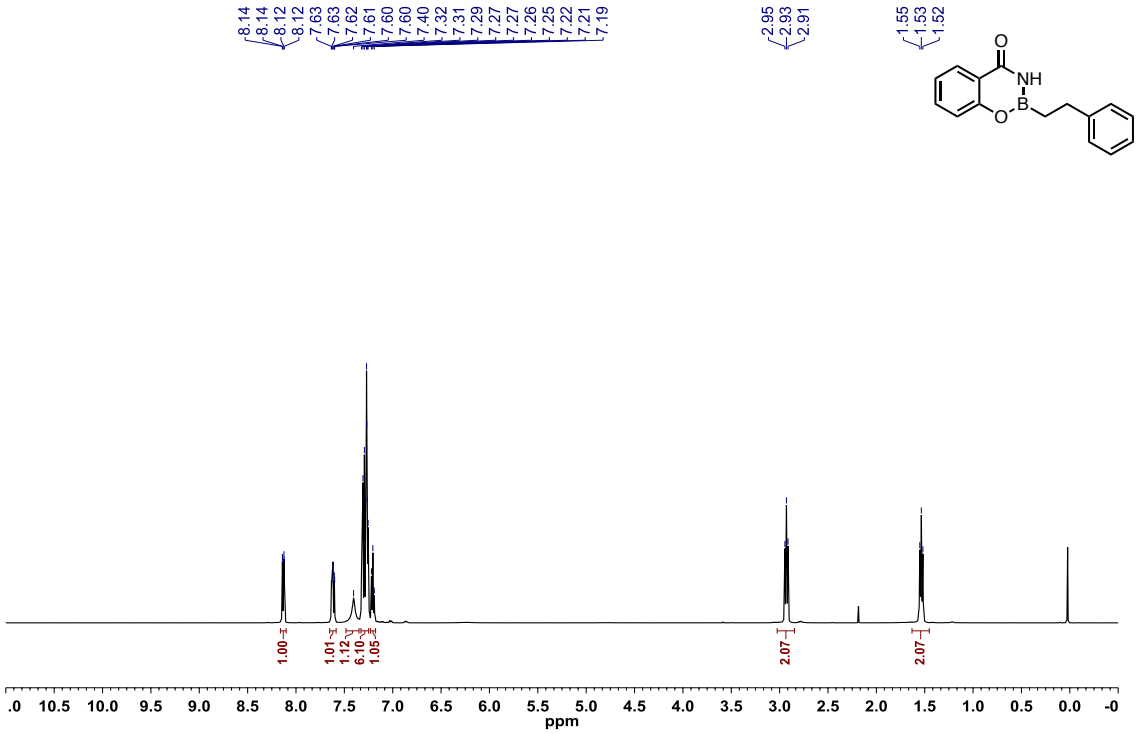

Figure A1.317: ^{13}C {^{1}H} NMR ($CDCl_3$, 125.8 MHz) of 2-phenethyl-1,3,2-benzoxazaborininone (**2.97**)

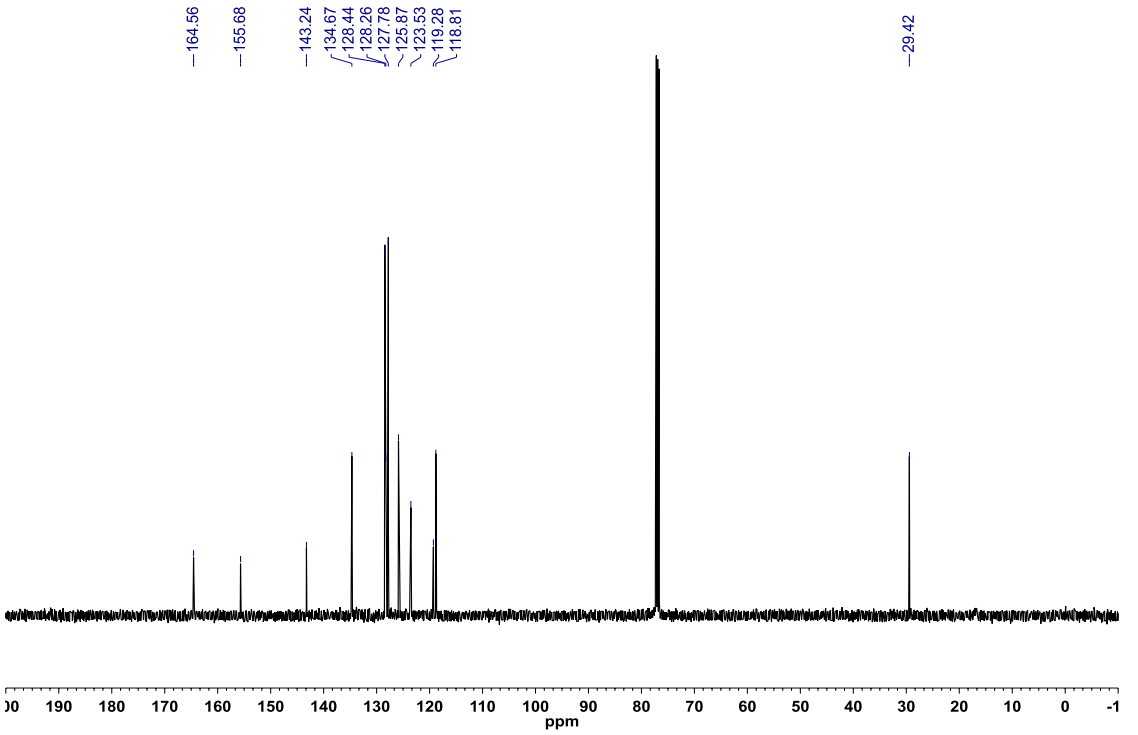

Figure A1.318: ^{11}B NMR ($CDCl_3$, 128.4 MHz) of 2-phenethyl-1,3,2-benzoxazaborininone (**2.97**)

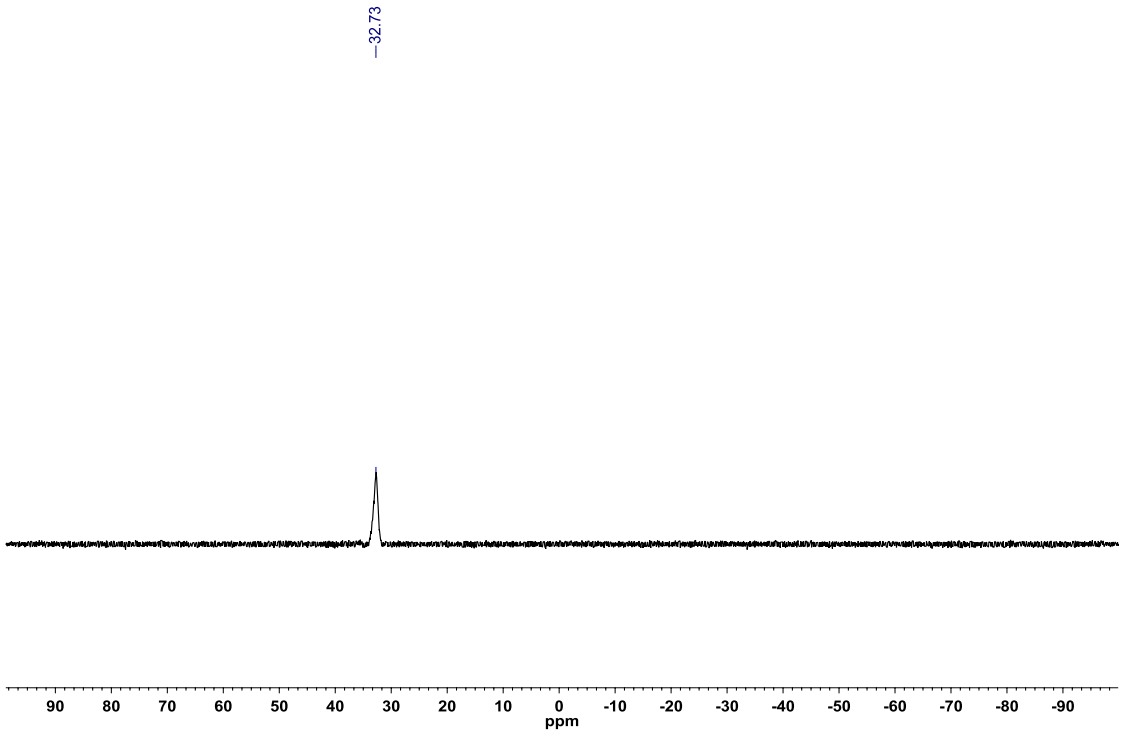

A1.5 – Computational data relevant to Chapter 2.4

Figure A1.319: Decomposition data for 2-Pheny-2,1-borazaronaphthalene (**2.111**)[a]

	IS	Prod-1	Prod:IS-1	%Δ-1	Prod-2	Prod:IS-2	%Δ-2	Average %Δ
Start	1.00	0.94	0.94	0	1.18	1.18	0	0.00
4 days	1.00	0.91	0.91	3.19	1.13	1.13	4.24	3.71
12 days	1.00	0.82	0.82	12.77	1.05	1.05	11.02	11.89
18 days	1.00	0.80	0.80	14.89	1.01	1.01	14.41	14.65
27 days	1.00	0.76	0.76	19.15	0.98	0.98	16.95	18.05

[a]Percent change in product (Average **%Δ**) is determined as an average of two separate integrals of protons 1H NMR of product (Prod-1, Prod-2) compared to an internal standard (IS, 4,4′-di-*tert*-butylbiphenyl).

Figure A1.320: Decomposition data for 2-(4-(methoxy)phenyl)-2,1-borazaronaphthalene (**2.112**)[a]

	IS	Prod-1	Prod:IS-1	%Δ-1	Prod-2	Prod:IS-2	%Δ-2	Average %Δ
Start	1.00	1.35	1.35	0	3.17	3.17	0	0.00
4 days	1.00	1.31	1.31	2.96	3.05	3.05	3.79	3.37
12 days	1.00	1.20	1.20	11.11	2.86	2.86	9.78	10.45
18 days	1.00	1.17	1.17	13.33	2.78	2.78	12.30	12.82
27 days	1.00	1.12	1.12	17.04	2.67	2.67	15.77	16.41

[a]Percent change in product (Average **%Δ**) is determined as an average of two separate integrals of protons 1H NMR of product (Prod-1, Prod-2) compared to an internal standard (IS, 4,4′-di-*tert*-butylbiphenyl).

Figure A1.321: Decomposition data for 2-(4-(triflouromethyl)phenyl)-2,1-borazaronaphthalene (**2.113**)[a]

	IS	Prod-1	Prod:IS-1	%Δ-1	Prod-2	Prod:IS-2	%Δ-2	Average %Δ
Start	1.00	2.79	2.79	0	6.71	6.71	0	0.00
4 days	1.00	2.65	2.65	5.02	6.36	6.36	5.22	5.12
12 days	1.00	2.43	2.43	12.90	5.90	5.90	12.07	12.49
18 days	1.00	2.27	2.27	18.64	5.50	5.50	18.03	18.34
27 days	1.00	2.18	2.18	21.86	5.31	5.31	20.86	21.36

[a]Percent change in product (Average **%Δ**) is determined as an average of two separate integrals of protons 1H NMR of product (Prod-1, Prod-2) compared to an internal standard (IS, 4,4′-di-*tert*-butylbiphenyl).

Figure A1.322: Computationally derived values for 2,1-borazaonapthalenes

	Bond Lengths (Å)			NICS (ppm)					
Compound	**B-N**	**B-C**	**B-R**	**A(0)**	**B(0)**	**Center (0)**	**A(1)**	**B(1)**	**Center(1)**
Reference[a]	*1.421*	*1.524*	*N.A.*	*-8.86*	*-3.63*	*-38.59*	*-10.31*	*-6.33*	*-15.23*
2.112	1.430	1.532	1.563	-8.35	-2.68	-37.72	-9.83	-5.28	-14.49
2.114	1.429	1.531	1.566	-8.31	-2.49	-37.92	-9.93	-5.38	-14.56
2.115	1.432	1.534	1.559	-8.13	-2.39	-37.39	-9.75	-5.08	-14.36
2.111	1.428	1.531	1.568	-8.46	-2.73	-38.15	-9.91	-5.44	-14.70
2.113	1.428	1.528	1.571	-8.45	-2.91	-38.19	-10.01	-5.63	-14.77
2.116	1.428	1.530	1.568	-8.49	-2.67	-38.21	-10.03	-5.42	-14.65
2.117	1.425	1.526	1.573	-8.53	-3.09	-38.35	-10.04	-5.74	-14.90

[a]Referenced to 2-*H*-2,1-borazaronaphthalene

Figure A1.323: Atomic coordinates for [B3LYP/6-311+G(2d,p)] optimized geometry value of total energy of 2-Pheny-2,1-borazaronaphthalene (**2.111**)

Center Number	Atomic Number	Atomic Type	Coordinates (Angstroms) X	Y	Z
1	6	0	0.086561	0.202013	-0.036955
2	6	0	0.026913	0.033910	1.352941
3	6	0	1.195754	-0.108455	2.072217
4	6	0	2.452521	-0.089342	1.439985
5	6	0	2.498552	0.076874	0.034600
6	6	0	1.304008	0.223700	-0.687804
7	1	0	1.347108	0.352829	-1.764383
8	7	0	3.726262	0.092819	-0.596849
9	5	0	4.987828	-0.044286	0.057713
10	6	0	4.898666	-0.207408	1.576886
11	6	0	3.680753	-0.229026	2.176163
12	1	0	3.587484	-0.357495	3.252347
13	1	0	5.775352	-0.329741	2.205054
14	6	0	6.310016	-0.025534	-0.785154
15	6	0	6.347483	-0.419662	-2.132469
16	6	0	7.525574	-0.394328	-2.869779
17	6	0	8.708157	0.035675	-2.275525
18	6	0	8.702017	0.430109	-0.941263
19	6	0	7.520385	0.391639	-0.209636
20	1	0	7.536439	0.703170	0.828988
21	1	0	9.619444	0.765116	-0.470927
22	1	0	9.628627	0.058446	-2.847258
23	1	0	7.523926	-0.713961	-3.905642
24	1	0	5.444052	-0.779008	-2.616182
25	1	0	3.681651	0.238217	-1.596722
26	1	0	1.160908	-0.237387	3.148541
27	1	0	-0.931209	0.017124	1.857227
28	1	0	-0.827491	0.315329	-0.607615

E_{Tot}: -620.571318032 Hartree

Figure A1.324: Atomic coordinates for [B3LYP/6-311+G(2d,p)] optimized geometry value of total energy of 2-(4-(methoxy)phenyl)-2,1-borazaronaphthalene (**2.112**)

Center Number	Atomic Number	Atomic Type	Coordinates (Angstroms) X	Y	Z
1	6	0	0.097234	-0.049873	0.109554
2	8	0	0.126902	0.047549	1.526218
3	6	0	1.337426	0.037143	2.152470
4	6	0	2.566526	-0.058538	1.499825
5	6	0	3.739607	-0.063070	2.249632
6	6	0	3.746114	0.030649	3.646546
7	6	0	2.486773	0.137521	4.266403
8	6	0	1.306102	0.134838	3.546328
9	1	0	0.344671	0.209771	4.039590
10	1	0	2.429672	0.213939	5.346418
11	5	0	5.061306	0.025713	4.491832
12	6	0	5.215635	0.595767	5.905815
13	6	0	6.423846	0.545150	6.521449
14	6	0	7.584672	-0.039428	5.903431
15	6	0	8.831467	-0.090393	6.552517
16	6	0	9.934278	-0.660087	5.949121
17	6	0	9.814799	-1.200874	4.662285
18	6	0	8.604884	-1.165123	3.997456
19	6	0	7.477947	-0.585882	4.601672
20	7	0	6.259622	-0.539846	3.954053
21	1	0	6.256625	-0.973607	3.040662
22	1	0	8.515740	-1.584412	3.000445
23	1	0	10.675899	-1.650741	4.182479
24	1	0	10.885783	-0.690523	6.465176
25	1	0	8.912474	0.330397	7.548927
26	1	0	6.562158	0.954362	7.519890
27	1	0	4.395959	1.064873	6.440860
28	1	0	4.677736	-0.118809	1.705470
29	1	0	2.622480	-0.122995	0.421974
30	1	0	0.613815	0.793264	-0.358903
31	1	0	0.543451	-0.987751	-0.234684
32	1	0	-0.954314	-0.027564	-0.168419

E_{Tot}: -735.131831765 Hartree

Figure A1.325: Atomic coordinates for [B3LYP/6-311+G(2d,p)] optimized geometry value of total energy of 2-(4-(triflouromethyl)phenyl)-2,1-borazaronaphthalene (**2.113**)

Center Number	Atomic Number	Atomic Type	Coordinates (Angstroms) X	Y	Z
1	6	0	-0.003294	-0.005970	0.042118
2	6	0	-0.001309	-0.014793	1.543945
3	6	0	1.205893	0.054219	2.234254
4	6	0	1.203131	0.087702	3.621631
5	6	0	0.010496	0.061418	4.361229
6	6	0	-1.188093	0.004274	3.634844
7	6	0	-1.202096	-0.038849	2.247011
8	1	0	-2.140850	-0.095389	1.711327
9	1	0	-2.133213	-0.019523	4.164877
10	5	0	-0.005907	0.096720	5.931985
11	6	0	-1.122542	0.682898	6.794449
12	6	0	-0.997072	0.665444	8.146721
13	6	0	0.146444	0.100980	8.810949
14	6	0	0.262237	0.083267	10.213491
15	6	0	1.362367	-0.468446	10.836129
16	6	0	2.389665	-1.024722	10.061760
17	6	0	2.307562	-1.021855	8.683820
18	6	0	1.193414	-0.460458	8.040838
19	7	0	1.092168	-0.444799	6.663105
20	1	0	1.864751	-0.885762	6.181676
21	1	0	3.104641	-1.452625	8.086663
22	1	0	3.255809	-1.460311	10.545325
23	1	0	1.433840	-0.473589	11.916544
24	1	0	-0.538589	0.515146	10.803621
25	1	0	-1.769174	1.086978	8.786358
26	1	0	-2.013176	1.137920	6.372941
27	1	0	2.157238	0.158309	4.133636
28	1	0	2.140216	0.079254	1.688048
29	9	0	1.075853	-0.634022	-0.473976
30	9	0	-1.096396	-0.605884	-0.474562
31	9	0	0.014749	1.255988	-0.455266

E_{Tot}: -957.729774257 Hartree

Figure A1.326: Atomic coordinates for [B3LYP/6-311+G(2d,p)] optimized geometry value of total energy of 2-(*p*-tolyl)-2,1-borazaronaphthalene (**2.114**)

Center Number	Atomic Number	Atomic Type	Coordinates (Angstroms) X	Y	Z
1	6	0	0.079489	-0.017798	0.024228
2	6	0	0.038581	-0.031274	1.530899
3	6	0	1.216063	-0.071450	2.281599
4	6	0	1.179684	-0.058174	3.669370
5	6	0	-0.029665	-0.000722	4.380547
6	6	0	-1.202434	0.045679	3.612695
7	6	0	-1.171658	0.023185	2.223423
8	1	0	-2.102893	0.048752	1.666908
9	1	0	-2.164867	0.086399	4.110909
10	5	0	-0.091679	0.010828	5.945428
11	6	0	-1.236231	0.578631	6.789597
12	6	0	-1.150466	0.544007	8.143696
13	6	0	-0.022065	-0.022107	8.834257
14	6	0	0.054742	-0.056487	10.238505
15	6	0	1.140991	-0.608642	10.886177
16	6	0	2.192855	-1.148351	10.134135
17	6	0	2.148638	-1.128834	8.754190
18	6	0	1.049299	-0.567174	8.085958
19	7	0	0.986424	-0.535723	6.707186
20	1	0	1.776196	-0.963655	6.242625
21	1	0	2.965190	-1.546756	8.174341
22	1	0	3.048462	-1.584266	10.636074
23	1	0	1.181896	-0.626379	11.968129
24	1	0	-0.765461	0.362905	10.811019
25	1	0	-1.943332	0.952381	8.766615
26	1	0	-2.118145	1.033532	6.349748
27	1	0	2.124214	-0.072043	4.205354
28	1	0	2.172911	-0.110758	1.770795
29	1	0	0.883839	-0.649671	-0.358430
30	1	0	-0.861164	-0.369162	-0.403272
31	1	0	0.253963	0.994547	-0.354213

E_{Tot}: -659.900257871 Hartree

Figure A1.327: Atomic coordinates for [B3LYP/6-311+G(2d,p)] optimized geometry value of total energy of 2-(4-(dimethylamino)phenyl)-2,1-borazaronaphthalene (**2.115**)

Center Number	Atomic Number	Atomic Type	Coordinates (Angstroms) X	Y	Z
1	6	0	-0.093562	0.136694	0.102381
2	7	0	-0.068150	0.216444	1.552457
3	6	0	1.174591	-0.136546	2.216733
4	1	0	1.350410	0.504442	3.083143
5	1	0	1.194351	-1.181924	2.555312
6	1	0	2.001366	0.014831	1.525181
7	6	0	-1.258511	0.142753	2.258095
8	6	0	-2.507558	0.239497	1.609938
9	6	0	-3.687899	0.207381	2.333517
10	6	0	-3.726113	0.063401	3.729556
11	6	0	-2.475031	-0.058447	4.354453
12	6	0	-1.278163	-0.021043	3.658224
13	1	0	-0.354634	-0.121801	4.210277
14	1	0	-2.428262	-0.181887	5.430917
15	5	0	-5.050232	0.027160	4.551804
16	6	0	-5.201798	-0.506292	5.982281
17	6	0	-6.420078	-0.497819	6.578668
18	6	0	-7.599504	0.007734	5.925680
19	6	0	-8.857303	0.015179	6.554192
20	6	0	-9.978280	0.508627	5.917005
21	6	0	-9.865294	1.014119	4.615610
22	6	0	-8.644134	1.019364	3.970171
23	6	0	-7.498732	0.518041	4.608698
24	7	0	-6.269911	0.514174	3.980826
25	1	0	-6.276101	0.915530	3.052956
26	1	0	-8.560155	1.411116	2.961537
27	1	0	-10.740065	1.404116	4.108770
28	1	0	-10.938296	0.506349	6.418059
29	1	0	-8.932994	-0.377916	7.562349
30	1	0	-6.553653	-0.882032	7.587740
31	1	0	-4.369173	-0.915688	6.545689
32	1	0	-4.614159	0.272460	1.769495
33	1	0	-2.560043	0.335225	0.534875
34	1	0	-0.699134	0.939858	-0.322846
35	1	0	0.919663	0.256173	-0.276910
36	1	0	-0.489003	-0.820694	-0.265340

E_{Tot}: -754.578544867 Hartree

Figure A1.328: Atomic coordinates for [B3LYP/6-311+G(2d,p)] optimized geometry value of total energy of 2-(4-(fluoro)phenyl)-2,1-borazaronaphthalene (**2.116**)

Center Number	Atomic Number	Atomic Type	Coordinates (Angstroms) X	Y	Z
1	6	0	0.016215	-0.011737	0.010647
2	6	0	-0.011118	0.034086	1.393105
3	6	0	1.199459	0.039956	2.075808
4	6	0	2.434460	-0.004815	1.409081
5	5	0	3.804037	0.002933	2.171698
6	6	0	5.115356	-0.589708	1.651526
7	6	0	6.227829	-0.534021	2.427528
8	6	0	6.234226	0.077707	3.729587
9	6	0	7.394704	0.133979	4.523130
10	6	0	7.386451	0.730657	5.767131
11	6	0	6.200324	1.294560	6.255634
12	6	0	5.043963	1.254387	5.502284
13	6	0	5.041519	0.647339	4.236805
14	7	0	3.895260	0.594691	3.467931
15	1	0	3.091769	1.045202	3.885276
16	1	0	4.126665	1.691081	5.883663
17	1	0	6.187302	1.765552	7.231292
18	1	0	8.289693	0.764915	6.363367
19	1	0	8.307733	-0.304151	4.134961
20	1	0	7.169606	-0.959819	2.088484
21	1	0	5.195523	-1.079662	0.686269
22	6	0	2.396829	-0.062070	0.006908
23	6	0	1.200995	-0.059480	-0.701521
24	1	0	1.176922	-0.095944	-1.783225
25	1	0	3.325550	-0.099141	-0.550714
26	1	0	1.168631	0.055313	3.160549
27	1	0	-0.961165	0.058025	1.911607
28	9	0	-1.156277	-0.015304	-0.666659

E_{Tot}: -719.843398396 Hartree

Figure A1.329: Atomic coordinates for [B3LYP/6-311+G(2d,p)] optimized geometry value of total energy of 2-(4-(nitro)phenyl)-2,1-borazaronaphthalene (**2.117**)

Center Number	Atomic Number	Atomic Type	Coordinates (Angstroms) X	Y	Z
1	6	0	0.096906	0.019708	-0.061134
2	6	0	0.041472	-0.005947	1.339364
3	6	0	1.212218	-0.015800	2.067906
4	6	0	2.469101	-0.000638	1.434141
5	6	0	2.510229	0.020860	0.019082
6	6	0	1.313098	0.033525	-0.713476
7	1	0	1.353146	0.052837	-1.797637
8	7	0	3.738594	0.032036	-0.613588
9	5	0	4.997491	0.031852	0.054481
10	6	0	4.917291	0.020019	1.578788
11	6	0	3.698456	-0.002110	2.178769
12	1	0	3.608665	-0.023327	3.262386
13	1	0	5.796661	0.006845	2.214653
14	6	0	6.325676	0.037973	-0.787506
15	6	0	6.410424	-0.552240	-2.059467
16	6	0	7.585393	-0.541996	-2.796552
17	6	0	8.703874	0.076660	-2.254373
18	6	0	8.672653	0.671456	-1.000180
19	6	0	7.488086	0.639995	-0.279093
20	1	0	7.464672	1.104972	0.699339
21	1	0	9.563679	1.142265	-0.610212
22	7	0	9.957212	0.097570	-3.027956
23	8	0	10.928346	0.652273	-2.525973
24	8	0	9.957241	-0.441018	-4.129451
25	1	0	7.650559	-1.004139	-3.771169
26	1	0	5.547602	-1.055953	-2.481906
27	1	0	3.688722	0.072876	-1.623088
28	1	0	1.179953	-0.033995	3.151677
29	1	0	-0.916487	-0.017147	1.843900
30	1	0	-0.819989	0.028320	-0.638113

E_{Tot}: -825.142040012 Hartree

Figure A1.330: Atomic coordinates for [B3LYP/6-311+G(2d,p)] optimized geometry value of total energy of 2-*H*-2,1-borazaronaphthalene

Center Number	Atomic Number	Atomic Type	Coordinates (Angstroms) X	Y	Z
1	6	0	0.000000	0.000000	0.000000
2	6	0	0.000000	0.000000	1.401867
3	6	0	1.198930	0.000000	2.083259
4	6	0	2.430573	0.000012	1.401055
5	6	0	2.415433	0.000012	-0.015086
6	6	0	1.189936	0.000010	-0.699319
7	1	0	1.187808	0.000016	-1.784435
8	7	0	3.619220	0.000030	-0.694126
9	5	0	4.896398	0.000038	-0.071211
10	6	0	4.883301	0.000051	1.452413
11	6	0	3.688031	0.000031	2.099425
12	1	0	3.636729	0.000031	3.186146
13	1	0	5.790191	0.000063	2.048002
14	1	0	5.861144	0.000024	-0.769069
15	1	0	3.537769	0.000022	-1.701454
16	1	0	1.209573	-0.000001	3.167759
17	1	0	-0.937235	0.000005	1.944326
18	1	0	-0.939023	0.000003	-0.540551

E_{Tot}: -389.442767914 Hartree

A1.6 – Spectral data relevant to Chapter 2.4

Figure A1.331: ^{1}H NMR ($CDCl_3$, 500.4 MHz) of 1-benzyl-2-(quinolin-6-yl)-2,1-borazaronaphthalene (**2.122**)

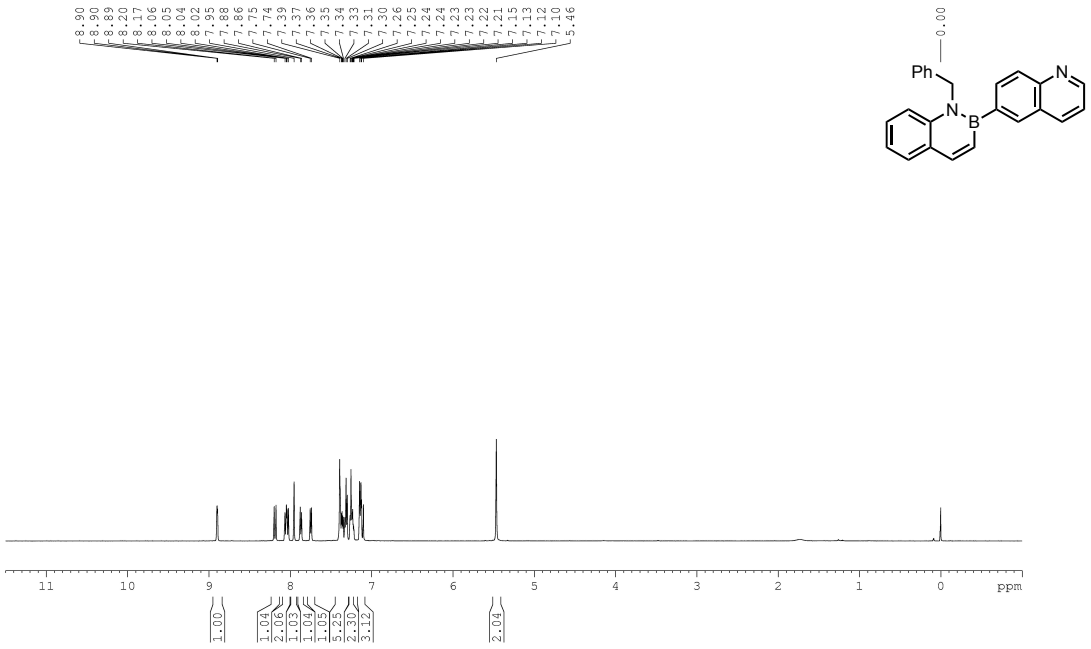

Figure A1.332: ^{13}C {^{1}H} NMR ($CDCl_3$, 125.8 MHz) of 1-benzyl-2-(quinolin-6-yl)-2,1-borazaronaphthalene (**2.122**)

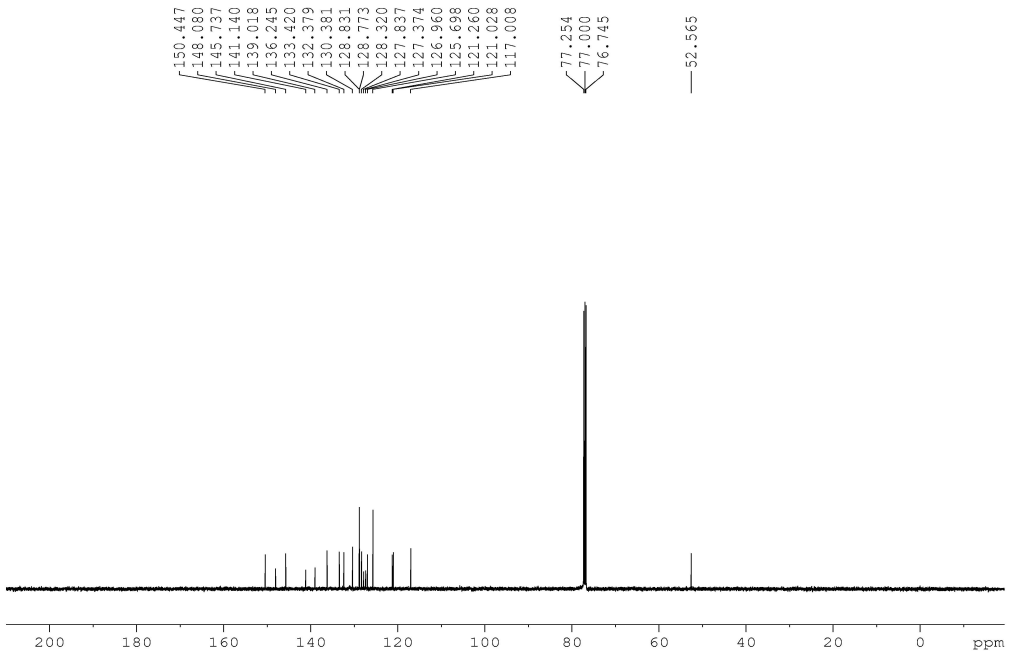

Figure A1.333: ^{11}B NMR ($CDCl_3$, 128.4 MHz) of 1-benzyl-2-(quinolin-6-yl)-2,1-borazaronaphthalene (**2.122**)

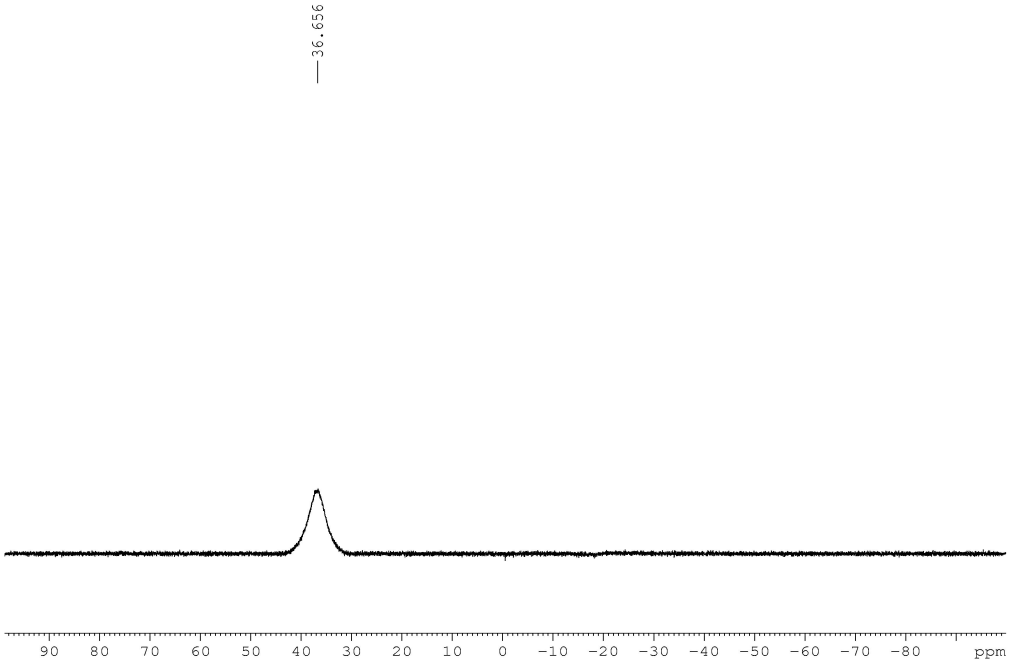

Figure A1.334: ^{1}H NMR ($CDCl_3$, 500.4 MHz) of 1-benzyl-2-(quinolin-3-yl)-2,1-borazaronaphthalene (**2.123**)

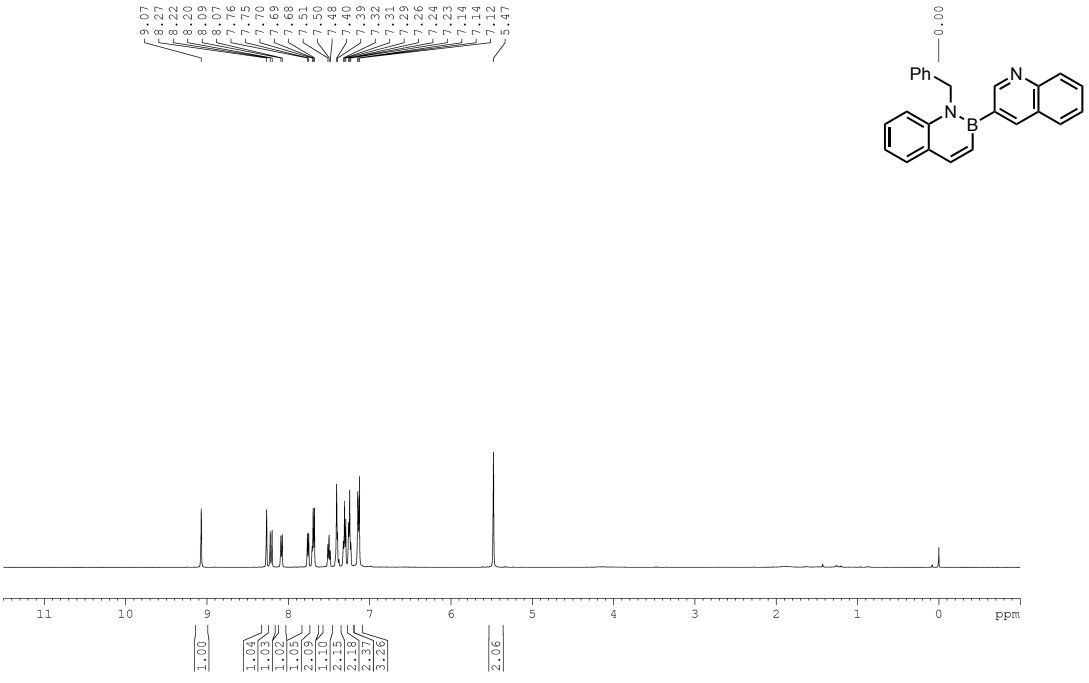

Figure A1.335: ^{13}C {^{1}H} NMR ($CDCl_3$, 125.8 MHz) of 1-benzyl-2-(quinolin-3-yl)-2,1-borazaronaphthalene (**2.123**)

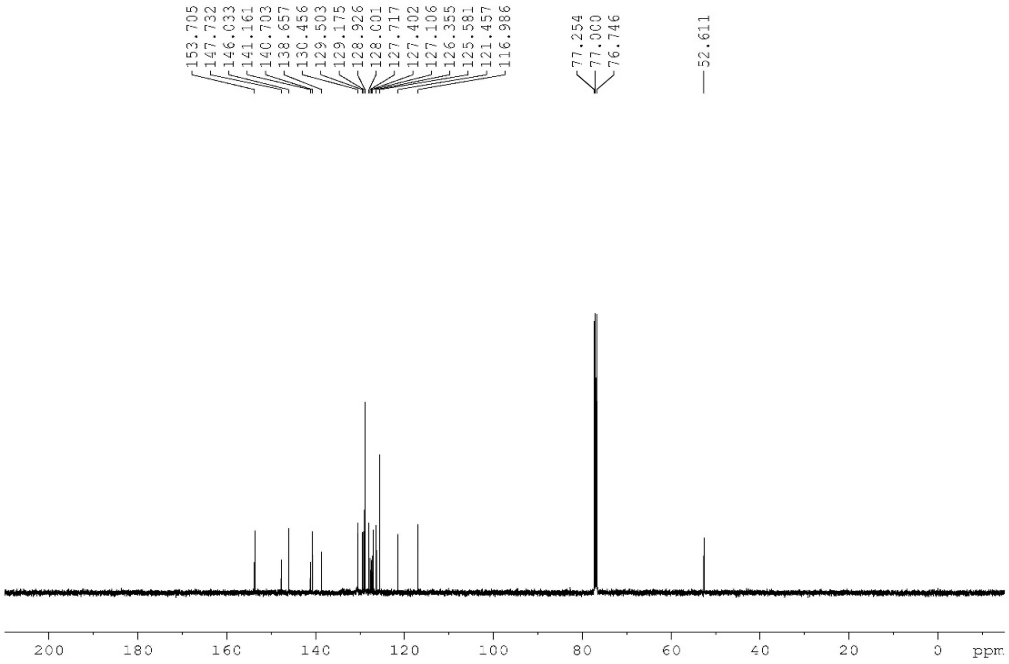

Figure A1.336: ^{11}B NMR ($CDCl_3$, 128.4 MHz) of 1-benzyl-2-(quinolin-3-yl)-2,1-borazaronaphthalene (**2.123**)

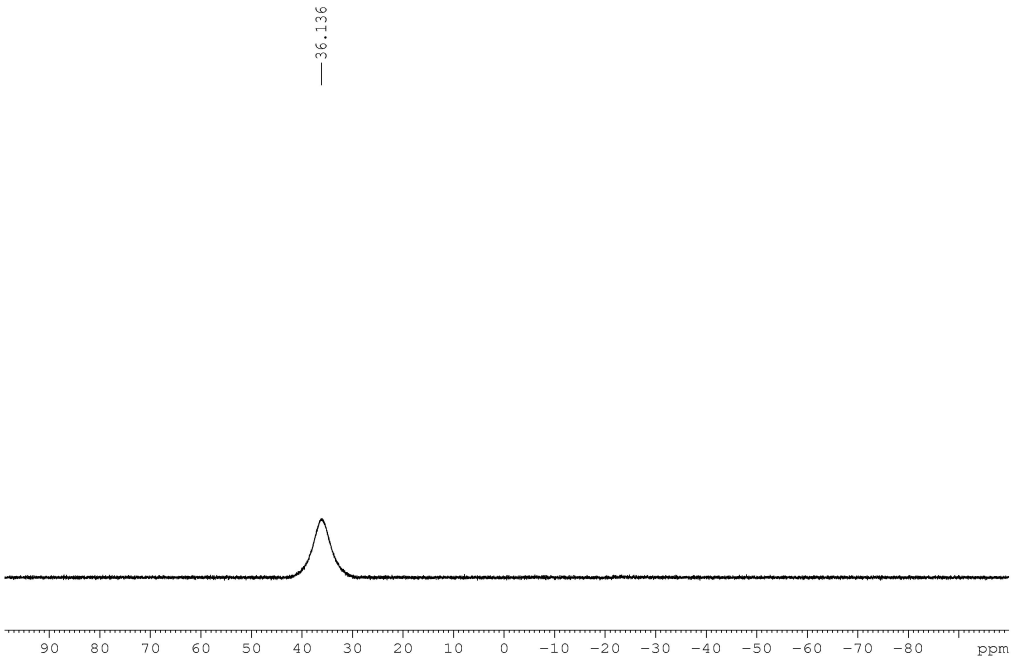

Figure A1.337: ^{1}H NMR ($CDCl_3$, 500.4 MHz) of 1-benzyl-2-(pyrimidin-5-yl)-2,1-borazaronaphthalene (**2.124**)

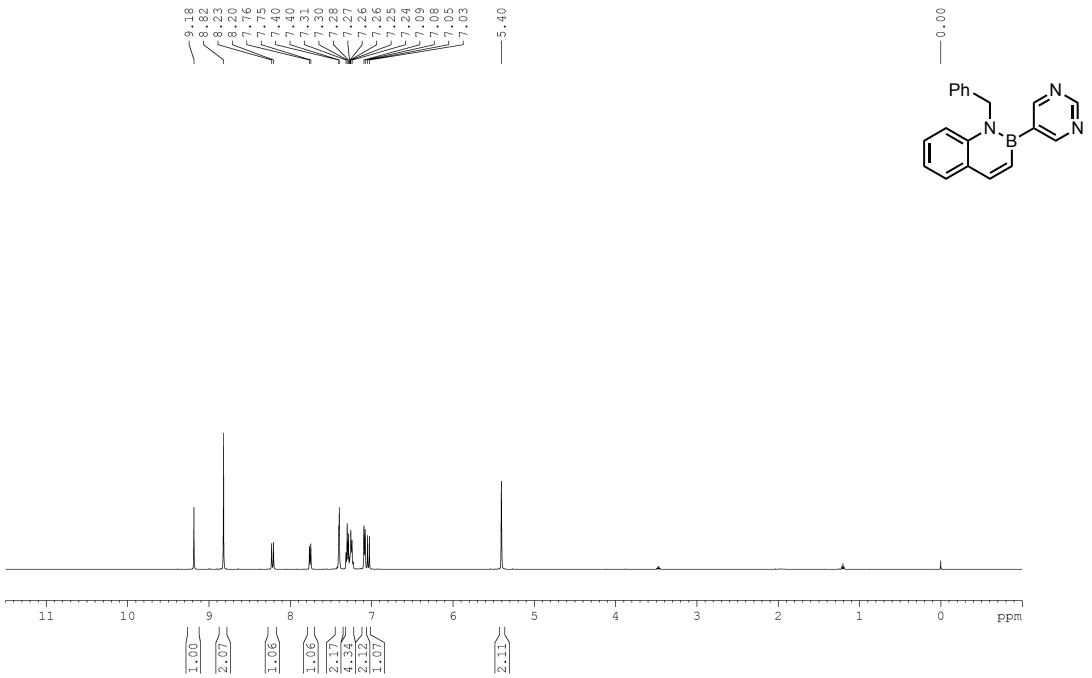

Figure A1.338: ^{13}C {^{1}H} NMR ($CDCl_3$, 125.8 MHz) of 1-benzyl-2-(pyrimidin-5-yl)-2,1-borazaronaphthalene (**2.124**)

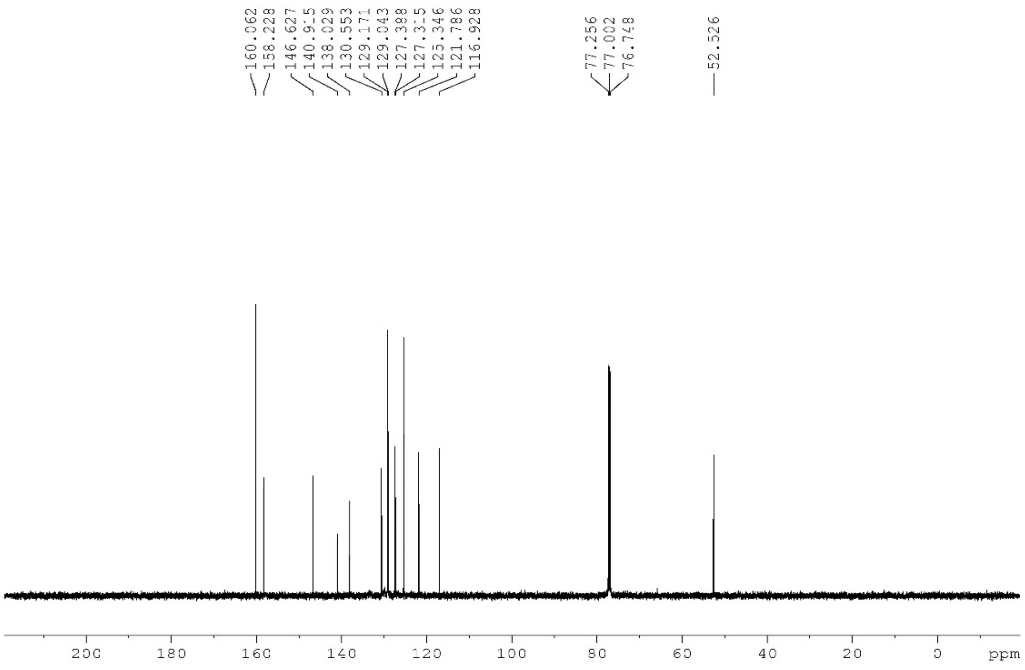

Figure A1.339: ^{11}B NMR ($CDCl_3$, 128.4 MHz) of 1-benzyl-2-(pyrimidin-5-yl)-2,1-borazaronaphthalene (**2.124**)

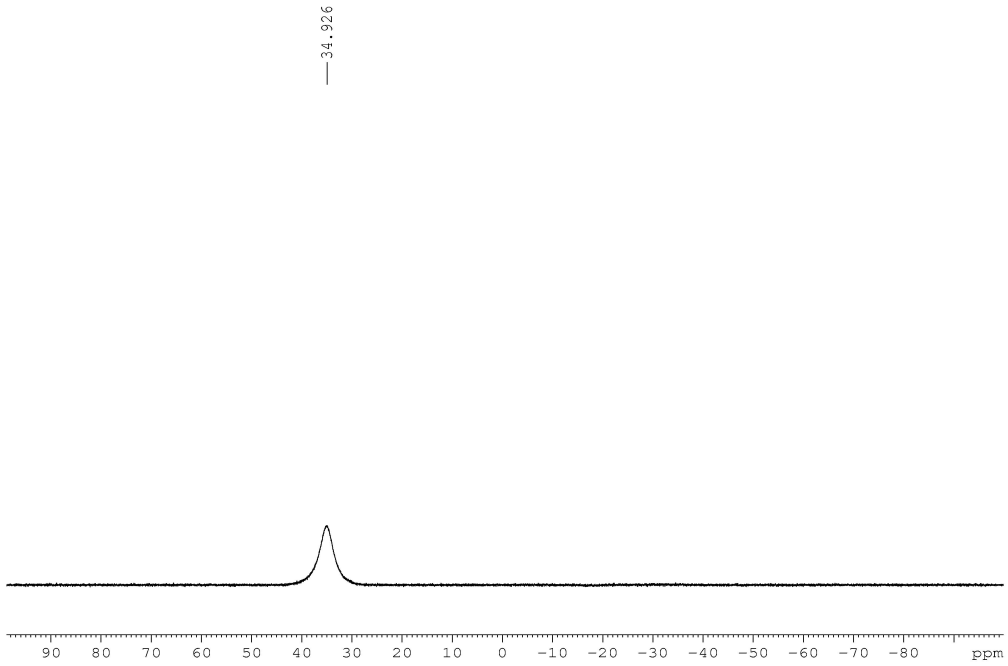

Figure A1.340: ^{1}H NMR ($CDCl_3$, 500.4 MHz) of 1-benzyl-2-(6-fluoropyridin-3-yl)-2,1-borazaronaphthalene (**2.125**)

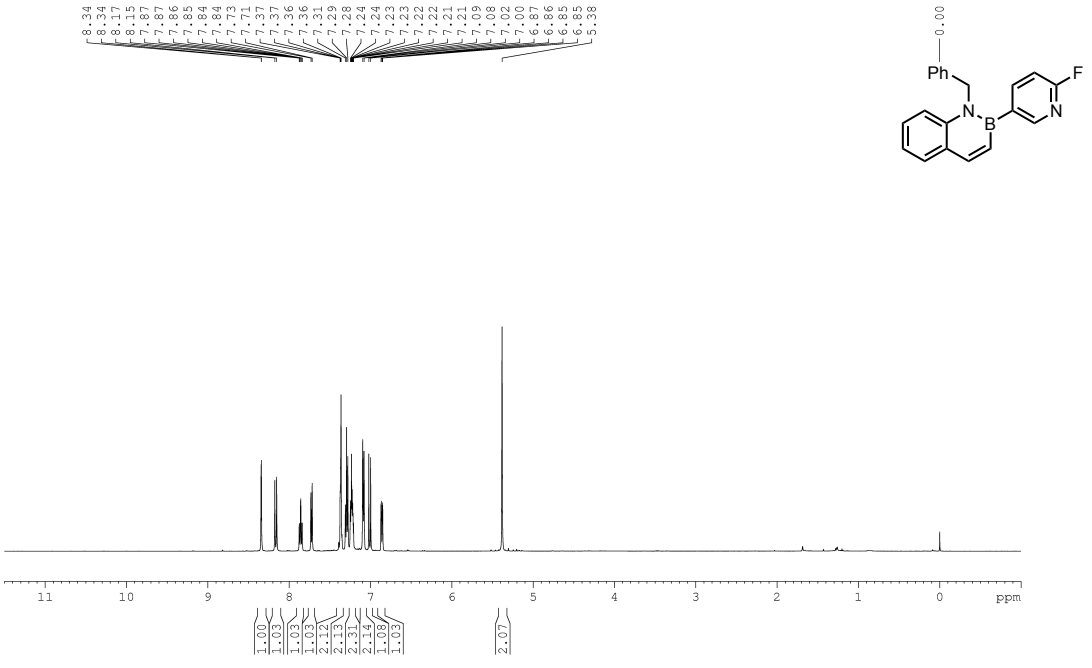

Figure A1.341: ^{13}C {^{1}H} NMR ($CDCl_3$, 125.8 MHz) of 1-benzyl-2-(6-fluoropyridin-3-yl)-2,1-borazaronaphthalene (**2.125**)

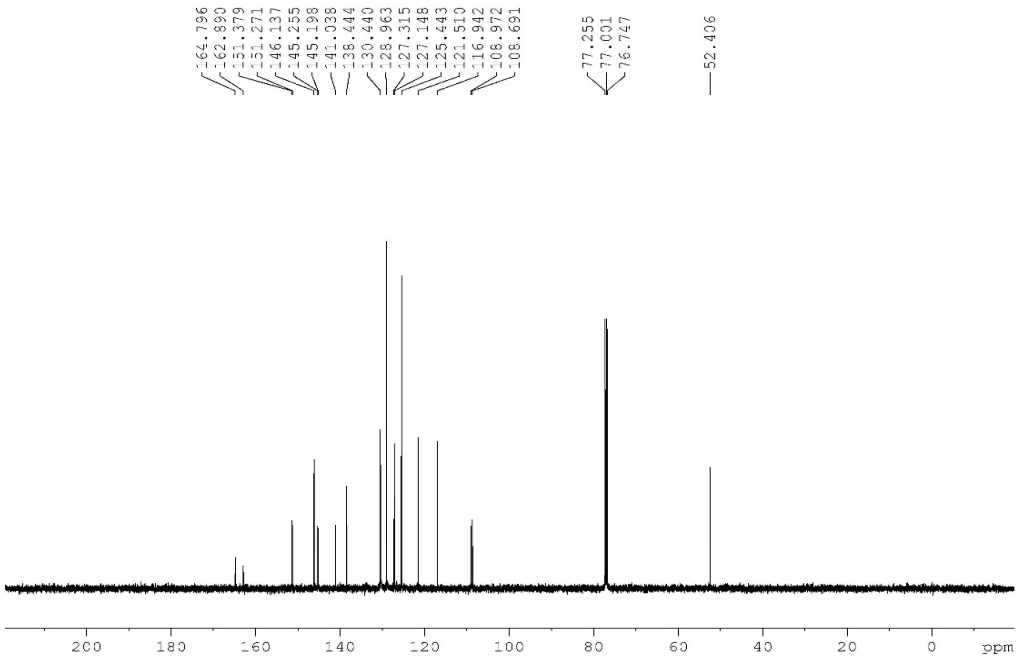

Figure A1.342: ^{19}F {^{1}H} NMR ($CDCl_3$, 470.8 MHz) of 1-benzyl-2-(6-fluoropyridin-3-yl)-2,1-borazaronaphthalene (**2.125**)

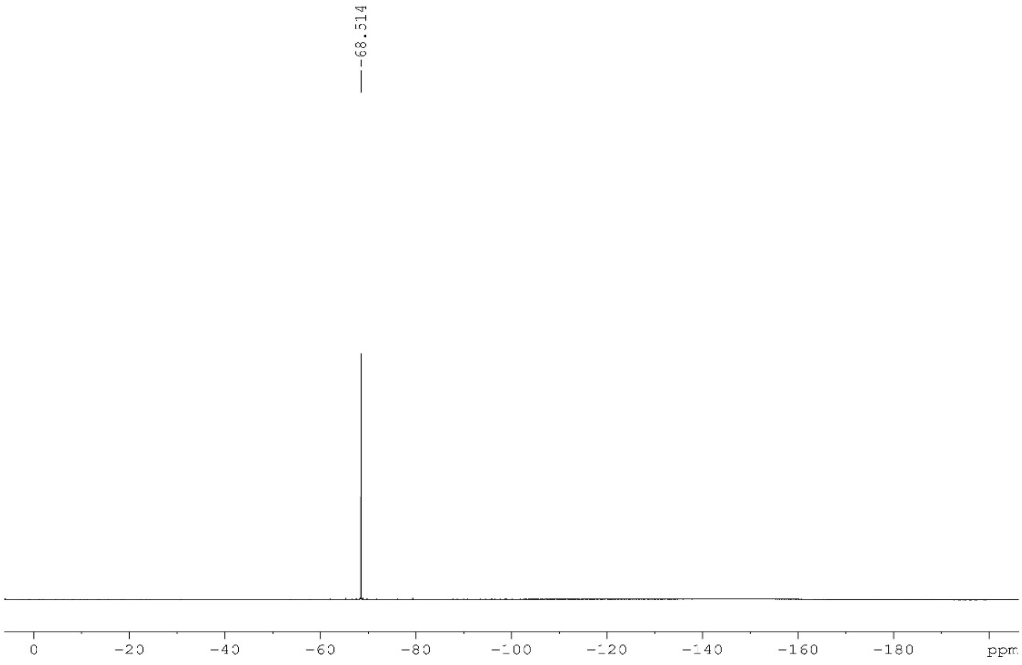

Figure A1.343: ^{11}B NMR ($CDCl_3$, 128.4 MHz) of 1-benzyl-2-(6-fluoropyridin-3-yl)-2,1-borazaronaphthalene (**2.125**)

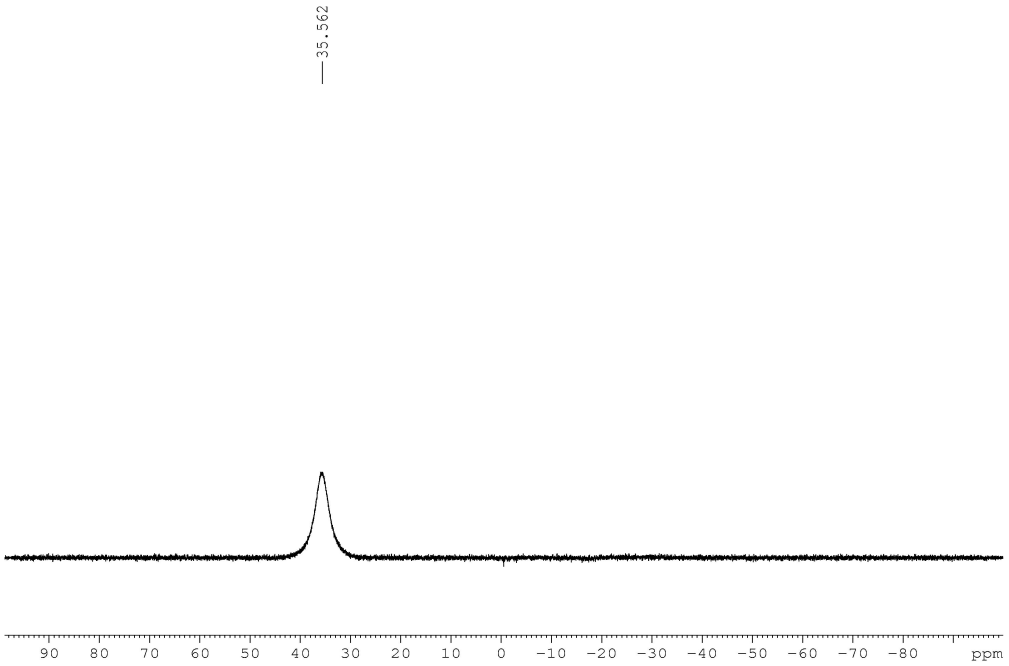

Figure A1.344: ^{1}H NMR ($CDCl_3$, 500.4 MHz) of 1-benzyl-2-(2-fluoropyridin-3-yl)-2,1-borazaronaphthalene (**2.126**)

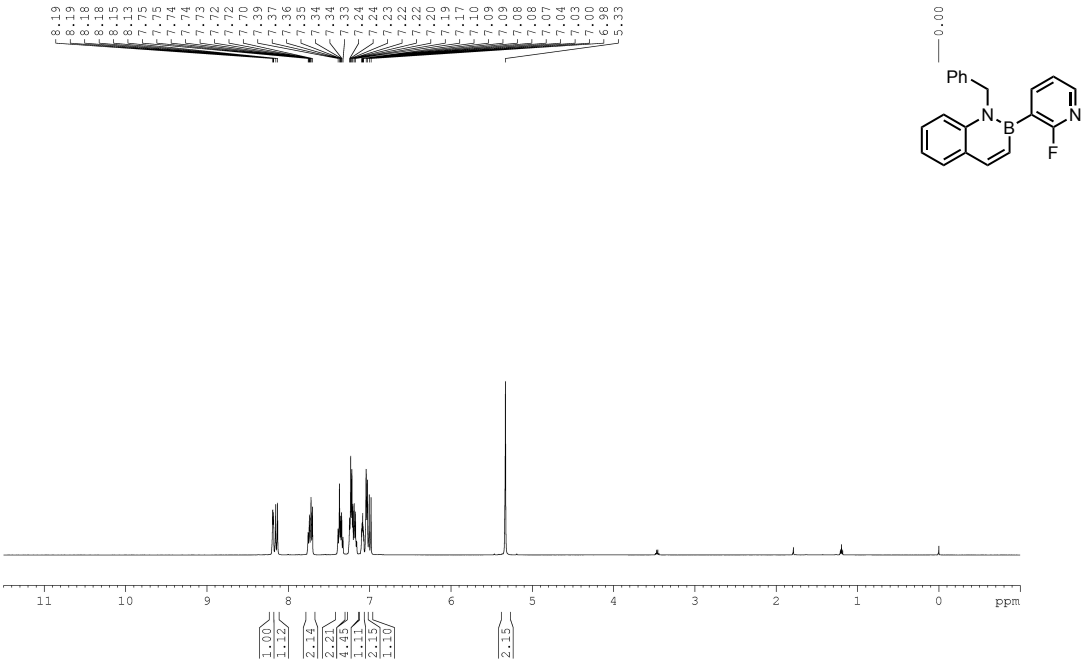

Figure A1.345: ^{13}C {^{1}H} NMR ($CDCl_3$, 125.8 MHz) of 1-benzyl-2-(2-fluoropyridin-3-yl)-2,1-borazaronaphthalene (**2.126**)

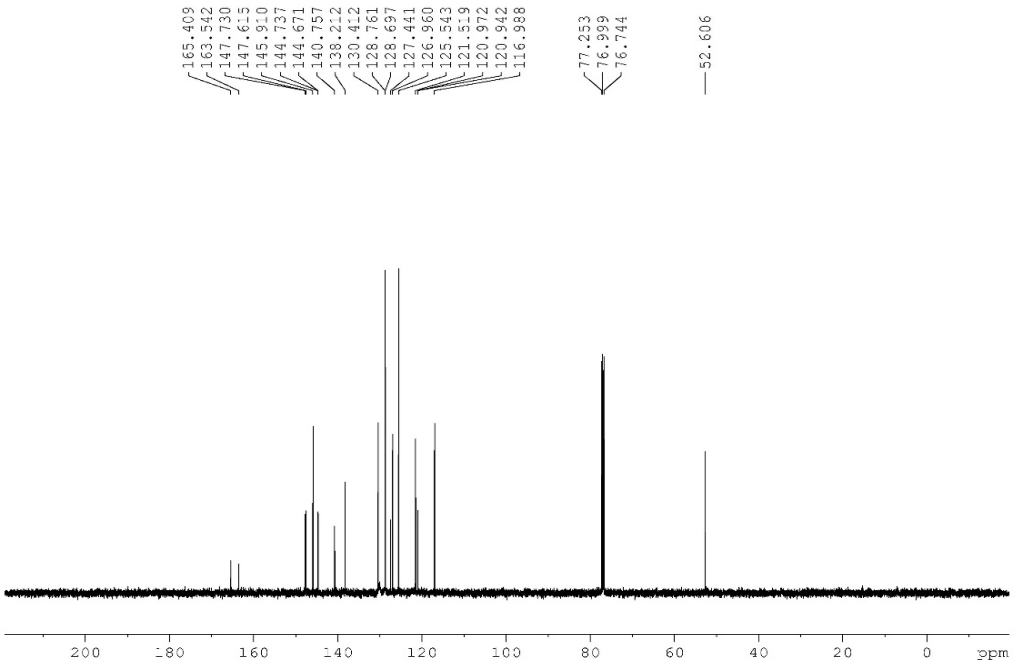

Figure A1.346: ^{19}F {^{1}H} NMR ($CDCl_3$, 470.8 MHz) of 1-benzyl-2-(2-fluoropyridin-3-yl)-2,1-borazaronaphthalene (**2.126**)

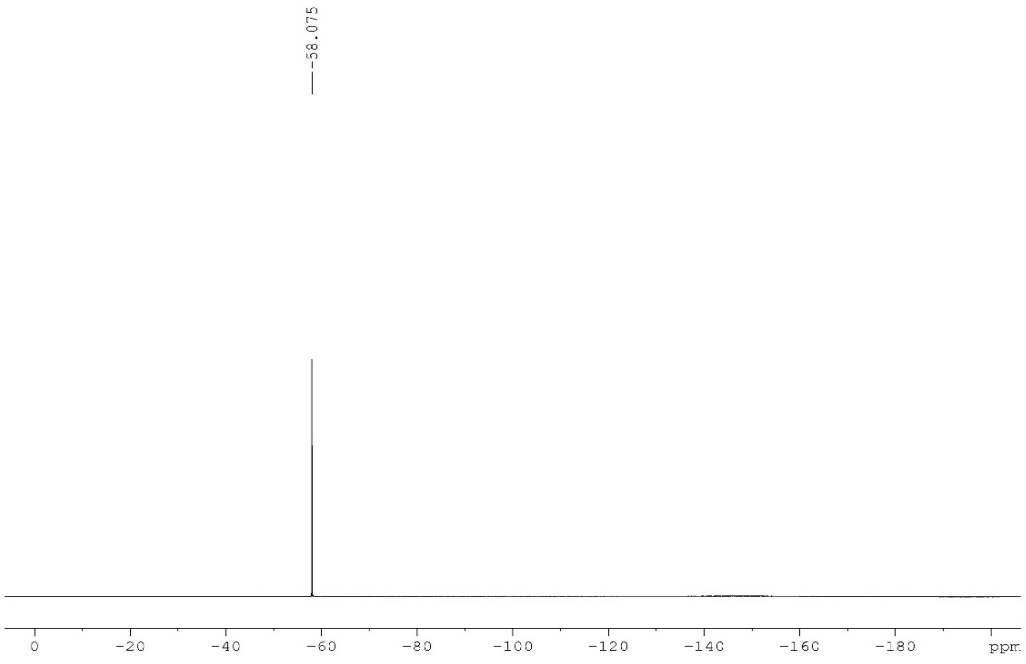

Figure A1.347: ^{11}B NMR ($CDCl_3$, 128.4 MHz) of 1-benzyl-2-(2-fluoropyridin-3-yl)-2,1-borazaronaphthalene (**2.126**)

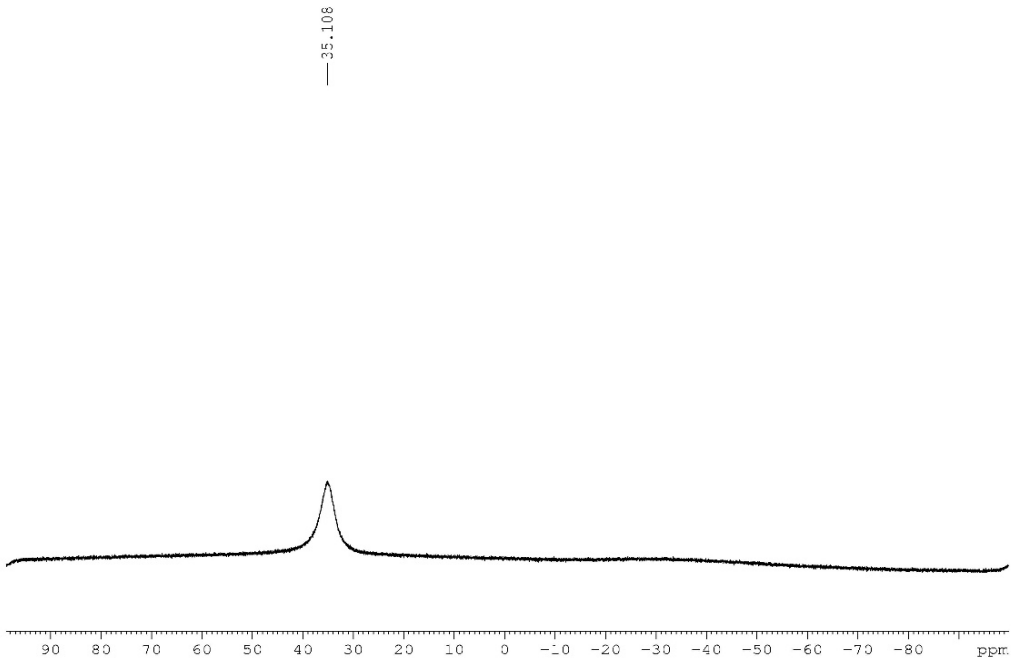

Figure A1.348: ^{1}H NMR ($CDCl_3$, 500.4 MHz) of 1-benzyl-2-(4-(N,N-dimethylamino)pyridin-5-yl)-2,1-borazaronaphthalene (**2.127**)

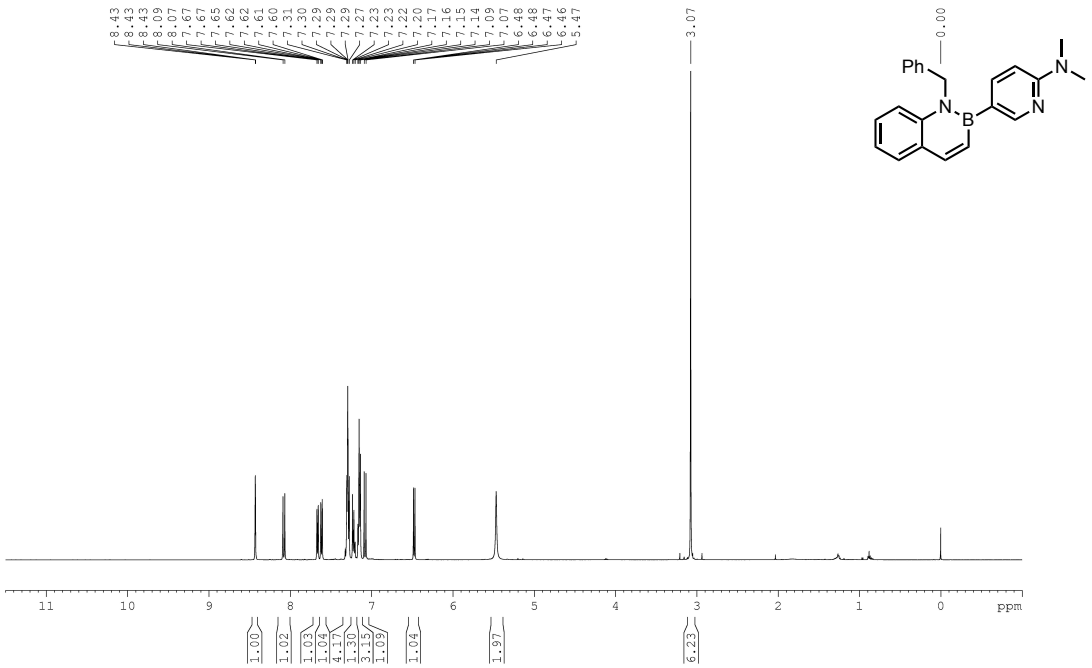

Figure A1.349: ^{13}C {^{1}H} NMR ($CDCl_3$, 125.8 MHz) of 1-benzyl-2-(4-(N,N-dimethylamino)pyridin-5-yl)-2,1-borazaronaphthalene (**2.127**)

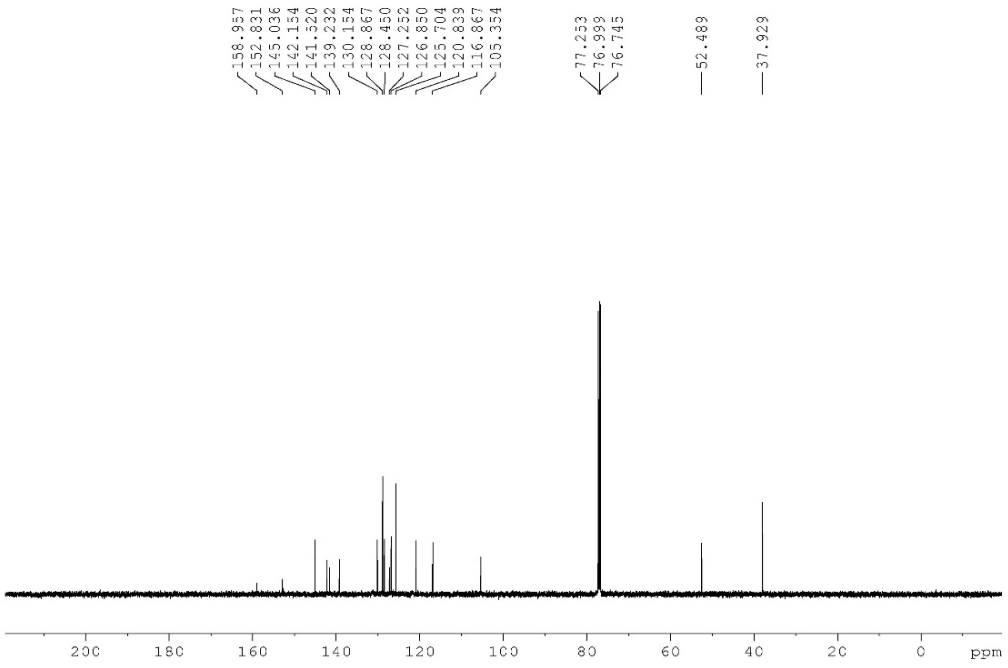

Figure A1.350: ^{11}B NMR ($CDCl_3$, 128.4 MHz) of 1-benzyl-2-(4-(N,N-dimethylamino)pyridin-5-yl)-2,1-borazaronaphthalene (**2.127**)

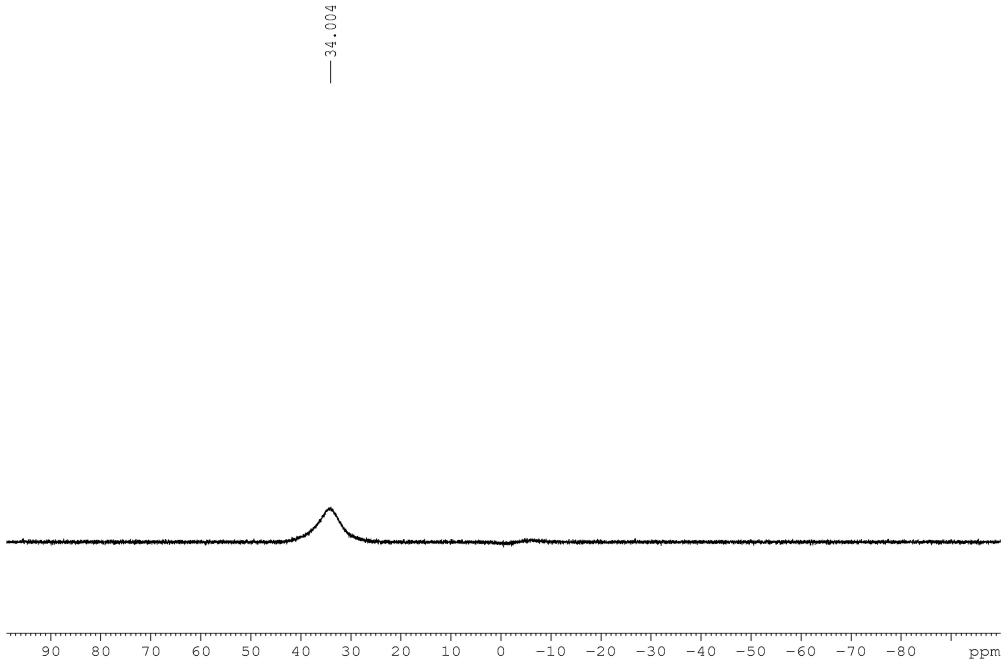

Figure A1.351: ^{1}H NMR ($CDCl_3$, 500.4 MHz) of 1-benzyl-2-(1-methyl-*1H*-pyrazol-4-yl)-2,1-borazaronaphthalene (**2.128**)

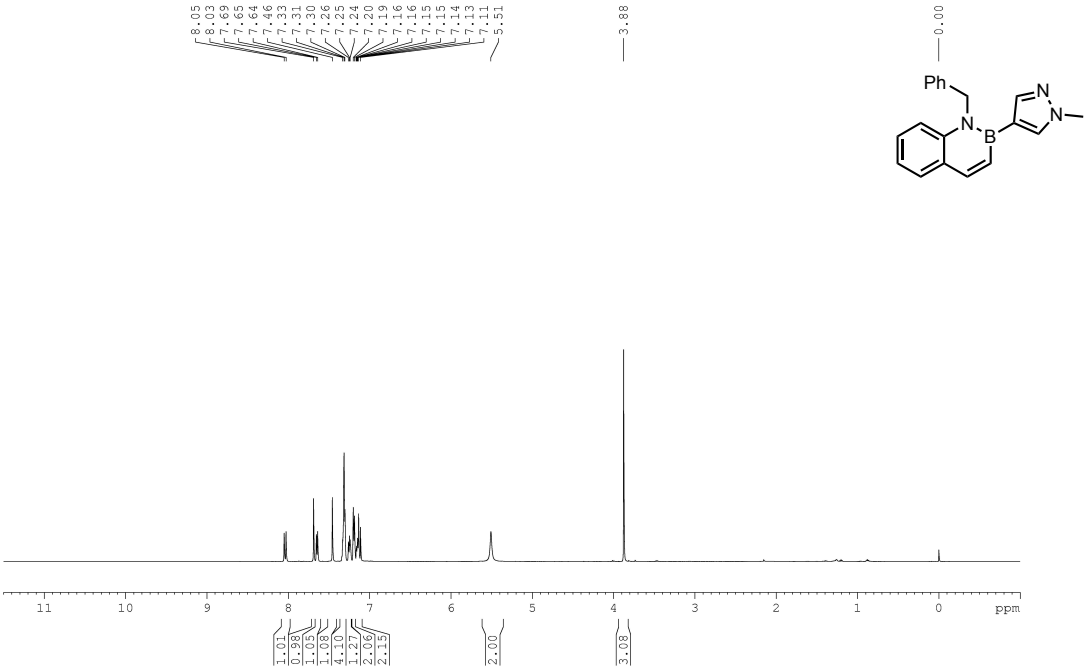

Figure A1.352: ^{13}C {^{1}H} NMR ($CDCl_3$, 125.8 MHz) of 1-benzyl-2-(1-methyl-*1H*-pyrazol-4-yl)-2,1-borazaronaphthalene (**2.128**)

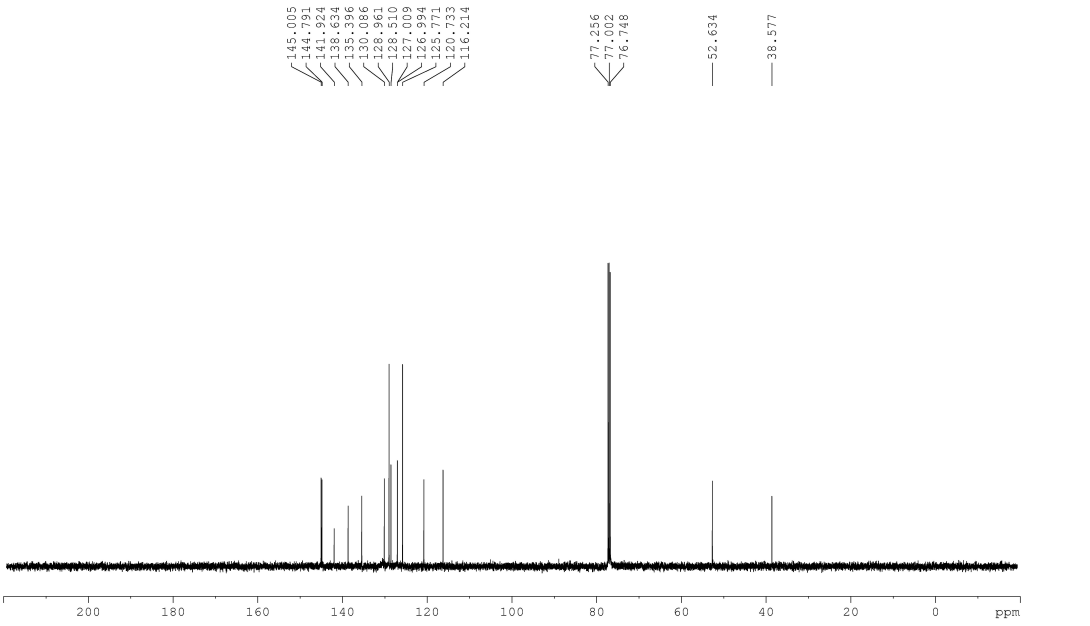

Figure A1.353: ^{11}B NMR ($CDCl_3$, 128.4 MHz) of 1-benzyl-2-(1-methyl-1H-pyrazol-4-yl)-2,1-borazaronaphthalene (**2.128**)

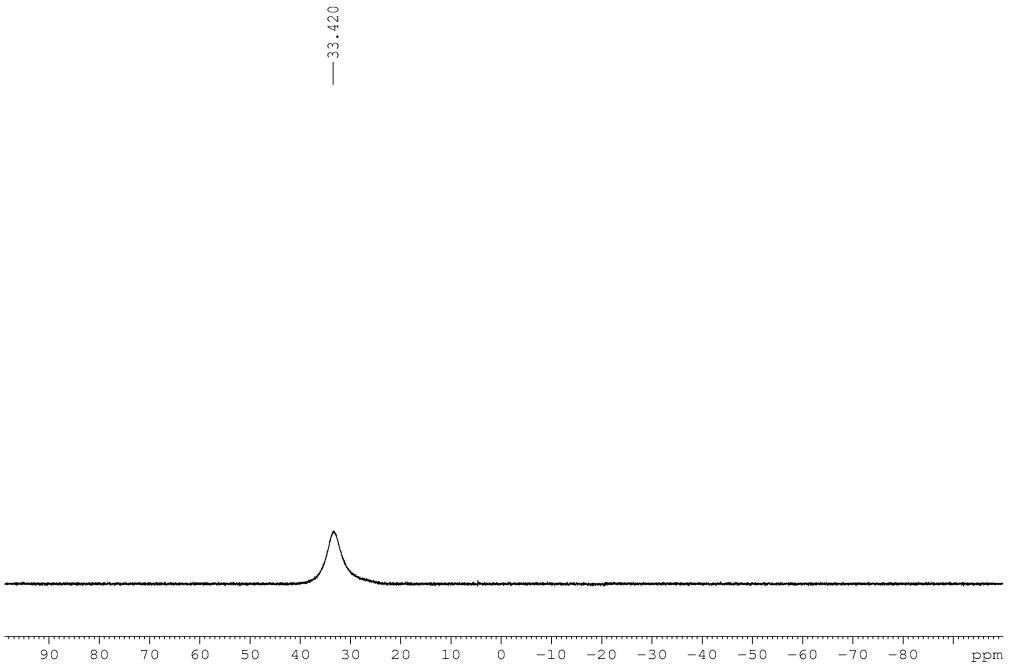

Figure A1.354: ^{1}H NMR ($CDCl_3$, 500.4 MHz) of 1-benzyl-2-(3,5-dimethylisoxazole-4-yl)-2,1-borazaronaphthalene (**2.129**)

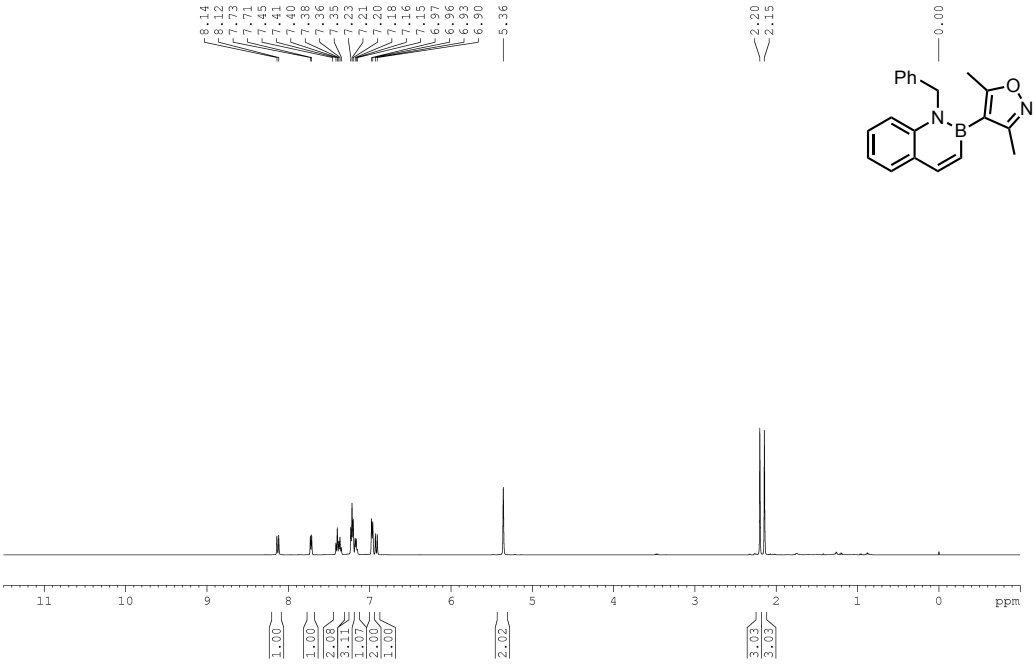

Figure A1.355: ^{13}C {^{1}H} NMR ($CDCl_3$, 125.8 MHz) of 1-benzyl-2-(3,5-dimethylisoxazole-4-yl)-2,1-borazaronaphthalene (**2.129**)

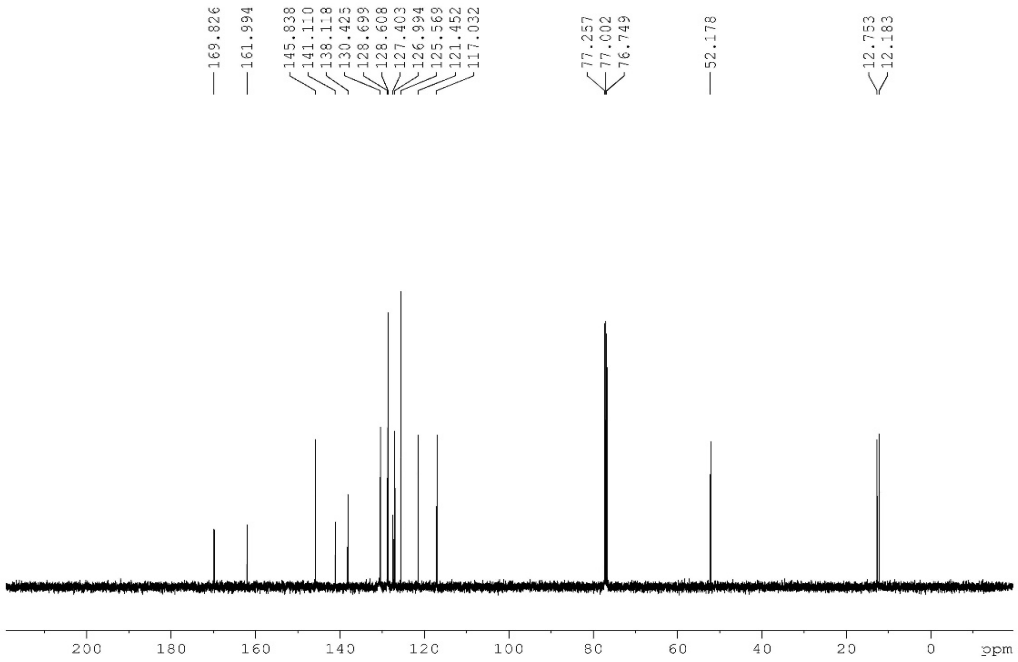

Figure A1.356: ^{11}B NMR ($CDCl_3$, 128.4 MHz) of 1-benzyl-2-(3,5-dimethylisoxazole-4-yl)-2,1-borazaronaphthalene (**2.129**)

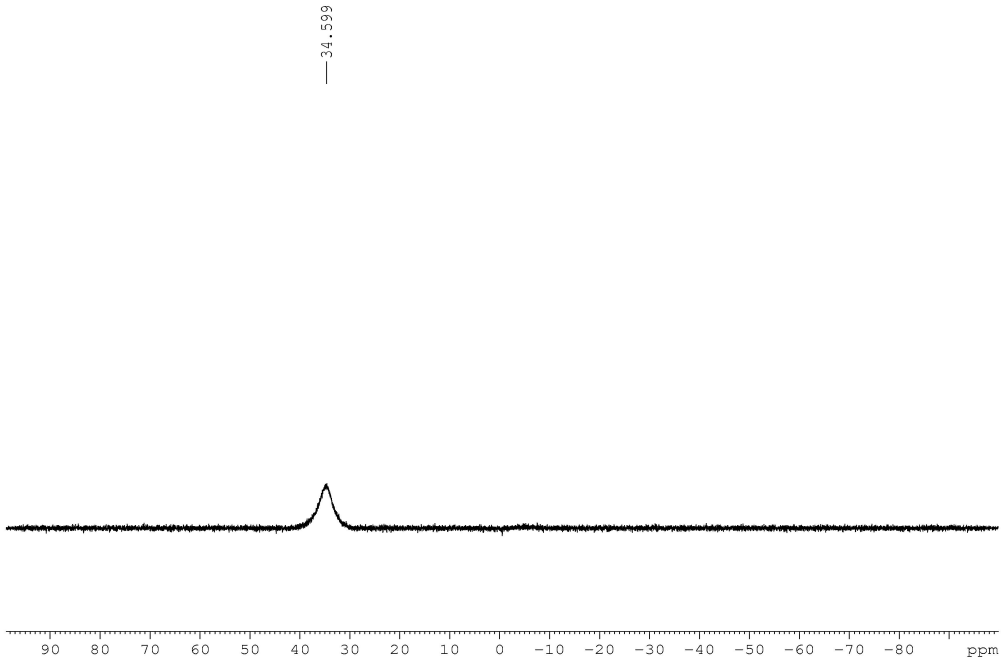

Figure A1.357: ^{1}H NMR ($CDCl_3$, 500.4 MHz) of 1-benzyl-2-(1-(phenylsulfonyl)-1H-indol-3-yl)-2,1-borazaronaphthalene (**2.130**)

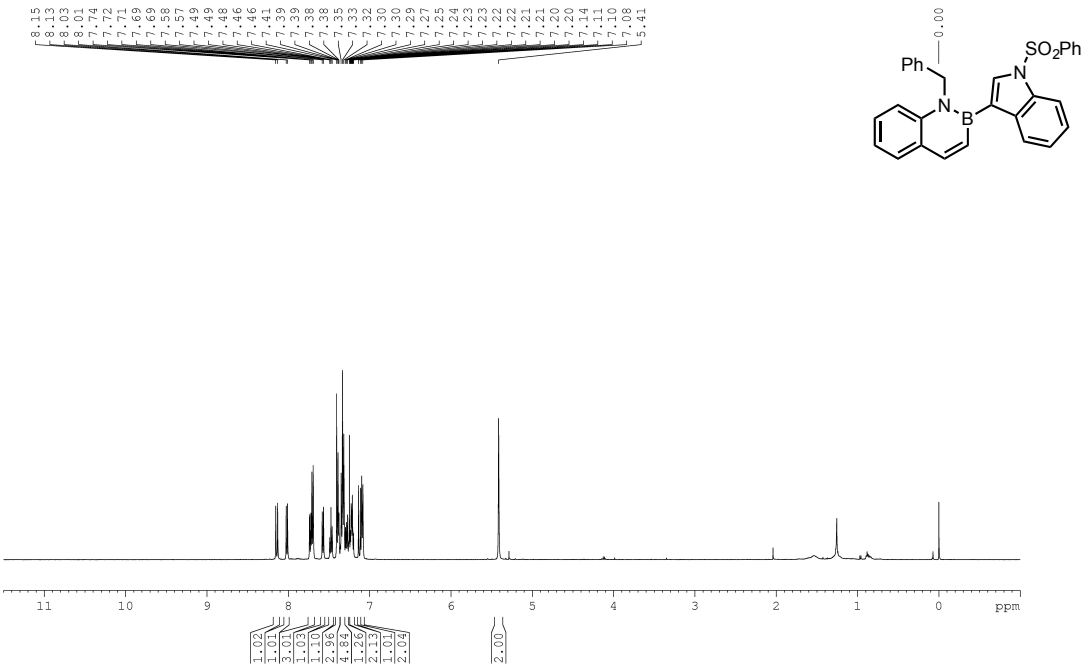

Figure A1.358: ^{13}C {^{1}H} NMR ($CDCl_3$, 125.8 MHz) of 1-benzyl-2-(1-(phenylsulfonyl)-1H-indol-3-yl)-2,1-borazaronaphthalene (**2.130**)

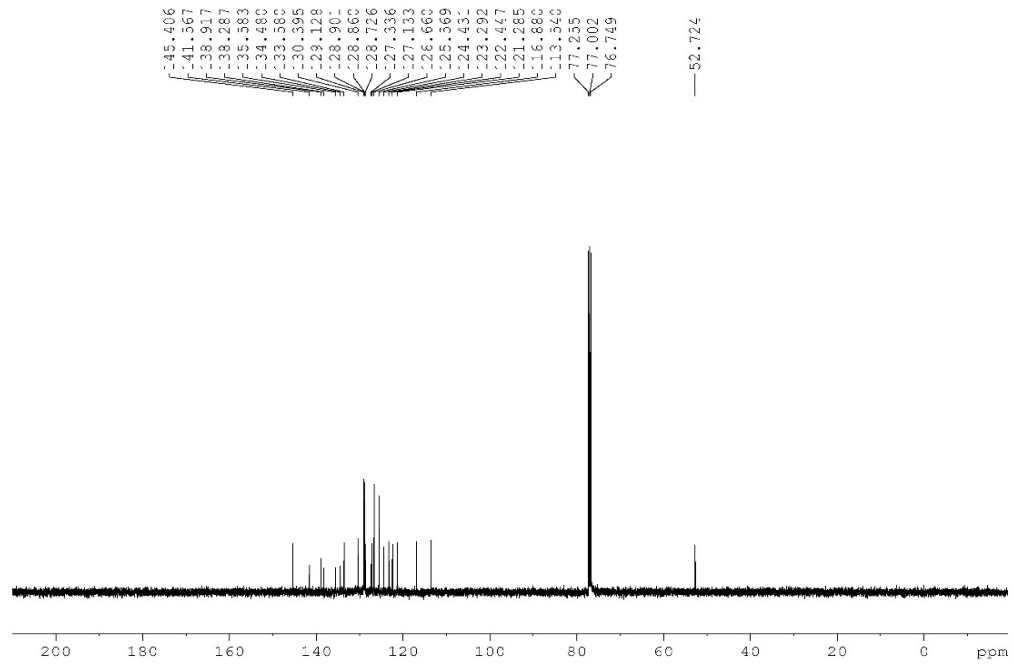

Figure A1.359: ^{11}B NMR ($CDCl_3$, 128.4 MHz) of 1-benzyl-2-(1-(phenylsulfonyl)-1H-indol-3-yl)-2,1-borazaronaphthalene (**2.130**)

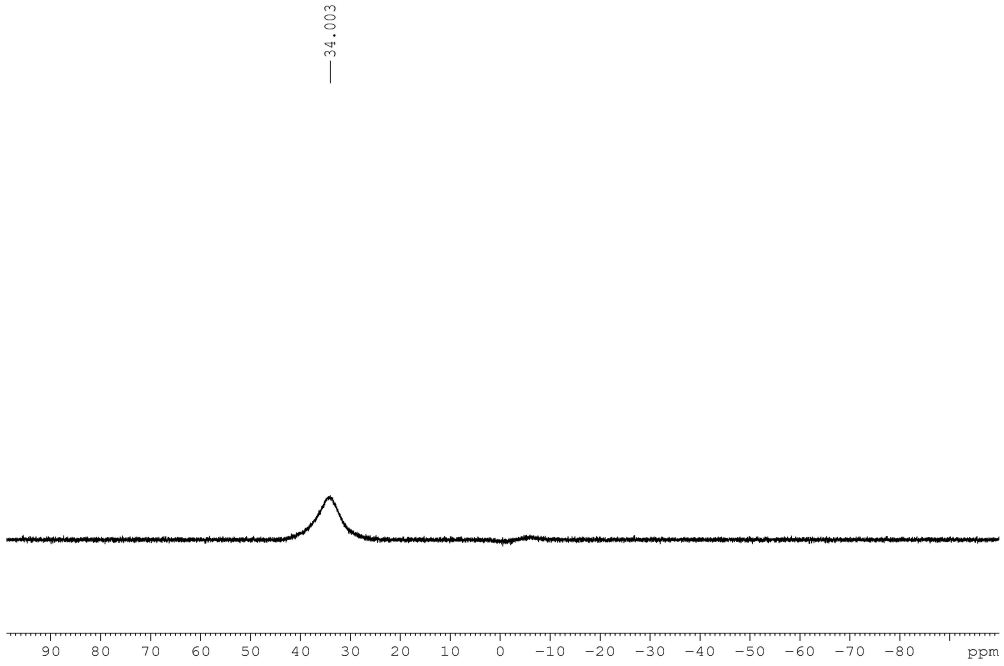

Figure A1.360: ^{1}H NMR ($CDCl_3$, 500.4 MHz) of 1-methyl-2-(quinolin-6-yl)-2,1-borazaronaphthalene (**2.131**)

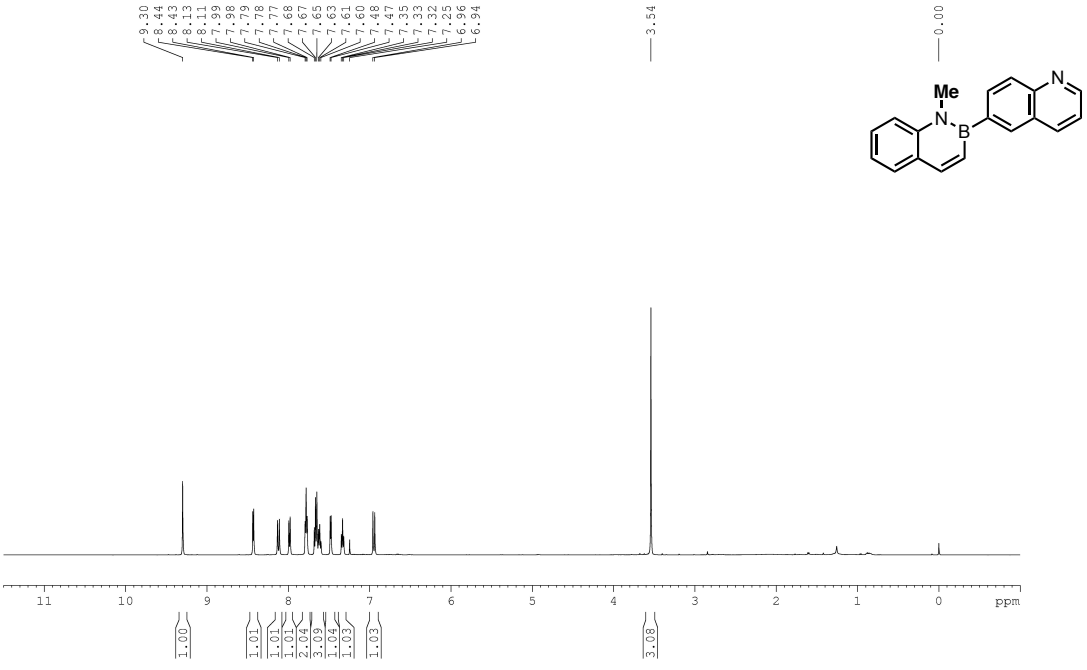

Figure A1.361: ^{13}C {^{1}H} NMR ($CDCl_3$, 125.8 MHz) of 1-methyl-2-(quinolin-6-yl)-2,1-borazaronaphthalene (**2.131**)

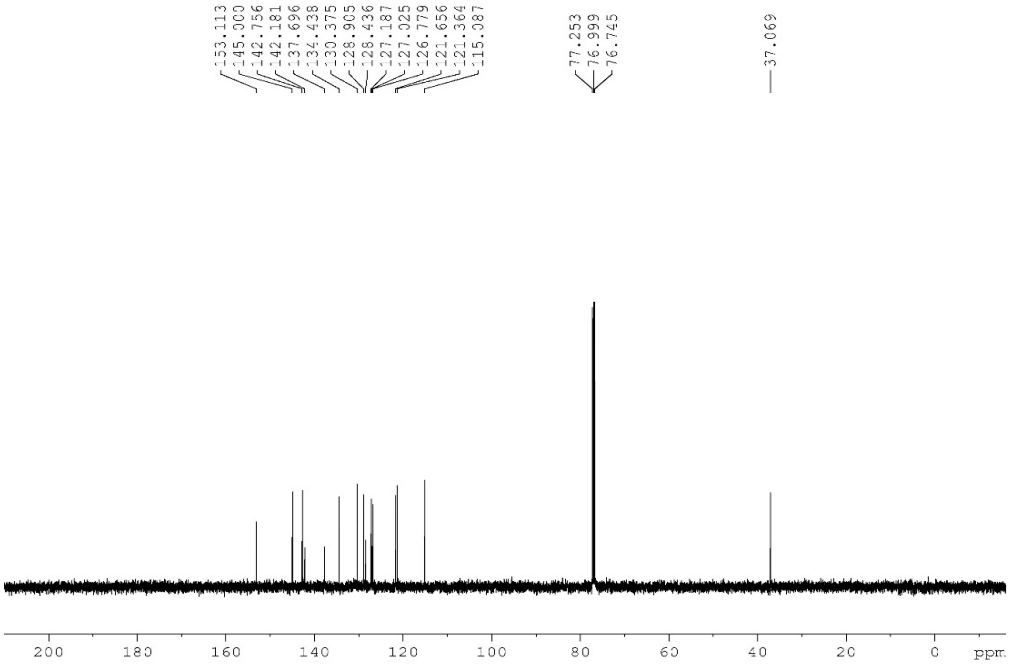

Figure A1.362: ^{11}B NMR ($CDCl_3$, 128.4 MHz) of 1-methyl-2-(quinolin-6-yl)-2,1-borazaronaphthalene (**2.131**) ‘

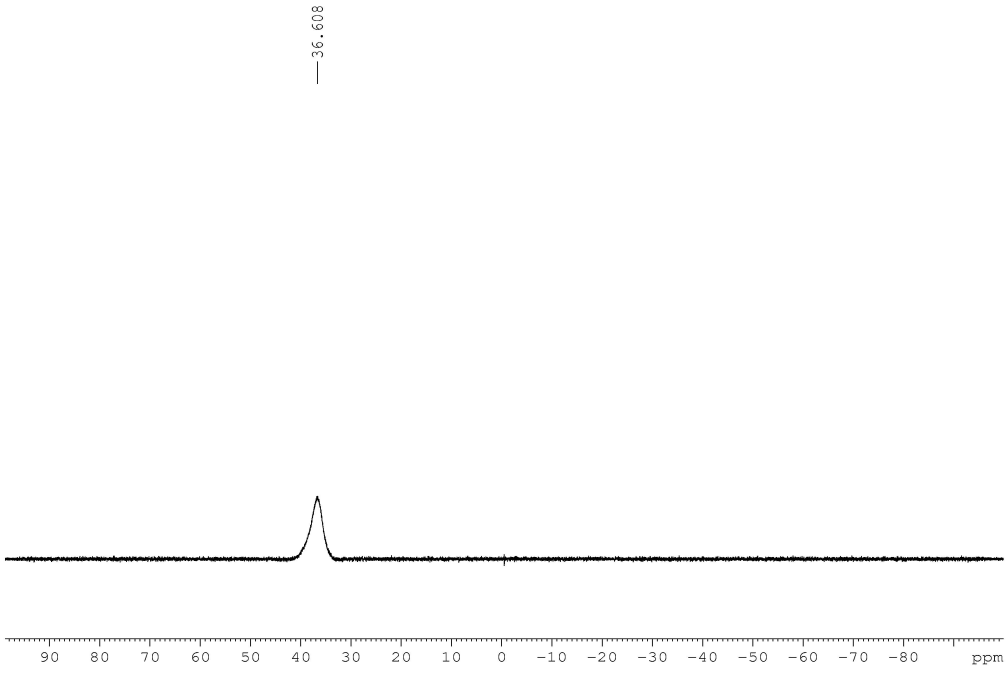

Figure A1.363: ^{1}H NMR ($CDCl_3$, 500.4 MHz) of 1-methyl-2-(quinolin-3-yl)-2,1-borazaronaphthalene (**2.132**)

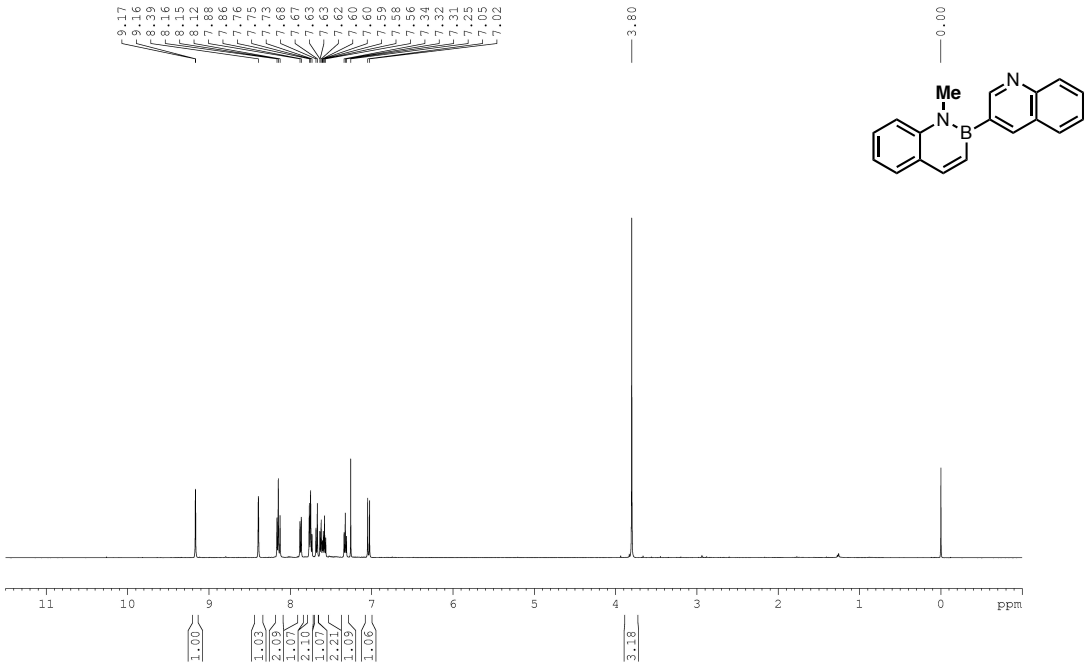

Figure A1.364: ^{13}C {^{1}H} NMR ($CDCl_3$, 125.8 MHz) of 1-methyl-2-(quinolin-3-yl)-2,1-borazaronaphthalene (**2.132**)

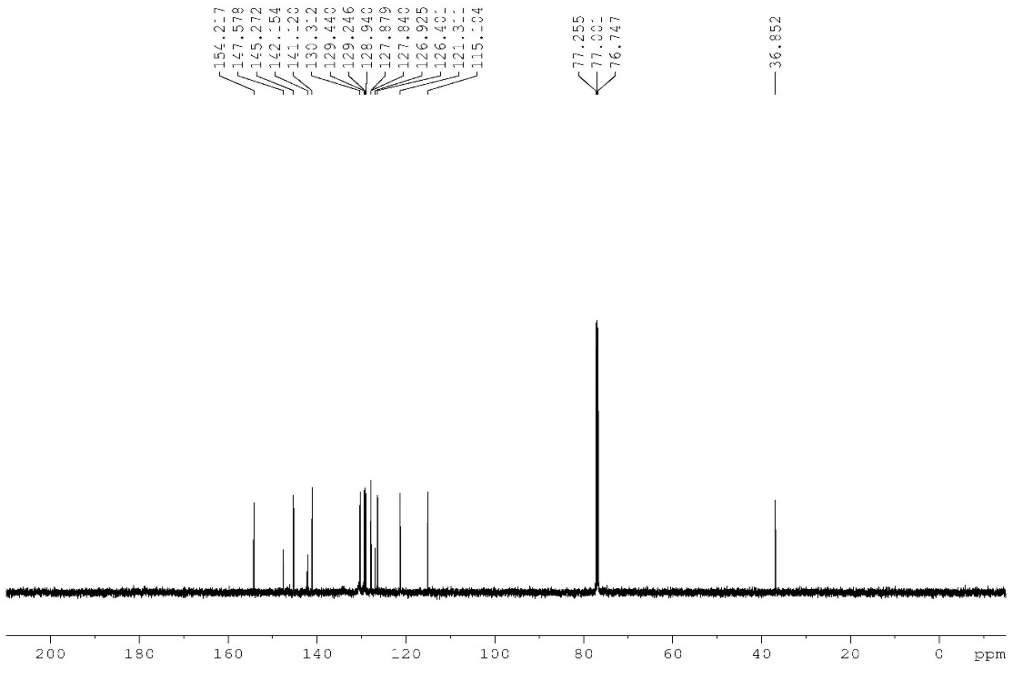

Figure A1.365: ^{11}B NMR ($CDCl_3$, 128.4 MHz) of 1-methyl-2-(quinolin-3-yl)-2,1-borazaronaphthalene (**2.132**)

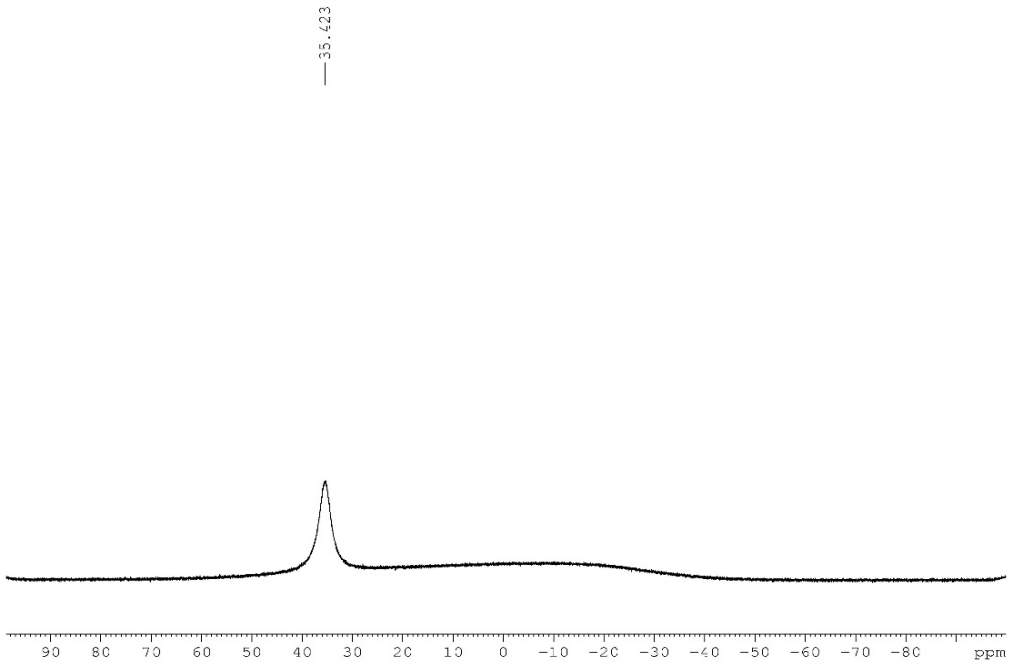

Figure A1.366: ^{1}H NMR ($CDCl_3$, 500.4 MHz) of 2-(isoquinolin-5-yl)-1-methyl-2,1-borazaronaphthalene (**2.132**)

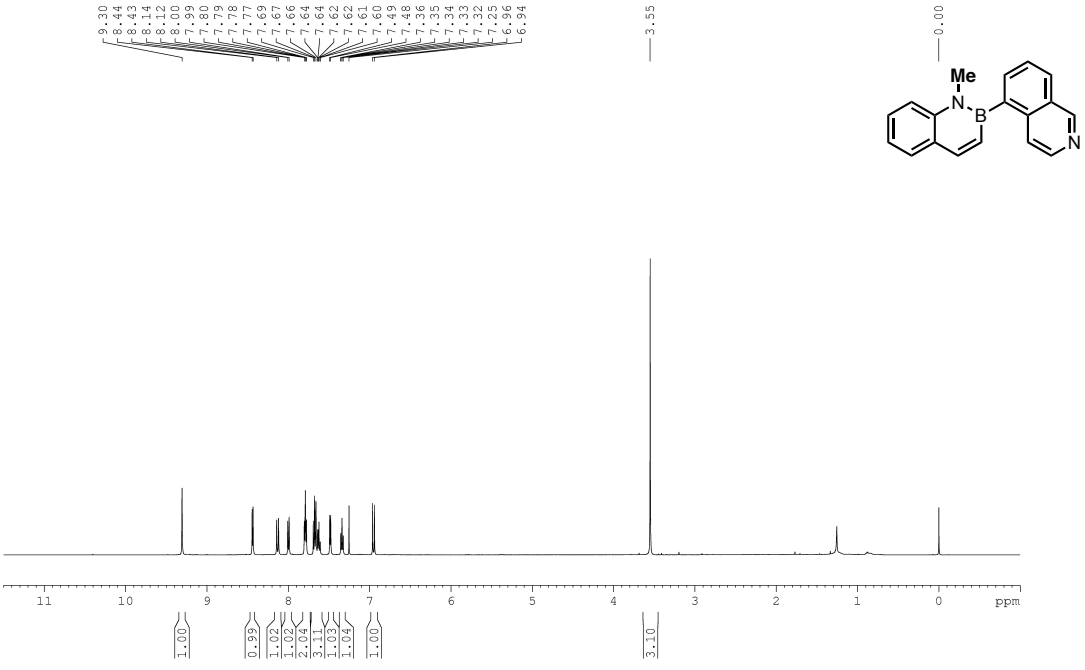

Figure A1.367: ^{13}C {^{1}H} NMR ($CDCl_3$, 125.8 MHz) of 2-(isoquinolin-5-yl)-1-methyl-2,1-borazaronaphthalene (**2.133**)

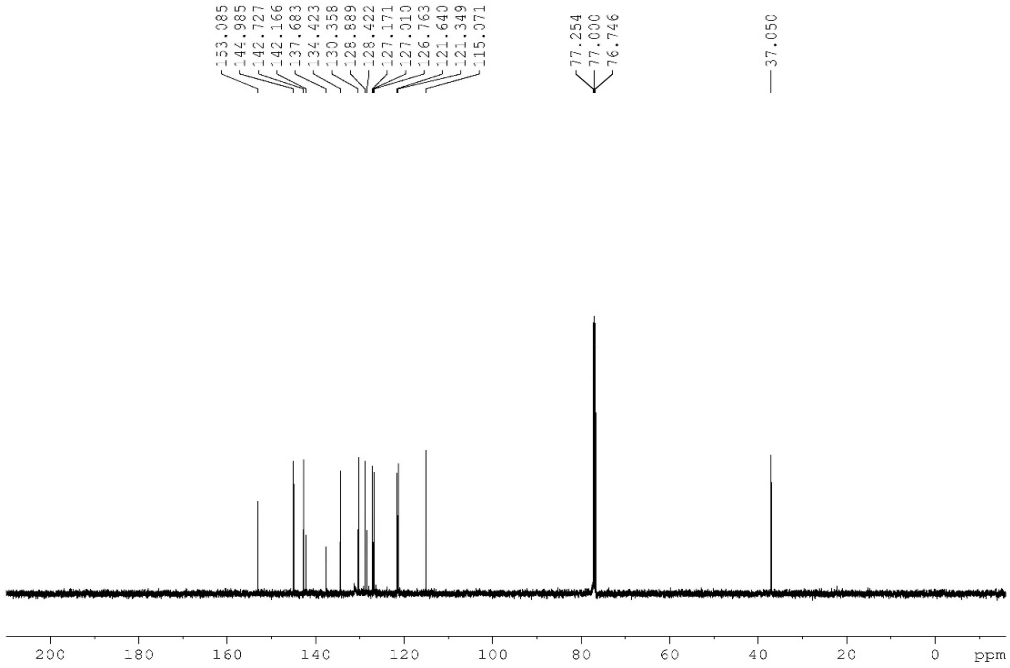

Figure A1.368: ^{11}B NMR ($CDCl_3$, 128.4 MHz) of 2-(isoquinolin-5-yl)-1-methyl-2,1-borazaronaphthalene (**2.133**)

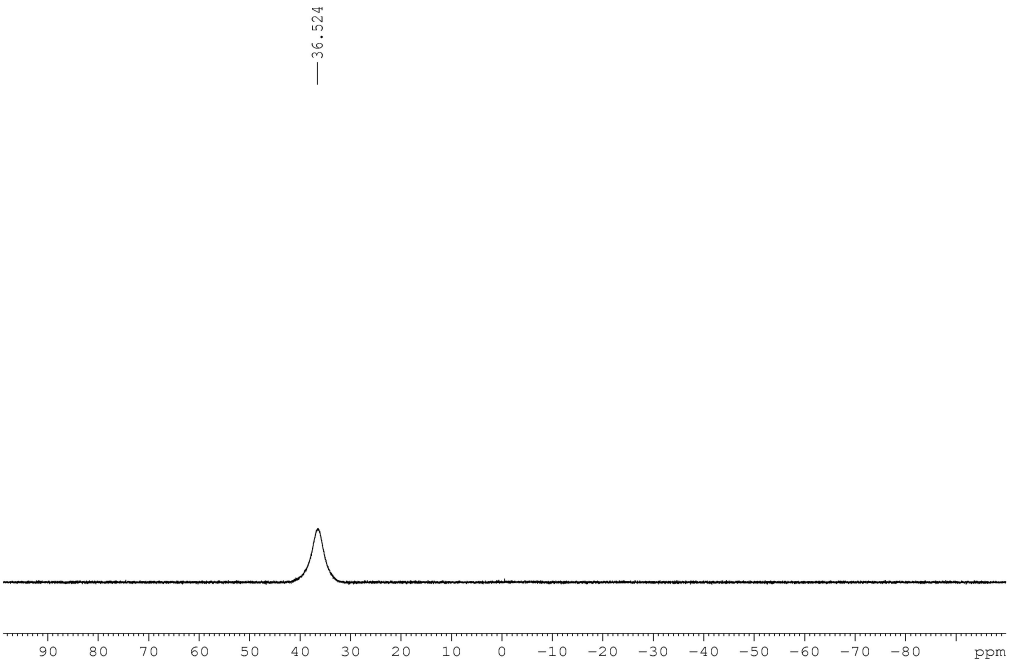

Figure A1.369: H NMR ($CDCl_3$, 500.4 MHz) of 2-(6-fluoropyridin-3-yl)-1-methyl-2,1-borazaronaphthalene (**2.134**)

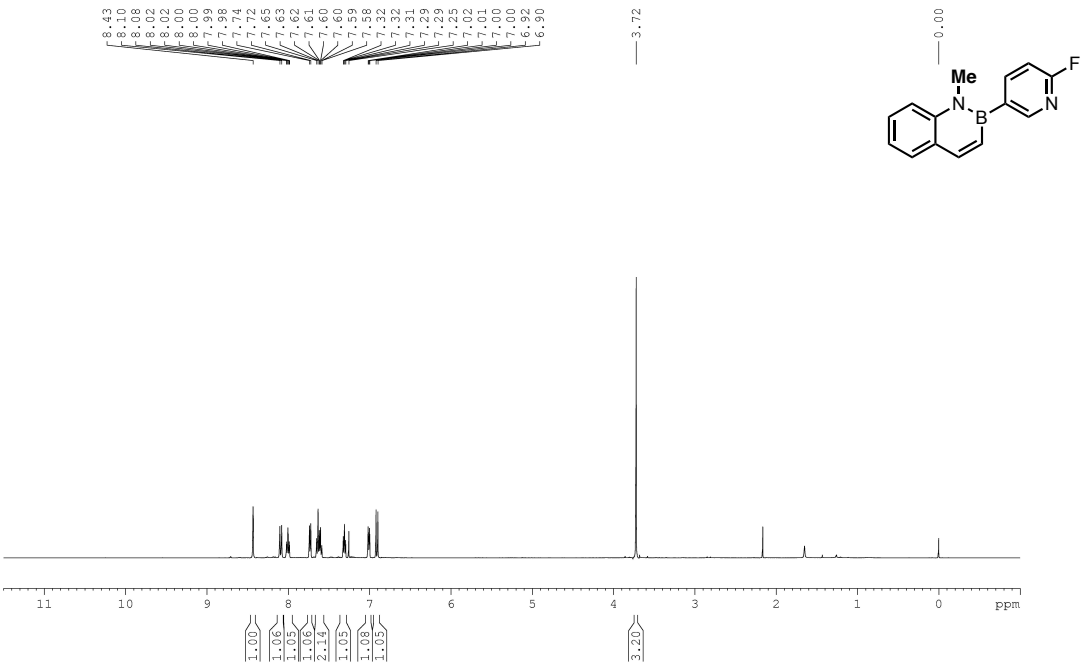

Figure A1.370: ^{3}C {^{1}H} NMR ($CDCl_3$, 125.8 MHz) of 2-(6-fluoropyridin-3-yl)-1-methyl-2,1-borazaronaphthalene (**2.134**)

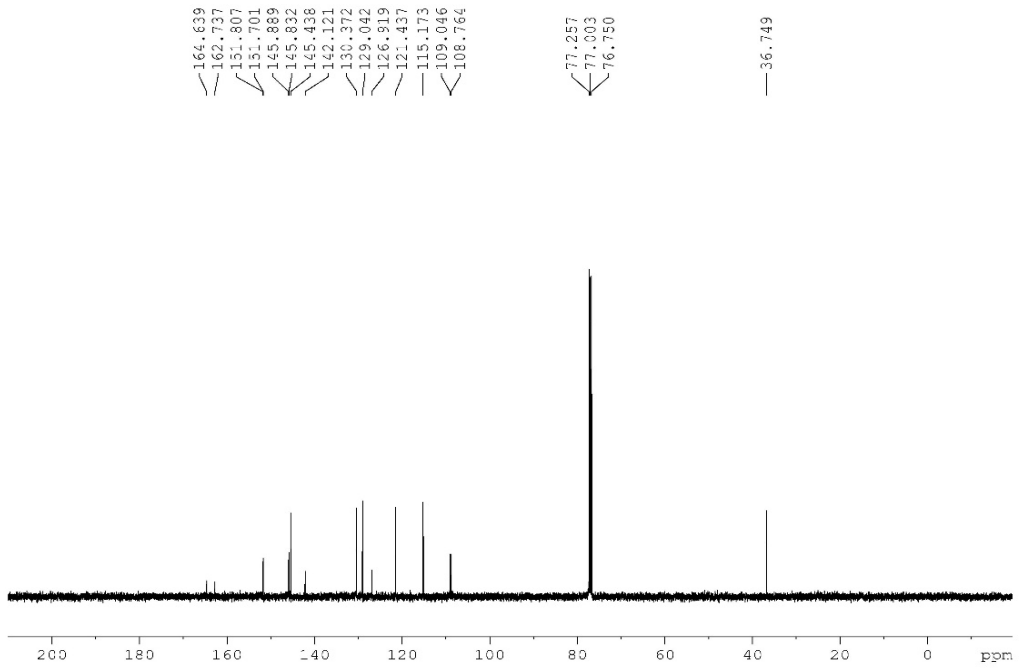

Figure A1.371: ^{19}F {^{1}H} NMR ($CDCl_3$, 470.8 MHz) of 2-(6-fluoropyridin-3-yl)-1-methyl-2,1-borazaronaphthalene (**2.134**)

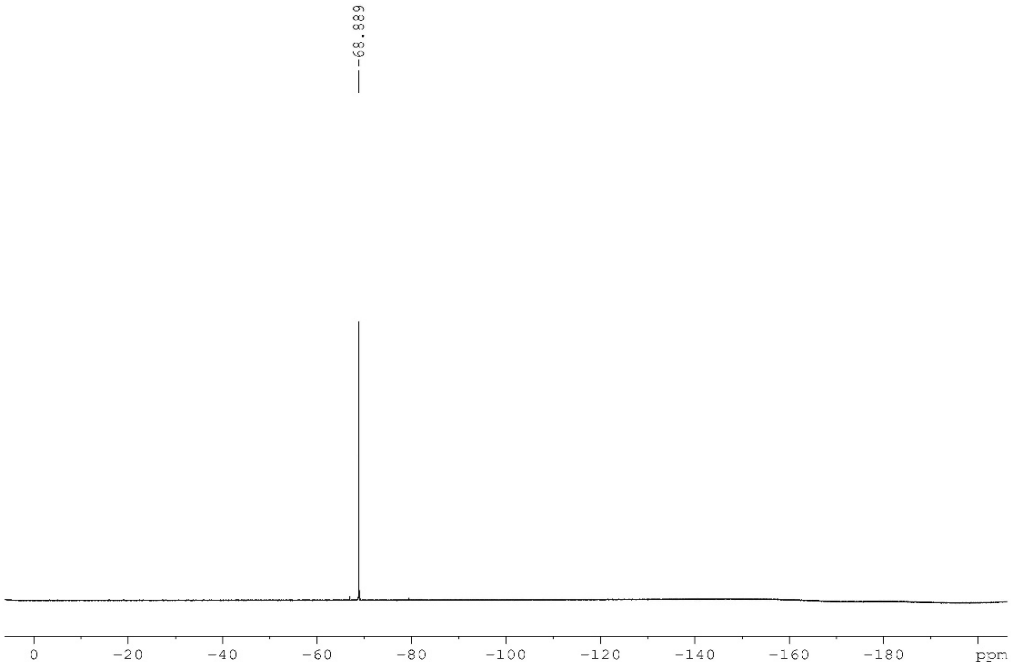

Figure A1.372: ^{11}B NMR ($CDCl_3$, 128.4 MHz) of 2-(6-fluoropyridin-3-yl)-1-methyl-2,1-borazaronaphthalene (**2.134**)

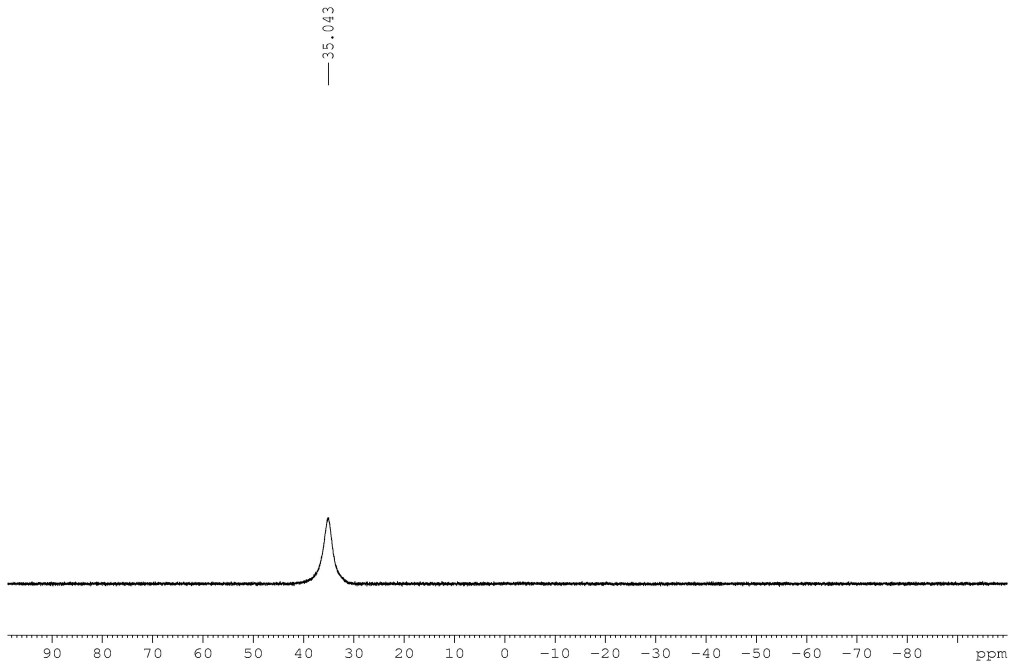

Figure A1.373: ^{1}H NMR ($CDCl_3$, 500.4 MHz) of 2-(3-fluoropyridin-4-yl)-1-methyl-2,1-borazaronaphthalene (**2.135**)

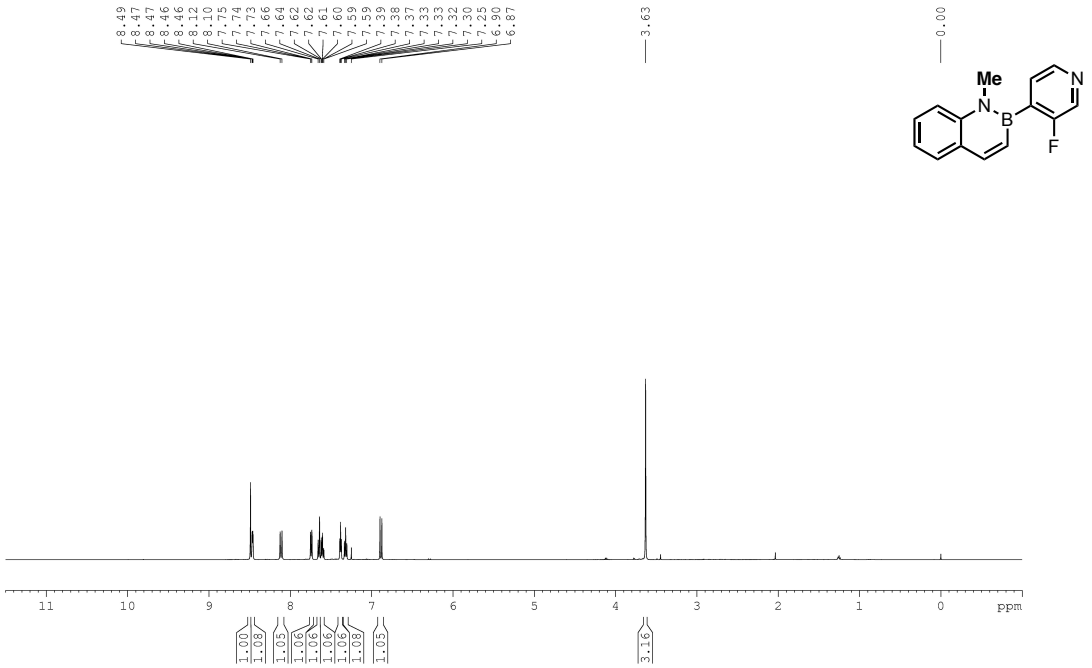

Figure A1.374: ^{13}C {^{1}H} NMR ($CDCl_3$, 125.8 MHz) of 2-(3-fluoropyridin-4-yl)-1-methyl-2,1-borazaronaphthalene (**2.135**)

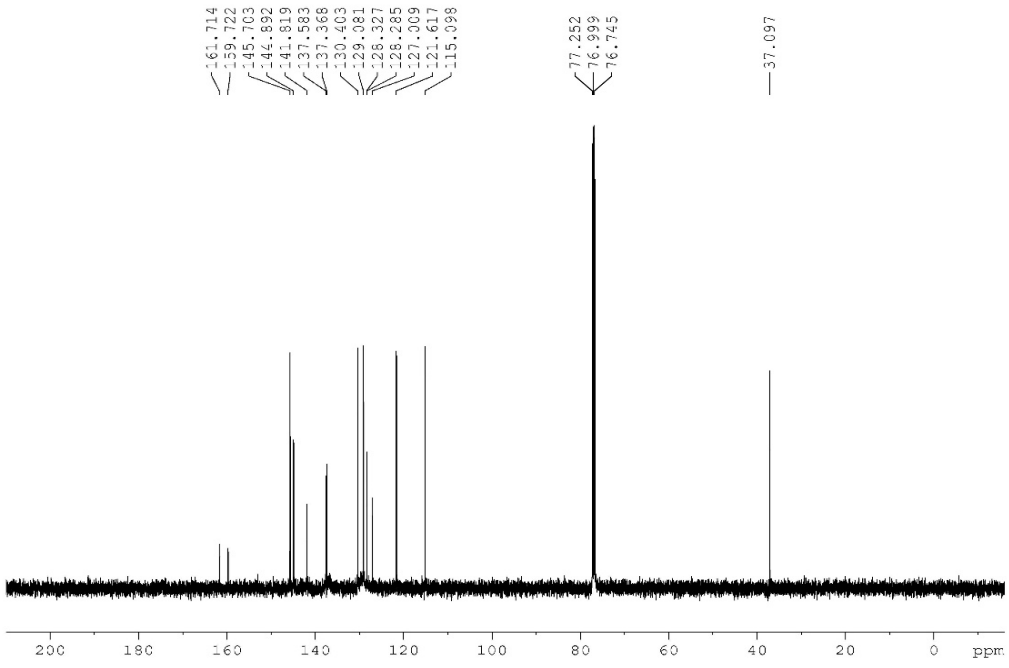

Figure A1.375: ^{19}F {^{1}H} NMR ($CDCl_3$, 470.8 MHz) of 2-(3-fluoropyridin-4-yl)-1-methyl-2,1-borazaronaphthalene (**2.135**)

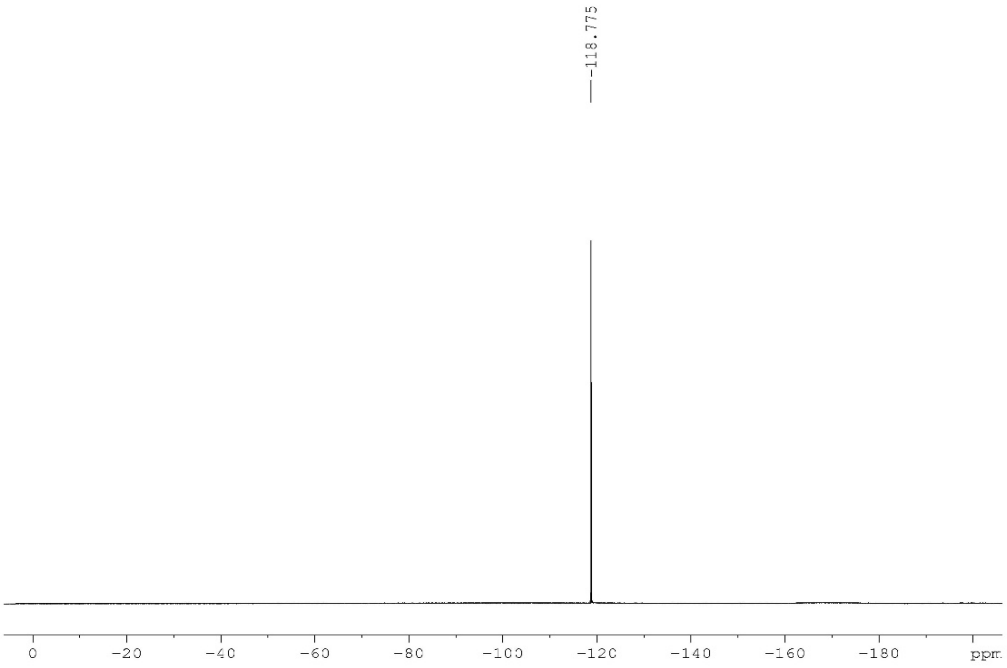

Figure A1.376: ^{11}B NMR ($CDCl_3$, 128.4 MHz) of 2-(3-fluoropyridin-4-yl)-1-methyl-2,1-borazaronaphthalene (**2.135**)

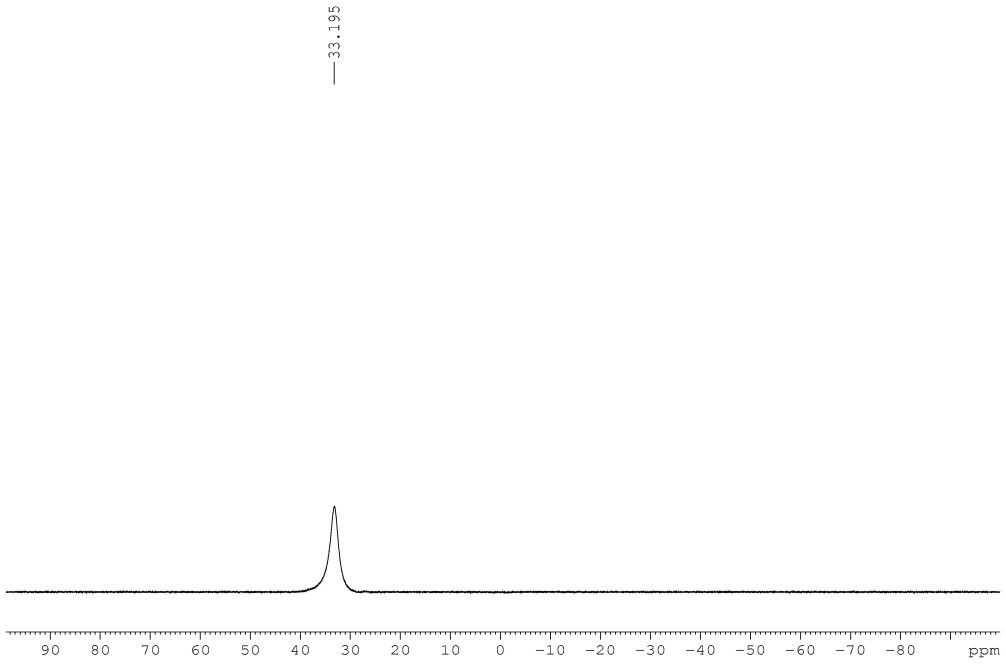

Figure A1.377: ^{1}H NMR ($CDCl_3$, 500.4 MHz) of 1-methyl-2-(2-(morpholino)pyridin-3-yl)-2,1-borazaronaphthalene (**2.136**)

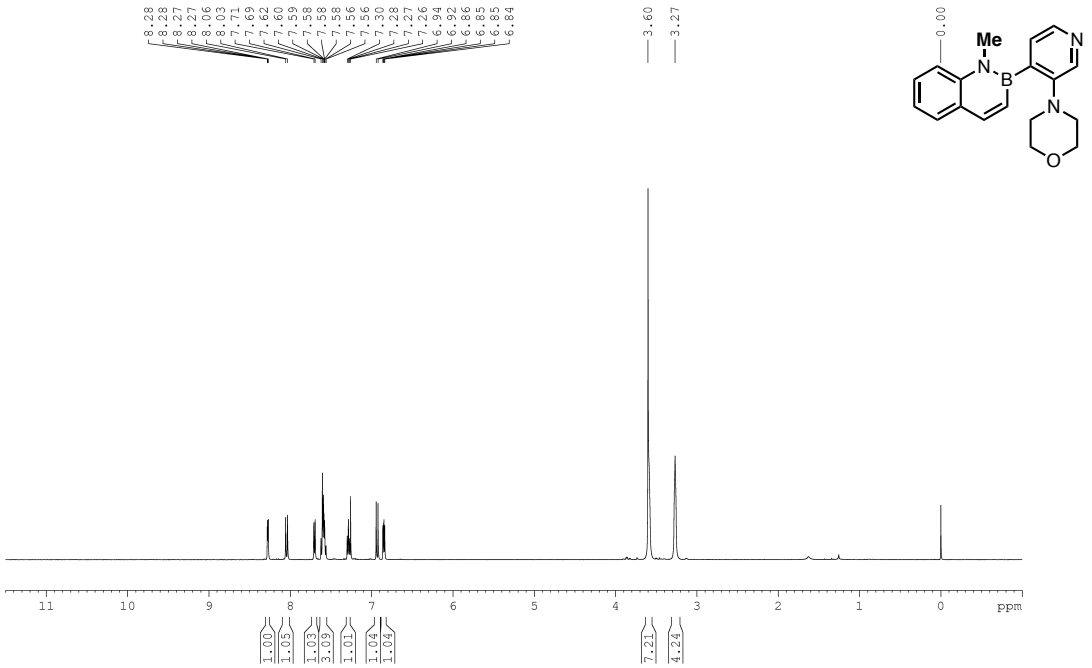

Figure A1.378: ^{13}C {^{1}H} NMR ($CDCl_3$, 125.8 MHz) of 1-methyl-2-(2-(morpholino)pyridin-3-yl)-2,1-borazaronaphthalene (**2.136**)

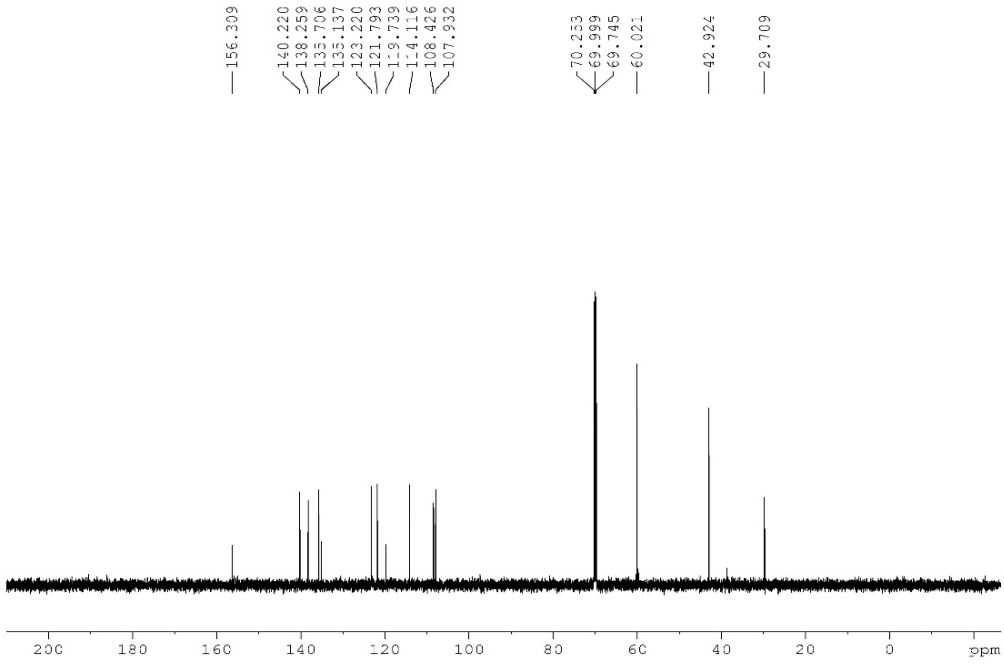

Figure A1.379: ^{11}B NMR ($CDCl_3$, 128.4 MHz) of 1-methyl-2-(2-(morpholino)pyridin-3-yl)-2,1-borazaronaphthalene (**2.136**)

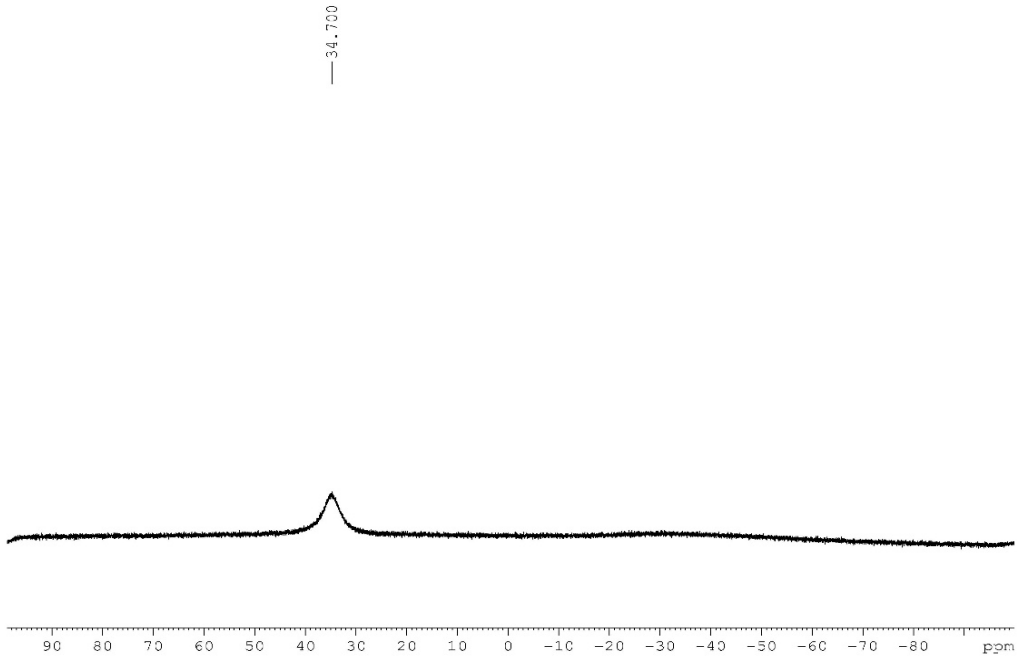

Figure A1.380: ^{1}H NMR ($CDCl_3$, 500.4 MHz) of 1-methyl-2-(pyrimidin-5-yl)-2,1-borazaronaphthalene (**2.137**)

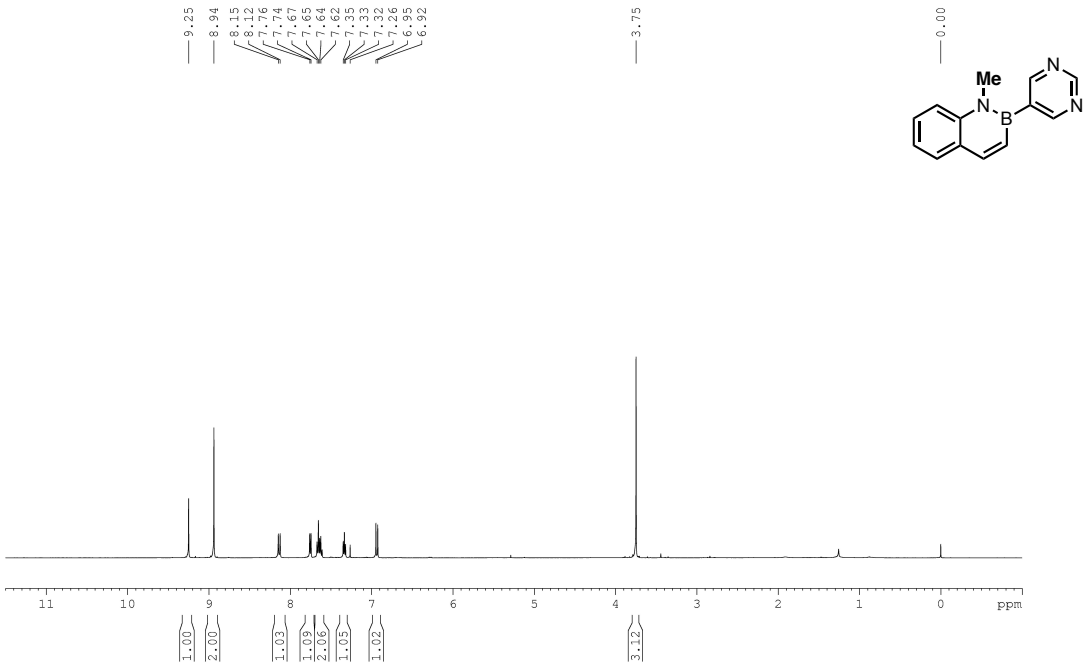

Figure A1.381: ^{13}C {^{1}H} NMR ($CDCl_3$, 125.8 MHz) of 1-methyl-2-(pyrimidin-5-yl)-2,1-borazaronaphthalene (**2.137**)

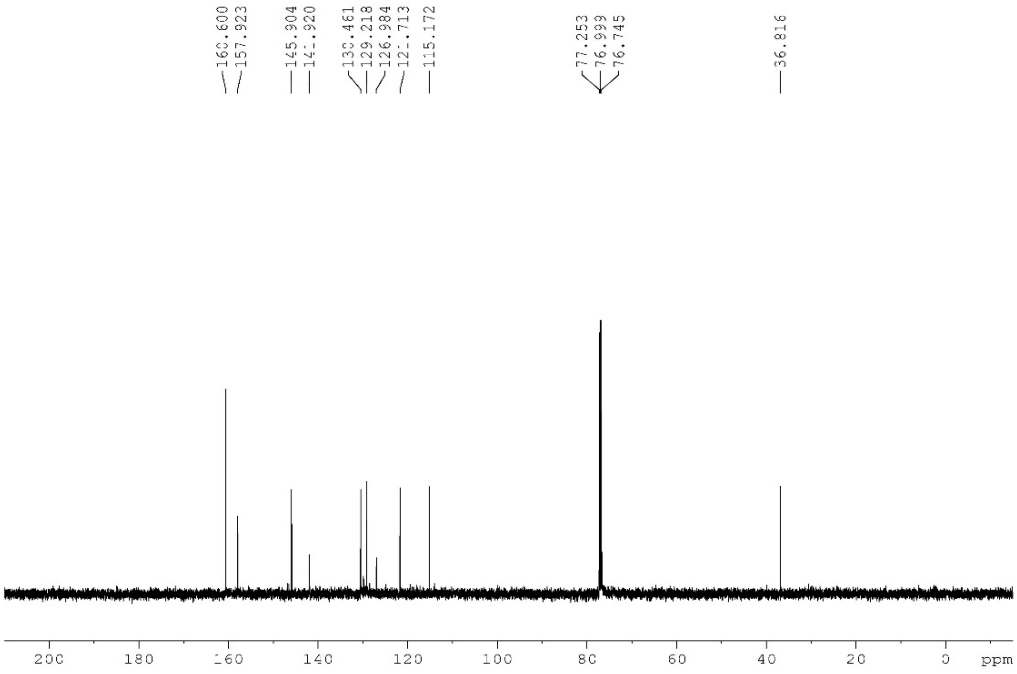

Figure A1.382: ^{11}B NMR ($CDCl_3$, 128.4 MHz) of 1-methyl-2-(pyrimidin-5-yl)-2,1-borazaronaphthalene (**2.137**)

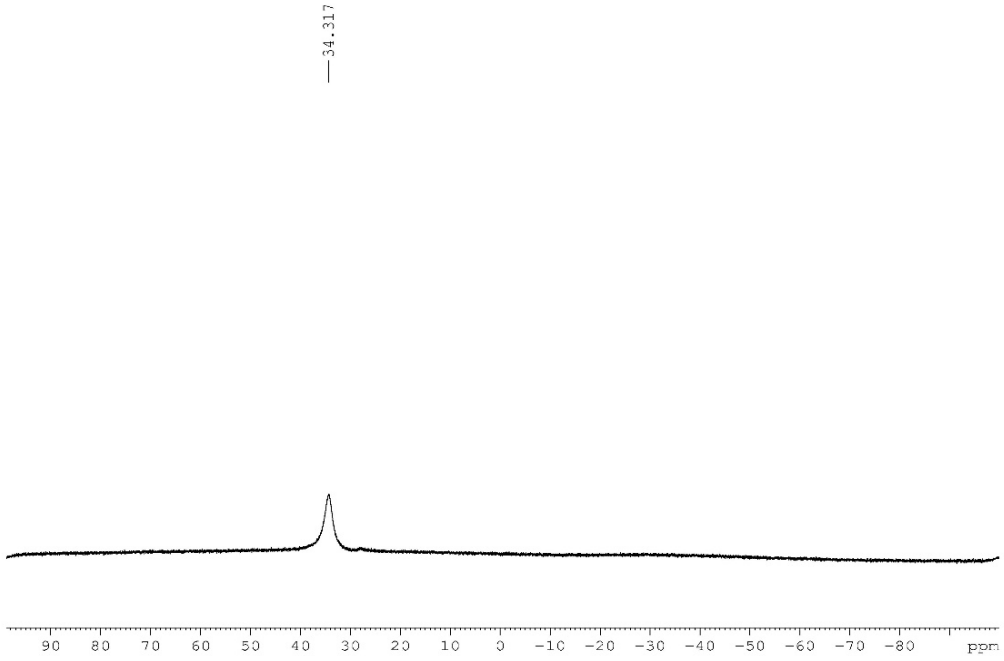

Figure A1.383: ^{1}H NMR ($CDCl_3$, 500.4 MHz) of 1-methyl-2-(3,5-dimethylisoxazole-4-yl)-2,1-borazaronaphthalene **(2.138)**

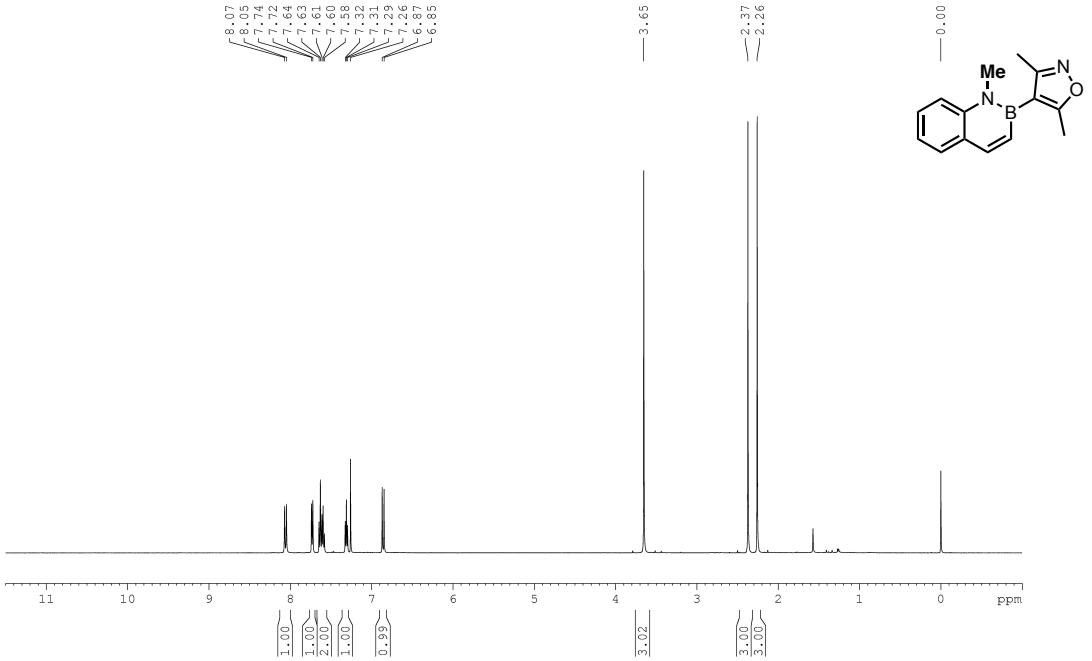

Figure A1.384: ^{13}C {^{1}H} NMR ($CDCl_3$, 125.8 MHz) of 1-methyl-2-(3,5-dimethylisoxazole-4-yl)-2,1-borazaronaphthalene **(2.138)**

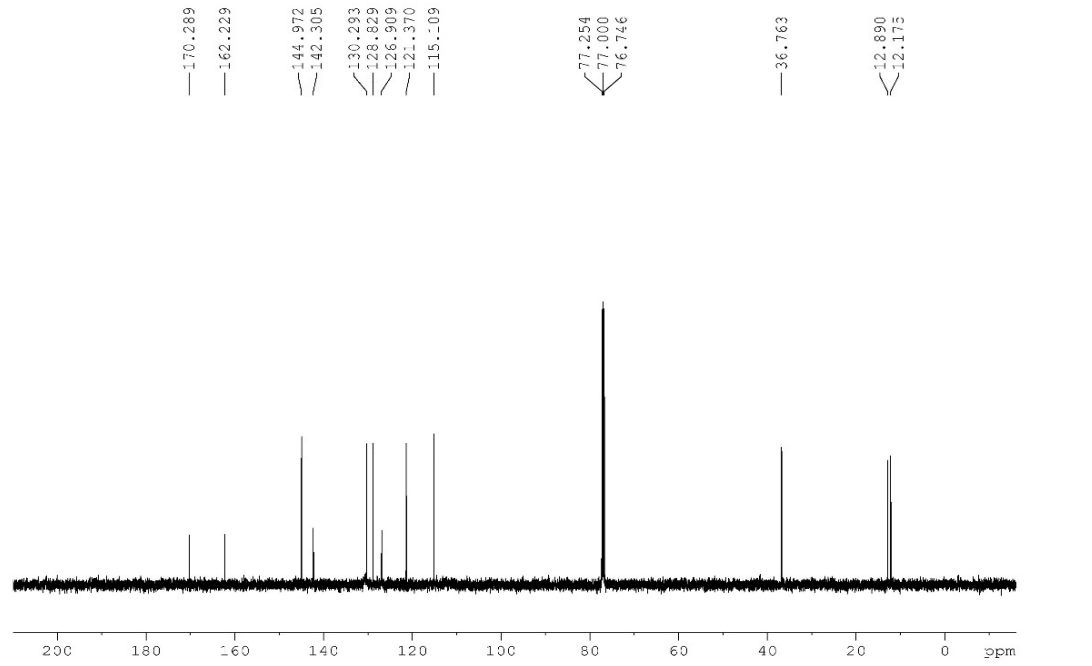

Figure A1.385: ^{11}B NMR ($CDCl_3$, 128.4 MHz) of 1-methyl-2-(3,5-dimethylisoxazole-4-yl)-2,1-borazaronaphthalene **(2.138)**

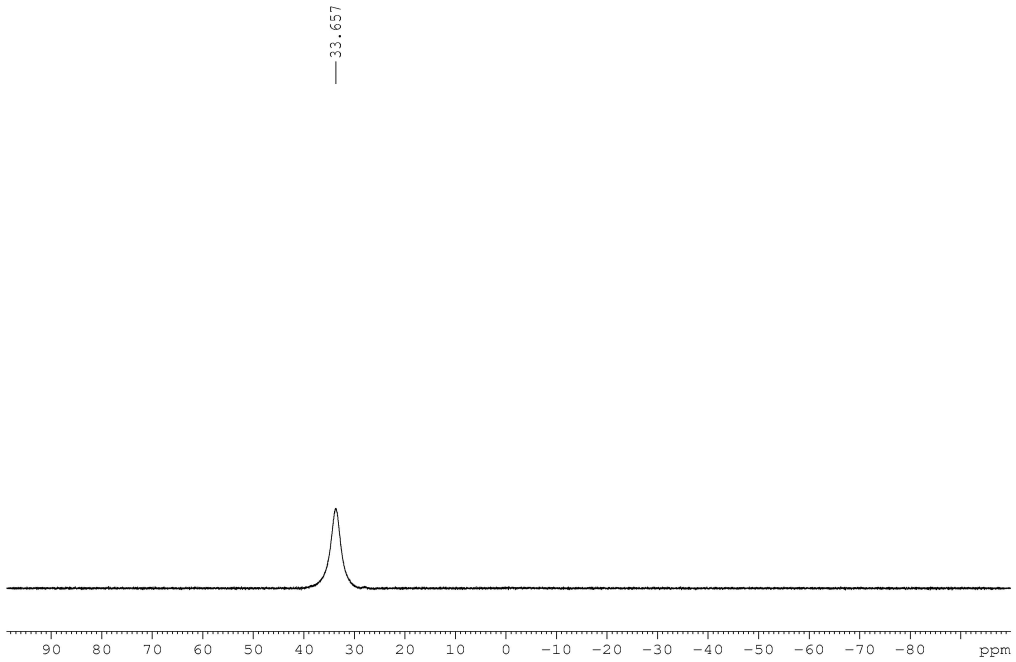

Figure A1.386: ^{1}H NMR ($CDCl_3$, 500.4 MHz) of 1-methyl-2-(1-methyl-1H-pyrazol-4-yl)-2,1-borazaronaphthalene **(2.139)**

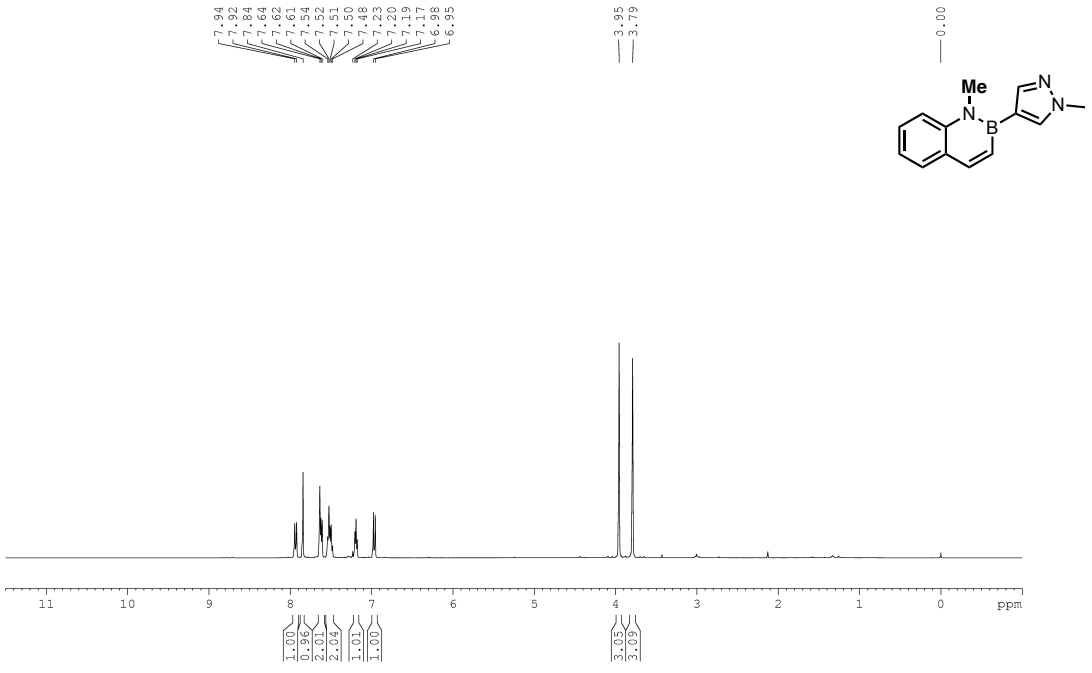

Figure A1.387: ^{13}C {^{1}H} NMR ($CDCl_3$, 125.8 MHz) of 1-methyl-2-(1-methyl-1H-pyrazol-4-yl)-2,1-borazaronaphthalene **(2.139)**

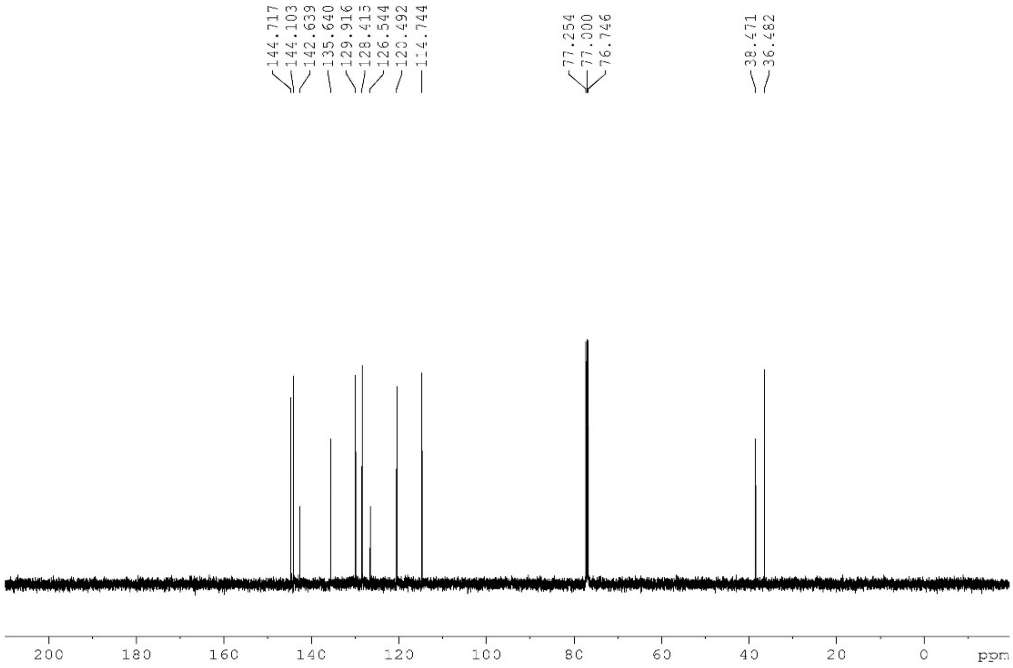

Figure A1.388: ^{1}B NMR ($CDCl_3$, 128.4 MHz) of 1-methyl-2-(1-methyl-1H-pyrazol-4-yl)-2,1-borazaronaphthalene **(2.139)**

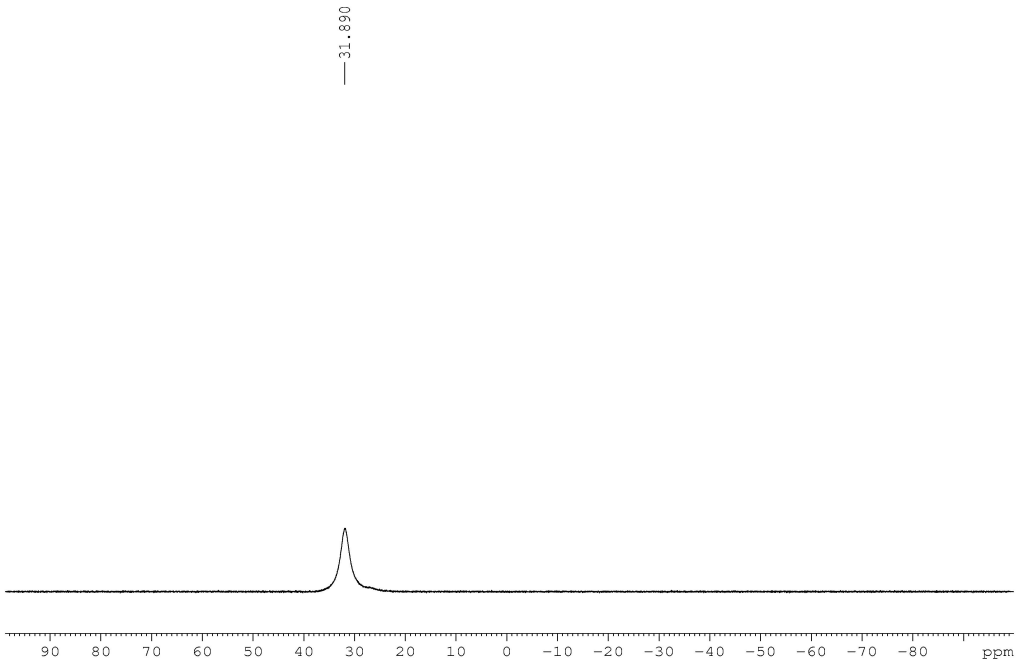

Figure A1.389: ^{1}H NMR ($CDCl_3$, 500.4 MHz) of 1-methyl-2-(1-tosyl-1H-pyrrol-2-yl)-2,1-borazaronaphthalene (**2.140**)

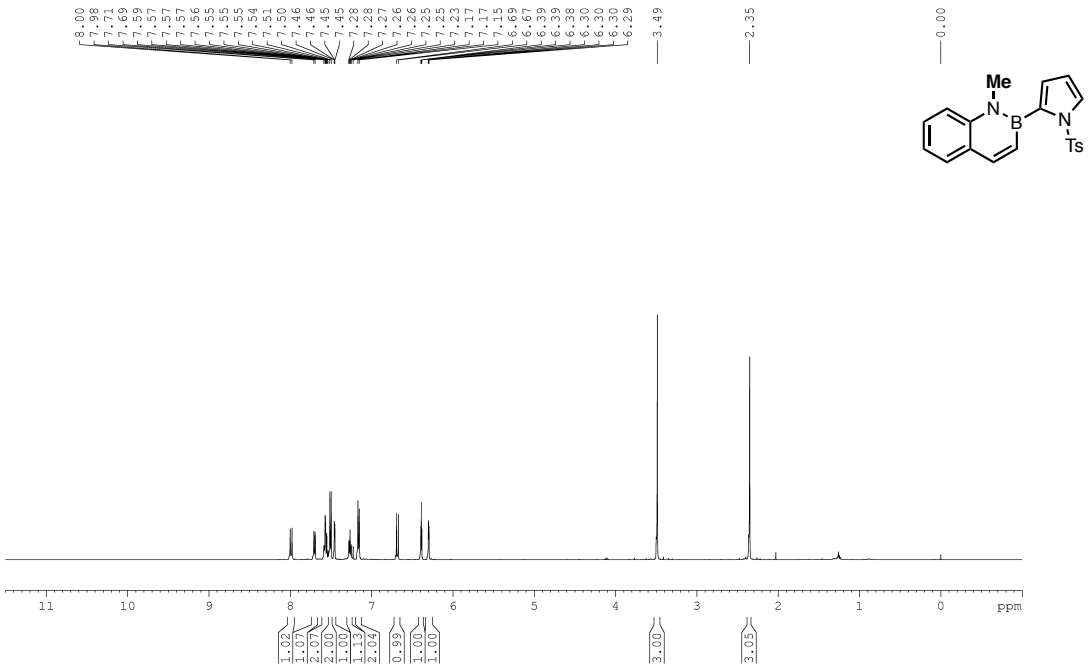

Figure A1.390: ^{13}C $\{^{1}H\}$ NMR ($CDCl_3$, 125.8 MHz) of 1-methyl-2-(1-tosyl-1H-pyrrol-2-yl)-2,1-borazaronaphthalene (**2.140**)

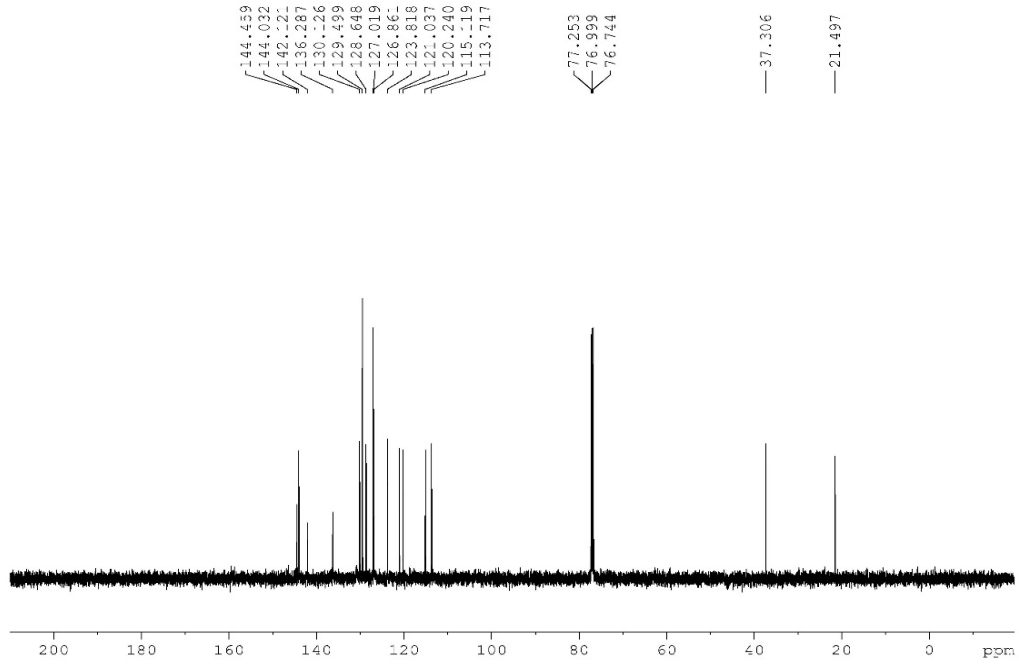

Figure A1.391: ^{11}B NMR ($CDCl_3$, 128.4 MHz) of 1-methyl-2-(1-tosyl-1H-pyrrol-2-yl)-2,1-borazaronaphthalene (**2.140**)

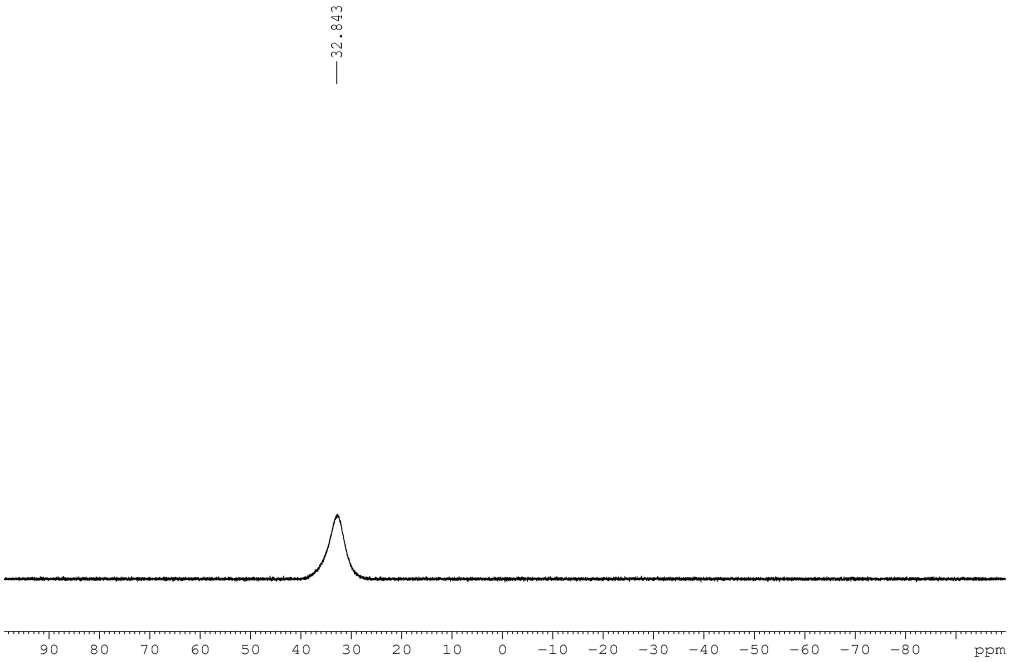

Figure A1.392: ^{1}H NMR ($CDCl_3$, 500.4 MHz) of 1-(4-(*tert*-butyl)phenyl)-2-(quinolin-6-yl)-2,1-borazaronaphthalene (**2.141**)

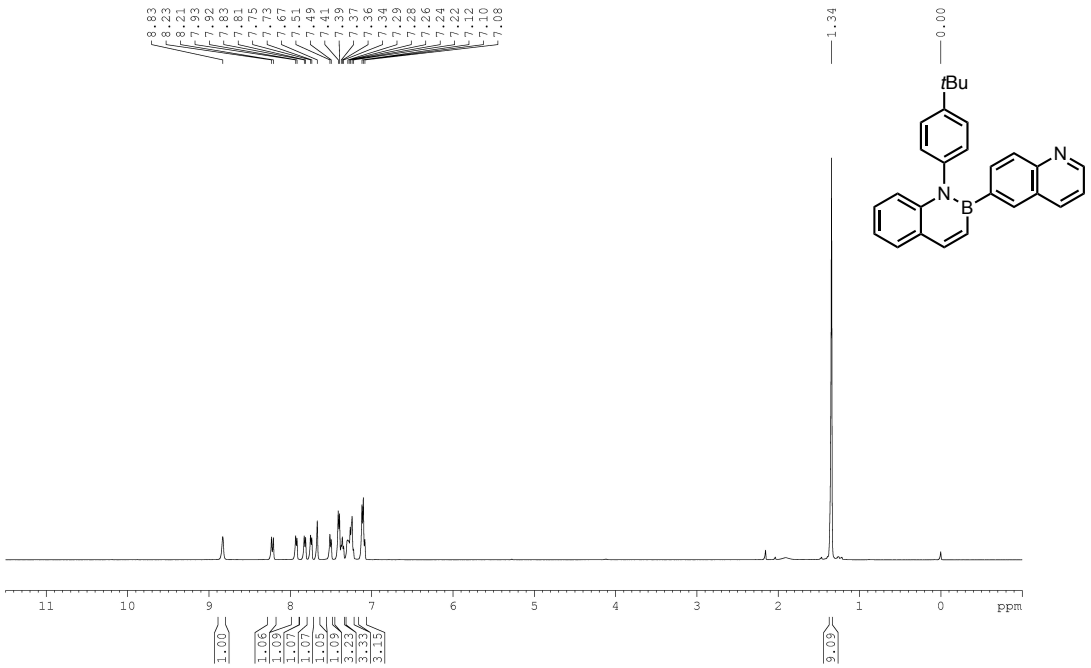

Figure A1.393: ^{13}C {^{1}H} NMR ($CDCl_3$, 125.8 MHz) of 1-(4-(*tert*-butyl)phenyl)-2-(quinolin-6-yl)-2,1-borazaronaphthalene (**2.141**)

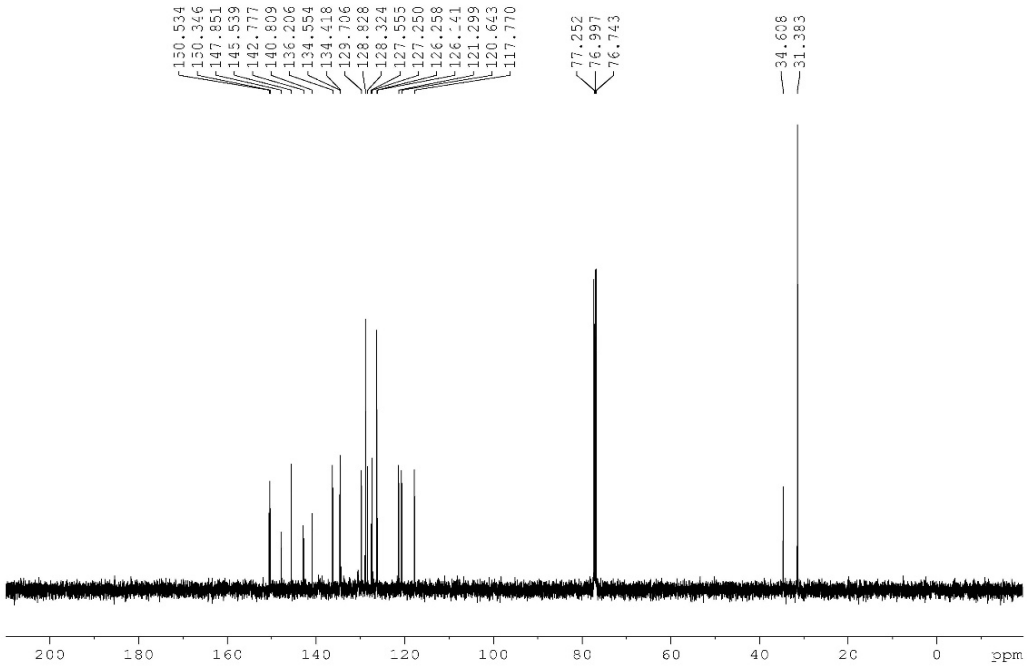

Figure A1.394: ^{11}B NMR ($CDCl_3$, 128.4 MHz) of 1-(4-(*tert*-butyl)phenyl)-2-(quinolin-6-yl)-2,1-borazaronaphthalene (**2.141**)

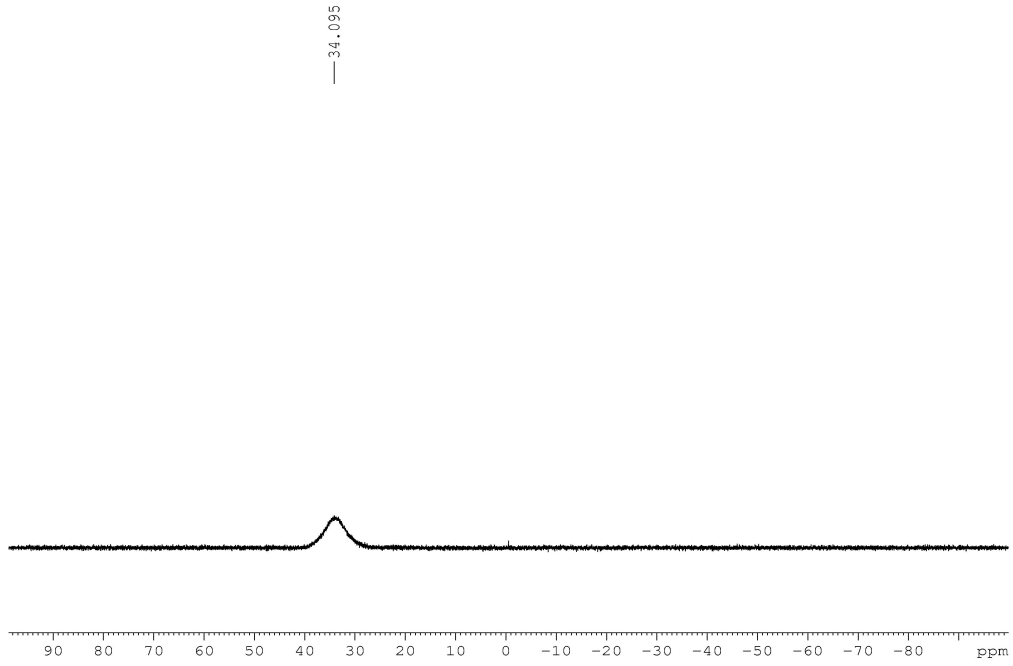

Figure A1.395: ^{1}H NMR ($CDCl_3$, 500.4 MHz) of 1-allyl-2-(quinolin-6-yl)-2,1-borazaronaphthalene (**2.142**)'

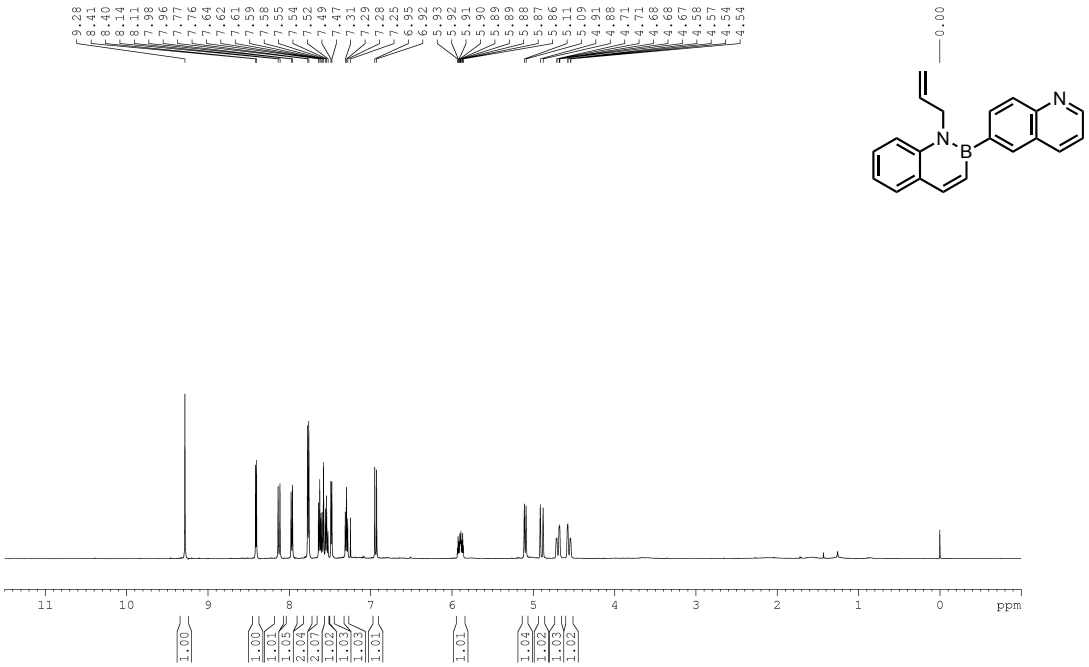

Figure A1.396: ^{13}C {^{1}H} NMR ($CDCl_3$, 125.8 MHz) of 1-allyl-2-(quinolin-6-yl)-2,1-borazaronaphthalene (**2.142**)

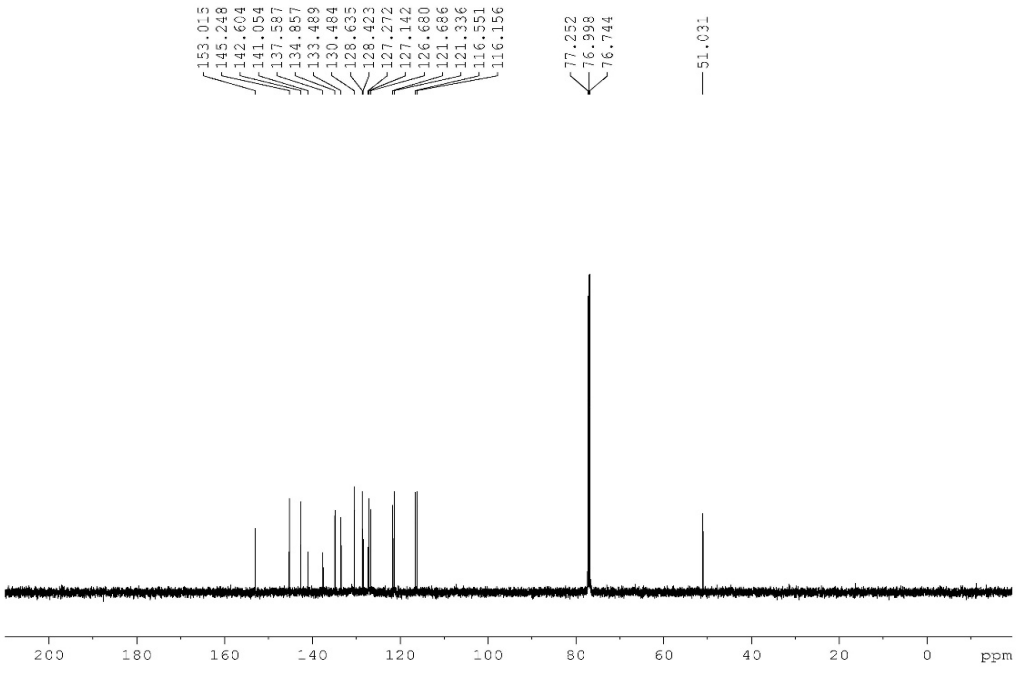

Figure A1.397: ^{11}B NMR ($CDCl_3$, 128.4 MHz) of 1-allyl-2-(quinolin-6-yl)-2,1-borazaronaphthalene (**2.142**)

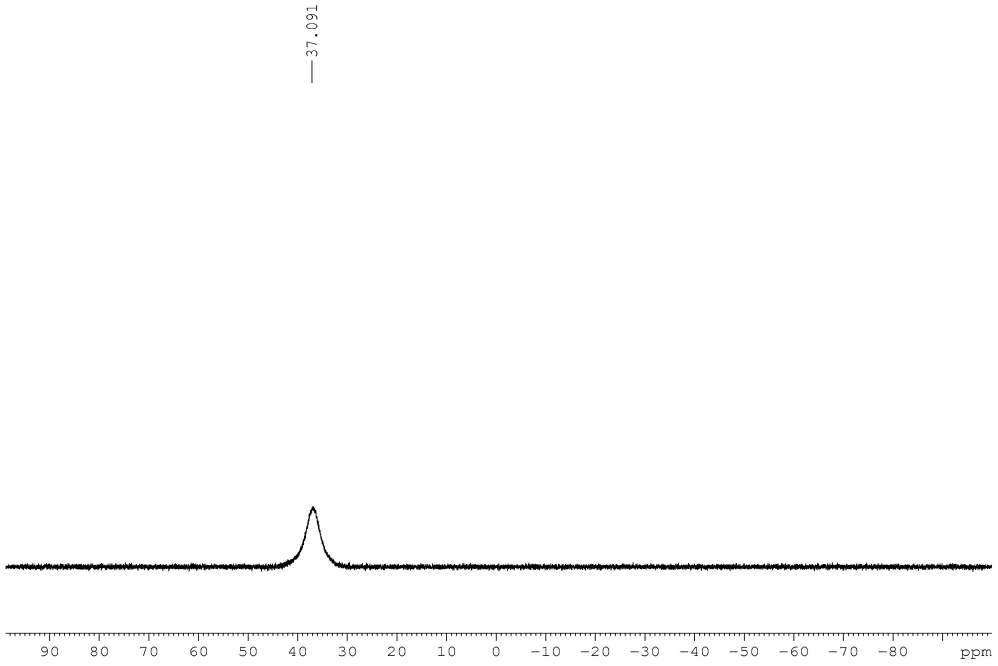

Figure A1.398: ^{1}H NMR (DMSO-d_6, 500.4 MHz) of 2-(quinolin-6-yl)-2,1-borazaronaphthalene (**2.143**)

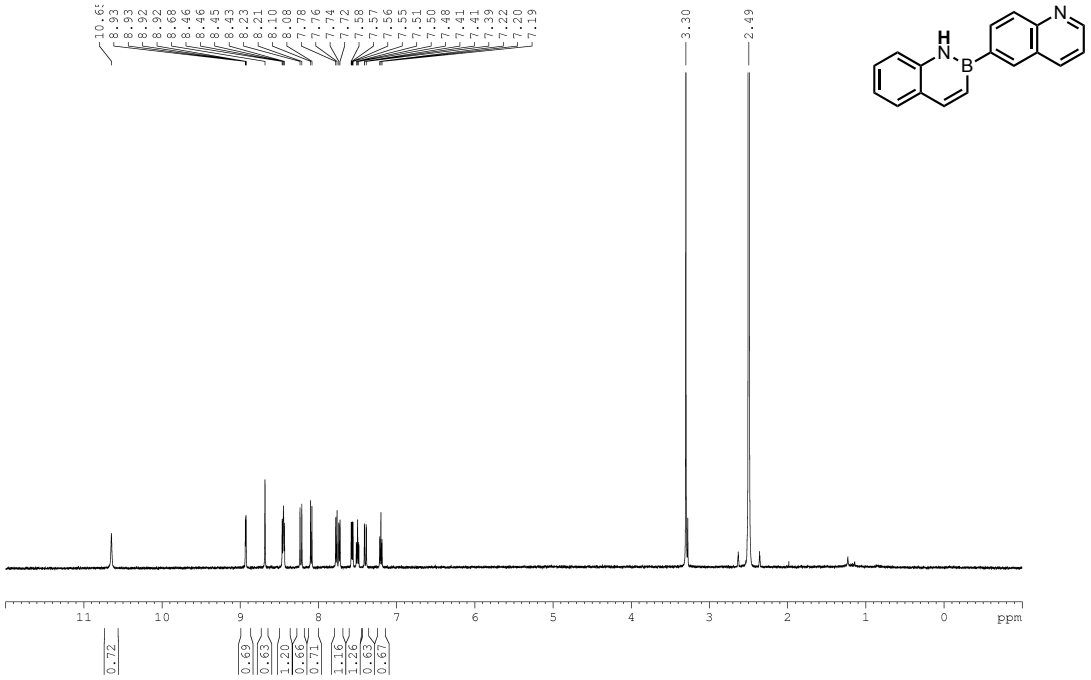

Figure A1.399: ^{13}C {^{1}H} NMR (DMSO-d_6, 125.8 MHz) of 2-(quinolin-6-yl)-2,1-borazaronaphthalene (**2.143**)

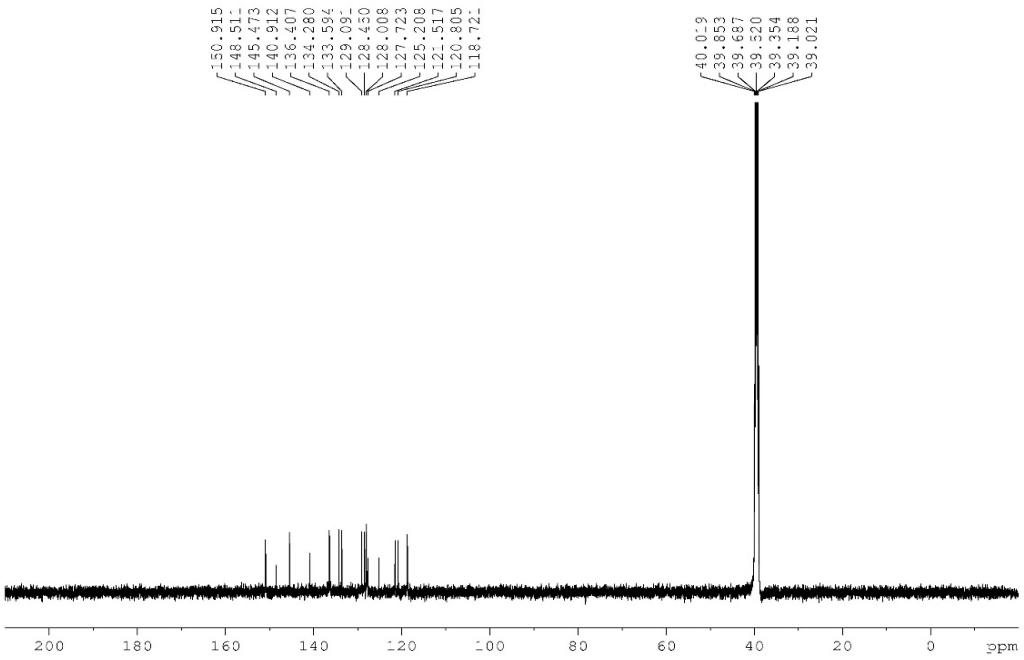

Figure A1.400: ^{11}B NMR (Acetone-d_6, 128.4 MHz) of 2-(quinolin-6-yl)-2,1-borazaronaphthalene (**2.143**)

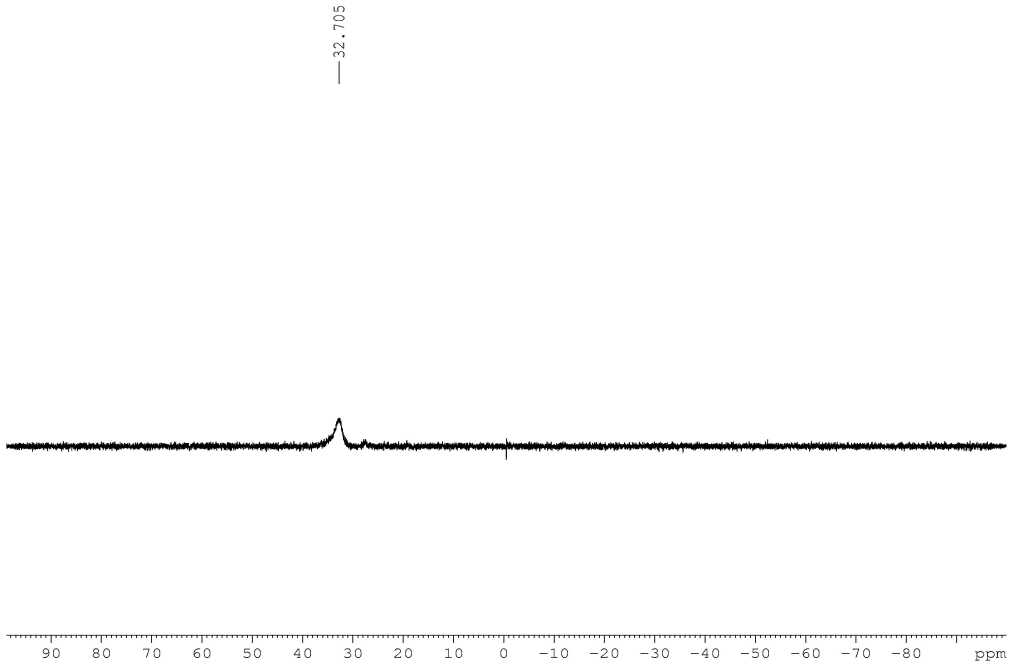

Figure A1.401: ^{1}H NMR ($CDCl_3$, 500.4 MHz) of 1-(3-phenylpropyl)-2-(quinolin-6-yl)-2,1-borazaronaphthalene (**2.144**)

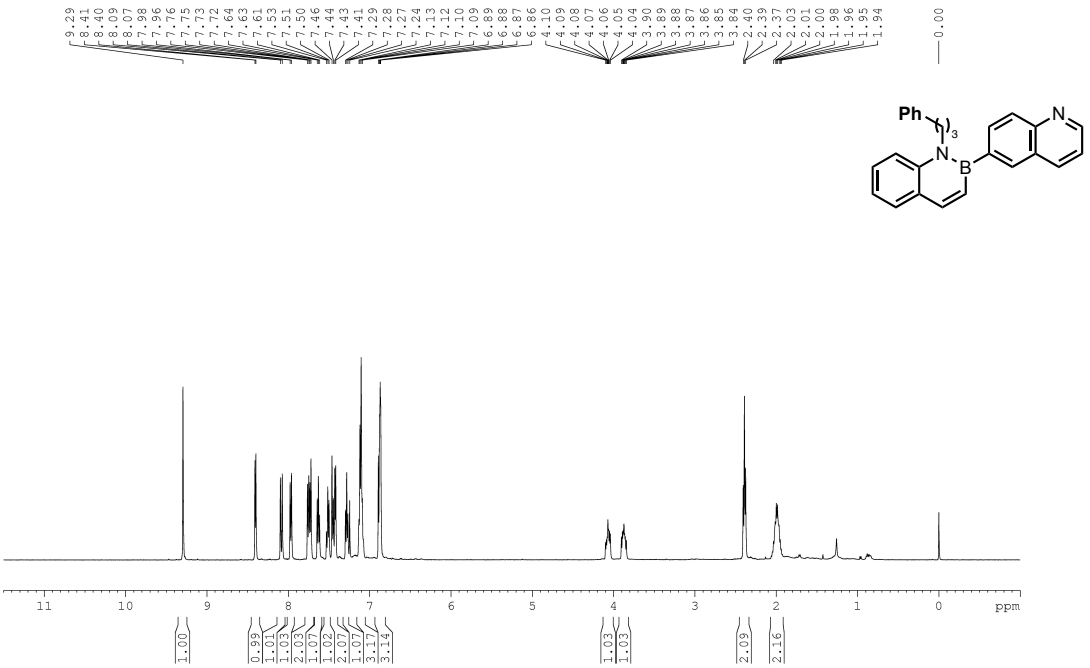

Figure A1.402: ^{13}C {^{1}H} NMR ($CDCl_3$, 125.8 MHz) of 1-(3-phenylpropyl)-2-(quinolin-6-yl)-2,1-borazaronaphthalene (**2.144**)

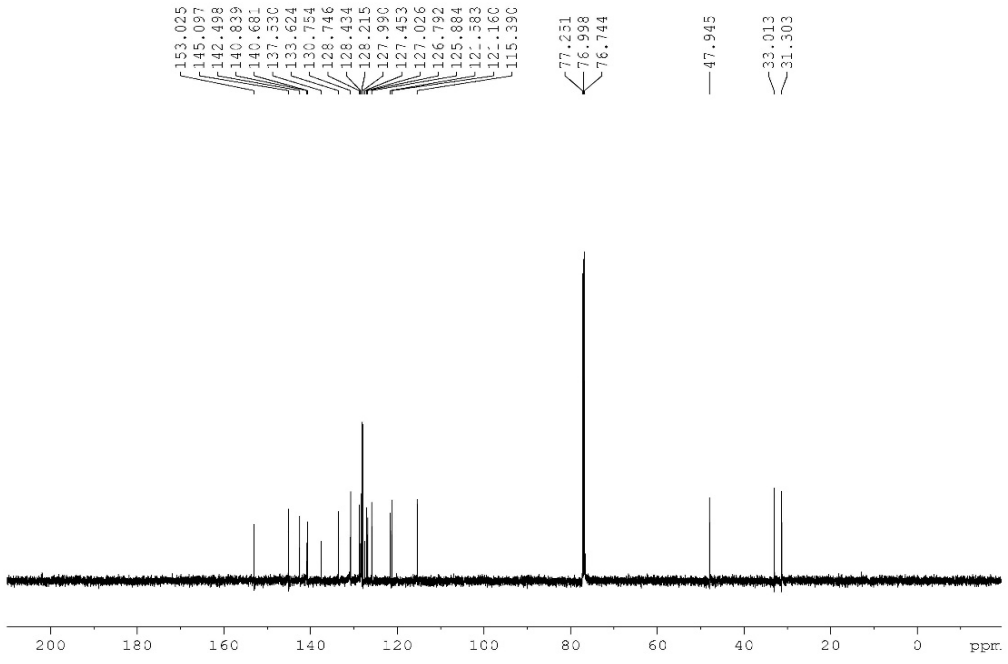

Figure A1.403: ^{11}B NMR ($CDCl_3$, 128.4 MHz) of 1-(3-phenylpropyl)-2-(quinolin-6-yl)-2,1-borazaronaphthalene (**2.144**)

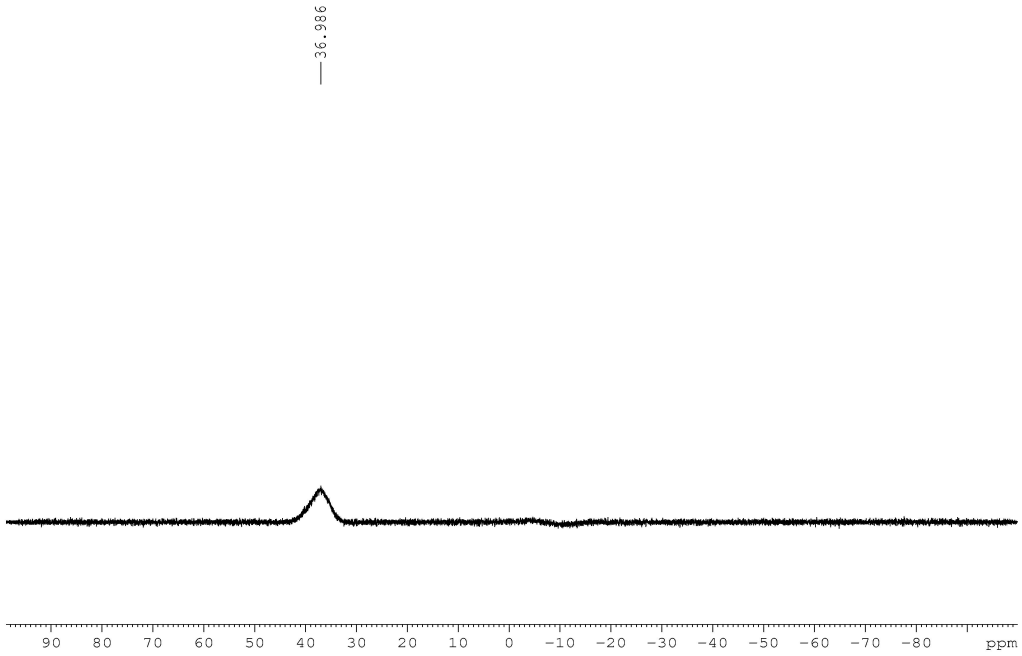

Figure A1.404: ^{1}H NMR ($CDCl_3$, 500.4 MHz) of 1-(3-phenylpropyl)-2-(quinolin-3-yl)-2,1-borazaronaphthalene (**2.145**)

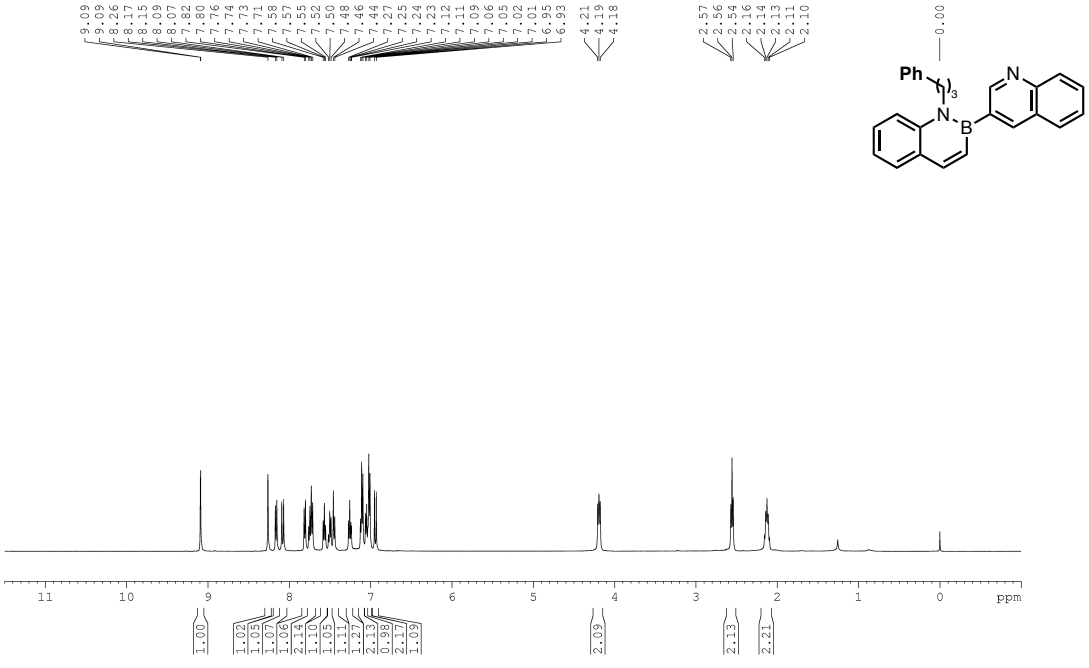

Figure A1.405: ^{13}C {^{1}H} NMR ($CDCl_3$, 125.8 MHz) of 1-(3-phenylpropyl)-2-(quinolin-3-yl)-2,1-borazaronaphthalene (**2.145**)

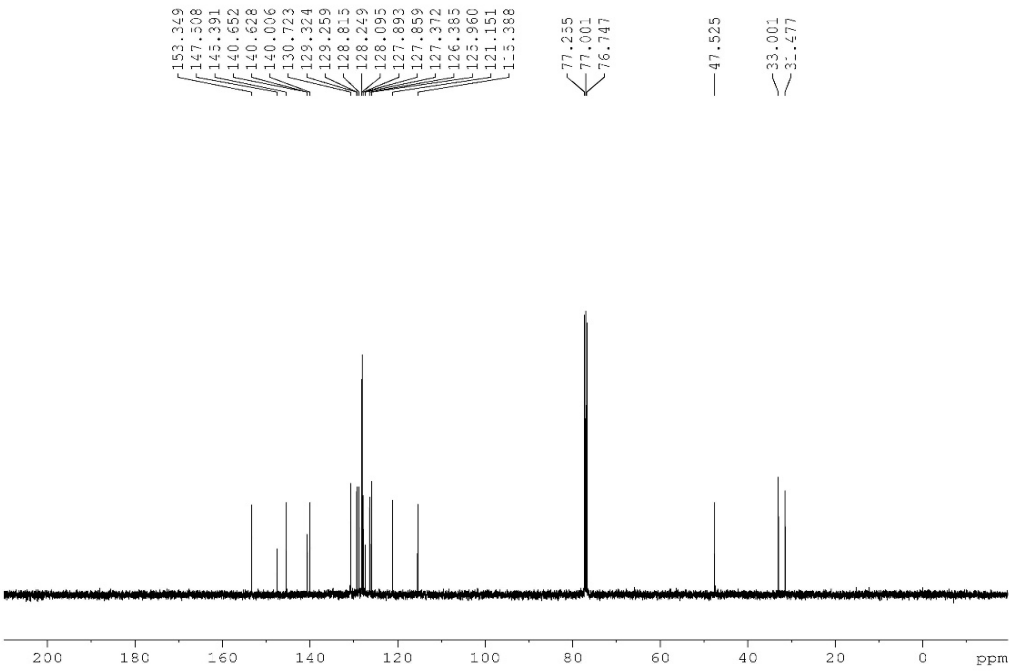

Figure A1.406: ^{11}B NMR ($CDCl_3$, 128.4 MHz) of 1-(3-phenylpropyl)-2-(quinolin-3-yl)-2,1-borazaronaphthalene (**2.145**)

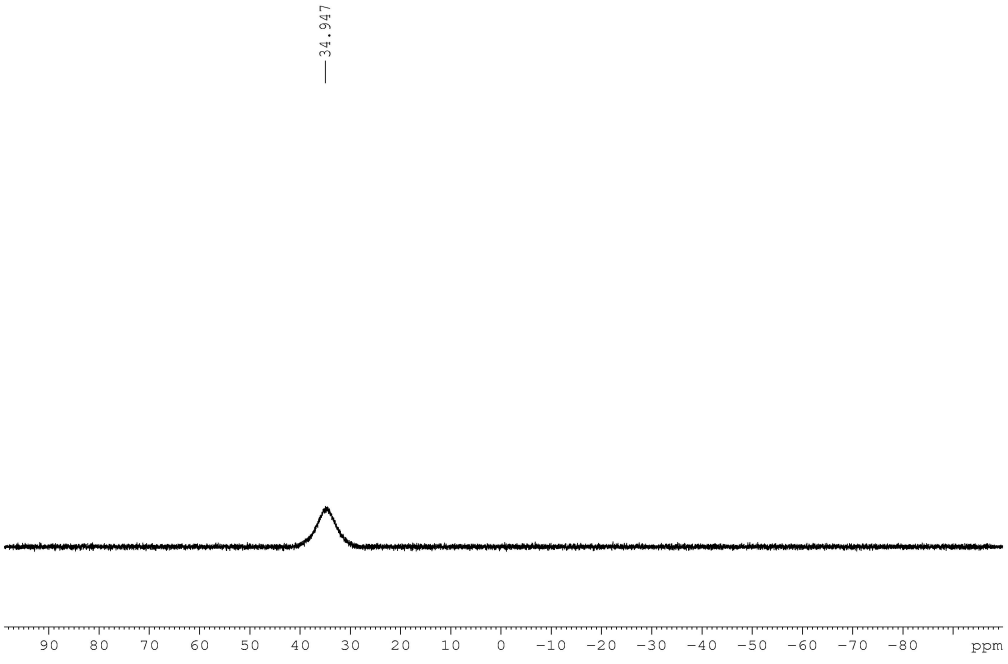

Figure A1.407: ^{1}H NMR ($CDCl_3$, 500.4 MHz) of 2-(isoquinolin-5-yl)-1-(3-phenylpropyl)-2,1-borazaronaphthalene (**2.146**)

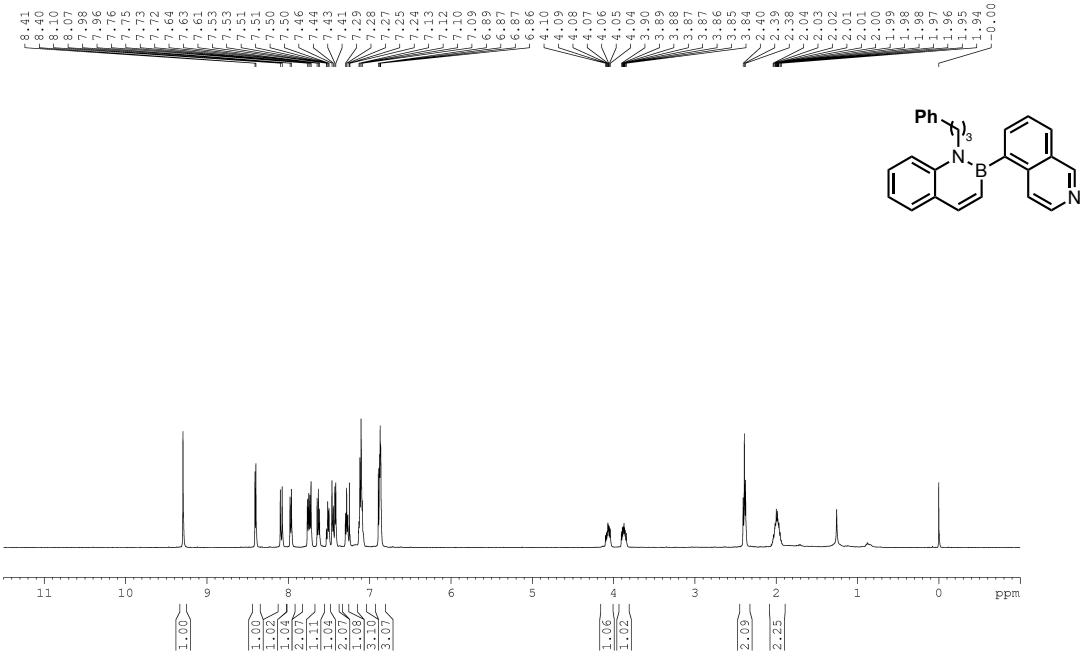

Figure A1.408: ^{13}C {^{1}H} NMR ($CDCl_3$, 125.8 MHz) of 2-(isoquinolin-5-yl)-1-(3-phenylpropyl)-2,1-borazaronaphthalene (**2.146)**

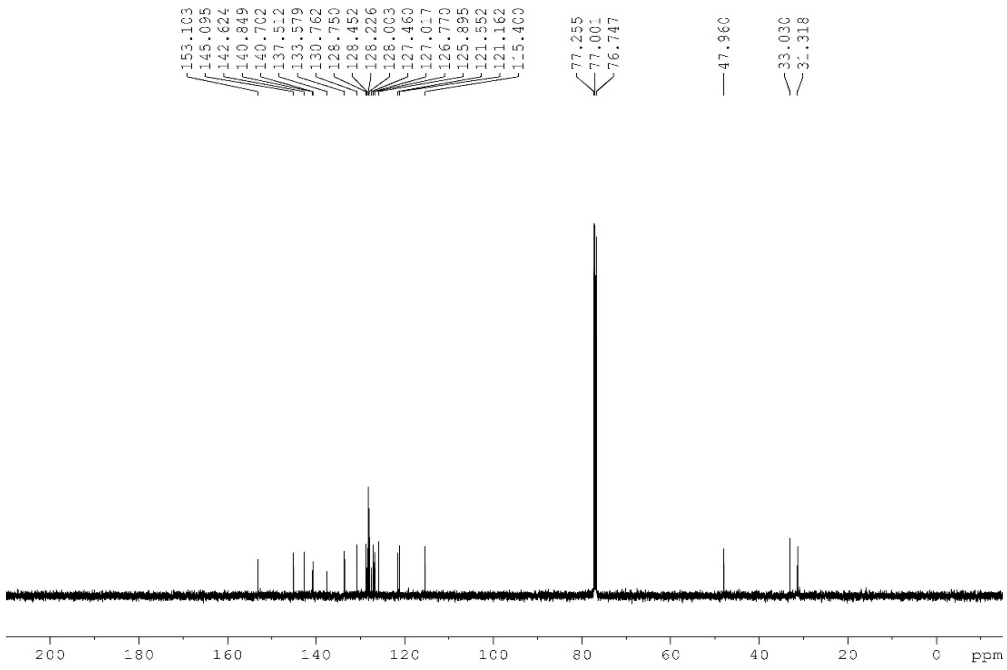

Figure A1.409: ^{11}B NMR ($CDCl_3$, 128.4 MHz) of 2-(isoquinolin-5-yl)-1-(3-phenylpropyl)-2,1-borazaronaphthalene (**2.146**)

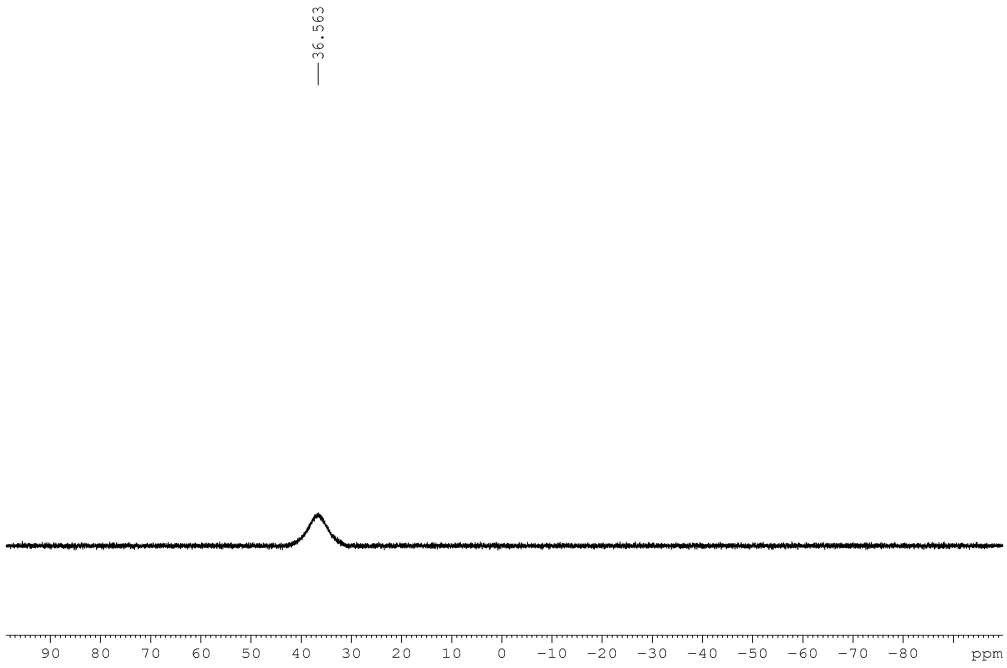

Figure A1.410: ^{1}H NMR ($CDCl_3$, 500.4 MHz) of 2-(quinolin-6-yl)-7-(trifluoromethyl)-2,1-borazaronaphthalene (**2.147**)

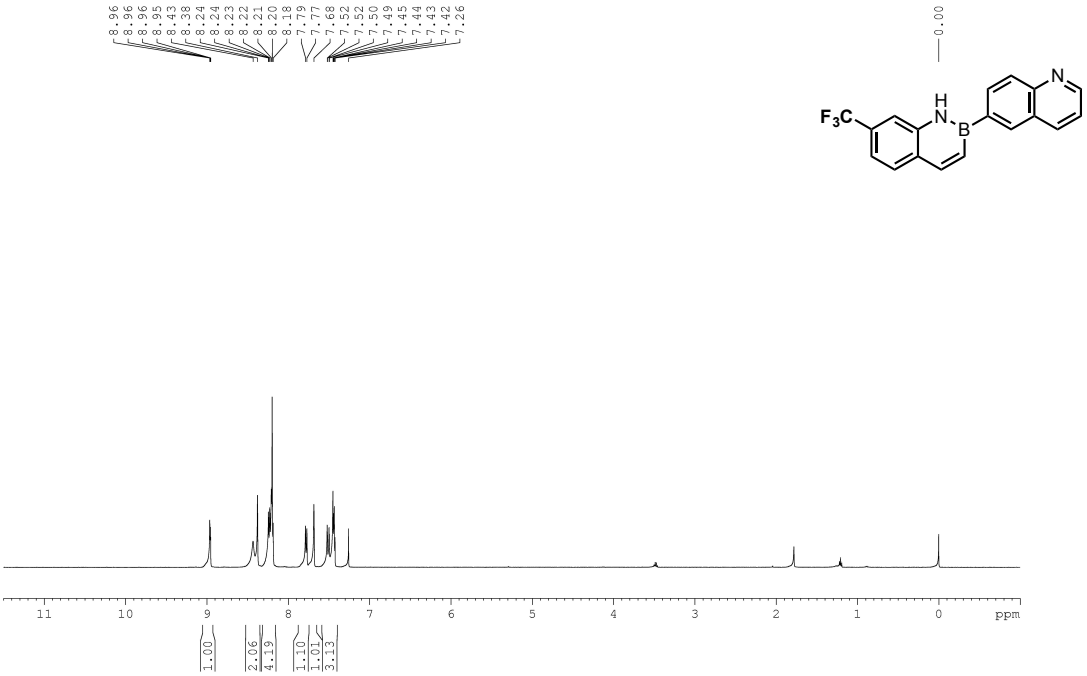

Figure A1.411: ^{13}C {^{1}H} NMR ($CDCl_3$, 125.8 MHz) of 2-(quinolin-6-yl)-7-(trifluoromethyl)-2,1-borazaronaphthalene (**2.147**)

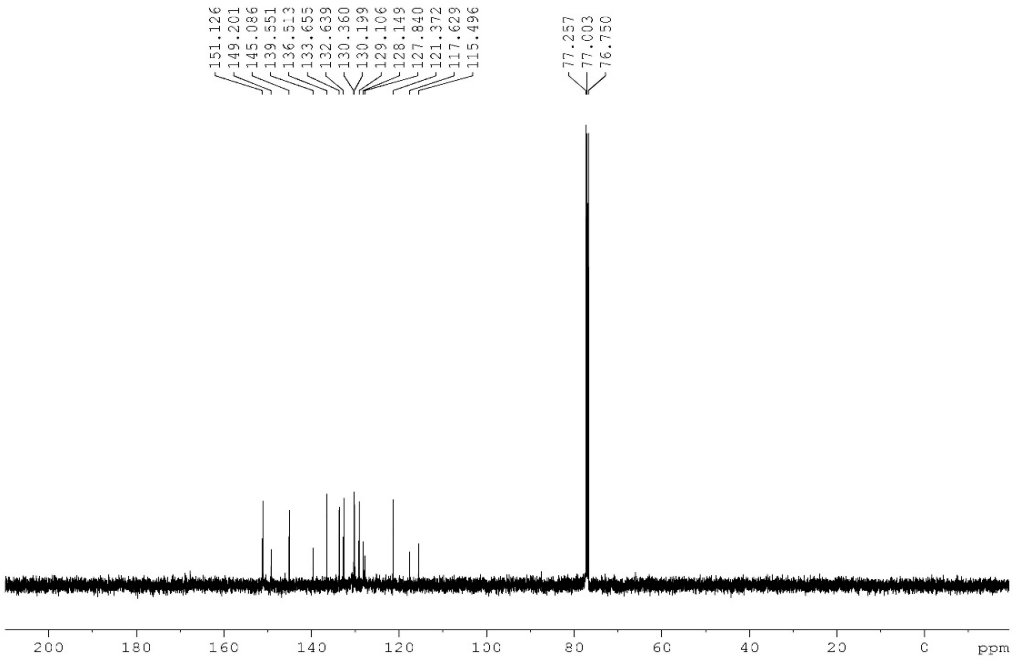

Figure A1.412: ^{19}F {^{1}H} NMR ($CDCl_3$, 470.8 MHz) of 2-(quinolin-6-yl)-7-(trifluoromethyl)-2,1-borazaronaphthalene (**2.147**)

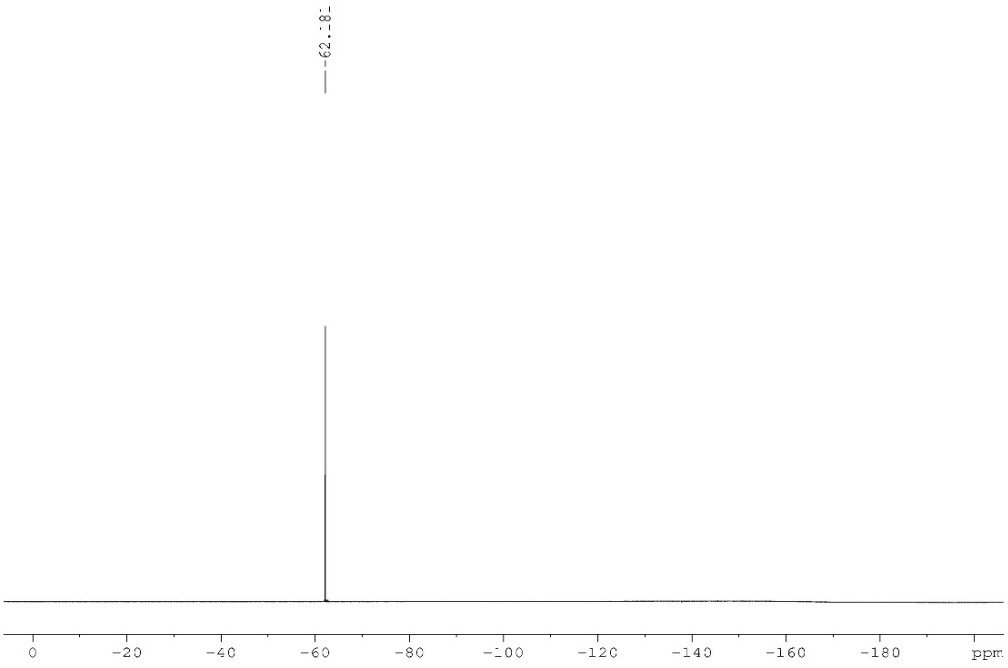

Figure A1.413: ^{11}B NMR ($CDCl_3$, 128.4 MHz) of 2-(quinolin-6-yl)-7-(trifluoromethyl)-2,1-borazaronaphthalene (**2.147**)

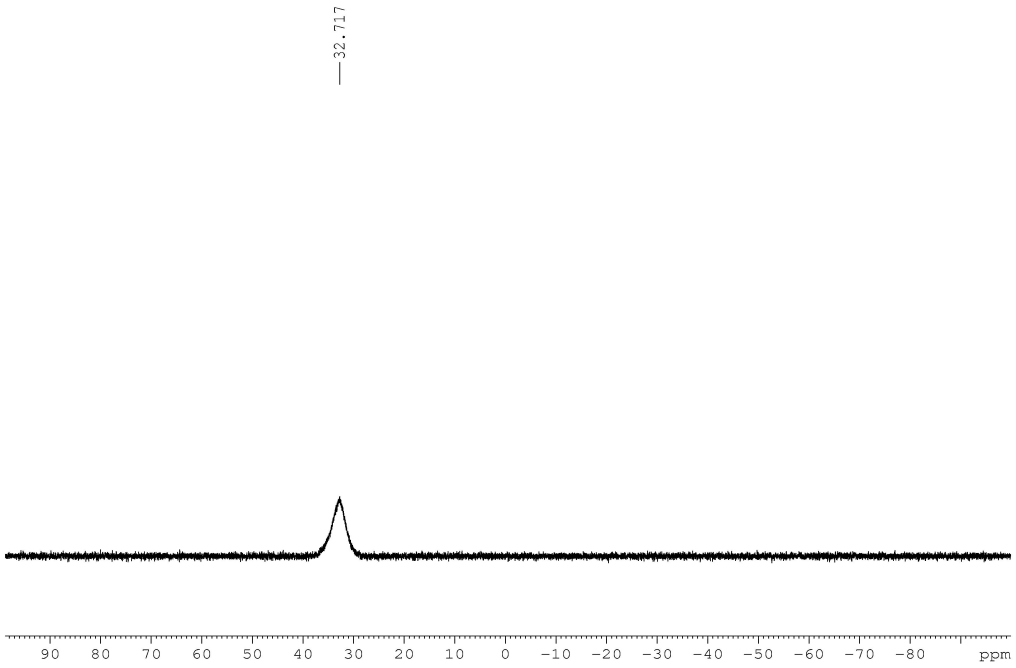

Figure A1.414: ^{1}H NMR (DMSO-d_6, 500.4 MHz) of 2-(quinolin-6-yl)-6-(trifluoromethoxy)-2,1-borazaronaphthalene (**2.148**)

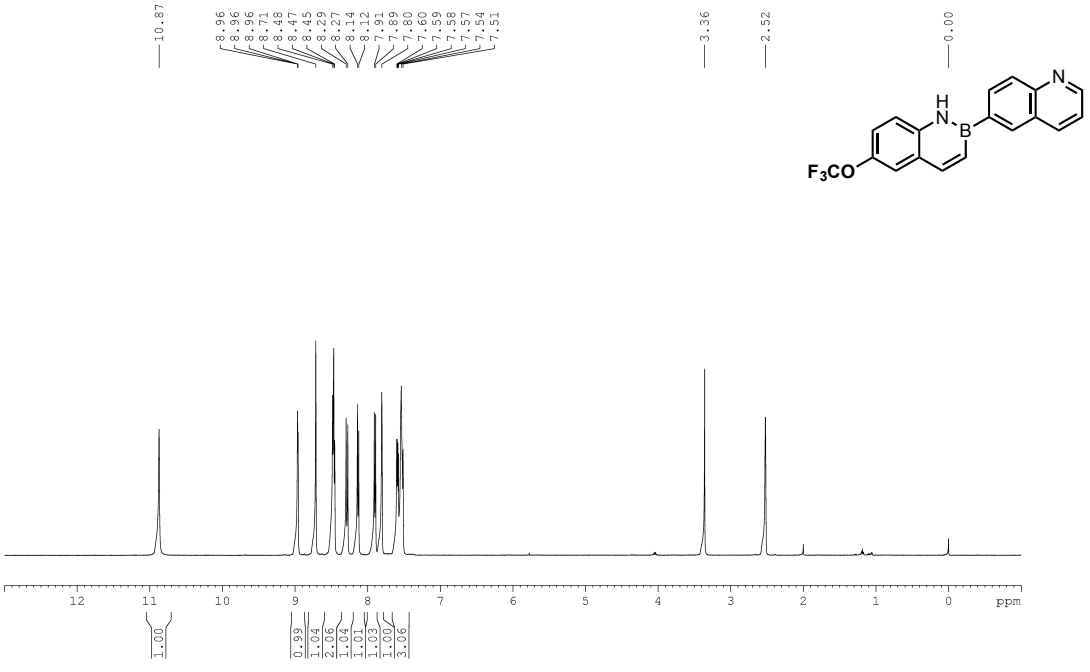

Figure A1.415: ^{13}C {^{1}H} NMR (DMSO-d_6, 125.8 MHz) of 2-(quinolin-6-yl)-6-(trifluoromethoxy)-2,1-borazaronaphthalene (**2.148**)

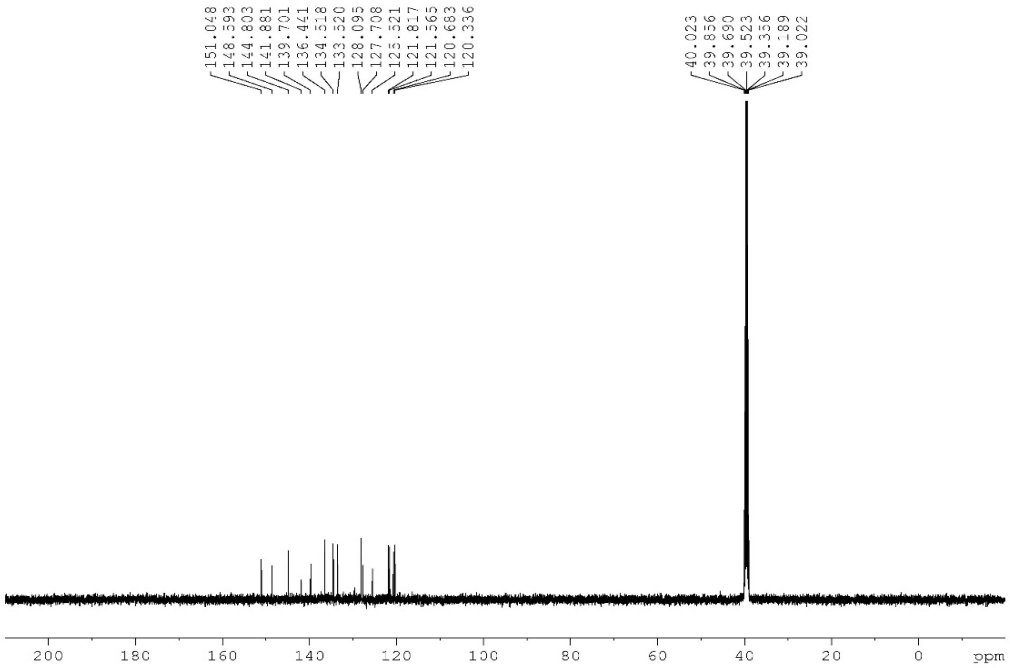

Figure A1.416: ^{19}F {^{1}H} NMR (DMSO-d_6, 470.8 MHz) of 2-(quinolin-6-yl)-6-(trifluoromethoxy)-2,1-borazaronaphthalene (**2.148**)

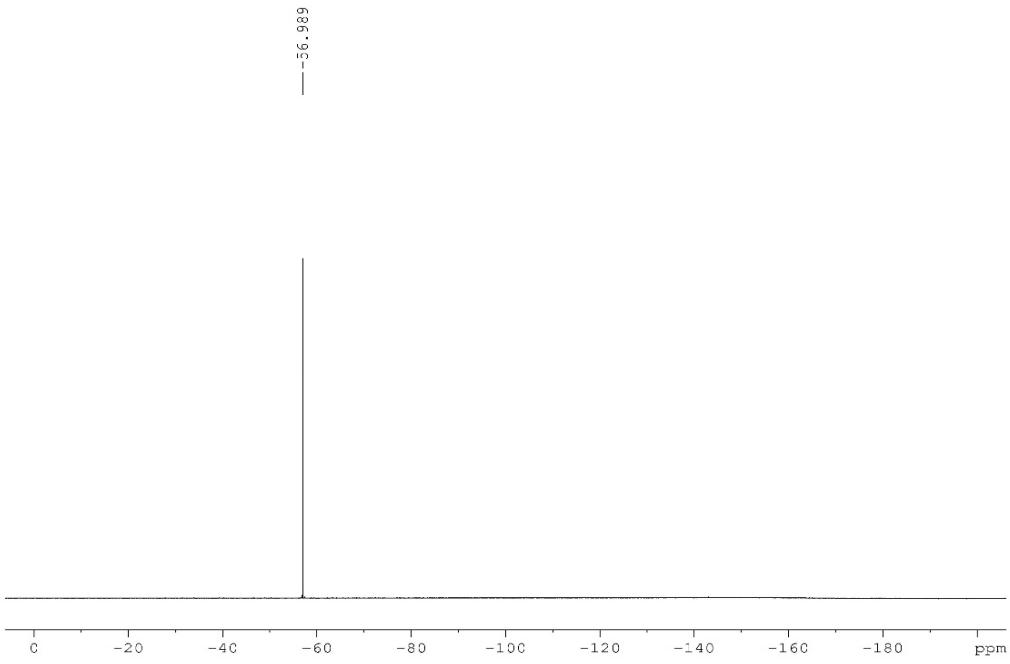

Figure A1.417: ^{11}B NMR ($CDCl_3$, 128.4 MHz) of 2-(quinolin-6-yl)-6-(trifluoromethoxy)-2,1-borazaronaphthalene (**2.148**)

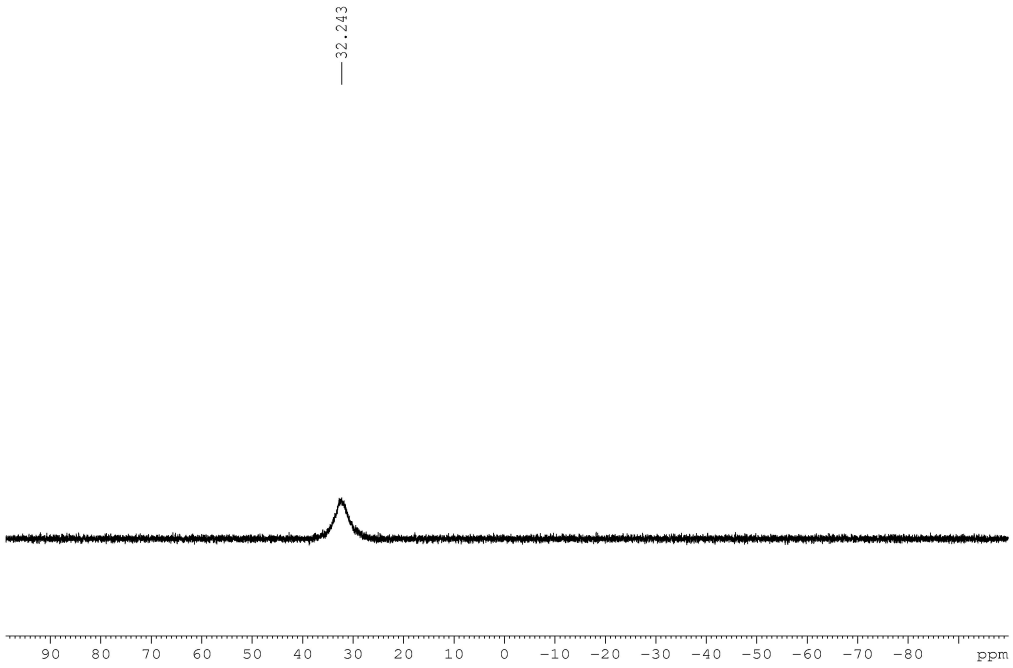

Figure A1.418: ^{1}H NMR ($CDCl_3$, 500.4 MHz) of 6,8-difluoro-2-(quinolin-6-yl)-2,1-borazaronaphthalene (**2.149**)

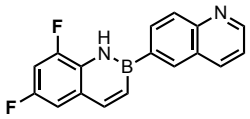

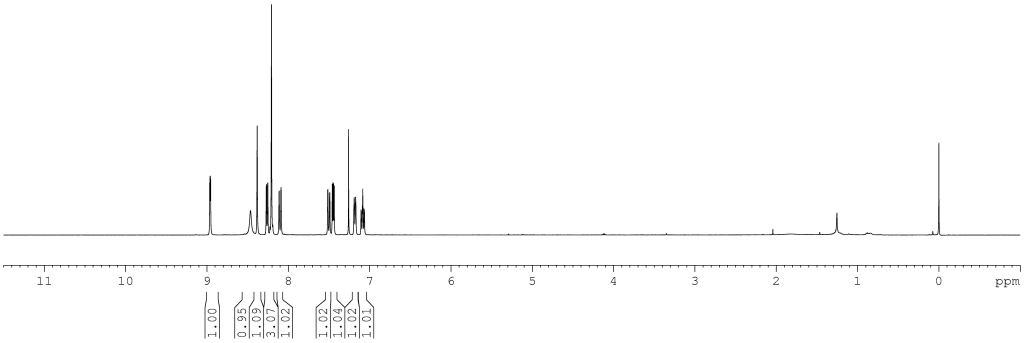

Figure A1.419: ^{13}C {^{1}H} NMR ($CDCl_3$, 125.8 MHz) of 6,8-difluoro-2-(quinolin-6-yl)-2,1-borazaronaphthalene (**2.149**)

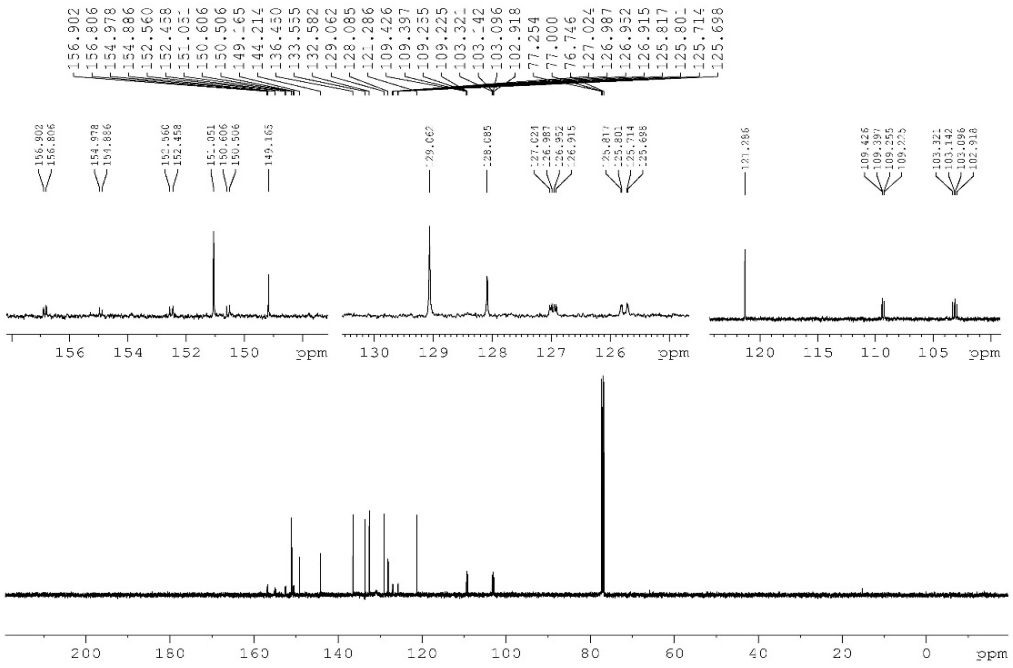

Figure A1.420: ^{19}F {^{1}H} NMR ($CDCl_3$, 470.8 MHz) of 6,8-difluoro-2-(quinolin-6-yl)-2,1-borazaronaphthalene (**2.149**)

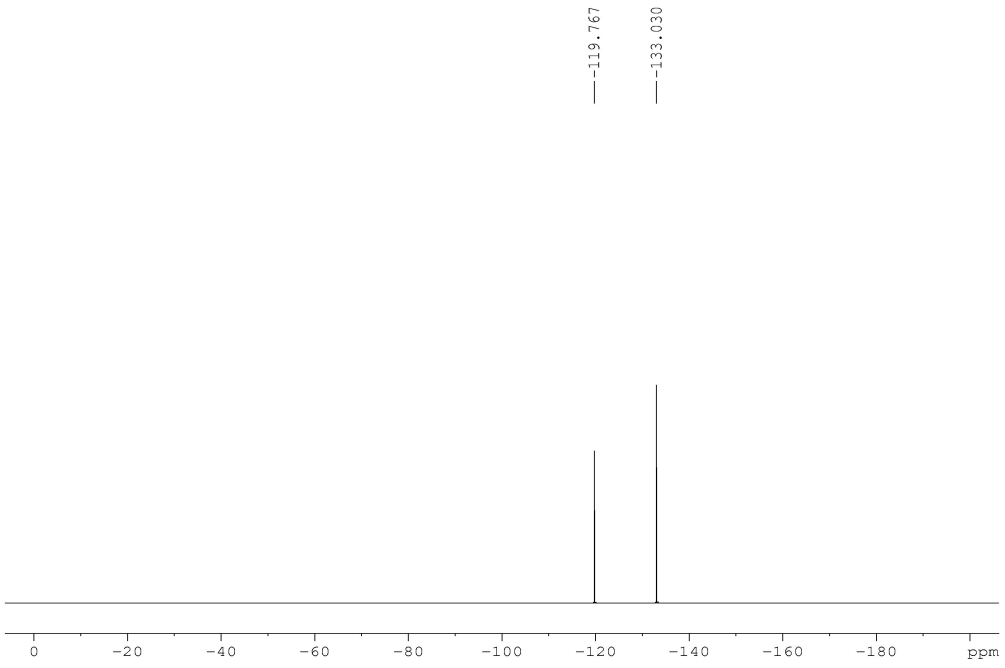

Figure A1.421: ^{11}B NMR ($CDCl_3$, 128.4 MHz) of 6,8-difluoro-2-(quinolin-6-yl)-2,1-borazaronaphthalene (**2.149**)

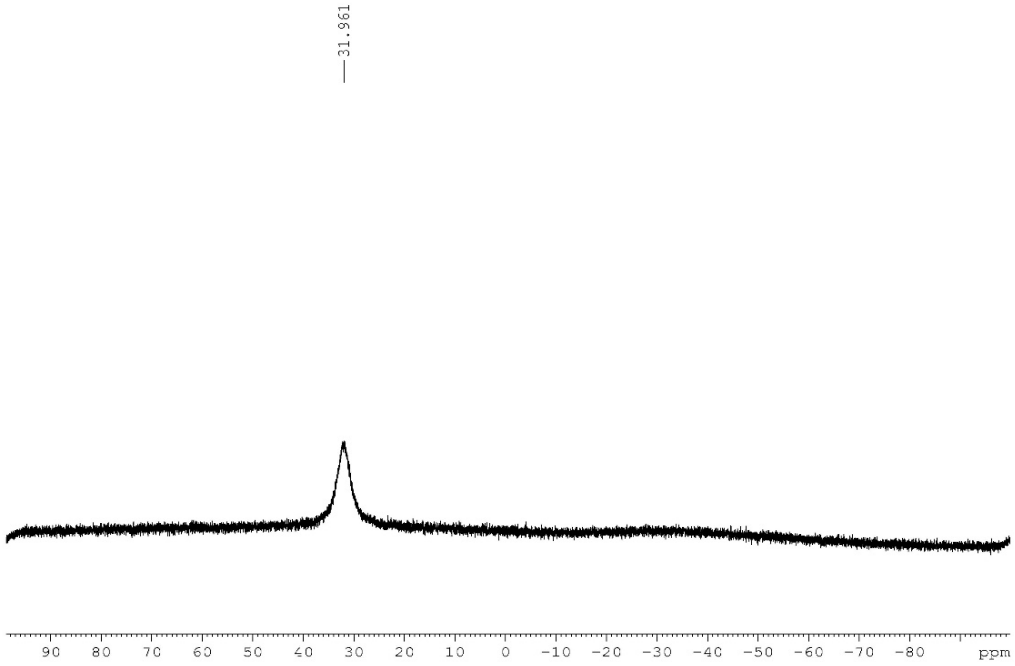

Figure A1.422: ^{1}H NMR ($CDCl_3$, 500.4 MHz) of 6-isopropyl-2-(quinolin-6-yl)-2,1-borazaronaphthalene (**2.150**)

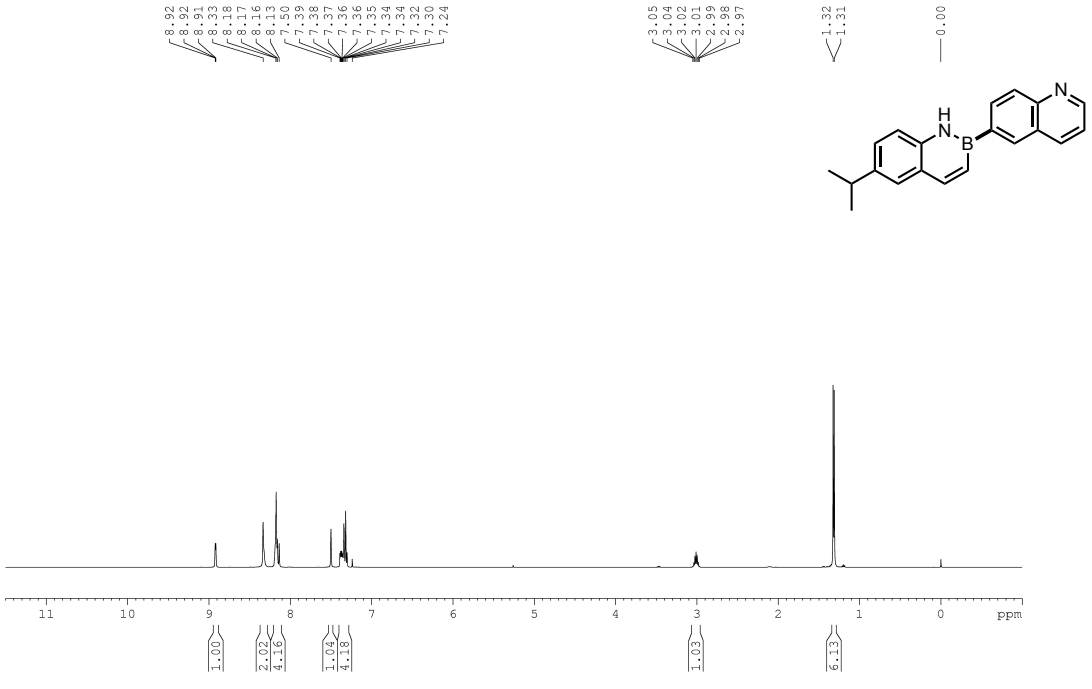

Figure A1.423: ^{13}C {^{1}H} NMR ($CDCl_3$, 125.8 MHz) of 6-isopropyl-2-(quinolin-6-yl)-2,1-borazaronaphthalene (**2.150**)

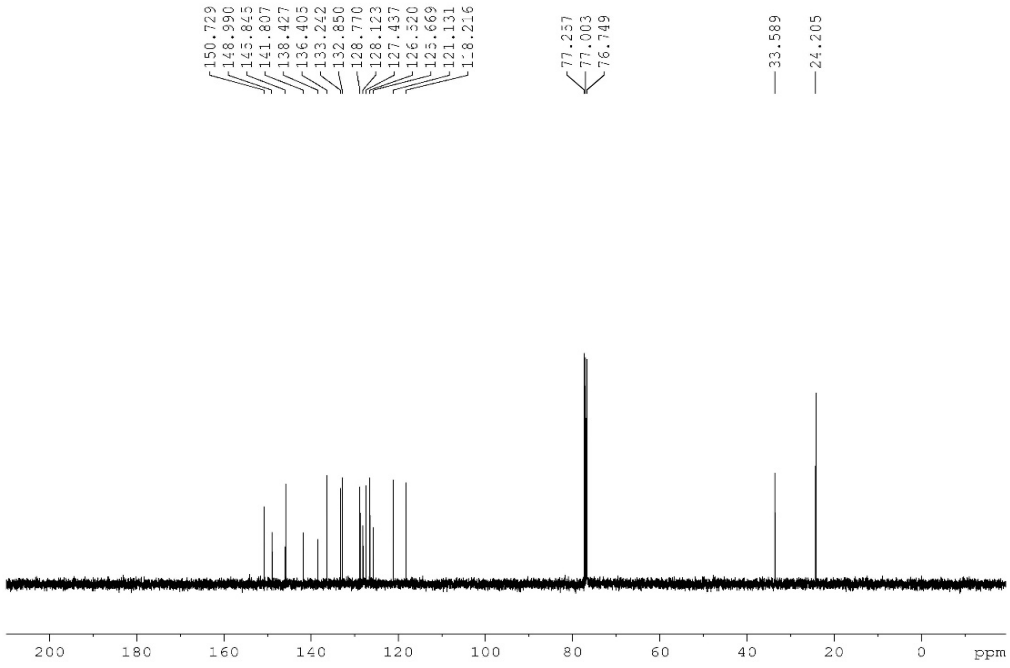

Figure A1.424: ^{11}B NMR ($CDCl_3$, 128.4 MHz) of 6-isopropyl-2-(quinolin-6-yl)-2,1-borazaronaphthalene (**2.150**)

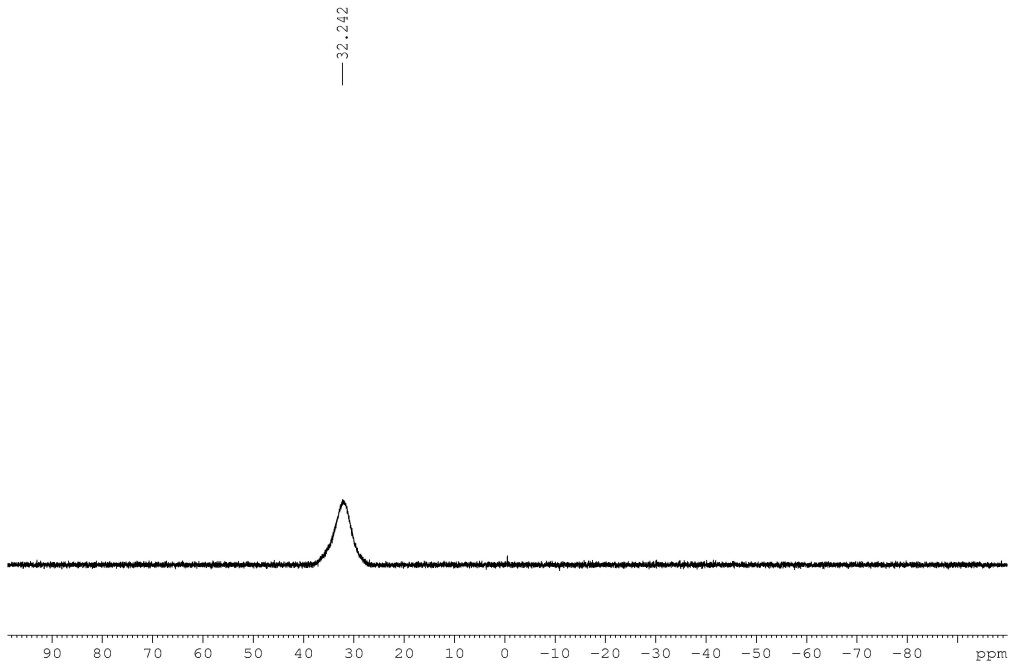

Figure A1.425: ^{1}H NMR (DMSO-d_6, 500.4 MHz) of 2-(quinolin-6-yl)-6-carbonitrile-2,1-borazaronaphthalene (**2.151**)

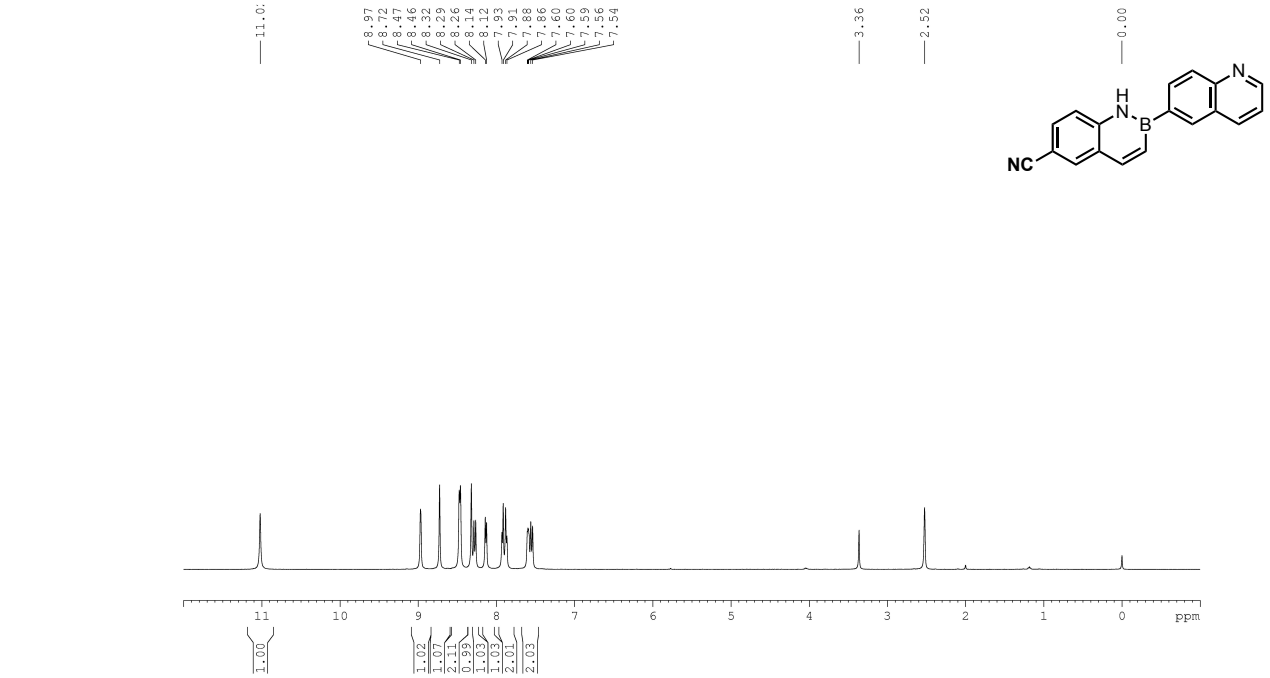

Figure A1.426: ^{13}C {^{1}H} NMR (DMSO-d_6, 125.8 MHz) of 2-(quinolin-6-yl)-6-carbonitrile-2,1-borazaronaphthalene (**2.151**)

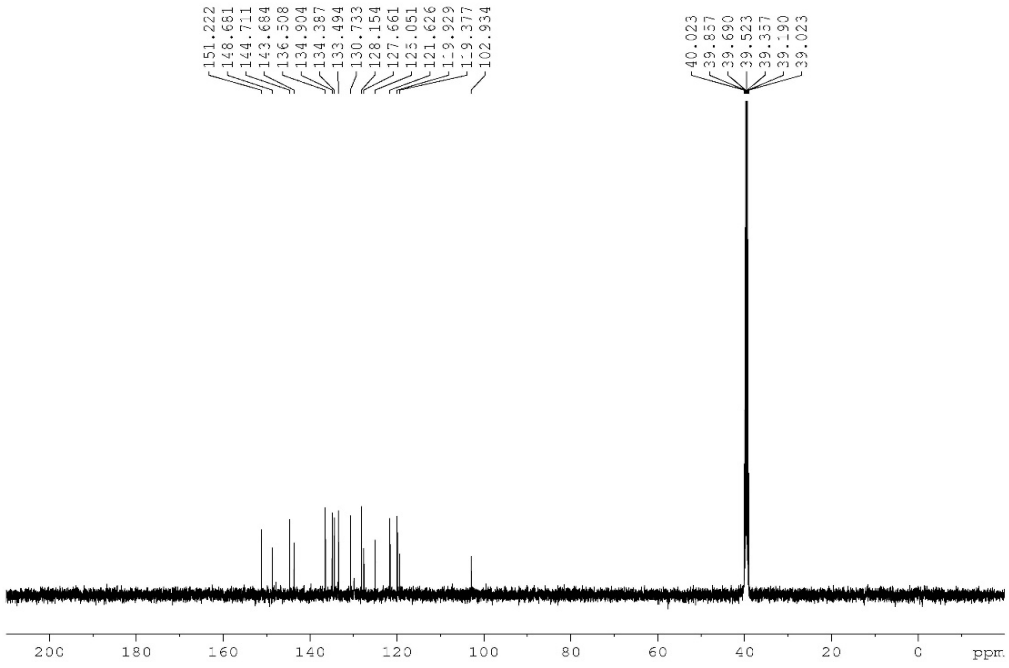

Figure A1.427: ^{11}B NMR ($CDCl_3$, 128.4 MHz) of 2-(quinolin-6-yl)-6-carbonitrile-2,1-borazaronaphthalene (**2.151**)

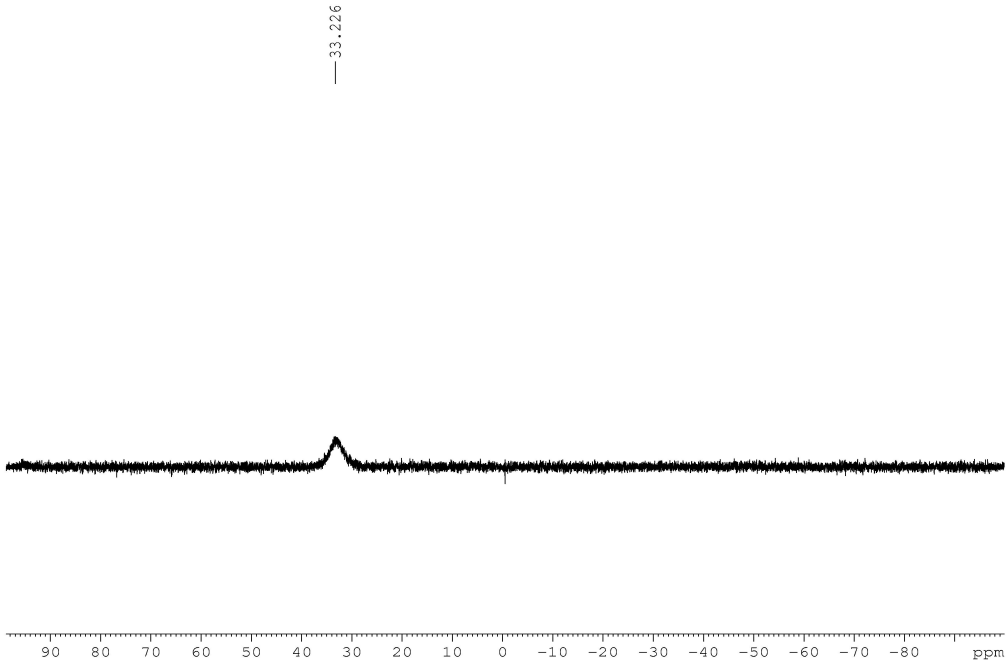

Figure A1.428: ^{1}H NMR (DMSO-d_6, 500.4 MHz) of 2-(quinolin-6-yl)-6,5-borazaroquinoline (**2.152**)

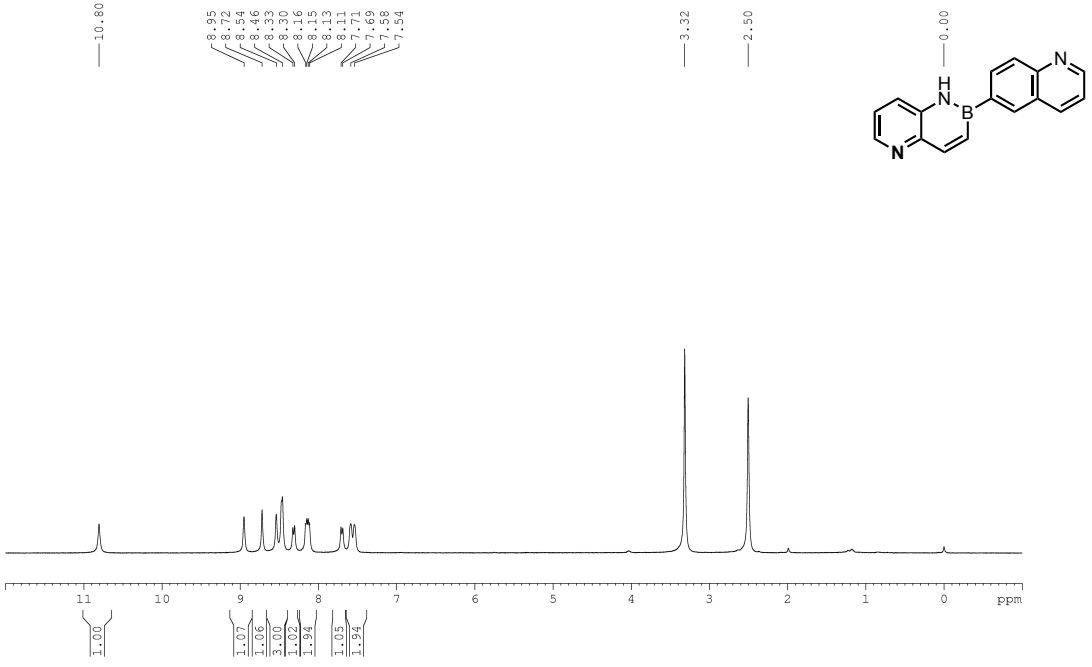

Figure A1.429: ^{13}C {^{1}H} NMR (DMSO-d_6, 125.8 MHz) of 2-(quinolin-6-yl)-6,5-borazaroquinoline (**2.152**)

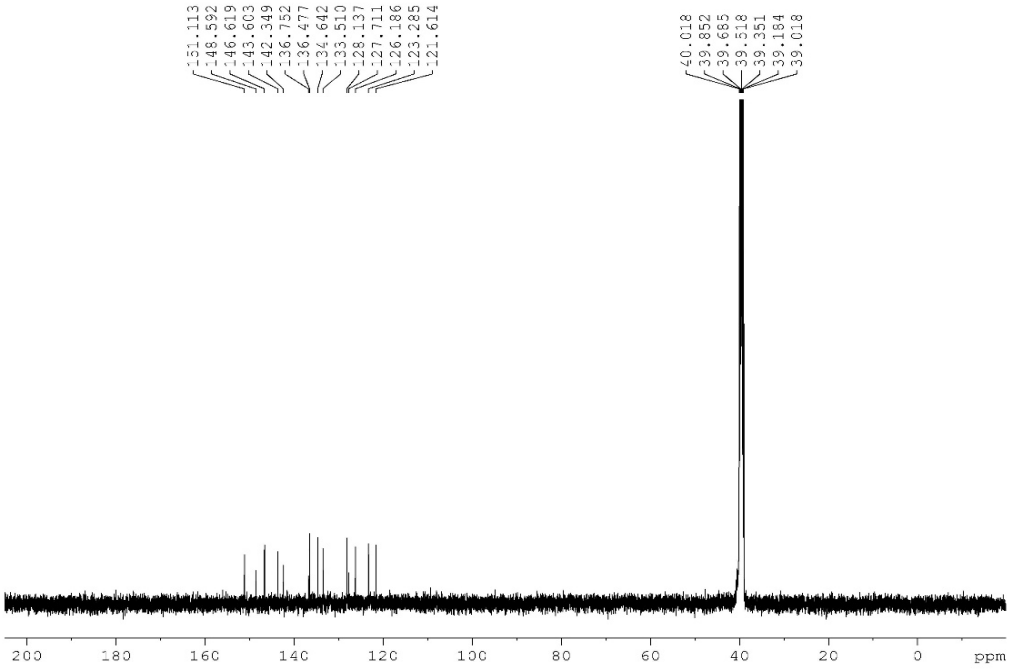

Figure A1.430: ^{11}B NMR ($CDCl_3$, 128.4 MHz) of 2-(quinolin-6-yl)-6,5-borazaroquinoline (**2.152**)

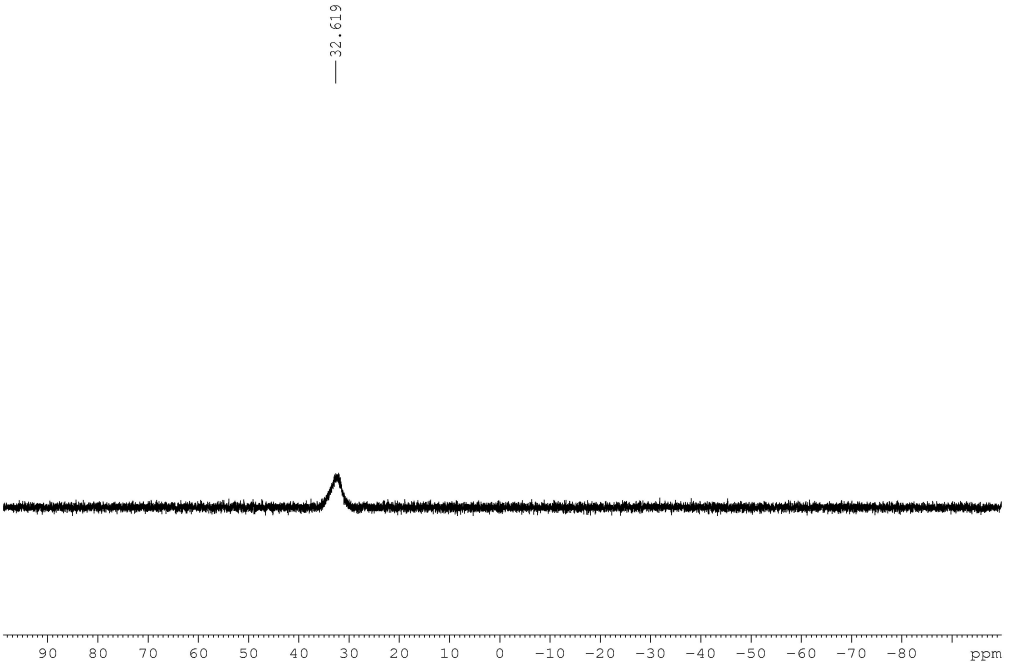

Figure A1.431: ^{1}H NMR ($CDCl_3$, 500.4 MHz) of 2-(3,5-dimethylisoxazole-4-yl)-6,5-borazaroisoquinoline (**2.153**)

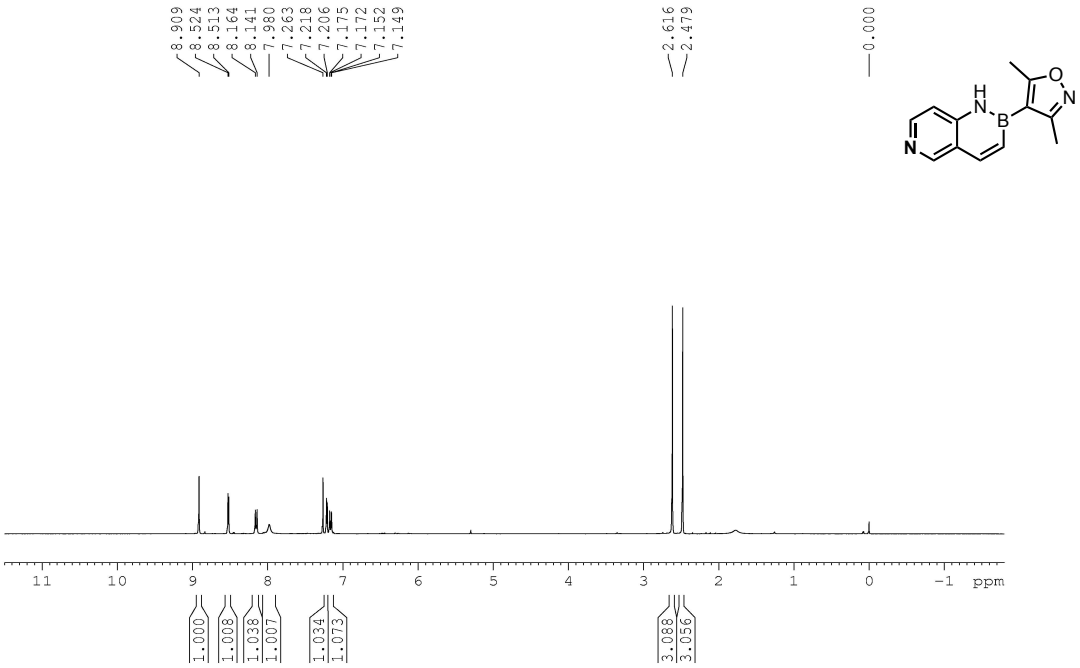

Figure A1.432: ^{3}C {^{1}H} NMR ($CDCl_3$, 125.8 MHz) of 2-(3,5-dimethylisoxazole-4-yl)-6,5-borazaroisoquinoline (**2.153**)

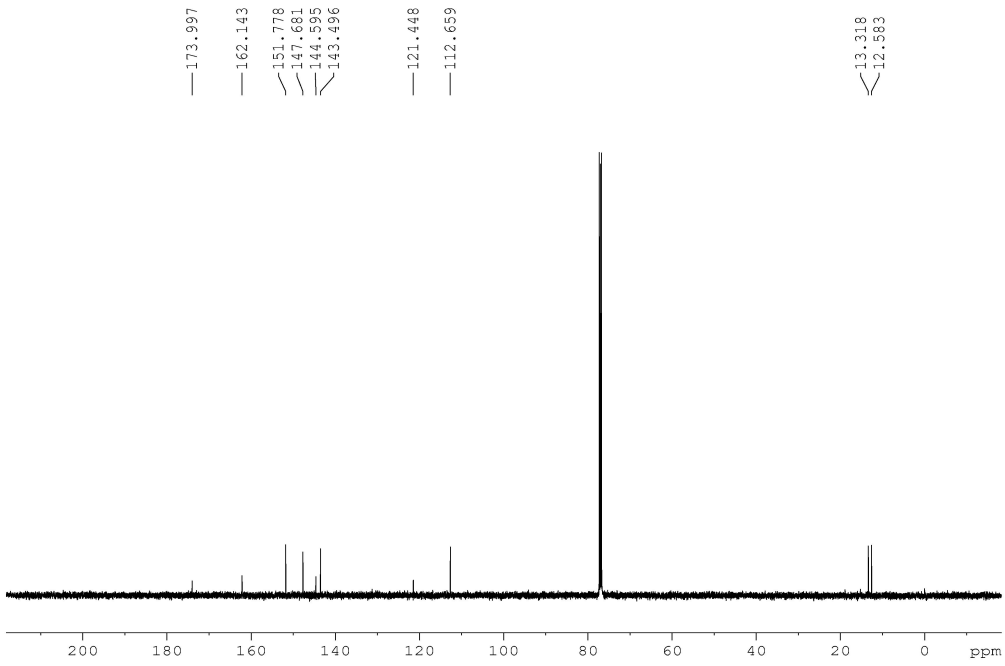

Figure A1.433: ^{11}B NMR ($CDCl_3$, 128.4 MHz) of 2-(3,5-dimethylisoxazole-4-yl)-6,5-borazaroisoquinoline (**2.153**)

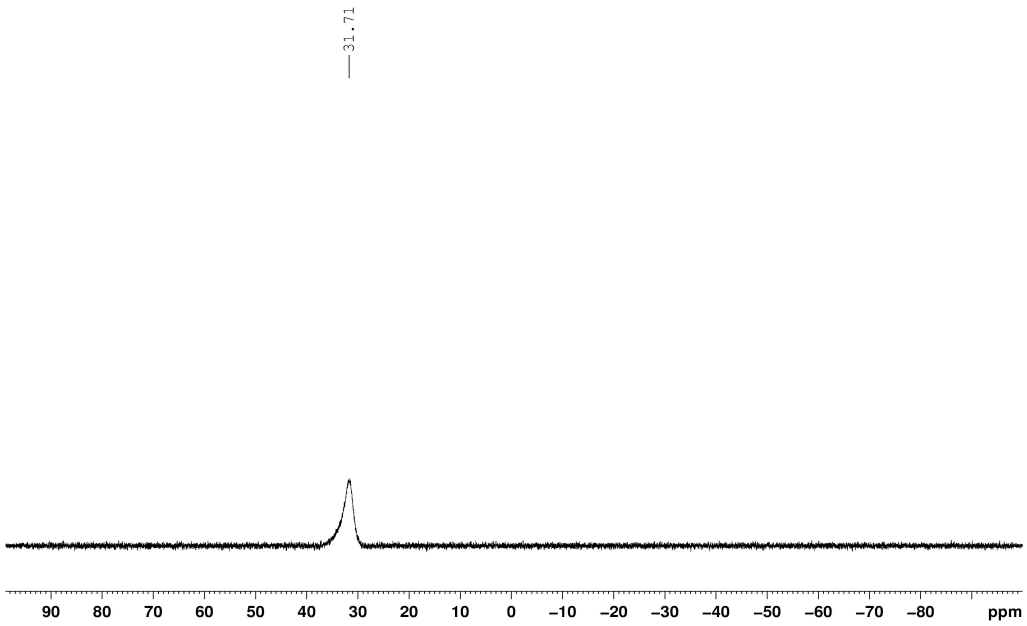

Figure A1.434: ^{1}H NMR ($CDCl_3$, 500.4 MHz) of 2-(3-fluorophenyl)-6,5-borazaroquinoline (**2.154**)

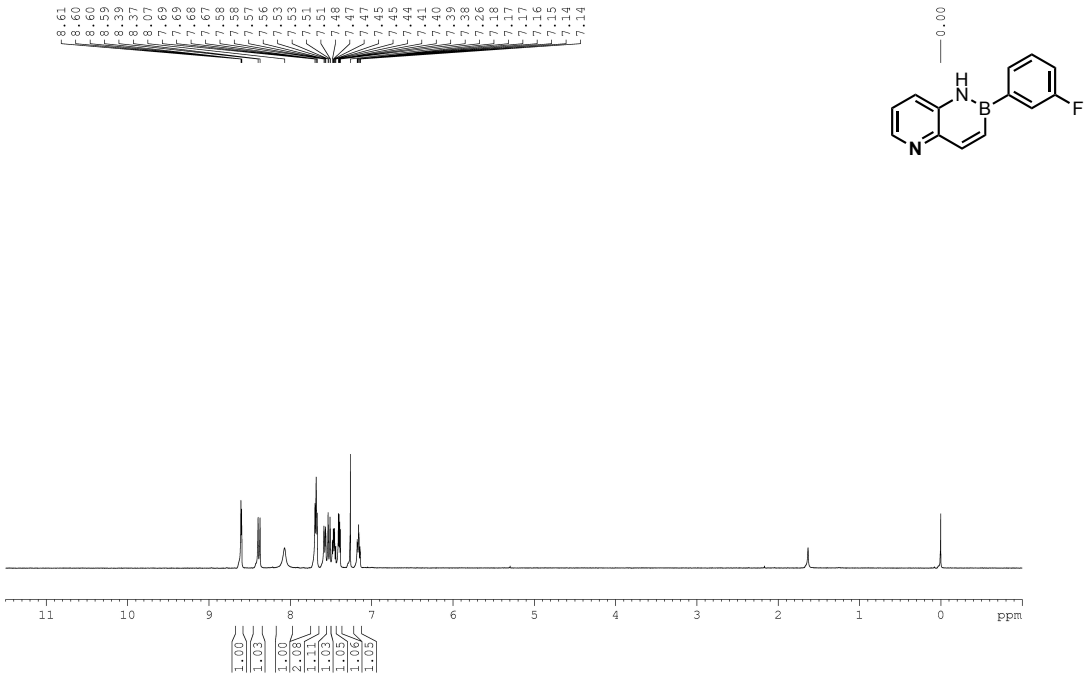

Figure A1.435: ^{13}C {^{1}H} NMR ($CDCl_3$, 125.8 MHz) of 2-(3-fluorophenyl)-6,5-borazaroquinoline (**2.154**)

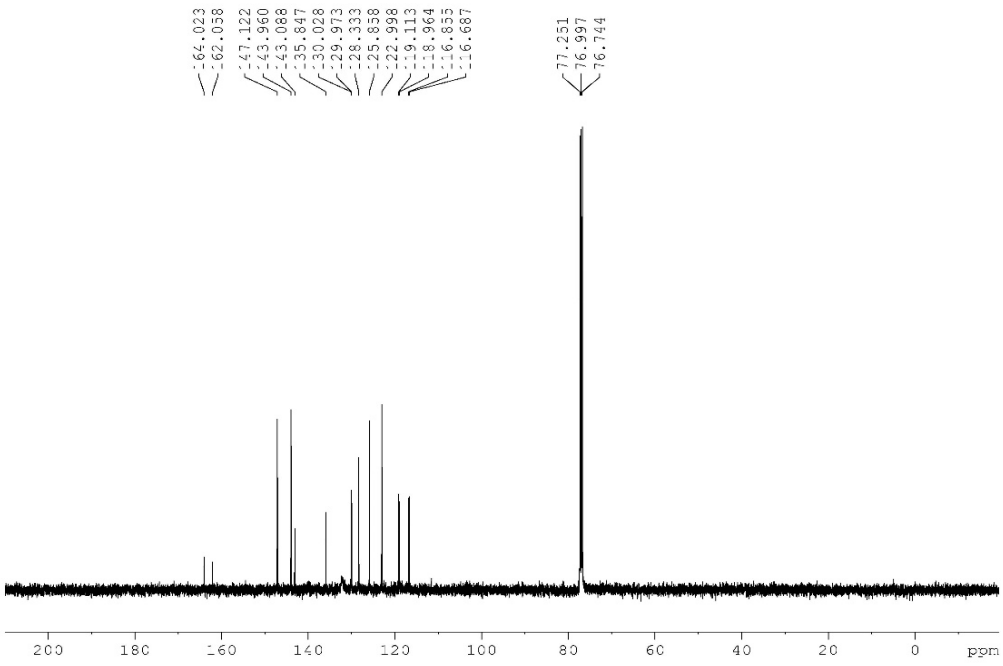

Figure A1.436: ^{19}F {^{1}H} NMR ($CDCl_3$, 470.8 MHz) of 2-(3-fluorophenyl)-6,5-borazaroquinoline (**2.154**)

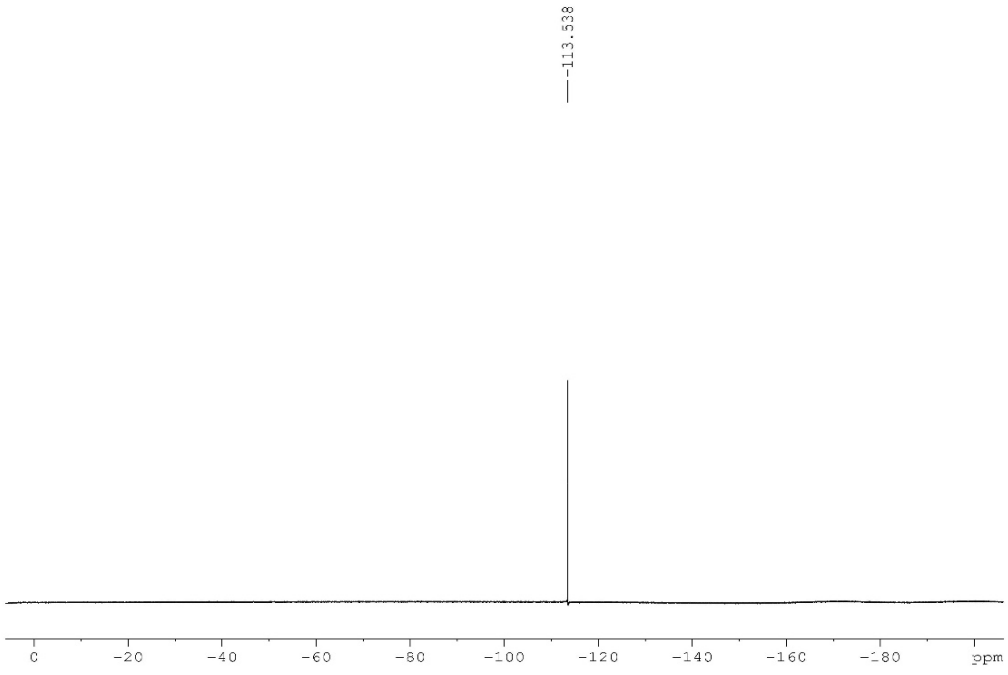

Figure A1.437: ^{11}B NMR ($CDCl_3$, 128.4 MHz) of 2-(3-fluorophenyl)-6,5-borazaroquinoline (**2.154**)

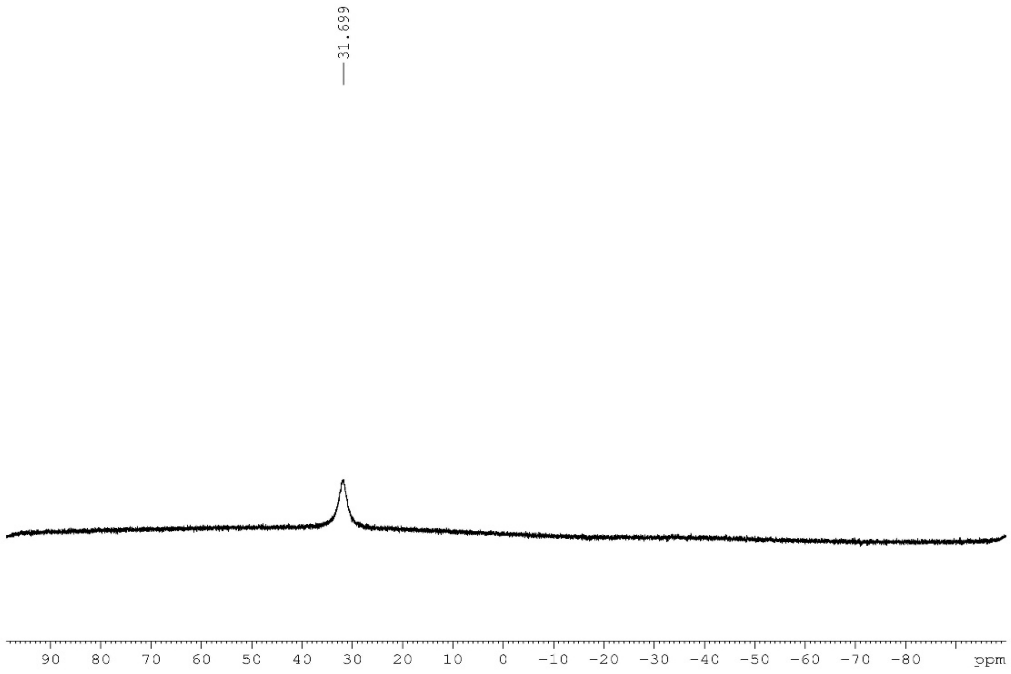

Figure A1.438: ^{1}H NMR ($CDCl_3$, 500.4 MHz) of 2-(thiophen-3-yl)-6,5-borazaroisoquinoline (**2.155**)

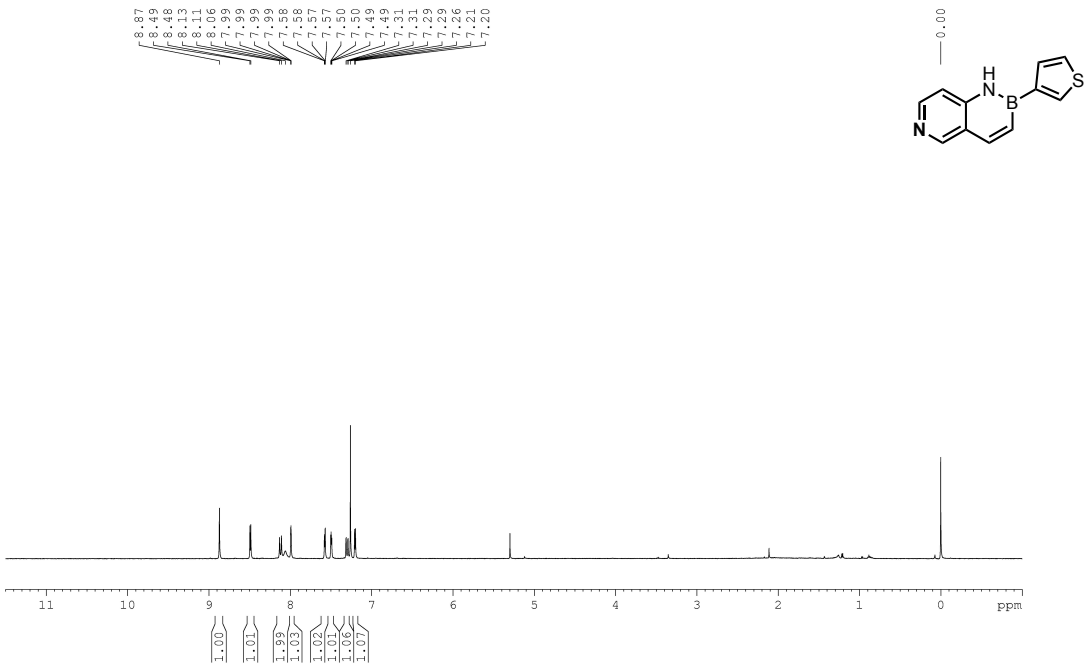

Figure A1.439: ^{13}C {^{1}H} NMR ($CDCl_3$, 125.8 MHz) of 2-(thiophen-3-yl)-6,5-borazaroisoquinoline (**2.155**)

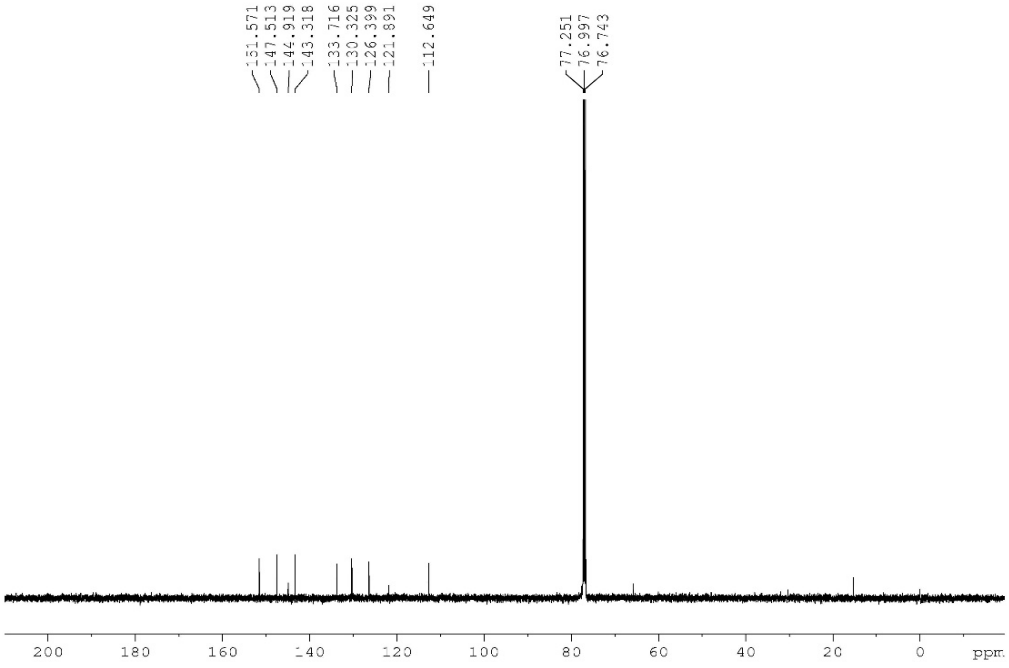

Figure A1.440: ^{11}B NMR ($CDCl_3$, 128.4 MHz) of 2-(thiophen-3-yl)-6,5-borazaroisoquinoline (**2.155**)

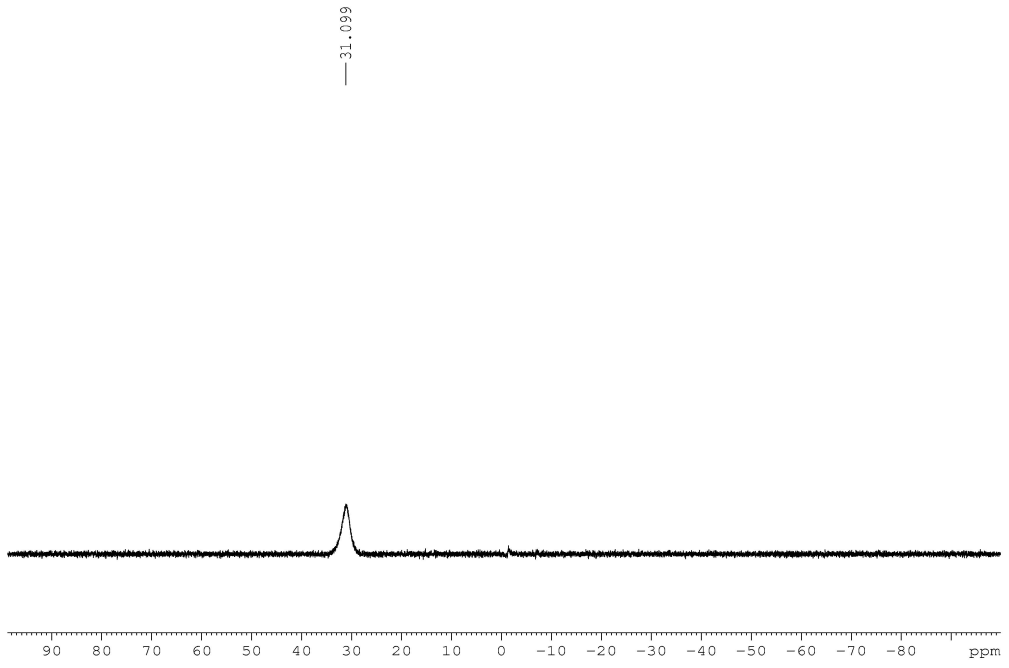

APPENDIX A2 – SUPPORTING DATA FOR CHAPTER 3

A2.1 – Spectral data relevant to Chapter 3.2

Figure A2.1: ^{1}H NMR ($CDCl_3$, 500.4 MHz) of 2-(4-cyclohexylphenyl)-2,1-borazanaphthalene (**3.2**)

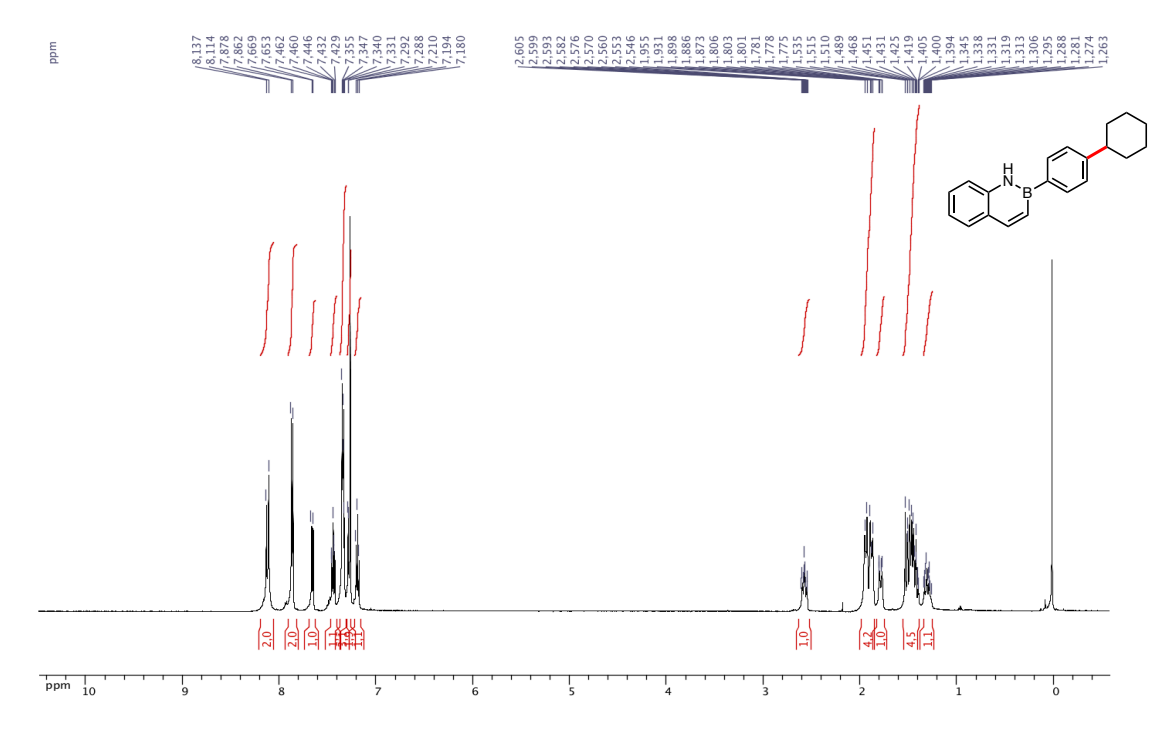

Figure A2.2: ^{13}C {^{1}H} NMR ($CDCl_3$, 125.8 MHz) of 2-(4-cyclohexylphenyl)-2,1-borazanaphthalene (**3.2**)

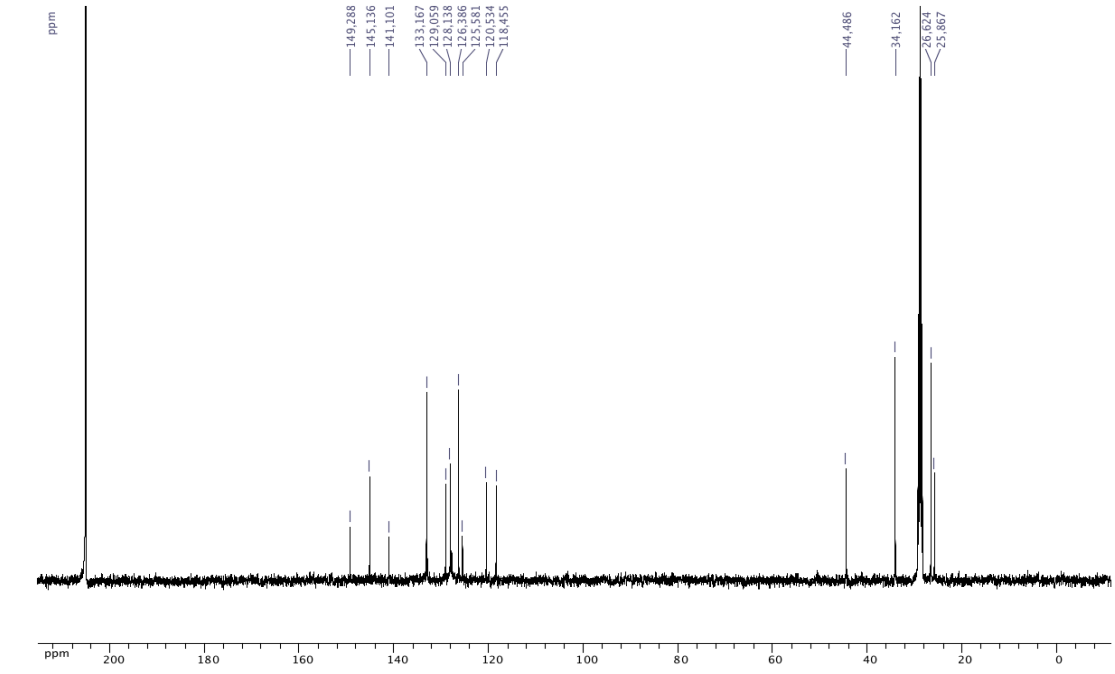

Figure A2.3: ^{11}B NMR (acetone, 128.4 MHz) of 2-(4-cyclohexylphenyl)-2,1-borazanaphthalene (**3.2**)

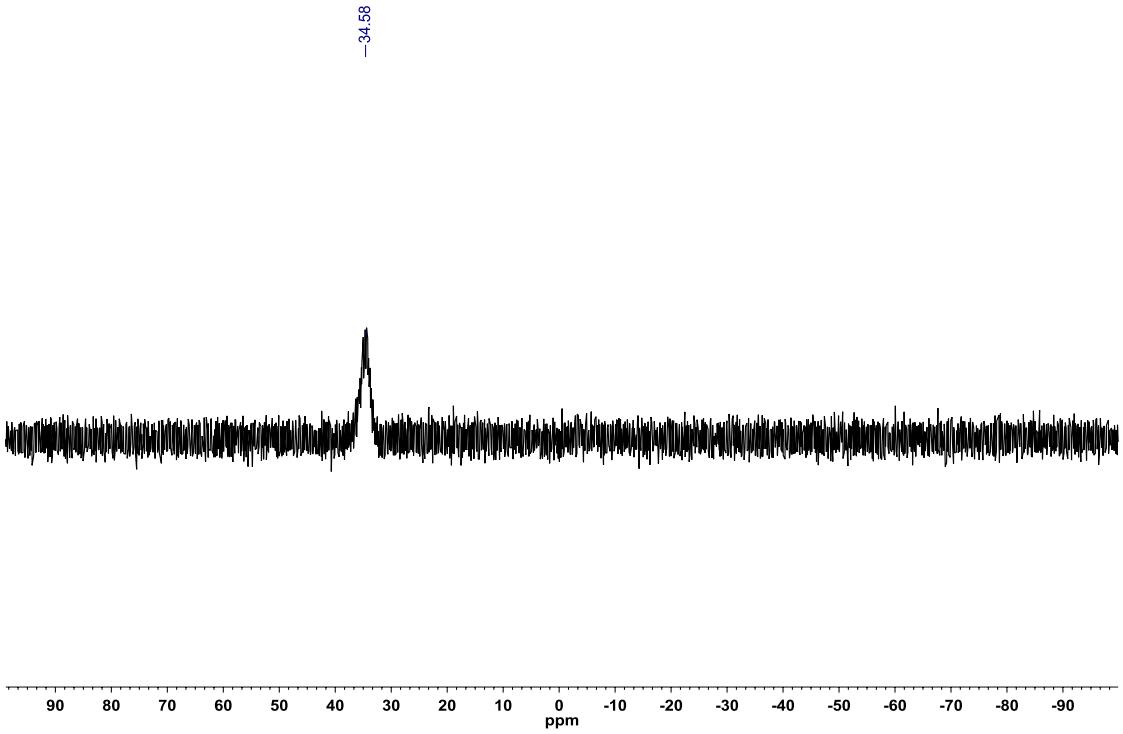

Figure A2.4: ^{1}H NMR (acetone-d_6, 500.4 MHz) of 2-(4-(*exo*-bicyclo[2.2.1]heptan-2-yl)phenyl)-2,1-borazanaphthalene (**3.3**)

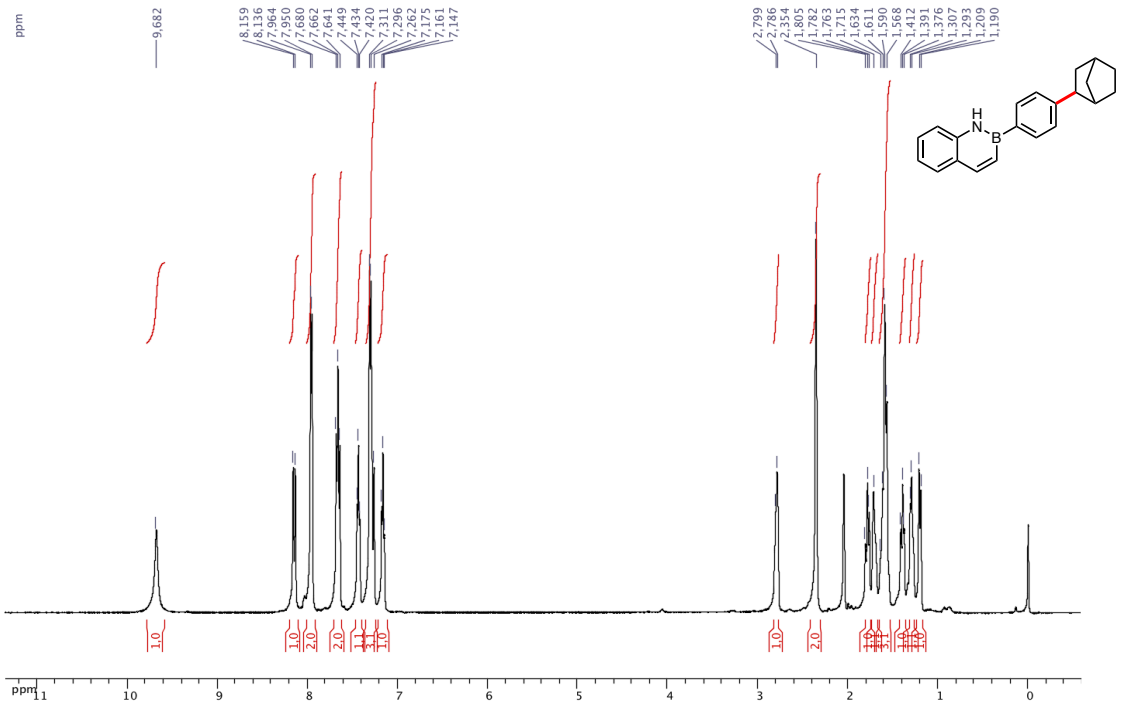

Figure A2.5: ^{13}C {^{1}H} NMR (acetone-d_6, 125.8 MHz) of 2-(4-(*exo*-bicyclo[2.2.1]heptan-2-yl)phenyl)-2,1-borazanaphthalene (**3.3**)

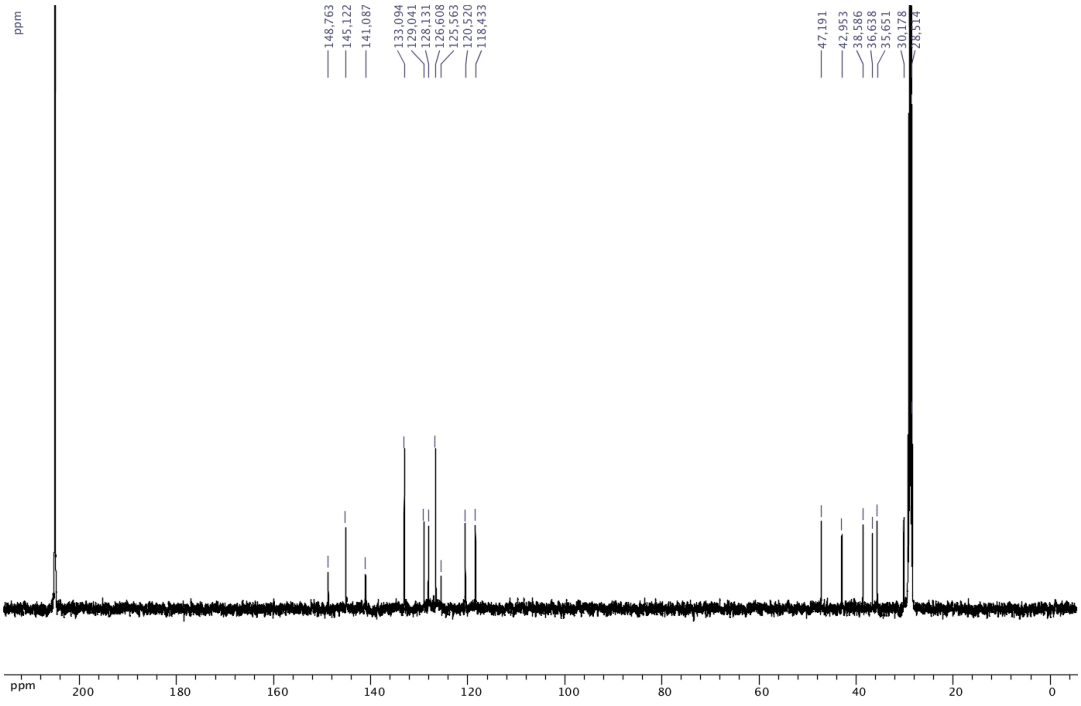

Figure A2.6: ^{11}B NMR (acetone, 128.4 MHz) of of 2-(4-(*exo*-bicyclo[2.2.1]heptan-2-yl)phenyl)-2,1-borazanaphthalene (**3.3**)

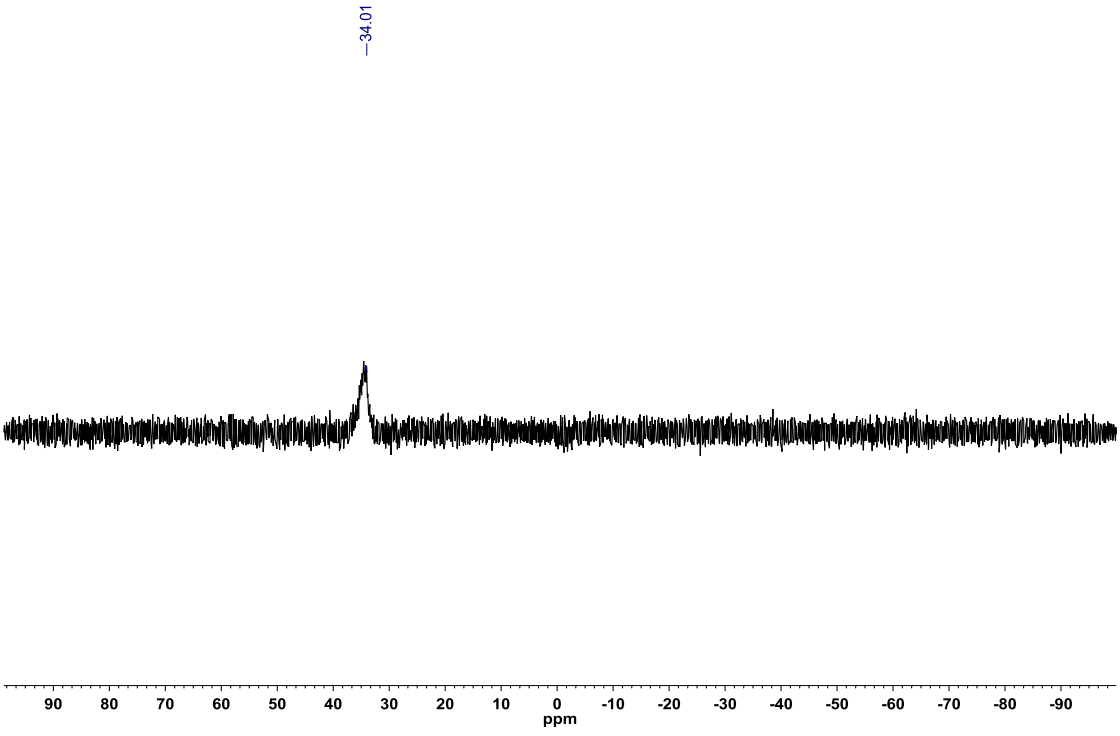

Figure A2.7: ^{1}H NMR (acetone-d_6, 500.4 MHz) of 2-(4-(3,3,3-trifluoropropyl)phenyl)-2,1-borazanaphthalene (**3.4**)

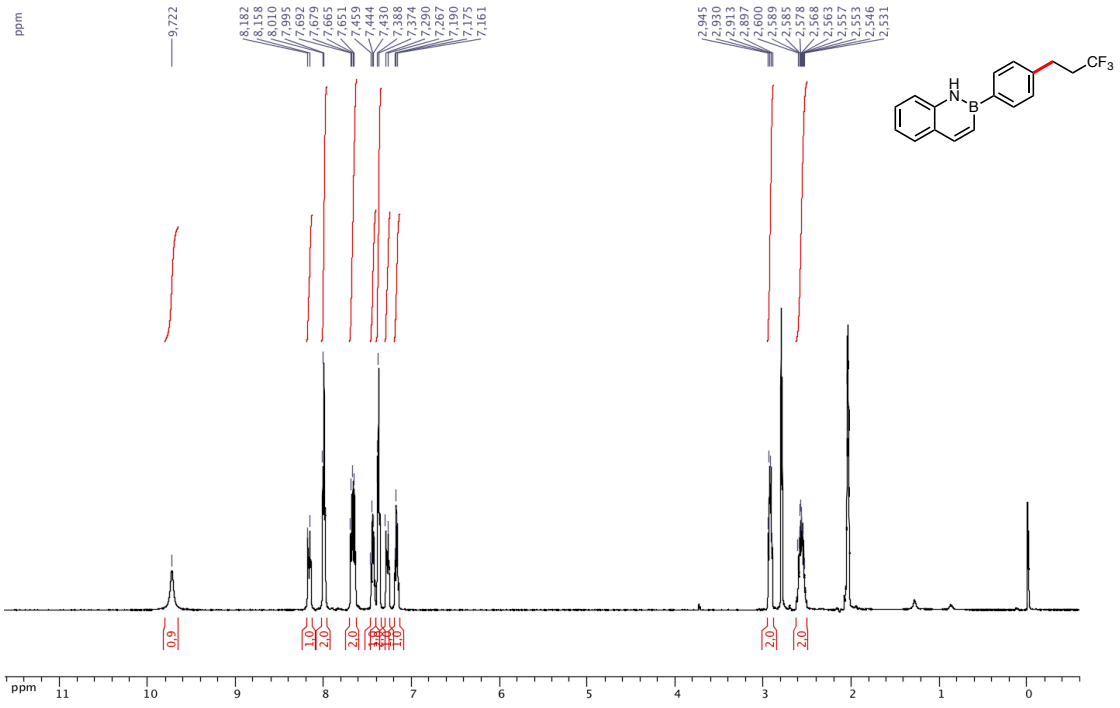

Figure A2.8: ^{13}C {^{1}H} ($CDCl_3$, 125.8 MHz) of 2-(4-(3,3,3-trifluoropropyl)phenyl)-2,1-borazanaphthalene (**3.4**)

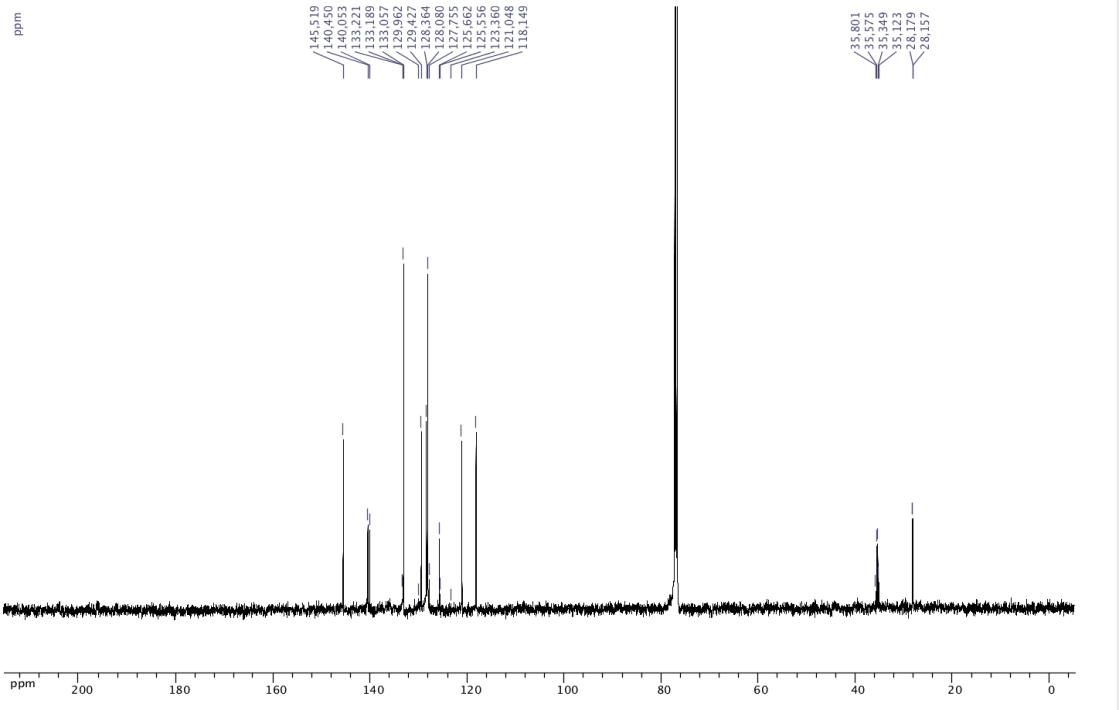

Figure A2.9: ^{19}F {^{1}H} NMR (acetone-d_6, 470.8 MHz) of 2-(4-(3,3,3-trifluoropropyl)phenyl)-2,1-borazanaphthalene (**3.4**)

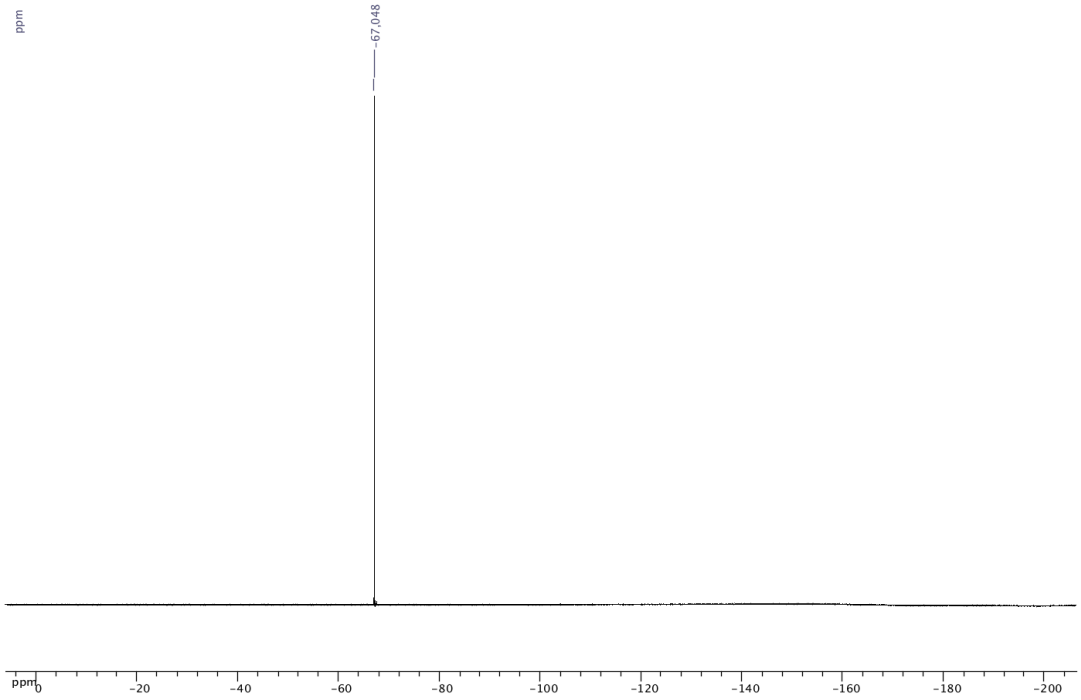

Figure A2.10: ^{11}B NMR (acetone, 128.4 MHz) of 2-(4-(3,3,3-trifluoropropyl)phenyl)-2,1-borazanaphthalene (**3.4**)

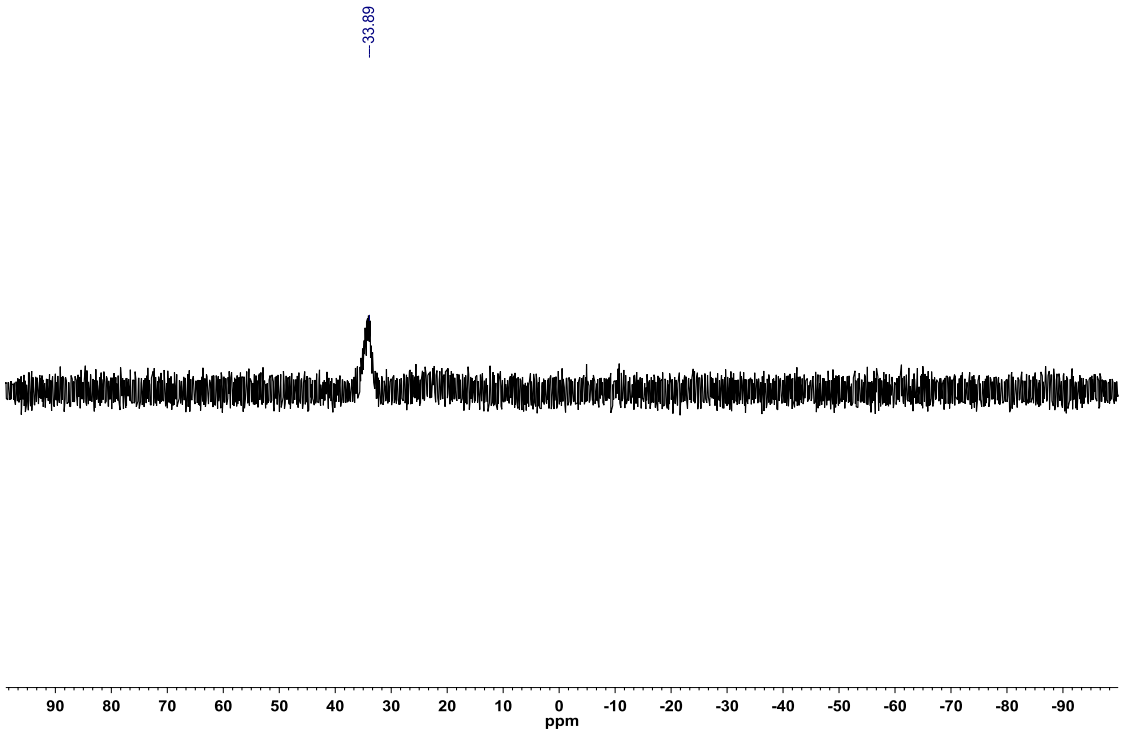

Figure A2.11: ^{1}H NMR (acetone-d_6, 500.4 MHz) of 2-(4-(3-methoxypropyl)phenyl)-2,1-borazanaphthalene (**3.5**)

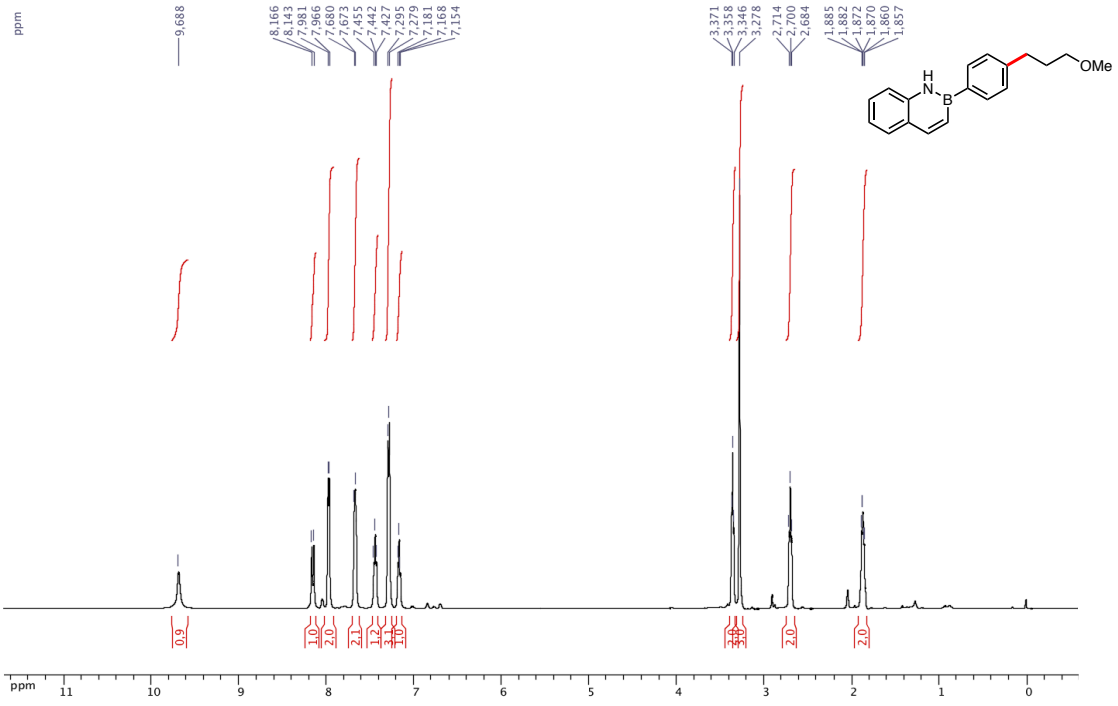

Figure A2.12: ^{13}C {^{1}H} (acetone-d_6, 125.8 MHz) of 2-(4-(3-methoxypropyl)phenyl)-2,1-borazanaphthalene (**3.5**)

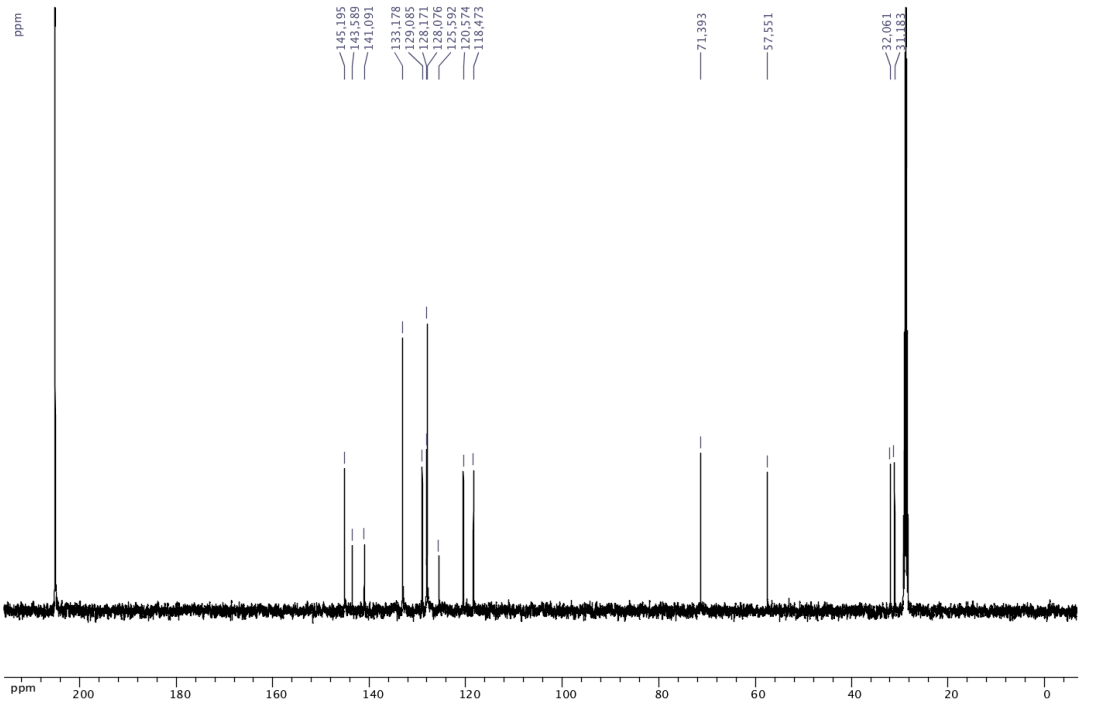

Figure A2.13: ^{11}B NMR (acetone, 128.4 MHz) of 2-(4-(3-methoxypropyl)phenyl)-2,1-borazanaphthalene (**3.5**)

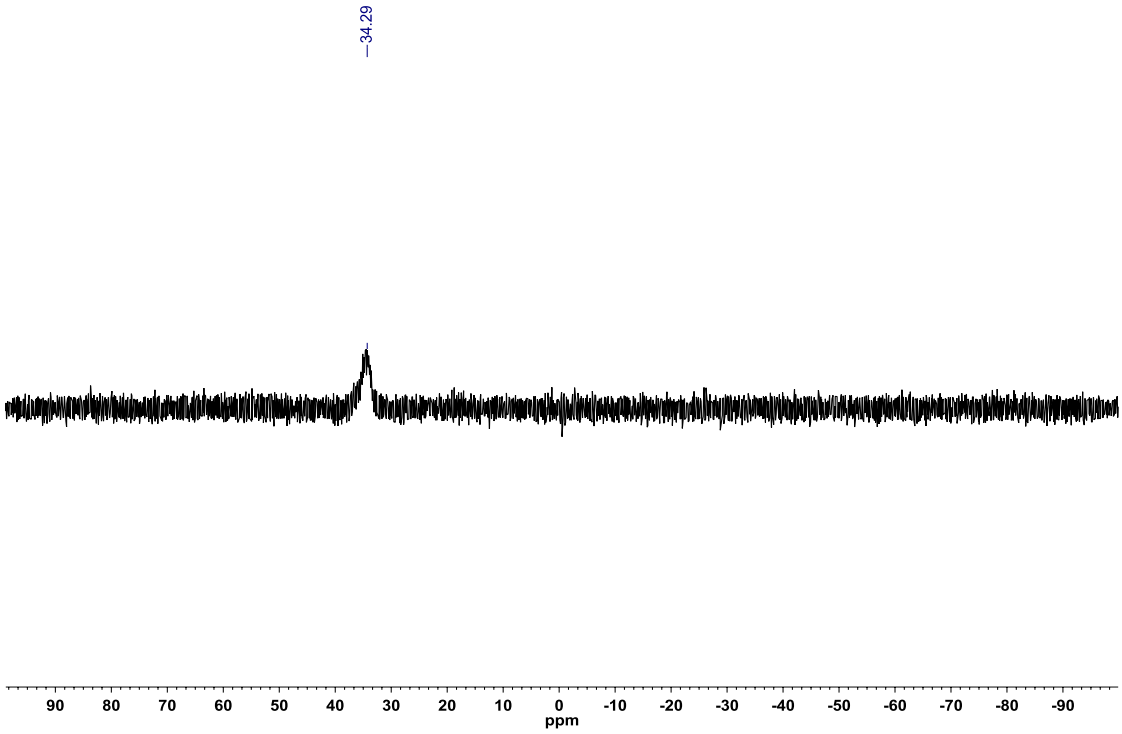

Figure A2.14: ^{1}H NMR (acetone-d_6, 500.4 MHz) of 2-(4-isobutylphenyl)-2,1-borazanaphthalene (**3.6**)

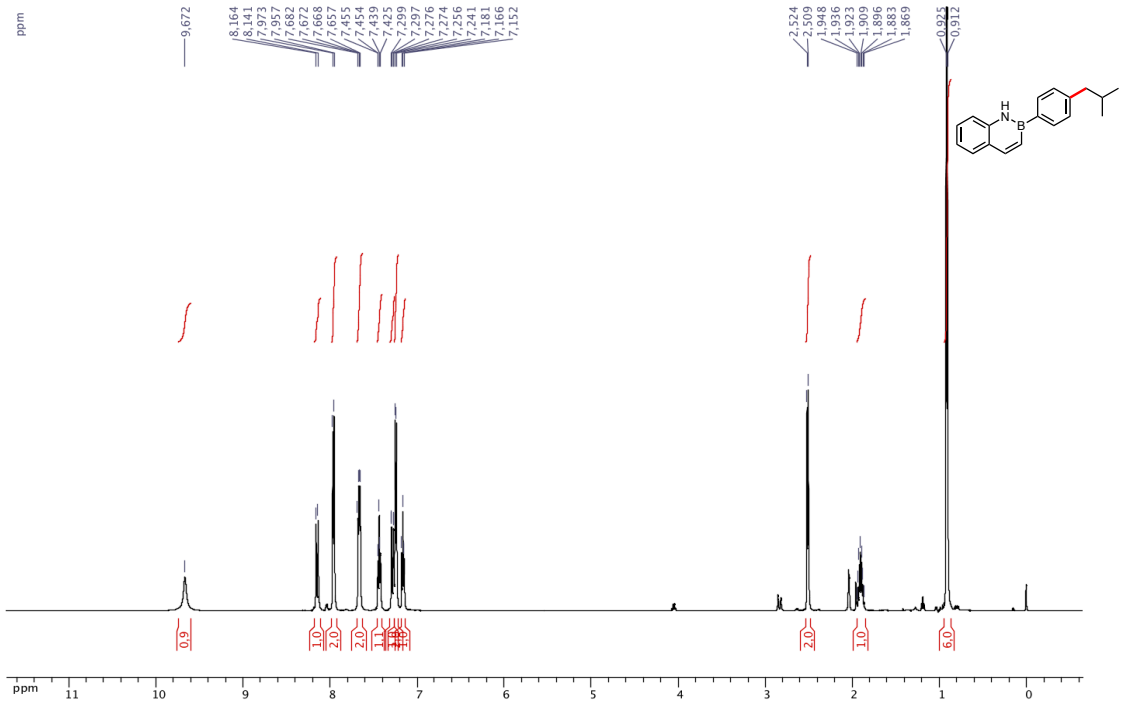

Figure A2.15: ^{13}C {^{1}H} NMR (acetone-d_6, 125.8 MHz) of 2-(4-isobutylphenyl)-2,1-borazanaphthalene (**3.6**)

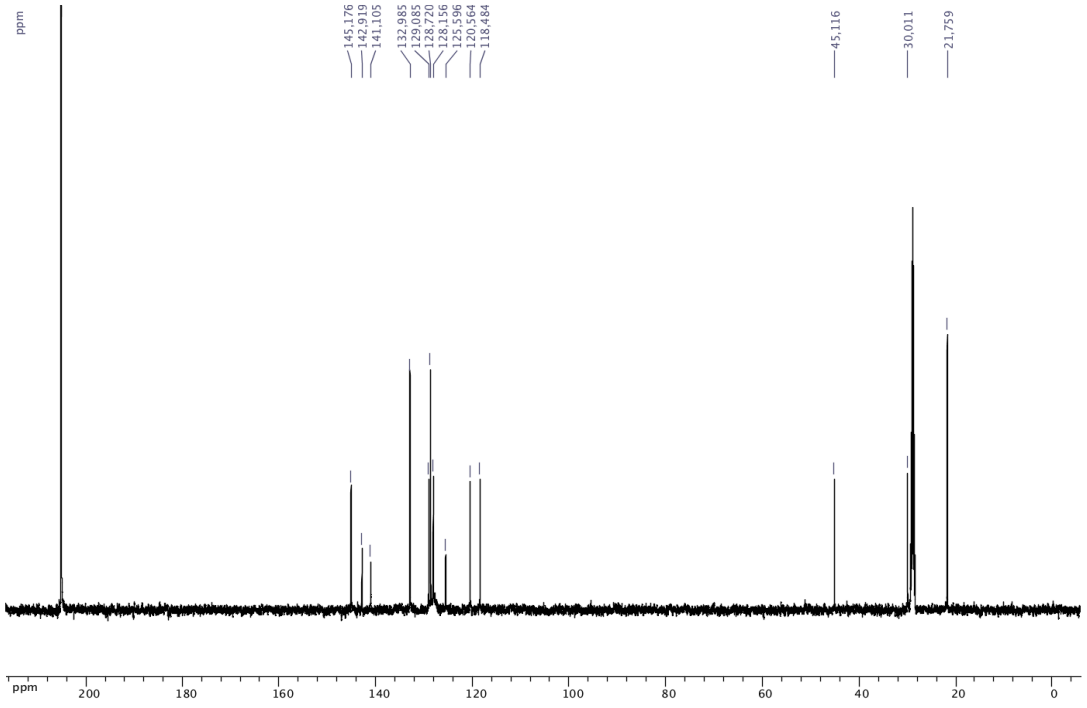

Figure A2.16: ^{11}B NMR (acetone, 128.4 MHz) of 2-(4-isobutylphenyl)-2,1-borazanaphthalene (**3.6**)

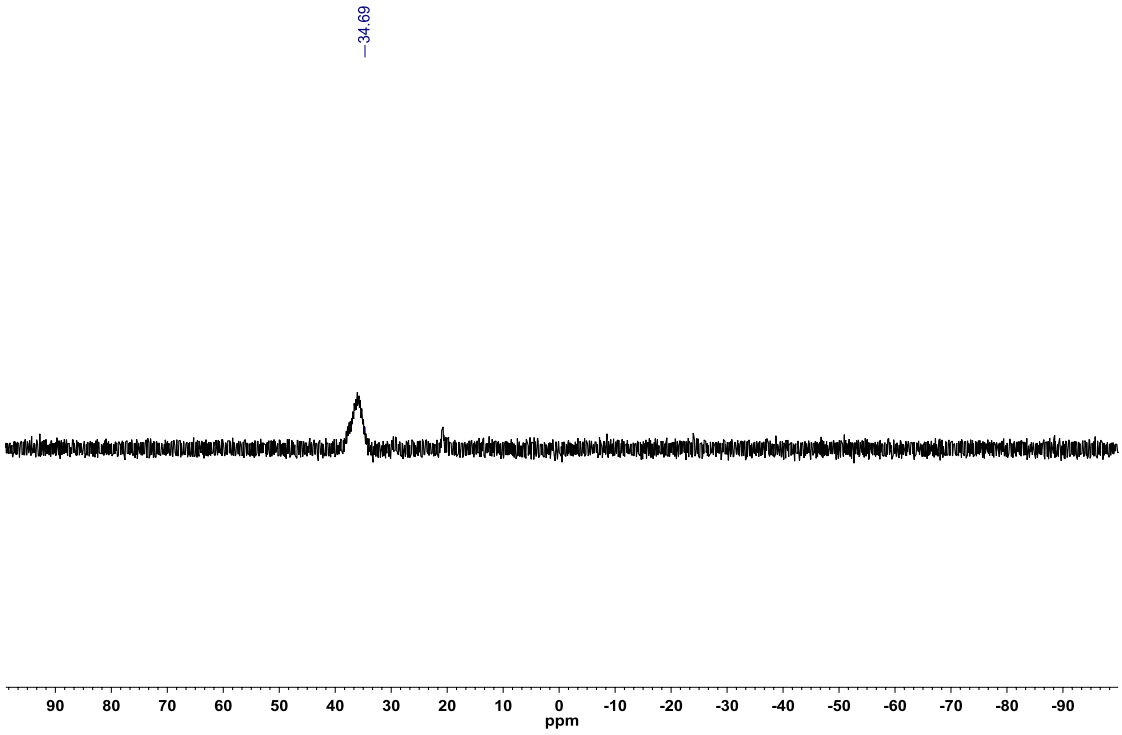

Figure A2.17: ^{1}H NMR (acetone-d_6, 500.4 MHz) of 2-(4-(acetoxymethyl)phenyl)-2,1-borazanaphthalene (**3.7**)

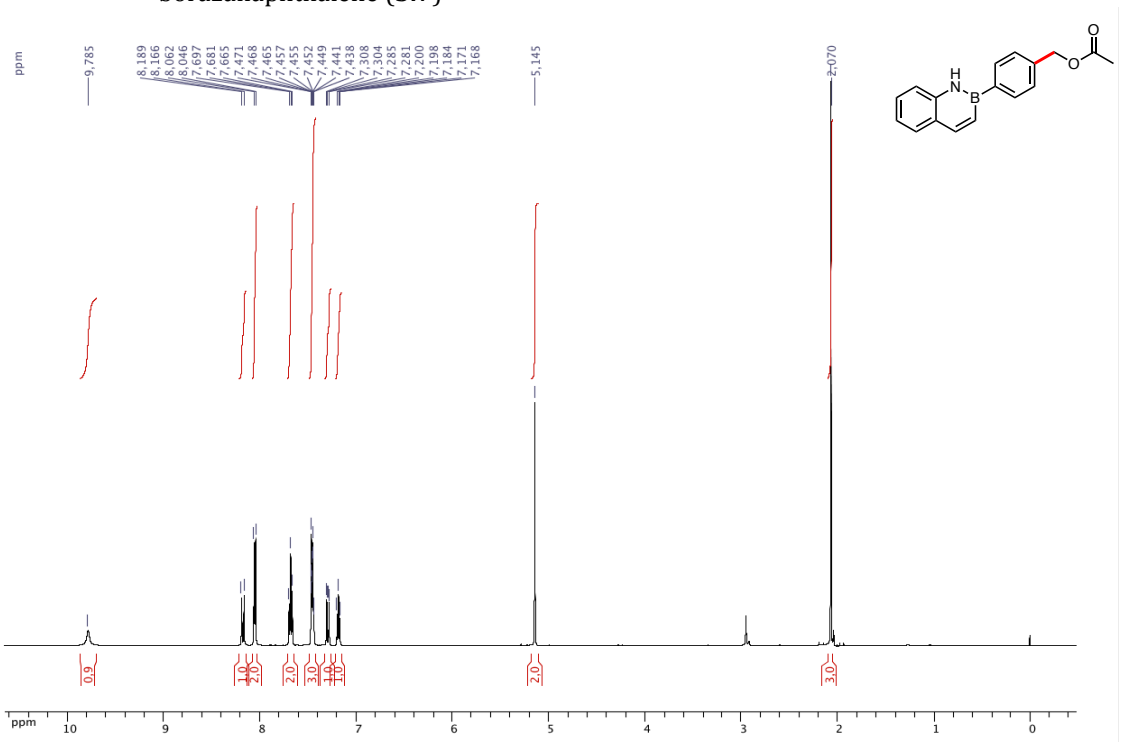

Figure A2.18: ^{13}C {^{1}H} NMR (acetone-d_6, 125.8 MHz) of 2-(4-(acetoxymethyl)phenyl)-2,1-borazanaphthalene (**3.7**)

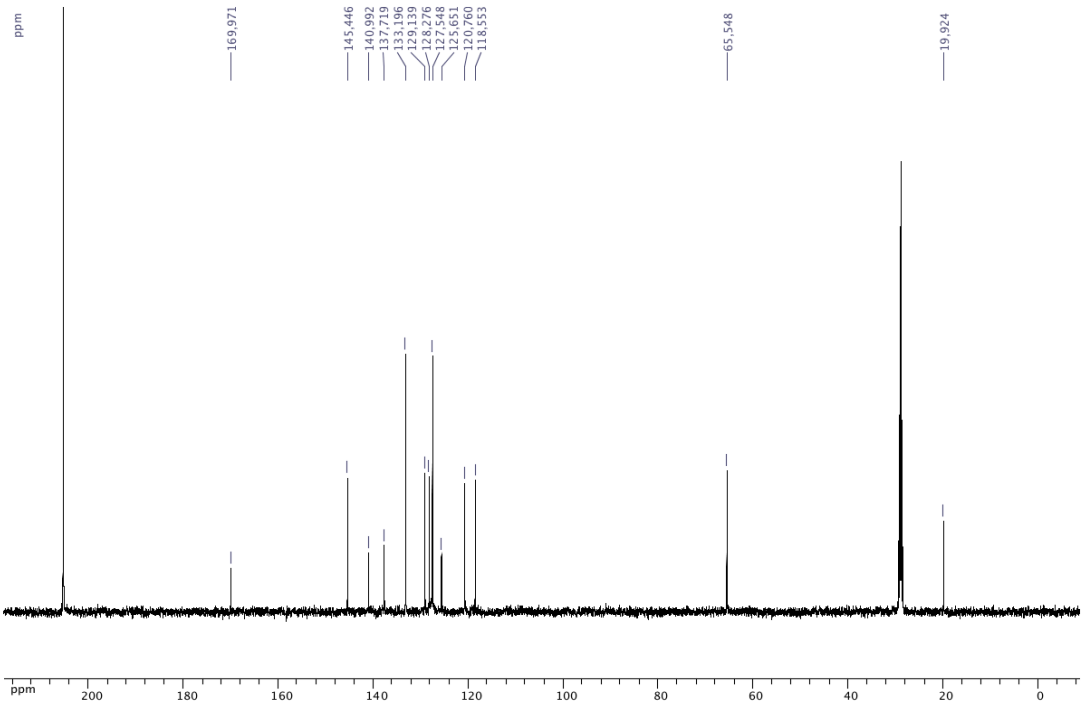

Figure A2.19: ^{11}B NMR (acetone, 128.4 MHz) of 2-(4-(acetoxymethyl)phenyl)-2,1-borazanaphthalene (**3.7**)

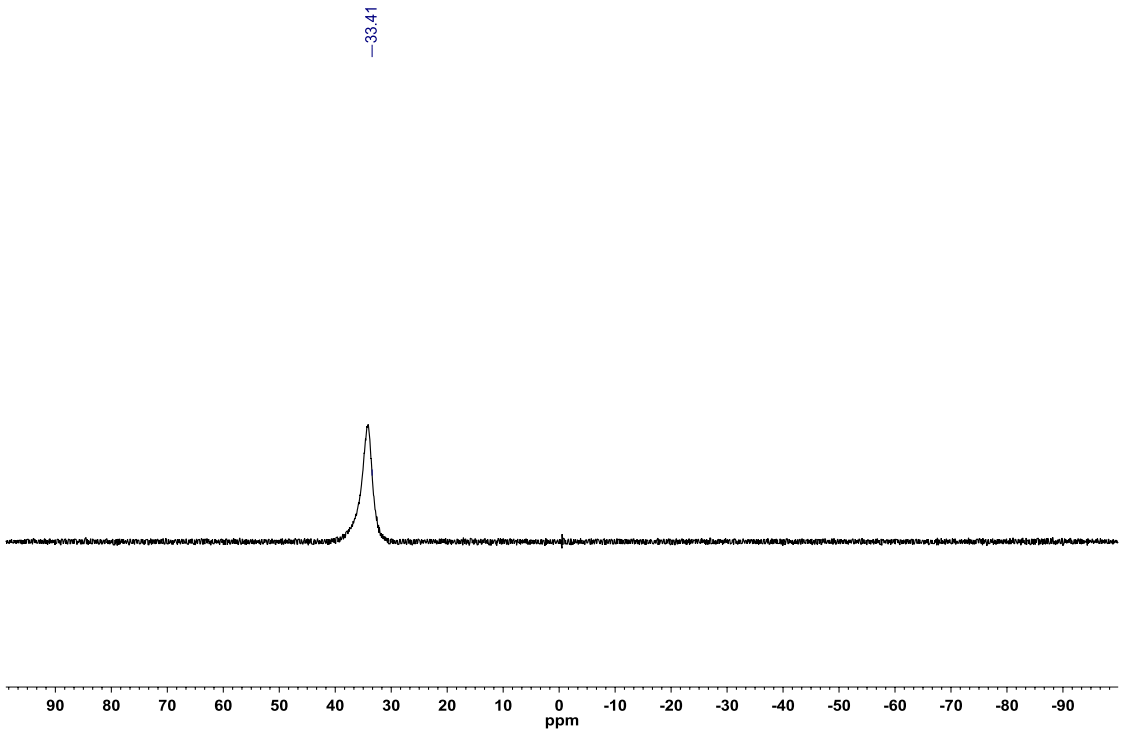

Figure A2.20: ^{1}H NMR (acetone-d_6, 500.4 MHz) of 2-(4-(3-acetoxypropyl)phenyl)-2,1-borazanaphthalene (**3.8**)

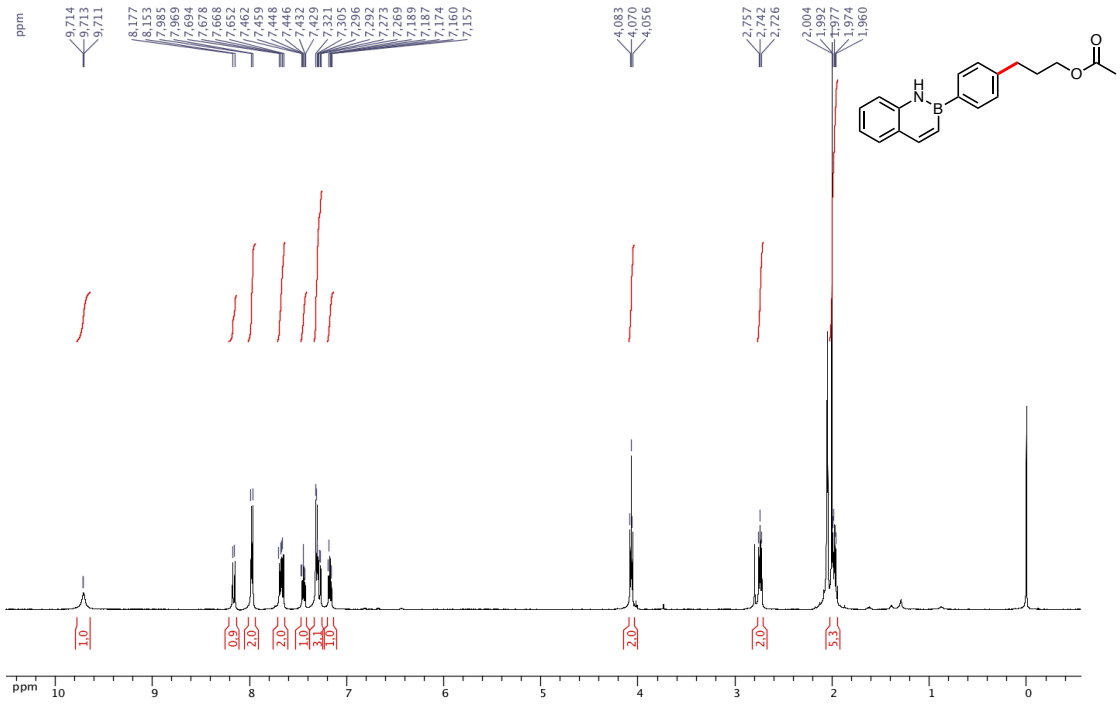

Figure A2.21: ^{13}C {^{1}H} NMR (acetone-d_6, 125.8 MHz) of 2-(4-(3-acetoxypropyl)phenyl)-2,1-borazanaphthalene (**3.8**)

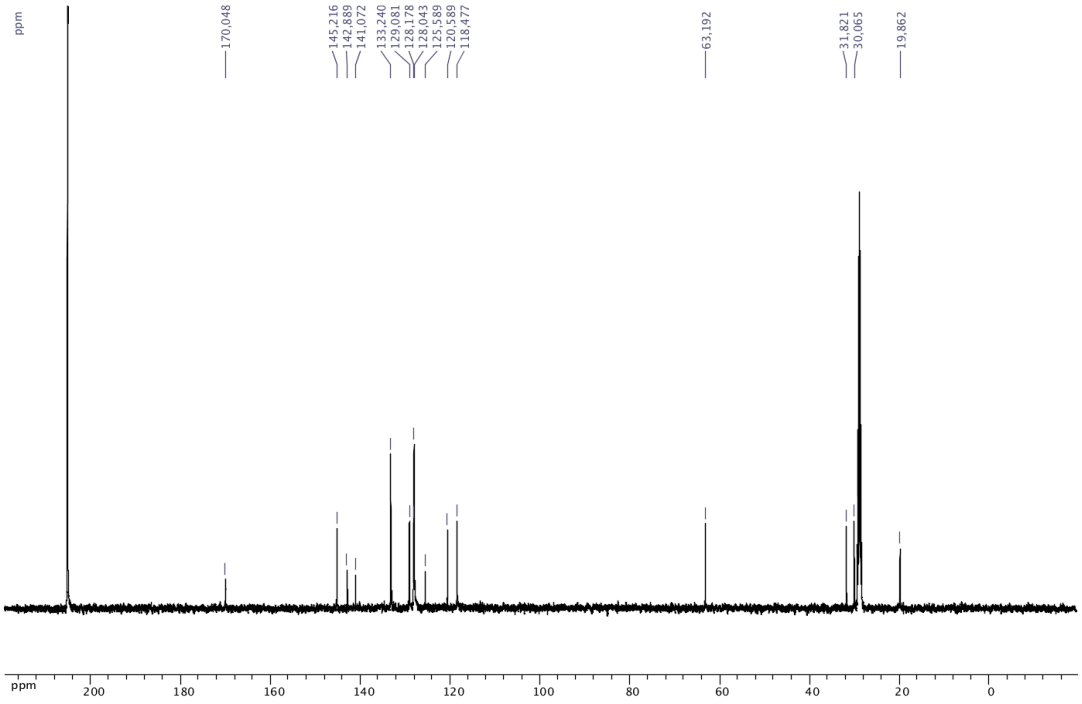

Figure A2.22: ^{11}B NMR (acetone, 128.4 MHz) of 2-(4-(3-acetoxypropyl)phenyl)-2,1-borazanaphthalene (**3.8**)

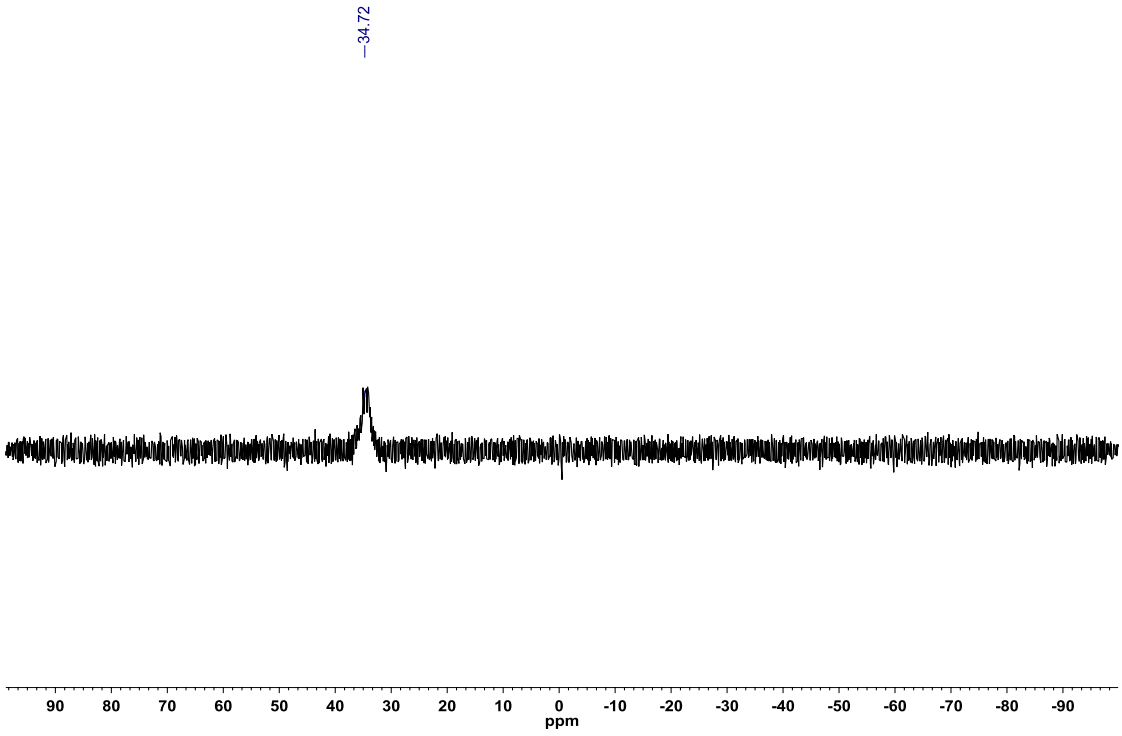

Figure A2.23: ^{1}H NMR ($CDCl_3$, 500.4 MHz) of 2-(4-(3-acetamidopropyl)phenyl)-2,1-borazanaphthalene (**3.9**)

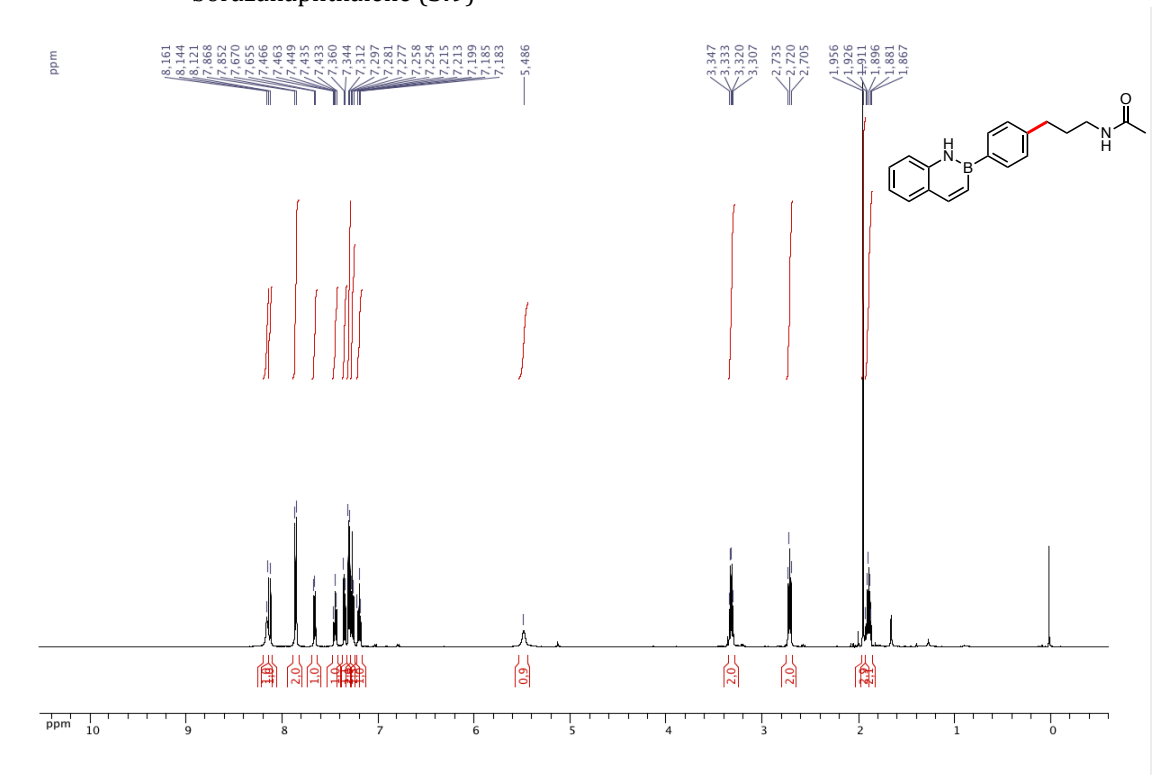

Figure A2.24: ^{13}C {^{1}H} NMR ($CDCl_3$, 125.8 MHz) of 2-(4-(3-acetamidopropyl)phenyl)-2,1-borazanaphthalene (**3.9**)

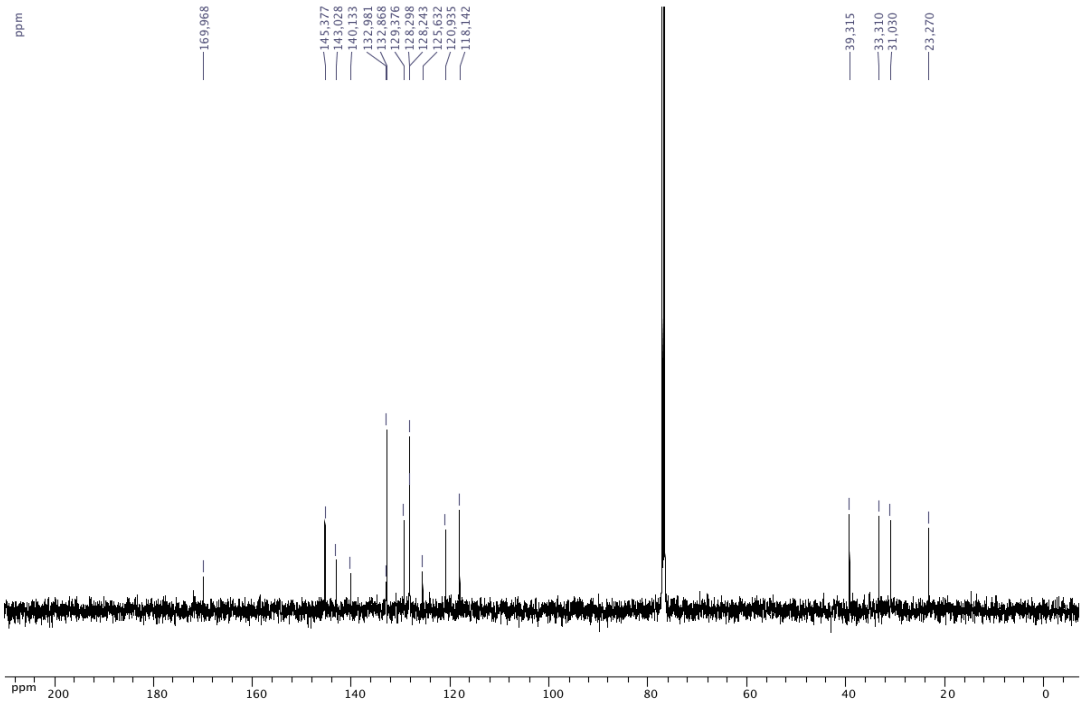

Figure A2.25: ^{11}B NMR (acetone, 128.4 MHz) of 2-(4-(3-acetamidopropyl)phenyl)-2,1-borazanaphthalene (**3.9**)

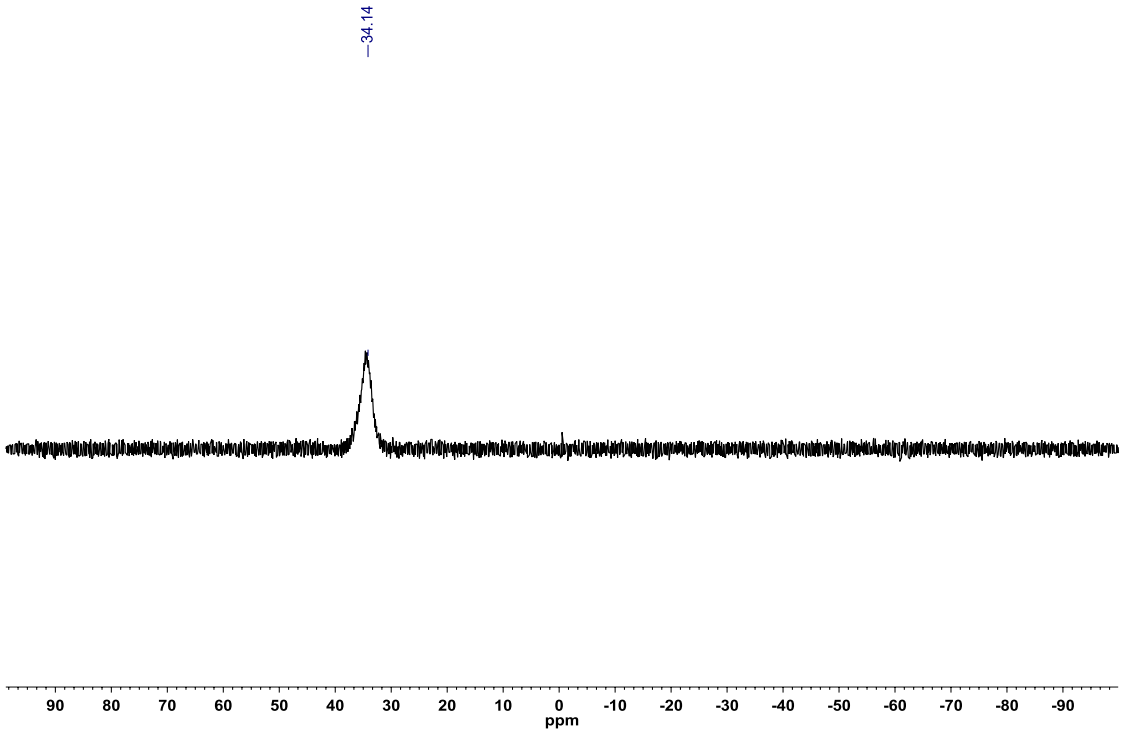

Figure A2.26: ^{1}H NMR (DMSO-d_6, 500.4 MHz) of 2-(4-(3-(2-oxoazepane-1-carboxamido)propyl)phenyl)-2,1-borazanaphthalene (**3.10**)

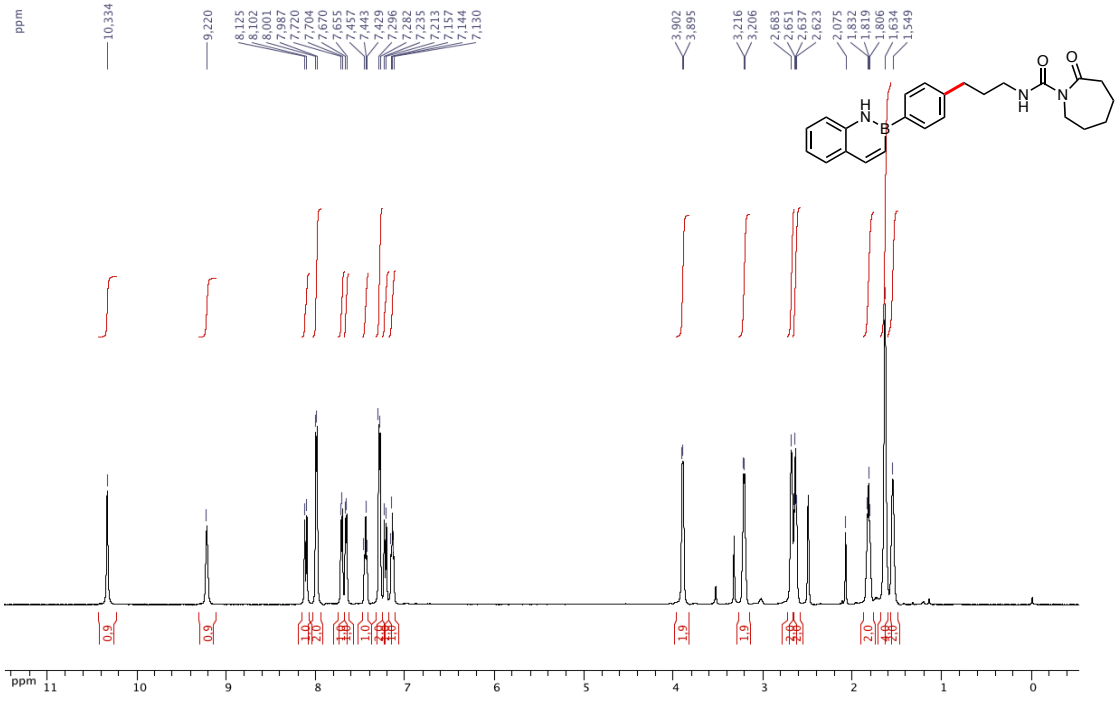

Figure A2.27: ^{13}C {^{1}H} NMR (DMSO-d_6, 125.8 MHz) of 2-(4-(3-(2-oxoazepane-1-carboxamido)propyl)phenyl)-2,1-borazanaphthalene (**3.10**)

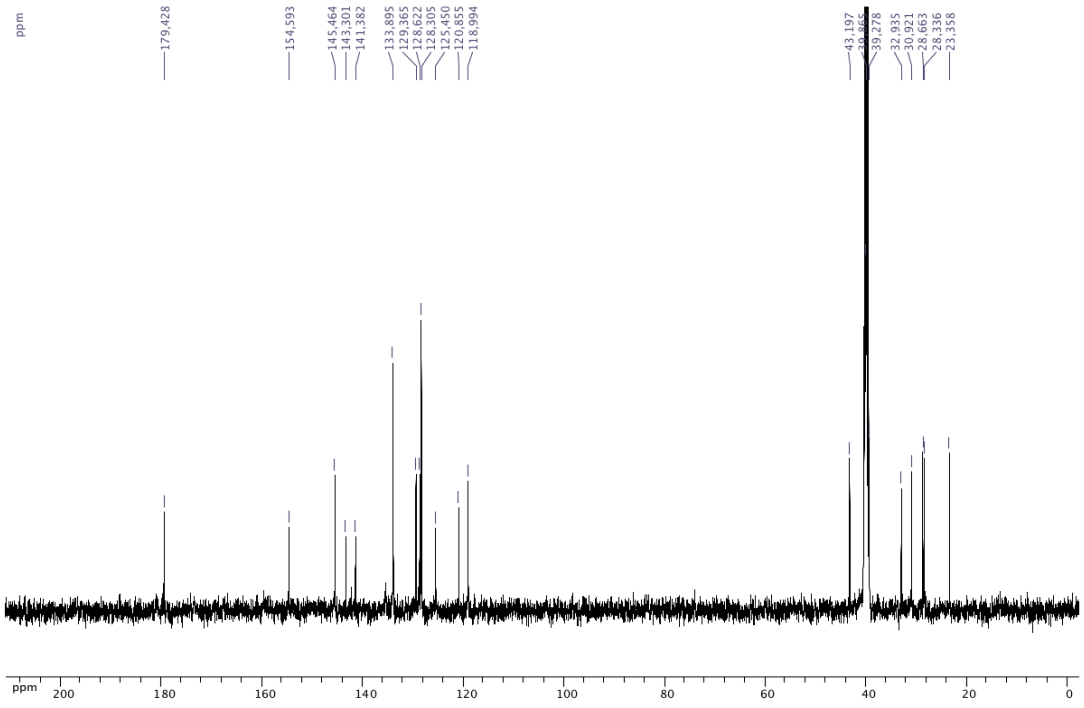

Figure A2.28: ^{11}B NMR (acetone, 128.4 MHz) of 2-(4-(3-(2-oxoazepane-1-carboxamido)propyl)phenyl)-2,1-borazanaphthalene (**3.10**)

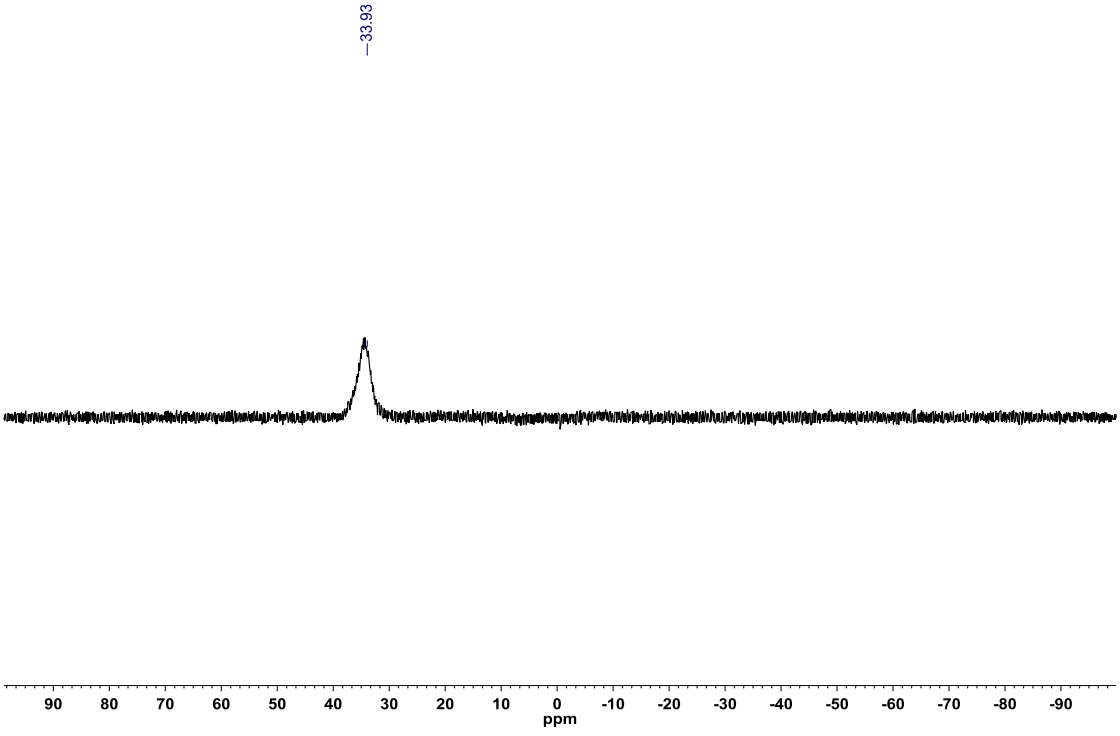

Figure A2.29: ^{1}H NMR (acetone-d_6, 500.4 MHz) of 2-(4-(2-pyridin-2-yl)ethyl)phenyl)-2,1-borazanaphthalene (**3.11**)

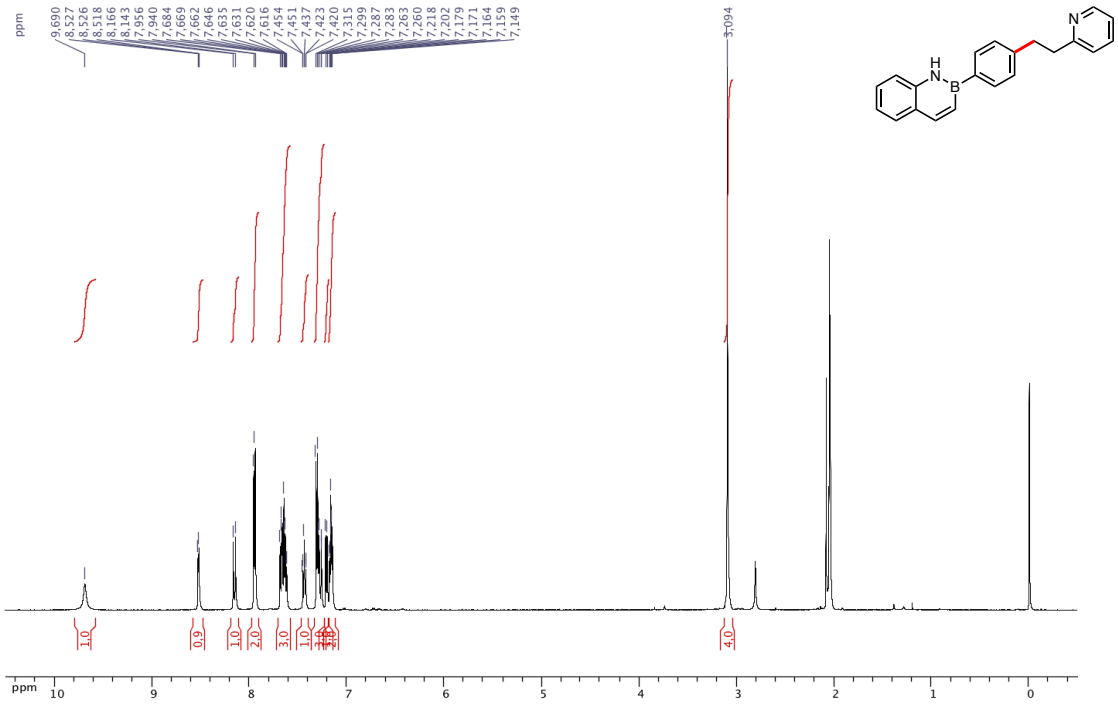

Figure A2.30: ^{13}C {^{1}H} NMR (acetone-d_6, 125.8 MHz) of 2-(4-(2-pyridin-2-yl)ethyl)phenyl)-2,1-borazanaphthalene (**3.11**)

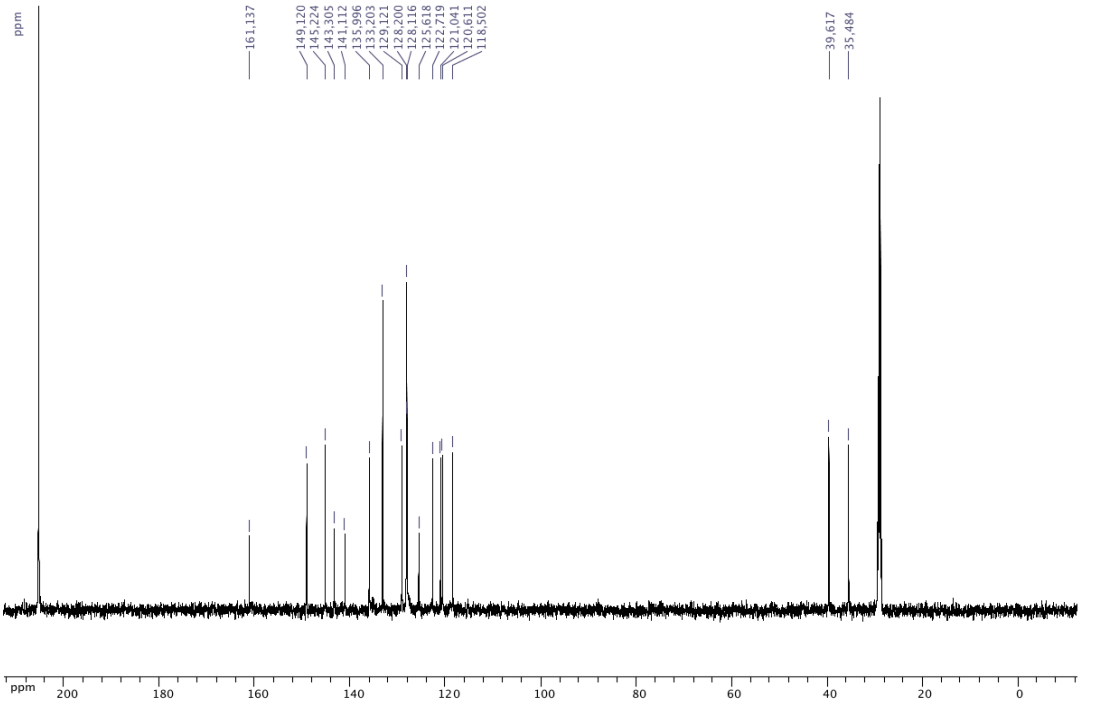

Figure A2.31: ^{11}B NMR (acetone, 128.4 MHz) of 2-(4-(2-pyridin-2-yl)ethyl)phenyl)-2,1-borazanaphthalene (**3.11**)

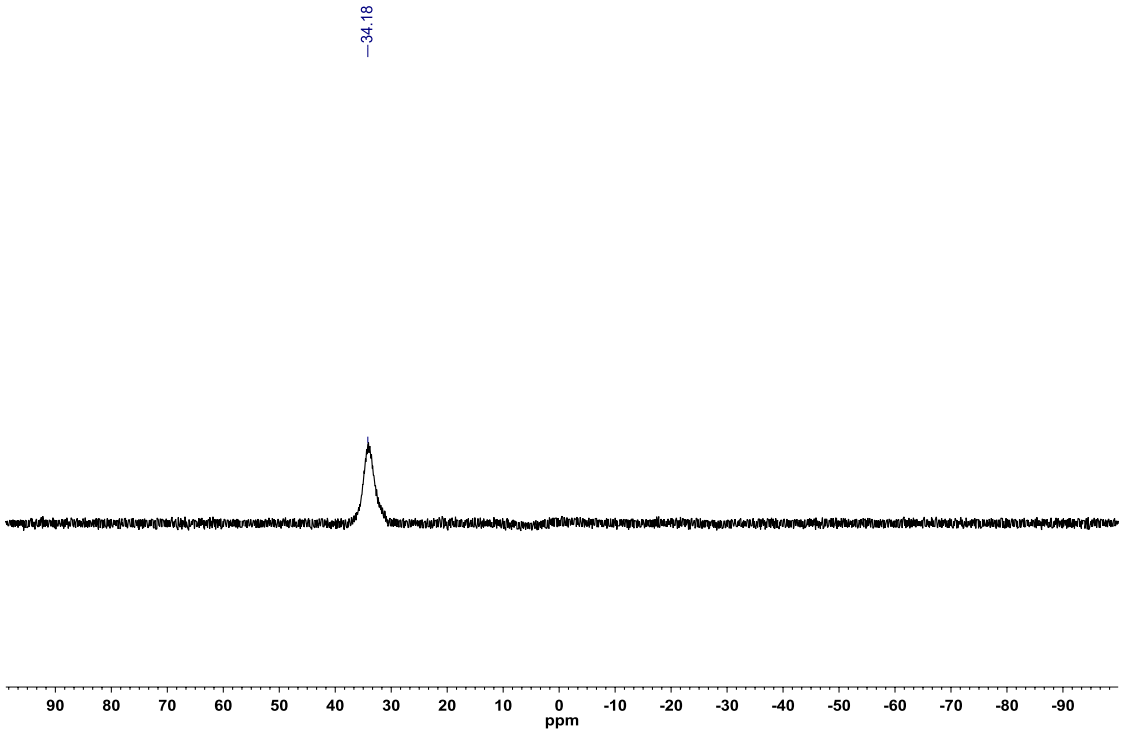

Figure A2.32: ^{1}H NMR (acetone-d_6, 500.4 MHz) of 2-(4-(3-(piperazin-1-yl)propyl)phenyl)-2,1-borazanaphthalene (**3.12**)

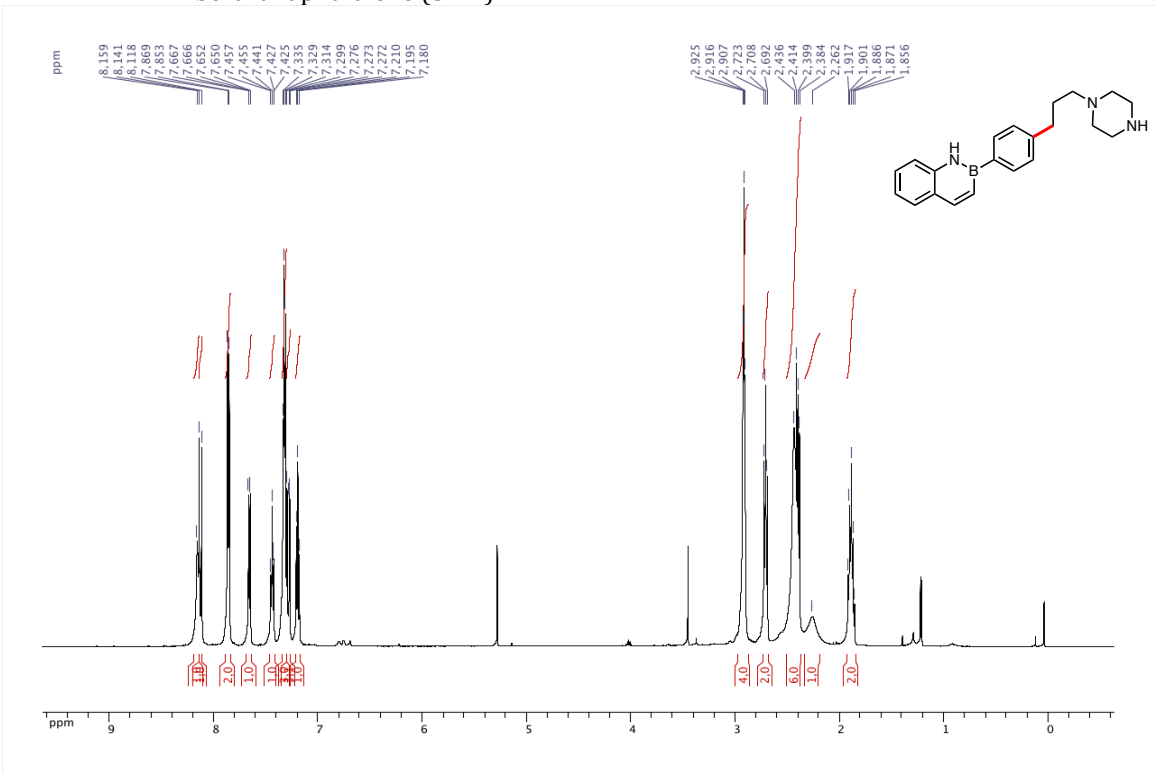

Figure A2.33: ^{13}C {^{1}H} NMR (acetone-d_6, 125.8 MHz) of 2-(4-(3-(piperazin-1-yl)propyl)phenyl)-2,1-borazanaphthalene (**3.12**)

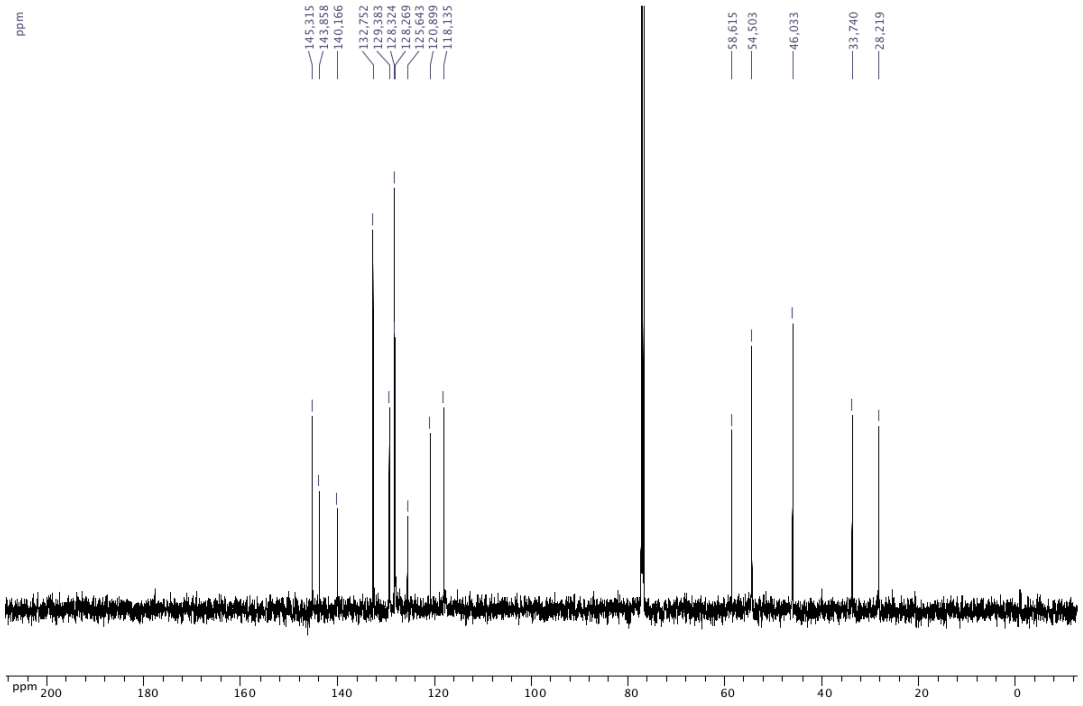

Figure A2.34: ^{11}B NMR (acetone, 128.4 MHz) of 2-(4-(3-(piperazin-1-yl)propyl)phenyl)-2,1-borazanaphthalene (**3.12**)

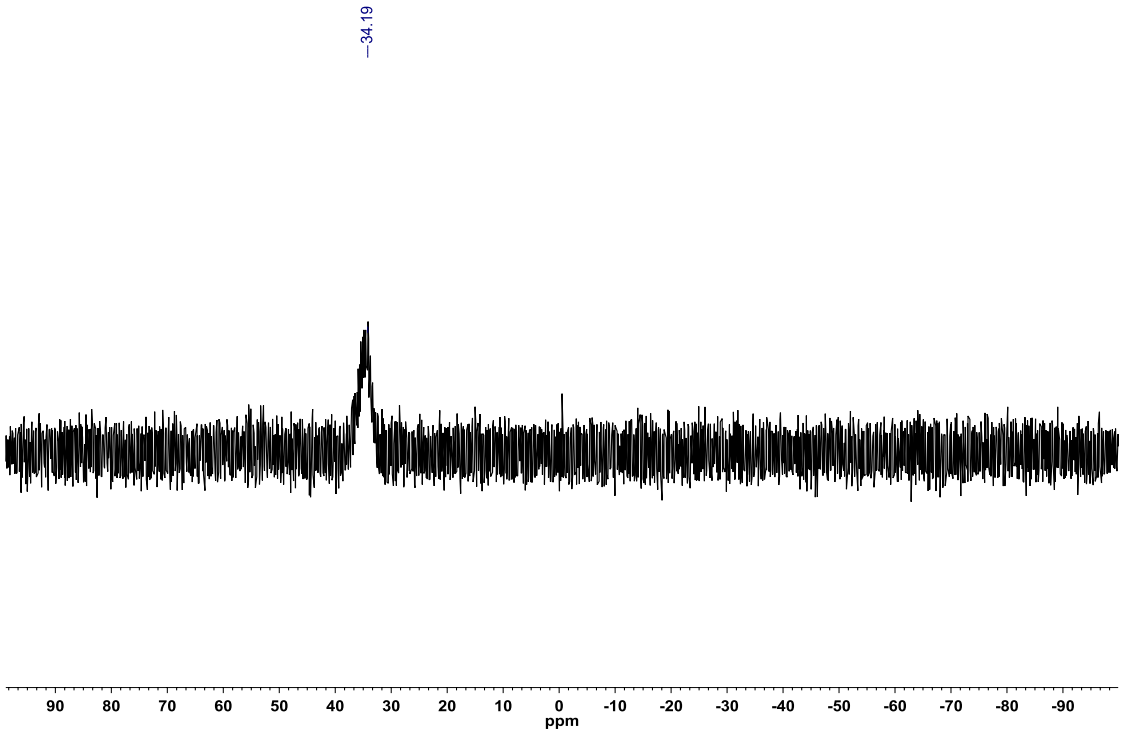

Figure A2.35: ^{1}H NMR (acetone-d_6, 500.4 MHz) of 2-(4-(3-(phenylamino)propyl)phenyl)-2,1-borazanaphthalene (**3.13**)

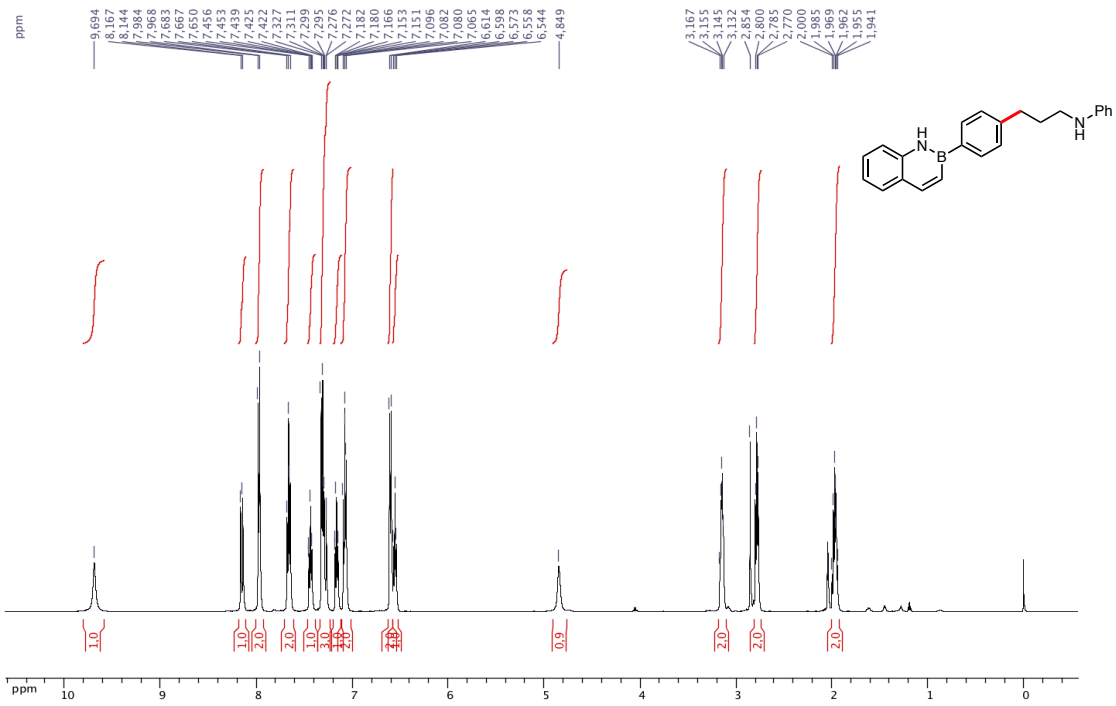

Figure A2.36: ^{13}C {^{1}H} NMR (acetone-d_6, 125.8 MHz) of 2-(4-(3-(phenylamino)propyl)phenyl)-2,1-borazanaphthalene (**3.13**)

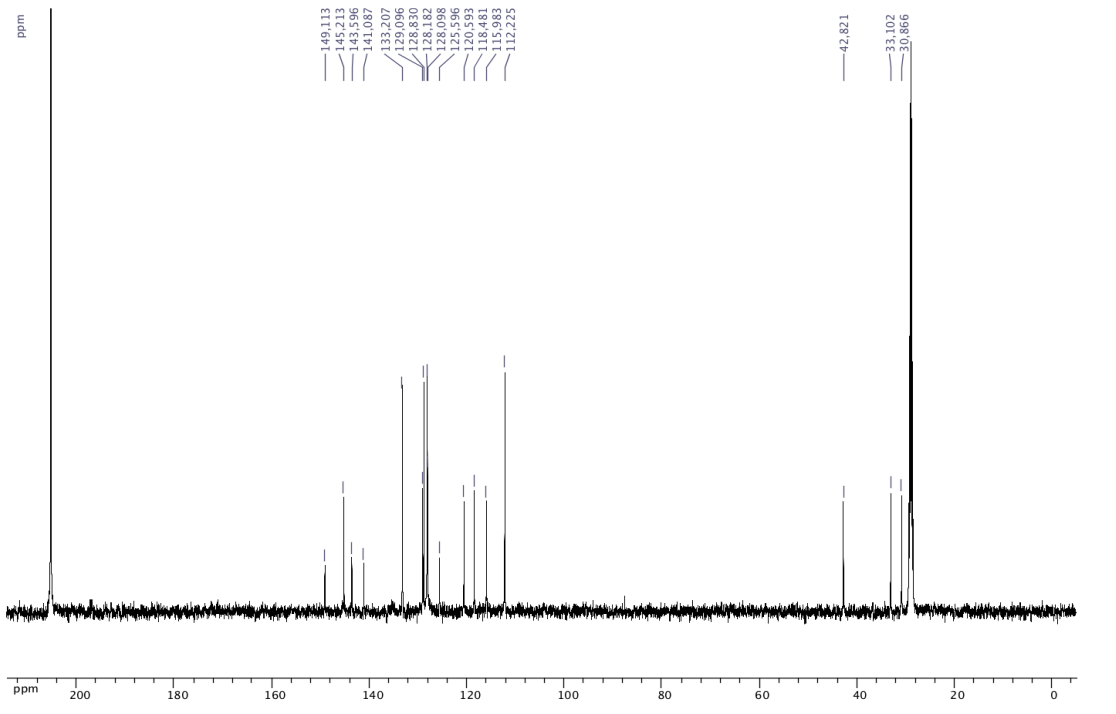

Figure A2.37: ^{11}B NMR (acetone, 128.4 MHz) of 2-(4-(3-(phenylamino)propyl)phenyl)-2,1-borazanaphthalene (**3.13**)

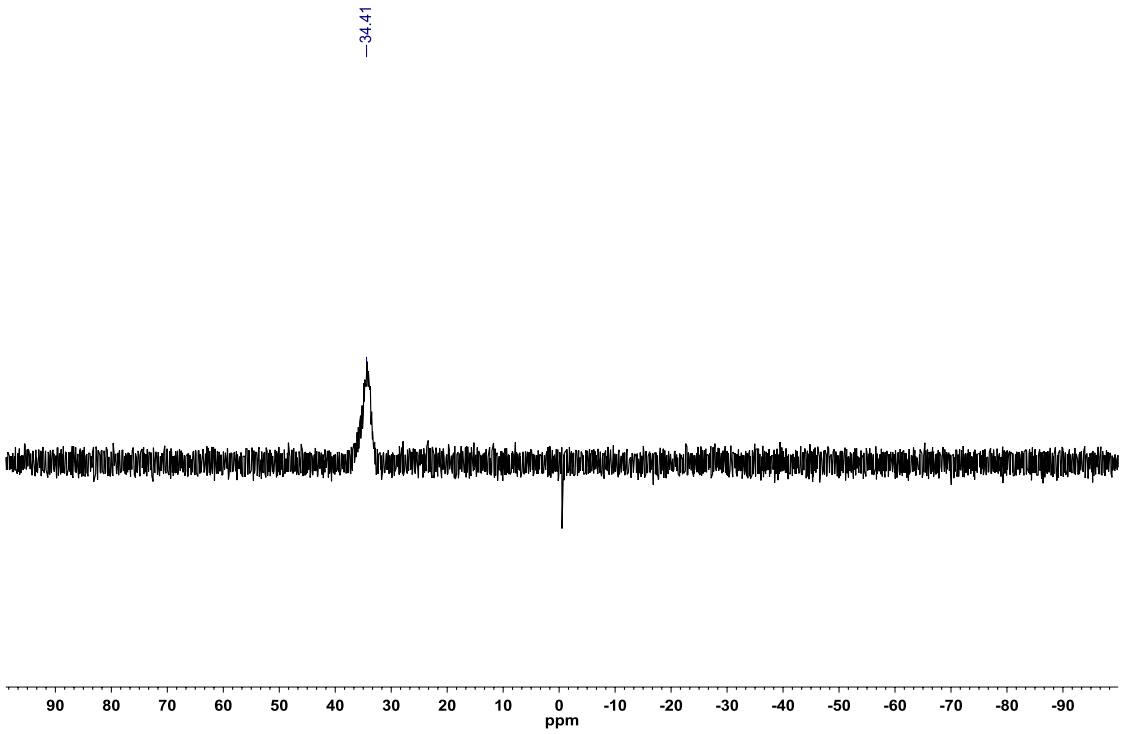

Figure A2.38: ^{1}H NMR ($CDCl_3$, 500.4 MHz) of 2-(4-(3-(butylamino)propyl)phenyl)-2,1-borazanaphthalene (**3.14**)

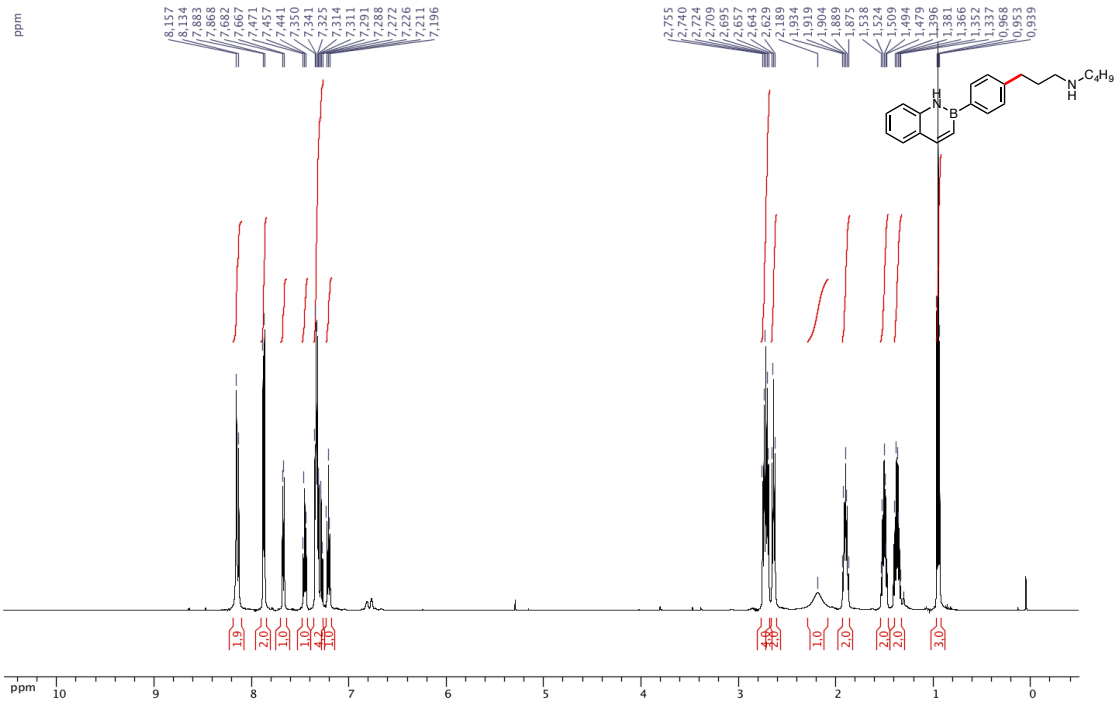

Figure A2.39: ^{13}C {^{1}H} NMR ($CDCl_3$, 125.8 MHz) of 2-(4-(3-(butylamino)propyl)phenyl)-2,1-borazanaphthalene (**3.14**)

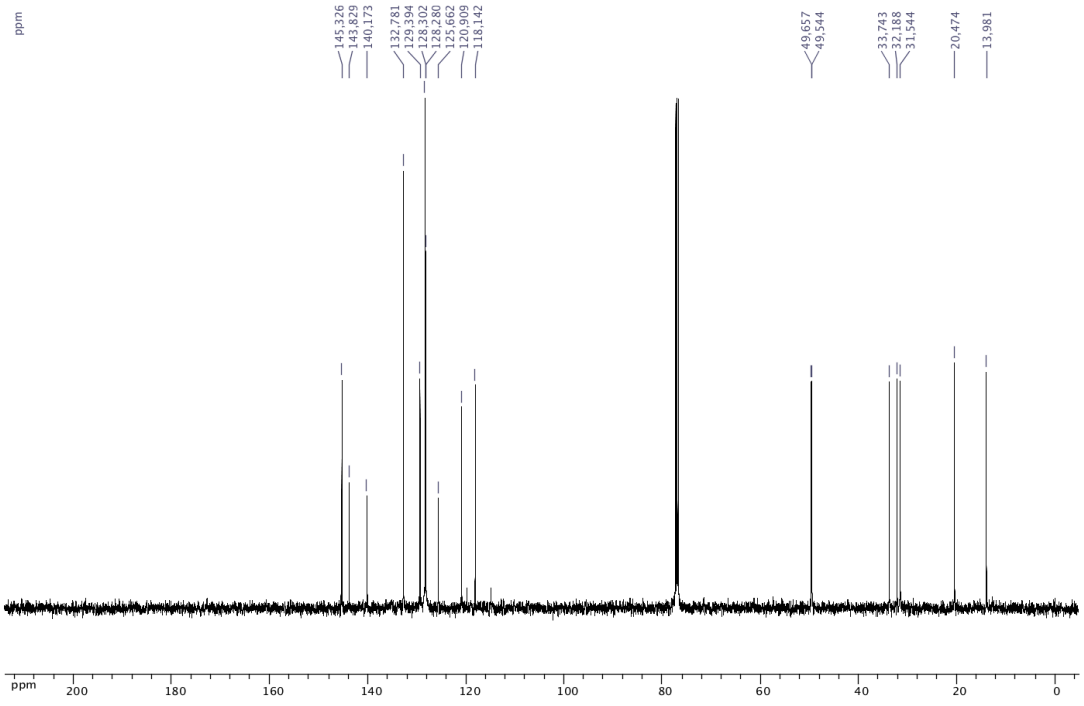

Figure A2.40: ^{11}B NMR (acetone, 128.4 MHz) of 2-(4-(3-(butylamino)propyl)phenyl)-2,1-borazanaphthalene (**3.14**)

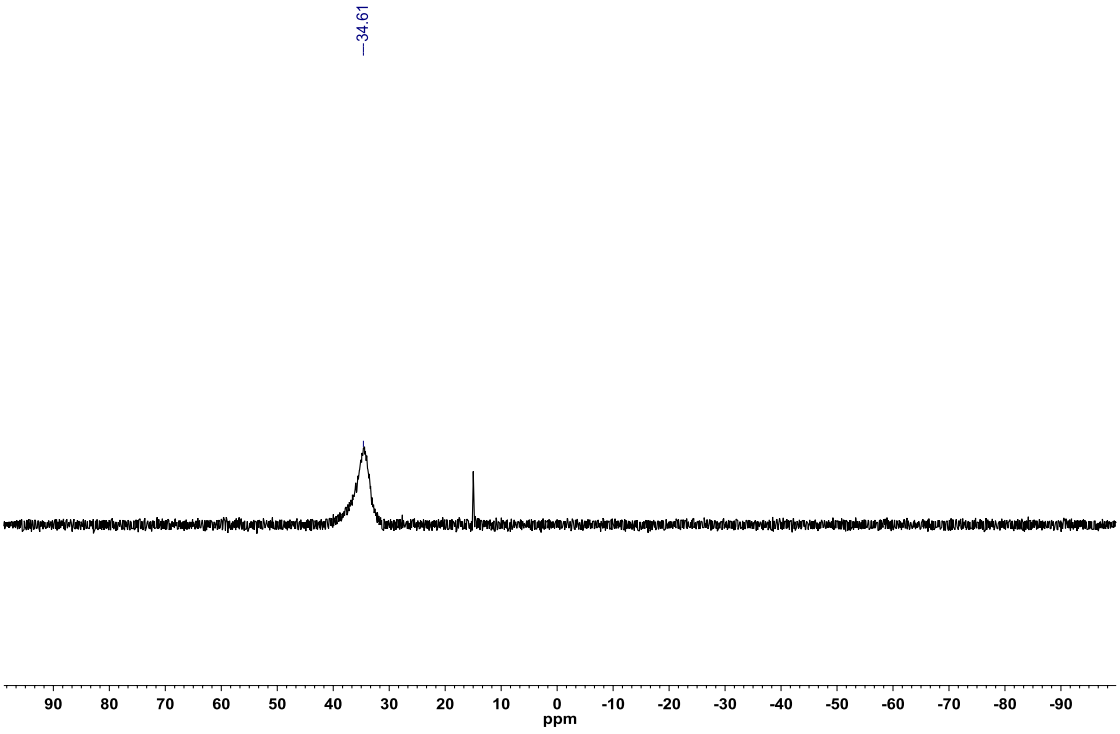

Figure A2.41: ^{1}H NMR (acetone-d_6, 500.4 MHz) of 2-(4-(3-aminopropyl)phenyl)-2,1-borazanaphthalene (**3.15**)

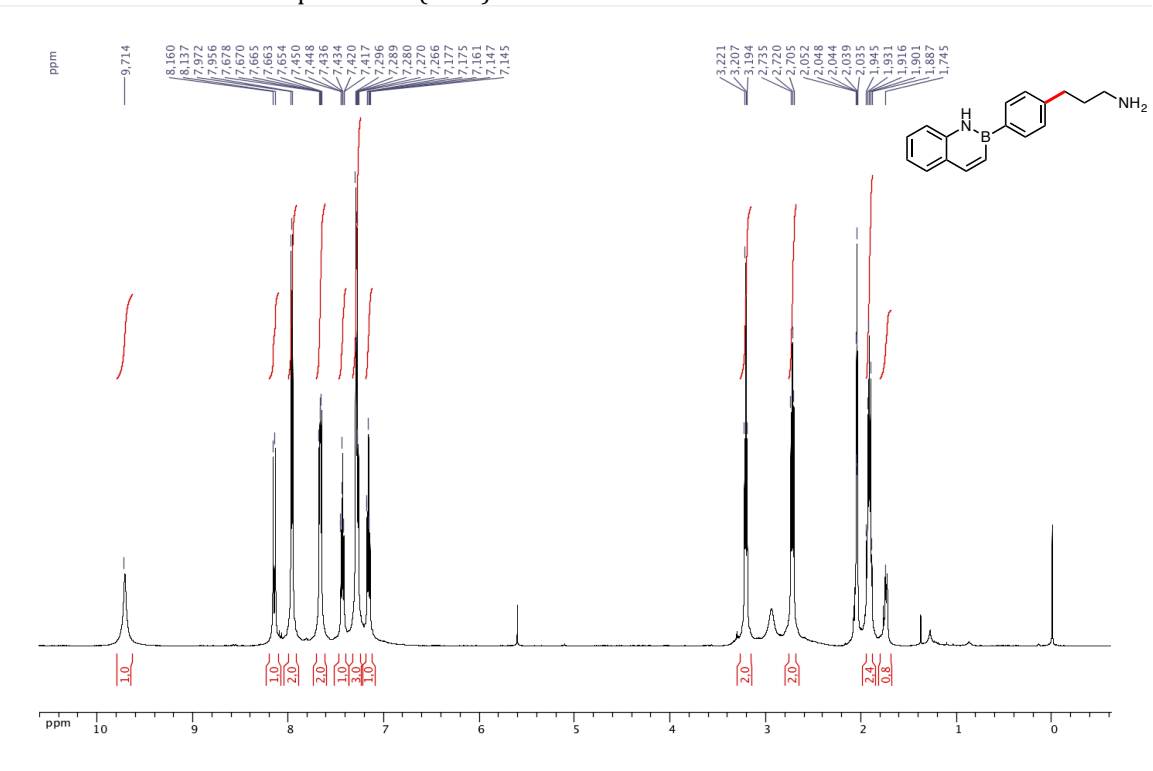

Figure A2.42: ^{13}C {^{1}H} NMR (acetone-d_6, 125.8 MHz) of 2-(4-(3-aminopropyl)phenyl)-2,1-borazanaphthalene (**3.15**)

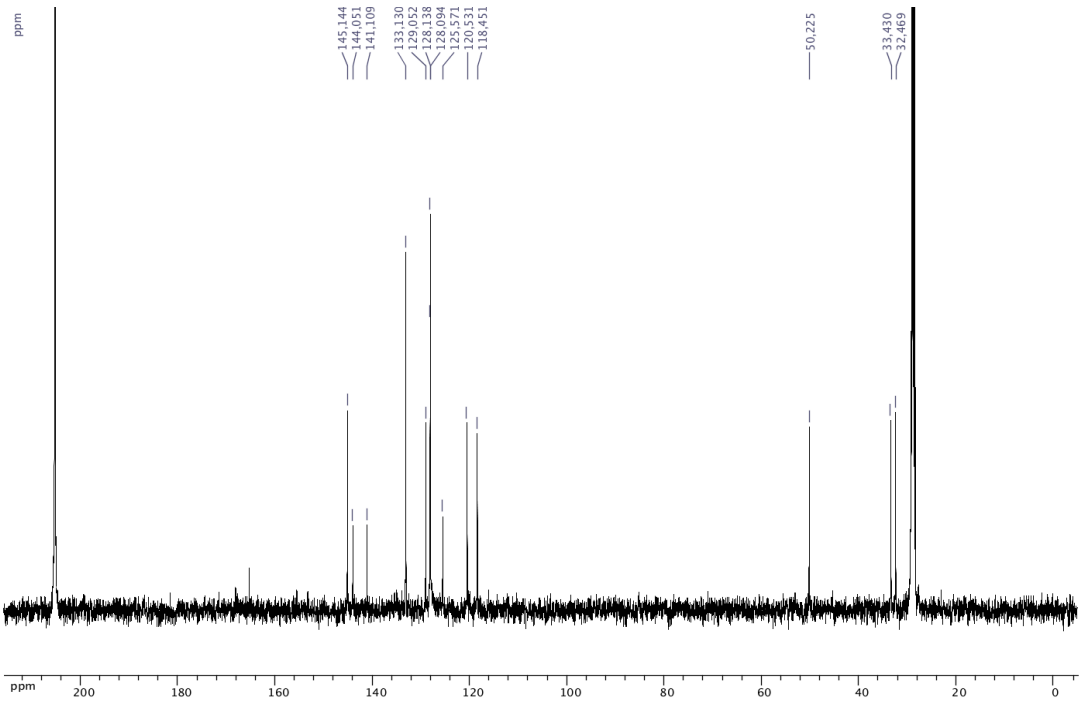

Figure A2.43: ^{11}B NMR (acetone, 128.4 MHz) of 2-(4-(3-aminopropyl)phenyl)-2,1-borazanaphthalene (**3.15**)

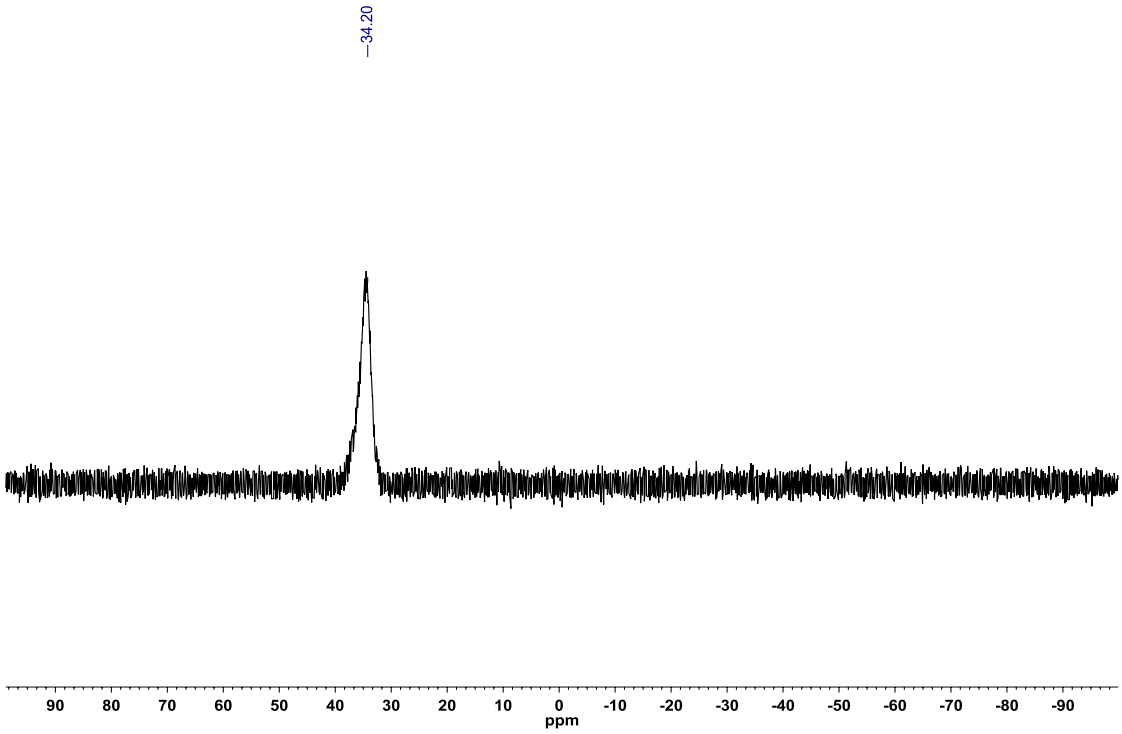

Figure A2.44: ^{1}H NMR ($CDCl_3$, 500.4 MHz) of 2-(3-(3-(phenylamino)propyl)phenyl)-2,1-borazanaphthalene (**3.16**)

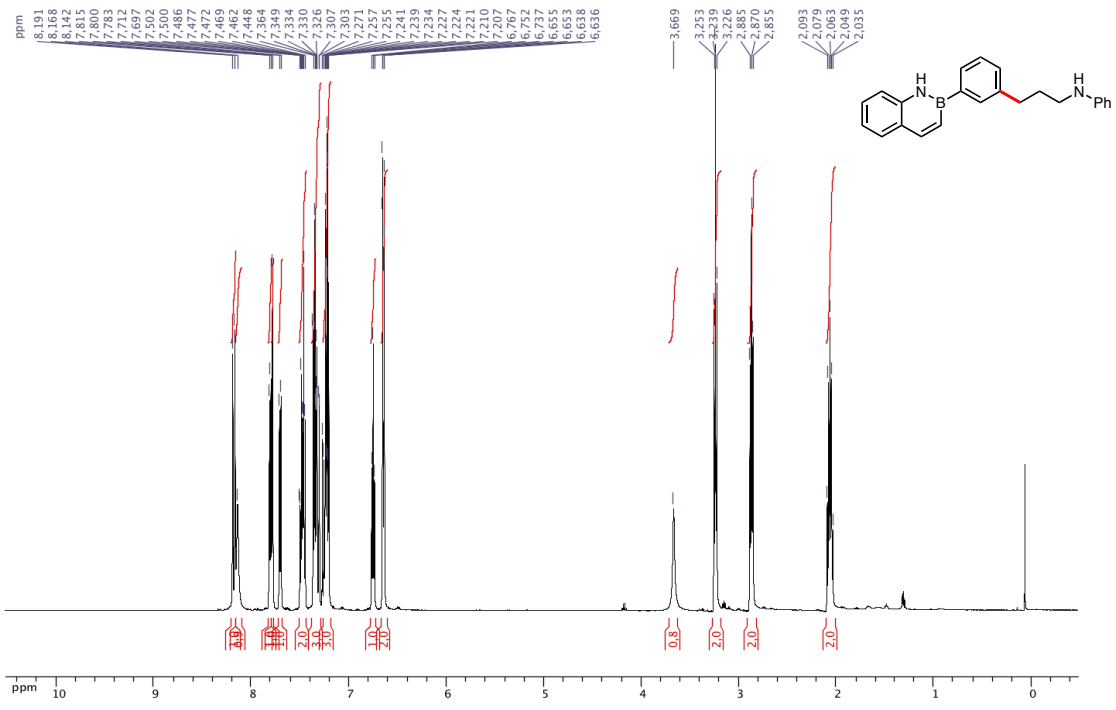

Figure A2.45: ^{13}C {^{1}H} NMR ($CDCl_3$, 125.8 MHz) of 2-(3-(3-(phenylamino)propyl)phenyl)-2,1-borazanaphthalene (**3.16**)

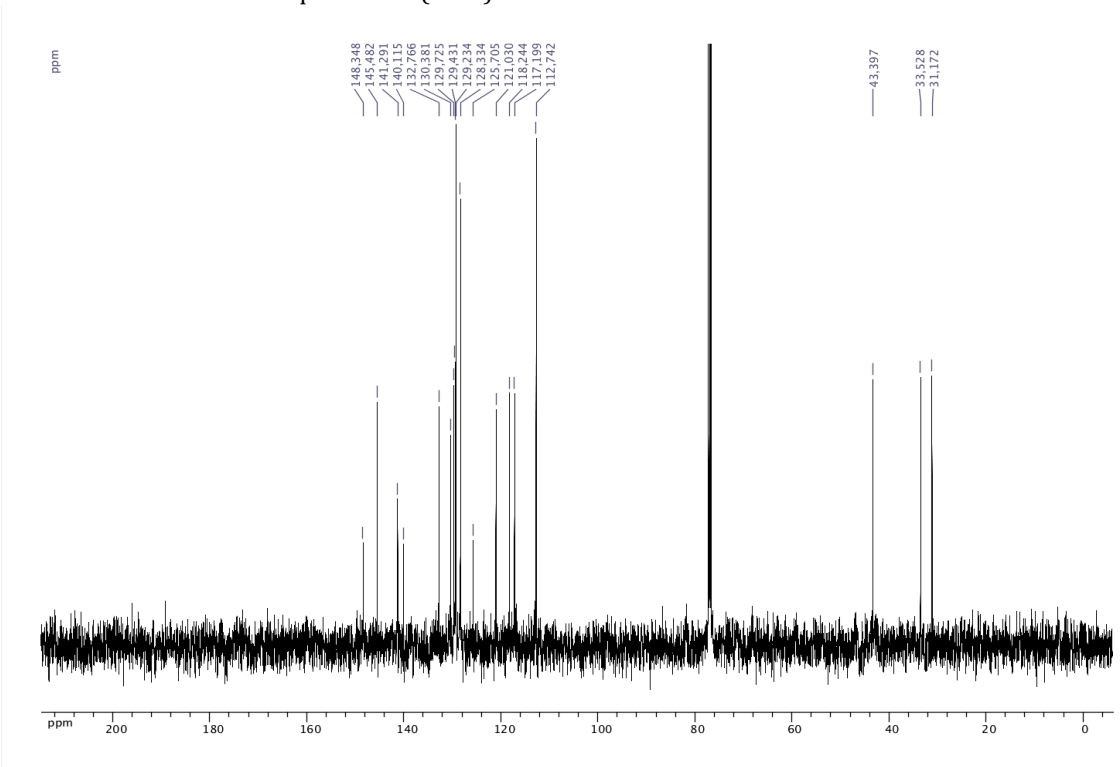

Figure A2.46: ^{11}B NMR (acetone, 128.4 MHz) of 2-(3-(3-(phenylamino)propyl)phenyl)-2,1-borazanaphthalene (**3.16**)

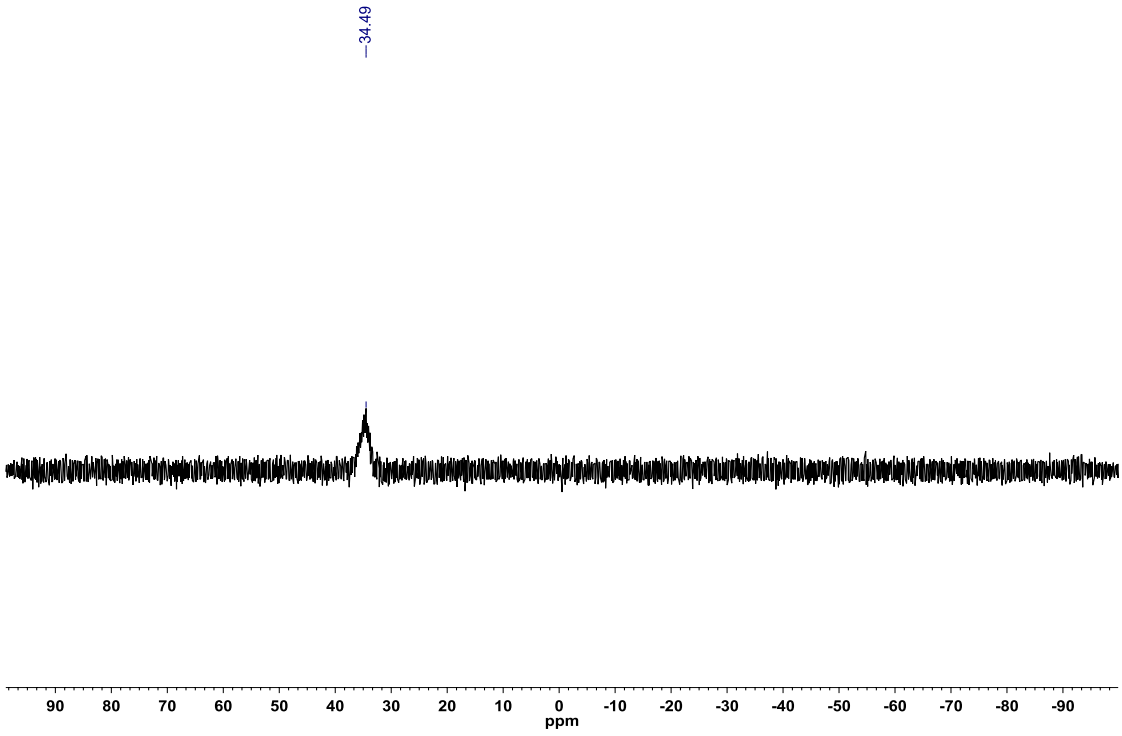

Figure A2.47: ^{1}H NMR ($CDCl_3$, 500.4 MHz) of 2-(3-(*exo*-bicyclo[2.2.1]heptan-2-yl)phenyl)-2,1-borazanaphthalene (**3.17**)

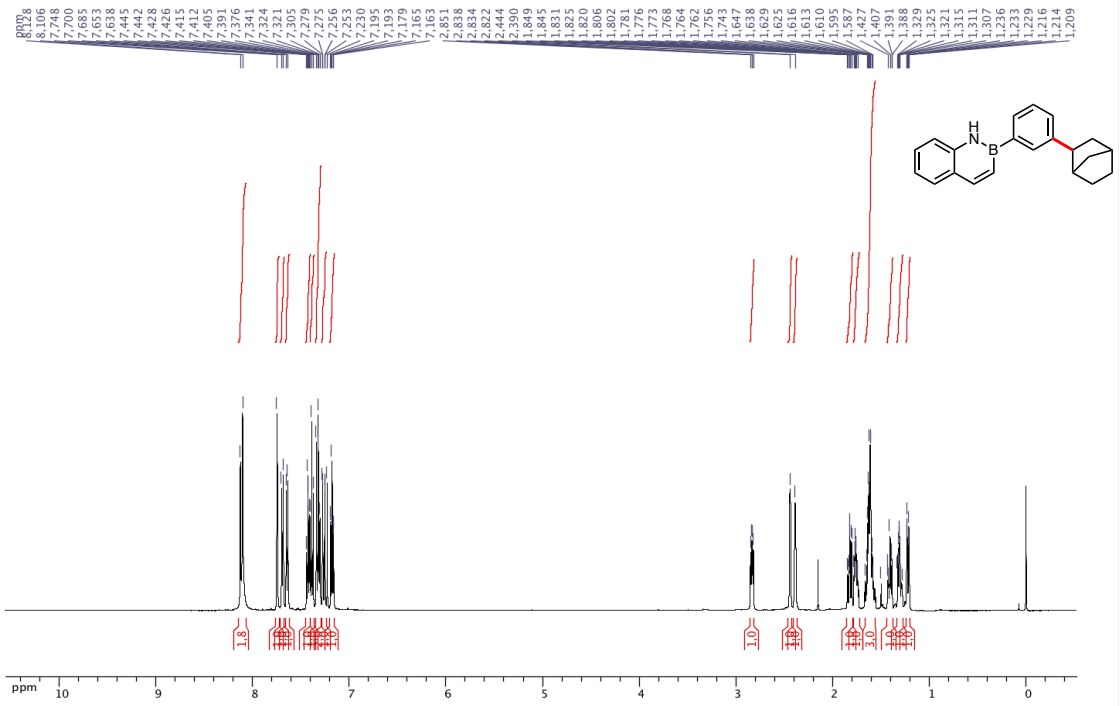

Figure A2.48: ^{13}C {^{1}H} NMR ($CDCl_3$, 125.8 MHz) of 2-(3-(*exo*-bicyclo[2.2.1]heptan-2-yl)phenyl)-2,1-borazanaphthalene (**3.17**)

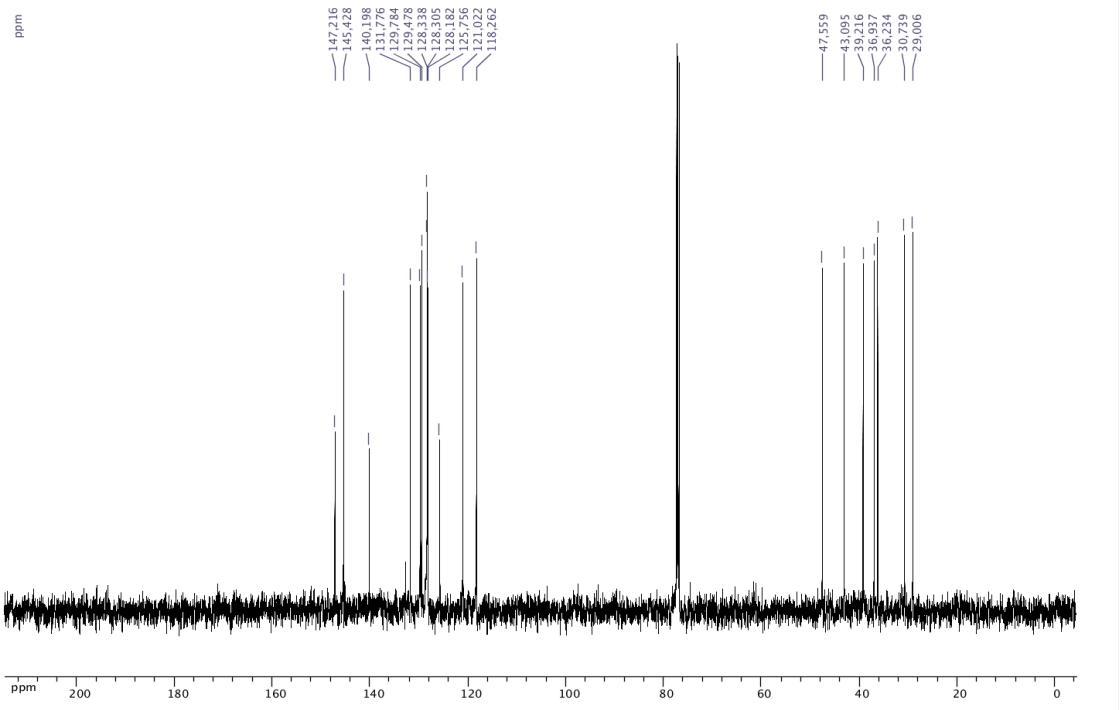

Figure A2.49: ^{11}B NMR (acetone, 128.4 MHz) of 2-(3-(*exo*-bicyclo[2.2.1]heptan-2-yl)phenyl)-2,1-borazanaphthalene (**3.17**)

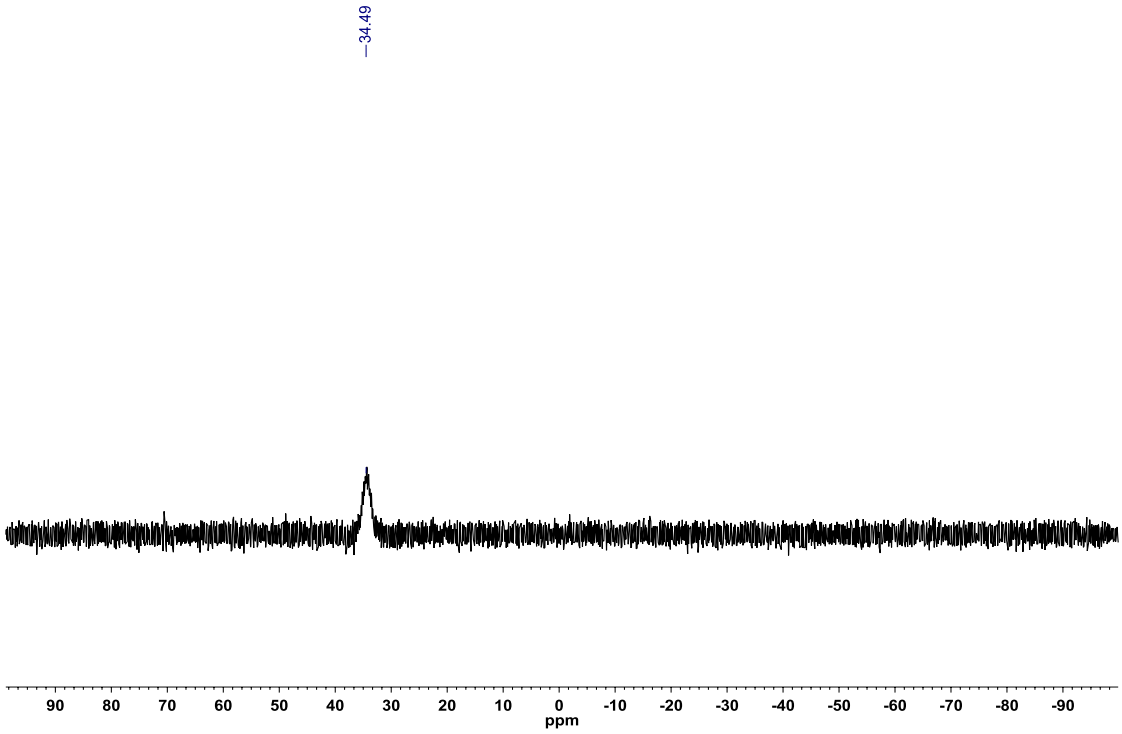

Figure A2.50: ^{1}H NMR ($CDCl_3$, 500.4 MHz) of 2-(3-(3-acetamidopropyl)phenyl)-2,1-borazanaphthalene (**3.18**)

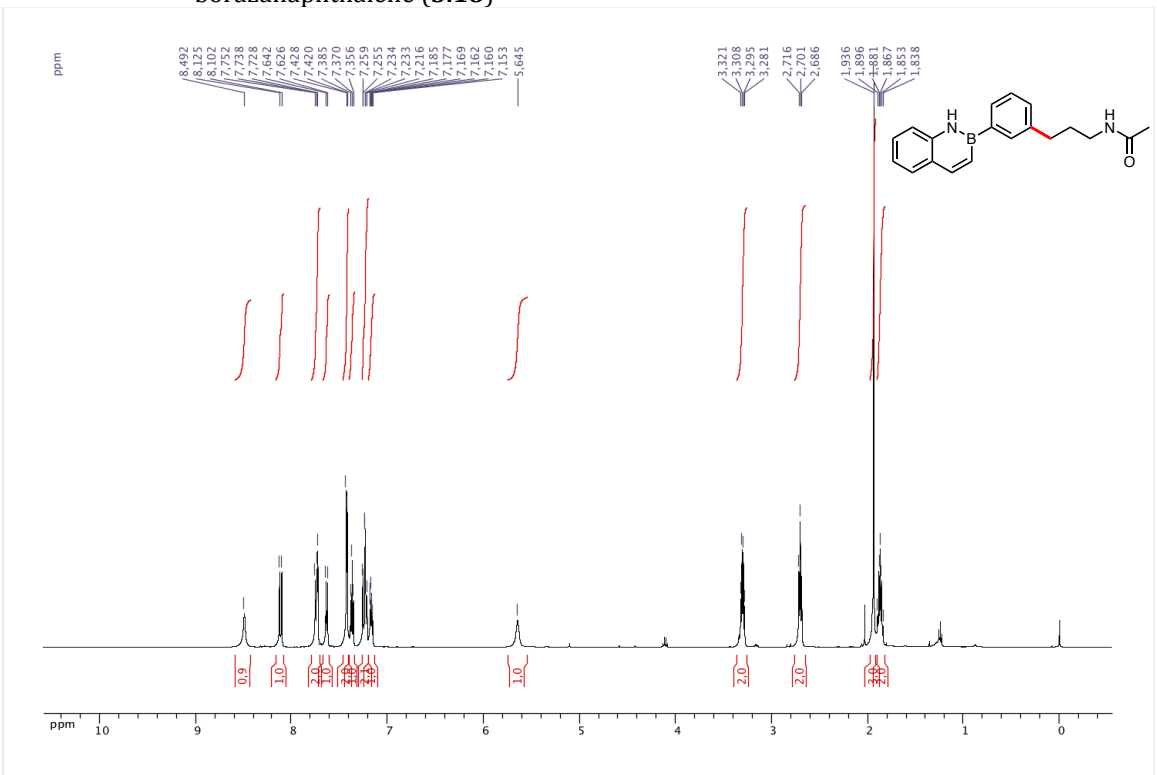

Figure A2.51: ^{13}C {^{1}H} NMR ($CDCl_3$, 125.8 MHz) of 2-(3-(3-acetamidopropyl)phenyl)-2,1-borazanaphthalene (**3.18**)

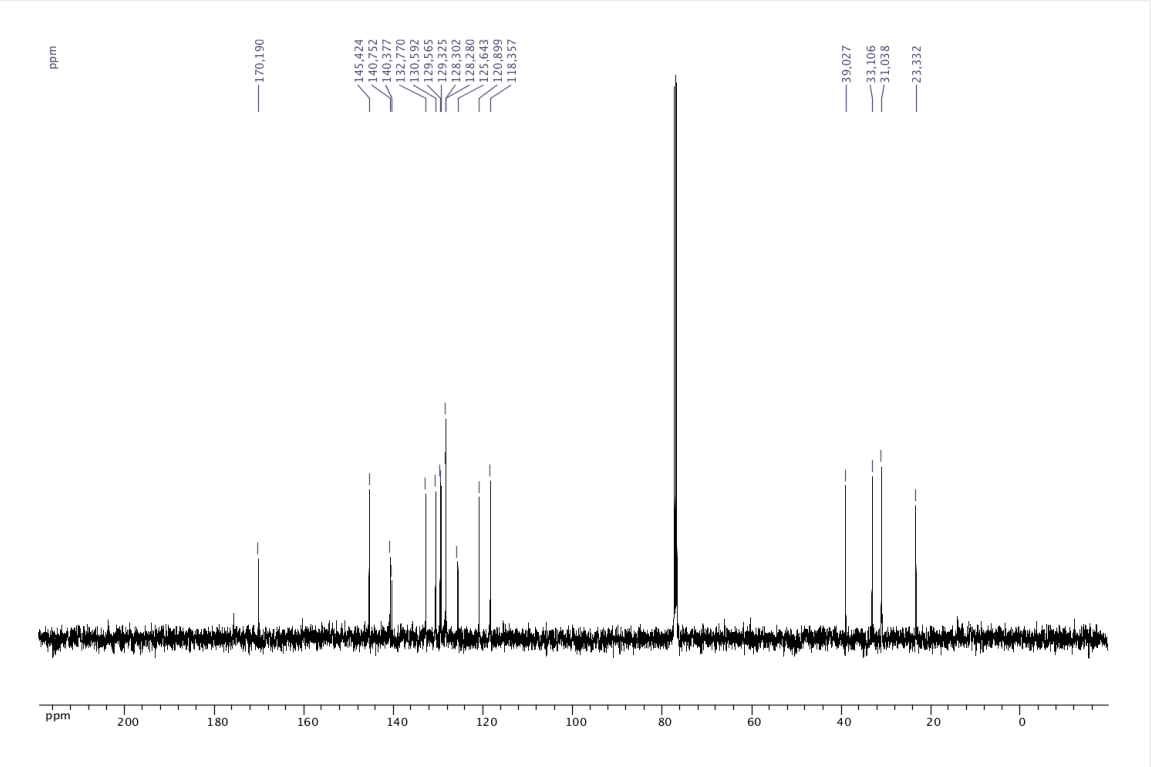

Figure A2.52: ^{11}B NMR (acetone, 128.4 MHz) of 2-(3-(3-acetamidopropyl)phenyl)-2,1-borazanaphthalene (**3.18**)

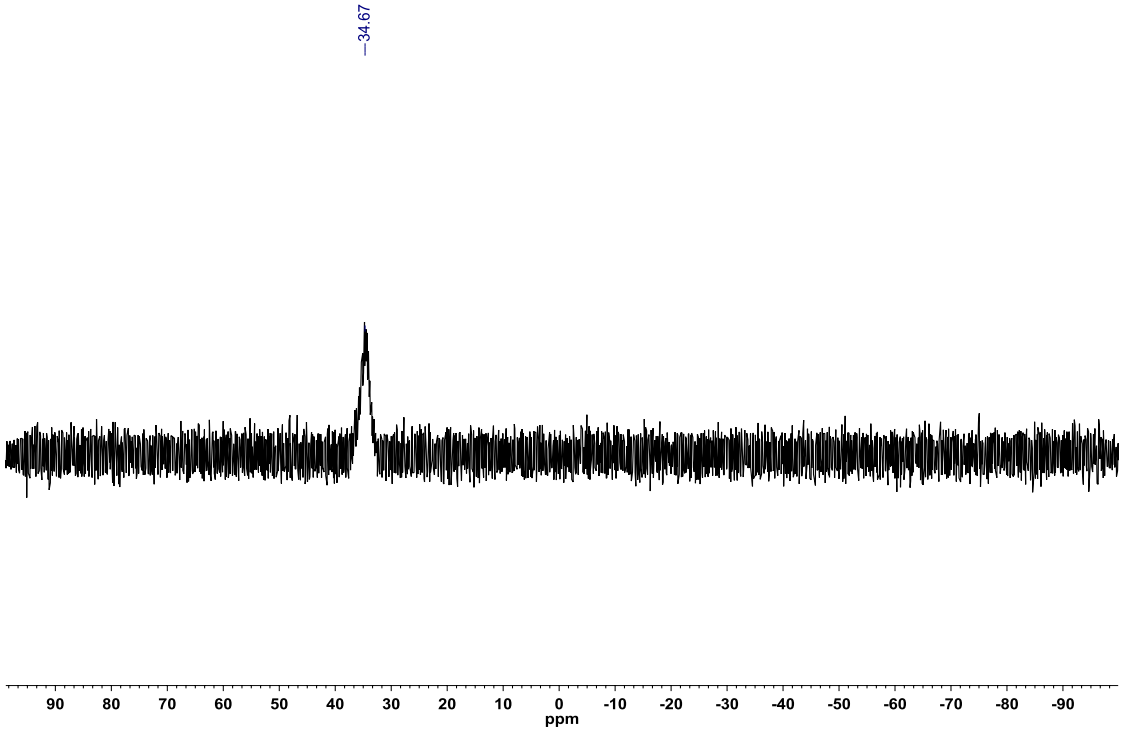

Figure A2.53: ^{1}H NMR ($CDCl_3$, 500.4 MHz) of 2-(2-(3-(phenylamino)propyl)phenyl)-2,1-borazanaphthalene (**3.19**)

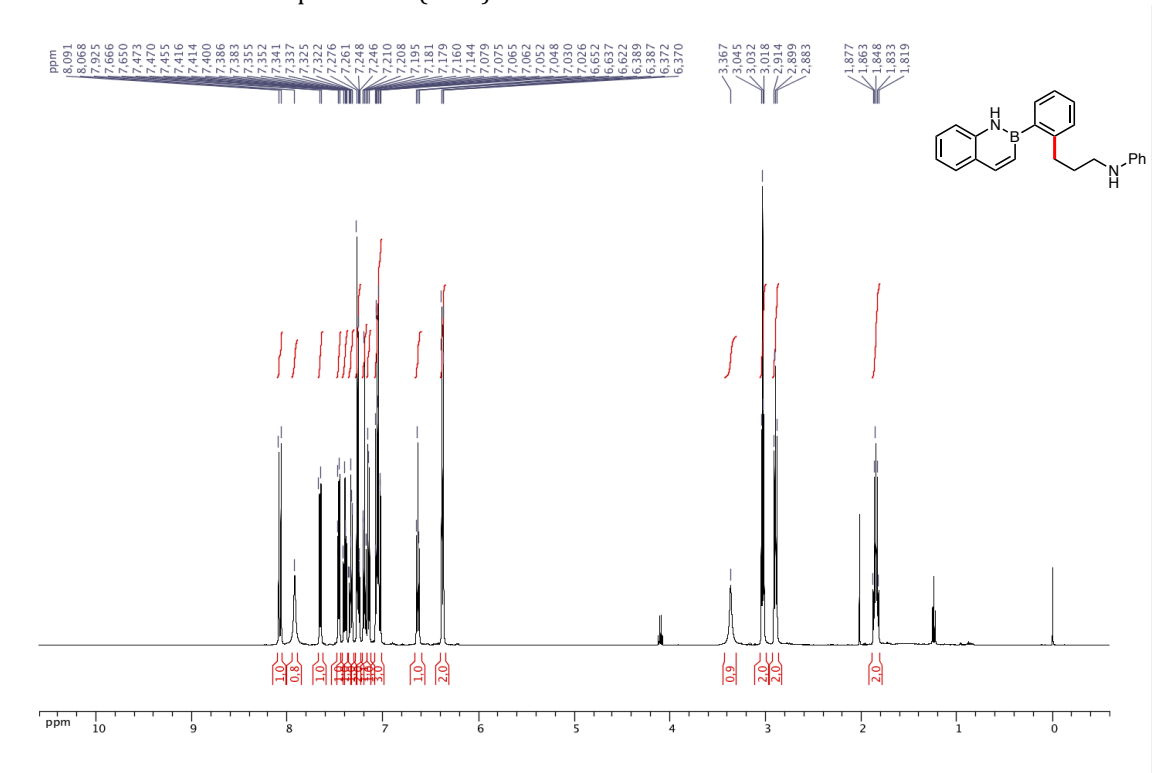

Figure A2.54: ^{13}C {^{1}H} NMR ($CDCl_3$, 125.8 MHz) of 2-(2-(3-(phenylamino)propyl)phenyl)-2,1-borazanaphthalene (**3.19**)

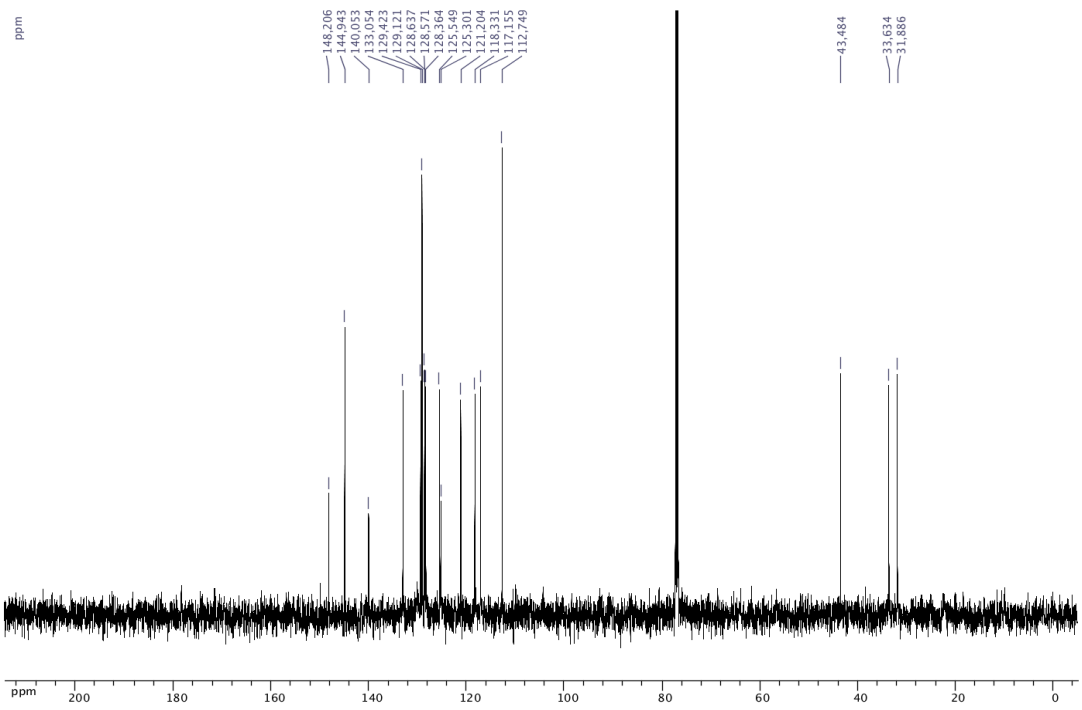

Figure A2.55: ^{11}B NMR (acetone, 128.4 MHz) of 2-(2-(3-(phenylamino)propyl)phenyl)-2,1-borazanaphthalene (**3.19**)

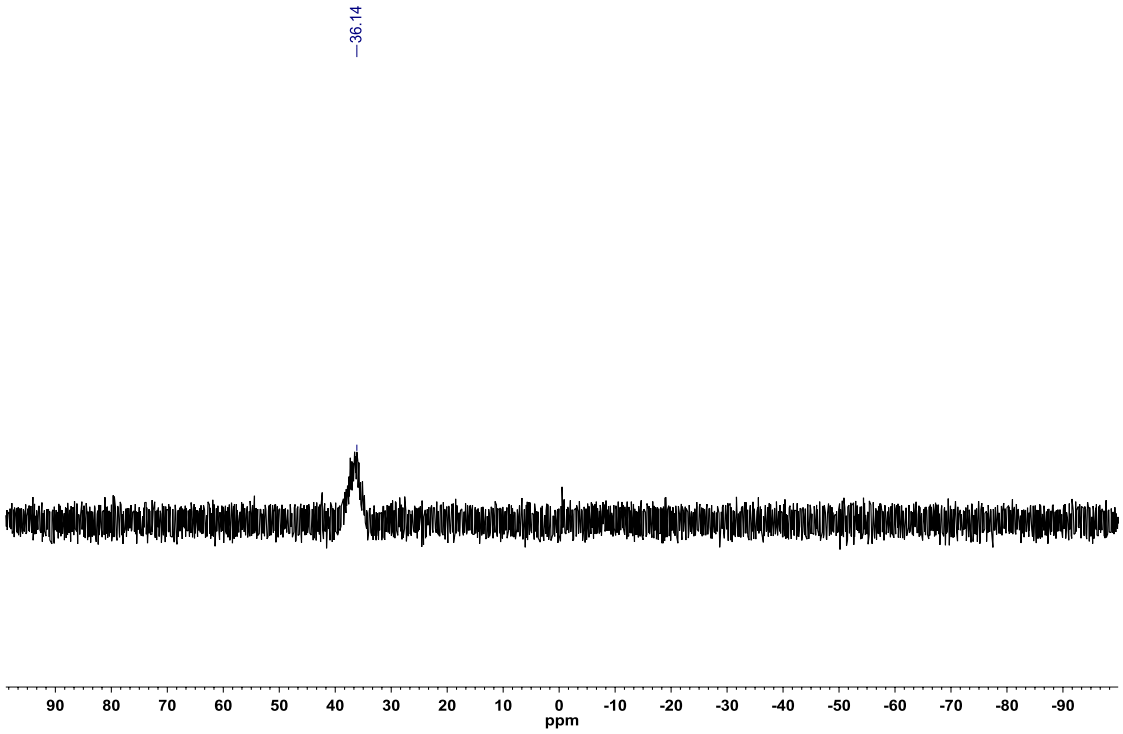

Figure A2.56: ^{1}H NMR ($CDCl_3$, 500.4 MHz) of 2-(2-hexylphenyl)-2,1-borazanaphthalene (**3.20**)

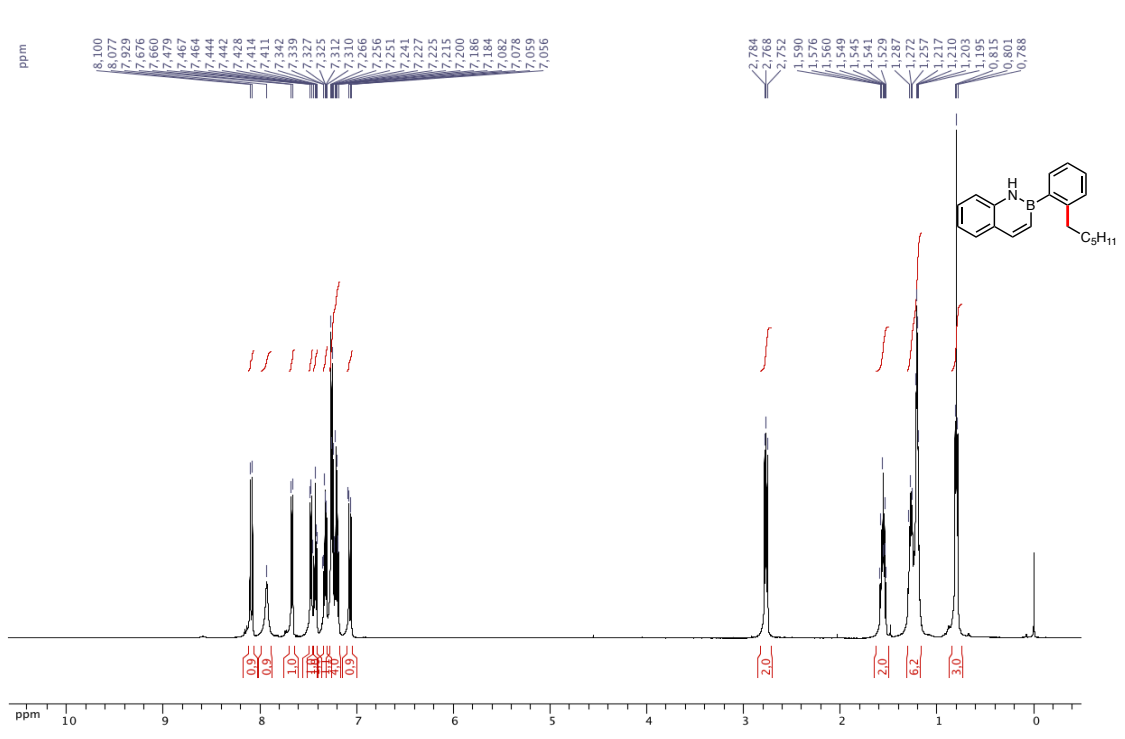

Figure A2.57: ^{13}C {^{1}H} NMR ($CDCl_3$, 125.8 MHz) of 2-(2-hexylphenyl)-2,1-borazanaphthalene (**3.20**)

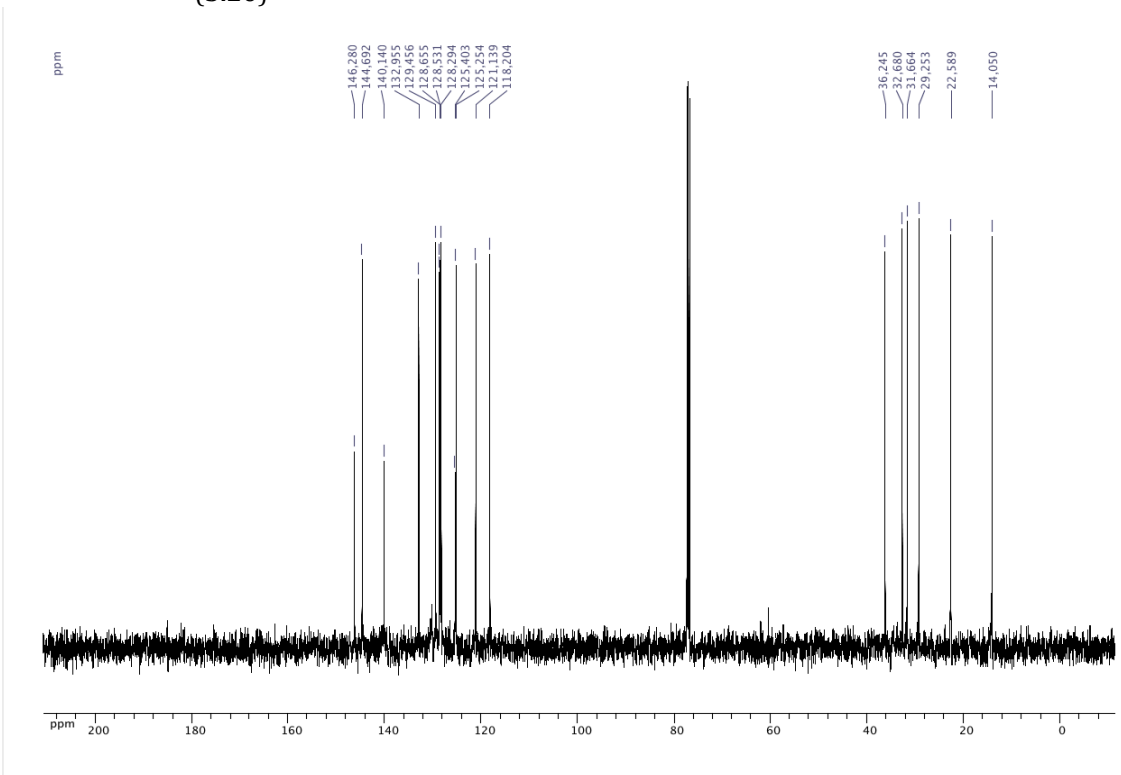

Figure A2.58: ^{11}B NMR (acetone, 128.4 MHz) of 2-(2-hexylphenyl)-2,1-borazanaphthalene (**3.20**)

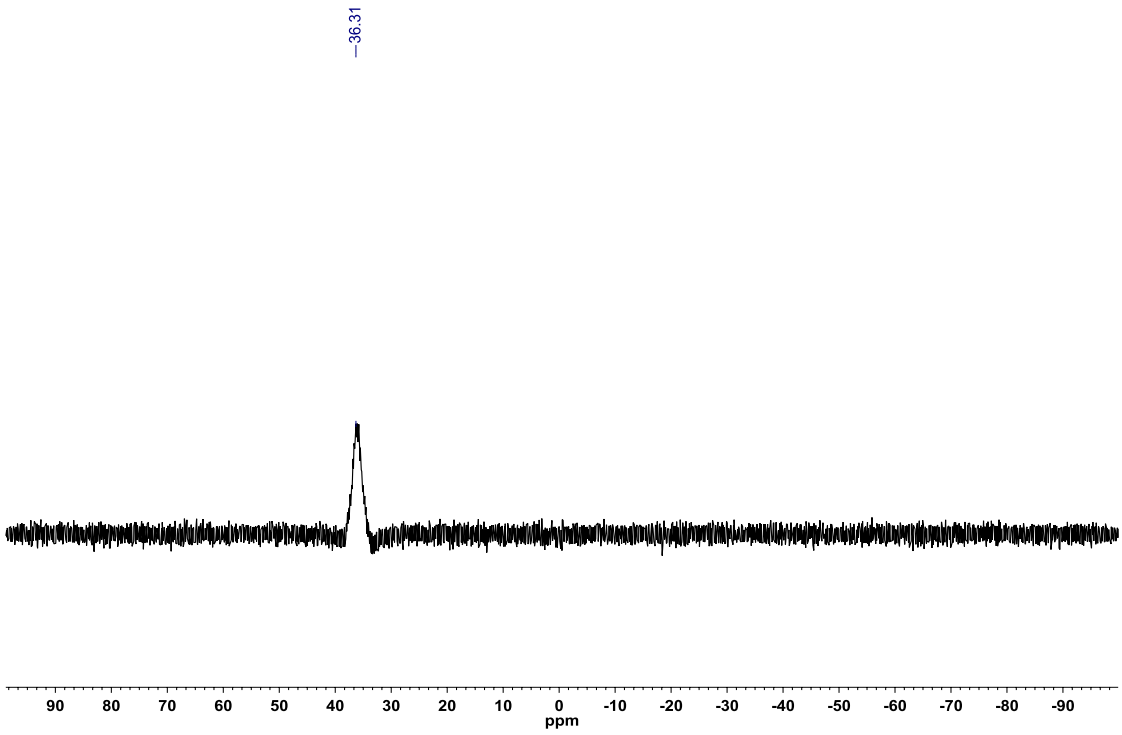

Figure A2.59: ^{1}H NMR ($CDCl_3$, 500.4 MHz) of 2-(2-(3-acetoxypropyl)phenyl)-2,1-borazanaphthalene (**3.21**)

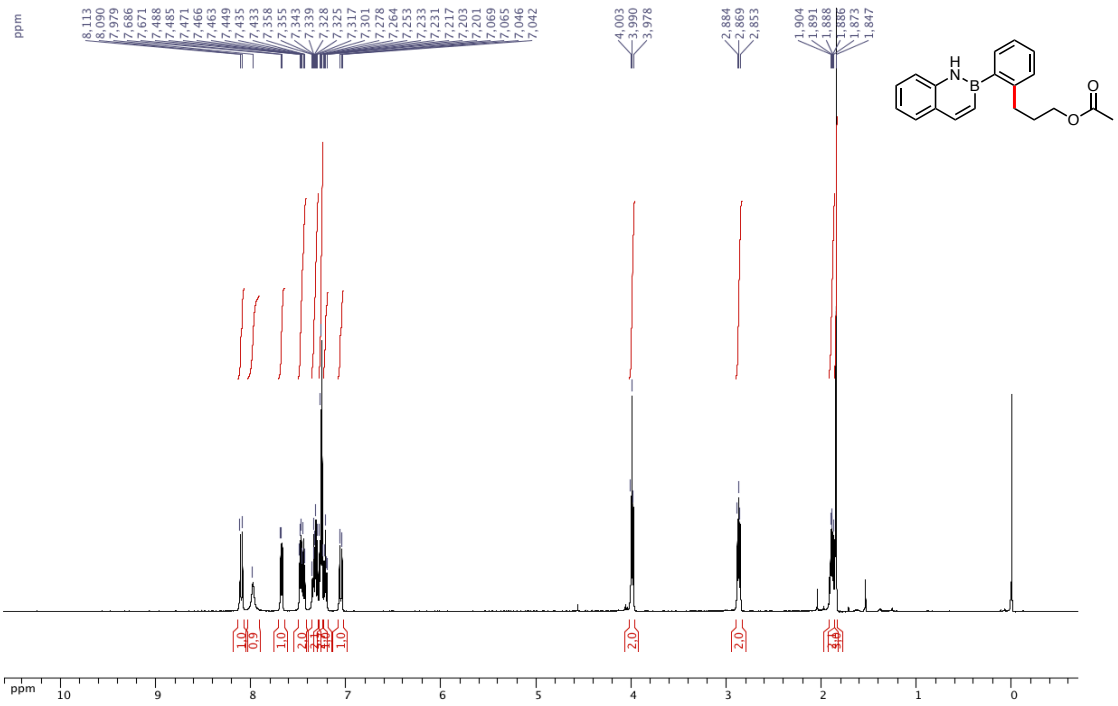

Figure A2.60: ^{13}C {^{1}H} NMR ($CDCl_3$, 125.8 MHz) of 2-(2-(3-acetoxypropyl)phenyl)-2,1-borazanaphthalene (**3.21**)

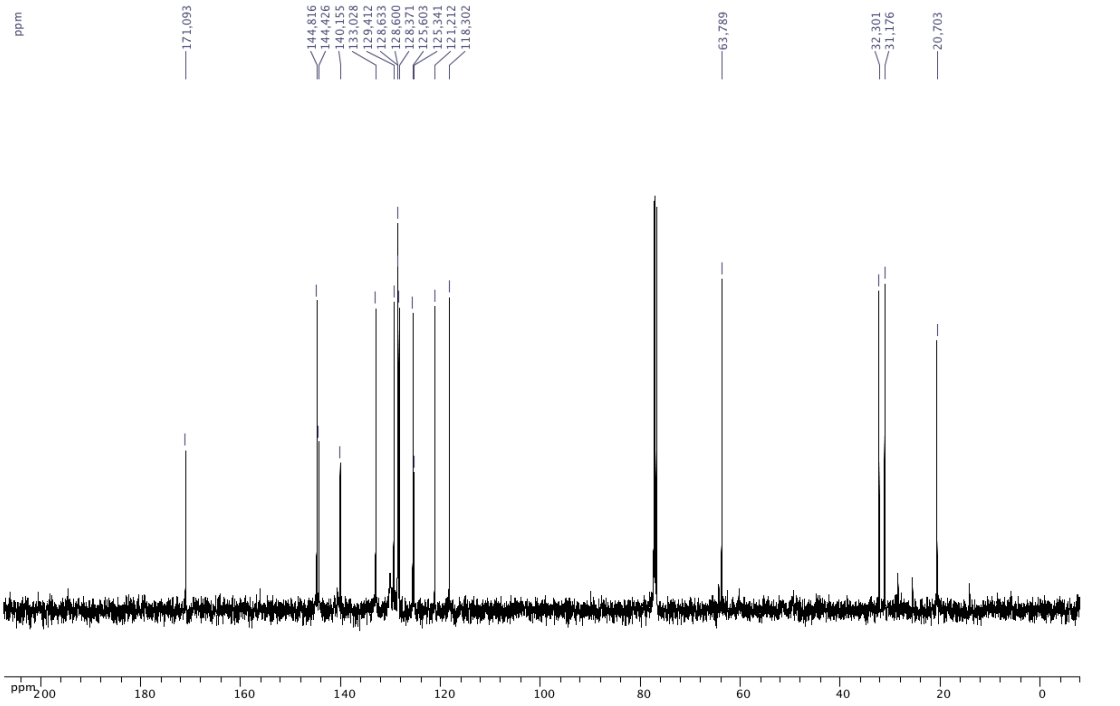

Figure A2.61: ^{11}B NMR (acetone, 128.4 MHz) of 2-(2-(3-acetoxypropyl)phenyl)-2,1-borazanaphthalene (**3.21**)

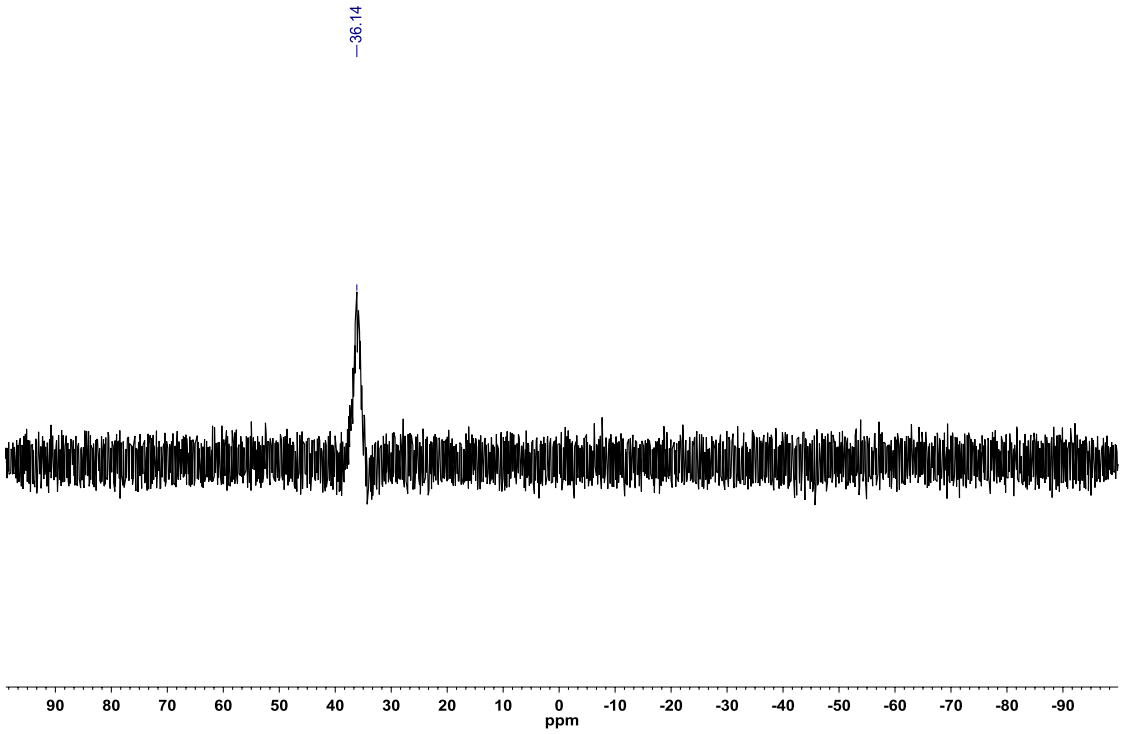

Figure A2.62: ^{1}H NMR ($CDCl_3$, 500.4 MHz) of 3-(3-aminopropyl)-2-phenyl-2,1-borazanaphthalene (**3.22**)

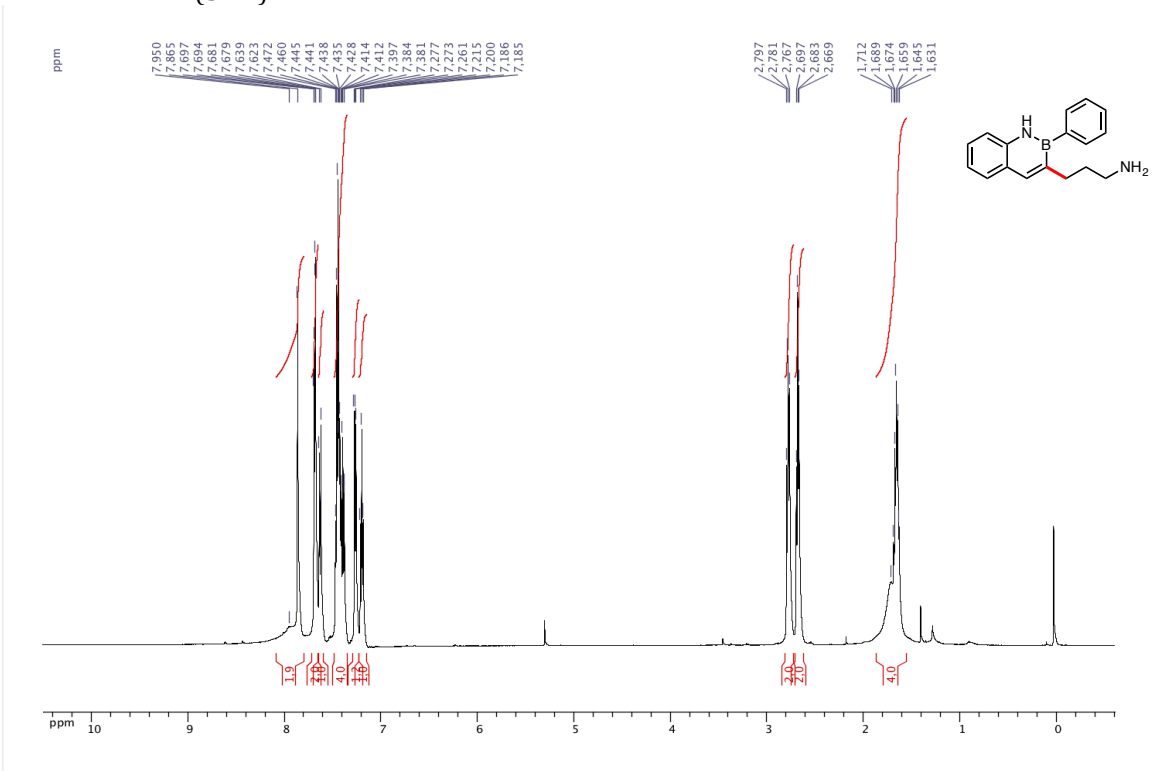

Figure A2.63: ^{13}C {^{1}H} NMR ($CDCl_3$, 125.8 MHz) of 3-(3-aminopropyl)-2-phenyl-2,1-borazanaphthalene (**3.22**)

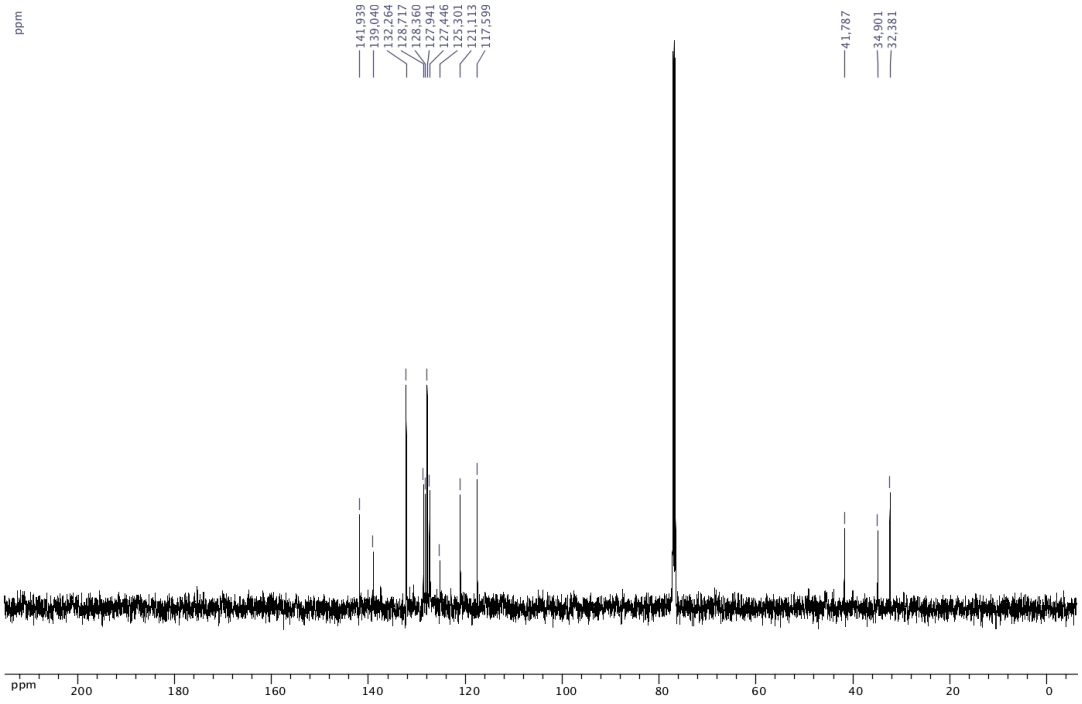

Figure A2.64: ^{11}B NMR (acetone, 128.4 MHz) of 3-(3-aminopropyl)-2-phenyl-2,1-borazanaphthalene (**3.22**)

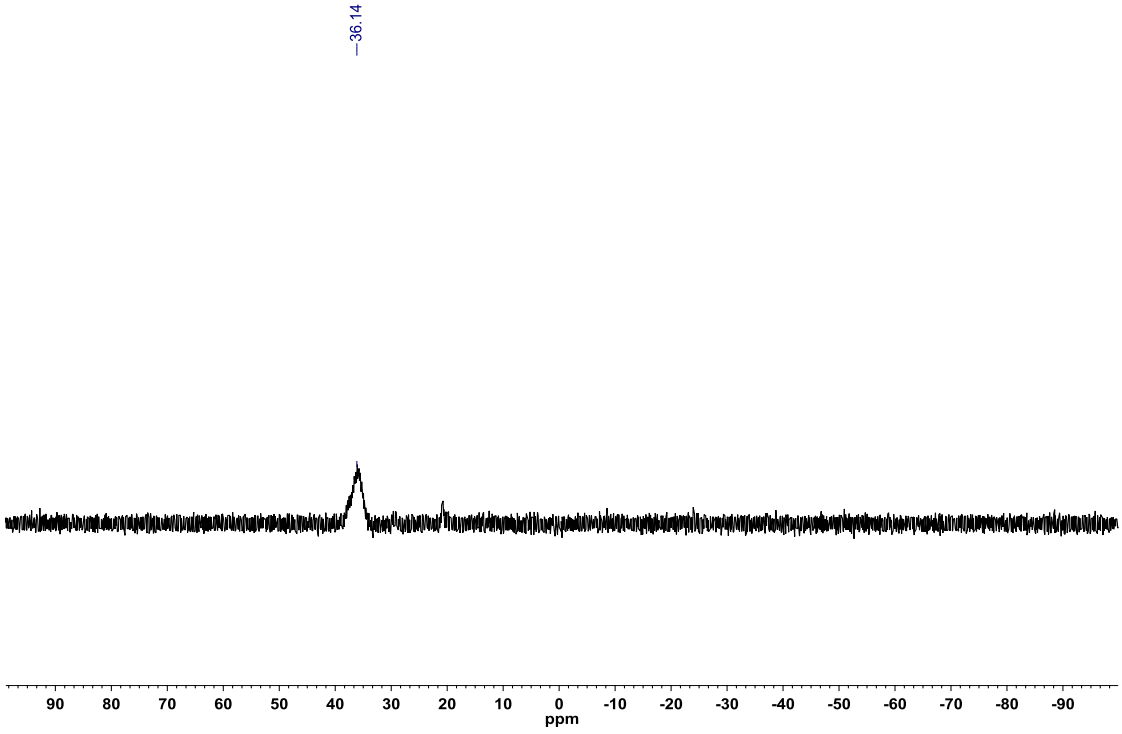

Figure A2.65: ^{1}H NMR ($CDCl_3$, 500.4 MHz) of 3-(3-acetamidopropyl)-2-phenyl-2,1-borazanaphthalene (**3.23**)

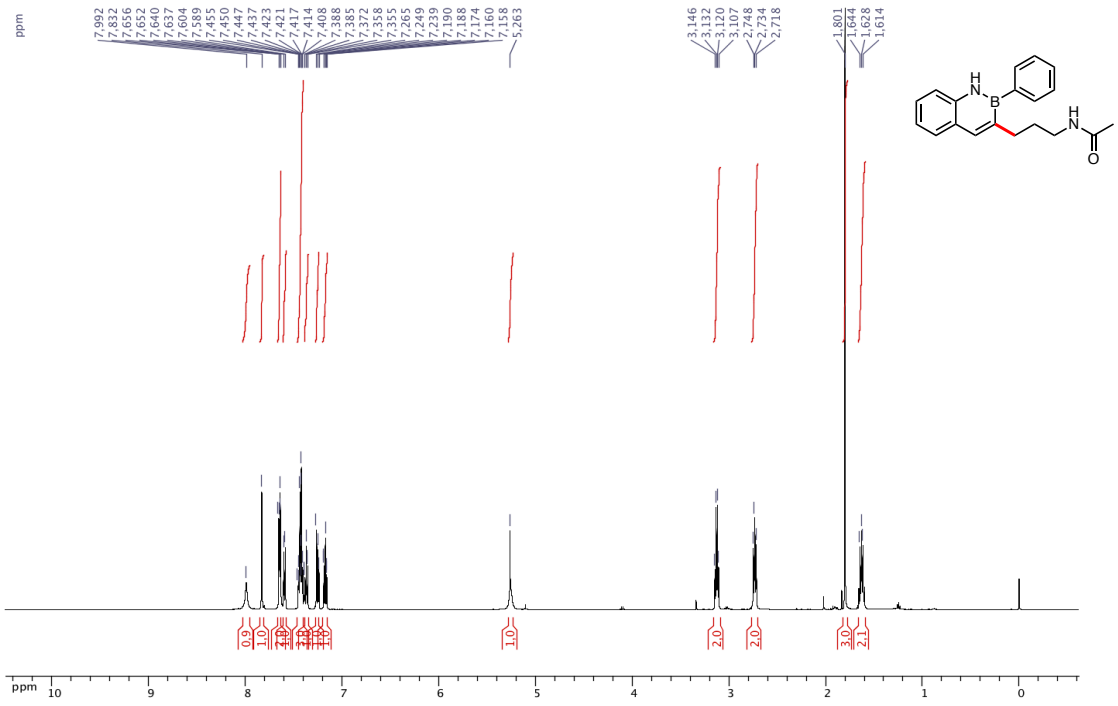

Figure A2.66: ^{13}C {^{1}H} ($CDCl_3$, 125.8 MHz) of 3-(3-acetamidopropyl)-2-phenyl-2,1-borazanaphthalene (**3.23**)

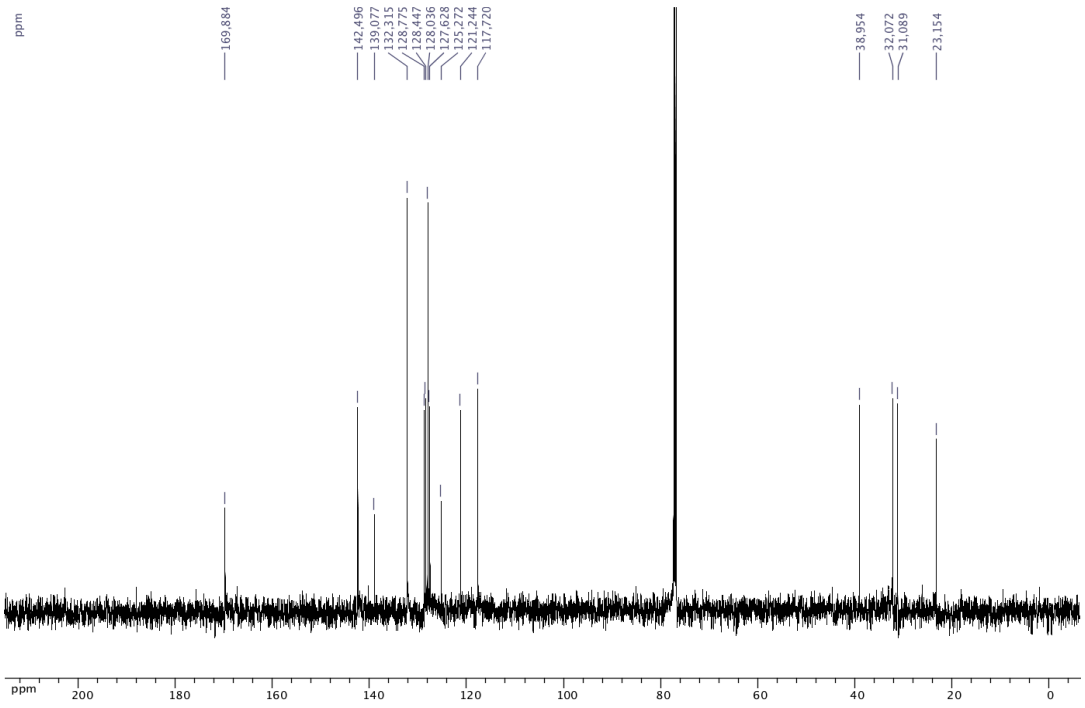

Figure A2.67: ^{11}B NMR (acetone, 128.4 MHz) of 3-(3-acetamidopropyl)-2-phenyl-2,1-borazanaphthalene (**3.23**)

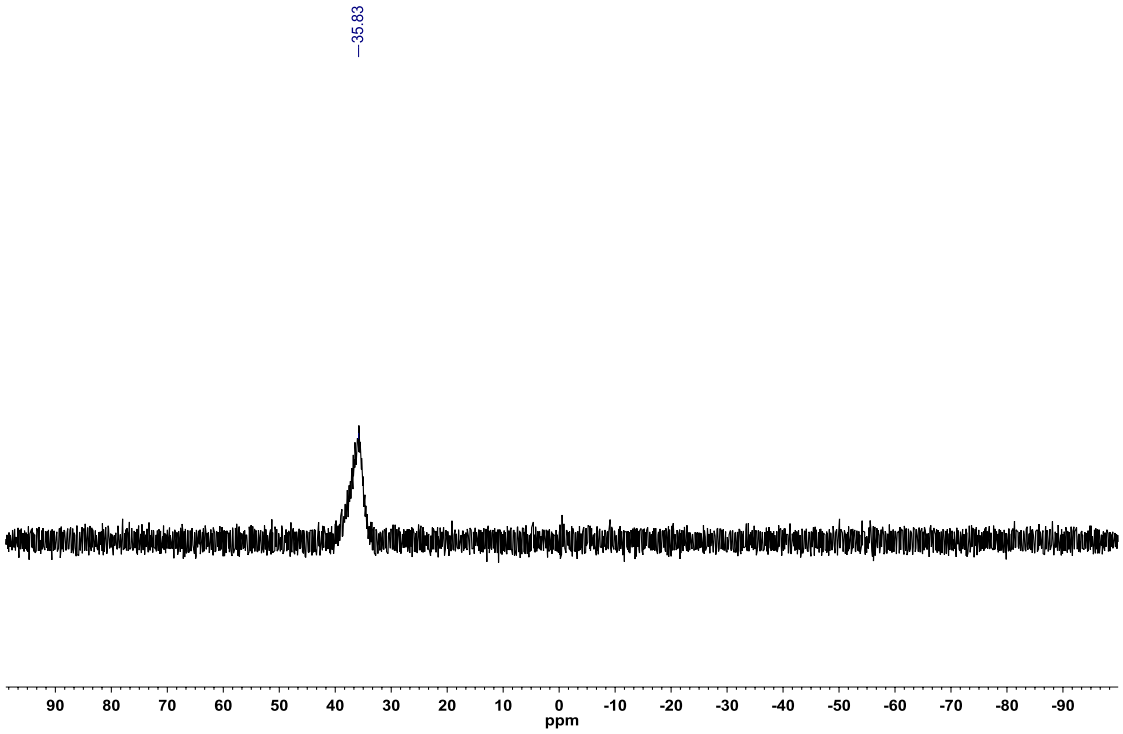

Figure A2.68: ^{1}H NMR ($CDCl_3$, 500.4 MHz) of 3-(3-acetoxypropyl)-2-phenyl-2,1-borazanaphthalene (**3.24**)

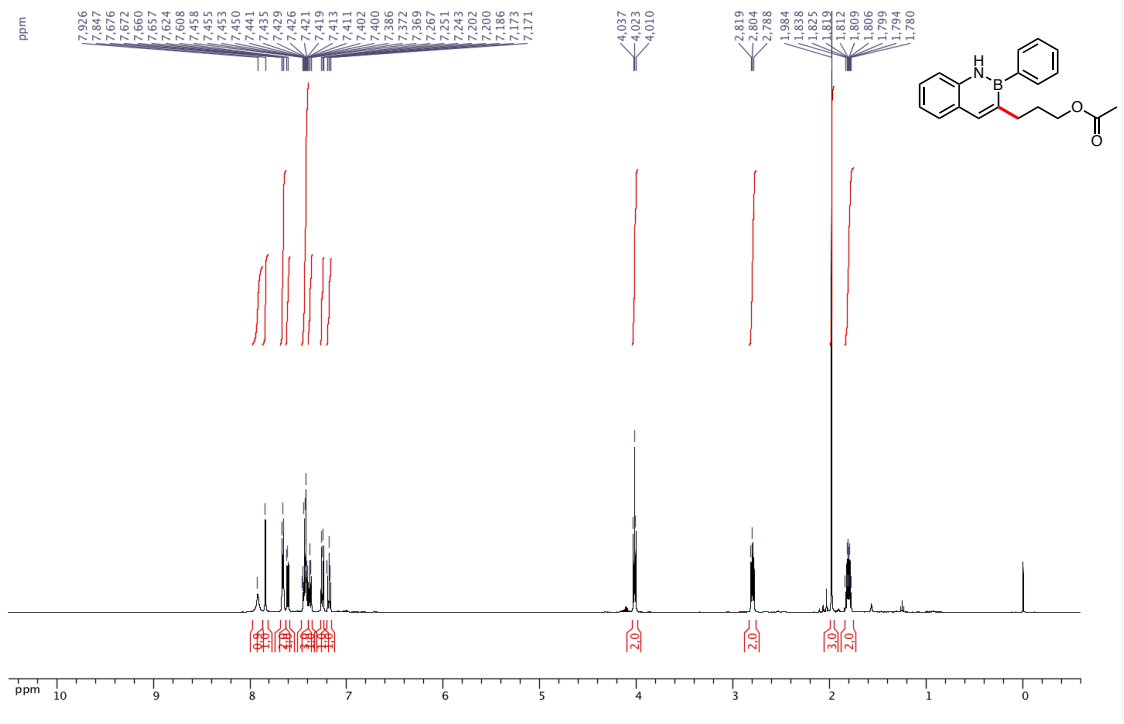

Figure A2.69: ^{13}C {^{1}H} NMR ($CDCl_3$, 125.8 MHz) of 3-(3-acetoxypropyl)-2-phenyl-2,1-borazanaphthalene (**3.24**)

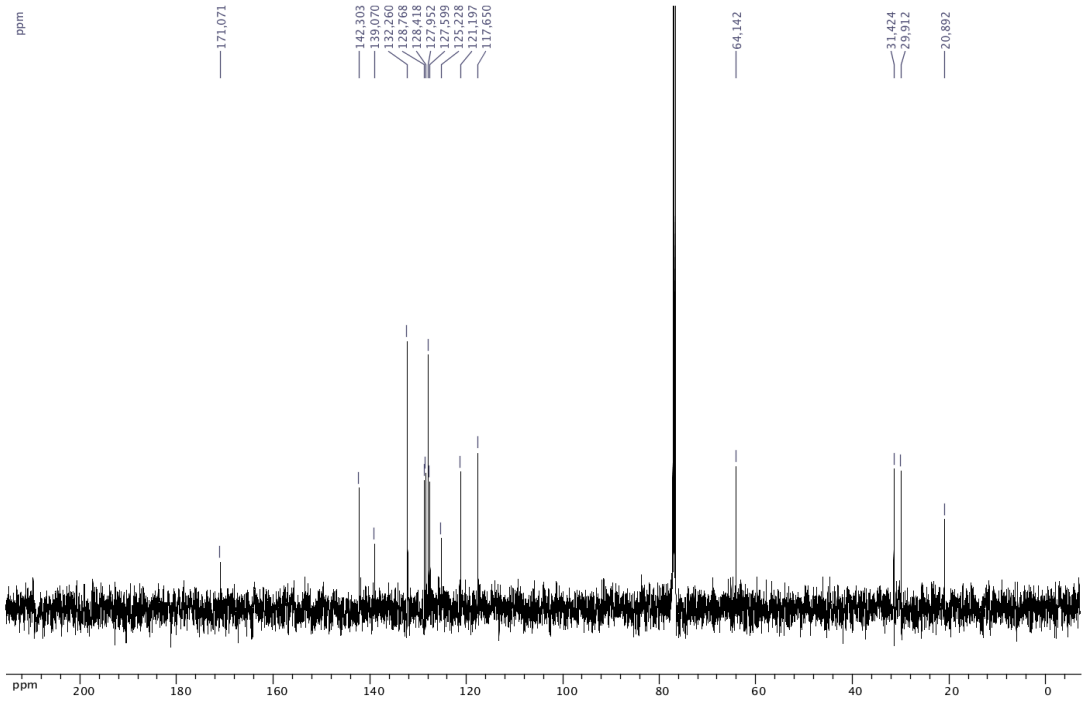

Figure A2.70: ^{11}B NMR (acetone, 128.4 MHz) of 3-(3-acetoxypropyl)-2-phenyl-2,1-borazanaphthalene (**3.24**)

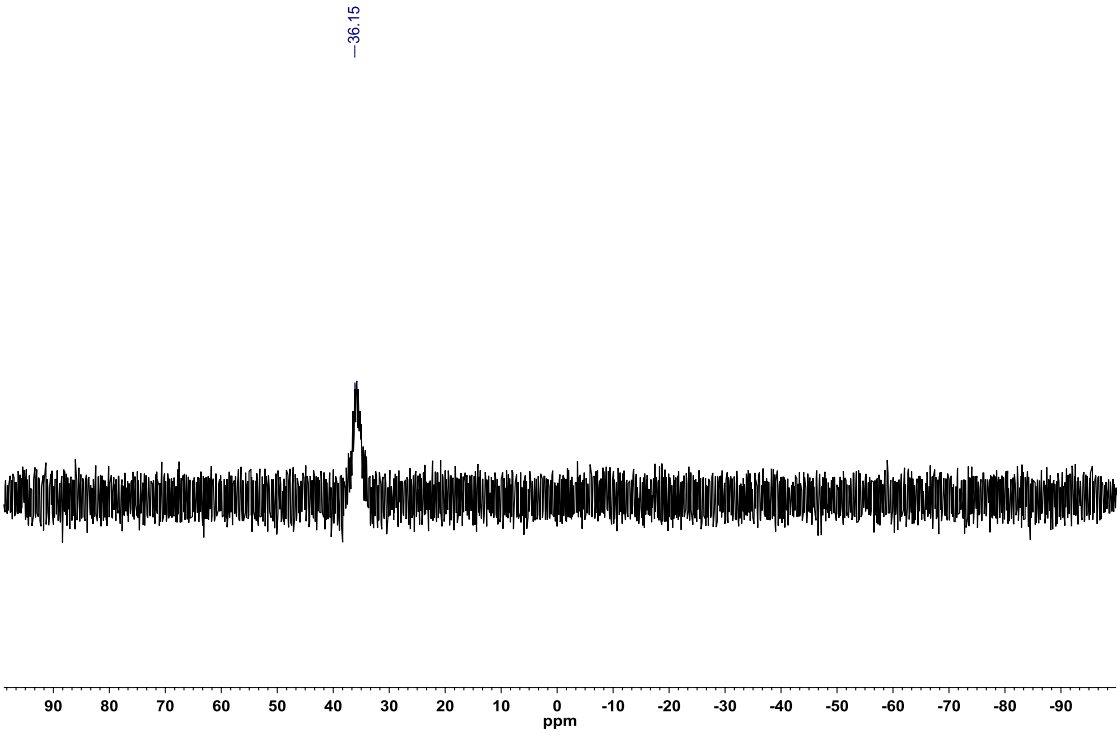

Figure A2.71: ^{1}H NMR ($CDCl_3$, 500.4 MHz) of 3-(3-(phenylamino)propyl)-2-phenyl-2,1-borazanaphthalene (**3.25**)

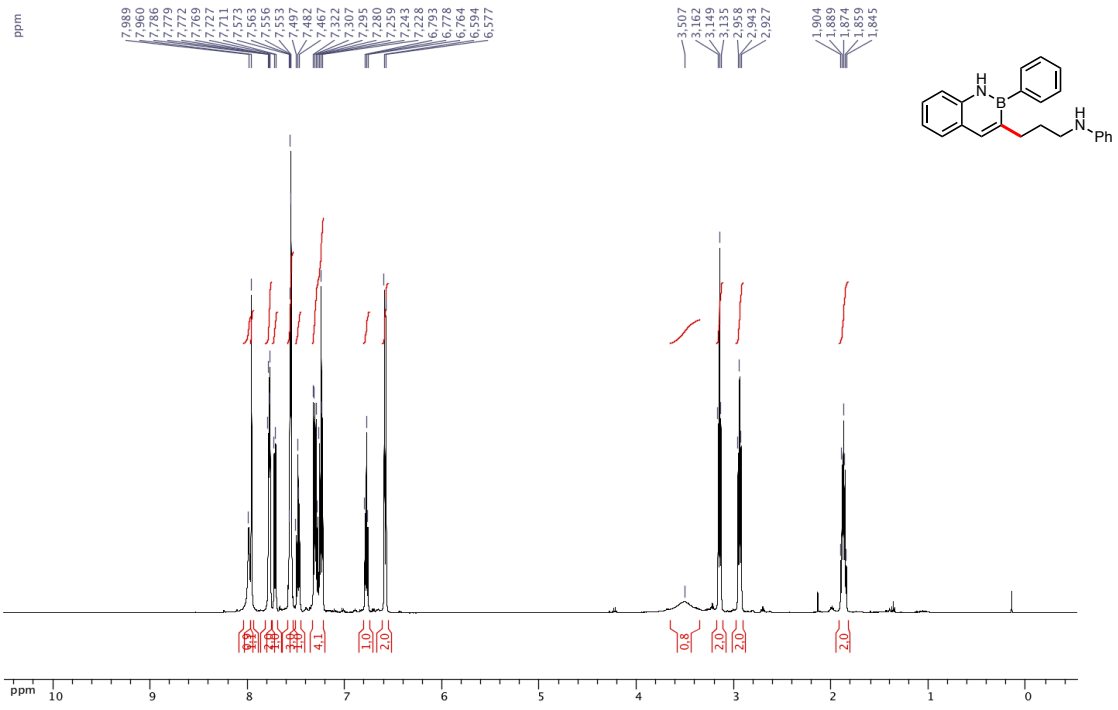

Figure A2.72: ^{13}C {^{1}H} NMR ($CDCl_3$, 125.8 MHz) of 3-(3-(phenylamino)propyl)-2-phenyl-2,1-borazanaphthalene (**3.25**)

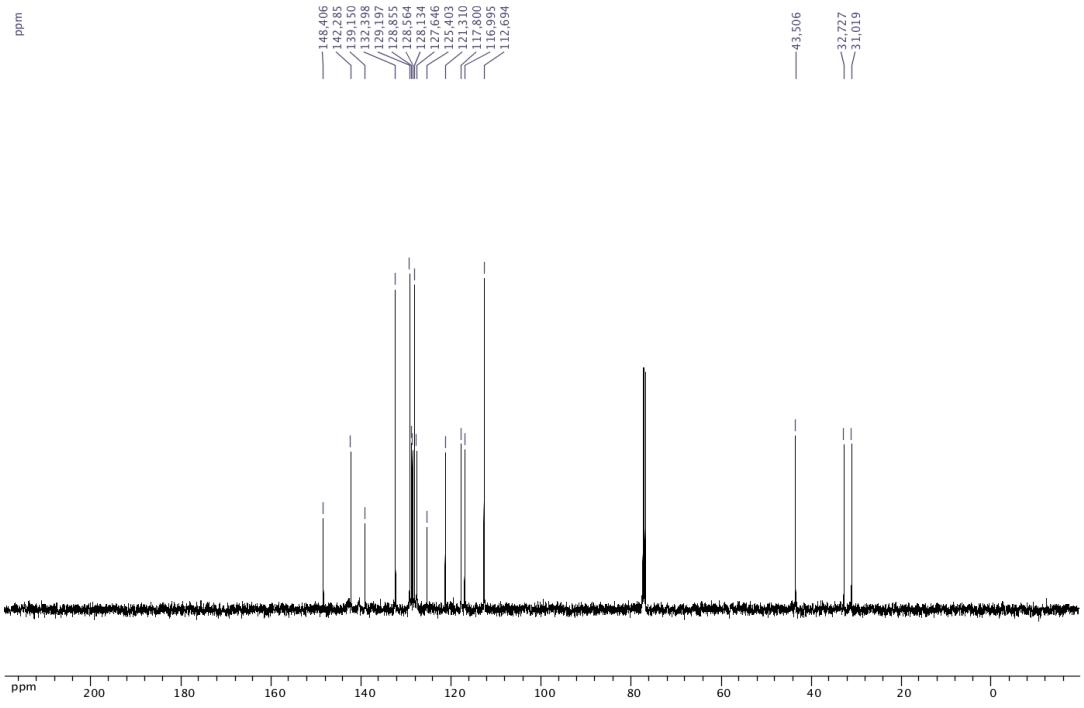

Figure A2.73: ^{11}B NMR (acetone, 128.4 MHz) of 3-(3-(phenylamino)propyl)-2-phenyl-2,1-borazanaphthalene (**3.25**)

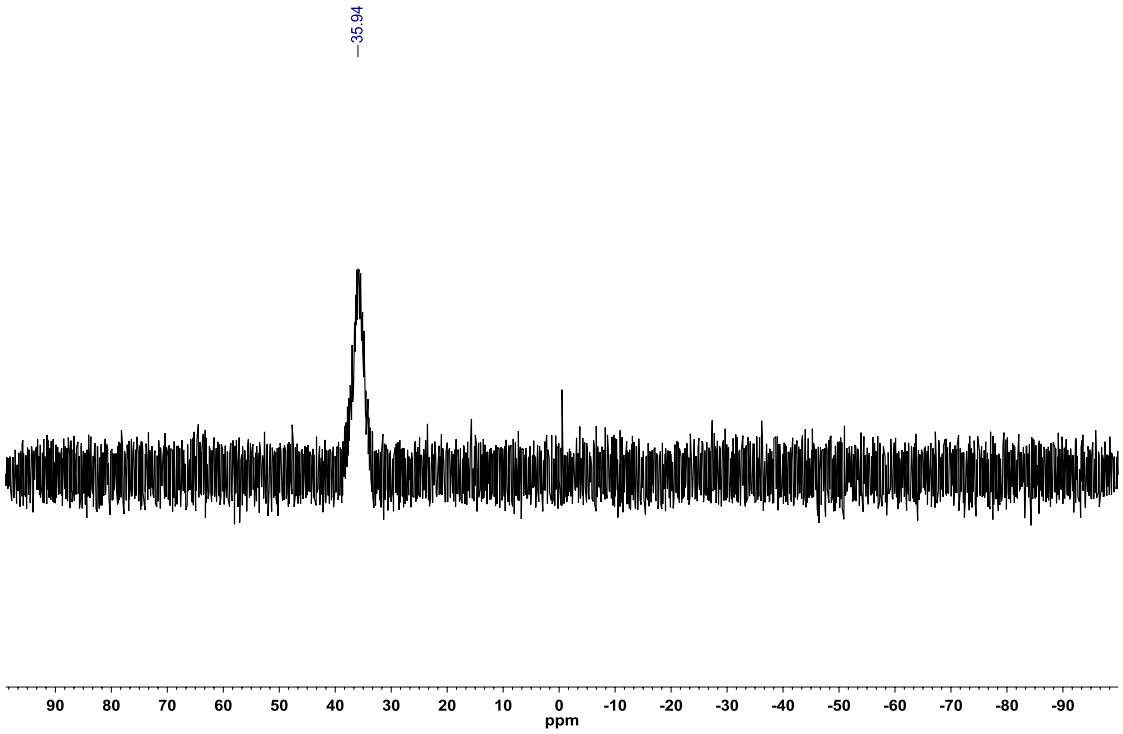

Figure A2.74: ^{1}H NMR ($CDCl_3$, 500.4 MHz) of 3-(3-(butylamino)propyl)-2-phenyl-2,1-borazanaphthalene (**3.26**)

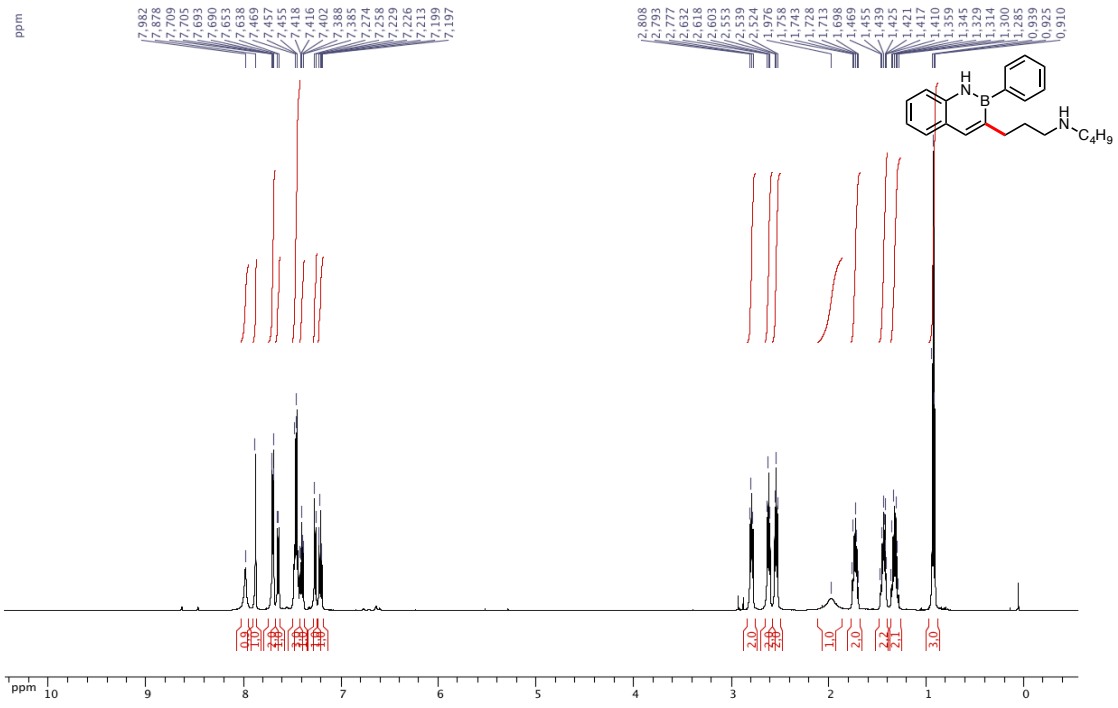

Figure A2.75: ^{13}C {^{1}H} NMR ($CDCl_3$, 125.8 MHz) of 3-(3-(butylamino)propyl)-2-phenyl-2,1-borazanaphthalene (**3.26**)

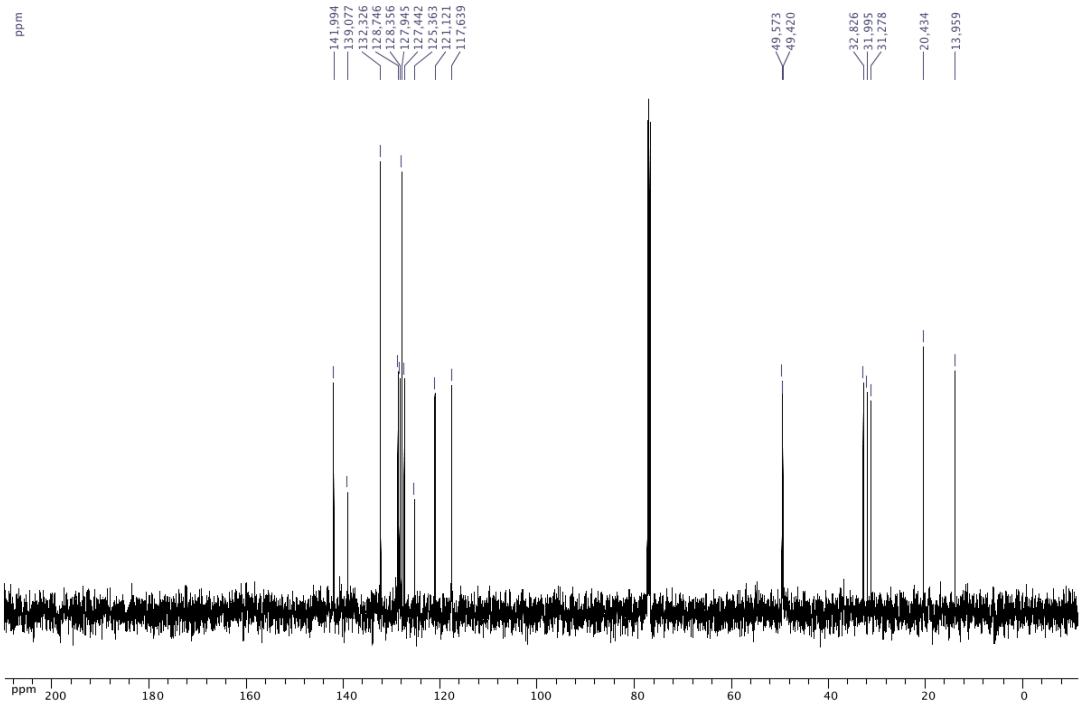

Figure A2.76: ^{11}B NMR (acetone, 128.4 MHz) of 3-(3-(butylamino)propyl)-2-phenyl-2,1-borazanaphthalene (**3.26**)

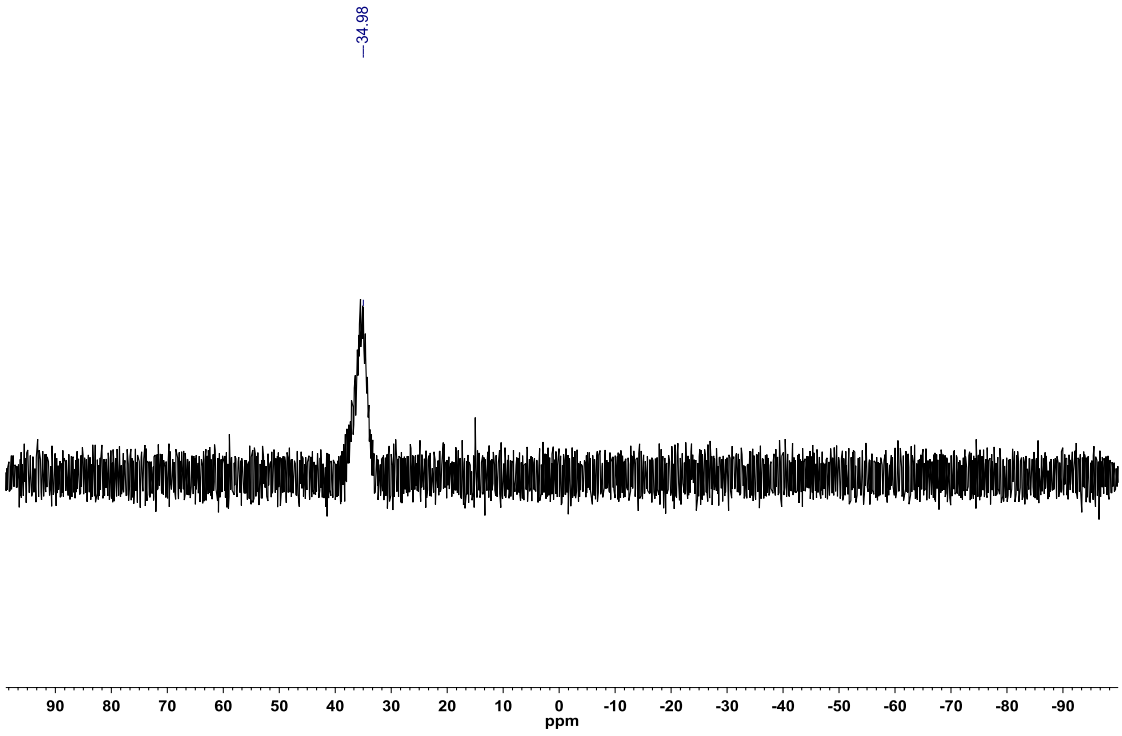

Figure A2.77: ^{1}H NMR ($CDCl_3$, 500.4 MHz) of 3-(*exo*-bicyclo[2.2.1]heptan-2-yl)-2-phenyl-2,1-borazanaphthalene (**3.27**)

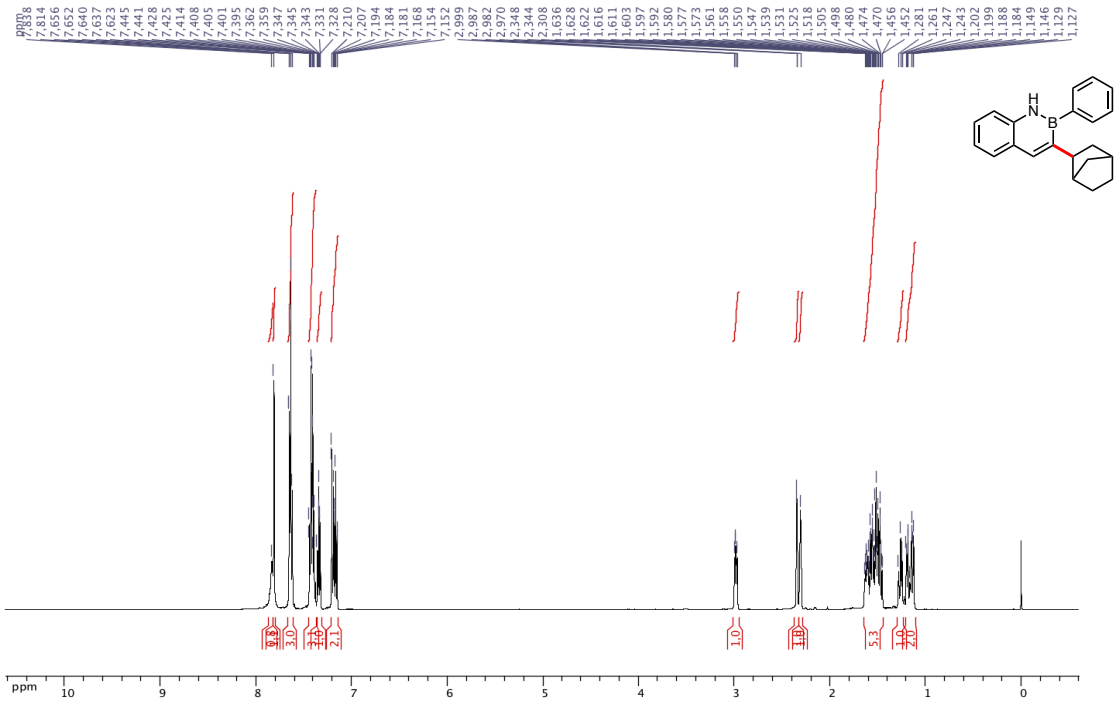

Figure A2.78: ^{13}C {^{1}H} NMR ($CDCl_3$, 125.8 MHz) of 3-(*exo*-bicyclo[2.2.1]heptan-2-yl)-2-phenyl-2,1-borazanaphthalene (**3.27**)

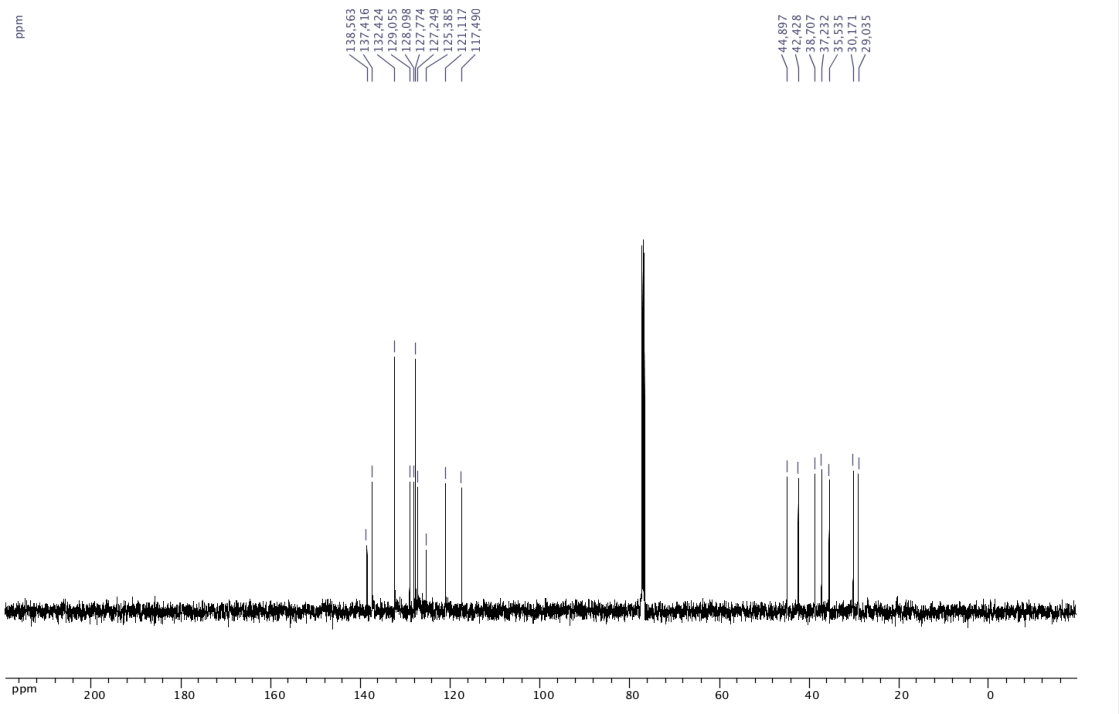

Figure A2.79: ^{11}B NMR (acetone, 128.4 MHz) of 3-(*exo*-bicyclo[2.2.1]heptan-2-yl)-2-phenyl-2,1-borazanaphthalene (**3.27**)

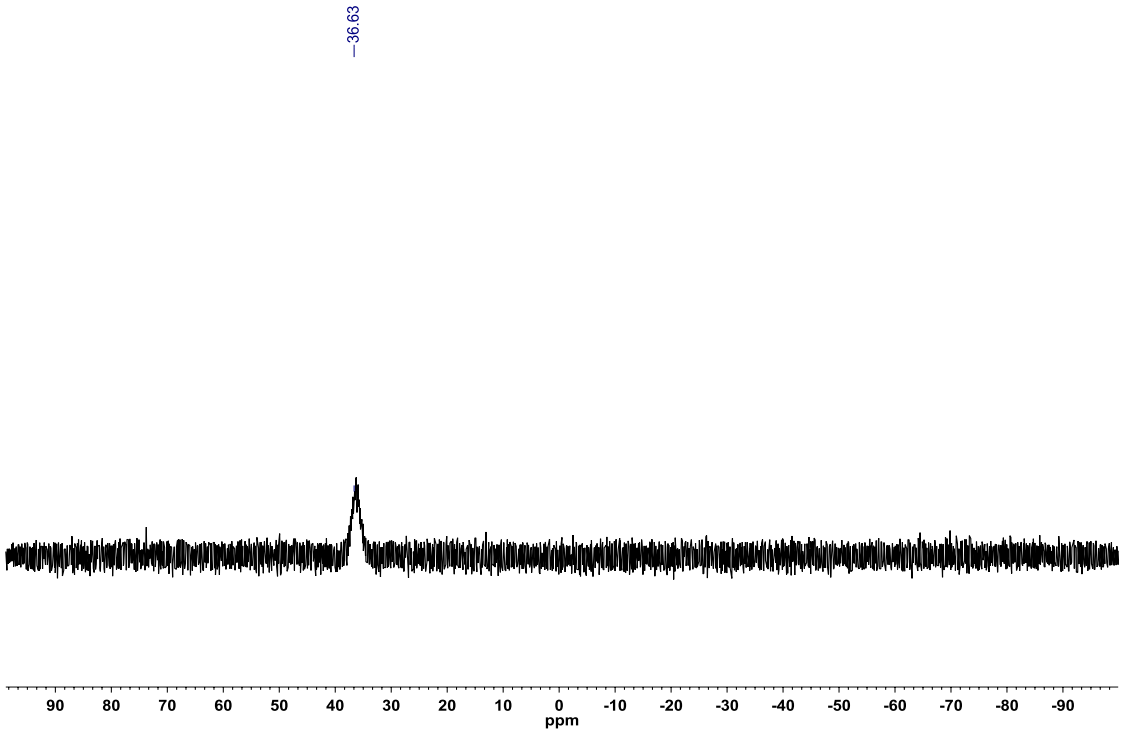

Figure A2.80: ^{1}H NMR (acetone-d_6, 500.4 MHz) of 3-(2-pyridin-2-yl)ethyl)-2-(4-trifluoromethylphenyl)-2,1-borazanaphthalene (**3.28**)

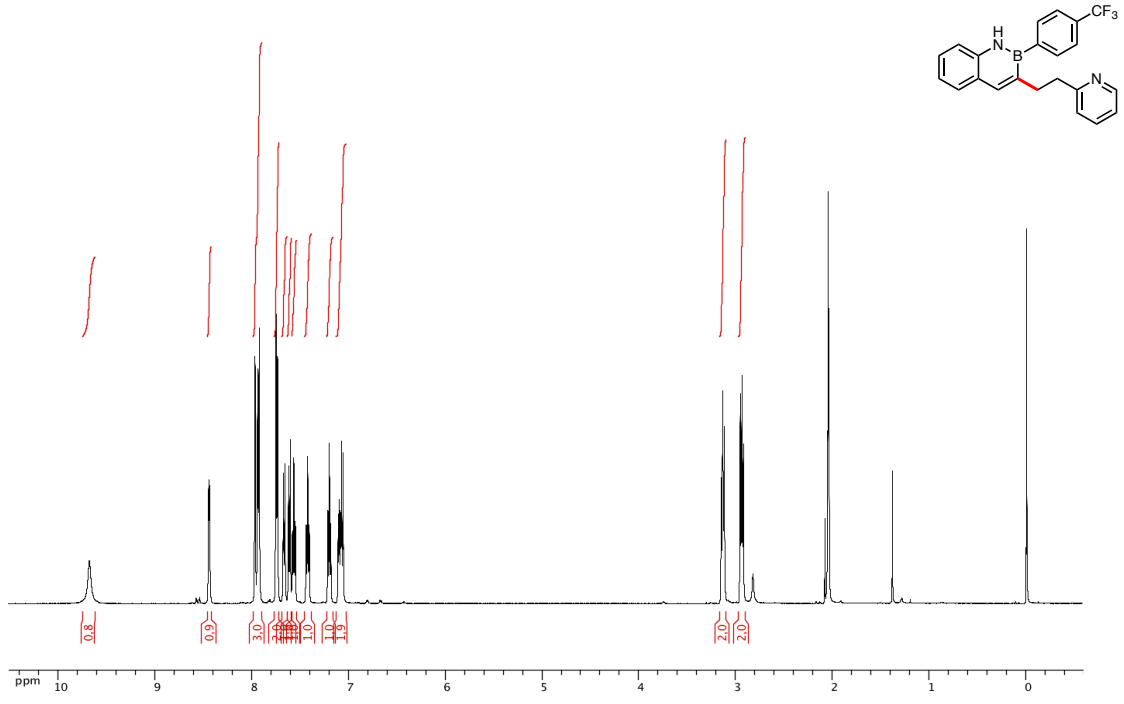

Figure A2.81: ^{13}C {^{1}H} NMR (acetone-d_6, 125.8 MHz) of 3-(2-pyridin-2-yl)ethyl)-2-(4-trifluoromethylphenyl)-2,1-borazanaphthalene (**3.28**)

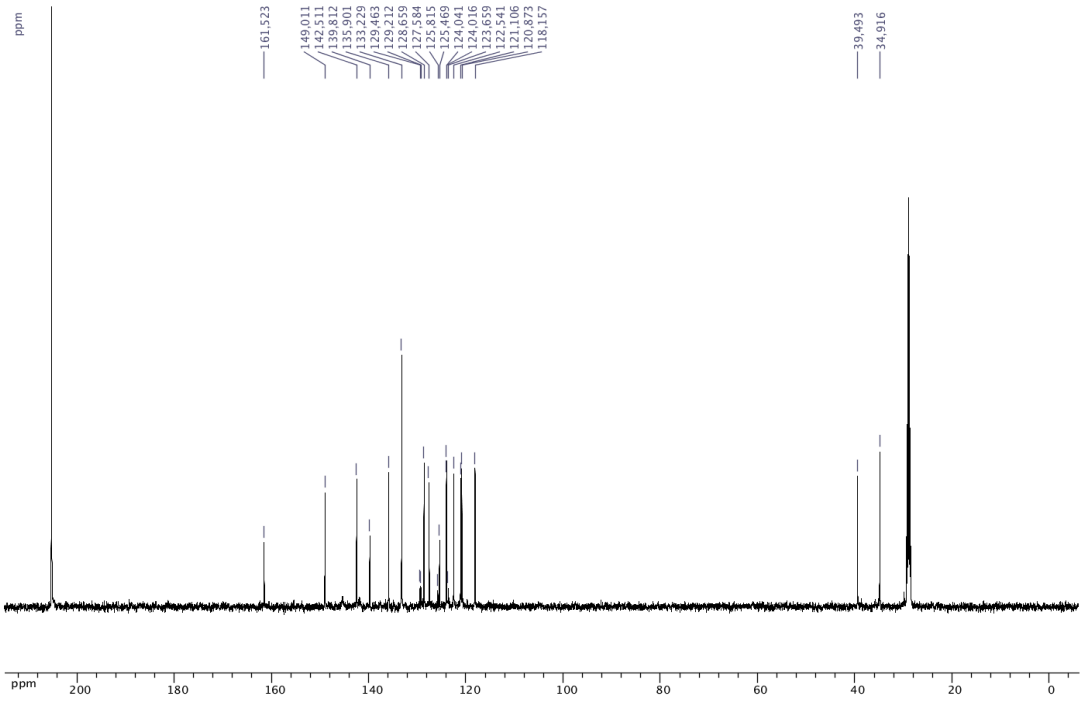

Figure A2.82: ^{19}F {^{1}H} NMR (acetone-d_6, 470.8 MHz) of 3-(2-pyridin-2-yl)ethyl)-2-(4-trifluoromethylphenyl)-2,1-borazanaphthalene (**3.28**)

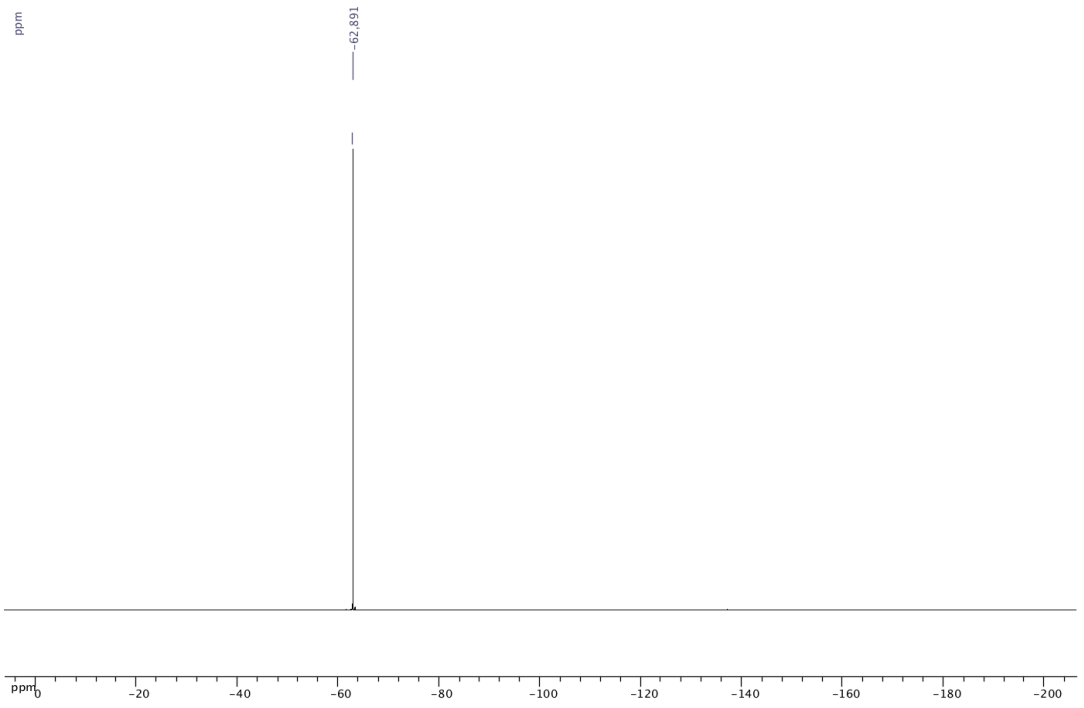

Figure A2.83: ^{11}B NMR (acetone, 128.4 MHz) of 3-(2-pyridin-2-yl)ethyl)-2-(4-trifluoromethylphenyl)-2,1-borazanaphthalene (**3.28**)

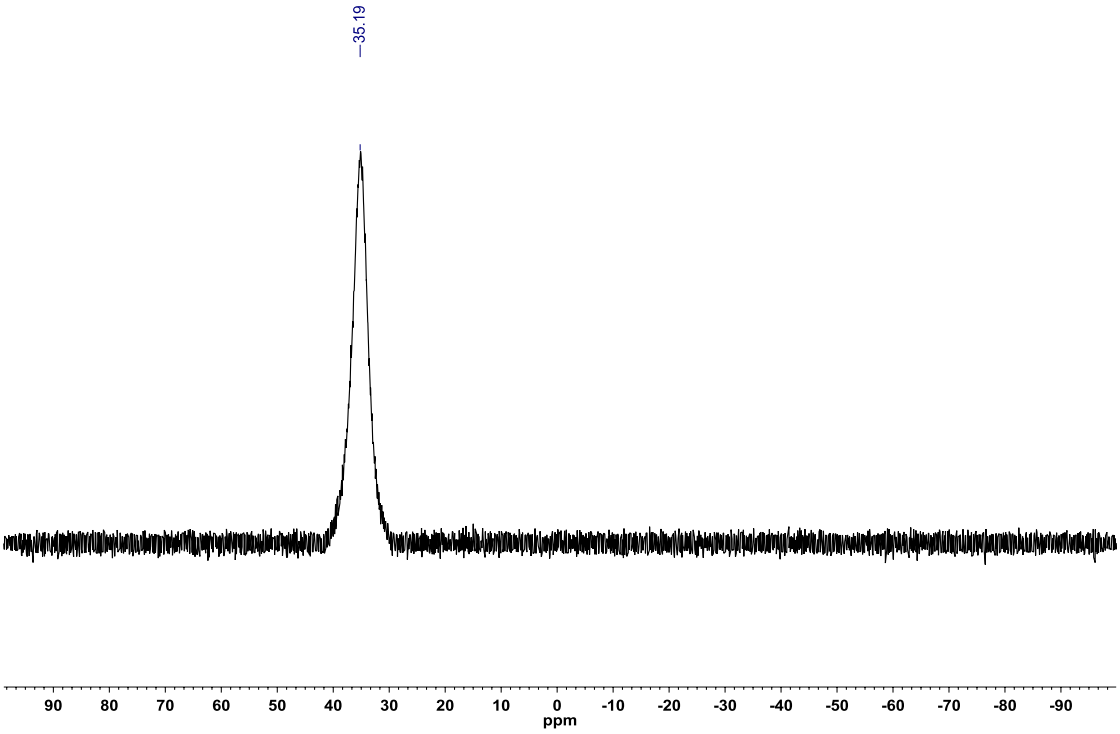

Figure A2.84: ^{1}H NMR ($CDCl_3$, 500.4 MHz) of 3-(isobutyl)-2-(2,3-dihydro-1,4-benzodioxin-6-yl)-2,1-borazanaphthalene (**3.29**)

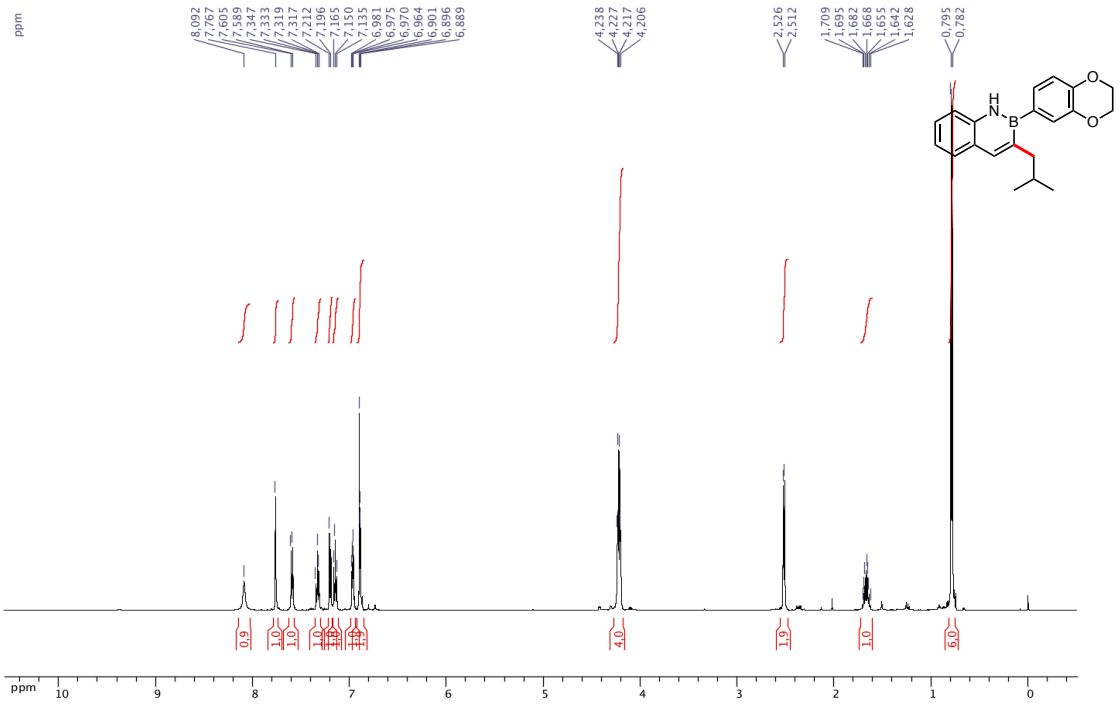

Figure A2.85: ^{13}C {^{1}H} NMR ($CDCl_3$, 125.8 MHz) of 3-(isobutyl)-2-(2,3-dihydro-1,4-benzodioxin-6-yl)-2,1-borazanaphthalene (**3.29**)

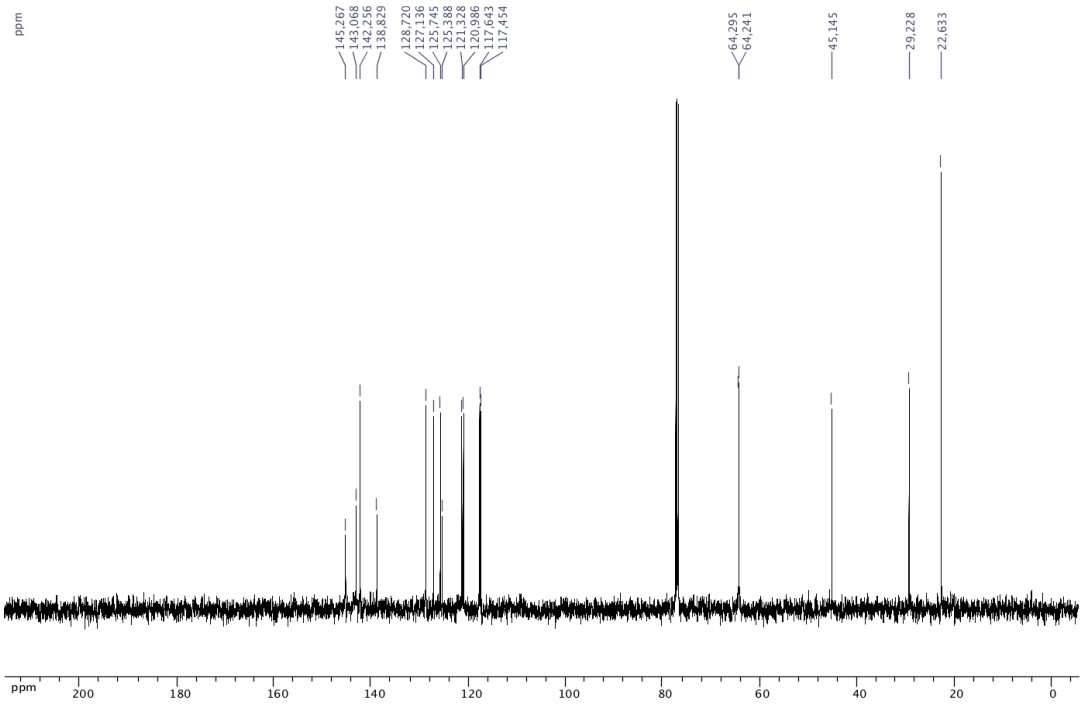

Figure A2.86: ^{11}B NMR (acetone, 128.4 MHz) of 3-(isobutyl)-2-(2,3-dihydro-1,4-benzodioxin-6-yl)-2,1-borazanaphthalene (**3.29**

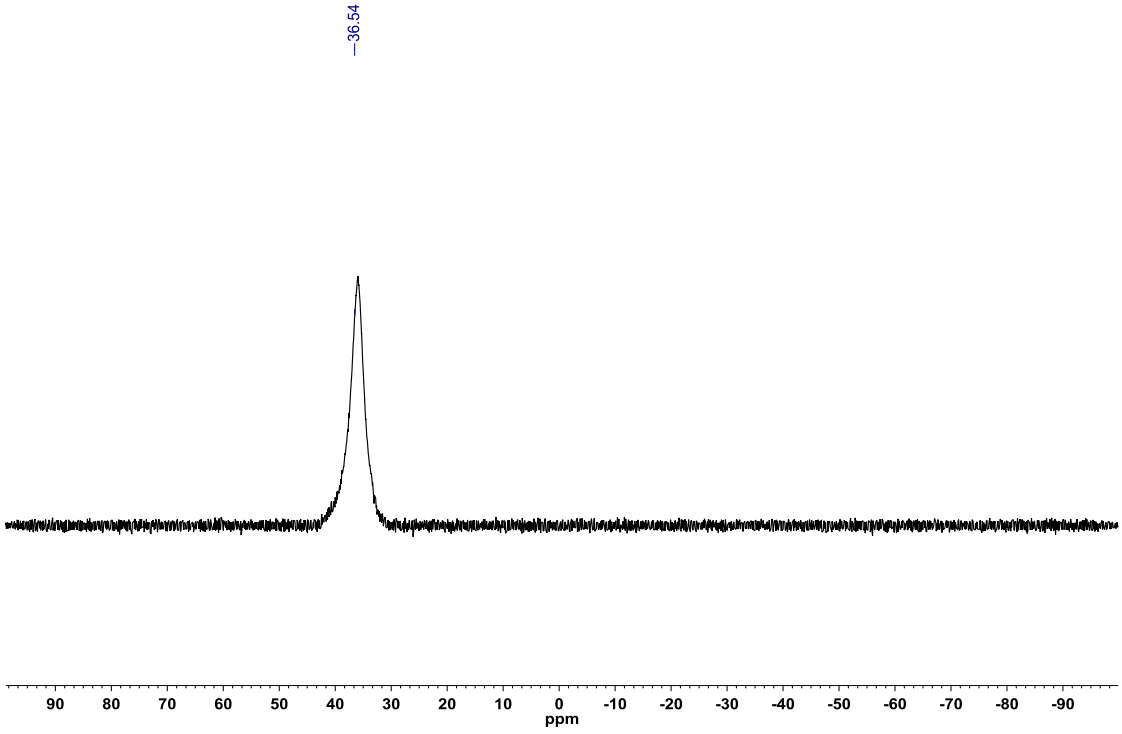

Figure A2.87: ^{1}H NMR (acetone-d_6, 500.4 MHz) of 3-(3-methoxypropyl)-2-(2,6-difluorophenyl)-2,1-borazanaphthalene (**3.30**)

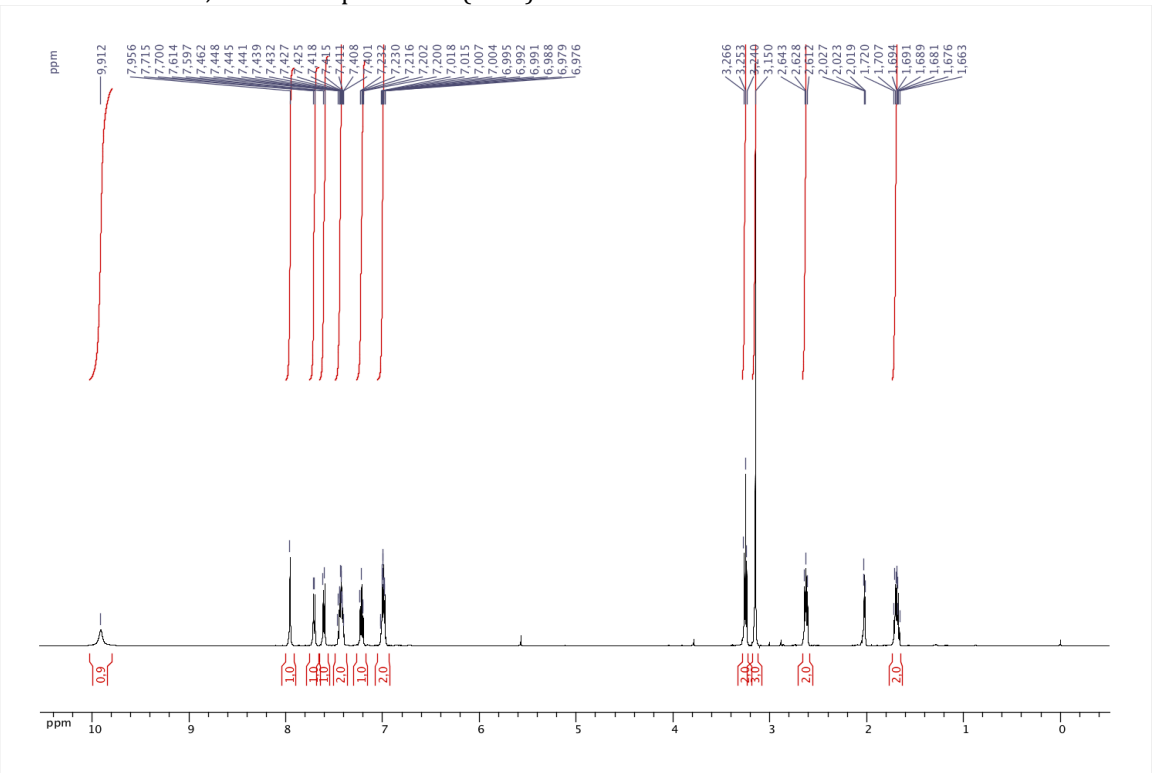

Figure A2.88: ^{13}C {^{1}H} NMR (acetone-d_6, 125.8 MHz) of 3-(3-methoxypropyl)-2-(2,6-difluorophenyl)-2,1-borazanaphthalene (**3.30**)

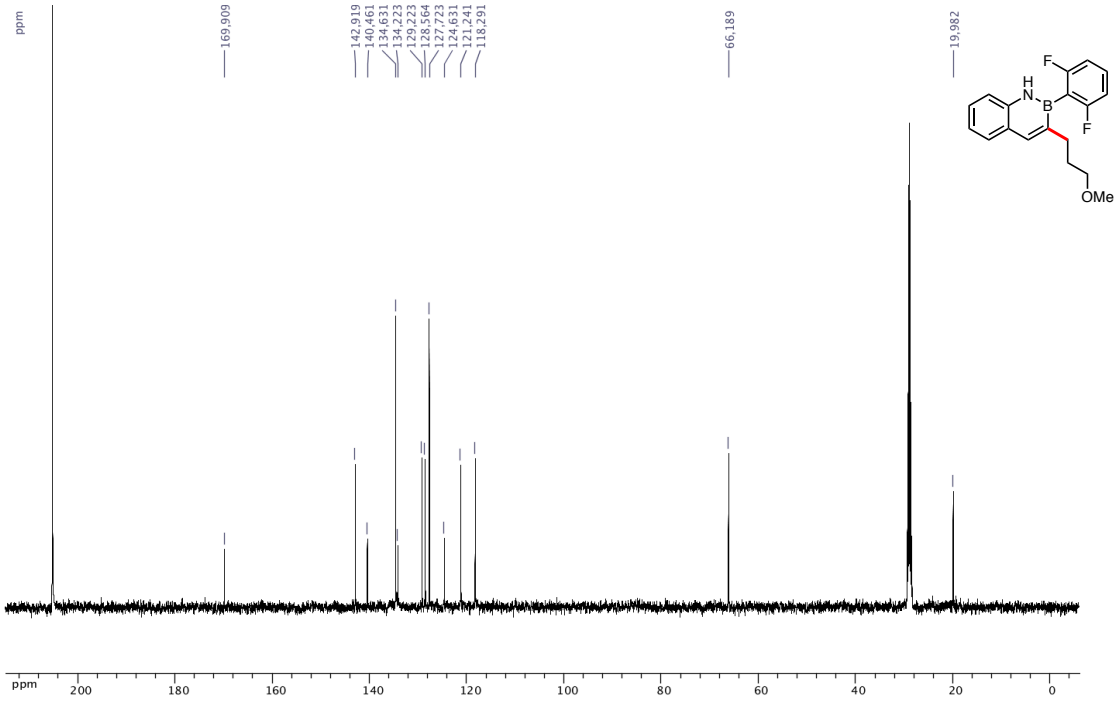

Figure A2.89: ^{19}F {^{1}H} NMR (acetone-d_6, 470.8 MHz) of 3-(3-methoxypropyl)-2-(2,6-difluorophenyl)-2,1-borazanaphthalene (**3.30**)

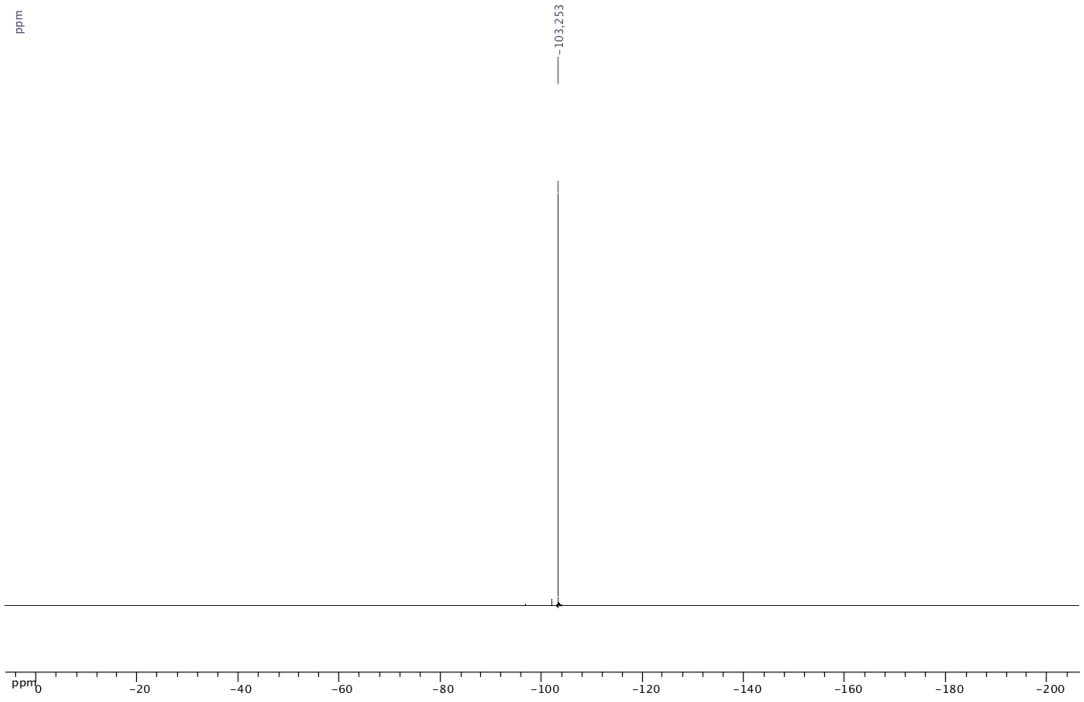

Figure A2.90: ^{11}B NMR (acetone, 128.4 MHz) of 3-(3-methoxypropyl)-2-(2,6-difluorophenyl)-2,1-borazanaphthalene (**3.30**)

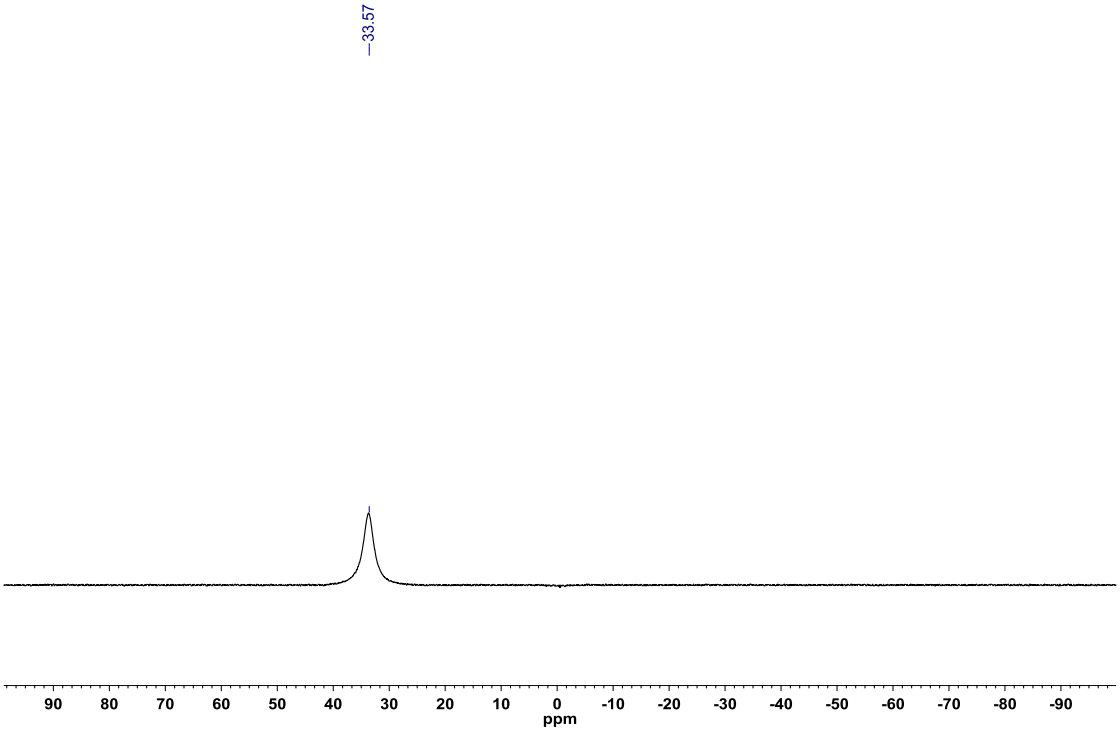

Figure A2.91: ^{1}H NMR (acetone-d_6, 500.4 MHz) of 3-(acetoxymethyl)-2-(4-chlorophenyl)-2,1-borazanaphthalene (**3.31**)

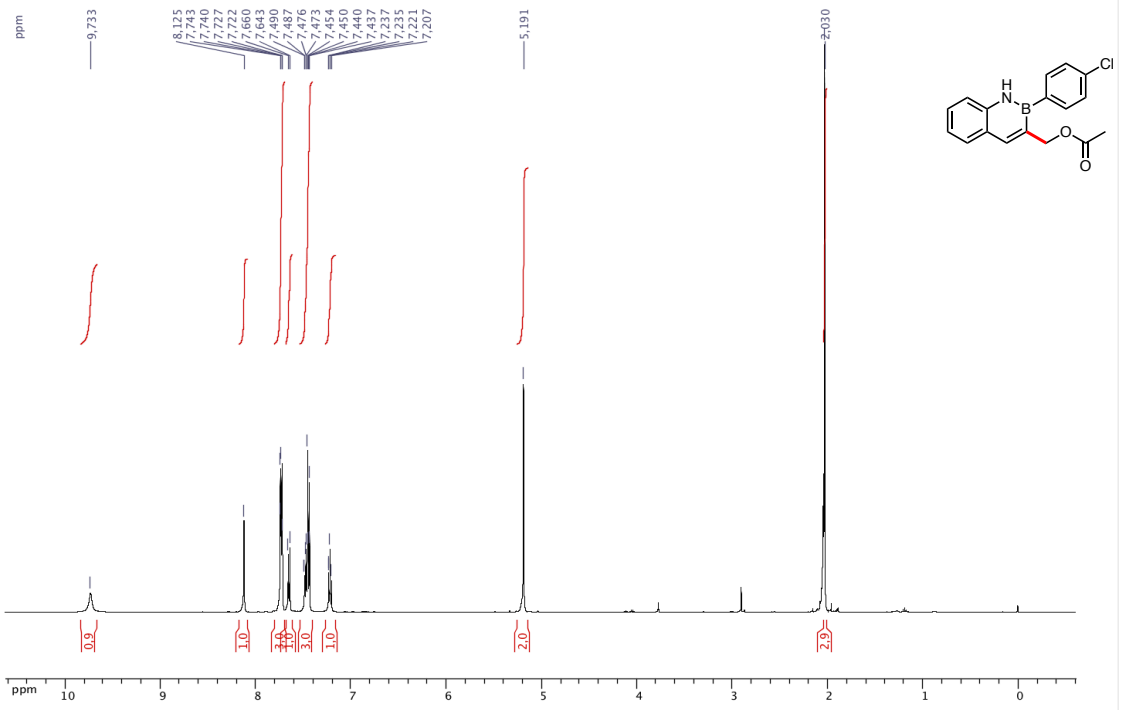

Figure A2.92: ^{13}C {^{1}H} NMR (acetone-d_6, 125.8 MHz) of 3-(acetoxymethyl)-2-(4-chlorophenyl)-2,1-borazanaphthalene (**3.31**)

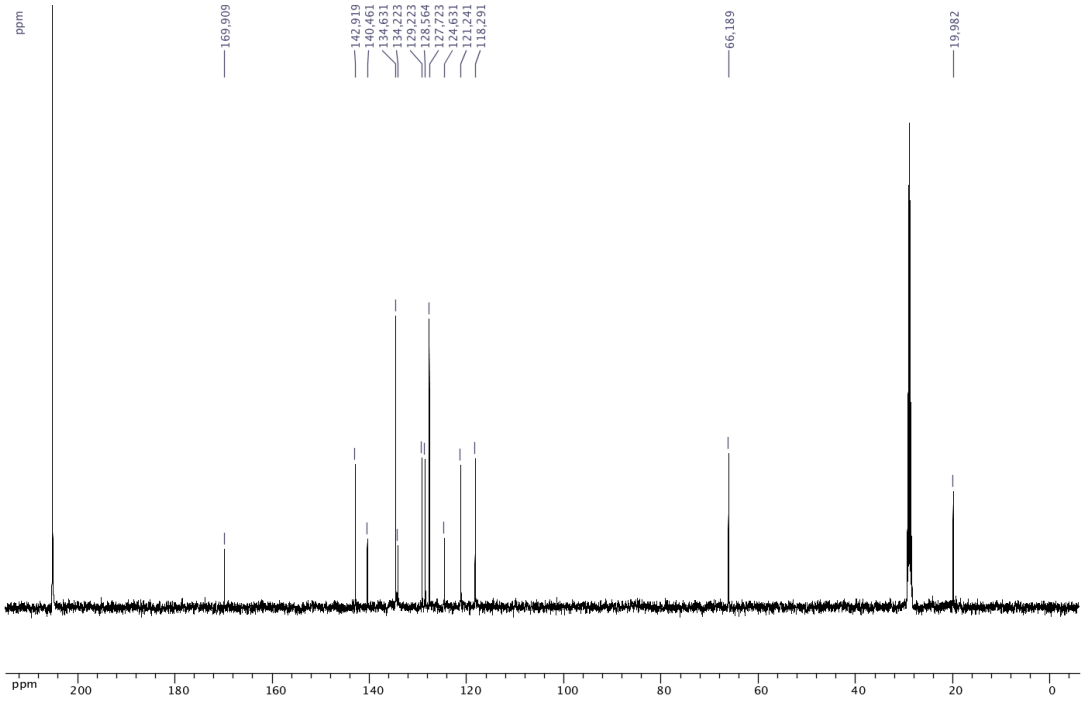

Figure A2.93: ^{11}B NMR (acetone, 128.4 MHz) of 3-(acetoxymethyl)-2-(4-chlorophenyl)-2,1-borazanaphthalene (**3.31**)

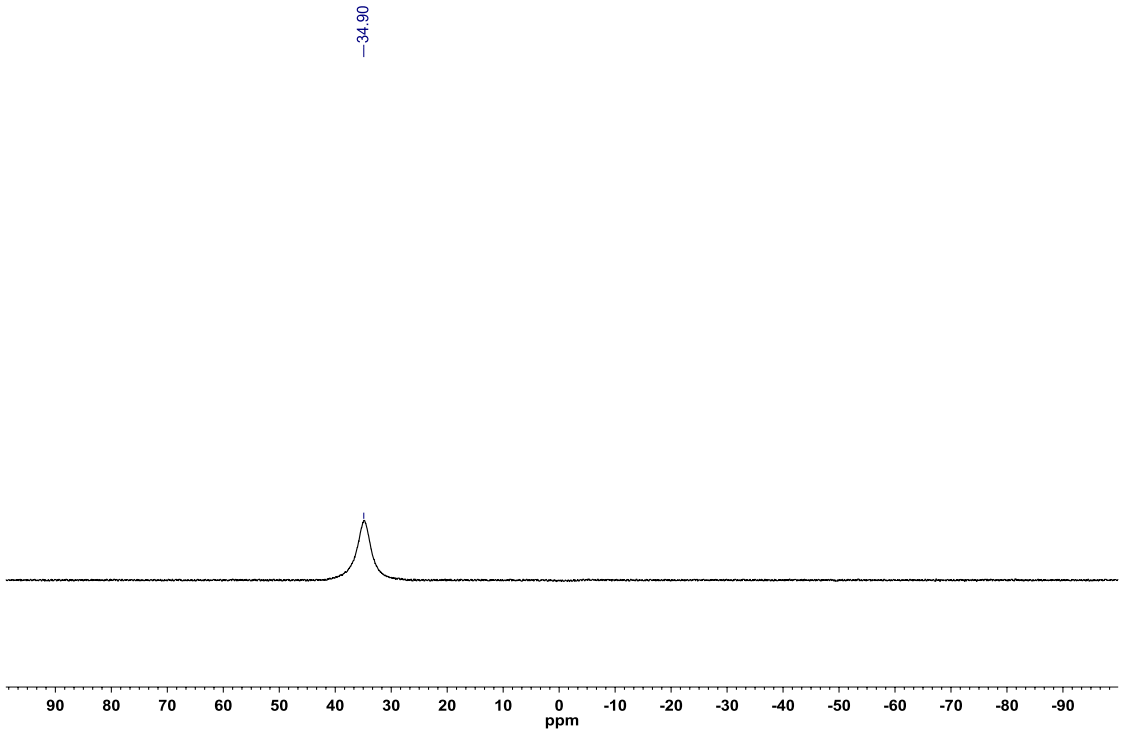

A2.2 – HTE screening data relevant to Chapter 3.3

Figure A2.94: Initial screen (96 well plate) – Lead condition hits *via* consumption of starting material

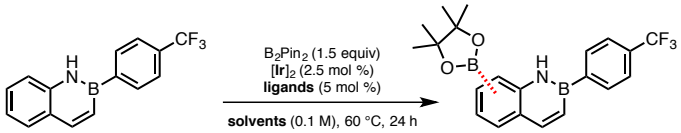

- *Iridium Sources*: $[Ir(\mu\text{-}OMe)(COD)]_2$, $[Ir(\mu\text{-}Cl)(COD)]_2$
- *Ligands*:

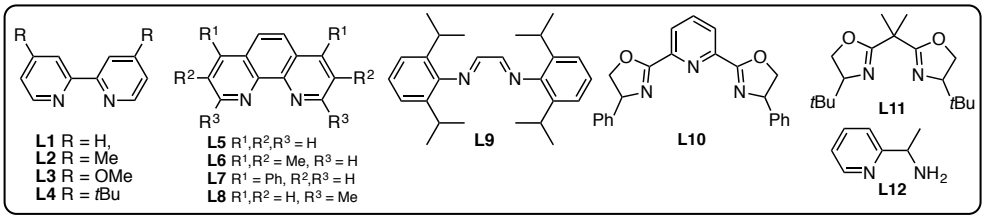

- *Solvents*: THF, dioxane, benzene, *n*-hexane

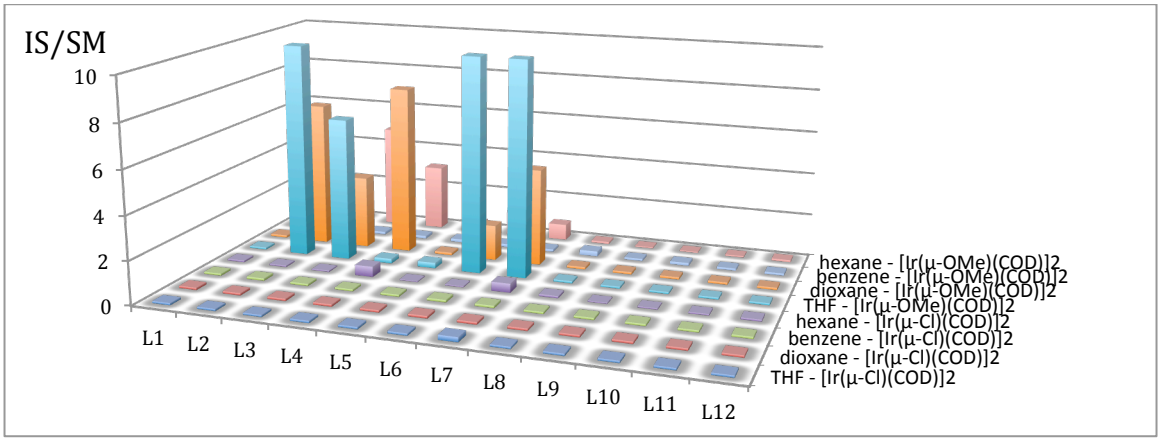

Results: Based on the ratio of internal standard (4,4′-di-*tert*-butylbiphenyl) to starting material ratio (IS/SM), full conversion was observed for $[Ir(\mu\text{-}OMe)(COD)]_2$ in THF using **L2**, **L6** or **L7** as ligands. Conversion was dependent of both the solvent and the ligand. Different product isomers were observed, all giving a mass hit for the expected BPin functionalized azaborine.

Figure A2.95: Second Screen (96 well plate) – Ligand / solvent effect on conversion and selectivity for 8-position borylation

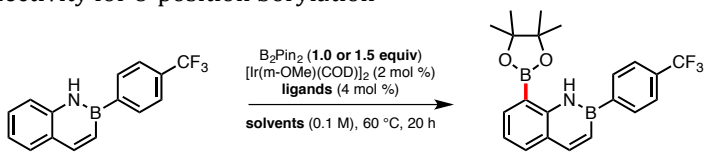

- *Ligands:* **L2**, **L3**, **L4**, **L5**, **L6**, **L7**
- *Solvents:* THF, dioxane, CPME, *n*-hexane, cyclohexane, methyl-cyclohexane, MTBE, EtOAc
- *Equiv B_2Pin_2:* 1.0, 1.5

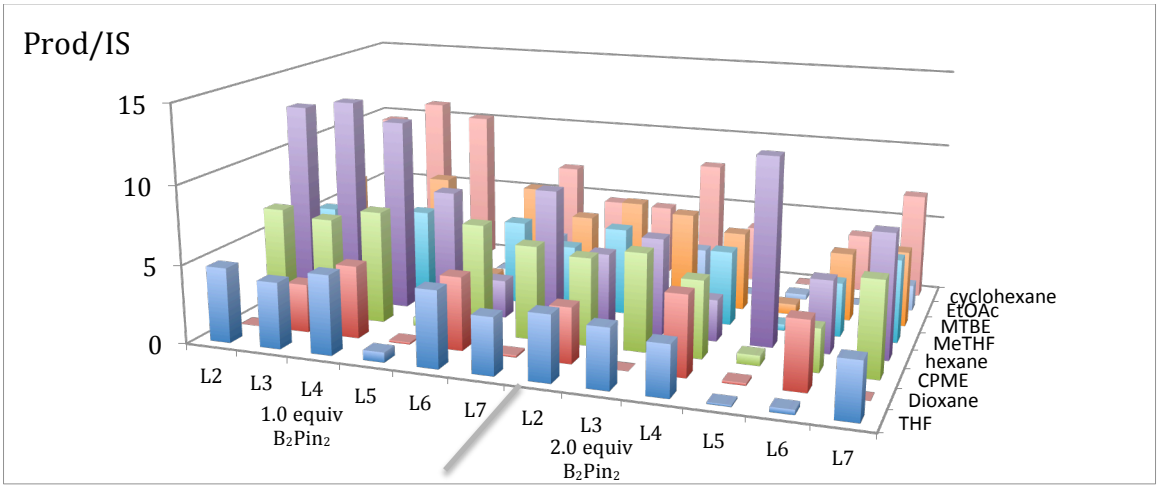

Results: - Based on the ratio of product to internal standard (Prod/IS), the best results were obtained while using **L4** in *n*-hexane *or* cyclohexane with 1.0 equiv of B_2Pin_2. **L2** and **L3** were less selective, causing non-regioselective borylation and lower conversion. 6,8-diborylated azaborine was observed as the predominant product when using the same reaction conditions, in cases of excess of B_2Pin_2. An additional set of reaction conditions, **L5** in *n*-hexane using 1.5 equiv of B_2Pin_2, also afforded reasonable product formation.

Figure A2.96: Third Screen (96 well plate) – Catalyst loading and metal to ligand ratios

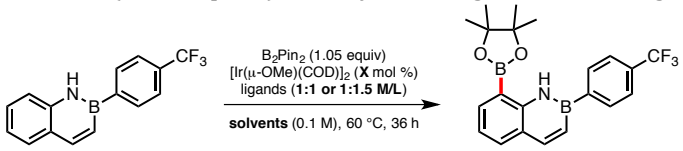

- *Ligands:* **L4, L7**
- *Solvents: n*-hexane, cyclohexane, methyl-cyclohexane, *n*-hexane/THF 5:1, *n*-hexane/THF 1:1, *n*-hexane/THF 1:5
- *Catalyst Loading:* 0.1%, 0.5%, 1%, 2%
- *Metal to Ligand Ratio:* 1:1 *or* 1:1.5

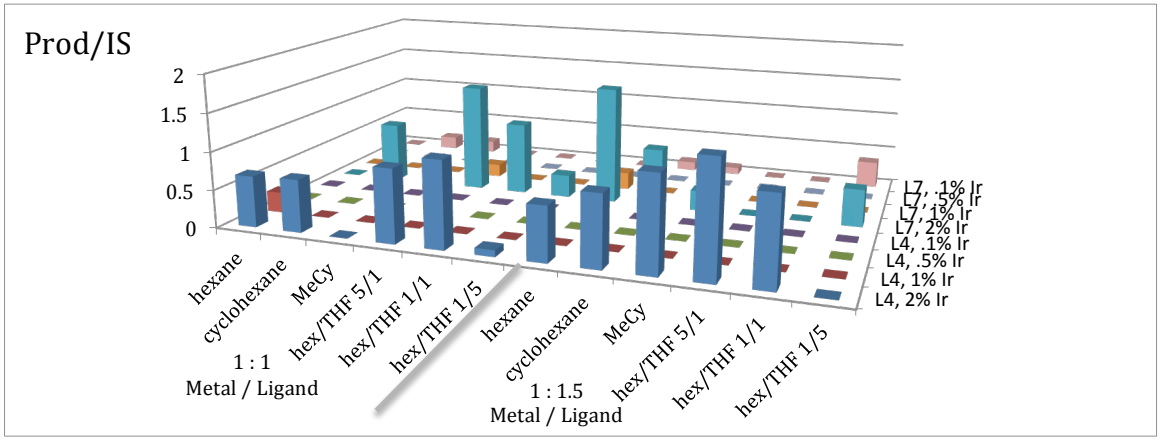

Results: Based on the ratio of product to internal standard, the best results were obtained while using **L4** at 1:1.5 iridium dimer to ligand ratio in *n*-hexane, cyclohexane or methylcyclohexane. More side products (notably *N*-borylated) and lower conversions are observed when using **L7**. Across the screen, no conditions allowed complete conversion, indicating at least 4% of Ir (2% of dimer) is required. Addition of THF is detrimental to the reaction, but a 20% mixture of THF in hexane allows a homogeneous reaction mixture.

Figure A2.97: Fourth Screen (24 well plate) – Mixed solvent systems

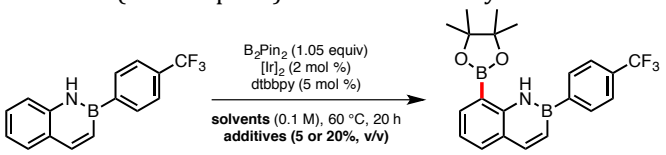

- *Solvents:* DCE, THF, DME, MeTHF, MeCN, CPME
- *Solvent mixtures:* 5% in methylcyclohexane, 5% in cyclohexane, 20% in methylcyclohexane, 20% in cyclohexane

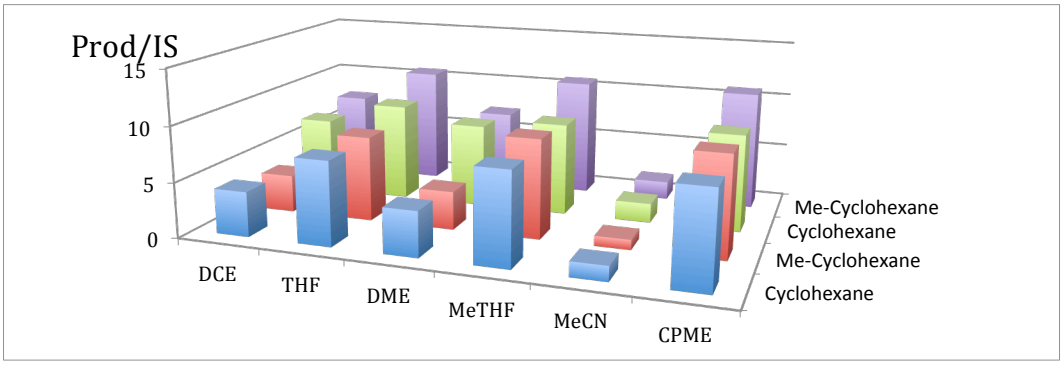

Results: Best results were obtained in methylcyclohexane using 5% of CPME, MeTHF or THF as additive. CPME is the least detrimental toward selectivity of the preferred borylated product.

Figure A2.98: Benchtop optimization

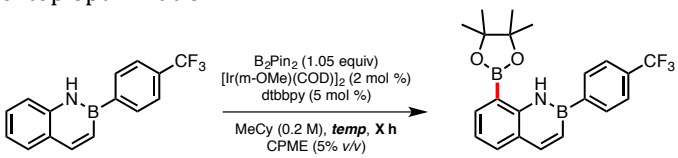

- *Temperature*: 40, 60 or 80 °C
- *Time*: 12 or 16 hours

Entry	Temperature (Time)	SM	NBPin	Product	bis-borylated	P/side P
1	40 °C (12 h)	3.08	4.96	42.63	3.87	4.83
2	60 °C (12 h)	0.69	5.76	47.13	6.81	3.75
3	80 °C (12 h)	1.12	4.61	33.94	12.44	1.99
4	40 °C (16 h)	0.82	3.78	37.88	4.22	4.73
5	60 °C (16 h)	0	5.30	40.12	7.48	3.14
6	80 °C (16 h)	0.99	5.81	41.66	17.88	1.76

Area % (HPLC, 210 nm)

Results: Lower temperature enhance selectivity, though the reaction takes longer.

A2.3 – Computationally data relevant to Chapter 3.3

Figure A2.99: Anionic stability energy values (kcal/mol) of 2-phenyl-2,1-borazaronaphthalene

2-phneyl-2,1-borazaronaphthalene			
Location	RB3LYP Energy	Free Energy	Enthalpy
C3	-388887.308	-388779.472	-388746.541
C4	-388889.394	-388781.389	-388748.576
C5	-388892.368	-388784.021	-388751.367
C6	-388889.335	-388781.148	-388748.407
C7	-388892.407	-388784.038	-388751.400
C8	-388899.266	-388790.628	-388758.053
pC	-388887.478	-388779.923	-388746.628
mC	-388885.855	-388777.883	-388745.134
oC	-388885.888	-388778.362	-388745.333

Figure A2.100: Anionic stability energy values (kcal/mol) of 2-phenylindole

2-phenylindole			
Location	RB3LYP Energy	Free Energy	Enthalpy
C3	-372882.763	-372783.637	-372753.278
C4	-372873.072	-372773.913	-372742.952
C5	-372868.753	-372770.001	-372738.770
C6	-372871.717	-372772.761	-372741.638
C7	-372880.226	-372780.959	-372749.922
pC	-372878.400	-372779.399	-372748.281
mC	-372877.299	-372778.247	-372747.203
oC	-372880.778	-372781.130	-372751.384

Figure A2.101: Atomic Coordinates for [B3LYP/6-31G(d)] optimized geometry value of total energy of 2-phenyl-2,1-borazaronaphthalene (**Figure 3.6-A**)

Center Number	Atomic Number	Atomic Type	Coordinates (Angstroms) X	Y	Z
1	6	0	0.000127	0.017870	0.005511
2	6	0	0.003296	0.019348	1.391256
3	6	0	1.219824	0.007427	2.099949
4	6	0	2.450570	-0.000906	1.389216
5	6	0	2.411215	-0.003622	-0.021130
6	6	0	1.210030	0.005403	-0.710047
7	1	0	1.200761	0.003759	-1.796025
8	1	0	3.353531	-0.011459	-0.564265
9	6	0	3.692334	-0.002387	2.121785
10	6	0	3.741596	0.004638	3.483707
11	5	0	2.434049	-0.000158	4.285607
12	7	0	1.248027	0.006406	3.482502
13	1	0	0.333665	0.039856	3.921053
14	6	0	2.313479	-0.017252	5.849692
15	6	0	3.332659	0.526190	6.655078
16	6	0	3.240587	0.535566	8.046801
17	6	0	2.121884	-0.014630	8.675870
18	6	0	1.099964	-0.571174	7.903713
19	6	0	1.199095	-0.567501	6.512704
20	1	0	0.399166	-1.026476	5.933109
21	1	0	0.230602	-1.011206	8.386134
22	1	0	2.048639	-0.014171	9.760480
23	1	0	4.040635	0.969611	8.641443
24	1	0	4.209899	0.960635	6.181091
25	1	0	4.722800	-0.008784	3.955801
26	1	0	4.604871	-0.012457	1.523964
27	1	0	-0.933930	0.027776	1.944196
28	1	0	-0.946254	0.025903	-0.528419

E_{Tot}: -620.396935451 Hartree

Figure A2.102: Atomic Coordinates for [B3LYP/6-31G(d)] optimized geometry value of total energy of 2-phenylindole (**Figure 3.6-B**)

Center Number	Atomic Number	Atomic Type	Coordinates (Angstroms) X	Y	Z
1	6	0	0.037354	0.273100	-0.015377
2	6	0	0.007361	0.155295	1.369784
3	6	0	1.178753	-0.121821	2.105392
4	6	0	2.404138	-0.279365	1.471723
5	6	0	2.470584	-0.155151	0.071956
6	6	0	1.272517	0.109958	-0.649987
7	7	0	1.603092	0.152642	-1.989329
8	6	0	2.975025	-0.028766	-2.141310
9	6	0	3.525757	-0.234318	-0.893099
10	1	0	4.563530	-0.465889	-0.695920
11	6	0	3.605651	-0.014110	-3.462698
12	6	0	4.965265	0.320956	-3.597769
13	6	0	5.575816	0.331717	-4.848710
14	6	0	4.841489	0.020616	-5.996235
15	6	0	3.490781	-0.310131	-5.877474
16	6	0	2.879794	-0.332185	-4.624872
17	1	0	1.838238	-0.633034	-4.545557
18	1	0	2.911560	-0.563641	-6.761478
19	1	0	5.317997	0.035616	-6.972493
20	1	0	6.626954	0.595668	-4.930101
21	1	0	5.534455	0.593058	-2.713742
22	1	0	0.997558	0.495841	-2.719266
23	1	0	3.301617	-0.490617	2.047528
24	1	0	1.117066	-0.211787	3.186543
25	1	0	-0.936465	0.275942	1.894423
26	1	0	-0.866769	0.481481	-0.581787

E_{Tot}: -594.878889823 Hartree

Figure A2.103: Atomic Coordinates for [B3LYP/6-31G(d)] optimized geometry value of total energy of 2-phenylnaphthalene (**Figure 3.6-C**)

Center Number	Atomic Number	Atomic Type	Coordinates (Angstroms) X	Y	Z
1	6	0	-0.003403	0.001932	0.000733
2	6	0	-0.001022	0.042356	1.417140
3	6	0	1.188155	0.051431	2.110444
4	6	0	2.432492	0.022223	1.423278
5	6	0	2.428341	-0.023185	-0.008543
6	6	0	1.184973	-0.030355	-0.694253
7	1	0	1.187081	-0.062710	-1.781430
8	6	0	3.676693	-0.058893	-0.685448
9	6	0	4.861927	-0.051428	0.009784
10	6	0	4.883517	-0.005009	1.435203
11	6	0	3.674024	0.029658	2.109249
12	1	0	3.662403	0.035880	3.196452
13	6	0	6.174904	0.002781	2.168462
14	6	0	6.344128	0.779532	3.327467
15	6	0	7.553337	0.779778	4.020824
16	6	0	8.623605	0.005331	3.569018
17	6	0	8.472391	-0.768744	2.417212
18	6	0	7.262416	-0.769046	1.724668
19	1	0	7.149160	-1.395534	0.844187
20	1	0	9.296372	-1.380923	2.059812
21	1	0	9.567035	0.006835	4.108230
22	1	0	7.662739	1.394697	4.910419
23	1	0	5.526972	1.407722	3.670954
24	1	0	5.803728	-0.052821	-0.531338
25	1	0	3.682502	-0.083060	-1.772820
26	1	0	1.191905	0.082766	3.197583
27	1	0	-0.944987	0.066390	1.955002
28	1	0	-0.948802	-0.004816	-0.534996

E_{Tot}: -616.95016201 Hartree

Figure A2.104: Atomic Coordinates for [B3LYP/6-31G(d)] optimized geometry value of total energy of 2-phenylquinoline (**Figure 3.6-D**)

Center Number	Atomic Number	Atomic Type	Coordinates (Angstroms) X	Y	Z
1	6	0	0.099110	0.064938	0.102351
2	6	0	0.191405	0.248840	1.504794
3	6	0	1.417469	0.263919	2.131188
4	6	0	2.611850	0.095220	1.380007
5	6	0	2.516017	-0.089836	-0.035713
6	6	0	1.239225	-0.100731	-0.652690
7	1	0	1.175718	-0.241200	-1.729448
8	6	0	3.734733	-0.243044	-0.743754
9	6	0	4.926008	-0.219940	-0.064240
10	6	0	4.926260	-0.046916	1.354018
11	7	0	3.802261	0.112113	2.039130
12	6	0	6.197694	-0.017797	2.127644
13	6	0	6.215840	0.555663	3.410586
14	6	0	7.391899	0.601547	4.153677
15	6	0	8.575132	0.069090	3.634909
16	6	0	8.568505	-0.513545	2.367118
17	6	0	7.391639	-0.555721	1.620137
18	1	0	7.405306	-1.036352	0.646597
19	1	0	9.479668	-0.942565	1.958579
20	1	0	9.493043	0.104663	4.215651
21	1	0	7.386712	1.055789	5.141144
22	1	0	5.291270	0.960737	3.806654
23	1	0	5.862070	-0.306741	-0.604227
24	1	0	3.714027	-0.367432	-1.824269
25	1	0	1.511532	0.401743	3.203853
26	1	0	-0.717070	0.378203	2.086963
27	1	0	-0.876919	0.055145	-0.374908

E_{Tot}: -632.991297333 Hartree

Figure A2.105: Atomic Coordinates for [B3LYP/6-31G(d)] optimized geometry value of total energy of 2-phenylindol-3-ide (**i-C3**)

Center Number	Atomic Number	Atomic Type	Coordinates (Angstroms) X	Y	Z
1	6	0	0.202752	-0.839045	0.330886
2	6	0	0.123020	-0.234238	1.587828
3	6	0	1.047210	0.756157	1.973926
4	6	0	2.070664	1.148855	1.110312
5	6	0	2.204514	0.560371	-0.160493
6	6	0	1.232518	-0.434825	-0.524759
7	7	0	1.531832	-0.826044	-1.808868
8	6	0	2.744793	-0.135503	-2.176886
9	6	0	3.191114	0.765866	-1.217337
10	6	0	3.327991	-0.401052	-3.483252
11	6	0	2.727730	-1.215365	-4.470987
12	6	0	3.347917	-1.447174	-5.700522
13	6	0	4.584450	-0.872271	-5.995626
14	6	0	5.189070	-0.049626	-5.031442
15	6	0	4.578466	0.180310	-3.807134
16	1	0	5.021795	0.814073	-3.043666
17	1	0	6.152100	0.413688	-5.244887
18	1	0	5.067227	-1.054301	-6.953922
19	1	0	2.852456	-2.079152	-6.437372
20	1	0	1.748066	-1.651752	-4.288058
21	1	0	1.265644	-1.737138	-2.161046
22	1	0	2.789160	1.910811	1.411053
23	1	0	0.957388	1.214545	2.958472
24	1	0	-0.668579	-0.531512	2.275108
25	1	0	-0.521563	-1.598982	0.035299

E_{Tot}: -594.226851264 Hartree

Figure A2.106: Atomic Coordinates for [B3LYP/6-31G(d)] optimized geometry value of total energy of 2-phenylindol-4-ide (**i-C4**)

Center Number	Atomic Number	Atomic Type	Coordinates (Angstroms) X	Y	Z
1	6	0	0.019992	0.160712	-0.025769
2	6	0	0.001774	0.095230	1.370918
3	6	0	1.181961	-0.104296	2.125440
4	6	0	2.491678	-0.258073	1.608100
5	6	0	2.456614	-0.164381	0.178171
6	6	0	1.278131	0.020959	-0.615536
7	7	0	1.635012	0.018187	-1.962322
8	6	0	3.039929	-0.054310	-2.052961
9	6	0	3.535783	-0.203245	-0.770231
10	1	0	4.573947	-0.372657	-0.507084
11	6	0	3.715317	-0.035318	-3.334406
12	6	0	5.110169	0.188784	-3.425128
13	6	0	5.762586	0.213380	-4.651644
14	6	0	5.054096	0.029510	-5.846093
15	6	0	3.676420	-0.190458	-5.779120
16	6	0	3.019223	-0.227768	-4.551201
17	1	0	1.954319	-0.443194	-4.522590
18	1	0	3.106072	-0.346857	-6.693485
19	1	0	5.566402	0.056899	-6.804950
20	1	0	6.836639	0.389392	-4.680003
21	1	0	5.670723	0.359577	-2.510394
22	1	0	1.091447	0.507665	-2.661401
23	1	0	1.033137	-0.139001	3.215010
24	1	0	-0.960446	0.197108	1.883106
25	1	0	-0.885782	0.308203	-0.614124

E_{Tot}: -594.211068629 Hartree

Figure A2.107: Atomic Coordinates for [B3LYP/6-31G(d)] optimized geometry value of total energy of 2-phenylindol-5-ide (**i-C5**)

Center Number	Atomic Number	Atomic Type	Coordinates (Angstroms) X	Y	Z
1	6	0	0.008838	-0.032831	-0.012403
2	6	0	0.012897	0.046890	1.387898
3	6	0	1.156375	0.017357	2.260636
4	6	0	2.360909	-0.112008	1.543500
5	6	0	2.448686	-0.188705	0.127449
6	6	0	1.250826	-0.160476	-0.637820
7	7	0	1.589105	-0.295142	-1.986584
8	6	0	2.987582	-0.296532	-2.101327
9	6	0	3.519981	-0.269919	-0.821898
10	1	0	4.574194	-0.363190	-0.585319
11	6	0	3.642176	-0.383974	-3.392171
12	6	0	5.011064	-0.059427	-3.542532
13	6	0	5.643512	-0.140646	-4.777592
14	6	0	4.937104	-0.534924	-5.920415
15	6	0	3.583330	-0.856220	-5.793911
16	6	0	2.948095	-0.788449	-4.556194
17	1	0	1.905634	-1.084377	-4.473682
18	1	0	3.016523	-1.175007	-6.667063
19	1	0	5.432505	-0.589857	-6.886807
20	1	0	6.698102	0.118247	-4.854297
21	1	0	5.566516	0.276824	-2.671547
22	1	0	1.000670	0.073492	-2.720672
23	1	0	3.319940	-0.144403	2.084034
24	1	0	-0.985414	0.137907	1.842946
25	1	0	-0.915047	-0.003235	-0.598127

E_{Tot}: -594.204186183 Hartree

Figure A2.108: Atomic Coordinates for [B3LYP/6-31G(d)] optimized geometry value of total energy of 2-phenylindol-6-ide (**i-C6**)

Center Number	Atomic Number	Atomic Type	Coordinates (Angstroms) X	Y	Z
1	6	0	0.027437	0.217392	-0.020326
2	6	0	-0.003838	0.164276	1.389653
3	6	0	1.310489	-0.034482	1.960713
4	6	0	2.510330	-0.163139	1.270886
5	6	0	2.482424	-0.094793	-0.141388
6	6	0	1.211758	0.079725	-0.761825
7	7	0	1.429858	0.066760	-2.140437
8	6	0	2.803259	-0.015234	-2.403033
9	6	0	3.454736	-0.144007	-1.182494
10	1	0	4.518044	-0.317361	-1.060783
11	6	0	3.331577	-0.021691	-3.750961
12	6	0	4.707860	0.197447	-4.002022
13	6	0	5.219555	0.194533	-5.293816
14	6	0	4.382396	-0.013006	-6.397377
15	6	0	3.020341	-0.227621	-6.172072
16	6	0	2.504045	-0.237433	-4.878694
17	1	0	1.448588	-0.449054	-4.729226
18	1	0	2.351227	-0.401147	-7.013218
19	1	0	4.784174	-0.006618	-7.407715
20	1	0	6.283596	0.368144	-5.445427
21	1	0	5.368438	0.389632	-3.161134
22	1	0	0.773682	0.473086	-2.790729
23	1	0	3.462325	-0.307994	1.790745
24	1	0	1.389327	-0.093000	3.056176
25	1	0	-0.902621	0.365400	-0.592460

E_{Tot}: -594.208908414 Hartree

Figure A2.109: Atomic Coordinates for [B3LYP/6-31G(d)] optimized geometry value of total energy of 2-phenylindol-7-ide (**i-C7**)

Center Number	Atomic Number	Atomic Type	Coordinates (Angstroms) X	Y	Z
1	6	0	0.011617	-0.149429	0.031783
2	6	0	0.031446	-0.245080	1.436609
3	6	0	1.369152	-0.094673	1.870507
4	6	0	2.565039	0.091156	1.101248
5	6	0	2.425004	0.180105	-0.304154
6	6	0	1.142050	0.058579	-0.815456
7	1	0	0.997232	0.118349	-1.898415
8	1	0	3.290003	0.330423	-0.950695
9	6	0	3.662090	0.136571	2.008796
10	6	0	3.158414	-0.006604	3.301777
11	7	0	1.782731	-0.114563	3.202591
12	1	0	1.140817	-0.387836	3.932563
13	6	0	3.859771	-0.001544	4.573594
14	6	0	5.259116	-0.197178	4.637322
15	6	0	5.939327	-0.189425	5.849839
16	6	0	5.252892	0.001316	7.054756
17	6	0	3.869476	0.192012	7.014231
18	6	0	3.185956	0.195575	5.800560
19	1	0	2.115264	0.380953	5.794520
20	1	0	3.315149	0.349663	7.937859
21	1	0	5.785475	-0.000362	8.002899
22	1	0	7.016834	-0.345319	5.857841
23	1	0	5.804194	-0.374330	3.714484
24	1	0	4.705096	0.311600	1.764556
25	1	0	-0.949259	-0.239884	-0.496736

E_{Tot}: -594.222468779 Hartree

Figure A2.110: Atomic Coordinates for [B3LYP/6-31G(d)] optimized geometry value of total energy of 2-(phenyl-2-ide)-indole (**i-*oC***)

Center Number	Atomic Number	Atomic Type	Coordinates (Angstroms) X	Y	Z
1	6	0	-0.025473	0.101559	0.051970
2	6	0	-0.049053	-0.082948	1.436755
3	6	0	1.149733	-0.161741	2.170377
4	6	0	2.389029	-0.061051	1.541177
5	6	0	2.451903	0.121922	0.146783
6	6	0	1.216197	0.202648	-0.575167
7	7	0	1.543906	0.389186	-1.898988
8	6	0	2.932548	0.417146	-2.063581
9	6	0	3.500841	0.258081	-0.810728
10	1	0	4.570545	0.247589	-0.663474
11	6	0	3.594315	0.590291	-3.365599
12	6	0	5.023901	0.513301	-3.371770
13	6	0	5.558478	0.678094	-4.674750
14	6	0	4.808771	0.886554	-5.840228
15	6	0	3.412664	0.963401	-5.762665
16	6	0	2.805840	0.818738	-4.516824
17	1	0	1.713860	0.902168	-4.467105
18	1	0	2.809687	1.137875	-6.653836
19	1	0	5.299147	0.996072	-6.812746
20	1	0	6.649999	0.641998	-4.805445
21	1	0	0.885294	0.427210	-2.659598
22	1	0	3.306422	-0.125074	2.123439
23	1	0	1.105453	-0.304410	3.248837
24	1	0	-1.004294	-0.165245	1.951205
25	1	0	-0.950333	0.165021	-0.519424

E_{Tot}: -594.223351816 Hartree

Figure A2.111: Atomic Coordinates for [B3LYP/6-31G(d)] optimized geometry value of total energy of 2-(phenyl-3-ide)-indole (**i-*m*C**)

Center Number	Atomic Number	Atomic Type	Coordinates (Angstroms) X	Y	Z
1	6	0	0.010235	-0.021191	-0.018130
2	6	0	-0.003988	-0.002715	1.378085
3	6	0	1.198325	0.017916	2.109169
4	6	0	2.433939	0.027046	1.465124
5	6	0	2.484945	0.019305	0.059380
6	6	0	1.248726	-0.014188	-0.660483
7	7	0	1.569575	-0.043782	-1.999326
8	6	0	2.954141	0.003354	-2.175548
9	6	0	3.531159	0.029977	-0.915278
10	1	0	4.595428	0.024954	-0.726635
11	6	0	3.541024	0.036241	-3.512201
12	6	0	4.789559	0.664581	-3.750120
13	6	0	5.464467	0.734499	-4.993775
14	6	0	4.700938	0.129240	-6.028490
15	6	0	3.431856	-0.453255	-5.871063
16	6	0	2.848902	-0.521638	-4.607126
17	1	0	1.905362	-1.049720	-4.460741
18	1	0	2.904383	-0.889932	-6.725020
19	1	0	5.118200	0.087982	-7.046456
20	1	0	5.233938	1.156949	-2.873728
21	1	0	0.922935	0.065733	-2.764877
22	1	0	3.354864	0.045188	2.044712
23	1	0	1.160242	0.027609	3.196828
24	1	0	-0.955878	-0.006409	1.904563
25	1	0	-0.917284	-0.041885	-0.587270

E_{Tot}: -594.217803952 Hartree

Figure A2.112: Atomic Coordinates for [B3LYP/6-31G(d)] optimized geometry value of total energy of 2-(phenyl-4-ide) -indole (**i-*p*C**)

Center Number	Atomic Number	Atomic Type	Coordinates (Angstroms) X	Y	Z
1	6	0	0.007950	0.133510	-0.034976
2	6	0	-0.019646	0.100854	1.361175
3	6	0	1.171400	-0.018406	2.100682
4	6	0	2.409537	-0.100948	1.466396
5	6	0	2.474317	-0.061725	0.061709
6	6	0	1.248255	0.049577	-0.667088
7	7	0	1.579062	0.046491	-2.003806
8	6	0	2.961233	-0.036584	-2.171263
9	6	0	3.525440	-0.114219	-0.904628
10	1	0	4.581425	-0.230872	-0.704180
11	6	0	3.559236	-0.030994	-3.498378
12	6	0	4.923774	0.274443	-3.684741
13	6	0	5.476517	0.287273	-4.966270
14	6	0	4.781753	0.014066	-6.182765
15	6	0	3.413670	-0.289411	-5.919240
16	6	0	2.810463	-0.318619	-4.659738
17	1	0	1.756446	-0.604732	-4.566501
18	1	0	2.751138	-0.534527	-6.763078
19	1	0	6.545573	0.543245	-5.013829
20	1	0	5.530862	0.525827	-2.810907
21	1	0	0.946386	0.218540	-2.769321
22	1	0	3.321685	-0.191364	2.053162
23	1	0	1.123047	-0.045835	3.187623
24	1	0	-0.973298	0.166677	1.880130
25	1	0	-0.911122	0.220663	-0.611357

E_{Tot}: -594.219559058 Hartree

Figure A2.113: Atomic Coordinates for [B3LYP/6-31G(d)] optimized geometry value of total energy of 2-phenyl-2,1-borazaronaphthalen-3-ide (**b-C3**)

Center Number	Atomic Number	Atomic Type	Coordinates (Angstroms) X	Y	Z
1	6	0	-0.005709	0.041983	0.002595
2	6	0	-0.000458	-0.031718	1.392417
3	6	0	1.207619	-0.048853	2.112040
4	6	0	2.456152	0.024067	1.421401
5	6	0	2.407818	0.100135	0.013455
6	6	0	1.210668	0.108440	-0.694360
7	1	0	1.214726	0.171951	-1.781859
8	1	0	3.356481	0.162993	-0.520487
9	6	0	3.694728	0.089889	2.188443
10	6	0	3.820781	-0.030337	3.551129
11	5	0	2.469279	-0.246684	4.241413
12	7	0	1.234490	-0.136125	3.491847
13	1	0	0.311825	-0.150610	3.922411
14	6	0	2.334947	-0.583992	5.793023
15	6	0	3.488015	-0.449498	6.593320
16	6	0	3.471594	-0.723587	7.960818
17	6	0	2.289290	-1.142552	8.580392
18	6	0	1.131923	-1.294213	7.812125
19	6	0	1.163645	-1.021106	6.442435
20	1	0	0.250227	-1.171232	5.865186
21	1	0	0.207998	-1.631628	8.281150
22	1	0	2.269976	-1.352781	9.648942
23	1	0	4.380687	-0.611677	8.551402
24	1	0	4.393644	-0.132713	6.076924
25	1	0	4.566685	0.301608	1.533580
26	1	0	-0.940902	-0.083991	1.943327
27	1	0	-0.951651	0.049123	-0.536382

E_{Tot}: -619.731378822 Hartree

Figure A2.114: Atomic Coordinates for [B3LYP/6-31G(d)] optimized geometry value of total energy of 2-phenyl-2,1-borazaronaphthalen-4-ide (**b-C4**)

Center Number	Atomic Number	Atomic Type	Coordinates (Angstroms) X	Y	Z
1	6	0	0.003105	0.022752	0.003194
2	6	0	0.006904	0.022950	1.392078
3	6	0	1.222141	0.004941	2.106264
4	6	0	2.484384	-0.013296	1.424688
5	6	0	2.415618	-0.008853	0.011053
6	6	0	1.220321	0.007230	-0.698434
7	1	0	1.221695	0.008903	-1.787728
8	1	0	3.377017	-0.020312	-0.499499
9	6	0	3.810095	-0.033428	2.069119
10	6	0	3.732549	-0.048714	3.466811
11	5	0	2.443880	-0.002643	4.260577
12	7	0	1.226531	0.015349	3.488065
13	1	0	0.312326	0.088944	3.921115
14	6	0	2.301757	0.005808	5.839342
15	6	0	3.267915	0.638221	6.649320
16	6	0	3.175264	0.650551	8.041503
17	6	0	2.104612	0.018797	8.681338
18	6	0	1.134750	-0.625018	7.908693
19	6	0	1.238410	-0.626822	6.516379
20	1	0	0.479111	-1.149885	5.935319
21	1	0	0.299135	-1.128478	8.393531
22	1	0	2.029463	0.024727	9.767317
23	1	0	3.939121	1.154200	8.632479
24	1	0	4.106889	1.131150	6.163290
25	1	0	4.688775	-0.101649	4.015291
26	1	0	-0.936531	0.033621	1.943427
27	1	0	-0.944375	0.034552	-0.534711

E_{Tot}: -619.734701766 Hartree

Figure A2.115: Atomic Coordinates for [B3LYP/6-31G(d)] optimized geometry value of total energy of 2-phenyl-2,1-borazaronaphthalen-5-ide (**b-C5**)

Center Number	Atomic Number	Atomic Type	Coordinates (Angstroms) X	Y	Z
1	6	0	0.002955	0.021445	0.007953
2	6	0	0.001230	0.024207	1.400689
3	6	0	1.236379	0.008181	2.067083
4	6	0	2.450841	-0.003650	1.306280
5	6	0	2.501912	-0.009019	-0.134884
6	6	0	1.213003	0.004351	-0.712172
7	1	0	1.115913	0.002773	-1.807266
8	6	0	3.683626	-0.004430	2.047145
9	6	0	3.779210	0.007956	3.420382
10	5	0	2.496243	0.008782	4.230981
11	7	0	1.292527	0.007971	3.460367
12	1	0	0.383388	0.050200	3.912413
13	6	0	2.394083	0.000912	5.811285
14	6	0	3.407247	0.573542	6.606023
15	6	0	3.339149	0.585230	7.999749
16	6	0	2.244928	0.012569	8.653432
17	6	0	1.227170	-0.570637	7.895151
18	6	0	1.307604	-0.573174	6.501588
19	1	0	0.511449	-1.051442	5.932498
20	1	0	0.373217	-1.028926	8.391402
21	1	0	2.187945	0.017363	9.740216
22	1	0	4.139615	1.042408	8.579189
23	1	0	4.263779	1.026757	6.111554
24	1	0	4.775616	-0.010406	3.867199
25	1	0	4.569660	-0.017249	1.408797
26	1	0	-0.928666	0.035329	1.972513
27	1	0	-0.957226	0.032147	-0.518336

E_{Tot}: -619.739441355 Hartree

Figure A2.116: Atomic Coordinates for [B3LYP/6-31G(d)] optimized geometry value of total energy of 2-phenyl-2,1-borazaronaphthalen-6-ide (**b-C6**)

Center Number	Atomic Number	Atomic Type	Coordinates (Angstroms) X	Y	Z
1	6	0	0.012431	0.025119	0.000648
2	6	0	0.005189	0.023239	1.397228
3	6	0	1.222325	0.008958	2.095333
4	6	0	2.434327	0.003735	1.349179
5	6	0	2.344683	0.008187	-0.073858
6	6	0	1.170740	0.019845	-0.846007
7	1	0	3.324857	0.005341	-0.578460
8	6	0	3.676734	0.001865	2.063069
9	6	0	3.771595	0.007437	3.434066
10	5	0	2.488562	0.002032	4.254399
11	7	0	1.285789	0.002775	3.486637
12	1	0	0.375940	0.038084	3.935542
13	6	0	2.399613	-0.012981	5.832937
14	6	0	3.427878	0.538564	6.623719
15	6	0	3.370414	0.542768	8.017811
16	6	0	2.271649	-0.015310	8.676343
17	6	0	1.238631	-0.576808	7.922122
18	6	0	1.308822	-0.573409	6.528330
19	1	0	0.500816	-1.036595	5.963572
20	1	0	0.380731	-1.023518	8.421839
21	1	0	2.222688	-0.015995	9.763414
22	1	0	4.182588	0.983363	8.593657
23	1	0	4.288082	0.982256	6.126863
24	1	0	4.769649	-0.010014	3.876744
25	1	0	4.578627	-0.006580	1.443647
26	1	0	-0.930127	0.029064	1.968855
27	1	0	-0.983703	0.031047	-0.467856

E_{Tot}: -619.734608411 Hartree

Figure A2.117: Atomic Coordinates for [B3LYP/6-31G(d)] optimized geometry value of total energy of 2-phenyl-2,1-borazaronaphthalen-7-ide (**b-C7**)

Center Number	Atomic Number	Atomic Type	Coordinates (Angstroms) X	Y	Z
1	6	0	0.008429	-0.028719	-0.001673
2	6	0	-0.003432	-0.029515	1.404975
3	6	0	1.336498	-0.008235	1.939129
4	6	0	2.502475	0.017200	1.193078
5	6	0	2.455199	0.018751	-0.225463
6	6	0	1.158509	-0.003202	-0.817259
7	7	0	1.082087	0.002093	-2.207864
8	5	0	2.194210	0.021011	-3.103682
9	6	0	3.559688	0.031771	-2.433878
10	6	0	3.613258	0.035920	-1.058271
11	1	0	4.577443	0.056295	-0.540887
12	1	0	4.503375	0.064012	-2.980867
13	6	0	1.933803	0.039586	-4.664202
14	6	0	2.871808	-0.503996	-5.564631
15	6	0	2.662385	-0.503283	-6.944182
16	6	0	1.495702	0.052226	-7.475821
17	6	0	0.548671	0.605296	-6.610795
18	6	0	0.770470	0.596411	-5.232860
19	1	0	0.026415	1.050945	-4.580407
20	1	0	-0.361121	1.048864	-7.011707
21	1	0	1.327990	0.056768	-8.551035
22	1	0	3.408522	-0.937713	-7.607519
23	1	0	3.783111	-0.945338	-5.166373
24	1	0	0.126636	-0.044506	-2.550026
25	1	0	3.487504	0.034282	1.671287
26	1	0	1.465419	-0.011888	3.031023
27	1	0	-0.946051	-0.043279	-0.558683

E_{Tot}: -619.739504482 Hartree

Figure A2.118: Atomic Coordinates for [B3LYP/6-31G(d)] optimized geometry value of total energy of 2-phenyl-2,1-borazaronaphthalen-8-ide (**b-C8**)

Center Number	Atomic Number	Atomic Type	Coordinates (Angstroms) X	Y	Z
1	6	0	0.005672	0.039502	0.018051
2	6	0	0.006471	0.044151	1.420022
3	6	0	1.338038	0.017429	1.933998
4	6	0	2.547376	-0.004354	1.173226
5	6	0	2.423607	-0.006989	-0.239662
6	6	0	1.163571	0.014285	-0.806885
7	1	0	1.064355	0.012890	-1.896047
8	1	0	3.325489	-0.024305	-0.852961
9	6	0	3.818327	-0.020827	1.835883
10	6	0	3.952316	-0.015180	3.201829
11	5	0	2.688361	-0.001265	4.060537
12	7	0	1.475313	0.014786	3.323496
13	1	0	0.540717	0.051584	3.730257
14	6	0	2.659981	-0.013392	5.643711
15	6	0	3.755405	0.452425	6.398070
16	6	0	3.751366	0.451120	7.793770
17	6	0	2.638934	-0.026961	8.490550
18	6	0	1.537968	-0.500698	7.772411
19	6	0	1.555124	-0.491709	6.377158
20	1	0	0.691102	-0.878234	5.839457
21	1	0	0.666061	-0.881318	8.302003
22	1	0	2.630452	-0.032213	9.578931
23	1	0	4.616084	0.824553	8.340396
24	1	0	4.628808	0.833368	5.872410
25	1	0	4.964415	-0.044278	3.611214
26	1	0	4.704116	-0.042009	1.191116
27	1	0	-0.954976	0.056631	-0.516888

E_{Tot}: -619.750434707 Hartree

Figure A2.119: Atomic Coordinates for [B3LYP/6-31G(d)] optimized geometry value of total energy of 2-(phenyl-2-ide)-2,1-borazaronaphthalene (**b-*o*C**)

Center Number	Atomic Number	Atomic Type	Coordinates (Angstroms) X	Y	Z
1	6	0	-0.006087	0.022310	0.021139
2	6	0	0.005872	0.021080	1.411651
3	6	0	1.219174	0.005918	2.127801
4	6	0	2.453056	0.000043	1.409158
5	6	0	2.403311	0.002038	0.002532
6	6	0	1.199381	0.011864	-0.694020
7	1	0	1.193743	0.012218	-1.781660
8	1	0	3.346363	-0.003295	-0.542453
9	6	0	3.702377	-0.012519	2.142293
10	6	0	3.745536	-0.006749	3.501953
11	5	0	2.443727	0.000024	4.332340
12	7	0	1.248160	-0.003376	3.504768
13	1	0	0.336953	0.021361	3.950144
14	6	0	2.387738	0.041832	5.877793
15	6	0	3.545293	0.622898	6.496900
16	6	0	3.413271	0.766496	7.904473
17	6	0	2.318131	0.312726	8.648323
18	6	0	1.216883	-0.267074	7.998534
19	6	0	1.250473	-0.377669	6.610923
20	1	0	0.379535	-0.810277	6.101572
21	1	0	0.355748	-0.617713	8.569145
22	1	0	2.309082	0.399861	9.740261
23	1	0	4.226760	1.237059	8.476249
24	1	0	4.697408	0.009647	4.028173
25	1	0	4.611659	-0.027580	1.534732
26	1	0	-0.930627	0.028709	1.968035
27	1	0	-0.956879	0.030534	-0.508139

E_{Tot}: -619.729115317 Hartree

Figure A2.120: Atomic Coordinates for [B3LYP/6-31G(d)] optimized geometry value of total energy of 2-(phenyl-3-ide)-2,1-borazaronaphthalene (**b-*m*C**)

Center Number	Atomic Number	Atomic Type	Coordinates (Angstroms) X	Y	Z
1	6	0	0.005258	-0.014799	0.002550
2	6	0	0.004145	-0.013206	1.390896
3	6	0	1.215149	-0.003978	2.115015
4	6	0	2.450325	0.005149	1.401544
5	6	0	2.414303	0.002431	-0.005619
6	6	0	1.215510	-0.007245	-0.707925
7	1	0	1.214564	-0.008938	-1.795150
8	1	0	3.361131	0.007925	-0.543684
9	6	0	3.691326	0.018121	2.144108
10	6	0	3.730314	0.014295	3.504247
11	5	0	2.419635	0.005892	4.329614
12	7	0	1.237972	0.003387	3.487084
13	1	0	0.330775	0.007464	3.942268
14	6	0	2.271785	-0.016665	5.863786
15	6	0	3.354413	0.325993	6.706976
16	6	0	3.187729	0.309035	8.089466
17	6	0	1.930229	-0.004921	8.638310
18	6	0	0.795685	-0.423251	7.895573
19	6	0	1.066990	-0.423932	6.508101
20	1	0	0.277646	-0.810335	5.837878
21	1	0	1.847186	0.099053	9.731721
22	1	0	4.028586	0.579124	8.736869
23	1	0	4.310789	0.627591	6.276760
24	1	0	4.710820	0.011409	3.980558
25	1	0	4.606370	0.026886	1.546133
26	1	0	-0.935208	-0.021274	1.940713
27	1	0	-0.941326	-0.022460	-0.533721

E_{Tot}: -619.729063047 Hartree

Figure A2.121: Atomic Coordinates for [B3LYP/6-31G(d)] optimized geometry value of total energy of 2-(phenyl-4-ide)-2,1-borazaronaphthalene (**b-*p*C**)

Center Number	Atomic Number	Atomic Type	Coordinates (Angstroms) X	Y	Z
1	6	0	-0.000398	0.000171	0.005910
2	6	0	0.004029	0.000106	1.394086
3	6	0	1.217597	-0.000009	2.114205
4	6	0	2.448740	-0.000084	1.395217
5	6	0	2.407823	-0.000011	-0.010753
6	6	0	1.206636	0.000117	-0.709578
7	1	0	1.201615	0.000170	-1.796676
8	1	0	3.353007	-0.000066	-0.551698
9	6	0	3.693127	-0.000263	2.134740
10	6	0	3.736699	-0.000364	3.492722
11	5	0	2.429169	-0.000135	4.329364
12	7	0	1.243970	-0.000066	3.486533
13	1	0	0.331725	-0.000128	3.930832
14	6	0	2.312675	-0.000186	5.859257
15	6	0	3.456754	-0.002222	6.696764
16	6	0	3.345805	-0.002448	8.087189
17	6	0	2.124049	-0.000539	8.825405
18	6	0	1.003116	0.001474	7.938352
19	6	0	1.072161	0.001634	6.546641
20	1	0	0.135170	0.003411	5.970975
21	1	0	-0.011318	0.002952	8.366763
22	1	0	4.297343	-0.004010	8.641221
23	1	0	4.449063	-0.003711	6.233441
24	1	0	4.719208	-0.000463	3.963832
25	1	0	4.606367	-0.000298	1.534350
26	1	0	-0.934115	0.000164	1.946533
27	1	0	-0.949343	0.000270	-0.526323

E_{Tot}: -619.731649391 Hartree

A2.4 – 2-D NMR data relevant to Chapter 3.3

Figure A2.122: 2-D NMR correlations of *8-(4,4,5,5-tetramethyl-1,3,2-dioxaboryl)-2-(4-(trifluoromethyl)phenyl)-2,1-borazaronaphthalene* (**3.32**)

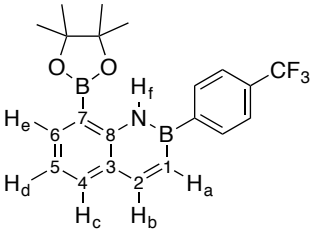

Proton	Chemical Shift
H_a	7.32
H_b	8.22
H_c	7.83
H_d	7.27
H_e	8.05
H_f	10.62

Carbon	Chemical Shift
C_1	127.37 – boron center
C_2	146.38
C_3	125.42 – quaternary center
C_4	133.57
C_5	120.68
C_6	137.11
C_7	116.18 – boron center
C_8	148.69 – quaternary center

COSY NMR Correlations

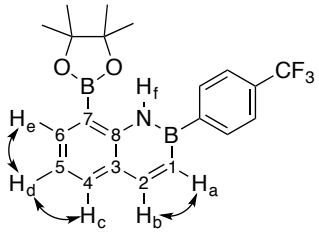

HMQC NMR Correlations

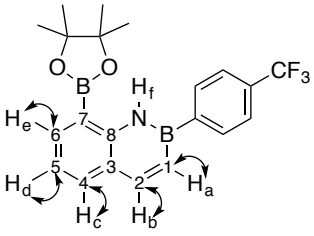

HMBC NMR Correlations

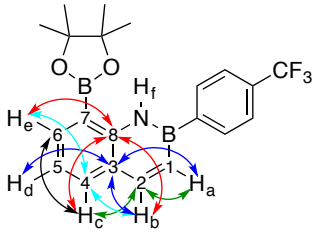

Figure A2.123: ^{1}H NMR ($CDCl_3$, 500.4 MHz) - *8-(4,4,5,5-tetramethyl-1,3,2-dioxaboryl)-2-(4-(trifluoromethyl)phenyl)-2,1-borazaronaphthalene* (**3.32**)

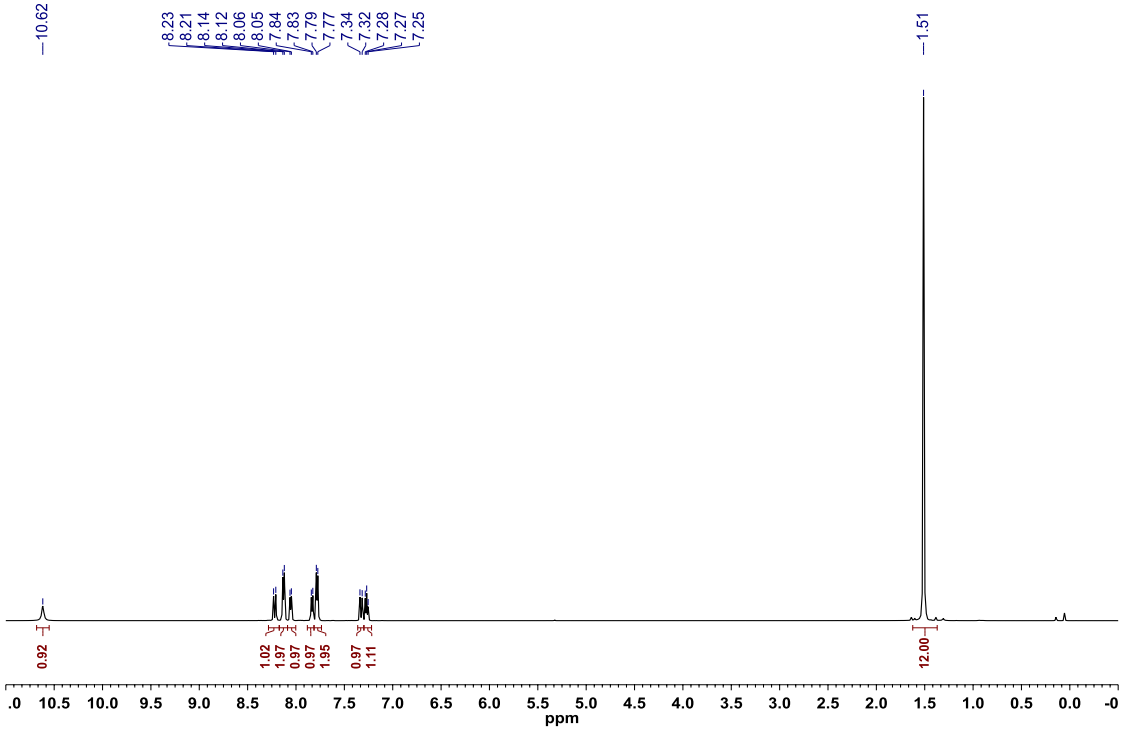

Figure A2.124: ^{13}C {^{1}H} NMR ($CDCl_3$, 125.8 MHz) - *8-(4,4,5,5-tetramethyl-1,3,2-dioxaboryl)-2-(4-(trifluoromethyl)phenyl)-2,1-borazaronaphthalene* (**3.32**)

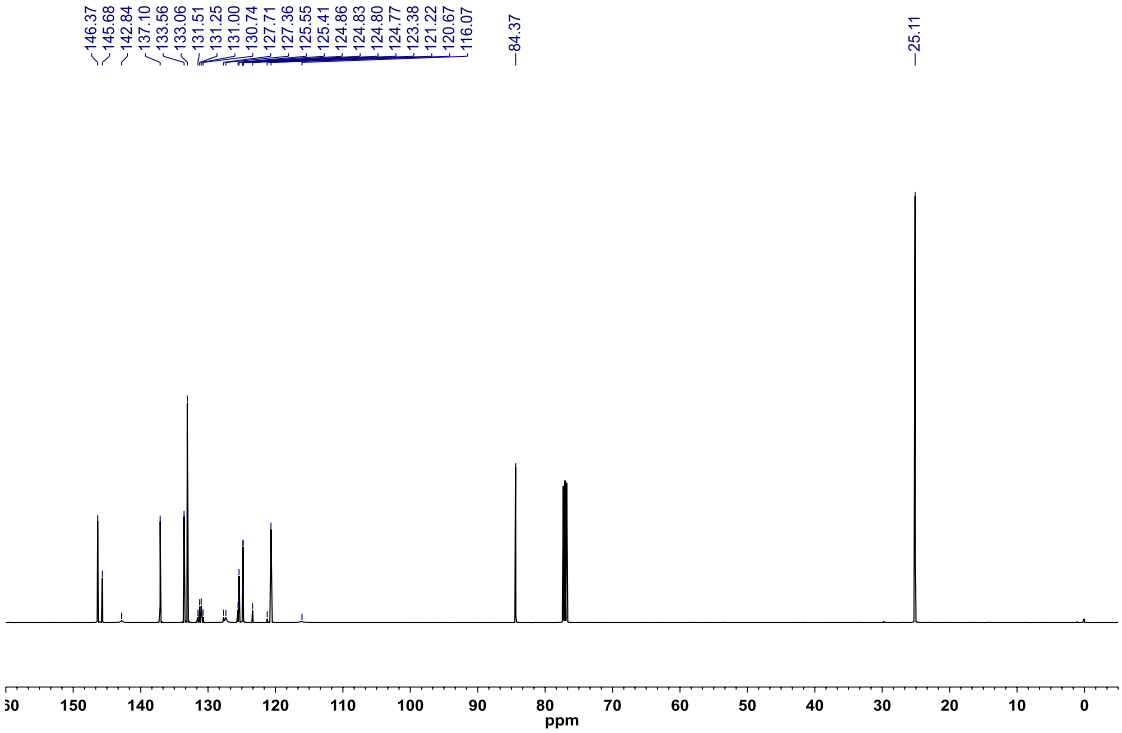

Figure A2.125: COSY - *8-(4,4,5,5-tetramethyl-1,3,2-dioxaboryl)-2-(4-(trifluoromethyl)phenyl)-2,1-borazaronaphthalene* (**3.32**)

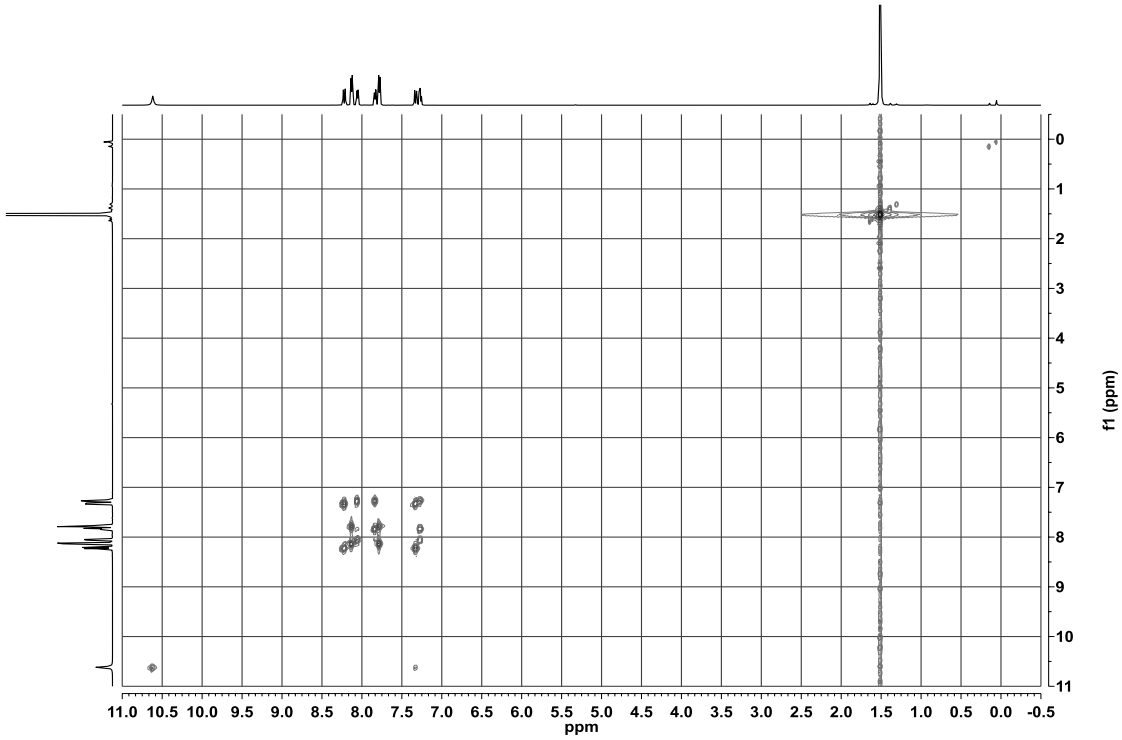

Figure A2.126: HSQC - *8-(4,4,5,5-tetramethyl-1,3,2-dioxaboryl)-2-(4-(trifluoromethyl)phenyl)-2,1-borazaronaphthalene* (**3.32**)

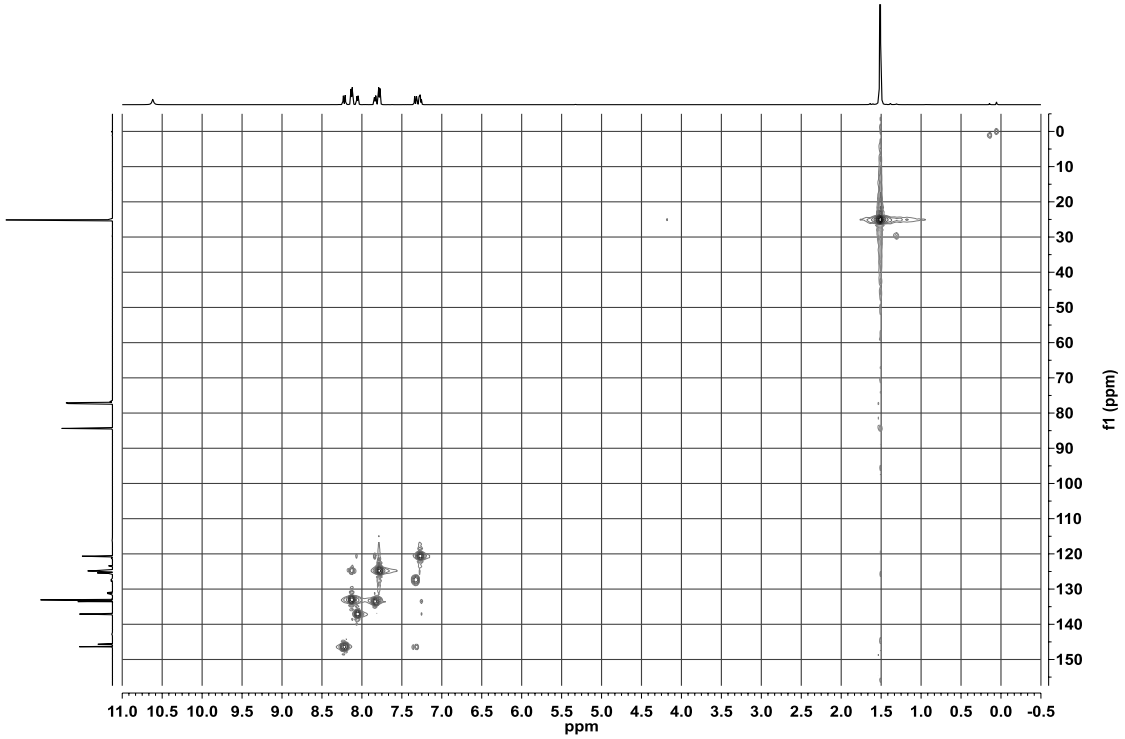

Figure A2.127: HMBC - *8-(4,4,5,5-tetramethyl-1,3,2-dioxaboryl)-2-(4-(trifluoromethyl)phenyl)-2,1-borazaronaphthalene* (**3.32**)

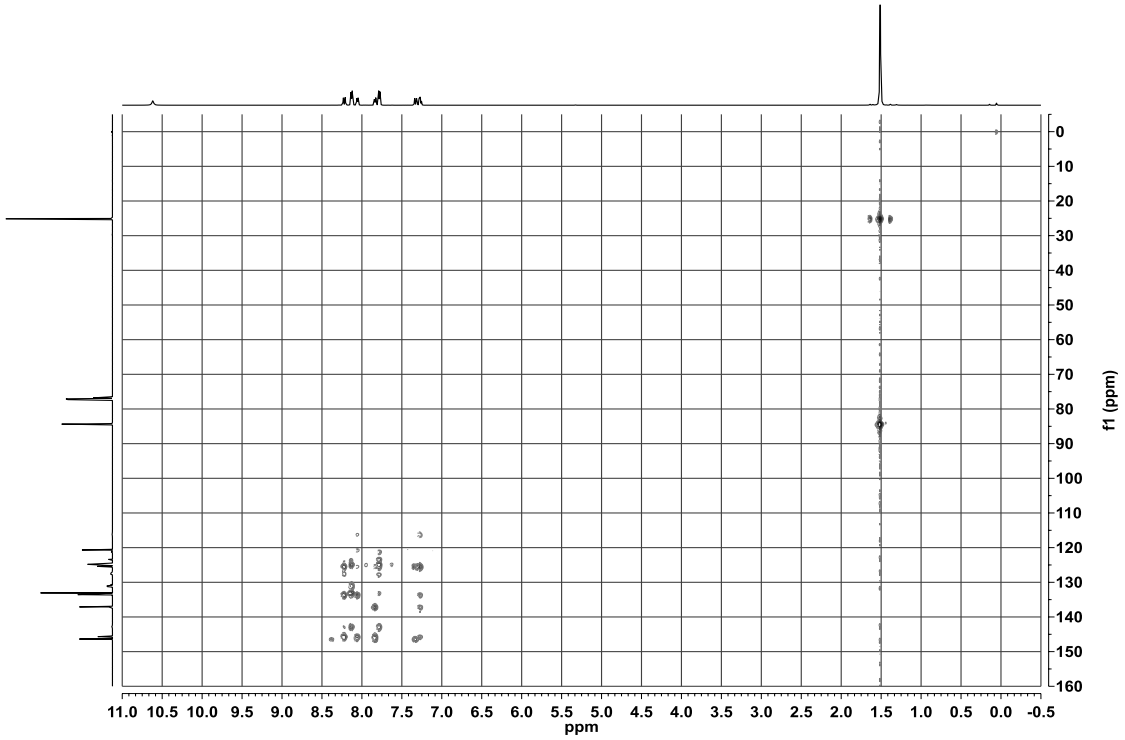

Figure A2.128: NMR correlations of mixture of *N-methyl-7-(4,4,5,5-tetramethyl-1,3,2-dioxaboryl)-2-(4-(trifluoromethyl)phenyl)-2,1-borazaronaphthalene* (**3.65**) and *N-methyl-6-(4,4,5,5-tetramethyl-1,3,2-dioxaboryl)-2-(4-(trifluoromethyl)phenyl)-2,1-borazaronaphthalene* (**3.66**)

N-methyl-7-(4,4,5,5-tetramethyl-1,3,2-dioxaboryl)-2-(4-(trifluoromethyl)phenyl)-2,1-borazaronaphthalene (**3.65**)

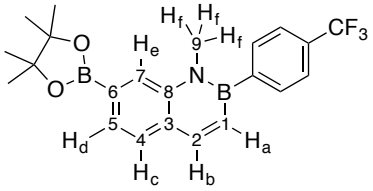

Proton	Chemical Shift
H_a	6.97
H_b	8.11
H_c	7.87
H_d	7.87
H_e	8.11
H_f	3.91

Carbon	Chemical Shift
C_1	132.13 – boron center
C_2	145.29
C_3	129.22 – quaternary center
C_4	127.29 or 129.76
C_5	127.29 or 129.76
C_6	Boron center
C_7	121.90
C_8	141.64 – quaternary center
C_9	37.09

COSY NMR Correlations

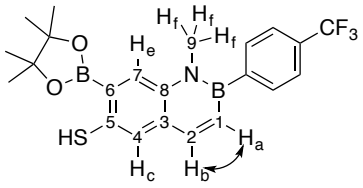

HMQC NMR Correlations

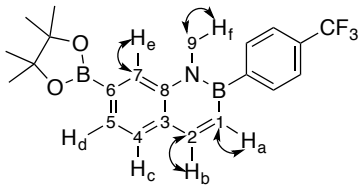

HMBC NMR Correlations

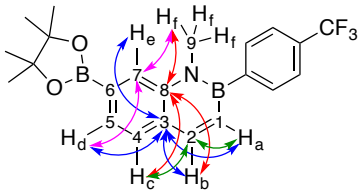

N-methyl-6-(4,4,5,5-tetramethyl-1,3,2-dioxaboryl)-2-(4-(trifluoromethyl)phenyl)-2,1-borazaronaphthalene (**3.66**)

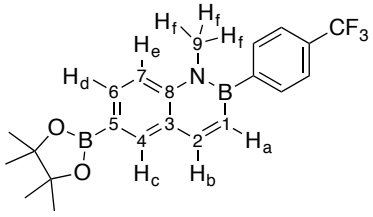

Proton	Chemical Shift
H_a	6.89
H_b	8.10
H_c	8.22
H_d	8.05
H_e	7.71
H_f	3.78

Carbon	Chemical Shift
C_1	Boron center
C_2	145.90
C_3	126.54 – quaternary center
C_4	138.11
C_5	Boron center
C_6	135.11
C_7	114.25
C_8	144.48– quaternary center
C_9	37.02

COSY NMR Correlations

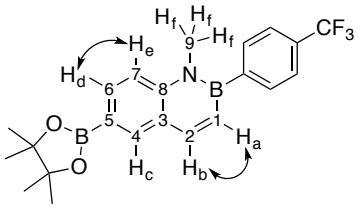

HMQC NMR Correlations

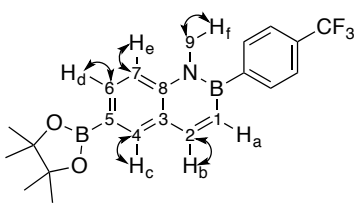

HMBC NMR Correlations

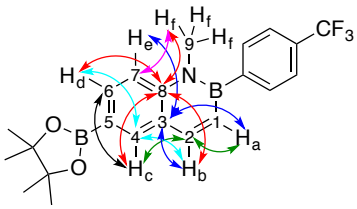

Figure A2.129: ^{1}H NMR ($CDCl_3$, 500.4 MHz) - *N-methyl-7-(4,4,5,5-tetramethyl-1,3,2-dioxaboryl)-2-(4-(trifluoromethyl)phenyl)-2,1-borazaronaphthalene* (**3.65**) and *N-methyl-6-(4,4,5,5-tetramethyl-1,3,2-dioxaboryl)-2-(4-(trifluoromethyl)phenyl)-2,1-borazaronaphthalene* (**3.66**)

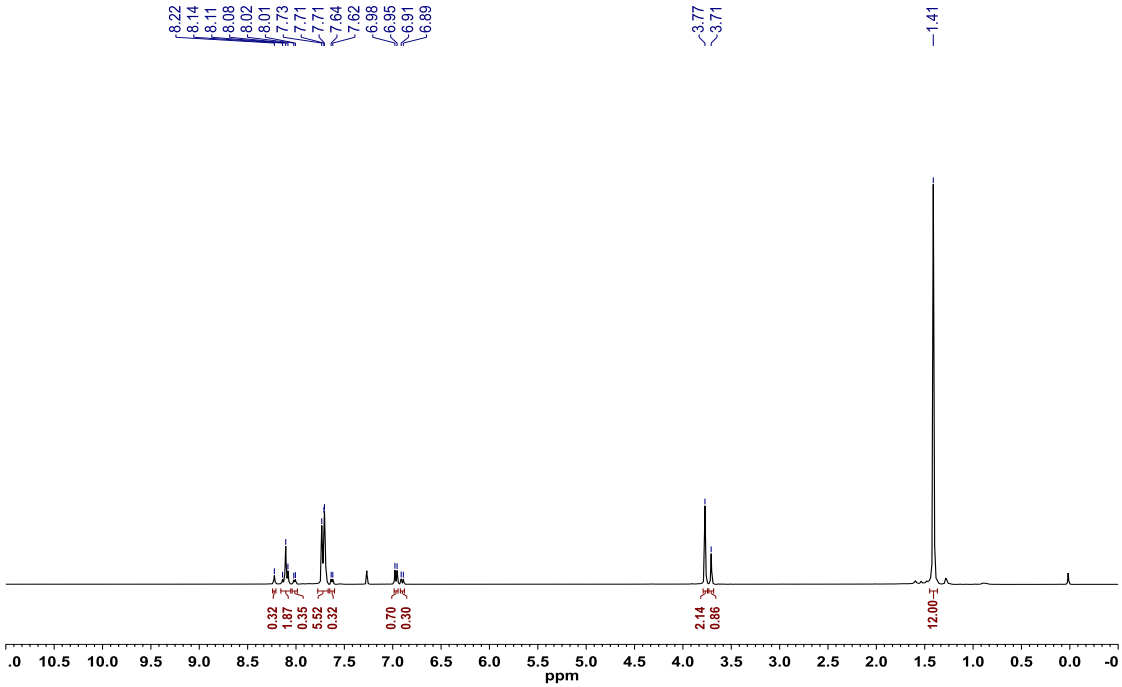

Figure A2.130: ^{13}C $\{^{1}H\}$ NMR ($CDCl_3$, 125.8 MHz) - *N-methyl-7-(4,4,5,5-tetramethyl-1,3,2-dioxaboryl)-2-(4-(trifluoromethyl)phenyl)-2,1-borazaronaphthalene* (**3.65**) and *N-methyl-6-(4,4,5,5-tetramethyl-1,3,2-dioxaboryl)-2-(4-(trifluoromethyl)phenyl)-2,1-borazaronaphthalene* (**3.66**)

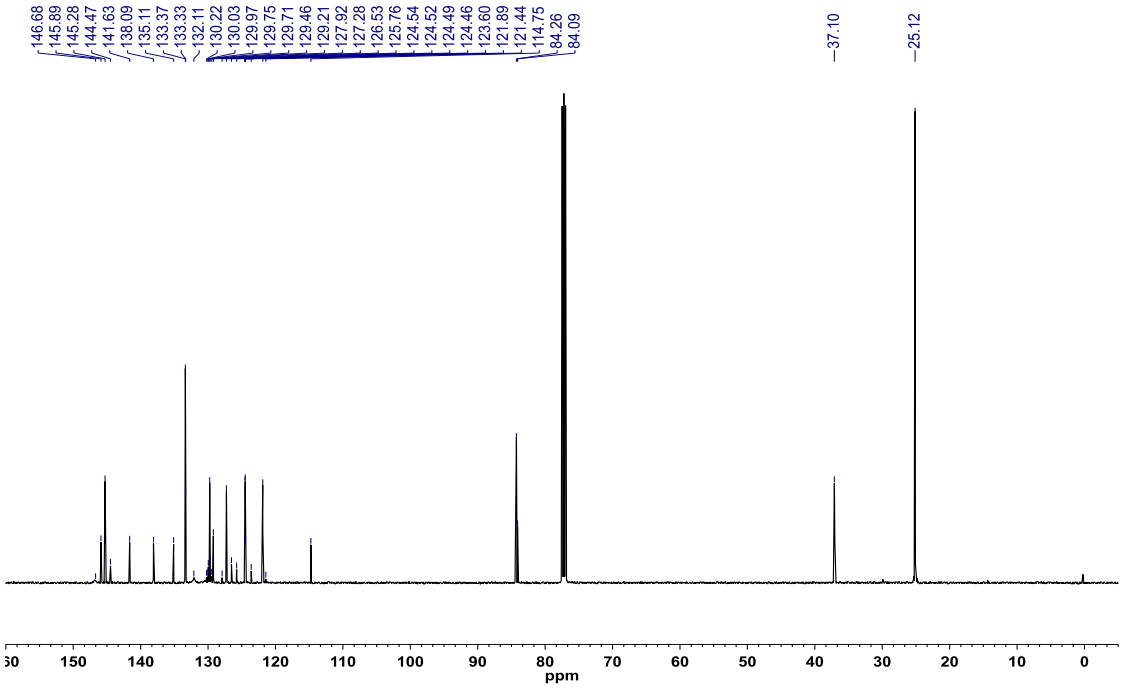

Figure A2.131: ^{19}F {^{1}H} NMR ($CDCl_3$, 470.8 MHz) - *N-methyl-7-(4,4,5,5-tetramethyl-1,3,2-dioxaboryl)-2-(4-(trifluoromethyl)phenyl)-2,1-borazaronaphthalene* (**3.65**) and *N-methyl-6-(4,4,5,5-tetramethyl-1,3,2-dioxaboryl)-2-(4-(trifluoromethyl)phenyl)-2,1-borazaronaphthalene* (**3.66**)

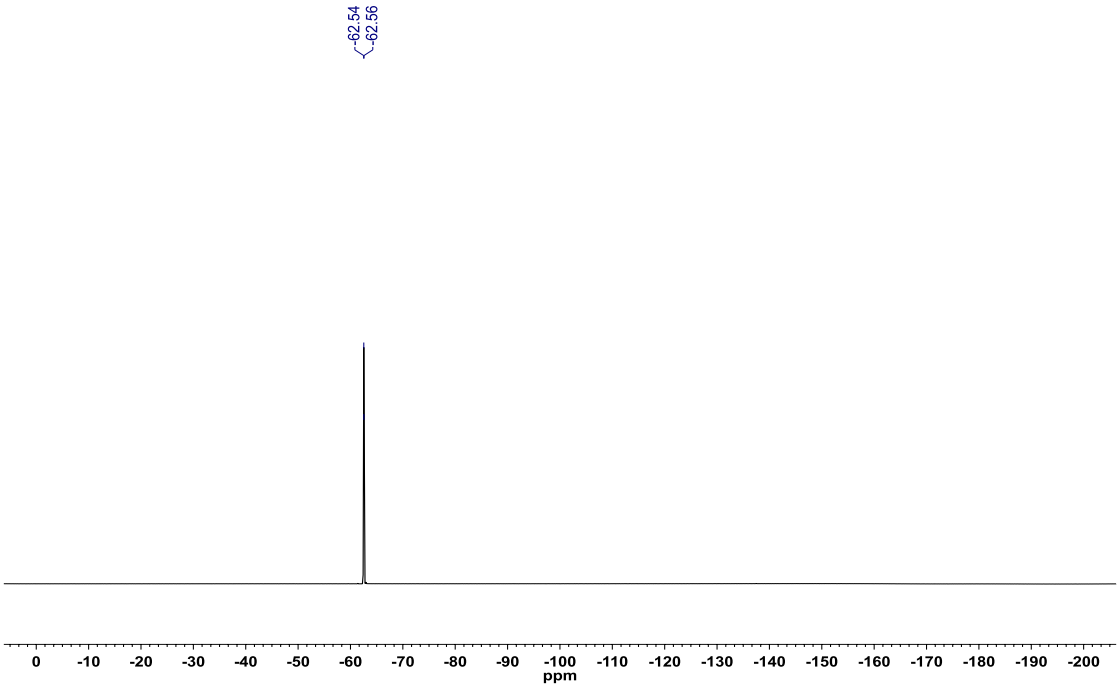

Figure A2.132: ^{11}B NMR ($CDCl_3$, 128.4 MHz) - *N-methyl-7-(4,4,5,5-tetramethyl-1,3,2-dioxaboryl)-2-(4-(trifluoromethyl)phenyl)-2,1-borazaronaphthalene* (**3.65**) and *N-methyl-6-(4,4,5,5-tetramethyl-1,3,2-dioxaboryl)-2-(4-(trifluoromethyl)phenyl)-2,1-borazaronaphthalene* (**3.66**)

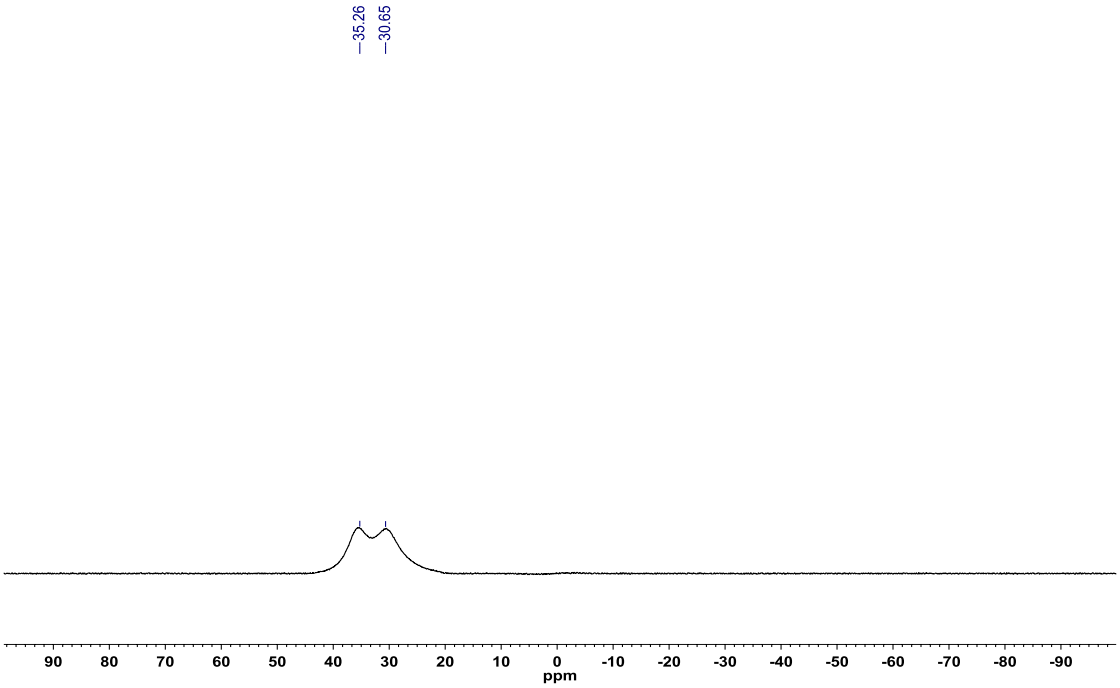

Figure A2.133: DEPT-135 - *N-methyl-7-(4,4,5,5-tetramethyl-1,3,2-dioxaboryl)-2-(4-(trifluoromethyl)phenyl)-2,1-borazaronaphthalene* (**3.65**) and *N-methyl-6-(4,4,5,5-tetramethyl-1,3,2-dioxaboryl)-2-(4-(trifluoromethyl)phenyl)-2,1-borazaronaphthalene* (**3.66**)

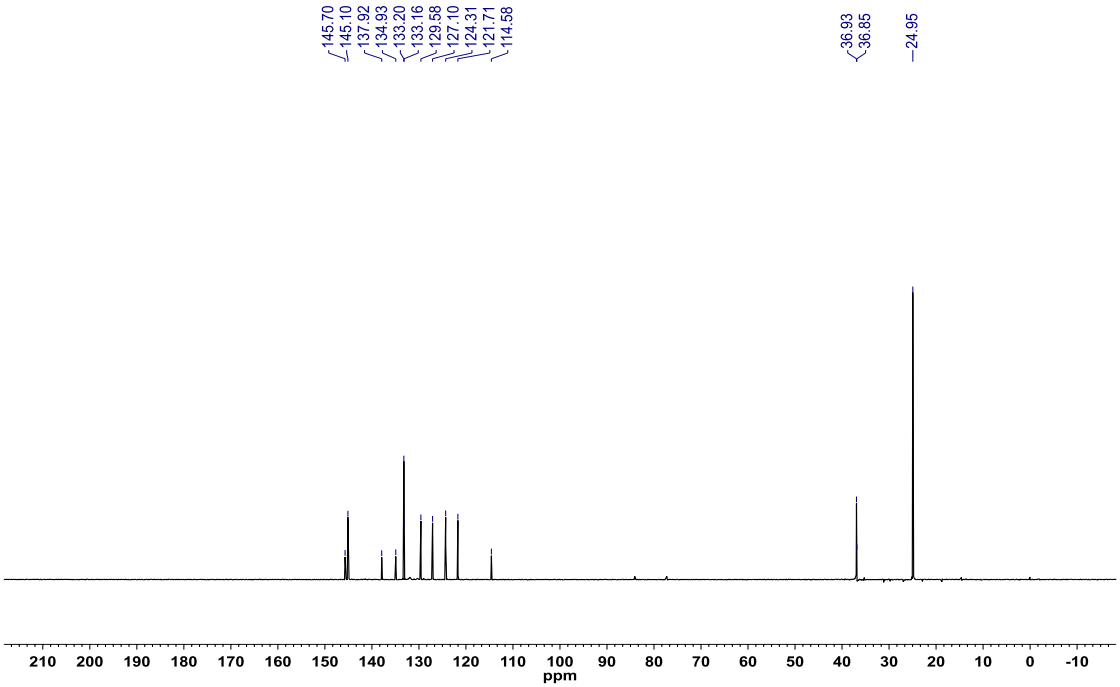

Figure A2.134: COSY - *N-methyl-7-(4,4,5,5-tetramethyl-1,3,2-dioxaboryl)-2-(4-(trifluoromethyl)phenyl)-2,1-borazaronaphthalene* (**3.65**) and *N-methyl-6-(4,4,5,5-tetramethyl-1,3,2-dioxaboryl)-2-(4-(trifluoromethyl)phenyl)-2,1-borazaronaphthalene* (**3.66**)

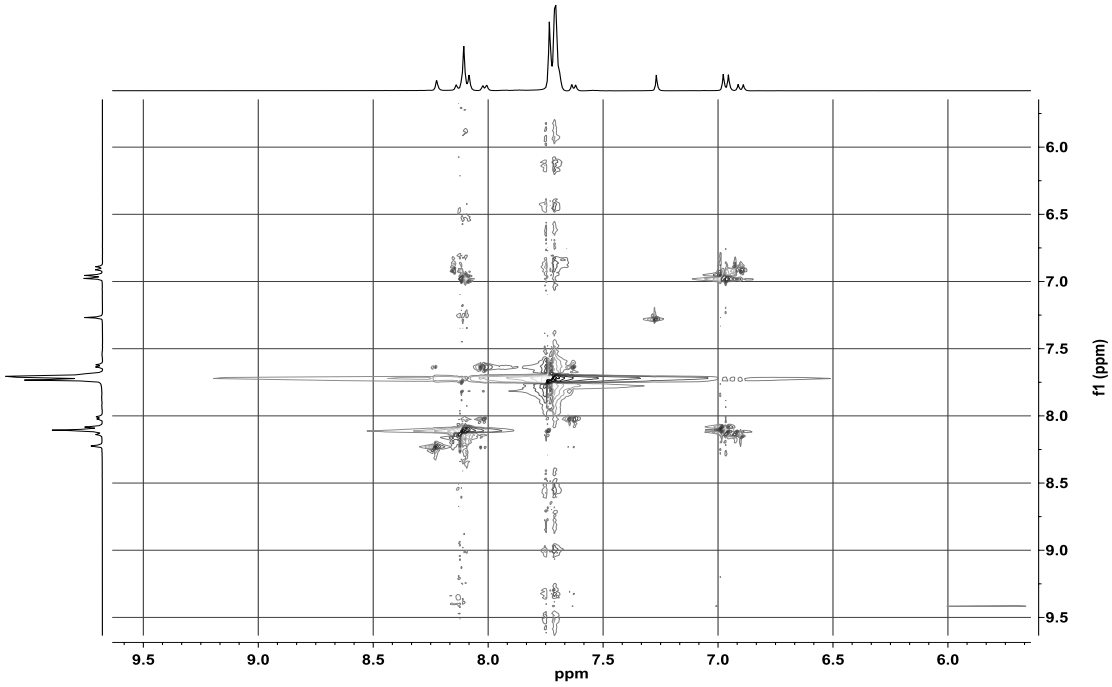

Figure A2.135: HSQC - *N-methyl-7-(4,4,5,5-tetramethyl-1,3,2-dioxaboryl)-2-(4-(trifluoromethyl)phenyl)-2,1-borazaronaphthalene* (**3.65**) and *N-methyl-6-(4,4,5,5-tetramethyl-1,3,2-dioxaboryl)-2-(4-(trifluoromethyl)phenyl)-2,1-borazaronaphthalene* (**3.66**)

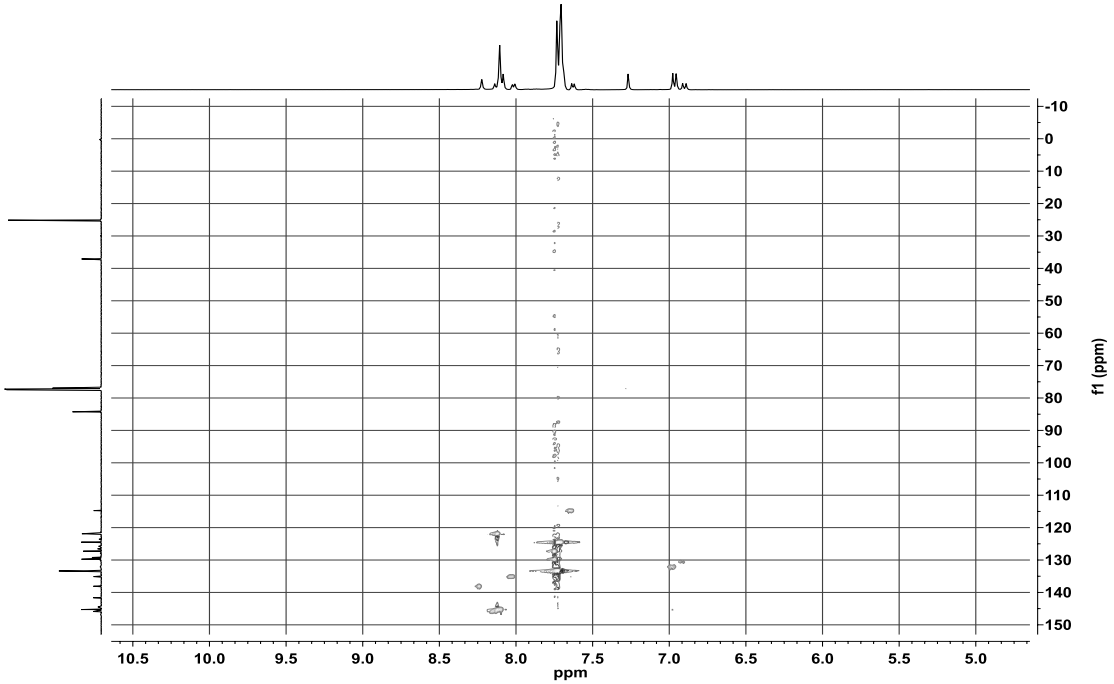

Figure A2.136: HMBC - *N-methyl-7-(4,4,5,5-tetramethyl-1,3,2-dioxaboryl)-2-(4-(trifluoromethyl)phenyl)-2,1-borazaronaphthalene* (**3.65**) and *N-methyl-6-(4,4,5,5-tetramethyl-1,3,2-dioxaboryl)-2-(4-(trifluoromethyl)phenyl)-2,1-borazaronaphthalene* (**3.66**)

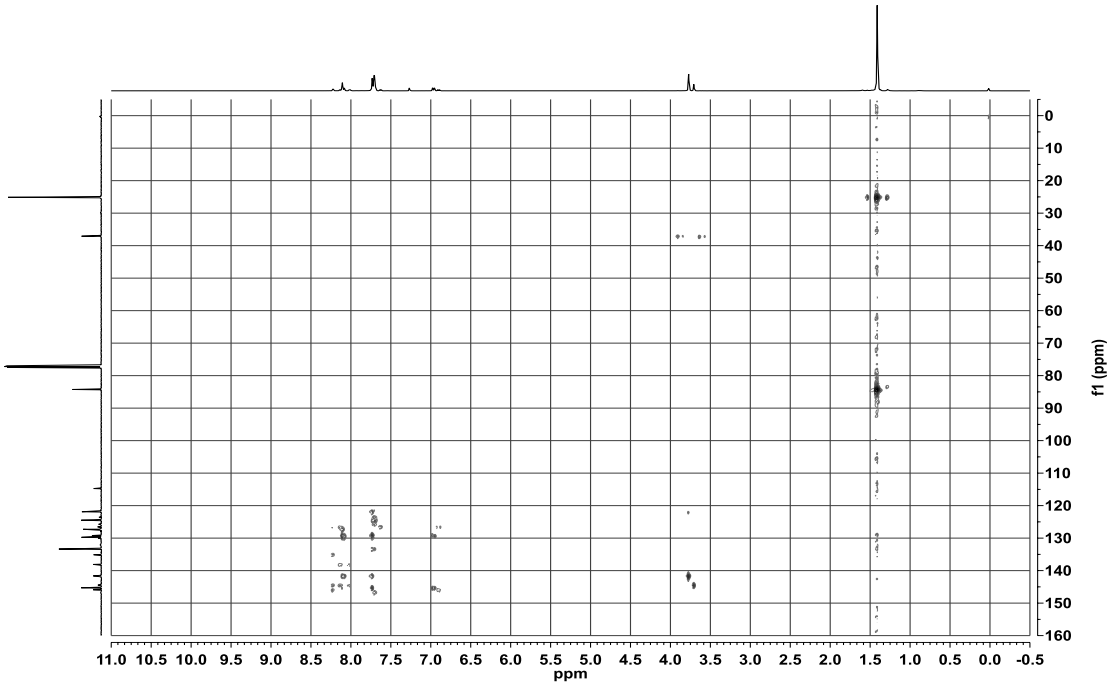

A2.5 – Spectral data relevant to Chapter 3.3

Figure A2.137: ^{1}H NMR ($CDCl_3$, 500.4 MHz) of *8-(4,4,5,5-tetramethyl-1,3,2-dioxaboryl)-2-(4-(trifluoromethyl)phenyl)-2,1-borazaronaphthalene* (**3.32**)

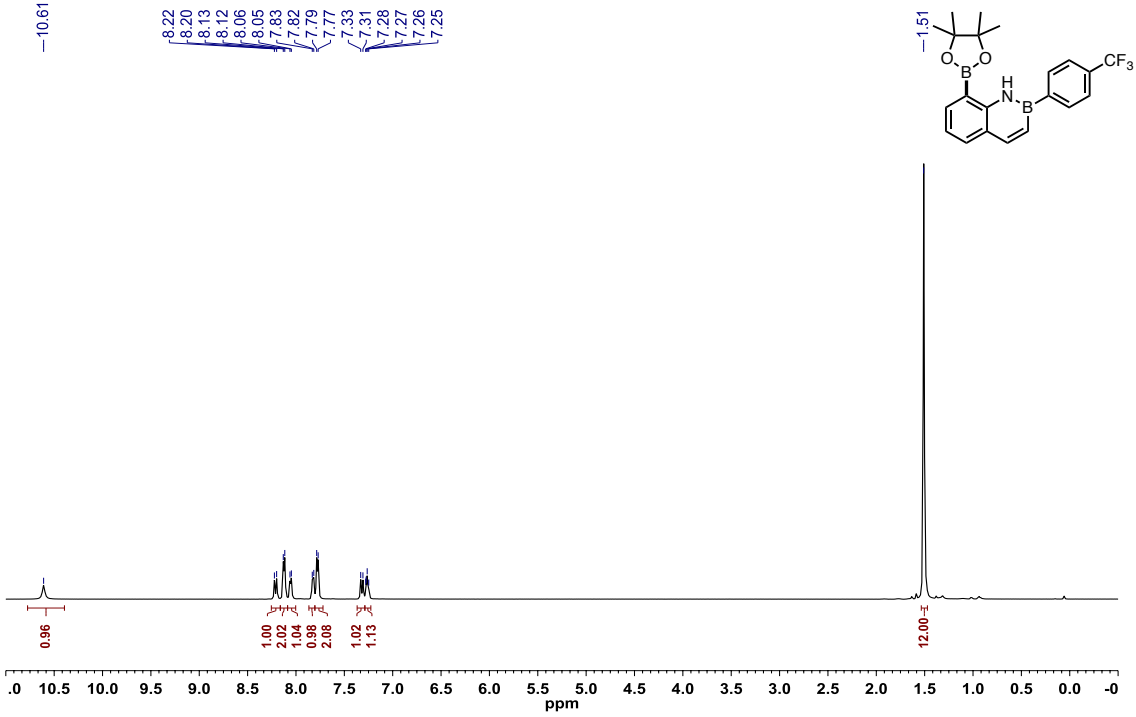

Figure A2.138: ^{13}C {^{1}H} NMR ($CDCl_3$, 125.8 MHz) of *8-(4,4,5,5-tetramethyl-1,3,2-dioxaboryl)-2-(4-(trifluoromethyl)phenyl)-2,1-borazaronaphthalene* (**3.32**)

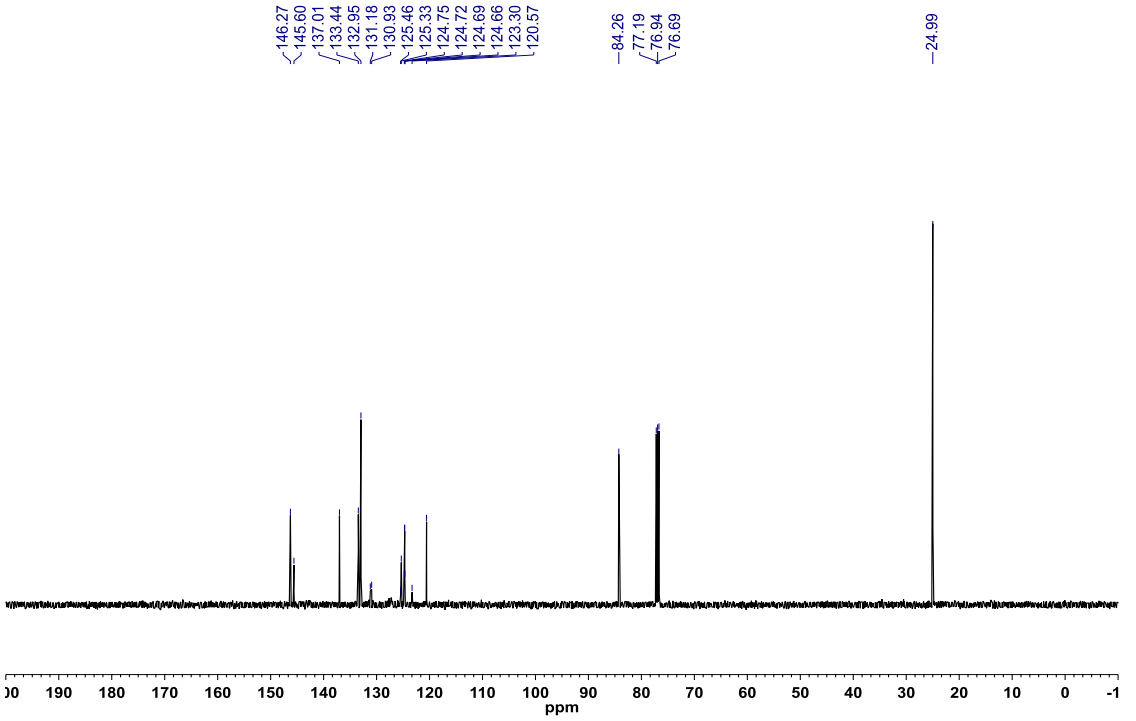

Figure A2.139: ^{19}F {^{1}H} NMR ($CDCl_3$, 470.8 MHz) of *8-(4,4,5,5-tetramethyl-1,3,2-dioxaboryl)-2-(4-(trifluoromethyl)phenyl)-2,1-borazaronaphthalene* (**3.32**)

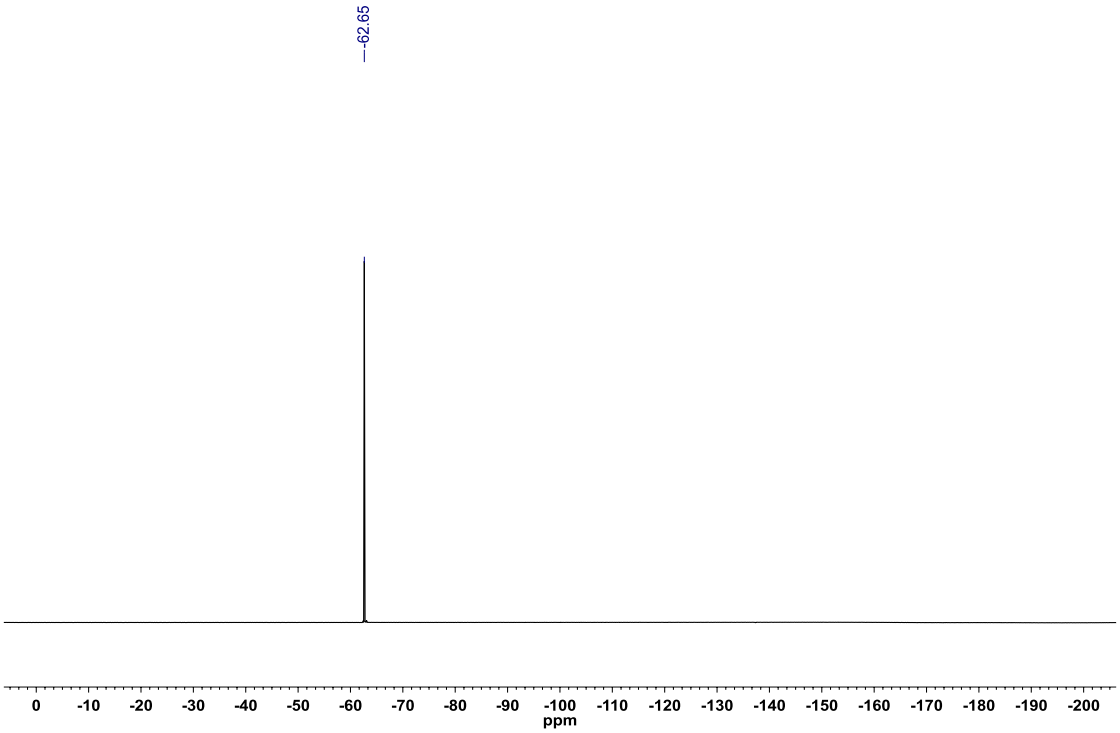

Figure A2.140: ^{11}B NMR ($CDCl_3$, 128.4 MHz) of *8-(4,4,5,5-tetramethyl-1,3,2-dioxaboryl)-2-(4-(trifluoromethyl)phenyl)-2,1-borazaronaphthalene* (**3.32**)

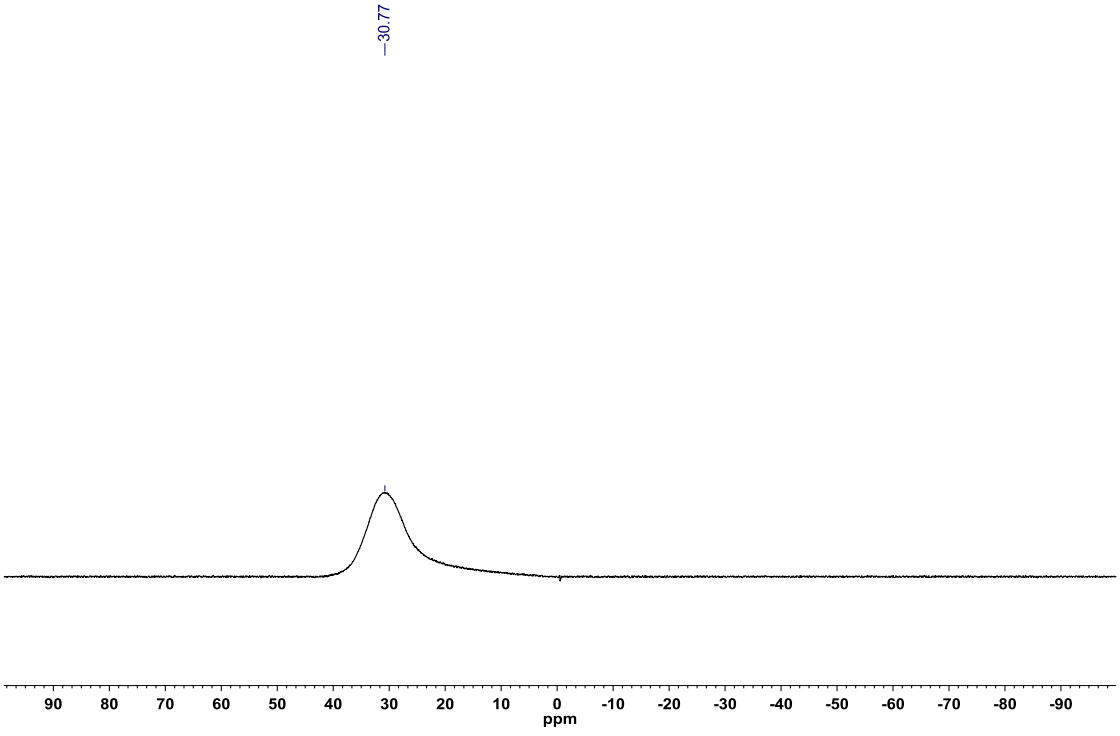

Figure A2.141: H NMR ($CDCl_3$, 500.4 MHz) of *2-(p-tolyl)-8-(4,4,5,5-tetramethyl-1,3,2-dioxaboryl)-2,1-borazaronaphthalene* (**3.33**)

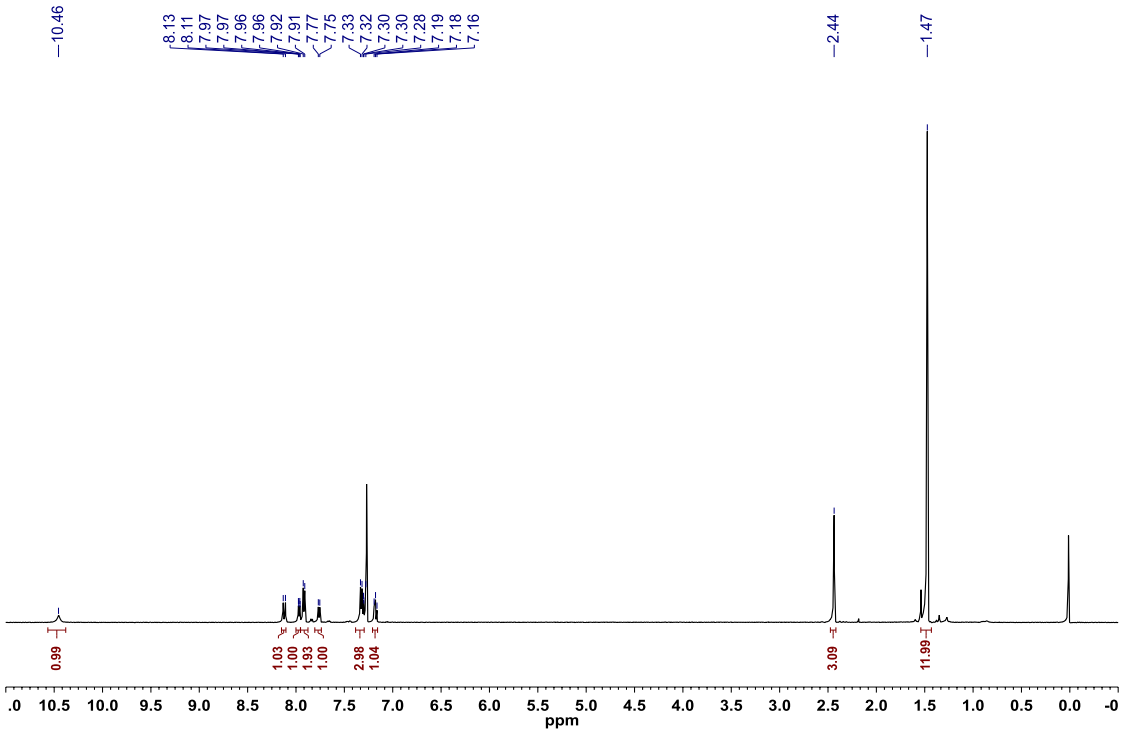

Figure A2.142: ^{13}C {^{1}H} NMR ($CDCl_3$, 125.8 MHz) of *2-(p-tolyl)-8-(4,4,5,5-tetramethyl-1,3,2-dioxaboryl)-2,1-borazaronaphthalene* (**3.33**)

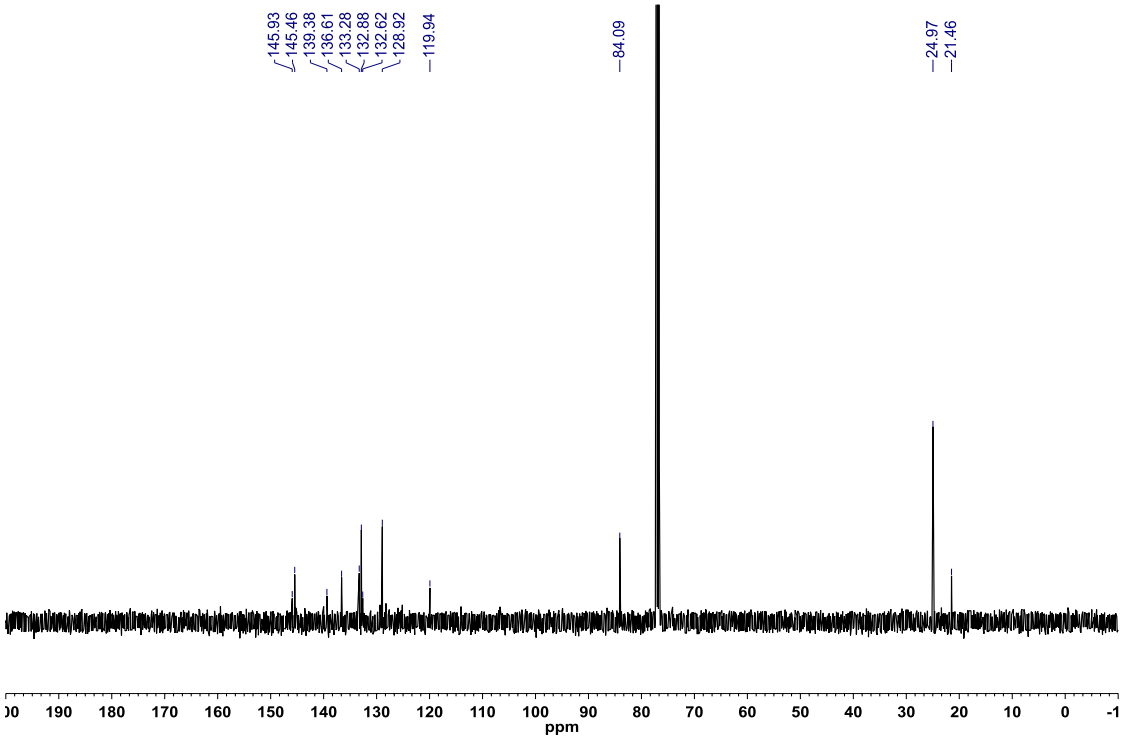

Figure A2.143: ^{11}B NMR ($CDCl_3$, 128.4 MHz) of *2-(p-tolyl)-8-(4,4,5,5-tetramethyl-1,3,2-dioxaboryl)-2,1-borazaronaphthalene* (**3.33**)

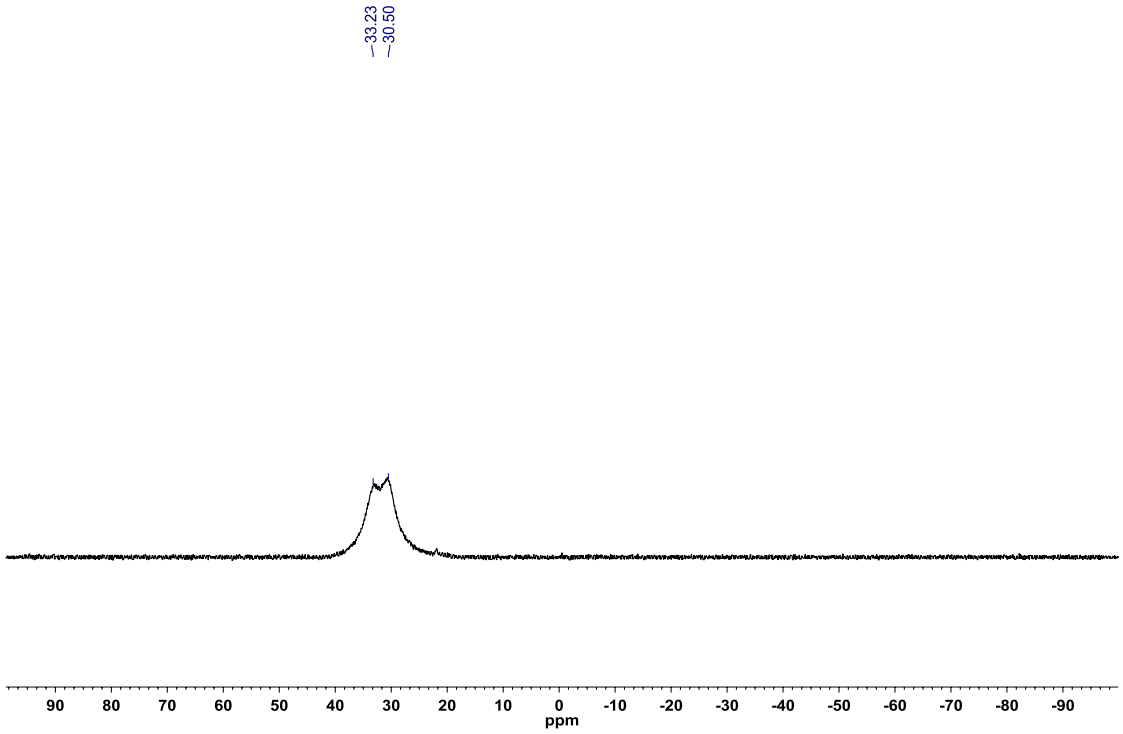

Figure A2.144: ^{1}H NMR ($CDCl_3$, 500.4 MHz) of *2-phenyl-8-(4,4,5,5-tetramethyl-1,3,2-dioxaboryl)-2,1-borazaronaphthalene* (**3.34**)

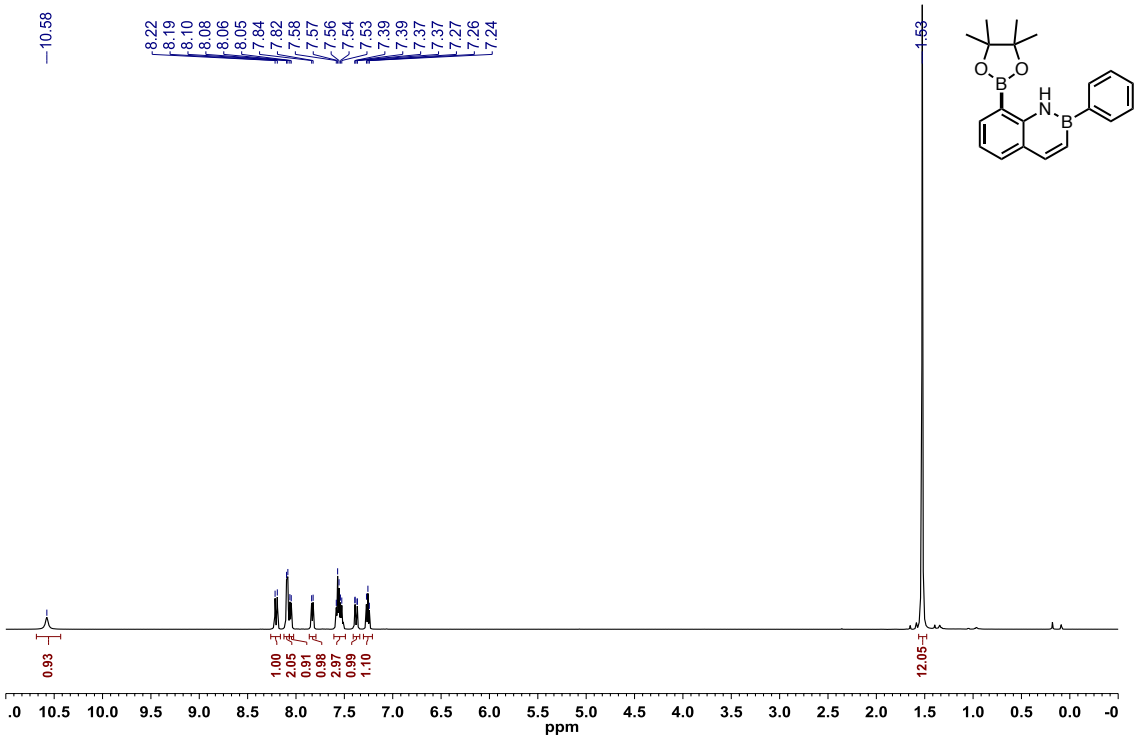

Figure A2.145: ^{13}C {^{1}H} NMR ($CDCl_3$, 125.8 MHz) of *2-phenyl-8-(4,4,5,5-tetramethyl-1,3,2-dioxaboryl)-2,1-borazaronaphthalene* (**3.34**)

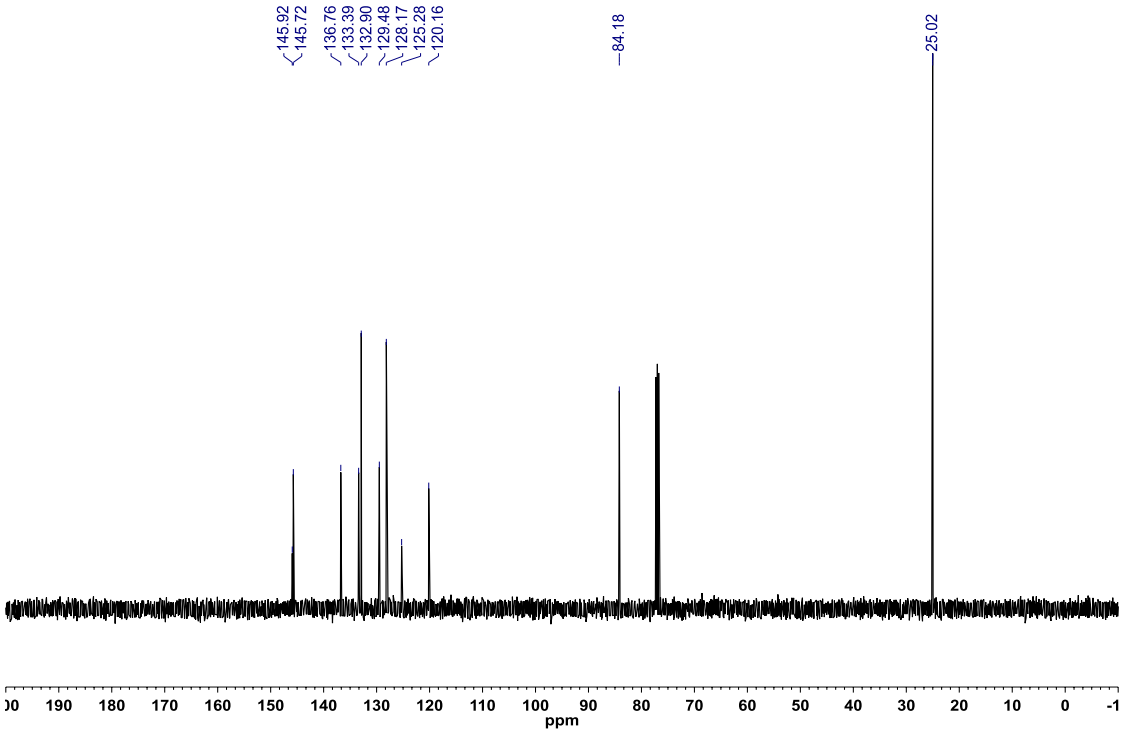

Figure A2.146: ^{11}B NMR ($CDCl_3$, 128.4 MHz) of *2-phenyl-8-(4,4,5,5-tetramethyl-1,3,2-dioxaboryl)-2,1-borazaronaphthalene* (**3.34**)

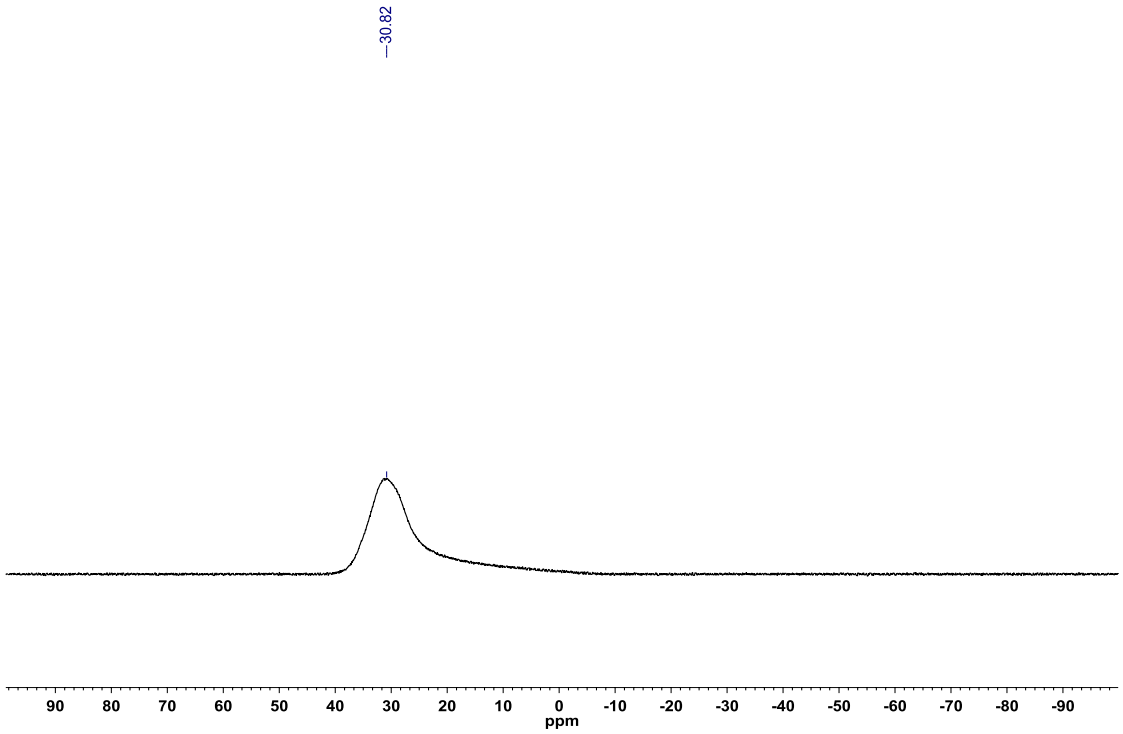

Figure A2.147: ^{1}H NMR ($CDCl_3$, 500.4 MHz) of *2-(4-methoxyphenyl)-8-(4,4,5,5-tetramethyl-1,3,2-dioxaboryl)-2,1-borazaronaphthalene* (**3.35**)

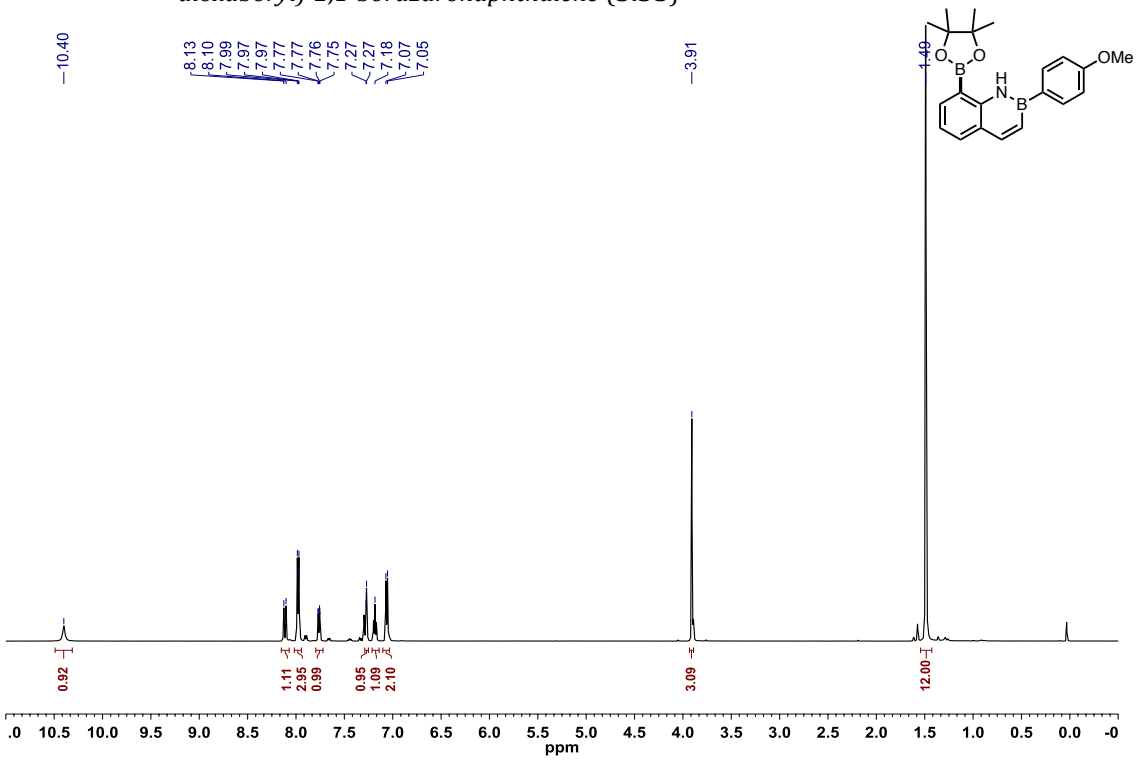

Figure A2.148: ^{13}C {^{1}H} NMR ($CDCl_3$, 125.8 MHz) of *2-(4-methoxyphenyl)-8-(4,4,5,5-tetramethyl-1,3,2-dioxaboryl)-2,1-borazaronaphthalene* (**3.35**)

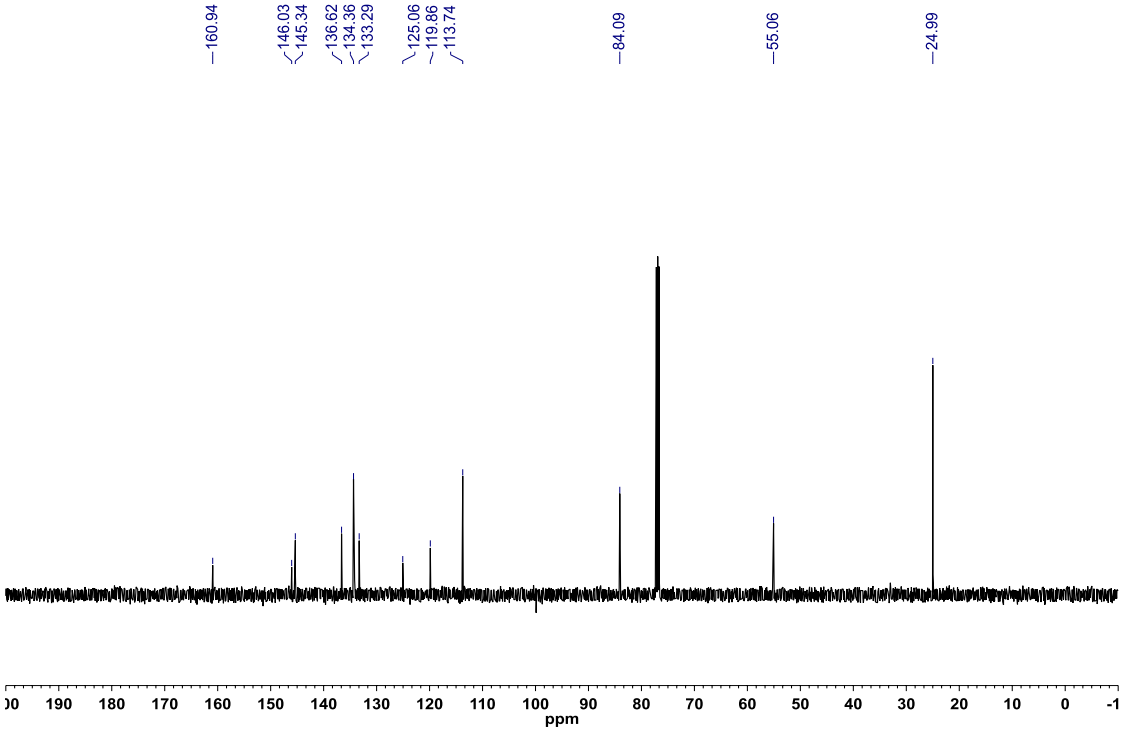

Figure A2.149: ^{11}B NMR ($CDCl_3$, 128.4 MHz) of *2-(4-methoxyphenyl)-8-(4,4,5,5-tetramethyl-1,3,2-dioxaboryl)-2,1-borazaronaphthalene* (**3.35**)

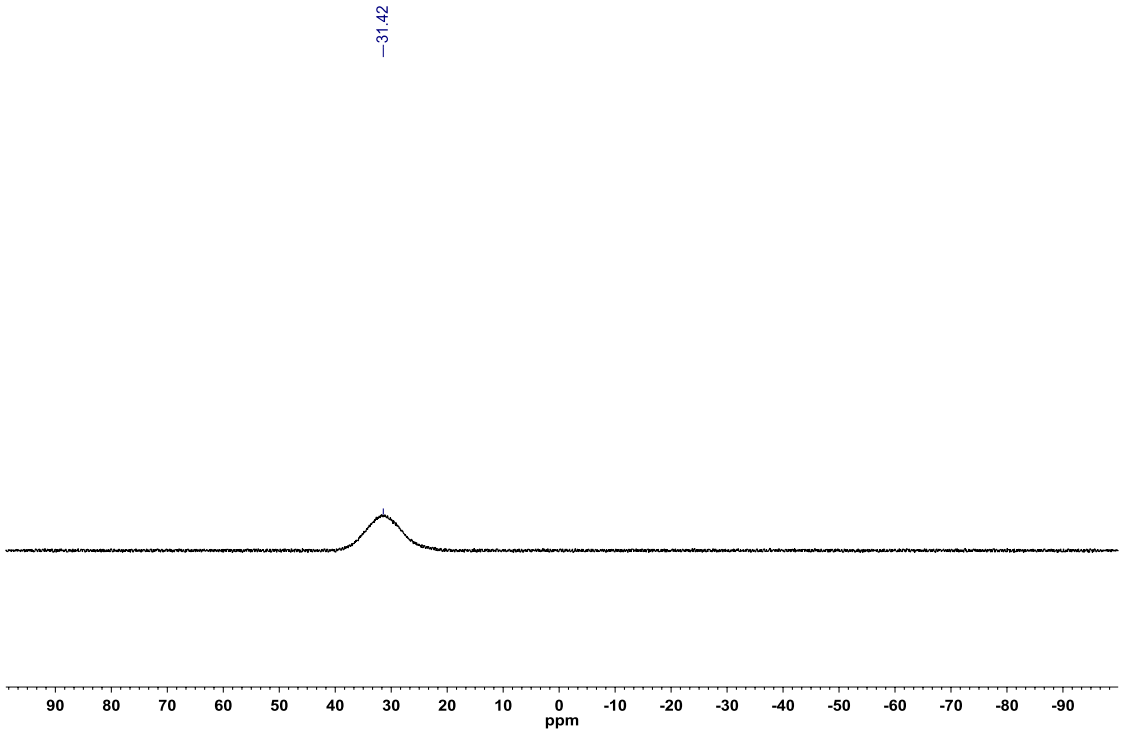

Figure A2.150: ^{1}H NMR ($CDCl_3$, 500.4 MHz) of *2-(3-methoxyphenyl)-8-(4,4,5,5-tetramethyl-1,3,2-dioxaboryl)-2,1-borazaronaphthalene* (**3.36**)

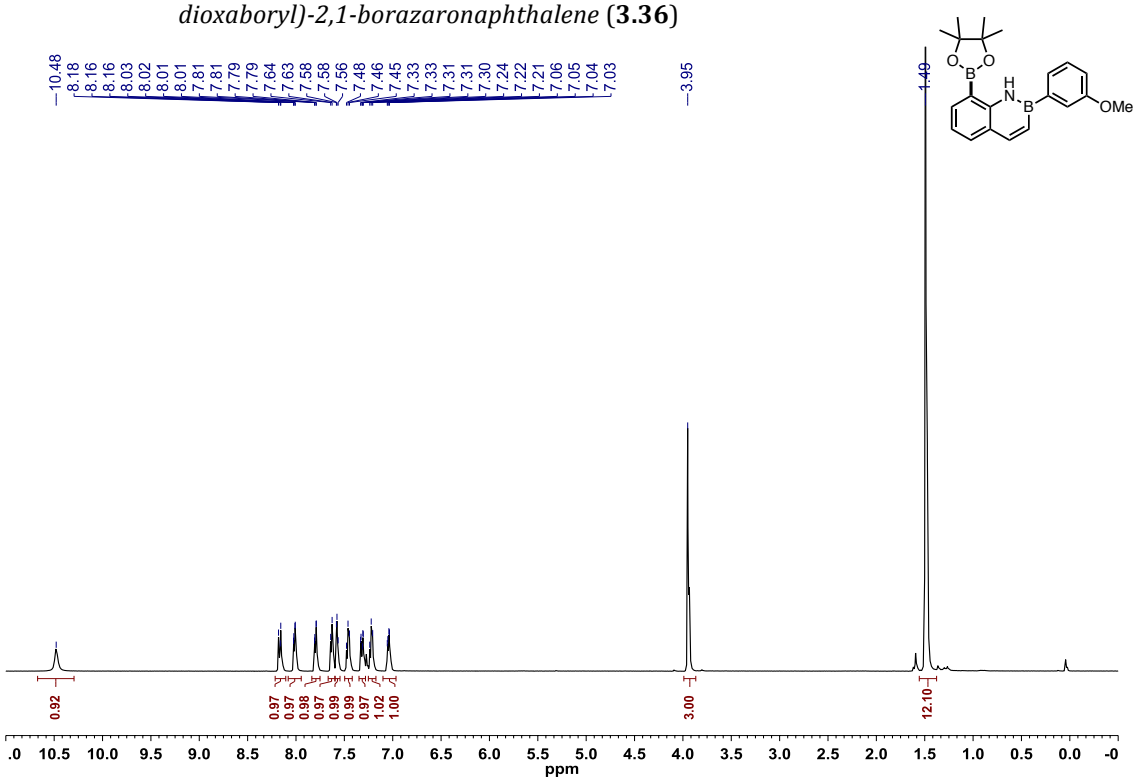

Figure A2.151: ^{13}C {^{1}H} NMR ($CDCl_3$, 125.8 MHz) of *2-(3-methoxyphenyl)-8-(4,4,5,5-tetramethyl-1,3,2-dioxaboryl)-2,1-borazaronaphthalene* (**3.36**)

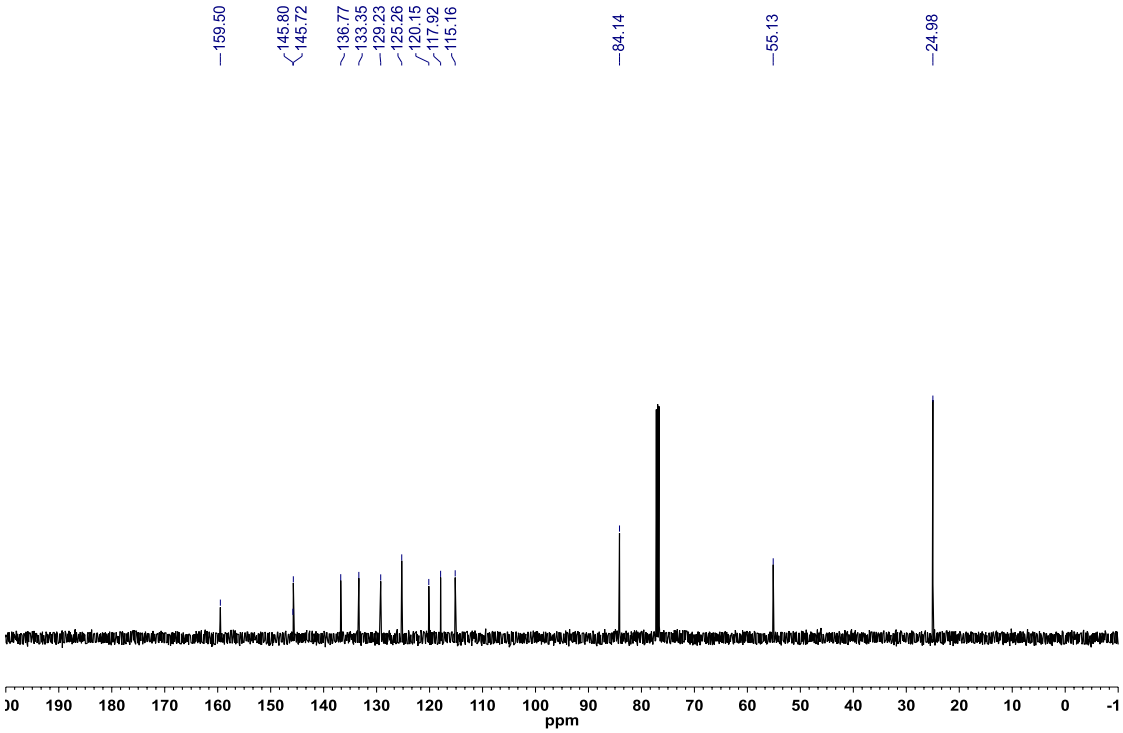

Figure A2.152: ^{11}B NMR ($CDCl_3$, 128.4 MHz) of *2-(3-methoxyphenyl)-8-(4,4,5,5-tetramethyl-1,3,2-dioxaboryl)-2,1-borazaronaphthalene* (**3.36**)

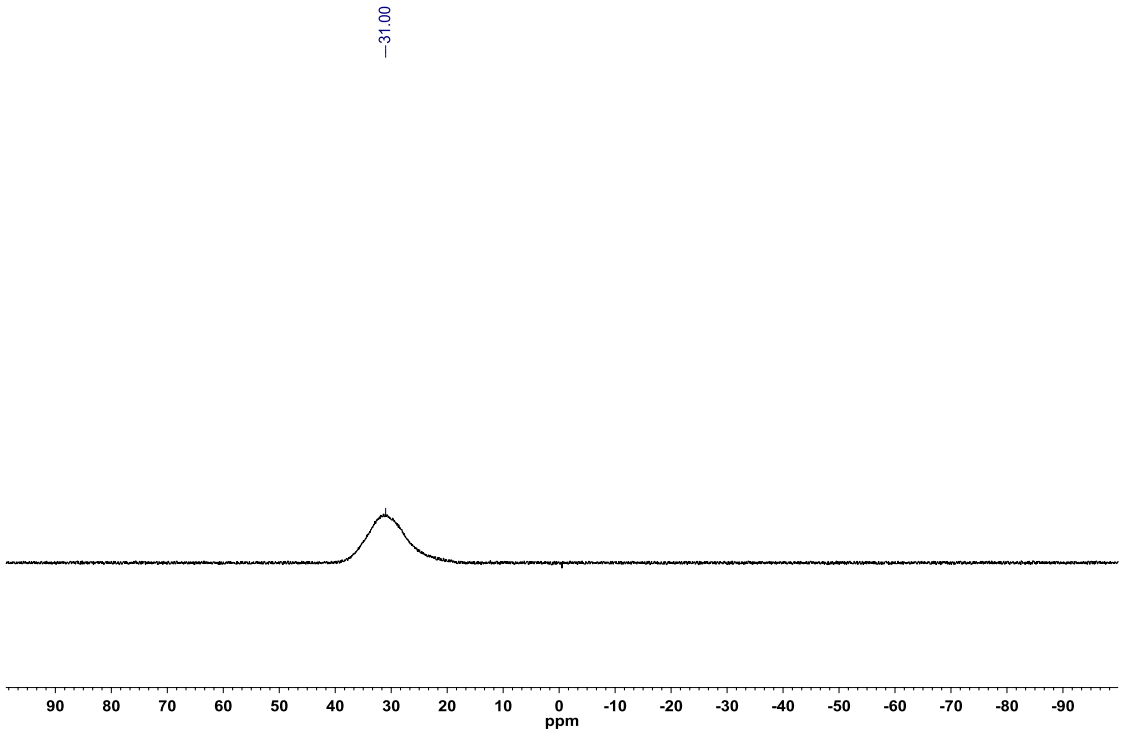

Figure A2.153: ^{1}H NMR ($CDCl_3$, 500.4 MHz) of *2-(2,3-dihydrobenzo[1,4]dioxine)-8-(4,4,5,5-tetramethyl-1,3,2-dioxaboryl)-2,1-borazaronaphthalene* (**3.37**)

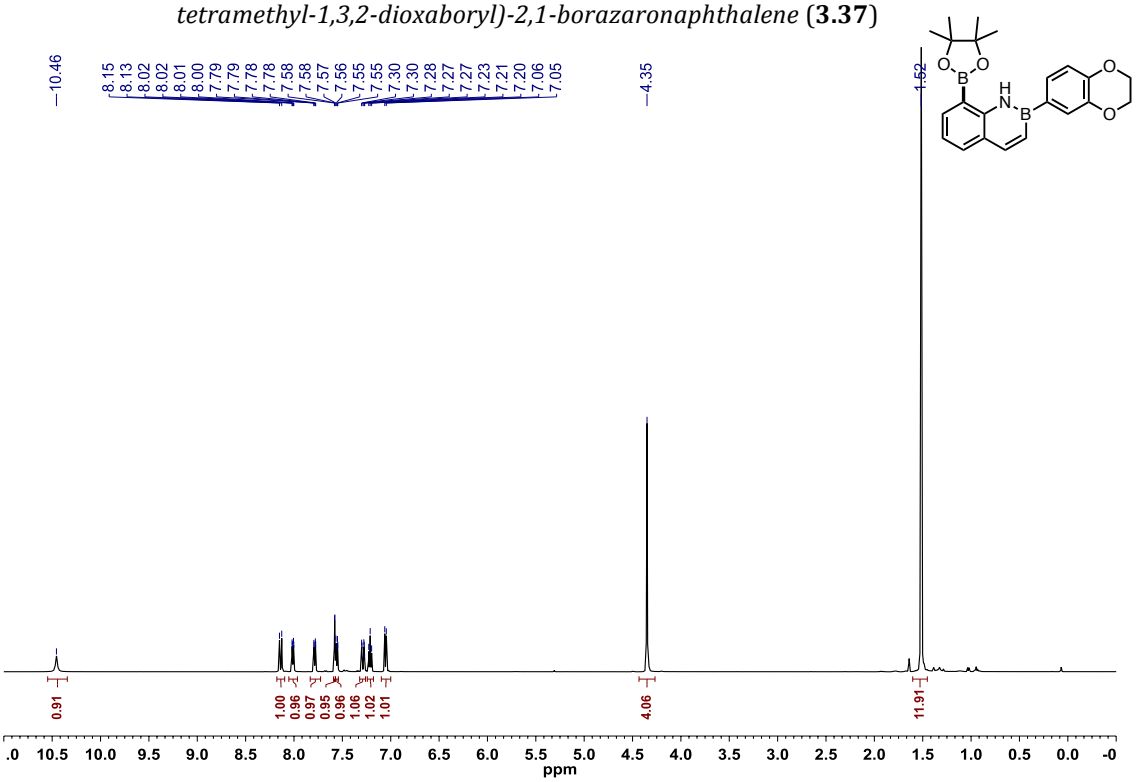

Figure A2.154: ^{13}C {^{1}H} NMR ($CDCl_3$, 125.8 MHz) of *2-(2,3-dihydrobenzo[1,4]dioxine)-8-(4,4,5,5-tetramethyl-1,3,2-dioxaboryl)-2,1-borazaronaphthalene* (**3.37**)

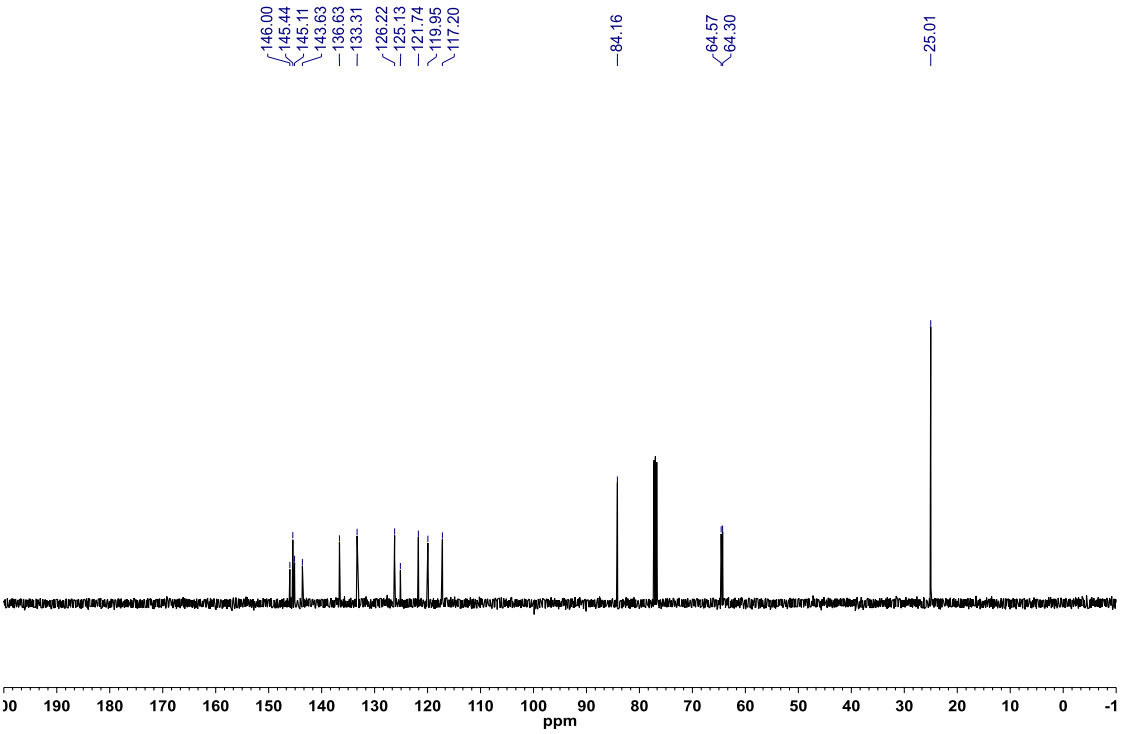

Figure A2.155: ^{11}B NMR ($CDCl_3$, 128.4 MHz) of *2-(2,3-dihydrobenzo[1,4]dioxine)-8-(4,4,5,5-tetramethyl-1,3,2-dioxaboryl)-2,1-borazaronaphthalene* (**3.37**)

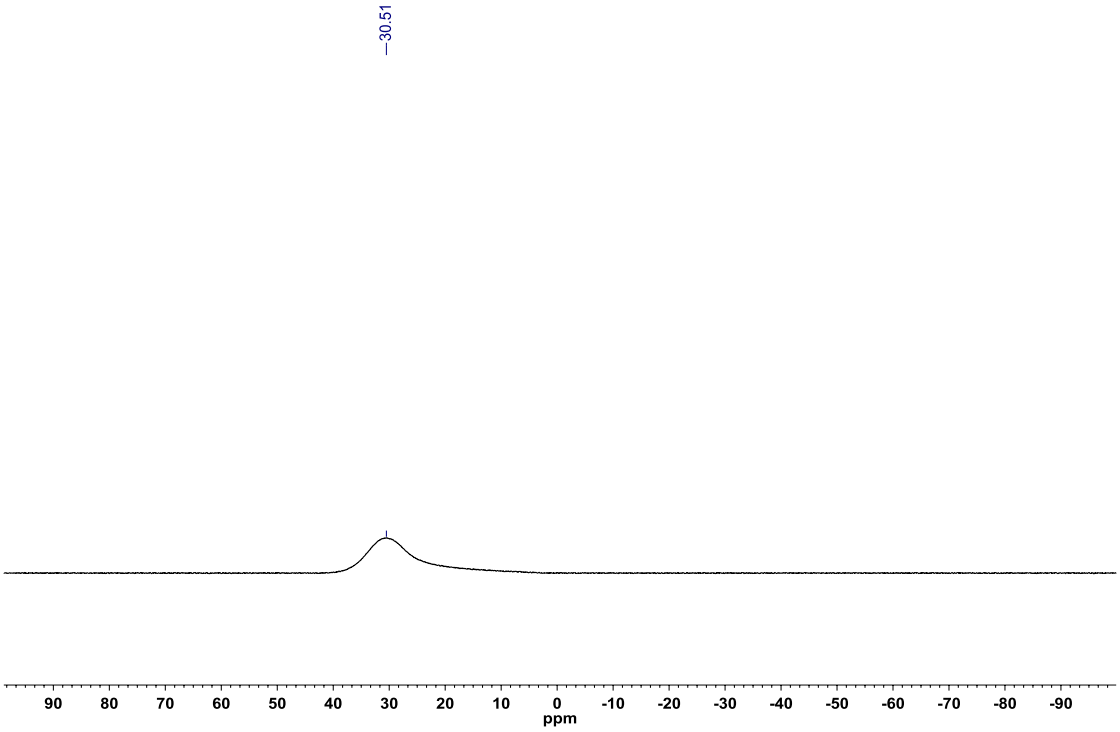

Figure A2.156: ^{1}H NMR ($CDCl_3$, 500.4 MHz) of *2-(4-iodophenyl)-8-(4,4,5,5-tetramethyl-1,3,2-dioxaboryl)-2,1-borazaronaphthalene* (**3.38**)

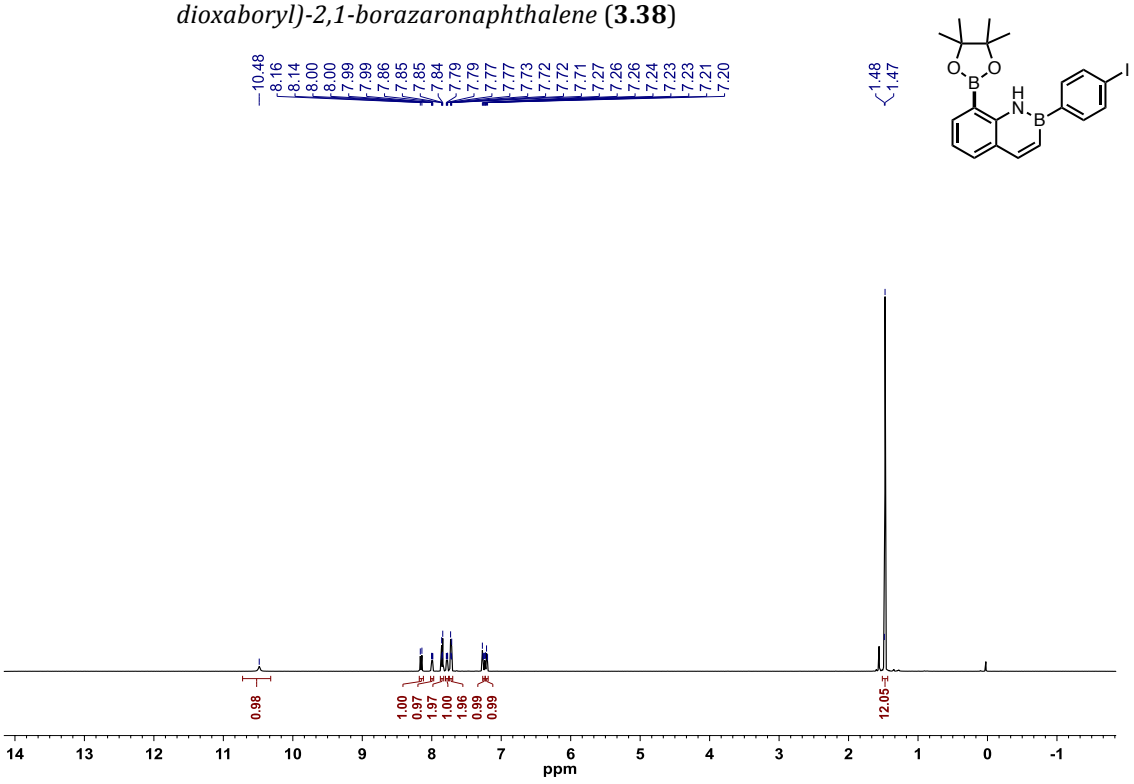

Figure A2.157: ^{13}C {^{1}H} NMR ($CDCl_3$, 125.8 MHz) of *2-(4-iodophenyl)-8-(4,4,5,5-tetramethyl-1,3,2-dioxaboryl)-2,1-borazaronaphthalene* (**3.38**)

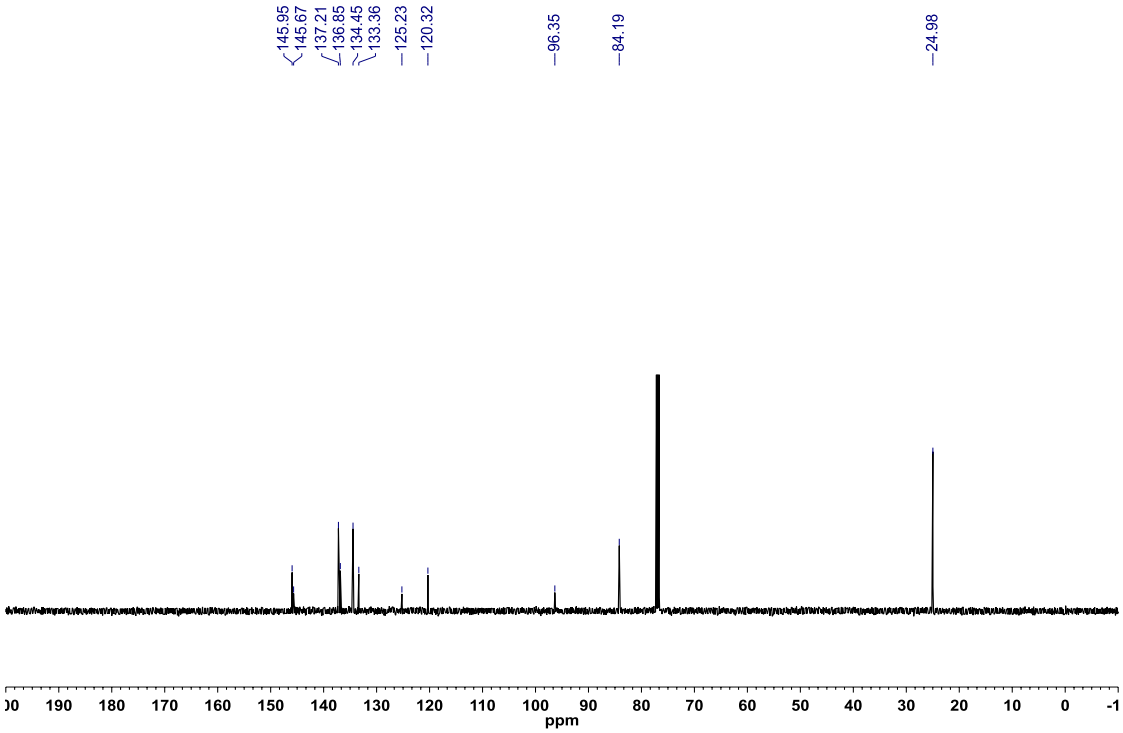

Figure A2.158: ^{11}B NMR ($CDCl_3$, 128.4 MHz) of *2-(4-iodophenyl)-8-(4,4,5,5-tetramethyl-1,3,2-dioxaboryl)-2,1-borazaronaphthalene* (**3.38**)

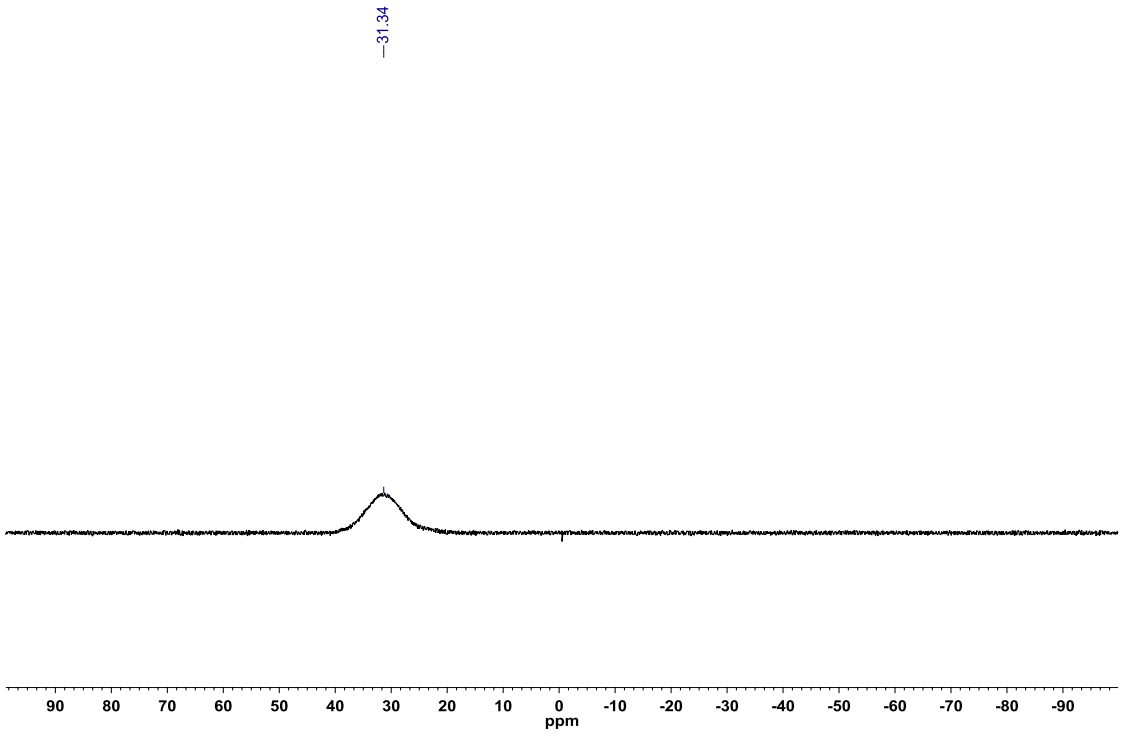

Figure A2.159: ^{1}H NMR ($CDCl_3$, 500.4 MHz) of *2-(4-bromophenyl)-8-(4,4,5,5-tetramethyl-1,3,2-dioxaboryl)-2,1-borazaronaphthalene* (**3.39**)

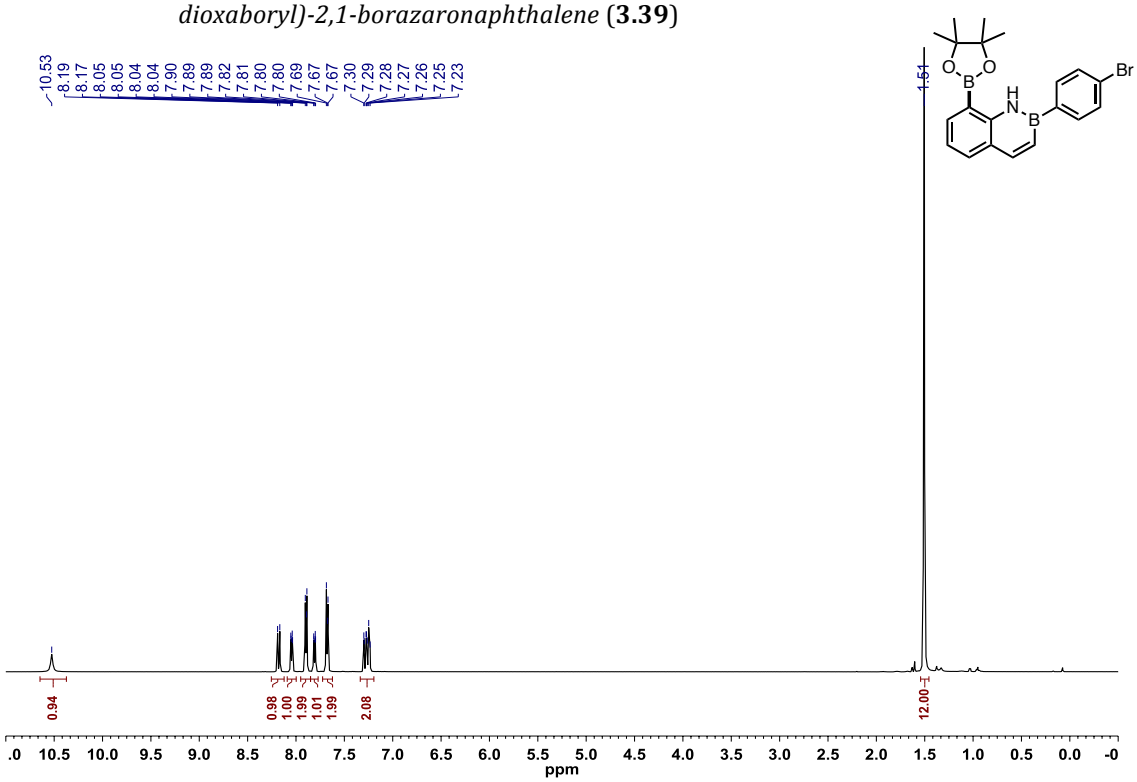

Figure A2.160: ^{13}C {^{1}H} NMR ($CDCl_3$, 125.8 MHz) of *2-(4-bromophenyl)-8-(4,4,5,5-tetramethyl-1,3,2-dioxaboryl)-2,1-borazaronaphthalene* (**3.39**)

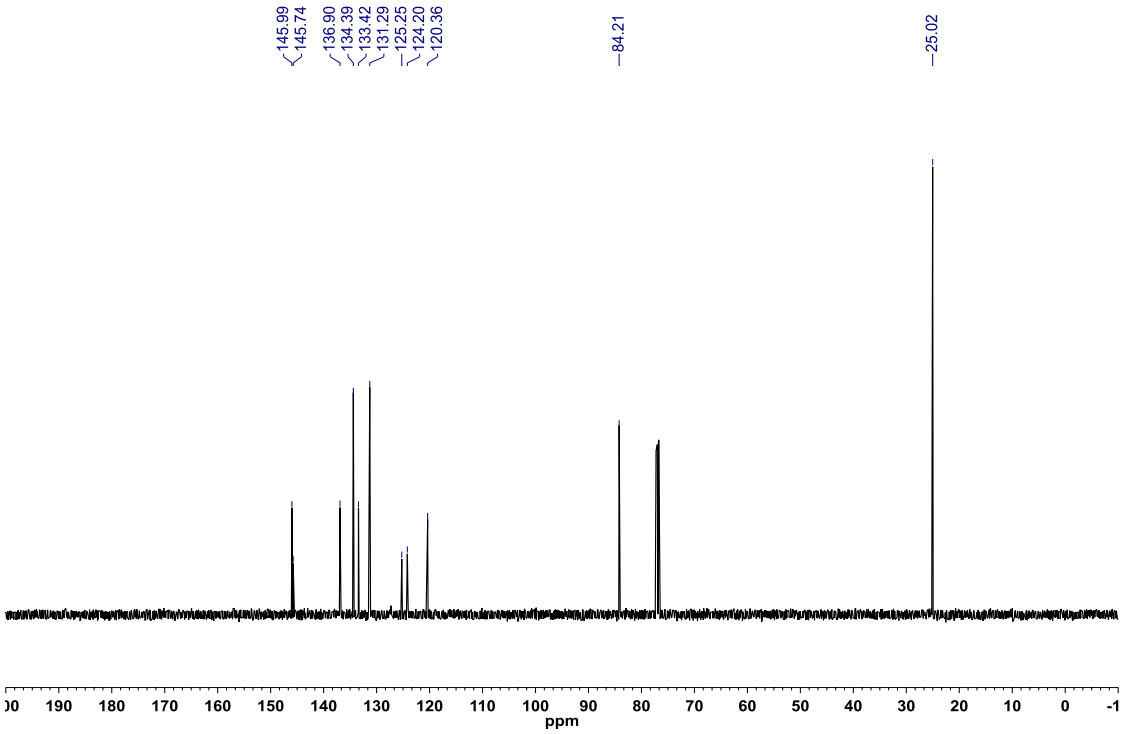

Figure A2.161: ^{11}B NMR ($CDCl_3$, 128.4 MHz) of *2-(4-bromophenyl)-8-(4,4,5,5-tetramethyl-1,3,2-dioxaboryl)-2,1-borazaronaphthalene* (**3.39**)

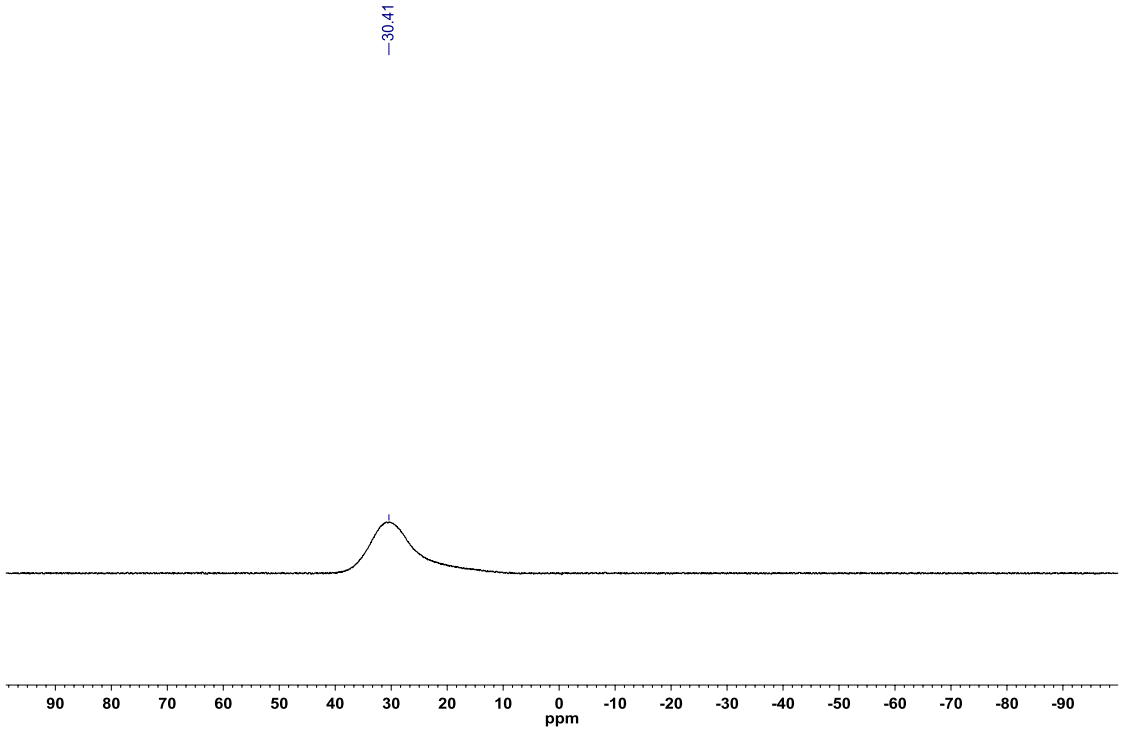

Figure A2.162: ^{1}H NMR ($CDCl_3$, 500.4 MHz) of *2-(3-bromophenyl)-8-(4,4,5,5-tetramethyl-1,3,2-dioxaboryl)-2,1-borazaronaphthalene* (**3.40**)

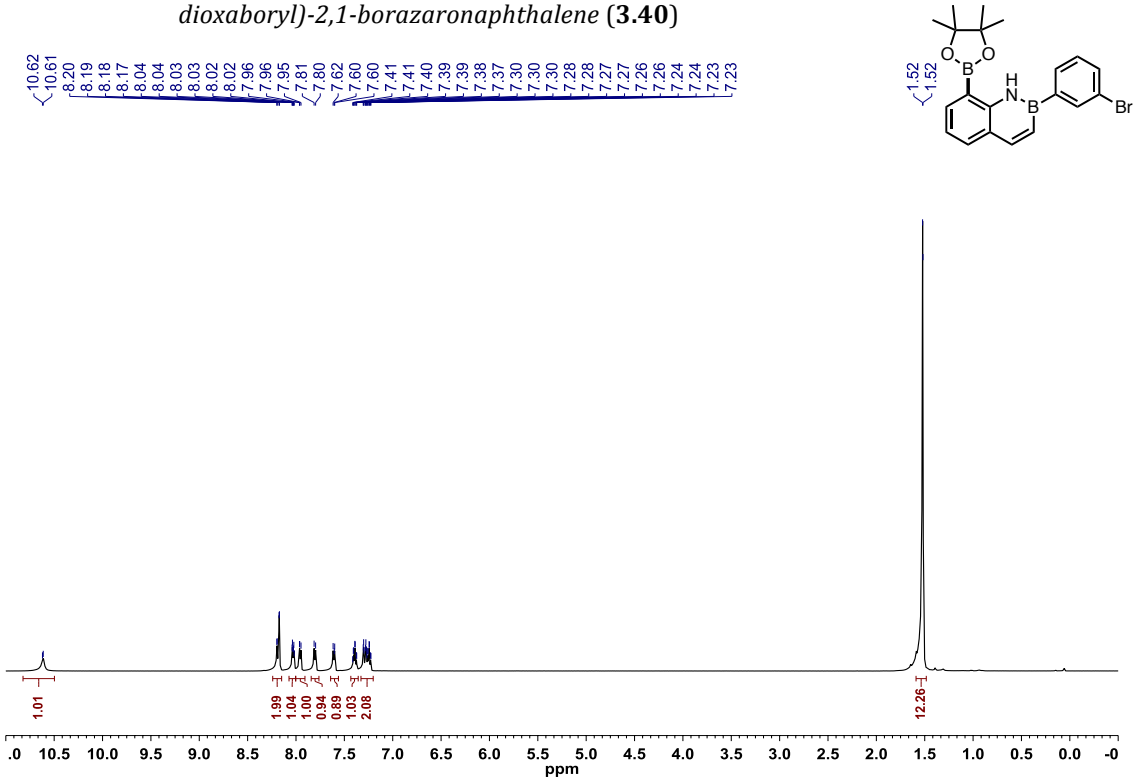

Figure A2.163: ^{13}C {^{1}H} NMR ($CDCl_3$, 125.8 MHz) of *2-(3-bromophenyl)-8-(4,4,5,5-tetramethyl-1,3,2-dioxaboryl)-2,1-borazaronaphthalene* (**3.40**)

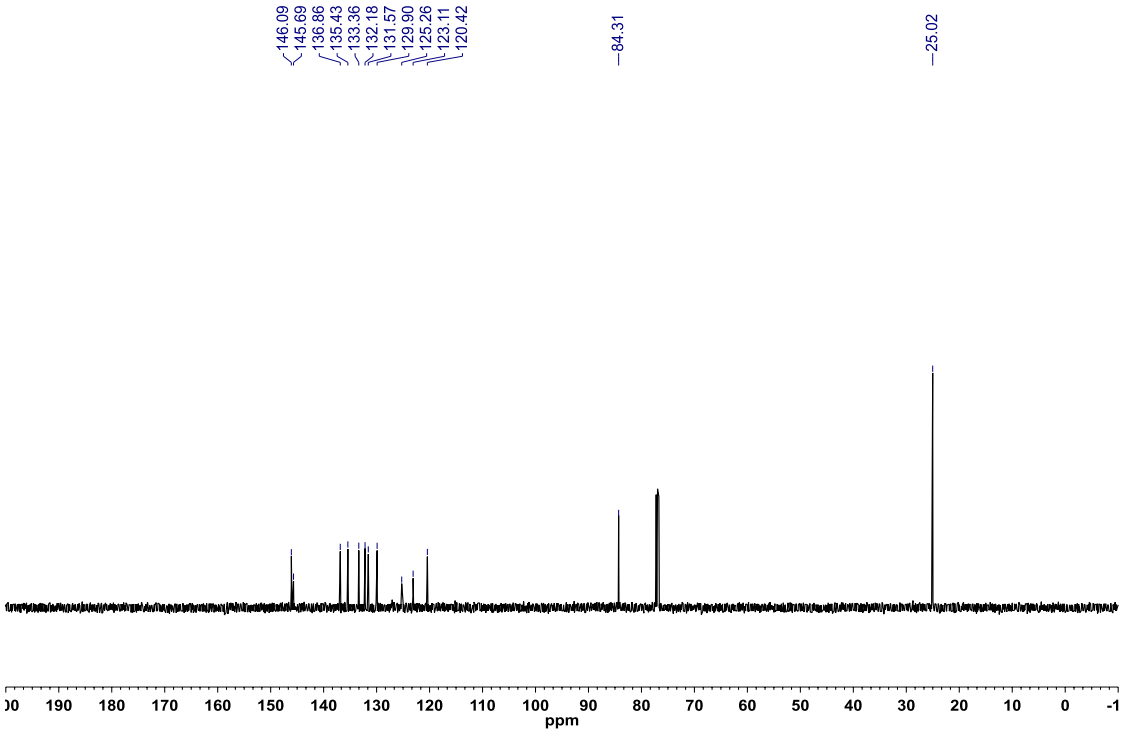

Figure A2.164: ^{11}B NMR ($CDCl_3$, 128.4 MHz) of *2-(3-bromophenyl)-8-(4,4,5,5-tetramethyl-1,3,2-dioxaboryl)-2,1-borazaronaphthalene* (**3.40**)

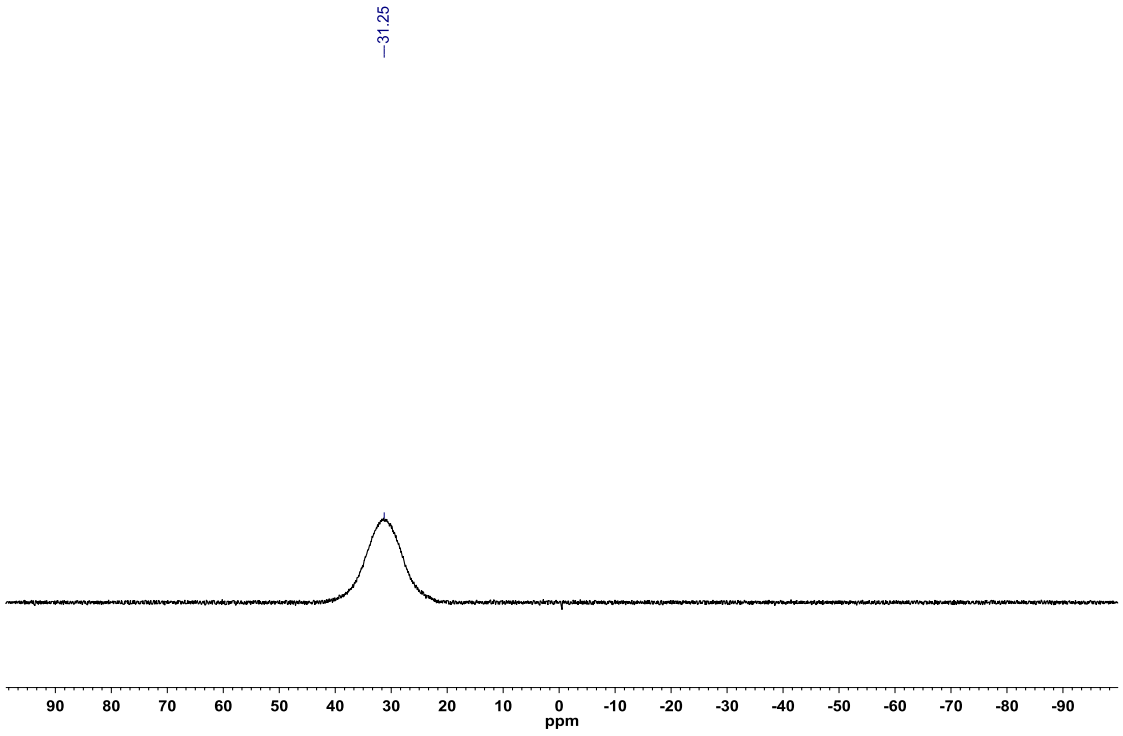

Figure A2.165: ^{1}H NMR ($CDCl_3$, 500.4 MHz) of *2-(2-bromophenyl)-8-(4,4,5,5-tetramethyl-1,3,2-dioxaboryl)-2,1-borazaronaphthalene* (**3.41**)

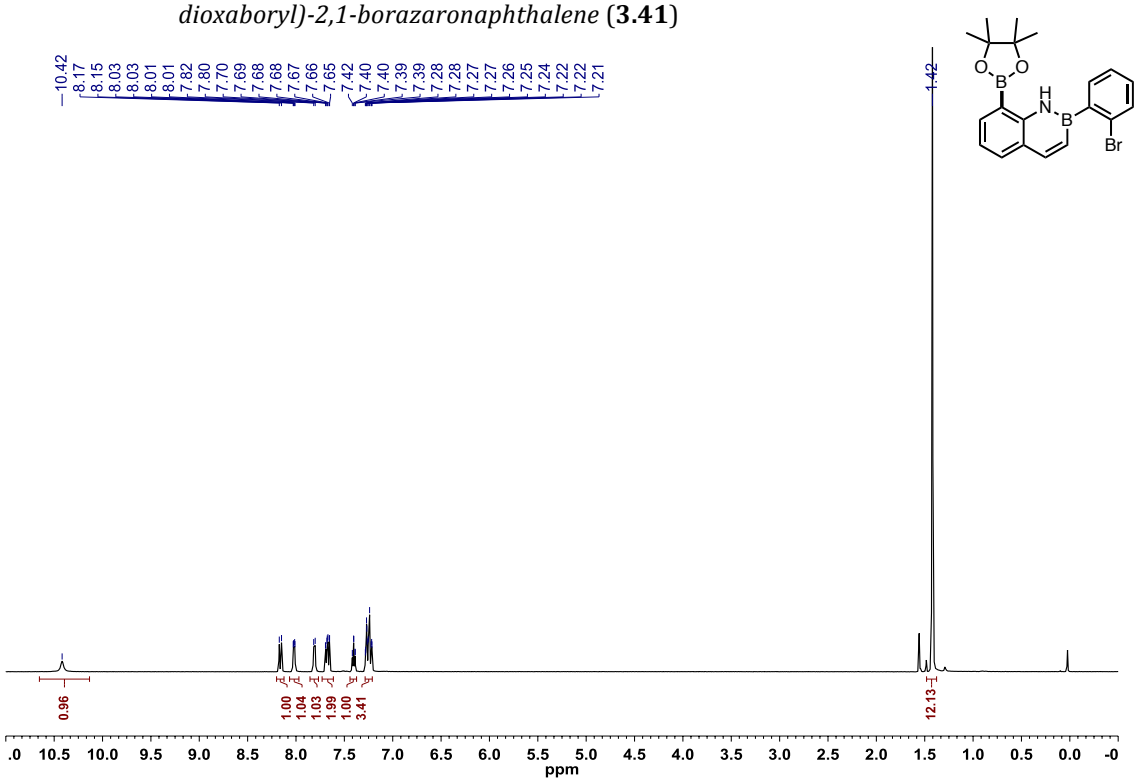

Figure A2.166: ^{13}C {^{1}H} NMR ($CDCl_3$, 125.8 MHz) of *2-(2-bromophenyl)-8-(4,4,5,5-tetramethyl-1,3,2-dioxaboryl)-2,1-borazaronaphthalene* (**3.41**)

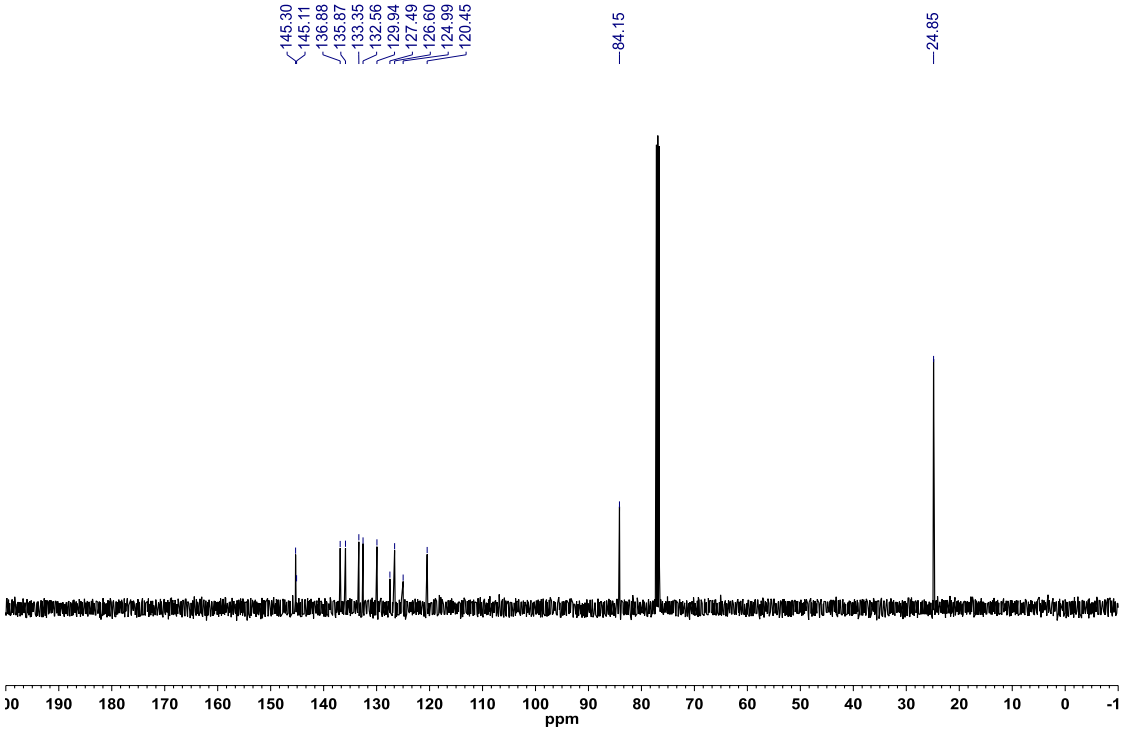

Figure A2.167: ^{11}B NMR ($CDCl_3$, 128.4 MHz) of *2-(2-bromophenyl)-8-(4,4,5,5-tetramethyl-1,3,2-dioxaboryl)-2,1-borazaronaphthalene* (**3.41**)

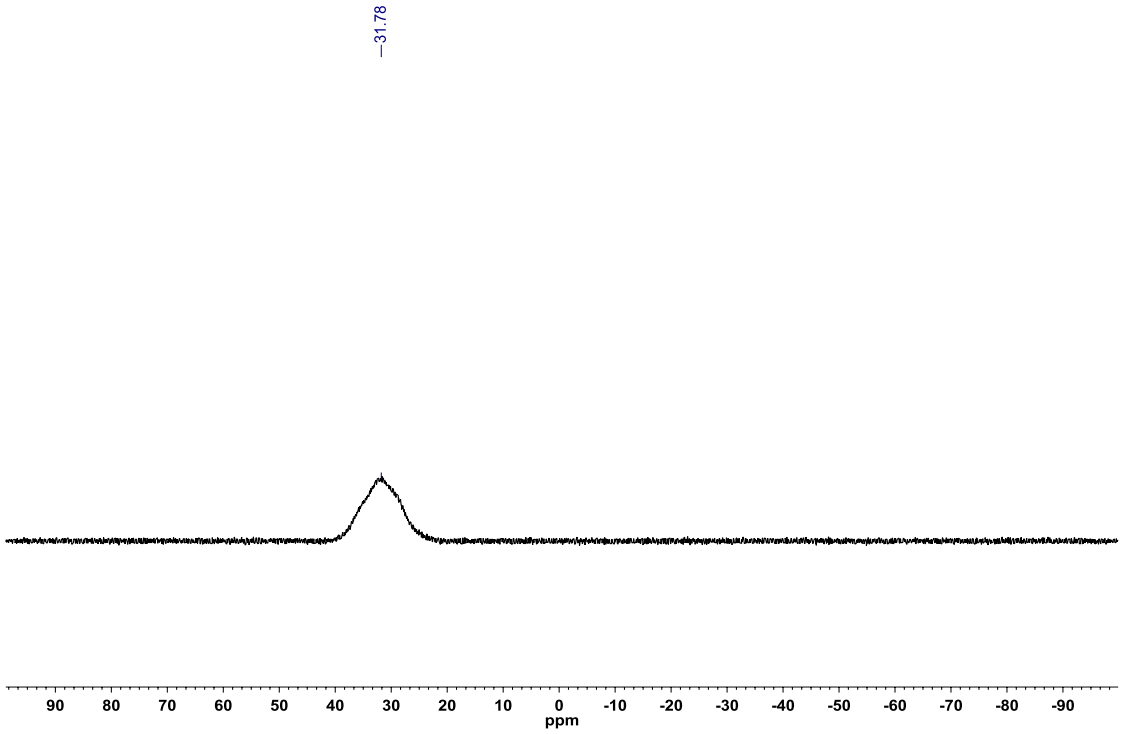

Figure A2.168: ^{1}H NMR ($CDCl_3$, 500.4 MHz) of *2-(3-chlorophenyl)-8-(4,4,5,5-tetramethyl-1,3,2-dioxaboryl)-2,1-borazaronaphthalene* (**3.42**)

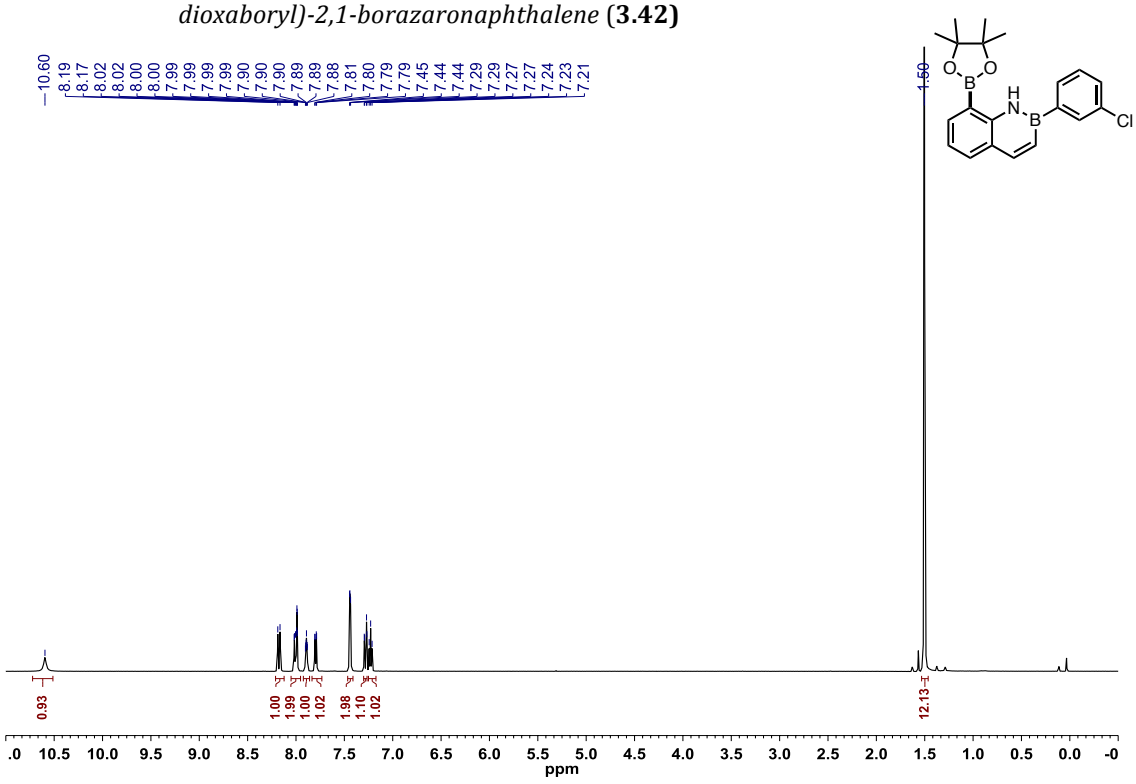

Figure A2.169: ^{13}C {^{1}H} NMR ($CDCl_3$, 125.8 MHz) of *2-(3-chlorophenyl)-8-(4,4,5,5-tetramethyl-1,3,2-dioxaboryl)-2,1-borazaronaphthalene* (**3.42)**

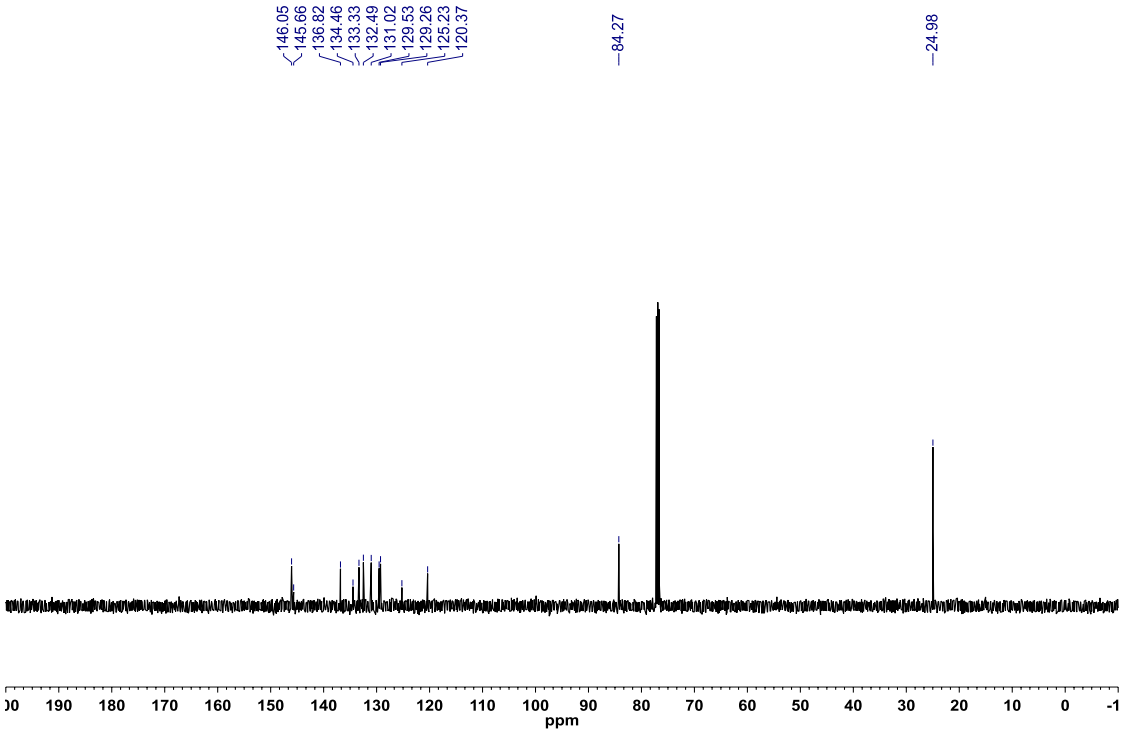

Figure A2.170: ^{11}B NMR ($CDCl_3$, 128.4 MHz) of *2-(3-chlorophenyl)-8-(4,4,5,5-tetramethyl-1,3,2-dioxaboryl)-2,1-borazaronaphthalene* (**3.42)**

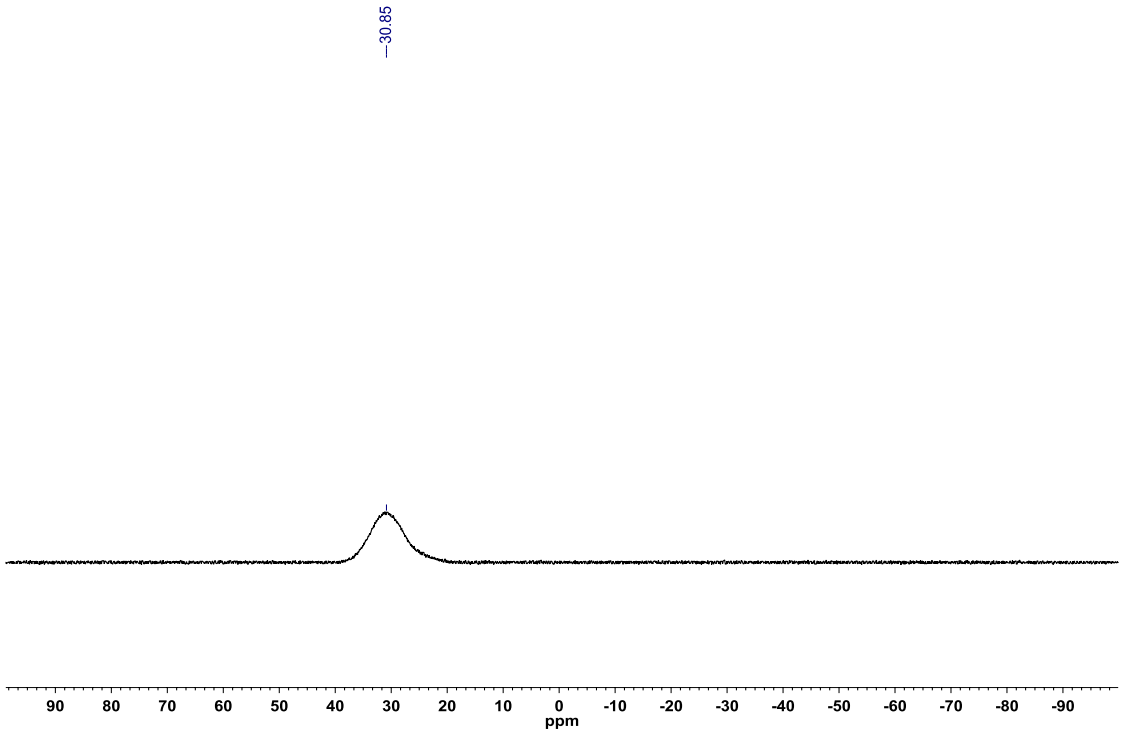

Figure A2.171: ^{1}H NMR ($CDCl_3$, 500.4 MHz) of *2-(benzothiophen-2-yl)-8-(4,4,5,5-tetramethyl-1,3,2-dioxaboryl)-2,1-borazaronaphthalene* (**3.43**)

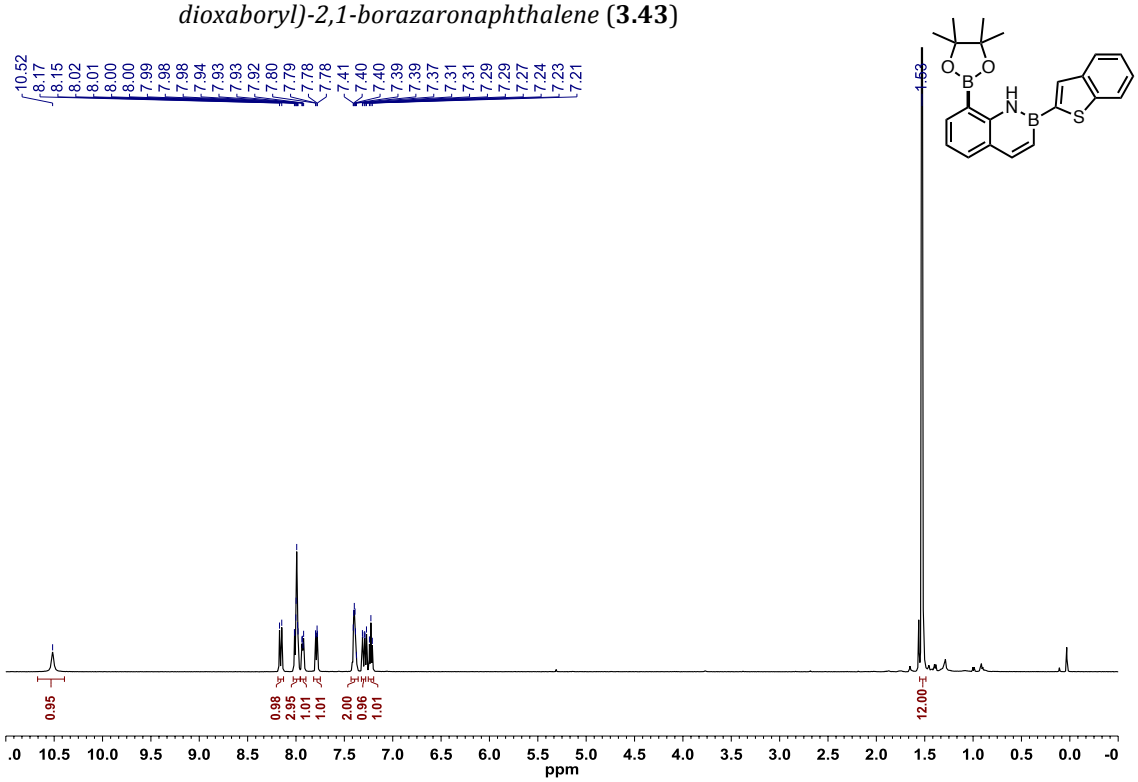

Figure A2.172: ^{13}C {^{1}H} NMR ($CDCl_3$, 125.8 MHz) of *2-(benzothiophen-2-yl)-8-(4,4,5,5-tetramethyl-1,3,2-dioxaboryl)-2,1-borazaronaphthalene* (**3.43**)

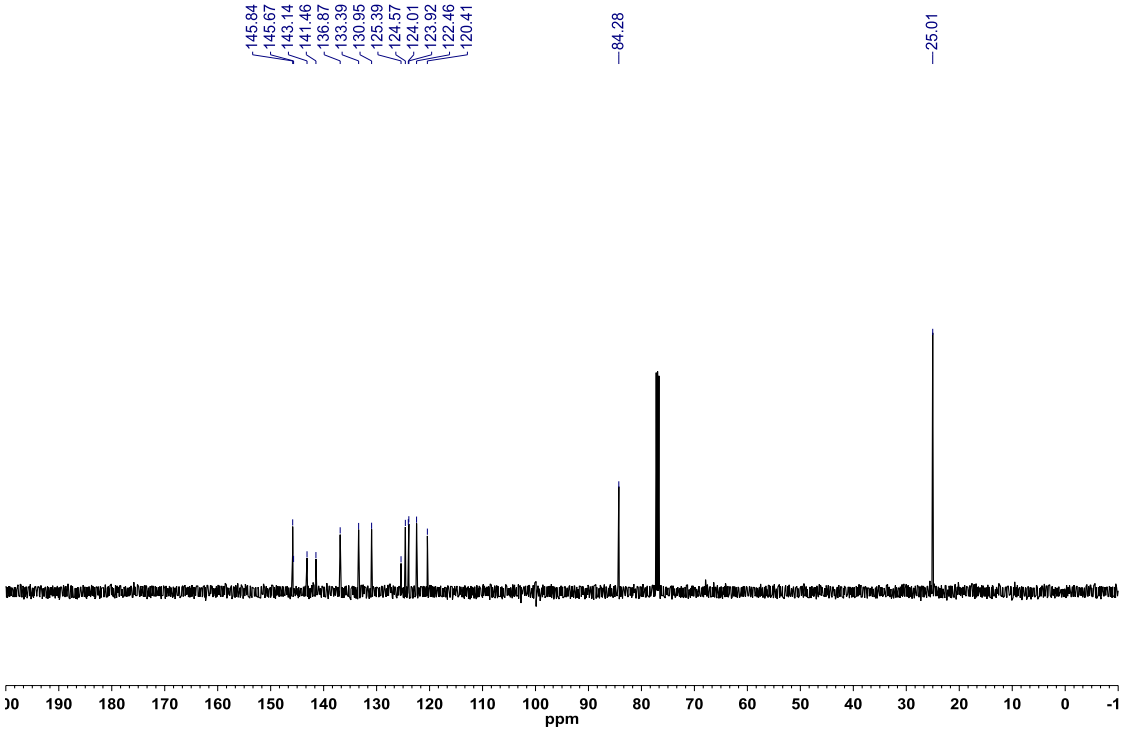

Figure A2.173: ^{11}B NMR ($CDCl_3$, 128.4 MHz) of *2-(benzothiophen-2-yl)-8-(4,4,5,5-tetramethyl-1,3,2-dioxaboryl)-2,1-borazaronaphthalene* (**3.43**)

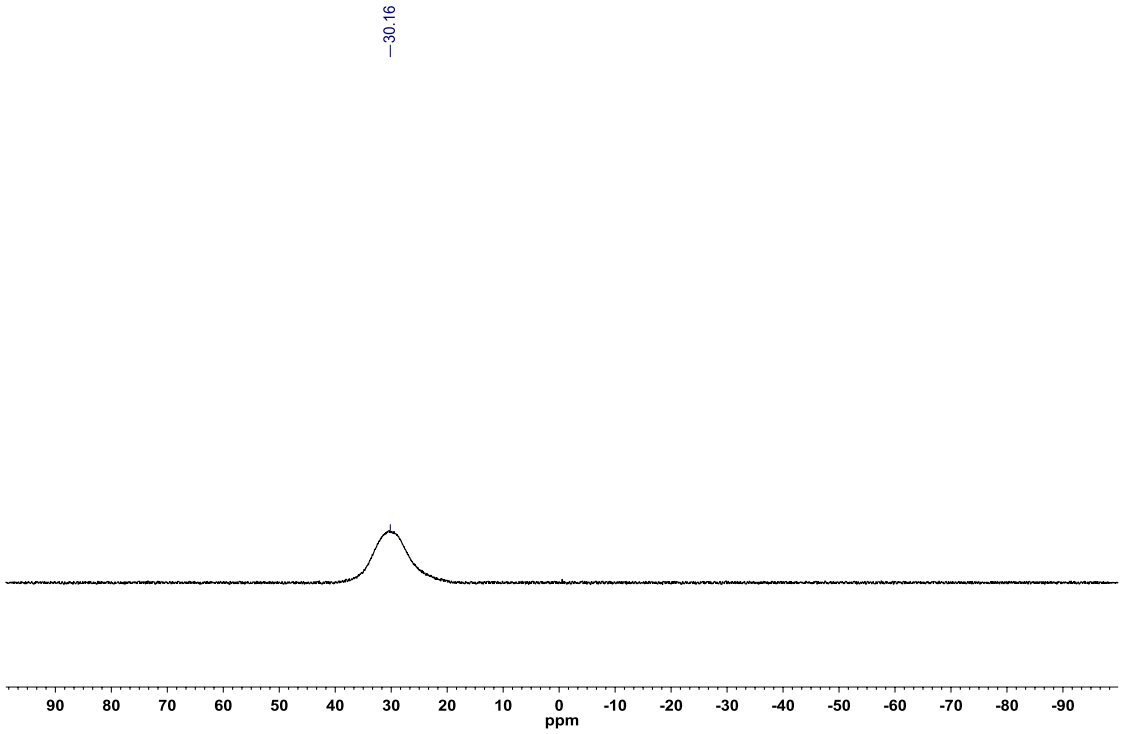

Figure A2.174: ^{1}H NMR ($CDCl_3$, 500.4 MHz) of *2-(furan-3-yl)-8-(4,4,5,5-tetramethyl-1,3,2-dioxaboryl)-2,1-borazaronaphthalene* (**3.44**)

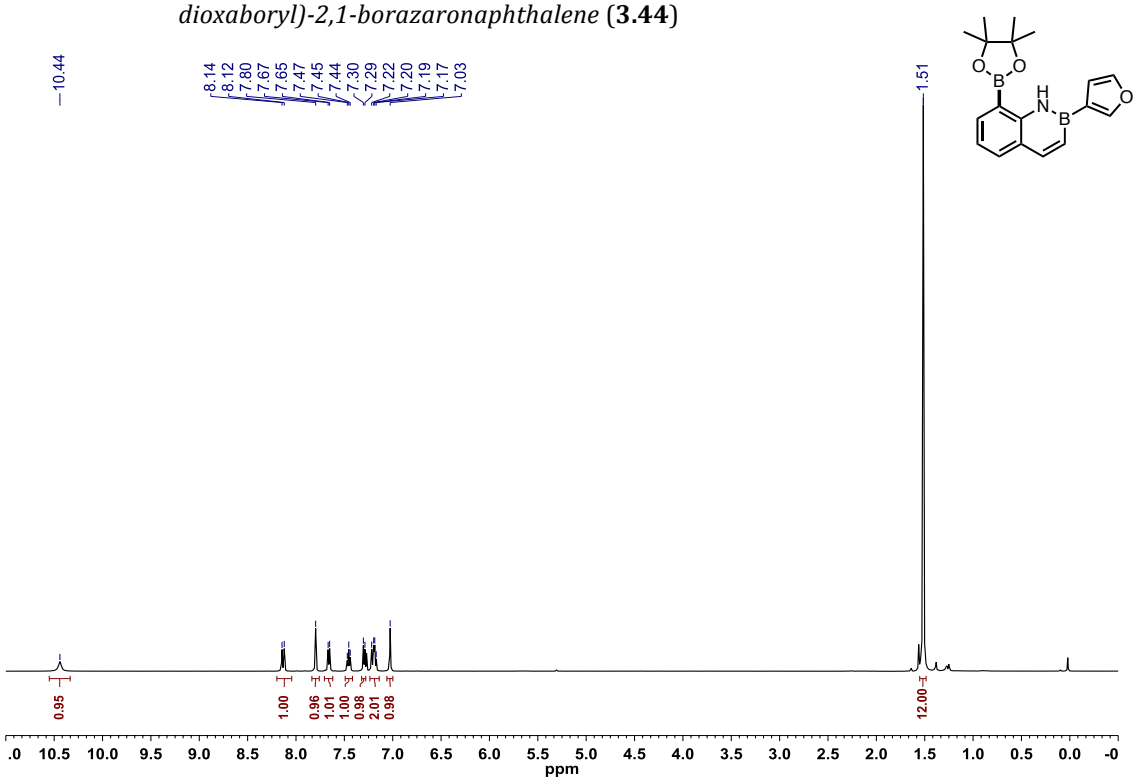

Figure A2.175: ^{13}C {^{1}H} NMR ($CDCl_3$, 125.8 MHz) of *2-(furan-3-yl)-8-(4,4,5,5-tetramethyl-1,3,2-dioxaboryl)-2,1-borazaronaphthalene* (**3.44**)

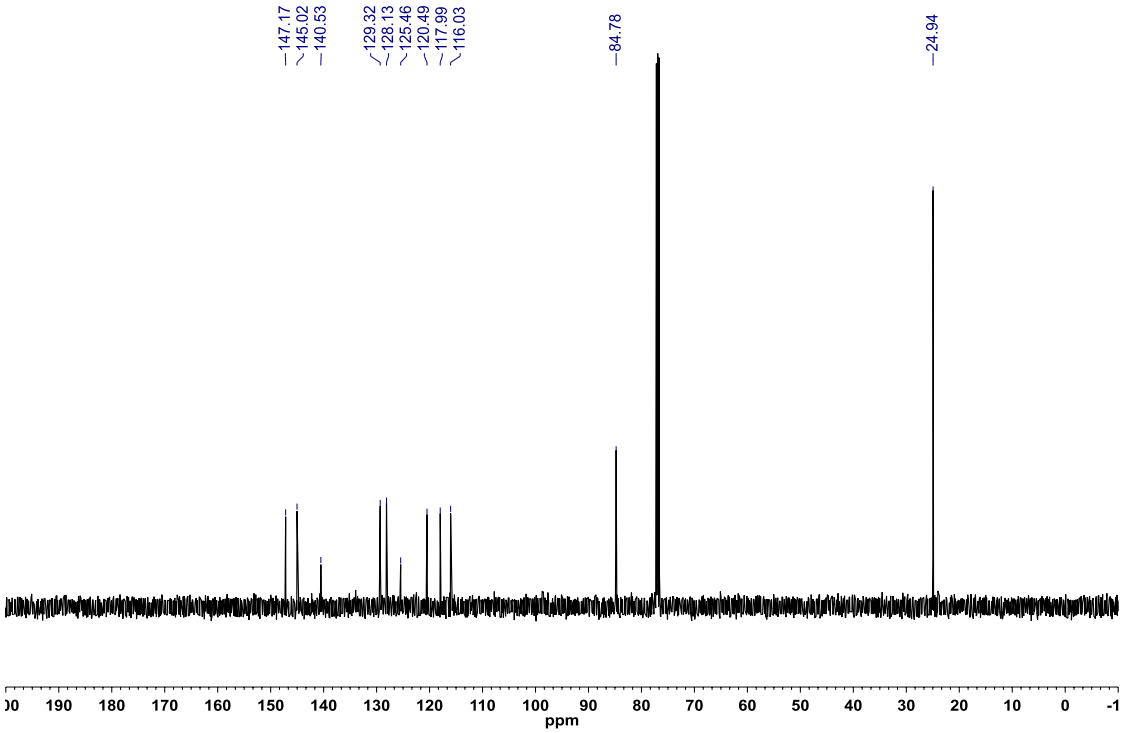

Figure A2.176: ^{11}B NMR ($CDCl_3$, 128.4 MHz) of *2-(furan-3-yl)-8-(4,4,5,5-tetramethyl-1,3,2-dioxaboryl)-2,1-borazaronaphthalene* (**3.44**)

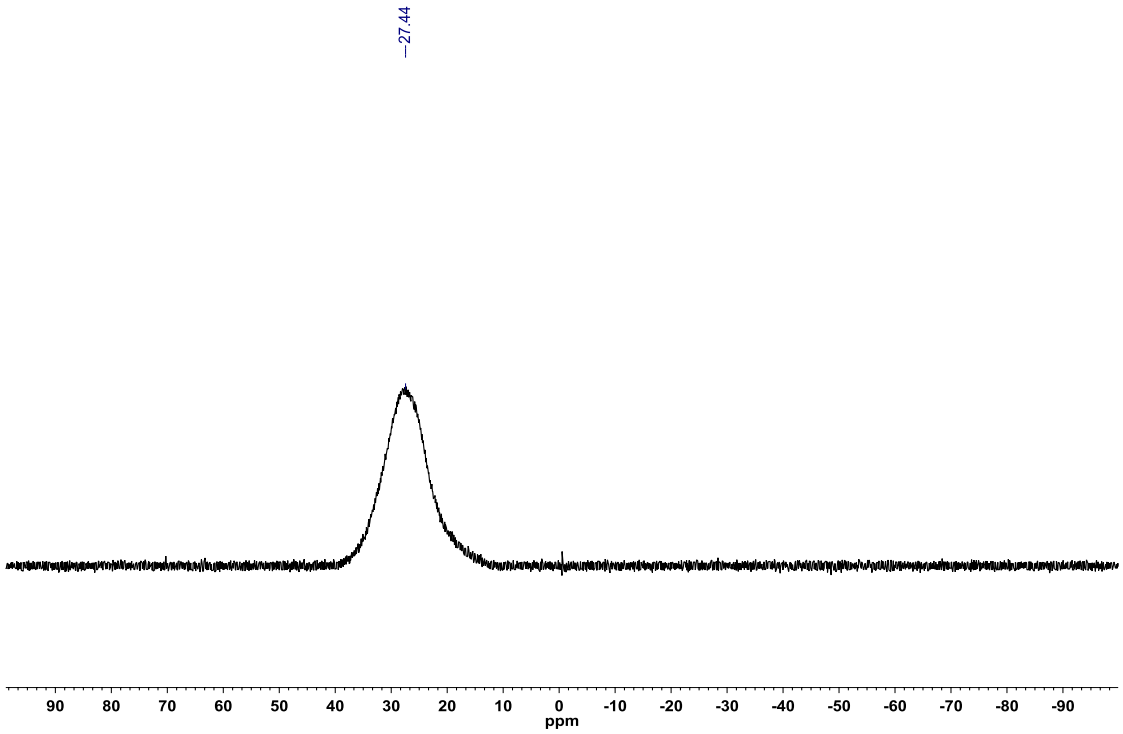

Figure A2.177: ^{1}H NMR ($CDCl_3$, 500.4 MHz) of *2-methyl-8-(4,4,5,5-tetramethyl-1,3,2-dioxaboryl)-2,1-borazaronaphthalene* (**3.45**)

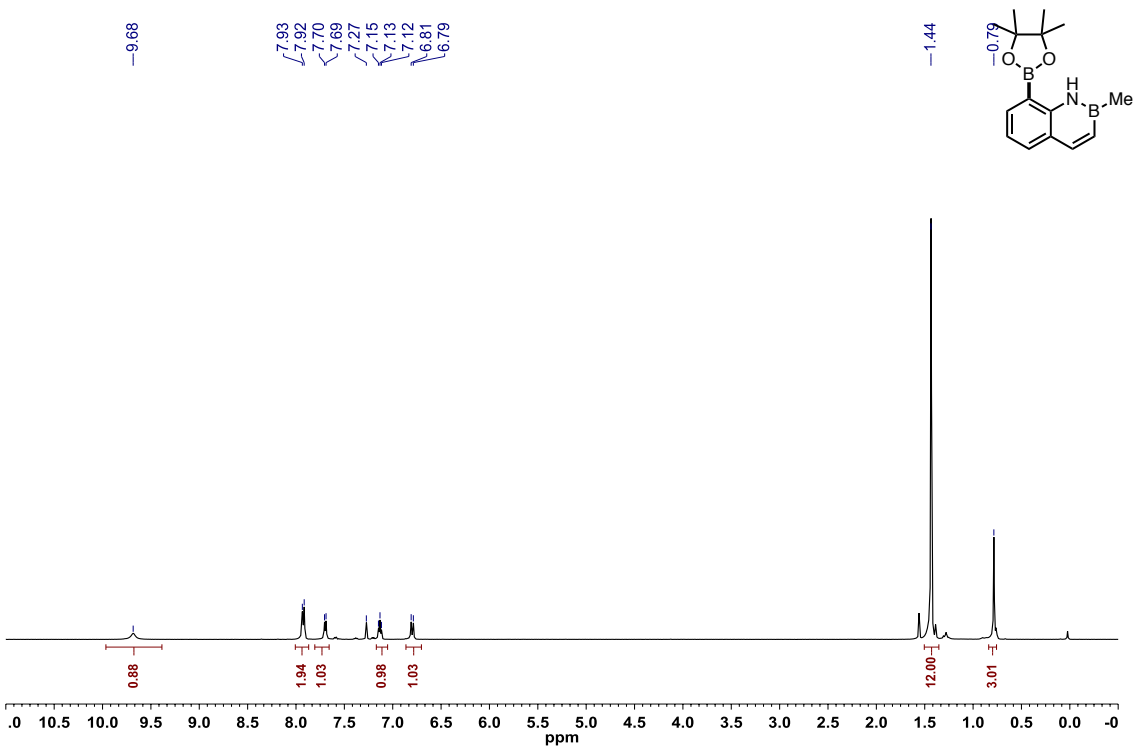

Figure A2.178: ^{13}C {^{1}H} NMR ($CDCl_3$, 125.8 MHz) of *2-methyl-8-(4,4,5,5-tetramethyl-1,3,2-dioxaboryl)-2,1-borazaronaphthalene* (**3.45**)

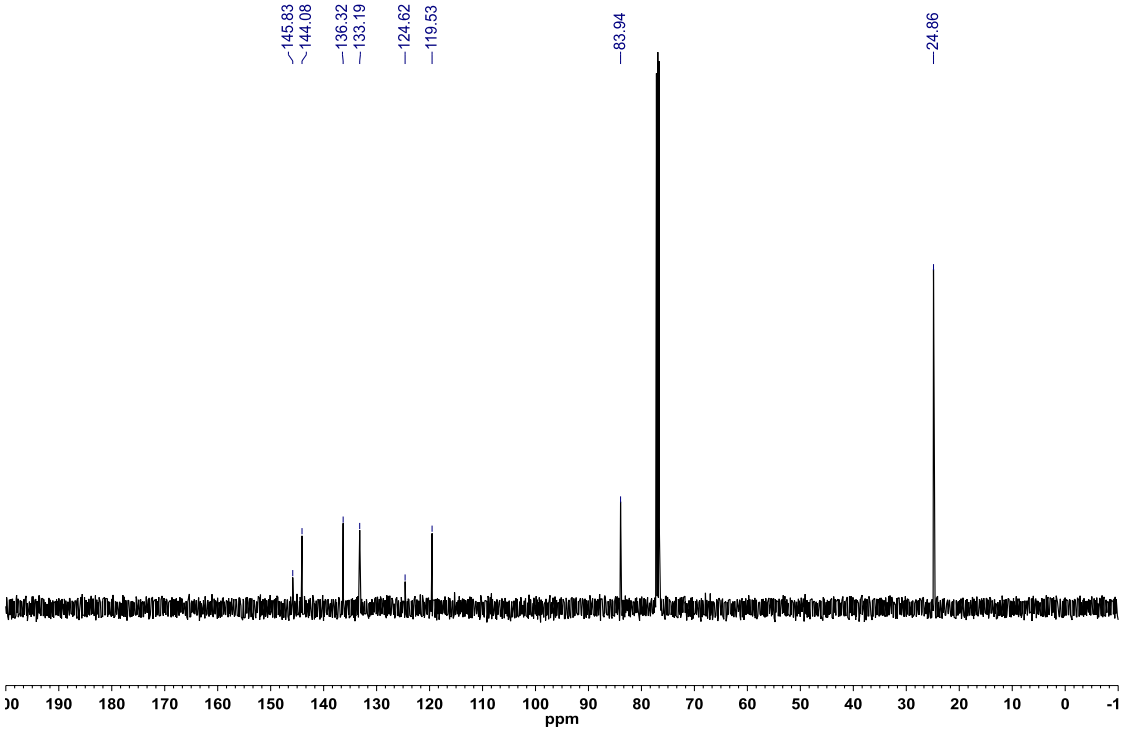

Figure A2.179: ^{11}B NMR ($CDCl_3$, 128.4 MHz) of *2-methyl-8-(4,4,5,5-tetramethyl-1,3,2-dioxaboryl)-2,1-borazaronaphthalene* (**3.45**)

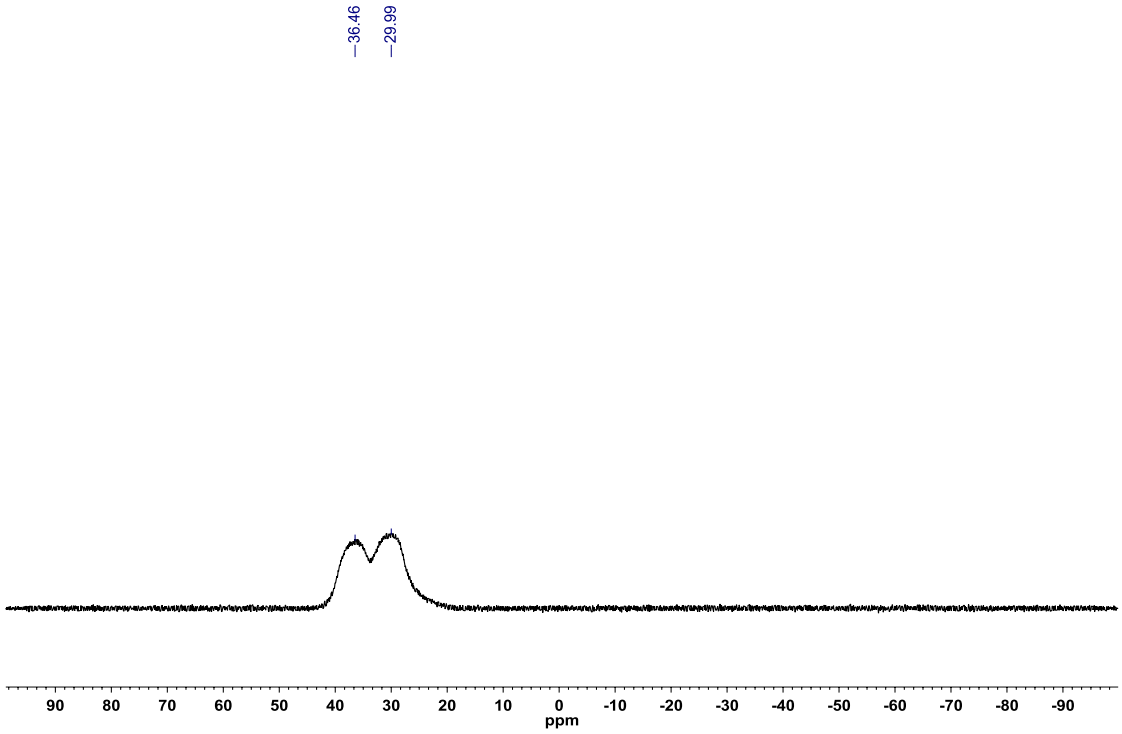

Figure A2.180: ^{1}H NMR ($CDCl_3$, 500.4 MHz) of *2-hexyl-8-(4,4,5,5-tetramethyl-1,3,2-dioxaboryl)-2,1-borazaronaphthalene* (**3.46**)

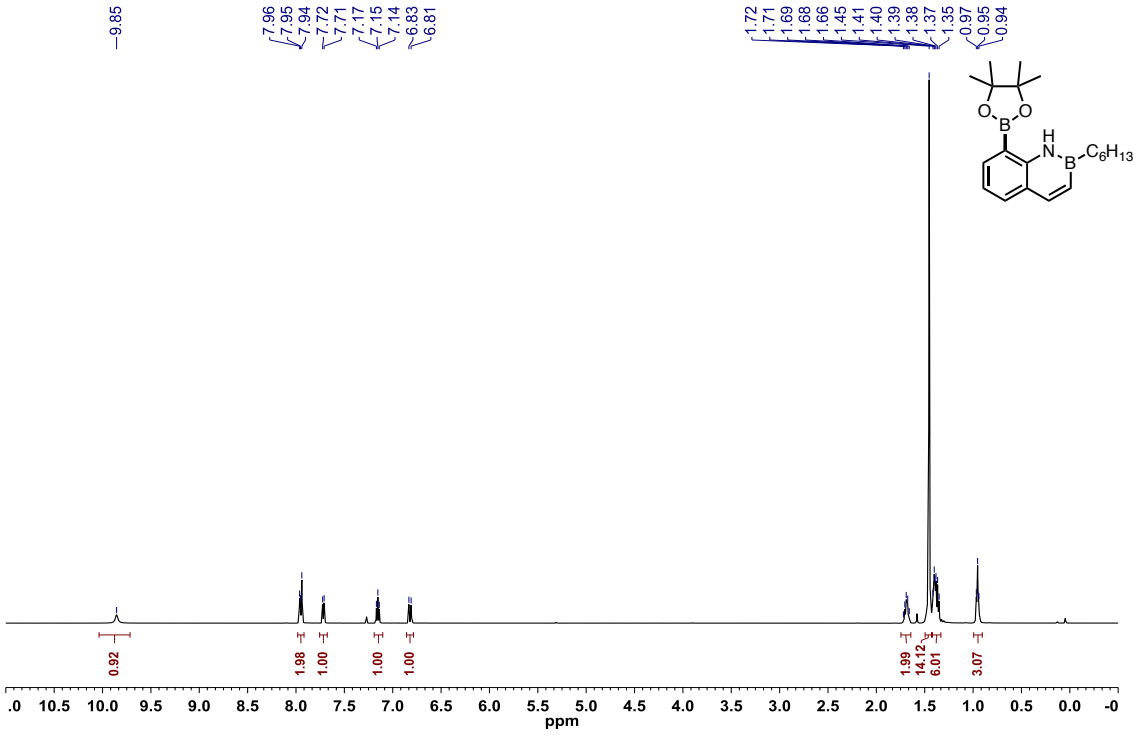

Figure A2.181: ^{13}C {^{1}H} NMR ($CDCl_3$, 125.8 MHz) of *2-hexyl-8-(4,4,5,5-tetramethyl-1,3,2-dioxaboryl)-2,1-borazaronaphthalene* (**3.46**)

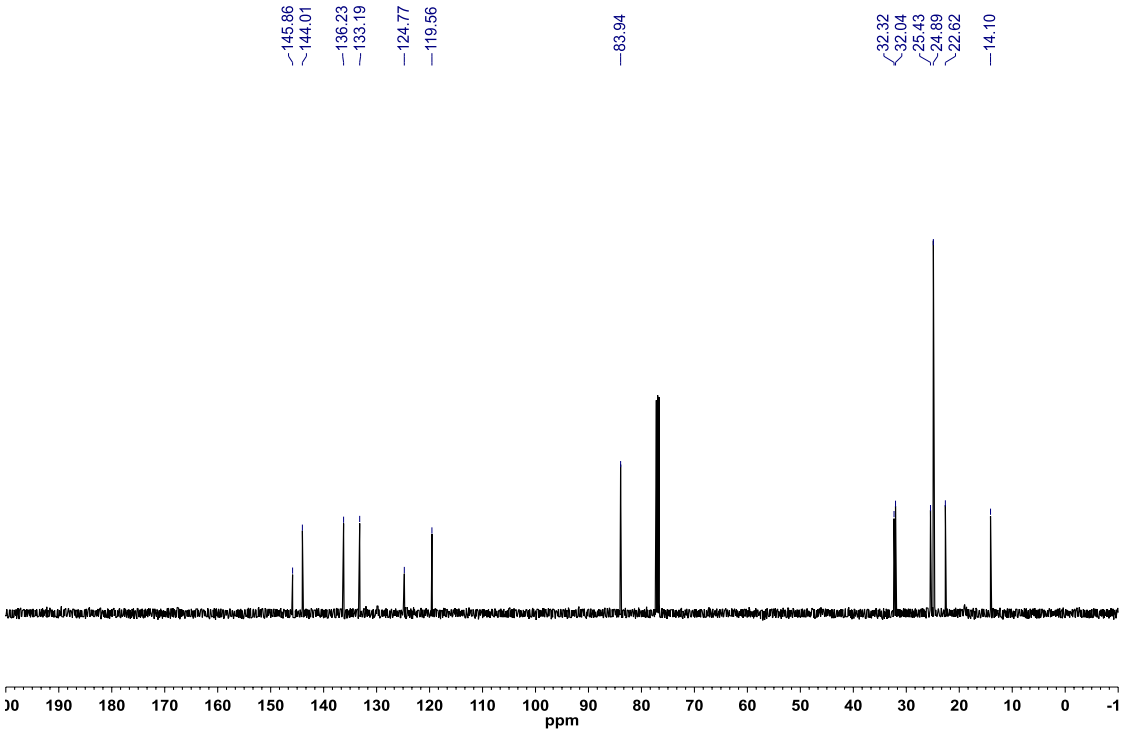

Figure A2.182: ^{11}B NMR ($CDCl_3$, 128.4 MHz) of *2-hexyl-8-(4,4,5,5-tetramethyl-1,3,2-dioxaboryl)-2,1-borazaronaphthalene* (**3.46**)

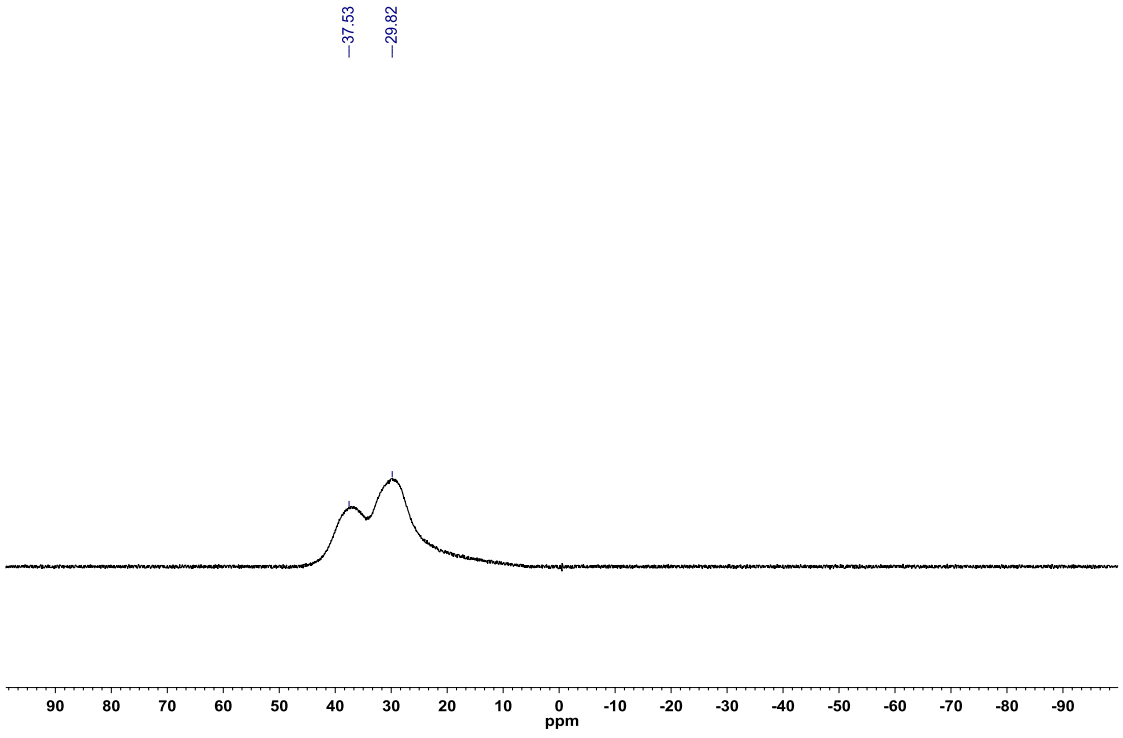

Figure A2.183: ^{1}H NMR ($CDCl_3$, 500.4 MHz) of *2-phenethyl-8-(4,4,5,5-tetramethyl-1,3,2-dioxaboryl)-2,1-borazaronaphthalene* (**3.47**)

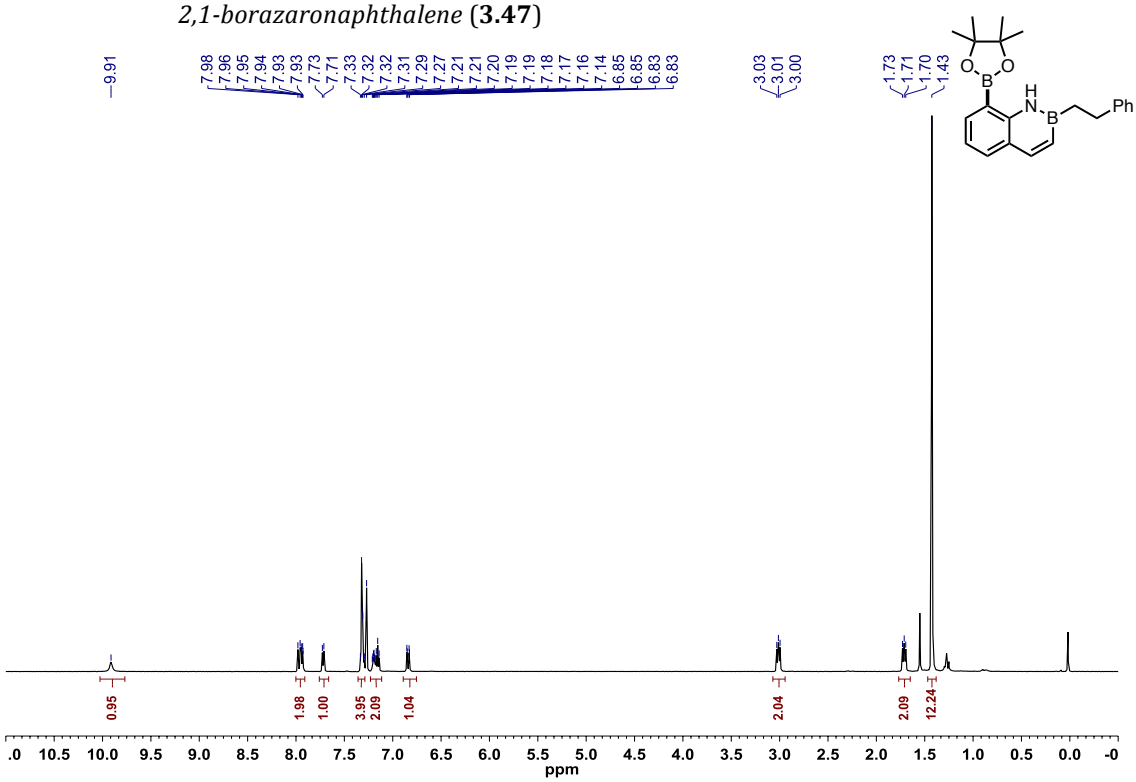

Figure A2.184: ^{13}C {^{1}H} NMR ($CDCl_3$, 125.8 MHz) of *2-phenethyl-8-(4,4,5,5-tetramethyl-1,3,2-dioxaboryl)-2,1-borazaronaphthalene* (**3.47**)

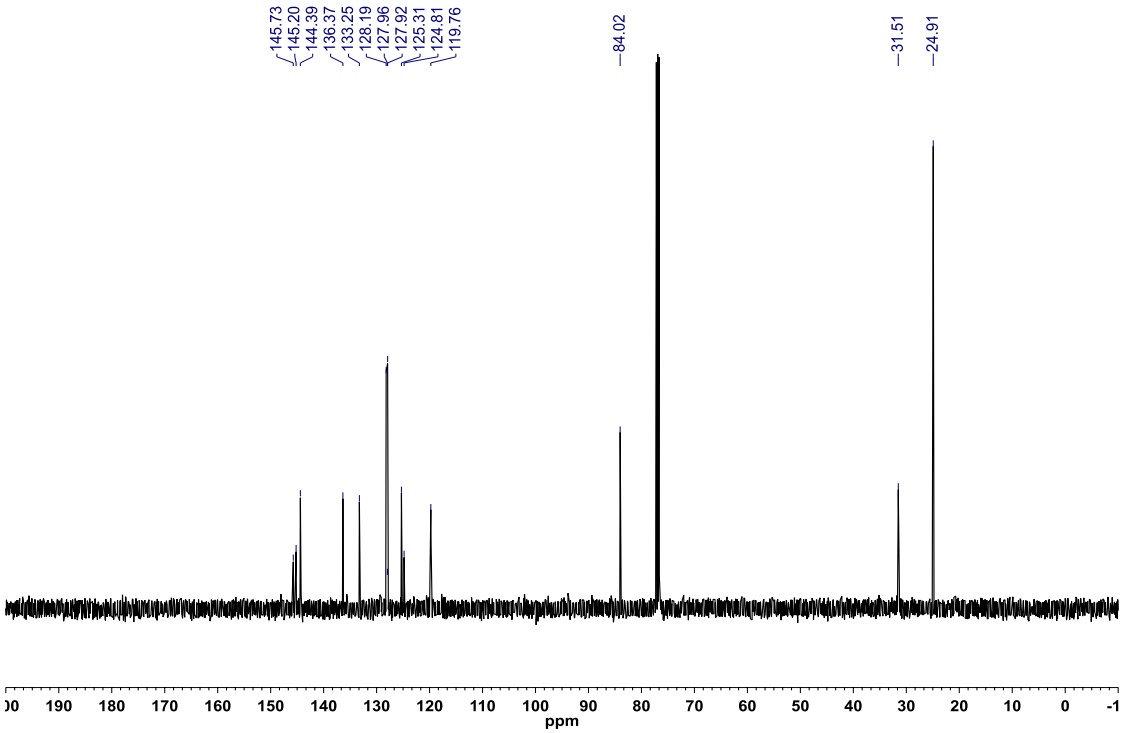

Figure A2.185: ^{11}B NMR ($CDCl_3$, 128.4 MHz) of *2-phenethyl-8-(4,4,5,5-tetramethyl-1,3,2-dioxaboryl)-2,1-borazaronaphthalene* (**3.47**)

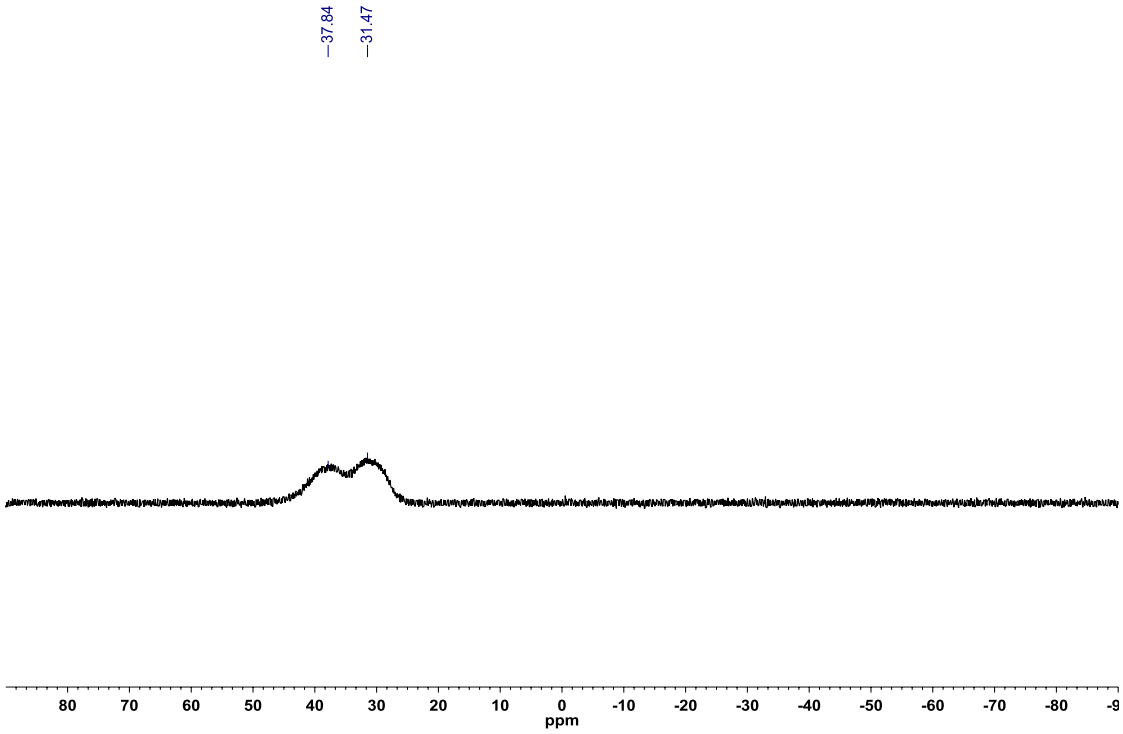

Figure A2.186: ^{1}H NMR ($CDCl_3$, 500.4 MHz) of *2-cyclopropyl-8-(4,4,5,5-tetramethyl-1,3,2-dioxaboryl)-2,1-borazaronaphthalene* (**3.48**)

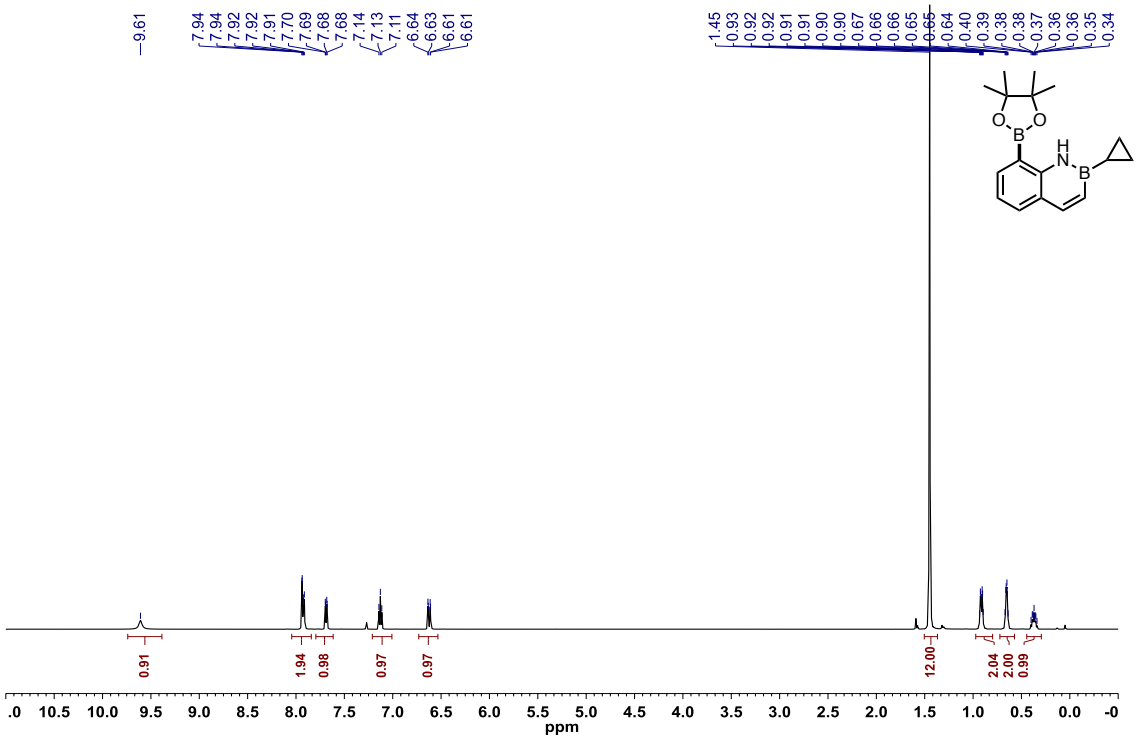

Figure A2.187: ^{13}C {^{1}H} NMR ($CDCl_3$, 125.8 MHz) of *2-cyclopropyl-8-(4,4,5,5-tetramethyl-1,3,2-dioxaboryl)-2,1-borazaronaphthalene* (**3.48**)

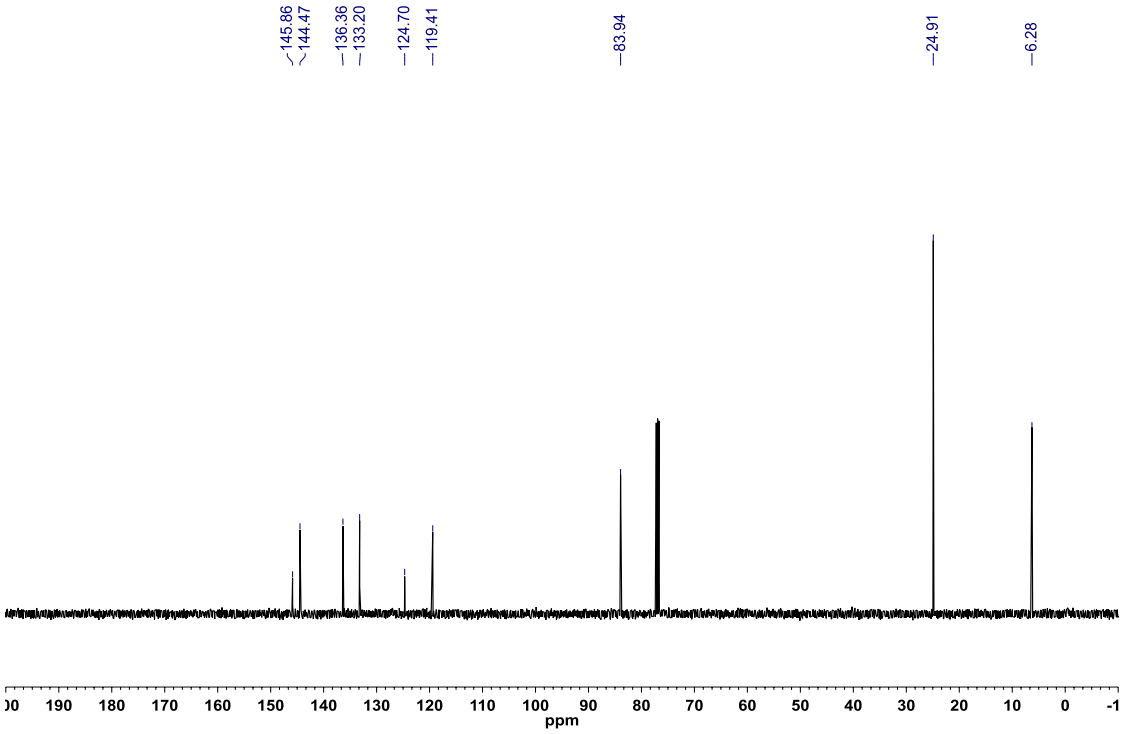

Figure A2.188: ^{11}B NMR ($CDCl_3$, 128.4 MHz) of *2-cyclopropyl-8-(4,4,5,5-tetramethyl-1,3,2-dioxaboryl)-2,1-borazaronaphthalene* (**3.48**)

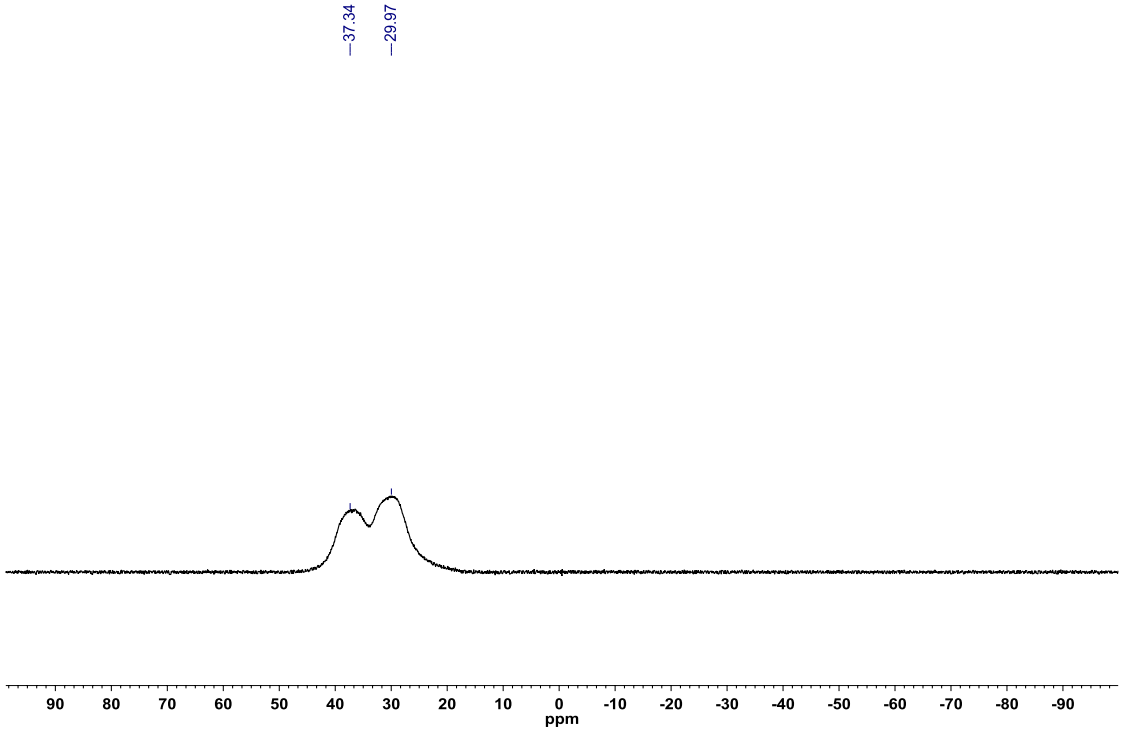

Figure A2.189: ^{1}H NMR ($CDCl_3$, 500.4 MHz) of *2-cyclohexyl-8-(4,4,5,5-tetramethyl-1,3,2-dioxaboryl)-2,1-borazaronaphthalene* (**3.49**)

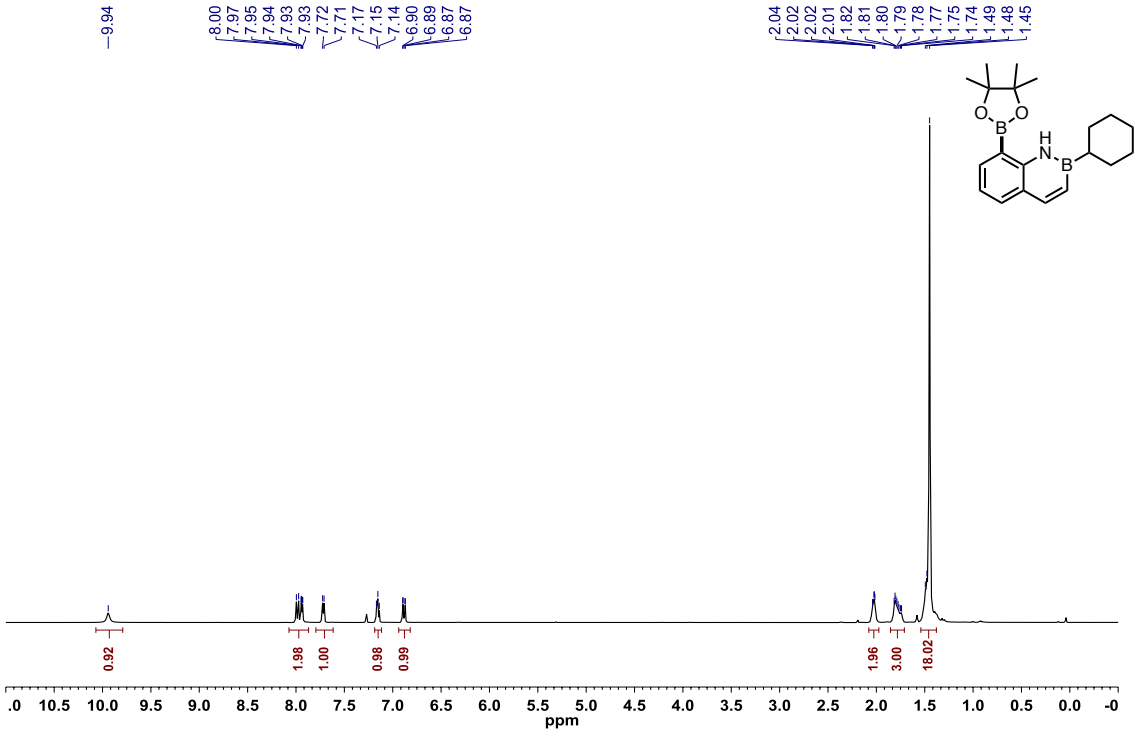

Figure A2.190: ^{13}C {^{1}H} NMR ($CDCl_3$, 125.8 MHz) of *2-cyclohexyl-8-(4,4,5,5-tetramethyl-1,3,2-dioxaboryl)-2,1-borazaronaphthalene* (**3.49**)

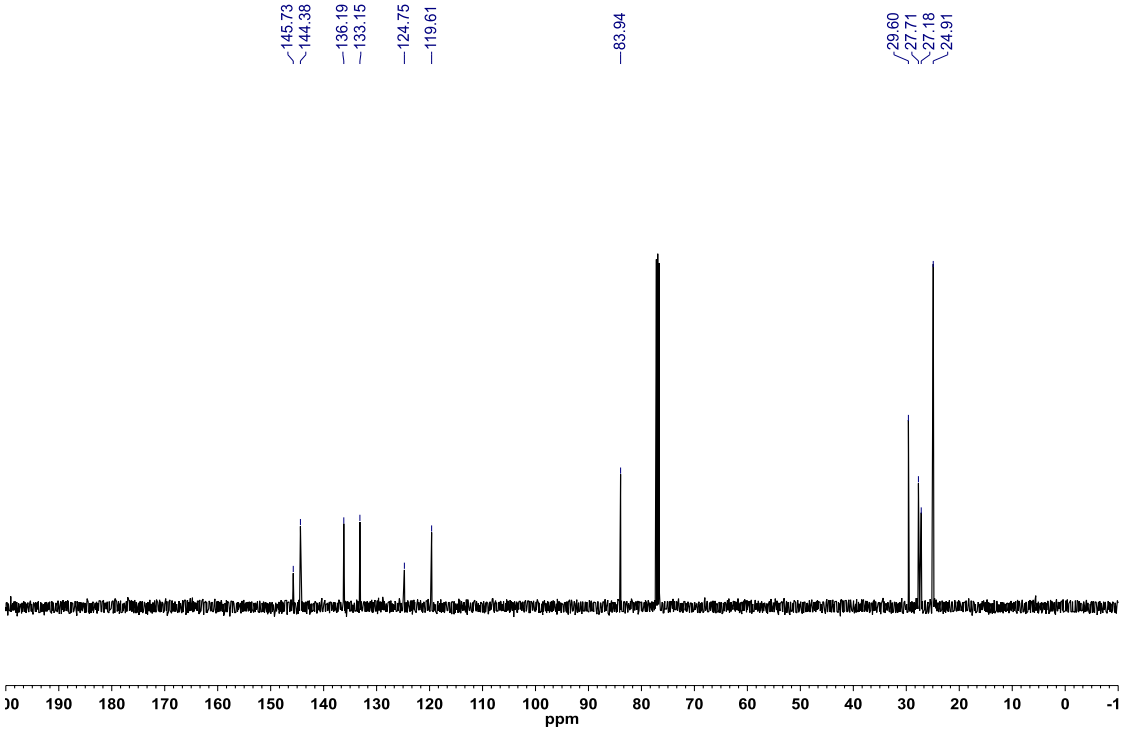

Figure A2.191: ^{11}B NMR ($CDCl_3$, 128.4 MHz) of *2-cyclohexyl-8-(4,4,5,5-tetramethyl-1,3,2-dioxaboryl)-2,1-borazaronaphthalene* (**3.49**)

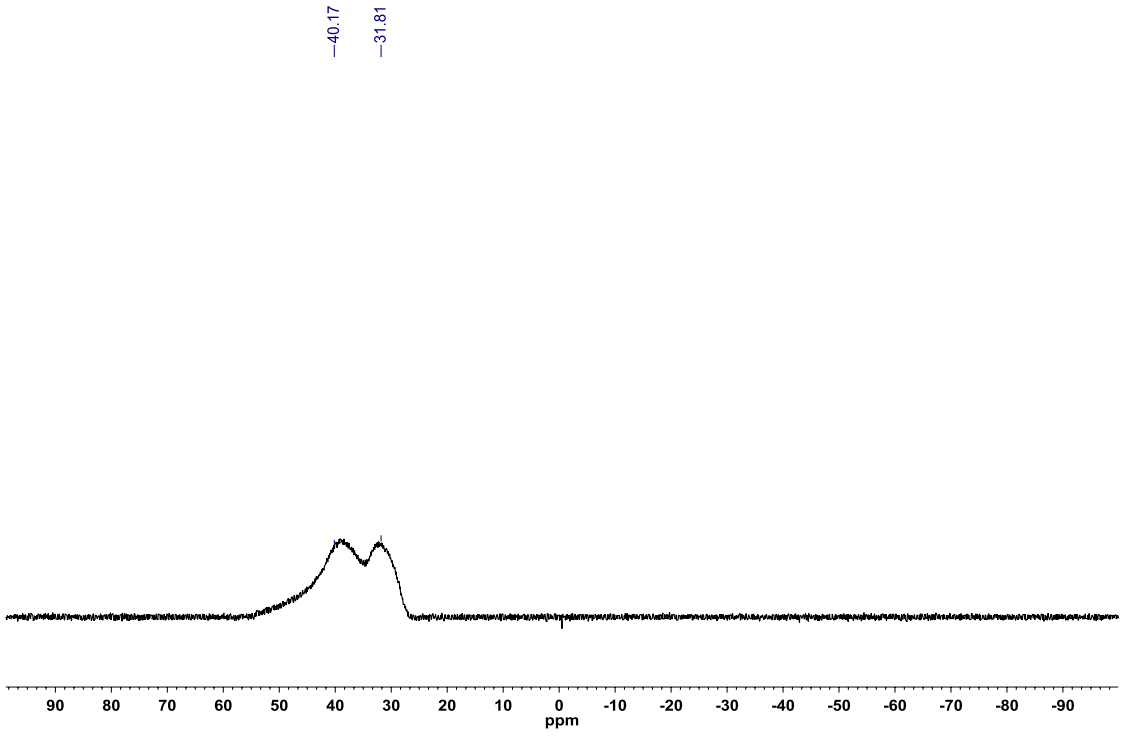

Figure A2.192: ^{1}H NMR ($CDCl_3$, 500.4 MHz) of *3-bromo-2-phenyl-8-(4,4,5,5-tetramethyl-1,3,2-dioxaboryl)-2,1-borazaronaphthalene* (**3.50**)

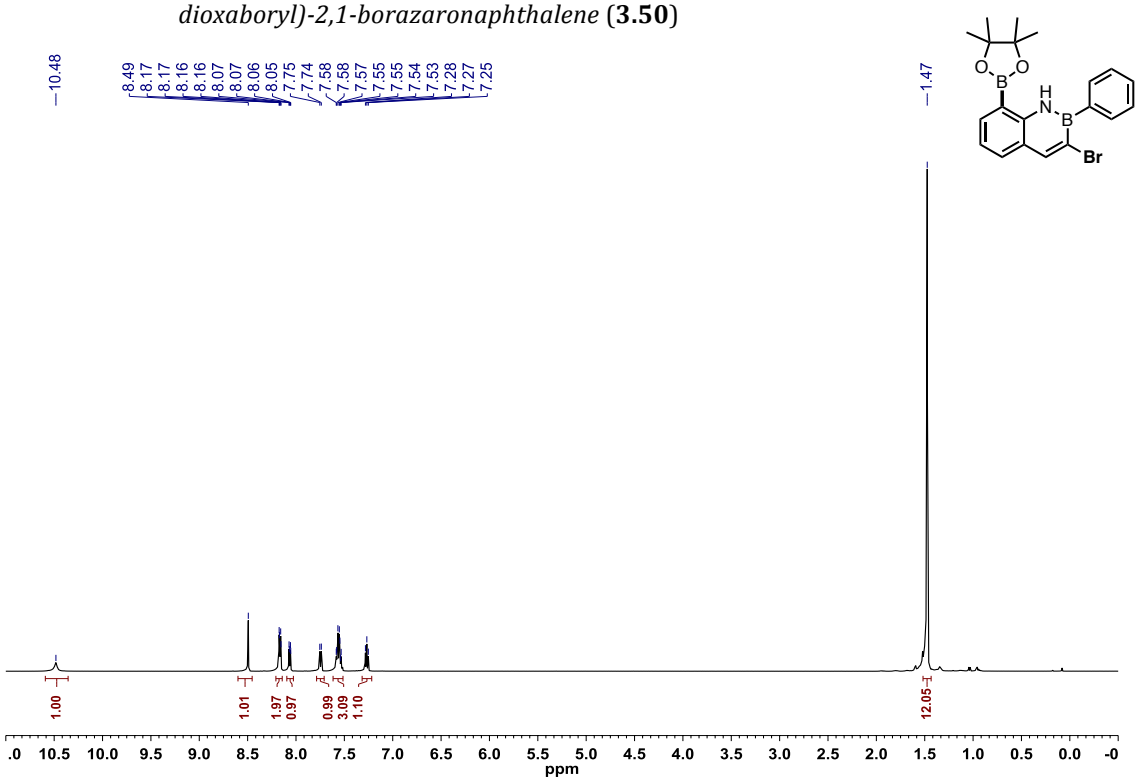

Figure A2.193: ^{13}C {^{1}H} NMR ($CDCl_3$, 125.8 MHz) of *3-bromo-2-phenyl-8-(4,4,5,5-tetramethyl-1,3,2-dioxaboryl)-2,1-borazaronaphthalene* (**3.50**)

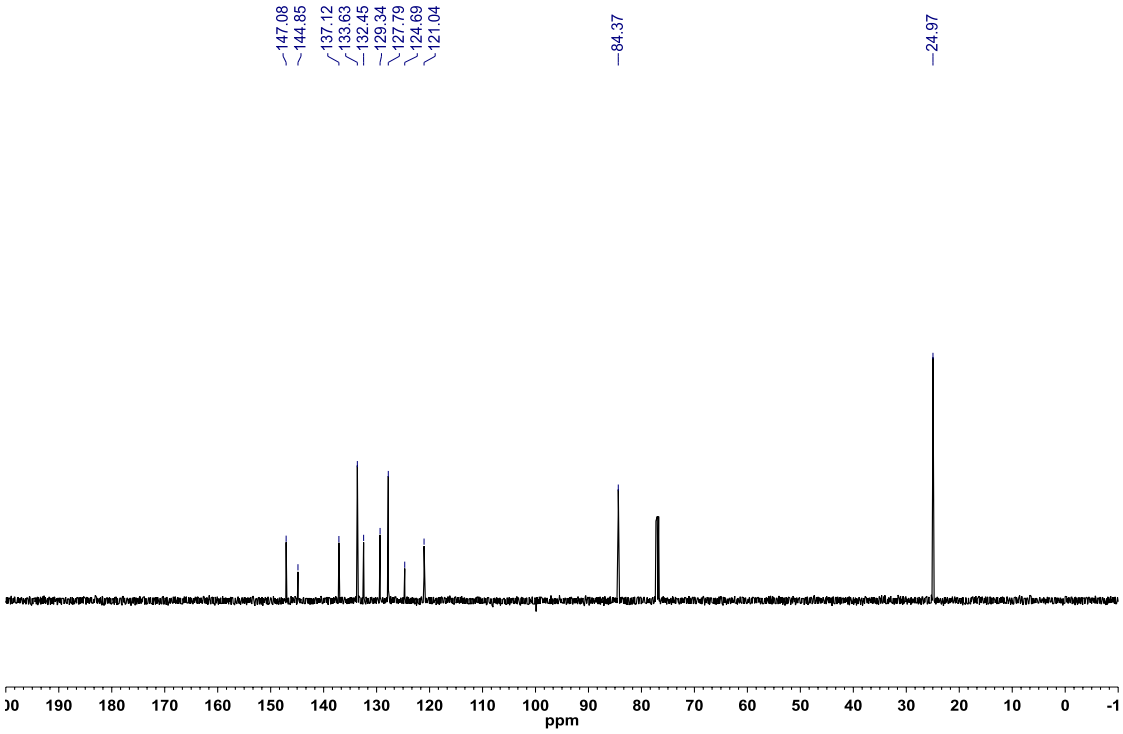

Figure A2.194: ^{11}B NMR ($CDCl_3$, 128.4 MHz) of *3-bromo-2-phenyl-8-(4,4,5,5-tetramethyl-1,3,2-dioxaboryl)-2,1-borazaronaphthalene* (**3.50**)

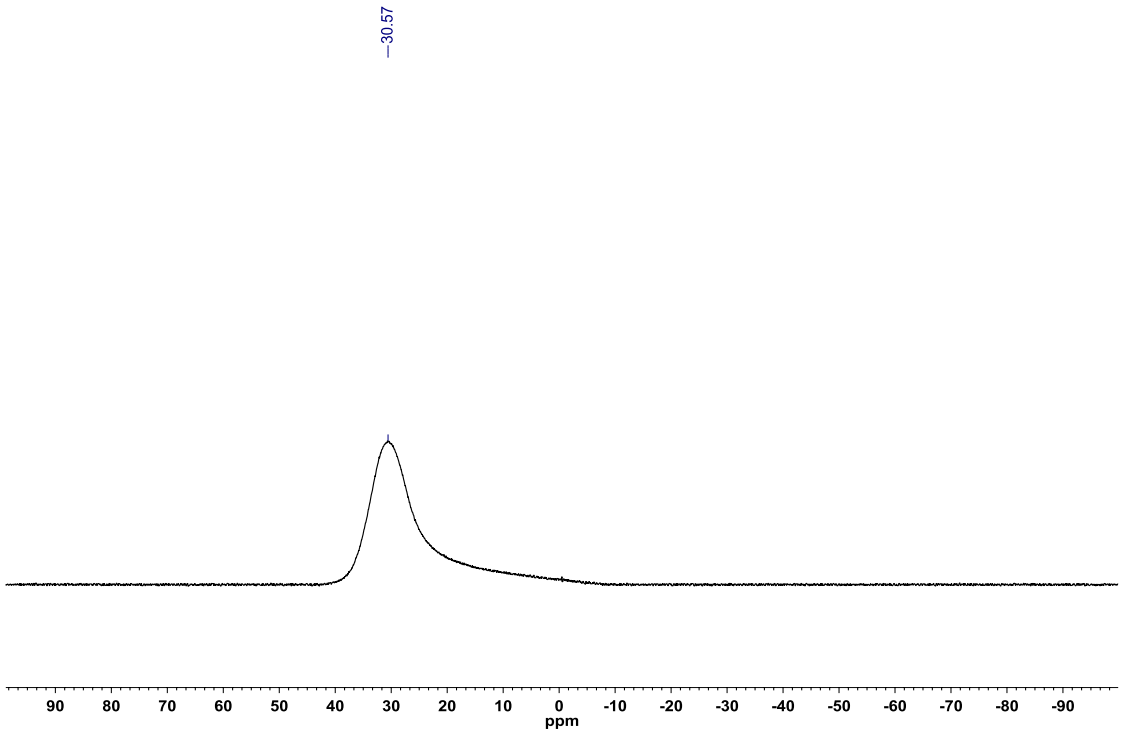

Figure A2.195: ^{1}H NMR ($CDCl_3$, 500.4 MHz) of *3-bromo-8-(4,4,5,5-tetramethyl-1,3,2-dioxaboryl)-2-(4-(trifluoromethyl)phenyl)-2,1-borazaronaphthalene* (**3.51**)

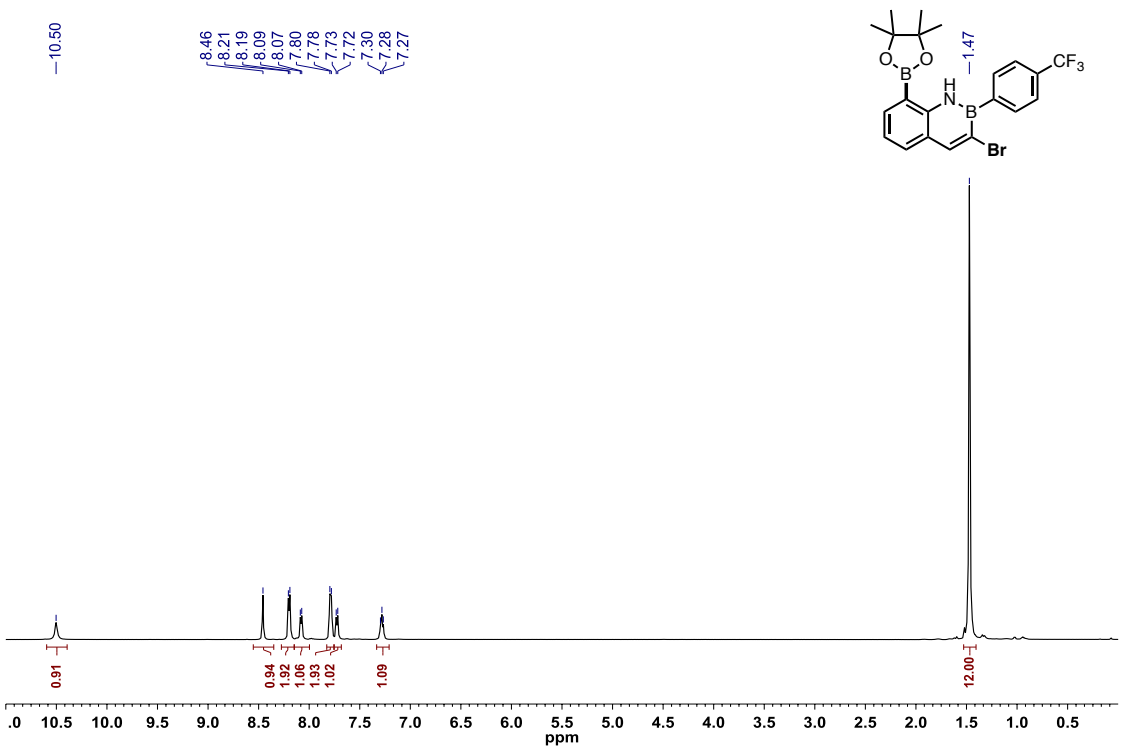

Figure A2.196: ^{13}C {^{1}H} NMR ($CDCl_3$, 125.8 MHz) of *3-bromo-8-(4,4,5,5-tetramethyl-1,3,2-dioxaboryl)-2-(4-(trifluoromethyl)phenyl)-2,1-borazaronaphthalene* (**3.51**)

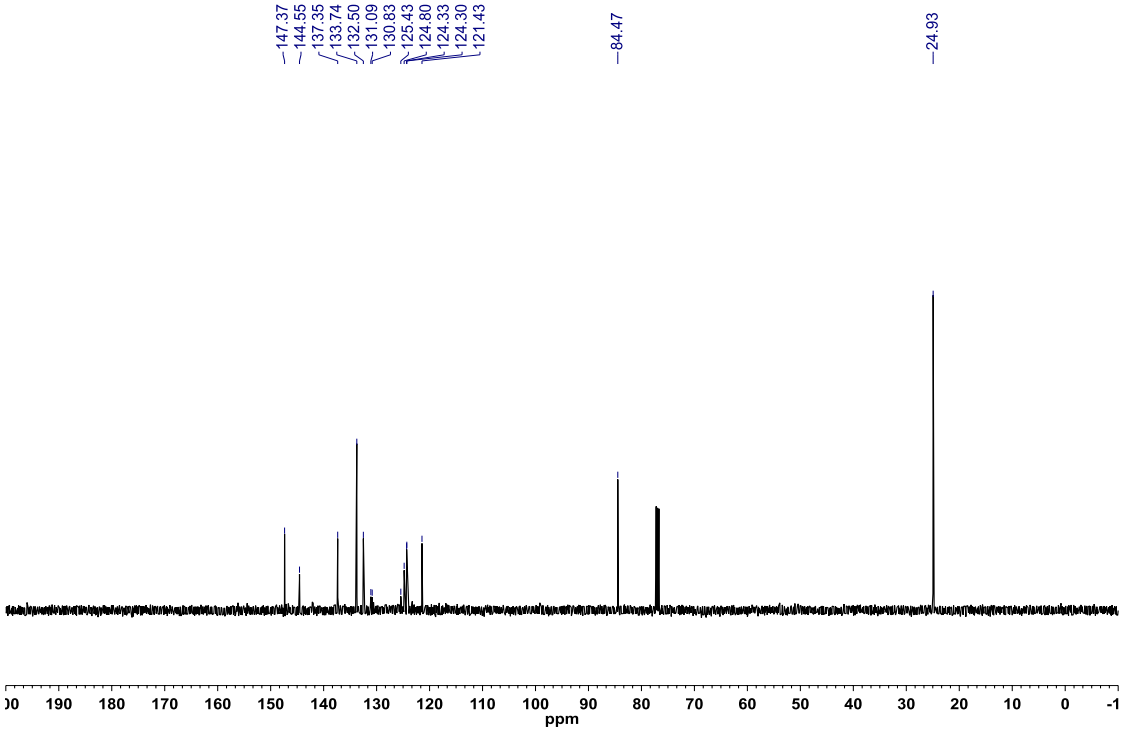

Figure A2.197: ^{19}F {^{1}H} NMR ($CDCl_3$, 470.8 MHz) of *3-bromo-8-(4,4,5,5-tetramethyl-1,3,2-dioxaboryl)-2-(4-(trifluoromethyl)phenyl)-2,1-borazaronaphthalene* (**3.51**)

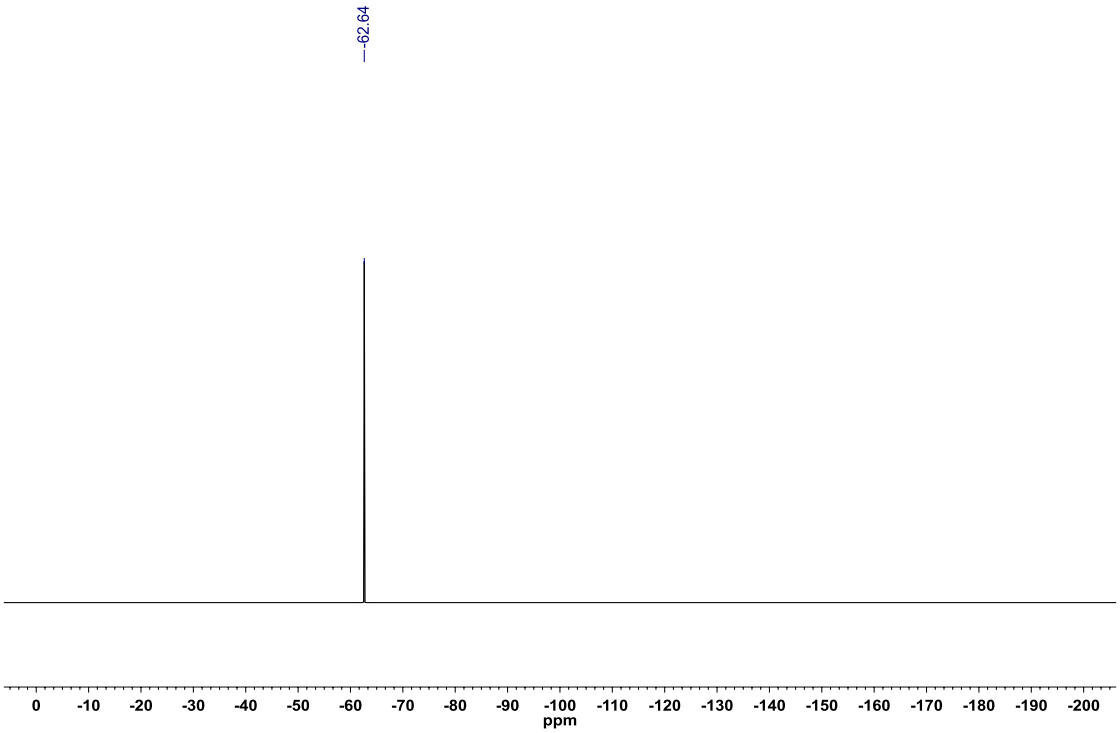

Figure A2.198: ^{11}B NMR ($CDCl_3$, 128.4 MHz) of *3-bromo-8-(4,4,5,5-tetramethyl-1,3,2-dioxaboryl)-2-(4-(trifluoromethyl)phenyl)-2,1-borazaronaphthalene* (**3.51**)

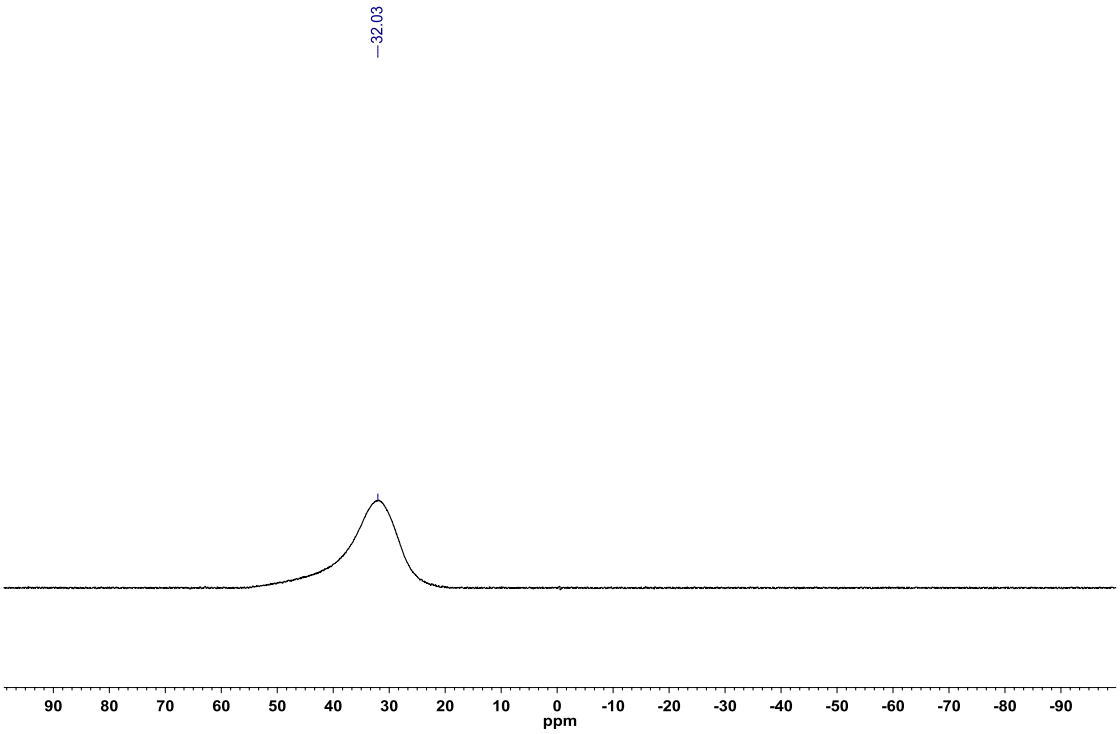

Figure A2.199: ^{1}H NMR ($CDCl_3$, 500.4 MHz) of *3,6-dibromo-2-phenyl-8-(4,4,5,5-tetramethyl-1,3,2-dioxaboryl)-2,1-borazaronaphthalene* (**3.52**)

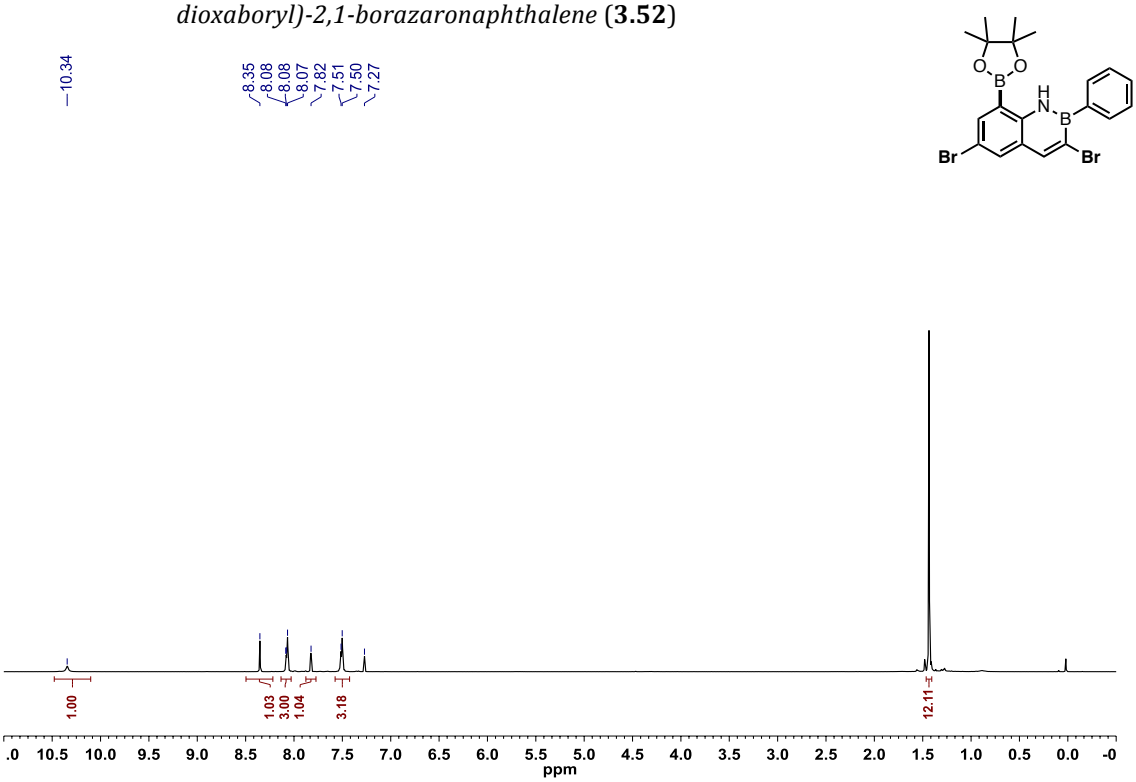

Figure A2.200: ^{13}C {^{1}H} NMR ($CDCl_3$, 125.8 MHz) of *3,6-dibromo-2-phenyl-8-(4,4,5,5-tetramethyl-1,3,2-dioxaboryl)-2,1-borazaronaphthalene* (**3.52**)

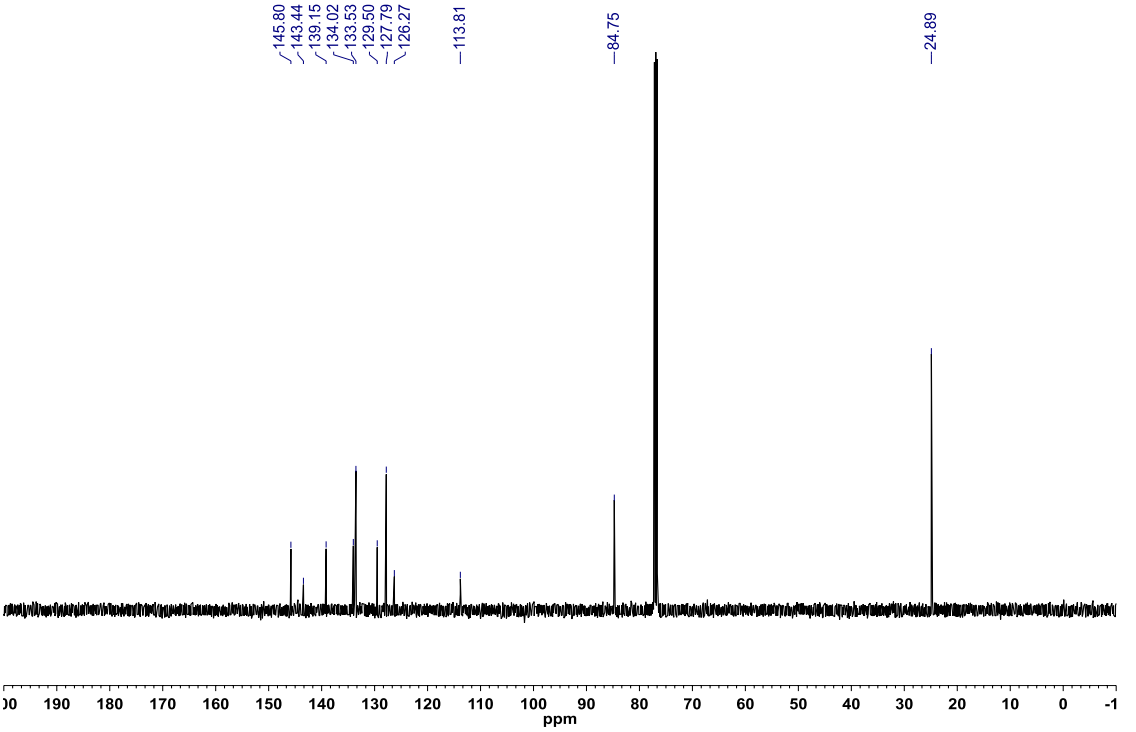

Figure A2.201: ^{11}B NMR ($CDCl_3$, 128.4 MHz) of *3,6-dibromo-2-phenyl-8-(4,4,5,5-tetramethyl-1,3,2-dioxaboryl)-2,1-borazaronaphthalene* (**3.52**)

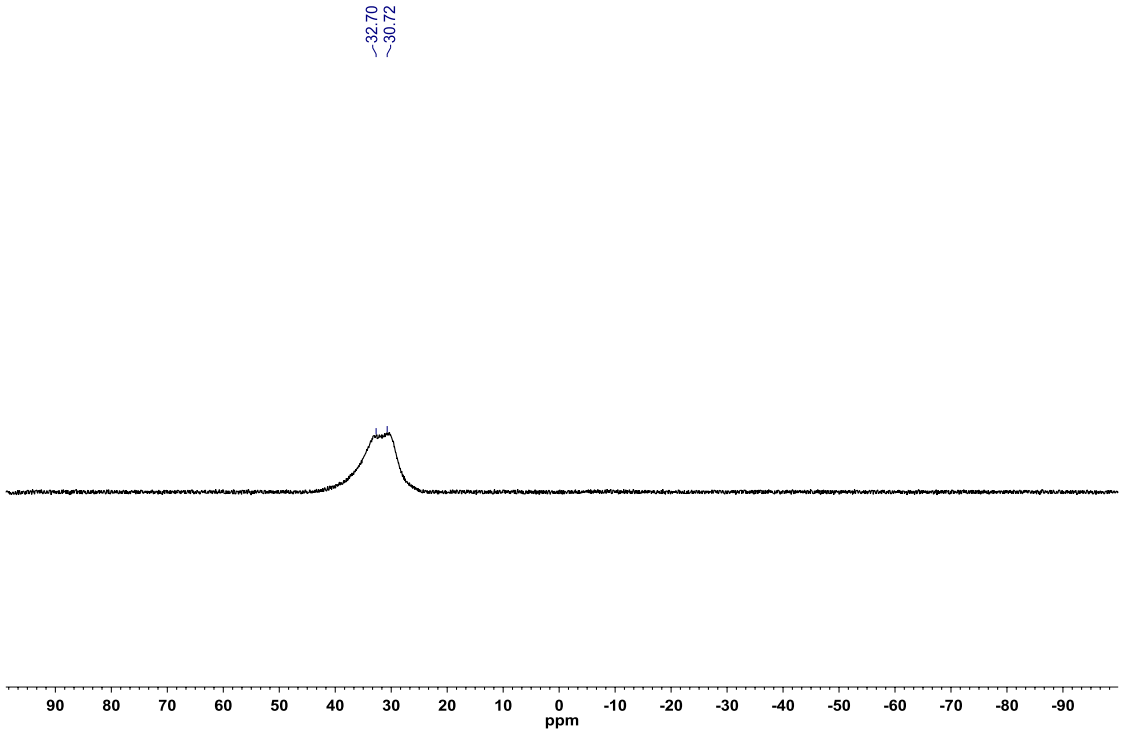

Figure A2.202: ^{1}H NMR ($CDCl_3$, 500.4 MHz) of *3-(4-fluorophenyl)-2-phenyl-8-(4,4,5,5-tetramethyl-1,3,2-dioxaboryl)-2,1-borazaronaphthalene* (**3.53**)

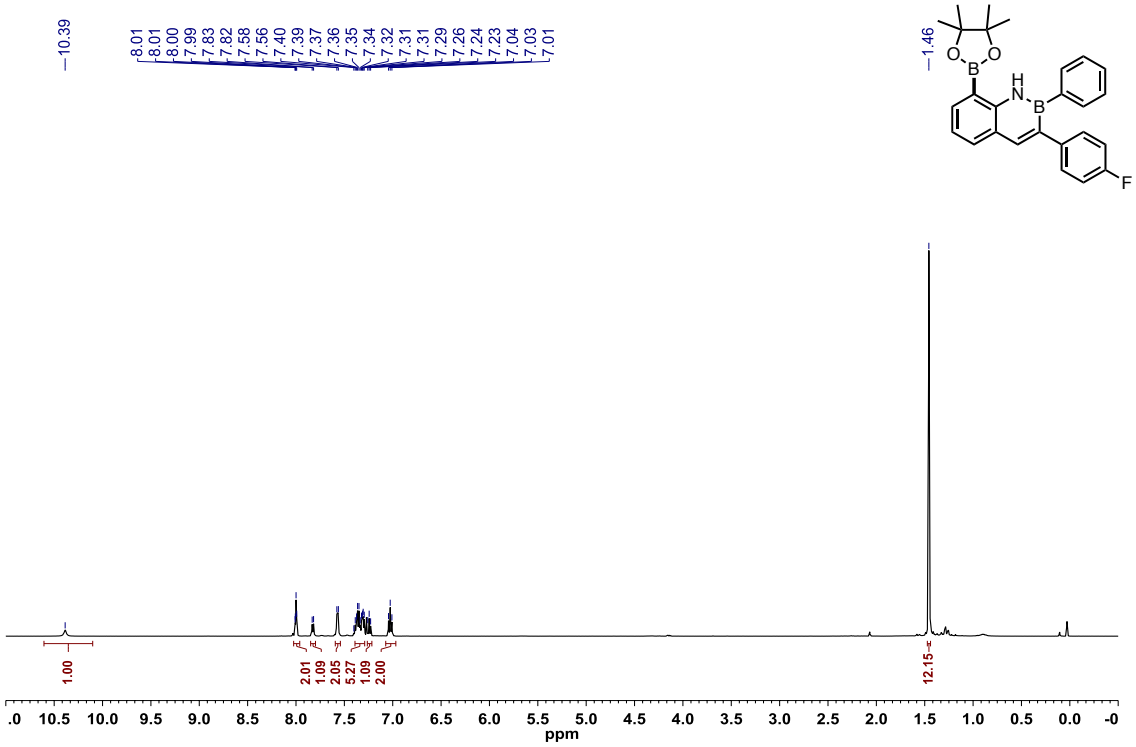

Figure A2.203: ^{13}C {^{1}H} NMR ($CDCl_3$, 125.8 MHz) of *3-(4-fluorophenyl)-2-phenyl-8-(4,4,5,5-tetramethyl-1,3,2-dioxaboryl)-2,1-borazaronaphthalene* (**3.53**)

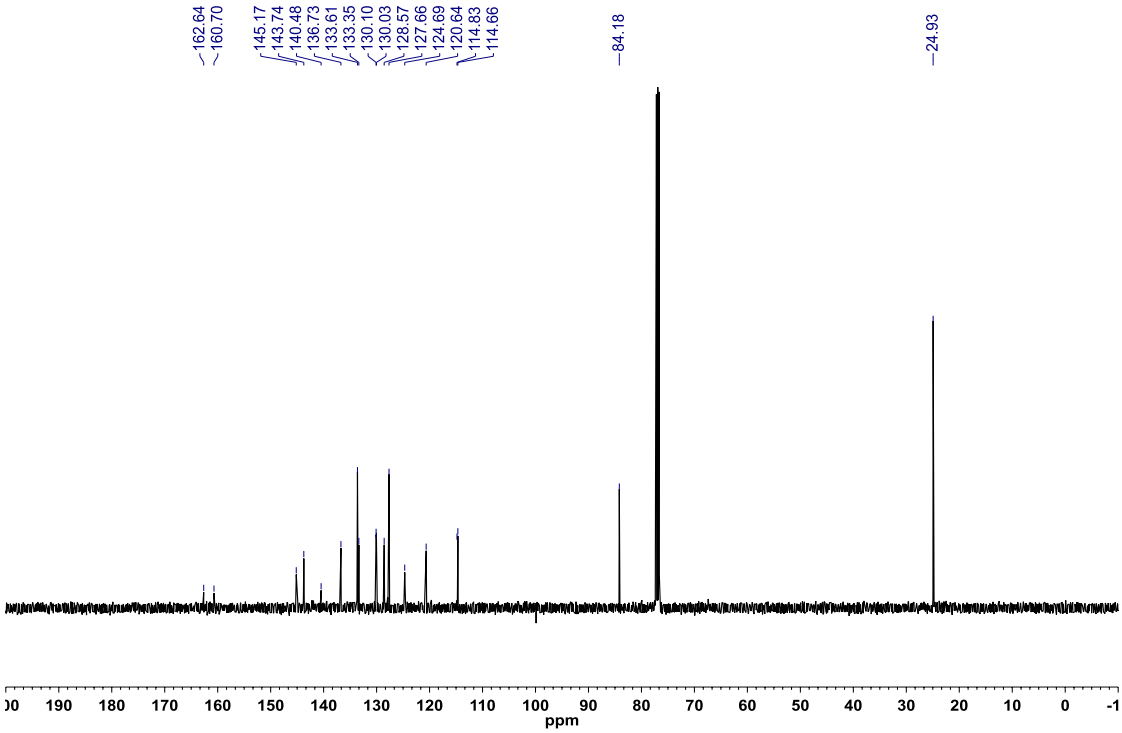

Figure A2.204: ^{19}F {^{1}H} NMR ($CDCl_3$, 470.8 MHz) of *3-(4-fluorophenyl)-2-phenyl-8-(4,4,5,5-tetramethyl-1,3,2-dioxaboryl)-2,1-borazaronaphthalene* (**3.53**)

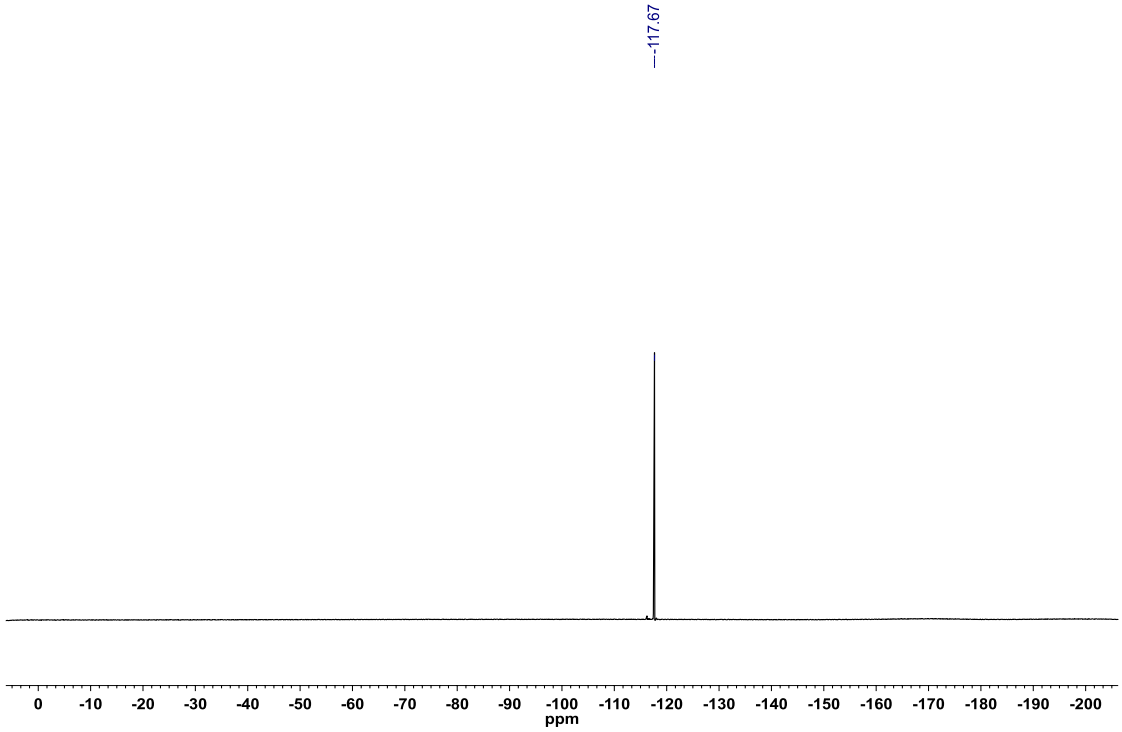

Figure A2.205: ^{11}B NMR ($CDCl_3$, 128.4 MHz) of *3-(4-fluorophenyl)-2-phenyl-8-(4,4,5,5-tetramethyl-1,3,2-dioxaboryl)-2,1-borazaronaphthalene* (**3.53**)

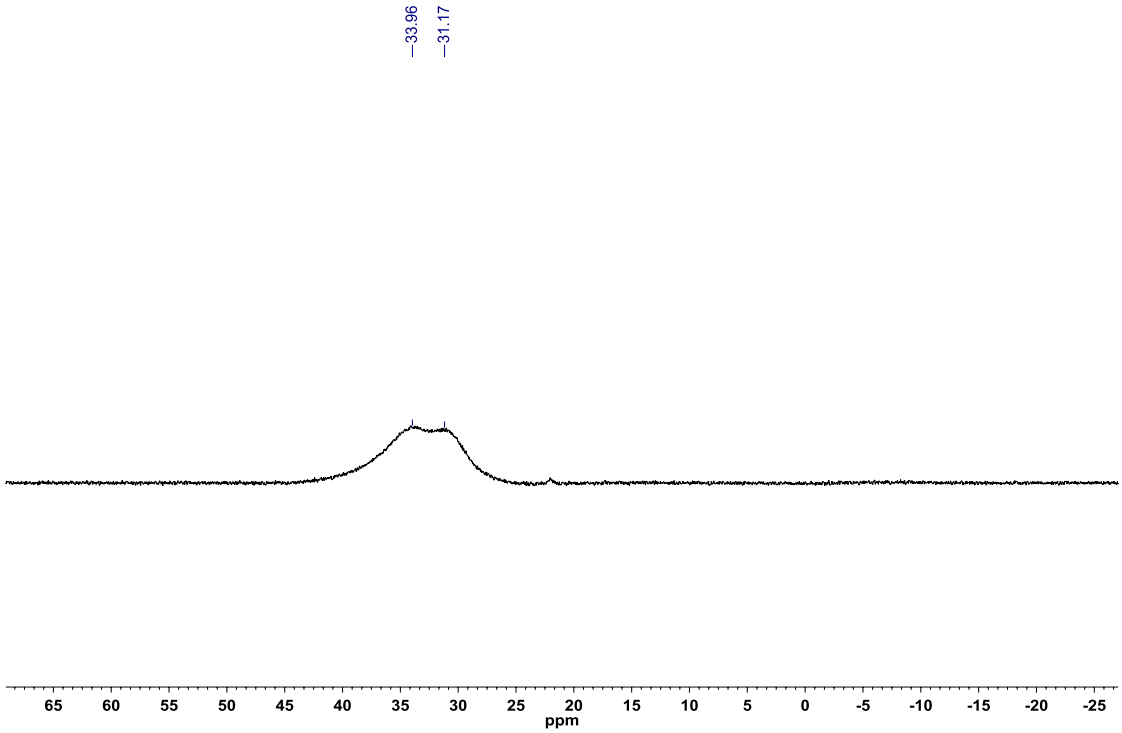

Figure A2.206: ^{1}H NMR ($CDCl_3$, 500.4 MHz) of *7-fluoro-8-(4,4,5,5-tetramethyl-1,3,2-dioxaboryl)-2-(4-(trifluoromethyl)phenyl)-2,1-borazaronaphthalene* (**3.54**)

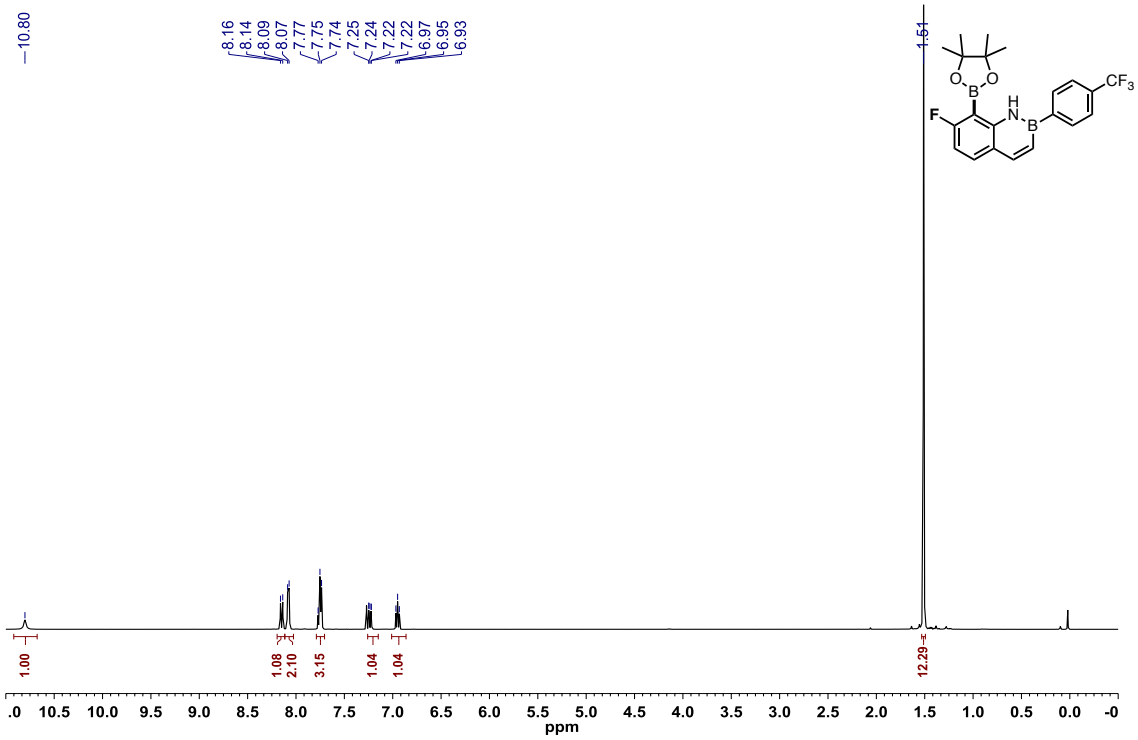

Figure A2.207: ^{13}C {^{1}H} NMR ($CDCl_3$, 125.8 MHz) of *7-fluoro-8-(4,4,5,5-tetramethyl-1,3,2-dioxaboryl)-2-(4-(trifluoromethyl)phenyl)-2,1-borazaronaphthalene* (**3.54**)

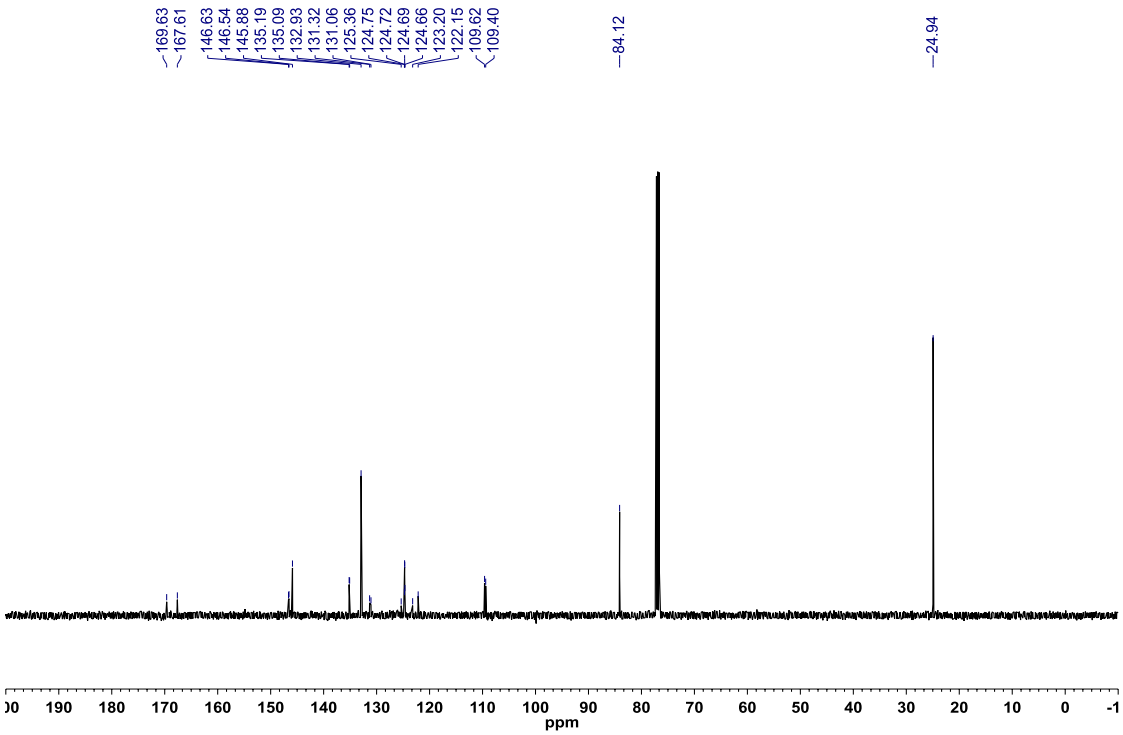

Figure A2.208: ^{19}F {^{1}H} NMR ($CDCl_3$, 470.8 MHz) of *7-fluoro-8-(4,4,5,5-tetramethyl-1,3,2-dioxaboryl)-2-(4-(trifluoromethyl)phenyl)-2,1-borazaronaphthalene* (**3.54**)

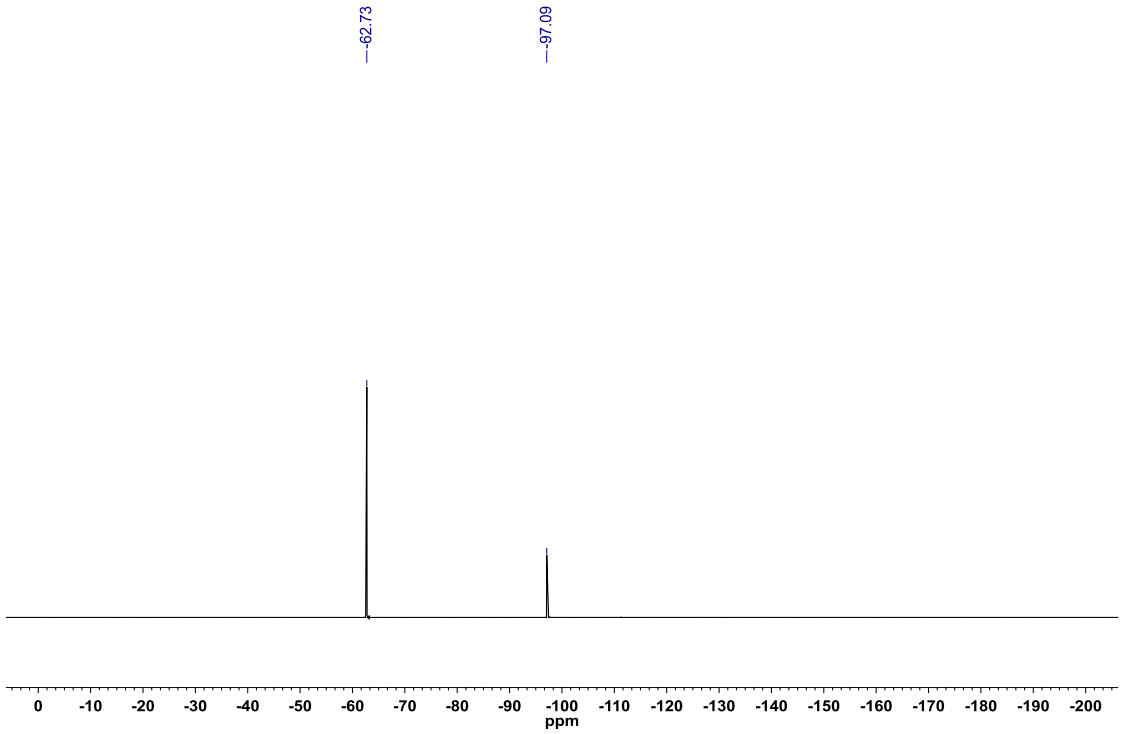

Figure A2.209: ^{11}B NMR ($CDCl_3$, 128.4 MHz) of *7-fluoro-8-(4,4,5,5-tetramethyl-1,3,2-dioxaboryl)-2-(4-(trifluoromethyl)phenyl)-2,1-borazaronaphthalene* (**3.54**)

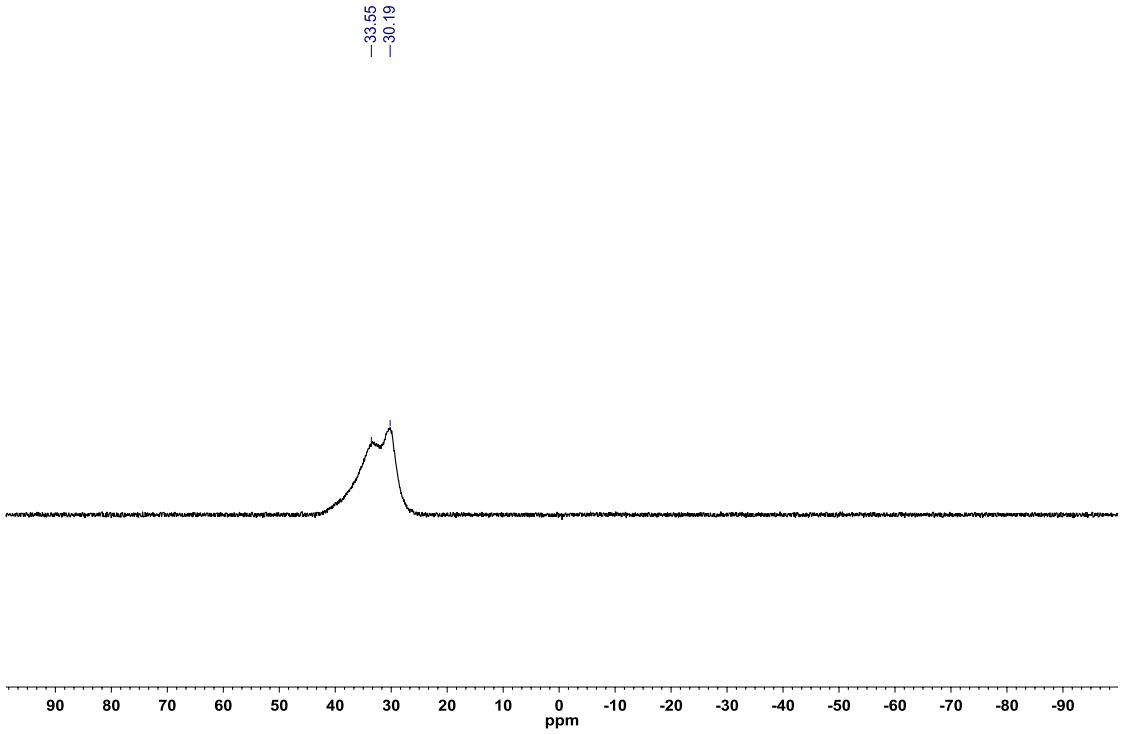

Figure A2.210: ^{1}H NMR ($CDCl_3$, 500.4 MHz) of *6-cyano-8-(4,4,5,5-tetramethyl-1,3,2-dioxaboryl)-2-(4-(trifluoromethyl)phenyl)-2,1-borazaronaphthalene* (**3.55**)

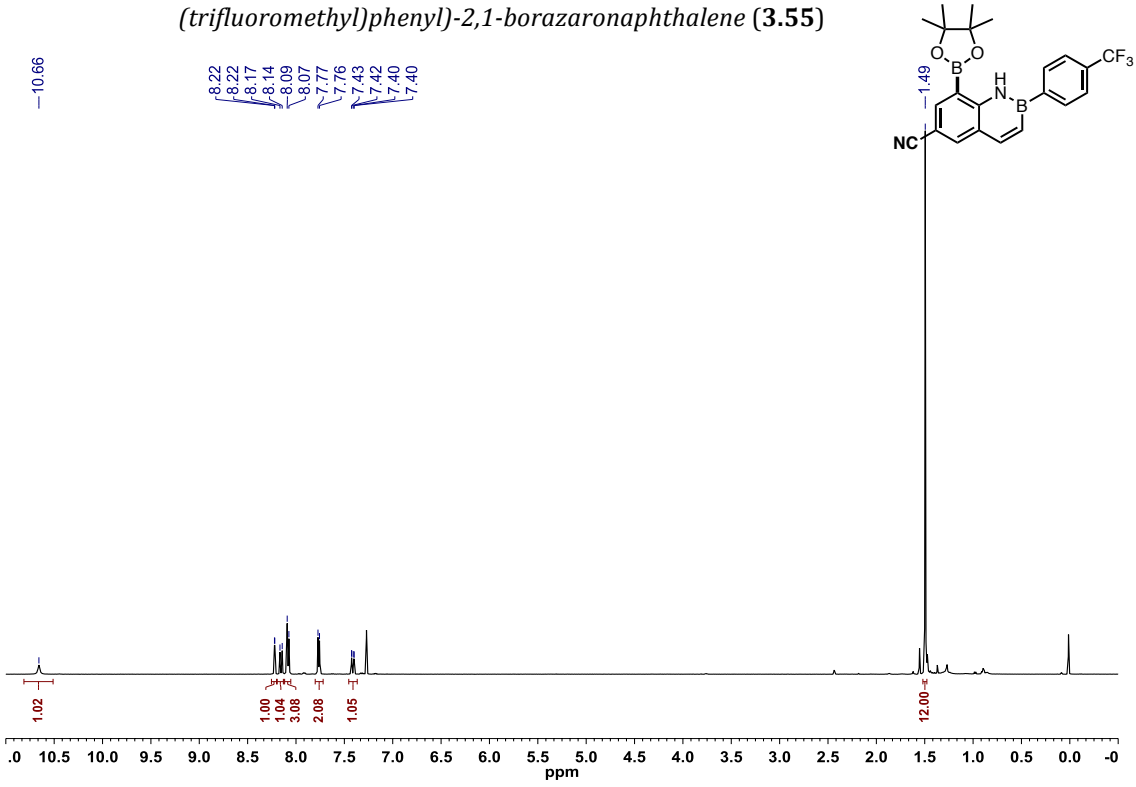

Figure A2.211: ^{13}C {^{1}H} NMR ($CDCl_3$, 125.8 MHz) of *6-cyano-8-(4,4,5,5-tetramethyl-1,3,2-dioxaboryl)-2-(4-(trifluoromethyl)phenyl)-2,1-borazaronaphthalene* (**3.55**)

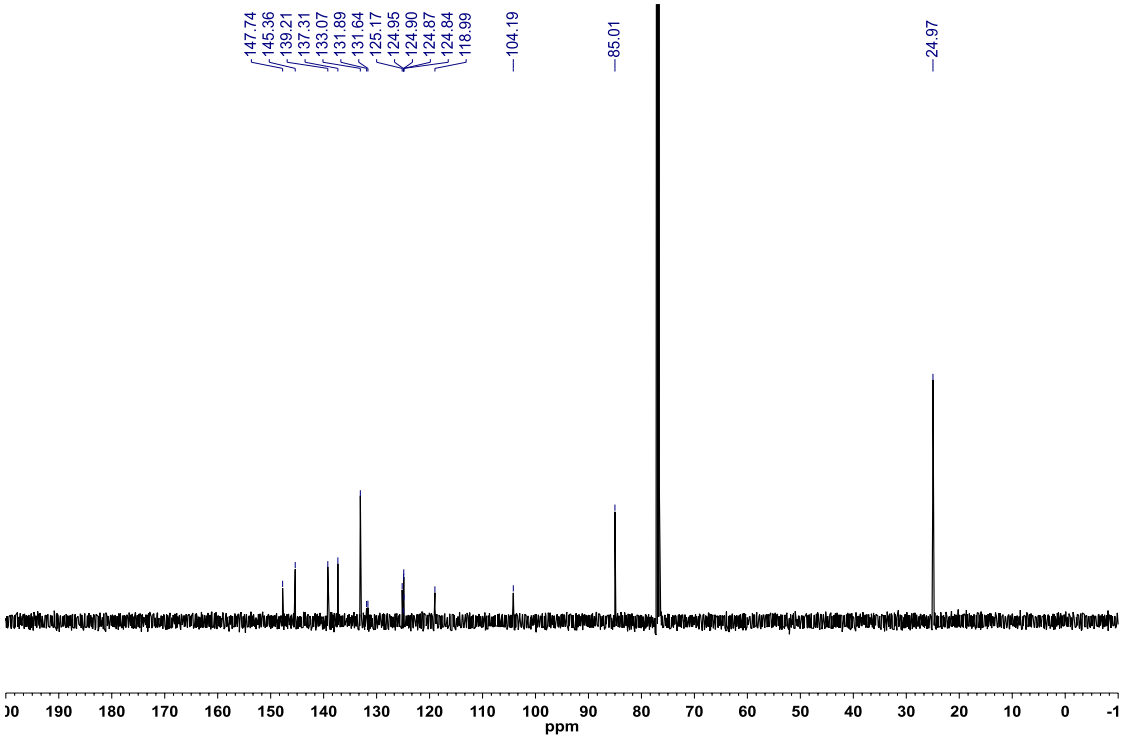

Figure A2.212: ^{19}F {^{1}H} NMR ($CDCl_3$, 470.8 MHz) of *6-cyano-8-(4,4,5,5-tetramethyl-1,3,2-dioxaboryl)-2-(4-(trifluoromethyl)phenyl)-2,1-borazaronaphthalene* (**3.55**)

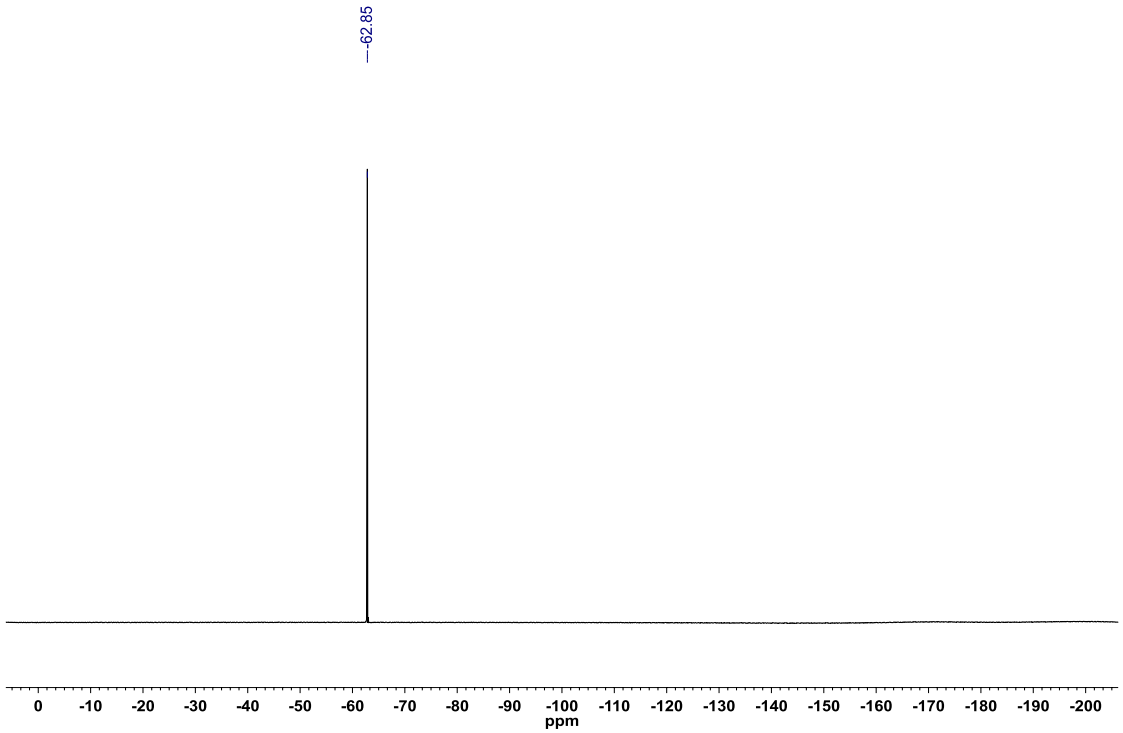

Figure A2.213: ^{11}B NMR ($CDCl_3$, 128.4 MHz) of *6-cyano-8-(4,4,5,5-tetramethyl-1,3,2-dioxaboryl)-2-(4-(trifluoromethyl)phenyl)-2,1-borazaronaphthalene* (**3.55**)

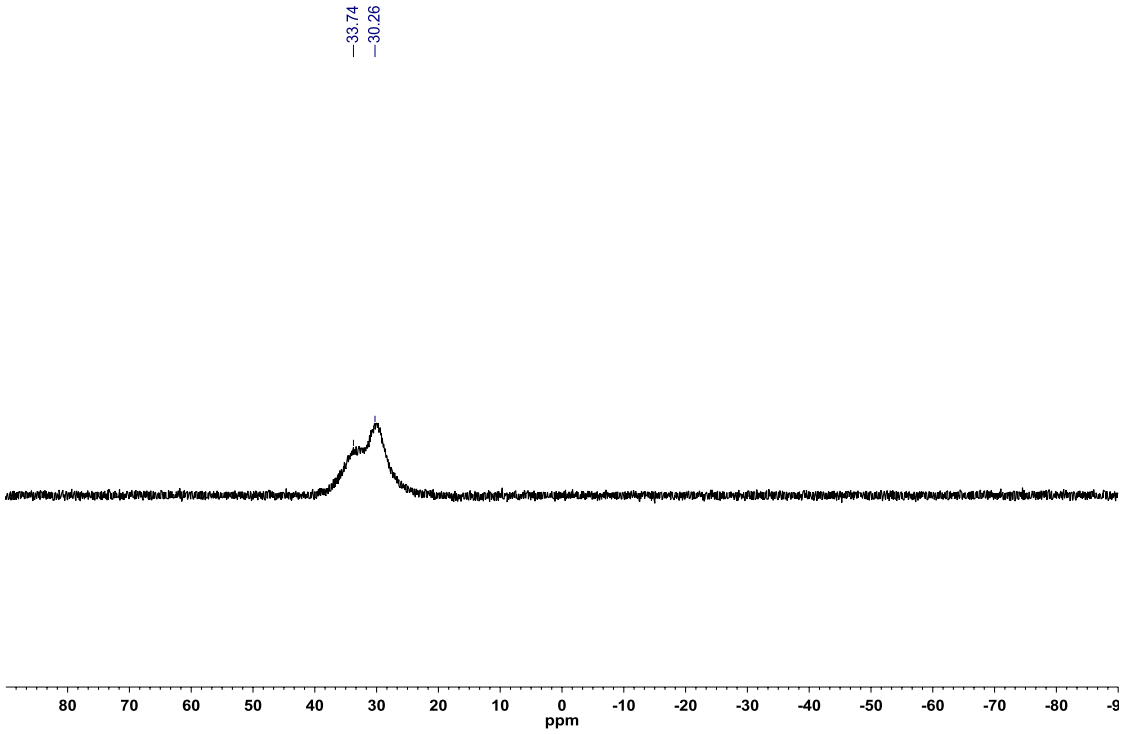

Figure A2.214: ^{1}H NMR ($CDCl_3$, 500.4 MHz) of *8-(4,4,5,5-tetramethyl-1,3,2-dioxaboryl)- 6-(trifluoromethyl)-2-(4-(trifluoromethyl)phenyl)-2,1-borazaronaphthalene* (**3.56**)

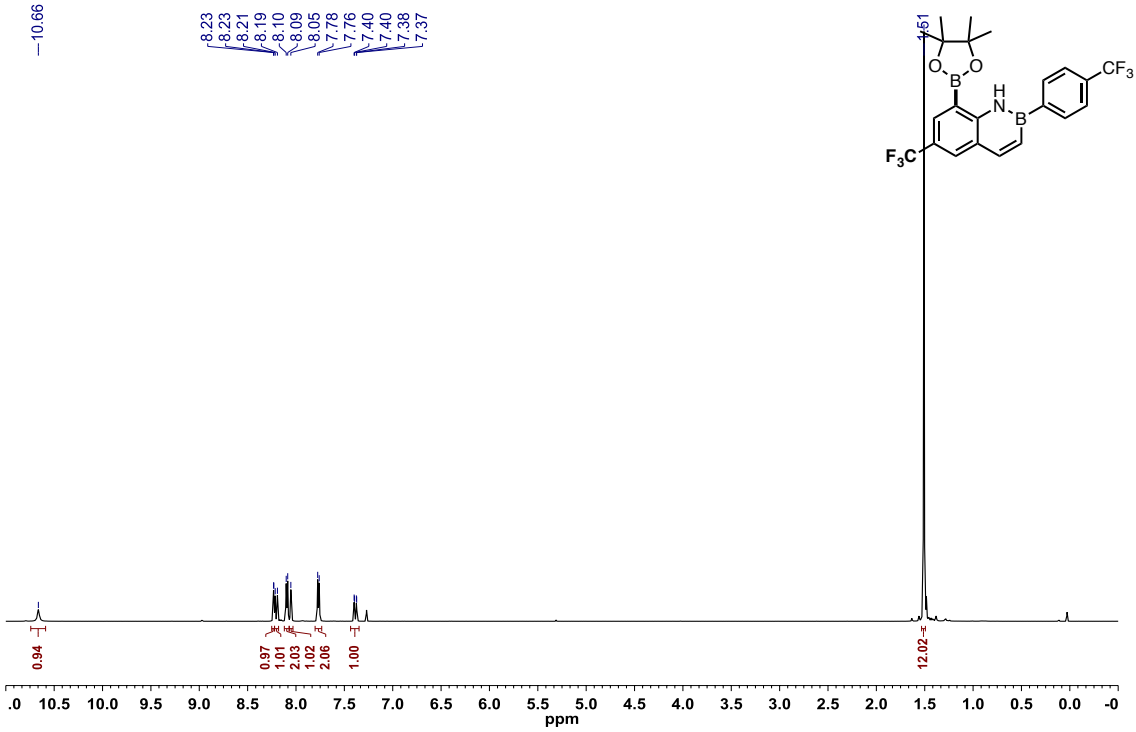

Figure A2.215: ^{13}C {^{1}H} NMR ($CDCl_3$, 125.8 MHz) of *8-(4,4,5,5-tetramethyl-1,3,2-dioxaboryl)- 6-(trifluoromethyl)-2-(4-(trifluoromethyl)phenyl)-2,1-borazaronaphthalene* (**3.56**)

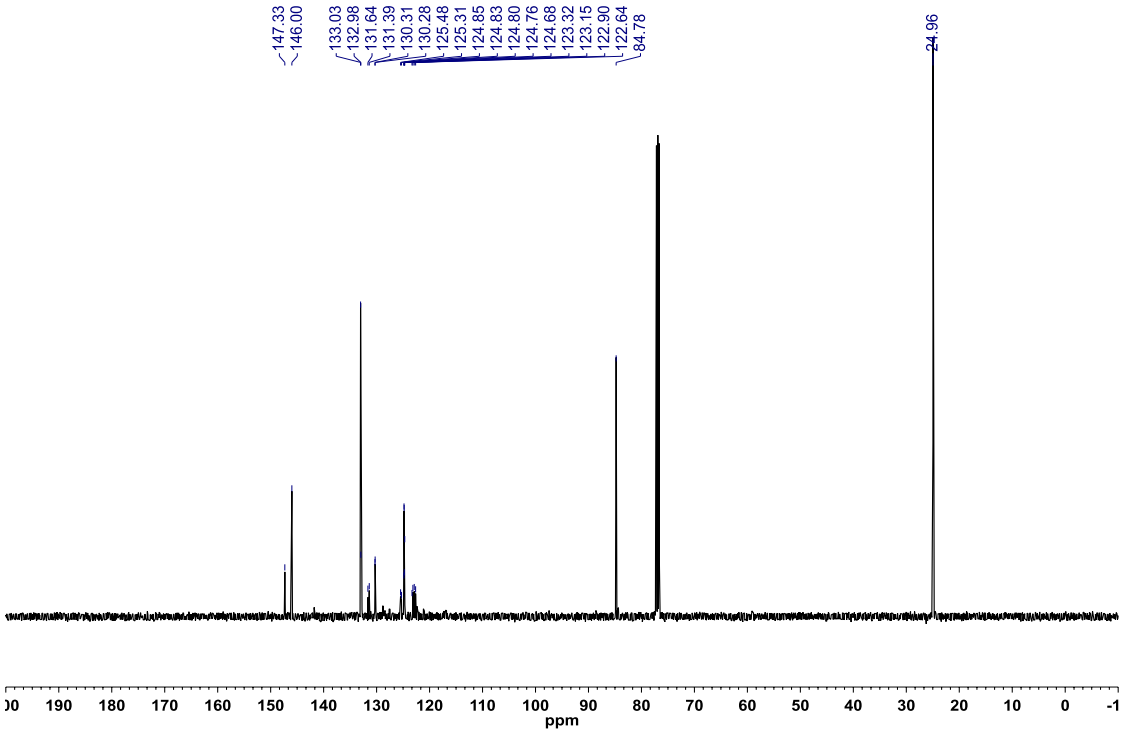

Figure A2.216: ^{19}F {^{1}H} NMR ($CDCl_3$, 470.8 MHz) of *8-(4,4,5,5-tetramethyl-1,3,2-dioxaboryl)- 6-(trifluoromethyl)-2-(4-(trifluoromethyl)phenyl)-2,1-borazaronaphthalene* (**3.56**)

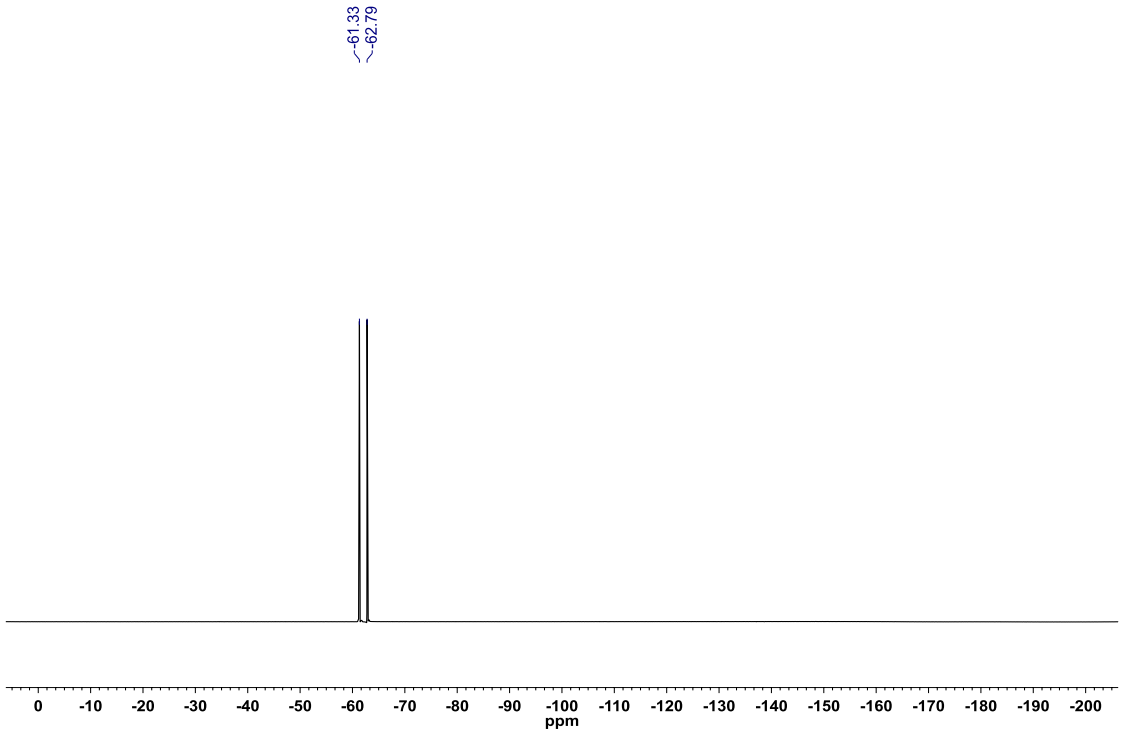

Figure A2.217: ^{11}B NMR ($CDCl_3$, 128.4 MHz) of *8-(4,4,5,5-tetramethyl-1,3,2-dioxaboryl)- 6-(trifluoromethyl)-2-(4-(trifluoromethyl)phenyl)-2,1-borazaronaphthalene* (**3.56**)

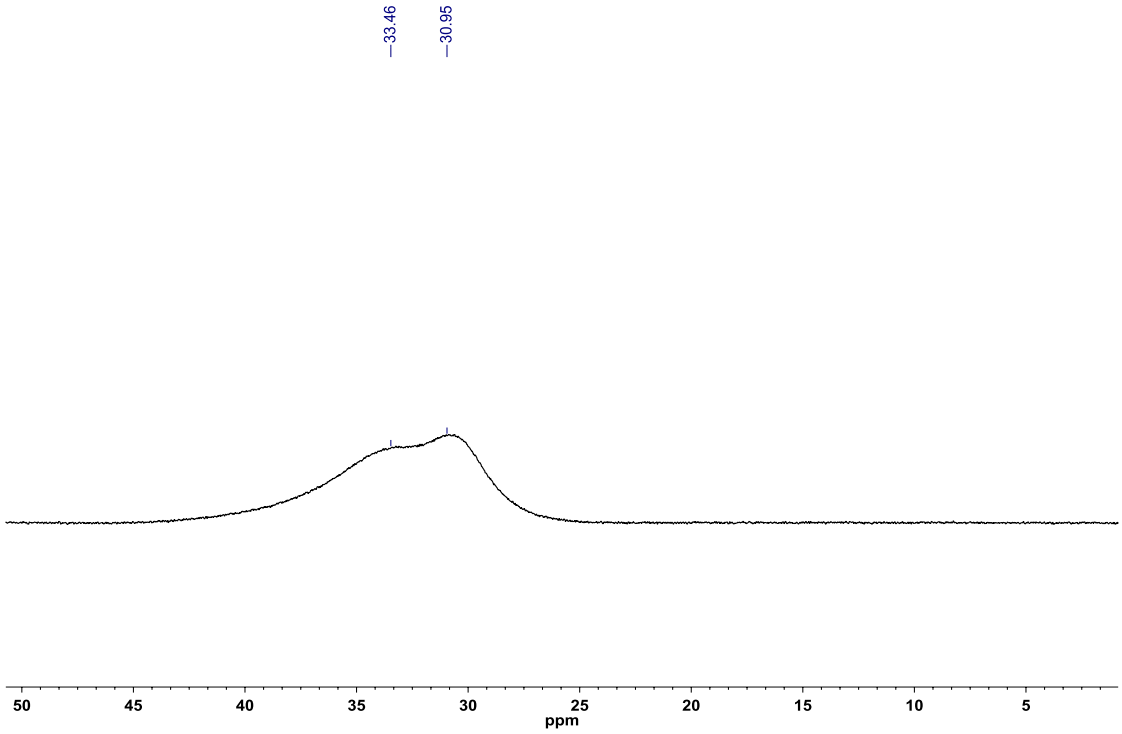

Figure A2.218: ^{1}H NMR ($CDCl_3$, 500.4 MHz) of *6-isopropy-8-(4,4,5,5-tetramethyl-1,3,2-dioxaboryl)-2-(4-(trifluoromethyl)phenyl)-2,1-borazaronaphthalene* (**3.57**)

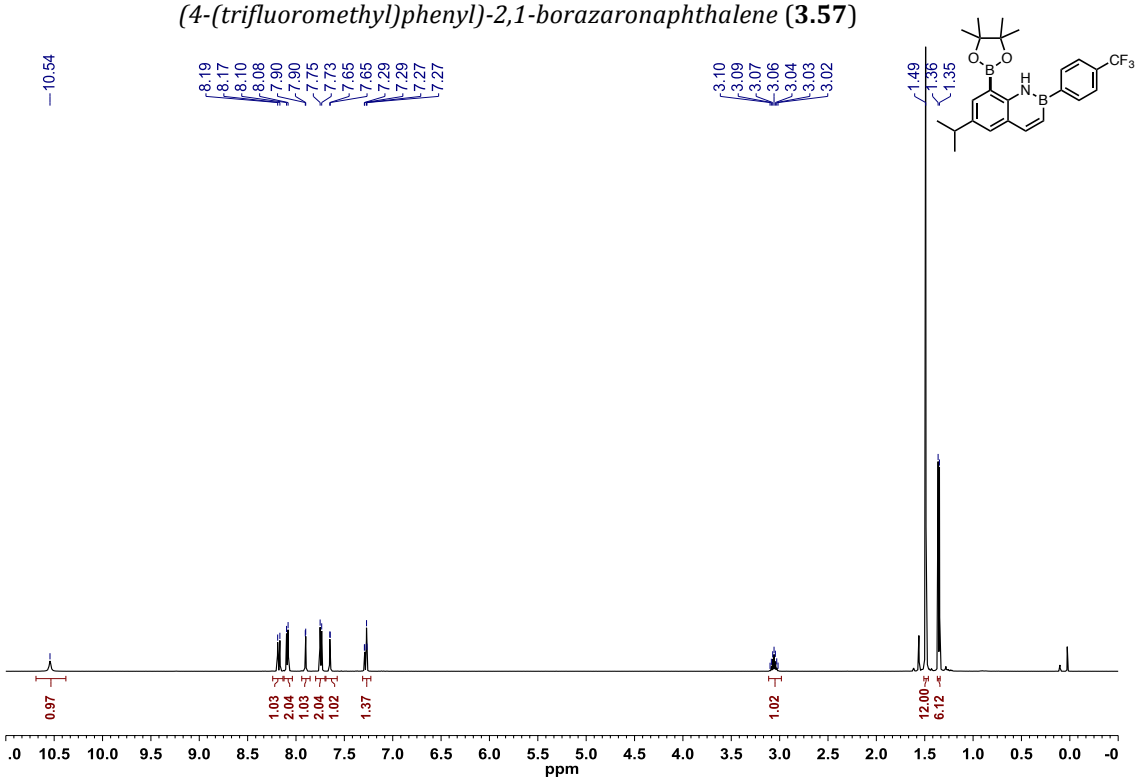

Figure A2.219: ^{13}C {^{1}H} NMR ($CDCl_3$, 125.8 MHz) of *6-isopropy-8-(4,4,5,5-tetramethyl-1,3,2-dioxaboryl)-2-(4-(trifluoromethyl)phenyl)-2,1-borazaronaphthalene* (**3.57**)

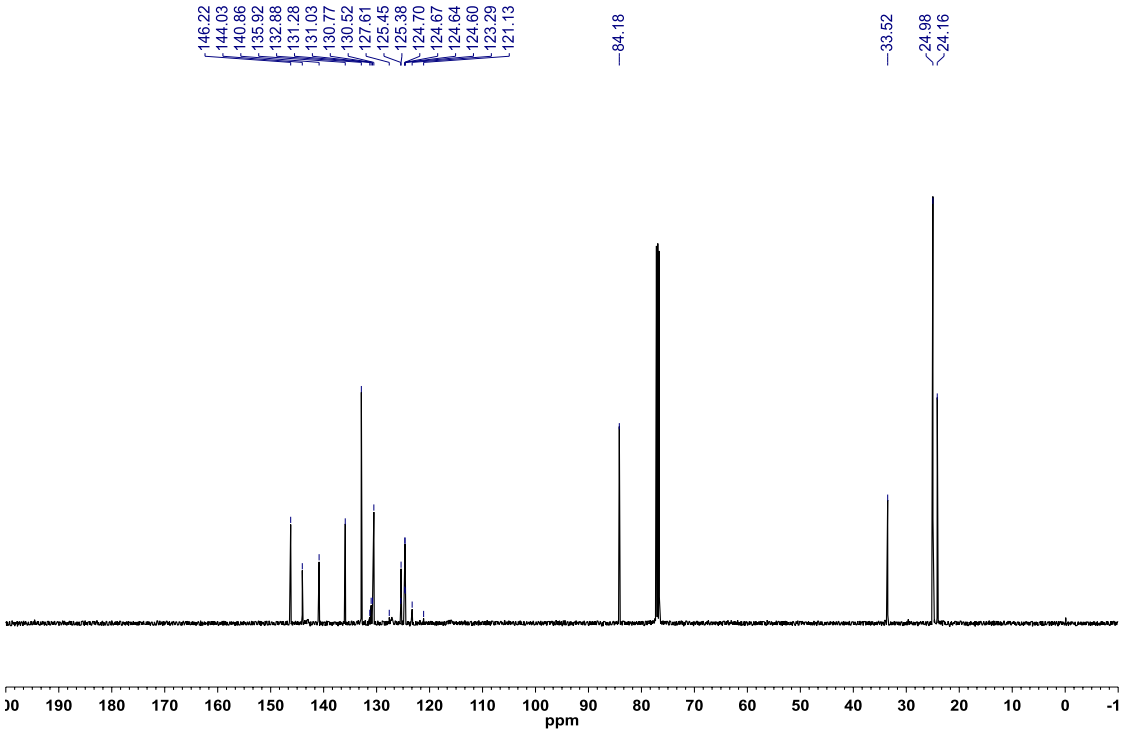

Figure A2.220: ^{19}F {^{1}H} NMR ($CDCl_3$, 470.8 MHz) of *6-isopropy-8-(4,4,5,5-tetramethyl-1,3,2-dioxaboryl)-2-(4-(trifluoromethyl)phenyl)-2,1-borazaronaphthalene* (**3.57**)

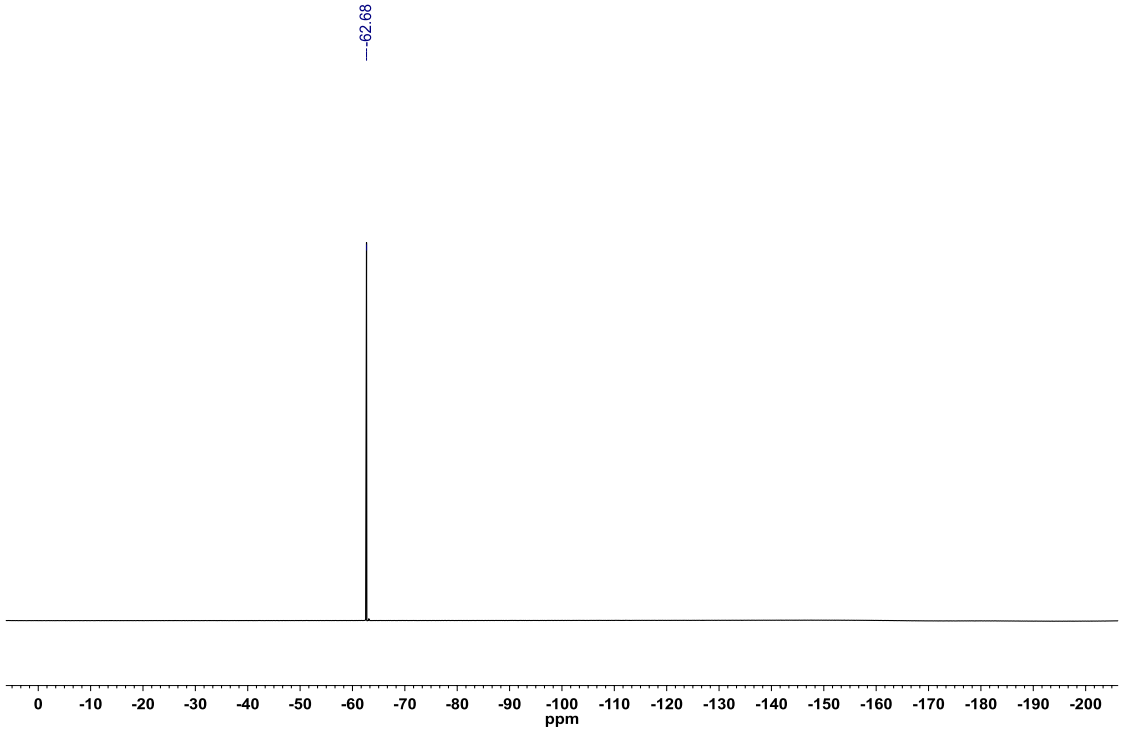

Figure A2.221: ^{11}B NMR ($CDCl_3$, 128.4 MHz) of *6-isopropy-8-(4,4,5,5-tetramethyl-1,3,2-dioxaboryl)-2-(4-(trifluoromethyl)phenyl)-2,1-borazaronaphthalene* (**3.57**)

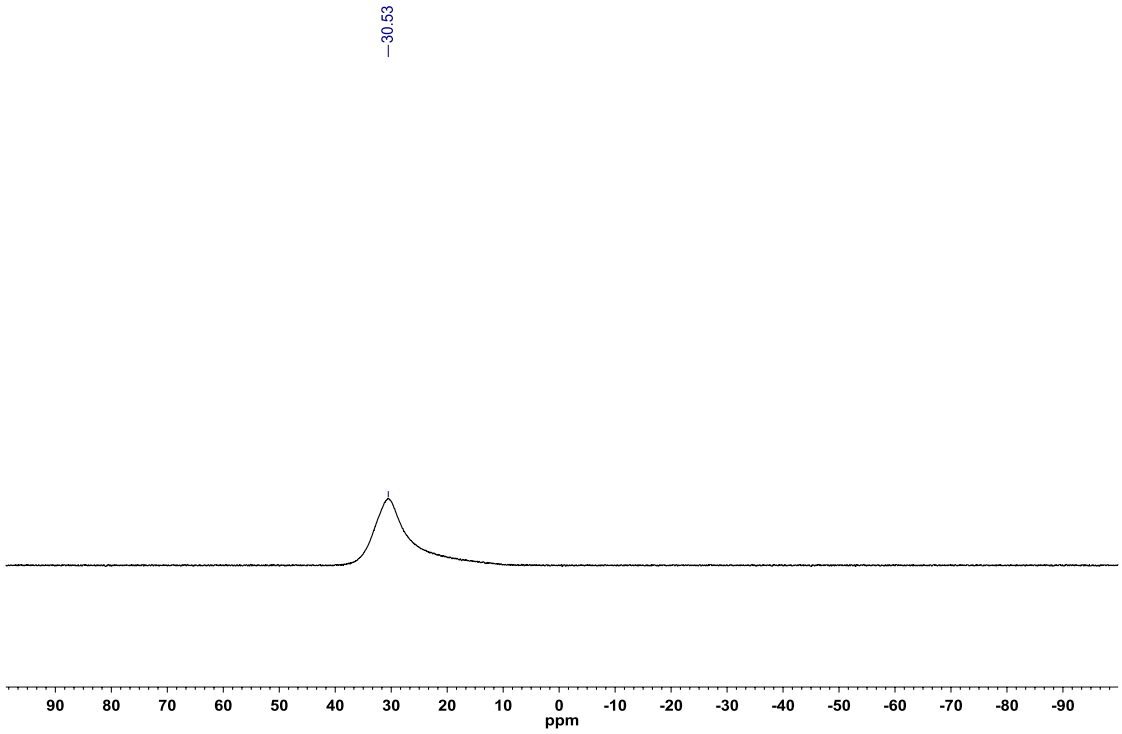

Figure A2.222: ^{1}H NMR ($CDCl_3$, 500.4 MHz) of *8-(4,4,5,5-tetramethyl-1,3,2-dioxaboryl)-6-(trifluoromethoxy)-2-(4-(trifluoromethyl)phenyl)-2,1-borazaronaphthalene* (**3.58**)

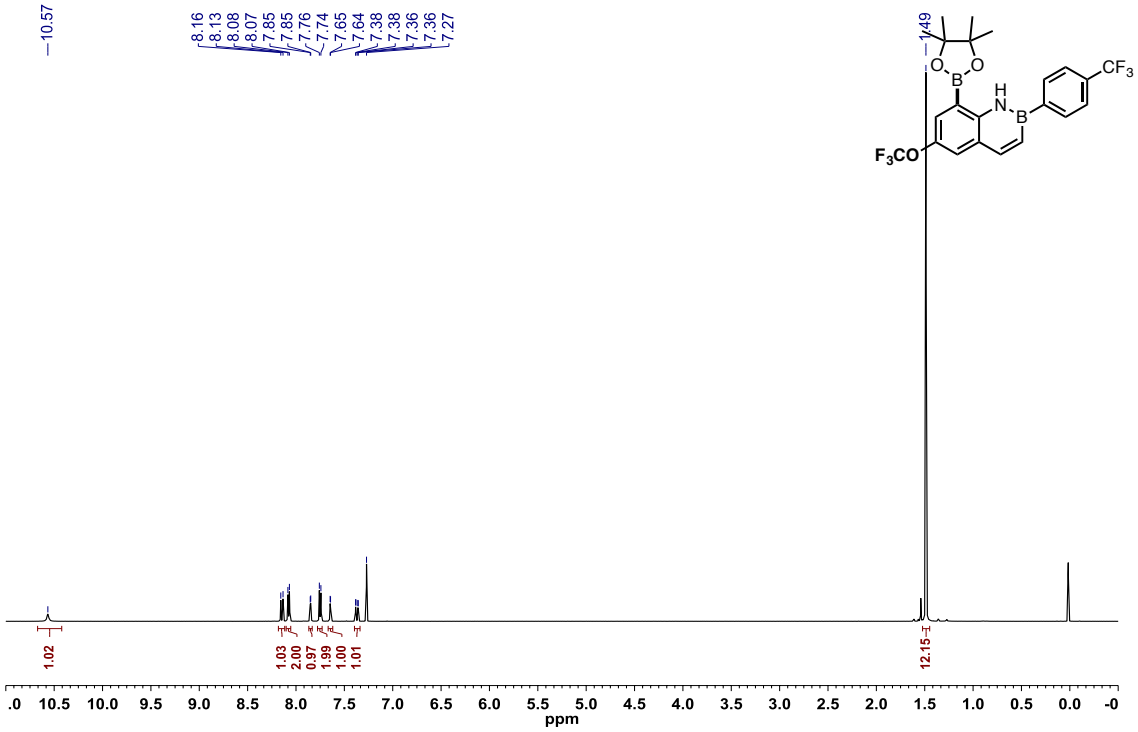

Figure A2.223: ^{13}C {^{1}H} NMR ($CDCl_3$, 125.8 MHz) of *8-(4,4,5,5-tetramethyl-1,3,2-dioxaboryl)-6-(trifluoromethoxy)-2-(4-(trifluoromethyl)phenyl)-2,1-borazaronaphthalene* (**3.58**)

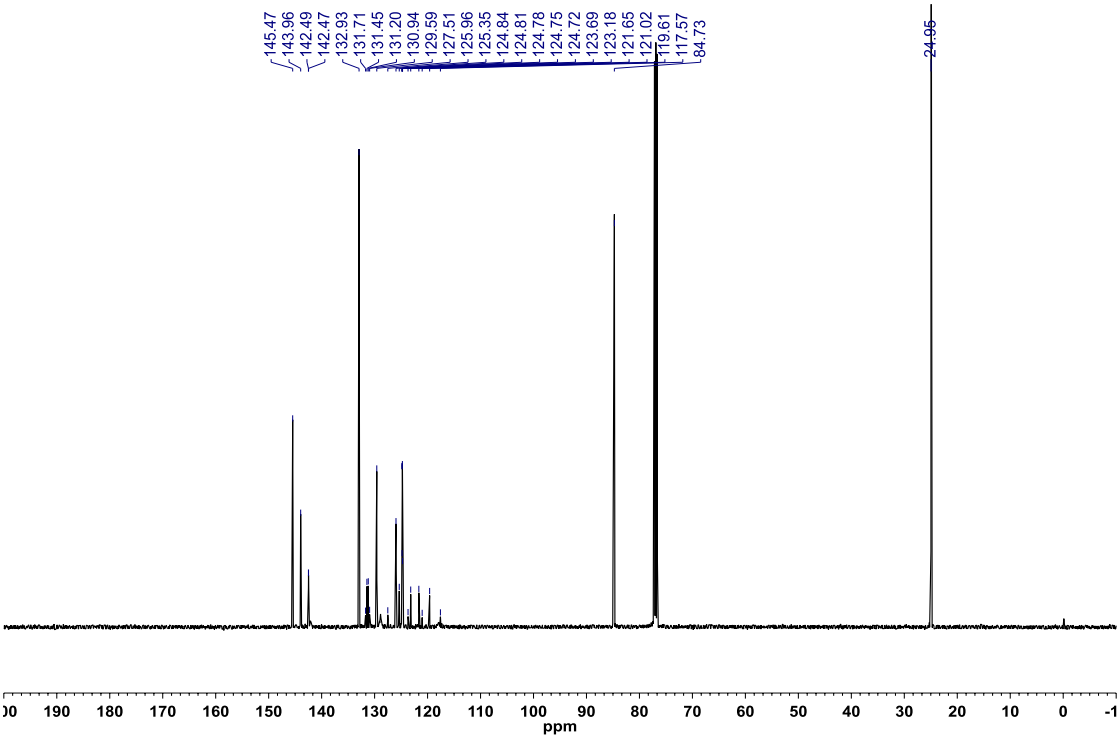

Figure A2.224: ^{19}F {^{1}H} NMR ($CDCl_3$, 470.8 MHz) of *8-(4,4,5,5-tetramethyl-1,3,2-dioxaboryl)-6-(trifluoromethoxy)-2-(4-(trifluoromethyl)phenyl)-2,1-borazaronaphthalene* (**3.58**)

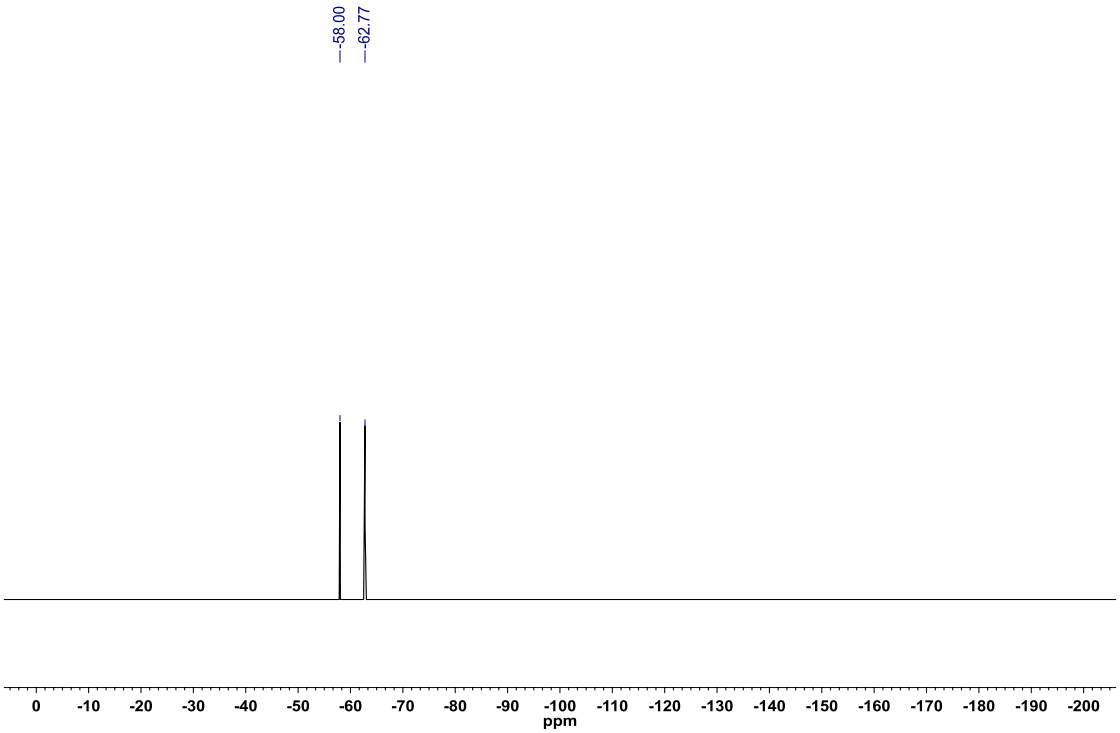

Figure A2.225: ^{11}B NMR ($CDCl_3$, 128.4 MHz) of *8-(4,4,5,5-tetramethyl-1,3,2-dioxaboryl)-6-(trifluoromethoxy)-2-(4-(trifluoromethyl)phenyl)-2,1-borazaronaphthalene* (**3.58**)

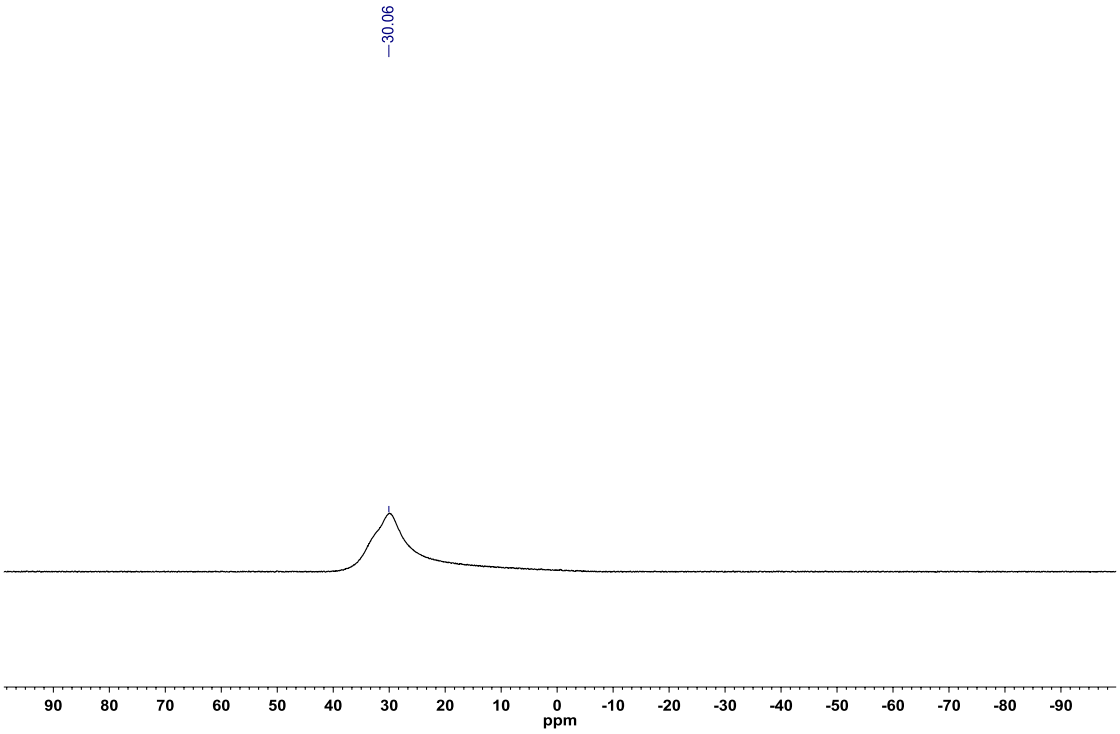

Figure A2.226: ^{1}H NMR ($CDCl_3$, 500.4 MHz) of *6,8-bis(4,4,5,5-tetramethyl-1,3,2-dioxaboryl)-2-(4-(trifluoromethyl)phenyl)-2,1-borazaronaphthalene* (**3.59**)

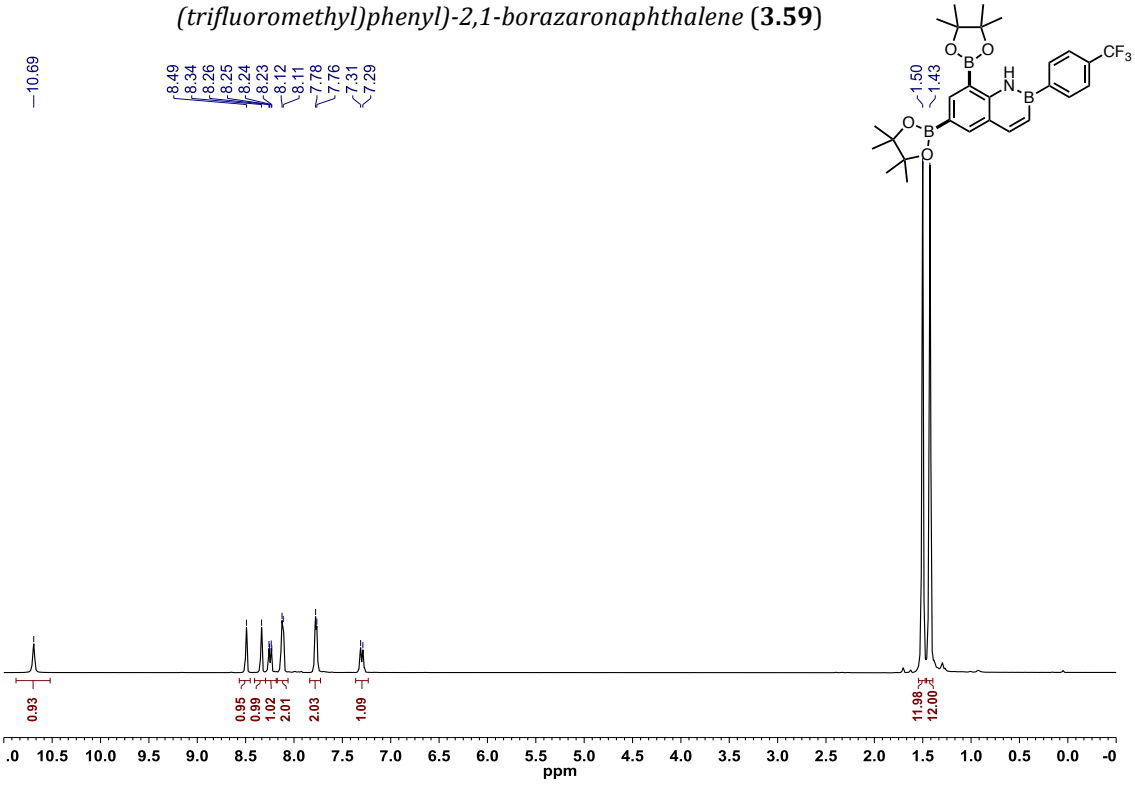

Figure A2.227: ^{13}C {^{1}H} NMR ($CDCl_3$, 125.8 MHz) of *6,8-bis(4,4,5,5-tetramethyl-1,3,2-dioxaboryl)-2-(4-(trifluoromethyl)phenyl)-2,1-borazaronaphthalene* (**3.59**)

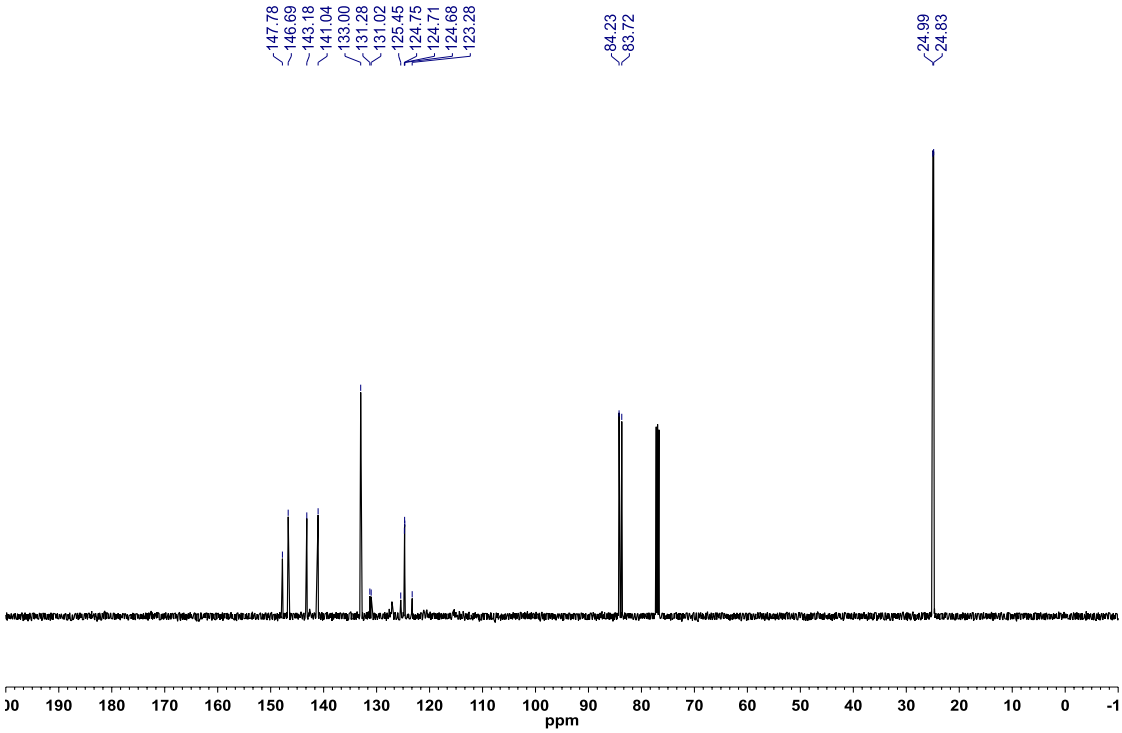

Figure A2.228: ^{19}F {^{1}H} NMR ($CDCl_3$, 470.8 MHz) of *6,8-bis(4,4,5,5-tetramethyl-1,3,2-dioxaboryl)-2-(4-(trifluoromethyl)phenyl)-2,1-borazaronaphthalene* (**3.59**)

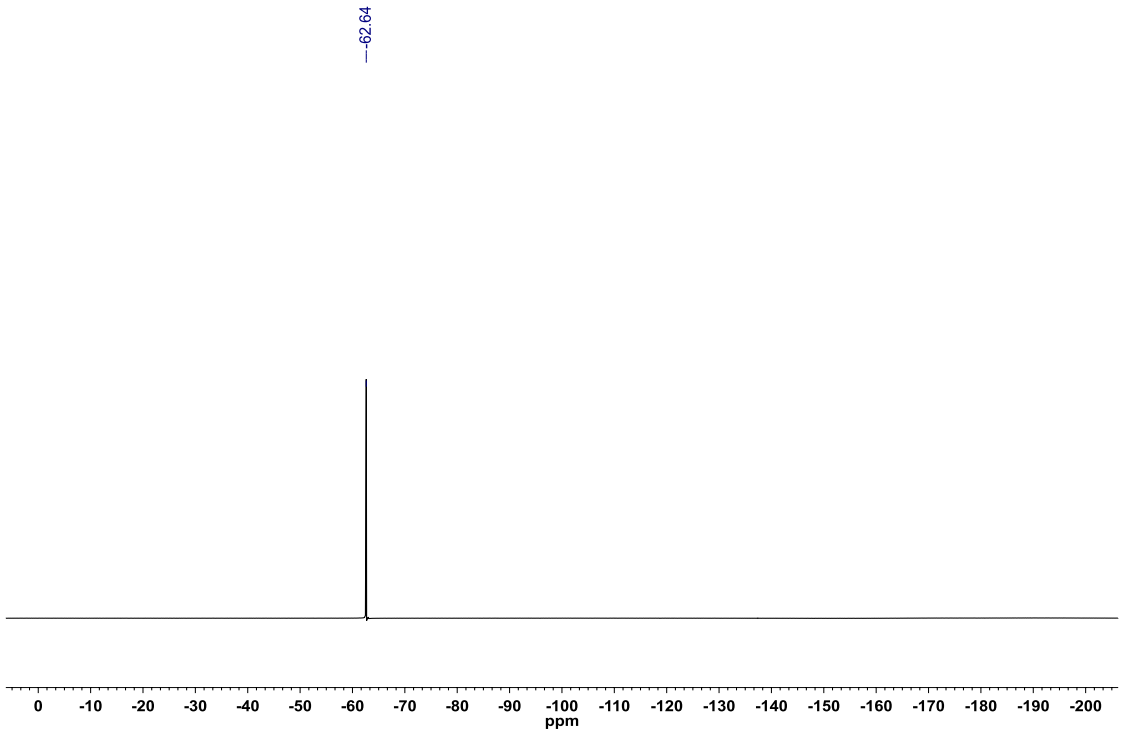

Figure A2.229: ^{11}B NMR ($CDCl_3$, 128.4 MHz) of *6,8-bis(4,4,5,5-tetramethyl-1,3,2-dioxaboryl)-2-(4-(trifluoromethyl)phenyl)-2,1-borazaronaphthalene* (**3.59**)

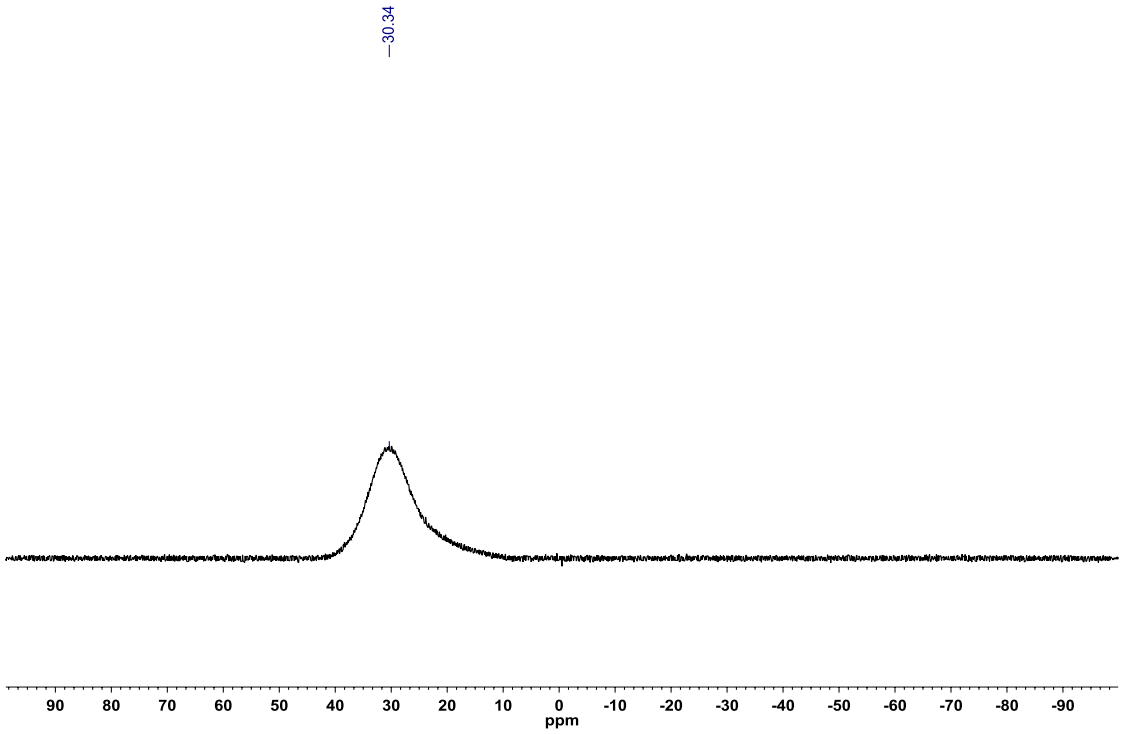

Figure A2.230: ^{1}H NMR ($CDCl_3$, 500.4 MHz) of *2-cyclopropyl-6,8-bis(4,4,5,5-tetramethyl-1,3,2-dioxaboryl)-2,1-borazaronaphthalene* (**3.60**)

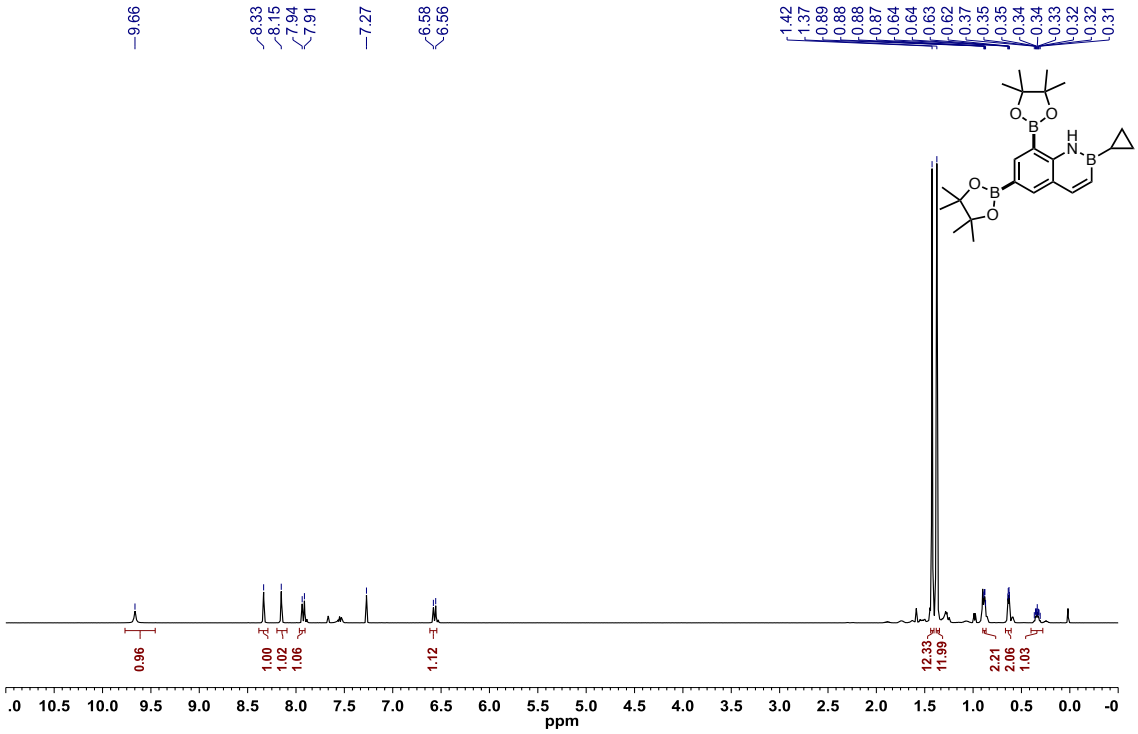

Figure A2.231: ^{13}C {^{1}H} NMR ($CDCl_3$, 125.8 MHz) of *2-cyclopropyl-6,8-bis(4,4,5,5-tetramethyl-1,3,2-dioxaboryl)-2,1-borazaronaphthalene* (**3.60**)

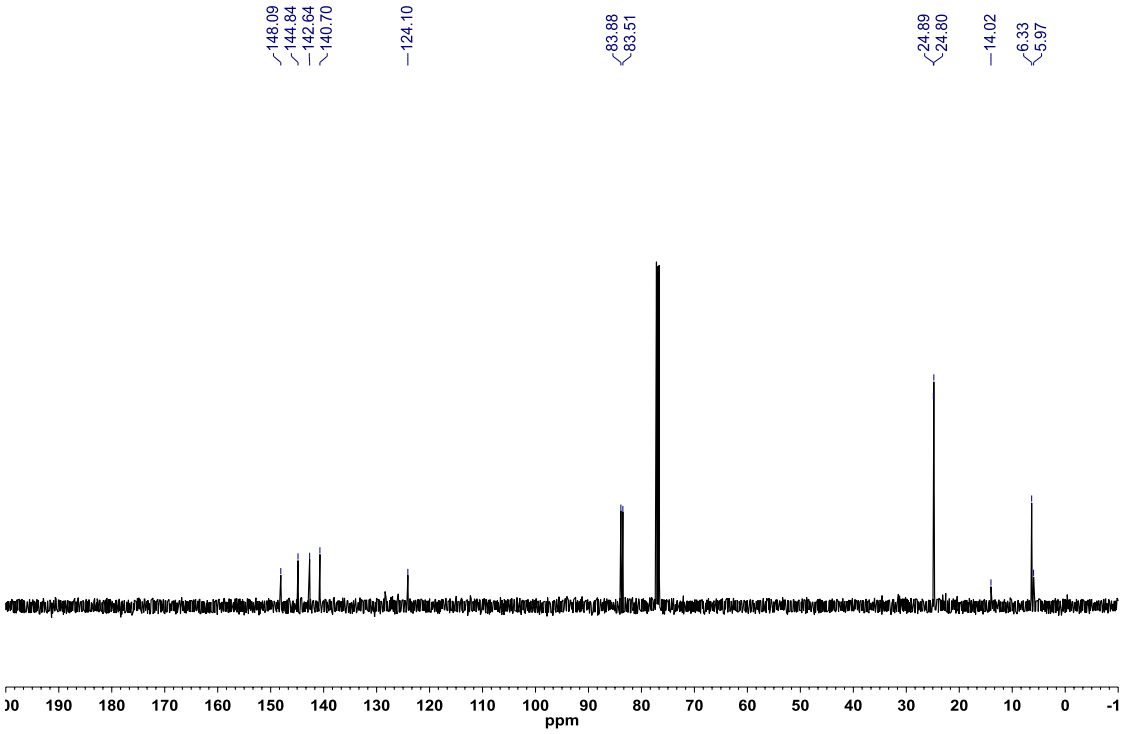

Figure A2.232: ^{11}B NMR ($CDCl_3$, 128.4 MHz) of *2-cyclopropyl-6,8-bis(4,4,5,5-tetramethyl-1,3,2-dioxaboryl)-2,1-borazaronaphthalene* (**3.60**)

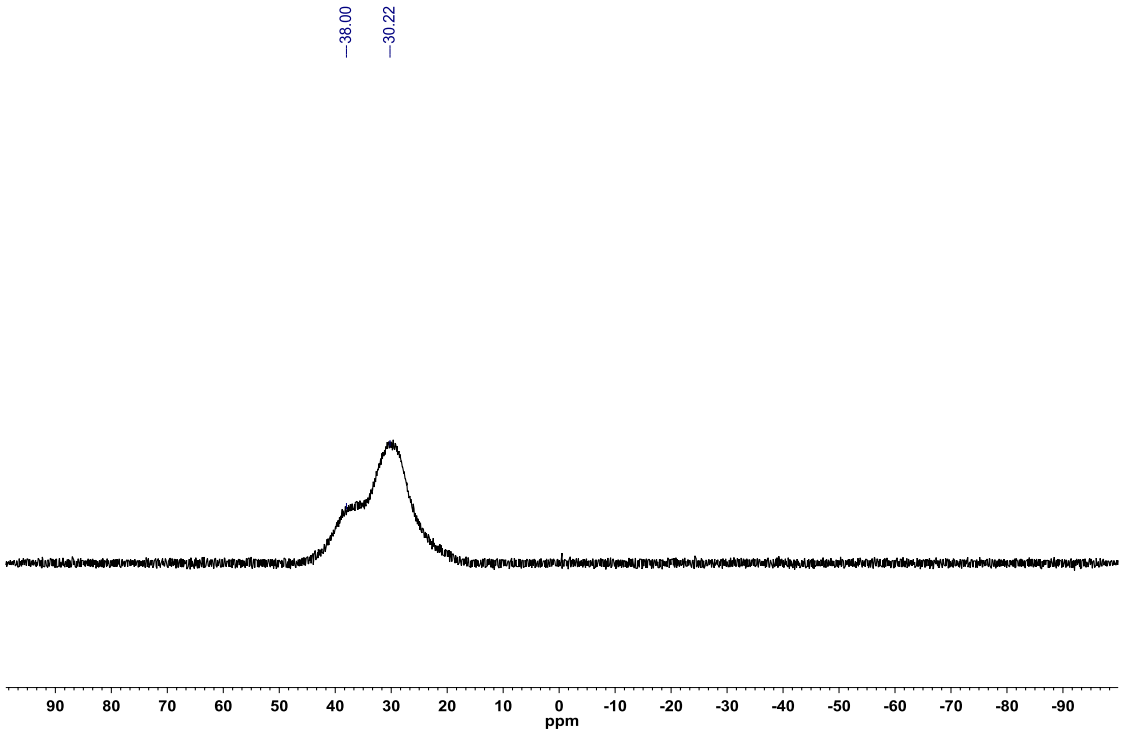

Figure A2.233: ^{1}H NMR ($CDCl_3$, 500.4 MHz) of *2-methyl-6,8-bis(4,4,5,5-tetramethyl-1,3,2-dioxaboryl)-2,1-borazaronaphthalene* (**3.61**)

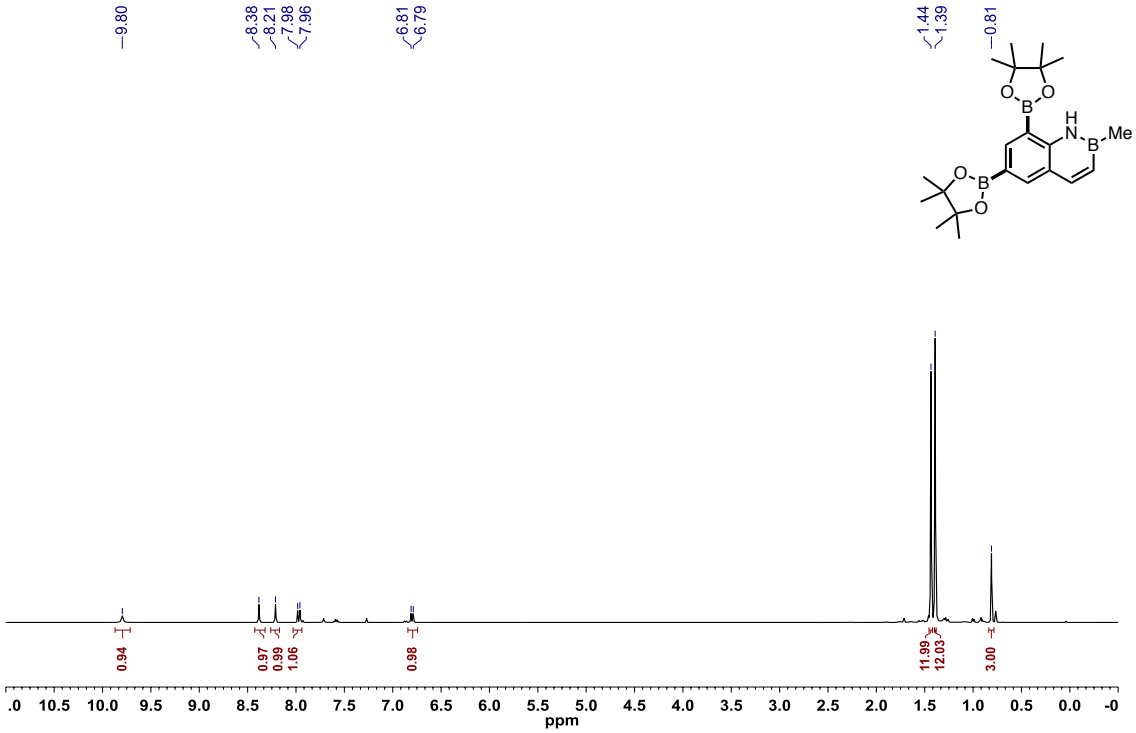

Figure A2.234: ^{13}C {^{1}H} NMR ($CDCl_3$, 125.8 MHz) of *2-methyl-6,8-bis(4,4,5,5-tetramethyl-1,3,2-dioxaboryl)-2,1-borazaronaphthalene* (**3.61**)

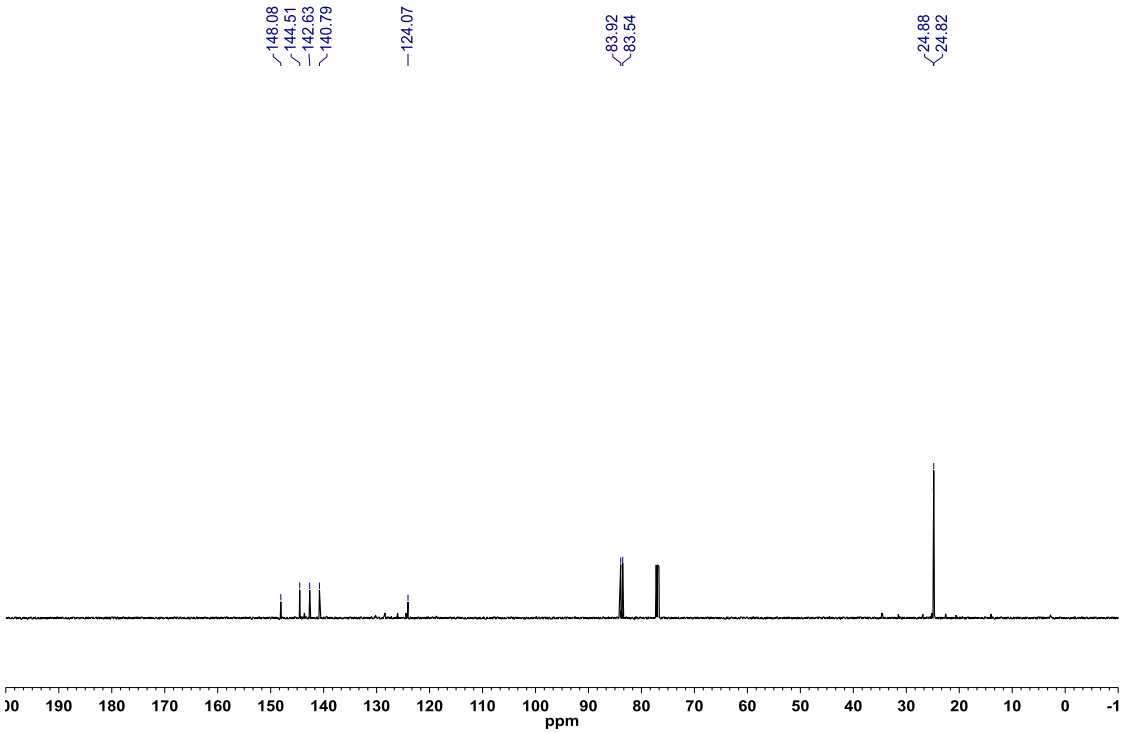

Figure A2.235: ^{11}B NMR ($CDCl_3$, 128.4 MHz) of *2-methyl-6,8-bis(4,4,5,5-tetramethyl-1,3,2-dioxaboryl)-2,1-borazaronaphthalene* (**3.61**)

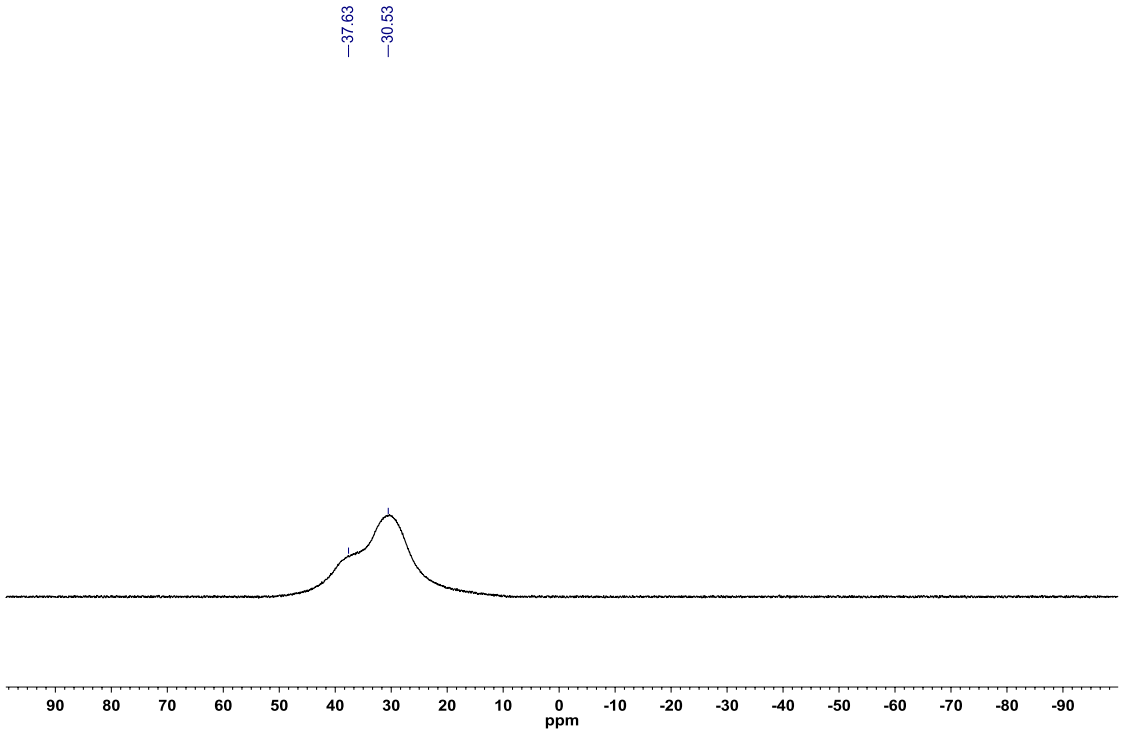

Figure A2.236: ^{1}H NMR ($CDCl_3$, 500.4 MHz) of *N-deuterio-2-(4-(trifluoromethyl)phenyl)-2,1-borazaronaphthalene* (**6**)

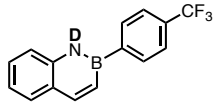

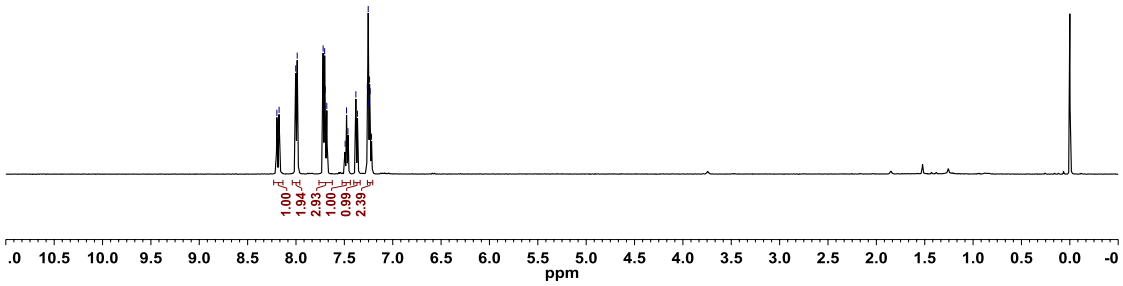

Figure A2.237: ^{13}C {^{1}H} NMR ($CDCl_3$, 125.8 MHz) of *N-deuterio-2-(4-(trifluoromethyl)phenyl)-2,1-borazaronaphthalene* (**6**)

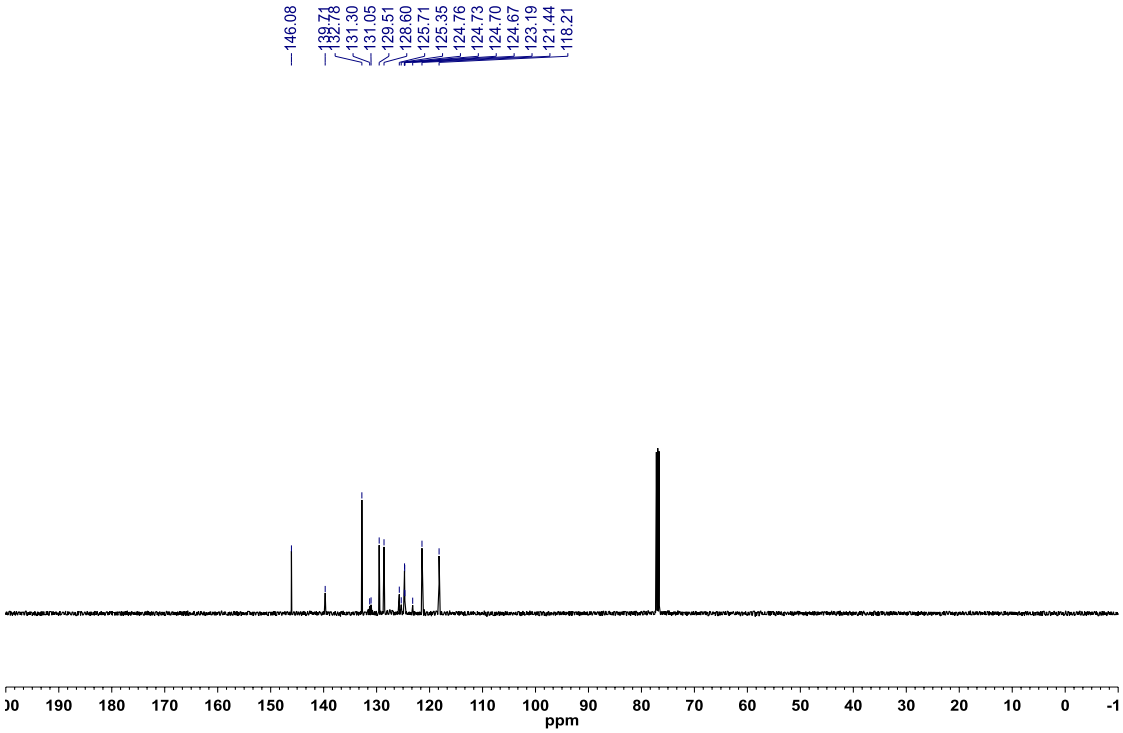

Figure A2.238: ^{19}F {^{1}H} NMR ($CDCl_3$, 470.8 MHz) of *N-deuterio-2-(4-(trifluoromethyl)phenyl)-2,1-borazaronaphthalene* (**6**)

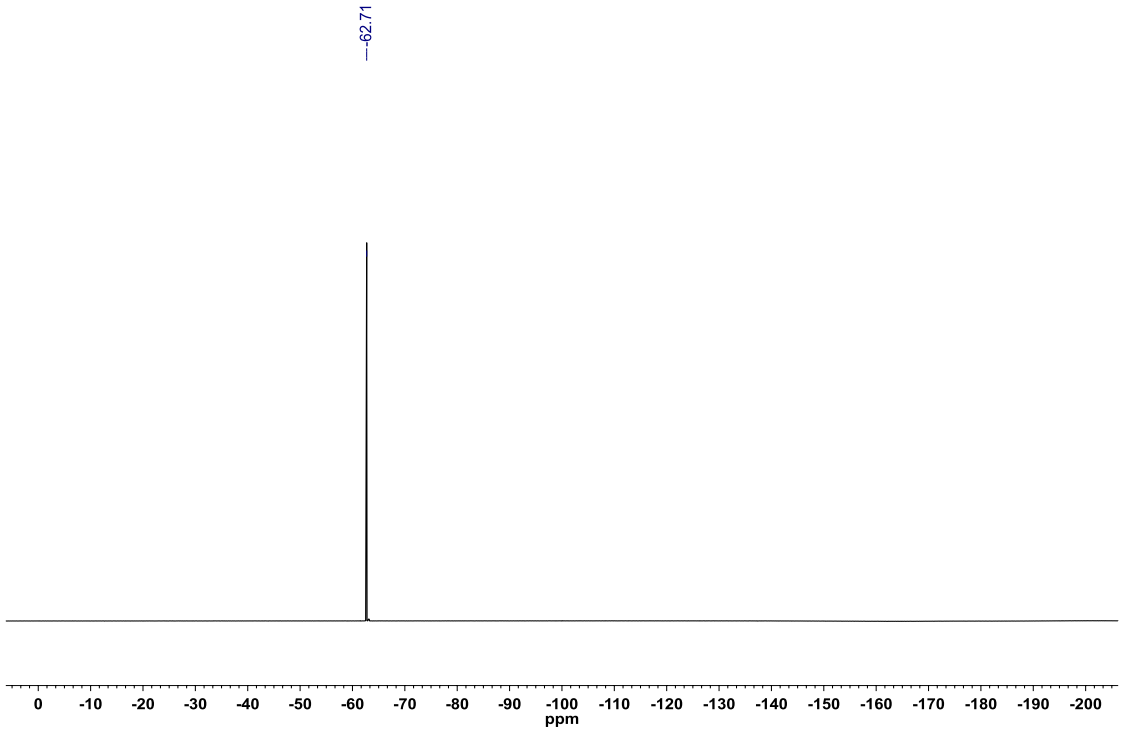

Figure A2.239: ^{11}B NMR ($CDCl_3$, 128.4 MHz) of *N-deuterio-2-(4-(trifluoromethyl)phenyl)-2,1-borazaronaphthalene* (**6**)

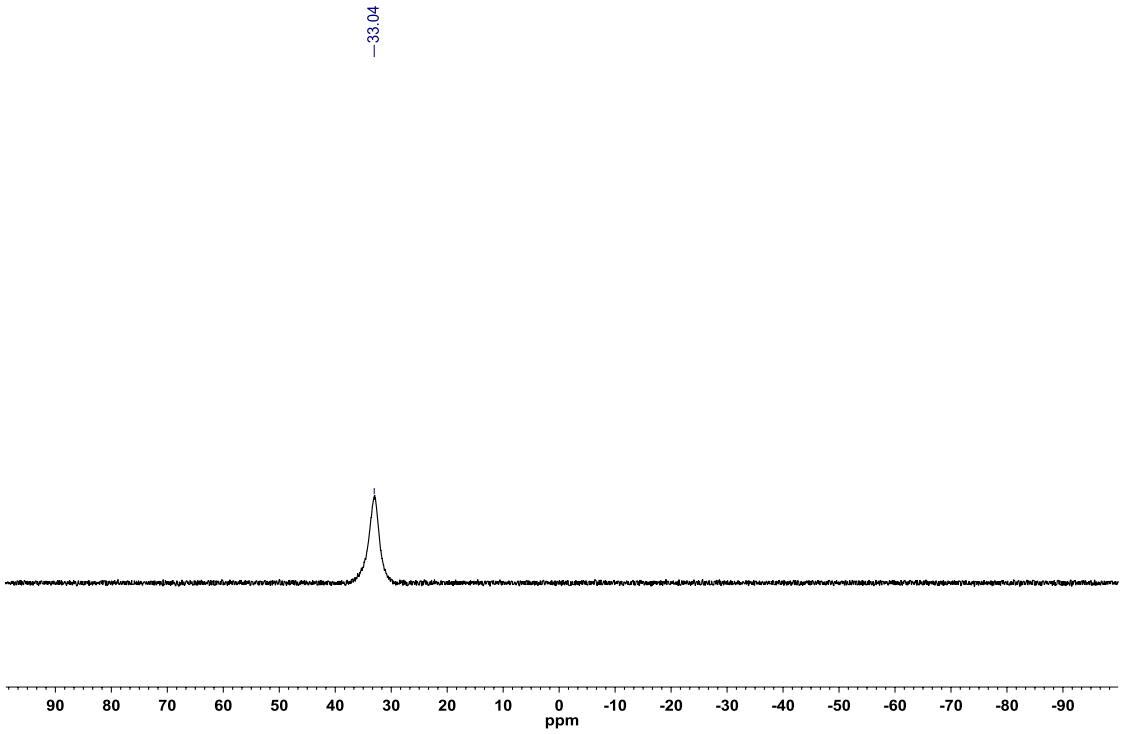

Figure A2.240: ^{1}H NMR ($CDCl_3$, 500.4 MHz) of *N-deuterio-8-(4,4,5,5-tetramethyl-1,3,2-dioxaboryl)*-2-*(4-(trifluoromethyl)phenyl)-2,1-borazaronaphthalene* (**7**)

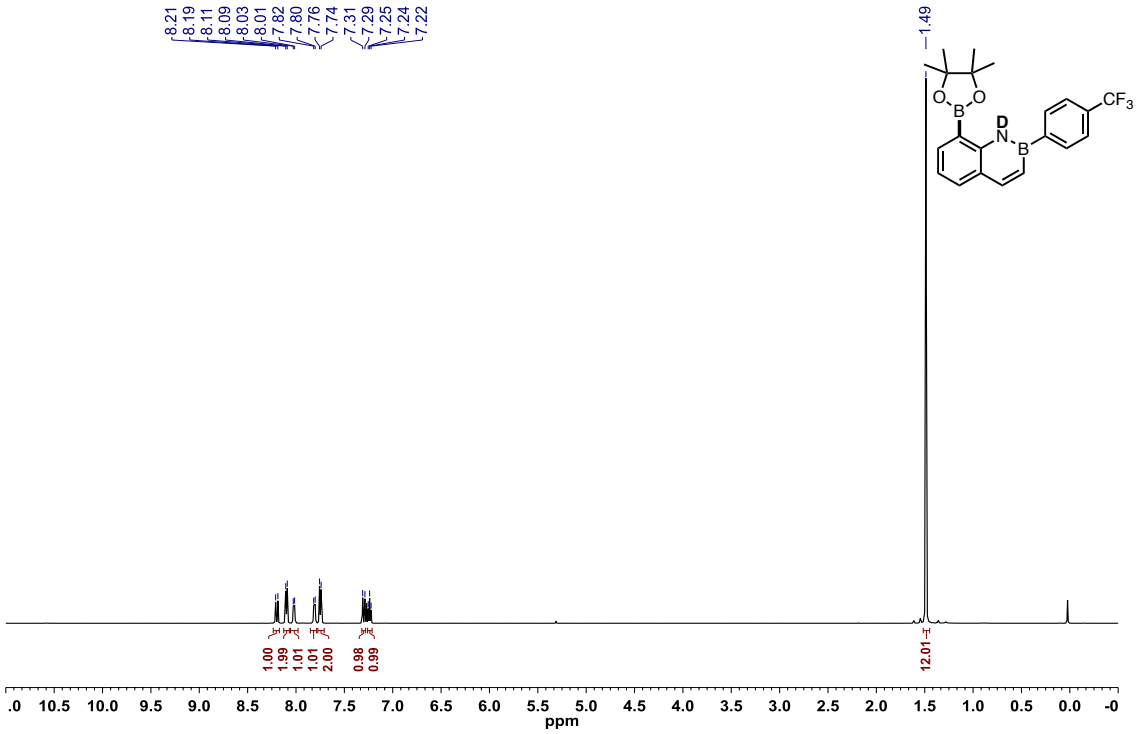

Figure A2.241: ^{13}C {^{1}H} NMR ($CDCl_3$, 125.8 MHz) of *N-deuterio-8-(4,4,5,5-tetramethyl-1,3,2-dioxaboryl)-2-(4-(trifluoromethyl)phenyl)-2,1-borazaronaphthalene* (**7**)

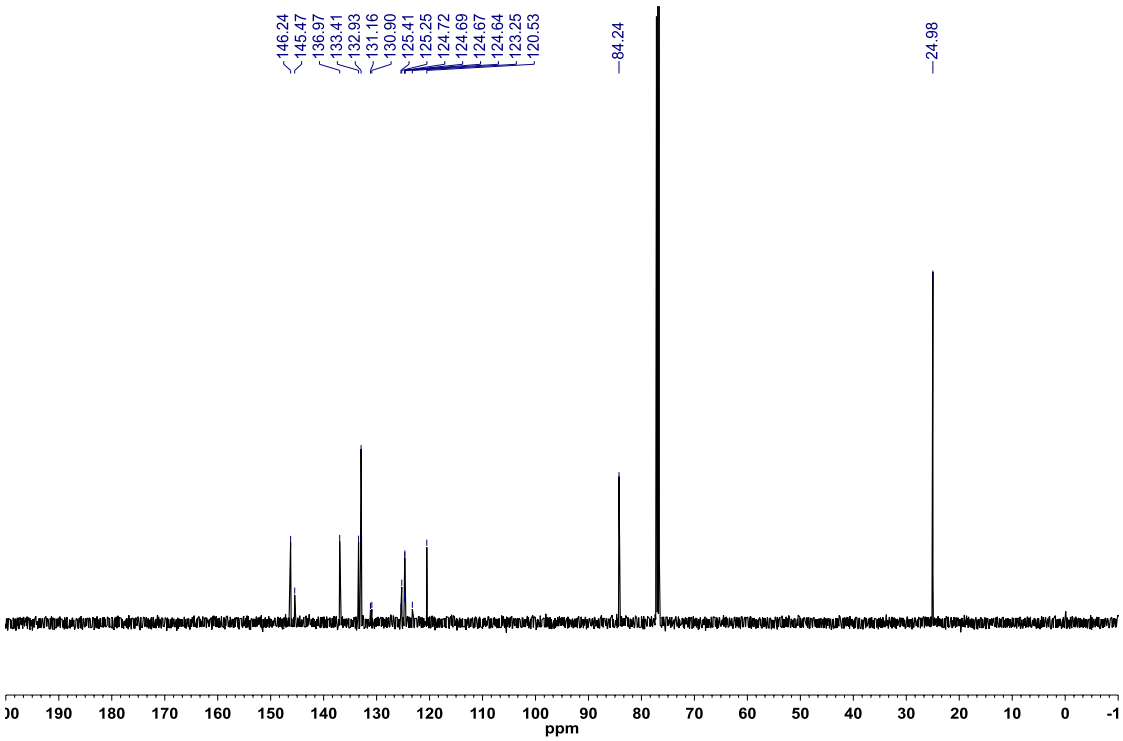

Figure A2.242: ^{19}F {^{1}H} NMR ($CDCl_3$, 470.8 MHz) of *N-deuterio-8-(4,4,5,5-tetramethyl-1,3,2-dioxaboryl)-2-(4-(trifluoromethyl)phenyl)-2,1-borazaronaphthalene* (**7**

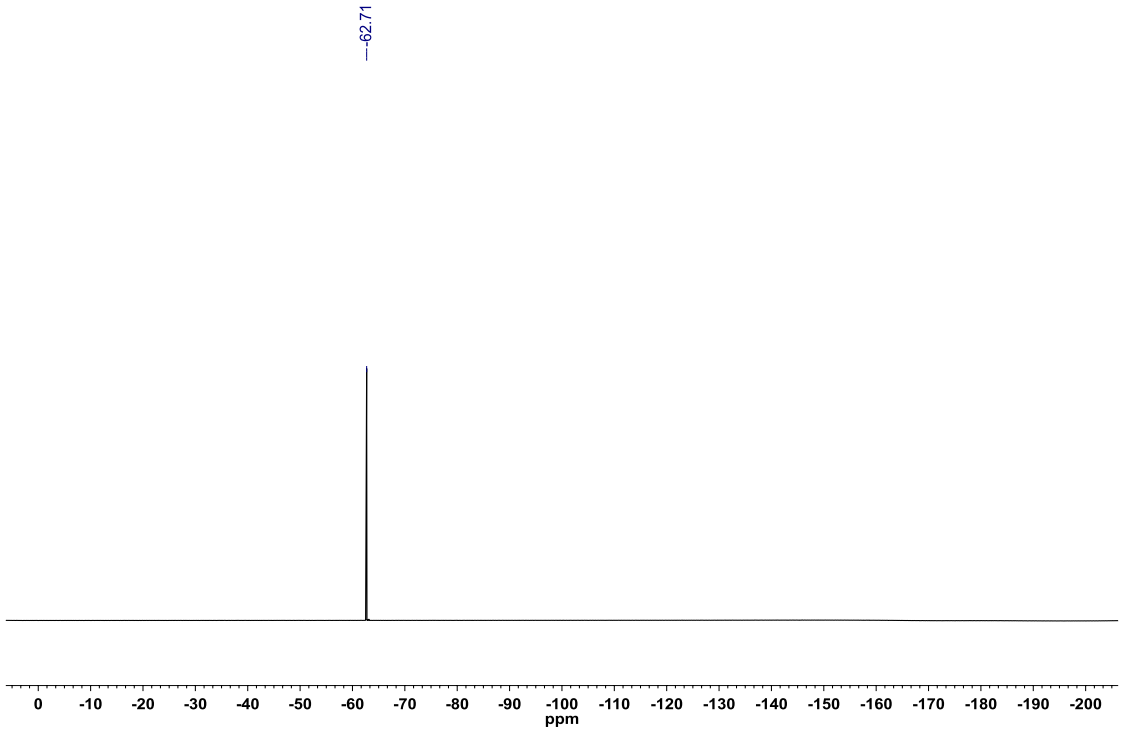

Figure A2.243: ^{11}B NMR ($CDCl_3$, 128.4 MHz) of *N-deuterio-8-(4,4,5,5-tetramethyl-1,3,2-dioxaboryl)-2-(4-(trifluoromethyl)phenyl)-2,1-borazaronaphthalene* (**7**)

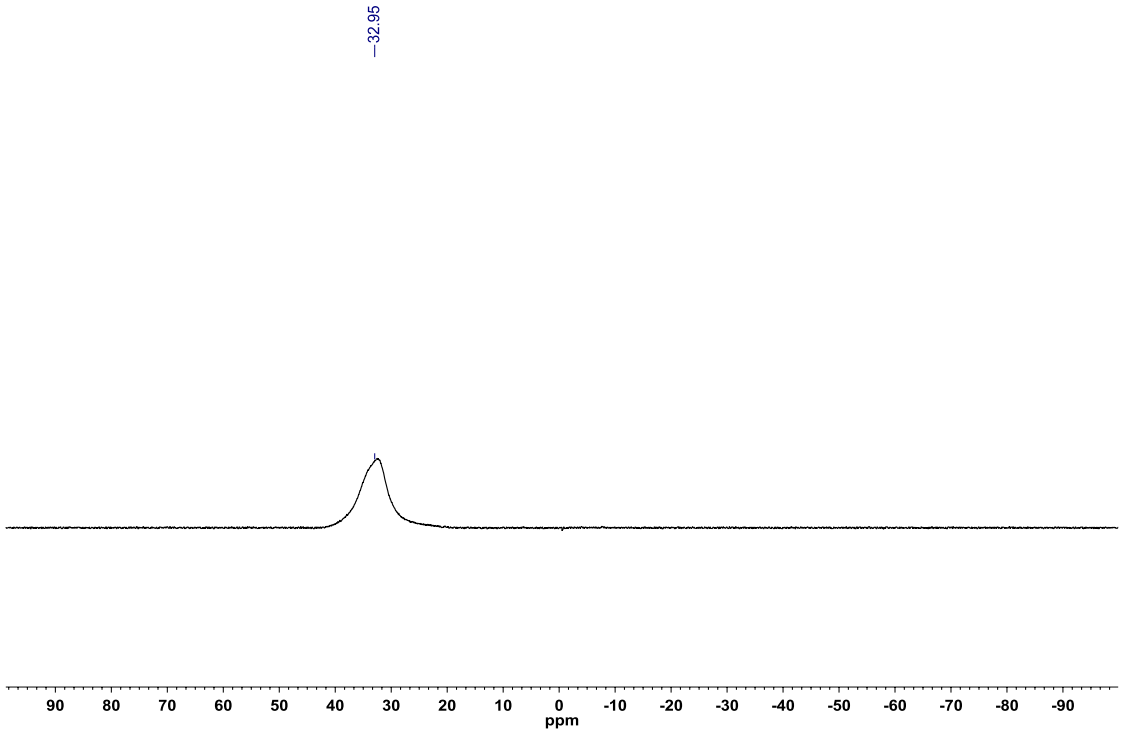

Figure A2.244: ^{1}H NMR ($CDCl_3$, 500.4 MHz) of *8-(pyrimidin-5-yl)-2-(4-(trifluoromethyl)phenyl)-2,1-borazaronaphthalene* (**3.67**)

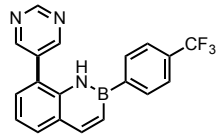

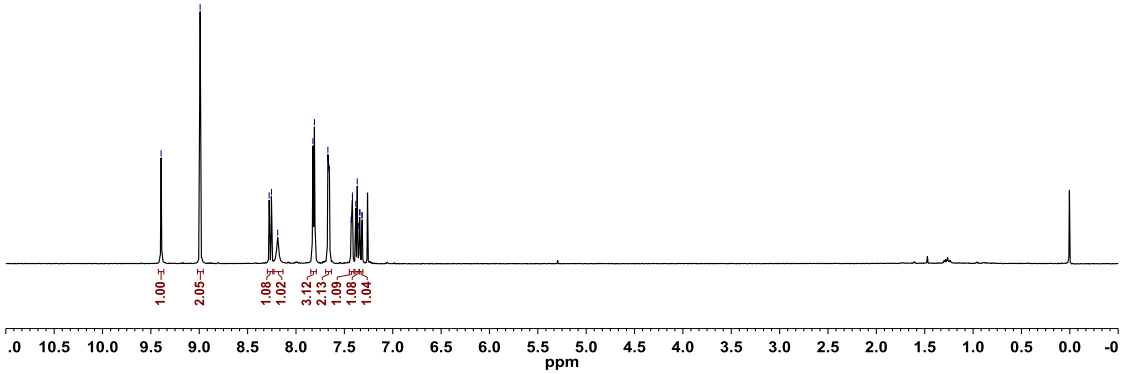

Figure A2.245: ^{13}C {^{1}H} NMR ($CDCl_3$, 125.8 MHz) of *8-(pyrimidin-5-yl)-2-(4-(trifluoromethyl)phenyl)-2,1-borazaronaphthalene* (**3.67**)

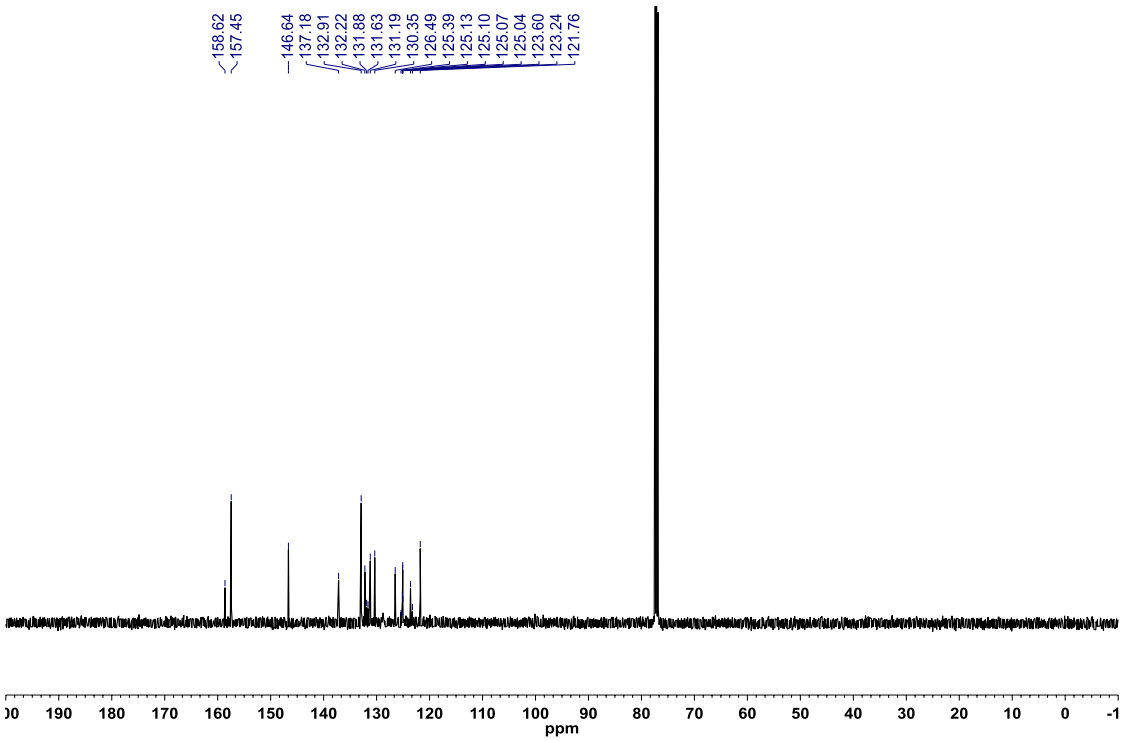

Figure A2.246: ^{19}F {^{1}H} NMR ($CDCl_3$, 470.8 MHz) of *8-(pyrimidin-5-yl)-2-(4-(trifluoromethyl)phenyl)-2,1-borazaronaphthalene* (**3.67**)

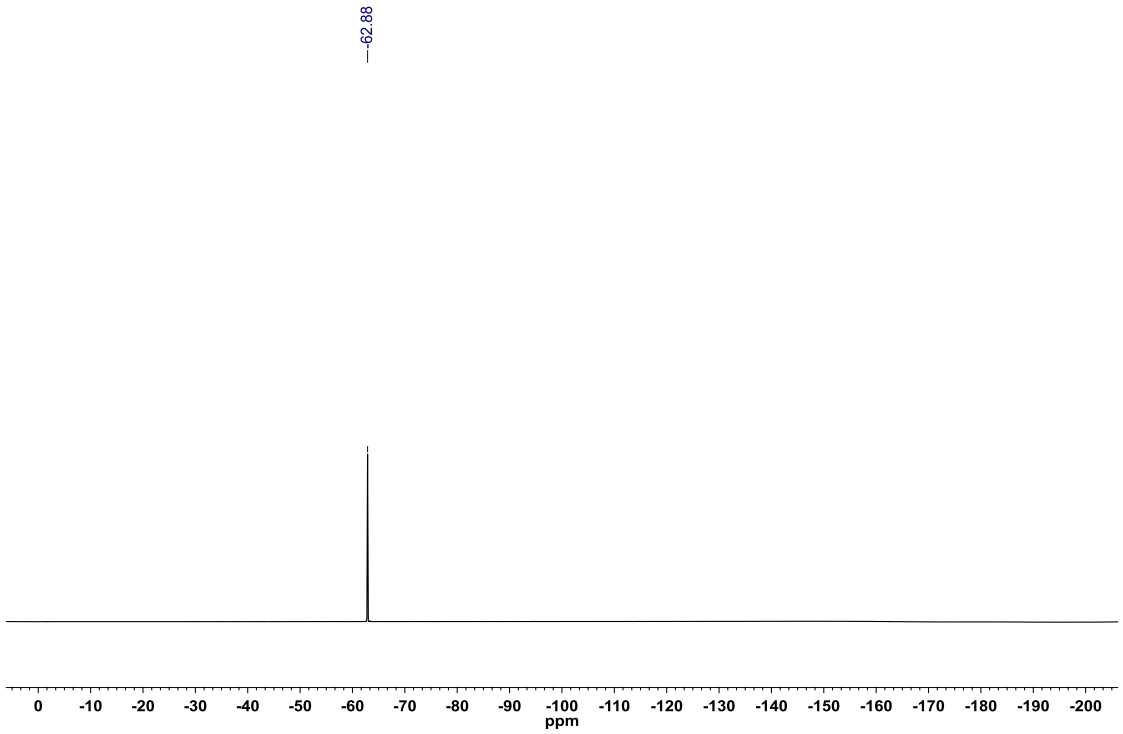

Figure A2.247: ^{11}B NMR ($CDCl_3$, 128.4 MHz) of *8-(pyrimidin-5-yl)-2-(4-(trifluoromethyl)phenyl)-2,1-borazaronaphthalene* (**3.67**)

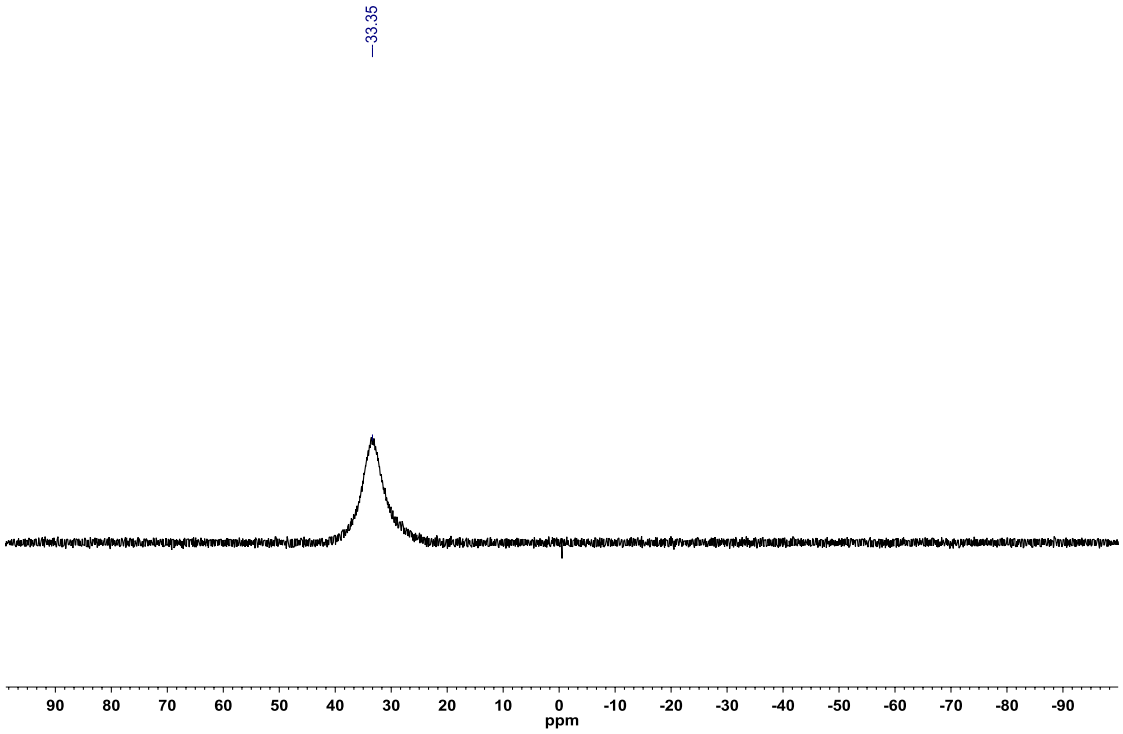

Figure A2.248: ^{1}H NMR ($CDCl_3$, 500.4 MHz) of *8-(pyrimidin-5-yl)-2-(p-tolyl)-2,1-borazaronaphthalene* (**3.68**)

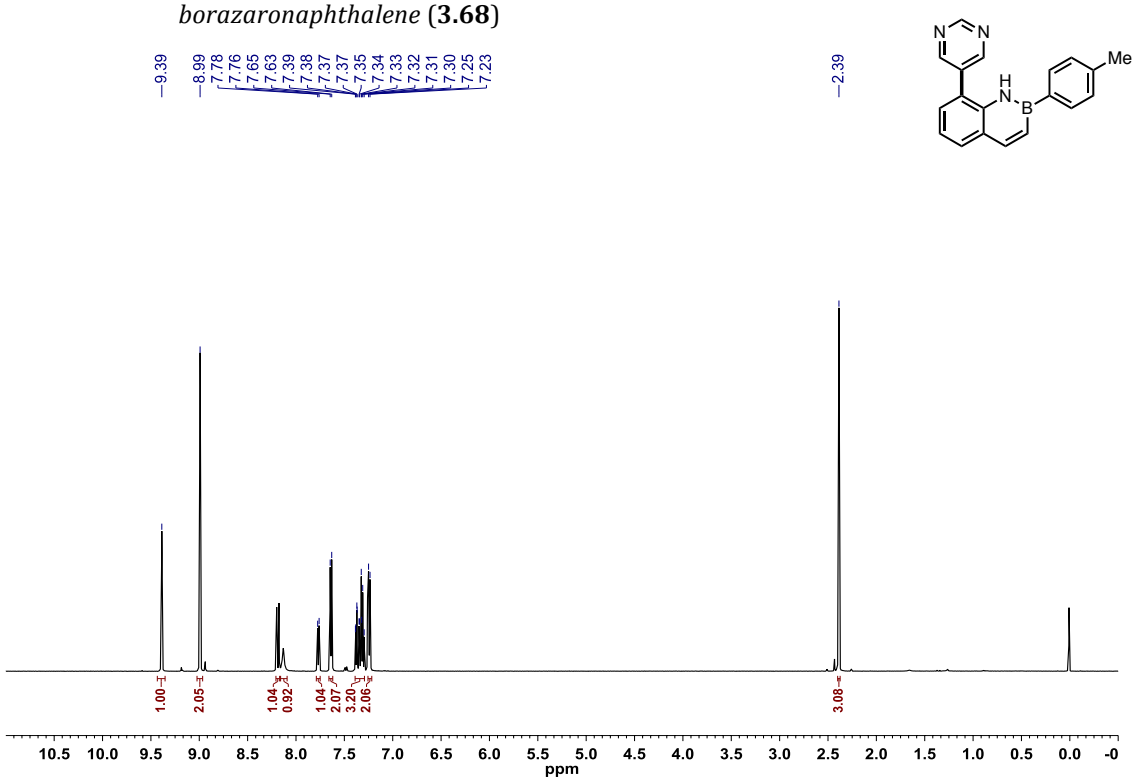

Figure A2.249: ^{13}C {^{1}H} NMR ($CDCl_3$, 125.8 MHz) of *8-(pyrimidin-5-yl)-2-(p-tolyl)-2,1-borazaronaphthalene* (**3.68**)

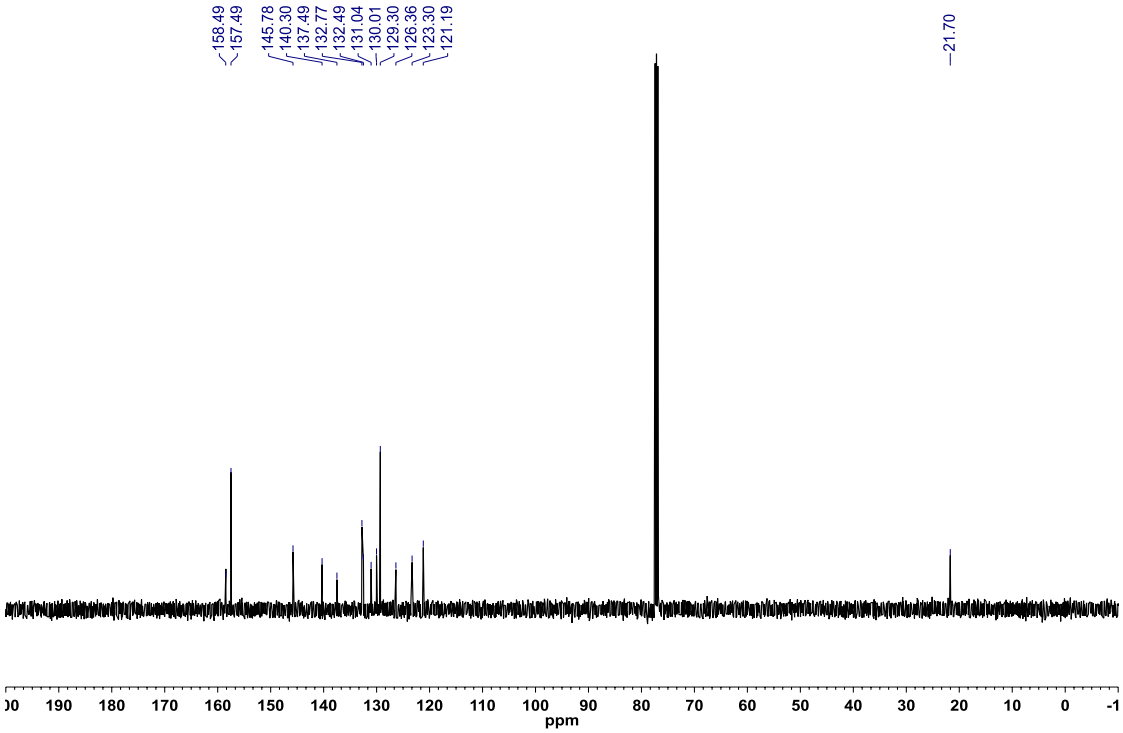

Figure A2.250: ^{11}B NMR ($CDCl_3$, 128.4 MHz) of *8-(pyrimidin-5-yl)-2-(p-tolyl)-2,1-borazaronaphthalene* (**3.68**)

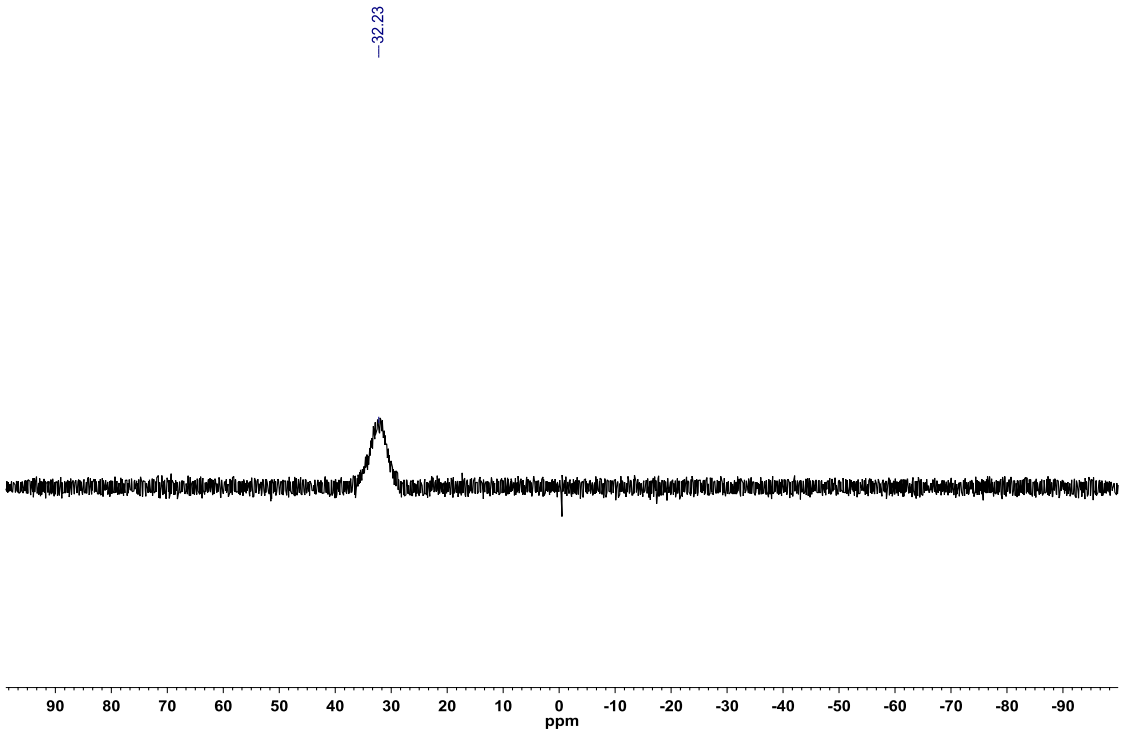

Figure A2.251: ^{1}H NMR ($CDCl_3$, 500.4 MHz) of *2-cyclopropyl-8-(pyrimidin-5-yl)-2,1-borazaronaphthalene* (**3.69**)

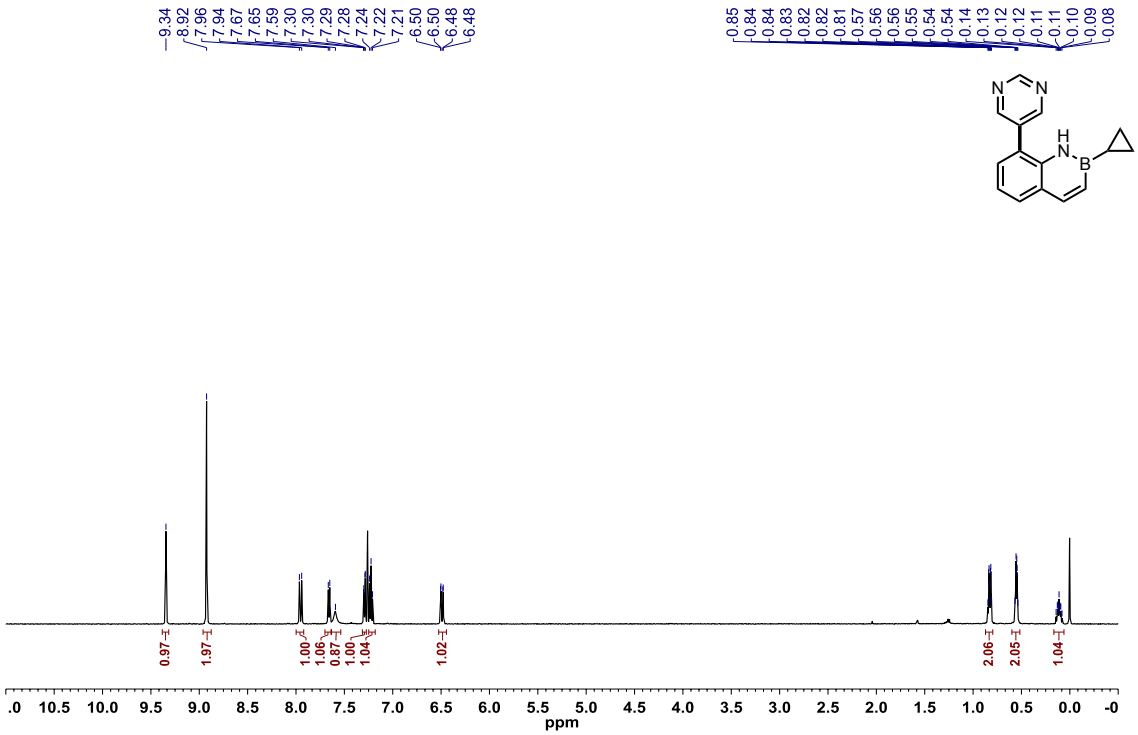

Figure A2.252: ^{13}C {^{1}H} NMR ($CDCl_3$, 125.8 MHz) of *2-cyclopropyl-8-(pyrimidin-5-yl)-2,1-borazaronaphthalene* (**3.69**)

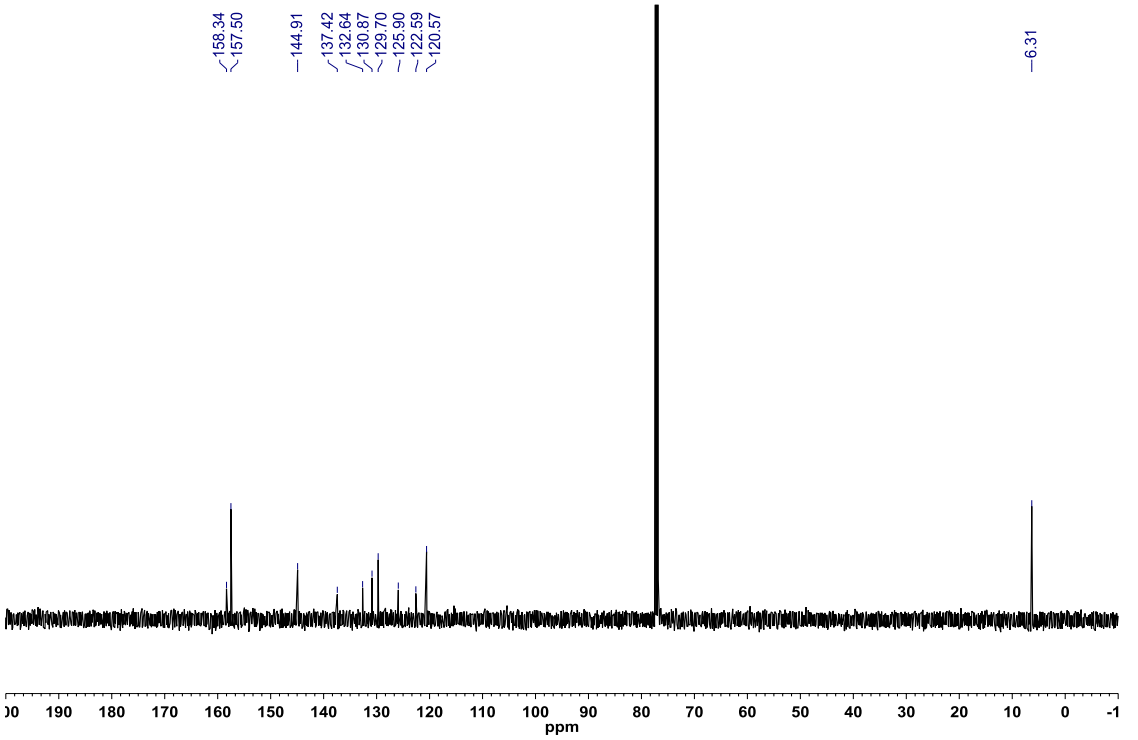

Figure A2.253: ^{11}B NMR ($CDCl_3$, 128.4 MHz) of *2-cyclopropyl-8-(pyrimidin-5-yl)-2,1-borazaronaphthalene* (**3.69**)

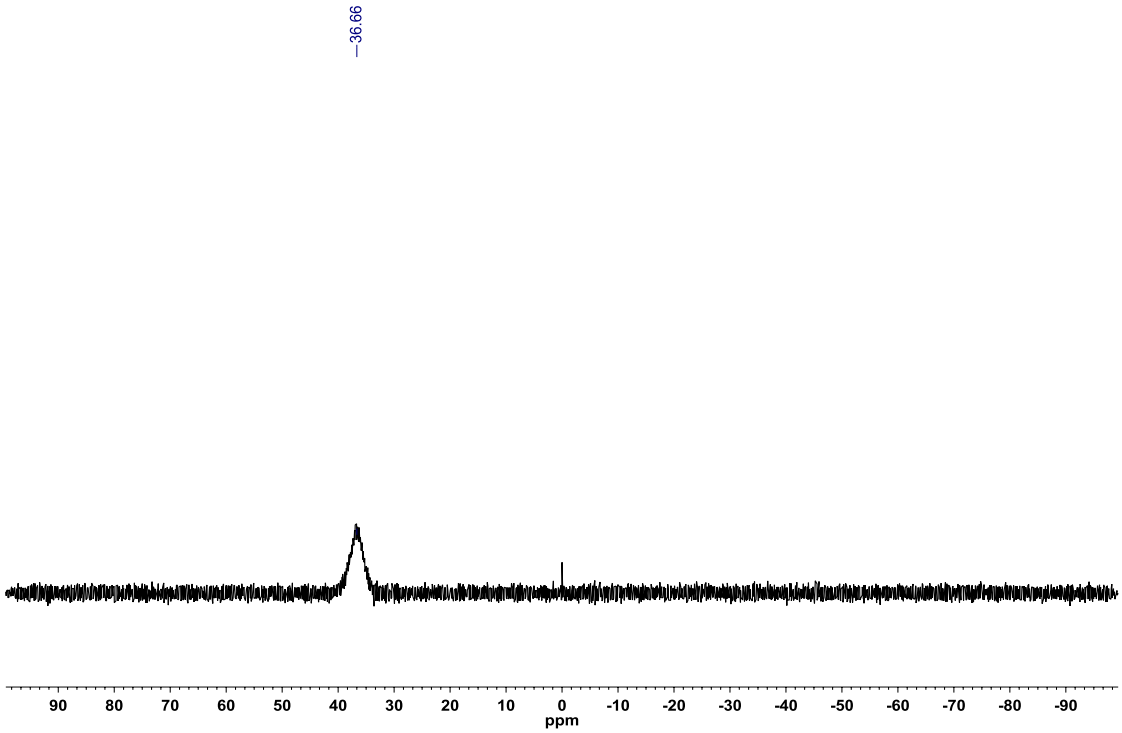

Figure A2.254: ^{1}H NMR ($CDCl_3$, 500.4 MHz) of *8-(pyridin-3-yl)-2-(4-(trifluoromethyl)phenyl)-2,1-borazaronaphthalene* (**3.70**)

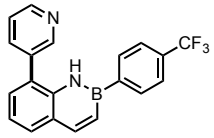

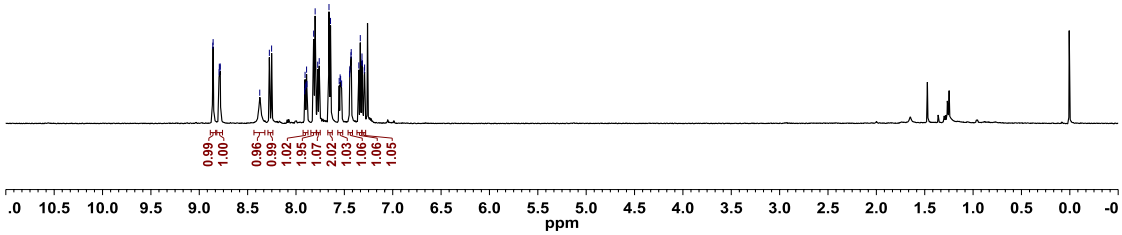

Figure A2.255: ^{13}C {^{1}H} NMR ($CDCl_3$, 125.8 MHz) of *8-(pyridin-3-yl)-2-(4-(trifluoromethyl)phenyl)-2,1-borazaronaphthalene* (**3.70**)

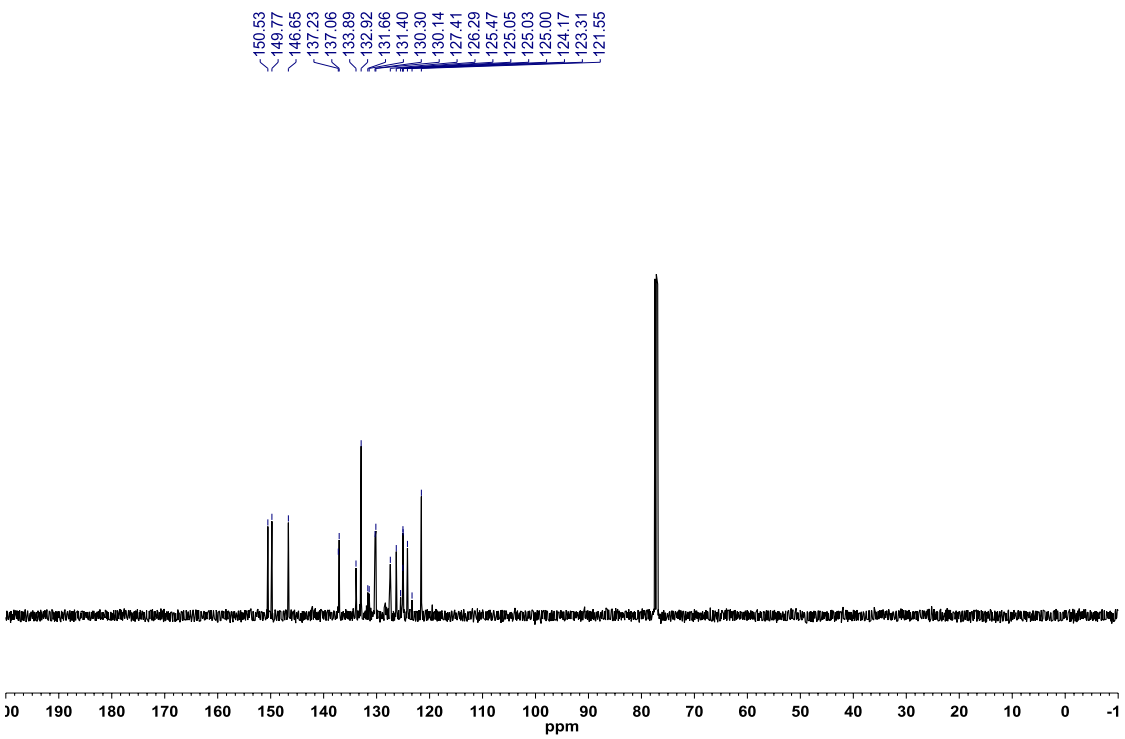

Figure A2.256: ^{19}F {^{1}H} NMR ($CDCl_3$, 470.8 MHz) of *8-(pyridin-3-yl)-2-(4-(trifluoromethyl)phenyl)-2,1-borazaronaphthalene* (**3.70**)

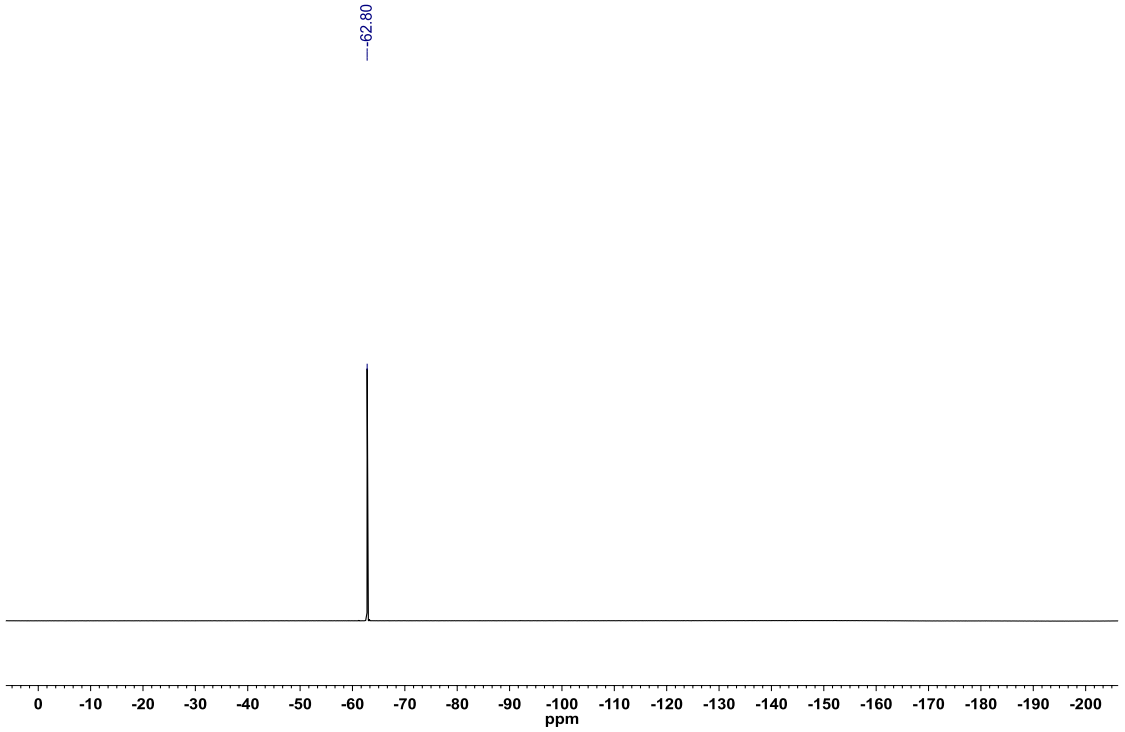

Figure A2.257: ^{11}B NMR ($CDCl_3$, 128.4 MHz) of *8-(pyridin-3-yl)-2-(4-(trifluoromethyl)phenyl)-2,1-borazaronaphthalene* (**3.70**)

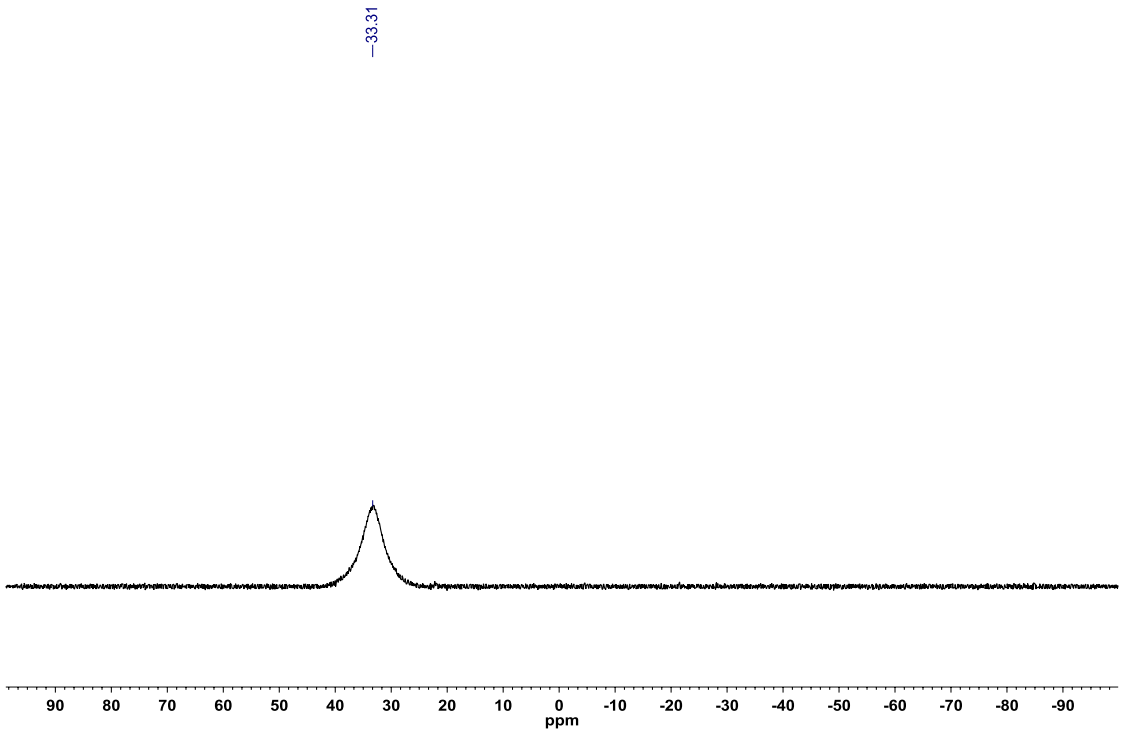

Figure A2.258: ^{1}H NMR ($CDCl_3$, 500.4 MHz) of *8-(quinolin-3-yl)-2-(4-(trifluoromethyl)phenyl)-2,1-borazaronaphthalene* (**3.71**)

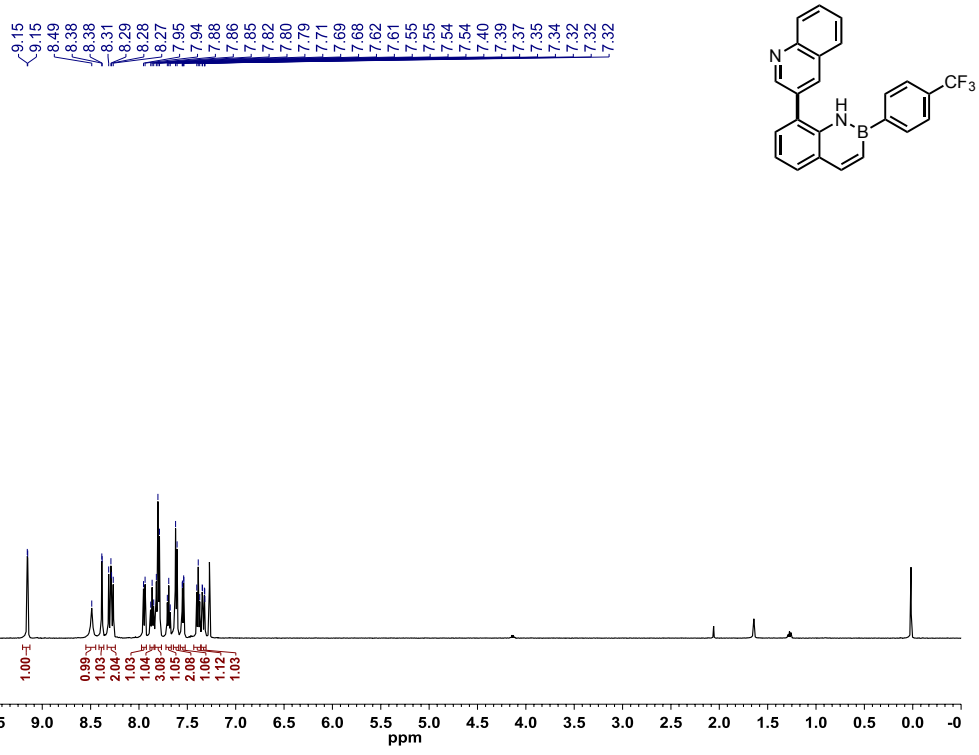

Figure A2.259: ^{13}C {^{1}H} NMR ($CDCl_3$, 125.8 MHz) of *8-(quinolin-3-yl)-2-(4-(trifluoromethyl)phenyl)-2,1-borazaronaphthalene* (**3.71**)

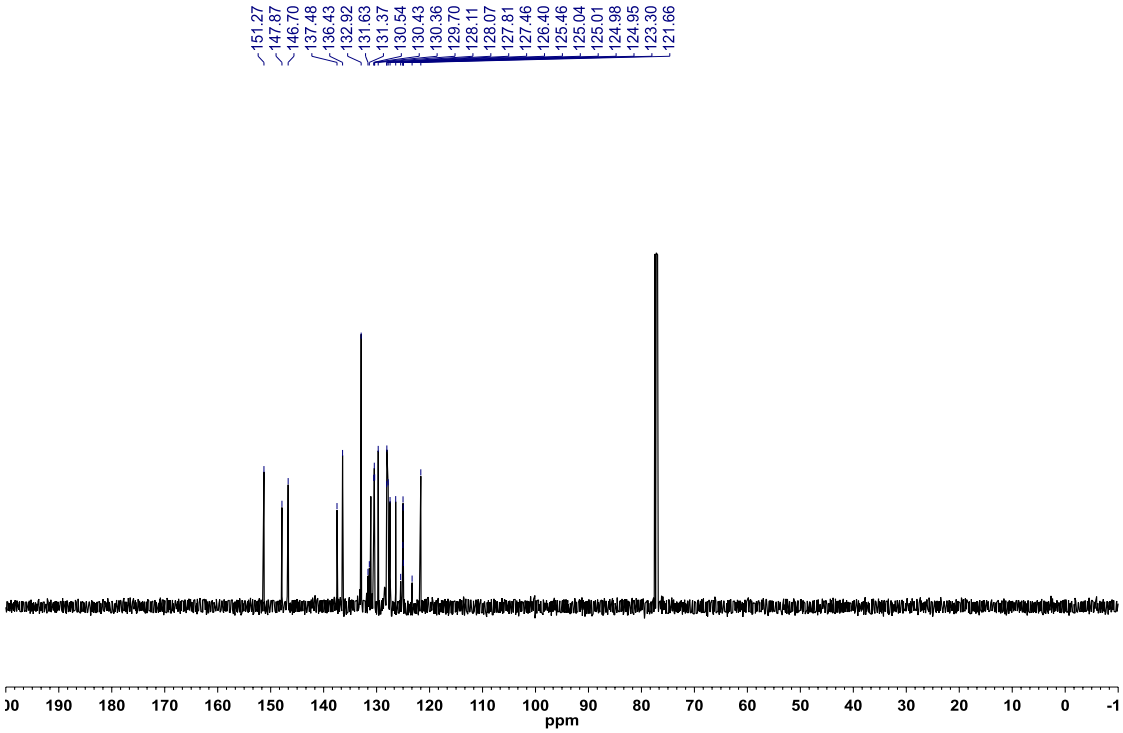

Figure A2.260: ^{19}F {^{1}H} NMR ($CDCl_3$, 470.8 MHz) of *8-(quinolin-3-yl)-2-(4-(trifluoromethyl)phenyl)-2,1-borazaronaphthalene* (**3.71**)

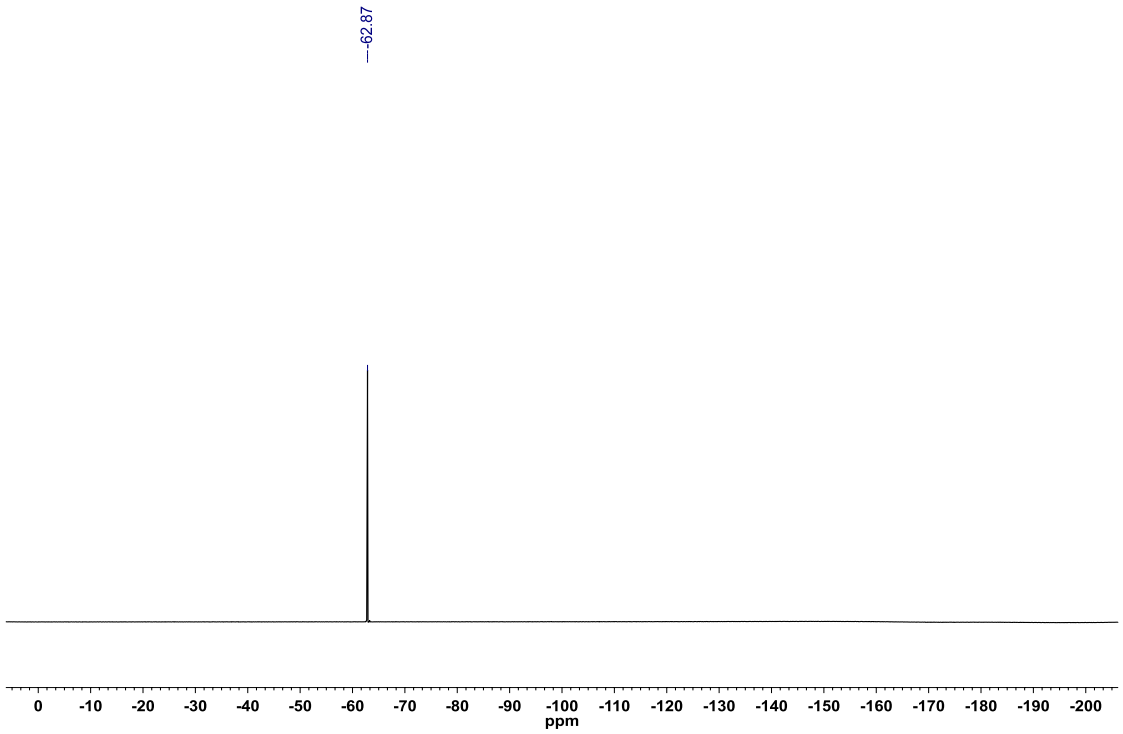

Figure A2.261: ^{11}B NMR ($CDCl_3$, 128.4 MHz) of *8-(quinolin-3-yl)-2-(4-(trifluoromethyl)phenyl)-2,1-borazaronaphthalene* (**3.71**)

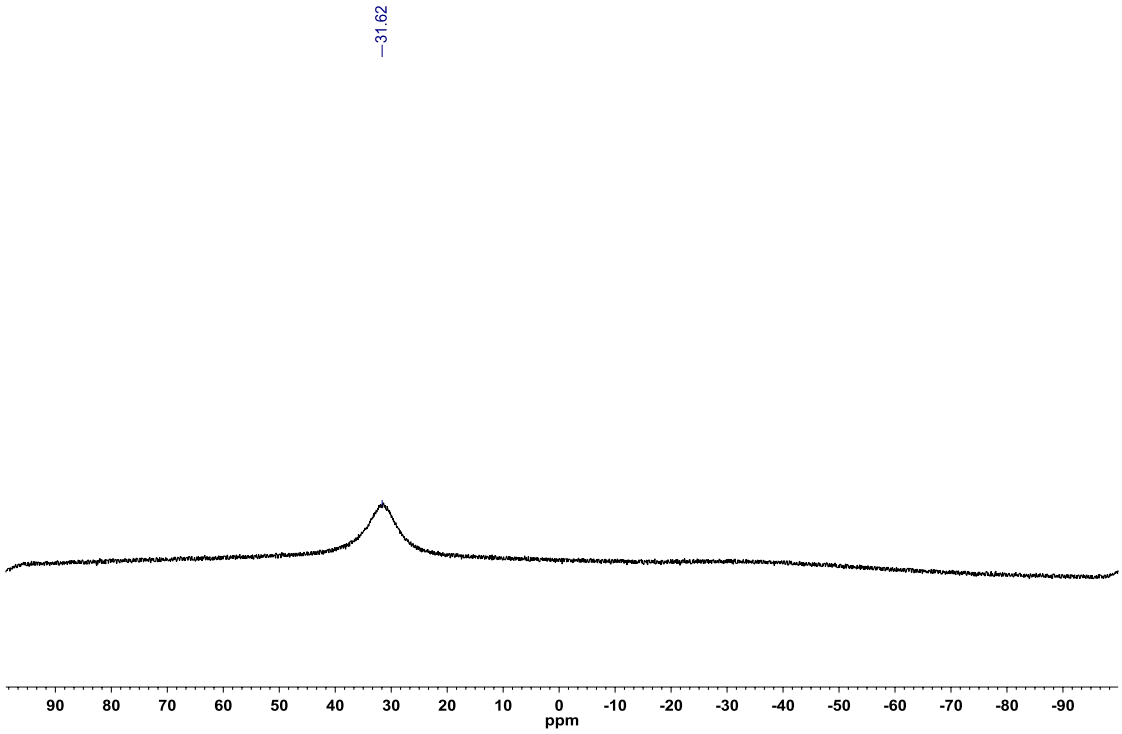

Figure A2.262: ^{1}H NMR ($CDCl_3$, 500.4 MHz) of *8-(thiophen-3-yl)-2-(4-(trifluoromethyl)phenyl)-2,1-borazaronaphthalene* (**3.72**)

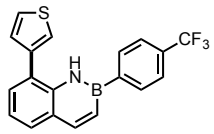

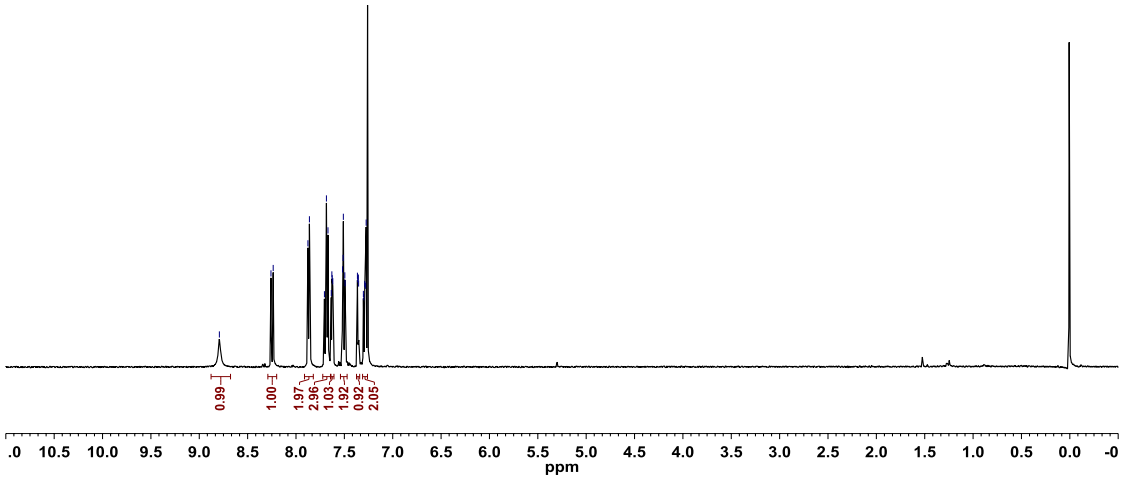

Figure A2.263: ^{13}C {^{1}H} NMR ($CDCl_3$, 125.8 MHz) of *8-(thiophen-3-yl)-2-(4-(trifluoromethyl)phenyl)-2,1-borazaronaphthalene* (**3.72**)

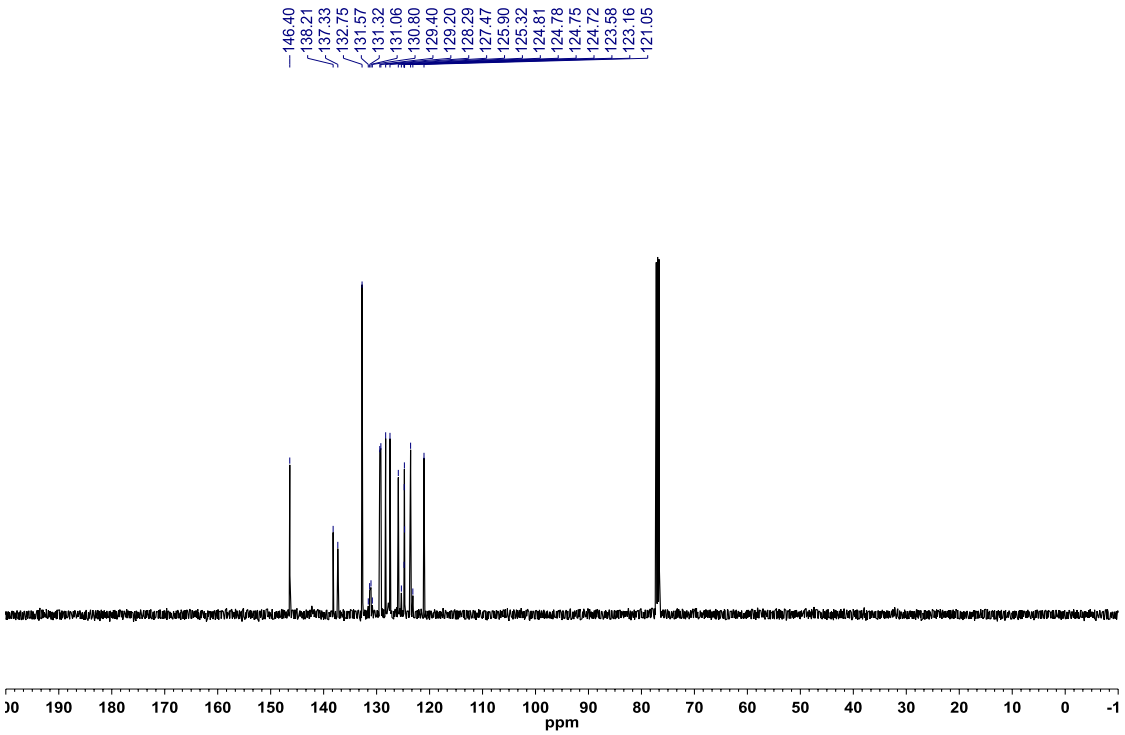

Figure A2.264: ^{19}F {^{1}H} NMR ($CDCl_3$, 470.8 MHz) of *8-(thiophen-3-yl)-2-(4-(trifluoromethyl)phenyl)-2,1-borazaronaphthalene* (**3.72**)

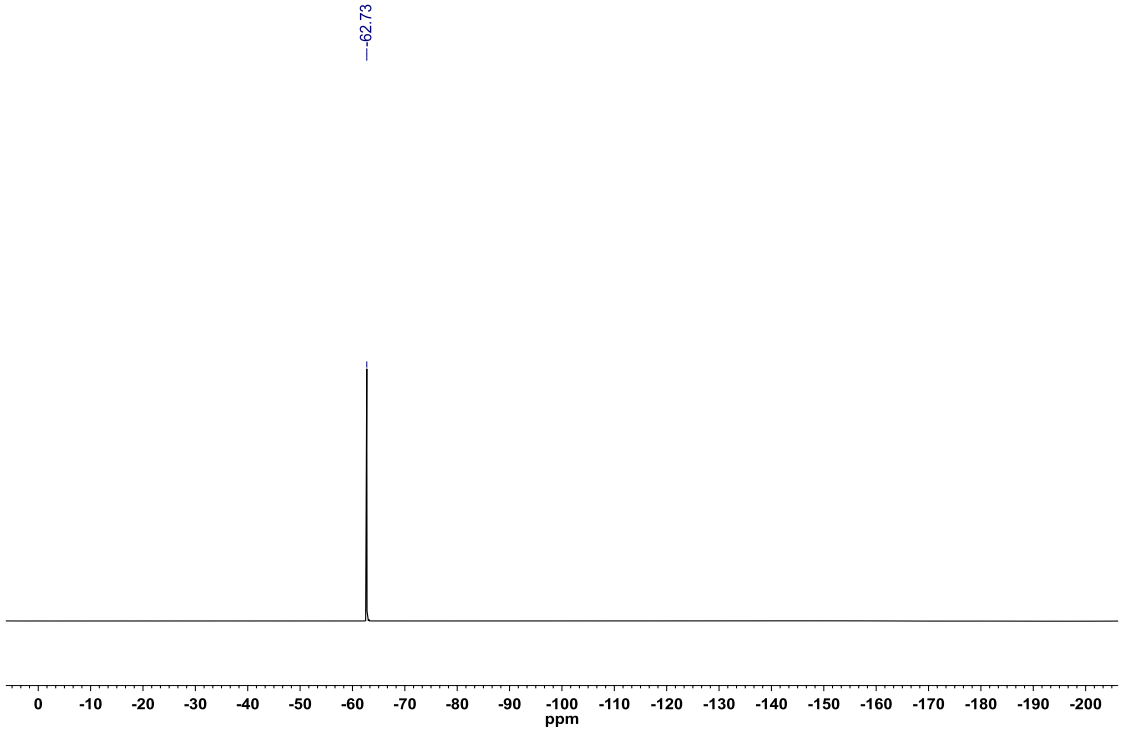

Figure A2.265: ^{11}B NMR ($CDCl_3$, 128.4 MHz) of *8-(thiophen-3-yl)-2-(4-(trifluoromethyl)phenyl)-2,1-borazaronaphthalene* (**3.72**)

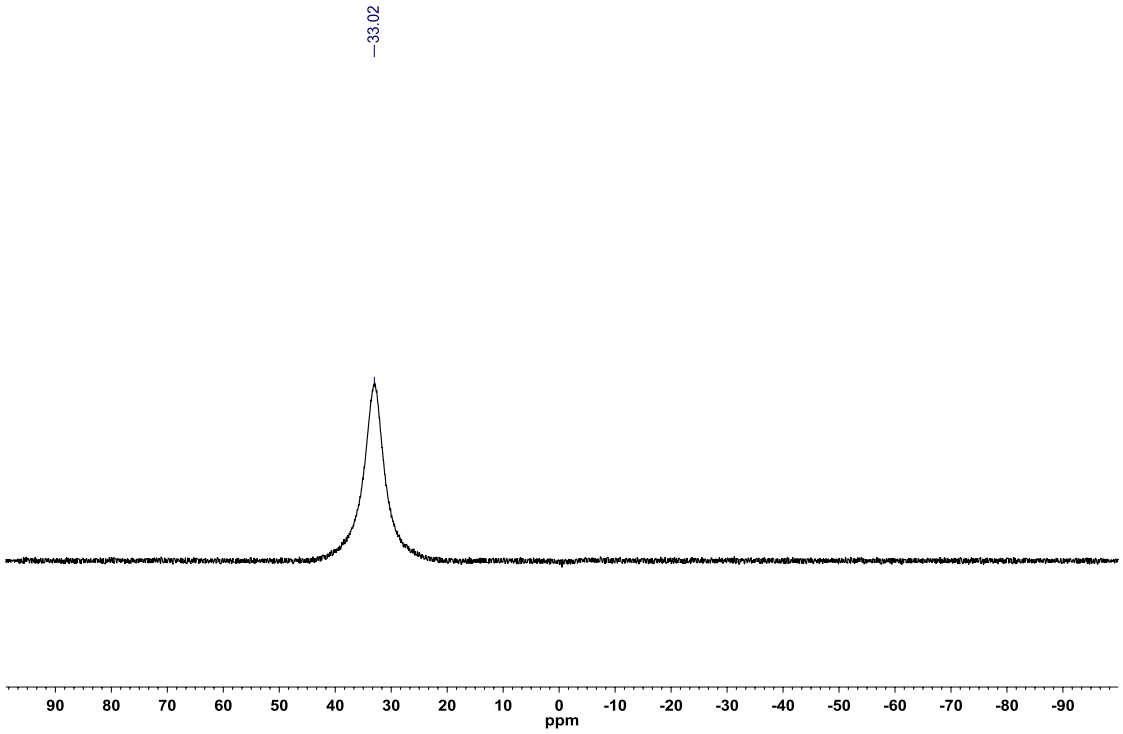

Figure A2.266: ^{1}H NMR ($CDCl_3$, 500.4 MHz) of *8-(thiophen-3-yl)-2-(3-methoxyphenyl)-2,1-borazaronaphthalene* (**3.73**)

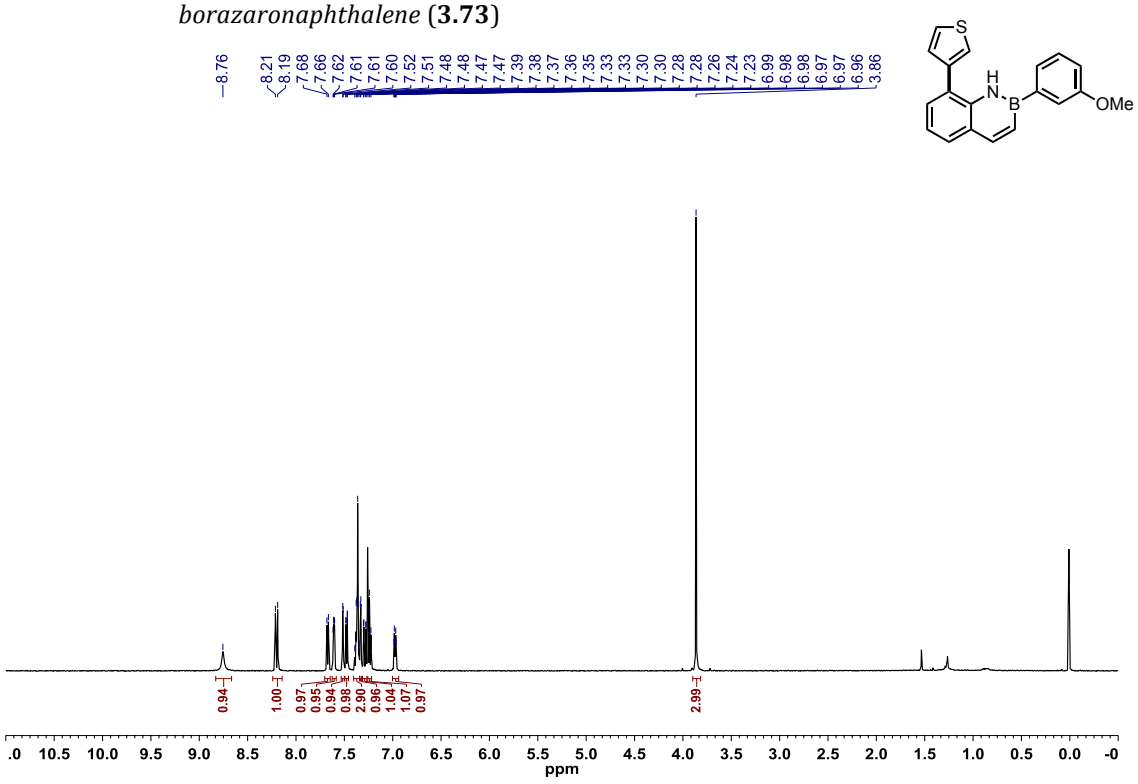

Figure A2.267: ^{13}C {^{1}H} NMR ($CDCl_3$, 125.8 MHz) of *8-(thiophen-3-yl)-2-(3-methoxyphenyl)-2,1-borazaronaphthalene* (**3.73**)

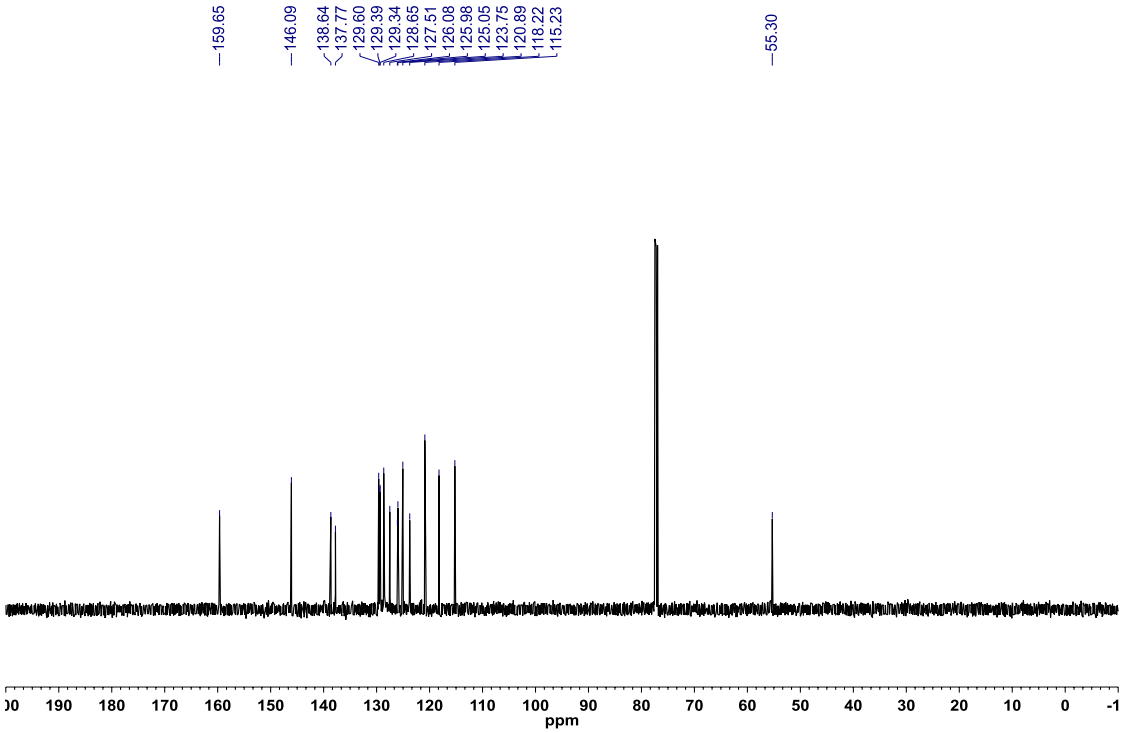

Figure A2.268: ^{11}B NMR ($CDCl_3$, 128.4 MHz) of *8-(thiophen-3-yl)-2-(3-methoxyphenyl)-2,1-borazaronaphthalene* (**3.73**)

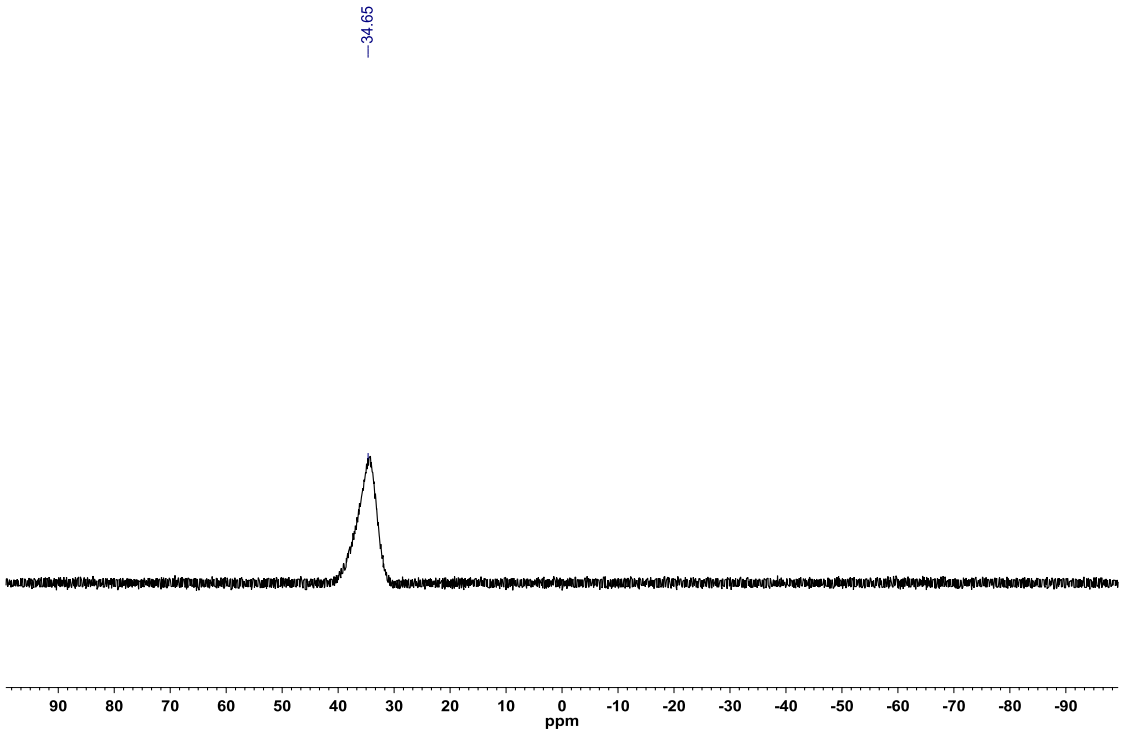

Figure A2.269: ^{1}H NMR ($CDCl_3$, 500.4 MHz) of *2-(4-(trifluoromethyl)phenyl)-8-(1,3,7-trimethyl-2,6-dioxo-2,3,6,7-tetrahydro-1H-purin-8-yl)-2,1-borazaronaphthalene* (**3.74**)

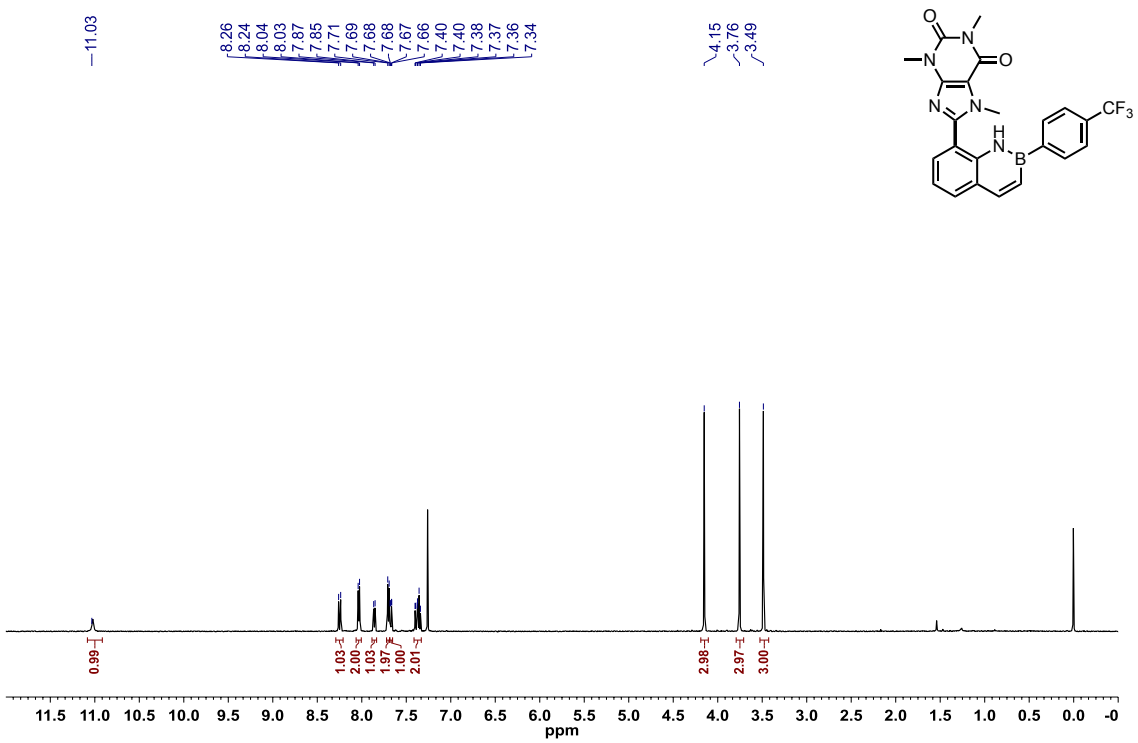

Figure A2.270: ^{13}C {^{1}H} NMR ($CDCl_3$, 125.8 MHz) of *2-(4-(trifluoromethyl)phenyl)-8-(1,3,7-trimethyl-2,6-dioxo-2,3,6,7-tetrahydro-1H-purin-8-yl)-2,1-borazaronaphthalene* (**3.74**)

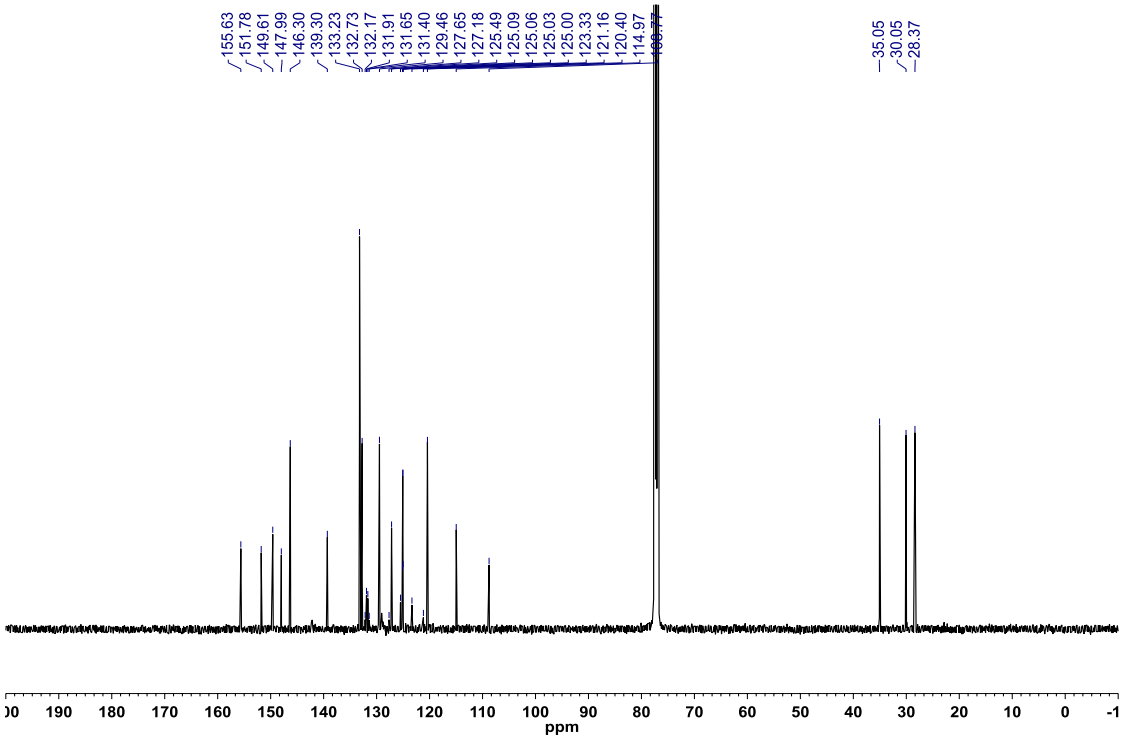

Figure A2.271: ^{19}F {^{1}H} NMR ($CDCl_3$, 470.8 MHz) of *2-(4-(trifluoromethyl)phenyl)-8-(1,3,7-trimethyl-2,6-dioxo-2,3,6,7-tetrahydro-1H-purin-8-yl)-2,1-borazaronaphthalene* (**3.74**)

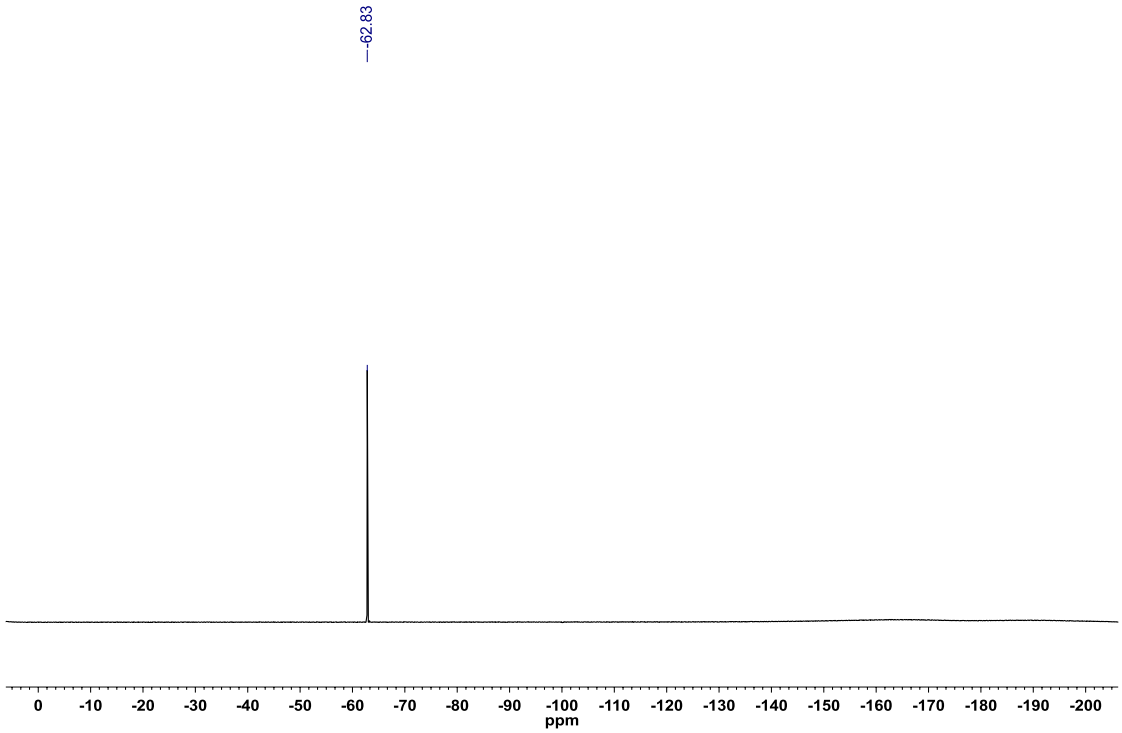

Figure A2.272: ^{11}B NMR ($CDCl_3$, 128.4 MHz) of *2-(4-(trifluoromethyl)phenyl)-8-(1,3,7-trimethyl-2,6-dioxo-2,3,6,7-tetrahydro-1H-purin-8-yl)-2,1-borazaronaphthalene* (**3.74**)

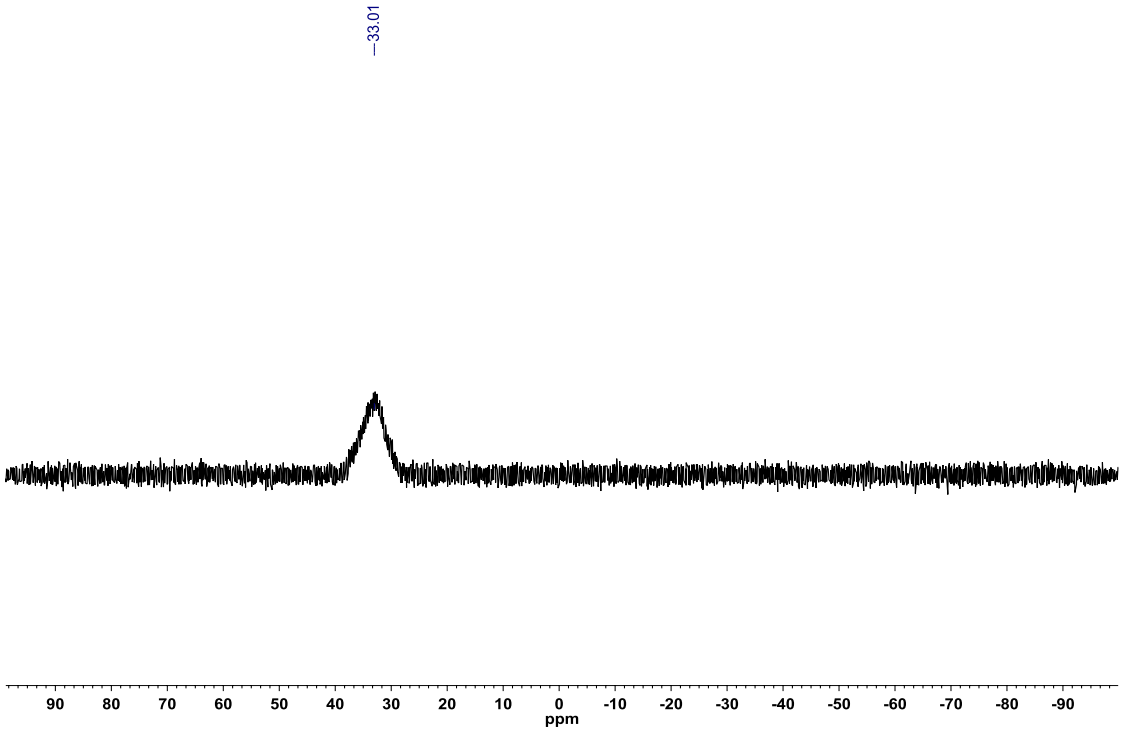

Figure A2.273: ^{1}H NMR ($CDCl_3$, 500.4 MHz) of *2-(4-methoxyphenyl)-8-(1,3,7-trimethyl-2,6-dioxo-2,3,6,7-tetrahydro-1H-purin-8-yl)-2,1-borazaronaphthalene* (**3.75**)

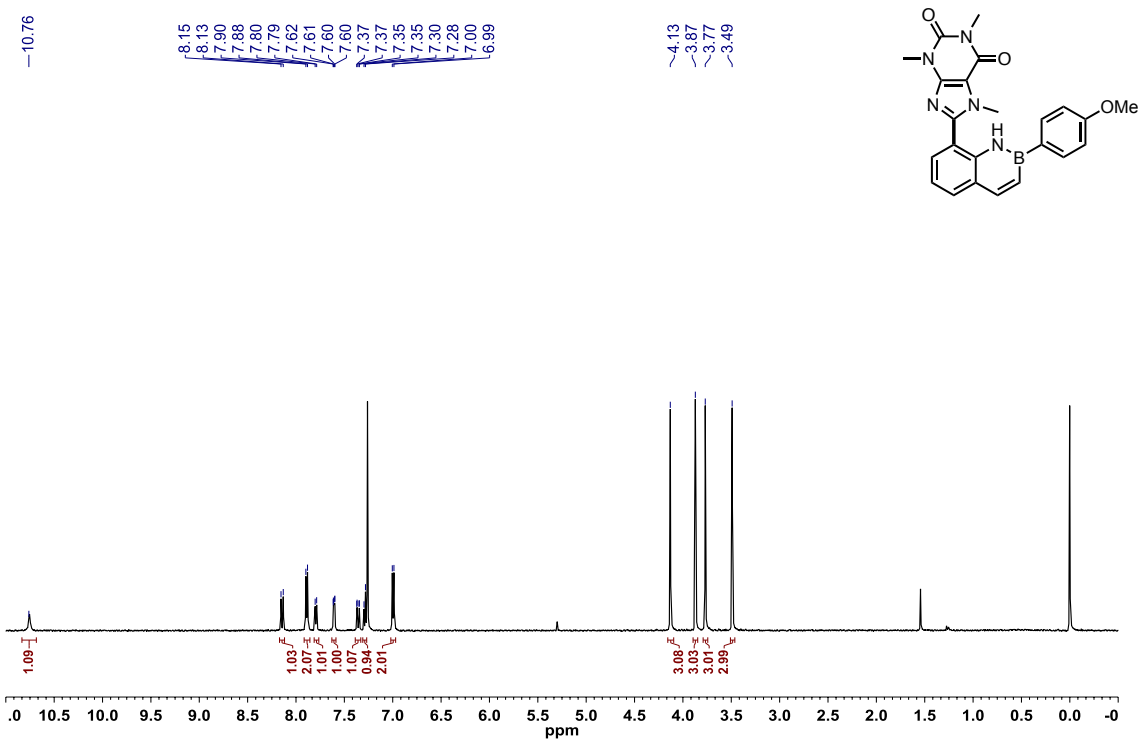

Figure A2.274: ^{13}C {^{1}H} NMR ($CDCl_3$, 125.8 MHz) of *2-(4-methoxyphenyl)-8-(1,3,7-trimethyl-2,6-dioxo-2,3,6,7-tetrahydro-1H-purin-8-yl)-2,1-borazaronaphthalene* (**3.75**)

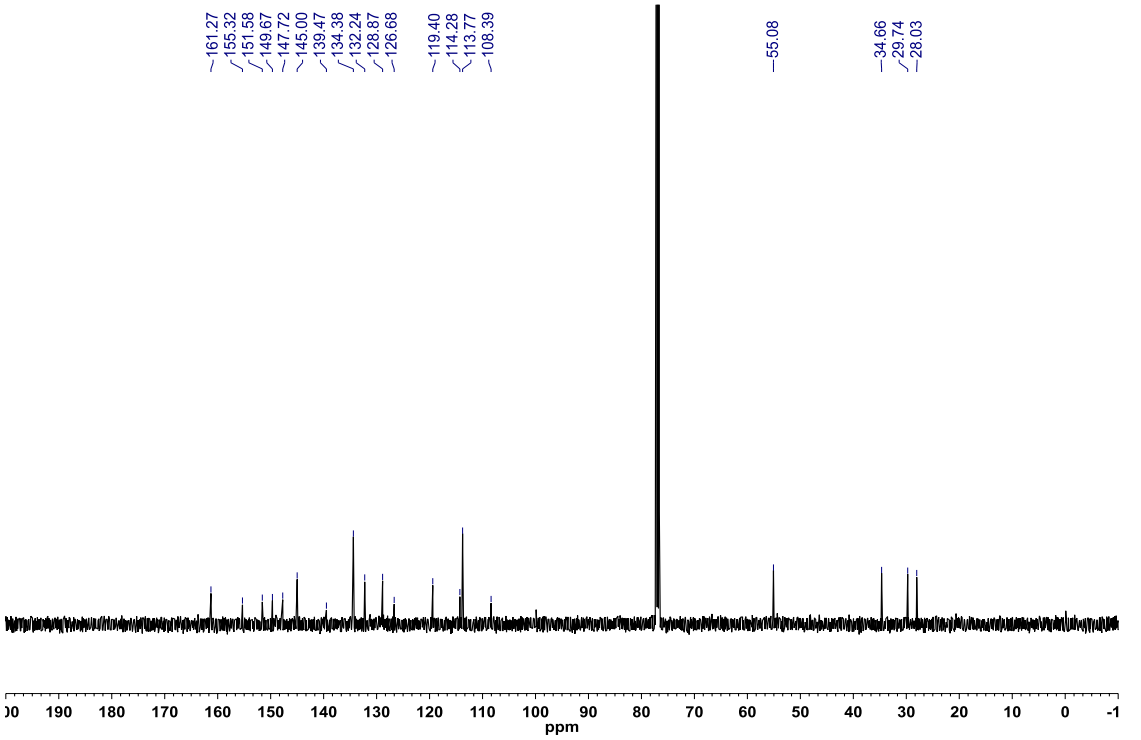

Figure A2.275: ^{11}B NMR ($CDCl_3$, 128.4 MHz) of *2-(4-methoxyphenyl)-8-(1,3,7-trimethyl-2,6-dioxo-2,3,6,7-tetrahydro-1H-purin-8-yl)-2,1-borazaronaphthalene* (**3.75**)

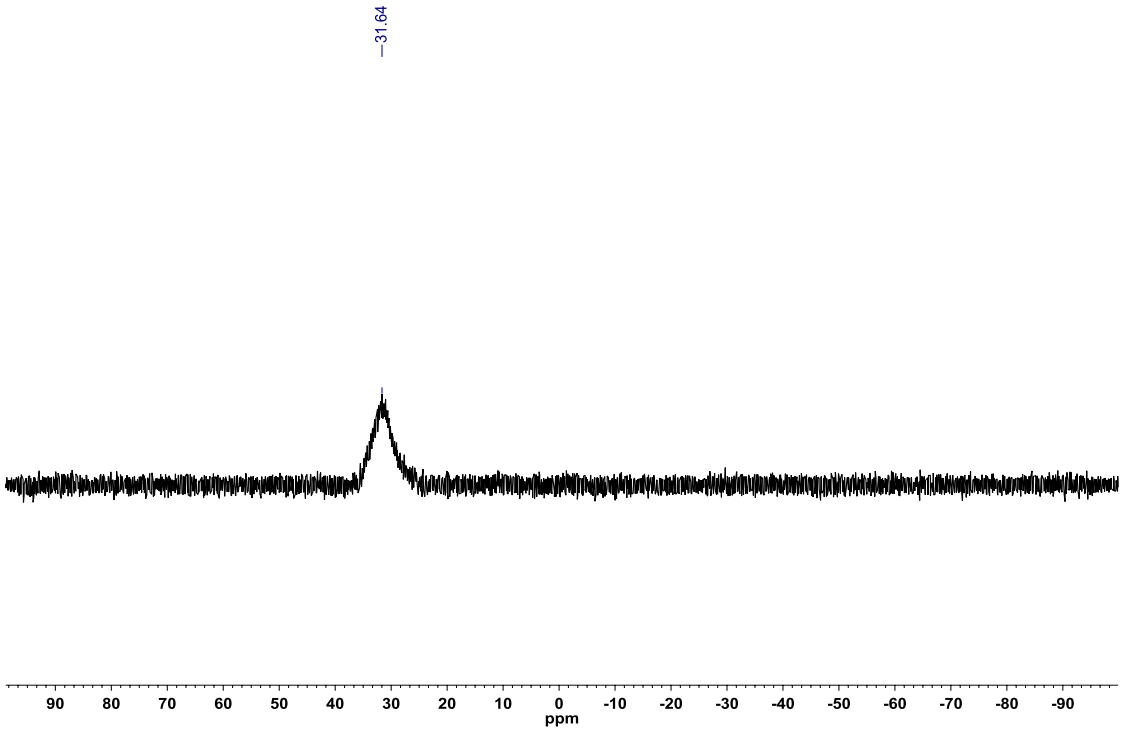

Figure A2.276: ^{1}H NMR ($CDCl_3$, 500.4 MHz) of *6-cyano-2-(4-(trifluoromethyl)phenyl)-8-(1,3,7-trimethyl-2,6-dioxo-2,3,6,7-tetrahydro-1H-purin-8-yl)-2,1-borazaronaphthalene* (**3.76**)

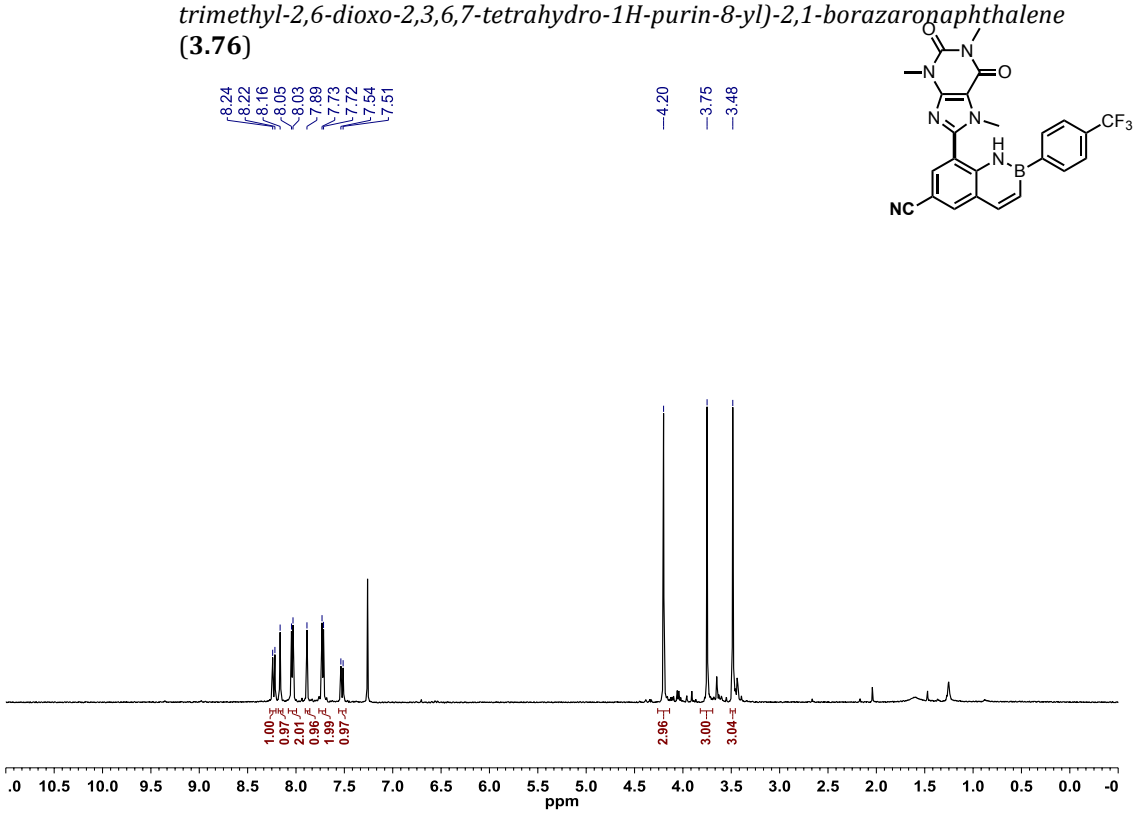

Figure A2.277: ^{13}C {^{1}H} NMR ($CDCl_3$, 125.8 MHz) of *6-cyano-2-(4-(trifluoromethyl)phenyl)-8-(1,3,7-trimethyl-2,6-dioxo-2,3,6,7-tetrahydro-1H-purin-8-yl)-2,1-borazaronaphthalene* (**3.76**)

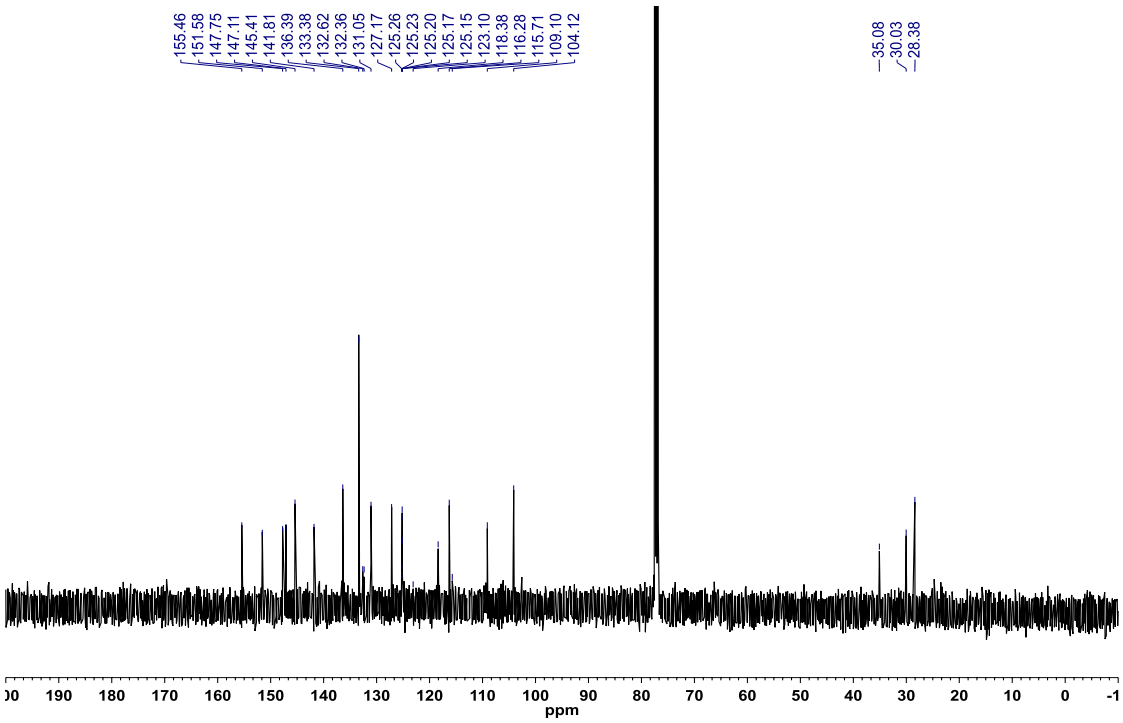

Figure A2.278: ^{19}F {^{1}H} NMR ($CDCl_3$, 470.8 MHz) of *6-cyano-2-(4-(trifluoromethyl)phenyl)-8-(1,3,7-trimethyl-2,6-dioxo-2,3,6,7-tetrahydro-1H-purin-8-yl)-2,1-borazaronaphthalene* (**3.76**)

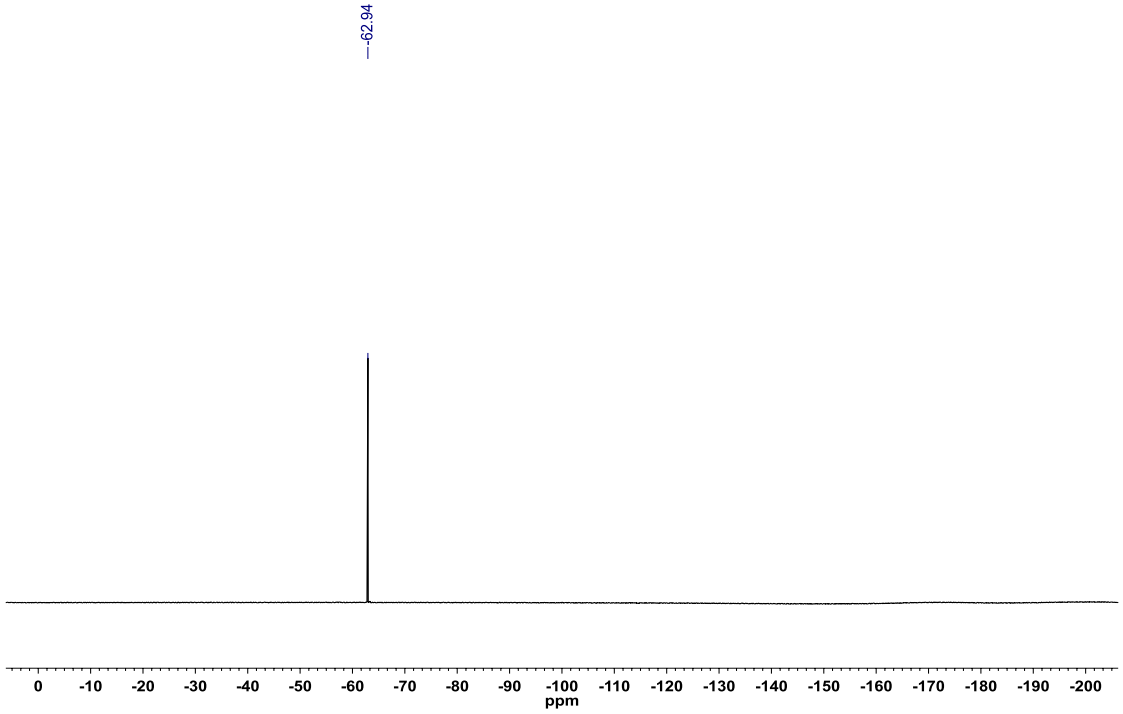

Figure A2.279: ^{11}B NMR ($CDCl_3$, 128.4 MHz) of *6-cyano-2-(4-(trifluoromethyl)phenyl)-8-(1,3,7-trimethyl-2,6-dioxo-2,3,6,7-tetrahydro-1H-purin-8-yl)-2,1-borazaronaphthalene* (**3.76**)

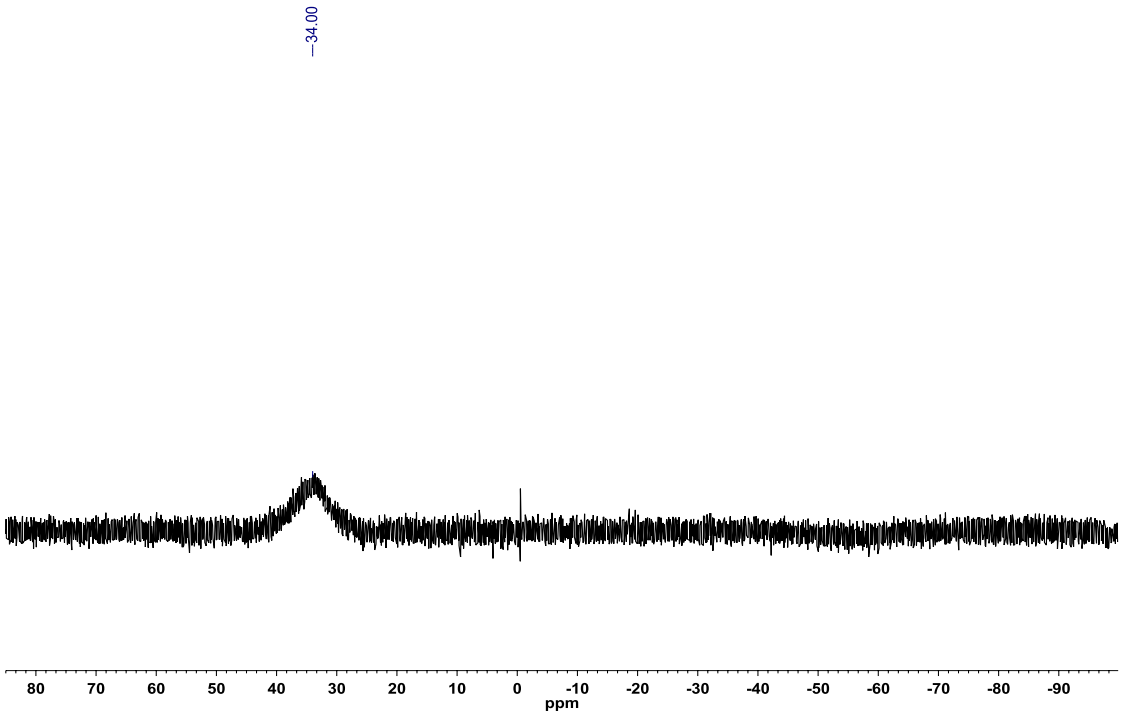

Figure A2.280: ^{1}H NMR ($CDCl_3$, 500.4 MHz) of *6-(trifluoromethoxy)-2-(4-(trifluoromethyl)phenyl)-8-(1,3,7-trimethyl-2,6-dioxo-2,3,6,7-tetrahydro-1H-purin-8-yl)-2,1-borazaronaphthalene* (**3.77**)

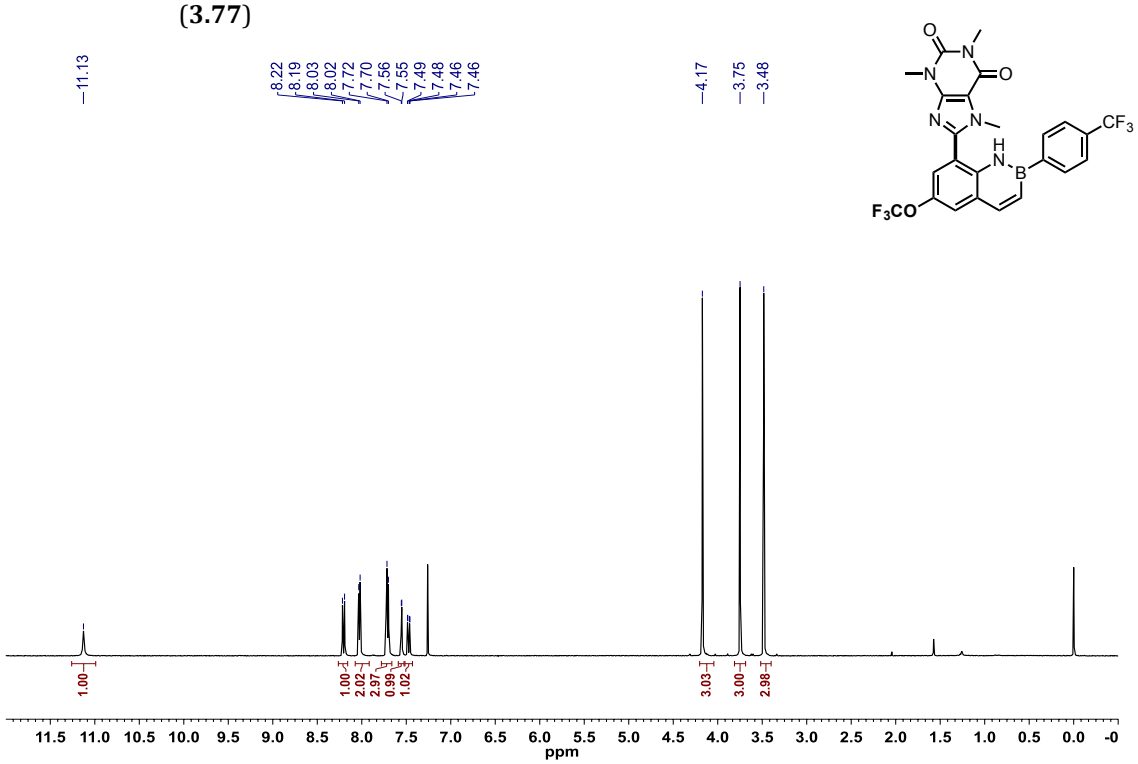

Figure A2.281: ^{13}C {^{1}H} NMR ($CDCl_3$, 125.8 MHz) of *6-(trifluoromethoxy)-2-(4-(trifluoromethyl)phenyl)-8-(1,3,7-trimethyl-2,6-dioxo-2,3,6,7-tetrahydro-1H-purin-8-yl)-2,1-borazaronaphthalene* (**3.77**)

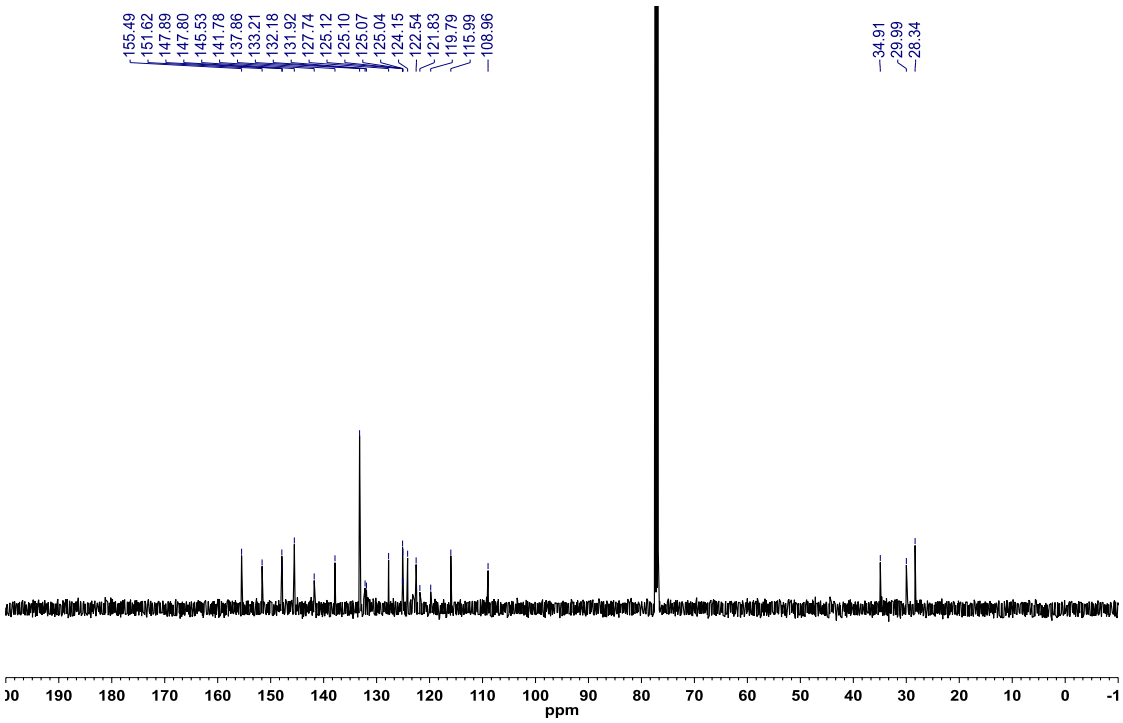

Figure A2.282: ^{19}F {^{1}H} NMR ($CDCl_3$, 470.8 MHz) of *6-(trifluoromethoxy)-2-(4-(trifluoromethyl)phenyl)-8-(1,3,7-trimethyl-2,6-dioxo-2,3,6,7-tetrahydro-1H-purin-8-yl)-2,1-borazaronaphthalene* (**3.77**)

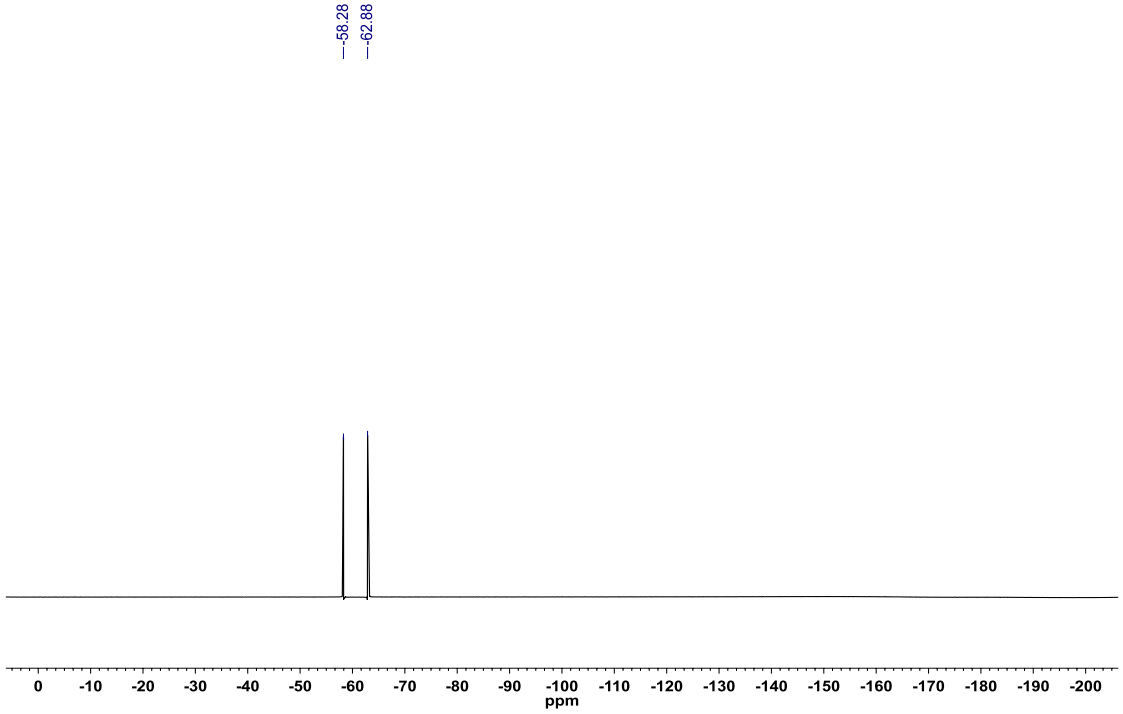

Figure A2.283: ^{11}B NMR ($CDCl_3$, 128.4 MHz) of *6-(trifluoromethoxy)-2-(4-(trifluoromethyl)phenyl)-8-(1,3,7-trimethyl-2,6-dioxo-2,3,6,7-tetrahydro-1H-purin-8-yl)-2,1-borazaronaphthalene* (**3.77**)

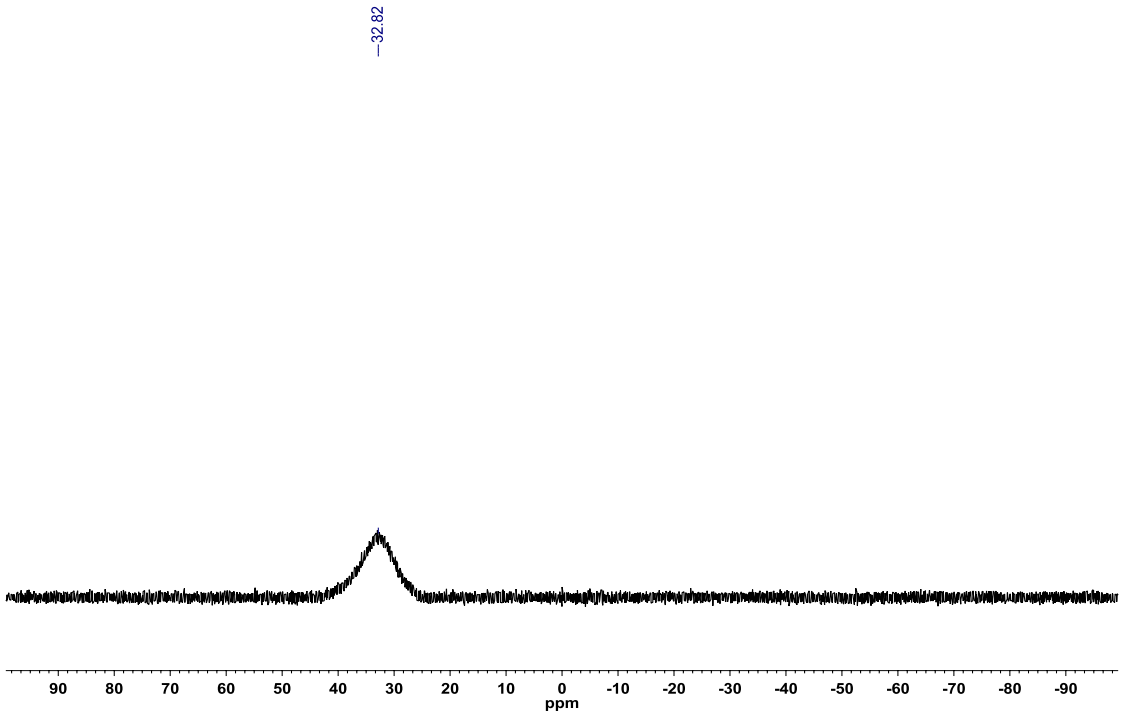

Figure A2.284: ^{1}H NMR ($CDCl_3$, 500.4 MHz) of *8-(4-(2,1-borazaronaphthalen-2-yl)phenyl)-2-(4-(trifluoromethyl)phenyl)-2,1-borazaronaphthalene* (**3.78**)

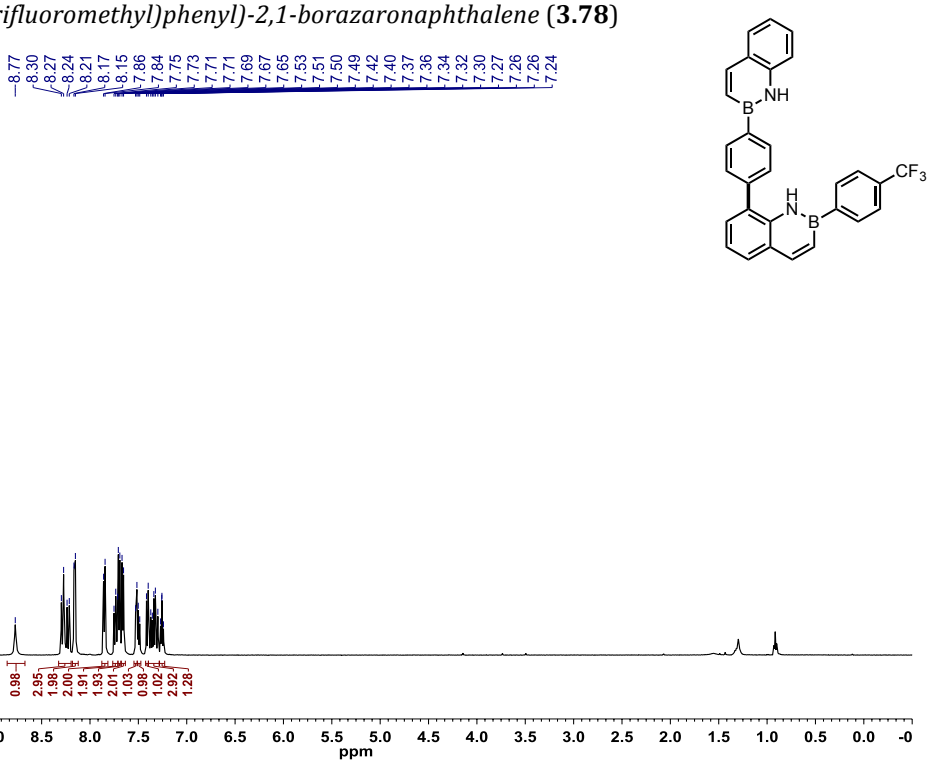

Figure A2.285: ^{13}C {^{1}H} NMR ($CDCl_3$, 125.8 MHz) of *8-(4-(2,1-borazaronaphthalen-2-yl)phenyl)-2-(4-(trifluoromethyl)phenyl)-2,1-borazaronaphthalene* (**3.78**)

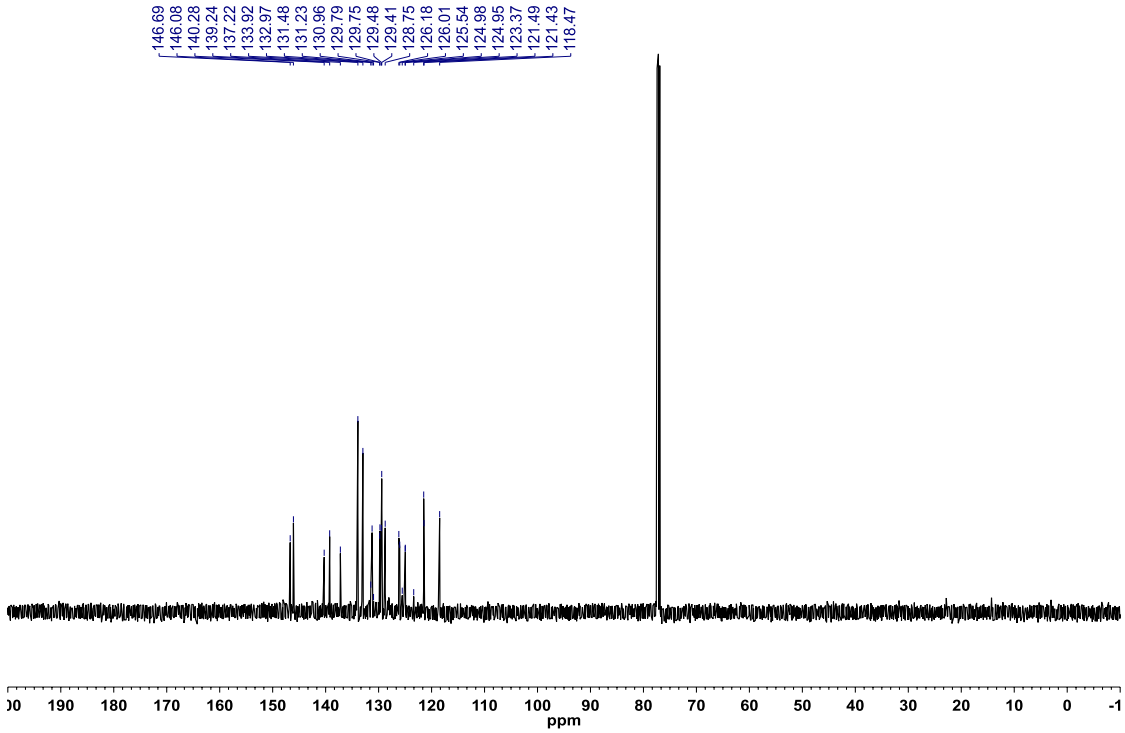

Figure A2.286: ^{19}F {^{1}H} NMR ($CDCl_3$, 470.8 MHz) of *8-(4-(2,1-borazaronaphthalen-2-yl)phenyl)-2-(4-(trifluoromethyl)phenyl)-2,1-borazaronaphthalene* (**3.78**)

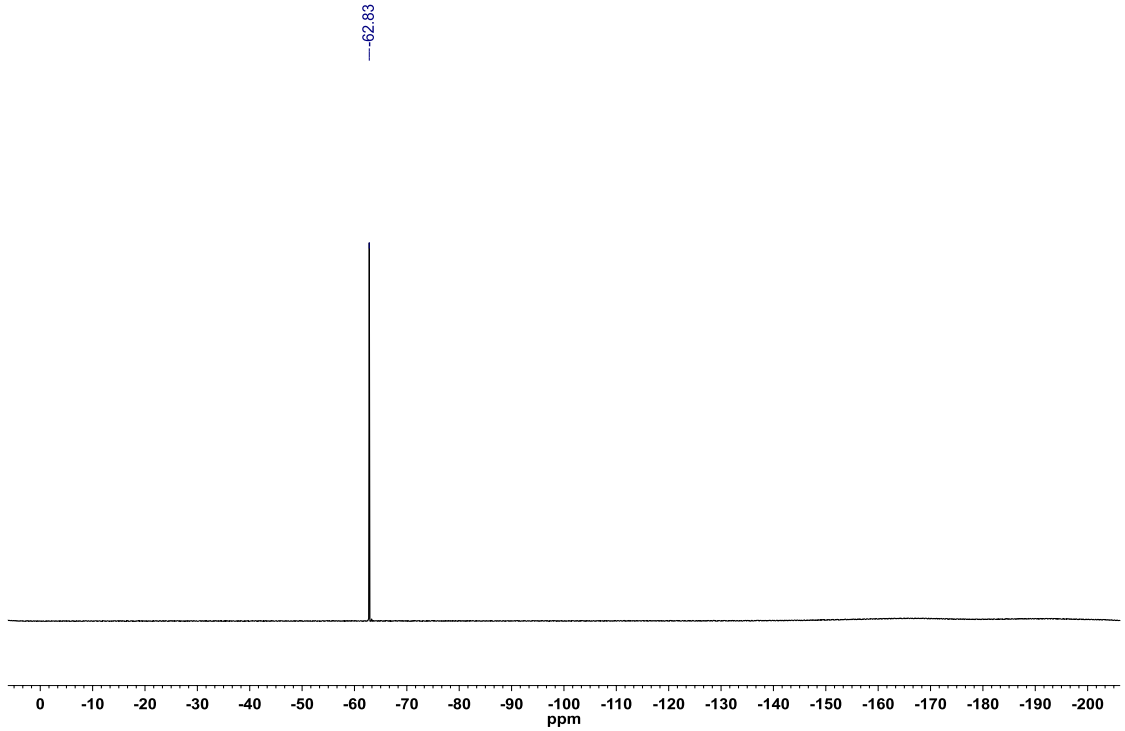

Figure A2.287: ^{11}B NMR ($CDCl_3$, 128.4 MHz) of *8-(4-(2,1-borazaronaphthalen-2-yl)phenyl)-2-(4-(trifluoromethyl)phenyl)-2,1-borazaronaphthalene* (**3.78**)

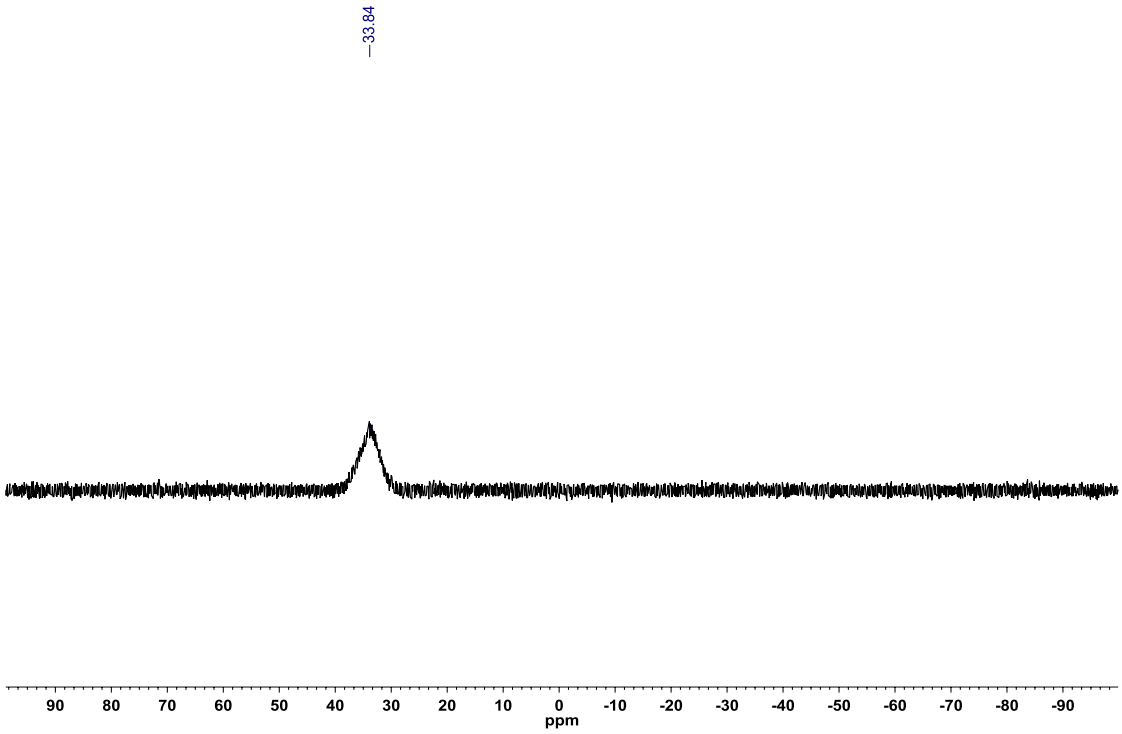

Figure A2.288: ^{1}H NMR ($CDCl_3$, 500.4 MHz) of *8-(2-methyl-2,1-borazaronaphthalen-3-yl)-2-(4-(trifluoromethyl)phenyl)-2,1-borazaronaphthalene* (**3.79**)

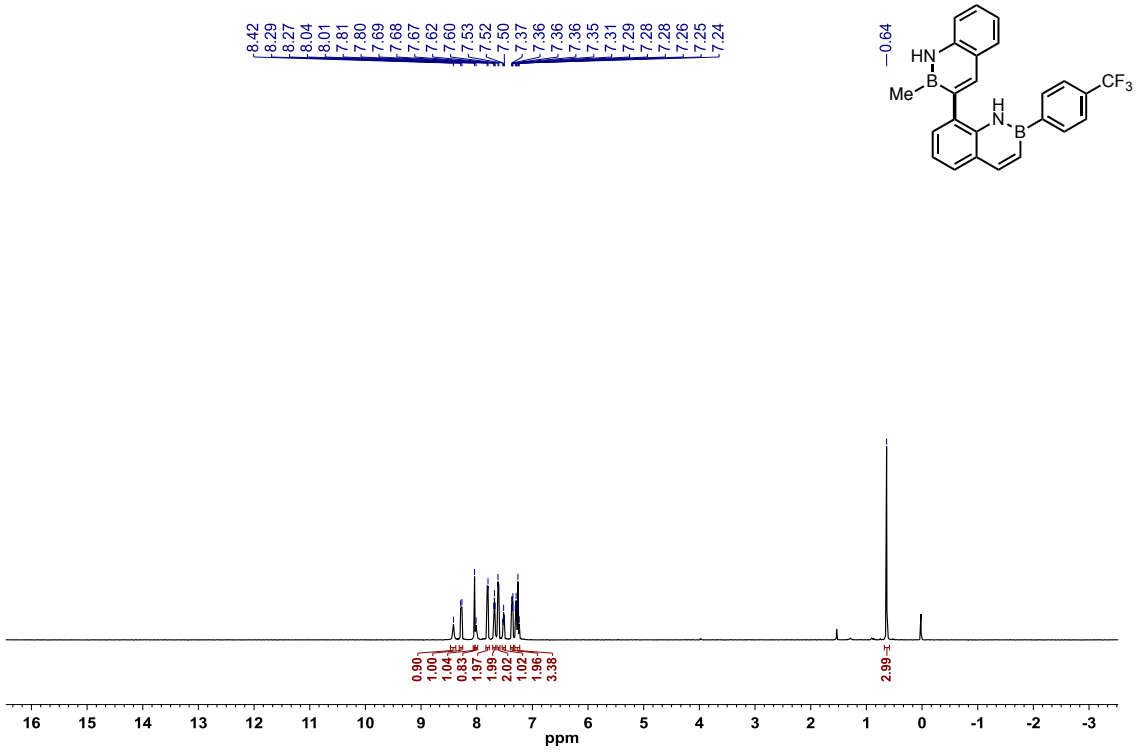

Figure A2.289: ^{13}C {^{1}H} NMR ($CDCl_3$, 125.8 MHz) of *8-(2-methyl-2,1-borazaronaphthalen-3-yl)-2-(4-(trifluoromethyl)phenyl)-2,1-borazaronaphthalene* (**3.79**)

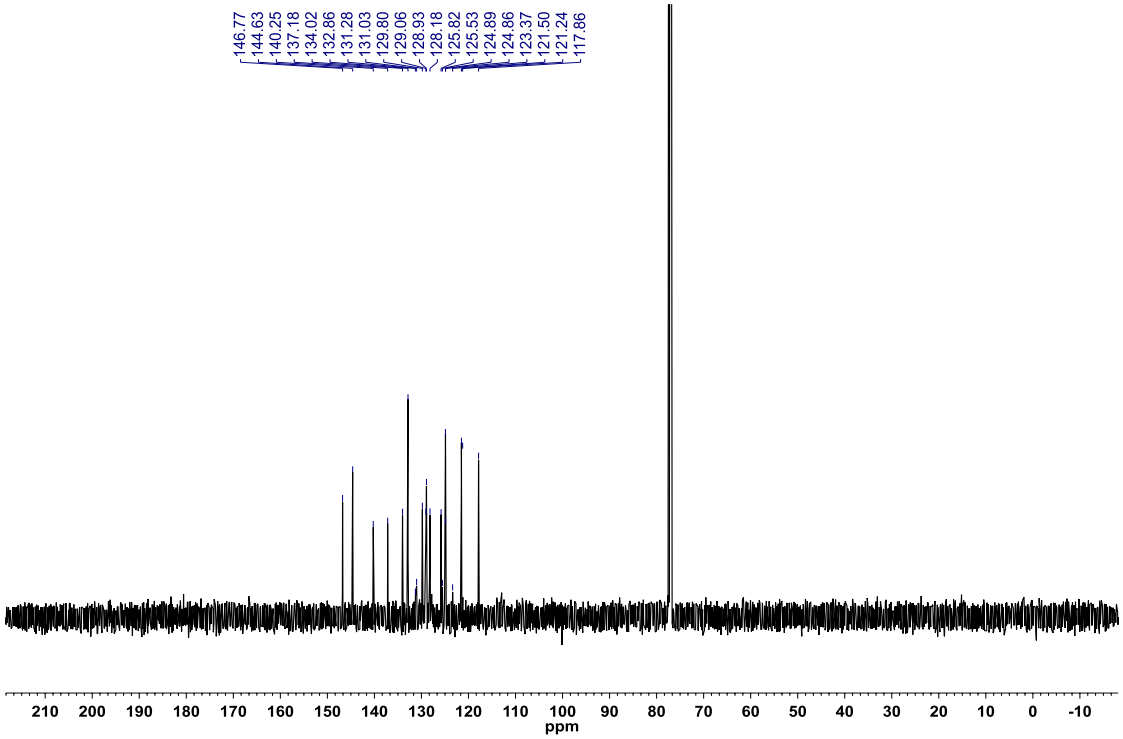

Figure A2.290: ^{19}F {^{1}H} NMR ($CDCl_3$, 470.8 MHz) of *8-(2-methyl-2,1-borazaronaphthalen-3-yl)-2-(4-(trifluoromethyl)phenyl)-2,1-borazaronaphthalene* (**3.79**)

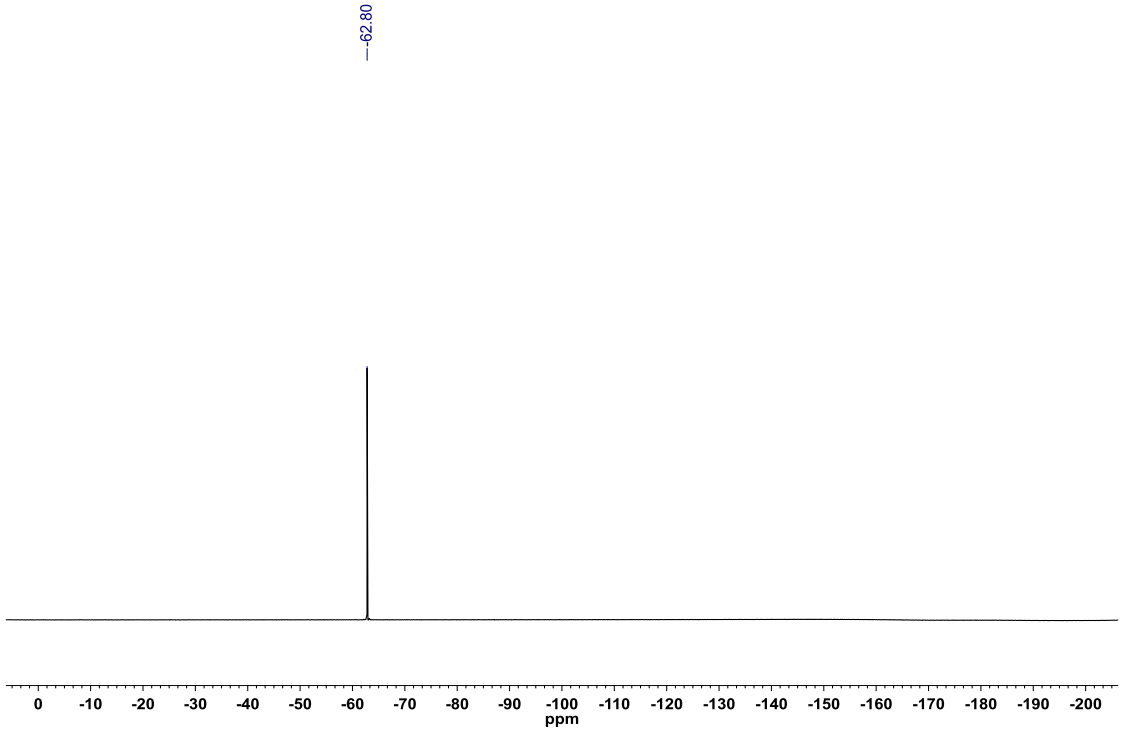

Figure A2.291: ^{11}B NMR ($CDCl_3$, 128.4 MHz) of *8-(2-methyl-2,1-borazaronaphthalen-3-yl)-2-(4-(trifluoromethyl)phenyl)-2,1-borazaronaphthalene* (**3.79**)

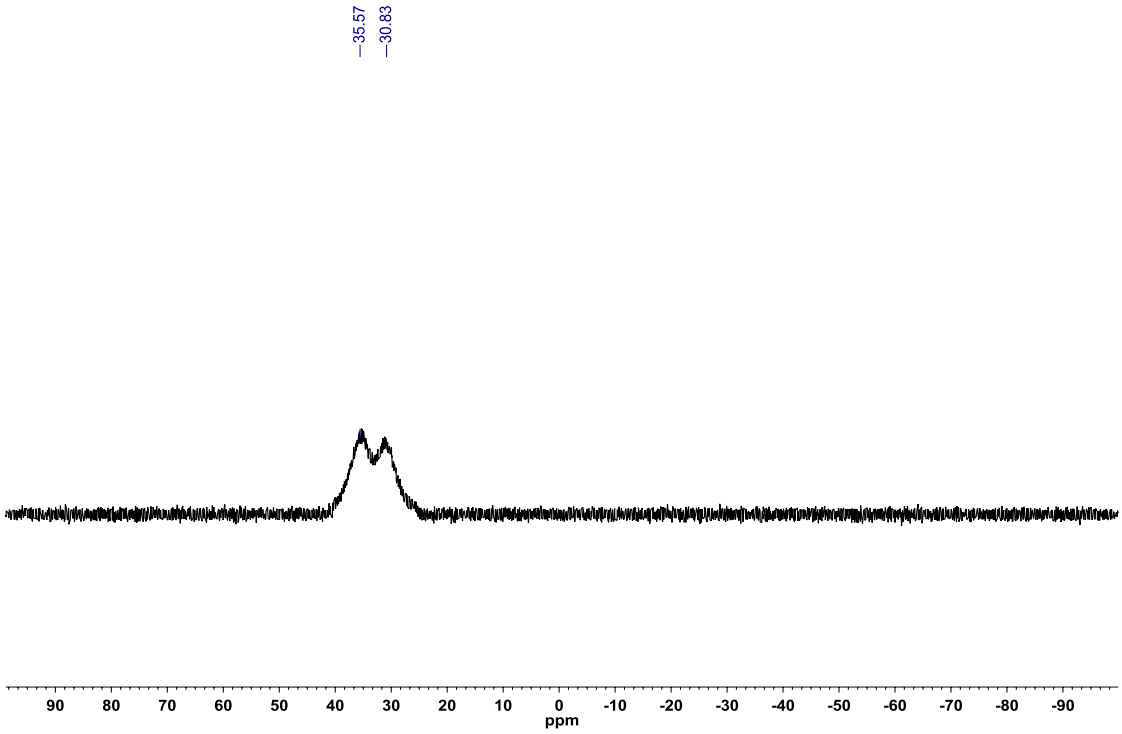

Figure A2.292: ^{1}H NMR (500.4 MHz, $CDCl_3$) of *8-(p-tolyl)-2-(4-(trifluoromethyl)phenyl)-2,1-borazaronaphthalene* (**3.80**)

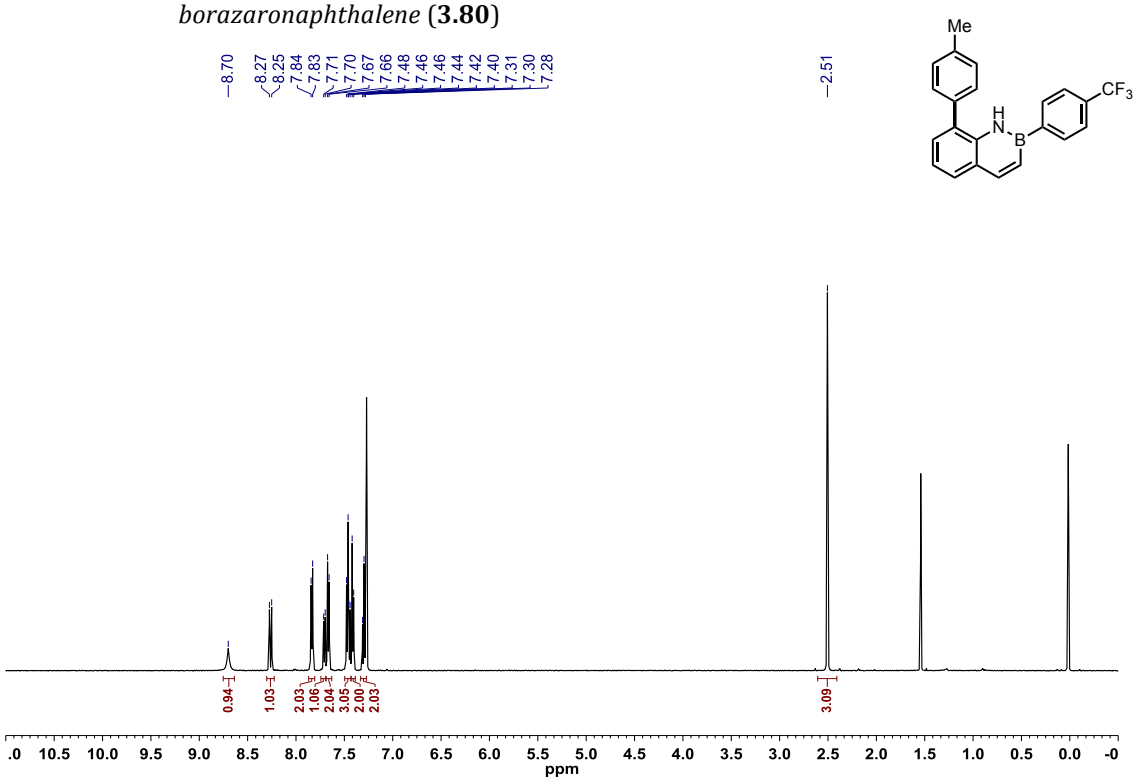

Figure A2.293: ^{13}C {^{1}H} NMR ($CDCl_3$, 125.8 MHz) of *8-(p-tolyl)-2-(4-(trifluoromethyl)phenyl)-2,1-borazaronaphthalene* (**3.80**)

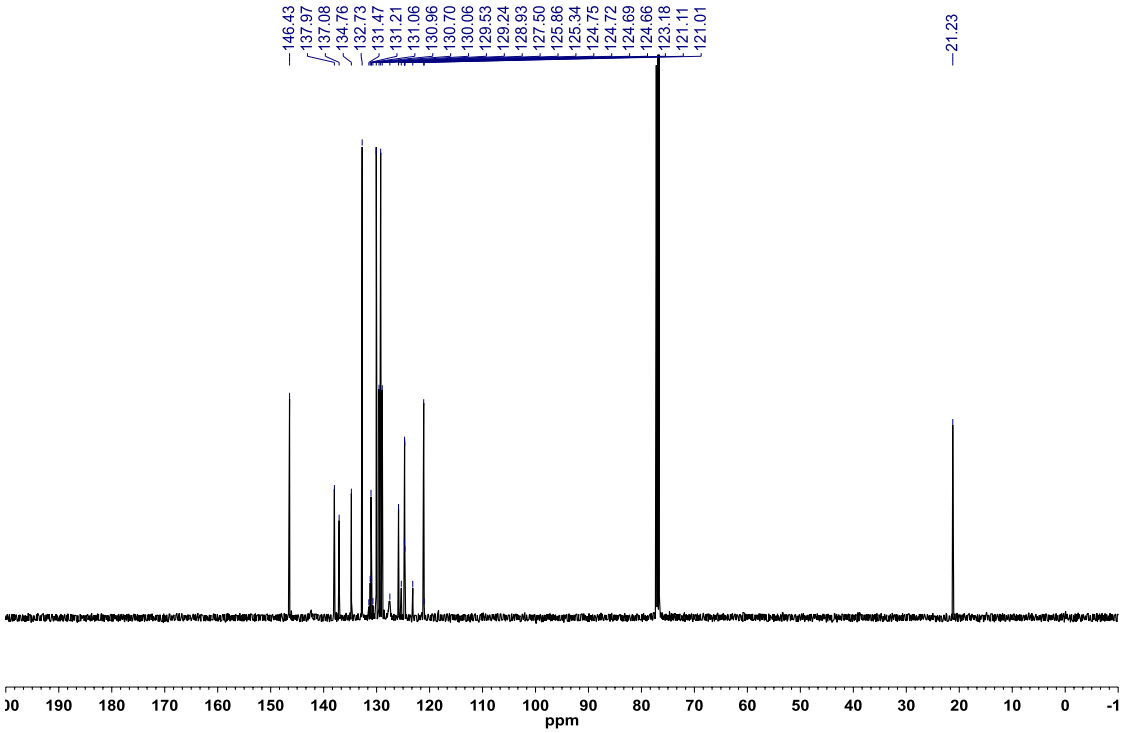

Figure A2.294: ^{19}F {^{1}H} NMR ($CDCl_3$, 470.8 MHz) of *8-(p-tolyl)-2-(4-(trifluoromethyl)phenyl)-2,1-borazaronaphthalene* (**3.80**)

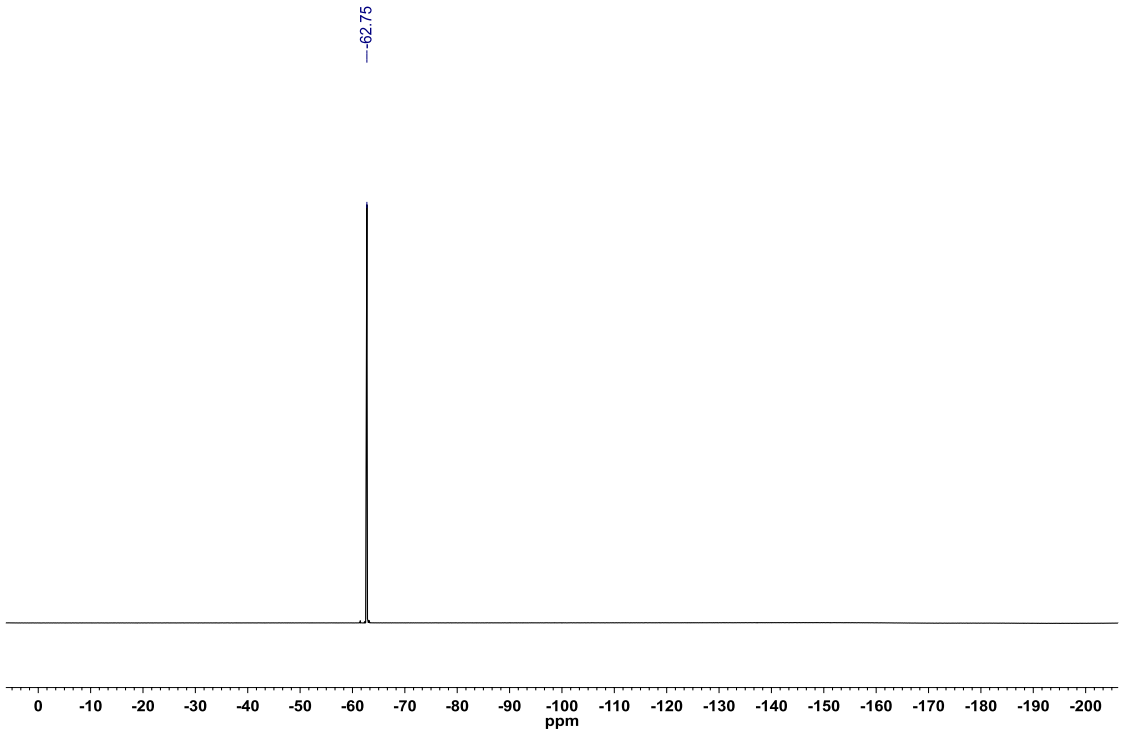

Figure A2.295: ^{11}B NMR ($CDCl_3$, 128.4 MHz) of *8-(p-tolyl)-2-(4-(trifluoromethyl)phenyl)-2,1-borazaronaphthalene* (**3.80**)

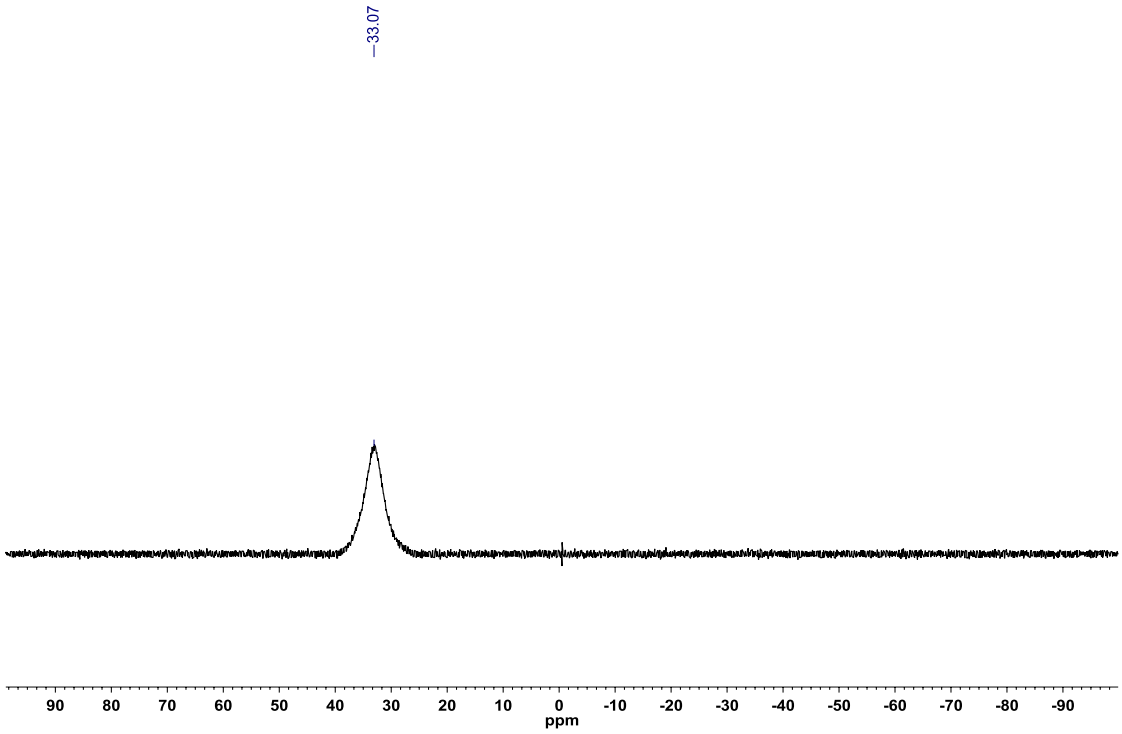

Figure A2.296: ^{1}H NMR (500.4 MHz, $CDCl_3$) of *2,8-bis(4-(trifluoromethyl)phenyl)-2,1-borazaronaphthalene* (**3.81**)

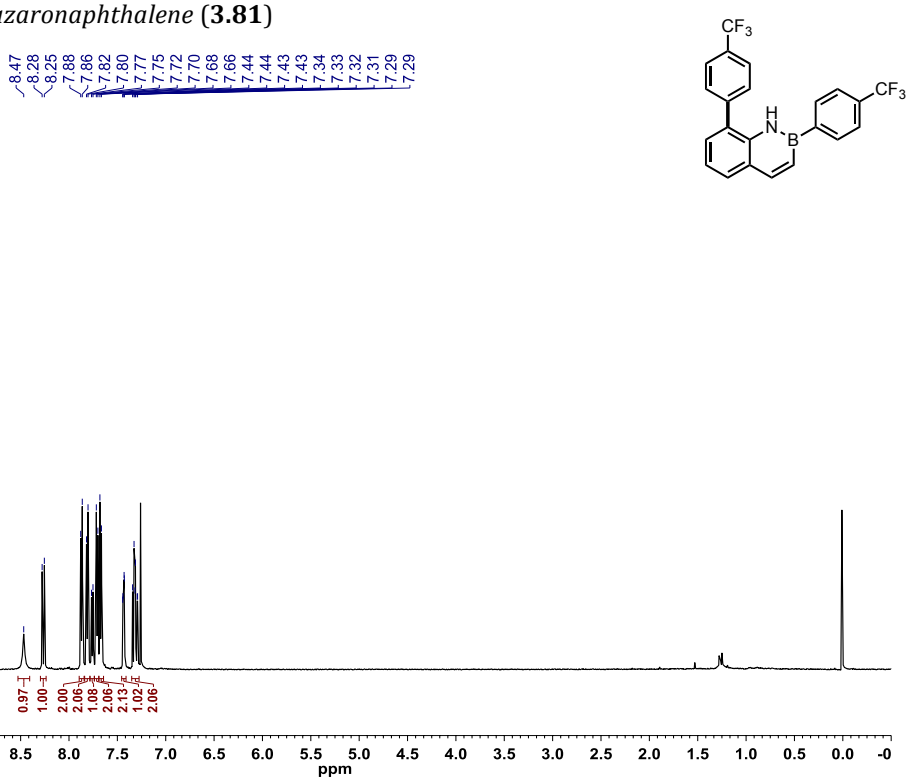

Figure A2.297: ^{13}C {^{1}H} NMR ($CDCl_3$, 125.8 MHz) of *2,8-bis(4-(trifluoromethyl)phenyl)-2,1-borazaronaphthalene* (**3.81**)

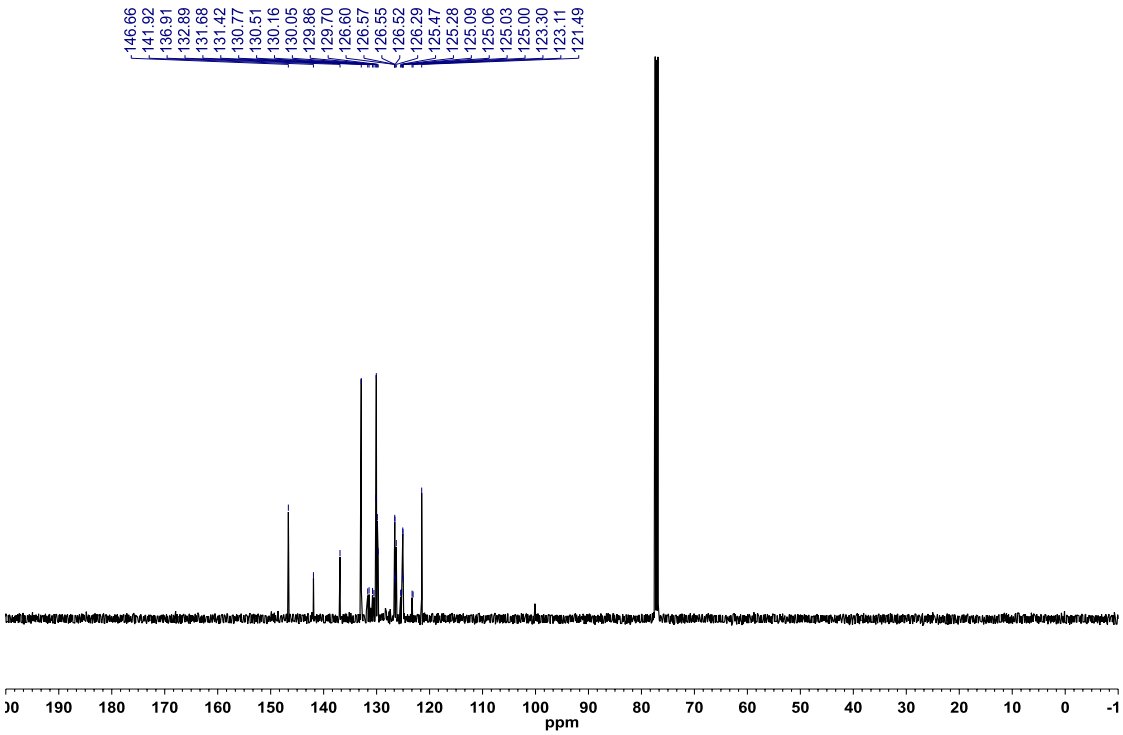

Figure A2.298: ^{19}F {^{1}H} NMR ($CDCl_3$, 470.8 MHz) of *2,8-bis(4-(trifluoromethyl)phenyl)-2,1-borazaronaphthalene* (**3.81**)

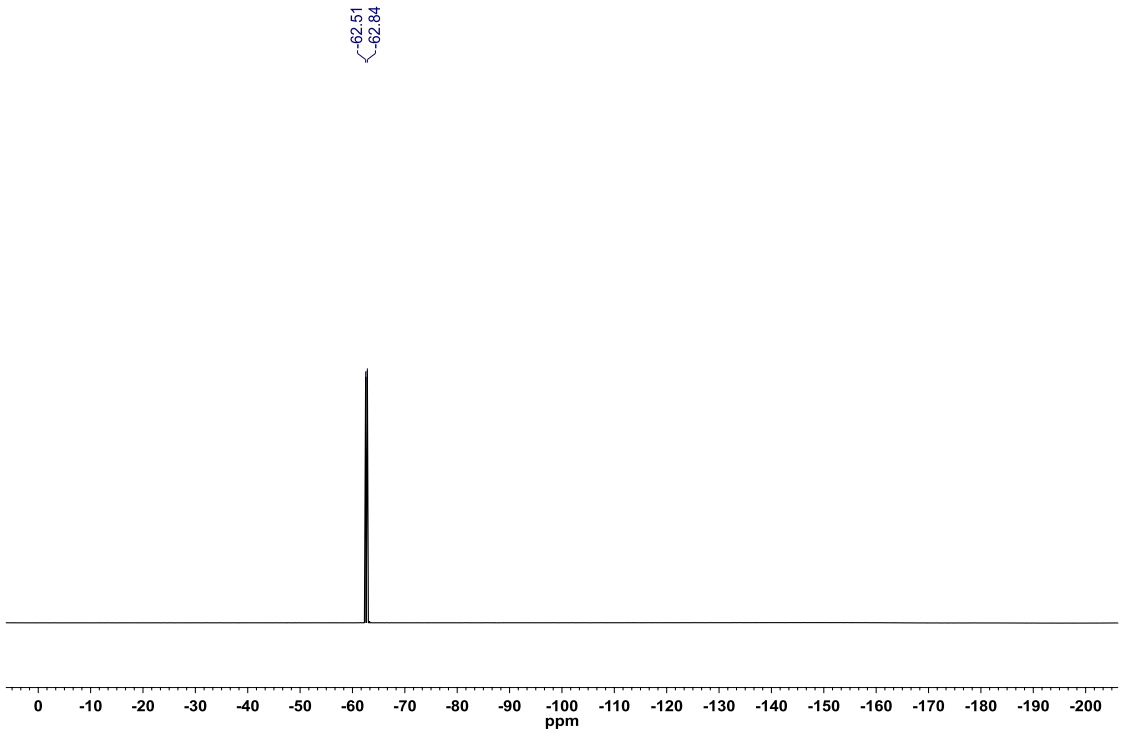

Figure A2.299: ^{11}B NMR ($CDCl_3$, 128.4 MHz) of *2,8-bis(4-(trifluoromethyl)phenyl)-2,1-borazaronaphthalene* (**3.81**)

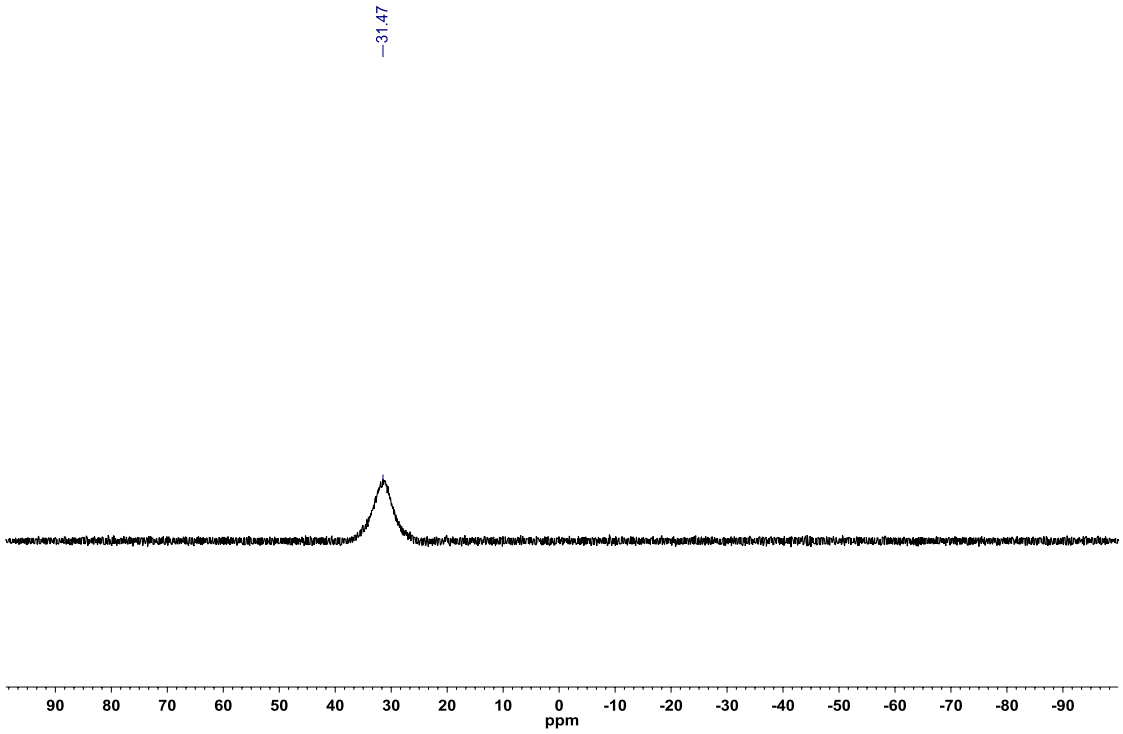

Figure A2.300: ^{1}H NMR (500.4 MHz, $CDCl_3$) of *8-(4-(dimethylamino)phenyl)-2-(4-(trifluoromethyl)phenyl)-2,1-borazaronaphthalene* (**3.82**)

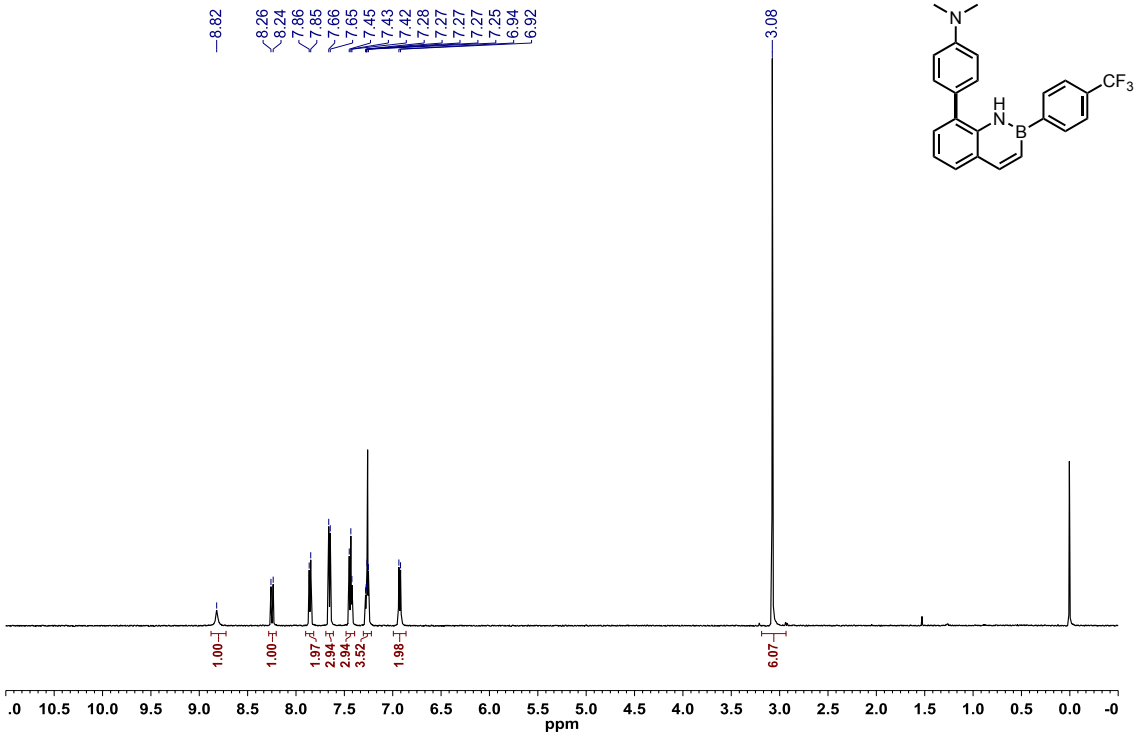

Figure A2.301: ^{13}C {^{1}H} NMR ($CDCl_3$, 125.8 MHz) of *8-(4-(dimethylamino)phenyl)-2-(4-(trifluoromethyl)phenyl)-2,1-borazaronaphthalene* (**3.82**)

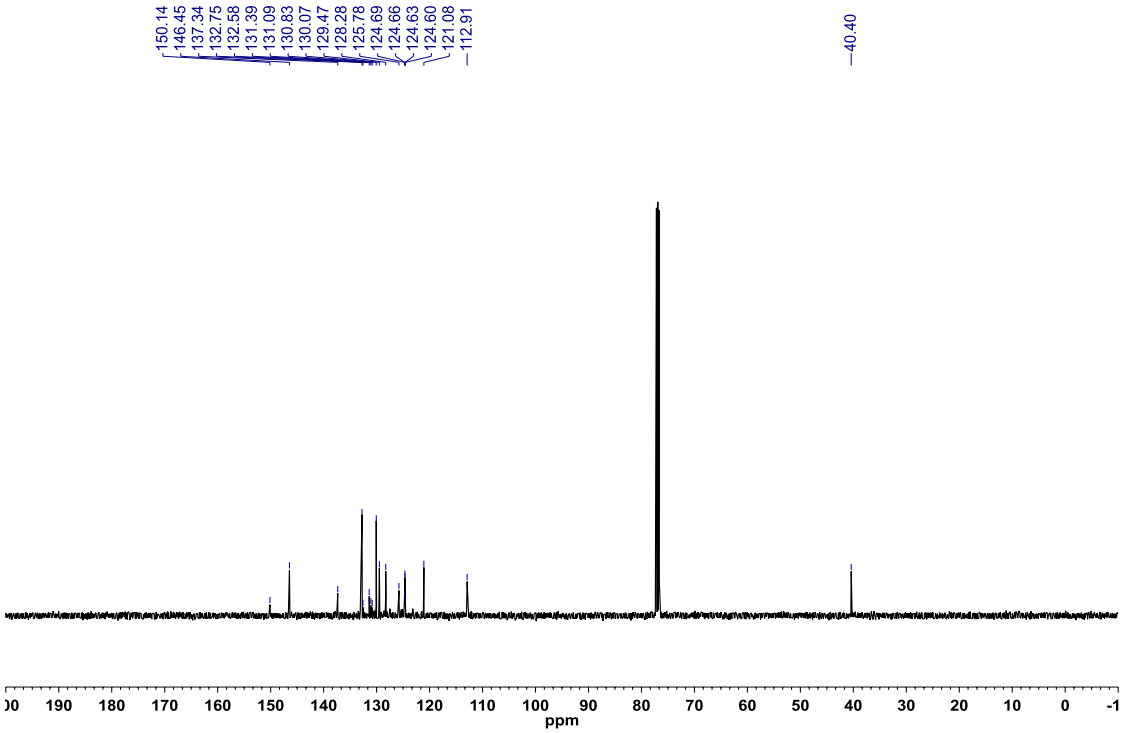

Figure A2.302: ^{19}F {^{1}H} NMR ($CDCl_3$, 470.8 MHz) of *8-(4-(dimethylamino)phenyl)-2-(4-(trifluoromethyl)phenyl)-2,1-borazaronaphthalene* (**3.82**)

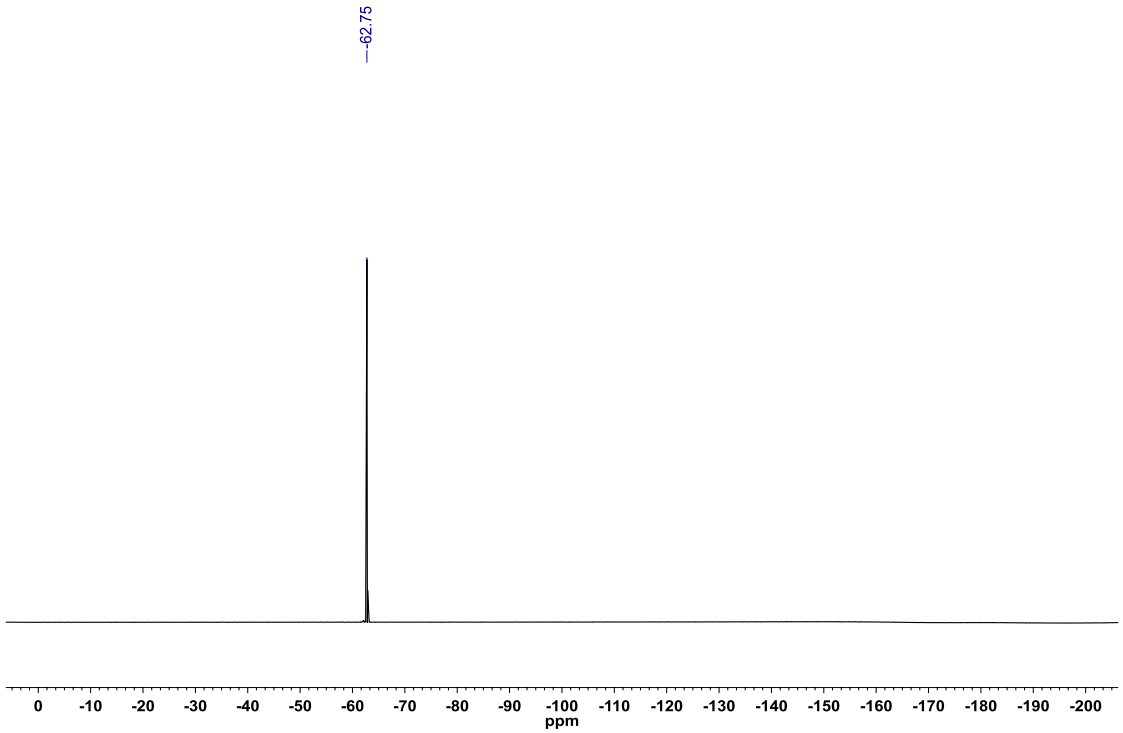

Figure A2.303: ^{11}B NMR ($CDCl_3$, 128.4 MHz) of *8-(4-(dimethylamino)phenyl)-2-(4-(trifluoromethyl)phenyl)-2,1-borazaronaphthalene* (**3.82**)

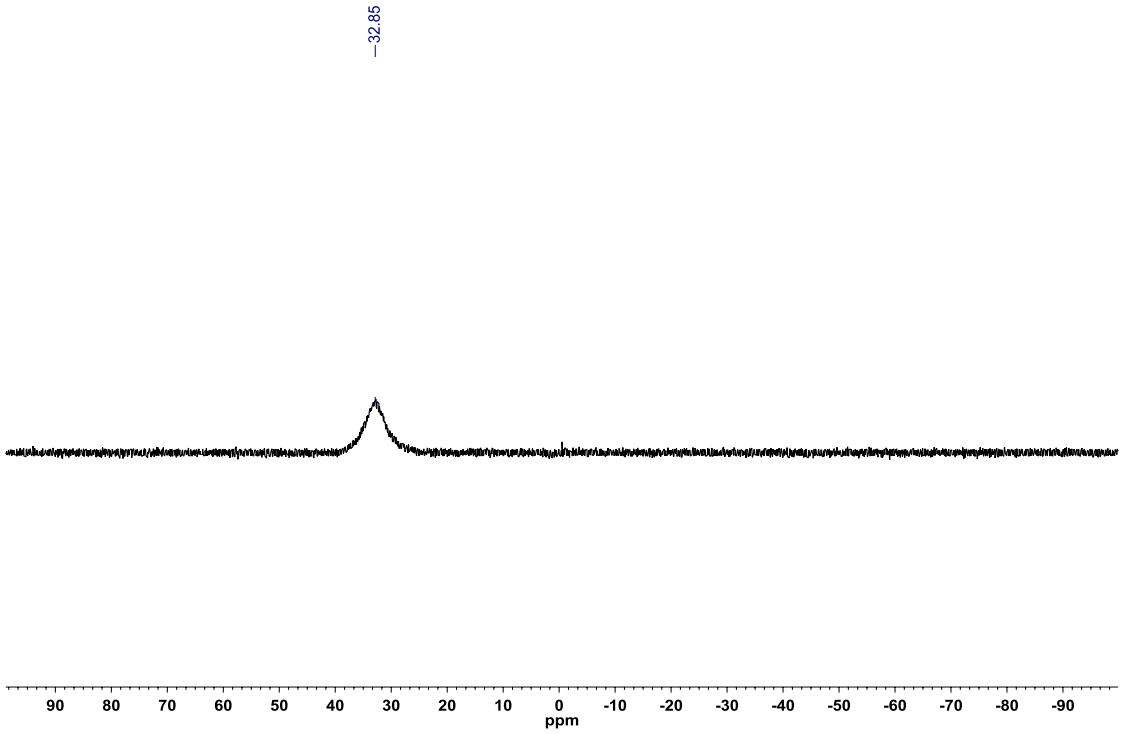

Figure A2.304: ^{1}H NMR (500.4 MHz, $CDCl_3$) of *8-(4-(dimethylamino)phenyl)-2-(4-methoxyphenyl)-2,1-borazaronaphthalene* (**3.83**)

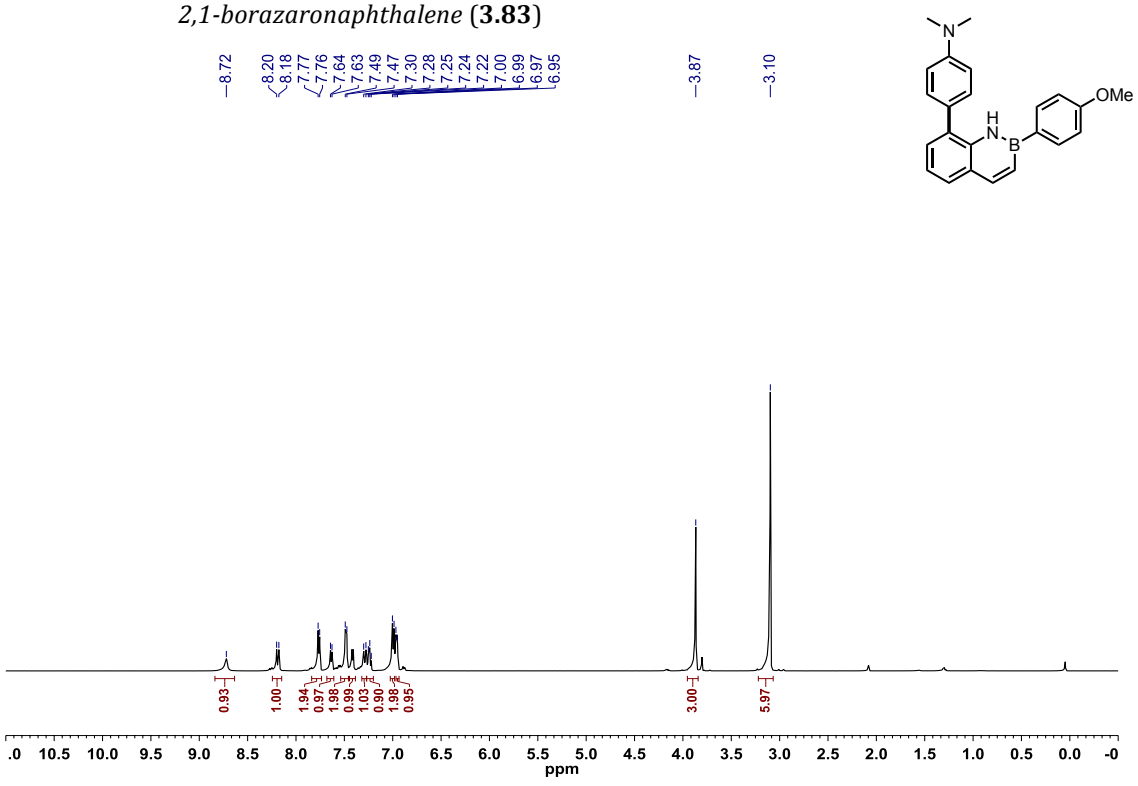

Figure A2.305: ^{13}C {^{1}H} NMR ($CDCl_3$, 125.8 MHz) of *8-(4-(dimethylamino)phenyl)-2-(4-methoxyphenyl)-2,1-borazaronaphthalene* (**3.83**)

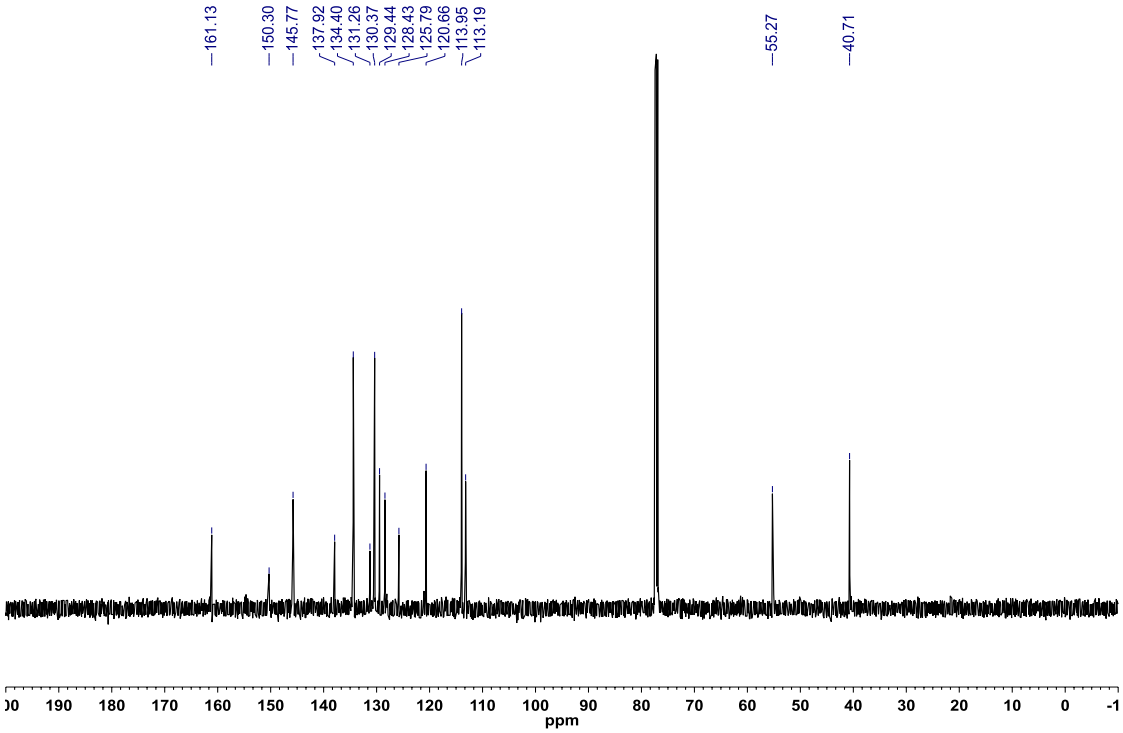

Figure A2.306: ^{11}B NMR ($CDCl_3$, 128.4 MHz) of *8-(4-(dimethylamino)phenyl)-2-(4-methoxyphenyl)-2,1-borazaronaphthalene* (**3.83**)

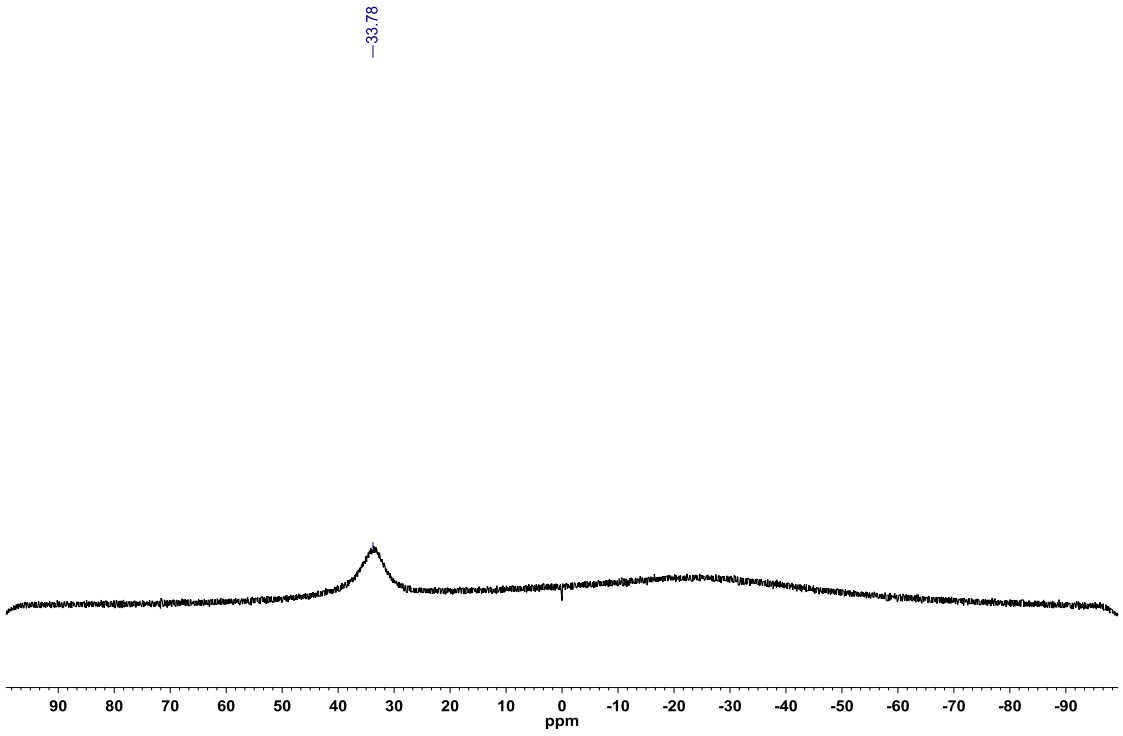

A2.6 – X-Ray crystallographic data relevant to Chapter 3.3

Figure A2.307: X-ray Structure Determination of 8-(4,4,5,5-tetramethyl-1,3,2-dioxaboryl)-2-(4-(trifluoromethyl)phenyl)-2,1-borazaronaphthalene (**3.32**)

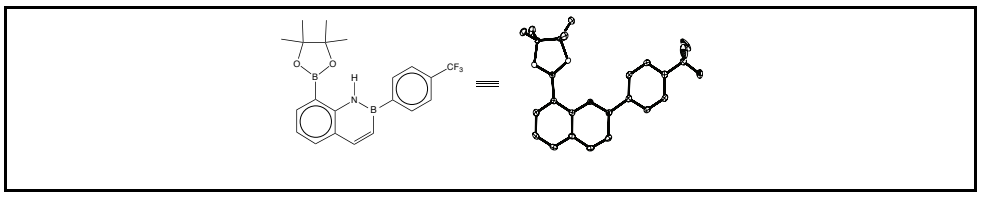

3.32, $C_{21}H_{22}B_2F_3NO_2$, crystallizes in the monoclinic space group $P2_1/c$ (systematic absences 0k0: k=odd and h0l: l=odd) with a=16.0412(6)Å, b=9.7859(3)Å, c=12.6241(5)Å, β=98.1930(10)°, V=1961.47(12)Å^3, Z=4, and d_{calc}=1.351 g/cm$_3$. X-ray intensity data were collected on a Bruker D8QUEST [1] CMOS area detector employing graphite-monochromated Mo-Kα radiation (λ=0.71073Å) at a temperature of 100K. Preliminary indexing was performed from a series of thirty-six 0.5° rotation frames with exposures of 10 seconds. A total of 1316 frames were collected with a crystal to detector distance of 34.1 mm, rotation widths of 0.5° and exposures of 10 seconds:

scan type	2θ	ω	φ	χ	Frames
w	0.00	195.50	90.00	54.72	298
w	0.00	195.50	0.00	54.72	298
f	-1.00	345.19	0.00	54.72	720

Rotation frames were integrated using SAINT [2], producing a listing of unaveraged F^2 and $\sigma(F^2)$ values. A total of 55761 reflections were measured over the ranges $6.078 \leq 2\theta \leq 55.074°$, $-20 \leq h \leq 20$, $-12 \leq k \leq 12$, $-16 \leq l \leq 16$ yielding 4531 unique reflections (R_{int} = 0.0277). The intensity data were corrected for Lorentz and polarization effects and for absorption using SADABS [3] (minimum and maximum transmission 0.7075, 0.7456). The structure was solved by direct methods - XT (Sheldrick, 2015) [4]. Refinement was by full-matrix least squares based on F^2 using SHELXL-2014 [5]. All reflections were used during refinement. The weighting scheme used was $w=1/[\sigma^2(F_o^2)+ (0.0576P)^2 + 1.0076P]$ where $P = (F_o^2 + 2F_c^2)/3$. Non-hydrogen atoms were refined anisotropically and hydrogen atoms were refined using a riding model. Refinement converged to R1=0.0398 and wR2=0.1062 for 4167 observed reflections for which $F > 4\sigma(F)$ and R1=0.0430 and wR2=0.1092 and GOF =1.036 for

all 4531 unique, non-zero reflections and 266 variables. The maximum Δ/σ in the final cycle of least squares was 0.000 and the two most prominent peaks in the final difference Fourier were +0.34 and -0.44 e/Å^3.

Table 1. lists cell information, data collection parameters, and refinement data. Final positional and equivalent isotropic thermal parameters are given in Tables 2. and 3. Anisotropic thermal parameters are in Table 4. Tables 5. and 6. list bond distances and bond angles. Figure 1. is an ORTEP representation of the molecule with 50% probability thermal ellipsoids displayed.

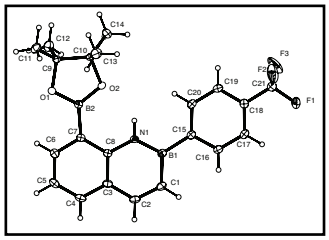

ORTEP drawing of the title compound with 50% thermal ellipsoids.

Figure A2.308: Summary of Structure Determination of Compound 8-(4,4,5,5-tetramethyl-1,3,2-dioxaboryl)-2-(4-(trifluoromethyl)phenyl)-2,1-borazaronaphthalene (**3.32**)

Empirical formula	$C_{21}H_{22}B_2F_3NO_2$
Formula weight	399.01
Temperature/K	100
Crystal system	monoclinic
Space group	$P2_1/c$
a	16.0412(6)Å
b	9.7859(3)Å
c	12.6241(5)Å
β	98.1930(10)°
Volume	1961.47(12)Å^3
Z	4
d_{calc}	1.351 g/cm^3
μ	0.104 mm^{-1}
F(000)	832.0
Crystal size, mm	0.3 × 0.3 × 0.12
2θ range for data collection	6.078 - 55.074°
Index ranges	-20 ≤ h ≤ 20, -12 ≤ k ≤ 12, -16 ≤ l ≤ 16

Reflections collected	55761
Independent reflections	4531[R(int) = 0.0277]
Data/restraints/parameters	4531/0/266
Goodness-of-fit on F^2	1.036
Final R indexes [I>=2σ (I)]	R_1 = 0.0398, wR_2 = 0.1062
Final R indexes [all data]	R_1 = 0.0430, wR_2 = 0.1092
Largest diff. peak/hole	0.34/-0.44 eÅ^{-3}

Figure A2.309: Refined Positional Parameters for Compound 8-(4,4,5,5-tetramethyl-1,3,2-dioxaboryl)-2-(4-(trifluoromethyl)phenyl)-2,1-borazaronaphthalene (**3.32**)

Atom	*x*	*y*	*z*	U(eq)
F1	0.06032(5)	0.71370(11)	0.77795(7)	0.0394(2)
F2	0.01403(7)	0.54008(10)	0.68800(9)	0.0508(3)
F3	-0.01407(6)	0.73932(14)	0.62547(8)	0.0604(4)
O1	0.32170(5)	0.39250(9)	0.04583(6)	0.01691(18)
O2	0.24823(5)	0.44892(9)	0.18181(6)	0.01764(18)
N1	0.34758(6)	0.57900(9)	0.36398(7)	0.01331(19)
C1	0.43716(7)	0.68681(12)	0.51976(9)	0.0178(2)
C2	0.50312(7)	0.67699(12)	0.46390(9)	0.0178(2)
C3	0.49489(7)	0.61872(11)	0.35822(9)	0.0150(2)
C4	0.56462(7)	0.60847(12)	0.30251(10)	0.0187(2)
C5	0.55792(7)	0.54929(12)	0.20271(10)	0.0198(2)
C6	0.48000(7)	0.49884(12)	0.15550(9)	0.0165(2)
C7	0.40823(7)	0.50688(11)	0.20601(8)	0.0133(2)
C8	0.41625(6)	0.5678(1)	0.30901(8)	0.0125(2)
C9	0.23402(6)	0.36517(11)	0.00314(8)	0.0126(2)
C10	0.18792(6)	0.37326(11)	0.10514(8)	0.0143(2)
C11	0.23190(8)	0.22602(12)	-0.05009(9)	0.0201(2)
C12	0.20714(8)	0.47573(12)	-0.07940(9)	0.0206(2)
C13	0.17449(8)	0.23458(13)	0.15464(10)	0.0236(3)
C14	0.10589(7)	0.45305(13)	0.08952(10)	0.0224(3)
C15	0.26828(7)	0.64409(10)	0.52237(8)	0.0136(2)
C16	0.27419(7)	0.67430(11)	0.63188(9)	0.0156(2)
C17	0.20321(7)	0.68191(11)	0.68349(9)	0.0162(2)
C18	0.12416(7)	0.65984(11)	0.62543(9)	0.0153(2)
C19	0.11566(7)	0.63107(11)	0.51616(9)	0.0164(2)
C20	0.18711(7)	0.62307(11)	0.46623(8)	0.0156(2)
C21	0.04677(7)	0.66422(13)	0.67910(9)	0.0200(2)
B1	0.35090(8)	0.63602(12)	0.46793(10)	0.0140(2)
B2	0.32459(7)	0.44933(12)	0.14491(9)	0.0133(2)

Figure A2.310: Positional Parameters for Hydrogens in 8-(4,4,5,5-tetramethyl-1,3,2-dioxaboryl)-2-(4-(trifluoromethyl)phenyl)-2,1-borazaronaphthalene (**3.32**)

Atom	*x*	*y*	*z*	U(eq)
H1a	0.2998	0.5494	0.333	0.018
H1	0.4443	0.7238	0.5883	0.024
H2	0.5555	0.709	0.495	0.024
H4	0.6165	0.6425	0.3338	0.025
H5	0.6047	0.543	0.1672	0.026
H6	0.4758	0.4586	0.0882	0.022
H11a	0.2643	0.2289	-0.1084	0.03
H11b	0.1747	0.2022	-0.0767	0.03
H11c	0.2554	0.159	0.0012	0.03
H12a	0.2124	0.5637	-0.0454	0.031
H12b	0.1496	0.4611	-0.1102	0.031
H12c	0.2424	0.4722	-0.1347	0.031
H13a	0.2274	0.1877	0.1696	0.035
H13b	0.1363	0.1814	0.1056	0.035
H13c	0.1513	0.2471	0.22	0.035
H14a	0.0843	0.4594	0.1565	0.034
H14b	0.0656	0.407	0.0381	0.034
H14c	0.1159	0.5432	0.0641	0.034
H16	0.327	0.6896	0.671	0.021
H17	0.2087	0.7016	0.7562	0.022
H19	0.0626	0.6174	0.4772	0.022
H20	0.1812	0.6032	0.3935	0.021

Figure A2.311: Refined Thermal Parameters (U's) for 8-(4,4,5,5-tetramethyl-1,3,2-dioxaboryl)-2-(4-(trifluoromethyl)phenyl)-2,1-borazaronaphthalene (**3.32**)

Atom	U_{11}	U_{22}	U_{33}	U_{23}	U_{13}	U_{12}
F1	0.0257(4)	0.0645(6)	0.0299(4)	-0.0257(4)	0.0111(3)	-0.0060(4)
F2	0.0606(6)	0.0399(5)	0.0625(7)	-0.0193(5)	0.0448(5)	-0.0281(5)
F3	0.0244(4)	0.1108(10)	0.0491(6)	0.0401(6)	0.0162(4)	0.0312(5)
O1	0.0113(4)	0.0241(4)	0.0154(4)	-0.0052(3)	0.0018(3)	-0.0008(3)
O2	0.0132(4)	0.0265(4)	0.0134(4)	-0.0071(3)	0.0023(3)	-0.0065(3)
N1	0.0112(4)	0.0142(4)	0.0141(4)	-0.0010(3)	0.0004(3)	-0.0028(3)
C1	0.0199(5)	0.0163(5)	0.0163(5)	-0.0031(4)	-0.0007(4)	-0.0042(4)
C2	0.0149(5)	0.0169(5)	0.0201(5)	-0.0006(4)	-0.0029(4)	-0.0049(4)
C3	0.0133(5)	0.0125(5)	0.0185(5)	0.0018(4)	0.0002(4)	-0.0018(4)
C4	0.0110(5)	0.0194(5)	0.0250(6)	0.0012(4)	0.0001(4)	-0.0029(4)
C5	0.0125(5)	0.0227(6)	0.0251(6)	0.0016(4)	0.0057(4)	-0.0003(4)
C6	0.0156(5)	0.0164(5)	0.0178(5)	0.0000(4)	0.0036(4)	0.0003(4)
C7	0.0127(5)	0.0122(5)	0.0148(5)	0.0011(4)	0.0012(4)	-0.0003(4)
C8	0.0123(5)	0.0104(4)	0.0145(5)	0.0023(4)	0.0011(4)	-0.0005(4)
C9	0.0116(5)	0.0144(5)	0.0113(4)	-0.0011(4)	0.0000(4)	0.0009(4)
C10	0.0126(5)	0.0177(5)	0.0122(5)	-0.0031(4)	0.0006(4)	-0.0034(4)
C11	0.0250(6)	0.0165(5)	0.0176(5)	-0.0046(4)	-0.0009(4)	0.0024(4)
C12	0.0257(6)	0.0193(5)	0.0167(5)	0.0043(4)	0.0026(4)	0.0040(5)
C13	0.0257(6)	0.0258(6)	0.0190(5)	0.0049(5)	0.0024(4)	-0.0080(5)
C14	0.0150(5)	0.0287(6)	0.0238(6)	-0.0061(5)	0.0043(4)	0.0017(5)
C15	0.0170(5)	0.0093(4)	0.0141(5)	0.0002(4)	0.0012(4)	-0.0002(4)
C16	0.0160(5)	0.0147(5)	0.0152(5)	-0.0012(4)	-0.0011(4)	-0.0005(4)
C17	0.0204(5)	0.0152(5)	0.0126(5)	-0.0008(4)	0.0007(4)	0.0002(4)
C18	0.0170(5)	0.0126(5)	0.0162(5)	0.0013(4)	0.0027(4)	0.0007(4)
C19	0.0157(5)	0.0165(5)	0.0158(5)	-0.0004(4)	-0.0019(4)	-0.0012(4)
C20	0.0198(5)	0.0143(5)	0.0123(5)	-0.0008(4)	0.0004(4)	-0.0010(4)
C21	0.0183(5)	0.0243(6)	0.0173(5)	-0.0006(4)	0.0023(4)	-0.0011(4)
B1	0.0154(5)	0.0116(5)	0.0146(5)	0.0001(4)	0.0008(4)	-0.0011(4)
B2	0.0137(5)	0.0124(5)	0.0138(5)	0.0009(4)	0.0018(4)	0.0002(4)

Figure A2.312: Bond Distances in 8-(4,4,5,5-tetramethyl-1,3,2-dioxaboryl)-2-(4-(trifluoromethyl)phenyl)-2,1-borazaronaphthalene (**3.32**), (**Å**)

F1-C21	1.3272(14)	F2-C21	1.3346(15)	F3-C21	1.3276(15)
O1-C9	1.4573(12)	O1-B2	1.3637(14)	O2-C10	1.4677(12)
O2-B2	1.3711(14)	N1-C8	1.3873(13)	N1-B1	1.4200(15)
C1-C2	1.3560(16)	C1-B1	1.5271(16)	C2-C3	1.4395(16)
C3-C4	1.4071(15)	C3-C8	1.4151(14)	C4-C5	1.3768(17)
C5-C6	1.3960(16)	C6-C7	1.3956(14)	C7-C8	1.4195(14)
C7-B2	1.5548(15)	C9-C10	1.5757(14)	C9-C11	1.5168(15)
C9-C12	1.5212(15)	C10-C13	1.5221(16)	C10-C14	1.5185(15)
C15-C16	1.4036(14)	C15-C20	1.4060(15)	C15-B1	1.5795(16)
C16-C17	1.3922(15)	C17-C18	1.3881(15)	C18-C19	1.3954(15)
C18-C21	1.4972(15)	C19-C20	1.3868(15)		

Figure A2.313: Bond Angles in 8-(4,4,5,5-tetramethyl-1,3,2-dioxaboryl)-2-(4-(trifluoromethyl)phenyl)-2,1-borazaronaphthalene (**3.32**), (°)

B2-O1-C9	108.60(8)	B2-O2-C10	108.32(8)	C8-N1-B1	124.43(9)
C2-C1-B1	118.74(10)	C1-C2-C3	122.32(10)	C4-C3-C2	121.13(10)
C4-C3-C8	118.55(10)	C8-C3-C2	120.30(10)	C5-C4-C3	121.55(10)
C4-C5-C6	119.21(10)	C7-C6-C5	122.11(10)	C6-C7-C8	117.99(10)
C6-C7-B2	117.56(9)	C8-C7-B2	124.45(9)	N1-C8-C3	118.32(9)
N1-C8-C7	121.10(9)	C3-C8-C7	120.58(10)	O1-C9-C10	103.25(8)
O1-C9-C11	106.75(8)	O1-C9-C12	106.69(9)	C11-C9-C10	115.06(9)
C11-C9-C12	110.41(9)	C12-C9-C10	113.81(9)	O2-C10-C9	102.84(8)
O2-C10-C13	107.31(9)	O2-C10-C14	107.69(9)	C13-C10-C9	113.64(9)
C14-C10-C9	114.75(9)	C14-C10-C13	109.94(10)	C16-C15-C20	117.07(10)
C16-C15-B1	119.73(9)	C20-C15-B1	123.19(9)	C17-C16-C15	121.81(10)
C18-C17-C16	119.42(10)	C17-C18-C19	120.44(10)	C17-C18-C21	120.70(10)
C19-C18-C21	118.86(10)	C20-C19-C18	119.35(10)	C19-C20-C15	121.91(10)
F1-C21-F2	105.46(10)	F1-C21-F3	106.71(11)	F1-C21-C18	113.62(10)
F2-C21-C18	111.94(10)	F3-C21-F2	106.10(12)	F3-C21-C18	112.44(10)
N1-B1-C1	115.86(10)	N1-B1-C15	119.91(9)	C1-B1-C15	124.24(10)
O1-B2-O2	113.27(9)	O1-B2-C7	121.13(10)	O2-B2-C7	125.60(10)

This report has been created with Olex2 [6], compiled on 2016.02.19 svn.r3266 for OlexSys.

Figure A2.314: X-ray Structure Determination of 6,8-bis(4,4,5,5-tetramethyl-1,3,2-dioxaboryl)-2-(4-(trifluoromethyl)phenyl)-2,1-borazaronaphthalene (**3.59**)

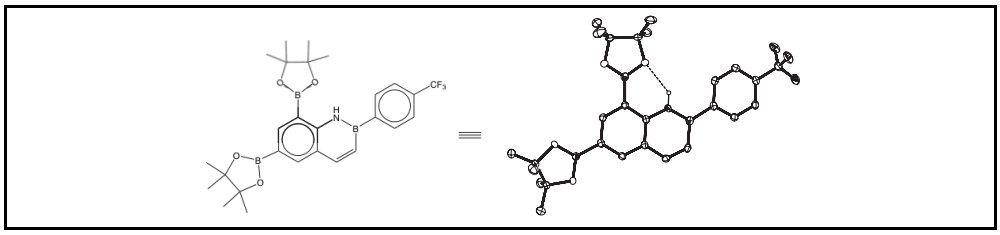

Compound 9220, $C_{27}H_{33}B_3NO_4F_3$, crystallizes in the monoclinic space group $P2_1/n$ (systematic absences 0k0: k=odd and h0l: h+l=odd) with a=21.6033(6)Å, b=13.3398(4)Å, c=28.3256(9)Å, β=94.209(2)°, V=8141.0(4)Å^3, Z=12, and d_{calc}=1.285 g/cm$_3$. X-ray intensity data were collected on a Bruker APEXII [1] CCD area detector employing graphite-monochromated Mo-Kα radiation (λ=0.71073Å) at a temperature of 100K. Preliminary indexing was performed from a series of thirty-six 0.5° rotation frames with exposures of 10 seconds. A total of 3389 frames were collected with a crystal to detector distance of 49.9 mm, rotation widths of 0.5° and exposures of 15 seconds:

scan type	2θ	ω	φ	χ	Frames
f	-30.50	251.25	9.11	21.36	739
f	-30.50	338.88	42.82	78.00	739
f	24.50	68.74	340.76	-42.87	739
f	29.50	288.30	17.77	39.97	739
w	-30.50	149.09	72.07	99.72	114
w	-23.00	326.67	91.95	-98.74	106
w	29.50	335.72	183.80	85.83	114
w	22.00	315.41	74.22	94.02	145

Rotation frames were integrated using SAINT [2], producing a listing of unaveraged F^2 and $\sigma(F^2)$ values. A total of 168625 reflections were measured over the ranges $2.292 \leq 2\theta \leq 50.802°$, $-26 \leq h \leq 26$, $-16 \leq k \leq 16$, $-34 \leq l \leq 34$ yielding 14977 unique reflections (R_{int} = 0.0372). The intensity data were corrected for Lorentz and polarization effects and for absorption using SADABS [3] (minimum and maximum transmission 0.7199, 0.7452). The structure was solved by direct methods - SHELXT [4]. Refinement was by full-matrix least squares based on F^2 using SHELXL-2014 [5]. All reflections were used during refinement. The weighting scheme used was $w=1/[\sigma^2(F_o^2)+ (0.0757P)^2 + 2.6606P]$

where P = $(F_o^2 + 2F_c^2)/3$. Non-hydrogen atoms were refined anisotropically and hydrogen atoms were refined using a riding model. Refinement converged to R1=0.0459 and wR2=0.1229 for 10825 observed reflections for which F > 4σ(F) and R1=0.0678 and wR2=0.1398 and GOF =1.009 for all 14977 unique, non-zero reflections and 1051 variables. The maximum Δ/σ in the final cycle of least squares was 0.001 and the two most prominent peaks in the final difference Fourier were +0.34 and -0.20 e/Å^3.

Table 1. lists cell information, data collection parameters, and refinement data. Final positional and equivalent isotropic thermal parameters are given in Tables 2. and 3. Anisotropic thermal parameters are in Table 4. Tables 5. and 6. list bond distances and bond angles. Figures 1., 2., and 3. are ORTEP representations of the molecule with 50% probability thermal ellipsoids displayed.

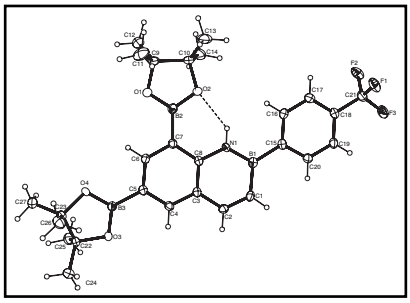

ORTEP drawing of molecule no. 1 of the asymmetric unit with 50% thermal ellipsoids.

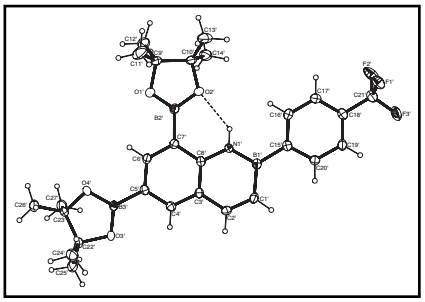

ORTEP drawing of molecule no. 2 of the asymmetric unit with 50% thermal ellipsoids.

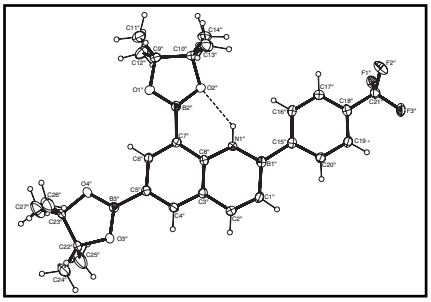

ORTEP drawing of molecule no. 3 of the asymmetric unit with 50% thermal ellipsoids.

Figure A2.315: Summary of Structure Determination of 6,8-bis(4,4,5,5-tetramethyl-1,3,2-dioxaboryl)-2-(4-(trifluoromethyl)phenyl)-2,1-borazaronaphthalene (**3.59**)

Empirical formula	$C_{27}H_{33}B_3NO_4F_3$
Formula weight	524.97
Temperature/K	100
Crystal system	monoclinic
Space group	$P2_1/n$
a	21.6033(6)Å
b	13.3398(4)Å
c	28.3256(9)Å
β	94.209(2)°
Volume	8141.0(4)Å^3
Z	12
d_{calc}	1.285 g/cm^3
μ	0.097 mm^{-1}
F(000)	3312.0
Crystal size, mm	0.25 × 0.2 × 0.15
2θ range for data collection	2.292 - 50.802°
Index ranges	-26 ≤ h ≤ 26, -16 ≤ k ≤ 16, -34 ≤ l ≤ 34
Reflections collected	168625
Independent reflections	14977[R(int) = 0.0372]
Data/restraints/parameters	14977/0/1051
Goodness-of-fit on F^2	1.009
Final R indexes [I>=2σ (I)]	R_1 = 0.0459, wR_2 = 0.1229
Final R indexes [all data]	R_1 = 0.0678, wR_2 = 0.1398
Largest diff. peak/hole	0.34/-0.20 eÅ^{-3}

Figure A2.316: Refined Positional Parameters for 6,8-bis(4,4,5,5-tetramethyl-1,3,2-dioxaboryl)-2-(4-(trifluoromethyl)phenyl)-2,1-borazaronaphthalene (**3.59**)

Atom	*x*	*y*	*z*	U(eq)
F1	0.21987(4)	0.27978(7)	0.99472(4)	0.0341(3)
F2	0.21801(4)	0.43973(7)	0.99837(4)	0.0318(2)
F3	0.22897(4)	0.3536(1)	1.06234(4)	0.0455(3)
O1	0.59842(5)	0.49393(9)	0.82698(4)	0.0234(3)
O2	0.51584(5)	0.42134(8)	0.85964(4)	0.0227(3)
O3	0.84680(4)	0.35807(8)	0.96493(4)	0.0183(2)
O4	0.82391(4)	0.39025(8)	0.88621(4)	0.0190(2)
N1	0.54062(5)	0.37799(9)	0.95903(4)	0.0170(3)
C1	0.56404(7)	0.32498(12)	1.04266(5)	0.0194(3)
C2	0.62483(7)	0.32550(12)	1.03433(5)	0.0189(3)
C3	0.64646(7)	0.35284(11)	0.98909(5)	0.0166(3)
C4	0.70964(7)	0.35318(11)	0.98127(5)	0.0175(3)
C5	0.73115(7)	0.37801(11)	0.93773(5)	0.0178(3)
C6	0.68670(7)	0.40493(11)	0.90108(5)	0.0174(3)
C7	0.62322(7)	0.40651(11)	0.90648(5)	0.0170(3)
C8	0.60298(7)	0.37919(11)	0.95126(5)	0.0159(3)
C9	0.54734(7)	0.49747(12)	0.79010(5)	0.0215(3)
C10	0.48937(7)	0.47730(12)	0.81833(5)	0.0214(3)
C11	0.56049(10)	0.41670(15)	0.75478(6)	0.0389(5)
C12	0.54814(8)	0.60006(13)	0.76705(6)	0.0319(4)
C13	0.43964(8)	0.41315(14)	0.79237(6)	0.0344(4)
C14	0.46071(8)	0.57154(14)	0.83745(6)	0.0332(4)
C15	0.44348(7)	0.35709(11)	1.00662(5)	0.0176(3)
C16	0.40155(7)	0.37639(13)	0.96772(6)	0.0236(4)
C17	0.33808(7)	0.37779(13)	0.97154(6)	0.0258(4)
C18	0.31495(7)	0.36096(11)	1.01534(6)	0.0191(3)
C19	0.35490(7)	0.34264(12)	1.05473(6)	0.0208(3)
C20	0.41831(7)	0.34015(12)	1.04997(5)	0.0206(3)
C21	0.24596(7)	0.35915(13)	1.01817(6)	0.0246(4)
C22	0.90617(7)	0.37898(12)	0.94525(5)	0.0189(3)
C23	0.89003(6)	0.36531(12)	0.89101(5)	0.0191(3)
C24	0.95458(7)	0.30759(13)	0.96720(6)	0.0261(4)
C25	0.92279(7)	0.48684(12)	0.95826(6)	0.0253(4)
C26	0.89550(7)	0.25701(13)	0.87515(6)	0.0280(4)
C27	0.92427(7)	0.43365(14)	0.85932(6)	0.0277(4)
B1	0.51586(8)	0.35375(13)	1.00280(6)	0.0181(4)
B2	0.57821(8)	0.44045(13)	0.86384(6)	0.0187(4)
B3	0.80162(8)	0.37564(13)	0.92970(6)	0.0170(4)
F1'	-0.11442(4)	0.29023(7)	0.66108(4)	0.0297(2)

F2'	-0.11529(4)	0.44933(8)	0.66904(4)	0.0392(3)
F3'	-0.10397(4)	0.35457(10)	0.73061(4)	0.0463(3)
O1'	0.26182(5)	0.48270(9)	0.48958(4)	0.0273(3)
O2'	0.17914(5)	0.42260(8)	0.52665(4)	0.0221(2)
O3'	0.51144(5)	0.35971(8)	0.62961(4)	0.0195(2)
O4'	0.48919(4)	0.39374(8)	0.55093(4)	0.0197(2)
N1'	0.20608(5)	0.38139(9)	0.62505(4)	0.0169(3)
C1'	0.23072(7)	0.33280(12)	0.70920(5)	0.0204(3)
C2'	0.29135(7)	0.33322(12)	0.70045(5)	0.0200(3)
C3'	0.31220(7)	0.35800(11)	0.65458(5)	0.0172(3)
C4'	0.37537(7)	0.35806(11)	0.64628(5)	0.0180(3)
C5'	0.39610(7)	0.38073(11)	0.60222(5)	0.0174(3)
C6'	0.35118(7)	0.40452(11)	0.56550(5)	0.0181(3)
C7'	0.28781(7)	0.40581(11)	0.57138(5)	0.0179(3)
C8'	0.26821(7)	0.38184(11)	0.61671(5)	0.0163(3)
C9'	0.20914(7)	0.48642(13)	0.45415(5)	0.0241(4)
C10'	0.15230(7)	0.47561(12)	0.48454(5)	0.0211(3)
C11'	0.21685(10)	0.39906(16)	0.42069(6)	0.0436(5)
C12'	0.21209(8)	0.58521(14)	0.42811(7)	0.0355(4)
C13'	0.09911(8)	0.41370(14)	0.46204(6)	0.0338(4)
C14'	0.12816(8)	0.57487(14)	0.50192(6)	0.0314(4)
C15'	0.10987(7)	0.36324(11)	0.67358(5)	0.0184(3)
C16'	0.06733(7)	0.37981(13)	0.63469(6)	0.0236(4)
C17'	0.00389(7)	0.38151(13)	0.63903(6)	0.0259(4)
C18'	-0.01873(7)	0.36767(11)	0.68310(6)	0.0203(3)
C19'	0.02171(7)	0.35243(12)	0.72252(6)	0.0222(3)
C20'	0.08512(7)	0.34969(12)	0.71727(5)	0.0214(3)
C21'	-0.08759(7)	0.36622(13)	0.68642(6)	0.0256(4)
C22'	0.56942(7)	0.34555(12)	0.60702(5)	0.0202(3)
C23'	0.55667(7)	0.40251(12)	0.55912(5)	0.0187(3)
C24'	0.57711(8)	0.23309(13)	0.60081(6)	0.0304(4)
C25'	0.62222(7)	0.38672(15)	0.63930(6)	0.0315(4)
C26'	0.58678(7)	0.35850(14)	0.51729(6)	0.0268(4)
C27'	0.57100(8)	0.51382(12)	0.56291(6)	0.0275(4)
B1'	0.18202(8)	0.35958(13)	0.66933(6)	0.0181(4)
B2'	0.24211(8)	0.43674(13)	0.52870(6)	0.0196(4)
B3'	0.46657(8)	0.37831(13)	0.59423(6)	0.0170(4)
F1"	0.45291(4)	0.72560(7)	0.67212(3)	0.0274(2)
F2"	0.45673(4)	0.56590(7)	0.66556(4)	0.0324(2)
F3"	0.44383(4)	0.65758(9)	0.60316(3)	0.0374(3)
O1"	0.07413(5)	0.52748(9)	0.84308(4)	0.0242(3)
O2"	0.15932(5)	0.58028(8)	0.80698(4)	0.0213(2)

O3"	-0.17244(5)	0.63976(9)	0.70406(4)	0.0267(3)
O4"	-0.14801(5)	0.64246(10)	0.78351(4)	0.0296(3)
N1"	0.13353(5)	0.62550(9)	0.70793(4)	0.0165(3)
C1"	0.10959(7)	0.67406(12)	0.62371(5)	0.0208(3)
C2"	0.04884(7)	0.67467(12)	0.63233(5)	0.0200(3)
C3"	0.02768(7)	0.65145(11)	0.67813(5)	0.0172(3)
C4"	-0.03540(7)	0.65408(11)	0.68655(5)	0.0182(3)
C5"	-0.05630(7)	0.63514(11)	0.73084(5)	0.0175(3)
C6"	-0.01159(7)	0.61073(11)	0.76764(5)	0.0181(3)
C7"	0.05156(7)	0.60533(11)	0.76165(5)	0.0168(3)
C8"	0.07135(7)	0.62730(11)	0.71605(5)	0.0155(3)
C9"	0.12562(7)	0.51842(12)	0.87909(5)	0.0203(3)
C10"	0.18401(7)	0.52654(12)	0.84956(5)	0.0206(3)
C11"	0.11852(8)	0.41882(13)	0.90375(6)	0.0285(4)
C12"	0.11937(9)	0.60463(13)	0.91349(6)	0.0325(4)
C13"	0.20725(8)	0.42614(13)	0.83290(6)	0.0301(4)
C14"	0.23732(8)	0.58706(14)	0.87286(6)	0.0302(4)
C15"	0.23010(7)	0.64345(11)	0.65975(5)	0.0174(3)
C16"	0.27250(7)	0.62788(12)	0.69875(6)	0.0235(4)
C17"	0.33598(7)	0.62800(13)	0.69469(6)	0.0246(4)
C18"	0.35885(7)	0.64298(11)	0.65059(6)	0.0191(3)
C19"	0.31833(7)	0.65686(12)	0.61104(5)	0.0205(3)
C20"	0.25487(7)	0.65743(12)	0.61596(5)	0.0202(3)
C21"	0.42745(7)	0.64735(12)	0.64750(6)	0.0219(4)
C22"	-0.23078(7)	0.65664(13)	0.72528(6)	0.0236(4)
C23"	-0.21516(7)	0.62687(14)	0.77760(6)	0.0259(4)
C24"	-0.28071(8)	0.59485(17)	0.69935(7)	0.0408(5)
C25"	-0.24471(9)	0.76755(16)	0.71908(9)	0.0559(7)
C26"	-0.22505(9)	0.51596(18)	0.78561(9)	0.0577(7)
C27"	-0.24609(9)	0.6874(2)	0.81364(8)	0.0684(9)
B1"	0.15792(8)	0.64702(13)	0.66367(6)	0.0179(4)
B2"	0.09607(8)	0.57156(13)	0.80431(6)	0.0181(4)
B3"	-0.12657(8)	0.63945(13)	0.73959(6)	0.0184(4)

Figure A2.317: Positional Parameters for Hydrogens 6,8-bis(4,4,5,5-tetramethyl-1,3,2-dioxaboryl)-2-(4-(trifluoromethyl)phenyl)-2,1-borazaronaphthalene (**3.59**)

Atom	*x*	*y*	*z*	U(eq)
H1a	0.5147	0.3931	0.9356	0.023
H1	0.5517	0.3073	1.0723	0.026
H2	0.6539	0.3075	1.0587	0.025
H4	0.7383	0.3362	1.0061	0.023
H6	0.7005	0.4225	0.8719	0.023
H11a	0.5297	0.4193	0.7286	0.058
H11b	0.5592	0.3522	0.7698	0.058
H11c	0.6009	0.4273	0.7436	0.058
H12a	0.585	0.6068	0.7503	0.048
H12b	0.5477	0.651	0.791	0.048
H12c	0.5123	0.6073	0.7452	0.048
H13a	0.4237	0.4472	0.7642	0.052
H13b	0.4065	0.4016	0.8125	0.052
H13c	0.4573	0.3501	0.784	0.052
H14a	0.4397	0.6081	0.8118	0.05
H14b	0.4928	0.6127	0.8526	0.05
H14c	0.4315	0.5534	0.86	0.05
H16	0.4168	0.3887	0.9384	0.031
H17	0.3111	0.3899	0.945	0.034
H19	0.3394	0.3321	1.0841	0.028
H20	0.445	0.3268	1.0765	0.027
H24a	0.9398	0.24	0.9636	0.039
H24b	0.9623	0.3227	1.0002	0.039
H24c	0.9924	0.3148	0.9517	0.039
H25a	0.9626	0.5028	0.9473	0.038
H25b	0.9242	0.4946	0.992	0.038
H25c	0.892	0.5311	0.9436	0.038
H26a	0.8783	0.2504	0.8431	0.042
H26b	0.8732	0.2144	0.8953	0.042
H26c	0.9384	0.2377	0.8771	0.042
H27a	0.9121	0.4187	0.8268	0.042
H27b	0.9682	0.4235	0.8652	0.042
H27c	0.9143	0.5021	0.8659	0.042
H1a'	0.1799	0.3954	0.6017	0.022
H1'	0.2188	0.3164	0.7391	0.027
H2'	0.3208	0.3169	0.7249	0.027
H4'	0.4044	0.3424	0.6711	0.024
H6'	0.3644	0.4201	0.5359	0.024
H11a'	0.1849	0.4018	0.3953	0.065

H11b'	0.2137	0.3371	0.4376	0.065
H11c'	0.2568	0.4031	0.408	0.065
H12a'	0.2472	0.5851	0.4092	0.053
H12b'	0.2162	0.6391	0.4506	0.053
H12c'	0.1747	0.5942	0.408	0.053
H13a'	0.0835	0.4447	0.433	0.051
H13b'	0.0666	0.4098	0.4833	0.051
H13c'	0.1136	0.3474	0.4556	0.051
H14a'	0.1074	0.6104	0.4759	0.047
H14b'	0.1623	0.6143	0.5153	0.047
H14c'	0.0995	0.5627	0.5256	0.047
H16'	0.0821	0.39	0.605	0.031
H17'	-0.0234	0.3919	0.6125	0.034
H19'	0.0067	0.3441	0.7522	0.03
H20'	0.1121	0.3384	0.7439	0.028
H24a'	0.5435	0.2078	0.5801	0.046
H24b'	0.5769	0.2007	0.6311	0.046
H24c'	0.6158	0.2198	0.5873	0.046
H25a'	0.6601	0.3833	0.6236	0.047
H25b'	0.6264	0.3477	0.6678	0.047
H25c'	0.6137	0.4552	0.6469	0.047
H26a'	0.5743	0.3961	0.4893	0.04
H26b'	0.5741	0.2899	0.513	0.04
H26c'	0.6311	0.3615	0.523	0.04
H27a'	0.6151	0.5234	0.5665	0.041
H27b'	0.5525	0.5412	0.5899	0.041
H27c'	0.5544	0.5472	0.5348	0.041
H1a"	0.1595	0.6103	0.7313	0.022
H1"	0.1218	0.6899	0.5938	0.028
H2"	0.0196	0.6907	0.6078	0.027
H4"	-0.0643	0.6691	0.6616	0.024
H6"	-0.025	0.5975	0.7975	0.024
H11a"	0.115	0.3661	0.8806	0.043
H11b"	0.0819	0.4202	0.921	0.043
H11c"	0.1542	0.407	0.9253	0.043
H12a"	0.1251	0.667	0.8975	0.049
H12b"	0.1503	0.5981	0.9395	0.049
H12c"	0.0788	0.6032	0.9252	0.049
H13a"	0.1729	0.3877	0.8192	0.045
H13b"	0.2268	0.3903	0.8593	0.045
H13c"	0.2367	0.4369	0.8096	0.045
H14a"	0.2707	0.5894	0.8523	0.045

H14b"	0.2515	0.5561	0.9023	0.045
H14c"	0.2234	0.654	0.8787	0.045
H16"	0.2576	0.6171	0.7283	0.031
H17"	0.3632	0.6181	0.7213	0.033
H19"	0.3335	0.6657	0.5814	0.027
H20"	0.2279	0.6675	0.5892	0.027
H24a"	-0.2881	0.6195	0.6676	0.061
H24b"	-0.3182	0.5995	0.7154	0.061
H24c"	-0.2676	0.5261	0.6985	0.061
H25a"	-0.2458	0.7846	0.6861	0.084
H25b"	-0.213	0.806	0.7363	0.084
H25c"	-0.2842	0.7823	0.7309	0.084
H26a"	-0.2687	0.5016	0.7832	0.087
H26b"	-0.2075	0.4978	0.8165	0.087
H26c"	-0.2052	0.4782	0.7621	0.087
H27a"	-0.2362	0.757	0.8099	0.103
H27b"	-0.2316	0.6657	0.8448	0.103
H27c"	-0.2902	0.6784	0.8093	0.103

Figure A2.318: Refined Thermal Parameters (U's) for 6,8-bis(4,4,5,5-tetramethyl-1,3,2-dioxaboryl)-2-(4-(trifluoromethyl)phenyl)-2,1-borazaronaphthalene (**3.59**)

Atom	U_{11}	U_{22}	U_{33}	U_{23}	U_{13}	U_{12}
F1	0.0201(5)	0.0303(6)	0.0516(7)	-0.0025(5)	0.0010(4)	-0.0071(4)
F2	0.0189(5)	0.0308(6)	0.0449(6)	-0.0030(5)	-0.0028(4)	0.0052(4)
F3	0.0180(5)	0.0926(10)	0.0271(6)	0.0050(6)	0.0091(4)	0.0009(5)
O1	0.0179(5)	0.0329(7)	0.0194(6)	0.0084(5)	0.0016(4)	0.0027(5)
O2	0.0174(5)	0.0339(7)	0.0163(6)	0.0068(5)	-0.0017(4)	-0.0029(5)
O3	0.0137(5)	0.0264(6)	0.0150(5)	0.0024(4)	0.0030(4)	0.0000(4)
O4	0.0106(5)	0.0298(6)	0.0166(5)	0.0035(5)	0.0011(4)	0.0029(4)
N1	0.0115(6)	0.0221(7)	0.0174(7)	0.0010(5)	0.0012(5)	-0.0002(5)
C1	0.0206(8)	0.0227(8)	0.0156(8)	0.0008(6)	0.0062(6)	-0.0017(6)
C2	0.0189(8)	0.0229(8)	0.0144(8)	-0.0009(6)	-0.0006(6)	0.0002(6)
C3	0.0156(7)	0.0178(8)	0.0168(8)	-0.0012(6)	0.0036(6)	-0.0011(6)
C4	0.0150(7)	0.0200(8)	0.0173(8)	-0.0014(6)	-0.0005(6)	-0.0009(6)
C5	0.0158(7)	0.0192(8)	0.0188(8)	-0.0008(6)	0.0032(6)	0.0003(6)
C6	0.0175(7)	0.0193(8)	0.0158(8)	0.0010(6)	0.0038(6)	-0.0001(6)
C7	0.0162(7)	0.0184(8)	0.0166(8)	-0.0007(6)	0.0028(6)	-0.0001(6)
C8	0.0145(7)	0.0162(8)	0.0173(8)	-0.0024(6)	0.0025(6)	-0.0011(6)
C9	0.0228(8)	0.0259(9)	0.0153(8)	0.0020(7)	-0.0014(6)	0.0045(7)
C10	0.0200(8)	0.0276(9)	0.0160(8)	0.0039(7)	-0.0036(6)	0.0010(7)
C11	0.0540(12)	0.0425(12)	0.0205(9)	-0.0029(8)	0.0048(8)	0.0183(10)
C12	0.0299(9)	0.0334(10)	0.0322(10)	0.0132(8)	0.0010(8)	-0.0006(8)
C13	0.0331(10)	0.0366(11)	0.0309(10)	0.0078(8)	-0.0149(8)	-0.0080(8)
C14	0.0256(9)	0.0453(11)	0.0285(10)	-0.0044(8)	0.0007(7)	0.0108(8)
C15	0.0173(8)	0.0159(8)	0.0201(8)	-0.0027(6)	0.0044(6)	-0.0012(6)
C16	0.0202(8)	0.0331(10)	0.0181(8)	0.0041(7)	0.0057(6)	0.0001(7)
C17	0.0179(8)	0.037(1)	0.0222(9)	0.0048(7)	-0.0001(6)	0.0030(7)
C18	0.0156(8)	0.0196(8)	0.0225(8)	-0.0021(6)	0.0035(6)	-0.0008(6)
C19	0.0183(8)	0.0258(9)	0.0187(8)	-0.0013(7)	0.0051(6)	-0.0037(6)
C20	0.0182(8)	0.0262(9)	0.0172(8)	-0.0003(7)	0.0001(6)	-0.0025(6)
C21	0.0177(8)	0.0316(10)	0.0244(9)	-0.0012(7)	0.0012(7)	-0.0013(7)
C22	0.0128(7)	0.0262(9)	0.0180(8)	0.0021(6)	0.0030(6)	0.0002(6)
C23	0.0101(7)	0.0292(9)	0.0179(8)	0.0018(7)	0.0010(6)	0.0019(6)
C24	0.0206(8)	0.0323(10)	0.0251(9)	0.0035(7)	-0.0006(7)	0.0038(7)
C25	0.0224(8)	0.0267(9)	0.0268(9)	-0.0017(7)	0.0024(7)	-0.0035(7)
C26	0.0226(8)	0.0318(10)	0.0294(9)	-0.0077(8)	0.0010(7)	0.0023(7)
C27	0.0198(8)	0.0416(11)	0.0220(9)	0.0054(8)	0.0027(7)	-0.0027(7)
B1	0.0196(9)	0.0160(9)	0.0191(9)	-0.0020(7)	0.0034(7)	-0.0012(7)
B2	0.0196(9)	0.0209(9)	0.0161(9)	-0.0028(7)	0.0036(7)	0.0020(7)
B3	0.0166(8)	0.0175(9)	0.0171(9)	0.0006(7)	0.0023(7)	-0.0003(7)
F1'	0.0198(5)	0.0280(5)	0.0408(6)	-0.0033(4)	-0.0006(4)	-0.0045(4)

F2'	0.0210(5)	0.0280(6)	0.0675(8)	-0.0077(5)	-0.0058(5)	0.0064(4)
F3'	0.0186(5)	0.0923(10)	0.0290(6)	-0.0084(6)	0.0085(4)	-0.0024(5)
O1'	0.0204(6)	0.0416(7)	0.0202(6)	0.0116(5)	0.0034(5)	0.0040(5)
O2'	0.0187(5)	0.0319(6)	0.0154(5)	0.0066(5)	-0.0008(4)	-0.0012(5)
O3'	0.0148(5)	0.0271(6)	0.0171(5)	0.0013(4)	0.0058(4)	0.0017(4)
O4'	0.0120(5)	0.0280(6)	0.0192(6)	0.0011(5)	0.0020(4)	0.0007(4)
N1'	0.0129(6)	0.0220(7)	0.0160(6)	0.0014(5)	0.0015(5)	-0.0003(5)
C1'	0.0217(8)	0.0245(9)	0.0155(8)	-0.0005(6)	0.0056(6)	-0.0030(7)
C2'	0.0196(8)	0.0245(9)	0.0154(8)	-0.0008(6)	-0.0011(6)	0.0002(6)
C3'	0.0174(7)	0.0163(8)	0.0182(8)	-0.0017(6)	0.0036(6)	-0.0012(6)
C4'	0.0172(7)	0.0181(8)	0.0187(8)	-0.0015(6)	0.0004(6)	-0.0011(6)
C5'	0.0166(8)	0.0155(8)	0.0203(8)	-0.0009(6)	0.0029(6)	0.0001(6)
C6'	0.0195(8)	0.0182(8)	0.0174(8)	0.0015(6)	0.0059(6)	0.0005(6)
C7'	0.0189(8)	0.0174(8)	0.0176(8)	0.0006(6)	0.0027(6)	0.0002(6)
C8'	0.0164(7)	0.0140(7)	0.0189(8)	-0.0016(6)	0.0037(6)	-0.0009(6)
C9'	0.0243(8)	0.0314(9)	0.0163(8)	0.0049(7)	0.0005(6)	0.0065(7)
C10'	0.0228(8)	0.0236(9)	0.0163(8)	0.0035(7)	-0.0025(6)	0.0002(7)
C11'	0.0603(13)	0.0491(13)	0.0216(10)	-0.0016(9)	0.0048(9)	0.0236(10)
C12'	0.0308(10)	0.0447(12)	0.0309(10)	0.0189(9)	0.0013(8)	-0.0020(8)
C13'	0.0332(10)	0.0360(11)	0.0301(10)	0.0075(8)	-0.0116(8)	-0.0078(8)
C14'	0.0291(9)	0.0378(11)	0.0267(9)	-0.0037(8)	-0.0010(7)	0.0084(8)
C15'	0.0181(8)	0.0174(8)	0.0200(8)	-0.0022(6)	0.0029(6)	-0.0008(6)
C16'	0.0217(8)	0.0311(9)	0.0186(8)	0.0025(7)	0.0053(6)	0.0001(7)
C17'	0.0199(8)	0.0371(10)	0.0203(8)	0.0033(7)	-0.0008(7)	0.0037(7)
C18'	0.0171(8)	0.0191(8)	0.0247(9)	-0.0033(7)	0.0019(6)	-0.0006(6)
C19'	0.0192(8)	0.0279(9)	0.0201(8)	-0.0015(7)	0.0058(6)	-0.0038(7)
C20'	0.0184(8)	0.0284(9)	0.0171(8)	-0.0008(7)	-0.0007(6)	-0.0027(7)
C21'	0.0198(8)	0.0301(10)	0.0269(9)	-0.0061(7)	0.0019(7)	-0.0005(7)
C22'	0.0156(7)	0.0285(9)	0.0171(8)	-0.0004(7)	0.0052(6)	0.0021(6)
C23'	0.0125(7)	0.0265(9)	0.0173(8)	0.0006(7)	0.0019(6)	-0.0002(6)
C24'	0.0280(9)	0.0285(10)	0.0353(10)	0.0059(8)	0.0064(8)	0.0079(7)
C25'	0.0195(8)	0.0537(12)	0.0214(9)	-0.0012(8)	0.0016(7)	-0.0020(8)
C26'	0.0198(8)	0.0393(10)	0.0217(9)	-0.0027(7)	0.0051(7)	-0.0005(7)
C27'	0.0237(8)	0.0274(9)	0.0322(10)	0.0024(7)	0.0074(7)	-0.0019(7)
B1'	0.0182(9)	0.0174(9)	0.0188(9)	-0.0023(7)	0.0031(7)	-0.0021(7)
B2'	0.0206(9)	0.0206(9)	0.0181(9)	0.0014(7)	0.0043(7)	0.0021(7)
B3'	0.0179(9)	0.0159(9)	0.0174(9)	-0.0014(7)	0.0031(7)	0.0009(7)
F1"	0.0200(5)	0.0271(5)	0.0349(6)	-0.0062(4)	0.0011(4)	-0.0052(4)
F2"	0.0204(5)	0.0274(5)	0.0487(6)	-0.0039(5)	-0.0020(4)	0.0057(4)
F3"	0.0179(5)	0.0722(8)	0.0230(5)	-0.0047(5)	0.0076(4)	-0.0030(5)
O1"	0.0182(6)	0.0361(7)	0.0184(6)	0.0093(5)	0.0013(4)	0.0018(5)
O2"	0.0168(5)	0.0312(6)	0.0156(5)	0.0056(5)	-0.0004(4)	-0.0007(5)
O3"	0.0141(5)	0.0502(8)	0.0161(6)	0.0021(5)	0.0038(4)	0.0036(5)

O4"	0.0127(5)	0.0594(9)	0.0166(6)	-0.0027(6)	0.0014(4)	0.0010(5)
N1"	0.0134(6)	0.0209(7)	0.0152(6)	0.0011(5)	0.0007(5)	0.0003(5)
C1"	0.0219(8)	0.0255(9)	0.0157(8)	0.0009(7)	0.0060(6)	-0.0027(7)
C2"	0.0199(8)	0.0245(9)	0.0156(8)	0.0003(6)	0.0001(6)	0.0003(6)
C3"	0.0180(7)	0.0173(8)	0.0164(8)	-0.0015(6)	0.0021(6)	-0.0013(6)
C4"	0.0152(7)	0.0209(8)	0.0183(8)	-0.0010(6)	-0.0004(6)	0.0008(6)
C5"	0.0173(8)	0.0171(8)	0.0183(8)	-0.0003(6)	0.0021(6)	0.0001(6)
C6"	0.0169(7)	0.0199(8)	0.0179(8)	0.0018(6)	0.0048(6)	0.0005(6)
C7"	0.0171(7)	0.0177(8)	0.0157(8)	0.0011(6)	0.0022(6)	-0.0001(6)
C8"	0.0146(7)	0.0140(7)	0.0182(8)	-0.0012(6)	0.0033(6)	-0.0005(6)
C9"	0.0210(8)	0.0233(8)	0.0163(8)	0.0021(6)	-0.0008(6)	0.0018(6)
C10"	0.0206(8)	0.0237(9)	0.0169(8)	0.0028(6)	-0.0022(6)	0.0020(6)
C11"	0.0320(9)	0.0297(10)	0.0232(9)	0.0058(7)	-0.0028(7)	-0.0043(7)
C12"	0.0490(11)	0.0291(10)	0.0200(9)	0.0002(7)	0.0076(8)	0.0064(8)
C13"	0.0279(9)	0.0348(10)	0.0271(9)	-0.0058(8)	-0.0009(7)	0.0085(8)
C14"	0.0263(9)	0.0343(10)	0.0286(9)	0.0060(8)	-0.0081(7)	-0.0046(8)
C15"	0.0192(8)	0.0153(8)	0.0182(8)	-0.0027(6)	0.0038(6)	-0.0014(6)
C16"	0.0201(8)	0.0316(9)	0.0197(8)	0.0026(7)	0.0071(7)	0.0002(7)
C17"	0.0195(8)	0.035(1)	0.0193(8)	0.0030(7)	0.0001(7)	0.0028(7)
C18"	0.0171(8)	0.0176(8)	0.0230(8)	-0.0026(6)	0.0046(6)	-0.0005(6)
C19"	0.0198(8)	0.0255(9)	0.0167(8)	-0.0017(7)	0.0046(6)	-0.0032(6)
C20"	0.0173(8)	0.0257(9)	0.0176(8)	-0.0014(7)	0.0007(6)	-0.0031(6)
C21"	0.0185(8)	0.0274(9)	0.0198(8)	-0.0041(7)	0.0021(6)	0.0008(7)
C22"	0.0127(7)	0.0381(10)	0.0205(8)	0.0056(7)	0.0050(6)	0.0046(7)
C23"	0.0096(7)	0.0491(11)	0.0189(8)	0.0049(8)	0.0012(6)	0.0000(7)
C24"	0.0194(9)	0.0732(15)	0.0295(10)	-0.0091(10)	0.0001(7)	-0.0017(9)
C25"	0.026(1)	0.0456(13)	0.0970(19)	0.0295(13)	0.0098(11)	0.0101(9)
C26"	0.0239(10)	0.0716(16)	0.0775(17)	0.0494(14)	0.0021(10)	-0.0008(10)
C27"	0.023(1)	0.144(3)	0.0387(12)	-0.0404(15)	0.0059(9)	0.0025(13)
B1"	0.0189(9)	0.0159(9)	0.0193(9)	-0.0023(7)	0.0042(7)	-0.0020(7)
B2"	0.0180(8)	0.0183(9)	0.0184(9)	0.0000(7)	0.0038(7)	0.0011(7)
B3"	0.0179(9)	0.0189(9)	0.0187(9)	0.0017(7)	0.0026(7)	0.0014(7)

Figure A2.319: Bond Distances in 6,8-bis(4,4,5,5-tetramethyl-1,3,2-dioxaboryl)-2-(4-(trifluoromethyl)phenyl)-2,1-borazaronaphthalene (**3.59**), (**Å**)

F1-C21	1.3509(19)	F2-C21	1.3361(19)	F3-C21	1.3313(19)
O1-C9	1.4637(18)	O1-B2	1.362(2)	O2-C10	1.4681(18)
O2-B2	1.368(2)	O3-C22	1.4624(17)	O3-B3	1.364(2)
O4-C23	1.4633(17)	O4-B3	1.369(2)	N1-C8	1.3810(18)
N1-B1	1.423(2)	C1-C2	1.351(2)	C1-B1	1.527(2)
C2-C3	1.443(2)	C3-C4	1.399(2)	C3-C8	1.417(2)
C4-C5	1.389(2)	C5-C6	1.408(2)	C5-B3	1.556(2)
C6-C7	1.391(2)	C7-C8	1.419(2)	C7-B2	1.561(2)
C9-C10	1.558(2)	C9-C11	1.511(2)	C9-C12	1.517(2)
C10-C13	1.520(2)	C10-C14	1.519(2)	C15-C16	1.398(2)
C15-C20	1.397(2)	C15-B1	1.576(2)	C16-C17	1.383(2)
C17-C18	1.389(2)	C18-C19	1.381(2)	C18-C21	1.499(2)
C19-C20	1.387(2)	C22-C23	1.561(2)	C22-C24	1.514(2)
C22-C25	1.522(2)	C23-C26	1.520(2)	C23-C27	1.510(2)
F1'-C21'	1.3483(19)	F2'-C21'	1.337(2)	F3'-C21'	1.3345(19)
O1'-C9'	1.4619(19)	O1'-B2'	1.362(2)	O2'-C10'	1.4688(18)
O2'-B2'	1.371(2)	O3'-C22'	1.4599(17)	O3'-B3'	1.365(2)
O4'-C23'	1.4639(17)	O4'-B3'	1.369(2)	N1'-C8'	1.3798(18)
N1'-B1'	1.423(2)	C1'-C2'	1.351(2)	C1'-B1'	1.528(2)
C2'-C3'	1.444(2)	C3'-C4'	1.402(2)	C3'-C8'	1.416(2)
C4'-C5'	1.390(2)	C5'-C6'	1.406(2)	C5'-B3'	1.556(2)
C6'-C7'	1.391(2)	C7'-C8'	1.418(2)	C7'-B2'	1.559(2)
C9'-C10'	1.557(2)	C9'-C11'	1.519(2)	C9'-C12'	1.514(2)
C10'-C13'	1.517(2)	C10'-C14'	1.518(2)	C15'-C16'	1.399(2)
C15'-C20'	1.395(2)	C15'-B1'	1.573(2)	C16'-C17'	1.385(2)
C17'-C18'	1.386(2)	C18'-C19'	1.381(2)	C18'-C21'	1.498(2)
C19'-C20'	1.389(2)	C22'-C23'	1.562(2)	C22'-C24'	1.521(2)
C22'-C25'	1.512(2)	C23'-C26'	1.511(2)	C23'-C27'	1.519(2)
F1"-C21"	1.3498(18)	F2"-C21"	1.3397(19)	F3"-C21"	1.3367(18)
O1"-C9"	1.4580(18)	O1"-B2"	1.361(2)	O2"-C10"	1.4693(18)
O2"-B2"	1.368(2)	O3"-C22"	1.4532(18)	O3"-B3"	1.359(2)
O4"-C23"	1.4628(18)	O4"-B3"	1.360(2)	N1"-C8"	1.3796(18)
N1"-B1"	1.424(2)	C1"-C2"	1.352(2)	C1"-B1"	1.526(2)
C2"-C3"	1.440(2)	C3"-C4"	1.401(2)	C3"-C8"	1.414(2)
C4"-C5"	1.387(2)	C5"-C6"	1.406(2)	C5"-B3"	1.557(2)
C6"-C7"	1.389(2)	C7"-C8"	1.421(2)	C7"-B2"	1.555(2)
C9"-C10"	1.568(2)	C9"-C11"	1.514(2)	C9"-C12"	1.520(2)
C10"-C13"	1.518(2)	C10"-C14"	1.517(2)	C15"-C16"	1.398(2)
C15"-C20"	1.399(2)	C15"-B1"	1.572(2)	C16"-C17"	1.385(2)
C17"-C18"	1.391(2)	C18"-C19"	1.383(2)	C18"-C21"	1.492(2)
C19"-C20"	1.388(2)	C22"-C23"	1.548(2)	C22"-C24"	1.505(2)
C22"-C25"	1.517(3)	C23"-C26"	1.514(3)	C23"-C27"	1.497(3)

Figure A2.320: Bond Angles in 6,8-bis(4,4,5,5-tetramethyl-1,3,2-dioxaboryl)-2-(4-(trifluoromethyl)phenyl)-2,1-borazaronaphthalene (**3.59**), (°)

B2-O1-C9	107.26(12)	B2-O2-C10	107.34(12)	B3-O3-C22	106.80(11)
B3-O4-C23	106.82(11)	C8-N1-B1	125.09(13)	C2-C1-B1	119.21(14)
C1-C2-C3	122.59(14)	C4-C3-C2	121.67(14)	C4-C3-C8	118.68(13)
C8-C3-C2	119.65(13)	C5-C4-C3	122.35(14)	C4-C5-C6	117.45(13)
C4-C5-B3	121.29(13)	C6-C5-B3	121.27(14)	C7-C6-C5	123.19(14)
C6-C7-C8	117.72(13)	C6-C7-B2	118.85(13)	C8-C7-B2	123.41(13)
N1-C8-C3	118.49(13)	N1-C8-C7	120.90(13)	C3-C8-C7	120.61(13)
O1-C9-C10	102.72(11)	O1-C9-C11	106.32(13)	O1-C9-C12	107.72(13)
C11-C9-C10	114.45(14)	C11-C9-C12	110.47(14)	C12-C9-C10	114.32(13)
O2-C10-C9	102.49(11)	O2-C10-C13	108.63(13)	O2-C10-C14	106.37(13)
C13-C10-C9	114.52(14)	C14-C10-C9	113.84(14)	C14-C10-C13	110.26(14)
C16-C15-B1	122.67(14)	C20-C15-C16	116.81(14)	C20-C15-B1	120.52(14)
C17-C16-C15	121.96(15)	C16-C17-C18	119.42(15)	C17-C18-C21	118.34(14)
C19-C18-C17	120.37(14)	C19-C18-C21	121.25(14)	C18-C19-C20	119.26(14)
C19-C20-C15	122.18(14)	F1-C21-C18	111.52(13)	F2-C21-F1	105.35(12)
F2-C21-C18	112.65(13)	F3-C21-F1	106.54(13)	F3-C21-F2	106.98(13)
F3-C21-C18	113.26(13)	O3-C22-C23	102.36(11)	O3-C22-C24	108.80(12)
O3-C22-C25	106.62(12)	C24-C22-C23	115.37(13)	C24-C22-C25	110.60(13)
C25-C22-C23	112.35(13)	O4-C23-C22	102.18(11)	O4-C23-C26	106.56(12)
O4-C23-C27	108.96(12)	C26-C23-C22	112.65(13)	C27-C23-C22	115.51(13)
C27-C23-C26	110.25(14)	N1-B1-C1	114.95(14)	N1-B1-C15	119.44(14)
C1-B1-C15	125.60(14)	O1-B2-O2	113.58(14)	O1-B2-C7	121.89(14)
O2-B2-C7	124.52(14)	O3-B3-O4	113.76(13)	O3-B3-C5	123.49(14)
O4-B3-C5	122.75(14)	B2'-O1'-C9'	107.44(12)	B2'-O2'-C10'	107.42(12)
B3'-O3'-C22'	106.71(12)	B3'-O4'-C23'	106.67(11)	C8'-N1'-B1'	125.08(13)
C2'-C1'-B1'	119.19(14)	C1'-C2'-C3'	122.45(14)	C4'-C3'-C2'	121.53(14)
C4'-C3'-C8'	118.69(14)	C8'-C3'-C2'	119.77(13)	C5'-C4'-C3'	122.20(14)
C4'-C5'-C6'	117.58(13)	C4'-C5'-B3'	120.63(14)	C6'-C5'-B3'	121.79(14)
C7'-C6'-C5'	123.10(14)	C6'-C7'-C8'	117.87(14)	C6'-C7'-B2'	118.88(13)
C8'-C7'-B2'	123.21(13)	N1'-C8'-C3'	118.46(13)	N1'-C8'-C7'	120.98(13)
C3'-C8'-C7'	120.55(13)	O1'-C9'-C10'	102.89(12)	O1'-C9'-C11'	106.67(13)
O1'-C9'-C12'	107.79(14)	C11'-C9'-C10'	113.64(15)	C12'-C9'-C10'	114.40(14)
C12'-C9'-C11'	110.69(15)	O2'-C10'-C9'	102.31(11)	O2'-C10'-C13'	108.71(13)
O2'-C10'-C14'	106.32(12)	C13'-C10'-C9'	114.95(14)	C13'-C10'-C14'	110.08(14)
C14'-C10'-C9'	113.71(14)	C16'-C15'-B1'	122.81(14)	C20'-C15'-C16'	116.52(14)
C20'-C15'-B1'	120.67(14)	C17'-C16'-C15'	121.97(15)	C16'-C17'-C18'	119.63(15)
C17'-C18'-C21'	118.42(14)	C19'-C18'-C17'	120.25(14)	C19'-C18'-C21'	121.30(14)
C18'-C19'-C20'	119.18(15)	C19'-C20'-C15'	122.44(14)	F1'-C21'-C18'	111.50(13)
F2'-C21'-F1'	105.31(13)	F2'-C21'-C18'	112.71(14)	F3'-C21'-F1'	106.18(13)
F3'-C21'-F2'	107.44(14)	F3'-C21'-C18'	113.17(13)	O3'-C22'-C23'	102.45(11)

O3'-C22'-C24'	106.43(12)	O3'-C22'-C25'	108.74(12)	C24'-C22'-C23'	113.15(13)
C25'-C22'-C23'	115.20(13)	C25'-C22'-C24'	110.14(14)	O4'-C23'-C22'	102.05(11)
O4'-C23'-C26'	109.00(12)	O4'-C23'-C27'	106.55(12)	C26'-C23'-C22'	115.68(13)
C26'-C23'-C27'	109.76(13)	C27'-C23'-C22'	113.08(13)	N1'-B1'-C1'	115.02(14)
N1'-B1'-C15'	119.31(14)	C1'-B1'-C15'	125.67(14)	O1'-B2'-O2'	113.35(14)
O1'-B2'-C7'	122.15(14)	O2'-B2'-C7'	124.50(14)	O3'-B3'-O4'	113.85(13)
O3'-B3'-C5'	123.14(14)	O4'-B3'-C5'	123.01(14)	B2"-O1"-C9"	107.90(12)
B2"-O2"-C10"	107.76(12)	B3"-O3"-C22"	107.55(12)	B3"-O4"-C23"	107.02(12)
C8"-N1"-B1"	124.82(13)	C2"-C1"-B1"	119.18(14)	C1"-C2"-C3"	122.53(14)
C4"-C3"-C2"	121.67(14)	C4"-C3"-C8"	118.65(14)	C8"-C3"-C2"	119.67(13)
C5"-C4"-C3"	122.33(14)	C4"-C5"-C6"	117.44(13)	C4"-C5"-B3"	121.54(13)
C6"-C5"-B3"	121.01(14)	C7"-C6"-C5"	123.29(14)	C6"-C7"-C8"	117.65(13)
C6"-C7"-B2"	118.50(13)	C8"-C7"-B2"	123.79(13)	N1"-C8"-C3"	118.74(13)
N1"-C8"-C7"	120.65(13)	C3"-C8"-C7"	120.61(13)	O1"-C9"-C10"	102.91(11)
O1"-C9"-C11"	107.31(13)	O1"-C9"-C12"	106.66(13)	C11"-C9"-C10"	114.80(13)
C11"-C9"-C12"	110.58(13)	C12"-C9"-C10"	113.75(14)	O2"-C10"-C9"	102.35(11)
O2"-C10"-C13"	106.49(12)	O2"-C10"-C14"	108.41(13)	C13"-C10"-C9"	113.74(13)
C14"-C10"-C9"	114.79(13)	C14"-C10"-C13"	110.30(14)	C16"-C15"-C20"	116.72(14)
C16"-C15"-B1"	122.98(14)	C20"-C15"-B1"	120.30(14)	C17"-C16"-C15"	121.99(15)
C16"-C17"-C18"	119.59(15)	C17"-C18"-C21"	118.55(14)	C19"-C18"-C17"	120.10(14)
C19"-C18"-C21"	121.31(14)	C18"-C19"-C20"	119.37(14)	C19"-C20"-C15"	122.22(14)
F1"-C21"-C18"	111.64(12)	F2"-C21"-F1"	105.48(12)	F2"-C21"-C18"	112.90(13)
F3"-C21"-F1"	106.29(13)	F3"-C21"-F2"	106.94(13)	F3"-C21"-C18"	113.05(13)
O3"-C22"-C23"	102.79(12)	O3"-C22"-C24"	109.00(14)	O3"-C22"-C25"	105.90(14)
C24"-C22"-C23"	115.14(15)	C24"-C22"-C25"	110.40(16)	C25"-C22"-C23"	112.86(16)
O4"-C23"-C22"	102.58(12)	O4"-C23"-C26"	105.75(14)	O4"-C23"-C27"	109.50(14)
C26"-C23"-C22"	111.78(16)	C27"-C23"-C22"	115.96(16)	C27"-C23"-C26"	110.49(19)
N1"-B1"-C1"	115.05(14)	N1"-B1"-C15"	119.28(14)	C1"-B1"-C15"	125.66(14)
O1"-B2"-O2"	113.43(14)	O1"-B2"-C7"	121.34(14)	O2"-B2"-C7"	125.22(14)
O3"-B3"-O4"	113.48(14)	O3"-B3"-C5"	123.27(14)	O4"-B3"-C5"	123.25(14)

Figure A2.321: Hydrogen Bonds for 6,8-bis(4,4,5,5-tetramethyl-1,3,2-dioxaboryl)-2-(4-(trifluoromethyl)phenyl)-2,1-borazaronaphthalene (**3.59**)

D	H	A	d(D-H)/Å	d(H-A)/Å	d(D-A)/Å	D-H-A/°
N1	H1a	O2	0.86	2.19	2.8851(16)	138.3
N1'	H1a'	O2'	0.86	2.15	2.8585(16)	138.9
N1"	H1a"	O2"	0.86	2.18	2.8838(16)	138.8

This report has been created with Olex2 [6], compiled on 2016.09.09 svn.r3337 for OlexSys

References [1] APEX2 2014.11-0 [2] SAINT v8.34A [3] SADABS v2014/5

[4] SHELXS-97 [5] SHELXL-2014/7 [6] Olex2 (Dolomanov et al., 2009)

ABOUT THE AUTHOR

Geraint H. M. Davies was born in Winston Salem, North Carolina to Huw and Angela Davies. He has a brother Evan, who is currently enrolled at Georgia Tech in the mechanical engineering doctoral program. Growing up in Clarence - a suburb of Buffalo, New York - he attended the Clarence School District and the University at Buffalo Gifted Math Program where, outside of academics, he was actively involved in both music (violin and piano) and athletics (cross country/track and field).

Upon graduating Clarence High School in 2008, Geraint went to Emory University where he studied both music performance (violin) and chemistry, along with preforming in the university orchestra and running on the varsity cross country/track and field teams. Geraint had the opportunity to do pursue several different avenues of research during his undergraduate tenure. At Emory, Geraint worked in the laboratory of Professor Simon Blakey studying Lewis-acid catalyzed asymmetric allylation, during which he completed the SURE program (Summer Undergraduate Research at Emory). Geraint also had the opportunity to do summer research at Princeton in the group of Professor Erik Sorensen under the tutelage of Dr. Chris Jeffrey (University of Reno) and at Bristol-Myers Squibb in the process research and development under the guidance of Dr. Omid Soltani (Seattle Genetics) and Dr. Caroline Wei.

After completing degrees in both chemistry (B.S. - with highest honors) and music (B.A.) in 2012, Geraint started his doctoral studies at the University of Pennsylvania. Since joining the Molander Group in the spring of 2009, he has studied synthetic methods for accessing azaborine isosteres of heteroaromatic systems and developed computational strategies for analyzing them. Outside of chemistry, Geraint is an avid runner competing for the Penn Running Club and Philadelphia Runner Track Club. His proudest running accomplishments include finishing 8th overall in the 2015 Broad Street run and being a 2-time winner (2015, 2013) of the Atlanta Half Marathon. For the past 3 years Geraint has also been the coach of the Penn Running Club. After completion of his graduate studies, Geraint will be joining Celgene as a medicinal chemist in Cambridge, Massachusetts.

BIBLIOGRAPHY

Abbey, E. R.; Lamm, A. N.; Baggett, A. W.; Zakharov, L. N.; Liu, S.-Y. *J. Am. Chem. Soc.* **2013**, *135*, 12908.

Abbey, E. R.; Liu, S.-Y. *Org. Biomol. Chem.* **2013**, *11*, 2060.

Abbey, E. R.; Zakharov, L. N.; Liu, S.-Y. *J. Am. Chem. Soc.* **2011**, *133*, 11508.

Amaike, K.; Loach, R. P.; Movassaghi, M. *Org. Synth.* **2015**, *92*, 373.

Ashley, J. D.; Stefanick, J. F.; Schroeder, V. A.; Suckow, M. A.; Kiziltepe, T.; Bilgicer B. *J. Med. Chem.* **2014**, *57*, 5282.

Atkinson, I. B.; Clapp, D. B.; Beck, C.A.; Currell, B. R. *J. Chem. Soc., Dalton Trans.* **1972**, 182.

Bagget, A. W.; Gou, F.; Li, B.; Liu, S.-Y. Jäkle, F. *Angew. Chem., Int. Ed.* **2015**, *54*, 11191.

Baggett, A. W.; Vasiliu, M.; Li, B.; Dixon, D. A.; Liu, S.-L. *J. Am. Chem. Soc.* **2015**, *137*, 5536.

Baker, S. J.; Ding, C. Z.; Akama, T.; Zhang, Y.-K.; Hernandez, V.; Xia, Y. *Future Med. Chem.* **2009**, *1*, 2375.

Baker, S. J.; Tomsho, J. W.; Benkovic, S. J. *Chem. Soc. Rev.* **2011**, *40*, 4279.

Balaban, A. T.; Oniciu, D. C.; Katritzky, A. R. *Chem. Rev.* **2004**, *104*, 2777.

Balasubramaniyan, V. *Chem. Rev.* **1966**, *66*, 567.

Baldock, C.; Rafferty, J. B.; Sedelnikova, S. E.; Baker, P. J.; Stuitje, A. R.; Slabas, A. R.; Hawkes, T. R.; Rice, D. W. *Science* **1996**, *274*, 2107.

Bandyopadhyay, A.; Cambray, S.; Gao, J. *J. Am. Chem. Soc.* **2017**, *139*, 871.

Bocchi, V.; Palla, G.; *Synthesis* **1982**, *12*, 1096.

Becke, A. D. J. *Chem. Phys*. **1993**, *98*, 5648.

Bikiaris, D.; Koutris, E.; Karavas, E. *Recent Pat. Drug Deliv. Formul.* **2007**, *1*, 201.

Bordwell, F. G.; Drucker, G. E.; Fried, H. E. *J. Org. Chem.* **1981**, *46*, 632.

Bosdet, M. J. D.; Jaska, C. A.; Piers, W. E.; Sorensen, T. S.; Parvez, M. *Org. Lett.* **2007**, *9*, 1395.

Bosdet, M. J. D.; Piers, W. E. *Can. J. Chem.* **2009**, *87*, 8.

Braunschweig, H.; Damme, A.; Jimenez-Halla, J. O. C.; Pfaffinger, B.; Radacki, K.; Wolf, J. *Angew. Chem., Int. Ed.* **2012**, *51*, 10034.

Brooks, K. P.; Bowden, M. E.; Karkamkar, A. J.; Houghton, A. Y.; Autrey, S. T. *J. Power Sources* **2016**, *324*, 170.

Bua, R.; Shrivastava, S.; Sonwane, S. K.; Srivastava, S. K. *Advan. Biol. Res.* **2011**, *5*, 120.

Campbell, P. G.; Marwits, A. J. V.; Liu, S.-Y. *Angew. Chem., Int. Ed.* **2012**, *51,* 6074.

Carvalho, I.; Borges, Á. D. L.; Bernardes, L. S. C. *J. Chem. Educ.* **2005**, *82*, 588.

Casasnovas, R.; Fernández, D.; Ortega-Castro, J.; Frau, J.; Donoso, J.; Muñoz, F. *Theor. Chem. Acc.* **2011**, *130*, 1.

Casado, M. R. S.; Jimeńez, M. C.; Bueno, M. A.; Barriol, M.; Leenaerts, J. E.; Pagliuca, C.; Lamenca, C. M.; Lucas, A. I. D.; García, A.; Trabanco, A. A.; Rombouts, F. J. R. *Eur. J. Org. Chem*. **2015**, *23*, 5221.

Chen, Z.; Tian, Z.; Kallio, K.; Oleson, A. L.; Ji. A.; Borchardt, D.; Jiang, D.; Remington, S. J.; Ai, H. *J Am. Chem. Soc.* **2016**, *138*, 4900.

Chen, Z.; Wannere, C. S.; Corminboeuf, C.; Puchta, R.; Schleyer, P. v. R. *Chem. Rev.* **2005**, *105*, 3842.

Chinchill, R.; Nájera, C.; Yus, M.; *Chem. Rev.* **2004**, *104*, 2667.

Corce, V.; Chamoreau, L.-M.; Derat, E.; Goddard, J.-P.; Ollivier, C.; Fensterbank, L. *Angew. Chem., Int. Ed.* **2015**, *54*, 11414.

Chrostawska, A.; Xu, S.; Maziére, A.; Bokenvitz, K.; Li, B.; Abbey, E. R.; Cargelos, A.; Graciaa, A.; Liu, S.-Y. *J. Am. Chem. Soc.* **2014**, *136*, 11813.

Chu, J.-H.; Tsai, S.-L.; Wu, M.-J. *Synthesis* **2009**, *22*, 3757.

Chu, L.; Lipshultz, J. M.; MacMillan, D. W. C. *Angew. Chem., Int. Ed.* **2015**, *54*, 7929.

Churches, Q. I.; Hooper, J. F.; Hutton, C. A.; *J. Org. Chem.* **2015**, *80*, 5428.

Clark, T.; Kranz, *J. Org. Chem.* **1992**, *57*, 5492.

Coventry, D. N.; Batsanov, A. S.; Goeta, A. E.; Howard, J. A. K.; Marder, T. B.; Perutz, R. N. *Chem. Commun.* **2005**, 2172.

Cragg, R. H.; Miller, T. J. *J. Organomet. Chem.* **1985**, *294*, 1.

Crudden, C. M.; Ziebenhaus, C.; Rygus, J. P. G.; Ghozati, K.; Unsworth, P. J.; Nambo, M.; Voth, S.; Hutchinson, M.; Laberge, V. S.; Maekawa, Y.; Imao, D. *Nat. Chem.* **2016**, *7*, doi:10.1038/ncomms11065.

Currel, B.R.; Gerrard, W.; Khodabocus, M. *J. Organomet. Chem.* **1967**, *8*, 411.

Davie, M. C.; Franzblau, S. G.; Martin A. R.; *Bioorg. Med. Chem. Lett.* **1998**, *8*, 843.

Davies, G. H. M.; Molander, G. A. *J. Org. Chem.* **2016**, *81*, 3771.

Davies, G. H. M.; Mukhtar, A.; Fatemeh, S.; Kelly, C. B.; Molander, G. A.; *J. Org. Chem.* **2017**, *82*, 5380.

Davies, G. H. M.; Zhou, Z.-Z.; Jouffroy, M.; Molander, G. A. *J. Org. Chem.* **2017**, *82*, 549.

Dewar, M. J. S.; Dietz, R. *J. Chem. Soc.* **1959**, 2728.

Dewar, M. J. S.; Dietz, R. *Tetrahedron* **1961**, *15*, 26.

Dewar, M. J. S.; Kubba, V. P.; Pettit, R. *J. Chem. Soc.* **1958**, 3073**.**

Ditchfield, R.; Hehre, W. J.; Pople, J. A. *J. Chem. Phys.* **1971**, *54*, 724.

Dohr, A. D.; Kampf, J. W.; Ashe, A. J. *Organometallics* **2014**, *33*, 1318.

Dosdet, M. J. D.; Piers, W. E. *Can. J. Chem.* **2009**, *87*, 8.

El Khatib, M.; Serafim, R. A. M.; Molander, G. A. *Angew. Chem., Int. Ed.* **2016**, *55*, 254.

Eid, S. Zalewski, A.; Smieško, M.; Ernst, B.; Vedani, A. *Int. J. Mol. Sci.* **2013**, *14*, 684.

Firth, N. C.; Brown, N.; Blagg, J. *J. Chem. Inf. Model.* **2012**, *52*, 2516.

Frisch, M. J.; Trucks, G. W.; Schlegel, H. B.; Scuseria, G. E.; Robb, M. A.; Cheeseman, J. R.; Scalmani, G.; Barone, V.; Mennucci, B.; Petersson, G. A.; Nakatsuji, H.; Caricato, M.; Li, X.; Hratchian, H. P.; Izmaylov, A. F.; Bloino, J.; Zheng, G.; Sonnenberg, J. L.; Hada, M.; Ehara, M.; Toyota, K.; Fukuda, R.; Hasegawa, J.; Ishida, M.; Nakajima, T.; Honda, Y.; Kitao, O.; Nakai, H.; Vreven, T.; Montgomery, J. A., Jr.; Peralta, J. E.; Ogliaro, F.; Bearpark, M.; Heyd, J. J.; Brothers, E.; Kudin, K. N.; Staroverov, V. N.; Kobayashi, R.; Normand, J.; Raghavachari, K.; Rendell, A.; Burant, J. C.; Iyengar, S. S.; Tomasi, J.; Cossi, M.; Rega, N.; Millam, J. M.; Klene, M.; Knox, J. E.; Cross, J. B.; Bakken, V.; Adamo, C.; Jaramillo, J.; Gomperts, R.; Stratmann, R. E.; Yazyev, O.; Austin, A. J.; Cammi, R.; Pomelli, C.; Ochterski, J. W.; Martin, R. L.; Morokuma, K.; Zakrzewski, V. G.; Voth, G. A.; Salvador, P.; Dannenberg, J. J.; Dapprich, S.; Daniels, A. D.; Farkas, Ö.; Foresman, J. B.; Ortiz, J. V.; Cioslowski, J.; Fox, D. J. *Gaussian 09*, revision D.01; Gaussian, Inc.: Wallingford CT, 2009.

Foye, W. O.; Lemke, T. L.; Williams, D. A. *Foye's Principles of Medicinal Chemistry*; Wolters Kluwer Health/Lippincott Williams & Wilkins: Philadelphia, 2013.

Fu, H.; Fang, H.; Sun, J.; Wang, H.; Liu, A.; Sun, J.; Wu, Z. *Curr. Med. Chem.* **2014**, *21*, 3271.

Gellrich, U.; Diskin-Posner, Y.; Shimon, L. J. W.; Milstein, D. *J. Am. Chem. Soc.* **2016**, *138*, 13307.

Ghosh, D.; Periyasamy, G.; Pati, S. K. *Phys. Chem. Chem. Phys.* **2011**, *13*, 20627.

Goldberg, A. R.; Northrop, B. H. *J. Org. Chem.* ***20*16, *81***, *9*69.

Hariharan, P. C.; Pople, J. A. *Theor. Chim. Acta* **1973**, *28*, 213.

Hashimoto, S.; Ikurta, T.; Shiren, K.; Nakatsuka, S.; Ni, J.; Nakamura, M.; Hatakeyama, T. *Chem. Mater.* **2014**, *26*, 6265.

Hartwig, J. F. *Acc. Chem. Res.* **2012**, *45*, 864.

Hawthorne, M. F. *J. Am. Chem. Soc.* **1961**, *83*, 831.

Hehre, W. J.; Ditchfield, R.; Pople, J. A. *J. Chem. Phys.* **1972**, *56*, 2257.

Hernandez, V.; Crépin, C.; Palencia, A.; Cusack, S.; Akama, T.; Baker, S. J.; Bu, W.; Feng, L.; Freund, Y. R.; Liu, L.; Meewan, M.; Mohan, M.; Mao, W.; Rock, F. L.; Sexton, H.; Sheoran, A.; Zhang, Y.; Zhang, Y.-K.; Zhou, Y.; Nieman, J. A.; Anugula, M. R.; Keramane, E. M.; Savariraj, K.; Reddy, D. S.; Sharma, R.; Subedi, R.; Singh, R.; O'Leary, A.; Simon, N. L.; De Marsh, Peter, L.; Mushtaq, S.; Warner, M.; Livermore, D. M.; Alley, M. R. K.; Plattnera, J. J. *Antimicrob. Agents Chemother.* **2013**, *57*, 1394.

Hughes, J. P.; Rees, S.; Kalindjina, S. B.; Philpott, K. L. *Br. J. Pharmacol.* **2011**, *162*, 1239.

Hunter, P. *EMBO Rep.* **2009**, *10*, 125.

Igarashi, T.; Tobisu, M.; Chatani, N. *Angew. Chem., Int. Ed.* **2017**, *56*, 2069.

Ihara, H.; Koyanagi, M.; Suginome, M. *Org. Lett.* **2011**, *13*, 2662.

Ihara, H.; Ueda, A.; Suginome, M. *Chem. Lett.* **2011**, *40*, 916.

Ishiyama, T.; Takagi, J.; Yonekawa, Y.; Hartwig, J. F.; Miyaura, N. *Adv. Synth. Catal.* **2003**, *345*, 1103.

Jolibois, H.; Doucet, A.; Dubry, J. L. J. *Inorg. Nucl. Chem. Lett.* **1976**, *12*, 759.

Jouffroy, M.; Davies, G. H. M.; Molander, G. A. *Org. Lett.* **2016**, *18*, 1606.

Jouffroy, M.; Primer, D. N.; Molander, G. A. *J. Am. Chem. Soc.* **2016**, *138*, 475.

Kalyani, D.; McMurtrey, K. B.; Neufeldt, S. R.; Sanford, M. S. *J. Am. Chem. Soc.* **2011**, *133*, 18566.

Karakaya, I.; Primer, D. N.; Molander, G. A. *Org. Lett.* **2015**, *17*, 3294.

Kaupp, G.; Naimi-Jamal, M. R.; Stepanenko, V. *Chem. Eur. J.* **2003**, *9*, 4156.

Kaushi, N. K.; Kaushik, N.; Attri, P.; Kumar, N.; Kim, C. H.; Verma, A. K.; Choi, E. H. *Molecules* **2013**, *18*, 6620.

Kerns, E. H.; Di, L. *Drug-like Properties: Concepts, Structure Design and Methods*; 1st Edn, Elsevier: Burlington, MA, 2008.

Kim, B. J.; Matteson, D. S. *Angew. Chem. Int. Ed.* **2004**, *43*, 3056.

Knack, D. H.; Marshall, J. L.; Harlow, G. P.; Dudzik A.; Szaleniec, M.; Liu, S.-Y.; Heider, J. *Angew. Chem., Int. Ed.* **2013**, *52*, 2599.

Konishi, S.; Kawamorita, S.; Iwai, T.; Steel, P. G.; Marder, T. B.; Masaya S. *Chem. Asian J.* **2014**, *9*, 434.

Koyanagi, M.; Sichenauer, N.; Ihara, H.; Yamamoto, T.; Suginome, M. *Chem. Lett.* **2013**, *42*, 541.

Kurata, R.; Kaneda, K.; Ito, A. *Org. Lett.* **2017**, *19*, 392.

Langmuir, I. *J. Am. Chem. Soc.* **1919**, *41*, 1543.

Larsen, M. A.; Hartwig, J. F. *J. Am. Chem. Soc.* **2014**, *136*, 4287.

Le, C. C.; MacMillan, D. W. C. *J. Am. Chem. Soc.* **2015**, *137*, 11938.

Lee, C.; Yang, W.; Parr, R. G. *Phys. Rev. B: Condens. Matter Mater. Phys.* **1988**, *37*, 785.

Lee, H.; Fischer, M.; Shoichet, B. K.; Liu, Liu, S.-Y. *J. Am. Chem. Soc.* **2016**, *138*, 12021.

Lee, Y.-S.; Cheon, C.-H. *Adv. Synth. Catal.* **2015**, *13*, 2951.

Leeson, P. *Nature* **2012**, *481*, 455.

Li, X.; Zhang, Y.-K.; Plattner, J. J.; Mao, W.; Alley, M.R.K.; Xia, Y.; Hernandez, V.; Zhou, Y.; Ding, C. Z.; Li, J.; Shao, Z.; Zhang, H.; Xu, M. *Bioorg. Med. Chem. Lett.* **2013**, *23*, 963.

Lima, L. M.; Berreiro, E. J. *Curr. Med. Chem.* **2005**, *12*, 23.

Liptak, M. D.; Shields, G. C. *J. Am. Chem. Soc.* **2001**, *123*, 7314.

Liu, L.; Marwitz, A. J.; Matthews, B. W.; Liu, S. Y. *Angew. Chem., Int. Ed.* **2009**, *48*, 6817.

Liu, S.-Y.; Hills I. D.; Fu, G. C. *Organometallics* **2002**, *21*, 4323.

Liu, W.; Wu, P.; Li, J.; Cui, C. *J. Org. Chem.* **2015**, *80*, 3737.

Liu, X.; Zhang, Y.; Li, B.; Zakharove, L. N.; Vasiliu, M.; Dixon, D. A.; Liu, S.-Y. *Angew. Chem., Int. Ed.* **2016**, *55*, 8333.

Liu, Z.; Xu, J.; Ruan, W.; Fu, C.; Zhang, H.-J.; Wen, T.-B. *Dalton Trans.* **2013**, *42*, 11976.

Lu, J.-S., Ko, S.-B.; Walters N. R.; Kang, Y.; Sauriol, F.; Wang, S. *Angew. Chem., Int. Ed.* **2013**, *52*, 4544.

Macarron, R.; Banks, M. N.; Bojanic, D.; Burns, D. J.; Cirovic, D. A.; Garyantes, T.; Green, D. V. S.; Herzberg, R. P.; Janzen, W. P.; Paslay, J. W.; Schopfer, U.; Sittampalam, G. S. *Nat. Rev. Drug Descov.* **2011**, *10*, 188.

Mahdavi, M.; Asadi, M.; Saeedi, M.; Tehrani M. H.; Sara Mirfazli, S. S.; Abbas Shafiee, A.; Foroumadi A. *Synth. Commun.* **2013**, *43*, 2936.

Maitlis, P. M. *Chem. Rev.* **1962**, *62*, 223.

Manallack, D. T.; Prankerd, R. J.; Yuriev, E.; Oprea, T. I.; Chalmers D. K. *Chem. Soc. Rev.* **2013**, *42*, 485.

Martinez, C. R.; Iverson, B. L. *Chem. Sci.* **2012**, *3*, 2191.

Meanwell, N. A. *J. Med. Chem.* **2011**, *54*, 2529.

Meriam, J. S.; Niedenzu, K. *J. Organomet. Chem.* **1973**, *51*, 21.

Miertuš S. *Chem. Phys.* **1981**, *55*, 117.

Mkhalid, I. A. I.; Barnard, J. H.; Marder, T. B.; Murphy, J. M.; Hartwig, J. F. *Chem. Rev.* **2010**, *110*, 890.

Molander, G. A. *J. Org. Chem.* **2015**, *80*, 7837.

Molander, G. A.; Amani, J.; Wisniewski, S. R. *Org. Lett.* **2014**, *16*, 6024.

Molander, G. A.; Cavalcanti, L. N.; Canturk, B.; Pan, P.-S.; Kennedy, L. E. *J. Org. Chem.* **2009**, *74*, 7364.

Molander, G. A.; Wisniewski, S. R. *J. Org. Chem.* **2014**, *79*, 6663.

Molander, G. A.; Wisniewski, S. R. *J. Org. Chem.* **2014**, *79*, 8339.

Molander, G. A.; Wisniewski, S. R.; Amani, J. *Org. Lett.* **2014**, *16*, 5636.

Molander, G. A.; Wisniewski, S. R.; Etemadi-Davan, E. *J. Org. Chem.* **2014**, *79*, 11199.

Molander, G. A.; Wisniewski, S. R.; Traister, K. M. *Org. Lett.* **2014**, *16*, 3692.

Morgan, M. M.; Piers, W. E. *Dalton Trans.* **2016**, *45*, 5920.

Morrison, R. T.; Boyd, R. N. *Organic Chemistry*, 6th ed.; Prentice-Hall: Eaglewood Cliffs, New Jersey, 1992.

Muckerman, J. T.; Skone, J. H.; Ning, M.; Wasada-Tsutsui, Y. *Biochim. Biophys. Acta* **2013**, *1827*, 882.

Müller, K.; Völkl, J.; Arlt, W. *Energy Technol.* **2013**, *1*, 20.

Murugan, K.; Chinnapattu, M.; Khan, F.-R. N.; Lyer, P. S. *RCS Adv.* **2015**, *5*, 36902.

Nare, B.; Wring, S.; Bacchi, C.; Beaudet, B.; Bowling, T.; Brun, R.; Chen, D.; Ding, C.; Freund, Y.; Gaukel, E.; Hussain, A.; Jarnagin, K.; Jenks, M.; Kaiser, M.; Mercer, M.; Mejia, E.; Noe, A.; Orr, M.; Parham, R.; Plattner, J.; Randolph, R.; Rattendi, D.; Rewerts, C.; Sligar, J.; Nigel Yarlett, N.; Don, R.; Jacobs, R. *Antimicrob. Agents Chemother*. **2010**, *54*, 4379.

Nicolaou, C. A.; Brown, N. *Drug Discov. Today* **2013**, *10*, 427.

Noble, A.; McCarver, S. J.; MacMillan, D. W. C. *J. Am. Chem. Soc.* **2015**, *137*, 624.

Noda H.; Bode, J. W. *J. Am. Chem. Soc.* **2015**, *137*, 3958.

Nyilas, E.; Soloway, A. H. *J. Am. Chem. Soc.* **1959**, *81*, 2681.

Papadopoulos, A. G.; Charistos, N. D.; Kyriakidou, K.; Sigalas, M. P. *J. Phys. Chem. A* **2015**, *119*, 10091.

Patani, G. A.; LaVoie, E. J. *Chem. Rev.* **1996**, *96*, 3147.

Patel, N. R.; Kelly, C. B.; Jouffroy, M.; Molander, G. A. *Org. Lett.* **2016**, *18*, 764**.**

Paul, S.; Chotana, G. A.; Holmes, D.; Reichle, R. C.; Maleczka, R. E., Jr., Smith, M. R., III *J. Am. Chem. Soc.* **2006**, *128*, 15552.

Pérez, Y A.; Usista, C. M.; Martínez, J. I.; Nava, M. D. C. D.; Rodríguez, F. A. R. *Polymers* **2016**, *8*, 214.

Plumley, J. A.; Evanseck, J. D. *J. Phys. Chem. A* **2009**, *113*, 5985.

Preshlokc, S. M.; Ghaffari, B.; Maligres, P, E.; Krska, S. W.; Maleczka, R. E., Jr.; Smith, M. R., III *J. Am. Chem. Soc.* **2013**, *135*, 7572.

Preshlock, S. M.; Plattner, D. L.; Malegres, P. E.; Krska, S. W.; Maleczka, R. E., Jr.; Smith, M. R., III *Angew. Chem., Int. Ed.* **2013**, *52*, 12915.

Primer, D. N.; Karakaya, I.; Tellis, J. C.; Molander, G. A. *J. Am. Chem. Soc.* **2015**, *137*, 2195.

Ramachandran, P. V. *Future Med. Chem.* **2013**, *5*, 611.

Ramadhar, T. R.; Bansagi, J.; Batey, R. A. *J. Org. Chem.* **2013**, *78*, 1216.

Rami, T.; Hensen, K. *J. Inorg. Nucl. Chem.* **1971**, *33*, 937.

Robbins, D. W.; Boebel, T. A.; Hartwig, J. F. *J. Am. Chem. Soc.* **2010**, *132*, 4068.

Rombouts, F. J. R.; Tovar, F.; Austin, N.; Tresadern, G.; Trabanco, A. A. *J. Med. Chem.* **2015**, *58*, 9287.

Roosen, P. C.; Kallepalli, B. A.; Chattopadhyay, B.; Singleton, D. A.; Maleczka, R. E., Jr.; Smith, M. R., III *J. Am. Chem. Soc.* **2012**, *134*, 11350.

Rueping, M.; Koenigs, R. M.; Poscharny, K.; Fabry, D. C.; Leonori, D.; Vila, C. *Chem.–Eur. J.* **2012**, *18*, 5170.

Ros A.; Fernández, R.; Lassaletta, J. M. *Chem. Soc. Rev.* **2014**, *43*, 3229.

Sahoo, B.; Hopkinson, M. N.; Glorius, F. *J. Am. Chem. Soc.* **2013**, *135*, 5505.

Saint-Louis, C. J.; Magill, L. L.; Wilson, J. A.; Schroeder, A. R.; Harrell, S. E.; Jackson, N. S.; Trindell, J. A.; Kim, S.; Fisch, A. R.; Munro, L.; J. Catalano, V. J.; Webster, C. E.; Vaughan, P. P.; Molek, K. S.; Schrock, A. K.; Huggins, M. T. *J. Org. Chem.* **2016**, *81*, 10955.

Saito, Y.; Segawa, Y.; Itami, K. *J. Am. Chem. Soc.* **2015**, *137,* 5193.

Schmidt, J.R.; Polik, W.F. *WebMO Enterprise*, version 14.0.004e; WebMO LLC: Holland, MI, USA, 2013; http://www.webmo.net.

Scott, H. K.; Aggarwall, V. K. *Chem. Eur. J.* **2011**, *17*, 13124.

Settepani, J. A.;Stokes, J. B.; Borkovec, A. *J. Med. Chem.* **1970**, *13*, 128.

Shinokubo, H. *Proc. Jpn. Acad. Ser. B Phys. Biol. Sci.* **2014**, *90*, 1.

Shu, X. Z.; Zhang, M.; He, Y.; Frei, H.; Toste, F. D. *J. Am. Chem. Soc.* **2014**, *136*, 5844.

Slabber, C. A.; Grimmer, C. D.; Robinson, R. S. *J. Organomet. Chem.* **2013**, *723*, 122.

Srivastava, A. K.; Pandey, S. K.; Misra, N. *Mol. Phys.* **2016**, *114*, 1763.

Stanger, A. *Phys. Chem. Chem. Phys.* **2011**, *13*, 12652-12654.

Stephens, P. J.; Devlin, F. J.; Chabalowski, C. F.; Frisch, M. J. *J. Phys. Chem*. **1994**, *98*, 11623.

Stock, A.; Pohland, E. *Ber. Dtsch. Chem. Ges.* **1926**, *59*, 2215-2223.

Su, F.; Lv, L.; Huang, M.; Shou, Z.; Fang, X. *Org. Lett.* **2014**, *16*, 5024.

Suchy, M.; Hudson, R. H. E. *J. Org. Chem.* **2014**, *79*, 3336.

Tajuddin, H.; Harrisson, P.; Bitterlich, B.; Collings, J. C.; Sim, N.; Batsanov, A. S.; Cheung, M. S.; Kawamorita, S.; Maxwell, A. C.; Shukla, L.; Morris, J.; Lin, Z.; Marder, T. B.; Steel, P. G. *Chem. Sci.* **2012**, *3*, 3505.

Tellis, J. C.; Primer, D. N.; Molander, G. A. *Science* **2014**, *345*, 433.

Thiedemann, B.; Gliese, P. J.; Hoffmann, J.; Lawrence, P. G.; Sönnichsen, F. D.; Staubitz, A. *Chem. Commun.* **2017**, *Advance Article*, DOI: 10.1039/C6CC08599G.

Tomasi, J.; Mennucci, B.; Cammi, R. *Chem. Rev.* **2005**, *105*, 2999.

Ulmschneider, D.; Goubeau, J. *Chem. Ber.* **1957**, *90*, 2733.

Van de Wouw, H. L.; Lee, J. Y.; Klausen, R. S. *Org. Biomol. Chem.* **2016**, *14*, 3256.

Vlasceanu, A.; Jessing, M.; Kilburn, J. P. *Bioorg. Med. Chem.* **2015**, *23*, 4453.

Vanchura, B. A.; Preshlock, S. M.; Roosen, P. C.; Kallepalli, V. A.; Staples, R. J.; Maleczka, R. E., Jr.; Singleton, D. A.; Smith, M. R., III. *Chem. Commun.* **2010**, *46*, 7724.

Vara, B. A.; Jouffroy, M.; Molander, G. A.; *Chem. Sci.* **2017**, *8*, 530.

Vosko, S. H.; Wilk, L.; Nusair, M. *Can. J. Phys.* **1980**, *58*, 1200.

Wan, W.-M.; Baggett, A. W.; Cheng, F.; Lin, H.; Liu, S.-Y.; Jäkle, F. *Chem. Commun.* **2016**, *52*, 13616.

Wang, J.-Y.; Pei, J. *Chin. Chem. Lett.* **2016**, *27*, 1139.

Wang, X.; Zhang, F.; Schellhammer, K. S.; Machata, P.; Ortmann, F.; Cuniberti, G.; Fu, Y.; Hunger, J.; Tang, R.; Popov, A. A.; Berger, R.; Müllen, K.; Feng, X. *J. Am. Chem. Soc.* **2016**, *138*, 11606.

Wang, X.-Y.; Ahuang, F.-D.; Wang, J.-Y.; Pei, J. *Chem. Commun.* **2015**, *51*, 17532.

Wang, X.-Y.; Wang, J.-Y.; Pei, J. *Chem. Eur. J.* **2015**, *21*, 3528.

Weber, L. *Coord. Chem. Rev.* **2008**, *252*, 1.

Weber, L.; Böhling, L. *Coord. Chem. Rev.* **2015**, *284*, 236.

Weber, L.; Schmid, G. *Angew. Chem., Int. Ed.* **1974**, *13*, 467.

Welsch, M. E.; Snyder, S. A.; Stockwell, B. R. *Curr. Opin. Chem. Biol.* **2010**, *14*, 347.

Wisniewski, S. R.; Guenther, C. L.; Argintaru, O. A.; Molander, G. A. *J. Org. Chem.* **2014**, *79*, 365.

Xu, S.; Haeffner, F. Bo, L.; Zakharove, L. N.; Liu, S.-Y. *Angew. Chem., Int. Ed.* **2014**, *53*, 6795.

Xu, S.; Mikulas, T. C.; Zakharov, L. N.; Dixon, D. A.; Liu, S.-Y. *Angew. Chem., Int. Ed.* **2013**, *52*, 7527.

Xu, S.; Zakharov, L. N.; Liu, S.-Y. *J. Am. Chem. Soc.* **2011**, *133*, 20152.

Xu, S.; Zhang, Y.; Li, B.; Liu, S.-Y. *J. Am. Chem. Soc.* **2016**, *138*, 14566.

Yale, H. L. *J. Heterocyclic Chem.* **1971**, *8*, 193.

Yang, J.; Johnson, B. J.; Letourneau, A. A.; Vogels, C. M.; Decken, A.; Baerlocher, F. J.; Westcott, S. A.; *Aust. J. Chem.* **2015**, *68*, 366.

Ye, Y.; Sanford, M. S. *J. Am. Chem. Soc.* **2012**, *134*, 9034.

Zhao, P.; Nettleton, D. O.; Karki, R. G.; Zécri, F. J.; Liu, S.-L. *Chem. Med. Chem.* **2017**, *12*, 358.

Zhu, Q.-L.; Xu, Q. *Energy Environ. Sci.* **2015**, *8*, 478.

Zhuang, F.-D.; Han, J.-M.; Tang, S.; Yang, J.-H.; Chen, Q.-R.; Wang, J.-Y.; Pei, J. *Organometallics* **2016,** *ASAP*, DIO: 10.1021/acs.organomet.6b00811.

Zuo, Z. W.; Ahneman, D. T.; Chu, L. L.; Terrett, J. A.; Doyle, A. G.; MacMillan, D. W. C. *Science* **2014**, *345*, 437.